

# Ferroptosis in cancer and beyond

**Edited by**

Yanqing Liu, Guo Chen, Chaoyun Pan and Xin Wang

**Published in**

Frontiers in Molecular Biosciences



## FRONTIERS EBOOK COPYRIGHT STATEMENT

The copyright in the text of individual articles in this ebook is the property of their respective authors or their respective institutions or funders. The copyright in graphics and images within each article may be subject to copyright of other parties. In both cases this is subject to a license granted to Frontiers.

The compilation of articles constituting this ebook is the property of Frontiers.

Each article within this ebook, and the ebook itself, are published under the most recent version of the Creative Commons CC-BY licence. The version current at the date of publication of this ebook is CC-BY 4.0. If the CC-BY licence is updated, the licence granted by Frontiers is automatically updated to the new version.

When exercising any right under the CC-BY licence, Frontiers must be attributed as the original publisher of the article or ebook, as applicable.

Authors have the responsibility of ensuring that any graphics or other materials which are the property of others may be included in the CC-BY licence, but this should be checked before relying on the CC-BY licence to reproduce those materials. Any copyright notices relating to those materials must be complied with.

Copyright and source acknowledgement notices may not be removed and must be displayed in any copy, derivative work or partial copy which includes the elements in question.

All copyright, and all rights therein, are protected by national and international copyright laws. The above represents a summary only. For further information please read Frontiers' Conditions for Website Use and Copyright Statement, and the applicable CC-BY licence.

ISSN 1664-8714  
ISBN 978-2-83251-342-2  
DOI 10.3389/978-2-83251-342-2

## About Frontiers

Frontiers is more than just an open access publisher of scholarly articles: it is a pioneering approach to the world of academia, radically improving the way scholarly research is managed. The grand vision of Frontiers is a world where all people have an equal opportunity to seek, share and generate knowledge. Frontiers provides immediate and permanent online open access to all its publications, but this alone is not enough to realize our grand goals.

## Frontiers journal series

The Frontiers journal series is a multi-tier and interdisciplinary set of open-access, online journals, promising a paradigm shift from the current review, selection and dissemination processes in academic publishing. All Frontiers journals are driven by researchers for researchers; therefore, they constitute a service to the scholarly community. At the same time, the *Frontiers journal series* operates on a revolutionary invention, the tiered publishing system, initially addressing specific communities of scholars, and gradually climbing up to broader public understanding, thus serving the interests of the lay society, too.

## Dedication to quality

Each Frontiers article is a landmark of the highest quality, thanks to genuinely collaborative interactions between authors and review editors, who include some of the world's best academicians. Research must be certified by peers before entering a stream of knowledge that may eventually reach the public - and shape society; therefore, Frontiers only applies the most rigorous and unbiased reviews. Frontiers revolutionizes research publishing by freely delivering the most outstanding research, evaluated with no bias from both the academic and social point of view. By applying the most advanced information technologies, Frontiers is catapulting scholarly publishing into a new generation.

## What are Frontiers Research Topics?

Frontiers Research Topics are very popular trademarks of the *Frontiers journals series*: they are collections of at least ten articles, all centered on a particular subject. With their unique mix of varied contributions from Original Research to Review Articles, Frontiers Research Topics unify the most influential researchers, the latest key findings and historical advances in a hot research area.

Find out more on how to host your own Frontiers Research Topic or contribute to one as an author by contacting the Frontiers editorial office: [frontiersin.org/about/contact](https://frontiersin.org/about/contact)



# Ferroptosis in cancer and beyond

## Topic editors

Yanqing Liu — Columbia University, United States

Guo Chen — China Pharmaceutical University, China

Chaoyun Pan — Sun Yat-sen University, China

Xin Wang — National Institutes of Health (NIH), United States

## Citation

Liu, Y., Chen, G., Pan, C., Wang, X., eds. (2023). *Ferroptosis in cancer and beyond*. Lausanne: Frontiers Media SA. doi: 10.3389/978-2-83251-342-2

# Table of contents

06	<b>Editorial: Ferroptosis in cancer and beyond</b> Xin Wang, Guo Chen, Chaoyun Pan and Yanqing Liu
10	<b>SLC7A11, a Potential Therapeutic Target Through Induced Ferroptosis in Colon Adenocarcinoma</b> Xin Cheng, Yadong Wang, Liangchao Liu, Chenggang Lv, Can Liu and Jingyun Xu
21	<b>Ferroptosis Biology and Implication in Cancers</b> Chi Qu, Yang Peng and Shengchun Liu
32	<b>Post-Translational Modification of GPX4 is a Promising Target for Treating Ferroptosis-Related Diseases</b> Can Cui, Fei Yang and Qian Li
38	<b>Therapeutic Implications of Ferroptosis in Renal Fibrosis</b> Yao Zhang, Yanhua Mou, Jianjian Zhang, Chuanjian Suo, Hai Zhou, Min Gu, Zengjun Wang and Ruoyun Tan
59	<b>Ferroptosis in Chronic Liver Diseases: Opportunities and Challenges</b> Xiaoxi Zhou, Yadong Fu, Wei Liu, Yongping Mu, Hua Zhang, Jiamei Chen and Ping Liu
69	<b>Comprehensive Analyses of Ferroptosis-Related Alterations and Their Prognostic Significance in Glioblastoma</b> Yuan Tian, Hongtao Liu, Caiqing Zhang, Wei Liu, Tong Wu, Xiaowei Yang, Junyan Zhao and Yuping Sun
86	<b>New Insights on Ferroptosis and Gynecological Malignancies</b> Ruiqi Fan, Yujun Sun, Mengxue Wang, Qian Wang, Aifang Jiang and Tingting Yang
94	<b>Multifaceted Roles of Ferroptosis in Lung Diseases</b> Yi Li, Ying Yang and Yongfeng Yang
110	<b>The Role of Ferroptosis in Acute Kidney Injury</b> Jinshi Zhang, Binqi Wang, Shizhu Yuan, Qiang He and Juan Jin
119	<b>Development and Validation of a Novel Ferroptosis-Related Gene Signature for Prognosis and Immunotherapy in Hepatocellular Carcinoma</b> Bo Zhang, Jilong Zhao, Bing Liu, Yanan Shang, Fei Chen, Sidi Zhang, Jiayao He, Yumei Fan and Ke Tan
141	<b>Ferroptosis: Opportunities and Challenges in Treating Endometrial Cancer</b> Jianfa Wu, Li Zhang, Suqin Wu and Zhou Liu
154	<b>Modified Iron Deposition in Nigrosomes by Pharmacotherapy for the Management of Parkinson's Disease</b> Mengdi Wang, Hongxia Wang, Jing Wang, Shujun Lu, Chen Li, Xiaofei Zhong, Nan Wang, Ruli Ge, Qi Zheng, Jinbo Chen and Hongcai Wang

- 165 **Screening for Potential Therapeutic Agents for Non-Small Cell Lung Cancer by Targeting Ferroptosis**  
Xin Zhao, Lijuan Cui, Yushan Zhang, Chao Guo, Lijiao Deng, Zhitong Wen, Zhihong Lu, Xiaoyuan Shi, Haojie Xing, Yunfeng Liu and Yi Zhang
- 178 **The Mechanisms of Ferroptosis and the Applications in Tumor Treatment: Enemies or Friends?**  
Shuzheng Tan, Ying Kong, Yongtong Xian, Pengbo Gao, Yue Xu, Chuzhong Wei, Peixu Lin, Weilong Ye, Zesong Li and Xiao Zhu
- 191 **Hydrogen Sulfide Inhibits Ferroptosis in Cardiomyocytes to Protect Cardiac Function in Aging Rats**  
Zihui Liang, Yuxin Miao, Xu Teng, Lin Xiao, Qi Guo, Hongmei Xue, Danyang Tian, Sheng Jin and Yuming Wu
- 208 **NPC1 Deficiency Contributes to Autophagy-Dependent Ferritinophagy in HEI-OC1 Auditory Cells**  
Lihong Liang, Hongshun Wang, Jun Yao, Qinqun Wei, Yajie Lu, Tianming Wang and Xin Cao
- 221 **The potential interplay between G-quadruplex and p53: their roles in regulation of ferroptosis in cancer**  
Lulu Zhang, Yi Lu, Xiaoli Ma, Yuanxin Xing, Jinbo Sun and Yanfei Jia
- 229 **Neuronal ferroptosis after intracerebral hemorrhage**  
Siying Ren, Yue Chen, Likun Wang and Guofeng Wu
- 241 **Characterizing the role of SLC3A2 in the molecular landscape and immune microenvironment across human tumors**  
Jiajun He, Dong Liu, Mei Liu, Rong Tang and Dongqing Zhang
- 255 **Single-cell transcriptomics uncover the key ferroptosis regulators contribute to cancer progression in head and neck squamous cell carcinoma**  
Fei Liu, Lindong Tang, Qing Li, Leihui Chen, Yuyue Pan, Zhao Yin, Jingjun He and Junzhang Tian
- 268 **Ferroptosis-related gene signature predicts the clinical outcome in pediatric acute myeloid leukemia patients and refines the 2017 ELN classification system**  
Yu Tao, Li Wei and Hua You
- 285 **A ferroptosis-related gene signature and immune infiltration patterns predict the overall survival in acute myeloid leukemia patients**  
Zhao Yin, Fang Li, Qinqun Zhou, Jianfang Zhu, Zhi Liu, Jing Huang, Huijuan Shen, Ruiming Ou, Yangmin Zhu, Qing Zhang and Shuang Liu
- 295 **Perspectives and mechanisms for targeting ferroptosis in the treatment of hepatocellular carcinoma**  
Lanqing Li, Xiaoqiang Wang, Haiying Xu, Xianqiong Liu and Kang Xu

- 311 **Emerging role of ferroptosis in glioblastoma: Therapeutic opportunities and challenges**  
Shenghua Zhuo, Guiying He, Taixue Chen, Xiang Li, Yunheng Liang, Wenkai Wu, Lingxiao Weng, Jigao Feng, Zhenzhong Gao and Kun Yang
- 326 **The link between ferroptosis and airway inflammatory diseases: A novel target for treatment**  
Zhiwei Lin, Xiaojing Yang, Lili Guan, Lijie Qin, Jiabin Ding and Luqian Zhou
- 339 **The mechanisms of ferroptosis and its role in alzheimer's disease**  
Hongyue Ma, Yan Dong, Yanhui Chu, Yanqin Guo and Luxin Li
- 356 **Current progress of ferroptosis study in ovarian cancer**  
Zhuomin Tan, Hui Huang, Wenyan Sun, Ya Li and Yinnong Jia
- 368 **Mechanisms and inhibitors of ferroptosis in psoriasis**  
Qiao Zhou, Lijing Yang, Ting Li, Kaiwen Wang, Xiaobo Huang, Jingfen Shi and Yi Wang
- 377 **Screening of ferroptosis-related genes with prognostic effect in colorectal cancer by bioinformatic analysis**  
Dongzhi Hu, Zhengyang Zhou, Junyi Wang and Kegan Zhu
- 390 **Ferroptosis and its emerging role in esophageal cancer**  
Rezeye Maimaitizunong, Kai Wang and Hui Li
- 405 **The role of microRNAs in ferroptosis**  
Liqing Guo, Qingkun Zhang and Yuehui Liu
- 415 **Ferroptosis and its role in skeletal muscle diseases**  
Ying Wang, Zepeng Zhang, Weikai Jiao, Yanyan Wang, Xiuge Wang, Yunyun Zhao, Xuechun Fan, Lulu Tian, Xiangyan Li and Jia Mi
- 434 **Indocyanine green as a near-infrared theranostic agent for ferroptosis and apoptosis-based, photothermal, and photodynamic cancer therapy**  
Hsiang-Ching Tseng, Chan-Yen Kuo, Wei-Ting Liao, Te-Sen Chou and Jong-Kai Hsiao



## OPEN ACCESS

## EDITED BY

William C. Cho,  
QEH, Hong Kong SAR, China

## REVIEWED BY

Lu Ding,  
Tongji University, China

## \*CORRESPONDENCE

Yanqing Liu,  
✉ [lyanqing321@163.com](mailto:lyanqing321@163.com)

## SPECIALTY SECTION

This article was submitted to Molecular  
Diagnostics and Therapeutics,  
a section of the journal  
Frontiers in Molecular Biosciences

RECEIVED 04 December 2022

ACCEPTED 19 December 2022

PUBLISHED 04 January 2023

## CITATION

Wang X, Chen G, Pan C and Liu Y (2023),  
Editorial: Ferroptosis in cancer  
and beyond.  
*Front. Mol. Biosci.* 9:1115974.  
doi: 10.3389/fmolb.2022.1115974

## COPYRIGHT

© 2023 Wang, Chen, Pan and Liu. This is an  
open-access article distributed under the  
terms of the [Creative Commons  
Attribution License \(CC BY\)](#). The use,  
distribution or reproduction in other  
forums is permitted, provided the original  
author(s) and the copyright owner(s) are  
credited and that the original publication in  
this journal is cited, in accordance with  
accepted academic practice. No use,  
distribution or reproduction is permitted  
which does not comply with these terms.

# Editorial: Ferroptosis in cancer and beyond

Xin Wang<sup>1</sup>, Guo Chen<sup>2</sup>, Chaoyun Pan<sup>3</sup> and Yanqing Liu<sup>4\*</sup>

<sup>1</sup>National Institute of Neurological Disorders and Stroke, Bethesda, MD, United States, <sup>2</sup>School of Biopharmacy, China Pharmaceutical University, Nanjing, China, <sup>3</sup>Department of Biochemistry and Molecular Biology, Zhongshan School of Medicine, Sun Yat-sen University, Guangzhou, China, <sup>4</sup>Herbert Irving Comprehensive Cancer Center, Columbia University, New York, NY, United States

## KEYWORDS

ferroptosis, oxidative stress, cancer, neurodegenerative disease, organ injury, disease therapy

## Editorial on the Research Topic Ferroptosis in cancer and beyond

## Introduction

To die or not to die, that's not a question for eukaryotic cells. The issues that really matter are WHEN and HOW to die. Cell death has been observed for quite a long time. Historically, this process was taken for granted as passive and uncontrolled, until the discovery of regulated cell death (RCD) (Galluzzi et al., 2018). RCD is a generic term referring to cell death types that can be modulated genetically or pharmacologically, which is contrast to accidental cell death (ACD, which is caused by chemical, physical, or mechanical stresses and cannot be regulated) (Galluzzi et al., 2018). RCD is an evolutionary strategy for both unicellular and multicellular lives to orchestrate normal development and growth (programmed cell death, PCD) or cope with extracellular or intracellular insults (stress-driven RCD) (Galluzzi et al., 2016). Over a long period, RCD and PCD were synonymous to apoptosis—the first discovered RCD type (Hengartner, 2000). In the last two decades, many more types of novel RCDs were identified, such as necroptosis (Vandenabeele et al., 2010), pyroptosis (Shi et al., 2017), and ferroptosis (Stockwell et al., 2017; Dixon and Stockwell, 2019). According to the Nomenclature Committee on Cell Death (NCCD), to date there are more than ten RCD modalities (Galluzzi et al., 2018). All of these cell death processes are featured by specific cellular morphology, molecular mechanism and physiological/pathological significance, while they may also share some similarities in these aspects. Among them, ferroptosis stands out as one of the most interesting Research Topics in the RCD field and shows critical roles in development along with great therapeutic potential for various pathological disorders (Stockwell et al., 2017; Dixon and Stockwell, 2019).

Ferroptosis is caused by the unchecked oxidative perturbation within the cell. Since its discovery, ferroptosis field has caught much attention for not only its significance in basic life sciences as a novel RCD, but also its great potential in clinical use. Actually, many disorders have been linked to ferroptosis (Qiu et al., 2020; Stockwell et al., 2020), such as cancer (Hassannia et al., 2019), ischemia-reperfusion injury (Pefanis et al., 2019), and neurodegenerative disease (Ratan, 2020). Although some molecular mechanisms for the initiation and regulation of ferroptosis have been dug out, there are still many critical questions await to be addressed, along with more and more emerging new research results



that are refreshing our knowledge about the role of ferroptosis in cancer and other diverse disorders. Based on whatever purpose, scientifically or clinically, this field deserves much more devotion to harvest more fruitful achievements. To summarize and advance the development of this field, we organized this Research Topic titled “*Ferroptosis in cancer and beyond*”, aiming to report on the basic mechanisms underlying ferroptosis, how ferroptosis is regulated, and how ferroptosis pathways can be targeted therapeutically in various diseases, particularly in cancer. This Research Topic has shown great success, as we have collected 33 papers in total. These papers include cutting-edge research articles and reviews about the regulation and pathological function of ferroptosis. We would like to briefly introduce these papers below.

## Regulation of ferroptosis

Ferroptosis is delicately regulated, with many factors and pathways involved in its initiation, propagation, and termination (Dixon and Stockwell, 2019; Liu and Gu, 2022a). Among them, GPX4 and p53 are the two core regulators of ferroptosis (Liu and Gu, 2022a; Liu and Gu, 2022b). Cui et al. discussed how post-translational protein modification modulates GPX4 expression and activity, thereby influencing its role to antagonize ferroptosis. For p53, the review by Zhang et al. focuses on the potential crosstalk between p53 and G-quadruplex of DNA or RNA, adding new mechanism to the regulation of p53 function in ferroptosis (Liu et al., 2019). SLC7A11 is a repressive target of p53, and also an upstream regulator of GPX4, therefore linking p53- and GPX4-mediated ferroptosis pathways (Jiang et al., 2015). Cheng et al. found that SLC7A11 is upregulated in colon adenocarcinoma than in normal colon tissues and is associated with various tumor hallmarks of colon adenocarcinoma. SLC3A2 and SLC7A11 form a complex called System Xc<sup>-</sup> to import cystine into the cell. He et al. analyzed the expression of SLC3A2 across different tumor types and investigated its correlation with tumor microenvironment, especially the immune cell function. Autophagy-dependent ferritinophagy contributes to ferroptosis initiation. Liang et al. discovered that NPC intracellular cholesterol transporter 1 (NPC1) has a role in regulating ferritinophagy, ferroptosis, and hearing loss. MicroRNA is a type of pleiotropic small RNA to regulate various biological processes, including cancer (Liu et al., 2016; Liu et al., 2017; Liu et al., 2018; Ma et al., 2019). In the review by Guo et al. authors introduced how different microRNAs participate in the regulation of ferroptosis. In addition, Liu et al. used single-cell transcriptomics technology to identify many key regulators of ferroptosis in head and neck squamous cell carcinoma.

## Ferroptosis and tumor

Ferroptosis is associated with the development of many diseases, with tumor as a notable example. In fact, till now there are numerous papers reporting that ferroptosis involves the transformation processes of distinct tumor types. In this Research Topic, Qu et al. wrote a good review to summarize the role of ferroptosis in different cancers. They firstly introduced the basic mechanism and regulation of ferroptosis. Then, they discussed how ferroptosis participates in the regulation of tumor development. They also touched the therapeutic

potential by targeting ferroptosis in tumors, with a summary of the available ferroptosis inducers. Maimaitizunong et al. contributed a comprehensive review about ferroptosis and esophagus cancer. In their paper, the regulators and signaling pathways of ferroptosis are discussed in detail. They also depicted various applications related to ferroptosis in esophagus cancer. The figures and tables in this paper are well-presented and informative. In addition, Fan et al. focused on ferroptosis and gynecological malignancies. Due to the significant role of ferroptosis, it is obvious that targeting ferroptosis can be an effective way to treat cancer. Tan et al. proposed a question: is ferroptosis enemy or friend in tumor therapy? On one side, they thought targeting ferroptosis may be good to many tumor patients. On the other side, they warned the researchers to take possible side effect of inducing ferroptosis into consideration when treating cancers. Indocyanine green is a near-infrared fluorescent molecule used in the imaging of residual tumor removal during surgery. A study by Tseng et al. found that OATP1B3-mediated uptake of indocyanine green facilitated ferroptosis when exposed to 808-nm laser irradiation in HT1080 cell. This result is consolidated by *in vivo* data. These results suggested that indocyanine green plus laser radiation may be a new treatment method for chemo-resistant cancers by inducing ferroptosis. To identify efficient agents to target ferroptosis in non-small cell lung cancer, Zhao et al. used bioinformatics to screen lead compounds that induce ferroptosis in tumor cells. By doing so, they identified flufenamic acid could promote ferroptosis and suppress growth and migration in A549 cell line. Moreover, three excellent reviews by Zhuo et al., Wu et al., and Li et al. discussed the therapeutic potential by modulating ferroptosis in glioblastoma, endometrial cancer, and hepatocellular carcinoma, respectively. Beyond as treatment target, ferroptosis-related genes can also have prognostic potential in cancer and other disorders (Liu et al., 2022; Ye et al., 2022). In hepatocellular carcinoma, Zhang et al. analyzed the differentially expressed ferroptosis-related genes by using the TCGA database. Based on the analysis result, they constructed a gene signature that is associated with immune cell infiltration in hepatocellular carcinoma. Importantly, their signature can effectively reflect the prognosis of hepatocellular carcinoma patients. In addition, this model also works well when considering other different characteristics of hepatocellular carcinoma. This study flow encourages the mining of prognostic usage of ferroptosis-related gene signatures in other tumor types. Indeed, by using similar approaches, Tian et al., Yin et al., and Hu et al. expanded the prognostic potential of ferroptosis to glioblastoma, acute myeloid leukemia, and colorectal cancer, respectively. What should not be missed is Tao et al.'s result. Their ferroptosis-related mRNAs and lncRNAs model is a wonderful supplement to the classic 2017 European LeukemiaNet (ELN) classification system of pediatric acute myeloid leukemia.

## Ferroptosis and other diseases

Unlike its tumor-suppressive role that can be leveraged in tumor treatment, ferroptosis is often one of the causes in neurodegenerative diseases and organ injury, which should be avoided. In this Research Topic, there is an excellent review by Ma et al. to summarize connection between Alzheimer's disease and the ferroptosis signaling pathways. To begin with, the authors introduced the major regulators and signaling pathways in ferroptosis. Next, they

introduced in detail the link between these factors (including iron metabolism, lipid metabolism, amino acid metabolism, and GPX4) with Alzheimer's disease. Then, they suggested that ferroptosis inhibitors could be used to treat Alzheimer's disease. In Parkinson's disease, Wang et al. found that increased iron deposition in nigrosome might be a critical pathological cause for Parkinson's disease. Mechanistically, iron deposition may increase the sensitivity of neuron to ferroptosis. Development of iron deposit modulation drug is a practical way to prevent and treat Parkinson's disease. Ferroptosis in brain may also happen after intracerebral hemorrhage. Ren et al. in their review discussed the risk of brain injury after intracerebral hemorrhage. They concluded that the induction of ferroptosis is a risk factor for after intracerebral hemorrhage-related brain injury and should be monitored and inhibited in clinical practice. In kidney, the occurrence of ferroptosis is associated with acute kidney injury and renal fibrosis. In Zhang et al.'s and Zhang et al.'s reviews respectively, the readers can find detailed information how ferroptosis contribute to these kidney disorders and how to prevent it. Beyond brain and kidney, ferroptosis also functions in liver, lung, heart, and skeletal muscle. Zhou et al. concluded the effect of ferroptosis in multiple chronic liver diseases, including alcoholic liver disease, non-alcoholic fatty liver disease, liver fibrosis, hepatocellular carcinoma. Remarkably, they proposed some limitations in the current ferroptosis studies in chronic liver diseases. Li et al. discussed extensively the contribution of ferroptosis to the pathologic process of lung diseases, such as obstructive lung diseases (chronic obstructive pulmonary disease, asthma, and cystic fibrosis), interstitial lung diseases (pulmonary fibrosis of different causes), pulmonary diseases of vascular origin (ischemia-reperfusion injury and pulmonary hypertension), pulmonary infections (bacteria, viruses, and fungi), acute lung injury, acute respiratory distress syndrome, obstructive sleep apnea, pulmonary alveolar proteinosis, and lung cancer. In another review, Lin et al. focused on ferroptosis and airway inflammatory diseases. Noteworthy, they also discussed the potential link between ferroptosis and COVID-19 infection. Ageing is along with cardiac dysfunction. Liang et al. found that ageing-associated ferroptosis is a reason for this process. In addition, hydrogen sulfide was demonstrated to protect aging rat from cardiac dysfunction by suppressing cardiomyocyte ferroptosis. Wang et al.'s review reports the correlation between ferroptosis and various skeletal muscle diseases, including sarcopenia, rhabdomyolysis, rhabdomyosarcoma, exhaustive exercise-induced fatigue, and idiopathic inflammatory myopathy. Ferroptosis even has a role in

psoriasis. The review by Zhou et al. depicts the pathogenesis of psoriasis, the mechanisms of ferroptosis, and the connection between these two processes. Moreover, authors also discussed the therapeutic potential of ferroptosis inhibitors in psoriasis.

## Conclusion and perspective

To sum up, this Research Topic covers a batch of up-to-date papers about ferroptosis research, with an emphasis on the role of ferroptosis in tumor and other multiple diseases. We believe our Research Topic could provide invaluable information to the readers interested in ferroptosis field. We also look forward more exciting and important research results could come out in the near future.

## Author contributions

YL and XW wrote the manuscript. GC and CP reviewed and revised the manuscript. The authors read and approved the final manuscript.

## Acknowledgments

We are grateful to all the authors and reviewers for their contributions to this Research Topic.

## Conflict of interest

The authors declare that the research was conducted in the absence of any commercial or financial relationships that could be construed as a potential conflict of interest.

## Publisher's note

All claims expressed in this article are solely those of the authors and do not necessarily represent those of their affiliated organizations, or those of the publisher, the editors and the reviewers. Any product that may be evaluated in this article, or claim that may be made by its manufacturer, is not guaranteed or endorsed by the publisher.

## References

- Dixon, S. J., and Stockwell, B. R. (2019). The hallmarks of ferroptosis. *Annu. Rev. Canc. Biol.* 3, 35–54. doi:10.1146/annurev-cancerbio-030518-055844
- Galluzzi, L., Pedro, J. M. B. S., Kepp, O., and Kroemer, G. (2016). Regulated cell death and adaptive stress responses. *Cell Mol. Life Sci.* 73 (11–12), 2405–2410. doi:10.1007/s00018-016-2209-y
- Galluzzi, L., Vitale, I., Aaronson, S. A., Abrams, J. M., Adam, D., Agostinis, P., et al. (2018). Molecular mechanisms of cell death: Recommendations of the nomenclature committee on cell death 2018. *Cell death Differ.* 25 (3), 486–541. doi:10.1038/s41418-017-0012-4
- Hassannia, B., Vandenabeele, P., and Vanden Berghe, T. (2019). Targeting ferroptosis to iron out cancer. *Cancer Cell* 35 (6), 830–849. doi:10.1016/j.ccell.2019.04.002
- Hengartner, M. O. (2000). The biochemistry of apoptosis. *Nature* 407 (6805), 770–776. doi:10.1038/35037710
- Jiang, L., Kon, N., Li, T. Y., Wang, S. J., Su, T., Hibshoosh, H., et al. (2015). Ferroptosis as a p53-mediated activity during tumour suppression. *Nature* 520 (7545), 57–62. doi:10.1038/nature14344
- Liu, Y., and Gu, W. (2022). The complexity of p53-mediated metabolic regulation in tumor suppression. *Seminars cancer Biol.* 85, 4–32. doi:10.1016/j.semcancer.2021.03.010
- Liu, Y., and Gu, W. (2022). p53 in ferroptosis regulation: the new weapon for the old guardian. *Cell death Differ.* 29 (5), 895–910. doi:10.1038/s41418-022-00943-y
- Liu, Y., Liu, Y., Ye, S., Feng, H., and Ma, L. (2022). Development and validation of cuproptosis-related gene signature in the prognostic prediction of liver cancer. *Front. Oncol.* 12, 985484. doi:10.3389/fonc.2022.985484
- Liu, Y. Q., Chen, X. R., Cheng, R. J., Yang, F., Yu, M. C., Wang, C., et al. (2018). The Jun/miR-22/HuR regulatory axis contributes to tumorigenesis in colorectal cancer. *Mol. Cancer* 17, 11. doi:10.1186/s12943-017-0751-3

- Liu, Y. Q., Liu, R., Yang, F., Cheng, R. J., Chen, X. R., Cui, S. F., et al. (2017). miR-19a promotes colorectal cancer proliferation and migration by targeting TIA1. *Mol. Cancer* 16, 53. doi:10.1186/s12943-017-0625-8
- Liu, Y. Q., Tavana, O., and Gu, W. (2019). p53 modifications: exquisite decorations of the powerful guardian. *J. Mol. Cell Biol.* 11 (7), 564–577. doi:10.1093/jmcb/mjz060
- Liu, Y. Q., Uzair-ur-RehmanGuo, Y., Liang, H. W., Cheng, R. J., Yang, F., et al. (2016). miR-181b functions as an oncomiR in colorectal cancer by targeting PDCD4. *Protein Cell* 7 (10), 722–734. doi:10.1007/s13238-016-0313-2
- Ma, L. J., Chen, X. R., Li, C., Cheng, R. J., Gao, Z., Meng, X. B., et al. (2019). miR-129-5p and-3p co-target WWP1 to suppress gastric cancer proliferation and migration. *J. Cell. Biochem.* 120 (5), 7527–7538. doi:10.1002/jcb.28027
- Pefanis, A., Ierino, F. L., Murphy, J. M., and Cowan, P. J. (2019). Regulated necrosis in kidney ischemia-reperfusion injury. *Kidney Int.* 96 (2), 291–301. doi:10.1016/j.kint.2019.02.009
- Qiu, Y. M., Cao, Y., Cao, W. J., Jia, Y. F., and Lu, N. (2020). The application of ferroptosis in diseases. *Pharmacol. Res.* 159, 104919. doi:10.1016/j.phrs.2020.104919
- Ratan, R. R. (2020). The chemical biology of ferroptosis in the central nervous system. *Cell Chem. Biol.* 27 (5), 479–498. doi:10.1016/j.chembiol.2020.03.007
- Shi, J. J., Gao, W. Q., and Shao, F. (2017). Pyroptosis: Gasdermin-Mediated programmed necrotic cell death. *Trends Biochem. Sci.* 42 (4), 245–254. doi:10.1016/j.tibs.2016.10.004
- Stockwell, B. R., Angeli, J. P. F., Bayir, H., Bush, A. I., Conrad, M., Dixon, S. J., et al. (2017). Ferroptosis: A regulated cell death nexus linking metabolism, redox biology, and disease. *Cell* 171 (2), 273–285. doi:10.1016/j.cell.2017.09.021
- Stockwell, B. R., Jiang, X. J., and Gu, W. (2020). Emerging mechanisms and disease relevance of ferroptosis. *Trends Cell Biol.* 30 (6), 478–490. doi:10.1016/j.tcb.2020.02.009
- Vandenabeele, P., Galluzzi, L., Vanden Berghe, T., and Kroemer, G. (2010). Molecular mechanisms of necroptosis: An ordered cellular explosion. *Nat. Rev. Mol. Cell Bio* 11 (10), 700–714. doi:10.1038/nrm2970
- Ye, S., Liu, Y., Zhang, T., Feng, H., Liu, Y., and Ma, L. (2022). Analysis of the correlation between non-alcoholic fatty liver disease and the risk of colorectal neoplasms. *Front. Pharmacol.* 13, 1068432. doi:10.3389/fphar.2022.1068432



# SLC7A11, a Potential Therapeutic Target Through Induced Ferroptosis in Colon Adenocarcinoma

Xin Cheng<sup>1</sup>, Yadong Wang<sup>1</sup>, Liangchao Liu<sup>1</sup>, Chenggang Lv<sup>1</sup>, Can Liu<sup>2</sup> and Jingyun Xu<sup>3\*</sup>

<sup>1</sup>General Surgery Department, Wuhu Hospital of Traditional Chinese Medicine, Wuhu, China, <sup>2</sup>The First Affiliated Hospital of Wannan Medical College, Wuhu, China, <sup>3</sup>School of Basic Medicine, Wannan Medical College, Wuhu, China

**Background:** Ferroptosis induced by SLC7A11 has an important translational value in the treatment of cancers. However, the mechanism of SLC7A11 in the pathogenesis of colon adenocarcinoma (COAD) is rarely studied in detail.

**Methods:** SLC7A11 expression was explored with The Cancer Genome Atlas (TCGA), Gene Expression Omnibus (GEO) databases, and Western blot assay. The correlation of SLC7A11 expression with the abundance of infiltrating immune cells was evaluated via the TIMER database. The relation of SLC7A11 expression with immune cell markers was investigated via Gene Expression Profiling Interactive Analysis (GEPIA). The co-expression genes of SLC7A11 were screened by R packages, and the PPI was constructed via the STRING database. SLC7A11 and co-expressed gene modulators were selected by NetworkAnalyst and DSigDB database. The correlations between SLC7A11 and cancer immune characteristics were analyzed via the TIMER and TISIDB databases.

**Results:** SLC7A11 is overexpressed in most tumors, including COAD. The expression level of SLC7A11 has a significant correlation with the infiltration levels of CD8<sup>+</sup> T cells, neutrophils, and dendritic cells in COAD. The infiltrated lymphocyte markers of Th1 cell such as TBX21, IL12RB2, IL27RA, STAT1, and IFN- $\gamma$  were strongly correlated with SLC7A11 expression. Five hub genes co-expressed with SLC7A11 that induce ferroptosis were identified, and mir-335-5p, RELA, and securinine have regulatory effects on it. SLC7A11 was negatively correlated with the expression of chemokines and chemokine receptors, such as CCL17, CCL19, CCL22, CCL23, CXCL14, CCR10, CX3CR1, and CXCR3, in COAD.

**Conclusion:** SLC7A11 may play a role in induced ferroptosis and regulating tumor immunity, which can be considered as potential therapeutic targets in COAD.

**Keywords:** SLC7A11, ferroptosis, immune infiltrate, immune microenvironment, COAD

## INTRODUCTION

Colon adenocarcinoma (COAD) is one of the most common malignant tumors of the digestive system; the diagnosis rate and the mortality rate represent about 1/10 of the total cancer cases (El Kinany et al., 2020). In recent years, the incidence of COAD is increasing annually, with the highest incidence in China (Roslan et al., 2019). Traditional treatments for COAD include radiation, chemotherapy, and surgery.

## OPEN ACCESS

### Edited by:

Xin Wang,  
National Institutes of Health (NIH),  
United States

### Reviewed by:

Wenjuan Wang,  
National Institutes of Health (NIH),  
United States  
Zhenyi Su,  
Columbia University, United States

### \*Correspondence:

Jingyun Xu  
20200011@wnmc.edu.cn

### Specialty section:

This article was submitted to  
Molecular Diagnostics and  
Therapeutics,  
a section of the journal  
Frontiers in Molecular Biosciences

**Received:** 04 March 2022

**Accepted:** 23 March 2022

**Published:** 20 April 2022

### Citation:

Cheng X, Wang Y, Liu L, Lv C, Liu C  
and Xu J (2022) SLC7A11, a Potential  
Therapeutic Target Through Induced  
Ferroptosis in Colon Adenocarcinoma.  
Front. Mol. Biosci. 9:889688.  
doi: 10.3389/fmolb.2022.889688

Currently, new therapeutic methods such as bio-targeted therapy, precision therapy, and immunotherapy have been gradually applied in the treatment of colon cancer (Sandhu et al., 2019; Bao et al., 2020). However, drug resistance and immune escape restrict the therapeutic effect of these therapies (Fidelle et al., 2020). Therefore, finding new therapeutic targets to halt or slow disease progression is an urgent priority.

Studies showed that ferroptosis as a novel-induced programmed cell death, which can effectively inhibit tumor growth by inducing ferroptosis of tumor cells (Mou et al., 2019), and it also plays a critical role in reversing cisplatin resistance of tumors (Guo et al., 2018). Therefore, modulating ferroptosis may have important transforming significance in various ferroptosis-associated diseases. Glutathione peroxidase 4 (GPX4) was shown to be a central regulator of ferroptosis; glutathione (GSH) is a necessary cofactor for the biological activity of GPX4; GSH synthesis depends on the Gys/Glu reverse transfer system (Xc-); System Xc- consists of two subunits, including solute carrier family 7, membrane 11 (SLC7A11), and heavy chain subunit SLC3A2; SLC7A11 is responsible for the primary activity of System Xc-, while SLC3A2 plays an auxiliary coordinating role (Xie et al., 2016; Koppula et al., 2018; Song et al., 2018). Latest studies have shown that 2-imino-6-methoxy-2H-chromene-3-carbothioamide (IMCA) downregulates SLC7A11 expression through the AMPK/mTOR pathway and induces ferroptosis (Zhang et al., 2020). However, whether SLC7A11 can be an effective target for COAD treatment needs more theoretical support.

In this study, bioinformatics methods were used to analyze SLC7A11 expression and clinical information in COAD patients. Then, we used the TIMER and GEPIA databases to study the relationship between SLC7A11 expression and infiltrating immune cells and their corresponding gene marker sets. In addition, the protein-protein interaction network of SLC7A11 was explored by STRING. The results showed that the overexpression of SLC7A11 inhibited the ferroptosis of tumor cells and promoted the development and metastasis of COAD. Targeted inhibition of SLC7A11 may be a promising therapeutic strategy for inducing ferroptosis or in combination with immunotherapy for COAD.

## MATERIALS AND METHODS

### Clinical Samples and Ethics

Six patients undergoing radical resection of colon cancer were collected in the First Affiliated Hospital of Wannan Medical College and pathologically diagnosed with colon cancer. None of them received chemotherapy or immunotherapy before surgery. Tumor tissues and paracancerous tissues were collected from the six patients (the adjacent normal tissues were extracted >3 cm from the tumor margin). This study was approved by the Ethics Committee of Wannan Medical College (NO. 2021081).

### Data Source

The Cancer Genome Atlas (TCGA) (<https://genomecancer.ucsc.edu/>), a free data portal of largescale cancer genome project. The

data of COAD patients with the expression of RNA-Seq and matching clinical information (include pathologic stage, histologic grade, OS time, gender, and age) were obtained by the TCGA tools.

### Retrieval of Datasets

In order to compare the expression level of SLC7A11 in cancer and normal tissues, two datasets were involved in this study, GSE21510 and GSE24514, where both were from the GEO database (<https://www.ncbi.nlm.nih.gov/geo/>). In GSE21510, the expression profiles of cancer cells in 104 patients with colorectal cancer were examined by laser microdissection and oligonucleotide microarray analysis (Tsukamoto et al., 2011). GSE24514 illustrated microsatellite instability in colorectal cancer patients (Alhopuro et al., 2012).

### Western Blot (WB)

Total proteins were extracted from the cancer and paracancerous tissues, after protein concentration was detected, WB assay was performed. The primary antibodies used were as follows: SLC7A11 antibody (Abcam, ab175186) (diluted at 1:5,000) and GAPDH recombinant antibody (proteintech, 80570-1-RR) (diluted at 1:5,000) at room temperature (RT) for 1 h. After washing three times with TBST, 5 min/wash, the membrane was incubated with HRP-labeled goat antirabbit IgG (Beyotime, A0208) (diluted at 1:1,000) as the secondary antibody for 1 h at RT. Finally, the signal was detected by chemiluminescence, and the bands' gray value was measured using ImageJ software.

### Correlation Analysis Between SLC7A11 Expression and Immune Cell Infiltration

The correlation of SLC7A11 expression with the abundance of infiltrating immune cells, including tumor-associated macrophage (TAM), neutrophils, macrophages, dendritic cells, B cells, CD8<sup>+</sup> T cells, CD4<sup>+</sup> T cells, and their subtypes in COAD patients was evaluated *via* the TIMER database (<http://cistrome.org/TIMER/>). The relationship between the expression of the SLC7A11 gene and tumor purity was also displayed.

### Correlation Analysis of SLC7A11 Expression and Immune Cell Markers

The relation of SLC7A11 expression with multiple markers for immune cells was investigated *via* The Gene Expression Profiling Interactive Analysis (GEPIA) (<http://gepia.cancer-pku.cn/index.html>). Moreover, we used TIMER data to validate the genes which were of significant correlation with SLC7A11 expression in the GEPIA web.

### Co-Expression Network Establishment of SLC7A11 and GO-KEGG Analysis

The co-expression genes of SLC7A11 were screened by R packages (limma). The correlation between the SLC7A11 expression level and co-expression genes were examined by Pearson correlation coefficients and the Z-test from the TCGA databases (related parameter settings: |Pearson correlation coefficient| > 0.5 and p-value < 0.001). The STRING database (v11.5, <https://www>.



string-db.org/) was used to construct the protein–protein interactions (PPI). In addition, GO–KEGG enrichment analysis was performed by Bioconductor package “clusterProfiler.”

## Construction of the TF-miRNA Co-Regulatory Network

The NetworkAnalyst database (<https://www.networkanalyst.ca/>) was used to identify TF-miRNA co-regulate with co-expression genes. The common network topology measures were also computed based on well-established igraph R package. TF and gene target data were derived from ENCODE ChIP-seq data. Only the peak intensity signal <500 and the predicted regulatory potential score <1 were used.

## Screening of Potential Therapeutic Drugs

The Enrichr platform was used for drug screening of SLC7A11 and co-expression genes. The access of the DSigDB database was acquired using Enrichr (<https://amp.pharm.mssm.edu/Enrichr/>). Potential therapeutic agents were determined by the adj. *p* values and the abundance of acting on SLC7A11 and co-expression genes.

## TISIDB Database Analysis

To study the association between SLC7A11 and chemokine/chemokine receptor expression, we evaluated the expression levels of chemokine/chemokine receptors of tumor-infiltrating immune cells through the “chemokine” module of the TISIDB database (<http://cis.hku.hk/TISIDB/>). To further clarify the immune correlation of SLC7A11 in cancer, the “immunomodulator” module was used to analyze and evaluate the correlation between SLC7A11 expression and the levels of immune checkpoint genes.

## Enzyme-Linked Immunosorbent Assay (ELISA)

The levels of CCL17, CXCL14, and CXCR3 in cancer and paracancerous tissues were measured by ELISA kits from Yuanju, Inc. (Shanghai, China) (Yuanju, YJ779969/YJ714549/YJ719414) according to the manufacturer’s protocol.

## RESULTS

### Patient Characteristics

In total, the RNA-sequencing data and detailed clinical prognostic information resources of 478 COAD samples were obtained from the TCGA database. The clinical information including tumor extent (T), lymph node invasion (N), detectable metastasis (M), histologic grade, age at diagnosis, overall survival (OS), and lymphatic invasion are summarized in Table 1.

### Higher SLC7A11 Expression in Tumor Samples Than That in Normal Tissues

The mRNA expression level of SLC7A11 was analyzed in various cancer types (Figure 1A). The gene expression level of SLC7A11 was significantly higher in tumor samples than that in normal

**TABLE 1 |** Clinical characteristics of the COAD patients.

Characteristic	Levels	Overall
N		478
Tumor extent (T) stage, n (%)	T1	11 (2.3%)
	T2	83 (17.4%)
	T3	323 (67.7%)
	T4	60 (12.6%)
Lymph node invasion (N) stage, n (%)	N0	284 (59.4%)
	N1	108 (22.6%)
	N2	86 (18%)
Detectable metastasis (M) stage, n (%)	M0	349 (84.1%)
	M1	66 (15.9%)
Pathologic stage, n (%)	Stage I	81 (17.3%)
	Stage II	187 (40%)
	Stage III	133 (28.5%)
	Stage IV	66 (14.1%)
Age, n (%)	<=65	194 (40.6%)
	>65	284 (59.4%)
Lymphatic invasion, n (%)	NO	266 (61.3%)
	YES	168 (38.7%)
Overall survival (OS) event, n (%)	Alive	375 (78.5%)
	Dead	103 (21.5%)
Gender, n (%)	Female	226 (47.3%)
	Male	252 (52.7%)
Age, median (IQR)		69 (58, 77)

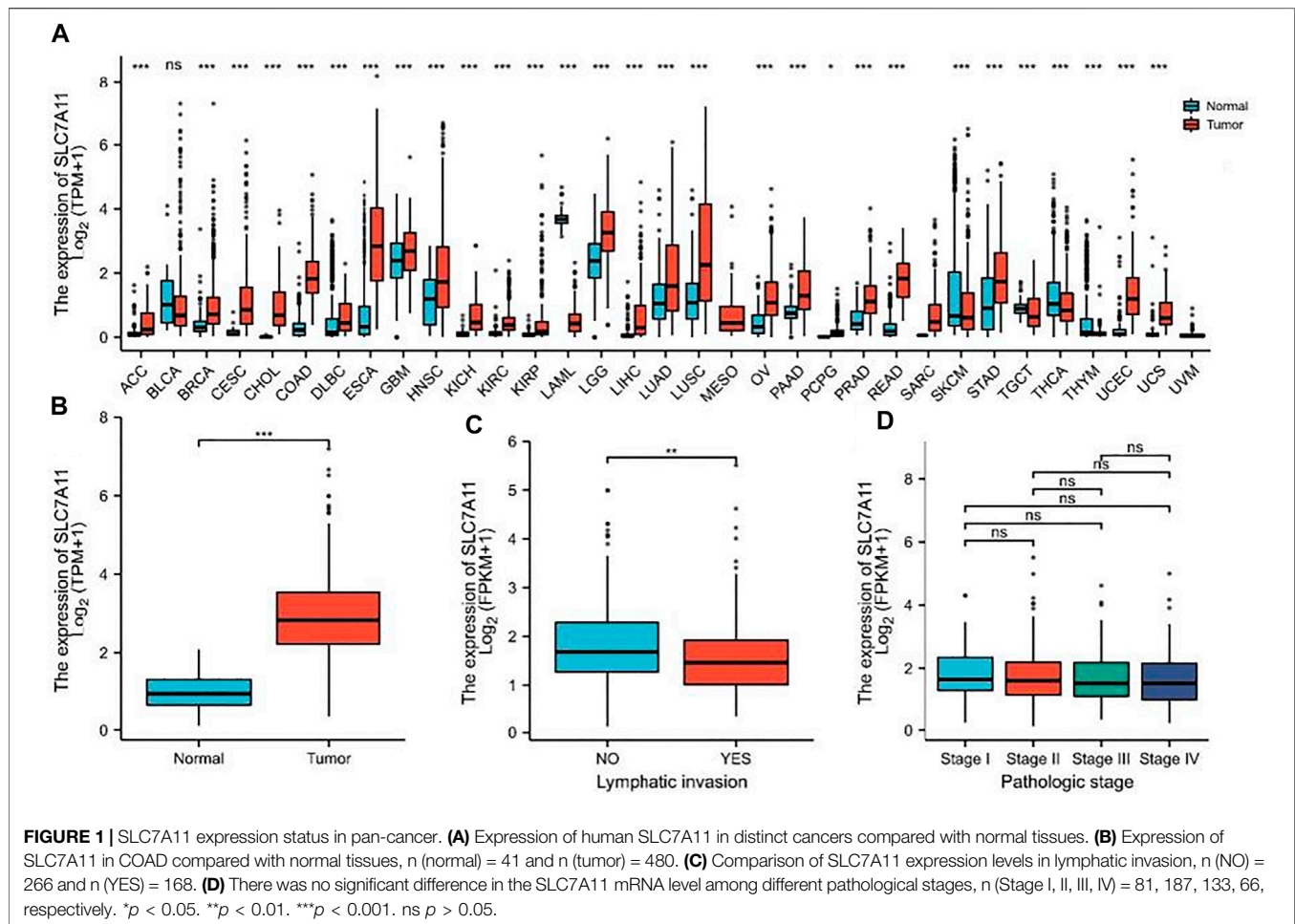
**Note:** A small amount of samples may be lost during the statistics of different clinical variables in the TCGA database. T1, the carcinoma invaded the submucosa but not involve the lamina propria; T2, the carcinoma invaded the lamina propria; T3, the carcinoma penetrated the lamina propria; T4, the carcinoma invaded the visceral peritoneum or adhered to adjacent organs; N0, no regional lymph node metastasis; N1, limited to 1–3 regional lymph node metastases, or no regional lymph node metastasis, but any number of tumor nodules; N2, four or more regional lymph nodes metastases; M0, imaging showed no distant metastasis; M1, metastases to one or more distant sites, organs, or peritoneum; Stage I, the carcinoma confined within the intestinal wall; Stage II, the carcinoma penetrated the intestinal wall and invaded the mucosa or serosa without lymph node metastasis; Stage III, local lymph node metastasis; and Stage IV, invasion of adjacent organs or distant metastasis.

tissues of COAD in TCGA and GEO databases ( $p < 0.01$ , Figure 1B). The expression of SLC7A11 is downregulated in COAD tissue when lymphatic invasion occurs ( $p < 0.01$ , Figure 1C). However, SLC7A11 expression is relatively stable in all pathologic stages of COAD ( $p > 0.05$ , Figure 1D).

In addition, the high expression of SLC7A11 in COAD was also observed in two datasets of the GEO database (Figure 2A), and the aforementioned results were also verified by WB (Figure 2B).

The expression level of SLC7A11 had obviously positive correlation with infiltrating levels of CD8<sup>+</sup> T cells ( $r = 0.358$ ,  $p = 1.03e-13$ ), neutrophils ( $r = 0.267$ ,  $p = 5.72e-08$ ), and dendritic cells ( $r = 0.171$ ,  $p = 5.65e-04$ ) in COAD, but it was negatively correlated with tumor purity ( $r = -0.104$ ,  $p = 3.59e-02$ ) (Figure 3).

To intensely explore the possible role of SLC7A11 in the infiltration of various immune cells in COAD, the GEPIA and TIMER databases were used to execute the relationships between SLC7A11 and several immune marker sets. Furthermore, various functional T cells including Th1, Th2, Th17, and Treg were also been examined in this study. Results showed that the levels of most immune sets marking different T cells, TAMs, macrophages, monocytes, and DCs were associated with the SLC7A11 expression in COAD (Table 2).



## Network Establishment for SLC7A11-Correlated Genes in COAD

To further study the genes closely associated with SLC7A11 in COAD, the top 50 co-expressed genes were showed in a heatmap (Figure 4). Of note, 25 of 50 genes were negatively correlated with SLC7A11 (such as PRDX5, CLDN3, ROMO1, and VEGFB), and 25 genes were positively correlated (such as LARP1B, AHR, AP1S3, IBTK, and SPATA5) (Figure 4A). GO-KEGG enrichment analysis showed that the co-expression genes of SLC7A11 were mainly involved in the proteasomal protein catabolic process, Golgi vesicle transport, chromosome segregation, and other signaling pathways (Figure 4B).

## PPI and the TF-miRNA Co-regulatory Network

To determine the role of SLC7A11 protein interactions in COAD progression, protein-protein interaction (PPI) was constructed by the STRING tool. The proteins that interact most closely with SLC7A11 include GPX4, GCLC, GCLM, SLC3A2, SLC1A7, SLC1A5, SLC3A1, SLC1A2, CD44, and BECN1; among which SLC7A11, GPX4, GCLC, GCLM, and SLC3A2 are involved in the ferroptosis signaling pathway (Figure 5A). Furthermore, 193

miRNAs were identified that regulated the expression level of co-expression genes by NetworkAnalyst analysis, and the main co-regulated genes were SLC7A11, SLC1A2, SLC1A5, BECN1, GCLC, and CD44. The miRNA that hit more frequently were hsa-mir-335-5p, hsa-mir-155-5p, hsa-mir-34a-5p, hsa-mir-16-5p, hsa-mir-20a-5p, hsa-mir-93-5p, hsa-mir-98-5p, and hsa-mir-24-3p. The TF that hit more frequently were RELA, SP1, NFKB1, TP53, BRCA1, JUN, and ESR1 (Figure 5B).

## Screening of Potential Therapeutic Drugs

Enrichr platform analysis found that F0447-0125 PC3 UP, semustine PC3 UP, securinine PC3 UP, alpha-tocopherol CTD 00007387, ampicillin CTD 00005394 *etc.* have been identified as drugs that regulate action for both SLC7A11 and co-expression genes (Table 3).

## Correlation of SLC7A11 Expression With Immune Characteristics

The correlation between the expression level of SLC7A11 and immune cell chemokines (or receptors) in COAD were analyzed *via* the TISIDB database. The results showed that several chemokines and chemokine receptors were significantly

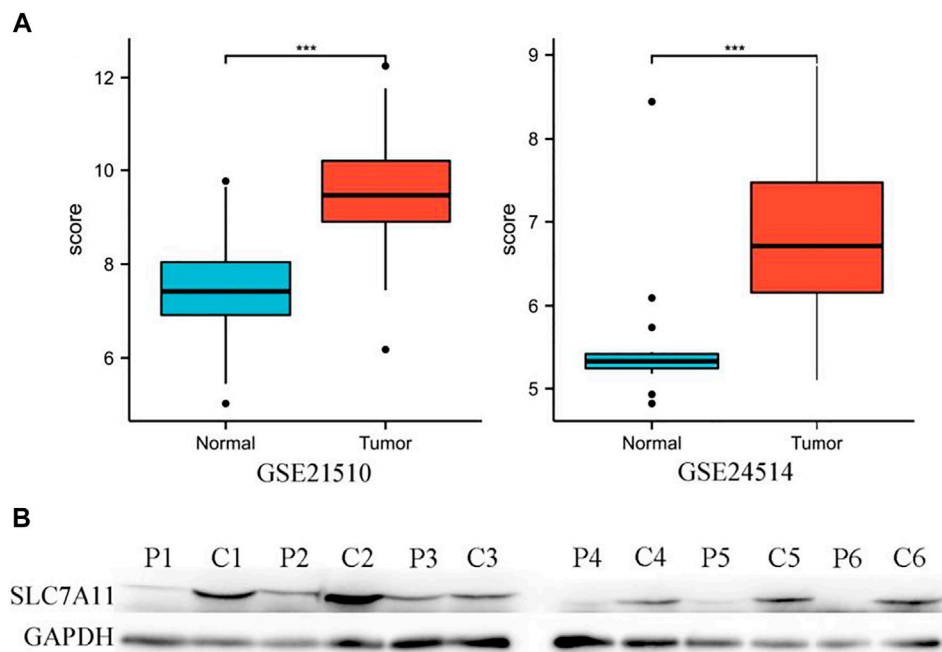


**FIGURE 2 |** High expression of SLC7A11 in colon cancer. **(A)** Analysis of SLC7A11 gene expression in GEO datasets, n (normal) = 25 and n (tumor) = 123 in GSE21510, n (normal) = 15 and n (tumor) = 34 in GSE24514. \*\*\* $p < 0.001$ . **(B)** Expression levels of SLC7A11 were detected by Western blot analysis, P1-6: paracancerous tissues of patients 1–6, C1-6: cancer tissues of patients 1–6, the bands gray value of C1-6 significantly higher than the P1-6 ( $p < 0.01$ ). Correlation analysis between SLC7A11 expression and infiltrating immune cells.

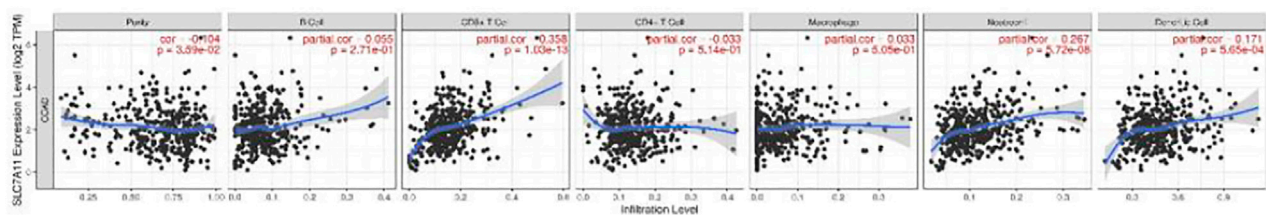


**FIGURE 3 |** Correlation of SLC7A11 expression with immune cell-infiltrated in COAD.

correlated with the expression of SLC7A11 in COAD. Concretely, SLC7A11 expression was negatively correlated with CCL17 ( $r = -0.24$  and  $p = 2.07e-07$ ), CCL19 ( $r = -0.201$  and  $p = 1.44e-05$ ), CCL23 ( $r = -0.27$  and  $p = 4.96e-09$ ), CXCL14 ( $r = -0.289$  and  $p = 3.25e-10$ ), CCR10 ( $r = -0.33$  and  $p = 5.11e-13$ ), CX3CR1 ( $r = -0.203$  and  $p = 1.2e-05$ ), CXCR3 ( $r = -0.332$  and  $p = 4.17e-13$ ) etc (Figures 6A,B). Subsequently, the correlation between SLC7A11 and the expressions of immunoinhibitors (or immunostimulators) in different cancers were analyzed. The results showed that SLC7A11 was negatively correlated with the expression of several immunoinhibitors and immunostimulators, such as ADORA2A ( $r = -0.224$ ,  $p = 1.36e-06$ ), CSF1R ( $r = -0.176$ ,  $p = 1.54e-04$ ), TGFB1 ( $r = -0.162$ ,  $p = 4.95e-04$ ), CD27 ( $r = -0.247$ ,  $p = 9.01e-08$ ), LTA ( $r = -0.181$ ,  $p = 1.01e-04$ ), TMIGD2 ( $r = -0.141$ ,  $p = 2.47e-03$ ), TNFRSF13B ( $r = -0.248$ ,  $p = 7.64e-08$ ) et al. Interestingly, SLC7A11 was positively correlated with the expression of several

immunostimulators, such as TNFSF9 ( $r = 0.209$ ,  $p = 6.41e-06$ ), ULBP1 ( $r = 0.303$ ,  $p = 4.09e-11$ ), and NT5E ( $r = 0.337$ ,  $p = 1.59e-13$ ) (Figures 6C,D). Therefore, these results suggest that SLC7A11 may play a role in regulating tumor immunity.

### Overexpressed SLC7A11-Inhibited Chemokine and Receptors Expression

For validation, we examined the expression of CCL17, CXCL14, and CXCR3 in cancer and adjacent tissues of six patients with SLC7A11 overexpression by ELISA. The results showed that the levels of CCL17, CXCL14, and CXCR3 in cancer were  $1.558 \pm 0.104$  ng/ml,  $2.169 \pm 0.214$  ng/ml, and  $2.843 \pm 0.423$  ng/ml, respectively, significantly lower than the corresponding adjacent tissues  $1.795 \pm 0.207$  ng/ml,  $2.625 \pm 0.093$  ng/ml, and  $6.868 \pm 0.455$  ng/ml ( $p < 0.05$  or  $0.01$ , Figure 7).

**TABLE 2 |** Correlation analysis between SLC7A11 and immune cell markers in TIMER and GEPIA.

Cell Type	Gene Symbol	None		Purity		Tumor		Normal	
		Core	P	Core	P	R	P	R	P
Tumor associated	MS4A4A	0.08	0.087	-0.379	**	0.06	0.32	0.15	0.34
Macrophage (TAM)	CCL2	0.127	**	-0.354	**	0.003	0.96	0.14	0.38
	CCR5	0.091	0.052	-0.436	**	0.11	0.058	0.38	0.14
	CD80	0.103	*	-0.313	**	0.028	0.64	0.41	**
	CD86	0.131	**	-0.42	**	0.081	0.15	0.2	0.22
Monocyte	CD14	0.003	0.954	-0.394	**	0.07	0.25	0.13	0.43
	CD16	-0.027	0.567	-0.222	**	0.11	0.065	0.2	0.22
	CD115	-0.034	0.468	-0.366	**	0.022	0.72	0.18	0.25
Neutrophil	CD11b	-0.098	*	-0.25	**	0.013	0.83	0.25	0.11
	CD15	0.219	**	0.019	0.699	*	0.86	0.37	*
	CD66b	-0.259	**	0.103	*	-0.045	0.46	0.27	0.09
NK	CD7	0.013	0.783	-0.472	**	0.11	0.061	-0.084	0.6
	XCL1	-0.021	0.66	-0.241	**	0.019	0.76	-0.14	0.39
	KIR3DL1	0.113	*	-0.249	**	0.36	**	0.099	0.54
Dendritic cell	CD1C	-0.073	0.121	-0.331	**	-0.076	0.21	0.085	0.6
	CD11c	0.061	0.196	-0.427	**	0.06	0.32	0.45	**
	CD141	0.038	0.42	-0.361	**	0.018	0.77	0.2	0.21
B cell	CD19	-0.132	**	-0.414	**	-0.0096	0.87	0.23	0.14
	CD20	0.005	0.917	-0.023	0.64	-0.014	0.82	0.31	*
	CD38	-0.023	0.621	-0.384	**	0.05	0.4	0.19	0.23
CD8 <sup>+</sup> T cell	CD8A	0.114	*	-0.397	**	0.22	**	0.043	0.79
	CD8B	0.01	0.832	0.221	**	0.05	0.41	-0.1	0.52
Th1	TBX21	0.123	**	-0.4	**	0.17	**	0.13	0.4
	STAT4	0.147	**	-0.377	**	0.12	0.053	0.095	0.55
	IL12RB2	0.113	*	-0.238	**	0.17	**	0.1	0.52
	IL27RA	0.039	0.408	-0.24	**	0.13	*	0.22	0.16
	STAT1	0.259	**	-0.274	**	0.29	**	0.096	0.55
	IFN- $\gamma$	0.176	**	-0.241	**	0.27	**	0.1	0.53
	TNF- $\alpha$	-0.02	0.67	-0.255	**	0.022	0.72	-0.026	0.87
Th2	GATA3	-0.065	0.16	-0.364	**	-0.028	0.64	0.22	0.17
	CCR3	-0.068	0.15	-0.173	**	0.006	0.92	-0.25	0.12
	STAT6	-0.005	0.91	0.012	0.815	0.012	0.85	-0.03	0.85
	STAT5A	-0.096	*	-0.161	**	0.039	0.52	0.078	0.63
Th17	STAT3	0.187	**	-0.225	**	0.067	0.27	0.28	0.073
	IL-17 A	-0.064	0.175	-0.012	0.814	-0.038	0.53	0.27	0.092
	IL-21R	-0.023	0.626	-0.441	**	0.058	0.34	0.32	*
	IL-23R	0.024	0.61	0.023	0.65	-0.041	0.5	0.098	0.54
Treg	FOXP3	-0.095	*	-0.382	**	-0.038	0.53	0.26	0.1
	IL2RA	0.098	*	-0.401	**	0.11	0.075	0.4	**
	CCR8	0.014	0.76	-0.336	**	-0.029	0.63	0.33	*
Macrophage	CD68	0.031	0.51	-0.317	**	0.047	0.44	0.24	0.14
	CD11b	-0.006	0.89	-0.355	**	0.013	0.83	0.25	0.11

Note: None, Correlation without adjustment. Purity, correlation adjusted by purity. Cor, R value of Spearman's correlation. \*p < 0.05; \*\*p < 0.01.

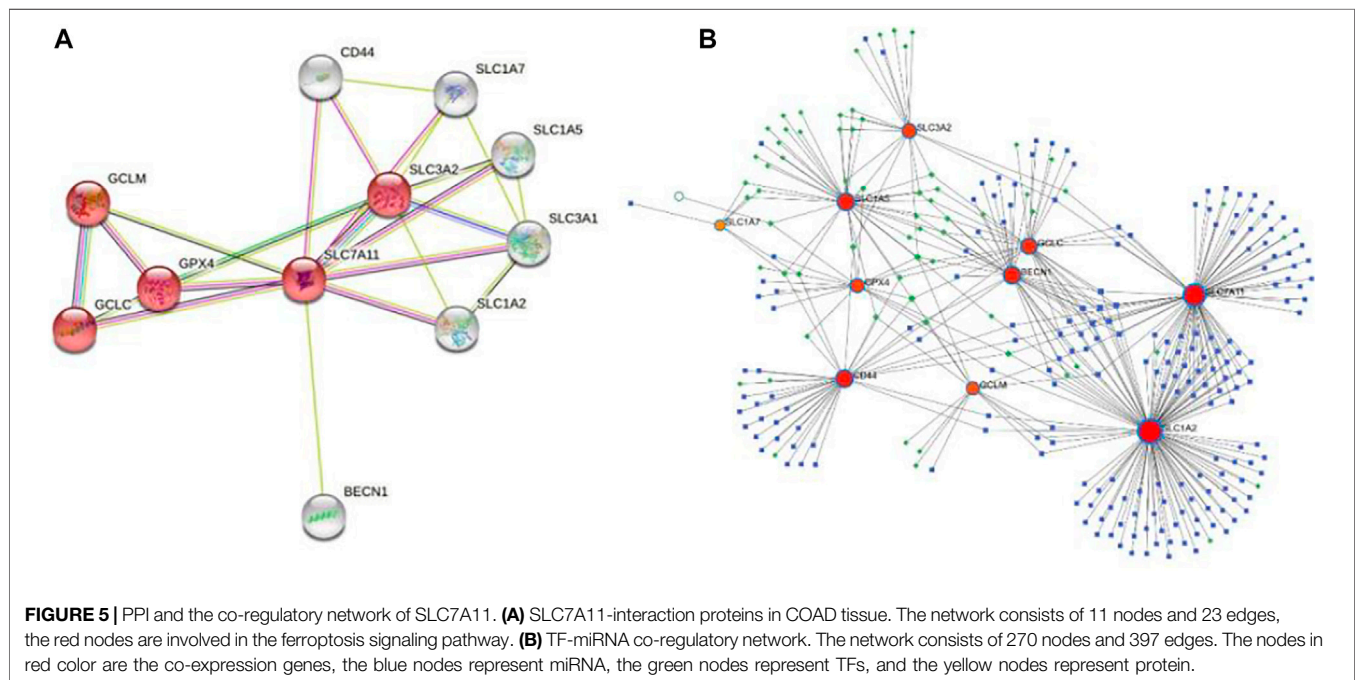
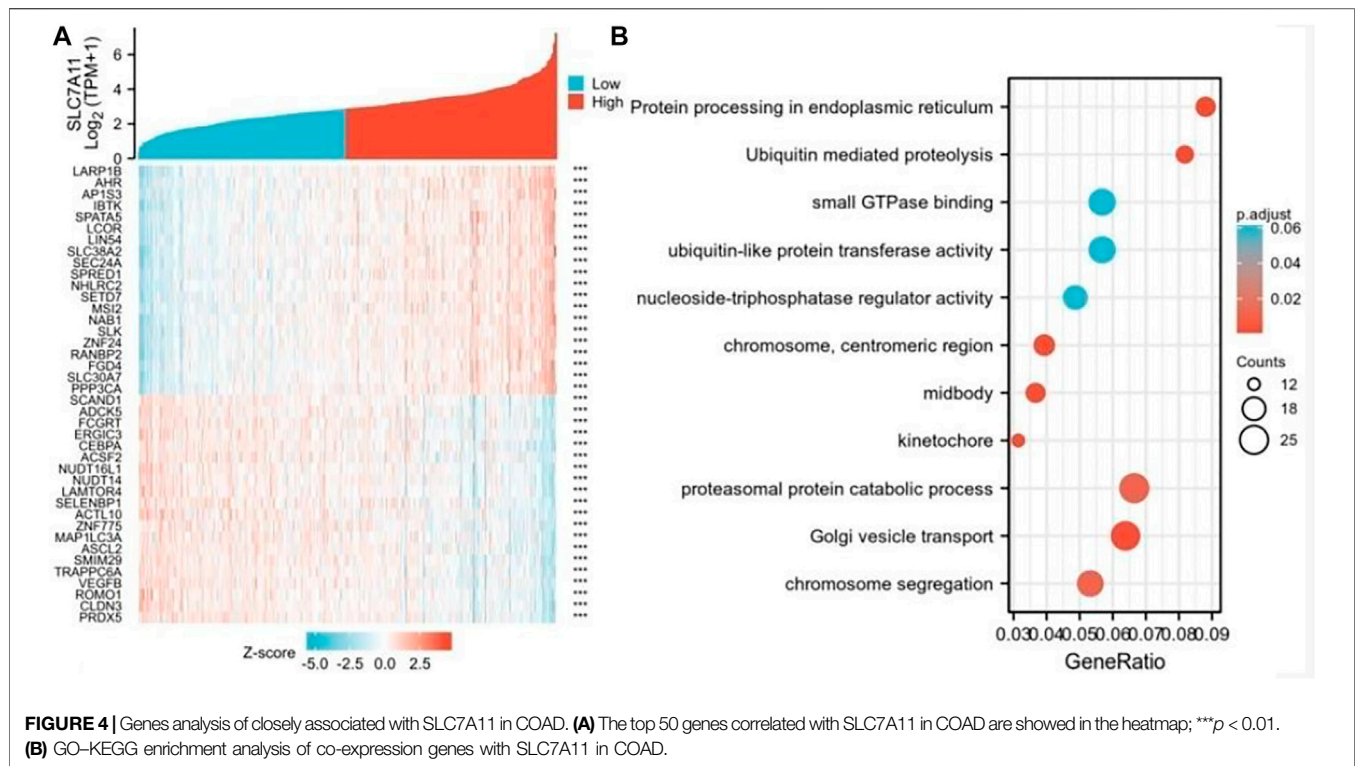
## DISCUSSION

Despite adjuvant chemotherapy, immunotherapy, and other anticancer therapies in early cancer treatment have shown encouraging efficacy, the middle and later stages of treatment in most cases are challenging. Therefore, it is necessary and urgent to find a more effective strategy to treat cancer. The ideal therapeutic target to be inhibited by an anticancer drug should have a selective effect on tumor growth, allowing the corresponding drug to produce the desired toxic effect in cancer cells without side effects on normal cells. Ferroptosis is a newly discovered mechanism of iron-dependent cell death, characterized by increased reactive oxygen species (ROS) and lipid peroxidation due to metabolic dysfunction, which is considered as a powerful weapon in the elimination of cancer

cells (Tang et al., 2020). SLC7A11 is a core target-regulating ferroptosis, and its overexpression leads to downregulation of the sensitivity of cancer cells to ferroptosis. Recent research suggests that cancer therapies, such as immunotherapy and radiotherapy, can induce ferroptosis partly through modulating SLC7A11 expression (Lang et al., 2019; Lei et al., 2020); knockout or inhibition of SLC7A11 has a significant inhibitory effect on lung cancer and pancreatic cancer cells (Ji et al., 2018; Sharbeen et al., 2021). SLC7A11 has become a central hub linking ferroptosis to its suppressive function on tumor.

The study showed that SLC7A11 is essential to elicit tumor formation and maintain tumorigenicity by relieving oxidative stress in COAD, pancreatic ductal adenocarcinoma (PDAC), and lung adenocarcinoma (LUAD) (Lim et al., 2019). This study found that SLC7A11 is highly expressed in most cancers, such as COAD,





LUAD, and esophageal cancer (ESCA). This notion is further supported by the GEO database. The results indicated that many cases may shrink ferroptosis by upregulating SLC7A11 expression. Interestingly, the expression of SLC7A11 was relatively stable in all pathological stages of COAD, but decreased after lymphatic

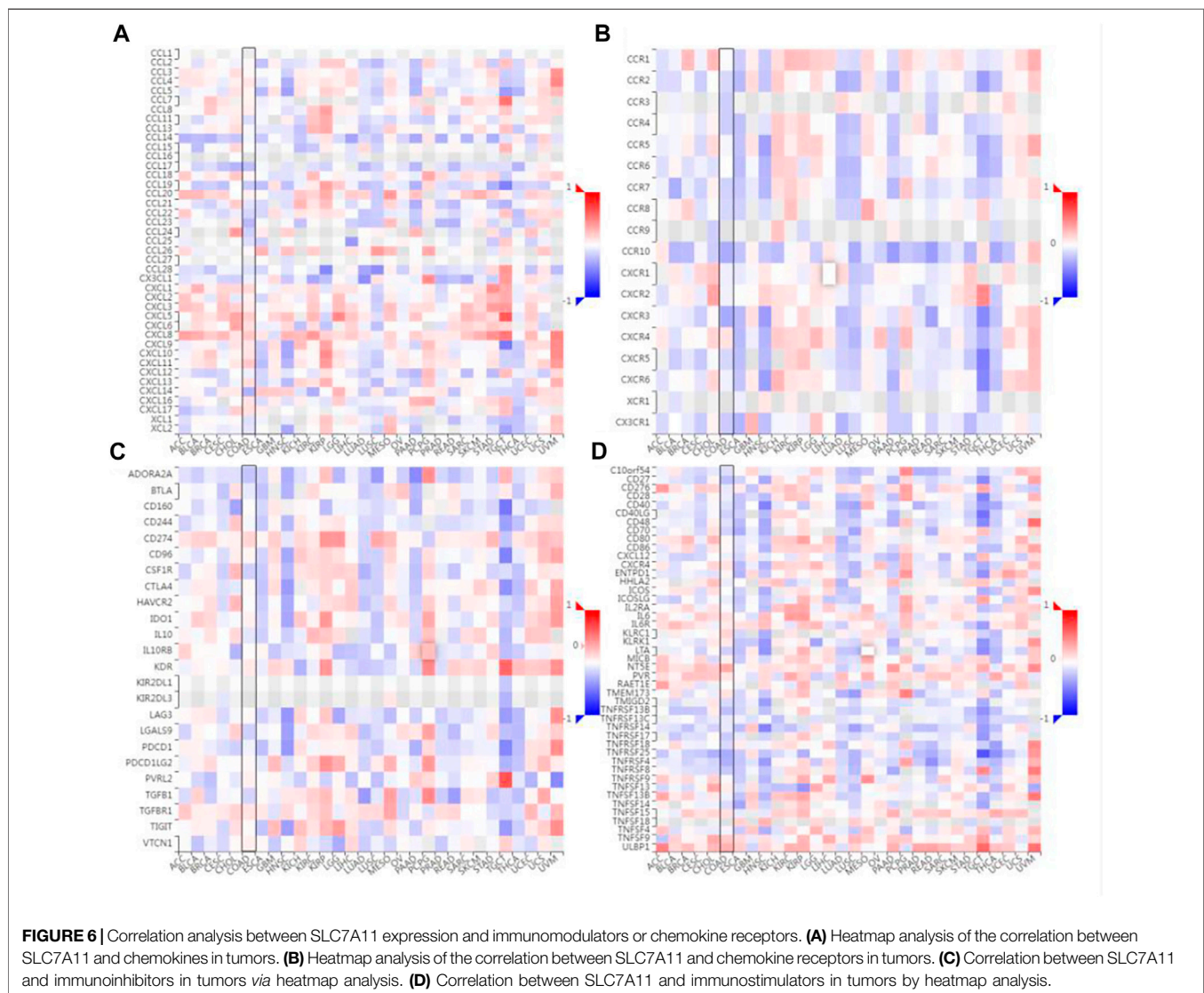
invasion. These results suggest that the overexpression of SLC7A11 promotes lymphatic metastasis of tumor cells, which was also confirmed in pancreatic carcinoma (Zhu et al., 2020).

Our study demonstrated that the expression level of SLC7A11 has a significant correlation with the infiltration levels of CD8<sup>+</sup>



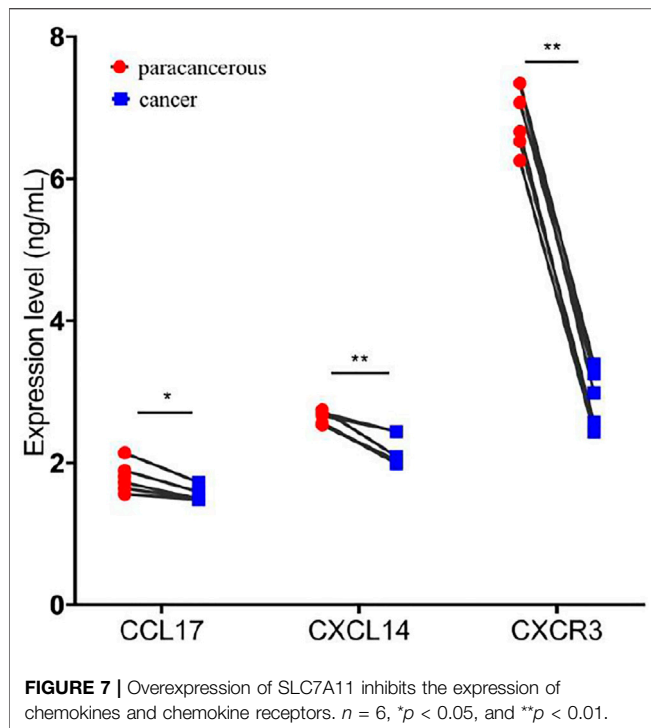
**TABLE 3 |** Potential drugs that regulate action for both SLC7A11 and co-expression genes.

Drug	Adjusted <i>p</i> -value	Odds ratio	Combined score	Target genes
F0447-0125 PC3 UP	2.47E-06	369.94	3,921.13	SLC7A11 and GCLM
Semustine PC3 UP	2.47E-06	325.53	4,868.78	GCLC; SLC7A11; and GCLM
Securinine PC3 UP	2.99E-06	308.14	5,892.08	GCLC; SLC3A2; SLC7A11; and GCLM
Alpha-tocopherol CTD 00007387	3.51E-06	728.02	5,209.14	GCLC; SLC3A2; SLC7A11; and GCLM
Ampicillin CTD 00005394	1.75E-05	277.40	2,796.46	SLC7A11 and GCLM
Ebselen MCF7 UP	3.26E-05	277.40	2,796.46	SLC7A11 and GCLM
17-Ethynyl estradiol CTD 00005932	3.26E-05	241.43	3,410.20	GCLC; SLC7A11; and GCLM
N-acetyl-L-cysteine CTD 00005305	3.40E-05	237.39	4,306.60	GCLC; SLC3A2; SLC7A11; and GCLM
Glutathione CTD 00006035	4.90E-05	233.57	2,280.80	SLC7A11 and GCLM
Vanillin CTD 00003324	4.97E-05	221.88	2,145.57	SLC7A11 and GCLM



T cells, neutrophils, and dendritic cells in COAD. Studies show that immunotherapy-activated CD8<sup>+</sup> T cells enhance ferroptosis-specific lipid peroxidation in tumor cells, and that increased ferroptosis contributes to the antitumor efficacy of immunotherapy (Wang

et al., 2019). Further analysis of infiltrated lymphocyte markers showed that the markers of Th1 cell such as TBX21, IL12RB2, IL27RA, STAT1, and IFN- $\gamma$  were strongly correlated with SLC7A11 expression, as well as the CD8<sup>+</sup> T cell marker CD8A and the NK cell



marker KIR3DL1. Intriguingly, IFN- $\gamma$  upregulates the level of intracellular Fe<sup>2+</sup> and decreases the level of GPX4, which lead the cells to be more sensitive to ferroptosis; STAT1 inhibitors could reverse the reduction of SLC7A11 expression induced by IFN- $\gamma$  and induces ferroptosis *via* activation of the JAK1-2/STAT1/SLC7A11 signaling pathway (Wei et al., 2021). Meanwhile, SLC7A11 also affects the infiltration of immune cells in rectal cancer, such as CD8<sup>+</sup> T cells (Supplementary Figure S1). These results further implied that SLC7A11 was the key molecule for bridging the ferroptosis process and immunotherapy. Moreover, we noticed that most of the immune cells or their markers were weak in the prediction of correlations *via* the TIMER and GEPIA databases. A similar situation has occurred in some recent studies (Zhao et al., 2021). This weak correlation does not mean that the detected target molecule can be ignored. If the correlations of target molecules, which are considered to be highly reliable, are calculated with consistent results in different databases (positive or negative), and  $p$  values indicate significant differences.

SLC7A11 is a key gene regulating ferroptosis and is overexpressed in COAD. Further study found that the genes closely associated with SLC7A11, such as PRDX5, CLDN3, ROMO1, and VEGFB genes were also overexpressed; LARP1B, AP1S3, IBTK, and SPATA5 genes were under-expressed. PRX5 can promote epithelial-to-mesenchymal transition (EMT) properties by inducing the expression of EMT-inducing transcription factors in colorectal cancer (Ahn et al., 2017). Li, et al. study found that CLDN3 is overexpressed in colorectal cancer tissues, and its high expression may promote the occurrence and progression of colorectal cancer (Li et al., 2017). VEGFB overexpression is thought to be highly associated with poor prognosis (Lautenschlaeger et al., 2013). In contrast, among

the genes that are under-expressed, IBTK inhibits the survival and proliferation of tumor cells by influencing the tumor microenvironment (Pal Singh et al., 2018). These results suggest that SLC7A11 and its co-expressed gene may be an important gene promoting the development of COAD.

TFs-miRNAs can jointly regulate target gene expression in the forms of feed-forward loops or feedback loops; these regulatory loops play an important role in gene regulatory networks and disease processes (Zhang et al., 2015). In this study, miRNA (such as hsa-mir-335-5p, hsa-mir-155-5p, and hsa-mir-34a-5p) and TFs (such as RELA, SP1, and NFKB1) with high frequency of action were identified. Studies have shown that mir-335-5P mediates the proliferation, apoptosis, and invasion of osteosarcoma and breast cancer cells (Chen et al., 2018; Zhang et al., 2021). RELA of NF- $\kappa$ B-driven cytokine by myeloid cells is required for colitis-associated cancer growth (Greten et al., 2004). Therefore, it is assumed that targeting TFs and miRNAs to regulate the expression of SLC7A11 may have a potential role in the treatment of COAD.

The construction of the PPI network is of great significance in analyzing protein signal transduction, gene expression regulation, and functional relationship among proteins. According to the PPIs network, SLC7A11, GPX4, GCLC, GCLM, and SLC3A2 were declared as hub genes involved in ferroptosis. Further examination of the hub genes of the PPI network revealed that these genes were also highly expressed in COAD (Supplementary Figure S2). As can be seen from the ferroptosis signaling pathway (Supplementary Figure S3), SLC7A11 is the upstream gene, and its expression level is positively correlated with hub genes. These results further suggest that SLC7A11 was a central regulator of ferroptosis in COAD. Furthermore, securinine PC3 UP, alpha-tocopherol CTD 00007387, and N-acetyl-L-cysteine CTD 00005305 are the peak drug candidates for regulating hub genes. Growing evidence suggest that securinine and alpha-tocopherol have anticancer and antimetastasis properties (Middha et al., 2019; Ashraf et al., 2021).

Chemokines and chemokine receptors are essential for the infiltration of immune cells into tumors. In this study, it is proved that the expression level of SLC7A11 was negatively correlated with the expressions of CCL17, CCL19, CCL22, CCL23, CXCL14, CCR10, CX3CR1, and CXCR3, suggesting that the high expression of SLC7A11 may inhibit the migration of immune cells. In contrast, the SLC7A11 expression level was positively correlated with the expressions of CXCL1-6/8-11. Studies have shown that CXCL9/10/11 are the main chemokines of CD8<sup>+</sup> T cells (Shigeta et al., 2020; Marcovecchio et al., 2021); CXCL2/8 are the main chemokines of neutrophil (Xu et al., 2021). This further confirmed the results of immune cell infiltration. However, a high proportion of neutrophils can inhibit the function of immune cells such as CD8<sup>+</sup> T cells, and promote tumor growth (Zhou et al., 2018). This may explain the poor immunotherapy response in patients with SLC7A11 high expression. CCL17 and CCL22 are the ligands for CCR4, which effect on the recruitment of Treg, Th2, and Th17 into the tumor (Korbecki et al., 2020). In addition, they exert an anticancer effect by causing the infiltration of tumor-infiltrating lymphocytes (TIL) into the tumor (Kanagawa et al., 2007).

Chemokine CXCL14 is a key regulatory factor in cancer and represents a potential target for future cancer immunotherapies (Westrich et al., 2020). The CXCR3 and CX3CR1 are mainly responsible for the tumor-suppressive lymphocytic infiltration into the tumor microenvironment (Bronger et al., 2019). Interestingly, the high expression of SLC7A11 also affects the expression of immunoinhibitors and immunostimulators. Therefore, these results suggest that SLC7A11 may play a role in regulating tumor immunity.

## CONCLUSION

In summary, our study found that the expression of SLC7A11 and genes interact with it are significantly upregulated in COAD, and results in more GSH synthesis. GPX4 uses GSH to improve the antioxidant activity of tumor cells, thereby suppressing ferroptosis. Meanwhile, the overexpression of SLC7A11 can affect the expression of chemokines, leading to the infiltration of immune cells such as CD8<sup>+</sup> T cells/neutrophils, and deficiency of other immune cells, and causes immunosuppression of tumor cells. Regulation of SLC7A11 expression would be a potential therapeutic approach in inducing ferroptosis and/or immunotherapy for tumors.

## DATA AVAILABILITY STATEMENT

The original contributions presented in the study are included in the article/**Supplementary Material**; further inquiries can be directed to the corresponding author.

## REFERENCES

- Ahn, H.-M., Yoo, J.-W., Lee, S., Lee, H. J., Lee, H.-S., and Lee, D.-S. (2017). Peroxiredoxin 5 Promotes the Epithelial-Mesenchymal Transition in colon Cancer. *Biochem. Biophysical Res. Commun.* 487 (3), 580–586. doi:10.1016/j.bbrc.2017.04.094
- Alhopuro, P., Sammalkorpi, H., Niittymäki, I., Biström, M., Raitila, A., Saharinen, J., et al. (2012). Candidate Driver Genes in Microsatellite-Unstable Colorectal Cancer. *Int. J. Cancer* 130 (7), 1558–1566. doi:10.1002/ijc.26167
- Ashraf, S. M., Mahanty, S., and Rathinasamy, K. (2021). Securinine Induces Mitotic Block in Cancer Cells by Binding to Tubulin and Inhibiting Microtubule Assembly: A Possible Mechanistic Basis for its Anticancer Activity. *Life Sci.* 287, 120105. doi:10.1016/j.lfs.2021.120105
- Bao, X., Zhang, H., Wu, W., Cheng, S., Dai, X., Zhu, X., et al. (2020). Analysis of the Molecular Nature Associated with Microsatellite Status in colon Cancer Identifies Clinical Implications for Immunotherapy. *J. Immunother. Cancer* 8 (2), e001437. doi:10.1136/jitc-2020-001437
- Bronger, H., Magdolen, V., Goettig, P., and Dreyer, T. (2019). Proteolytic Chemokine Cleavage as a Regulator of Lymphocytic Infiltration in Solid Tumors. *Cancer Metastasis Rev.* 38 (3), 417–430. doi:10.1007/s10555-019-09807-3
- Chen, Y., Chen, Q., Zou, J., Zhang, Y., and Bi, Z. (2018). Construction and Analysis of a ceRNA-ceRNA Network Reveals Two Potential Prognostic Modules Regulated by hsa-miR-335-5p in Osteosarcoma. *Int. J. Mol. Med.* 42 (3), 1237–1246. doi:10.3892/ijmm.2018.3709
- El Kinany, K., Mint Sidi Deoula, M., Hatime, Z., Boudouaya, H. A., Huybrechts, I., El Asri, A., et al. (2020). Consumption of Modern and Traditional Moroccan

## ETHICS STATEMENT

The studies involving human participants were reviewed and approved by the ethics committee of the First Affiliated Hospital of Wannan Medical College, Wuhu, Anhui, China. The patients provided their written informed consent to participate in this study.

## AUTHOR CONTRIBUTIONS

XC and JX participated in study design and drafted the manuscript. YW and LL performed the statistical analysis. CL (4th author) and CL (5th author) collected the samples and clinical data. JX contributed for overall editing and supervision. All authors approved the final manuscript.

## FUNDING

This work was supported by the Key Project in Natural Science Research in Higher Education Institutions of Anhui Province (KJ 2019A0403) and the Natural Science Foundation of Wannan Medical College (WK202123).

## SUPPLEMENTARY MATERIAL

The Supplementary Material for this article can be found online at: <https://www.frontiersin.org/articles/10.3389/fmolb.2022.889688/full#supplementary-material>

- Dairy Products and Colorectal Cancer Risk: a Large Case Control Study. *Eur. J. Nutr.* 59 (3), 953–963. doi:10.1007/s00394-019-01954-1
- Fidelle, M., Yonekura, S., Picard, M., Cogdill, A., Hollebecque, A., Roberti, M. P., et al. (2020). Resolving the Paradox of Colon Cancer through the Integration of Genetics, Immunology, and the Microbiota. *Front. Immunol.* 11, 600886. doi:10.3389/fimmu.2020.600886
- Greten, F. R., Eckmann, L., Greten, T. F., Park, J. M., Li, Z.-W., Egan, L. J., et al. (2004). IKK $\beta$  Links Inflammation and Tumorigenesis in a Mouse Model of Colitis-Associated Cancer. *Cell* 118 (3), 285–296. doi:10.1016/j.cell.2004.07.013
- Guo, J., Xu, B., Han, Q., Zhou, H., Xia, Y., Gong, C., et al. (2018). Ferroptosis: A Novel Anti-tumor Action for Cisplatin. *Cancer Res. Treat.* 50 (2), 445–460. doi:10.4143/crt.2016.572
- Ji, X., Qian, J., Rahman, S. M. J., Siska, P. J., Zou, Y., Harris, B. K., et al. (2018). xCT (SLC7A11)-Mediated Metabolic Reprogramming Promotes Non-small Cell Lung Cancer Progression. *Oncogene* 37 (36), 5007–5019. doi:10.1038/s41388-018-0307-z
- Kanagawa, N., Niwa, M., Hatanaka, Y., Tani, Y., Nakagawa, S., Fujita, T., et al. (2007). CC-chemokine Ligand 17 Gene Therapy Induces Tumor Regression through Augmentation of Tumor-Infiltrating Immune Cells in a Murine Model of Preexisting CT26 colon Carcinoma. *Int. J. Cancer* 121 (9), 2013–2022. doi:10.1002/ijc.22908
- Koppula, P., Zhang, Y., Zhuang, L., and Gan, B. (2018). Amino Acid Transporter SLC7A11/xCT at the Crossroads of Regulating Redox Homeostasis and Nutrient Dependency of Cancer. *Cancer Commun.* 38 (1), 12. doi:10.1186/s40880-018-0288-x
- Korbecki, J., Kojder, K., Simińska, D., Bohatyrewicz, R., Gutowska, I., Chlubek, D., et al. (2020). CC Chemokines in a Tumor: A Review of Pro-cancer and Anti-cancer Properties of the Ligands of Receptors CCR1, CCR2, CCR3, and CCR4. *Ijms* 21 (21), 8412. doi:10.3390/ijms21218412



- Lang, X., Green, M. D., Wang, W., Yu, J., Choi, J. E., Jiang, L., et al. (2019). Radiotherapy and Immunotherapy Promote Tumoral Lipid Oxidation and Ferroptosis via Synergistic Repression of SLC7A11. *Cancer Discov.* 9 (12), 1673–1685. doi:10.1158/2159-8290.CD-19-0338
- Lautenschlaeger, T., George, A., Klimowicz, A. C., Efstathiou, J. A., Wu, C.-L., Sandler, H., et al. (2013). Bladder Preservation Therapy for Muscle-Involving Bladder Cancers on Radiation Therapy Oncology Group Trials 8802, 8903, 9506, and 9706: Vascular Endothelial Growth Factor B Overexpression Predicts for Increased Distant Metastasis and Shorter Survival. *Oncologist* 18 (6), 685–686. doi:10.1634/theoncologist.2012-0461
- Lei, G., Zhang, Y., Koppula, P., Liu, X., Zhang, J., Lin, S. H., et al. (2020). The Role of Ferroptosis in Ionizing Radiation-Induced Cell Death and Tumor Suppression. *Cell Res* 30 (2), 146–162. doi:10.1038/s41422-019-0263-3
- Li, J. Y., Xie, F., Xu, X. P., Ma, J. J., Zhou, D. C., Liao, Y., et al. (2017). Claudin-3 Expression in Colorectal Carcinoma and its Significance. *Nan Fang Yi Ke Da Xue Xue Bao* 37 (1), 63–67. doi:10.3969/j.issn.1673-4254.2017.01.11
- Lim, J. K. M., Delaidelli, A., Minaker, S. W., Zhang, H.-F., Colovic, M., Yang, H., et al. (2019). Cystine/glutamate Antiporter xCT (SLC7A11) Facilitates Oncogenic RAS Transformation by Preserving Intracellular Redox Balance. *Proc. Natl. Acad. Sci. U.S.A.* 116 (19), 9433–9442. doi:10.1073/pnas.1821323116
- Marcovecchio, P. M., Thomas, G., and Salek-Ardakani, S. (2021). CXCL9-expressing Tumor-Associated Macrophages: New Players in the Fight against Cancer. *J. Immunother. Cancer* 9 (2), e002045. doi:10.1136/jitc-2020-002045
- Middha, P., Weinstein, S. J., Männistö, S., Albanes, D., and Mondul, A. M. (2019).  $\beta$ -Carotene Supplementation and Lung Cancer Incidence in the Alpha-Tocopherol, Beta-Carotene Cancer Prevention Study: The Role of Tar and Nicotine. *Nicotine Tob. Res.* 21 (8), 1045–1050. doi:10.1093/ntr/nty115
- Mou, Y., Wang, J., Wu, J., He, D., Zhang, C., Duan, C., et al. (2019). Ferroptosis, a New Form of Cell Death: Opportunities and Challenges in Cancer. *J. Hematol. Oncol.* 12 (1), 34. doi:10.1186/s13045-019-0720-y
- Pal Singh, S., Dammeijer, F., and Hendriks, R. W. (2018). Role of Bruton's Tyrosine Kinase in B Cells and Malignancies. *Mol. Cancer* 17 (1), 57. doi:10.1186/s12943-018-0779-z
- Roslan, N. H., Makpol, S., and Mohd Yusof, Y. A. (2019). A Review on Dietary Intervention in Obesity Associated Colon Cancer. *Asian Pac. J. Cancer Prev.* 20 (5), 1309–1319. doi:10.31557/APJCP.2019.20.5.1309
- Sandhu, J., Lavingia, V., and Fakih, M. (2019). Systemic Treatment for Metastatic Colorectal Cancer in the Era of Precision Medicine. *J. Surg. Oncol.* 119 (5), 564–582. doi:10.1002/jso.25421
- Sharbeen, G., McCarroll, J. A., Akerman, A., Kopecky, C., Youkhana, J., Kokkinos, J., et al. (2021). Cancer-Associated Fibroblasts in Pancreatic Ductal Adenocarcinoma Determine Response to SLC7A11 Inhibition. *Cancer Res.* 81 (13), 3461–3479. doi:10.1158/0008-5472.CAN-20-2496
- Shigeta, K., Matsui, A., Kikuchi, H., Klein, S., Mamessier, E., Chen, I. X., et al. (2020). Regorafenib Combined with PD1 Blockade Increases CD8 T-Cell Infiltration by Inducing CXCL10 Expression in Hepatocellular Carcinoma. *J. Immunother. Cancer* 8 (2), e001435. doi:10.1136/jitc-2020-001435
- Song, X., Zhu, S., Chen, P., Hou, W., Wen, Q., Liu, J., et al. (2018). AMPK-mediated BECN1 Phosphorylation Promotes Ferroptosis by Directly Blocking System Xc- Activity. *Curr. Biol.* 28 (15), 2388–2399. doi:10.1016/j.cub.2018.05.094
- Tang, R., Xu, J., Zhang, B., Liu, J., Liang, C., Hua, J., et al. (2020). Ferroptosis, Necroptosis, and Pyroptosis in Anticancer Immunity. *J. Hematol. Oncol.* 13 (1), 110. doi:10.1186/s13045-020-00946-7
- Tsukamoto, S., Ishikawa, T., Iida, S., Ishiguro, M., Mogushi, K., Mizushima, H., et al. (2011). Clinical Significance of Osteoprotegerin Expression in Human Colorectal Cancer. *Clin. Cancer Res.* 17 (8), 2444–2450. doi:10.1158/1078-0432.CCR-10-2884
- Wang, W., Green, M., Choi, J. E., Gijón, M., Kennedy, P. D., Johnson, J. K., et al. (2019). CD8+ T Cells Regulate Tumour Ferroptosis during Cancer Immunotherapy. *Nature* 569 (7755), 270–274. doi:10.1038/s41586-019-1170-y
- Wei, T. T., Zhang, M. Y., Zheng, X. H., Xie, T. H., Wang, W., Zou, J., et al. (2021). Interferon- $\gamma$  Induces Retinal Pigment Epithelial Cell Ferroptosis by a JAK1-2/STAT1/SLC7A11 Signaling Pathway in Age-related Macular Degeneration. *FEBS J.* 289 (7), 1968–1983. doi:10.1111/febs.16272
- Westrich, J. A., Vermeer, D. W., Colbert, P. L., Spanos, W. C., and Pyeon, D. (2020). The Multifarious Roles of the Chemokine CXCL14 in Cancer Progression and Immune Responses. *Mol. Carcinogenesis* 59 (7), 794–806. doi:10.1002/mc.23188
- Xie, Y., Hou, W., Song, X., Yu, Y., Huang, J., Sun, X., et al. (2016). Ferroptosis: Process and Function. *Cell Death Differ.* 23 (3), 369–379. doi:10.1038/cdd.2015.158
- Xu, X., Ye, L., Zhang, Q., Shen, H., Li, S., Zhang, X., et al. (2021). Group-2 Innate Lymphoid Cells Promote HCC Progression through CXCL2-Neutrophil-Induced Immunosuppression. *Hepatology* 74 (5), 2526–2543. doi:10.1002/hep.31855
- Zhang, D., An, X., Yu, H., and Li, Z. (2021). The Regulatory Effect of 6-TG on lncRNA-miRNA-mRNA ceRNA Network in Triple-Negative Breast Cancer Cell Line. *Biosci. Rep.* 41 (2), BSR20203890. doi:10.1042/BSR20203890
- Zhang, H.-M., Kuang, S., Xiong, X., Gao, T., Liu, C., and Guo, A.-Y. (2015). Transcription Factor and microRNA Co-regulatory Loops: Important Regulatory Motifs in Biological Processes and Diseases. *Brief. Bioinform.* 16 (1), 45–58. doi:10.1093/bib/bbt085
- Zhang, L., Liu, W., Liu, F., Wang, Q., Song, M., Yu, Q., et al. (2020). IMCA Induces Ferroptosis Mediated by SLC7A11 through the AMPK/mTOR Pathway in Colorectal Cancer. *Oxidative Med. Cell Longevity* 2020, 1–14. doi:10.1155/2020/1675613
- Zhao, H., Xu, Y., Xie, Y., Zhang, L., Gao, M., Li, S., et al. (2021). m6A Regulators Is Differently Expressed and Correlated with Immune Response of Esophageal Cancer. *Front. Cell Dev. Biol.* 9, 650023. doi:10.3389/fcell.2021.650023
- Zhou, J., Nefedova, Y., Lei, A., and Gabrilovich, D. (2018). Neutrophils and PMN-MDSC: Their Biological Role and Interaction with Stromal Cells. *Semin. Immunol.* 35, 19–28. doi:10.1016/j.smim.2017.12.004
- Zhu, J.-H., De Mello, R. A., Yan, Q.-L., Wang, J.-W., Chen, Y., Ye, Q.-H., et al. (2020). MiR-139-5p/SLC7A11 Inhibits the Proliferation, Invasion and Metastasis of Pancreatic Carcinoma via PI3K/Akt Signaling Pathway. *Biochim. Biophys. Acta (Bba) - Mol. Basis Dis.* 1866 (6), 165747. doi:10.1016/j.bbdis.2020.165747

**Conflict of Interest:** The authors declare that the research was conducted in the absence of any commercial or financial relationships that could be construed as a potential conflict of interest.

**Publisher's Note:** All claims expressed in this article are solely those of the authors and do not necessarily represent those of their affiliated organizations, or those of the publisher, the editors, and the reviewers. Any product that may be evaluated in this article, or claim that may be made by its manufacturer, is not guaranteed or endorsed by the publisher.

Copyright © 2022 Cheng, Wang, Liu, Lv, Liu and Xu. This is an open-access article distributed under the terms of the Creative Commons Attribution License (CC BY). The use, distribution or reproduction in other forums is permitted, provided the original author(s) and the copyright owner(s) are credited and that the original publication in this journal is cited, in accordance with accepted academic practice. No use, distribution or reproduction is permitted which does not comply with these terms.



# Ferroptosis Biology and Implication in Cancers

Chi Qu, Yang Peng and Shengchun Liu\*

Department of Endocrine and Breast Surgery, The First Affiliated Hospital of Chongqing Medical University, Chongqing, China

Ferroptosis, a novel form of regulated cell death (RCD), has garnered increasing attention in studies on numerous human diseases in the last decade. Emerging evidence has indicated that the pathological process of ferroptosis involves the overloaded production of reactive oxygen species (ROS), followed by aberrant accumulation of lipid peroxidation in an iron-dependent manner, accompanied with an increased uptake of polyunsaturated fatty acids into the cellular membrane, further unfolding an ancient vulnerability in multiple context. The unique nature of ferroptosis differentiates it from other forms of RCD, as it is intricately associated with several biological processes, including the metabolism of iron, amino acids, synthesis of ROS and lipid peroxidation. Accordingly, inducers and inhibitors designed to target the key processes of ferroptosis have been extensively studied. Characterized by its distinct properties as mentioned above and its inducible nature, ferroptosis has been widely implicated in several diseases, and numerous studies have focused on identifying effective therapeutic targets for multiple human diseases, including in cancer, by targeting this process. In the present review, recent studies on the involvement of ferroptosis in several types of cancer are summarized and the findings discussed, highlighting the need for increased contemplation of its involvement in the study of cancer, particularly in the clinical setting. A comprehensive summary of the biological mechanisms underlying ferroptosis, the implications of the multiple inducers of ferroptosis, as well as immunotherapy targeting ferroptosis in different types of cancer is provided in this review to highlight the pathophysiological role of ferroptosis in carcinogenesis, to serve as an aid in future studies on the role of ferroptosis in cancer.

**Keywords:** ferroptosis, iron metabolism, lipid peroxidation, ether lipid, glutathione peroxidase 4, ferroptosis suppressor protein 1, AT-rich interaction domain 1A, chromatin accessibility

## OPEN ACCESS

### Edited by:

Yanqing Liu,  
Columbia University, United States

### Reviewed by:

Min Nie,  
Nanjing Drum Tower Hospital, China  
Mengchao Yu,  
Qingdao University Medical College,  
China

### \*Correspondence:

Shengchun Liu  
liushengchun1968@163.com

### Specialty section:

This article was submitted to  
Molecular Diagnostics and  
Therapeutics,  
a section of the journal  
Frontiers in Molecular Biosciences

**Received:** 09 March 2022

**Accepted:** 22 March 2022

**Published:** 20 April 2022

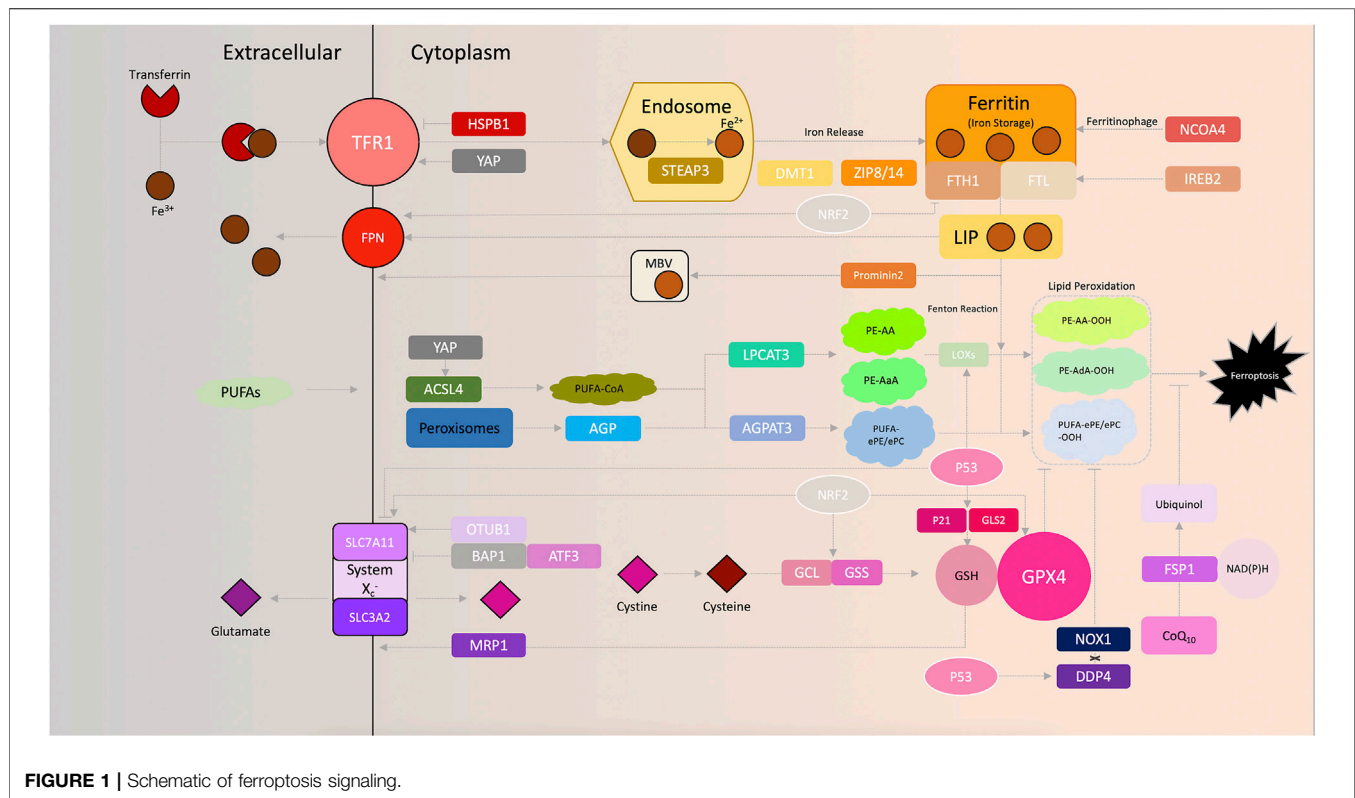
### Citation:

Qu C, Peng Y and Liu S (2022)  
Ferroptosis Biology and Implication  
in Cancers.  
Front. Mol. Biosci. 9:892957.  
doi: 10.3389/fmolb.2022.892957

## INTRODUCTION

Death, by one of several means, is the eventual fate of cells, and it is physiologically associated with the development and maintenance of the human body, and pathologically associated with the development of numerous diseases (Gao and Jiang, 2018). Certain forms of cell death have been extensively studied and are relatively well understood, and can be inhibited by exposure to treatments that genetically or pharmacologically regulate these processes; these types of cell deaths are therefore termed regulated cell death (RCD) (Galluzzi et al., 2018). The traditional understanding of RCD allows for its stratification into three morphologically distinct types: Apoptosis, autophagy and necrosis. Clinically, chemotherapeutic regimens targeting caspase-dependent apoptosis for the treatment of cancer can result in the acquisition of resistance, thus reducing the efficacy of a chemotherapeutic regimen long term (Gottesman et al., 2002; Angeli et al., 2017). More recently, the





discovery of a novel form of RCD highlighted novel opportunities for alternate approaches to treatment of a range of diseases, including cancer (Berghe et al., 2014). Exclusively iron-dependent, ferroptosis is biologically characterized by the overloaded production of reactive oxygen species (ROS) and aberrant accumulation of lipid peroxidation. In addition, cytological changes, including the disappearance of the mitochondrial cristae, outer mitochondrial membrane rupture and the condensation of the mitochondrial membrane, are commonly observed during ferroptosis (Dixon et al., 2012; Stockwell et al., 2017).

Metabolic reprogramming of cancer cells, which results in the changes associated with ferroptosis, were initially described in the 1920s. To prevent the excessive production of ROS, cancer cells preferentially switch from aerobic glycolysis to anaerobic lactate-dependent glycolysis, which in turn increases the requirements of glucose or other energy providing substrates to sustain their proliferative activity, due to the reduced efficiency of anaerobic glycolysis (Goodwin et al., 2014). Correspondingly, the increased metabolic activity enhances the demands on the antioxidant capacity of cancer cells, thus leading the evolution of cells with a reduced sensitivity to conditions of increased oxidative stress (Diebold and Chandel, 2016; Gwangwa et al., 2018). Ferroptosis, unlike other forms of RCD, can trigger the collapse of the antioxidant defense system in cancer cells and potentially presents a more recently evolved but regulatable target for cancer treatment (Dixon et al., 2012).

Studies on ferroptosis address the essential signaling pathways and biomarkers that may serve as therapeutic targets and for

prediction of prognosis of certain diseases. Whilst previous studies on this novel form of RCD have highlighted the importance of numerous biological processes, including iron metabolism and the biosynthesis of a range of amino acids and phospholipids (Galluzzi et al., 2018), more recent investigations have provided a broader and clearer insight into the molecular mechanisms underlying ferroptosis. As ferroptosis has been discovered more recently than the other forms of RCD, its value as a targetable mechanism for management of diseases remains to be further studied. In the present review, a systematic, comprehensive and up-to-date summary of the studies in this field is provided, with the aim of providing an integrated understanding of ferroptosis biology, both metabolically and molecularly.

## FERROPTOSIS BIOLOGY

Recent studies on ferroptosis have improved our understanding of the biological principles and regulatory mechanisms underlying ferroptosis-based oncotherapy. In this section, the key regulators and metabolic mechanisms involved in ferroptosis biology are summarized (Figure 1), with an emphasis on the implications of targeting ferroptotic cell death in cancer treatments. In addition, the metabolic alterations triggered by chromatin remodeling are also discussed and novel perspectives in this area are considered, to highlight potential means of exploiting ferroptosis to improve patient outcomes.

**Metabolism of iron.** The Fenton reaction, exclusively catalyzed by redox-active iron ( $\text{Fe}^{2+}$ ), has been shown to be obligatory for excessive ROS production, which further sensitizes cells to ferroptosis. The delicate nature of intracellular iron transport serves as a key operator of ferroptosis (Dixon and Stockwell, 2014). The addition of the iron chelator deferoxamine, which functionally disables iron utilization, rescues cells from erastin-induced ferroptosis (Dixon et al., 2012). Complexes of extracellular ferric iron ( $\text{Fe}^{3+}$ ) and transferrin can be specifically imported by the transferrin receptor (TFR1) and further shuttled to the endosome, where  $\text{Fe}^{3+}$  is reduced to ferrous iron ( $\text{Fe}^{2+}$ ) by the six-transmembrane epithelial antigen of the prostate 3 (Gao et al., 2015a). Increased iron uptake consequently enhances the susceptibility of cancer cells to oxidative damage and ferroptosis. Ferroptosis-sensitive cells exhibit increased levels of TFR1 (Yang and Stockwell, 2008), whereas inhibition of iron uptake by silencing TFR1, the gene encoding TFR1, results in impaired ferroptosis induced by erastin (Gao et al., 2015a). Overexpression of heat shock protein  $\beta$ -1 (HSPB1) downregulates TFR1 and concurrently inhibits erastin-induced ferroptosis while antagonizing Merlin-Hippo signaling, synchronously activating YAP, leads an upregulated expression of TFR1 and, vice versa, prompts ferroptosis (Sun et al., 2015; Wu et al., 2019).  $\text{Fe}^{2+}$  is released into the cellular labile iron pool by divalent metal transporter 1 (DMT1) or zinc-iron regulatory protein family 8/14, and is stored in ferritin, a complex of ferritin light chain (FTL) and ferritin heavy chain (FTH1) (Bogdan et al., 2016). Interestingly, our previous study also found that DMT1 was significantly upregulated upon induction of ferroptosis (Yu et al., 2019a). Finally, redundant  $\text{Fe}^{2+}$  is exported and oxidized to  $\text{Fe}^{3+}$  by ferroportin to ensure cellular iron homeostasis (Bogdan et al., 2016). Induction of prominin 2, a pentaspanin protein involved in lipid dynamics, facilitates the formation of ferritin-containing multivesicular bodies and exosomes to export iron out of the cells, thereby impeding ferroptosis in breast cancer cells (Brown et al., 2019). Similarly, knockdown of nuclear receptor coactivator 4 decreased the degradation of ferritin, which in-turn reduces the sensitivity to ferroptosis in human pancreatic carcinoma cells (Hou et al., 2016). Additionally, suppression of iron responsive element binding protein 2, a master transcription factor of iron metabolism, increases the iron storage capacity of cancer cells by upregulating FTL and FTH1, thereby inhibiting erastin-induced ferroptosis (Dixon et al., 2012; Gammella et al., 2015). Moreover, RAS signaling was found to be vital for regulating ferroptosis sensitivity by regulating iron metabolism in certain cancer cell lines (Yagoda et al., 2007). As mentioned above, cancer cells have a significantly higher demand for energy and iron, which in turn make them more vulnerable to accumulation of iron and ROS (Hassannia et al., 2019). This biological phenomenon addresses the involvement of iron utilization in carcinogenesis, and reinforces the importance of ferroptosis in future cancer treatments.

**Role of amino acids in ferroptosis.** Transmembrane transport of amino acids, such as facilitated diffusion, requires specific transporters on the cell membrane. System  $\text{X}_c^-$ , a heterodimeric

transporter consists of two functional subunits: Solute carrier family 3 member 2 (SLC3A2) and solute carrier family 7 member 11 (SLC7A11), which are prevalently expressed on phospholipid bilayers (Dixon et al., 2012). With the assistance of system  $\text{X}_c^-$ , glutamate and cystine are exchanged across the plasma membrane and cystine is immediately reduced to cysteine once imported, which is followed by the synthesis of reduced glutathione (GSH). Since glutamate and cystine transport are the most upstream events in ferroptosis, targeting system  $\text{X}_c^-$  provides a suitable method for induction of ferroptosis (Toyokuni et al., 2017). Erastin was one of the first ferroptosis inducers identified, and functions by directly inhibiting system  $\text{X}_c^-$  by binding to the mitochondrial voltage-dependent anion channel 2/3 and activating the endoplasmic reticulum (ER) stress response (Dixon et al., 2014). Sulfasalazine, commonly used for treatment of chronic inflammation, was also found to trigger ferroptosis by inhibiting the cystine transporter (Gout et al., 2001; Yu et al., 2019a). In certain cancer cells, sorafenib exerts its toxic effects by suppressing system  $\text{X}_c^-$  to induce ferroptosis as well (Dixon et al., 2014). The bioactivity of system  $\text{X}_c^-$  also varies based on the genetic variants of the catalytic subunit, SLC7A11. For example, ubiquitin aldehyde binding 1 (OTUB1) was found to directly interact with and stabilize SLC7A11 in cancer cells. Reducing the cellular SLC7A11 levels by knocking down OTUB1 significantly increased the sensitivity of cells to ferroptosis (Liu et al., 2019). In fibrosarcoma HT-1080 cells, overexpression of activating transcription factor 3 reduced SLC7A11 by directly binding to its promoter region and thereby increasing the sensitivity of cells to erastin-mediated ferroptosis (Wang et al., 2020). Moreover, the tumor suppressor gene, BRCA1-associated protein 1 (BAP1), was found to reduce SLC7A11 expression by decreasing histone 2A ubiquitination occupancy on its promoter in human cancer, which consequently resulted in increased ferroptosis (Zhang et al., 2018).

GSH is on the most abundantly present antioxidants in mammals, where it serves as an electron donor for glutathione peroxidase 4 (GPX4) and thereby reduces lipid hydroperoxide levels. On the basis of glutamate, cysteine and glycine levels, GSH synthesis is strictly dependent on the concentration of substrates and the biological availability of two catalytic enzymes, glutamate-cysteine ligase and GSH synthetase (Meister, 1983). Consistently, inhibitors that prevent GSH biosynthesis can induce ferroptosis. Buthioninesulfoximine (BSO), an inhibitor of  $\gamma$ -glutamyl cysteine synthetase, has been shown to effectively induce ferroptosis in RAS-mutated cells (Yang et al., 2014). By depleting GSH, acetaminophen was found to synchronously induce apoptosis and ferroptosis in specific cell lines as well (Lőrincz et al., 2015). Moreover, a recent study demonstrated that most  $\text{CD8}^+$  memory T cells physiologically possess upregulated levels of cytosolic phosphoenolpyruvate carboxykinase, which consistently ensures high levels of GSH and consequently quenches ROS production to favor cell survival, and GSH has been implicated in the molecular mechanism underlying this protective effect in cancer immunotherapy (Ma et al., 2018). Additionally, cancer cells overexpressing multidrug resistance protein 1, an ATP binding cassette-family transporter, possess increased GSH efflux capacity and thereby exhibit higher

susceptibility to ferroptosis (Cao et al., 2019). Together, these observations summarize the potential of targeting glutamate and cystine transport, as well as GSH synthesis as a method of cancer treatment.

**Lipid peroxidation.** Oxygen ( $O_2$ ), which is required for aerobic respiration and is vital for life, receives electrons from NADH, and in the process, is reduced to water (Papa et al., 2012). Simultaneously, a proportion of the electrons may react with oxygen molecules and generate reactive superoxide ( $O_2^{\cdot-}$ ) in the mitochondria (Sullivan and Chandel, 2014). The high antioxidant capacity present in cells, mediated by certain antioxidant molecules, such as superoxide dismutase, can catalyze  $O_2^{\cdot-}$  into hydrogen peroxide ( $H_2O_2$ ) which is less reactive (Sullivan and Chandel, 2014). In the presence of redox-active divalent iron ( $Fe^{2+}$ ) and  $H_2O_2$ , the Fenton reaction can be conditionally triggered and hydroxyl radicals ( $HO\cdot$ ) may thus be generated (Cheng and Li, 2007). These molecules containing a partially reduced oxygen are collectively referred to as ROS, and they can cause aberrant oxidation of DNA/RNA, lipids and proteins, and thus induce cell death (Lin et al., 2018). Indeed, induction of ferrostatin-1 and liproxtatin-1 efficiently inhibit ROS accumulation in multiple types of cancer cells and consequently counteract ferroptosis induced by erastin and RSL3 (Dixon et al., 2012; Friedmann Angeli et al., 2014).

Another hallmark of ferroptosis is the aberrant accumulation of lipid peroxidation (D'Herde and Krysko, 2017). Mechanistically, extensive lipid peroxidation can destabilize and thin the lipid bilayer, which consequently leads to the loss of biomembrane integrity and causes cell death (Agmon et al., 2018). The decomposed lipid peroxides can reactively disrupt and devastate nucleic acids and proteins, further triggering ferroptotic death (Gaschler and Stockwell, 2017). Fueling cells with polyunsaturated fatty acids (PUFA), instead of unsaturated or monounsaturated fatty acids, significantly enhances a cells susceptibility to ferroptosis (Yang et al., 2016); the mechanistic explanation of this phenomena revolves around the increased sensitivity of PUFAs to lipid peroxidation, as they possess highly reactive hydrogen atoms in the methylene bridges (Emerit and Michelson, 1982; Aruoma et al., 2006). Esterification of PUFAs requires the action of Acyl-CoA synthetase long-chain family member 4 (ACSL4), which functionally promotes the synthesis of PUFA-coenzyme A (CoA), particularly arachidonic acid-CoA (AA-CoA) and adrenic acid-CoA (AdA-CoA). In fact, upregulated ACSL4 upon YAP activation prompts ferroptosis (Wu et al., 2019) and ACSL4-knockout cancer cells exhibit significantly decreased levels of AA-CoA and AdA-CoA, and in-turn, induction of ferroptosis by RSL3 is reduced (Doll et al., 2017). Incorporation of PUFAs into the cell membrane contributes to lysophosphatidyl-choline acyltransferase 3, and substrates consisting of AA- and AdA containing phosphatidylethanolamine species are simultaneously generated and presented for lipid peroxidation (Dixon et al., 2015; Hashidate-Yoshida et al., 2015). Interestingly, recent lipidomic profiling revealed that polyunsaturated ether phospholipids (PUFA-ePLs) may serve as another important substrate for lipid peroxidation; peroxisomes were identified to exclusively contribute to ferroptosis by catalyzing the

biosynthesis of ether lipids (Zou et al., 2020). In fact, peroxisome components, such as peroxisomal enzymes alkylglycerone phosphate synthase, fatty acyl-CoA reductase 1 and glyceronephosphate O-acyltransferase synergistically promote the biosynthesis of the ether lipids precursor, 1-O-alkyl-glycerol-3-phosphate, which is then transported to the ER (Honsho and Fujiki, 2017). The ER-resident enzyme 1, acylglycerol-3-phosphate O-acyltransferase 3, acylates AGP by adding an ester-linked PUFA, which ACSL4 cooperatively incorporates into the sn-2 position in PUFA-ePL containing PUFA-ether-linked phosphatidylethanolamine, resulting in the generation of PUFA-ether-linked phosphatidylcholine. As a result, sufficient intracellular concentrations of peroxisomes and PUFA-ePL guarantee adequate susceptibility to ferroptosis, and conversely, the biochemical plasticity in attenuating PUFA-ePL in cancer cells allows them to subsequently evade ferroptosis (Zou et al., 2020). Ferroptotic lipid peroxidation specifically requires for divalent iron ( $Fe^{2+}$ ) and hydroxyl radicals ( $HO\cdot$ ) generated from the Fenton reaction to directly react with and oxidize PUFAs that have been incorporated into membrane phospholipids to trigger ferroptotic cell death. The  $Fe^{2+}$  coadjutant lipoxygenase (LOX) can enzymatically facilitate the generation of doubly and triply-oxygenated (15-hydroperoxy)-diacylated PE species as well, which induces ferroptosis (Yang et al., 2016; Kagan et al., 2017). Recently, the LOX family member (ALOX)12 was found to facilitate P53-mediated ferroptosis in an ACSL4-independent manner (Chu et al., 2019), whereas Raf1 kinase inhibitory protein induces activation of ALOX15 and increases the sensitivity of cells to ferroptosis (Anthonymuthu et al., 2018).

Increasing the antioxidant capacity of cells and preventing lipid peroxidation protects cells from ferroptosis. GPX4 was first identified as a mammalian GPX in 1982 (Ursini et al., 1982), and subsequently shown to be a key upstream regulator of ferroptosis in 2014 (Friedmann Angeli et al., 2014; Yang et al., 2014). GPX4 functions to continuously hydrolyze complex lipid hydroperoxides, and GSH serves as an electron donor to constitutively reduce phospholipid hydroperoxides (such as PE-AA-OOH and PE-AdA-OOH) to less oxidative phospholipid alcohols (such as PE-AA-OH and PE-AdA-OH), thus reducing induction of ferroptosis (Ursini et al., 1985). Serving as one of the most important biomarkers of ferroptosis signaling, GPX4 can potentially be targeted pharmacologically or genetically to trigger ferroptotic cell death. Inhibitors, such as RSL3 directly bind and inactivate GPX4 via alkylation of the selenocysteine, and thereby increases lipid peroxidation (Yang et al., 2014). Several ferroptosis-inducing agents (FINs) reduce GPX4 activity without GSH depletion, and the PC-OOH is not reduced, thus inducing ferroptosis (Yang et al., 2014). Moreover, the molecular and metabolic alterations in different cells provides a foundation for understanding the differences in ferroptosis susceptibility, further highlighting other potential exploitable targets for the treatment of cancer. In this regard, studies have used CRISPR-Cas9 screens in GPX4 pharmacologically or genetically attenuated cells, and consequently determined the essential molecules that were potentially responsible for ferroptosis

susceptibility, and these studies reinforced the importance of GPX4 in ferroptotic signaling (Havas et al., 2001; Clapier and Cairns, 2009; Gilbert et al., 2014; Yang et al., 2014).

Two recent studies have concurrently determined and described a novel regulator that confers potent protection against ferroptosis induced by GPX4 depletion, termed ferroptosis suppressor protein 1 (FSP1), which was previously referred to as apoptosis-inducing factor mitochondria associated 2 (Bersuker et al., 2019; Doll et al., 2019). In addition to the GPX4-GSH antioxidant capacity, which functions by converting lipid hydroperoxides into non-toxic lipid alcohols, N-terminal myristoylation recruits FSP1, which functions as a lipophilic radical-trapping antioxidant, to reduce coenzyme Q<sub>10</sub> (CoQ<sub>10</sub>; also known as ubiquinone) to ubiquinol by shuttling reducing equivalents from NAD(P)H into the lipid bilayer, and this consequently inhibits lipid peroxidation and halts ferroptosis. These studies first elaborated the importance of the NADH-FSP1-CoQ<sub>10</sub> pathway in ferroptosis signaling, and highlighted its potential as a target in oncotherapy. In lung cancer cells, FSP1 expression is significantly upregulated, which allows cells to evade ferroptosis. This result highlights the importance of FSP1 in cell protection and as a potential target for inducing ferroptosis as a treatment for cancer (Bersuker et al., 2019; Doll et al., 2019).

Essential genes comprehensively cross-talking with ferroptosis. P53, conventionally emerged and recognized as a tumor suppressor which exerts its biological essence in regulating cell cycle arrest, apoptosis, senescence (Vousden and Prives, 2009; Kasthuber and Lowe, 2017), is now identified as the interest of ferroptosis cascade (Liu and Gu, 2022). By binding to the specific p53 response element in the 5' untranslated region of SLC7A11 and subsequently recruiting chromatin-modifying enzymes, P53 transcriptionally inhibits SLC7A11 and therefore upregulates ferroptosis susceptibility (Brady et al., 2011; Li et al., 2012). ALOX12, which helps to fuel lipid peroxidation by enzymatically facilitating the generation of doubly and triply-oxygenated (15-hydroperoxy)-diacylated PE species during ferroptosis, is also proved a target of P53 (Chu et al., 2019). Moreover, P53-transcriptionally-activated glutaminase 2 (GLS2), promotes cellular antioxidant capacity by increasing GSH production and subsequently regulates ferroptosis (Hu et al., 2010; Bieging et al., 2014; Gao et al., 2015b), while P21, a well-known target of P53, is also claimed to augment cellular GSH (Tarangelo et al., 2018). In mechanical addition, by sequestering dipeptidyl peptidase-4 (DDP4), P53 unleashes NADPH oxidase 1 (NOX1) from plasma membrane and consequently decreases lipid peroxidation (Xie et al., 2017). Further studies aimed at understanding the specific molecular mechanism by which p53 mediates ferroptosis may highlight novel avenues for treatment of cancer, through identification of novel targets.

Nuclear factor erythroid 2-related factor 2 (NRF2), named to initiate antioxidant capacity after being translocated to nucleus, captured its momentous status in ferroptosis signaling due to its comprehensive regulation in iron metabolism and lipid peroxidation (Kerins and Ooi, 2018; Dodson et al., 2019). By transcriptionally upregulating ferroportin1 (FPN1) for iron efflux whilst downregulating ferritin to cut down iron storage, NRF2

impairs ferroptosis fundamentally by means of eliminating iron supply (Harada et al., 2011; Tomiotto-Pellissier et al., 2018). Moreover, important genes involved in glutathione synthesis including glutathione synthetase (GSS), glutamate-cysteine ligase (GCL) and the transporter SLC7A11, are also targeted by NRF2 (Chan and Kwong, 2000; Ishii et al., 2000; Kwak et al., 2002; Sasaki et al., 2002; Yang et al., 2005). Other mechanism by which NRF2 mitigates ferroptosis incorporates upregulation of GPX4, an integral anti-ferroptotic agent as mentioned priorly and impacting on heme oxygenase 1 (HMOX1), to promote ROS production ((Abdalkader et al., 2018; Hassannia et al., 2018; Zou et al., 2019), (Takahashi et al., 2020)). Thus, NRF2 is deemed as a critical factor for ferroptosis due to its uniformed regulation on these vital biological processes and is potentially turned as a target for triggering ferroptosis.

Chromatin accessibility and ROS production. The switching defective/sucrose nonfermenting family (SWI/SNF), equipped with two substantially catalytic ATPase subunits, a helicase-SANT (which contains an N-terminal domain that is bound to actin and a C-terminal bromodomain) induces chromatin remodeling, promotes unfolding and thereby exposes binding sites for transcription factors (Kadoch et al., 2013; Mashtalir et al., 2018). ARID1A, which encodes an important SWI/SNF component, was found to be frequently mutated in several types of cancer, and significantly contributes to tumorigenesis (Kadoch et al., 2013). Recently, ARID1A was shown to be an essential regulator for the maintenance of GSH metabolism in cancer cells. Inhibitors, such as APR-246, PRIMA-1 (which devitalizes cysteine by covalently binding to its residues) and BSO exhibit significantly higher sensitivity in ARID1A-deficient ovarian cancer cells, and thus increase ROS-accumulation-induced cell death. Indeed, cysteine levels are significantly reduced in ARID1A-deficient cells compared with ARID1A-proficient cells, confirming the ability of ARID1A to affect GSH metabolism by regulating the import of cysteine (Ogiwara et al., 2019). Additionally, ARID1A-deficient patient-derived gastric cancer cells are more sensitive to GSH attenuation induced by inhibitors, such as APR-246 and BSO, as well the SLC7A11 inhibitor, erastin (Sasaki et al., 2020). In fact, the expression of SLC7A11 is significantly lower in ARID1A-deficient cells. Mechanistically, combined with BRG1 (the catalytic subunit of the SWI/SNF chromatin remodeling complex), ARID1A exposes the transcription start site of SLC7A11, and colocalizes with the transcription factor NRF2, which consequently triggers the transcription of SLC7A11, and thus increases the import of cysteine for GSH synthesis (Ogiwara et al., 2019). These studies provide a novel perspective into the association between epigenetic regulation and ROS production, which may further improve targeting of ferroptosis for oncotherapy.

Other participants involved in ferroptosis. The RAS family members (HRAS, NRAS and KRAS) are frequently mutated in several types of cancer and potentially activate oncogenic pathways to promote tumorigenesis. Small molecules that are specifically lethal to cells bearing oncogenic mutant RAS expression have been successfully identified (Torrance et al., 2001; Shaw et al., 2011; Weïwer et al., 2012). Two oncogenic



RAS selective lethal (RSL) molecules termed RSL3 and erastin were first isolated in the 2000s, and were later demonstrated to trigger ferroptosis (Dolma et al., 2003; Yang and Stockwell, 2008). However, induction of ferroptosis proceeded in a both Ras-dependent and independent manner, whereas inhibition of the RAS/RAF/MEK/ERK (all of which are members of the MAPK family), results in inhibition of ferroptosis in cancer cells with Ras mutations (Yagoda et al., 2007). However, associations between Ras and ferroptosis signaling remain contested, and thus require further study.

## FERROPTOSIS IN CANCER THERAPY

Implications of ferroptosis inducers in cancer. Plasticity of the cell state enables cancer cells to become resistant to various types of cancer therapies; however, the adapted genetic alterations could unexpectedly and concurrently increase the cancer cells susceptibility to other forms of death, or even induce these forms of cell death more directly. Cancer cells with a mesenchymal phenotype are typically associated with property of metastasis and resistance to cancer therapies, mostly incorporating classical apoptosis-induced manners, across different cancer lineages, and this cell state is specifically characterized by elevated synthesis of polyunsaturated lipids, which, coincidentally, are acquiescent substrates for lipid peroxidation during ferroptosis and therefore converges a dependency on GPX4. Featuring with high mesenchymal phenotypes, cancer cells of melanoma, prostate cancer and sarcomas, which are respectively resistant to the original cancer therapy, show upregulated susceptibility to GPX4-targeted ferroptosis (Hangauer et al., 2017; Viswanathan et al., 2017). These studies demonstrate that cells with significant resistance to other forms of RCD may in fact become selectively more sensitive to ferroptosis. Considering the frequent mutations of SLC7A11 in several types of cancer, triggering ferroptosis for cancer therapy may be a promising approach (Koppula et al., 2018; Combs and DeNicola, 2019).

System  $X_c^-$  is essential for the transport of small molecule nutrients required for maintenance of cell proliferation and survival, which in turn makes system  $X_c^-$  a promising target in oncotherapy (Lu et al., 2017). Erastin, which directly inhibits system  $X_c^-$ , is the most commonly used approach for induction of ferroptosis; however, the poor water solubility and unstable metabolic properties of erastin substantially impair its use clinically (Yang et al., 2014). Efforts have been made to overcome this difficulty; in triple negative breast cancer (TNBC) cells, erastin was encapsulated into exosomes and covered with folate, as folate receptors are extensively present throughout TNBC cells, and using this modified erastin complex, ferroptosis was effectively induced *in vivo* (Yu et al., 2019b). Piperazine erastin, erastin with a piperazine moiety attached to the aniline ring, was shown to possess improved solubility and stability compared with erastin, and displayed improved anti-tumor activity in a xenograft model established using HT-1080 cells (Dixon et al., 2012; Yang et al., 2014). Similarly, an Food and Drug Administration approved drug, sulfasalazine, which is

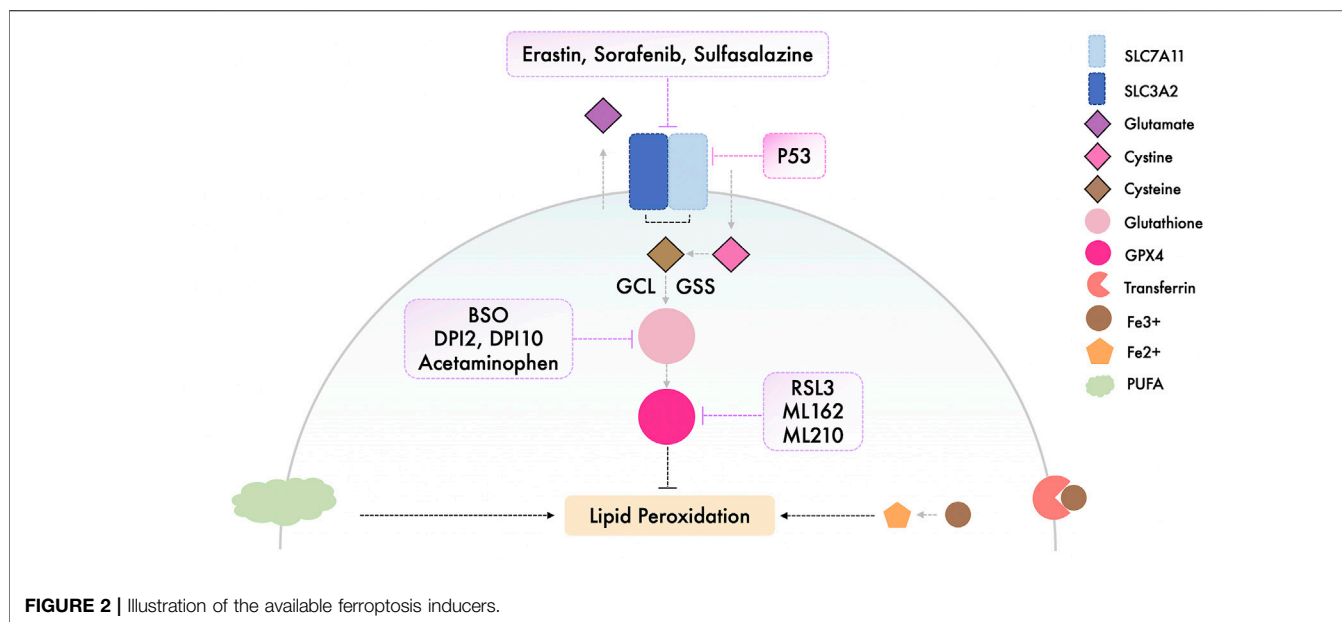
normally used as an anti-inflammatory drug, can inhibit system  $X_c^-$  and trigger ferroptosis in a range of cancer cell lines (Yang et al., 2014; Yu et al., 2019a), whereas sorafenib, a multi-kinase inhibitor, efficaciously induced ferroptotic cell death in hepatocellular carcinoma, and this was pharmacologically rescued by ferroptostatin-1, and genetically suppressed by retinoblastoma protein overexpression (Louandre et al., 2013; Louandre et al., 2015).

Synthesizing cysteine from methionine, which bypasses system  $X_c^-$ , enables cells to evade ferroptosis induced by inhibition of system  $X_c^-$  (Stockwell et al., 2017). Targeting the key regulator - GPX4, has thus become an alternate option to trigger ferroptosis (Gao et al., 2016). RSL3 can target enzymes, such as cysteine and selenocysteine, and directly inactivates GPX4 by alkylating selenocysteine (Yang et al., 2014). Conversely, overexpression of GPX4 counteracts RSL-3 induced ferroptosis in several different cancer cell lines. In addition to RSL3, the class 2 FINs, consisting of other synthetic small molecules, such as ML162 and ML210, impair GPX4 enzymatic activity without attenuating GSH synthesis. The class 1 FINs, such as DPI2 and DPI10, elicit similar mechanisms to that of erastin to functionally prevent GPX4 activity via GSH depletion (Yang et al., 2014; Lei et al., 2020).

Triggering ferroptosis has shown to be an efficient method both *in vivo* and *in vitro* as a method of targeting and killing cancer cells, and these potential inducers should be studied further with regard to their suitability in a clinical setting (Floresan et al., 2019; Hassannia et al., 2019). The currently available inducers of ferroptosis are illustrated and summarized respectively in **Figure 2** and **Table 1**.

Immunotherapy and ferroptosis. Immunogenic apoptosis (IA), which is characterized by the release of damage-associated molecular patterns, such as ATP and chromatin-binding protein high-mobility group B1 (HMGB1) (Apetoh et al., 2007; Michaud et al., 2011; Garg et al., 2012), underline the importance of immune response activation in triggering death of malignant cancer cells (Zhang et al., 2019). Interestingly, it was found that HMGB1 is released during ferroptosis, which is respectively induced by erastin, RSL3, sorafenib and FIN56, in an autophagy-dependent manner (Dixon et al., 2012). This discovery consequently addresses the hypothesis that induction of ferroptosis in cancer cells can potentially trigger the innate immune response. Immunotherapy-activated CD8<sup>+</sup> T cells have been shown to facilitate ferroptosis by enhancing lipid peroxidation in cancer cells, which in-turn increases the anti-tumor efficiency of immunotherapy. The IFN $\gamma$  secreted by CD8<sup>+</sup> T cells downregulates the expression of SLC7A11 and SLC3A2, and therefore attenuates the uptake of cystine by tumor cells, consequently enhancing lipid peroxidation in tumor cells, ultimately increasing ferroptosis (Dolma et al., 2003; Wang et al., 2019). With regard to this mechanism, increasing IFN $\gamma$  levels in the tumor microenvironment appears to be a promising approach to remodel susceptibility of cancer cells to ferroptosis. Combined use of checkpoint immunotherapy and radiotherapy significantly increases Ki67<sup>+</sup>CD8<sup>+</sup> T cell infiltration and concurrently increases expression of the Ataxia-Telangiectasia mutated gene. As a result, IFN $\gamma$  is abundantly secreted in to the



**TABLE 1 |** Summary of the available ferroptosis inducers.

Compounds	Targets	Applied Cells/Animals	Reference
Erastin	VDAC2/3 and System $X_c^-$	BJeLR, HT1080, Calu-1, A-673, Hela, Jurkat T cells, U2PS, DU-145	Chan and Kwong (2000); Yang et al. (2005); Harada et al. (2011); Tomiotto-Pellissier et al. (2018); Dodson et al. (2019)
Piperazine Erastin (PE)	VDAC2/3 and System $X_c^-$	BJeLR, Nude mice	Yang et al. (2005)
Sorafenib	System $X_c^-$	HT1080, Calu-1, DU-145, Huh7, ACHN cells, Nude mice	Chan and Kwong (2000); Kastenhuber and Lowe (2017); Wu et al. (2019); Takahashi et al. (2020)
Sulfasalazine	System $X_c^-$	BJeLR, HT1080, Calu-1, DU-145, MDA-MB-231, BT54, MCF7, T47D	Dodson et al. (2019); Chan and Kwong (2000); Toyokuni et al. (2017)
Buthioninesulfoximine (BSO)	GSH	BJeLR, HTC116, A549	Yang et al. (2005); Chan and Kwong (2000)
Acetaminophen	GSH	HepG2, mouse hepatocytes	Lőrincz et al. (2015); Ishii et al. (2000)
FINs I (DPI2, DPI10)	GSH	BJeLR, HT1080	Yang et al. (2014)
RSL3	GPX4	BJeLR, HT1080, A549, Calu-1, HCT116, MIA PaCa-2, KBM7	Kwak et al. (2002); Sasaki et al. (2002)
FINs II (ML162, ML210)	GPX4	BJeLR, A549	Yang et al. (2014); Lei et al. (2020)

tumor microenvironment, which further promotes ferroptosis (Lang et al., 2019). In addition to apoptosis, ferroptosis provides a novel mechanism by which  $CD8^+$  T cells mediate tumor elimination *in vivo*. These studies suggest that targeting the mechanisms underlying ferroptosis may improve the efficiency of cancer immunotherapy.

## CONCLUSION

Ferroptosis is a more recently discovered form of RCD, that has been implicated as a target for cancer due to its

pharmacologically/genetically accessible characteristics. Significant progress has been made to better exploit ferroptosis, including the development of inducers of death of cancer cells; however, notable challenges remain to be overcome. The machinery underlying ferroptosis is not fully understood; however, targeting the key modulators of this unique signaling method has provided promising efficacy in inducing/inhibiting ferroptotic death. High intracellular levels of redox-active iron ( $Fe^{2+}$ ) is a prerequisite for induction of ferroptosis. In fact, hydroxyl radicals generated by the Fenton reaction are the primary source of ROS facilitating ferroptotic lipid peroxidation. Esterification of carbohydrate based energy

sources, such as PUFAs, is essential for the synthesis of lipid peroxidation substrates, which include AA-PE, Ada-PE and the more recently identified PUFA-ePLs. However, the antioxidant capacity of cells is regulated by GSH-GPX4 and NADH-FSP1-CoQ<sub>10</sub> signaling axis, which efficiently counteracts intracellular lipid peroxidation and thereby prevents ferroptosis. Moreover, P53 and NRF2 are also shown to comprehensively interact with ferroptosis signaling, which consequently exploits candidate targets for management of ferroptotic cascade. Targeting the biological processes described above indeed trigger/attenuate ferroptosis; however, plasticity and heterogeneity of cancer cells enables them to potentially become resistant to ferroptosis. Thus, developing a means of increasing ferroptosis susceptibility alongside the use of ferroptosis inducers may improve the efficacy of the inducers. Interestingly, ferroptosis is found to actively participate in cancer immunotherapy, providing a novel perspective for treatment of cancer by combining the therapeutic approaches for regulating ferroptosis with immunotherapy-based approaches. Moreover,

associations between chromatin accessibility and ROS production may also provide alternative methods for exploitation of ferroptosis clinically. Nevertheless, further studies are required to assess, develop and test these methods.

As the understanding of ferroptosis and its association with several other biological processes increases, targeting ferroptosis in cancer treatment may prove to be a clinically viable method, either alone or as an adjuvant. Studies on ferroptosis in oncotherapy are thus encouraged, and it is considered that an interdisciplinary approach may improve the impact of the studies, and thus the clinical value of the outcomes.

## AUTHOR CONTRIBUTIONS

CQ was in charge of reference collecting and writing the whole essay; YP was dedicated in sorting and organizing the sentences and writing abstract; SL reviewed and revised the whole article.

## REFERENCES

- Abdalkader, M., Lampinen, R., Kanninen, K. M., Malm, T. M., and Liddell, J. R. (2018). Targeting Nrf2 to Suppress Ferroptosis and Mitochondrial Dysfunction in Neurodegeneration. *Front. Neurosci.* 12, 466. doi:10.3389/fnins.2018.00466
- Agmon, E., Solon, J., Bassereau, P., and Stockwell, B. R. (2018). Modeling the Effects of Lipid Peroxidation during Ferroptosis on Membrane Properties. *Sci. Rep.* 8, 5155. doi:10.1038/s41598-018-23408-0
- Angeli, J. P. F., Shah, R., Pratt, D. A., and Conrad, M. (2017). Ferroptosis Inhibition: Mechanisms and Opportunities. *Trends Pharmacological Sciences* 38, 489–498. doi:10.1016/j.tips.2017.02.005
- Anthonymuthu, T. S., Kenny, E. M., Shrivastava, I., Tyurina, Y. Y., Hier, Z. E., Ting, H.-C., et al. (2018). Empowerment of 15-Lipoxygenase Catalytic Competence in Selective Oxidation of Membrane ETE-PE to Ferroptotic Death Signals, HpETE-PE. *J. Am. Chem. Soc.* 140, 17835–17839. doi:10.1021/jacs.8b09913
- Apetoh, L., Ghiringhelli, F., Tesniere, A., Obeid, M., Ortiz, C., Criollo, A., et al. (2007). Toll-like Receptor 4-dependent Contribution of the Immune System to Anticancer Chemotherapy and Radiotherapy. *Nat. Med.* 13, 1050–1059. doi:10.1038/nm1622
- Aruoma, O. I., Grootveld, M., and Bahorun, T. (2006). Free Radicals in Biology and Medicine: from Inflammation to Biotechnology. *BioFactors* 27, 1–3. doi:10.1002/biof.5520270101
- Berghe, T. V., Linkermann, A., Jouan-Lanhuet, S., Walczak, H., and Vandenabeele, P. (2014). Regulated Necrosis: the Expanding Network of Non-apoptotic Cell Death Pathways. *Nat. Rev. Mol. Cell Biol.* 15, 135–147. doi:10.1038/nrm3737
- Bersuker, K., Hendricks, J. M., Li, Z., Magtanong, L., Ford, B., Tang, P. H., et al. (2019). The CoQ Oxidoreductase FSP1 Acts Parallel to GPX4 to Inhibit Ferroptosis. *Nature* 575, 688–692. doi:10.1038/s41586-019-1705-2
- Biegging, K. T., Mello, S. S., and Attardi, L. D. (2014). Unravelling Mechanisms of P53-Mediated Tumour Suppression. *Nat. Rev. Cancer* 14, 359–370. doi:10.1038/nrc3711
- Bogdan, A. R., Miyazawa, M., Hashimoto, K., and Tsuji, Y. (2016). Regulators of Iron Homeostasis: New Players in Metabolism, Cell Death, and Disease. *Trends Biochemical Sciences* 41, 274–286. doi:10.1016/j.tibs.2015.11.012
- Brady, C. A., Jiang, D., Mello, S. S., Johnson, T. M., Jarvis, L. A., Kozak, M. M., et al. (2011). Distinct P53 Transcriptional Programs Dictate Acute DNA-Damage Responses and Tumor Suppression. *Cell* 145, 571–583. doi:10.1016/j.cell.2011.03.035
- Brown, C. W., Amante, J. J., Chhoy, P., Elaimy, A. L., Liu, H., Zhu, L. J., et al. (2019). Prominin2 Drives Ferroptosis Resistance by Stimulating Iron Export. *Dev. Cell* 51, 575–586. doi:10.1016/j.devcel.2019.10.007
- Cao, J. Y., Poddar, A., Magtanong, L., Lumb, J. H., Mileur, T. R., Reid, M. A., et al. (2019). A Genome-wide Haploid Genetic Screen Identifies Regulators of Glutathione Abundance and Ferroptosis Sensitivity. *Cel. Rep.* 26, 1544–1556. doi:10.1016/j.celrep.2019.01.043
- Chan, J. Y., and Kwong, M. (2000). Impaired Expression of Glutathione Synthetic Enzyme Genes in Mice with Targeted Deletion of the Nrf2 Basic-Leucine Zipper Protein. *Biochim. Biophys. Acta (Bba) - Gene Struct. Expr.* 1517 (1), 19–26. doi:10.1016/s0167-4781(00)00238-4
- Cheng, Z., and Li, Y. (2007). What Is Responsible for the Initiating Chemistry of Iron-Mediated Lipid Peroxidation: an Update. *Chem. Rev.* 107, 748–766. doi:10.1021/cr040077w
- Chu, B., Kon, N., Chen, D., Li, T., Liu, T., Jiang, L., et al. (2019). ALOX12 Is Required for P53-Mediated Tumour Suppression through a Distinct Ferroptosis Pathway. *Nat. Cell Biol.* 21, 579–591. doi:10.1038/s41556-019-0305-6
- Clapier, C. R., and Cairns, B. R. (2009). The Biology of Chromatin Remodeling Complexes. *Annu. Rev. Biochem.* 78, 273–304. doi:10.1146/annurev.biochem.77.062706.153223
- Combs, J. A., and DeNicola, G. M. (2019). The Non-essential Amino Acid Cysteine Becomes Essential for Tumor Proliferation and Survival. *Cancers (Basel)* 11, 678. doi:10.3390/cancers11050678
- D'Herde, K., and Krysko, D. V. (2017). Oxidized PEs Trigger Death. *Nat. Chem. Biol.* 13, 4–5. doi:10.1038/nchembio.2261
- Diebold, L., and Chandel, N. S. (2016). Mitochondrial ROS Regulation of Proliferating Cells. *Free Radic. Biol. Med.* 100, 86–93. doi:10.1016/j.freeradbiomed.2016.04.198
- Dixon, S. J., Patel, D. N., Welsch, M., Skouta, R., Lee, E. D., Hayano, M., et al. (2014). Pharmacological Inhibition of Cystine-Glutamate Exchange Induces Endoplasmic Reticulum Stress and Ferroptosis. *eLife* 3, e02523. doi:10.7554/eLife.02523
- Dixon, S. J., Lemberg, K. M., Lamprecht, M. R., Skouta, R., Zaitsev, E. M., Gleason, C. E., et al. (2012). Ferroptosis: an Iron-dependent Form of Nonapoptotic Cell Death. *Cell* 149, 1060–1072. doi:10.1016/j.cell.2012.03.042
- Dixon, S. J., and Stockwell, B. R. (2014). The Role of Iron and Reactive Oxygen Species in Cell Death. *Nat. Chem. Biol.* 10, 9–17. doi:10.1038/nchembio.1416
- Dixon, S. J., Winter, G. E., Musavi, L. S., Lee, E. D., Snijder, B., Rebsamen, M., et al. (2015). Human Haploid Cell Genetics Reveals Roles for Lipid

- Metabolism Genes in Nonapoptotic Cell Death. *ACS Chem. Biol.* 10, 1604–1609. doi:10.1021/acschembio.5b00245
- Dodson, M., Castro-Portuguez, R., and Zhang, D. D. (2019). NRF2 Plays a Critical Role in Mitigating Lipid Peroxidation and Ferroptosis. *Redox Biol.* 23 (17), 101107–101773. doi:10.1016/j.redox.2019.101107
- Doll, S., Freitas, F. P., Shah, R., Aldrovandi, M., da Silva, M. C., Ingold, I., et al. (2019). FSP1 Is a Glutathione-independent Ferroptosis Suppressor. *Nature* 575, 693–698. doi:10.1038/s41586-019-1707-0
- Doll, S., Proneth, B., Tyurina, Y. Y., Panzilius, E., Kobayashi, S., Ingold, I., et al. (2017). ACSL4 Dictates Ferroptosis Sensitivity by Shaping Cellular Lipid Composition. *Nat. Chem. Biol.* 13, 91–98. doi:10.1038/nchembio.2239
- Dolma, S., Lessnick, S. L., Hahn, W. C., and Stockwell, B. R. (2003). Identification of Genotype-Selective Antitumor Agents Using Synthetic Lethal Chemical Screening in Engineered Human Tumor Cells. *Cancer cell* 3, 285–296. doi:10.1016/s1535-6108(03)00050-3
- Emerit, J., and Michelson, A. M. (1982). Free Radicals in Medicine and Biology. *Sem Hop* 58, 2670–2675.
- Floean, C., Song, S., Dicato, M., and Diederich, M. (2019). Redox Biology of Regulated Cell Death in Cancer: A Focus on Necroptosis and Ferroptosis. *Free Radic. Biol. Med.* 134, 177–189. doi:10.1016/j.freeradbiomed.2019.01.008
- Friedmann Angeli, J. P., Schneider, M., Proneth, B., Tyurina, Y. Y., Tyurin, V. A., Hammond, V. J., et al. (2014). Inactivation of the Ferroptosis Regulator Gpx4 Triggers Acute Renal Failure in Mice. *Nat. Cell Biol.* 16, 1180–1191. doi:10.1038/ncb3064
- Galluzzi, L., Vitale, I., Aaronson, S. A., Abrams, J. M., Adam, D., Agostinis, P., et al. (2018). Molecular Mechanisms of Cell Death: Recommendations of the Nomenclature Committee on Cell Death 2018. *Cell Death Differ* 25, 486–541. doi:10.1038/s41418-017-0012-4
- Gammella, E., Recalcati, S., Rybinska, I., Buratti, P., and Cairo, G. (2015). Iron-induced Damage in Cardiomyopathy: Oxidative-dependent and Independent Mechanisms. *Oxid Med. Cell Longev* 2015, 230182. doi:10.1155/2015/230182
- Gao, M., and Jiang, X. (2018). To Eat or Not to Eat - the Metabolic Flavor of Ferroptosis. *Curr. Opin. Cell Biol.* 51, 58–64. doi:10.1016/jceb.2017.11.001
- Gao, M., Monian, P., Pan, Q., Zhang, W., Xiang, J., and Jiang, X. (2016). Ferroptosis Is an Autophagic Cell Death Process. *Cell Res* 26, 1021–1032. doi:10.1038/cr.2016.95
- Gao, M., Monian, P., Quadri, N., Ramasamy, R., and Jiang, X. (2015). Glutaminolysis and Transferrin Regulate Ferroptosis. *Mol. Cell* 59, 298–308. doi:10.1016/j.molcel.2015.06.011
- Gao, M., Monian, P., Quadri, N., Ramasamy, R., and Jiang, X. (2015). Glutaminolysis and Transferrin Regulate Ferroptosis. *Mol. Cell* 59, 298–308. doi:10.1016/j.molcel.2015.06.011
- Garg, A. D., Krysko, D. V., Verfaillie, T., Kaczmarek, A., Ferreira, G. B., Marysaal, T., et al. (2012). A Novel Pathway Combining Calreticulin Exposure and ATP Secretion in Immunogenic Cancer Cell Death. *EMBO J.* 31, 1062–1079. doi:10.1038/emboj.2011.497
- Gaschler, M. M., and Stockwell, B. R. (2017). Lipid Peroxidation in Cell Death. *Biochem. biophysical Res. Commun.* 482, 419–425. doi:10.1016/j.bbrc.2016.10.086
- Gilbert, L. A., Horlbeck, M. A., Adamson, B., Villalta, J. E., Chen, Y., Whitehead, E. H., et al. (2014). Genome-Scale CRISPR-Mediated Control of Gene Repression and Activation. *Cell* 159, 647–661. doi:10.1016/j.cell.2014.09.029
- Goodwin, M. L., Gladden, L. B., Nijsten, M. W., and Jones, K. B. (2014). Lactate and Cancer: Revisiting the Warburg Effect in an Era of Lactate Shuttling. *Front. Nutr.* 27, 27. doi:10.3389/fnut.2014.00027
- Gottesman, M. M., Fojo, T., and Bates, S. E. (2002). Multidrug Resistance in Cancer: Role of ATP-dependent Transporters. *Nat. Rev. Cancer* 2, 48–58. doi:10.1038/nrc706
- Gout, P., Buckley, A., Simms, C., and Bruchovsky, N. (2001). Sulfasalazine, a Potent Suppressor of Lymphoma Growth by Inhibition of the Xc<sup>-</sup> Cystine Transporter: a New Action for an Old Drug. *Leukemia* 15, 1633–1640. doi:10.1038/sj.leu.2402238
- Gwangwa, M. V., Joubert, A. M., and Visagie, M. H. (2018). Crosstalk between the Warburg Effect, Redox Regulation and Autophagy Induction in Tumorigenesis. *Cell Mol Biol Lett* 23, 20. doi:10.1186/s11658-018-0088-y
- Hangauer, M. J., Viswanathan, V. S., Ryan, M. J., Bole, D., Eaton, J. K., Matov, A., et al. (2017). Drug-tolerant Persister Cancer Cells Are Vulnerable to GPX4 Inhibition. *Nature* 551, 247–250. doi:10.1038/nature24297
- Harada, N., Kanayama, M., Maruyama, A., Yoshida, A., Tazumi, K., Hosoya, T., et al. (2011). Nrf2 Regulates Ferroportin 1-mediated Iron Efflux and Counteracts Lipopolysaccharide-Induced Ferroportin 1 mRNA Suppression in Macrophages. *Arch. Biochem. Biophys.* 508 (1), 101–109. doi:10.1016/j.abb.2011.02.001
- Hashidate-Yoshida, T., Harayama, T., Hishikawa, D., Morimoto, R., Hamano, F., Tokuoka, S. M., et al. (2015). Fatty Acid Remodeling by LPCAT3 Enriches Arachidonate in Phospholipid Membranes and Regulates Triglyceride Transport. *eLife* 4, e06328. doi:10.7554/eLife.06328
- Hassannia, B., Vandenabeele, P., and Vanden Berghe, T. (2019). Targeting Ferroptosis to Iron Out Cancer. *Cancer cell* 35, 830–849. doi:10.1016/j.ccell.2019.04.002
- Hassannia, B., Wiernicki, B., Ingold, I., Qu, F., Van Herck, S., Tyurina, Y. Y., et al. (2018). Nano-targeted Induction of Dual Ferroptotic Mechanisms Eradicates High-Risk Neuroblastoma. *J. Clin. Invest.* 128, 3341–3355. doi:10.1172/jci99032
- Havas, K., Whitehouse, I., and Owen-Hughes, T. (2001). ATP-dependent Chromatin Remodeling Activities. *Cmls, Cel. Mol. Life Sci.* 58, 673–682. doi:10.1007/pl00000891
- Honsho, M., and Fujiki, Y. (2017). Plasmalogen Homeostasis - Regulation of Plasmalogen Biosynthesis and its Physiological Consequence in Mammals. *FEBS Lett.* 591, 2720–2729. doi:10.1002/1873-3468.12743
- Hou, W., Xie, Y., Song, X., Sun, X., Lotze, M. T., Zeh, H. J., et al. (2016). Autophagy Promotes Ferroptosis by Degradation of Ferritin. *Autophagy* 12, 1425–1428. doi:10.1080/15548627.2016.1187366
- Hu, W., Zhang, C., Wu, R., Sun, Y., Levine, A., and Feng, Z. (2010). Glutaminase 2, a Novel P53 Target Gene Regulating Energy Metabolism and Antioxidant Function. *Proc. Natl. Acad. Sci. U.S.A.* 107, 7455–7460. doi:10.1073/pnas.1001006107
- Ishii, T., Itoh, K., Takahashi, S., Sato, H., Yanagawa, T., Katoh, Y., et al. (2000). Transcription Factor Nrf2 Coordinately Regulates a Group of Oxidative Stress-Inducible Genes in Macrophages. *J. Biol. Chem.* 275 (21), 16023–16029. doi:10.1074/jbc.275.21.16023
- Kadoch, C., Hargreaves, D. C., Hodges, C., Elias, L., Ho, L., Ranish, J., et al. (2013). Proteomic and Bioinformatic Analysis of Mammalian SWI/SNF Complexes Identifies Extensive Roles in Human Malignancy. *Nat. Genet.* 45, 592–601. doi:10.1038/ng.2628
- Kagan, V. E., Mao, G., Qu, F., Angeli, J. P. F., Doll, S., Croix, C. S., et al. (2017). Oxidized Arachidonic and Adrenic PEs Navigate Cells to Ferroptosis. *Nat. Chem. Biol.* 13, 81–90. doi:10.1038/nchembio.2238
- Kastenhuber, E. R., and Lowe, S. W. (2017). Putting P53 in Context. *Cell* 170, 1062–1078. doi:10.1016/j.cell.2017.08.028
- Kerins, M. J., and Ooi, A. (2018). The Roles of NRF2 in Modulating Cellular Iron Homeostasis. *Antioxid. Redox Signaling* 29 (17), 1756–1773. doi:10.1089/ars.2017.7176
- Koppula, P., Zhang, Y., Zhuang, L., and Gan, B. (2018). Amino Acid Transporter SLC7A11/xCT at the Crossroads of Regulating Redox Homeostasis and Nutrient Dependency of Cancer. *Cancer Commun. (Lond)* 38 (12), 12. doi:10.1186/s40880-018-0288-x
- Kwak, M.-K., Itoh, K., Yamamoto, M., and Kensler, T. W. (2002). Enhanced Expression of the Transcription Factor Nrf2 by Cancer Chemopreventive Agents: Role of Antioxidant Response Element-like Sequences in the Nrf2 Promoter. *Mol. Cell Biol.* 22 (9), 2883–2892. doi:10.1128/mcb.22.9.2883-2892.2002
- Lang, X., Green, M. D., Wang, W., Yu, J., Choi, J. E., Jiang, L., et al. (2019). Radiotherapy and Immunotherapy Promote Tumoral Lipid Oxidation and Ferroptosis via Synergistic Repression of SLC7A11. *Cancer Discov.* 9, 1673–1685. doi:10.1158/2159-8290.cd-19-0338
- Lei, G., Zhang, Y., Koppula, P., Liu, X., Zhang, J., Lin, S. H., et al. (2020). The Role of Ferroptosis in Ionizing Radiation-Induced Cell Death and Tumor Suppression. *Cel Res* 30 (2), 146–162. doi:10.1038/s41422-019-0263-3
- Li, T., Kon, N., Jiang, L., Tan, M., Ludwig, T., Zhao, Y., et al. (2012). Tumor Suppression in the Absence of P53-Mediated Cell-Cycle Arrest, Apoptosis, and Senescence. *Cell* 149, 1269–1283. doi:10.1016/j.cell.2012.04.026
- Lin, L.-S., Song, J., Song, L., Ke, K., Liu, Y., Zhou, Z., et al. (2018). Simultaneous Fenton-like Ion Delivery and Glutathione Depletion by MnO<sub>2</sub>-Based Nanoagent to Enhance Chemodynamic Therapy. *Angew. Chem. Int. Ed.* 57, 4902–4906. doi:10.1002/anie.201712027

- Liu, T., Jiang, L., Tavana, O., and Gu, W. (2019). The Deubiquitylase OTUB1 Mediates Ferroptosis via Stabilization of SLC7A11. *Cancer Res.* 79, 1913–1924. doi:10.1158/0008-5472.can-18-3037
- Liu, Y., and Gu, W. (2022). p53 in Ferroptosis Regulation: the New Weapon for the Old Guardian. *Cel Death Differ.* doi:10.1038/s41418-022-00943-y
- Lőrincz, T., Jemnitz, K., Kardón, T., Mandl, J., and Szarka, A. (2015). Ferroptosis Is Involved in Acetaminophen Induced Cell Death. *Pathol. Oncol. Res.* 21, 1115–1121. doi:10.1007/s12253-015-9946-3
- Louandre, C., Ezzoukhray, Z., Godin, C., Barbare, J.-C., Mazière, J.-C., Chaffert, B., et al. (2013). Iron-dependent Cell Death of Hepatocellular Carcinoma Cells Exposed to Sorafenib. *Int. J. Cancer* 133, 1732–1742. doi:10.1002/ijc.28159
- Louandre, C., Marcq, I., Bouhlal, H., Lachaier, E., Godin, C., Saidak, Z., et al. (2015). The Retinoblastoma (Rb) Protein Regulates Ferroptosis Induced by Sorafenib in Human Hepatocellular Carcinoma Cells. *Cancer Lett.* 356, 971–977. doi:10.1016/j.canlet.2014.11.014
- Lu, B., Chen, X. B., Ying, M. D., He, Q. J., Cao, J., and Yang, B. (2017). The Role of Ferroptosis in Cancer Development and Treatment Response. *Front. Pharmacol.* 8, 992. doi:10.3389/fphar.2017.00992
- Ma, R., Ji, T., Zhang, H., Dong, W., Chen, X., Xu, P., et al. (2018). A Pck1-Directed Glycogen Metabolic Program Regulates Formation and Maintenance of Memory CD8+ T Cells. *Nat. Cell Biol.* 20, 21–27. doi:10.1038/s41556-017-0002-2
- Mashtalir, N., D'Avino, A. R., Michel, B. C., Luo, J., Pan, J., Otto, J. E., et al. (2018). Modular Organization and Assembly of SWI/SNF Family Chromatin Remodeling Complexes. *Cell* 175, 1272–1288. doi:10.1016/j.cell.2018.09.032
- Meister, A. (1983). Selective Modification of Glutathione Metabolism. *Science* 220, 472–477. doi:10.1126/science.6836290
- Michaud, M., Martins, I., Sukkurwala, A. Q., Adjemian, S., Ma, Y., Pellegatti, P., et al. (2011). Autophagy-dependent Anticancer Immune Responses Induced by Chemotherapeutic Agents in Mice. *Science* 334, 1573–1577. doi:10.1126/science.1208347
- Ogiwara, H., Takahashi, K., Sasaki, M., Kuroda, T., Yoshida, H., Watanabe, R., et al. (2019). Targeting the Vulnerability of Glutathione Metabolism in ARID1A-Deficient Cancers. *Cancer cell* 35, 177–190. doi:10.1016/j.ccell.2018.12.009
- Papa, S., Martino, P. L., Capitanio, G., Gaballo, A., De Rasmio, D., Signorile, A., et al. (2012). The Oxidative Phosphorylation System in Mammalian Mitochondria. *Adv. Exp. Med. Biol.* 942, 3–37. doi:10.1007/978-94-007-2869-1\_1
- Sasaki, H., Sato, H., Kuriyama-Matsumura, K., Sato, K., Maebara, K., Wang, H., et al. (2002). Electrophile Response Element-Mediated Induction of the Cystine/glutamate Exchange Transporter Gene Expression. *J. Biol. Chem.* 277 (47), 44765–44771. doi:10.1074/jbc.m208704200
- Sasaki, M., Chiwaki, F., Kuroda, T., Komatsu, M., Matsusaki, K., Kohno, T., et al. (2020). Efficacy of Glutathione Inhibitors for the Treatment of ARID1A-Deficient Diffuse-type Gastric Cancers. *Biochem. biophysical Res. Commun.* 522, 342–347. doi:10.1016/j.bbrc.2019.11.078
- Shaw, A. T., Winslow, M. M., Magendantz, M., Ouyang, C., Dowdle, J., Subramanian, A., et al. (2011). Selective Killing of K-Ras Mutant Cancer Cells by Small Molecule Inducers of Oxidative Stress. *Proc. Natl. Acad. Sci. U.S.A.* 108, 8773–8778. doi:10.1073/pnas.1105941108
- Stockwell, B. R., Friedmann Angeli, J. P., Bayir, H., Bush, A. I., Conrad, M., Dixon, S. J., et al. (2017). Ferroptosis: A Regulated Cell Death Nexus Linking Metabolism, Redox Biology, and Disease. *Cell* 171, 273–285. doi:10.1016/j.cell.2017.09.021
- Sullivan, L. B., and Chandel, N. S. (2014). Mitochondrial Reactive Oxygen Species and Cancer. *Cancer Metab.* 2, 17. doi:10.1186/2049-3002-2-17
- Sun, X., Ou, Z., Xie, M., Kang, R., Fan, Y., Niu, X., et al. (2015). HSPB1 as a Novel Regulator of Ferroptotic Cancer Cell Death. *Oncogene* 34, 5617–5625. doi:10.1038/onc.2015.32
- Takahashi, N., Cho, P., Selfors, L. M., Kuiken, H. J., Kaul, R., Fujiwara, T., et al. (2020). 3D Culture Models with CRISPR Screens Reveal Hyperactive NRF2 as a Prerequisite for Spheroid Formation via Regulation of Proliferation and Ferroptosis. *Mol. Cell* 80 (5), 828–844. doi:10.1016/j.molcel.2020.10.010
- Tarangelo, A., Magtanong, L., Bieling-Rolett, K. T., Li, Y., Ye, J., Attardi, L. D., et al. (2018). p53 Suppresses Metabolic Stress-Induced Ferroptosis in Cancer Cells. *Cel Rep.* 22, 569–575. doi:10.1016/j.celrep.2017.12.077
- Tomiott-Pellissier, F., Alves, D. R., Miranda-Sapla, M. M., de Moraes, S. M., Assolini, J. P., da Silva Bortoleti, B. T., et al. (2018). Caryocar Coriaceum Extracts Exert Leishmanicidal Effect Acting in Promastigote Forms by Apoptosis-like Mechanism and Intracellular Amastigotes by Nrf2/HO-1/ ferritin Dependent Response and Iron Depletion. *Biomed. Pharmacother.* 98, 662–672. doi:10.1016/j.biopha.2017.12.083
- Torrance, C. J., Agrawal, V., Vogelstein, B., and Kinzler, K. W. (2001). Use of Isogenic Human Cancer Cells for High-Throughput Screening and Drug Discovery. *Nat. Biotechnol.* 19, 940–945. doi:10.1038/nbt1001-940
- Toyokuni, S., Ito, F., Yamashita, K., Okazaki, Y., and Akatsuka, S. (2017). Iron and Thiol Redox Signaling in Cancer: An Exquisite Balance to Escape Ferroptosis. *Free Radic. Biol. Med.* 108, 610–626. doi:10.1016/j.freeradbiomed.2017.04.024
- Ursini, F., Maiorino, M., and Gregolin, C. (1985). The Selenoenzyme Phospholipid Hydroperoxide Glutathione Peroxidase. *Biochim. Biophys. Acta (Bba) - Gen. Subjects* 839, 62–70. doi:10.1016/0304-4165(85)90182-5
- Ursini, F., Maiorino, M., Valente, M., Ferri, L., and Gregolin, C. (1982). Purification from Pig Liver of a Protein Which Protects Liposomes and Biomembranes from Peroxidative Degradation and Exhibits Glutathione Peroxidase Activity on Phosphatidylcholine Hydroperoxides. *Biochim. Biophys. Acta (Bba) - Lipids Lipid Metab.* 710, 197–211. doi:10.1016/0005-2760(82)90150-3
- Viswanathan, V. S., Ryan, M. J., Dhruv, H. D., Gill, S., Eichhoff, O. M., Seashore-Ludlow, B., et al. (2017). Dependency of a Therapy-Resistant State of Cancer Cells on a Lipid Peroxidase Pathway. *Nature* 547, 453–457. doi:10.1038/nature23007
- Vousden, K. H., and Prives, C. (2009). Blinded by the Light: The Growing Complexity of P53. *Cell* 137, 413–431. doi:10.1016/j.cell.2009.04.037
- Wang, L., Liu, Y., Du, T., Yang, H., Lei, L., Guo, M., et al. (2020). ATF3 Promotes Erastin-Induced Ferroptosis by Suppressing System Xc-. *Cel Death Differ* 27, 662–675. doi:10.1038/s41418-019-0380-z
- Wang, W., Green, M., Choi, J. E., Gijón, M., Kennedy, P. D., Johnson, J. K., et al. (2019). CD8+ T Cells Regulate Tumour Ferroptosis during Cancer Immunotherapy. *Nature* 569, 270–274. doi:10.1038/s41586-019-1170-y
- Weißer, M., Bittker, J. A., Lewis, T. A., Shimada, K., Yang, W. S., MacPherson, L., et al. (2012). Development of Small-Molecule Probes that Selectively Kill Cells Induced to Express Mutant RAS. *Bioorg. Med. Chem. Lett.* 22, 1822–1826. doi:10.1016/j.bmcl.2011.09.047
- Wu, J., Minikes, A. M., Gao, M., Bian, H., Li, Y., Stockwell, B. R., et al. (2019). Intercellular Interaction Dictates Cancer Cell Ferroptosis via NF2-YAP Signalling. *Nature* 572 (7769), 402–406. doi:10.1038/s41586-019-1426-6
- Xie, Y., Zhu, S., Song, X., Sun, X., Fan, Y., Liu, J., et al. (2017). The Tumor Suppressor P53 Limits Ferroptosis by Blocking DPP4 Activity. *Cel Rep.* 20, 1692–1704. doi:10.1016/j.celrep.2017.07.055
- Yagoda, N., von Rechenberg, M., Zaganjor, E., Bauer, A. J., Yang, W. S., Fridman, D. J., et al. (2007). RAS-RAF-MEK-dependent Oxidative Cell Death Involving Voltage-dependent Anion Channels. *Nature* 447, 864–868. doi:10.1038/nature05859
- Yang, H., Magilnick, N., Lee, C., Kalmaz, D., Ou, X., Chan, J. Y., et al. (2005). Nrf1 and Nrf2 Regulate Rat Glutamate-Cysteine Ligase Catalytic Subunit Transcription Indirectly via NF-Kb and AP-1. *Mol. Cell Biol.* 25 (14), 5933–5946. doi:10.1128/mcb.25.14.5933-5946.2005
- Yang, W. S., Kim, K. J., Gaschler, M. M., Patel, M., Shchepinov, M. S., and Stockwell, B. R. (2016). Peroxidation of Polyunsaturated Fatty Acids by Lipoxygenases Drives Ferroptosis. *Proc. Natl. Acad. Sci. U S A.* 113, E4966–E4975. doi:10.1073/pnas.1603244113
- Yang, W. S., SriRamaratnam, R., Welsch, M. E., Shimada, K., Skouta, R., Viswanathan, V. S., et al. (2014). Regulation of Ferroptotic Cancer Cell Death by GPX4. *Cell* 156, 317–331. doi:10.1016/j.cell.2013.12.010
- Yang, W. S., and Stockwell, B. R. (2008). Synthetic Lethal Screening Identifies Compounds Activating Iron-dependent, Nonapoptotic Cell Death in Oncogenic-RAS-Harboring Cancer Cells. *Chem. Biol.* 15, 234–245. doi:10.1016/j.chembiol.2008.02.010
- Yu, H., Yang, C., Jian, L., Guo, S., Chen, R., Li, K., et al. (2019). Sulfasalazine-induced Ferroptosis in B-reast C-ancer C-ells I-s R-educed by the I-nhibitory E-ffect of E-strogen R-eceptor on the T-ransferrin R-eceptor. *Oncol. Rep.* 42, 826–838. doi:10.3892/or.2019.7189

- Yu, M., Gai, C., Li, Z., Ding, D., Zheng, J., Zhang, W., et al. (2019). Targeted Exosome-encapsulated Erastin Induced Ferroptosis in Triple Negative Breast Cancer Cells. *Cancer Sci.* 110, 3173–3182. doi:10.1111/cas.14181
- Zhang, F., Jia, Y., Zheng, X., Shao, D., Zhao, Y., Wang, Z., et al. (2019). Janus Nanocarrier-Based Co-delivery of Doxorubicin and Berberine Weakens Chemotherapy-Exacerbated Hepatocellular Carcinoma Recurrence. *Acta Biomater.* 100, 352–364. doi:10.1016/j.actbio.2019.09.034
- Zhang, Y., Shi, J., Liu, X., Feng, L., Gong, Z., Koppula, P., et al. (2018). BAP1 Links Metabolic Regulation of Ferroptosis to Tumour Suppression. *Nat. Cell Biol.* 20, 1181–1192. doi:10.1038/s41556-018-0178-0
- Zou, Y., Henry, W. S., Ricq, E. L., Graham, E. T., Phadnis, V. V., Maretich, P., et al. (2020). Plasticity of Ether Lipids Promotes Ferroptosis Susceptibility and Evasion. *Nature* 585, 603–608. doi:10.1038/s41586-020-2732-8
- Zou, Y., Palte, M. J., Deik, A. A., Li, H., Eaton, J. K., Wang, W., et al. (2019). A GPX4-dependent Cancer Cell State Underlies the clear-cell Morphology and Confers Sensitivity to Ferroptosis. *Nat. Commun.* 10, 1617. doi:10.1038/s41467-019-09277-9

**Conflict of Interest:** The authors declare that the research was conducted in the absence of any commercial or financial relationships that could be construed as a potential conflict of interest.

**Publisher's Note:** All claims expressed in this article are solely those of the authors and do not necessarily represent those of their affiliated organizations, or those of the publisher, the editors, and the reviewers. Any product that may be evaluated in this article, or claim that may be made by its manufacturer, is not guaranteed or endorsed by the publisher.

Copyright © 2022 Qu, Peng and Liu. This is an open-access article distributed under the terms of the Creative Commons Attribution License (CC BY). The use, distribution or reproduction in other forums is permitted, provided the original author(s) and the copyright owner(s) are credited and that the original publication in this journal is cited, in accordance with accepted academic practice. No use, distribution or reproduction is permitted which does not comply with these terms.





# Post-Translational Modification of GPX4 is a Promising Target for Treating Ferroptosis-Related Diseases

Can Cui<sup>1</sup>, Fei Yang<sup>2,3</sup> and Qian Li<sup>2,4,5\*</sup>

<sup>1</sup>School of Basic Medical Sciences, Capital Medical University, Beijing, China, <sup>2</sup>Advanced Innovation Center for Human Brain Protection, Beijing Key Laboratory of Neural Regeneration and Repair, Capital Medical University, Beijing, China, <sup>3</sup>Department of Neurobiology, School of Basic Medical Sciences, Capital Medical University, Beijing, China, <sup>4</sup>Department of Biochemistry and Molecular Biology, School of Basic Medical Sciences, Capital Medical University, Beijing, China, <sup>5</sup>Beijing Key Laboratory of Cancer Invasion and Metastasis Research, Capital Medical University, Beijing, China

## OPEN ACCESS

### Edited by:

Xin Wang,  
National Institutes of Health (NIH),  
United States

### Reviewed by:

Yanqing Liu,  
Columbia University, United States  
Marina Ayres Pereira,  
Columbia University, United States

### \*Correspondence:

Qian Li  
qianli@ccmu.edu.cn

### Specialty section:

This article was submitted to  
Molecular Diagnostics and  
Therapeutics,  
a section of the journal  
Frontiers in Molecular Biosciences

**Received:** 22 March 2022

**Accepted:** 28 April 2022

**Published:** 12 May 2022

### Citation:

Cui C, Yang F and Li Q (2022) Post-Translational Modification of GPX4 is a Promising Target for Treating Ferroptosis-Related Diseases. *Front. Mol. Biosci.* 9:901565. doi: 10.3389/fmolb.2022.901565

Glutathione peroxidase 4 (GPX4) is one of the most important antioxidant enzymes. As the key regulator of ferroptosis, GPX4 has attracted considerable attention in the fields of cancer, cardiovascular, and neuroscience research in the past 10 years. How to regulate GPX4 activity has become a hot topic nowadays. GPX4 protein level is regulated transcriptionally by transcription factor SP2 or Nrf2. GPX4 activity can be upregulated by supplementing intracellular selenium or glutathione, and also be inhibited by ferroptosis inducers such as ML162 and RSL3. These regulatory mechanisms of GPX4 level/activity have already shown a great potential for treating ferroptosis-related diseases in preclinical studies, especially in cancer cells. Until recently, research show that GPX4 can undergo post-translational modifications (PTMs), such as ubiquitination, succination, phosphorylation, and glycosylation. PTMs of GPX4 affect the protein level/activity of GPX4, indicating that modifying these processes can be a potential therapy for treating ferroptosis-related diseases. This article summarizes the protein characteristics, enzyme properties, and PTMs of GPX4. It also provides a hypothetical idea for treating ferroptosis-related diseases by targeting the PTMs of GPX4.

**Keywords:** ferroptosis, post-translational modifications, cancer, enzyme, GPX4

## INTRODUCTION

In 1982, a new glutathione peroxidase was first isolated from the pig liver (Ursini et al., 1982). Unlike previously discovered glutathione peroxidase 1-3 (GPX1-3), this new enzyme, phospholipid hydroperoxide glutathione peroxidase (PHGPX), acts directly on peroxidized phospholipids in the membrane. GPX1-3 are tetramers that mainly reduce H<sub>2</sub>O<sub>2</sub> and fatty acid hydroperoxide (Gladyshev and Hatfield, 1999; Olson et al., 2010), whereas PHGPX is a monomeric protein and reduces lipid hydroperoxides specifically (Schuckelt et al., 1991). Later, PHGPX was renamed glutathione peroxidase 4 (GPX4) (Nam et al., 1998). Until 2014, GPX4 was identified as the central regulator of ferroptosis, which is an iron-dependent, non-apoptotic, programmed necroptotic cell death form (Dixon et al., 2012). How to regulate the protein level of GPX4 and its activity has become a hot topic to discover the potential treatment of ferroptosis-related diseases recently.

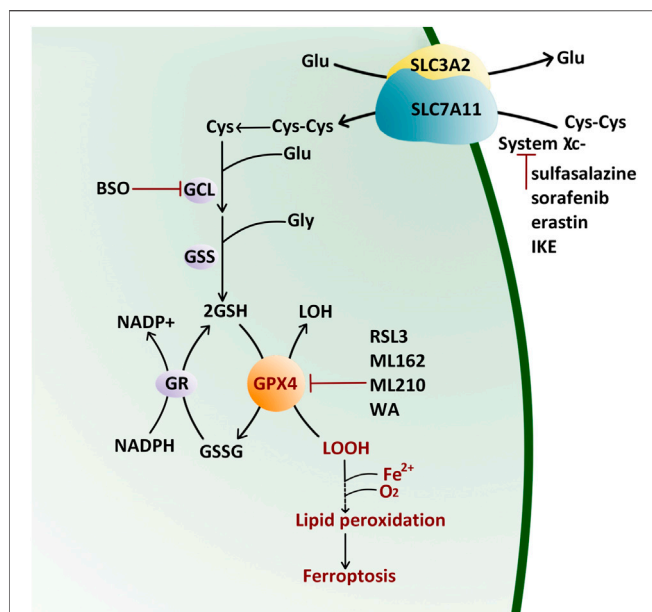


**FIGURE 1 |** Antioxidant Reaction of GPX4 by the Ping-Pong Pattern. GPX4 reduces lipid hydroperoxide (LOOH) to alcohol (LOH) and then supplements its active site residues through glutathione (GSH) which is synthesized from cystine (Cys-Cys) pumped by the (system  $\chi_c^-$ ). Glu: glutamate; Gly: glycine; GCL: glutamate-cysteine ligase; GSS: glutathione synthetase; BSO: L-buthionine sulfoximine; GR: glutathione reductase; NADP: nicotinamide adenine dinucleotide phosphate; GSSG: oxidized glutathione; IKE: imidazole ketone erastin; RSL3: Ras-selective lethal small molecule three; WA: withaferin A.

## ENZYME PROPERTIES OF GPX4 AND ITS ROLE IN CANCER THERAPIES

The selenoprotein GPX4 has high antioxidant activity. It directly reduces phospholipid hydroperoxide through a conserved catalytic triad of selenocysteine 46, asparagine 81, and tryptophane 136 (Maiorino et al., 1995). The reaction kinetics of GPX4 is described as a Ping-Pong pattern that is embodied in two phases (Takebe et al., 2002) (**Figure 1**). Firstly, the peroxide is reduced through the active site selenocysteine 46 and then converted to the oxidized form (selenenic acid derivative). The second stage is to recharge the oxidized catalytic site via glutathione (GSH) (Takebe et al., 2002). The content of GSH and nicotinamide adenine dinucleotide phosphate (NADPH) directly affect the GPX4 activity.

Cystine/glutamate transporter (system  $\chi_c^-$ ) on the cell membrane, composed of a catalytic subunit SLC7A11 and a chaperone subunit SLC3A2, pumps cystine from extracellular into cells for GSH biosynthesis (Bannai, 1986; Sato et al., 1999). Therefore, classic ferroptosis inducers (FINs) are divided into two classes (**Figure 1**): class I FIN such as sorafenib (Louandre et al., 2013), sulfasalazine (Gout et al., 2001), erastin (Dixon et al., 2012) and its analog imidazole ketone erastin (IKE) (Zhang et al., 2019), can block the GSH synthesis through inhibiting system  $\chi_c^-$ , and then reduce the GPX4 enzyme activity by GSH depletion; class II FIN such as Ras-selective lethal small molecule 3 (RSL3) (Yang

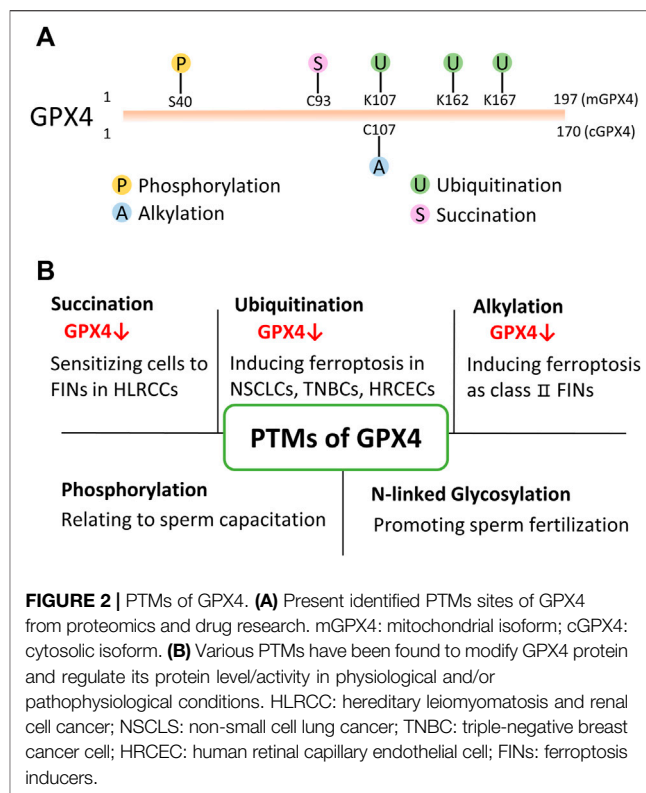


**FIGURE 2 |** PTMs of GPX4. (A) Present identified PTMs sites of GPX4 from proteomics and drug research. mGPX4: mitochondrial isoform; cGPX4: cytosolic isoform. (B) Various PTMs have been found to modify GPX4 protein and regulate its protein level/activity in physiological and/or pathophysiological conditions. HLRCC: hereditary leiomyomatosis and renal cell cancer; NSCLC: non-small cell lung cancer; TNBC: triple-negative breast cancer cell; HRCEC: human retinal capillary endothelial cell; FINs: ferroptosis inducers.

and Stockwell, 2008), ML162 (Weiwier et al., 2012), and ML210 (Eaton et al., 2020), can directly inhibit GPX4 activity. They eventually lead to the accumulation of lipid peroxides without the reduction of GSH (Yang et al., 2014). Apart from these two types of FINs, other methods or compounds can also induce ferroptosis (**Figure 1**): L-buthionine sulfoximine (BSO) suppresses glutamate-cysteine ligase (GCL) and induces GSH depletion (Seiler et al., 2008; Sun et al., 2018), driving cells to ferroptosis; Cystine starvation leads to glutamate accumulation, GSH biosynthesis reduction, and GPX4 translation blockage, therefore sensitizing cancer cells to ferroptosis (Zhang Y. et al., 2021). FINs and other compounds that cause ferroptosis drive tumor cell death, sensitizing cancer cells to radiotherapy and chemotherapy in prostate cancer (Li et al., 2021), colorectal cancer (Sui et al., 2018), osteosarcoma (Liu and Wang, 2019), and leukemia (Yu et al., 2015). Therefore, traditional chemotherapy/radiotherapy combined with FINs treatment is beneficial to reverse multidrug resistance.

## POST-TRANSLATIONAL MODIFICATIONS OF GPX4 IN CANCER CELLS

Besides small molecular compounds like FINs, post-translational modifications (PTMs) also provide an emerging perspective to regulate its protein level/activity (**Figure 2**). Thus, studying and targeting PTMs of GPX4 has a great potential to treat cancers in the future.

## Succination of GPX4

Succination was discovered in 2006 as a non-enzymatic, irreversible protein modification (Alderson et al., 2006). This post-translational modification is mediated by fumarate. Fumarate is an intermediate of the Krebs cycle in mitochondria. It binds to the sulfhydryl group of the cysteine residue and forms a thioether bond in the absence of an enzyme (Blatnik et al., 2008; Manuel and Frizzell, 2013). An elegant study showed that intracellular fumarate aggregation led to the succination of GPX4 at cysteine 93 (mono- and disuccination), which significantly reduced the enzymatic activity of GPX4 and sensitized cancer cells to FINs (Kerins et al., 2018). In addition, fumarate hydratase (FH)-inactivated cells were shown to be synthetic lethal with FINs (Kerins et al., 2018). This study suggests that targeting PTMs of GPX4 is a promising therapeutic strategy for ferroptosis-related diseases for the first time.

## Ubiquitination of GPX4

Ubiquitination is a reversible process in which the ubiquitin is added to lysine residue(s) of the substrate protein by three different types of enzymes, E1, E2, and E3. The process of ubiquitination ultimately renders proteins to degradation by the proteasome thereby affecting intracellular protein levels (Popovic et al., 2014). On the other hand, deubiquitinases (DUBs) remove ubiquitin chains from ubiquitinated proteins (Ronau et al., 2016). E3 ligase and DUB are both having substrate specificity.

Proteomic analyses reveal that GPX4 could be ubiquitinated at lysine 107, 162, and 167 (Wagner et al., 2011; Akimov et al., 2018). However, those hypothetically ubiquitinated residues have not been verified in bench works. Whereas, a study showed that when treating non-small cell lung cancer cells with the DUB inhibitor, pyridinium sulfur palladium complex (PdPT), GPX4 was ubiquitinated and degraded (Yang et al., 2020). Subsequently, cancer cell growth was restrained by inducing GPX4-dependent ferroptosis (Yang et al., 2020). Later, another study showed that a Parthenolide (PTL)-derived drug DMOCPYL directly bound to the GPX4 active site (selenocysteine 46), and led to GPX4 ubiquitination in triple-negative breast cancer cells (Ding et al., 2021). Unfortunately, the above-mentioned studies did not reveal the ubiquitinated residue(s) of GPX4.

Discovering the E3 ligase is also very important for understanding the regulatory mechanisms of protein ubiquitination. A very recent study discovered that the E3 motif-containing 46 (TRIM46) might be one of the E3 ligases of GPX4 in human retinal capillary endothelial cells with high glucose treatment (Zhang J. et al., 2021). Whether GPX4 has other E3 ligases is needed further investigation. These findings indicate that GPX4 can be ubiquitinated under certain circumstances. Importantly, treating cells with PdPT, DMOCPYL, or other similar compounds could potentially kill cancer cells by inducing ferroptosis.

## Alkylation of GPX4

Alkylation is a chemical process of introducing one or more alkyl groups into a protein or a compound. An alkyl group is an alkane

molecule that is missing a hydrogen atom. For example, methyl groups are the simplest alkyl and are added to various proteins including core histones (Chen et al., 1999; Strahl et al., 1999). Previous studies have shown several class II FINs such as RSL3 (Yang and Stockwell, 2008) and ML162 (Weiwier et al., 2012) exerted covalent inhibition activity. These class II FINs bound to selenocysteine 46 residue of GPX4 via an electrophilic alkyl chloride moiety, mediating alkylation on GPX4 (Eaton et al., 2020; Vučković et al., 2020). Besides selenocysteine 46, GPX4 contains several cysteine residues which are also nucleophilic sites. A report showed that GPX4 was most likely alkylated at cysteine 107 with the addition of withaferin A (Grossman et al., 2017). In addition, the alkylation of GPX4 resulted in ferroptosis in high-risk neuroblastoma (Hassannia et al., 2017). However, Hassaniia et al did not further investigate the specifically modified residue(s) of GPX4 or which kind(s) of alkylation occurs on GPX4.

## POST-TRANSLATIONAL MODIFICATIONS OF GPX4 IN OTHER CONDITIONS

### Phosphorylation of GPX4 is Involved in Sperm Maturation

Phosphorylation is one of the most common PTMs involved in the regulation of protein stability and activity. It occurs on serine, tyrosine, and threonine residues of target proteins and is regulated by protein kinases and phosphatases (Olsen et al., 2006). Phosphorylation of GPX4 has been found in the pig heart (Brigelius-Flohé et al., 1994), golden hamster's sperms (Nagdas et al., 2005), and rat testicles (Lundby et al., 2012). Notably, the mature testicle is the organ with the highest GPX4 activity in mammals (Vernet et al., 2004), and sperm express high levels of GPX4 (Nam et al., 1998). Studies showed that GPX4 lost its enzyme activity during the differentiation and maturation of sperm (Ursini et al., 1999). Meanwhile, the phosphorylation of GPX4 on tyrosine has been found in capacitated sperm of the golden hamster (Nagdas et al., 2005). Several proteomic analyses also revealed that human GPX4 might be phosphorylated at serine 40 (Mertins et al., 2014; Mertins et al., 2016). These data indicate that phosphorylation of GPX4 participates in the GPX4 activity regulation. However, the exact phosphorylated residues, the corresponding phosphatases, and the biological effects of phosphorylation on GPX4 need to be further investigated.

### N-Linked Glycosylation of GPX4 is Related to the Fertilization of Sperm

Glycosylation (N-linked and O-linked) is under the reaction of glycosyltransferases (Reily et al., 2019). Protein glycosylation affects protein stability and folding (Molinari, 2007) and leads to changes in protein function. GPX4 has been identified as a membrane glycoprotein in an N-linked glycoproteome study in human sperm. The modification site was at the asparagine residue of GPX4 (Wang et al., 2013). In addition, deglycosylation treatment was also found to significantly decrease sperm fertilization rate (Wang et al., 2013). This study suggests that

N-linked glycosylation plays an important role in modifying membrane GPX4 activity and enables sperm to exert their normal fertilization functions.

## SUMOylation of GPX4 Might Mediate Lipid Peroxidation Inhibition

In addition to phosphorylation and glycosylation, SUMOylation is also predicted to occur on GPX4. SUMOylation is a small ubiquitin-like modifier (SUMO) connected to the substrate protein through a tertiary enzymatic reaction (Tatham et al., 2001). It often modifies lysine residues of substrate proteins (Tatham et al., 2001). SUMOylation regulates the protein-protein interactions, mediates the function and localization of substrate proteins, and increases protein stability (Ouyang et al., 2009; Li et al., 2016; Han et al., 2018). A study using software resources (SUMOplot) for bioinformatics analysis predicted that the residues of GPX4 most likely to be modified by SUMO were lysine 74, 106, and 125 (Sheng et al., 2021). The cationic region of GPX4, including lysine 125, has the potential to interact with the phospholipid bilayer. Then the redox-active center of GPX4 was directed to the H<sub>2</sub>O<sub>2</sub> group in the phospholipid fatty acid chain, resulting in the inhibition of lipid peroxidation of the cell membrane *in silico* (Cozza et al., 2017; Sheng et al., 2021).

Since GPX4 is a core regulator of ferroptosis, although it is unknown whether the phosphorylation, glycosylation or SUMOylation of GPX4 affect ferroptosis, it would be of interest to investigate it in future translational studies.

## DISCUSSION AND FUTURE DIRECTION

PTMs are an important regulator of protein level and activity with huge potential in translational and clinical research. For instance, S-farnesylation is one of the post-translational protein lipid modifications (Nagase et al., 1997; Berndt et al., 2011). Hutchinson–Gilford progeria syndrome (HGPS) is a genetic rare disease caused by progerin formation due to a deficiency of removing a farnesylcysteine-containing peptide from prelamin A (Eriksson et al., 2003). Consequently, prelamin A turned into farnesylated and non-functional progerin instead of lamin A (Young et al., 2005). However, progerin was identified to be the critical target of farnesyltransferase inhibitors (FTIs) (Yang et al., 2010) and one FTI called lonafarnib have been tested in a cohort study which showed a significantly lower mortality rate (hazard ratio, 0.12) after a median of 2.2 years of follow-up (Gordon et al., 2018). S-palmitoylation is also an important PTM in many oncoproteins such as RAS-family GTPases (Dekker et al., 2010) and epidermal growth factor receptor (EGFR) and

tumor suppressors such as melanocortin one receptor (MRC1) (Chen et al., 2017), which serves as an important target pathway to inhibit tumor growth and prevent tumorigenesis (Hernandez et al., 2017). Inducing palmitoylation in MRC1 variant individuals can lower their risk to develop melanoma (Chen et al., 2017). Targeting inhibition of palmitoylation has also shown sensitization to gefitinib in cancer cells (Bollu et al., 2015).

The investigation of the GPX4 function was far ahead of the emergence of ferroptosis. A variety of PTMs of GPX4 has been observed in both physiological and pathophysiological conditions. Targeting PTMs of GPX4 could be a promising strategy for treating diseases, including ferroptosis-related diseases such as cancers, neurodegenerative disorders, and ischemic-reperfusion diseases as well as other important players in ferroptosis (Wei et al., 2020). However, in contrast to other proteins, such as TP53 (Liu et al., 2019), studies on PTMs of GPX4 have only just started. At this point, we believe it is important to explore several aspects in future studies, such as to discover whether some of the PTMs summarized above affect GPX4 activity in bench works and GPX4 dysfunction-relative diseases. What are the corresponding enzymes of the above-mentioned PTMs? If other PTMs, such as methylation, lipoylation, or newly identified lactation also modify GPX4 protein? Since ferroptosis is an important cell death form in various conditions, and GPX4 is its core regulator, more in-depth studies are urgently needed to assist GPX4-based clinical therapeutic strategies for tumor killing and neuronal protection.

## AUTHOR CONTRIBUTIONS

Writing-original draft: CC and QL. Writing-review and editing: CC, FY, and QL. All authors have agreed on the final version to be published.

## FUNDING

This work was supported by the National Natural Science Foundation of China (32070735 to QL, 81971037 to FY), the Beijing Natural Science Foundation Program and Scientific Research Key Program of Beijing Municipal Commission of Education (KZ202010025033 to QL, KZ201910025026 to FY).

## ACKNOWLEDGMENTS

We thank Wenten Yi (Beijing University of Aeronautics and Astronautics) for his figure drafting assistance.

## REFERENCES

- Akimov, V., Barrio-Hernandez, I., Hansen, S. V. F., Hallenborg, P., Pedersen, A.-K., Bekker-Jensen, D. B., et al. (2018). UbiSite Approach for Comprehensive Mapping of Lysine and N-Terminal Ubiquitination Sites. *Nat. Struct. Mol. Biol.* 25 (7), 631–640. doi:10.1038/s41594-018-0084-y
- Alderson, N. L., Wang, Y., Blatnik, M., Frizzell, N., Walla, M. D., Lyons, T. J., et al. (2006). S-(2-Succinyl)cysteine: a Novel Chemical Modification of Tissue Proteins by a Krebs Cycle Intermediate. *Archives Biochem. Biophysics* 450 (1), 1–8. doi:10.1016/j.abb.2006.03.005
- Bannai, S. (1986). Exchange of Cystine and Glutamate across Plasma Membrane of Human Fibroblasts. *J. Biol. Chem.* 261 (5), 2256–2263. doi:10.1016/s0021-9258(17)35926-4



- Berndt, N., Hamilton, A. D., and Sebti, S. M. (2011). Targeting Protein Prenylation for Cancer Therapy. *Nat. Rev. Cancer* 11 (11), 775–791. doi:10.1038/nrc3151
- Blatnik, M., Thorpe, S. R., and Baynes, J. W. (2008). Succination of Proteins by Fumarate. *Ann. N. Y. Acad. Sci.* 1126, 272–275. doi:10.1196/annals.1433.047
- Bollu, L. R., Katreddy, R. R., Blessing, A. M., Pham, N., Zheng, B., Wu, X., et al. (2015). Intracellular Activation of EGFR by Fatty Acid Synthase Dependent Palmitoylation. *Oncotarget* 6 (33), 34992–35003. doi:10.18632/oncotarget.5252
- Brigelius-Flohé, R., Aumann, K. D., Blöcker, H., Gross, G., Kiess, M., Klöppel, K. D., et al. (1994). Phospholipid-hydroperoxide Glutathione Peroxidase. Genomic DNA, cDNA, and Deduced Amino Acid Sequence. *J. Biol. Chem.* 269 (10), 7342–7348.
- Chen, D., Ma, H., Hong, H., Koh, S. S., Huang, S.-M., Schurter, B. T., et al. (1999). Regulation of Transcription by a Protein Methyltransferase. *Science* 284 (5423), 2174–2177. doi:10.1126/science.284.5423.2174
- Chen, S., Zhu, B., Yin, C., Liu, W., Han, C., Chen, B., et al. (2017). Palmitoylation-dependent Activation of MC1R Prevents Melanomagenesis. *Nature* 549 (7672), 399–403. doi:10.1038/nature23887
- Cozza, G., Rossetto, M., Bosello-Travain, V., Maiorino, M., Roveri, A., Toppo, S., et al. (2017). Glutathione Peroxidase 4-catalyzed Reduction of Lipid Hydroperoxides in Membranes: The Polar Head of Membrane Phospholipids Binds the Enzyme and Addresses the Fatty Acid Hydroperoxide Group toward the Redox Center. *Free Radic. Biol. Med.* 112, 1–11. doi:10.1016/j.freeradbiomed.2017.07.010
- Dekker, F. J., Rocks, O., Vartak, N., Menninger, S., Hedberg, C., Balamurugan, R., et al. (2010). Small-molecule Inhibition of APT1 Affects Ras Localization and Signaling. *Nat. Chem. Biol.* 6 (6), 449–456. doi:10.1038/nchembio.362
- Ding, Y., Chen, X., Liu, C., Ge, W., Wang, Q., Hao, X., et al. (2021). Identification of a Small Molecule as Inducer of Ferroptosis and Apoptosis through Ubiquitination of GPX4 in Triple Negative Breast Cancer Cells. *J. Hematol. Oncol.* 14 (1), 19. doi:10.1186/s13045-020-01016-8
- Dixon, S. J., Lemberg, K. M., Lamprecht, M. R., Skouta, R., Zaitsev, E. M., Gleason, C. E., et al. (2012). Ferroptosis: an Iron-dependent Form of Nonapoptotic Cell Death. *Cell* 149 (5), 1060–1072. doi:10.1016/j.cell.2012.03.042
- Eaton, J. K., Furst, L., Ruberto, R. A., Moosmayer, D., Hilpmann, A., Ryan, M. J., et al. (2020). Selective Covalent Targeting of GPX4 Using Masked Nitrile-Oxide Electrophiles. *Nat. Chem. Biol.* 16 (5), 497–506. doi:10.1038/s41589-020-0501-5
- Eriksson, M., Brown, W. T., Gordon, L. B., Glynn, M. W., Singer, J., Scott, L., et al. (2003). Recurrent De Novo Point Mutations in Lamin A Cause Hutchinsonin-Gilford Progeria Syndrome. *Nature* 423 (6937), 293–298. doi:10.1038/nature01629
- Gladyshev, V. N., and Hatfield, D. L. (1999). Selenocysteine-containing Proteins in Mammals. *J. Biomed. Sci.* 6 (3), 151–160. doi:10.1007/bf02255899
- Gordon, L. B., Shappell, H., Massaro, J., D'Agostino, R. B., Brazier, C., Campbell, S. E., et al. (2018). Association of Lonafarnib Treatment vs No Treatment with Mortality Rate in Patients with Hutchinsonin-Gilford Progeria Syndrome. *Jama* 319 (16), 1687–1695. doi:10.1001/jama.2018.3264
- Gout, P., Buckley, A., Simms, C., and Bruchovsky, N. (2001). Sulfasalazine, a Potent Suppressor of Lymphoma Growth by Inhibition of the Xc<sup>-</sup> Cystine Transporter: a New Action for an Old Drug. *Leukemia* 15 (10), 1633–1640. doi:10.1038/sj.leu.2402238
- Grossman, E. A., Ward, C. C., Spradlin, J. N., Bateman, L. A., Huffman, T. R., Miyamoto, D. K., et al. (2017). Covalent Ligand Discovery against Druggable Hotspots Targeted by Anti-cancer Natural Products. *Cell Chem. Biol.* 24 (11), 1368–1376. doi:10.1016/j.chembiol.2017.08.013
- Han, Z.-J., Feng, Y.-H., Gu, B.-H., Li, Y.-M., and Chen, H. (2018). The Post-translational Modification, SUMOylation, and Cancer (Review). *Int. J. Oncol.* 52 (4), 1081–1094. doi:10.3892/ijo.2018.4280
- Hassannia, B., Wiernicki, B., Ingold, I., Qu, F., Van Herck, S., Tyurina, Y. Y., et al. (2018). Nano-Targeted Induction of Dual Ferroptotic Mechanisms Eradicates High-Risk Neuroblastoma. *J. Clin. Invest* 128 (8), 3341–3355. doi:10.1172/jci99032
- Hernandez, J. L., Davda, D., Cheung See Kit, M., Majmudar, J. D., Won, S. J., Gang, M., et al. (2017). APT2 Inhibition Restores Scribble Localization and S-Palmitoylation in Snail-Transformed Cells. *Cell Chem. Biol.* 24 (1), 87–97. doi:10.1016/j.chembiol.2016.12.007
- Kerins, M. J., Milligan, J., Wohlschlegel, J. A., and Ooi, A. (2018). Fumarate Hydratase Inactivation in Hereditary Leiomyomatosis and Renal Cell Cancer Is Synthetic Lethal with Ferroptosis Induction. *Cancer Sci.* 109 (9), 2757–2766. doi:10.1111/cas.13701
- Li, M., Chen, X., Wang, X., Wei, X., Wang, D., Liu, X., et al. (2021). RSL3 Enhances the Antitumor Effect of Cisplatin on Prostate Cancer Cells via Causing Glycolysis Dysfunction. *Biochem. Pharmacol.* 192, 114741. doi:10.1016/j.bcp.2021.114741
- Li, S., Wang, M., Qu, X., Xu, Z., Yang, Y., Su, Q., et al. (2016). SUMOylation of PES1 Upregulates its Stability and Function via Inhibiting its Ubiquitination. *Oncotarget* 7 (31), 50522–50534. doi:10.18632/oncotarget.10494
- Liu, Q., and Wang, K. (2019). The Induction of Ferroptosis by Impairing STAT3/Nrf2/GPX4 Signaling Enhances the Sensitivity of Osteosarcoma Cells to Cisplatin. *Cell Biol. Int.* 43 (11), 1245–1256. doi:10.1002/cbin.11121
- Liu, Y., Tavana, O., and Gu, W. (2019). p53 Modifications: Exquisite Decorations of the Powerful Guardian. *J. Mol. Cell Biol.* 11 (7), 564–577. doi:10.1093/jmcb/mjz060
- Louandre, C., Ezzoukhry, Z., Godin, C., Barbare, J.-C., Mazière, J.-C., Chauffert, B., et al. (2013). Iron-dependent Cell Death of Hepatocellular Carcinoma Cells Exposed to Sorafenib. *Int. J. Cancer* 133 (7), 1732–1742. doi:10.1002/ijc.28159
- Lundby, A., Secher, A., Lage, K., Nordsborg, N. B., Dmytriiev, A., Lundby, C., et al. (2012). Quantitative Maps of Protein Phosphorylation Sites across 14 Different Rat Organs and Tissues. *Nat. Commun.* 3, 876. doi:10.1038/ncomms1871
- Maiorino, M., Aumann, K.-D., Brigelius-Flohé, R., Doria, D., van den Heuvel, J., McCarthy, J., et al. (1995). Probing the Presumed Catalytic Triad of Selenium-Containing Peroxidases by Mutational Analysis of Phospholipid Hydroperoxide Glutathione Peroxidase (PHGPx). *Biol. Chem. Hoppe-Seyler* 376 (11), 651–660. doi:10.1515/bchm3.1995.376.11.651
- Manuel, A. M., and Frizzell, N. (2013). Adipocyte Protein Modification by Krebs Cycle Intermediates and Fumarate Ester-Derived Succination. *Amino Acids* 45 (5), 1243–1247. doi:10.1007/s00726-013-1568-z
- Mertins, P., Mani, D. R., Mani, D. R., Ruggles, K. V., Gillette, M. A., Clauser, K. R., et al. (2016). Proteogenomics Connects Somatic Mutations to Signalling in Breast Cancer. *Nature* 534 (7605), 55–62. doi:10.1038/nature18003
- Mertins, P., Yang, F., Liu, T., Mani, D. R., Petyuk, V. A., Gillette, M. A., et al. (2014). Ischemia in Tumors Induces Early and Sustained Phosphorylation Changes in Stress Kinase Pathways but Does Not Affect Global Protein Levels. *Mol. Cell. Proteomics* 13 (7), 1690–1704. doi:10.1074/mcp.M113.036392
- Molinari, M. (2007). N-glycan Structure Dictates Extension of Protein Folding or Onset of Disposal. *Nat. Chem. Biol.* 3 (6), 313–320. doi:10.1038/nchembio880
- Nagase, T., Kawata, S., Tamura, S., Matsuda, Y., Inui, Y., Yamasaki, E., et al. (1997). Manumycin and Gliotoxin Derivative KT7595 Block Ras Farnesylation and Cell Growth but Do Not Disturb Lamin Farnesylation and Localization in Human Tumour Cells. *Br. J. Cancer* 76 (8), 1001–1010. doi:10.1038/bjc.1997.499
- Nagdas, S. K., Winfrey, V. P., and Olson, G. E. (2005). Tyrosine Phosphorylation Generates Multiple Isoforms of the Mitochondrial Capsule Protein, Phospholipid Hydroperoxide Glutathione Peroxidase (PHGPx), during Hamster Sperm Capacitation. *Biol. Reprod.* 72 (1), 164–171. doi:10.1095/biolreprod.104.033530
- Nam, S.-Y., Fujisawa, M., Kim, J.-S., Kurohmaru, M., and Hayashi, Y. (1998). Expression Pattern of Phospholipid Hydroperoxide Glutathione Peroxidase Messenger Ribonucleic Acid in Mouse Testis. *Biol. Reprod.* 58 (5), 1272–1276. doi:10.1095/biolreprod58.5.1272
- Olsen, J. V., Blagoev, B., Gnäd, F., Macek, B., Kumar, C., Mortensen, P., et al. (2006). Global, In Vivo, and Site-specific Phosphorylation Dynamics in Signaling Networks. *Cell* 127 (3), 635–648. doi:10.1016/j.cell.2006.09.026
- Olson, G. E., Whitin, J. C., Hill, K. E., Winfrey, V. P., Motley, A. K., Austin, L. M., et al. (2010). Extracellular Glutathione Peroxidase (Gpx3) Binds Specifically to Basement Membranes of Mouse Renal Cortex Tubule Cells. *Am. J. Physiology-Renal Physiology* 298 (5), F1244–F1253. doi:10.1152/ajprenal.00662.2009
- Ouyang, K. J., Woo, L. L., Zhu, J., Huo, D., Matunis, M. J., and Ellis, N. A. (2009). SUMO Modification Regulates BLM and RAD51 Interaction at Damaged Replication Forks. *PLoS Biol.* 7 (12), e1000252. doi:10.1371/journal.pbio.1000252
- Popovic, D., Vucic, D., and Dikic, I. (2014). Ubiquitination in Disease Pathogenesis and Treatment. *Nat. Med.* 20 (11), 1242–1253. doi:10.1038/nm.3739
- Reilly, C., Stewart, T. J., Renfrow, M. B., and Novak, J. (2019). Glycosylation in Health and Disease. *Nat. Rev. Nephrol.* 15 (6), 346–366. doi:10.1038/s41581-019-0129-4



- Ronau, J. A., Beckmann, J. F., and Hochstrasser, M. (2016). Substrate Specificity of the Ubiquitin and Ubl Proteases. *Cell Res.* 26 (4), 441–456. doi:10.1038/cr.2016.38
- Sato, H., Tamba, M., Ishii, T., and Bannai, S. (1999). Cloning and Expression of a Plasma Membrane Cystine/glutamate Exchange Transporter Composed of Two Distinct Proteins. *J. Biol. Chem.* 274 (17), 11455–11458. doi:10.1074/jbc.274.17.11455
- Schuckelt, R., Brigelius-Flohé, R., Maiorino, M., Roveri, A., Reumkens, J., Strabburger, W., et al. (1991). Phospholipid Hydroperoxide Glutathione Peroxidase Is a Seleno-Enzyme Distinct from the Classical Glutathione Peroxidase as Evident from Cdna and Amino Acid Sequencing. *Free Radic. Res. Commun.* 14 (5–6), 343–361. doi:10.3109/10715769109093424
- Seiler, A., Schneider, M., Förster, H., Roth, S., Wirth, E. K., Culmsee, C., et al. (2008). Glutathione Peroxidase 4 Senses and Translates Oxidative Stress into 12/15-lipoxygenase Dependent- and AIF-Mediated Cell Death. *Cell Metab.* 8 (3), 237–248. doi:10.1016/j.cmet.2008.07.005
- Sheng, Z., Zhu, J., Deng, Y.-n., Gao, S., and Liang, S. (2021). SUMOylation Modification-Mediated Cell Death. *Open Biol.* 11 (7), 210050. doi:10.1098/rsob.210050
- Strahl, B. D., Ohba, R., Cook, R. G., and Allis, C. D. (1999). Methylation of Histone H3 at Lysine 4 Is Highly Conserved and Correlates with Transcriptionally Active Nuclei in Tetrahymena. *Proc. Natl. Acad. Sci. U.S.A.* 96 (26), 14967–14972. doi:10.1073/pnas.96.26.14967
- Sui, X., Zhang, R., Liu, S., Duan, T., Zhai, L., Zhang, M., et al. (2018). RSL3 Drives Ferroptosis through GPX4 Inactivation and ROS Production in Colorectal Cancer. *Front. Pharmacol.* 9, 1371. doi:10.3389/fphar.2018.01371
- Sun, Y., Zheng, Y., Wang, C., and Liu, Y. (2018). Glutathione Depletion Induces Ferroptosis, Autophagy, and Premature Cell Senescence in Retinal Pigment Epithelial Cells. *Cell Death Dis.* 9 (7), 753. doi:10.1038/s41419-018-0794-4
- Takebe, G., Yarimizu, J., Saito, Y., Hayashi, T., Nakamura, H., Yodoi, J., et al. (2002). A Comparative Study on the Hydroperoxide and Thiol Specificity of the Glutathione Peroxidase Family and Selenoprotein P. *J. Biol. Chem.* 277 (43), 41254–41258. doi:10.1074/jbc.M202773200
- Tatham, M. H., Jaffray, E., Vaughan, O. A., Desterro, J. M. P., Botting, C. H., Naismith, J. H., et al. (2001). Polymeric Chains of SUMO-2 and SUMO-3 Are Conjugated to Protein Substrates by SAE1/SAE2 and Ubc9. *J. Biol. Chem.* 276 (38), 35368–35374. doi:10.1074/jbc.M104214200
- Ursini, F., Heim, S., Kiess, M., Maiorino, M., Roveri, A., Wissing, J., et al. (1999). Dual Function of the Selenoprotein PHGPx during Sperm Maturation. *Science* 285 (5432), 1393–1396. doi:10.1126/science.285.5432.1393
- Ursini, F., Maiorino, M., Valente, M., Ferri, L., and Gregolin, C. (1982). Purification from Pig Liver of a Protein Which Protects Liposomes and Biomembranes from Peroxidative Degradation and Exhibits Glutathione Peroxidase Activity on Phosphatidylcholine Hydroperoxides. *Biochimica Biophysica Acta (BBA) - Lipids Lipid Metabolism* 710 (2), 197–211. doi:10.1016/0005-2760(82)90150-3
- Vernet, P., Aitken, R. J., and Drevet, J. R. (2004). Antioxidant Strategies in the Epididymis. *Mol. Cell. Endocrinol.* 216 (1–2), 31–39. doi:10.1016/j.mce.2003.10.069
- Vučković, A. M., Bosello Travain, V., Bordin, L., Cozza, G., Miotto, G., Rossetto, M., et al. (2020). Inactivation of the Glutathione Peroxidase GPx4 by the Ferroptosis-inducing Molecule RSL3 Requires the Adaptor Protein 14-3-3 $\epsilon$ . *FEBS Lett.* 594 (4), 611–624. doi:10.1002/1873-3468.13631
- Wagner, S. A., Beli, P., Weinert, B. T., Nielsen, M. L., Cox, J., Mann, M., et al. (2011). A Proteome-wide, Quantitative Survey of *In Vivo* Ubiquitylation Sites Reveals Widespread Regulatory Roles. *Mol. Cell. Proteomics* 10 (10), M111. doi:10.1074/mcp.M111.013284
- Wang, G., Wu, Y., Zhou, T., Guo, Y., Zheng, B., Wang, J., et al. (2013). Mapping of the N-Linked Glycoproteome of Human Spermatozoa. *J. Proteome Res.* 12 (12), 5750–5759. doi:10.1021/pr400753f
- Wei, X., Yi, X., Zhu, X.-H., and Jiang, D.-S. (2020). Posttranslational Modifications in Ferroptosis. *Oxidative Med. Cell. Longev.* 2020, 1–12. doi:10.1155/2020/8832043
- Weiwier, M., Bittker, J. A., Lewis, T. A., Shimada, K., Yang, W. S., MacPherson, L., et al. (2012). Development of Small-Molecule Probes that Selectively Kill Cells Induced to Express Mutant RAS. *Bioorg. Med. Chem. Lett.* 22 (4), 1822–1826. doi:10.1016/j.bmcl.2011.09.047
- Yang, L., Chen, X., Yang, Q., Chen, J., Huang, Q., Yao, L., et al. (2020). Broad Spectrum Deubiquitinase Inhibition Induces Both Apoptosis and Ferroptosis in Cancer Cells. *Front. Oncol.* 10, 949. doi:10.3389/fonc.2020.00949
- Yang, S. H., Chang, S. Y., Andres, D. A., Spielmann, H. P., Young, S. G., and Fong, L. G. (2010). Assessing the Efficacy of Protein Farnesyltransferase Inhibitors in Mouse Models of Progeria. *J. Lipid Res.* 51 (2), 400–405. doi:10.1194/jlr.M002808
- Yang, W. S., SriRamaratnam, R., Welsch, M. E., Shimada, K., Skouta, R., Viswanathan, V. S., et al. (2014). Regulation of Ferroptotic Cancer Cell Death by GPX4. *Cell* 156 (1–2), 317–331. doi:10.1016/j.cell.2013.12.010
- Yang, W. S., and Stockwell, B. R. (2008). Synthetic Lethal Screening Identifies Compounds Activating Iron-dependent, Nonapoptotic Cell Death in Oncogenic-RAS-Harboring Cancer Cells. *Chem. Biol.* 15 (3), 234–245. doi:10.1016/j.chembiol.2008.02.010
- Young, S. G., Fong, L. G., and Michaelis, S. (2005). Thematic Review Series: Lipid Posttranslational Modifications. Prelamin A, Zmpste24, Missshapen Cell Nuclei, and Progeria—New Evidence Suggesting that Protein Farnesylation Could Be Important for Disease Pathogenesis. *J. Lipid Res.* 46 (12), 2531–2558. doi:10.1194/jlr.R500011-JLR200
- Yu, Y., Xie, Y., Cao, L., Yang, L., Yang, M., Lotze, M. T., et al. (2015). The Ferroptosis Inducer Erastin Enhances Sensitivity of Acute Myeloid Leukemia Cells to Chemotherapeutic Agents. *Mol. Cell. Oncol.* 2 (4), e1054549. doi:10.1080/23723556.2015.1054549
- Zhang, J., Qiu, Q., Wang, H., Chen, C., and Luo, D. (2021a). TRIM46 Contributes to High Glucose-Induced Ferroptosis and Cell Growth Inhibition in Human Retinal Capillary Endothelial Cells by Facilitating GPX4 Ubiquitination. *Exp. Cell Res.* 407 (2), 112800. doi:10.1016/j.yexcr.2021.112800
- Zhang, Y., Swanda, R. V., Nie, L., Liu, X., Wang, C., Lee, H., et al. (2021b). mTORC1 couples cyst(e)ine availability with GPX4 protein synthesis and ferroptosis regulation. *Nat. Commun.* 12 (1), 1589. doi:10.1038/s41467-021-21841-w
- Zhang, Y., Tan, H., Daniels, J. D., Zandkarimi, F., Liu, H., Brown, L. M., et al. (2019). Imidazole Ketone Erastin Induces Ferroptosis and Slows Tumor Growth in a Mouse Lymphoma Model. *Cell Chem. Biol.* 26 (5), 623–633. doi:10.1016/j.chembiol.2019.01.008

**Conflict of Interest:** The authors declare that the research was conducted in the absence of any commercial or financial relationships that could be construed as a potential conflict of interest.

**Publisher's Note:** All claims expressed in this article are solely those of the authors and do not necessarily represent those of their affiliated organizations, or those of the publisher, the editors and the reviewers. Any product that may be evaluated in this article, or claim that may be made by its manufacturer, is not guaranteed or endorsed by the publisher.

Copyright © 2022 Cui, Yang and Li. This is an open-access article distributed under the terms of the Creative Commons Attribution License (CC BY). The use, distribution or reproduction in other forums is permitted, provided the original author(s) and the copyright owner(s) are credited and that the original publication in this journal is cited, in accordance with accepted academic practice. No use, distribution or reproduction is permitted which does not comply with these terms.



# Therapeutic Implications of Ferroptosis in Renal Fibrosis

Yao Zhang<sup>1</sup>, Yanhua Mou<sup>2</sup>, Jianjian Zhang<sup>1</sup>, Chuanjian Suo<sup>1</sup>, Hai Zhou<sup>3</sup>, Min Gu<sup>3</sup>, Zengjun Wang<sup>1</sup> and Ruoyun Tan<sup>1\*</sup>

<sup>1</sup>Department of Urology, The First Affiliated Hospital of Nanjing Medical University, Nanjing, China, <sup>2</sup>Department of Oncology, Xiangyang Central Hospital, Affiliated Hospital of Hubei University of Arts and Science, Xiangyang, China, <sup>3</sup>Department of Urology, The Second Affiliated Hospital of Nanjing Medical University, Nanjing, China

## OPEN ACCESS

### Edited by:

Yanqing Liu,  
Columbia University, United States

### Reviewed by:

Zhenyi Su,  
Columbia University, United States  
Qiaosi Tang,  
Calico Life Sciences LLC,  
United States  
Yanchun Zhang,  
Icahn School of Medicine at Mount  
Sinai, United States

### \*Correspondence:

Ruoyun Tan  
tanruoyun112@vip.sina.com

### Specialty section:

This article was submitted to  
Molecular Diagnostics and  
Therapeutics,  
a section of the journal  
Frontiers in Molecular Biosciences

**Received:** 06 March 2022

**Accepted:** 12 April 2022

**Published:** 17 May 2022

### Citation:

Zhang Y, Mou Y, Zhang J, Suo C,  
Zhou H, Gu M, Wang Z and Tan R  
(2022) Therapeutic Implications of  
Ferroptosis in Renal Fibrosis.  
Front. Mol. Biosci. 9:890766.  
doi: 10.3389/fmolb.2022.890766

Renal fibrosis is a common feature of chronic kidney disease (CKD), and can lead to the destruction of normal renal structure and loss of kidney function. Little progress has been made in reversing fibrosis in recent years. Ferroptosis is more immunogenic than apoptosis due to the release and activation of damage-related molecular patterns (DAMPs) signals. In this paper, the relationship between renal fibrosis and ferroptosis was reviewed from the perspective of iron metabolism and lipid peroxidation, and some pharmaceuticals or chemicals associated with both ferroptosis and renal fibrosis were summarized. Other programmed cell death and ferroptosis in renal fibrosis were also firstly reviewed for comparison and further investigation.

**Keywords:** renal fibrosis, ferroptosis, iron homeostasis, lipid peroxidation, programmed cell death

## 1 INTRODUCTION

Chronic kidney disease (CKD) is an important public health concern causing a high economic cost to the health systems, with an overall prevalence of more than 10% (Hill et al., 2016). Progressive CKD often results in end-stage renal failure and the only options are dialysis or kidney transplantation. Renal fibrosis is a common characteristic of CKD independent of the underlying etiology, leading to the destruction of normal kidney structure and loss of renal function. Renal fibrosis, one of the common characteristics of CKD, includes tubulointerstitial fibrosis and glomerulosclerosis, regardless of the underlying etiology, is synthesized from an imbalance between excessive synthesis and reduced breakdown of the extracellular matrix, and it may be due to normal wound healing response become uncontrolled, with an uncontrolled inflammatory response and myofibroblast proliferation, eventually leading to destruction of normal kidney structure and loss of renal function (el Nahas et al., 1997). Currently, therapies against renal fibrosis exhibit limited effectiveness, and little progress has been made in reversing fibrosis in recent years.

In 2003, Sonam Dolma et al. discovered a new form of cell death induced by erastin without nuclear morphological changes, DNA fragmentation, and caspase-3 activation, which could not be reversed by caspase inhibitors (Dolma et al., 2003) but could be inhibited by iron chelator (Yang and Stockwell, 2008). Subsequently, Dixon named this cell death “ferroptosis” in 2012 (Dixon et al., 2012), which is characterized by lipid peroxidation-mediated membrane damage, leading to iron-dependent regulated necrosis (Stockwell et al., 2017). Different from autophagy, necrosis, pyroptosis, and apoptosis, ferroptosis morphologically exhibits normal nuclei and shrinking mitochondria with condensed mitochondrial membrane, diminished or abolished mitochondria cristae, and ruptured outer mitochondrial membrane (Yagoda et al., 2007; Cao and Dixon, 2016; Latunde-Dada, 2017). The connection between necrotic cell death and long-term renal fibrosis may be dominated by the inflammatory infiltration, which could be defined by the type of necrotic death (Tang et al., 2020).

Although our knowledge about the role of ferroptosis in renal fibrosis is still in its infancy, the cytotoxicity of iron and lipid peroxidation has been known since the 1900s and 1950s, respectively (Moore and Hawkes, 1908; Bieri, 1959). Before the proposing of ferroptosis, many studies confirmed that the ferroptosis-related indicators, including GPXs, iron, and lipid peroxides are participated in renal fibrosis (Sponsel et al., 1996; Ueda et al., 1996; Zachara et al., 2004; Himmelfarb, 2005; Dominguez et al., 2006; Seiler et al., 2008). This review is to summarize the relationship between renal fibrosis and ferroptosis from the perspective of iron metabolism and lipid peroxidation.

## 2 MECHANISM OF FERROPTOSIS

### 2.1 Oxidative Stress and Lipid Peroxidation in Ferroptosis

Ferroptosis is a regulated form of cell death characterized by iron-dependent oxidative stress induced lipid peroxidation (Stockwell et al., 2017). In general, ferroptosis is mainly caused by the inactivation of cellular antioxidant system; it is caspase- and necrosome-independent, which is precisely regulated at epigenetic, transcriptional, post-transcriptional and post-translational levels (Galluzzi et al., 2018).

#### 2.1.1 Oxidative Stress

Oxidative stress is a disruption of redox signaling and control (Jones, 2006), resulting from either excessive free radicals or insufficient degradation of these free radicals. Oxidative stress is a causative factor in the pathogenesis and pathophysiology of numerous degenerative disorders.

Firstly, ROS and reactive nitrogen species (RNS) are the most common oxidative compounds, which can mediate oxidative stress under various pathophysiological conditions, and are removed by antioxidant defense mechanisms. Secondly, reduced glutathione, is an essential intracellular antioxidant synthesized by the ATP-dependent cytosolic enzymes glutamate-cysteine ligase (GCL) and glutathione synthetase (GSS) in a two-step synthesis of cysteine, glutamate and glycine (Stockwell et al., 2017). Thirdly, extracellular cystine and intracellular cysteine are essential for the maintenance of glutathione biosynthesis and for the inhibition of a type of cell death, which can also be prevented by iron chelators or lipophilic antioxidants ( $\alpha$ -tocopherol) (Bannai et al., 1977; Murphy et al., 1989). Cysteine is imported into cells through the oxidized form-cystine of system Xc<sup>-</sup> where cystine is immediately reduced to cysteine within the cells. Finally, GSH is a major soluble non-enzymatic antioxidant, which relieves the oxidative damage and protects cellular macromolecules, including membrane lipids, against ROS by donating electrons to free radicals. This donation leads to its own oxidation, which converts GSH into glutathione disulfide (GSSG). In this process, glutathione peroxidases (GPXs) play an antioxidant role and converts potentially toxic lipid hydroperoxides (L-OOH) to non-toxic lipid alcohols (L-OH) by buffering H<sub>2</sub>O<sub>2</sub> with GSH (Battin and Brumaghim, 2009).

#### 2.1.2 Lipid Peroxidation

Oxidative stress might impact various macromolecules including lipids, proteins and nucleic acid, leading to the formation of oxidative damage products. Lipid peroxidation, broadly defined as the insertion of hydroperoxyl group into a lipid, has recently been identified as a major driver of ferroptosis (Yang and Stockwell, 2016). This process can be induced by a variety of oxidants (superoxides, H<sub>2</sub>O<sub>2</sub>, and highly reactive hydroxyl radicals) or by exposure to xenobiotics and environmental pollutants. As the main component of cellular membranes, lipids have an indispensable role in maintaining cell structural integrity. Polyunsaturated fatty acids (PUFAs), especially arachidonic acid (AA) or adrenic acid (AdA), are most susceptible to peroxidation, which is quite important for the maintenance of cellular membrane fluidity (Figure 1; de Carvalho and Caramujo, 2018).

In the non-enzymatic pathway, lipid peroxidation can be mediated by carbon- and oxygen-centered radicals initiated by Fenton reaction (see below) or it can also be carried out in an orderly manner by enzyme pathway. Acyl-CoA Synthetase Long Chain Family Member 4 (ACSL4) catalyzes the addition of CoA to the long-chain polyunsaturated bonds of AA or AdA to produce AA or AdA acyl Co-A derivatives, thereby promoting the esterification of PUFA into phospholipids (Kagan et al., 2017). It incorporates cellular membranes with PUFAs and drives ferroptosis through the accumulation of oxidized cellular membrane phospholipids (Doll et al., 2017). Then these derivatives are esterified into phosphatidylethanolamines (PEs) containing AA or AdA (AA-PE or AdA-PE) by Lysophosphatidylcholine Acyltransferase 3 (LPCAT3). Lipoygenases (LOXs) form a family of iron-containing lipid peroxide enzymes with highly conserved Fe-coordination sphere positioned in a helical core and shows the substrate specificity (Newcomer and Brash, 2015). According to the location specificity of arachidonic acid oxidation, lipoxygenase was named and classified as ALOXE3 (arachidonate lipoxygenase 3), ALOX5 (arachidonate 5-lipoxygenase), ALOX12 (arachidonate 12-lipoxygenase, 12S type), ALOX12B (arachidonate 12-lipoxygenase, 12R type), ALOX15 (arachidonate 15-lipoxygenase), and ALOX15B (arachidonate 15-lipoxygenase type B) in humans. Finally, AA-PE and AdA-PE, were oxidized by lipoxygenases (LOXs) to generate lipid hydroperoxides, thus proximately execute ferroptosis. The antioxidant  $\alpha$ -tocopherol and  $\alpha$ -tocotrienol could regulate ferroptosis by suppressing the LOX, then generating doubly and triply-oxygenated (15-hydroperoxy)-diacylated phosphatidylethanolamine (PE) species (Kagan et al., 2017). Furthermore, cytochrome P450 oxidoreductase (POR) were recently reported to generate lipid hydroperoxides by an ALOX-independent manner (Figure 1; Zou et al., 2020).

The GPX4, an antioxidant enzyme and a central blocker of ferroptosis, is the only glutathione peroxidase that uses GSH as a co-substrate to reduce phospholipid hydroperoxides to hydroxy phospholipid in the membranes (Yang et al., 2014). Decreased detoxification of GPX4, depletion of GSH and increased LOXs activity are the main driving factors of ferroptosis (Seiler et al., 2008; Yang and Stockwell, 2016). Selenium is a component of selenocysteine at the catalytic site of GPX4. Similar to ferrostatin-1, selenium has a strong inhibitory effect on cerebral hemorrhage and can reduce the concentration of ferroptosis, which is a

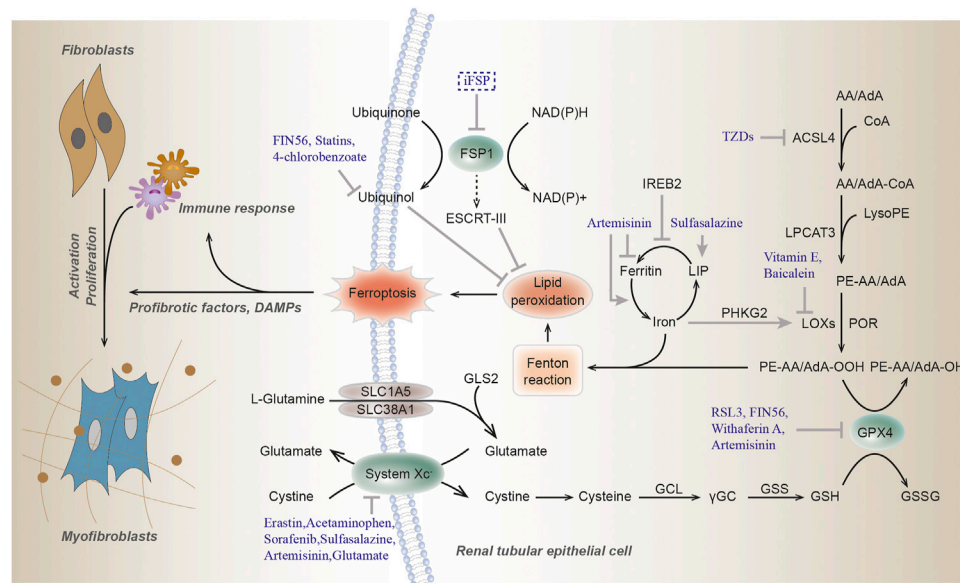


**FIGURE 1 |** Molecular mechanisms of ferroptosis. Ferroptosis is triggered by lethal lipid peroxidation caused by accumulation of intracellular free iron and/or dysfunction of antioxidant system. The commonly used ferroptosis regulators are shown here. Arrows indicate activation, while blunt lines indicate inhibition. GSH, glutathione; GPX4, glutathione peroxidase 4; GSSG, glutathione disulfide; GCL, glutamate-cysteine ligase; γGC, γ-glutamyl cysteine; GSS, glutathione synthetase; AA, arachidonic acid; AdA, adrenic acid; ACSL4, acyl-CoA synthetase 4; TZDs, thiazolidinediones; LPCAT3, lysophosphatidylcholine acyltransferase 3; LOXs, lipoxygenase; POR, cytochrome P450 oxidoreductase; FSP1, Ferroptosis suppressor protein 1; IREB2, iron responsive element binding protein 2; PHKG2, phosphorylase kinase G2; LIP, labile iron pool; GLS2, glutaminase 2; SLC1A5, solute carrier family 1 member 5; SLC38A1, solute carrier family 38 member A; NAD(P)H, nicotinamide adenine dinucleotide phosphate; ESCRT-III, endosomal sorting complex required for transport-III; RSL3, (1S,3R)-RSL3.

specific ferroptosis inhibitor (Ingold et al., 2018). In addition, lipophilic antioxidant ubiquinol (CoQ10) exerts a fundamental role in the mitochondrial electron transport chain and can hamper ferroptosis in a GSH-independent manner (Doll et al., 2019). Glutamate is converted from glutamine by glutaminase and is required for the induction of ferroptosis during serum-induced injury after amino acid starvation (Gao et al., 2015; Altman et al., 2016). Then glutamate can also be exchanged for cystine via xCT. Ferroptosis suppressor protein 1 (FSP1), also named as apoptosis-inducing factor mitochondria associated 2 (AIFM2), acts as an NADH-dependent oxidoreductase to catalyze oxidase ubiquinol into reduced ubiquinol and prevents lipid peroxides and incorporation into membranes and lipoproteins, in parallel to the canonical glutathione-based GPX4 pathway (Bersuker et al., 2019; Doll et al., 2019). The newly found Dihydroorotate dehydrogenase (DHODH), inhibits ferroptosis in the mitochondrial intima by reducing the ubiquitin ketone to ubiquitin alcohol, operating in parallel to mitochondrial GPX4, but not to cytosolic GPX4 or FSP1 (Mao et al., 2021; **Figure 1**).

## 2.2 Iron Homeostasis and Ferroptosis

Iron is an important trace element that plays an important role in many key biological processes. Iron is a key cofactor in electron transfer processes and redox reactions because of its ability to switch between specific oxidative forms; however, iron's redox potential might lead to cytotoxicity when iron is overloaded (Gozzelino and Arosio, 2016).

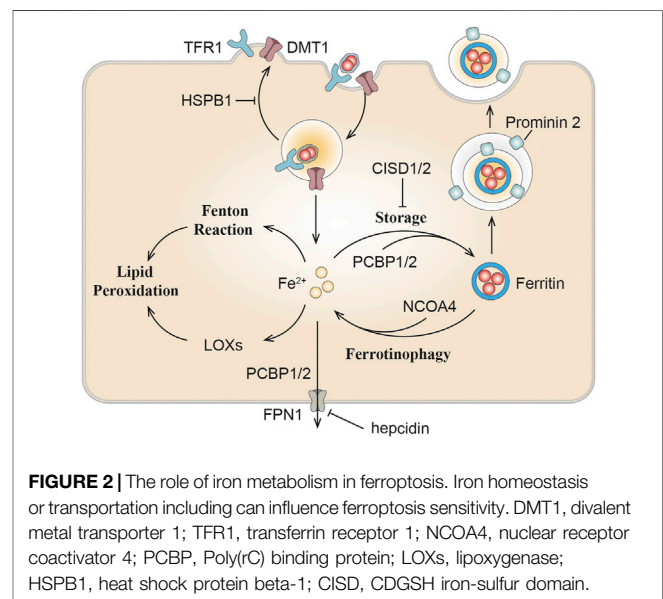


**FIGURE 2 |** The role of iron metabolism in ferroptosis. Iron homeostasis or transportation including can influence ferroptosis sensitivity. DMT1, divalent metal transporter 1; TFR1, transferrin receptor 1; NCOA4, nuclear receptor coactivator 4; PCBP, Poly(rC) binding protein; LOXs, lipoxygenase; HSPB1, heat shock protein beta-1; C1SD, CDGSH iron-sulfur domain.

### 2.2.1 Iron Overload Induces Ferroptosis

The excessive intracellular labile iron can directly participate in the redox cycle, providing electrons to expedite ROS production and lipid peroxidation via the Fenton reaction, a series of reactions in which this labile iron reacts with endogenous hydrogen peroxide or superoxide to form oxygen centered



radicals ( $\text{Fe}^{2+} + \text{H}_2\text{O}_2 \rightarrow \text{Fe}^{3+} + \text{OH}^- + \cdot\text{OH}$ ) (Koppenol, 1993; Neyens and Baeyens, 2003). GSH is necessary for the assembly of Fe-S clusters and can act as a coordinating ligand for [2Fe-2S] clusters when bound to a glutaredoxin scaffold (Hider and Kong, 2013). Interestingly, studies in yeast support the prime actor of GSH in maintaining iron balance during iron-sulfur cluster assembly, challenging the traditional view of its primary role in redox balance (Kumar et al., 2011).

Compelling evidence indicated that ferroptosis can be motivated by elevated iron levels and inhibited by iron chelation (Dixon et al., 2012). Several proteins impacting iron homeostasis or transportation can influence the sensitivity of ferroptosis (Figure 2; Dixon et al., 2012; Sun et al., 2015; Yuan et al., 2016; Kim et al., 2018). Ferritin plays a major role in protecting against ferroptosis through storing intracellular iron (Fang et al., 2020). It further emphasizes the essentiality of iron in ferroptosis, which requires transferrin and TFR1 as specific markers of ferroptosis (Gao et al., 2015; Feng et al., 2020). DMT1 inhibition could block the translocation of lysosomal iron, leading to the accumulation of lysosomal iron and cell death with ferroptotic features (Song et al., 2021). NCOA4-mediated ferritinophagy promotes ferroptosis by degradation of ferritin (Hou et al., 2016). In kidney, the liver-derived hormone hepcidin serves as a promising therapeutic target in conditions such as post-cardiopulmonary bypass AKI and delayed graft function after renal transplantation (Scindia et al., 2019). Reportedly, it could promote erastin-induced ferroptosis by degrading ferroportin, the sole iron export protein (Geng et al., 2018). Recently, prominin 2 has been found to facilitate the formation of ferritin-containing multivesicular bodies (MVB) and exosomes in mammary epithelial, thus driving ferroptosis resistance (Belavgeni et al., 2019; Brown et al., 2019). Heat shock protein beta-1 (HSPB1) can inhibit TFR1 recycling (Chen et al., 2006), its up-regulation can confine erastin-induced iron uptake through suppressing the ferroptosis (Sun et al., 2015). In addition to participating in Fenton reaction, iron is also transported to several iron-containing enzymes involved in lipid peroxidation, thus in turn actuating ferroptosis. For instance, phosphorylase kinase G2 (PHKG2) plays a significant role in promoting iron accumulation and regulating iron availability to LOXs (Yang et al., 2016). CDGSH iron-sulfur domain (CISD) has also been shown to bind a redox-active [2Fe-2S] cluster and participates in regulating iron storage and redox reactions (Fidai et al., 2016). Down-regulating CISD1 level can promote iron-mediated intramitochondrial lipid peroxidation contributing to erastin-induced ferroptosis (Yuan et al., 2016). Silencing CISD2 gene can raise lipid ROS production and mitochondrial iron content, making drug-resistant head and neck cancer cells sensitive to sulfasalazine-induced ferroptosis (Kim et al., 2018). Accumulation of iron responsive element binding protein 2 (IREB2) can induce iron aggregation, thus contributing to the ferroptosis (Li Y. et al., 2020), while the silencing of IREB2 gene leads to mutual changes in the expression of known iron absorption, metabolism and storage genes TFR1, iron-sulfur cluster assembly enzyme (ISCU), FTH1, FTL and in erastin sensitivity (Salahudeen et al., 2009; Vashisht et al., 2009).

## 3 FERROPTOSIS IN CHRONIC RENAL INJURY AND FIBROSIS

### 3.1 Lipid Peroxidation in Chronic Kidney Disease

The final common pathological denominator in the case of chronic kidney injury is renal fibrosis, and the extent of tubulointerstitial fibrosis is the best predictor of renal survival for CKD patients (Zeisberg and Neilson, 2010). Oxidative stress is present from the early stages of CKD and continues to increase as kidney function deteriorate due to antioxidant consumption and increased ROS production (Sureshbabu et al., 2015; Daenen et al., 2019; Duni et al., 2019; Gyuraszova et al., 2019).

Diverse renal abnormalities can trigger oxidative stress and accelerate the kidney disorders. Fibrotic and damaged tubular and glomerular cells in CKD may enhance ROS production, which is a major agent of oxidative stress (Daenen et al., 2019). Compared with healthy control group, the levels of GPX and GSH in renal cortex of CKD model rats and CKD patients were significantly decreased, while the levels of ROS and MDA were significantly increased (Zachara et al., 2004; Tbahriti et al., 2013). Lipid aldehydes, the end product of many oxidation reactions, including 4-hydroxy-2-hexenal (4-HHE) and 4-hydroxy-2-nonenal (4-HNE) (Himmelfarb, 2005), and their plasma concentrations are significantly higher in CKD patients (Soulage et al., 2020). Malondialdehyde (MDA), is the final product of peroxidation of polyfluorinated fatty acids and an indicator of ferroptosis (Kim et al., 2018), which is commonly raised in the serum of CKD patients (Taccone-Gallucci et al., 1989; Pei et al., 2016). These markers, including 4-HHE, 4-HNE, and MDA have all been widely used in the detection of ferroptosis recently. In HEK-293T cells, GPX4 was shown to block TNF $\alpha$ -mediated activation of NF- $\kappa$ B (Li et al., 2018). Moreover, recent researches have reflected that ferroptosis could facilitate renal damage in diabetic nephropathy (DN), and lipid peroxidation is increased in DN mice, and the expressions of ACSL4, SLC7A11, and SLC3A2 are up-regulated, while GPX4 is down-regulated (Wang Y. et al., 2020). ACSL4 inhibitor rosiglitazone alleviated renal impairment in DN by suppressing ferroptosis (Wang Y. et al., 2020). It is established that pathological changes of DN include renal hypertrophy, enlargement of glomerular capillaries, mesangial expansion, and glomerular basement membrane thickening caused by ECM deposition, which ultimately lead to inflammation, endothelial dysfunction, and renal fibrosis (Jha et al., 2016).

### 3.2 Iron Metabolism in Kidney

#### 3.2.1 Iron Homeostasis in Kidney

Normally, nutritional iron, which consists of both ferric iron ( $\text{Fe}^{3+}$ ) and ferrous iron ( $\text{Fe}^{2+}$ ), is absorbed by duodenal enterocytes.  $\text{Fe}^{3+}$  could bind to transferrin (TF) on the cell membrane to form transferrin-bound iron (TBI), which is captured by transferrin receptor 1 (TFR1) into the endosomes. Intracellular  $\text{Fe}^{3+}$  is reduced to  $\text{Fe}^{2+}$  by iron reductase (represented by Steap3).  $\text{Fe}^{2+}$  would then be released into the labile iron pool (LIP) in the cytoplasm by the divalent metal transporter 1 (DMT1) (Dhungana et al., 2004; Knutson, 2007).



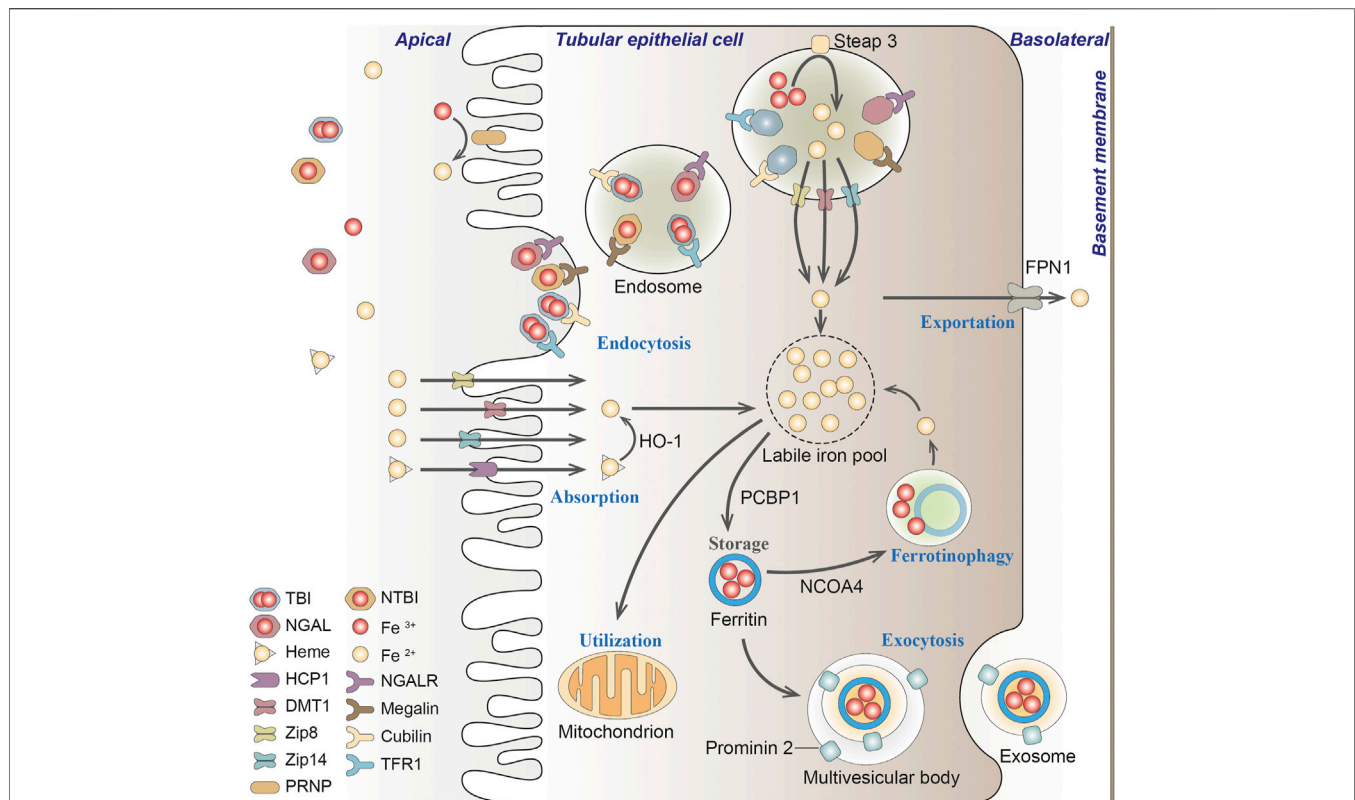


**FIGURE 3 |** Iron transportation in renal tubules. Filtered iron is almost completely reabsorbed in renal tubular, where it would be then stored in ferritin, utilized in the mitochondria or exported from the cell. TBI, transferrin-bound iron; NTBI, non-transferrin-bound iron; NGAL, neutrophil gelatinase-associated lipocalin; HO-1, heme oxygenase-1; PCBP1, Poly(rC) binding protein 1; NCOA4, nuclear receptor coactivator 4; FPN1, protein ferroportin 1; HCP1, heme carrier protein 1; DMT1, divalent metal transporter 1; Zip8, zinc transporter ZIP8; Zip14, zinc transporter ZIP14; PRNP, prion protein; NGALR, neutrophil gelatinase-associated lipocalin receptor; TFR1, transferrin receptor 1.

Endosomal  $\text{Fe}^{3+}$  is quickly reduced to  $\text{Fe}^{2+}$  by an oxidoreductase activity. Excess iron ions are either released through the basal membrane protein ferroportin 1 (FPN1) to the circulation or stored in ferritin, the major iron storage protein (Arosio et al., 2009). Ferritin is a spherical heteropolymer capable of storing 4,500 iron atoms, consisting of a ferritin heavy chain (FTH1) and a ferritin light chain (FTL), both of which can sequester and store iron in a non-toxic and bioavailable form. Iron is incorporated into ferritin via ferritin iron pores as  $\text{Fe}^{2+}$ , which could be formed by intestinal absorption or erythrocyte degradation. FTH1 catalyzes the oxidation of  $\text{Fe}^{2+}$  to  $\text{Fe}^{3+}$ , while FTL promotes the nucleation of ferrihydrite, enabling inert deposits of  $\text{Fe}^{3+}$ , which can hardly be used in cells or generate ROS (Philpott, 2018). Poly(rC) binding proteins (PCBPs) (especially PCBP1 and PCBP2), are important iron chaperones to regulate the metalation of iron-containing proteins and the storage and export of  $\text{Fe}^{2+}$  (Shi et al., 2008). They directly bind ferritin and deliver labile irons to ferritin for storage (Philpott et al., 2017). For intracellular utilization, iron needs to be released from ferritin and reduced to  $\text{Fe}^{2+}$  again. Ferritin degradation mediated by nuclear receptor coactivator 4 (NCOA4) is required for the maintenance of mitochondrial respiratory activity, respiratory chain complex assembly,

mitochondrial iron storage, and membrane potential (Figure 3; Fujimaki et al., 2019). However, it has been reported that iron excess in red blood cells in turn triggers the ubiquitin-mediated NCOA4 degradation by the E3-9 ligase HERC2 (Ryu et al., 2018).

In the kidney, circulating iron can be filtered through the glomeruli into the tubules under physiological conditions (Zhang et al., 2007; Smith and Thevenod, 2009). The filtered iron is almost completely reabsorbed in the renal tubules, and then stored in ferritin, utilized in the mitochondria or exported from the cell (Smith and Thevenod, 2009). If systemic iron is overloaded and transferrin is mostly saturated, iron would loosely bind to other filterable non-transferrin proteins, such as neutrophil gelatinase-associated lipocalin (NGAL), albumin, hemoglobin, myoglobin and hepcidin, or small molecules such as citrate, acetate, and phosphate (Swinkels et al., 2006; Smith and Thevenod, 2009; Brittenham, 2011; Kroot et al., 2011; Paragas et al., 2012; de Swart et al., 2016; Rosa et al., 2017; Figure 3).

The reabsorption of filtered transferrin-bound iron (TBI), hemoglobin and myoglobin in the renal tubules is mainly through megalin-dependent cubilin-mediated endocytosis via binding to TFR1 expressed in the apical membrane (Kozyraki et al., 2001). Renal TFR1 expression is decreased during

parenterally induced iron loading (Weiss et al., 2018), but increased under low iron conditions (Smith et al., 2019). NGAL is a promising biomarker for acute or chronic kidney disease, where iron binds to NGAL and is enucleated by neutrophil gelatinase-associated lipocalin receptor (NGALR) in distal tubules (Langelueddecke et al., 2012). Heme is reabsorbed through the heme importer, namely, heme carrier protein 1 (HCP1), in proximal and distal tubules (Le Blanc et al., 2012). Transporters in different nephron segments that promote the uptake of other non-transferrin proteins binding iron on the plasma membrane has not been fully elucidated (Thévenod and Wolff, 2016). Reportedly, zinc transporter ZIP8 (Zip8), zinc transporter ZIP14 (Zip14) and DMT1 were present in the apical membrane of human proximal and distal tubules (Canonne-Hergaux and Gros, 2002; Veuthey et al., 2014; van Raaij et al., 2018b). The endocytic iron is released from the transport protein, and is then reduced and exported to the cytosol mainly through DMT1, where  $\text{Fe}^{3+}$  is excluded under the excitation of an  $\text{H}^+$  electrochemical potential gradient, and potentially pass through the Zip14 or Zip8 (He et al., 2006; Pinilla-Tenas et al., 2011). Since DMT1 optimally transports ferrous iron at pH 5.0–6.0, whereas Zip8 and Zip14 at pH 6.5–7.5 (He et al., 2006; Pinilla-Tenas et al., 2011), it is speculated that DMT1 may mainly facilitate the uptake of free iron distal tubules, while Zip8 and Zip14 may play a better role in the proximal tubules (Figure 3; van Swelm et al., 2020).

There is no evidence for basolateral uptake of TBI, heme, hemoglobin, or non-transferrin-bound iron (NTBI) in the basolateral renal tubules so far, whereas the iron exporter-ferroportin exists in the basolateral membrane of proximal tubules (van Raaij et al., 2018a). As a master regulator of iron homeostasis, hepcidin regulates this ferroportin-mediated iron export and intracellular H-ferritin levels (Vyoral and Jiri, 2017). In podocytes, hemoglobin can be taken up by megalin-cubilin endocytosis catabolized by heme oxygenase-1 (HO-1), thus resulting in increased oxidative stress (Rubio-Navarro et al., 2018; Duann et al., 2019). In addition, iron transport and regulation also exist in mesangial cells, since ferritin, TFR1, HO-1, and IRP1 are all expressed in these cells (Cheng et al., 2015; Liu and Templeton, 2015).

### 3.2.2 Iron Overload and Toxicity in Kidney

Iron plays a key role in mitochondria, promoting oxidative stress and ROS production, leading to cell apoptosis, mitochondrial damage and vascular calcification (Nakanishi et al., 2020). In 1988, the deleterious role of iron in renal disease was first described as being involved in free radical mediated renal damage after ischemia and lipid peroxidation, while iron chelators can reduce these injury (Paller and Hedlund, 1988), suggesting the existence of ferroptosis. Mitochondria are extremely dependent on iron metabolism and are the target of iron transport in these cells. The tubular epithelium possesses abundance of mitochondria to support active transport, but quite susceptible to hypoxia, toxic compounds, proteinuria, metabolic disorders. Kidneys can be exposed to toxic levels of bound iron (e.g., transferrin), or free iron, due to redundant filtration of iron into renal tubules, alterations in cellular iron localization or

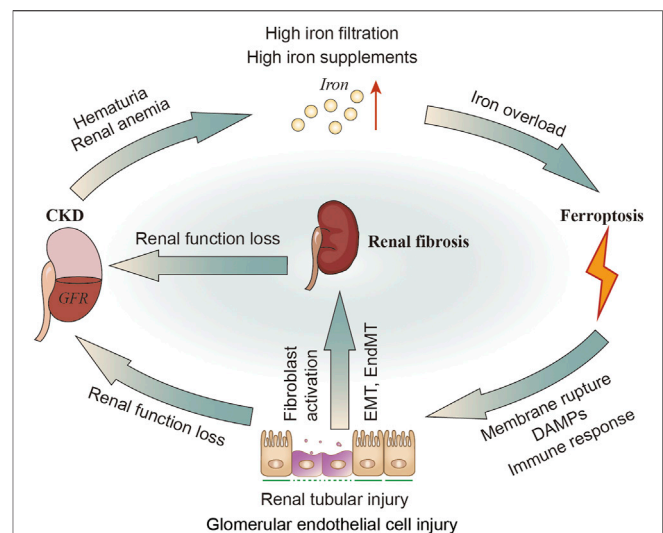


**FIGURE 4 |** The relationship of CKD, iron metabolism, ferroptosis in renal tubular cells and renal fibrosis. In patients with CKD, hematuria and renal anemia could cause increased iron filtration in renal tubules and excessive exogenous intake of iron. Iron overload may induce ferroptosis, leading to renal injury and DAMPs signals release as well as inflammatory and immune responses. The injured tubular can then activate fibroblasts or directly transform into myofibroblasts through EMT. Kidney injury or renal fibrosis can further reduce the GFR. DAMPs, damage-related molecular patterns; GFR, glomerular filtration rate.

compartmentalization in the kidney (Martines et al., 2013; van Raaij et al., 2018b; Figure 4).

It was found that kidney and urinary iron content are elevated in patients with CKD (Sears et al., 1966; Wang et al., 2001; Shah et al., 2007; van Raaij et al., 2018b) and animal models of CKD (Nankivell et al., 1994; Ueda et al., 1996; Harris and Tay, 1997; Naito et al., 2015). Altered molecular iron handling may lead to iron deposition in kidney (van Raaij et al., 2018b). When these iron or iron-containing molecules exceed the storage capacity of ferritin or the cell's ability to export iron, they damage renal tubular cells (Sponsel et al., 1996; Zager and Burkhart, 1997; Martines et al., 2013; Naito et al., 2015). Exposure to either the  $\text{Fe}^{2+}$  or  $\text{Fe}^{3+}$  (100  $\mu\text{M}$ , 30–80 h) may impair healing of denuded areas made within confluent monolayers of renal tubular epithelial cell lines (Sponsel et al., 1996).  $\text{Fe}^{2+}$  ( $\text{FeSO}_4$  100  $\mu\text{M}$ ) can stimulate  $\text{H}_2\text{O}_2$  production in renal tubular cells *in vitro* (Zager and Burkhart, 1997).  $\text{Fe}^{2+}$  can also cause cytopathic changes including numerous iron-particles-containing lysosomes and distortional mitochondria (Sponsel et al., 1996; Figure 4). Apart from the tubules, cultured human glomerular endothelial cells (HGECS) have been shown to express TFR1, FPN1 and DMT1. The endothelial injury factor-Ang II could induce iron incorporation followed by an increase in labile iron in HGECS (Tajima et al., 2010). Iron chelators have been confirmed to improve renal function in patients with glomerular disease, and minimize the reactivity of iron and remove iron from the kidneys or relieving iron-related oxidative stress (Rajapurkar et al., 2013). Iron restriction can also delay the progress of DN in diabetic rats (Matsumoto et al., 2013). In addition, administration of iron

chelation can alleviate renal interstitial fibrosis and suppress the increments of collagen type III and TGF- $\beta$  (Naito et al., 2015).

Iron-mediated cell injury or ferroptosis is considered as a core of the pathogenesis of acute kidney injury (Scindia et al., 2019). Iron homeostasis is becoming the focus of new therapeutic interventions for kidney diseases. Although iron overload or toxicity are not equivalent to ferroptosis, there is reason to believe that these “iron induced oxidative stress or lipid peroxidation” are at least related to ferroptotic events.

### 3.3 Ferroptosis in Renal Fibrosis

ROS play a wide role in the oxidation of lipids, proteins, and DNA, resulting in damage to the tubules and vascular endothelium, thus secreting profibrotic factors (Pisani et al., 2013; Daenen et al., 2019). Inhibition of oxidative stress has always been an anti-fibrotic target (Wang et al., 2019). Oxidative stress can cause fibroblast/pericyte activation (Bondi et al., 2010), tubular epithelial-mesenchymal transition (EMT) (He et al., 2015; Song et al., 2018), fibrocyte/macrophage recruitment (Wagner et al., 2012; Lee et al., 2016), and endothelial-mesenchymal transition (EndMT) (Echeverria et al., 2013; Montorfano et al., 2014). Reportedly, HK2 (human kidney tubular cell) has been reported to secrete profibrotic factors and facilitate fibroblast proliferation and activation during ferroptosis (Zhang et al., 2021). Oxidative stress induced glomerular endothelial cell dysfunction (Sol et al., 2020), mesangial sclerosis (Lu et al., 2018), podocyte abnormality (Okamura and Pennathur, 2015; Zschiedrich et al., 2017), and parietal epithelial cell injury (Odaci et al., 2015; Su et al., 2015) can lead to glomerulosclerosis (Tang et al., 2011; Su et al., 2019). Increased production of ROS (including  $\text{OH}^-$ ,  $\text{H}_2\text{O}_2$ , lipid peroxides, and superoxide anion free radicals) in podocytes can directly damage podocytes themselves, which consequently mediate glomerular injury (Gwinner et al., 1997; Marshall et al., 2006). Numerous pathologic processes mediated by oxidative stress associated factors can stimulate glomerular endothelial cells to undergo EndMT, which is consistent with increased mesenchymal marker expression including  $\alpha$ -smooth muscle actin ( $\alpha$ SMA) and fibroblast specific protein 1, and the production of ECM proteins (Liang et al., 2016; Dejana et al., 2017; **Figure 4**).

Although oxidative stress is known as an inducer for ferroptosis, we have to notice it is the “lipid ROS” and subsequently membrane rupture that represent the occurrence of ferroptosis, instead of the “ROS” (Dixon et al., 2012). Ferroptosis triggers inflammatory and immune responses through the release and activation of damage-related molecular patterns (DAMPs) signals, which makes it to be an attractive therapeutic target for renal fibrosis especially renal graft fibrosis (Linkermann et al., 2013; Martin-Sanchez et al., 2017). Synchronous tubule necrosis can be induced in renal ischemia/reperfusion (I/R) injury model, oxalate crystal-induced AKI model and diabetic nephropathy (DN) tubule cell death model (Linkermann et al., 2014; Wang Y. et al., 2020; Li S. et al., 2021). Erastin or TGF- $\beta$  can induce ferroptosis, promote fibroblast-to-myofibroblast differentiation resulting in fibrosis (Gong et al., 2019). Recent studies have shown that ureteral obstruction can induce ferroptosis in renal tubular epithelial cells *in vivo*, and HK-

2 cells (human proximal tubular cell line) to secrete various profibrotic factors which further promoted the proliferation and activation of fibroblast during ferroptosis (Zhang et al., 2021). Here, we first briefly summarize the role of several key regulators of ferroptosis in renal fibrosis, though the specific mechanism of these prooxidative factor in triggering ferroptosis and mediating renal fibrosis has far been elucidated.

#### 3.3.1 HO-1

HO-1, an inducible enzyme, catabolizes the heme group into carbon monoxide (CO) and biliverdin, which can further convert to bilirubin, and ferrous iron. HO-1 induction could protect the kidney from oxidative stress showing anti-inflammatory and anti-apoptotic activity in DN (Abo El Gheit and Emam, 2016), which was also proved to reduce glomerular sclerosis and intimal hyperplasia, being a therapeutic target to improve the long-term outcomes after kidney transplantation (Bedard et al., 2005; Corona et al., 2020). Additionally, compared with wild-type mice, HO-1<sup>-/-</sup> mice had higher levels of renal fibrosis (Kovtunovych et al., 2010), and more susceptible to myocardial I/R (Abo El Gheit and Emam, 2016). Absence of HO-1 was associated with immune response deficiency, such as Th1-weighted shift in cytokine responses (Kapturczak et al., 2004), and defects in erythrophagocytosing macrophages (Kovtunovych et al., 2010), thus supporting it a protective role in kidney diseases. However, activation of HO-1 triggers ferroptosis through iron overloading and excessive lipid peroxides, thus promoting renal fibrosis area and collagen I in DN mice (Chang et al., 2018; Feng et al., 2021). Increased HIF-1 $\alpha$ /HO-1 level, iron content, ferritin level and lipid peroxides were detected in this DN kidneys, indicating that ferroptosis might enhance DN and damage renal tubules through HIF-1 $\alpha$ /HO-1 pathway (Feng et al., 2021). Researches on neurodegenerative diseases and neoplastic disorders also demonstrated HO-1 has pro-ferroptotic effects on cells through iron accumulation and pro-oxidant effects (Chang et al., 2018; Li R. et al., 2020; Fernández-Mendivil et al., 2021).

Resultingly, though induction of HO-1 has been a potential therapeutic target in kidney diseases, attention must be paid to the safe range of HO-1 induction, owing to the pro-ferroptotic role of HO-1 in raising intracellular ferrous load and redox homeostasis (Chang et al., 2018; Li R. et al., 2020; Fernández-Mendivil et al., 2021).

#### 3.3.2 NOX4

NADPH oxidase (NOXs) plays the most important role in many enzyme systems involved in ROS production in the kidney (Jha et al., 2016). Nox4 is a major source of ROS in the renal cells, linking with myofibroblast differentiation and tubulointerstitial fibrosis through various pathways. Although Nox4 is expressed in a variety of kidney cells, including epithelial, endothelial, podocytes, mesangial cells, and fibroblasts, its role in fibrosis is controversial (Yang et al., 2018). Inhibition of NOX4 could protect from ferroptosis in various cells via suppressing  $\text{H}_2\text{O}_2$  and lipid peroxides production (Dixon et al., 2012; Wang et al., 2018; Chen et al., 2019). Manipulating Nox4 expression in mice proximal tubules cells could upregulate renal fibronectin and TGF- $\beta$  level (Seddek et al., 2010). It is confirmed that rapamycin can decrease MDA and NOX4 levels, inhibit the NADPH oxidase activity, and elevate the GSH level and SOD activity, thus



inhibiting the ROS production of mesangial cells in DN (Lu et al., 2018). Nrf2 is known to regulate the antioxidant response and the activity of several ferroptosis-related proteins, involving iron homeostasis, intermediate metabolism, and GSH metabolism; Nrf2-mediated up-regulation of HO-1, as described above, could facilitate heme degradation, free iron release, and lipid peroxidation, thus inducing ferroptosis (Dodson et al., 2019; Fang et al., 2019). The up-regulation of Nrf2 expression by Fenofibrate can inhibit iron droop, thus alleviating renal pathological changes in DN mice (Li S. et al., 2021). HIF-1 $\alpha$  could negatively regulate ferroptosis induction in human cancer cells (Yang M. et al., 2019), which is also mechanically antithetical to oxidative stress mentioned above (Nlandu Khodo et al., 2012). This is contrary to the traditional view that NOXs promotes ferroptosis by oxidative stress-induced lipid peroxidation (Xie et al., 2016a; Wang J. et al., 2020; Park et al., 2021). Different subcellular localization, cell types, molecular concentrations, disease types or/and stages may be responsible for this functional variability, and more research is warranted on cell-specific and inducible overexpression or knockout systems *in vivo*.

### 3.3.3 TP53

TP53 (p53) is considered as a tumor suppressor due to its ability to promote cell death or permanently inhibit cell proliferation. P53 can negative regulate SLC7A11, leading to reduced glutathione production and increased ROS (Jiang et al., 2015), target SAT1 which increase the level of ALOX15 (Ou et al., 2016), suggesting that p53 represents a novel inducer of ferroptosis. However, p53 can also regulate GSL2 (glutaminase 2) to influence glutamine metabolism and block dipeptidyl-peptidase-4 (DPP4) activity, which finally defense lipid peroxidation and ferroptosis (Hu et al., 2010; Xie et al., 2017). Reportedly, CRISPR/Cas9 mediated p53 deletion cells were sensitive to ferroptosis, implying that p53 hold a pro-survival function in ferroptosis, which requires p53 targeting CDKN1A (P21) expression (Tarangelo et al., 2018). These context-dependent roles of p53 in ferroptosis may result from fine-tuning its phosphorylation, ubiquitination, methylation, acetylation, and other modifications.

P53 also plays a critical role in non-neoplastic diseases including renal fibrosis and CKD, which acts as a critical co-factor for several key fibrotic and cell cycle effectors including TGF- $\beta$ 1, CTGF, PAI-1, P21 (Kortlever et al., 2006; Yang et al., 2010; Samarakoon et al., 2012). P53 inhibitor pifithrin- $\alpha$  was proved to alleviate renal experimental fibrogenesis consistent with decreased CTGF and TGF- $\beta$ 1 levels (Yang et al., 2010). Interestingly, the p53-dependent P21, shows both effect in ferroptosis and renal fibrosis (Tarangelo et al., 2018; Das et al., 2020), but whether a direct link exists between ferroptosis, renal fibrosis, and P21 has not been reported.

## 4 FERROPTOSIS REGULATORS AND RENAL FIBROSIS

### 4.1 Ferroptosis Inhibitors

Many drugs or compounds have been reported to inhibit renal fibrosis *in vitro* (Table 1) or *in vivo* (Table 2) and have also been proved to inhibit ferroptosis (Table 3).

#### 4.1.1 Antioxidants

Several antioxidants can suppress ferroptosis through limiting lipid peroxidation and have been verified to alleviate renal fibrosis from different causes *in vivo* and/or *in vitro* through different targets and mechanisms, including Vitamin E, CoQ10, N-acetylcysteine (NAC), Trolox, Diphenylene iodonium, and Zileuton (Jenkins et al., 2001; Ho et al., 2007; Piao et al., 2013; Shen et al., 2016; Atmaca et al., 2017; Giam et al., 2017; Gonzalez et al., 2017; Helmy et al., 2018; Zhao et al., 2018; Li C. et al., 2019; Montford et al., 2019; Farias et al., 2020).

#### 4.1.2 Iron Chelators

Reportedly, deferoxamine prevents renal interstitial fibrosis in the UUO mice (Ikeda et al., 2014). Long-term oral administration of deferiprone have been shown to have renal protective effects in both diabetic and non-diabetic glomerular disease (Rajapurkar et al., 2013). These two iron chelating agents have anti-iron toxicity at 100  $\mu$ M (Do Van et al., 2016).

#### 4.1.3 CYP450 Substrate

Certain cytochrome P450 substrate drugs have the anti-ferroptotic effect by scavenging activity against lipid peroxy radicals in various cell lines including NRK49F (rat kidney fibroblast), NRK52E (rat kidney tubular cell), and HK2 (Mishima et al., 2020). These drugs inhibit the ferroptotic pathological changes of different renal cell types and ameliorates renal damage, indicating the therapeutic promise of this repurposed drugs (e.g., Triiodothyronine, and Carvedilol) (Wong et al., 2001; Jovanovic et al., 2005; Lu et al., 2013; Adedoyin et al., 2018; El Agaty, 2018).

#### 4.1.4 Thiazolidinediones

The PPAR- $\gamma$  agonists thiazolidinediones (TZDs), including rosiglitazone, troglitazone, and pioglitazone, could prevent ferroptosis probably by inhibiting ACSL4, even in PPAR $\gamma$  KO cells (Doll et al., 2017; Kagan et al., 2017; Wang Y. et al., 2020). However, non-thiazolidinediones PPAR $\gamma$  agonists failed to rescue cells from RSL3-induced ferroptosis, suggesting that thiazolidinediones might exert anti-ferroptosis effect regardless of PPAR $\gamma$  (Doll et al., 2017). Reportedly, these drugs can alleviate the glomerulosclerosis and tubulointerstitial fibrosis of various renal disease models (McCarthy et al., 2000; Chung et al., 2005; Panchapakesan et al., 2005; Omasu et al., 2007; Kawai et al., 2009; Han et al., 2010; Bilan et al., 2011; Koch et al., 2012; Shui et al., 2017; Sun et al., 2017; Németh et al., 2019; Sun et al., 2019; Wei et al., 2020), and ameliorate chronic renal allograft dysfunction (Kiss et al., 2010; Deng et al., 2019).

#### 4.1.5 DPP4 Inhibitors

In the absence of TP53, ferroptosis can be inhibited by downregulation of DPP4 or administration of DPP4 inhibitors (e.g., alogliptin, linagliptin, and vildagliptin) (Xie et al., 2017). Additionally, DPP4 represents a precise druggable target in CKD. These DPP4 inhibitors were proved to exhibit renoprotective effects and ameliorate the glomerulosclerosis and tubulointerstitial fibrosis in different diseases (Kanasaki et al., 2014; Vavrinec et al., 2014; Tanaka et al., 2016; Tsuprykov et al.,

**TABLE 1 |** Evidence of ferroptosis inhibitors alleviates renal fibrosis *in vitro*.

Agents	Work concentration	Cell line model	Effects	References
Rosiglitazone	1 $\mu$ M	NRK-52E (Rat renal tubule epithelial cells)/HK2 Cells (Human Kidney 2)	Blocks ferroptosis by Inhibiting ACSL4-mediated lipid peroxidation	Wang Y et al. (2020)
	1–50 $\mu$ M	Rat mesangial cells	Causes an anti-fibrotic effect in renal mesangial cells by increasing sphingosine kinase 1 levels	Koch et al. (2012)
Troglitazone	1–20 $\mu$ M	Rat mesangial cells	Causes an anti-fibrotic effect in renal mesangial cells by increasing sphingosine kinase 1 levels	Koch et al. (2012)
Pioglitazone	10 $\mu$ M	High glucose-induced profibrotic HK-2 Cell model	Reverses the high glucose-induced profibrotic by intervention of AP-1, TGF- $\beta$ 1, and the extracellular matrix protein fibronectin	Panchapakesan et al. (2005)
	5 $\mu$ M	TGF- $\beta$ 1-induced HK-2 Cell model	Improves mitochondrial functions and protects against renal fibrosis	Sun et al. (2017)
Vitamin E	100 $\mu$ M	TGF- $\beta$ 1-induced HK-2 Cell model	Inhibits TGF- $\beta$ 1-induced renal fibrosis	Wang et al. (2010)
Baicalein	20–80 $\mu$ M	TGF- $\beta$ 1-induced NRK-49F cells	Suppresses the TGF- $\beta$ 1 signaling and inducing mitochondrion-associated myofibroblast apoptosis	Wang et al. (2016); Hu et al. (2017)
Ferrostatin-1	10 $\mu$ M	TGF- $\beta$ 1-induced HK-2 Cell model	Inhibits TGF- $\beta$ 1-induced expression of $\alpha$ -SMA, col1a1 and fibronectin	Li et al. (2022)
Diphenylene iodonium	20 $\mu$ M	RMC (Rat kidney mesangial cells)	Suppresses methylglyoxal-induced renal fibrosis by inhibiting superoxide, and expression of TGF- $\beta$ 1 and fibronectin	Ho et al. (2007)
N-acetylcysteine	10 mM	Cisplatin-induced NRK-52E	Decreases cisplatin-induced renal interstitial fibrosis via sirtuin1 activation and p53 deacetylation	Li C et al. (2019)
Puerarin	50 $\mu$ M or 100 $\mu$ M	HK2	Ameliorates renal fibrosis by reducing oxidative stress induced-epithelial cell apoptosis via MAPK signal pathways	Zhou et al. (2017)
Trolox	1 $\mu$ M	Mouse renal CD cell line (M-1)	Blunts prorenin-dependent ROS formation and augmentation of profibrotic factors	Gonzalez et al. (2017)
Triiodothyronine	1 nM	HK2	Inhibits TGF $\beta$ 1 induced renal tubular epithelial to mesenchymal transition by increasing miR34a expression	Lu et al. (2013)
Linagliptin	100–251 $\mu$ M	Mouse proximal tubular cell	Attenuates FFA-bound albumin-induced tubular inflammation, fibrosis and apoptosis	Tanaka et al. (2016)
U0126	10 $\mu$ M	HRPTECs (human renal proximal tubular epithelial cells)	Reverses Interleukin-17A induces renal fibrosis	Weng et al. (2020)
	20 mM	Primary PTECs from mice kidneys and pig kidney proximal tubule (LLC-PK1) cell line	Inhibits TGF- $\beta$ 1-induced renal fibrosis	Chen et al. (2014)
Chloroquine	50 $\mu$ M	HKC-8 cells (human tubular epithelial cell line)	Reduces renal fibrosis via increasing extracellular urokinase and collagen degradation	Fox et al. (2016)
Lipoxstatin-1	0.5 $\mu$ M	HK2 and fibroblasts	Inhibits the proliferation and differentiation of fibroblasts by inhibiting the release of profibrotic factors released by ferroptotic tubular epithelial cells	Zhang et al. (2021)

2016; Uchida et al., 2017; Oraby et al., 2019; Pengrattachot et al., 2020; Tang et al., 2021).

#### 4.1.6 Others

Recent studies have demonstrated that lipoxstatin-1 attenuates renal fibrosis induced by UUO through inhibiting ferroptosis in renal tubular epithelial cells (Zhang et al., 2021). Ferrostatin-1 is a widely used ferroptosis blocker, which exhibits renoprotective effects in obesity-induced renal fibrosis, inflammatory cell infiltration by inhibiting ferroptosis in high-fat diet mice (Li et al., 2022). It might reverse pathological parameters and improve renal function of folic acid-induced AKI mice, which is a model for studying nephrotoxic tubule damage and gradual progression of renal fibrosis (Li X. et al., 2020). Puerarin has been demonstrated to protect against heart failure via mitigating ferroptosis (Liu et al., 2018), which also ameliorates renal fibrosis by reducing oxidative stress induced-epithelial cell apoptosis via MAPK signal pathways (Zhou et al., 2017).

Baicalein restrains ferroptosis by abrogating ALOX-mediated lipid peroxidation (Xie et al., 2016b; Yang et al., 2016), and can inhibit renal fibrosis in a variety of ways (Wang W. et al., 2015; Wang et al., 2016; Hu et al., 2017). U0126, the ERK inhibitor, was proved to protect against cell death induced by erastin in MEFs (Gao et al., 2015). It has also been reported to ameliorate renal fibrosis in different renal proximal tubular epithelial cells (Chen et al., 2014; Weng et al., 2020). FG-4592 pretreatment plays a protective role at the early stage of folic acid-induced renal fibrosis and other kidney injury through alleviating ferroptosis (Li X. et al., 2020). However, in the UUO mice model, even high dose treatment of FG-4592 has little effect on renal fibrosis (Kabei et al., 2020).

#### 4.2 Ferroptosis Inducers

Interventions preventing cell death could initially prevent parenchymal cell loss thus protecting the kidney early in the course of kidney damage, but they may also facilitate fibrosis by



**TABLE 2 |** Evidence of ferroptosis inhibitors alleviates renal fibrosis *in vivo*.

Agents	Dosage regimen	Animal or patient model	Effects	References
Rosiglitazone	5 mg/kg/day, for 12 weeks; 3 or 30 mg/kg/day for 8 weeks)	Chronic renal allograft dysfunction rats	Inhibits TGF- $\beta$ signaling and the renal tubular EMT	Kiss et al. (2010); Deng et al. (2019)
	3 mg/kg/day, for 4 weeks	Cyclosporine-induced renal injury rats	Inhibits TGF- $\beta$ signaling and apoptosis	Chung et al. (2005)
	5 mg/kg/day in drinking water, for 24 weeks	Diabetic nephropathy (DN) rats	Alleviates the glomerulosclerosis and tubulointerstitial fibrosis	Bilan et al. (2011)
Troglitazone	5 mg/kg/day, for 4 weeks	Aristolochic acid nephropathy mice	Reduces renal fibrosis	Shui et al. (2017)
	150 or 300 mg/kg/day, for 14 days	UUO mice	Attenuates renal interstitial fibrosis and inflammation through reduction of TGF- $\beta$	Kawai et al. (2009)
	6 mg/g chow for the first 12 weeks and 12 mg/g chow between weeks 13 and 25	Type 2 diabetes mellitus rats	Ameliorates mesangial expansion thus preventing development of glomerulosclerosis	McCarthy et al. (2000)
Pioglitazone	20 mg/kg/day, for 5 weeks	TGF- $\beta$ overexpressing transgenic mice	Prevents TGF- $\beta$ induced renal fibrosis by repressing EGR-1 and STAT3	Németh et al. (2019)
	10 mg/kg/day, for 2 weeks	UUO mice	Reduces renal tubulointerstitial fibrosis via miR-21-5p modulation	Han et al. (2010); Sun et al. (2019)
	10 mg/kg/day, for 8 weeks	5/6 nephrectomized rats	Reduces renal fibrosis by downregulating TGF- $\beta$ 1, fibronectin and collagen I	Sun et al. (2017)
Vitamin E	5 mg/kg/day, for 24 weeks	Spontaneously hypercholesterolemic rats	Exerts renoprotective effects and inhibits plasminogen activator inhibitor-1 level	Omasu et al. (2007)
	350 mg/kg, for 2 weeks	UUO mice	Inhibits the TGF- $\beta$ 1/Smad2/3 during EMT	Farias et al. (2020)
	100 mg/kg/day, for 9 weeks	Renal interstitial fibrosis rats	Inhibits renal interstitial fibrosis via alleviation of autophagic stress	Zhao et al. (2018)
Baicalein	25 mg/kg	Cyclosporine nephrotoxicity rats	Inhibits renal interstitial fibrosis by suppressing renal mRNA expression of COX II, HO I, TGF- $\beta$ , and osteopontin	Jenkins et al. (2001)
	50 or 100 mg/kg/day, for 7 days	UUO mice	Attenuates renal fibrosis by inhibiting inflammation via down-regulating NF-kappaB and MAPK signaling mitochondrion-associated myofibroblast apoptosis	Wang W et al. (2015)
	20 and 30 mg/kg/day in 2–3 divided doses	Patients with ADCK4-related glomerulopathy	Appeared renoprotective effects with preserved eGFR and reduced proteinuria	Atmaca et al. (2017)
N-acetylcysteine	500 mg/kg/day, for 9–11 weeks	Cisplatin-induced mice	Decrease cisplatin-induced renal interstitial fibrosis via sirtuin1 activation and p53 deacetylation	Li C et al. (2019)
	40 mg/kg/day; 8 weeks	Dilated Cardiomyopathy mice	Attenuates tubulointerstitial and glomerular fibrosis and renal oxidized glutathione levels	Giam et al. (2017)
	250 mg/kg/day, for 7 days	UUO mice	Alleviate angiotensin II-mediated renal fibrosis	Shen et al. (2016)
Puerarin	150 mg/kg/day, for 4 weeks	Chronic cyclosporine nephropathy mice	Attenuated tubulointerstitial fibrosis in p-AKT/p-FoxO1 pathway	Piao et al. (2013)
	50 mg/kg or 100 mg/kg, for 7 days	UUO mice	Ameliorates renal fibrosis by reducing oxidative stress induced-epithelial cell apoptosis via MAPK signal pathways	Zhou et al. (2017)
	30 mg/kg/day, for 7 or 14 days	UUO mice	Reduced renal fibrosis through manipulation of 5-lipoxygenase pathway	Montford et al. (2019)
Zileuton	10 mg/kg, given twice; 1 h before and 12 h after cisplatin	Cisplatin-induced mice	Alleviates cisplatin nephrotoxicity, including tubular necrosis and interstitial fibrosis via renal oxidative/inflammatory/caspase-3 axis	Helmy et al. (2018)
	100 mg/kg/day, for 7 days	UUO mice	Prevents renal tubulointerstitial fibrosis by regulating TGF- $\beta$ -Smad signaling, oxidative stress, and inflammatory responses	Ikeda et al. (2014)
	100 mg/kg/day, for 7 days	UUO mice	Exhibits renoprotective role in human	Rajapurkar et al. (2013)
Deferiprone	50 mg/kg/day; for 6 months or 150 mg/kg/day; for 9 months	Patients with diabetes and non-diabetic glomerular disease	Exhibits renoprotective effects	Rajapurkar et al. (2013)
Ferrostatin-1	5 mg/kg, single use	FA-induced mice	Attenuates renal fibrosis with reduced NF- $\kappa$ B level and increased HO-1 level	Li Y et al. (2020)
Triiodothyronine	100 $\mu$ g/kg/day, for 2 weeks	5/6 nephrectomized rats	Plays a protective role at the early stage of FA-induced renal fibrosis through alleviating ferroptosis via Akt/GSK-3 $\beta$ -mediated Nrf2 activation	El Agaty, (2018)
FG-4592	10 mg/kg/day, for 2 days	FA-induced mice	Exhibits renoprotective effects by modulating macrophages M1/2	Li Y et al. (2020)
Alogliptin	40 mg/kg/day for 10 days	UUO mice	Exhibits renoprotective effects by modulating macrophages M1/2	Uchida et al. (2017)
Linagliptin	3 mg/kg/day, for 16 weeks	5/6 nephrectomized rats		Tsuprykov et al. (2016)

(Continued on following page)

**TABLE 2 |** (Continued) Evidence of ferroptosis inhibitors alleviates renal fibrosis *in vivo*.

Agents	Dosage regimen	Animal or patient model	Effects	References
	5 mg/kg/day, for 4 weeks	DN mice	Decreased interstitial fibrosis with decreased urine albumin-to-creatinine ratio	
Vildagliptin	3 mg/kg/day, for 4 weeks	High-fat diet-induced obese rats	Attenuated renal fibrosis by inhibiting EndMT, apoptosis and blocking the blocked the DPP4/CD32b/NF- $\kappa$ B signaling circuit	Kanasaki et al. (2014); Oraby et al. (2019); Tang et al. (2021)
	3 mg/kg/day, for 15 weeks	Zucker Diabetic Fatty (ZDF) rat	Attenuate renal lipid accumulation-induced lipotoxicity and reduced the TGF- $\beta$ level	Pengrattanachot et al. (2020)
Carvedilol	Chow supplemented with 2,400 p.p.m., for 6 weeks	Spontaneously hypertensive stroke-prone (SHR-SP) rats	Effectively prevent glomerulosclerosis and restored myogenic constriction	Vavrinec et al. (2014)
	60 mg/kg/day	Hypertensive rats	Shows renoprotective effects by inhibiting TGF- $\beta$	Wong et al. (2001)
Chloroquine	20 mg/kg, 3 times a week, for 15 days	UUO mice and chronic ischemia reperfusion injury mice	Slows down the development of interstitial fibrosis and tubular atrophy	Jovanovic et al. (2005)
			Reduces renal fibrosis via increasing extracellular urokinase and collagen degradation	Fox et al. (2016)
Liproxstatin-1	10 mg/kg/d for 14 consecutive days	UUO mice	Attenuates the expression of profibrotic factors	Zhang et al. (2021)

blocking the downregulation of fibroblast numbers later in the course of the renal disease. EMT, characterized by loss of E-cadherin, can facilitate ferroptosis, and upregulate transcription factors, including SNAI1, ZEB1, and, TWIST1, inducing EMT-mediated tumor metastasis, elevates ferroptosis sensitivity in turn (Wu et al., 2019), while E-cadherin-mediated cell-cell contacts has been demonstrated to protect against ferroptosis (Yang W.-H. et al., 2019; Wenz et al., 2019; Wu et al., 2019). Furthermore, human cancer cell lines and organoids with a highly mesenchymal-like cell state are selectively vulnerable to ferroptosis (Viswanathan et al., 2017). It is speculated that EMT might confer susceptibility to ferroptosis-based therapies in cancers (Chen et al., 2021). Analogizing to cancer cells, it is possible that induction of ferroptosis could also attenuate renal fibrosis by selectively killing mesenchymal-like cells transited from epithelium and endothelium.

Interestingly, some ferroptosis inducers (e.g., Acetaminophen, artemisinin and its derivatives, sorafenib, sulfasalazine, and withaferin A) have also been demonstrated to alleviate renal fibrosis in various models, suggesting a complex relationship between ferroptosis and renal fibrosis (Table 4). Reportedly, sorafenib, an xCT inhibitor, can inhibit the TGF- $\beta$ /Smad3-induced EMT signaling (Jia et al., 2015) and suppress the CXCR3/CXCL11-mediated macrophage infiltration (Ma et al., 2016), ameliorating renal fibrosis. Besides, an xCT inhibitor-sulfasalazine also play a protective role against renal fibrosis in the UUO rats, with decreased level of TGF- $\beta$ 1, ROS, and lipid peroxides (Demirbilek et al., 2007). Acetaminophen, a resistance indicator of fibrosis, and a reduction of tubular EMT in glomerular sclerosis may prevent renal oxidative stress in an obese Zucker mouse model (Wang et al., 2013; Lőrincz et al., 2015), and exerts renoprotective effects (Wang C. et al., 2015). In different models, artemisinin and its derivatives have been reported to induce ferroptosis by triggering ROS, promoting ferritin degradation, and regulating xCT/GPX4 axis (Louandre et al., 2013; Louandre et al., 2015; Sun et al., 2016), thus alleviating

renal fibrosis (Cao et al., 2016; Zhang et al., 2017; Wen et al., 2019; Zhang et al., 2019; Liu et al., 2020). Withaferin A can down-regulate pro-fibrotic factors, inflammatory signaling molecules, and ER stress-related molecules and improve kidney function by decreasing uric acid (Chen et al., 2020; Zhao et al., 2021), it could also induce ferroptosis via the NRF2 pathway by targeting KEAP1 or inactivating GPX4 (Hassannia et al., 2018).

Besides, erastin and sorafenib could induce ferroptosis in hepatic stellate cells and are potential drugs for the treatment of hepatic fibrosis (Zhang et al., 2018). Neratinib, a demonstrated ferroptosis inducer in breast cancer (Nagpal et al., 2019), has also been shown to inhibit liver fibrosis (Park et al., 2020). Fluvastatin suppressed interstitial renal fibrosis and oxidative stress in UUO mice model (Moriyama et al., 2001) and NRK-49F cells (Ikeuchi et al., 2004). Overall, these highlight the possibility of inducing ferroptosis to achieve remission of renal fibrosis.

## 5 OTHER PROGRAMMED CELL DEATH AND FERROPTOSIS IN RENAL FIBROSIS

It is considered that ferroptosis interacts extensively with other modes of cell death, and even distinct from other types of programmed cell death (PCD). Multiple types of PCD have been discovered and well-studied, including apoptosis, necroptosis, pyroptosis and ferroptosis, which we would like to briefly overview their relationship with renal fibrosis.

Apoptosis is regarded as a mechanism of self-protection that eliminates dead or damaged cells that form during the physiological process of aging, and is the best-known form of PCD which was first described in 1972 (Argüelles et al., 2019). Inhibition of apoptosis has been shown to reduce kidney fibrosis (Tanaka et al., 2003; Portilla, 2014), and a number of molecules or drugs have been reported to protect the kidneys by inhibiting apoptosis (Tanaka et al., 2005).

**TABLE 3 |** Mechanisms of ferroptosis inhibitors restraining ferroptosis.

Agents	Work concentration	Effects	Model	References
Rosiglitazone	1 $\mu$ M 10–30 $\mu$ M  0.4–0.5 mg/kg	Inhibits ACSL4-mediated lipid peroxidation Inhibits ACSL4-mediated lipid peroxidation  Inhibits ACSL4-mediated lipid peroxidation	NRK-52E/HK2 Cells Pfa1 cells (Breast cancer cell line)  Ischemia/reperfusion (I/R) injury mice	Wang Y et al. (2020) Doll et al. (2017); Kagan et al. (2017)  Li Y et al. (2019); Xu et al. (2020)
Troglitazone	10–30 $\mu$ M	Inhibits ACSL4-mediated lipid peroxidation	Breast cancer cell lines	Doll et al. (2017)
Pioglitazone	10–30 $\mu$ M 10 $\mu$ M	Inhibits ACSL4-mediated lipid peroxidation Suppresses sulfasalazine-induced ferroptosis	Breast cancer cell lines HNC/SNU cell lines	Doll et al. (2017) Kim et al. (2018)
Vitamin E	100 $\mu$ M	Inhibits lipid peroxidation by scavenging ROS	HT-1080/BJ cell lines	Yang et al. (2014); Shimada et al. (2016)
Baicalein	10 $\mu$ M	Inhibits ALOX-mediated lipid peroxidation	G-401 cell line (a human renal carcinoma cell line)	Yang et al. (2016)
CoQ10	10 $\mu$ M	May involve reprogramming of lipid metabolism in a way that is not conducive to the execution of ferroptosis	HT-1080 cells	Shimada et al. (2016)
Diphenylene iodonium	1 $\mu$ M	Inhibits NOX-mediated lipid peroxidation	SHSY5Y cells	Hou et al. (2019)
N-acetylcysteine	1 mM  40 mg/kg/day, for 7 days  1 mM	Inhibits toxic arachidonic acid products of nuclear ALOX5 Inhibits toxic arachidonic acid products of nuclear ALOX5 Inhibits erastin-induced ferroptosis through supplementing GSH	Primary cortical neurons Collagenase-induced intracerebral hemorrhage mice HT-1080 cells	Karuppagounder et al. (2018) Karuppagounder et al. (2018) Yang et al. (2014)
Puerarin	20 $\mu$ M  100 mg/kg/day or 200 mg/kg/day, for 12 weeks	Suppresses erastin- or isoprenaline-induced ferroptosis Suppresses erastin- or isoprenaline-induced ferroptosis	H9c2 cells Heart failure rats	Liu et al. (2018) Liu et al. (2018)
Trolox	100 $\mu$ M	Inhibits lipid peroxidation	HT-1080 cells	Dixon et al. (2012)
Zileuton	10–100 $\mu$ M	Inhibits lipid peroxidation by suppressing ALOX5	HT22 neuronal cells	Liu et al. (2015)
Deferoxamine	100 $\mu$ M	Inhibits iron-mediated lipid peroxidation	HT-1080 cells	Dixon et al. (2012)
Deferoxamine	100 mg/kg/day, for 7 days	Inhibits lipid peroxidation via ferroptotic-specific mitochondria genes	Spinal cord injury rats	Yao et al. (2019)
Deferiprone	100 $\mu$ M	Inhibits iron-mediated lipid peroxidation	LUHMES cells (Lund human mesencephalic cells)	Do Van et al. (2016)
Ferrostatin-1	0.1–10 $\mu$ M	Scavenge initiating alkoxyl radicals produced by ferrous iron from lipid hydroperoxides	HT-1080/HEK293T/LUHMES cells	Dixon et al. (2012); Do Van et al. (2016); Miotto et al. (2020)
Triiodothyronine	10 $\mu$ M	Inhibits lipid peroxidation	H9c2 cells	Mishima et al. (2020)
FG-4592	10 mg/kg	Alleviates ferroptosis via Akt/GSK-3 $\beta$ -mediated Nrf2 activation	FA-induced mice	Li Y et al. (2020)
Alogliptin	10 $\mu$ M	inhibits NOX1-mediated lipid peroxidation	TP53 <sup>-/-</sup> or TP53-deficient CRC cells (HCT116 and SW48)	Xie et al. (2017)
Linagliptin	10 $\mu$ M	inhibits NOX1-mediated lipid peroxidation	TP53 <sup>-/-</sup> or TP53-deficient CRC cells (HCT116 and SW48)	Xie et al. (2017)
Vildagliptin	10 $\mu$ M	inhibits NOX1-mediated lipid peroxidation	TP53 <sup>-/-</sup> or TP53-deficient CRC cells (HCT116 and SW48)	Xie et al. (2017)
U0126	10 $\mu$ M	Inhibits lipid peroxidation independent from MEK activity	MEFs (mouse embryonic fibroblasts)	Gao et al. (2015)
Carvedilol	0.1, 1, and 1 $\mu$ M	Inhibits lipid peroxidation	H9C2 cells	Mishima et al. (2020)
Chloroquine	50 $\mu$ M	Blocks ferroptosis at earlier time points, but the inhibitory effect will be gradually lost at later time points	MEFs and HT1080 cells	Gao et al. (2016)

Necroptosis, a mode of cell death dependent on the activity of RIPK1 and RIPK3 kinases, which is characterized by permeable and rupture of cell membranes can also trigger necroinflammation and release of DAMPs (Belavgeni et al., 2020). Inhibiting necroptosis was demonstrated to attenuate different type of renal fibrosis (Zhu et al., 2015; Zhu et al., 2016; Xiao et al., 2017; Dai et al., 2020; Huang et al., 2020).

Pyroptosis is caused by the cleavage of Gasdermins by various caspases, and is subsequently executed by the insertion of the N-terminal fragment of cleaved Gasdermins into the plasma membrane, facilitate plasma membrane rupture and the release of pro-inflammatory products, which has been considered as a key fibrotic mechanism in the kidney pathology development (Kesavardhana et al., 2020; Cuevas and Pelegrin, 2021). It is a form of lytic programmed cell death

**TABLE 4 |** Evidence of ferroptosis inducers alleviates renal fibrosis *in vitro* and *in vivo*.

Agents	Dosage	Model	Effects	References
Acetaminophen	30 mg/kg/day via drinking water for 26 weeks 3 $\mu$ M or 10 $\mu$ M	Obese Zucker rat model	Prevents tubulointerstitial fibrosis and glomerulosclerosis by alleviating tubular EMT and inhibiting renal oxidative stress	Wang et al. (2013)
		Human renal mesangial cells (HRMCs)	Exerts renoprotective effects by diminishing renal oxidative stress and p38/MAPK hyper-phosphorylation	Wang C et al. (2015)
Artemisinin	100 mg/kg/day for 16 weeks 25, 50, 100 $\mu$ M	Rats with 5/6 nephrectomy	Attenuates tubulointerstitial inflammation and fibrosis via the NF-kappaB/NLRP3 pathway	Wen et al. (2019)
		Ang II-induced HK2	Attenuates tubulointerstitial inflammation and fibrosis via the NF-kappaB/NLRP3 pathway	Wen et al. (2019)
Artesunate	30 or 60 mg/kg/day for 2 weeks 0.01, 0.1, and 1 $\mu$ g/ml	UUO rats	Attenuates renal fibrosis with the up-regulation of BMP-7 and down-regulation of USAG-1	Cao et al. (2016)
		TGF- $\beta$ 1-induced NRK-52E cells	Ameliorates TGF- $\beta$ 1-induced renal interstitial fibrosis by inhibition of EMT.	Zhang et al. (2017)
Dihydroartemisinin	40 mg/kg/day for 2 weeks 10 $\mu$ M	UUO mice	Attenuates renal fibrosis through regulation of fibroblast proliferation and differentiation via PI3K/AKT pathway and MALAT1/miR-145/FAK axis	Zhang et al. (2019); Liu et al. (2020)
		Primary human kidney fibroblasts/HK2 cells	Attenuates renal fibrosis through regulation of fibroblast proliferation and differentiation via PI3K/AKT pathway and MALAT1/miR-145/FAK axis	Zhang et al. (2019); Liu et al. (2020)
Sorafenib	20, 40, 80 mg/kg/day, for 14 or 21 days 5 mg/kg/day, for 10 days 1, 5, and 10 $\mu$ M	UUO rats	Ameliorates renal fibrosis by inhibiting TGF- $\beta$ /Smad3-induced EMT signaling	Jia et al. (2015)
		UUO mice	Ameliorates renal fibrosis by inhibition of macrophage infiltration via the CXCR3/CXCL11 pathway	Ma et al. (2016)
		NRK-52E cells	Ameliorates renal fibrosis by inhibiting TGF- $\beta$ /Smad3-induced EMT signaling	Jia et al. (2015)
Sulfasalazine	100 mg/kg/day, for 7 days	UUO rats	Protects against the renal interstitial inflammation and tissue damage	Demirbilek et al. (2007)
Withaferin A	3 mg/kg/day, for 14 days 0.1, 0.5, and 1 $\mu$ M 3, 5, 10 mg/kg/day, for 7 days	UUO mice	Reverses the increases in the protein levels of pro-fibrotic factors, inflammatory signaling molecules, and ER stress-related molecules	Chen et al. (2020)
		UA-induced NRK-52E cells	Improves kidney function by decreasing uric acid via regulation of xanthine oxidase and transporter genes in renal tubular cells	Zhao et al. (2021)
		Hypouricemic mouse model	Improves kidney function by decreasing uric acid via regulation of xanthine oxidase and transporter genes in renal tubular cells	Zhao et al. (2021)

initiated by inflammasomes, and HMGB1 released from pyroptotic renal tubular cells amplified inflammatory responses, which recruits immune cells to promote tissue healing and contributes to renal fibrogenesis (Raupach et al., 2006; Li Y. et al., 2021). GSDME-mediated pyroptosis is responsible for renal tubule injury and subsequently fibrosis induced by ureteral obstruction, 5/6 nephrectomy, and DN (Li W. et al., 2021; Li Y. et al., 2021; Wu et al., 2021). For more details, interested readers may refer to these excellent recently published reviews.

In general, apoptosis is a non-lytic form of cell death and is described as an active programmed cell division process to avoid triggering inflammation to remain immunologically silent, which may confine the contribution of subsequently renal fibrosis (Fink and Cookson, 2005). However, ferroptosis, pyroptosis, and necroptosis are all considered as lytic cell death, which can contribute to the release of several immune-stimulatory DAMPs, that trigger immune responses (Tang et al., 2020). Different lytic cell deaths serve distinct purposes, determine different profiles of the inflammatory infiltrate and thus determine the association between cell death and long-term renal fibrosis (Belavgeni et al., 2020).

The critical role of necroptotic pathway lies in the host response to pathogen infection, which is triggered when apoptosis is hindered

(Upton et al., 2010; Brault and Oberst, 2017). Pyroptosis is a primary cellular response following the sensing of pathogens as well as danger signals, which mainly includes DAMPs, pathogen-associated molecular patterns (PAMPs). The most significant initiator of pyroptosis is NLRP3 inflammasome which can be activated by various stimuli (Jo et al., 2016). However, as mentioned above, a key feature of ferroptosis is intracellular overload iron and catalysis of lipid peroxidation, which are both common and worsen in CKD with disease progression (Naito et al., 2015). In addition, proactive high-dose iron supplementation due to renal anemia also led to renal iron toxicity (Tanaka and Tanaka, 2015; van Raaij et al., 2018b). Thus, diverse chronic kidney disease creates an appropriate condition for the occurrence of ferroptosis. Although these different types of PCD have multiple functions in various physiological states and in a host's response to external damage, there is clear evidence of crosstalk or interactions (Wang and Kanneganti, 2021).

## 6 CONCLUSION AND PERSPECTIVE

We have witnessed an outbreak of ferroptosis research in biomedicine over the past decades. Generally, it is a form of iron-dependent, lipid peroxidation-mediated regulated necrosis, which is strictly under controlled. This type of cell death may play a fairly important role

in a wider range of physiological and pathophysiological processes (Qiu et al., 2020). On the other hand, a variety of studies on ferroptosis have detected only a few non-specific indicators, such as glutathione (GSH) levels and GPX4 levels, to demonstrate the presence of ferroptosis, which may possibly exaggerate the role of ferroptosis to some extent due to the variety of oxidative stress.

Despite a large number of recent studies have implicated that ferroptosis is related to renal fibrosis, its complex and finely concrete mechanism is still far from being resolved. More research is warranted to elucidate whether and how pharmaceuticals or chemicals mentioned in this article affect renal fibrosis by regulating ferroptosis.

## REFERENCES

- Abo El Gheit, R., and Emam, M. (2016). Targeting Heme Oxygenase-1 in Early Diabetic Nephropathy in Streptozotocin-Induced Diabetic Rats. *Acta Physiol. Hung* 103 (4), 413–427. doi:10.1556/2060.103.2016.4.001
- Adedoyin, O., Boddu, R., Traylor, A., Lever, J. M., Bolisetty, S., George, J. F., et al. (2018). Heme Oxygenase-1 Mitigates Ferroptosis in Renal Proximal Tubule Cells. *Am. J. Physiology-Renal Physiol.* 314 (5), F702–F714. doi:10.1152/ajprenal.00044.2017
- Altman, B. J., Stine, Z. E., and Dang, C. V. (2016). From Krebs to Clinic: Glutamine Metabolism to Cancer Therapy. *Nat. Rev. Cancer.* 16 (10), 619–634. doi:10.1038/nrc.2016.71
- Argüelles, S., Guerrero-Castilla, A., Cano, M., Muñoz, M. F., and Ayala, A. (2019). Advantages and Disadvantages of Apoptosis in the Aging Process. *Ann. N.Y. Acad. Sci.* 1443 (1), 20–33. doi:10.1111/nyas.14020
- Arosio, P., Ingrassia, R., and Cavadini, P. (2009). Ferritins: a Family of Molecules for Iron Storage, Antioxidation and More. *Biochim. Biophys. Acta (Bba) - Gen. Subjects* 1790 (7), 589–599. doi:10.1016/j.bbagen.2008.09.004
- Atmaca, M., Gulhan, B., Korkmaz, E., Inozu, M., Soylemezoglu, O., Candan, C., et al. (2017). Follow-up Results of Patients with ADCK4 Mutations and the Efficacy of CoQ10 Treatment. *Pediatr. Nephrol.* 32 (8), 1369–1375. doi:10.1007/s00467-017-3634-3
- Bannai, S., Tsukeda, H., and Okumura, H. (1977). Effect of Antioxidants on Cultured Human Diploid Fibroblasts Exposed to Cystine-Free Medium. *Biochem. Biophysical Res. Commun.* 74 (4), 1582–1588. doi:10.1016/0006-291x(77)90623-4
- Battin, E. E., and Brumaghim, J. L. (2009). Antioxidant Activity of Sulfur and Selenium: a Review of Reactive Oxygen Species Scavenging, Glutathione Peroxidase, and Metal-Binding Antioxidant Mechanisms. *Cell Biochem Biophys.* 55 (1), 1–23. doi:10.1007/s12013-009-9054-7
- Bedard, E. L. R., Jiang, J., Parry, N., Wang, H., Liu, W., Garcia, B., et al. (2005). Peritransplant Treatment with Cobalt Protoporphyrin Attenuates Chronic Renal Allograft Rejection. *Transpl. Int* 18 (3), 341–349. doi:10.1111/j.1432-2277.2004.00062.x
- Belavgeni, A., Bornstein, S. R., and Linkermann, A. (2019). Prominin-2 Suppresses Ferroptosis Sensitivity. *Developmental Cell* 51 (5), 548–549. doi:10.1016/j.devcel.2019.11.004
- Belavgeni, A., Meyer, C., Stumpf, J., Hugo, C., and Linkermann, A. (2020). Ferroptosis and Necroptosis in the Kidney. *Cell Chem. Biol.* 27 (4), 448–462. doi:10.1016/j.chembiol.2020.03.016
- Bersuker, K., Hendricks, J. M., Li, Z., Magtanong, L., Ford, B., Tang, P. H., et al. (2019). The CoQ Oxidoreductase FSP1 Acts Parallel to GPX4 to Inhibit Ferroptosis. *Nature* 575 (7784), 688–692. doi:10.1038/s41586-019-1705-2
- Bieri, J. G. (1959). An Effect of Selenium and Cystine on Lipid Peroxidation in Tissues Deficient in Vitamin E. *Nature* 184 (Suppl. 15), 1148–1149. doi:10.1038/1841148a0
- Bilan, V. P., Salah, E. M., Bastacky, S., Jones, H. B., Mayers, R. M., Zinker, B., et al. (2011). Diabetic Nephropathy and Long-Term Treatment Effects of Rosiglitazone and Enalapril in Obese ZSF1 Rats. *J. Endocrinol.* 210 (3), 293–308. doi:10.1530/JOE-11-0122
- Bondi, C. D., Manickam, N., Lee, D. Y., Block, K., Gorin, Y., Abboud, H. E., et al. (2010). NAD(P)H Oxidase Mediates TGF- $\beta$ 1-Induced Activation of Kidney

## AUTHOR CONTRIBUTIONS

RYT, MG, YHM and YZ developed the theoretical formalism. ZJW, JJZ, HZ and CJS contributed to the final version of the manuscript.

## FUNDING

This study was supported by the National Natural Science Foundation of China (Grant no. 82070769).

- Myofibroblasts. *J. Am. Soc. Nephrol.* 21 (1), 93–102. doi:10.1681/ASN.2009020146
- Brault, M., and Oberst, A. (2017). Controlled Detonation: Evolution of Necroptosis in Pathogen Defense. *Immunol. Cell Biol.* 95 (2), 131–136. doi:10.1038/icb.2016.117
- Brittenham, G. M. (2011). Iron-Chelating Therapy for Transfusional Iron Overload. *N. Engl. J. Med.* 364 (2), 146–156. doi:10.1056/NEJMc1004810
- Brown, C. W., Amante, J. J., Chhoy, P., Elaimy, A. L., Liu, H., Zhu, L. J., et al. (2019). Prominin2 Drives Ferroptosis Resistance by Stimulating Iron Export. *Developmental Cell* 51 (5), 575–586. doi:10.1016/j.devcel.2019.10.007
- Canonne-Hergaux, F., and Gros, P. (2002). Expression of the Iron Transporter DMT1 in Kidney from Normal and Anemic Mice. *Kidney Int.* 62 (1), 147–156. doi:10.1046/j.1523-1755.2002.00405.x
- Cao, J., Wang, W., Li, Y., Xia, J., Peng, Y., Zhang, Y., et al. (2016). Artesunate Attenuates Unilateral Ureteral Obstruction-Induced Renal Fibrosis by Regulating the Expressions of Bone Morphogenetic Protein-7 and Uterine Sensitization-Associated Gene-1 in Rats. *Int. Urol. Nephrol.* 48 (4), 619–629. doi:10.1007/s11255-016-1232-0
- Cao, J. Y., and Dixon, S. J. (2016). Mechanisms of Ferroptosis. *Cell. Mol. Life Sci.* 73 (11–12), 2195–2209. doi:10.1007/s00018-016-2194-1
- Chang, L., Chiang, S.-K., Chen, S.-E., Yu, Y.-L., Chou, R.-H., and Chang, W.-C. (2018). Heme Oxygenase-1 Mediates BAY 11-7085 Induced Ferroptosis. *Cancer Lett.* 416, 124–137. doi:10.1016/j.canlet.2017.12.025
- Chen, C.-M., Chung, Y.-P., Liu, C.-H., Huang, K.-T., Guan, S.-S., Chiang, C.-K., et al. (2020). Withaferin A Protects against Endoplasmic Reticulum Stress-Associated Apoptosis, Inflammation, and Fibrosis in the Kidney of a Mouse Model of Unilateral Ureteral Obstruction. *Phytomedicine* 79, 153352. doi:10.1016/j.phymed.2020.153352
- Chen, H., Zheng, C., Zhang, Y., Chang, Y.-Z., Qian, Z.-M., and Shen, X. (2006). Heat Shock Protein 27 Downregulates the Transferrin Receptor 1-mediated Iron Uptake. *Int. J. Biochem. Cell Biol.* 38 (8), 1402–1416. doi:10.1016/j.biocel.2006.02.006
- Chen, W.-C., Lin, H.-H., and Tang, M.-J. (2014). Regulation of Proximal Tubular Cell Differentiation and Proliferation in Primary Culture by Matrix Stiffness and ECM Components. *Am. J. Physiology-Renal Physiol.* 307 (6), F695–F707. doi:10.1152/ajprenal.00684.2013
- Chen, X., Kang, R., Kroemer, G., and Tang, D. (2021). Broadening Horizons: the Role of Ferroptosis in Cancer. *Nat. Rev. Clin. Oncol.* 18, 280–296. doi:10.1038/s41571-020-00462-0
- Chen, X., Xu, S., Zhao, C., and Liu, B. (2019). Role of TLR4/NADPH Oxidase 4 Pathway in Promoting Cell Death Through Autophagy and Ferroptosis During Heart Failure. *Biochem. Biophysical Res. Commun.* 516 (1), 37–43. doi:10.1016/j.bbrc.2019.06.015
- Cheng, H.-T., Yen, C.-J., Chang, C.-C., Huang, K.-T., Chen, K.-H., Zhang, R.-Y., et al. (2015). Ferritin Heavy Chain Mediates the Protective Effect of Heme Oxygenase-1 Against Oxidative Stress. *Biochim. Biophys. Acta (Bba) - Gen. Subjects.* 1850 (12), 2506–2517. doi:10.1016/j.bbagen.2015.09.018
- Chung, B. H., Li, C., Sun, B. K., Lim, S. W., Ahn, K. O., Yang, J. H., et al. (2005). Rosiglitazone Protects against Cyclosporine-Induced Pancreatic and Renal Injury in Rats. *Am. J. Transpl.* 5 (8), 1856–1867. doi:10.1111/j.1600-6143.2005.00979.x



- Corona, D., Ekser, B., Gioco, R., Caruso, M., Schipa, C., Veroux, P., et al. (2020). Heme-Oxygenase and Kidney Transplantation: A Potential for Target Therapy? *Biomolecules* 10 (6), 840. doi:10.3390/biom10060840
- Cuevas, S., and Pelegrin, P. (2021). Pyroptosis and Redox Balance in Kidney Diseases. *Antioxid. Redox Signaling* 35 (1), 40–60. doi:10.1089/ars.2020.8243
- Daenen, K., Andries, A., Mekahli, D., Van Schepdael, A., Jouret, F., and Bammens, B. (2019). Oxidative Stress in Chronic Kidney Disease. *Pediatr. Nephrol.* 34 (6), 975–991. doi:10.1007/s00467-018-4005-4
- Dai, Q., Zhang, Y., Liao, X., Jiang, Y., Lv, X., Yuan, X., et al. (2020). Fluorofenidone Alleviates Renal Fibrosis by Inhibiting Necroptosis through RIPK3/MLKL Pathway. *Front. Pharmacol.* 11, 534775. doi:10.3389/fphar.2020.534775
- Das, S., Neelamegam, K., Peters, W. N., Periyasamy, R., and Pandey, K. N. (2020). Depletion of cyclic-GMP Levels and Inhibition of cGMP-dependent Protein Kinase Activate P21<sup>Cip1</sup>/p27<sup>Kip1</sup> Pathways and lead to Renal Fibrosis and Dysfunction. *FASEB J.* 34 (9), 11925–11943. doi:10.1096/fj.202000754R
- de Carvalho, C., and Caramujo, M. (2018). The Various Roles of Fatty Acids. *Molecules* 23 (10), 2583. doi:10.3390/molecules23102583
- de Swart, L., Hendriks, J. C. M., van der Vorm, L. N., Cabantchik, Z. I., Evans, P. J., Hod, E. A., et al. (2016). Second International Round Robin for the Quantification of Serum Non-transferrin-bound Iron and Labile Plasma Iron in Patients with Iron-Overload Disorders. *Haematologica* 101 (1), 38–45. doi:10.3324/haematol.2015.133983
- Dejana, E., Hirschi, K. K., and Simons, M. (2017). The Molecular Basis of Endothelial Cell Plasticity. *Nat. Commun.* 8, 14361. doi:10.1038/ncomms14361
- Demirbilek, S., Emre, M. H., Aydin, E. N., Edali, M. N., Aksoy, R. T., Akin, M., et al. (2007). Sulfasalazine Reduces Inflammatory Renal Injury in Unilateral Ureteral Obstruction. *Pediatr. Nephrol.* 22 (6), 804–812. doi:10.1007/s00467-006-0416-8
- Deng, J., Xia, Y., Zhou, Q., Wang, X., Xiong, C., Shao, X., et al. (2019). Protective Effect of Rosiglitazone on Chronic Renal Allograft Dysfunction in Rats. *Transpl. Immunol.* 54, 20–28. doi:10.1016/j.trim.2019.01.002
- Dhungana, S., Taboy, C. H., Zak, O., Larvie, M., Crumbliss, A. L., and Aisen, P. (2004). Redox Properties of Human Transferrin Bound to its Receptor. *Biochemistry* 43 (1), 205–209. doi:10.1021/bi0353631
- Dixon, S. J., Lemberg, K. M., Lamprecht, M. R., Skouta, R., Zaitsev, E. M., Gleason, C. E., et al. (2012). Ferroptosis: an Iron-dependent Form of Nonapoptotic Cell Death. *Cell* 149 (5), 1060–1072. doi:10.1016/j.cell.2012.03.042
- Do Van, B., Gouel, F., Jonneaux, A., Timmerman, K., Gelé, P., Pétrault, M., et al. (2016). Ferroptosis, a Newly Characterized Form of Cell Death in Parkinson's Disease that Is Regulated by PKC. *Neurobiol. Dis.* 94, 169–178. doi:10.1016/j.nbd.2016.05.011
- Dodson, M., Castro-Portuguez, R., and Zhang, D. D. (2019). NRF2 Plays a Critical Role in Mitigating Lipid Peroxidation and Ferroptosis. *Redox Biol.* 23, 101107. doi:10.1016/j.redox.2019.101107
- Doll, S., Freitas, F. P., Shah, R., Aldrovandi, M., da Silva, M. C., Ingold, I., et al. (2019). FSP1 Is a Glutathione-independent Ferroptosis Suppressor. *Nature* 575 (7784), 693–698. doi:10.1038/s41586-019-1707-0
- Doll, S., Proneth, B., Tyurina, Y. Y., Panzilius, E., Kobayashi, S., Ingold, I., et al. (2017). ACSL4 Dictates Ferroptosis Sensitivity by Shaping Cellular Lipid Composition. *Nat. Chem. Biol.* 13 (1), 91–98. doi:10.1038/nchembio.2239
- Dolma, S., Lessnick, S. L., Hahn, W. C., and Stockwell, B. R. (2003). Identification of Genotype-Selective Antitumor Agents Using Synthetic Lethal Chemical Screening in Engineered Human Tumor Cells. *Cancer cell* 3 (3), 285–296. doi:10.1016/s1535-6108(03)00050-3
- Dominguez, J. H., Wu, P., Hawes, J. W., Deeg, M., Walsh, J., Packer, S. C., et al. (2006). Renal Injury: Similarities and Differences in Male and Female Rats with the Metabolic Syndrome. *Kidney Int.* 69 (11), 1969–1976. doi:10.1038/sj.ki.5000406
- Duann, P., Lin, P.-H., and Lianos, E. A. (2019). Data on Characterization of Metalloporphyrin-Mediated HO-1 and DAF Induction in Rat Glomeruli and Podocytes. *Data in brief* 22, 279–285. doi:10.1016/j.dib.2018.11.108
- Duni, A., Liakopoulos, V., Roumeliotis, S., Peschos, D., and Dounousi, E. (2019). Oxidative Stress in the Pathogenesis and Evolution of Chronic Kidney Disease: Untangling Ariadne's Thread. *Int. J. Mol. Sci.* 20 (15), 3711. doi:10.3390/ijms20153711
- Echeverría, C., Montorfano, I., Sarmiento, D., Becerra, A., Nuñez-Villena, F., Figueroa, X. F., et al. (2013). Lipopolysaccharide Induces a Fibrotic-like Phenotype in Endothelial Cells. *J. Cell. Mol. Med.* 17 (6), 800–814. doi:10.1111/jcmm.12066
- El Agaty, S. M. (2018). Triiodothyronine Attenuates the Progression of Renal Injury in a Rat Model of Chronic Kidney Disease. *Can. J. Physiol. Pharmacol.* 96 (6), 603–610. doi:10.1139/cjpp-2017-0252
- el Nahas, A. M., Muchaneta-Kubara, E. C., Essaway, M., and Soylemezoglu, O. (1997). Renal Fibrosis: Insights into Pathogenesis and Treatment. *Int. J. Biochem. Cell Biol.* 29 (1), 55–62. doi:10.1016/s1357-2725(96)00119-7
- Fang, X., Cai, Z., Wang, H., Han, D., Cheng, Q., Zhang, P., et al. (2020). Loss of Cardiac Ferritin H Facilitates Cardiomyopathy via Slc7a11-Mediated Ferroptosis. *Circ. Res.* 127 (4), 486–501. doi:10.1161/circresaha.120.316509
- Fang, X., Wang, H., Han, D., Xie, E., Yang, X., Wei, J., et al. (2019). Ferroptosis as a Target for protection against Cardiomyopathy. *Proc. Natl. Acad. Sci. U.S.A.* 116 (7), 2672–2680. doi:10.1073/pnas.1821022116
- Farias, J. S., Santos, K. M., Lima, N. K. S., Cabral, E. V., Aires, R. S., Veras, A. C., et al. (2020). Maternal Endotoxemia Induces Renal Collagen Deposition in Adult Offspring: Role of NADPH oxidase/TGF- $\beta$ 1/mmp-2 Signaling Pathway. *Arch. Biochem. Biophys.* 684, 108306. doi:10.1016/j.abb.2020.108306
- Feng, H., Schorpp, K., Jin, J., Yozwiak, C. E., Hoffstrom, B. G., Decker, A. M., et al. (2020). Transferrin Receptor Is a Specific Ferroptosis Marker. *Cell Rep.* 30 (10), 3411–3423. e3417. doi:10.1016/j.celrep.2020.02.049
- Feng, X., Wang, S., Sun, Z., Dong, H., Yu, H., Huang, M., et al. (2021). Ferroptosis Enhanced Diabetic Renal Tubular Injury via HIF-1 $\alpha$ /HO-1 Pathway in Db/db Mice. *Front. Endocrinol.* 12, 626390. doi:10.3389/fendo.2021.626390
- Fernández-Mendivil, C., Luengo, E., Trigo-Alonso, P., García-Magro, N., Negro, P., and López, M. G. (2021). Protective Role of Microglial HO-1 Blockade in Aging: Implication of Iron Metabolism. *Redox Biol.* 38, 101789. doi:10.1016/j.redox.2020.101789
- Fidai, I., Wachnowsky, C., and Cowan, J. A. (2016). Mapping Cellular Fe-S Cluster Uptake and Exchange Reactions - Divergent Pathways for Iron-Sulfur Cluster Delivery to Human Ferredoxins. *Metallomics* 8 (12), 1283–1293. doi:10.1039/c6mt00193a
- Fink, S. L., and Cookson, B. T. (2005). Apoptosis, Pyroptosis, and Necrosis: Mechanistic Description of Dead and Dying Eukaryotic Cells. *Infect. Immun.* 73 (4), 1907–1916. doi:10.1128/iai.73.4.1907-1916.2005
- Fox, C., Cocchiari, P., Oakley, F., Howarth, R., Callaghan, K., Leslie, J., et al. (2016). Inhibition of Lysosomal Protease Cathepsin D Reduces Renal Fibrosis in Murine Chronic Kidney Disease. *Sci. Rep.* 6, 20101. doi:10.1038/srep20101
- Fujimaki, M., Furuya, N., Saiki, S., Amo, T., Imamichi, Y., and Hattori, N. (2019). Iron Supply via NCOA4-Mediated Ferritin Degradation Maintains Mitochondrial Functions. *Mol. Cell Biol.* 39 (14), e00010. doi:10.1128/mcb.00010-19
- Galluzzi, L., Vitale, I., Aaronson, S. A., Abrams, J. M., Adam, D., Agostinis, P., et al. (2018). Molecular Mechanisms of Cell Death: Recommendations of the Nomenclature Committee on Cell Death 2018. *Cell Death Differ.* 25 (3), 486–541. doi:10.1038/s41418-017-0012-4
- Gao, M., Monian, P., Pan, Q., Zhang, W., Xiang, J., and Jiang, X. (2016). Ferroptosis Is an Autophagic Cell Death Process. *Cell Res* 26 (9), 1021–1032. doi:10.1038/cr.2016.95
- Gao, M., Monian, P., Quadri, N., Ramasamy, R., and Jiang, X. (2015). Glutaminolysis and Transferrin Regulate Ferroptosis. *Mol. Cell* 59 (2), 298–308. doi:10.1016/j.molcel.2015.06.011
- Geng, N., Shi, B. J., Li, S. L., Zhong, Z. Y., Li, Y. C., Xua, W. L., et al. (2018). Knockdown of Ferroportin Accelerates Erastin-Induced Ferroptosis in Neuroblastoma Cells. *Eur. Rev. Med. Pharmacol. Sci.* 22 (12), 3826–3836. doi:10.26355/eurrev\_201806\_15267
- Giam, B., Kuruppu, S., Chu, P.-Y., Smith, A. I., Marques, F. Z., Fiedler, A., et al. (2017). N-Acetylcysteine Attenuates the Development of Renal Fibrosis in Transgenic Mice with Dilated Cardiomyopathy. *Sci. Rep.* 7 (1), 17718. doi:10.1038/s41598-017-17927-5
- Gong, Y., Wang, N., Liu, N., and Dong, H. (2019). Lipid Peroxidation and GPX4 Inhibition Are Common Causes for Myofibroblast Differentiation and Ferroptosis. *DNA Cell Biol.* 38 (7), 725–733. doi:10.1089/dna.2018.4541
- Gonzalez, A. A., Zamora, L., Reyes-Martinez, C., Salinas-Parra, N., Roldan, N., Cuevas, C. A., et al. (2017). (Pro)renin Receptor Activation Increases Profibrotic Markers and Fibroblast-Like Phenotype through MAPK-dependent ROS Formation in Mouse Renal Collecting Duct Cells. *Clin. Exp. Pharmacol. Physiol.* 44 (11), 1134–1144. doi:10.1111/1440-1681.12813
- Gozzelino, R., and Arosio, P. (2016). Iron Homeostasis in Health and Disease. *Int. J. Mol. Sci.* 17 (1), 130. doi:10.3390/ijms17010130

- Gwinner, W., Landmesser, U., Brandes, R. P., Kubat, B., Plasger, J., Eberhard, O., et al. (1997). Reactive Oxygen Species and Antioxidant Defense in Puromycin Aminonucleoside Glomerulopathy. *J. Am. Soc. Nephrol.* 8 (11), 1722–1731. doi:10.1681/asn.v8i111722
- Gyurászová, M., Kovalčíková, A. G., Renczés, E., Kmeťová, K., Celec, P., Bábičková, J., et al. (2019). Oxidative Stress in Animal Models of Acute and Chronic Renal Failure. *Dis. Markers* 2019, 1–10. doi:10.1155/2019/8690805
- Han, J.-Y., Kim, Y.-J., Kim, L., Choi, S.-J., Park, I.-S., Kim, J.-M., et al. (2010). PPAR $\gamma$  Agonist and Angiotensin II Receptor Antagonist Ameliorate Renal Tubulointerstitial Fibrosis. *J. Korean Med. Sci.* 25 (1), 35–41. doi:10.3346/jkms.2010.25.1.35
- Harris, D. C., and Tay, Y.-C. (1997). Mitochondrial Function in Rat Renal Cortex in Response to Proteinuria and Iron. *Clin. Exp. Pharmacol. Physiol.* 24 (12), 916–922. doi:10.1111/j.1440-1681.1997.tb02719.x
- Hassannia, B., Wiernicki, B., Ingold, I., Qu, F., Van Herck, S., Tyurina, Y. Y., et al. (2018). Nano-Targeted Induction of Dual Ferroptotic Mechanisms Eradicates High-Risk Neuroblastoma. *J. Clin. Invest.* 128 (8), 3341–3355. doi:10.1172/jci99032
- He, L., Girijashanker, K., Dalton, T. P., Reed, J., Li, H., Soleimani, M., et al. (2006). ZIP8, Member of the Solute-Carrier-39 (SLC39) Metal-Transporter Family: Characterization of Transporter Properties. *Mol. Pharmacol.* 70 (1), 171–180. doi:10.1124/mol.106.024521
- He, T., Guan, X., Wang, S., Xiao, T., Yang, K., Xu, X., et al. (2015). Resveratrol Prevents High Glucose-Induced Epithelial-Mesenchymal Transition in Renal Tubular Epithelial Cells by Inhibiting NADPH oxidase/ROS/ERK Pathway. *Mol. Cell Endocrinol.* 402, 13–20. doi:10.1016/j.mce.2014.12.010
- Helmy, M. M., Hashim, A. A., and Mounier, S. M. (2018). Zileuton Alleviates Acute Cisplatin Nephrotoxicity: Inhibition of Lipoxigenase Pathway Favorably Modulates the Renal Oxidative/Inflammatory/Caspase-3 axis. *Prostaglandins & other lipid mediators* 135, 1–10. doi:10.1016/j.prostaglandins.2018.01.001
- Hider, R. C., and Kong, X. (2013). Iron Speciation in the Cytosol: an Overview. *Dalton Trans.* 42 (9), 3220–3229. doi:10.1039/c2dt32149a
- Hill, N. R., Fatoba, S. T., Oke, J. L., Hirst, J. A., O'Callaghan, C. A., Lasserson, D. S., et al. (2016). Global Prevalence of Chronic Kidney Disease - A Systematic Review and Meta-Analysis. *Plos One* 11 (7), e0158765. doi:10.1371/journal.pone.0158765
- Himmelfarb, J. (2005). Relevance of Oxidative Pathways in the Pathophysiology of Chronic Kidney Disease. *Cardiol. Clin.* 23 (3), 319–330. doi:10.1016/j.ccl.2005.03.005
- Ho, C., Lee, P.-H., Huang, W.-J., Hsu, Y.-C., Lin, C.-L., and Wang, J.-Y. (2007). Methylglyoxal-induced Fibronectin Gene Expression through Ras-Mediated NADPH Oxidase Activation in Renal Mesangial Cells. *Nephrology* 12 (4), 348–356. doi:10.1111/j.1440-1797.2007.00809.x
- Hou, L., Huang, R., Sun, F., Zhang, L., and Wang, Q. (2019). NADPH Oxidase Regulates Paraquat and Maneb-Induced Dopaminergic Neurodegeneration through Ferroptosis. *Toxicology* 417, 64–73. doi:10.1016/j.tox.2019.02.011
- Hou, W., Xie, Y., Song, X., Sun, X., Lotze, M. T., Zeh, H. J., 3rd, et al. (2016). Autophagy Promotes Ferroptosis by Degradation of Ferritin. *Autophagy* 12 (8), 1425–1428. doi:10.1080/15548627.2016.1187366
- Hu, Q., Gao, L., Peng, B., and Liu, X. (2017). Baicalin and Baicalein Attenuate Renal Fibrosis *In Vitro* via Inhibition of the TGF- $\beta$ 1 Signaling Pathway. *Exp. Ther. Med.* 14 (4), 3074–3080. doi:10.3892/etm.2017.4888
- Hu, W., Zhang, C., Wu, R., Sun, Y., Levine, A., and Feng, Z. (2010). Glutaminase 2, a Novel P53 Target Gene Regulating Energy Metabolism and Antioxidant Function. *Proc. Natl. Acad. Sci. U.S.A.* 107 (16), 7455–7460. doi:10.1073/pnas.1001006107
- Huang, H., Jin, W. W., Huang, M., Ji, H., Capen, D. E., Xia, Y., et al. (2020). Gentamicin-Induced Acute Kidney Injury in an Animal Model Involves Programmed Necrosis of the Collecting Duct. *J. Am. Soc. Nephrol.* 31 (9), 2097–2115. doi:10.1681/ASN.2019020204
- Ikeda, Y., Ozono, I., Tajima, S., Imao, M., Horinouchi, Y., Izawa-Ishizawa, Y., et al. (2014). Iron Chelation by Deferoxamine Prevents Renal Interstitial Fibrosis in Mice with Unilateral Ureteral Obstruction. *PloS one* 9 (2), e89355. doi:10.1371/journal.pone.0089355
- Ikeuchi, H., Kuroiwa, T., Yamashita, S., Hiramatsu, N., Maeshima, A., Kaneko, Y., et al. (2004). Fluvastatin Reduces Renal Fibroblast Proliferation and Production of Type III Collagen: Therapeutic Implications for Tubulointerstitial Fibrosis. *Nephron Exp. Nephrol.* 97 (4), e115–e122. doi:10.1159/000079176
- Ingold, I., Berndt, C., Schmitt, S., Doll, S., Poschmann, G., Buday, K., et al. (2018). Selenium Utilization by GPX4 Is Required to Prevent Hydroperoxide-Induced Ferroptosis. *Cell* 172 (3), 409–422. doi:10.1016/j.cell.2017.11.048
- Jenkins, J. K., Huang, H., Ndebele, K., and Salahudeen, A. K. (2001). Vitamin e Inhibits Renal Mrna Expression of cox ii, ho i, tgf $\beta$ ?, and Osteopontin in the Rat model of Cyclosporine Nephrotoxicity. *Transplantation* 71 (2), 331–334. doi:10.1097/00007890-200101270-00028
- Jha, J. C., Banal, C., Chow, B. S. M., Cooper, M. E., and Jandeleit-Dahm, K. (2016). Diabetes and Kidney Disease: Role of Oxidative Stress. *Antioxid. Redox Signaling* 25 (12), 657–684. doi:10.1089/ars.2016.6664
- Jia, L., Ma, X., Gui, B., Ge, H., Wang, L., Ou, Y., et al. (2015). Sorafenib Ameliorates Renal Fibrosis through Inhibition of TGF- $\beta$ -Induced Epithelial-Mesenchymal Transition. *Plos One* 10 (2), e0117757. doi:10.1371/journal.pone.0117757
- Jiang, L., Kon, N., Li, T., Wang, S.-J., Su, T., Hibshoosh, H., et al. (2015). Ferroptosis as a P53-Mediated Activity during Tumour Suppression. *Nature* 520 (7545), 57–62. doi:10.1038/nature14344
- Jo, E.-K., Kim, J. K., Shin, D.-M., and Sasakawa, C. (2016). Molecular Mechanisms Regulating NLRP3 Inflammasome Activation. *Cell Mol Immunol* 13 (2), 148–159. doi:10.1038/cmi.2015.95
- Jones, D. P. (2006). Redefining Oxidative Stress. *Antioxid. Redox Signal.* 8 (9–10), 1865–1879. doi:10.1089/ars.2006.8.1865
- Jovanovic, D., Jovovic, D., Mihailovic-Stanojevic, N., Miloradovic, Z., Dimitrijevic, J., Maksic, N., et al. (2005). Influence of Carvedilol on Chronic Renal Failure Progression in Spontaneously Hypertensive Rats with Adriamycin Nephropathy. *Clin. Nephrol.* 63 (6), 446–453. doi:10.5414/cnp63446
- Kabei, K., Tateishi, Y., Shiota, M., Osada-Oka, M., Nishide, S., Uchida, J., et al. (2020). Effects of Orally Active Hypoxia Inducible Factor Alpha Prolyl Hydroxylase Inhibitor, FG4592 on Renal Fibrogenic Potential in Mouse Unilateral Ureteral Obstruction Model. *J. Pharmacol. Sci.* 142 (3), 93–100. doi:10.1016/j.jphs.2019.12.002
- Kagan, V. E., Mao, G., Qu, F., Angeli, J. P. F., Doll, S., Croix, C. S., et al. (2017). Oxidized Arachidonic and Adrenic PEs Navigate Cells to Ferroptosis. *Nat. Chem. Biol.* 13 (1), 81–90. doi:10.1038/nchembio.2238
- Kanasaki, K., Shi, S., Kanasaki, M., He, J., Nagai, T., Nakamura, Y., et al. (2014). Linagliptin-mediated DPP-4 Inhibition Ameliorates Kidney Fibrosis in Streptozotocin-Induced Diabetic Mice by Inhibiting Endothelial-To-Mesenchymal Transition in a Therapeutic Regimen. *Diabetes* 63 (6), 2120–2131. doi:10.2337/db13-1029
- Kapturczak, M. H., Wasserfall, C., Brusko, T., Campbell-Thompson, M., Ellis, T. M., Atkinson, M. A., et al. (2004). Heme Oxygenase-1 Modulates Early Inflammatory Responses: Evidence From the Heme Oxygenase-1-Deficient Mouse. *Am. J. Pathol.* 165 (3), 1045–1053. doi:10.1016/s0002-9440(10)63365-2
- Karuppagounder, S. S., Alin, L., Chen, Y., Brand, D., Bourassa, M. W., Dietrich, K., et al. (2018). N-Acetylcysteine Targets 5 Lipoxigenase-Derived, Toxic Lipids and can Synergize With Prostaglandin E $_2$  to Inhibit Ferroptosis And Improve Outcomes Following Hemorrhagic Stroke in Mice. *Ann. Neurol.* 84 (6), 854–872. doi:10.1002/ana.25356
- Kawai, T., Masaki, T., Doi, S., Arakawa, T., Yokoyama, Y., Doi, T., et al. (2009). PPAR- $\gamma$  Agonist Attenuates Renal Interstitial Fibrosis and Inflammation Through Reduction of TGF- $\beta$ . *Lab. Invest.* 89 (1), 47–58. doi:10.1038/labinvest.2008.104
- Kesavardhana, S., Malireddi, R. K. S., and Kanneganti, T.-D. (2020). Caspases in Cell Death, Inflammation, and Pyroptosis. *Annu. Rev. Immunol.* 38, 567–595. doi:10.1146/annurev-immunol-073119-095439
- Kim, E. H., Shin, D., Lee, J., Jung, A. R., and Roh, J.-L. (2018). Cisd2 Inhibition Overcomes Resistance to Sulfasalazine-Induced Ferroptotic Cell Death in Head and Neck Cancer. *Cancer Lett.* 432, 180–190. doi:10.1016/j.canlet.2018.06.018
- Kiss, E., Popovic, Z. V., Bedke, J., Adams, J., Bonrouhi, M., Babelova, A., et al. (2010). Peroxisome Proliferator-Activated Receptor (Ppar) Gamma Can Inhibit Chronic Renal Allograft Damage. *Am. J. Pathol.* 176 (5), 2150–2162. doi:10.2353/ajpath.2010.090370
- Knutson, M. D. (2007). Steap Proteins: Implications for Iron and Copper Metabolism. *Nut. Rev.* 65 (7), 335–340. doi:10.1111/j.1753-4887.2007.tb00311.x
- Koch, A., Wölzke, A., Wünsche, C., Meyer zu Heringdorf, D., Huwiler, A., and Pfeilschifter, J. (2012). Thiazolidinedione-dependent Activation of Sphingosine Kinase 1 Causes an Anti-fibrotic Effect in Renal Mesangial Cells. *Br. J. Pharmacol.* 166 (3), 1018–1032. doi:10.1111/j.1476-5381.2012.01824.x

- Koppenol, W. H. (1993). The Centennial of the Fenton Reaction. *Free Radic. Biol. Med.* 15 (6), 645–651. doi:10.1016/0891-5849(93)90168-t
- Kortlever, R. M., Higgins, P. J., and Bernards, R. (2006). Plasminogen Activator Inhibitor-1 Is a Critical Downstream Target of P53 in the Induction of Replicative Senescence. *Nat. Cell Biol.* 8 (8), 877–884. doi:10.1038/ncb1448
- Kovtunovych, G., Eckhaus, M. A., Ghosh, M. C., Ollivierre-Wilson, H., and Rouault, T. A. (2010). Dysfunction of the Heme Recycling System in Heme Oxygenase 1-deficient Mice: Effects on Macrophage Viability and Tissue Iron Distribution. *Blood* 116 (26), 6054–6062. doi:10.1182/blood-2010-03-272138
- Kozyraki, R., Fyfe, J., Verroust, P. J., Jacobsen, C., Dautry-Varsat, A., Gburek, J., et al. (2001). Megalin-Dependent Cubilin-Mediated Endocytosis Is a Major Pathway for the Apical Uptake of Transferrin in Polarized Epithelia. *Proc. Natl. Acad. Sci. U.S.A.* 98 (22), 12491–12496. doi:10.1073/pnas.211291398
- Kroot, J. J., Tjalsma, H., Fleming, R. E., and Swinkels, D. W. (2011). Hpcidin in Human Iron Disorders: Diagnostic Implications. *Clin. Chem.* 57 (12), 1650–1669. doi:10.1373/clinchem.2009.140053
- Kumar, C., Igbaria, A., D'Autreaux, B., Planson, A.-G., Junot, C., Godat, E., et al. (2011). Glutathione Revisited: A Vital Function in Iron Metabolism and Ancillary Role in Thiol-Redox Control. *EMBO J.* 30 (10), 2044–2056. doi:10.1038/emboj.2011.105
- Langelueddecke, C., Roussa, E., Fenton, R. A., Wolff, N. A., Lee, W.-K., and Thévenod, F. (2012). Lipocalin-2 (24p3/Neutrophil Gelatinase-Associated Lipocalin (NGAL)) Receptor Is Expressed in Distal Nephron and Mediates Protein Endocytosis. *J. Biol. Chem.* 287 (1), 159–169. doi:10.1074/jbc.M111.308296
- Latunde-Dada, G. O. (2017). Ferroptosis: Role of Lipid Peroxidation, Iron and Ferritinophagy. *Biochim. Biophys. Acta (Bba) - Gen. Subjects* 1861 (8), 1893–1900. doi:10.1016/j.bbagen.2017.05.019
- Le Blanc, S., Garrick, M. D., and Arredondo, M. (2012). Heme Carrier Protein 1 Transports Heme and Is Involved in Heme-Fe Metabolism. *Am. J. Physiology-Cell Physiol.* 302 (12), C1780–C1785. doi:10.1152/ajpcell.00080.2012
- Lee, W.-J., Liu, S.-H., Chiang, C.-K., Lin, S.-Y., Liang, K.-W., Chen, C.-H., et al. (2016). Aryl Hydrocarbon Receptor Deficiency Attenuates Oxidative Stress-Related Mesangial Cell Activation and Macrophage Infiltration and Extracellular Matrix Accumulation in Diabetic Nephropathy. *Antioxid. Redox Signaling* 24 (4), 217–231. doi:10.1089/ars.2015.6310
- Li, C., Deng, X., Xie, X., Liu, Y., Friedmann Angeli, J. P., and Lai, L. (2018). Activation of Glutathione Peroxidase 4 as a Novel Anti-inflammatory Strategy. *Front. Pharmacol.* 9, 1120. doi:10.3389/fphar.2018.01120
- Li, C., Xie, N., Li, Y., Liu, C., Hou, F. F., and Wang, J. (2019). N-Acetylcysteine Ameliorates Cisplatin-Induced Renal Senescence and Renal Interstitial Fibrosis through Sirtuin1 Activation and P53 Deacetylation. *Free Radic. Biol. Med.* 130, 512–527. doi:10.1016/j.freeradbiomed.2018.11.006
- Li, Y., Feng, D., Wang, Z., Zhao, Y., Sun, R., Tian, D., et al. (2019). Ischemia-induced ACSL4 Activation Contributes to Ferroptosis-Mediated Tissue Injury in Intestinal Ischemia/reperfusion. *Cell Death Differ* 26 (11), 2284–2299. doi:10.1038/s41418-019-0299-4
- Li, J., Yang, J., Zhu, B., Fan, J., Hu, Q., and Wang, L. (2022). Tectorigenin Protects against Unilateral Ureteral Obstruction by Inhibiting Smad3-mediated Ferroptosis and Fibrosis. *Phytotherapy Res.* 36 (1), 475–487. doi:10.1002/ptr.7353
- Li, R., Zhang, J., Zhou, Y., Gao, Q., Wang, R., Fu, Y., et al. (2020). Transcriptome Investigation and *In Vitro* Verification of Curcumin-Induced HO-1 as a Feature of Ferroptosis in Breast Cancer Cells. *Oxidative Med. Cell Longevity* 2020, 1–18. doi:10.1155/2020/3469840
- Li, X., Zou, Y., Xing, J., Fu, Y.-Y., Wang, K.-Y., Wan, P.-Z., et al. (2020). Pretreatment with Roxadustat (Fg-4592) Attenuates Folic Acid-Induced Kidney Injury Through Antiferroptosis Via Akt/Gsk-3 B/Nrf2 Pathway. *Oxidative Med. Cell. longevity* 2020, 1–17. doi:10.1155/2020/6286984
- Li, Y., Jin, C., Shen, M., Wang, Z., Tan, S., Chen, A., et al. (2020). Iron Regulatory Protein 2 Is Required for Artemether -mediated Anti-hepatic Fibrosis through Ferroptosis Pathway. *Free Radic. Biol. Med.* 160, 845–859. doi:10.1016/j.freeradbiomed.2020.09.008
- Li, S., Zheng, L., Zhang, J., Liu, X., and Wu, Z. (2021). Inhibition of Ferroptosis by Up-Regulating Nrf2 Delayed the Progression of Diabetic Nephropathy. *Free Radic. Biol. Med.* 162, 435–449. doi:10.1016/j.freeradbiomed.2020.10.323
- Li, W., Sun, J., Zhou, X., Lu, Y., Cui, W., and Miao, L. (2021). Mini-Review: GSDME-Mediated Pyroptosis in Diabetic Nephropathy. *Front. Pharmacol.* 12, 780790. doi:10.3389/fphar.2021.780790
- Li, Y., Yuan, Y., Huang, Z.-X., Chen, H., Lan, R., Wang, Z., et al. (2021). GSDME-mediated Pyroptosis Promotes Inflammation and Fibrosis in Obstructive Nephropathy. *Cell Death Differ* 28 (8), 2333–2350. doi:10.1038/s41418-021-00755-6
- Liang, X., Duan, N., Wang, Y., Shu, S., Xiang, X., Guo, T., et al. (2016). Advanced Oxidation Protein Products Induce Endothelial-To-Mesenchymal Transition in Human Renal Glomerular Endothelial Cells through Induction of Endoplasmic Reticulum Stress. *J. Diabetes its Complications* 30 (4), 573–579. doi:10.1016/j.jdiacomp.2016.01.009
- Linkermann, A., Bräsen, J. H., Darding, M., Jin, M. K., Sanz, A. B., Heller, J.-O., et al. (2013). Two Independent Pathways of Regulated Necrosis Mediate Ischemia-Reperfusion Injury. *Proc. Natl. Acad. Sci. U.S.A.* 110 (29), 12024–12029. doi:10.1073/pnas.1305538110
- Linkermann, A., Skouta, R., Himmerkus, N., Mulay, S. R., Dewitz, C., De Zen, F., et al. (2014). Synchronized Renal Tubular Cell Death Involves Ferroptosis. *Proc. Natl. Acad. Sci. U.S.A.* 111 (47), 16836–16841. doi:10.1073/pnas.1415518111
- Liu, B., Zhao, C., Li, H., Chen, X., Ding, Y., and Xu, S. (2018). Puerarin Protects against Heart Failure Induced by Pressure Overload through Mitigation of Ferroptosis. *Biochem. biophysical Res. Commun.* 497 (1), 233–240. doi:10.1016/j.bbrc.2018.02.061
- Liu, P., Zhang, B., Chen, Z., He, Y., Du, Y., Liu, Y., et al. (2020). m6A-Induced lncRNA MALAT1 Aggravates Renal Fibrogenesis in Obstructive Nephropathy through the miR-145/FAK Pathway. *Aging* 12 (6), 5280–5299. doi:10.18632/aging.102950
- Liu, Y., and Templeton, D. M. (2015). Iron-Dependent Turnover of IRP-1/ c-Aconitase in Kidney Cells. *Metalomics* 7 (5), 766–775. doi:10.1039/c4mt00315b
- Liu, Y., Wang, W., Li, Y., Xiao, Y., Cheng, J., and Jia, J. (2015). The 5-Lipoxygenase Inhibitor Zileuton Confers Neuroprotection against Glutamate Oxidative Damage by Inhibiting Ferroptosis. *Biol. Pharm. Bull.* 38 (8), 1234–1239. doi:10.1248/bpb.b15-00048
- Lőrincz, T., Jemnitz, K., Kardon, T., Mandl, J., and Szarka, A. (2015). Ferroptosis Is Involved in Acetaminophen Induced Cell Death. *Pathol. Oncol. Res.* 21 (4), 1115–1121. doi:10.1007/s12253-015-9946-3
- Louandre, C., Ezzoukhry, Z., Godin, C., Barbare, J.-C., Mazière, J.-C., Chaffert, B., et al. (2013). Iron-Dependent Cell Death of Hepatocellular Carcinoma Cells Exposed to Sorafenib. *Int. J. Cancer* 133 (7), 1732–1742. doi:10.1002/ijc.28159
- Louandre, C., Marcq, I., Bouhlal, H., Lachaier, E., Godin, C., Saidak, Z., et al. (2015). The Retinoblastoma (Rb) Protein Regulates Ferroptosis Induced by Sorafenib in Human Hepatocellular Carcinoma Cells. *Cancer Lett.* 356 (2 Pt B), 971–977. doi:10.1016/j.canlet.2014.11.014
- Lu, Q., Zhou, Y., Hao, M., Li, C., Wang, J., Shu, F., et al. (2018). The mTOR Promotes Oxidative Stress-Induced Apoptosis of Mesangial Cells in Diabetic Nephropathy. *Mol. Cell Endocrinol.* 473, 31–43. doi:10.1016/j.mce.2017.12.012
- Lu, X., Chen, Z., Liang, H., Li, Z., Zou, X., Luo, H., et al. (2013). Thyroid Hormone Inhibits TGFβ1 Induced Renal Tubular Epithelial to Mesenchymal Transition by Increasing miR34a Expression. *Cell Signal.* 25 (10), 1949–1954. doi:10.1016/j.cellsig.2013.06.005
- Ma, W., Tao, L., Wang, X., Liu, Q., Zhang, W., Li, Q., et al. (2016). Sorafenib Inhibits Renal Fibrosis Induced by Unilateral Ureteral Obstruction via Inhibition of Macrophage Infiltration. *Cell Physiol Biochem* 39 (5), 1837–1849. doi:10.1159/000447883
- Mao, C., Liu, X., Zhang, Y., Lei, G., Yan, Y., Lee, H., et al. (2021). DHODH-mediated Ferroptosis Defence Is a Targetable Vulnerability in Cancer. *Nature* 593, 586–590. doi:10.1038/s41586-021-03539-7
- Marshall, C. B., Pippin, J. W., Krofft, R. D., and Shankland, S. J. (2006). Puromycin Aminonucleoside Induces Oxidant-dependent DNA Damage in Podocytes *In Vitro* and *In Vivo*. *Kidney Int.* 70 (11), 1962–1973. doi:10.1038/sj.ki.5001965
- Martin-Sanchez, D., Ruiz-Andres, O., Poveda, J., Carrasco, S., Cannata-Ortiz, P., Sanchez-Niño, M. D., et al. (2017). Ferroptosis, but Not Necroptosis, Is Important in Nephrotoxic Folic Acid-Induced AKI. *J. Am. Soc. Nephrol.* 28 (1), 218–229. doi:10.1681/asn.2015121376
- Martines, A. M. F., Masereeuw, R., Tjalsma, H., Hoenderop, J. G., Wetzels, J. F. M., and Swinkels, D. W. (2013). Iron Metabolism in the Pathogenesis of Iron-



- Induced Kidney Injury. *Nat. Rev. Nephrol.* 9 (7), 385–398. doi:10.1038/nrneph.2013.98
- Matsumoto, M., Sasaki, N., Tsujino, T., Akahori, H., Naito, Y., and Masuyama, T. (2013). Iron Restriction Prevents Diabetic Nephropathy in Otsuka Long-Evans Tokushima Fatty Rat. *Ren. Fail.* 35 (8), 1156–1162. doi:10.3109/0886022X.2013.819729
- McCarthy, K. J., Routh, R. E., Shaw, W., Walsh, K., Welbourne, T. C., and Johnson, J. H. (2000). Troglitazone Halts Diabetic Glomerulosclerosis by Blockade of Mesangial Expansion. *Kidney Int.* 58 (6), 2341–2350. doi:10.1046/j.1523-1755.2000.00418.x
- Miotto, G., Rossetto, M., Di Paolo, M. L., Orian, L., Venerando, R., Roveri, A., et al. (2020). Insight into the Mechanism of Ferroptosis Inhibition by Ferrostatin-1. *Redox Biol.* 28, 101328. doi:10.1016/j.redox.2019.101328
- Mishima, E., Sato, E., Ito, J., Yamada, K.-i., Suzuki, C., Oikawa, Y., et al. (2020). Drugs Repurposed as Antiferroptosis Agents Suppress Organ Damage, Including AKI, by Functioning as Lipid Peroxyl Radical Scavengers. *J. Am. Soc. Nephrol.* 31 (2), 280–296. doi:10.1681/ASN.2019060570
- Montford, J. R., Bauer, C., Dobrinskikh, E., Hopp, K., Levi, M., Weiser-Evans, M., et al. (2019). Inhibition of 5-Lipoxygenase Decreases Renal Fibrosis and Progression of Chronic Kidney Disease. *Am. J. Physiology-Renal Physiology* 316 (4), F732–F742. doi:10.1152/ajprenal.00262.2018
- Montorfano, I., Becerra, A., Cerro, R., Echeverría, C., Sáez, E., Morales, M. G., et al. (2014). Oxidative Stress Mediates the Conversion of Endothelial Cells into Myofibroblasts via a TGF- $\beta$ 1 and TGF- $\beta$ 2-Dependent Pathway. *Lab. Invest.* 94 (10), 1068–1082. doi:10.1038/abinvest.2014.100
- Moore, B., and Hawkes, J. L. (1908). An Investigation of the Toxic Actions of Dilute Solutions of the Salts of Certain Heavy Metals (viz.: Copper, Iron, Nickel, Cobalt, Manganese, Zinc, Silver, and Lead) Upon the *Bacillus Typhosus*, with a View to Practical Application in the Purification of Shell-Fish. *Biochem. J.* 3 (6-8), 313–345. doi:10.1042/bj0030313
- Moriyama, T., Kawada, N., Nagatoya, K., Takeji, M., Horio, M., Ando, A., et al. (2001). Fluvastatin Suppresses Oxidative Stress and Fibrosis in the Interstitium of Mouse Kidneys with Unilateral Ureteral Obstruction. *Kidney Int.* 59 (6), 2095–2103. doi:10.1046/j.1523-1755.2001.05906.2095.x
- Murphy, T. H., Miyamoto, M., Sastre, A., Schnaar, R. L., and Coyle, J. T. (1989). Glutamate Toxicity in a Neuronal Cell Line Involves Inhibition of Cystine Transport Leading to Oxidative Stress. *Neuron* 2 (6), 1547–1558. doi:10.1016/0896-6273(89)90043-3
- Nagpal, A., Redvers, R. P., Ling, X., Ayton, S., Fuentes, M., Tavanché, E., et al. (2019). Neoadjuvant Neratinib Promotes Ferroptosis and Inhibits Brain Metastasis in a Novel Syngeneic Model of Spontaneous Her2<sup>+</sup> Breast Cancer Metastasis. *Breast Cancer Res.* 21 (1), 94. doi:10.1186/s13058-019-1177-1
- Naito, Y., Fujii, A., Sawada, H., Oboshi, M., Iwasaku, T., Okuhara, Y., et al. (2015). Association Between Renal Iron Accumulation and Renal Interstitial Fibrosis in a Rat Model of Chronic Kidney Disease. *Hypertens. Res.* 38 (7), 463–470. doi:10.1038/hr.2015.14
- Nakanishi, T., Nanami, M., and Kuragano, T. (2020). The Pathogenesis of CKD Complications: Attack of Dysregulated Iron and Phosphate Metabolism. *Free Radic. Biol. Med.* 157, 55–62. doi:10.1016/j.freeradbiomed.2020.01.024
- Nankivell, B. J., Chen, J., Boadle, R. A., and Harris, D. C. (1994). The Role of Tubular Iron Accumulation in the Remnant Kidney. *J. Am. Soc. Nephrol.* 4 (8), 1598–1607. doi:10.1681/asn.v4i81598
- Németh, Á., Mózes, M. M., Calvier, L., Hansmann, G., and Kókény, G. (2019). The PPAR $\gamma$  Agonist Pioglitazone Prevents TGF- $\beta$  Induced Renal Fibrosis by Repressing EGR-1 and STAT3. *BMC Nephrol.* 20 (1), 245. doi:10.1186/s12882-019-1431-x
- Newcomer, M. E., and Brash, A. R. (2015). The Structural Basis for Specificity in Lipoxygenase Catalysis. *Protein Sci.* 24 (3), 298–309. doi:10.1002/pro.2626
- Neyens, E., and Baeyens, J. (2003). A Review of Classic Fenton's Peroxidation as an Advanced Oxidation Technique. *J. Hazard. Mater.* 98 (1-3), 33–50. doi:10.1016/s0304-3894(02)00282-0
- Nlandu Khodo, S., Dizin, E., Sossauer, G., Szanto, I., Martin, P.-Y., Feraille, E., et al. (2012). NADPH-oxidase 4 Protects against Kidney Fibrosis during Chronic Renal Injury. *J. Am. Soc. Nephrol.* 23 (12), 1967–1976. doi:10.1681/ASN.2012040373
- Odaci, E., Ünal, D., Mercantepe, T., Topal, Z., Hanci, H., Türedi, S., et al. (2015). Pathological Effects of Prenatal Exposure to a 900 MHz Electromagnetic Field on the 21-Day-Old Male Rat Kidney. *Biotech. Histochem.* 90 (2), 93–101. doi:10.3109/10520295.2014.947322
- Okamura, D. M., and Pennathur, S. (2015). The Balance of powers: Redox Regulation of Fibrogenic Pathways in Kidney Injury. *Redox Biol.* 6, 495–504. doi:10.1016/j.redox.2015.09.039
- Omasu, F., Oda, T., Yamada, M., Yoshizawa, N., Yamakami, K., Sakurai, Y., et al. (2007). Effects of Pioglitazone and Candesartan on Renal Fibrosis and the Intrarenal Plasmin cascade in Spontaneously Hypercholesterolemic Rats. *Am. J. Physiology-Renal Physiol.* 293 (4), F1292–F1298. doi:10.1152/ajprenal.00232.2007
- Oraby, M. A., El-Yamany, M. F., Safar, M. M., Assaf, N., and Ghoneim, H. A. (2019). Amelioration of Early Markers of Diabetic Nephropathy by Linagliptin in Fructose-Streptozotocin-Induced Type 2 Diabetic Rats. *Nephron* 141 (4), 273–286. doi:10.1159/000495517
- Ou, Y., Wang, S. J., Li, D., Chu, B., and Gu, W. (2016). Activation of SAT1 Engages Polyamine Metabolism with P53-Mediated Ferroptotic Responses. *Proc. Natl. Acad. Sci. U S A.* 113 (44), E6806–E6812. doi:10.1073/pnas.1607152113
- Paller, M. S., Hedlund, B. E., Sikora, J. J., Faassen, A., and Waterfield, R. (1988). Role of Iron in Postischemic Renal Injury in the Rat. *Kidney Int.* 34 (4), 474–480. doi:10.1038/ki.1988.205
- Panchapakesan, U., Sumual, S., Pollock, C. A., and Chen, X. (2005). PPAR $\gamma$  Agonists Exert Antifibrotic Effects in Renal Tubular Cells Exposed to High Glucose. *Am. J. Physiology-Renal Physiol.* 289 (5), F1153–F1158. doi:10.1152/ajprenal.00097.2005
- Paragas, N., Qiu, A., Hollmen, M., Nickolas, T. L., Devarajan, P., and Barasch, J. (2012). NGAL-siderocalin in Kidney Disease. *Biochim. Biophys. Acta (Bba) - Mol. Cell Res.* 1823 (9), 1451–1458. doi:10.1016/j.bbamcr.2012.06.014
- Park, M. W., Cha, H. W., Kim, J., Kim, J. H., Yang, H., Yoon, S., et al. (2021). NOX4 Promotes Ferroptosis of Astrocytes by Oxidative Stress-Induced Lipid Peroxidation via the Impairment of Mitochondrial Metabolism in Alzheimer's Diseases. *Redox Biol.* 41, 101947. doi:10.1016/j.redox.2021.101947
- Park, Y. J., An, H.-T., Park, J.-S., Park, O., Duh, A. J., Kim, K., et al. (2020). Tyrosine Kinase Inhibitor Neratinib Attenuates Liver Fibrosis by Targeting Activated Hepatic Stellate Cells. *Sci. Rep.* 10 (1), 14756. doi:10.1038/s41598-020-71688-2
- Pei, Y., Xu, Y., Ruan, J., Rong, L., Jiang, M., Mo, Y., et al. (2016). Plasma Oxidative Stress Level of IgA Nephropathy in Children and the Effect of Early Intervention with Angiotensin-Converting Enzyme Inhibitors. *J. Renin Angiotensin Aldosterone Syst.* 17 (2), 147032031664724. doi:10.1177/1470320316647240
- Penggrattanachot, N., Chergwelling, R., Jaikumkao, K., Pongchaidecha, A., Thongnak, L., Swe, M. T., et al. (2020). Atorvastatin Attenuates Obese-Induced Kidney Injury and Impaired Renal Organic Anion Transporter 3 Function through Inhibition of Oxidative Stress and Inflammation. *Biochim. Biophys. Acta (Bba) - Mol. Basis Dis.* 1866 (6), 165741. doi:10.1016/j.bbadis.2020.165741
- Philpott, C. C., Ryu, M.-S., Frey, A., and Patel, S. (2017). Cytosolic Iron Chaperones: Proteins Delivering Iron Cofactors in the Cytosol of Mammalian Cells. *J. Biol. Chem.* 292 (31), 12764–12771. doi:10.1074/jbc.R117.791962
- Philpott, C. C. (2018). The Flux of Iron Through Ferritin in Erythrocyte Development. *Curr. Opin. Hematol.* 25 (3), 183–188. doi:10.1097/MOH.0000000000000417
- Piao, S. G., Kang, S. H., Lim, S. W., Chung, B. H., Doh, K. C., Heo, S. B., et al. (2013). Influence of N-Acetylcysteine on Klotho Expression and its Signaling Pathway in Experimental Model of Chronic Cyclosporine Nephropathy in Mice. *Transplantation* 96 (2), 146–153. doi:10.1097/TP.0b013e318296c9a9
- Pinilla-Tenas, J. J., Sparkman, B. K., Shawki, A., Illing, A. C., Mitchell, C. J., Zhao, N., et al. (2011). Zip14 Is a Complex Broad-Scope Metal-Ion Transporter Whose Functional Properties Support Roles in the Cellular Uptake of Zinc and Nontransferrin-Bound Iron. *Am. J. Physiology-Cell Physiol.* 301 (4), C862–C871. doi:10.1152/ajpcell.00479.2010
- Pisani, A., Riccio, E., Andreucci, M., Faga, T., Ashour, M., Di Nuzzi, A., et al. (2013). Role of Reactive Oxygen Species in Pathogenesis of Radiocontrast-Induced Nephropathy. *Biomed. Res. Int.* 2013, 1–6. doi:10.1155/2013/868321
- Portilla, D. (2014). Apoptosis, Fibrosis and Senescence. *Nephron Clin. Pract.* 127 (1-4), 65–69. doi:10.1159/000363717
- Qiu, Y., Cao, Y., Cao, W., Jia, Y., and Lu, N. (2020). The Application of Ferroptosis in Diseases. *Pharmacol. Res.* 159, 104919. doi:10.1016/j.phrs.2020.104919



- Rajapurkar, M. M., Hegde, U., Bhattacharya, A., Alam, M. G., and Shah, S. V. (2013). Effect of Deferiprone, an Oral Iron Chelator, in Diabetic and Non-diabetic Glomerular Disease. *Toxicol. Mech. Methods* 23 (1), 5–10. doi:10.3109/15376516.2012.730558
- Raupach, B., Peuschel, S.-K., Monack, D. M., and Zychlinsky, A. (2006). Caspase-1-Mediated Activation of Interleukin-1 $\beta$  (IL-1 $\beta$ ) and IL-18 Contributes to Innate Immune Defenses against Salmonella Enterica Serovar Typhimurium Infection. *Infect. Immun.* 74 (8), 4922–4926. doi:10.1128/iai.00417-06
- Rosa, L., Cutone, A., Lepanto, M., Paesano, R., and Valenti, P. (2017). Lactoferrin: A Natural Glycoprotein Involved in Iron and Inflammatory Homeostasis. *Int. J. Mol. Sci.* 18 (9), 1985. doi:10.3390/ijms18091985
- Rubio-Navarro, A., Sanchez-Niño, M. D., Guerrero-Hue, M., García-Caballero, C., Gutiérrez, E., Yuste, C., et al. (2018). Podocytes Are New Cellular Targets of Haemoglobin-Mediated Renal Damage. *J. Pathol.* 244 (3), 296–310. doi:10.1002/path.5011
- Ryu, M.-S., Duck, K. A., and Philpott, C. C. (2018). Ferritin Iron Regulators, PCBP1 and NCOA4, Respond to Cellular Iron Status in Developing Red Cells. *Blood Cell Mol. Dis.* 69, 75–81. doi:10.1016/j.bcmd.2017.09.009
- Salahudeen, A. A., Thompson, J. W., Ruiz, J. C., Ma, H.-W., Kinch, L. N., Li, Q., et al. (2009). An E3 Ligase Possessing an Iron-Responsive Hemerythrin Domain Is a Regulator of Iron Homeostasis. *Science* 326 (5953), 722–726. doi:10.1126/science.1176326
- Samarakoon, R., Overstreet, J. M., Higgins, S. P., and Higgins, P. J. (2012). TGF- $\beta$ 1  $\rightarrow$  SMAD/p53/USF2  $\rightarrow$  PAI-1 Transcriptional axis in Ureteral Obstruction-Induced Renal Fibrosis. *Cell Tissue Res* 347 (1), 117–128. doi:10.1007/s00441-011-1181-y
- Scindia, Y., Leeds, J., and Swaminathan, S. (2019). Iron Homeostasis in Healthy Kidney and its Role in Acute Kidney Injury. *Semin. Nephrol.* 39 (1), 76–84. doi:10.1016/j.semnephrol.2018.10.006
- Sears, D. A., Anderson, P. R., Foy, A. L., Williams, H. L., and Crosby, W. H. (1966). Urinary Iron Excretion and Renal Metabolism of Hemoglobin in Hemolytic Diseases. *Blood* 28 (5), 708–725. doi:10.1182/blood.v28.5.708.708
- Sedeek, M., Callera, G., Montezano, A., Gutsol, A., Heitz, F., Szyndralewicz, C., et al. (2010). Critical Role of Nox4-Based NADPH Oxidase in Glucose-Induced Oxidative Stress in the Kidney: Implications in Type 2 Diabetic Nephropathy. *Am. J. Physiology-Renal Physiol.* 299 (6), F1348–F1358. doi:10.1152/ajprenal.00028.2010
- Seiler, A., Schneider, M., Förster, H., Roth, S., Wirth, E. K., Culmsee, C., et al. (2008). Glutathione Peroxidase 4 Senses and Translates Oxidative Stress into 12/15-lipoxygenase Dependent- and AIF-Mediated Cell Death. *Cell Metab.* 8 (3), 237–248. doi:10.1016/j.cmet.2008.07.005
- Shah, S. V., Baliga, R., Rajapurkar, M., and Fonseca, V. A. (2007). Oxidants in Chronic Kidney Disease. *J. Am. Soc. Nephrol.* 18 (1), 16–28. doi:10.1681/ASN.2006050500
- Shen, Y., Miao, N.-J., Xu, J.-L., Gan, X.-X., Xu, D., Zhou, L., et al. (2016). N-acetylcysteine Alleviates Angiotensin II-Mediated Renal Fibrosis in Mouse Obstructed Kidneys. *Acta Pharmacol. Sin* 37 (5), 637–644. doi:10.1038/aps.2016.12
- Shi, H., Bencze, K. Z., Stemmler, T. L., and Philpott, C. C. (2008). A Cytosolic Iron Chaperone that Delivers Iron to Ferritin. *Science* 320 (5880), 1207–1210. doi:10.1126/science.1157643
- Shimada, K., Skouta, R., Kaplan, A., Yang, W. S., Hayano, M., Dixon, S. J., et al. (2016). Global Survey of Cell Death Mechanisms Reveals Metabolic Regulation of Ferroptosis. *Nat. Chem. Biol.* 12 (7), 497–503. doi:10.1038/nchembio.2079
- Shui, G.-X., Sang, D., Yin, X., Cai, Y., and Sun, W. (2017). Dahuang Fuzi Decoction Attenuates Renal Fibrosis and Ameliorates Mitochondrial Dysfunction in Chronic Aristolochic Acid Nephropathy. *Evid Based. Complement. Altern. medicine. eCAM* 2017, 1–8. doi:10.1155/2017/9536458
- Smith, C. P., Lee, W.-K., Haley, M., Poulsen, S. B., Thévenod, F., and Fenton, R. A. (2019). Proximal Tubule Transferrin Uptake Is Modulated by Cellular Iron and Mediated by Apical Membrane Megalin-Cubilin Complex and Transferrin Receptor 1. *J. Biol. Chem.* 294 (17), 7025–7036. doi:10.1074/jbc.RA118.006390
- Smith, C. P., and Thévenod, F. (2009). Iron Transport and the Kidney. *Biochim. Biophys. Acta (Bba) - Gen. Subjects* 1790 (7), 724–730. doi:10.1016/j.bbagen.2008.10.010
- Sol, M., Kamps, J. A. A. M., van den Born, J., van den Heuvel, M. C., van der Vlag, J., Krenning, G., et al. (2020). Glomerular Endothelial Cells as Instigators of Glomerular Sclerotic Diseases. *Front. Pharmacol.* 11, 573557. doi:10.3389/fphar.2020.573557
- Song, Y., Tao, Q., Yu, L., Li, L., Bai, T., Song, X., et al. (2018). Activation of Autophagy Contributes to the Renoprotective Effect of Postconditioning on Acute Kidney Injury and Renal Fibrosis. *Biochem. Biophys. Res. Commun.* 504 (4), 641–646. doi:10.1016/j.bbrc.2018.09.003
- Song, Y., Wang, B., Zhu, X., Hu, J., Sun, J., Xuan, J., et al. (2021). Human Umbilical Cord Blood-Derived MSCs Exosome Attenuate Myocardial Injury by Inhibiting Ferroptosis in Acute Myocardial Infarction Mice. *Cell Biol Toxicol* 37 (1), 51–64. doi:10.1007/s10565-020-09530-8
- Soulage, C. O., Pelletier, C. C., Florens, N., Lemoine, S., Dubourg, L., Juillard, L., et al. (2020). Two Toxic Lipid Aldehydes, 4-Hydroxy-2-Hexenal (4-HHE) and 4-Hydroxy-2-Nonenal (4-HNE), Accumulate in Patients with Chronic Kidney Disease. *Toxins* 12 (9), 567. doi:10.3390/toxins12090567
- Sponsel, H. T., Alfrey, A. C., Hammond, W. S., Durr, J. A., Ray, C., and Anderson, R. J. (1996). Effect of Iron on Renal Tubular Epithelial Cells. *Kidney Int.* 50 (2), 436–444. doi:10.1038/ki.1996.334
- Stockwell, B. R., Friedmann Angeli, J. P., Bayir, H., Bush, A. I., Conrad, M., Dixon, S. J., et al. (2017). Ferroptosis: A Regulated Cell Death Nexus Linking Metabolism, Redox Biology, and Disease. *Cell* 171 (2), 273–285. doi:10.1016/j.cell.2017.09.021
- Su, H., Chen, S., He, F.-F., Wang, Y.-M., Bondzie, P., and Zhang, C. (2015). New Insights into Glomerular Parietal Epithelial Cell Activation and its Signaling Pathways in Glomerular Diseases. *Biomed. Res. Int.* 2015, 1–8. doi:10.1155/2015/318935
- Su, H., Wan, C., Song, A., Qiu, Y., Xiong, W., and Zhang, C. (2019). Oxidative Stress and Renal Fibrosis: Mechanisms and Therapies. *Adv. Exp. Med. Biol.* 1165, 585–604. doi:10.1007/978-981-13-8871-2\_29
- Sun, L., Xu, T., Chen, Y., Qu, W., Sun, D., Song, X., et al. (2019). Pioglitazone Attenuates Kidney Fibrosis via miR-21-5p Modulation. *Life Sci.* 232, 116609. doi:10.1016/j.lfs.2019.116609
- Sun, L., Yuan, Q., Xu, T., Yao, L., Feng, J., Ma, J., et al. (2017). Pioglitazone Improves Mitochondrial Function in the Remnant Kidney and Protects against Renal Fibrosis in 5/6 Nephrectomized Rats. *Front. Pharmacol.* 8, 545. doi:10.3389/fphar.2017.00545
- Sun, X., Ou, Z., Chen, R., Niu, X., Chen, D., Kang, R., et al. (2016). Activation of the P62-Keap1-NRF2 Pathway Protects against Ferroptosis in Hepatocellular Carcinoma Cells. *Hepatology* 63 (1), 173–184. doi:10.1002/hep.28251
- Sun, X., Ou, Z., Xie, M., Kang, R., Fan, Y., Niu, X., et al. (2015). HSPB1 as a Novel Regulator of Ferroptotic Cancer Cell Death. *Oncogene* 34 (45), 5617–5625. doi:10.1038/onc.2015.32
- Sureshbabu, A., Rytter, S. W., and Choi, M. E. (2015). Oxidative Stress and Autophagy: Crucial Modulators of Kidney Injury. *Redox Biol.* 4, 208–214. doi:10.1016/j.redox.2015.01.001
- Swinkels, D. W., Janssen, M. C., Bergmans, J., and Marx, J. J. (2006). Hereditary Hemochromatosis: Genetic Complexity and New Diagnostic Approaches. *Clin. Chem.* 52 (6), 950–968. doi:10.1373/clinchem.2006.068684
- Taccone-Gallucci, M., Lubrano, R., Belli, A., Meloni, C., Morosetti, M., Meschini, L., et al. (1989). Disappearance of Oxidative Damage to Red Blood Cell Membranes in Uremic Patients Following Renal Transplant. *ASAIO Trans.* 35 (3), 533–534. doi:10.1097/00002216-198907000-00116
- Tajima, S., Tsuchiya, K., Horinouchi, Y., Ishizawa, K., Ikeda, Y., Kihira, Y., et al. (2010). Effect of Angiotensin II on Iron-Transporting Protein Expression and Subsequent Intracellular Labile Iron Concentration in Human Glomerular Endothelial Cells. *Hypertens. Res.* 33 (7), 713–721. doi:10.1038/hr.2010.63
- Tanaka, S., and Tanaka, T. (2015). How to Supplement Iron in Patients with Renal Anemia. *Nephron* 131 (2), 138–144. doi:10.1159/000440773
- Tanaka, T., Matsumoto, M., Inagi, R., Miyata, T., Kojima, I., Ohse, T., et al. (2005). Induction of Protective Genes by Cobalt Ameliorates Tubulointerstitial Injury in the Progressive Thy1 Nephritis. *Kidney Int.* 68 (6), 2714–2725. doi:10.1111/j.1523-1755.2005.00742.x
- Tanaka, T., Miyata, T., Inagi, R., Kurokawa, K., Adler, S., Fujita, T., et al. (2003). Hypoxia-induced Apoptosis in Cultured Glomerular Endothelial Cells: Involvement of Mitochondrial Pathways. *Kidney Int.* 64 (6), 2020–2032. doi:10.1046/j.1523-1755.2003.00301.x
- Tanaka, Y., Kume, S., Chin-Kanasaki, M., Araki, H., Araki, S.-i., Ugi, S., et al. (2016). Renoprotective Effect of DPP-4 Inhibitors against Free Fatty Acid-

- Bound Albumin-Induced Renal Proximal Tubular Cell Injury. *Biochem. Biophysical Res. Commun.* 470 (3), 539–545. doi:10.1016/j.bbrc.2016.01.109
- Tang, D.-q., Wei, Y.-q., Yin, X.-x., Lu, Q., Hao, H.-h., Zhai, Y.-p., et al. (2011). *In Vitro* suppression of Quercetin on Hypertrophy and Extracellular Matrix Accumulation in Rat Glomerular Mesangial Cells Cultured by High Glucose. *Fitoterapia* 82 (6), 920–926. doi:10.1016/j.fitote.2011.05.001
- Tang, P. M.-K., Zhang, Y.-Y., Hung, J. S.-C., Chung, J. Y.-F., Huang, X.-R., To, K.-F., et al. (2021). DPP4/CD32b/NF- $\kappa$ B Circuit: A Novel Druggable Target for Inhibiting CRP-Driven Diabetic Nephropathy. *Mol. Ther.* 29 (1), 365–375. doi:10.1016/j.ymthe.2020.08.017
- Tang, R., Xu, J., Zhang, B., Liu, J., Liang, C., Hua, J., et al. (2020). Ferroptosis, Necroptosis, and Pyroptosis in Anticancer Immunity. *J. Hematol. Oncol.* 13 (1), 110. doi:10.1186/s13045-020-00946-7
- Tarangelo, A., Magtanong, L., Biegling-Rolett, K. T., Li, Y., Ye, J., Attardi, L. D., et al. (2018). p53 Suppresses Metabolic Stress-Induced Ferroptosis in Cancer Cells. *Cell Rep.* 22 (3), 569–575. doi:10.1016/j.celrep.2017.12.077
- Tbahriti, H. F., Kaddous, A., Bouchenak, M., and Mekki, K. (2013). Effect of Different Stages of Chronic Kidney Disease and Renal Replacement Therapies on Oxidant-Antioxidant Balance in Uremic Patients. *Biochem. Res. Int.* 2013, 1–6. doi:10.1155/2013/358985
- Thévenod, F., and Wolff, N. A. (2016). Iron Transport in the Kidney: Implications for Physiology and Cadmium Nephrotoxicity. *Metallomics* 8 (1), 17–42. doi:10.1039/c5mt00021j
- Tsuprykov, O., Ando, R., Reichetzer, C., von Websky, K., Antonenko, V., Sharkovska, Y., et al. (2016). The Dipeptidyl Peptidase Inhibitor Linagliptin and the Angiotensin II Receptor Blocker Telmisartan Show Renal Benefit by Different Pathways in Rats with 5/6 Nephrectomy. *Kidney Int.* 89 (5), 1049–1061. doi:10.1016/j.kint.2016.01.016
- Uchida, T., Oda, T., Matsubara, H., Watanabe, A., Takechi, H., Oshima, N., et al. (2017). Renoprotective Effects of a Dipeptidyl Peptidase 4 Inhibitor in a Mouse Model of Progressive Renal Fibrosis. *Ren. Fail.* 39 (1), 340–349. doi:10.1080/0886022X.2017.1279553
- Ueda, N., Baliga, R., and Shah, S. V. (1996). Role of 'catalytic' Iron in an Animal Model of Minimal Change Nephrotic Syndrome. *Kidney Int.* 49 (2), 370–373. doi:10.1038/ki.1996.54
- Upton, J. W., Kaiser, W. J., and Mocarski, E. S. (2010). Virus Inhibition of RIP3-dependent Necrosis. *Cell Host & Microbe* 7 (4), 302–313. doi:10.1016/j.chom.2010.03.006
- van Raaij, S., van Swelm, R., Bouman, K., Cliteur, M., van den Heuvel, M. C., Pijts, J., et al. (2018a). Publisher Correction: Tubular Iron Deposition and Iron Handling Proteins in Human Healthy Kidney and Chronic Kidney Disease. *Sci. Rep.* 8 (1), 13390. doi:10.1038/s41598-018-31457-8
- van Raaij, S., van Swelm, R., Bouman, K., Cliteur, M., van den Heuvel, M. C., Pijts, J., et al. (2018b). Tubular Iron Deposition and Iron Handling Proteins in Human Healthy Kidney and Chronic Kidney Disease. *Sci. Rep.* 8 (1), 9353. doi:10.1038/s41598-018-27107-8
- van Swelm, R. P. L., Wetzels, J. F. M., and Swinkels, D. W. (2020). The Multifaceted Role of Iron in Renal Health and Disease. *Nat. Rev. Nephrol.* 16 (2), 77–98. doi:10.1038/s41581-019-0197-5
- Vashisht, A. A., Zumbrennen, K. B., Huang, X., Powers, D. N., Durazo, A., Sun, D., et al. (2009). Control of Iron Homeostasis by an Iron-Regulated Ubiquitin Ligase. *Science* 326 (5953), 718–721. doi:10.1126/science.1176333
- Vavrinec, P., Henning, R., Landheer, S., Wang, Y., Deelman, L., Dokkum, R., et al. (2014). Vildagliptin Restores Renal Myogenic Function and Attenuates Renal Sclerosis Independently of Effects on Blood Glucose or Proteinuria in Zucker Diabetic Fatty Rat. *Curr. Vasc. Pharmacol.* 12 (6), 836–844. doi:10.2174/1570161113116660151
- Veuthey, T., Hoffmann, D., Vaidya, V. S., and Wessling-Resnick, M. (2014). Impaired Renal Function and Development in Belgrade Rats. *Am. J. Physiology-Renal Physiol.* 306 (3), F333–F343. doi:10.1152/ajprenal.00285.2013
- Viswanathan, V. S., Ryan, M. J., Dhruv, H. D., Gill, S., Eichhoff, O. M., Seashore-Ludlow, B., et al. (2017). Dependency of a Therapy-Resistant State of Cancer Cells on a Lipid Peroxidase Pathway. *Nature* 547 (7664), 453–457. doi:10.1038/nature23007
- Vyoral, D., and Jiri Petrak, P. (2017). Therapeutic Potential of Hepcidin – the Master Regulator of Iron Metabolism. *Pharmacol. Res.* 115, 242–254. doi:10.1016/j.phrs.2016.11.010
- Wagner, B., Tan, C., Barnes, J. L., Ahuja, S., Davis, T. L., Gorin, Y., et al. (2012). Nephrogenic Systemic Fibrosis. *Am. J. Pathol.* 181 (6), 1941–1952. doi:10.1016/j.ajpath.2012.08.026
- Wang, C., Blough, E., Arvapalli, R., Dai, X., Triest, W. E., Leidy, J. W., et al. (2015). Acetaminophen Attenuates Glomerulosclerosis in Obese Zucker Rats via Reactive Oxygen species/p38MAPK Signaling Pathways. *Free Radic. Biol. Med.* 81, 47–57. doi:10.1016/j.freeradbiomed.2015.01.008
- Wang, W., Zhou, P.-h., Xu, C.-g., Zhou, X.-j., Hu, W., and Zhang, J. (2015). Baicalein Attenuates Renal Fibrosis by Inhibiting Inflammation via Down-Regulating NF-Kb and MAPK Signal Pathways. *J. Mol. Hist.* 46 (3), 283–290. doi:10.1007/s10735-015-9621-8
- Wang, C., Blough, E. R., Arvapalli, R., Dai, X., Paturi, S., Manne, N., et al. (2013). Metabolic Syndrome-Induced Tubulointerstitial Injury: Role of Oxidative Stress and Preventive Effects of Acetaminophen. *Free Radic. Biol. Med.* 65, 1417–1426. doi:10.1016/j.freeradbiomed.2013.10.005
- Wang, H., Nishiya, K., Ito, H., Hosokawa, T., Hashimoto, K., and Moriki, T. (2001). Iron Deposition in Renal Biopsy Specimens from Patients with Kidney Diseases. *Am. J. Kidney Dis.* 38 (5), 1038–1044. doi:10.1053/ajkd.2001.28593
- Wang, J., Deng, B., Liu, Q., Huang, Y., Chen, W., Li, J., et al. (2020). Pyroptosis and Ferroptosis Induced by Mixed Lineage Kinase 3 (MLK3) Signaling in Cardiomyocytes Are Essential for Myocardial Fibrosis in Response to Pressure Overload. *Cell Death Dis* 11 (7), 574. doi:10.1038/s41419-020-02777-3
- Wang, Y., Bi, R., Quan, F., Cao, Q., Lin, Y., Yue, C., et al. (2020). Ferroptosis Involves in Renal Tubular Cell Death in Diabetic Nephropathy. *Eur. J. Pharmacol.* 888, 173574. doi:10.1016/j.ejphar.2020.173574
- Wang, Q.-L., Yuan, J.-L., Tao, Y.-Y., Zhang, Y., Liu, P., and Liu, C.-H. (2010). Fuzheng Huayu Recipe and Vitamin E Reverse Renal Interstitial Fibrosis through Counteracting TGF-B1-Induced Epithelial-To-Mesenchymal Transition. *J. ethnopharmacology* 127 (3), 631–640. doi:10.1016/j.jep.2009.12.011
- Wang, W., Zhou, P.-h., Xu, C.-g., Zhou, X.-j., Hu, W., and Zhang, J. (2016). Baicalein Ameliorates Renal Interstitial Fibrosis by Inducing Myofibroblast Apoptosis in Vivo and in Vitro. *BJU Int.* 118 (1), 145–152. doi:10.1111/bju.13219
- Wang, Y., and Kanneganti, T.-D. (2021). From Pyroptosis, Apoptosis and Necroptosis to PANoptosis: A Mechanistic Compendium of Programmed Cell Death Pathways. *Comput. Struct. Biotechnol. J.* 19, 4641–4657. doi:10.1016/j.csbj.2021.07.038
- Wang, Y., Pang, L., Zhang, Y., Lin, J., and Zhou, H. (2019). Fenofibrate Improved Interstitial Fibrosis of Renal Allograft through Inhibited Epithelial-Mesenchymal Transition Induced by Oxidative Stress. *Oxidative Med. Cell Longevity* 2019, 1–12. doi:10.1155/2019/8936856
- Wang, Z., Ding, Y., Wang, X., Lu, S., Wang, C., He, C., et al. (2018). Pseudolaric Acid B Triggers Ferroptosis in Glioma Cells via Activation of Nox4 and Inhibition of xCT. *Cancer Lett.* 428, 21–33. doi:10.1016/j.canlet.2018.04.021
- Wei, S., Xu, C., Zhang, Y., Shi, Z., Wu, M., and Yang, B. (2020). Ultrasound Assisted a Peroxisome Proliferator-Activated Receptor (PPAR) $\gamma$  Agonist-Loaded Nanoparticle-Microbubble Complex to Attenuate Renal Interstitial Fibrosis. *Int. J. nanomedicine* 15, 7315–7327. doi:10.2147/IJN.S262052
- Weiss, A., Spektor, L., A. Cohen, L., Magid Gold, I., Zhang, D.-L., Truman-Rosentsvit, M., et al. (2018). Orchestrated Regulation of Iron Trafficking Proteins in the Kidney during Iron Overload Facilitates Systemic Iron Retention. *Plos One* 13 (10), e0204471. doi:10.1371/journal.pone.0204471
- Wen, Y., Pan, M. M., Lv, L. L., Tang, T. T., Zhou, L. T., Wang, B., et al. (2019). Artemisinin Attenuates Tubulointerstitial Inflammation and Fibrosis via the NF- $\kappa$ B/NLRP3 Pathway in Rats with 5/6 Subtotal Nephrectomy. *J. Cell Biochem* 120 (3), 4291–4300. doi:10.1002/jcb.27714
- Weng, C.-H., Li, Y.-J., Wu, H.-H., Liu, S.-H., Hsu, H.-H., Chen, Y.-C., et al. (2020). Interleukin-17A Induces Renal Fibrosis through the ERK and Smad Signaling Pathways. *Biomed. Pharmacother.* 123, 109741. doi:10.1016/j.biopha.2019.109741
- Wenz, C., Faust, D., Linz, B., Turmann, C., Nikolova, T., and Dietrich, C. (2019). Cell-cell Contacts Protect against T-BuOOH-Induced Cellular Damage and Ferroptosis *In Vitro*. *Arch. Toxicol.* 93 (5), 1265–1279. doi:10.1007/s00204-019-02413-w
- Wong, V. Y., Laping, N. J., Nelson, A. H., Contino, L. C., Olson, B. A., Gygielko, E., et al. (2001). Renoprotective Effects of Carvedilol in Hypertensive-Stroke Prone

- Rats May Involve Inhibition of TGF $\beta$  Expression. *Br. J. Pharmacol.* 134 (5), 977–984. doi:10.1038/sj.bjp.0704329
- Wu, J., Minikes, A. M., Gao, M., Bian, H., Li, Y., Stockwell, B. R., et al. (2019). Intercellular Interaction Dictates Cancer Cell Ferroptosis via NF2-YAP Signalling. *Nature* 572 (7769), 402–406. doi:10.1038/s41586-019-1426-6
- Wu, M., Xia, W., Jin, Q., Zhou, A., Wang, Q., Li, S., et al. (2021). Gasdermin E Deletion Attenuates Ureteral Obstruction- and 5/6 Nephrectomy-Induced Renal Fibrosis and Kidney Dysfunction. *Front. Cell Dev. Biol.* 9, 754134. doi:10.3389/fcell.2021.754134
- Xiao, X., Du, C., Yan, Z., Shi, Y., Duan, H., and Ren, Y. (2017). Inhibition of Necroptosis Attenuates Kidney Inflammation and Interstitial Fibrosis Induced by Unilateral Ureteral Obstruction. *Am. J. Nephrol.* 46 (2), 131–138. doi:10.1159/000478746
- Xie, Y., Hou, W., Song, X., Yu, Y., Huang, J., Sun, X., et al. (2016a). Ferroptosis: Process and Function. *Cell Death Differ* 23 (3), 369–379. doi:10.1038/cdd.2015.158
- Xie, Y., Song, X., Sun, X., Huang, J., Zhong, M., Lotze, M. T., et al. (2016b). Identification of Baicalein as a Ferroptosis Inhibitor by Natural Product Library Screening. *Biochem. Biophysical Res. Commun.* 473 (4), 775–780. doi:10.1016/j.bbrc.2016.03.052
- Xie, Y., Zhu, S., Song, X., Sun, X., Fan, Y., Liu, J., et al. (2017). The Tumor Suppressor P53 Limits Ferroptosis by Blocking DPP4 Activity. *Cell Rep.* 20 (7), 1692–1704. doi:10.1016/j.celrep.2017.07.055
- Xu, Y., Li, X., Cheng, Y., Yang, M., and Wang, R. (2020). Inhibition of ACSL4 Attenuates Ferroptotic Damage after Pulmonary Ischemia-reperfusion. *FASEB j.* 34 (12), 16262–16275. doi:10.1096/fj.202001758R
- Yao, X., Zhang, Y., Hao, J., Duan, H.-Q., Zhao, C.-X., et al. (2019). Deferoxamine Promotes Recovery of Traumatic Spinal Cord Injury by Inhibiting Ferroptosis. *Neural Regen. Res.* 14 (3), 532–541. doi:10.4103/1673-5374.245480
- Yagoda, N., von Rechenberg, M., Zaganjor, E., Bauer, A. J., Yang, W. S., Fridman, D. J., et al. (2007). RAS-RAF-MEK-dependent Oxidative Cell Death Involving Voltage-dependent Anion Channels. *Nature* 447 (7146), 865–869. doi:10.1038/nature05859
- Yang, L., Besschetnova, T. Y., Brooks, C. R., Shah, J. V., and Bonventre, J. V. (2010). Epithelial Cell Cycle Arrest in G2/M Mediates Kidney Fibrosis after Injury. *Nat. Med.* 16 (5), 535–543. doi:10.1038/nm.2144
- Yang, M., Chen, P., Liu, J., Zhu, S., Kroemer, G., Klionsky, D. J., et al. (2019). Clockophagy Is a Novel Selective Autophagy Process Favoring Ferroptosis. *Sci. Adv.* 5 (7), eaaw2238. doi:10.1126/sciadv.aaw2238
- Yang, W.-H., Ding, C.-K. C., Sun, T., Rupprecht, G., Lin, C.-C., Hsu, D., et al. (2019). The Hippo Pathway Effector TAZ Regulates Ferroptosis in Renal Cell Carcinoma. *Cell Rep.* 28 (10), 2501–2508. e2504. doi:10.1016/j.celrep.2019.07.107
- Yang, Q., Wu, F.-r., Wang, J.-n., Gao, L., Jiang, L., Li, H.-D., et al. (2018). Nox4 in Renal Diseases: An Update. *Free Radic. Biol. Med.* 124, 466–472. doi:10.1016/j.freeradbiomed.2018.06.042
- Yang, W. S., Kim, K. J., Gschler, M. M., Patel, M., Shchepinov, M. S., and Stockwell, B. R. (2016). Peroxidation of Polyunsaturated Fatty Acids by Lipoygenases Drives Ferroptosis. *Proc. Natl. Acad. Sci. U.S.A.* 113 (34), E4966–E4975. doi:10.1073/pnas.1603244113
- Yang, W. S., SriRamaratnam, R., Welsch, M. E., Shimada, K., Skouta, R., Viswanathan, V. S., et al. (2014). Regulation of Ferroptotic Cancer Cell Death by GPX4. *Cell* 156 (1–2), 317–331. doi:10.1016/j.cell.2013.12.010
- Yang, W. S., and Stockwell, B. R. (2016). Ferroptosis: Death by Lipid Peroxidation. *Trends Cell Biol.* 26 (3), 165–176. doi:10.1016/j.tcb.2015.10.014
- Yang, W. S., and Stockwell, B. R. (2008). Synthetic Lethal Screening Identifies Compounds Activating Iron-dependent, Nonapoptotic Cell Death in Oncogenic-RAS-Harboring Cancer Cells. *Chem. Biol.* 15 (3), 234–245. doi:10.1016/j.chembiol.2008.02.010
- Yuan, H., Li, X., Zhang, X., Kang, R., and Tang, D. (2016). C1SD1 Inhibits Ferroptosis by protection against Mitochondrial Lipid Peroxidation. *Biochem. Biophysical Res. Commun.* 478 (2), 838–844. doi:10.1016/j.bbrc.2016.08.034
- Zachara, B. A., Włodarczyk, Z., Masztalerz, M., Adamowicz, A., Gromadzinska, J., and Wasowicz, W. (2004). Selenium Concentrations and Glutathione Peroxidase Activities in Blood of Patients before and after Allogeneic Kidney Transplantation. *Biol. Trace Elem. Res.* 97 (1), 1–14. doi:10.1385/BTER:97:1:1
- Zager, R. A., and Burkhart, K. (1997). Myoglobin Toxicity in Proximal Human Kidney Cells: Roles of Fe, Ca<sup>2+</sup>, H<sub>2</sub>O<sub>2</sub>, and Terminal Mitochondrial Electron Transport. *Kidney Int.* 51 (3), 728–738. doi:10.1038/ki.1997.104
- Zeisberg, M., and Neilson, E. G. (2010). Mechanisms of Tubulointerstitial Fibrosis. *J. Am. Soc. Nephrol.* 21 (11), 1819–1834. doi:10.1681/ASN.2010080793
- Zhang, B., Chen, X., Ru, F., Gan, Y., Li, B., Xia, W., et al. (2021). Liproxstatin-1 Attenuates Unilateral Ureteral Obstruction-Induced Renal Fibrosis by Inhibiting Renal Tubular Epithelial Cells Ferroptosis. *Cell Death Dis* 12 (9), 843. doi:10.1038/s41419-021-04137-1
- Zhang, B., Liu, P., Zhou, Y., Chen, Z., He, Y., Mo, M., et al. (2019). Dihydroartemisinin Attenuates Renal Fibrosis through Regulation of Fibroblast Proliferation and Differentiation. *Life Sci.* 223, 29–37. doi:10.1016/j.lfs.2019.03.020
- Zhang, D., Meyron-Holtz, E., and Rouault, T. A. (2007). Renal Iron Metabolism: Transferrin Iron Delivery and the Role of Iron Regulatory Proteins. *J. Am. Soc. Nephrol.* 18 (2), 401–406. doi:10.1681/ASN.2006080908
- Zhang, Y., Li, H., Zhu, J., Wei, T., Peng, Y., Li, R., et al. (2017). Role of Artesunate in TGF- $\beta$ 1-Induced Renal Tubular Epithelial-Mesenchymal Transdifferentiation in NRK-52E Cells. *Mol. Med. Rep.* 16 (6), 8891–8899. doi:10.3892/mmr.2017.7728
- Zhang, Z., Yao, Z., Wang, L., Ding, H., Shao, J., Chen, A., et al. (2018). Activation of Ferritinophagy Is Required for the RNA-Binding Protein ELAVL1/HuR to Regulate Ferroptosis in Hepatic Stellate Cells. *Autophagy* 14 (12), 2083–2103. doi:10.1080/15548627.2018.1503146
- Zhao, X., Wang, J., Tang, L., Li, P., Ru, J., and Bai, Y. (2021). Withaferin A Protects against Hyperuricemia Induced Kidney Injury and its Possible Mechanisms. *Bioengineered* 12 (1), 589–600. doi:10.1080/21655979.2021.1882761
- Zhao, Y., Zhang, W., Jia, Q., Feng, Z., Guo, J., Han, X., et al. (2018). High Dose Vitamin E Attenuates Diabetic Nephropathy via Alleviation of Autophagic Stress. *Front. Physiol.* 9, 1939. doi:10.3389/fphys.2018.01939
- Zhou, X., Bai, C., Sun, X., Gong, X., Yang, Y., Chen, C., et al. (2017). Puerarin Attenuates Renal Fibrosis by Reducing Oxidative Stress Induced-Epithelial Cell Apoptosis via MAPK Signal Pathways *In Vivo* and *In Vitro*. *Ren. Fail.* 39 (1), 423–431. doi:10.1080/0886022X.2017.1305409
- Zhu, Y., Cui, H., Gan, H., Xia, Y., Wang, L., Wang, Y., et al. (2015). Necroptosis Mediated by Receptor Interaction Protein Kinase 1 and 3 Aggravates Chronic Kidney Injury of Subtotal Nephrectomized Rats. *Biochem. biophysical Res. Commun.* 461 (4), 575–581. doi:10.1016/j.bbrc.2015.03.164
- Zhu, Y., Cui, H., Xia, Y., and Gan, H. (2016). RIPK3-Mediated Necroptosis and Apoptosis Contributes to Renal Tubular Cell Progressive Loss and Chronic Kidney Disease Progression in Rats. *PLoS one* 11 (6), e0156729. doi:10.1371/journal.pone.0156729
- Zou, Y., Li, H., Graham, E. T., Deik, A. A., Eaton, J. K., Wang, W., et al. (2020). Cytochrome P450 Oxidoreductase Contributes to Phospholipid Peroxidation in Ferroptosis. *Nat. Chem. Biol.* 16 (3), 302–309. doi:10.1038/s41589-020-0472-6
- Zschiedrich, S., Bork, T., Liang, W., Wanner, N., Eulenbruch, K., Munder, S., et al. (2017). Targeting mTOR Signaling Can Prevent the Progression of FSGS. *J. Am. Soc. Nephrol.* 28 (7), 2144–2157. doi:10.1681/ASN.2016050519

**Conflict of Interest:** The authors declare that the research was conducted in the absence of any commercial or financial relationships that could be construed as a potential conflict of interest.

**Publisher's Note:** All claims expressed in this article are solely those of the authors and do not necessarily represent those of their affiliated organizations, or those of the publisher, the editors and the reviewers. Any product that may be evaluated in this article, or claim that may be made by its manufacturer, is not guaranteed or endorsed by the publisher.

Copyright © 2022 Zhang, Mou, Zhang, Suo, Zhou, Gu, Wang and Tan. This is an open-access article distributed under the terms of the Creative Commons Attribution License (CC BY). The use, distribution or reproduction in other forums is permitted, provided the original author(s) and the copyright owner(s) are credited and that the original publication in this journal is cited, in accordance with accepted academic practice. No use, distribution or reproduction is permitted which does not comply with these terms.



# Ferroptosis in Chronic Liver Diseases: Opportunities and Challenges

Xiaoxi Zhou<sup>1,2†</sup>, Yadong Fu<sup>1,2,3,4†</sup>, Wei Liu<sup>1,2</sup>, Yongping Mu<sup>1,2</sup>, Hua Zhang<sup>1,2</sup>, Jiamei Chen<sup>1,2\*</sup> and Ping Liu<sup>1,2,3\*</sup>

<sup>1</sup>Key Laboratory of Liver and Kidney Diseases, Ministry of Education, Institute of Liver Diseases, Shuguang Hospital Affiliated to Shanghai University of Traditional Chinese Medicine, Shanghai, China, <sup>2</sup>Shanghai Key Laboratory of Traditional Chinese Clinical Medicine, Shanghai, China, <sup>3</sup>Institute of Interdisciplinary Medicine, Shanghai University of Traditional Chinese Medicine, Shanghai, China, <sup>4</sup>State Key Laboratory of Cell Biology, Center for Excellence in Molecular Cell Science, Shanghai Institute of Biochemistry and Cell Biology, Chinese Academy of Sciences, Shanghai, China

## OPEN ACCESS

### Edited by:

Yanqing Liu,  
Columbia University, United States

### Reviewed by:

Zhenyi Su,  
Columbia University, United States  
Min Nie,  
Nanjing Drum Tower Hospital, China  
Xin Wang,  
National Institutes of Health (NIH),  
United States

### \*Correspondence:

Jiamei Chen  
cjm0102@126.com  
Ping Liu  
liuliver@vip.sina.com

<sup>†</sup>These authors have contributed  
equally to this work and share first  
authorship

### Specialty section:

This article was submitted to  
Molecular Diagnostics and  
Therapeutics,  
a section of the journal  
Frontiers in Molecular Biosciences

**Received:** 25 April 2022

**Accepted:** 16 May 2022

**Published:** 03 June 2022

### Citation:

Zhou X, Fu Y, Liu W, Mu Y, Zhang H,  
Chen J and Liu P (2022) Ferroptosis in  
Chronic Liver Diseases: Opportunities  
and Challenges.  
Front. Mol. Biosci. 9:928321.  
doi: 10.3389/fmolb.2022.928321

Ferroptosis, an iron-dependent non-apoptotic cell death characterized by lipid peroxidation, is a cell death pathway discovered in recent years. Ferroptosis plays an important role in tumors, ischemia-reperfusion injury, neurological diseases, blood diseases, etc. Recent studies have shown the importance of ferroptosis in chronic liver disease. This article summarizes the pathological mechanisms of ferroptosis involved in System Xc<sup>-</sup>, iron metabolism, lipid metabolism, and some GPX4-independent pathways, and the latest research on ferroptosis in chronic liver diseases such as alcoholic liver disease, non-alcoholic fatty liver disease, liver fibrosis, hepatocellular carcinoma. In addition, the current bottleneck issues that restrict the research on ferroptosis are proposed to provide ideas and strategies for exploring new therapeutic targets for chronic liver diseases.

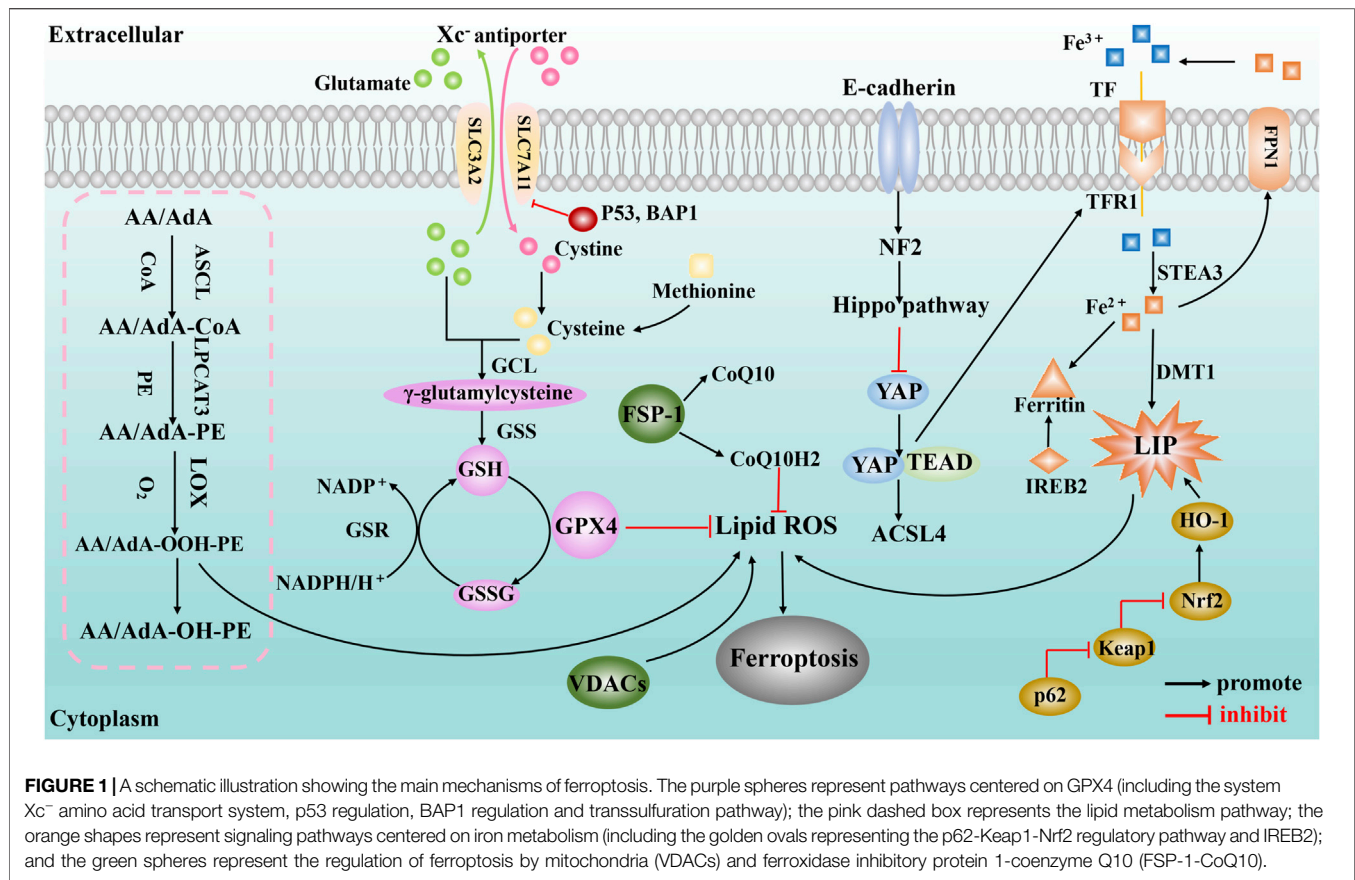
**Keywords:** ferroptosis, cell death, iron metabolism, lipid peroxidation, chronic liver diseases, liver fibrosis, hepatocellular carcinoma

## INTRODUCTION

Ferroptosis is a type of regulatory cell death discovered in recent years. It is an iron-dependent non-apoptotic cell death characterized by lipid peroxidation (Dixon et al., 2012), and was first proposed by Dixon et al. in 2012 (Li J. et al., 2020). Ferroptosis is distinct from apoptosis, necrosis, and other well-characterized types of regulated cell death, and is characterized by rounded cell morphology, smaller mitochondria, and rupture of the outer mitochondrial layer, but no rupture of the plasma membrane, reduced cristae, nuclei of normal size, and no chromatin condensation (Dixon et al., 2012).

There are many types of ferroptosis inducers, which can be roughly divided into four categories. The first type includes erastin, sulfasalazine, glutamate, and p53, which target the cystine/glutamate antiporter, and are associated with impaired cystine uptake, glutathione (GSH) depletion, and loss of glutathione peroxidase 4 (GPX4) activity. The second type of ferroptosis inducers, including RSL3 and DP17, directly inhibit the activity of GPX4, and their mechanism is related to the covalent interaction with GPX4 and the inhibition of enzyme activity. The third type of ferroptosis inducers are those that induce ferroptosis by depleting GPX4 and CoQ10, such as FIN56. The last type of ferroptosis inducers, such as FINO2 (1,2-dioxane-containing endoperoxide), induce ferroptosis by promoting iron oxidation, driving lipid peroxidation and indirect inactivation of GPX4 (Feng and Stockwell, 2018; Capelletti et al., 2020). The inhibitors of ferroptosis are mainly divided into lipid autooxidation inhibitors and





lipoygenase inhibitors, according to the lipid peroxidation pathway. The former includes compounds that react with chain free radicals and can inhibit the autoxidative chain reaction, such as ferrostatin-1 and liproxtatin-1 (Xie et al., 2016). The latter can inactivate the enzymatic activity by removing the active site that binds iron (e.g., iron chelators) (Angeli et al., 2017).

The liver is one of the main storage sites of iron, and is also the main source of hepcidin, an important hormone regulating iron metabolism (Capelletti et al., 2020). Many chronic liver diseases share the characteristics of ferroptosis such as abnormal iron metabolism and lipid peroxidation, indicating that ferroptosis is closely related to chronic liver disease. Current researches on the role and mechanisms of ferroptosis in the pathogenesis and progression of chronic liver diseases are sorted out, and the advantages and limitations of the existing researches are discussed, which may provide new ideas for the treatment of chronic liver diseases.

## PATHOLOGICAL MECHANISMS OF FERROPTOSIS

The pathological mechanism of ferroptosis is mainly related to System Xc<sup>-</sup> malfunction, abnormal iron metabolism, abnormal lipid metabolism, etc. (Figure 1).

### System Xc<sup>-</sup> Malfunction

System Xc<sup>-</sup> and GPX4 are the core regulatory targets in amino acid metabolism of ferroptosis. System Xc<sup>-</sup> is a sodium-independent antiporter composed of the heavy chain solute carrier family 3 member 2 (SLC3A2) and the light chain solute carrier family 7 member 11 (SLC7A11) (Lewerenz et al., 2013). System Xc<sup>-</sup> exchanges extracellular cystine and intracellular glutamate in a 1:1 ratio in an ATP-dependent manner; subsequently, the cystine transported into the cell is reduced to cysteine, which is used to synthesize the main antioxidant GSH in the cell (Dixon et al., 2012). Studies have shown (Wang L. et al., 2020) that inhibiting the activity of system Xc<sup>-</sup> can reduce the synthesis of intracellular GSH. The synthesis of GSH is essential to maintain the activity of GPX4, which is a physiological regulator of antioxidative damage (Capelletti et al., 2020). Once GPX4 is inactivated, it can cause severe lipid peroxidative damage, which, in turn, triggers ferroptosis (Ursini and Maiorino, 2020); hence, it is considered to be the main regulator of ferroptosis. Malfunctioning of system Xc<sup>-</sup> will affect the synthesis of intracellular GSH, limiting the superoxide-scavenging efficiency of GPX4, causing excessive lipid peroxidation and ferroptosis. The function of system Xc<sup>-</sup> is also affected by a variety of tumor suppressors. p53 is a tumor suppressor with extensive and powerful functions, and it has been reported to promote ferroptosis (Liu and Gu, 2022). Studies (Jiang et al., 2015) have shown that p53 (especially acetylation

deficient mutant p53) can suppress cystine uptake by inhibiting the expression of SLC7A11, resulting in insufficient intracellular GSH synthesis, affecting the normal function of GPX4 and rendering cells sensitive to ferroptosis. Another study (Zhang Y. et al., 2018) suggests that the tumor suppressor BRCA1-associated protein 1 (BAP1) also promotes ferroptosis by downregulating the expression of SLC7A11. BAP1 encodes a nuclear deubiquitination enzyme to reduce histone 2A ubiquitination (H2Aub) on chromatin, and inhibits cystine uptake by inhibition of SLC7A11 expression, which leads to lipid peroxidation and ferroptosis.

## Abnormal Iron Metabolism

Iron homeostasis is very important for maintaining the functions of various tissues and organs in the body (Yu et al., 2020). In the human body, iron exists mainly in two forms,  $\text{Fe}^{2+}$  and  $\text{Fe}^{3+}$ . After  $\text{Fe}^{3+}$  binds to transferrin in plasma, the iron-bearing transferrin binds to transferrin receptor 1 (TFR1) on cell membranes and enters cells by endocytosis. Then,  $\text{Fe}^{3+}$  is released from transferrin in an acidic environment and reduced to unstable and highly reactive  $\text{Fe}^{2+}$ , a part of which enters the cytoplasmic labile iron pool (LIP), and another part of  $\text{Fe}^{2+}$  can be absorbed by ferritin or hemoglobin-protein complexation. In addition,  $\text{Fe}^{2+}$  can be excreted through ferroportin 1 (FPN1) *via* ferritin to maintain iron homeostasis inside and outside the cell.

Iron overload is an important cause of ferroptosis. For example, intake of iron ions can accelerate the occurrence of ferroptosis, which is a phenomenon that does not occur when supplementing other metal elements (Dixon et al., 2012); while increasing the expression of FPN1 promotes the extracellular release of iron ions, it can significantly reduce iron overload and reverse the occurrence of ferroptosis (Zhao et al., 2020). The Fenton reaction is an important source of reactive oxygen species (ROS) in the process of ferroptosis, which means that the reaction between  $\text{Fe}^{2+}$  and  $\text{H}_2\text{O}_2$  can oxidize many known organic compounds such as carboxylic acids, alcohols, and esters to inorganic states and generate strong oxidative factors such as hydroxyl radicals (He et al., 2020). When the intracellular iron is overloaded, the excess  $\text{Fe}^{2+}$  exceeds the processing upper limit of the normal iron metabolism pathway and leads to the Fenton reaction, which can promote the production of lipid peroxidation and ROS, thereby triggering ferroptosis (Daher et al., 2017).

Other studies have shown that the p62-Keap1-Nrf2 signaling pathway may interfere with the occurrence and development of ferroptosis by affecting factors related to iron metabolism. Nrf2 is an important regulator of antioxidant responses, and studies have confirmed (Sun et al., 2016b) that under the intervention of ferroptosis inducers, the expression of p62 prevents the degradation of Nrf2 and increases the accumulation of Nrf2 protein by inactivating Keap1. Nrf2 protein further activates the expressions of retinoblastoma protein (Rb) and metallothionein-1G (MT-1G), and induces the transcriptional expressions of intracellular ferritin heavy chain (FTH1), NAD(P)H: quinone oxidoreductase 1

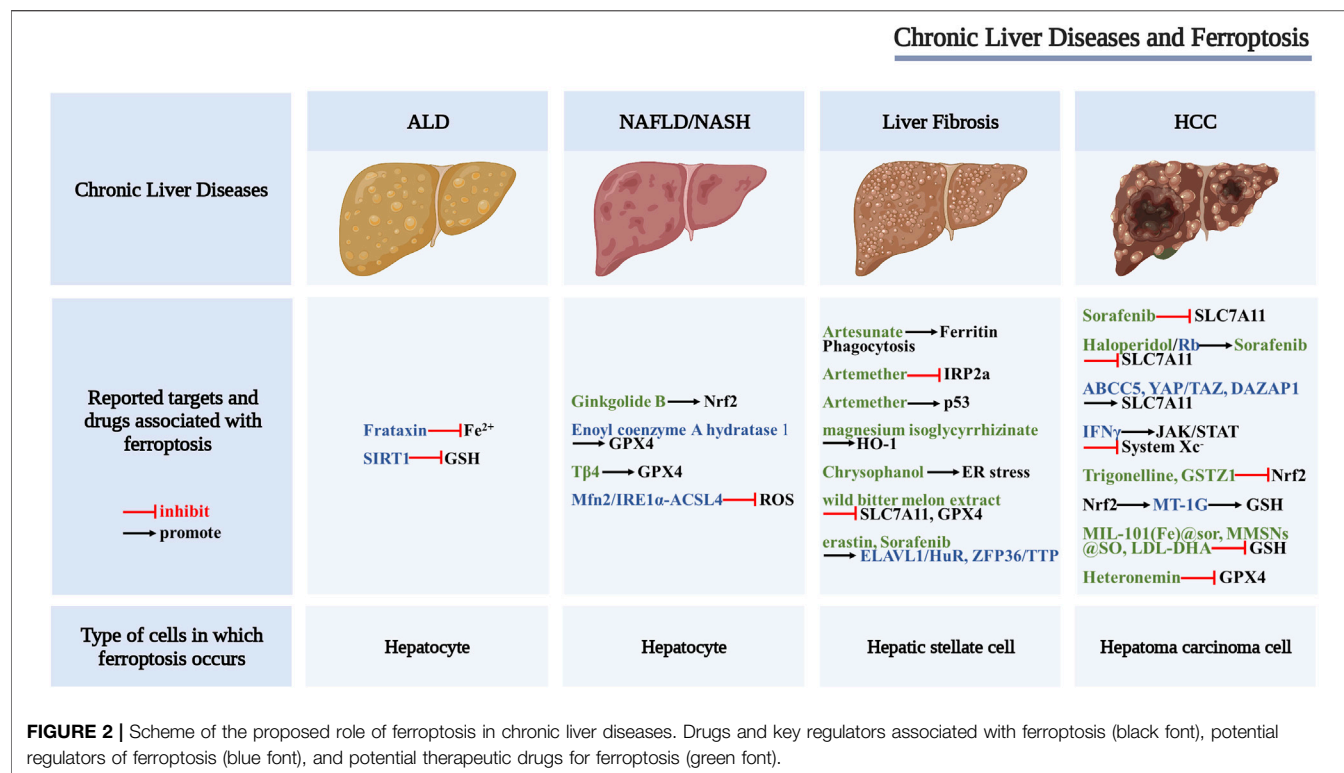
(NQO1), and heme oxygenase 1 (HO-1). The upregulation of HO-1 can promote the release of iron in heme and increase  $\text{Fe}^{2+}$  in LIP, thereby promoting the occurrence of lipid peroxidation and ferroptosis. Interestingly, in a recent study of 3D cancer spheroid models coupled with CRISPR-Cas9 screens (Takahashi et al., 2020), Nrf2 hyperactivation was shown to inhibit ferroptosis and promote the proliferation and survival of lung tumor spheroids. Targeting Nrf2 and GPX4 can kill tumor spheroids overall. This opens up a new perspective for studying the role of Nrf2 in the mechanism of ferroptosis, and also indicates the complexity of Nrf2 in ferroptosis. In addition, studies have reported that iron response element-binding protein 2 recombinant protein (IREB2) (Dixon et al., 2012) and heat shock 27 kDa protein 1 (Sun et al., 2016b) affect iron metabolism and downregulate the sensitivity of cells to ferroptosis by inhibiting the expression of TFR1.

## Abnormal Lipid Metabolism

Lipid peroxidation caused by abnormal lipid metabolism is one of the main mechanisms of ferroptosis, and lipid peroxidation of membrane phospholipids containing polyunsaturated fatty acid (PUFA) chains is the core of ferroptosis. Lipid peroxidation can oxidize PUFAs to peroxides, which affects the normal functions of cells. For example, it has been reported (Feng and Stockwell, 2018) that lipid peroxidation disrupts ion gradients and changes the fluidity and permeability of cell membranes.

However, the mechanism by which the lipid peroxidation of PUFAs affects cell ferroptosis warrants further exploration. As is known, overproduction of lipid peroxides can lead to their accumulation, triggering ferroptosis. The formation of lipid peroxides in PUFAs requires the participation of arachidonic acid lipid oxygenases (ALOXs), acyl-CoA synthase long-chain family 4 (ACSL4), and lysophosphatidylcholine acyltransferase 3 (LPCAT3) (Lei et al., 2019), and they are closely related to the occurrence of ferroptosis. Studies have found that ferroptosis in lung and intestinal tissue injury induced by ischemia-reperfusion is related to ACSL4 (Li et al., 2019; Xu et al., 2020). ACSL4 and LPCAT3 can regulate the sensitivity of cells to ferroptosis by affecting cellular lipid composition (Dixon et al., 2015; Doll et al., 2017). Silencing ALOXs can inhibit the occurrence and development of ferroptosis (Shintoku et al., 2017). Other pathways can also promote the synthesis of PUFAs, such as the decomposition of glutamine to glutamate, which is further converted into  $\alpha$ -ketoglutarate, which also promotes the production of lipids, thereby increasing the formation of lipid peroxides and promoting the progression of ferroptosis.

Lipid peroxidation products of PUFAs, such as malondialdehyde (MDA) and 4-hydroxynonenal (4-HNE), induce ferroptosis through their cytotoxicity. PUFAs produce large amounts of MDA through chemical and enzymatic reactions (Tsikas, 2017) and are the most commonly measured biomarkers of lipid peroxidation. Moreover, the accumulation of 4-HNE and the formation of 4-HNE adducts caused by redox imbalance also aggravate the cytotoxic effect (Wang F. X. et al., 2020), which, in turn, increases the permeability of the cell membrane and causes ferroptosis.



## Other Mechanisms Associated With Ferroptosis

Although GPX4 is a core regulatory protein of ferroptosis, the responses of GPX4 inhibitors in different cancer cell lines are inconsistent, suggesting that other factors may regulate ferroptosis. Recent studies (Doll et al., 2019) have identified GPX4-independent pathways that also trigger ferroptosis, such as ferroptosis-suppressing protein 1 (FSP1), which was originally identified as apoptosis-inducing factor, mitochondrion-associated 2 (AIFM2). It protects against ferroptosis caused by GPX4 deletion, and the mechanism is related to CoQ 10 catalyzing the capture of lipid peroxyl radicals by NAD(P)H.

The E-cadherin-NF2-Hippo-YAP signaling axis is a non-cell-autonomous regulation of ferroptosis. Studies have found that epithelial cell ferroptosis is suppressed by E-cadherin-mediated intercellular interactions through activation of the intracellular NF2 (also known as merlin) and Hippo signaling pathway. Antagonizing NF2 enhances YAP activity to promote ferroptosis by upregulating several ferroptosis modulators, including ACSL4 and TFR1 (Wu et al., 2019).

Tumor suppressor p53 inhibits the expression of SLC7A11 and is involved not only in GPX4-dependent ferroptosis but also in GPX4-independent ferroptosis by targeting ALOX12, iPLA2 $\beta$ , and SAT1/ALOX15 (Ou et al., 2016; Chu et al., 2019; Chen et al., 2021). It is worth noting that the role of p53 in ferroptosis is not only limited to the regulation of System Xc<sup>-</sup> function but also related to the regulation of lipid and iron metabolism (Liu and Gu, 2021). These results suggest that p53-mediated ferroptosis may be a basic and important ferroptosis pathway as GPX4-based

ferroptosis. In addition, it has been reported (Friedmann Angeli et al., 2014; Feng and Stockwell, 2018) that the occurrence of ferroptosis is closely related to mitochondria, in that mitochondrial respiration can promote the production of ROS in cells, thereby promoting ferroptosis. The related mechanism has also been studied. For example (Li J. et al., 2020), the ferroptosis inducer erastin can directly act on the mitochondrial voltage-dependent anion channel (VDAC), which is not dependent on the GPX4 pathway.

## ROLE OF FERROPTOSIS IN CHRONIC LIVER DISEASES

Many studies have shown that ferroptosis characterized by System Xc<sup>-</sup> malfunction, abnormal iron metabolism, and abnormal lipid metabolism can be found in different chronic liver diseases, such as alcoholic liver disease, non-alcoholic fatty liver disease, liver fibrosis, and hepatocellular carcinoma, suggesting that targeting ferroptosis may provide new strategies for the treatment of chronic liver diseases (Figure 2).

### Ferroptosis and Alcoholic Liver Disease

Alcoholic liver disease (ALD), including alcoholic fatty liver disease, alcoholic hepatitis, alcoholic liver cirrhosis and their complications, is one of the most common types of chronic liver disease (Singal et al., 2018). A prospective follow-up study of patients with alcoholic cirrhosis found that hepatic iron overload exacerbates alcohol-induced liver damage and is associated with various adverse outcomes (Ganne-Carrié et al.,

2000). Animal studies have shown that iron and alcohol can synergistically promote the development of ALD (Stål and Hultcrantz, 1993; Tsukamoto et al., 1995). Ferrostatin-1 can significantly reduce alcoholic liver injury *in vitro* and *in vivo* (Liu C.-Y. et al., 2020), suggesting that ferroptosis may play an important role in the progression of ALD.

Frataxin is a mitochondrial protein mainly involved in the body's iron homeostasis and oxidative stress response. Frataxin deficiency can increase the iron content and lipid peroxidation level of LIP, mediate alcohol-driven ferroptosis, and promote the occurrence of ALD (Liu J. et al., 2020). Other studies have found that the deletion of intestinal SIRT1 can protect mice from alcohol-induced liver inflammation, and the mechanism is related to improving iron metabolism disorder, increasing liver GSH content, and alleviating lipid peroxidation damage. These results suggest that targeting intestinal SIRT1 to inhibit liver ferroptosis may have the potential of treating ALD (Zhou et al., 2020). In addition, clinical studies found decreased hepcidin levels in the liver of patients with ALD, suggesting that long-term alcohol consumption may cause iron overload in the liver, inducing ferroptosis (Costa-Matos et al., 2012).

## Ferroptosis and Nonalcoholic Fatty Liver Disease

Nonalcoholic fatty liver disease (NAFLD) is a liver disease characterized by the accumulation of lipid droplets, hepatocyte death, immune/inflammatory cell infiltration, and a certain degree of fibrosis. In some cases, NAFLD may develop into non-alcoholic steatohepatitis (NASH), which is a progressive liver disease that can further develop into liver fibrosis, liver cirrhosis, and hepatocellular carcinoma (Chalasani et al., 2018; Eslam et al., 2020). NAFLD alters iron metabolism in the body, and the progression of NAFLD is accompanied by extensive lipid accumulation. Owing to the close relationship between iron, lipid metabolism, and ferroptosis (Bozzini et al., 2005), it is of great significance to explore the relationship between ferroptosis and NAFLD.

Neither the specific inhibitor of programmed necrosis nor the knockout of the mixed lineage kinase domain-like protein MLKL could inhibit cell death, while the ferroptosis inhibitors trolox and DFO inhibited cell death in a methionine-/choline-deficient (MCD), ethionine-supplemented (CDE) diet-induced NASH mouse model, suggesting that the ferroptosis pathway is activated in the liver of NASH mice (Tsurusaki et al., 2019). Similarly, arsenic-induced NASH is also related to ferroptosis. The researchers found that the content of ACSL4, a key regulator of ferroptosis, was increased in the arsenic-induced rat NASH model. Further research found that inhibiting the Mfn2/IRE1 $\alpha$ -ACSL4 pathway may be one of the important mechanisms to prevent the occurrence and development of NASH (Wei et al., 2020). It has been reported that the expression of GPX4 in mouse liver is decreased in the MCD combined with RSL3 mouse model, and treatment with GPX4 activator, iron chelator, or ferroptosis inhibitor can significantly slow the progression of NASH by enhancing GPX4 activity and affecting iron metabolism (Qi et al., 2020). In addition, the study by Li *et al.* showed that

inhibition of ferroptosis could reduce the degree of liver fibrosis in a mouse NASH model induced by MCD, and the mechanism was related to reduction the level of lipid peroxidation to inhibit ferroptosis (Li X. et al., 2020). The above studies suggest that ferroptosis promotes the progression of NASH, and inhibition of ferroptosis may be a new approach to the treatment of NASH.

Currently, targeted ferroptosis therapy for NAFLD has also achieved some progress. Researchers found that T $\beta$ 4 can effectively improve liver lipid metabolism-related indicators in high-fat diet (HFD)-induced NAFLD rat models and inhibit the palmitic acid (PA)-induced cell death in hepatocyte line LO2. Combining T $\beta$ 4 with ferrostatin-1 can enhance the effect of T $\beta$ 4. However, either erastin or siRNA interference with GPX4 expression could attenuate the protective effect of T $\beta$ 4. This study suggests that T $\beta$ 4 may protect hepatocytes by inhibiting the GPX4 depletion-mediated ferroptosis pathway (Zhu et al., 2021). As a lipid metabolism enzyme, enoyl coenzyme A hydratase 1 (ECH1) is a key component of mitochondrial fatty acid  $\beta$ -oxidation. Studies have shown that ECH1 knockdown can aggravate liver steatosis, inflammation, and fibrosis in mice, while ferrostatin-1 intervention can alleviate the pathological changes aggravated by ECH1 knockdown, suggesting that ECH1 may slow the progression of NASH in mice by inhibiting ferroptosis (Liu B. et al., 2021).

In addition, studies have shown that traditional Chinese medicines or components of traditional Chinese medicines also play an important role in the treatment of NAFLD. Both HFD-induced ApoE<sup>-/-</sup> mouse models and PA/OA-induced HepG2 cells showed iron overload, upregulation of TFR1 expression, and downregulation of FTH1 expression. Ginkgolide B (GB) treatment can significantly increase the expression of Nrf2 and alleviate iron overload. These results suggest that GB may inhibit the progression of NAFLD by regulating the Nrf2 signaling pathway, inhibiting lipid accumulation and oxidative stress-induced ferroptosis in hepatocytes (Yang et al., 2020).

## Ferroptosis and Liver Fibrosis

Although liver fibrosis has been a global health concern for a long time, there is no FDA-approved effective drug to treat this condition, and the discovery of ferroptosis provides a new strategy to address this issue (Pan et al., 2021). Studies (Daher et al., 2017) have shown that the ferroptosis inhibitor ferrostatin-1 could effectively reverse liver fibrosis induced by a high-iron diet or CCl<sub>4</sub> and ferroptosis induced by hepatic iron overload could aggravate acetaminophen-induced liver fibrosis in mice (Aldrovandi and Conrad, 2020), suggesting that hepatocyte ferroptosis promotes the progression of liver fibrosis. By contrast, when the target cells of ferroptosis are activated hepatic stellate cells (HSCs), the occurrence of ferroptosis can reduce liver fibrosis. SLC7A11 is a cystine/glutamate antiporter that can provide raw materials for intracellular synthesis of GSH (Dixon et al., 2012). Studies (Du et al., 2021) have shown that inhibiting the expression of SLC7A11 could induce ferroptosis in HSCs and alleviate liver fibrosis. Thus, ferroptosis acts as a “double-edged sword” in liver fibrosis. Given the important role of ferroptosis in the occurrence and development of liver



fibrosis, the development of some drugs targeting ferroptosis has become a new research hotspot. For example, Zhang *et al.* (Zhang Z. *et al.*, 2018; Zhang *et al.*, 2020) found that erastin and sorafenib could induce ferroptosis in HSCs, thereby reducing liver fibrosis in mice. Their mechanism of action is related to the regulation of RNA-binding proteins such as ZFP36/TTP and ELAVL1/HuR. ZFP36/TTP inhibits ferroptosis, while ELAVL1/HuR promotes ferroptosis, which broadens the new molecular mechanism of ferroptosis to a certain extent.

There is growing evidence that natural products are safe and effective in preventing and treating liver fibrosis. Medications such as artesunate, artemether, magnesium isoglycyrrhizinate, chrysophanol, and wild bitter gourd extract have been confirmed to act on ferroptosis-related pathways and affect the progression of liver fibrosis. As reported by *in vitro* and *in vivo* studies (Kong *et al.*, 2019), artesunate can alleviate liver fibrosis by triggering ferritin phagocytosis-mediated ferroptosis in HSCs. Artemether and magnesium isoglycyrrhizinate have also been shown to have good anti-fibrotic effects *in vitro* and *in vivo* (Sui *et al.*, 2018; Li Y. *et al.*, 2020), both of which can induce ferroptosis in HSCs. Artemether inhibits the ubiquitination of IRP2a and causes the accumulation of IRP2a in HSCs, thereby inducing the production of iron and ROS in HSCs and promoting the occurrence of ferroptosis. Other related studies (Wang *et al.*, 2019) showed that the tumor suppressor gene p53 is an upstream molecule of artemether-induced ferroptosis in HSCs, suggesting that artemether can alleviate CCl<sub>4</sub>-induced hepatic fibrosis by promoting p53-dependent ferroptosis in HSCs. Heme oxygenase 1 (HO-1) is the upstream molecule of magnesium isoglycyrrhizinate-induced ferroptosis in HSCs, and siRNA knockdown of HO-1 can block magnesium isoglycyrrhizinate-induced ferroptosis in HSCs, thereby promoting liver fibrosis (Li Y. *et al.*, 2020), suggesting that magnesium isoglycyrrhizinate alleviates CCl<sub>4</sub>-induced liver fibrosis by promoting HO-1-mediated ferroptosis in HSCs. Kuo *et al.* (2020) found that chrysophanol isolated from the rhizome of rhubarb can inhibit hepatitis B virus x protein (HBx)-induced activation of HSCs through ER stress and ferroptosis-dependent and GPX4-independent pathways, thereby reducing liver fibrosis. In addition, wild bitter melon extract can downregulate the protein levels of GPX4 and SLC7A11 in LPS-induced HSCs, suggesting that wild bitter melon extract can exert an anti-hepatic fibrosis effect by inducing ferroptosis (Ho *et al.*, 2021). The exact effect of ferroptosis on chronic liver diseases is related to the cell type and the specific disease environment. In liver fibrosis, ferroptosis exerts opposite effects on hepatocytes and HSCs; the former aggravates liver damage, while the latter reduces liver damage. Therefore, ferroptosis may have completely opposite effects in different cell types, and the possible side effects can be largely alleviated if drug delivery systems targeting specific cell types can be developed.

## Ferroptosis and Hepatocellular Carcinoma

Hepatocellular carcinoma (HCC) is a leading cancer worldwide (Hartke *et al.*, 2017). Sorafenib is an oral kinase inhibitor that inhibits tumor cell proliferation and angiogenesis, induces cancer cell apoptosis, and is a first-line molecular targeted drug for

advanced HCC (Kong F.-H. *et al.*, 2021). It is a ferroptosis inducer similar to erastin, which can induce ferroptosis in liver cancer cells, indicating that ferroptosis plays an important role in the killing effect of sorafenib on hepatoma carcinoma cells. The mechanism may be related to inhibiting the uptake of cystine by system Xc<sup>-</sup>, resulting in GSH depletion, loss of GPX4 activity, and accumulation of ROS (Galmiche *et al.*, 2014). The study also found that the mechanism of sorafenib-induced ferroptosis in hepatoma carcinoma cells is related to Rb, which is a major negative regulator of cell proliferation and cell cycle progression. Rb-deficient hepatoma carcinoma cells are exposed to sorafenib. The cell death rate is much higher than that of hepatoma carcinoma cells with normal Rb protein level, and the mechanism may be related to the exposure of mitochondrial respiratory chain to sorafenib, which produces a large amount of ROS (Louandre *et al.*, 2015).

Although sorafenib has a certain curative effect on the recurrence and metastasis of HCC, owing to the long-term exposure of patients to the drug, the sensitivity of hepatoma carcinoma cells to sorafenib gradually decreases. Therefore, the issue of drug resistance to sorafenib should be urgently addressed. The study of regulators that regulate SLC7A11, the core link of ferroptosis, will help to explore how to overcome the resistance to sorafenib in the treatment of HCC. For example, studies (Huang *et al.*, 2021) have shown that ABCC5, as a novel regulator of ferroptosis in hepatoma carcinoma cells, can stabilize the SLC7A11 protein, increase the generation of intracellular GSH, and reduce the accumulation of lipid peroxidation products, thereby inhibiting ferroptosis, while downregulation of ABCC5 expression can significantly reduce the resistance of hepatoma carcinoma cells to sorafenib. Another study showed that the key driver of HCC resistance to sorafenib is YAP/TAZ, which not only induces the expression of SLC7A11 in a TEAD-dependent manner but can also maintain the stability, nuclear localization, and transcriptional activity of ATF4 protein, and then synergistically induce the expression of SLC7A11, thereby inhibiting sorafenib-induced ferroptosis (Gao *et al.*, 2021) and increasing resistance to sorafenib. The chaperone molecule DAZAP1 of SLC7A11 mRNA plays an important role in HCC. DAZAP1 interacts with the 3'UTR (untranslated region) of SLC7A11 mRNA to regulate the stability of SLC7A11 (Wang *et al.*, 2021b). In addition, activation of the p62-Keap1-Nrf2 pathway can resist sorafenib-induced ferroptosis in hepatoma carcinoma cells (Sun *et al.*, 2016a). MT-1G is one of the target genes of the Nrf2 pathway. Clinical studies (Houessinon *et al.*, 2016) have shown that the serum MT-1G protein level increased in patients with HCC treated with sorafenib, and that the deletion of MT-1G gene accelerated GSH depletion and lipid peroxidation. This indicates that MT-1G may promote sorafenib resistance in hepatoma carcinoma cells by inhibiting ferroptosis, suggesting that it can be used as a potential prognostic indicator for patients with advanced HCC receiving sorafenib. Some researchers also found that trigonelline, the main active ingredient of the traditional Chinese medicine fenugreek,

and glutathione transferase zeta 1 (GSTZ1) can promote ferroptosis by acting on Nrf2, thereby reducing sorafenib resistance (Wang et al., 2021a). Some scholars have confirmed, for the first time, that exposure of hepatoma carcinoma cells to sorafenib can cause Nrf2 inactivation and passive upregulation of sigma receptor expression. Sigma receptor antagonist haloperidol can synergize with sorafenib to promote ferroptosis in hepatoma carcinoma cells (Bai et al., 2017; Bai et al., 2019).

In addition to the research on sorafenib, the development of drugs targeting ferroptosis-related pathways for the treatment of HCC has also become one of the research hotspots. Chang et al. (2021) discovered a marine terpenoid, heteronemin, which can reduce the expression of GPX4 and induce ferroptosis in hepatoma carcinoma cells, suggesting that heteronemin can be used as a potential drug for the treatment of HCC. IFN $\gamma$  has also been confirmed to inhibit system Xc<sup>-</sup> activity by activating JAK/STAT signaling and increase the sensitivity of hepatoma carcinoma cells to ferroptosis, which will provide a new mechanism for the use of IFN $\gamma$  in treating HCC (Kong R. et al., 2021). In addition, researchers have used nanotechnology to develop some HCC therapeutics based on the ferroptosis mechanism, such as sorafenib (sor)-loaded MIL-101(Fe) nanoparticles (NPs) [MIL-101(Fe)@sor] (Liu X. et al., 2021), MMSN@SO (Tang et al., 2019) and LDL nanoparticles reconstituted with the natural omega-3 fatty acid docosahexaenoic acid (LDL-DHA) (Ou et al., 2017). These substances can deplete GSH and reduce the level of GPX4, and induce ferroptosis in hepatoma carcinoma cells. In conclusion, ferroptosis could become a potential target for the treatment of HCC.

## LIMITATIONS IN CURRENT RESEARCHES OF FERROPTOSIS IN CHRONIC LIVER DISEASES

The current research on ferroptosis has some limitations. Firstly, the research results are mostly based on animal models and lack reliable clinical evidence, and most researches are limited to the observation of curative effect, owing to a lack of a mature ferroptosis model and systematic in-depth mechanism research. Despite the existence of various types of ferroptosis inducers and inhibitors, they are rarely used in clinical practice. Secondly, many chronic liver diseases may have multiple cell death modes at the same time, and further research is needed on the connection between ferroptosis and other cell deaths. When regulating a specific cell death pathway, the influence of other cell death pathways must be taken into account. Moreover, the current researches on ferroptosis mostly focus on HCC, and research on other liver diseases is relatively lacking. In addition to the types of liver diseases mentioned in this article, it has also been reported (Kain et al., 2020) that Nutlin-3 (a commonly used, highly selective, membrane-permeable MDM2 antagonist) can reduce the plasmodium liver stage infection

by activating the p53-SLC7A11-GPX4 signaling pathway. This indicates that the ferroptosis pathway is an effective immune barrier against parasites. The role of ferroptosis in many liver diseases is still largely unclear, and further in-depth research is warranted to reap more fruitful achievements in this field.

The most urgent issue to be addressed at present is the lack of specific and sensitive biomarkers and detection methods to clarify the characterization of ferroptosis. Currently, the occurrence of ferroptosis is usually judged by direct observation of cell morphological changes using transmission electron microscopy. Pathological tissue staining has been used to evaluate the accumulation of lipid peroxides, iron overload, etc., and the occurrence of ferroptosis was indirectly and comprehensively judged from different aspects by measuring lipid peroxidation and iron metabolism indicators related to ferroptosis.

## CONCLUSION

Ferroptosis, as a new form of cell death, is involved in the occurrence and development of various chronic liver diseases through a complex mechanism involving multiple pathways and links, which provides a new direction for the treatment of chronic liver diseases. In particular, it provides important ideas for combination therapy for HCC and the development of new drugs. The causes of cell ferroptosis include dysfunction of amino acid transporters, changes in iron homeostasis, and accumulation of lipid peroxidation. Many key proteins in the ferroptosis-related signaling pathway, such as GPX4, which regulate ferroptosis, may become drug targets. GPX4 is a key enzyme that has antioxidant properties and can catalyze the reduction reaction of lipid peroxides, thereby inhibiting the occurrence of ferroptosis. Previous studies on the mechanism of ferroptosis mostly relied on related mechanisms centered on GPX4. However, with the in-depth study of ferroptosis, more and more other ferroptosis regulations have been discovered. Surprisingly, p53 has been found to modulate ferroptosis by both the GPX4-dependent and GPX4-independent ferroptosis pathways, which suggests that targeting p53-mediated ferroptosis could be a potential treatment of chronic liver diseases, particularly HCC. In addition, recent studies have found that GPX4-independent mechanisms such as the FSP1 suppressor and the Hippo signaling pathway are also involved in the regulation of ferroptosis.

Existing research suggests that traditional Chinese medicine has a certain regulatory effect on ferroptosis. The occurrence of ferroptosis is inseparable from lipid accumulation and oxidative stress. There are many antioxidant components in traditional Chinese medicine, such as *Schisandra chinensis* and *Salvia miltiorrhiza*.

Targeting ferroptosis can be regarded as a new research idea for the treatment of chronic liver diseases. As a double-edged sword, inhibition of ferroptosis can be used to prevent and protect various chronic liver injuries caused by iron deposition and abnormal lipid metabolism, while induction of ferroptosis is helpful for the treatment of hepatocellular carcinoma. Further detailed studies on ferroptosis will provide important strategies for exploring new therapeutic targets and promoting new drug development for chronic liver diseases.

## AUTHOR CONTRIBUTIONS

XZ, YF, JC, and PL wrote the manuscript and were involved with project concept and submission; XZ, YF, WL, YM, and HZ performed data collection; JC and PL revised the manuscript and were responsible for final approval; all authors contributed to this manuscript.

## REFERENCES

- Aldrovandi, M., and Conrad, M. (2020). Ferroptosis: the Good, the Bad and the Ugly. *Cell Res.* 30(12), 1061–1062. doi:10.1038/s41422-020-00434-0
- Angeli, J. P. F., Shah, R., Pratt, D. A., and Conrad, M. (2017). Ferroptosis Inhibition: Mechanisms and Opportunities. *Trends Pharmacol. Sci.* 38(5), 489–498. doi:10.1016/j.tips.2017.02.005
- Bai, T., Lei, P., Zhou, H., Liang, R., Zhu, R., Wang, W., et al. (2019). Sigma-1 Receptor Protects against Ferroptosis in Hepatocellular Carcinoma Cells. *J. Cell Mol. Med.* 23(11), 7349–7359. doi:10.1111/jcmm.14594
- Bai, T., Wang, S., Zhao, Y., Zhu, R., Wang, W., and Sun, Y. (2017). Haloperidol, a Sigma Receptor 1 Antagonist, Promotes Ferroptosis in Hepatocellular Carcinoma Cells. *Biochem. Biophysical Res. Commun.* 491(4), 919–925. doi:10.1016/j.bbrc.2017.07.136
- Bozzini, C., Girelli, D., Olivieri, O., Martinelli, N., Bassi, A., De Matteis, G., et al. (2005). Prevalence of Body Iron Excess in the Metabolic Syndrome. *Diabetes Care* 28(8), 2061–2063. doi:10.2337/diacare.28.8.2061
- Capelletti, M. M., Manceau, H., Puy, H., and Peoc'h, K. (2020). Ferroptosis in Liver Diseases: An Overview. *Ijms* 21(14), 4908. doi:10.3390/ijms21144908
- Chalasan, N., Younossi, Z., Lavine, J. E., Charlton, M., Cusi, K., Rinella, M., et al. (2018). The Diagnosis and Management of Nonalcoholic Fatty Liver Disease: Practice Guidance from the American Association for the Study of Liver Diseases. *Hepatology* 67(1), 328–357. doi:10.1002/hep.29367
- Chang, W.-T., Bow, Y.-D., Fu, P.-J., Li, C.-Y., Wu, C.-Y., Chang, Y.-H., et al. (2021). A Marine Terpenoid, Heteronemin, Induces Both the Apoptosis and Ferroptosis of Hepatocellular Carcinoma Cells and Involves the ROS and MAPK Pathways. *Oxidative Med. Cell. Longev.* 2021, 1, 12. doi:10.1155/2021/7689045
- Chen, D., Chu, B., Yang, X., Liu, Z., Jin, Y., Kon, N., et al. (2021). iPLA2 $\beta$ -mediated Lipid Detoxification Controls P53-Driven Ferroptosis Independent of GPX4. *Nat. Commun.* 12(1), 3644. doi:10.1038/s41467-021-23902-6
- Chu, B., Kon, N., Chen, D., Li, T., Liu, T., Jiang, L., et al. (2019). ALOX12 Is Required for P53-Mediated Tumour Suppression through a Distinct Ferroptosis Pathway. *Nat. Cell Biol.* 21(5), 579–591. doi:10.1038/s41556-019-0305-6
- Costa-Matos, L., Batista, P., Monteiro, N., Simões, M., Egas, C., Pereira, J., et al. (2012). Liver Hepcidin mRNA Expression Is Inappropriately Low in Alcoholic Patients Compared with Healthy Controls. *Eur. J. Gastroenterology Hepatology* 24(10), 1158–1165. doi:10.1097/MEG.0b013e328355cfd0
- Daher, R., Manceau, H., and Karim, Z. (2017). Iron Metabolism and the Role of the Iron-Regulating Hormone Hepcidin in Health and Disease. *La Presse Médicale* 46(12 Pt 2), e272–e278. doi:10.1016/j.lpm.2017.10.006
- Dixon, S. J., Lemberg, K. M., Lamprecht, M. R., Skouta, R., Zaitsev, E. M., Gleason, C. E., et al. (2012). Ferroptosis: an Iron-dependent Form of Nonapoptotic Cell Death. *Cell* 149(5), 1060–1072. doi:10.1016/j.cell.2012.03.042
- Dixon, S. J., Winter, G. E., Musavi, L. S., Lee, E. D., Snijder, B., Rebsamen, M., et al. (2015). Human Haploid Cell Genetics Reveals Roles for Lipid Metabolism Genes in Nonapoptotic Cell Death. *ACS Chem. Biol.* 10(7), 1604–1609. doi:10.1021/acschembio.5b00245
- Doll, S., Freitas, F. P., Shah, R., Aldrovandi, M., da Silva, M. C., Ingold, I., et al. (2019). FSP1 Is a Glutathione-independent Ferroptosis Suppressor. *Nature* 575(7784), 693–698. doi:10.1038/s41586-019-1707-0
- Doll, S., Proneth, B., Tyurina, Y. Y., Panzilius, E., Kobayashi, S., Ingold, I., et al. (2017). ACSL4 Dictates Ferroptosis Sensitivity by Shaping Cellular Lipid Composition. *Nat. Chem. Biol.* 13(1), 91–98. doi:10.1038/nchembio.2239
- Du, K., Oh, S. H., Dutta, R. K., Sun, T., Yang, W. H., Chi, J. T., et al. (2021). Inhibiting xCT/SLC7A11 Induces Ferroptosis of Myofibroblastic Hepatic Stellate Cells but Exacerbates Chronic Liver Injury. *Liver Int.* 41(9), 2214–2227. doi:10.1111/liv.14945
- Eslam, M., Sanyal, A. J., George, J., Sanyal, A., Neuschwander-Tetri, B., Tiribelli, C., et al. (2020). MAFLD: A Consensus-Driven Proposed Nomenclature for Metabolic Associated Fatty Liver Disease. *Gastroenterology* 158(7), 1999–2014.e1991. doi:10.1053/j.gastro.2019.11.312
- Feng, H., and Stockwell, B. R. (2018). Unsolved Mysteries: How Does Lipid Peroxidation Cause Ferroptosis? *PLoS Biol.* 16(5), e2006203. doi:10.1371/journal.pbio.2006203
- Friedmann Angeli, J. P., Schneider, M., Proneth, B., Tyurina, Y. Y., Tyurin, V. A., Hammond, V. J., et al. (2014). Inactivation of the Ferroptosis Regulator Gpx4 Triggers Acute Renal Failure in Mice. *Nat. Cell Biol.* 16(12), 1180–1191. doi:10.1038/ncb3064
- Galmiche, A., Chaffert, B., and Barbare, J.-C. (2014). New Biological Perspectives for the Improvement of the Efficacy of Sorafenib in Hepatocellular Carcinoma. *Cancer Lett.* 346(2), 159–162. doi:10.1016/j.canlet.2013.12.028
- Ganne-Carrié, N., Christidis, C., Chastang, C., Ziolk, M., Chapel, F., and Imbert-Bismut, F. (2000). Liver Iron Is Predictive of Death in Alcoholic Cirrhosis: a Multivariate Study of 229 Consecutive Patients with Alcoholic And/or Hepatitis C Virus Cirrhosis: a Prospective Follow up Study. *Gut* 46(2), 277–282. doi:10.1136/gut.46.2.277
- Gao, R., Kalathur, R. K. R., Coto-Llerena, M., Ercan, C., Buechel, D., Shuang, S., et al. (2021). YAP/TAZ and ATF4 Drive Resistance to Sorafenib in Hepatocellular Carcinoma by Preventing Ferroptosis. *EMBO Mol. Med.* 13(12), e14351. doi:10.15252/emmm.202114351
- Hartke, J., Johnson, M., and Ghabril, M. (2017). The Diagnosis and Treatment of Hepatocellular Carcinoma. *Seminars Diagnostic Pathology* 34(2), 153–159. doi:10.1053/j.semdp.2016.12.011
- He, Y.-J., Liu, X.-Y., Xing, L., Wan, X., Chang, X., and Jiang, H.-L. (2020). Fenton Reaction-independent Ferroptosis Therapy via Glutathione and Iron Redox Couple Sequentially Triggered Lipid Peroxide Generator. *Biomaterials* 241, 119911. doi:10.1016/j.biomaterials.2020.119911
- Ho, C.-H., Huang, J.-H., Sun, M.-S., Tzeng, I.-S., Hsu, Y.-C., and Kuo, C.-Y. (2021). Wild Bitter Melon Extract Regulates LPS-Induced Hepatic Stellate Cell Activation, Inflammation, Endoplasmic Reticulum Stress, and Ferroptosis. *Evidence-Based Complementary Altern. Med.* 2021, 1, 11. doi:10.1155/2021/6671129
- Houesson, A., François, C., Sauzay, C., Louandre, C., Mongelard, G., Godin, C., et al. (2016). Metallothionein-1 as a Biomarker of Altered Redox Metabolism in Hepatocellular Carcinoma Cells Exposed to Sorafenib. *Mol. Cancer* 15(1), 38. doi:10.1186/s12943-016-0526-2
- Huang, W., Chen, K., Lu, Y., Zhang, D., Cheng, Y., Li, L., et al. (2021). ABCC5 Facilitates the Acquired Resistance of Sorafenib through the Inhibition of SLC7A11-Induced Ferroptosis in Hepatocellular Carcinoma. *Neoplasia* 23(12), 1227–1239. doi:10.1016/j.neo.2021.11.002
- Jiang, L., Kon, N., Li, T., Wang, S.-J., Su, T., Hibshoosh, H., et al. (2015). Ferroptosis as a P53-Mediated Activity during Tumour Suppression. *Nature* 520(7545), 57–62. doi:10.1038/nature14344
- Kain, H. S., Glennon, E. K. K., Vijayan, K., Arang, N., Douglass, A. N., Fortin, C. L., et al. (2020). Liver Stage Malaria Infection Is Controlled by Host Regulators of Lipid Peroxidation. *Cell Death Differ.* 27(1), 44–54. doi:10.1038/s41418-019-0338-1
- Kong, F.-H., Ye, Q.-F., Miao, X.-Y., Liu, X., Huang, S.-Q., Xiong, L., et al. (2021). Current Status of Sorafenib Nanoparticle Delivery Systems in the Treatment of Hepatocellular Carcinoma. *Theranostics* 11(11), 5464–5490. doi:10.7150/thno.54822

## FUNDING

This work is supported by National Natural Science Foundation of China (Nos 82130120 and 81973613), and Shanghai Rising-Star Program (19QA1408900). The Graduate Student Innovation Ability Project of Shanghai University of Traditional Chinese Medicine (Y2020059).

- Kong, R., Wang, N., Han, W., Bao, W., and Lu, J. (2021). Ifn $\gamma$ -mediated Repression of System Xc<sup>-</sup> Drives Vulnerability to Induced Ferroptosis in Hepatocellular Carcinoma Cells. *J. Leukoc. Biol.* 110(2), 301–314. doi:10.1002/jlb.3ma1220-815rrr
- Kong, Z., Liu, R., and Cheng, Y. (2019). Artesunate Alleviates Liver Fibrosis by Regulating Ferroptosis Signaling Pathway. *Biomed. Pharmacother.* 109, 2043–2053. doi:10.1016/j.biopha.2018.11.030
- Kuo, C.-Y., Chiu, V., Hsieh, P.-C., Huang, C.-Y., Huang, S. J., Tzeng, I.-S., et al. (2020). Chrysophanol Attenuates Hepatitis B Virus X Protein-Induced Hepatic Stellate Cell Fibrosis by Regulating Endoplasmic Reticulum Stress and Ferroptosis. *J. Pharmacol. Sci.* 144(3), 172–182. doi:10.1016/j.jphs.2020.07.014
- Lei, P., Bai, T., and Sun, Y. (2019). Mechanisms of Ferroptosis and Relations with Regulated Cell Death: A Review. *Front. Physiol.* 10, 139. doi:10.3389/fphys.2019.00139
- Lewerenz, J., Hewett, S. J., Huang, Y., Lambros, M., Gout, P. W., Kalivas, P. W., et al. (2013). The Cystine/Glutamate Antiporter System Xc<sup>-</sup> in Health and Disease: From Molecular Mechanisms to Novel Therapeutic Opportunities. *Antioxidants Redox Signal.* 18(5), 522–555. doi:10.1089/ars.2011.4391
- Li, J., Cao, F., Yin, H.-L., Huang, Z.-J., Lin, Z.-T., Mao, N., et al. (2020). Ferroptosis: Past, Present and Future. *Cell Death Dis.* 11(2), 88. doi:10.1038/s41419-020-2298-2
- Li, X., Wang, T. X., Huang, X., Li, Y., Sun, T., Zang, S., et al. (2020). Targeting Ferroptosis Alleviates Methionine-choline Deficient (MCD)-diet Induced NASH by Suppressing Liver Lipotoxicity. *Liver Int.* 40(6), 1378–1394. doi:10.1111/liv.14428
- Li, Y., Feng, D., Wang, Z., Zhao, Y., Sun, R., Tian, D., et al. (2019). Ischemia-induced ACSL4 Activation Contributes to Ferroptosis-Mediated Tissue Injury in Intestinal Ischemia/reperfusion. *Cell Death Differ.* 26(11), 2284–2299. doi:10.1038/s41418-019-0299-4
- Li, Y., Jin, C., Shen, M., Wang, Z., Tan, S., Chen, A., et al. (2020). Iron Regulatory Protein 2 Is Required for Artemether -mediated Anti-hepatic Fibrosis through Ferroptosis Pathway. *Free Radic. Biol. Med.* 160, 845–859. doi:10.1016/j.freeradbiomed.2020.09.008
- Liu, B., Yi, W., Mao, X., Yang, L., and Rao, C. (2021). Enoyl Coenzyme A Hydratase 1 Alleviates Nonalcoholic Steatohepatitis in Mice by Suppressing Hepatic Ferroptosis. *Am. J. Physiology-Endocrinology Metabolism* 320(5), E925–e937. doi:10.1152/ajpendo.00614.2020
- Liu, C.-Y., Wang, M., Yu, H.-M., Han, F.-X., Wu, Q.-S., Cai, X.-J., et al. (2020). Ferroptosis Is Involved in Alcohol-Induced Cell Death *In Vivo* and *In Vitro*. *Biosci. Biotechnol. Biochem.* 84(8), 1621–1628. doi:10.1080/09168451.2020.1763155
- Liu, J., He, H., Wang, J., Guo, X., Lin, H., Chen, H., et al. (2020). Oxidative Stress-dependent Frataxin Inhibition Mediated Alcoholic Hepatocytotoxicity through Ferroptosis. *Toxicology* 445, 152584. doi:10.1016/j.tox.2020.152584
- Liu, X., Zhu, X., Qi, X., Meng, X., and Xu, K. (2021). Co-Administration of iRGD with Sorafenib-Loaded Iron-Based Metal-Organic Framework as a Targeted Ferroptosis Agent for Liver Cancer Therapy. *Ijn* 16, 1037–1050. doi:10.2147/ijn.S292528
- Liu, Y., and Gu, W. (2022). p53 in Ferroptosis Regulation: the New Weapon for the Old Guardian. *Cell Death Differ.* 29, 895, 910. doi:10.1038/s41418-022-00943-y
- Liu, Y., and Gu, W. (2021). The Complexity of P53-Mediated Metabolic Regulation in Tumor Suppression. *Seminars Cancer Biol.* S1044-579X(21), 00060–00062. doi:10.1016/j.semcancer.2021.03.010
- Louandre, C., Marq, I., Bouhlal, H., Lachiaier, E., Godin, C., Saidak, Z., et al. (2015). The Retinoblastoma (Rb) Protein Regulates Ferroptosis Induced by Sorafenib in Human Hepatocellular Carcinoma Cells. *Cancer Lett.* 356(2 Pt B), 971–977. doi:10.1016/j.canlet.2014.11.014
- Ou, W., Mulik, R. S., Anwar, A., McDonald, J. G., He, X., and Corbin, I. R. (2017). Low-density Lipoprotein Docosahexaenoic Acid Nanoparticles Induce Ferroptotic Cell Death in Hepatocellular Carcinoma. *Free Radic. Biol. Med.* 112, 597–607. doi:10.1016/j.freeradbiomed.2017.09.002
- Ou, Y., Wang, S.-J., Li, D., Chu, B., and Gu, W. (2016). Activation of SAT1 Engages Polyamine Metabolism with P53-Mediated Ferroptotic Responses. *Proc. Natl. Acad. Sci. U.S.A.* 113(44), E6806–e6812. doi:10.1073/pnas.1607152113
- Pan, Q., Luo, Y., Xia, Q., and He, K. (2021). Ferroptosis and Liver Fibrosis. *Int. J. Med. Sci.* 18(15), 3361–3366. doi:10.7150/ijms.62903
- Qi, J., Kim, J.-W., Zhou, Z., Lim, C.-W., and Kim, B. (2020). Ferroptosis Affects the Progression of Nonalcoholic Steatohepatitis via the Modulation of Lipid Peroxidation-Mediated Cell Death in Mice. *Am. J. Pathology* 190(1), 68–81. doi:10.1016/j.ajpath.2019.09.011
- Shintoku, R., Takigawa, Y., Yamada, K., Kubota, C., Yoshimoto, Y., Takeuchi, T., et al. (2017). Lipoxigenase-mediated Generation of Lipid Peroxides Enhances Ferroptosis Induced by Erastin and RSL3. *Cancer Sci.* 108(11), 2187–2194. doi:10.1111/cas.13380
- Singal, A. K., Bataller, R., Ahn, J., Kamath, P. S., and Shah, V. H. (2018). ACG Clinical Guideline: Alcoholic Liver Disease. *Am. J. Gastroenterol.* 113(2), 175–194. doi:10.1038/ajg.2017.469
- Stål, P., and Hultcrantz, R. (1993). Iron Increases Ethanol Toxicity in Rat Liver. *J. Hepatology* 17(1), 108–115. doi:10.1016/s0168-8278(05)80530-6
- Sui, M., Jiang, X., Chen, J., Yang, H., and Zhu, Y. (2018). Magnesium Isoglycyrrhizinate Ameliorates Liver Fibrosis and Hepatic Stellate Cell Activation by Regulating Ferroptosis Signaling Pathway. *Biomed. Pharmacother.* 106, 125–133. doi:10.1016/j.biopha.2018.06.060
- Sun, X., Niu, X., Chen, R., He, W., Chen, D., Kang, R., et al. (2016a). Metallothionein-1G Facilitates Sorafenib Resistance through Inhibition of Ferroptosis. *Hepatology* 64(2), 488–500. doi:10.1002/hep.28574
- Sun, X., Ou, Z., Chen, R., Niu, X., Chen, D., Kang, R., et al. (2016b). Activation of the P62-Keap1-NRF2 Pathway Protects against Ferroptosis in Hepatocellular Carcinoma Cells. *Hepatology* 63(1), 173–184. doi:10.1002/hep.28251
- Takahashi, N., Cho, P., Selfors, L. M., Kuiken, H. J., Kaul, R., Fujiwara, T., et al. (2020). 3D Culture Models with CRISPR Screens Reveal Hyperactive NRF2 as a Prerequisite for Spheroid Formation via Regulation of Proliferation and Ferroptosis. *Mol. Cell* 80(5), 828–844.e826. doi:10.1016/j.molcel.2020.10.010
- Tang, H., Chen, D., Li, C., Zheng, C., Wu, X., Zhang, Y., et al. (2019). Dual GSH-Exhausting Sorafenib Loaded Manganese-Silica Nanodrugs for Inducing the Ferroptosis of Hepatocellular Carcinoma Cells. *Int. J. Pharm.* 572, 118782. doi:10.1016/j.ijpharm.2019.118782
- Tsikas, D. (2017). Assessment of Lipid Peroxidation by Measuring Malondialdehyde (MDA) and Relatives in Biological Samples: Analytical and Biological Challenges. *Anal. Biochem.* 524, 13–30. doi:10.1016/j.ab.2016.10.021
- Tsukamoto, H., Horne, W., Kamimura, S., Niemelä, O., Parkkila, S., Ylä-Herttuala, S., et al. (1995). Experimental Liver Cirrhosis Induced by Alcohol and Iron. *J. Clin. Invest.* 96(1), 620–630. doi:10.1172/jci118077
- Tsurusaki, S., Tsuchiya, Y., Koumura, T., Nakasone, M., Sakamoto, T., Matsuoka, M., et al. (2019). Hepatic Ferroptosis Plays an Important Role as the Trigger for Initiating Inflammation in Nonalcoholic Steatohepatitis. *Cell Death Dis.* 10(6), 449. doi:10.1038/s41419-019-1678-y
- Ursini, F., and Maiorino, M. (2020). Lipid Peroxidation and Ferroptosis: The Role of GSH and GPx4. *Free Radic. Biol. Med.* 152, 175–185. doi:10.1016/j.freeradbiomed.2020.02.027
- Wang, F. X., Li, H. Y., Li, Y. Q., and Kong, L. D. (2020). Can Medicinal Plants and Bioactive Compounds Combat Lipid Peroxidation Product 4-HNE-Induced Deleterious Effects? *Biomolecules* 10(1). doi:10.3390/biom10010146
- Wang, L., Liu, Y., Du, T., Yang, H., Lei, L., Guo, M., et al. (2020). ATF3 Promotes Erastin-Induced Ferroptosis by Suppressing System Xc<sup>-</sup>. *Cell Death Differ.* 27(2), 662–675. doi:10.1038/s41418-019-0380-z
- Wang, L., Zhang, Z., Li, M., Wang, F., Jia, Y., Zhang, F., et al. (2019). P53-dependent Induction of Ferroptosis Is Required for Artemether to Alleviate Carbon Tetrachloride-Induced Liver Fibrosis and Hepatic Stellate Cell Activation. *IUBMB Life* 71(1), 45–56. doi:10.1002/iub.1895
- Wang, Q., Bin, C., Xue, Q., Gao, Q., Huang, A., Wang, K., et al. (2021a). GSTZ1 Sensitizes Hepatocellular Carcinoma Cells to Sorafenib-Induced Ferroptosis via Inhibition of NRF2/GPx4 axis. *Cell Death Dis.* 12(5), 426. doi:10.1038/s41419-021-03718-4
- Wang, Q., Guo, Y., Wang, W., Liu, B., Yang, G., Xu, Z., et al. (2021b). RNA Binding Protein DAZAP1 Promotes HCC Progression and Regulates Ferroptosis by Interacting with SLC7A11 mRNA. *Exp. Cell Res.* 399(1), 112453. doi:10.1016/j.yexcr.2020.112453
- Wei, S., Qiu, T., Wang, N., Yao, X., Jiang, L., Jia, X., et al. (2020). Ferroptosis Mediated by the Interaction between Mfn2 and IRE $\alpha$  Promotes Arsenic-Induced Nonalcoholic Steatohepatitis. *Environ. Res.* 188, 109824. doi:10.1016/j.envres.2020.109824
- Wu, J., Minikes, A. M., Gao, M., Bian, H., Li, Y., Stockwell, B. R., et al. (2019). Intercellular Interaction Dictates Cancer Cell Ferroptosis via NF2-YAP Signalling. *Nature* 572(7769), 402–406. doi:10.1038/s41586-019-1426-6



- Xie, Y., Hou, W., Song, X., Yu, Y., Huang, J., Sun, X., et al. (2016). Ferroptosis: Process and Function. *Cell Death Differ.* 23(3), 369–379. doi:10.1038/cdd.2015.158
- Xu, Y., Li, X., Cheng, Y., Yang, M., and Wang, R. (2020). Inhibition of ACSL4 Attenuates Ferroptotic Damage after Pulmonary Ischemia-reperfusion. *FASEB J.* 34(12), 16262–16275. doi:10.1096/fj.202001758R
- Yang, Y., Chen, J., Gao, Q., Shan, X., Wang, J., and Lv, Z. (2020). Study on the Attenuated Effect of Ginkgolide B on Ferroptosis in High Fat Diet Induced Nonalcoholic Fatty Liver Disease. *Toxicology* 445, 152599. doi:10.1016/j.tox.2020.152599
- Yu, Y., Jiang, L., Wang, H., Shen, Z., Cheng, Q., Zhang, P., et al. (2020). Hepatic Transferrin Plays a Role in Systemic Iron Homeostasis and Liver Ferroptosis. *Blood* 136(6), 726–739. doi:10.1182/blood.2019002907
- Zhang, Y., Shi, J., Liu, X., Feng, L., Gong, Z., Koppula, P., et al. (2018). BAP1 Links Metabolic Regulation of Ferroptosis to Tumour Suppression. *Nat. Cell Biol.* 20(10), 1181–1192. doi:10.1038/s41556-018-0178-0
- Zhang, Z., Guo, M., Li, Y., Shen, M., Kong, D., Shao, J., et al. (2020). RNA-binding Protein ZFP36/TTP Protects against Ferroptosis by Regulating Autophagy Signaling Pathway in Hepatic Stellate Cells. *Autophagy* 16(8), 1482–1505. doi:10.1080/15548627.2019.1687985
- Zhang, Z., Yao, Z., Wang, L., Ding, H., Shao, J., Chen, A., et al. (2018). Activation of Ferritinophagy Is Required for the RNA-Binding Protein ELAVL1/HuR to Regulate Ferroptosis in Hepatic Stellate Cells. *Autophagy* 14(12), 2083–2103. doi:10.1080/15548627.2018.1503146
- Zhao, X., Liu, Z., Gao, J., Li, H., Wang, X., Li, Y., et al. (2020). Inhibition of Ferroptosis Attenuates Busulfan-Induced Oligospermia in Mice. *Toxicology* 440, 152489. doi:10.1016/j.tox.2020.152489
- Zhou, Z., Ye, T. J., DeCaro, E., Buehler, B., Stahl, Z., Bonavita, G., et al. (2020). Intestinal SIRT1 Deficiency Protects Mice from Ethanol-Induced Liver Injury by Mitigating Ferroptosis. *Am. J. Pathology* 190(1), 82–92. doi:10.1016/j.ajpath.2019.09.012
- Zhu, Z., Zhang, Y., Huang, X., Can, L., Zhao, X., Wang, Y., et al. (2021). Thymosin Beta 4 Alleviates Non-alcoholic Fatty Liver by Inhibiting Ferroptosis via Up-Regulation of GPX4. *Eur. J. Pharmacol.* 908, 174351. doi:10.1016/j.ejphar.2021.174351

**Conflict of Interest:** The authors declare that the research was conducted in the absence of any commercial or financial relationships that could be construed as a potential conflict of interest.

**Publisher's Note:** All claims expressed in this article are solely those of the authors and do not necessarily represent those of their affiliated organizations, or those of the publisher, the editors and the reviewers. Any product that may be evaluated in this article, or claim that may be made by its manufacturer, is not guaranteed or endorsed by the publisher.

Copyright © 2022 Zhou, Fu, Liu, Mu, Zhang, Chen and Liu. This is an open-access article distributed under the terms of the Creative Commons Attribution License (CC BY). The use, distribution or reproduction in other forums is permitted, provided the original author(s) and the copyright owner(s) are credited and that the original publication in this journal is cited, in accordance with accepted academic practice. No use, distribution or reproduction is permitted which does not comply with these terms.



# Comprehensive Analyses of Ferroptosis-Related Alterations and Their Prognostic Significance in Glioblastoma

Yuan Tian<sup>1\*†</sup>, Hongtao Liu<sup>2†</sup>, Caiqing Zhang<sup>3†</sup>, Wei Liu<sup>1</sup>, Tong Wu<sup>1</sup>, Xiaowei Yang<sup>4</sup>, Junyan Zhao<sup>5</sup> and Yuping Sun<sup>6\*</sup>

## OPEN ACCESS

### Edited by:

Yanqing Liu,  
Columbia University, United States

### Reviewed by:

Zhenyi Su,  
Columbia University, United States  
Yanchun Zhang,  
Icahn School of Medicine at Mount  
Sinai, United States  
迪王,  
Columbia University, United States

### \*Correspondence:

Yuan Tian  
tytytianyuan@allyun.com  
Yuping Sun  
13370582181@163.com

<sup>†</sup>These authors have contributed  
equally to this work

### Specialty section:

This article was submitted to  
Molecular Diagnostics and  
Therapeutics,  
a section of the journal  
Frontiers in Molecular Biosciences

Received: 25 March 2022

Accepted: 27 April 2022

Published: 03 June 2022

### Citation:

Tian Y, Liu H, Zhang C, Liu W, Wu T,  
Yang X, Zhao J and Sun Y (2022)  
Comprehensive Analyses of  
Ferroptosis-Related Alterations and  
Their Prognostic Significance  
in Glioblastoma.  
Front. Mol. Biosci. 9:904098.  
doi: 10.3389/fmolb.2022.904098

<sup>1</sup>Somatic Radiotherapy Department, Shandong Second Provincial General Hospital, Jinan, China, <sup>2</sup>Department of Pathology, Shandong Medicine and Health Key Laboratory of Clinical Pathology, The First Affiliated Hospital of Shandong First Medical University and Shandong Provincial Qianfoshan Hospital, Shandong Lung Cancer Institute, Shandong Institute of Nephrology, Jinan, China, <sup>3</sup>Department of Respiratory and Critical Care Medicine, Shandong Second Provincial General Hospital, Shandong University, Jinan, China, <sup>4</sup>Department of Hepatobiliary Intervention, Beijing Tsinghua Changgung Hospital, School of Clinical Medicine, Tsinghua University, Beijing, China, <sup>5</sup>Nursing Department, The First Affiliated Hospital of Shandong First Medical University & Shandong Provincial Qianfoshan Hospital, Jinan, China, <sup>6</sup>Phase I Clinical Trial Center, Shandong Cancer Hospital and Institute, Shandong First Medical University and Shandong Academy of Medical Sciences, Jinan, China

**Background:** This study was designed to explore the implications of ferroptosis-related alterations in glioblastoma patients.

**Method:** After obtaining the data sets CGGA325, CGGA623, TCGA-GBM, and GSE83300 online, extensive analysis and mutual verification were performed using R language-based analytic technology, followed by further immunohistochemistry staining verification utilizing clinical pathological tissues.

**Results:** The analysis revealed a substantial difference in the expression of ferroptosis-related genes between malignant and paracancerous samples, which was compatible with immunohistochemistry staining results from clinicopathological samples. Three distinct clustering studies were run sequentially on these data. All of the findings were consistent and had a high prediction value for glioblastoma. Then, the risk score predicting model containing 23 genes (*CP*, *EMP1*, *AKR1C1*, *FMOD*, *MYBPH*, *IFI30*, *SRPX2*, *PDLIM1*, *MMP19*, *SPOCD1*, *FCGBP*, *NAMPT*, *SLC11A1*, *S100A10*, *TNC*, *CSMD3*, *ATP1A2*, *CUX2*, *GALNT9*, *TNFAIP6*, *C15orf48*, *WSCD2*, and *CBLN1*) on the basis of “Ferroptosis.gene.cluster” was constructed. In the subsequent correlation analysis of clinical characteristics, tumor mutation burden, HRD, neoantigen burden and chromosomal instability, mRNAsi, TIDE, and GDSC, all the results indicated that the risk score model might have a better predictive efficiency.

**Abbreviations:** TMB, tumor mutational burden; PCA, principal component analysis; GSVA, gene set variation analysis; ssGSEA, single-sample gene set enrichment analysis; FPR, false-positive rate; TPR, true-positive rate; HRD, homologous recombination deficiency; TAI, telomeric-allelic imbalance; LST, large-scale state transitions; LOH, loss of heterozygosity; CNV, copy number variation; TIDE, tumor immune dysfunction and exclusion; GDSC, Genomics of Drug Sensitivity in Cancer; MSigDB, Molecular Signatures Database.

**Conclusion:** In glioblastoma, there were a large number of abnormal ferroptosis-related alterations, which were significant for the prognosis of patients. The risk score-predicting model integrating 23 genes would have a higher predictive value.

**Keywords:** ferroptosis, alterations, predictive models, prognosis, glioblastoma

## 1 INTRODUCTION

Ferroptosis, a kind of controlled cell death triggered by excessive lipid peroxidation (Jiang et al., 2021), has been implicated in tumor suppression mechanisms (Chen et al., 2021) and may play a critical role in carcinogenesis and precision medicine (Shen et al., 2018; Liang et al., 2019). Additionally, it has been implicated in the control of a variety of tumor-associated signaling pathways (Wu et al., 2019; Lee et al., 2020). CD8<sup>+</sup> T lymphocytes have been shown to be able to modulate tumor ferroptosis in studies in the field of tumor immunotherapy (Wang et al., 2019). Ferroptosis-related reports have been published in the fields of chemotherapy, radiation, and immunotherapy, demonstrating its distinct potential for tumor treatment (Yee et al., 2020; Liu et al., 2022; Zhao et al., 2022).

With the advancement of bioinformatics analysis and sequencing technology, it is becoming increasingly convenient for us to analyze the genomic alterations associated with certain diseases using publicly available data (Qu et al., 2016; Chen et al., 2021). Reports utilizing online data to uncover important genetic abnormalities in glioblastoma are frequent (Rutledge et al., 2013; Cimino et al., 2018) but seldom use ferroptosis. This study was created using R-based bioinformatics analytic tools and publicly available gene data from Internet sources.

## 2 MATERIALS AND METHODS

The flow diagram of the study is provided in **Supplementary Figure S1**. The specific details were listed as follows.

### 2.1 Data Download Collection

#### 2.1.1 TCGA-GBM Data Download

Gene expression data (<https://tcga-xena-hub.s3.us-east-1.amazonaws.com/latest/TCGA.GBM.sampleMap%2FHiSeqV2.gz>), genotype data ([https://tcga-xena-hub.s3.us-east-1.amazonaws.com/latest/TCGA.GBM.sampleMap%2FGBM\\_clinicalMatrix](https://tcga-xena-hub.s3.us-east-1.amazonaws.com/latest/TCGA.GBM.sampleMap%2FGBM_clinicalMatrix)), survival data of patient samples ([https://tcga-xena-hub.s3.us-east-1.amazonaws.com/latest/survival%2FGBM\\_survival.txt.gz](https://tcga-xena-hub.s3.us-east-1.amazonaws.com/latest/survival%2FGBM_survival.txt.gz)), TCGA-GBM mutant “maf” (mutation annotation format) file (<https://portal.gdc.cancer.gov/files/da904cd3-79d7-4ae3-b6c0-e7127998b3e6>), TCGA-GBM gene copy number data (<https://gdc-hub.s3.us-east-1.amazonaws.com/latest/TCGA-GBM.gistic.tsv.gz>), and the masked copy number segment file of TCGA-GBM were downloaded from the GDC database by the R package TCGAbiolinks (v 2.16.4).

#### 2.1.2 CGGA Data Download

The data of CGGA, including mRNAseq\_693, mRNAseq\_325, and mRNA sequencing data (non-glioma as control), were

downloaded from the following link: <http://www.cgga.org.cn/download.jsp>.

#### 2.1.3 GSE83300 Data Download

The GSE83300 data were downloaded from the GEO database by the R package “GEOquery (v2.54.1).”

#### 2.1.4 The Genomic Damage Information of TCGA Samples Was Mainly Collected From PMID: 29617664 (Knijnenburg et al., 2018)

mutLoad\_nonsilent (TMB): silent mutation load per Mb. CNA\_frac\_altered (CNV): fraction of genome altered (fraction of bps belonging to “altered” segments), where “altered” was defined as having relative CN >0.1 or <-0.1. HRD\_Score: homologous recombination deficiency score calculated from three scores (TAI + LST + HRD\_LOH). HRD\_TAI: number of subchromosomal regions with allelic imbalance extending to the telomere. HRD\_LST: number of chromosomal breaks between adjacent regions of at least 10 Mb. HRD\_LOH: the number of LOH regions of intermediate size (>15 MB but < whole chromosome in length) (Knijnenburg et al., 2018).

#### 2.1.5 Ferroptosis-Involved Information

Ferroptosis was mainly derived from the FerrDb database (<http://www.zhounan.org/ferrdb/>) [(PMID: 32760210) and (PMID: 33330074)] (Liang et al., 2020; Zhuo et al., 2020). Then, the three were merged.

#### 2.1.6 MSigDB Data Download

MSigDB data (Molecular Signatures Database) were downloaded from the following link: <https://www.gsea-msigdb.org/gsea/msigdb/index.jsp>.

#### 2.1.7 Human (Gene Transfer Format) Files Download

The human “gtf” file (Homo\_sapiens.GRCh38.99.gtf.gz) was downloaded from the Ensembl database, and then the symbol information was collected: (<http://www.ensembl.org/info/data/ftp/index.html>). The four data set samples were integrated, and the ComBat() function of the R package sva was used to remove the batch effect, and then subsequent analysis was performed.

## 2.2 Comprehensive Analysis of Ferroptosis-Related Genes

### 2.2.1 Comparison of Ferroptosis-Related Gene Diseases and Normal Expression

The “non-glioma as control” data downloaded from the CGGA database were regarded as the normal sample, and then the difference in ferroptosis-involved gene expression between

cancer and normal samples in the integrated data was compared; “wilcox.test()” was used to detect significant differences, and “ggpubr (v0.4.0)” was used to achieve visualization; \*\*\*\* means  $p < 0.0001$ , \*\*\* means  $p < 0.001$ , \*\* means  $p < 0.01$ , and \* means  $p < 0.05$ .

### 2.2.2 Mutation and Copy Number Variation Analysis

The gene-level CNV data of TCGA-GBM were downloaded, the copy number alterations of ferroptosis-related genes were counted, and then the variation frequency was calculated, and the R package ggplot2 (v 3.3.2) was used to draw the statistical graph.

### 2.2.3 Circos Display and Principal Component Analysis of the Position on the Chromosome

From the human chromosome “gtf” file, the location information of the ferroptosis gene was extracted. Then, the R package RCircos (v1.2.1) was used to draw a gene circos map for position display. The function “prcomp()” of R was used to perform the principal component analysis (PCA) of cancer and normal samples. Then, R packages pca3d (v0.10.2) and rgl (v0.105.22) were adopted to draw the 3D version of the PCA.

## 2.3 Ferroptosis-Involved Cluster Analysis

### 2.3.1 Cluster Analysis of Ferroptosis-Involved Genes

Based on the expression data of ferroptosis-involved genes in cancer samples, the package ConsensusClusterPlus (v1.50.0) was used to perform the unsupervised clustering of ferroptosis genes. The clustering algorithm used was k-means. Then, combined with the overall survival (OS) data, the R packages including survival (v3.2-7) and survminer (v0.4.8) were used to perform univariate Cox analysis on all ferroptosis-involved genes, and the differences and expression correlations (Pearson coefficient) among every ferroptosis genes would be calculated. Finally, the aforementioned results would be visualized by the Cytoscape (v3.7.2).

### 2.3.2 Unsupervised Cluster Analysis of Samples

Based on the expression data of ferroptosis-related genes, the R package ConsensusClusterPlus (v1.50.0) was used to perform the unsupervised clustering of cancer samples. The clustering algorithm used was “pam,” and the distance used was “pearson.” Then, the R packages of survival and survminer were used to analyze the survival of the obtained subtypes, and then the Kaplan–Meier curve would be drawn.

## 2.4 Gene Set Variation Analysis Function Enrichment Analyses

Using the R package GSEA (v1.34.0), based on the KEGG data in MSigDB, functional enrichment analysis were performed on the samples, and then “limma” (v3.42.2) was used to retrieve the differential enrichment entries among subtypes, and the relevant threshold was set as “adj.p.value<0.05 & |logFC|> 0.3”; Finally, the R package ComplexHeatmap (v2.2.0) was used to draw the heatmap for visualization.

## 2.5 The Proportion and Difference of Immune-Infiltrating Cells in Different Ferroptosis Clusters Evaluated by Single Sample Gene Set Enrichment Analysis

The R package “GSVA” was used to calculate the enrichment score of 28 immune-infiltrating cells in cancer samples. After the results were obtained, the data would be normalized by the “scale()” function. According to the formula “(x-min(x))/(max(x)-min(x)),” the data would be distributed from 0 to 1, and then the “wilcox.test()” was used to evaluate the significance of the difference in the proportion of immune cells among different ferroptosis cluster samples. “ggpubr” was used to achieve visualization. \*\*\*\* means  $p < 0.0001$ , \*\*\* means  $p < 0.001$ , \*\* means  $p < 0.01$ , and \* means  $p < 0.05$ . Finally, the Cox univariate regression analysis was performed on the proportion of immune cells, and  $p < 0.05$  was used as the threshold to select immune cells that were significantly related to the prognosis.

## 2.6 Correlation Analysis Between Different Ferroptosis Clusters and Clinical Characteristics

The proportion of age, gender, chemo\_therapy, and IDH1 mutations in different subtypes would be calculated, and relevant bar graphs would be drawn. Then, the “kruskal.test()” was used to test the significant difference in feature distributions among different subtypes.

## 2.7 Display of Ferroptosis-Related Genes in Different Ferroptosis Clusters

The expression differences of ferroptosis-related genes in different ferroptosis cluster subtypes would be counted, and then a heatmap for visualization would be drawn.

## 2.8 Screening of Differentially Expressed Genes in the Ferroptosis Cluster and Enrichment Analysis of DEGs

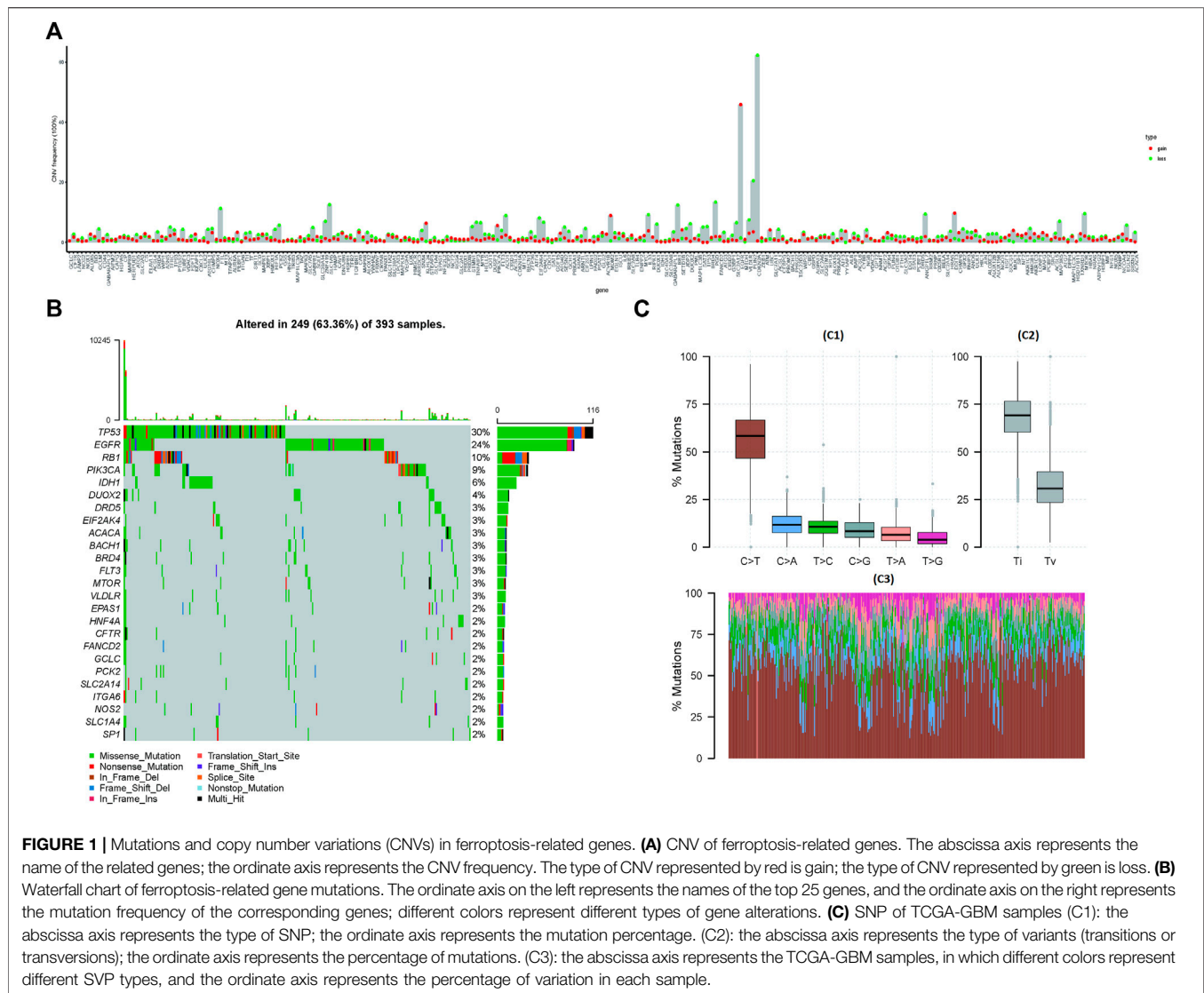
The R package “limma” was used to obtain DEGs among different subtypes. The threshold was set at “|logFC|> 1 and adj.p.val<0.05.” Afterward, the R package “clusterProfiler (v3.14.3)” was used for the functional enrichment analysis of DEGs. “ $p < 0.05$ ” and “ $q < 0.2$ ” were taken as the thresholds to filter the enrichment pathway, the enrichment factor would be calculated, and then the corresponding bubble chart would be drawn. The calculation formula of the enrichment factors is:

Enrichment factors = (the number of genes enriched into the pathway in the gene set)/(total number of genes in the pathway).

## 2.9 Ferroptosis.Gene.Cluster Obtained Based on the Cluster Analysis of DEGs

Through unsupervised clustering of samples based on DEGs, Ferroptosis.gene.cluster was obtained, and the heatmap of DEGs in different subtypes was drawn. Then, based on





Ferroptosis.gene.cluster for survival analysis, the Kaplan–Meier survival curve was drawn.

## 2.10 Construction of “Ferroptosis Gene Signatures” Based on the DEGs of the “Ferroptosis Cluster”

First, univariate Cox regression analyses on the DEGs in different “ferroptosis clusters” were performed, and  $p < 0.05$  was taken as the threshold to screen out genes that were significantly related to survival. Then, the R package “randomForest (v 4.614)” was used to perform random forest screening for survival significantly related genes. The related parameters used were “mtry = 2” and “ntree = 1,000.” Then, “MeanDecreaseGini > 0.72” was taken as the threshold to obtain key genes. Based on the expression of key genes, principal component analysis (PCA) on the sample was performed. The risk score is calculated by the following formula:

$$RScore_i = \sum (PC1_i + PC2_i). \quad (1)$$

Among them, PC1 and PC2 represent the scores of principal component 1 and component 2, respectively, and “i” represents the corresponding sample.

## 2.11 The Evaluation of the Prognostic Efficacy

After the sample risk score was obtained, the high- and low-risk score groups were divided by the median node, the survival analysis was performed in the high- and low-risk score groups, and then the Kaplan–Meier survival curve was drawn. At the same time, it was verified in the internal sub-data sets of TCGA, CGGA (CGGA325/CGGA693), and GSE83300.

After that, the time-based ROC curve was further drawn, and the AUC values of 1, 3, and 5 years were all greater than 0.6, indicating

that the predictive performance of the model was better. Finally, “ggalluvial (v0.12.3)” and “ggplot2” were used to draw Sankey diagrams to express the relationship of the data characteristics.

## 2.12 Correlation Analyses of Risk Score, “Ferroptosis Gene,” and Pathway Function

The correlation between the risk score and the differential enrichment pathway score (Pearson correlation coefficient) and the correlation between the “ferroptosis gene” and the differential enrichment pathway score (Pearson correlation coefficient) are further calculated, and the R package “corrplot (v 0.84)” was used to complete the visualization of relevance.

## 2.13 Difference Analysis of Risk Score in Different Groups

### 2.13.1 Differences in Enrichment Scores Between High- and Low-Risk Score Groups

The differences in enrichment scores between the high- and low-risk score groups would be calculated, and the significance of the difference would be calculated by the R package “wilcox.test()” and visualized by “ggpubr.” \*\*\*\* means  $p < 0.0001$ , \*\*\* means  $p < 0.001$ , \*\* means  $p < 0.01$ , and \* means  $p < 0.05$ .

### 2.13.2 Risk Score Differences in Different Ferroptosis.gene.clusters

The risk score differences in different Ferroptosis.gene.clusters would be counted. The significance of the difference would be calculated by the R package “wilcox.test()” and visualized by “ggpubr.” \*\*\*\* means  $p < 0.0001$ , \*\*\* means  $p < 0.001$ , \*\* means  $p < 0.01$ , and \* means  $p < 0.05$ .

### 2.13.3 Risk Score Differences in Different “Ferroptosis Clusters”

The risk score differences in different “ferroptosis cluster” would be counted. The significance of the difference would be calculated by the R package “wilcox.test()” and visualized by “ggpubr.” \*\*\*\* means  $p < 0.0001$ , \*\*\* means  $p < 0.001$ , \*\* means  $p < 0.01$ , and \* means  $p < 0.05$ .

## 2.14 Risk Score Differences in Clinical Characteristics and Different Molecular Types

The distribution of risk score in age, gender, chemo\_therapy, IDH1 mutation grouping, “ferroptosis cluster,” and “Ferroptosis.gene.cluster” was further checked. Then, the grouped box plot would be drawn, and the significant difference would be calculated by the R package “kruskal.test()” \*\*\*\* means  $p < 0.0001$ , \*\*\* means  $p < 0.001$ , \*\* means  $p < 0.01$ , and \* means  $p < 0.05$ .

The correlation between risk score and mutation load, homologous recombination deficiency, neoantigen load, chromosomal instability (TMB, CNV, HRD, HRD\_TAI, HRD\_LST, HRD\_LOH, DEL, INS, and SNP), and mRNAsi would be calculated. The linear correlation graph would be drawn.

## 2.15 The Landscape of the High- and Low-Risk Score Groups

The R package “TCGAbiolinks (v2.16.4)” was used for the GBM’s masked copy number segment data download, and the marker file data were downloaded from the GDC Reference File (<https://gdc.cancer.gov/about-data/gdc-data-processing/gdc-reference-files>); Then, “GenePattern GISTIC\_2.0” (<https://cloud.genepattern.org/gp/pages/index.jsf>) was used to analyze the alterations of CNV in the two groups online, and finally, the R package “maftools (v1.0.2)” was used for visualization.

Based on the “maf” (mutation annotation format) file of GBM mutation and risk score grouping, the mutation landscape of the two sets would be drawn by the R package “maftools.”

## 2.16 Immunotherapy Analysis Results in the High- and Low-Risk Score Groups (TIDE Prediction + GDSC)

### 2.16.1 Analysis Results of GDSC in the High- and Low-Risk Groups, Estimated by the IC<sub>50</sub> Value

The R package “pRRophetic (v0.5)” was used to predict drug treatment response in the high- and low-risk score groups, and then the box plot describing the difference would be drawn. Significant differences among groups were tested by the R package “wilcox.test()” \*\*\*\* means  $p < 0.0001$ , \*\*\* means  $p < 0.001$ , \*\* means  $p < 0.01$ , and \* means  $p < 0.05$ .

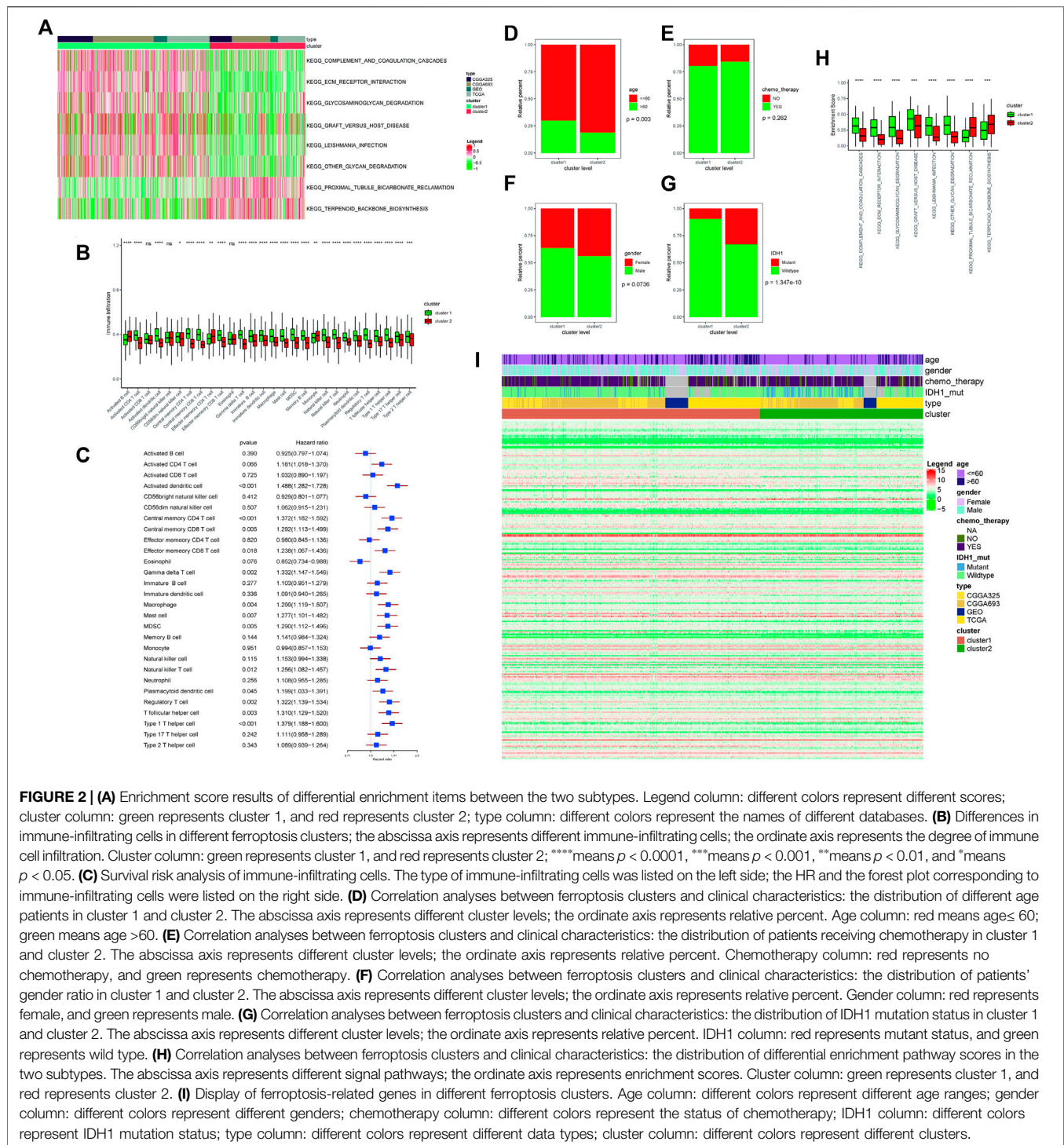
The TIDE score was used to predict the immunotherapy effect. The TIDE score could be obtained from the online website (<http://tide.dfci.harvard.edu>). Patients with higher TIDE scores enjoyed poorer therapeutic efficacy of immune checkpoint inhibitors and were related to the survival rate of those patients with worse anti-PD-1 and anti-CTLA-4 treatment results. After the TIDE score was obtained, the difference in different subtypes and risk groups would be calculated, and the significant difference would be tested by the R package “wilcox.test()” \*\*\*\* means  $p < 0.0001$ , \*\*\* means  $p < 0.001$ , \*\* means  $p < 0.01$ , and \* means  $p < 0.05$ .

### 2.16.2 Expression Differences of Immune Check Sites in the High- and Low-Risk Groups

The expression of immune checkpoints in the high- and low-risk groups would be further counted and drawn as a box-plot display; “wilcox.test()” was used to detect the significant difference. \*\*\*\* means  $p < 0.0001$ , \*\*\* means  $p < 0.001$ , \*\* means  $p < 0.01$ , and \* means  $p < 0.05$ .

## 2.17 Immunohistochemical Validation Results of Clinical Samples

The glioblastoma samples used for this study were collected from the First Affiliated Hospital of Shandong First Medical University & Shandong Provincial Qianfoshan Hospital from June 2019 to February 2022 with informed consent provided by all participants. All tumor tissue specimens were surgically resected followed by formalin fixation and paraffin embedding (FFPE) for histological evaluation. All HE-stained and immunohistochemical (IHC)-stained slides were examined and

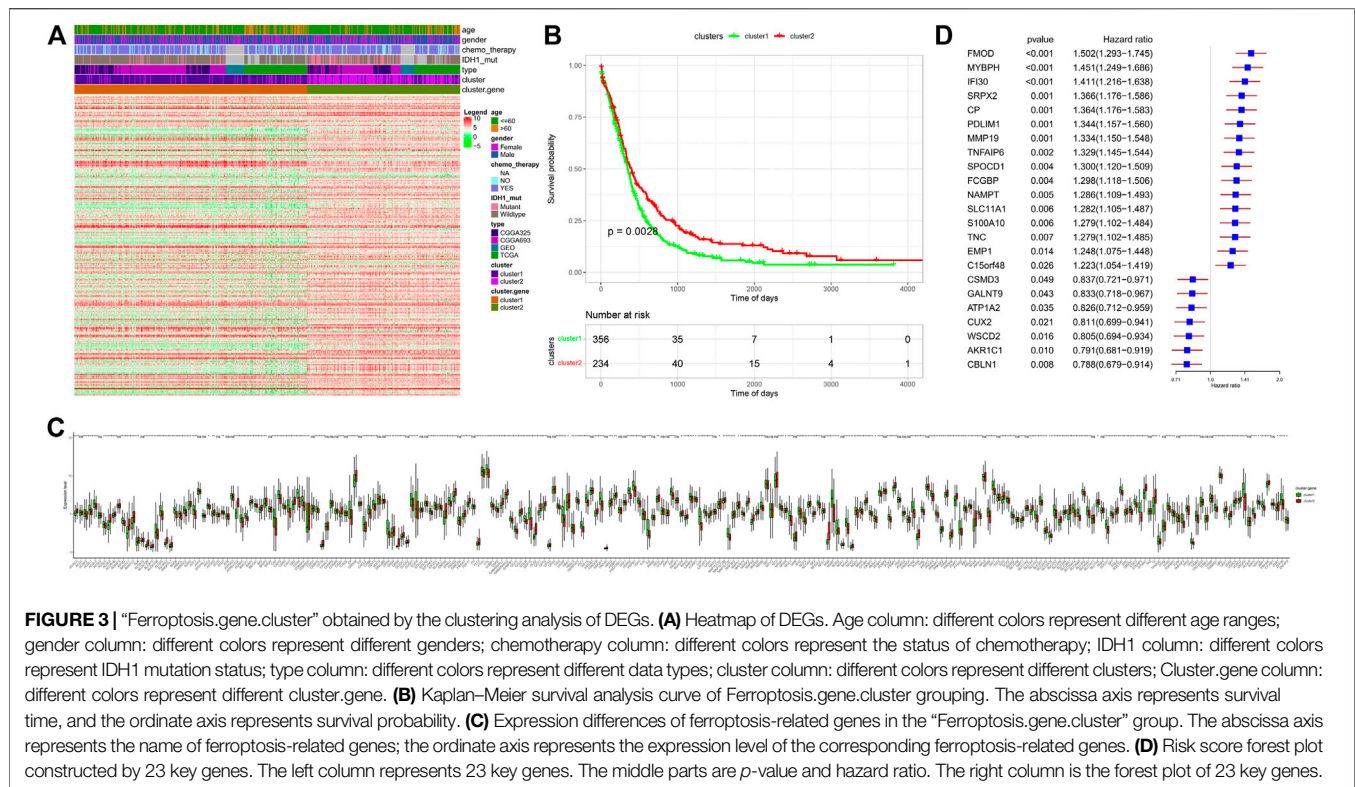


confirmed to be glioblastoma by two experienced pathologists independently according to WHO criteria.

Slides were IHC-stained with specific primary antibodies (mouse anti-human p53 monoclonal antibody: cat. No. MAB-0674, clone MX008; mouse anti-human IDH1 R132H monoclonal antibody: cat. No. MAB-0733, clone MX031; mouse anti-human Ki-67 monoclonal antibody: cat. No. MAB-0672, clone MX006; mouse anti-human

MGMT monoclonal antibody: cat. No. MAB-0361, clone MT3.1). All primary antibodies and secondary antibodies [sheep anti-mouse immunoglobulin G (IgG) polymer] were purchased from MXB Biotechnologies, Fuzhou, China. Slides were processed using an automated Roche BenchMark XT staining system according to the manufacturer's protocol. Other genes (Ki-67, MGMT, and IDH1) were immunohistochemically stained in the same way.





### 3 RESULTS

#### 3.1 Data Collation

The flow diagram of the study is provided in **Supplementary Figure S1**. TCGA-GBM data were downloaded from UCSC Xena. After removing the samples without survival data, the expression matrix of 116 cancer samples was obtained. CGGA325 and CGGA693 were downloaded from the CGGA database, and then GBM data were extracted. After removing the samples without survival data, expression matrices of 137 and 237 samples were obtained, respectively. The GSE83300 data were downloaded from the GEO database; survival data and expression matrices of 50 samples were obtained. After integrating the three data sets and removing the batch effects, a total of 590 cancer samples were obtained for subsequent analyses.

Ferroptosis-related genes were downloaded from the database and two literatures (Liang et al., 2020; Zhuo et al., 2020), and finally 291 ferroptosis-related genes were obtained, of which 257 ferroptosis-related genes were displayed with expression information. The expression matrix of ferroptosis-related genes was extracted for subsequent analyses. Basic characteristics of all the data were provided in (Table 1).

#### 3.2 The Overall Display of Ferroptosis-Related Genes

##### 3.2.1 Expression Display of Ferroptosis-Related Genes in Diseases and Normal Samples

Twenty non-glioma data were downloaded from the CGGA database and taken as the normal control, and then the

expression difference of ferroptosis-related genes between the cancer and normal samples in the integrated data was compared. Among them, 239 ferroptosis-related genes were found to be significantly different between cancer and normal samples ( $p < 0.05$ ), indicating that most of the expression of ferroptosis-related genes were related to GBM (**Supplementary Figure S2**).

##### 3.2.2 The Mutations and CNV of Ferroptosis-Related Genes

The copy number data of ferroptosis-related genes was extracted from the gene-level copy number variation (CNV) data of TCGA-GBM (including 628 samples), and then the CNV map was drawn. Among them, CDKN2A deletion was found in more than 60% samples, and EGFR duplication was found in 40% samples (**Figure 1A**). The mutations of ferroptosis-related genes were further extracted from the TCGA-GBM “maf” file (containing 393 samples), and then the top 25 genes were selected and drawn into a waterfall chart, among which TP53 and EGFR ranked the top two mutation frequencies (>20%). The C > T variation in SNP was the most common (**Figures 1B,C**).

##### 3.2.3 Positional Circos Display on Chromosomes and Principal Component Analysis

The location information of ferroptosis-related genes was extracted from human chromosomal “gtf” files, and then a gene circos diagram was drawn for location display. Finally, the PCA results of the cancer and normal samples were drawn (**Supplementary Figure S3A,B**).



### 3.3 Ferroptosis-Related Cluster Analyses

#### 3.3.1 Cluster Analyses of Ferroptosis-Related Genes

Based on the expression information of ferroptosis-related genes in cancer samples, the unsupervised clustering of ferroptosis-related genes was performed, and three subtypes were obtained. After that, batch Cox univariate regression analyses were performed on ferroptosis-related genes, and the Pearson coefficients among different ferroptosis-related genes were calculated at the same time. Finally, the aforementioned results were visualized by Cytoscape (Supplementary Figure S3C).

#### 3.3.2 Unsupervised Cluster Analyses of Cancer Samples

Based on the expression information of ferroptosis-related genes, unsupervised cluster analyses of cancer samples were performed, and two cluster subtypes were obtained. After the survival analysis was performed on the two subtypes, the survival difference between the two subtypes was significant ( $p < 0.05$ ) (Supplementary Figure S3D,E).

### 3.4 Gene Set Variation Analysis Function Enrichment Analysis

GSVA was used to perform functional enrichment analysis on the samples, and then the R package “limma” was used to retrieve differential enrichment items between the two subtypes; eight enrichment items were obtained according to the threshold, and then a heatmap was drawn. Among them, KEGG\_COMPLEMENT\_AND\_COAGULATION\_CASCADES, KEGG\_ECM\_RECEPTOR\_INTERACTION, KEGG\_GLYCOSAMINOGLYCAN\_DEGRADATION, KEGG\_GRAFT\_VERSUS\_HOST\_DISEASE, KEGG\_LEISHMANIA\_INFECTION, and KEGG\_OTHER\_GLYCAN\_DEGRADATION were found to be enriched with higher scores in cluster 1, while KEGG\_PROXIMAL\_TUBULE\_BICARBONATE\_RECLAMATION and KEGG\_TERPENOID\_BACKBONE\_BIOSYNTHESIS were found to be enriched with higher scores in cluster 2 (Figure 2A).

### 3.5 The Proportion and Difference of Immune-Infiltrating Cells in Different Ferroptosis Clusters Assessed by Single-Sample Gene Set Enrichment Analysis

The R package “GSVA” was used to calculate the enrichment score of 28 types of immune infiltration cells in cancer samples, and 25 types of immune infiltration cells were found to be significantly different between the two subtypes. Among them, activated CD4 T cell, activated dendritic cell, central memory CD4 T cell, effector memory CD8 T cell, gamma delta T cell, immature B cell, immature dendritic cell, macrophage, mast cell, MDSC, memory B cell, natural killer cell, natural killer T cell, neutrophil, plasmacytoid dendritic cell, regulatory T cell, T follicular helper cell, type 1 T helper cell, type 17 T helper cell, and type 2 T helper cell were found to be higher in cluster 1, while activated B cell, effector memory CD4 T cell, and monocyte were found to be higher in cluster 2 (Figure 2B).

After that, the univariate Cox regression analysis was performed on the proportion of immune cells, and the immune cells that were significantly related to the prognosis were screened with  $p < 0.05$  as the threshold. Among them, activated dendritic cell, central memory CD4 T cell, central memory CD8 T cell, effector memory CD8 T cell, gamma delta T cell, macrophage, mast cell, MDSC, natural killer T cell, plasmacytoid dendritic cell, regulatory T cell, and T cells of both follicular helper cell and type 1 T helper cell were found to have a significant impact on the survival (Figure 2C).

### 3.6 The Correlation Analysis Between Different Ferroptosis Clusters and Clinical Characteristics

The proportions of age, gender, chemo\_therapy, and IDH1 mutations in different subtypes would be calculated and plotted as a bar graph. Among them, only age was found to be significantly different between the two subtypes, and the remaining characteristics were not found to be significantly different. Between the two subtypes, seven of the eight differential enrichment pathway scores were found to be at a significantly different level, indicating that the two subtypes were closely related to the enrichment pathways (Figures 2D–H).

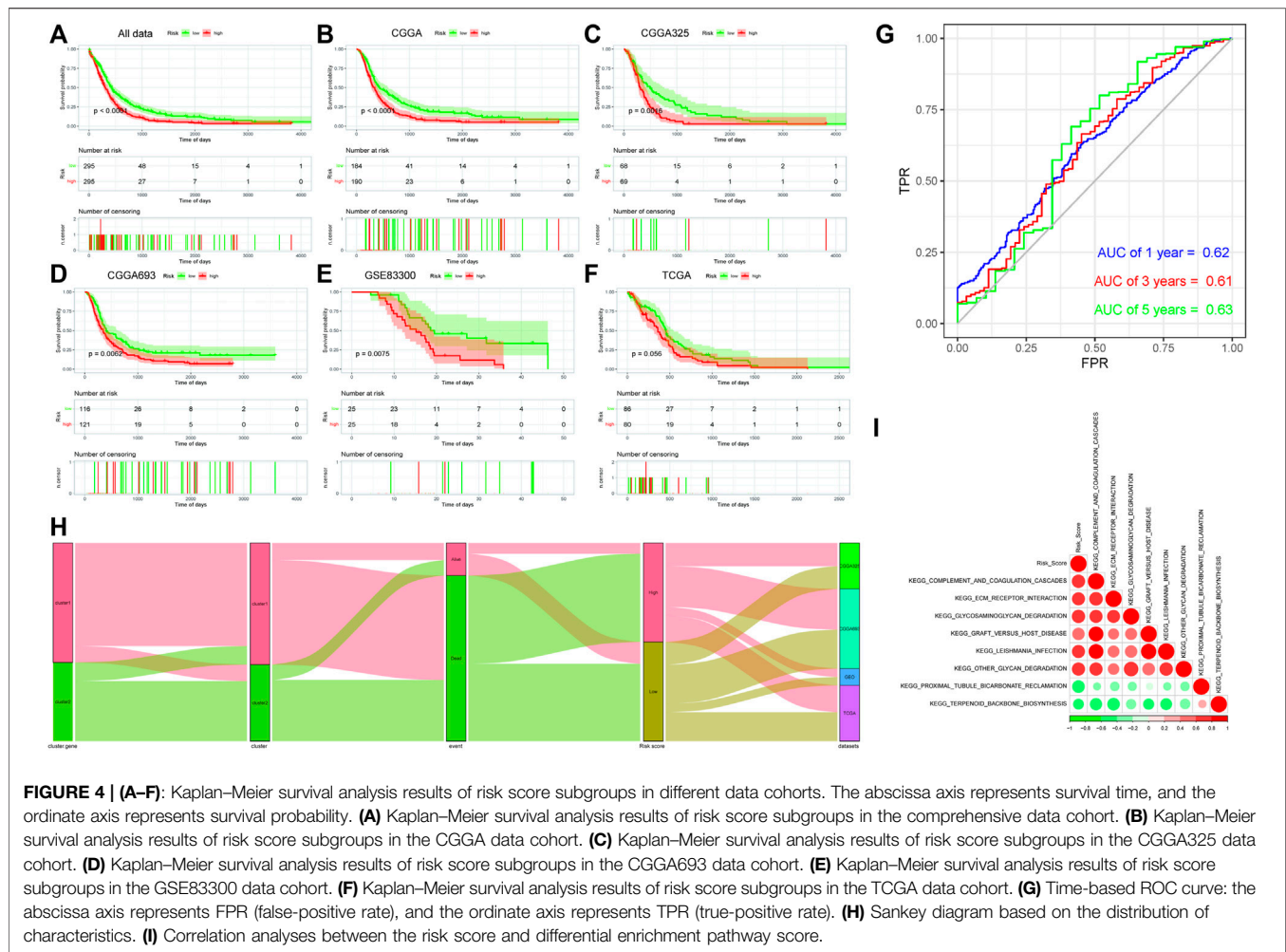
### 3.7 Display of Ferroptosis-Related Genes in Different “Ferroptosis Clusters”

The expression differences of ferroptosis-related genes among different “ferroptosis cluster” subtypes were counted and plotted as a heatmap (Figure 2I).

### 3.8 Screening for DEGs in “Ferroptosis Cluster” and Performing Enrichment Analysis for DEGs

The R package “limma” was used to screen for DEGs in different subtypes. Using  $|\log FC| > 1$  & FDR  $< 0.05$  as the thresholds, 491 DEGs were screened out, including 203 upregulated genes and 288 downregulated genes.

After that, GO and KEGG enrichment analyses of DEGs were performed. The GO enrichment analysis included three parts, namely: biological process (BP), cell component (CC), and molecular function (MF). Among them, the main pathways of BP enrichment were extracellular matrix organization and collagen fibril organization; the main pathways of CC enrichment were collagen-containing extracellular matrix and complex of collagen trimers; the main pathways of MF enrichment were extracellular matrix structural constituent, extracellular matrix structural constituent conferring tensile strength, and ion-gated channel activity. The main pathways of KEGG enrichment were ECM–receptor interaction and nicotine addiction. Relevant pathways were closely related to the ferroptosis process (Supplementary Figure S4).



### 3.9 “Ferroptosis.gene.cluster” Obtained by Cluster Analysis Based on DEGs

After unsupervised cluster analysis based on DEGs, two subtypes of “Ferroptosis.gene.cluster” were obtained, and the DEGs in different subtypes were displayed. Then, based on “Ferroptosis.gene.cluster” for survival analysis, the Kaplan–Meier survival curve was drawn, and the results showed that the survival curves of the two “Ferroptosis.gene.cluster” were significantly different. After that, the expression of ferroptosis-related genes in different “Ferroptosis.gene.cluster” was further analyzed, among which 196 ferroptosis-related genes were significantly different between the two “Ferroptosis.gene.clusters” (Figures 3A–C).

### 3.10 Construction of “Ferroptosis Gene Signatures” Based on the Risk Scores of DEGs in the “Ferroptosis Cluster”

Univariate Cox regression analysis was performed on the DEGs of different “ferroptosis clusters,” and 256 genes that were significantly related to the survival were screened out with  $p < 0.05$  as the threshold. Then, the R package “randomForest” was

used to perform random forest screening on genes that were significantly related to the survival, and 23 key genes (*FMOD*, *MYBPH*, *IFI30*, *SRPX2*, *CP*, *PDLIM1*, *MMP19*, *TNFAIP6*, *SPOCD1*, *FCGBP*, *NAMPT*, *SLC11A1*, *S100A10*, *TNC*, *EMP1*, *C15orf48*, *CSMD3*, *GALNT9*, *ATP1A2*, *CUX2*, *WSCD2*, *AKR1C1*, and *CBLN1*) were obtained with MeanDecreaseGini  $> 0.72$  as the threshold. Finally, based on the expression of these key genes, the PCA was performed on the samples, and the risk score of each sample was calculated (Figure 3D).

### 3.11 Prognostic Survival Assessment

After the sample risk score was obtained, the samples were divided into high- and low-risk score groups by the median node, and then survival analysis was performed on the two groups, and then the Kaplan–Meier curve was drawn. The significant difference of the survival could be found between the two groups. At the same time, they were verified by the CGGA (CGGA325/CGGA693), GSE83300, and TCGA internal sub-data sets. Significant differences were also found in the sub-data sets [except the TCGA data set ( $p = 0.056$ )] of the two subtype samples (Figures 4A–F).

After that, the time-based ROC curve was drawn, and the AUC values of 1, 3, and 5 years were all greater than 0.6, indicating that



**TABLE 1** | Basic characteristics of all the data.

	TCGA-GBM	CGGA325	CGGA693	GSE83300
Total	166	137	237	50
Age				
>60	81	14	52	4
≤60	85	123	185	46
Gender				
Male	107	87	139	25
Female	59	50	98	25
Chemo_therapy				
Yes	117	99	199	0
No	31	34	27	0
NA	18	4	11	50
IDH1_mut				
Mutant	6	39	45	0
Wild type	113	98	182	0
NA	47	0	10	50
Cluster				
cluster1	84	145	101	32
cluster2	53	92	65	18
Cluster.gene				
Cluster1	80	151	96	29
Cluster2	57	86	70	21
Event				
Dead	133	124	197	39
Alive	33	13	40	11

**TABLE 2** | Basic characteristics of all enrolled clinical samples.

Characteristic	P53 Wild-type	P53 mutation	p-value
N	27	15	-
Age, mean ± SD	57.89 ± 11.14	59.93 ± 9.92	0.557
Gender, n (%)	-	-	0.708
Female	12 (28.6%)	5 (11.9%)	-
Male	15 (35.7%)	10 (23.8%)	-
IDH1 mutation, n (%)	-	-	0.649
Wild-type	24 (57.1%)	12 (28.6%)	-
Mutation	3 (7.1%)	3 (7.1%)	-
Ki-67 expression, n (%)	-	-	0.085
≤30%	21 (50%)	7 (16.7%)	-
-	6 (14.3%)	8 (19%)	-
MGMT expression, n (%)	-	-	0.740
Low or negative	14 (35.9%)	10 (25.6%)	-
Positive	10 (25.6%)	5 (12.8%)	-

scores than those of the high-risk group. However, the scores of KEGG\_PROXIMAL\_TUBULE\_BICARBONATE\_RECLAMATION and KEGG\_TERPENOID\_BACKBONE\_BIOSYNTHESIS in the high-risk group were significantly higher than those of the low-risk group, which was consistent with the results of the previous analysis (Figure 5B).

### 3.13.2 Differential Analysis of the Risk Score in Different “Ferroptosis.gene.clusters”

By analyzing the risk score differences in different “Ferroptosis.gene.clusters,” it was found that the risk score in gene.cluster 1 was significantly higher than that of gene.cluster 2 (Figure 5C), and the relevant conclusions were consistent with the previous analysis.

### 3.13.3 Differential Analysis of the Risk Score in Different “Ferroptosis Clusters”

Through differential analysis of the risk score in different “Ferroptosis clusters,” it was indicated that the risk score in cluster 1 was significantly higher than that of cluster 2 (Figure 5D), and the relevant conclusions were consistent with the previous analysis.

### 3.14 Differential Analysis of the Risk Score in Clinical Features and Different Molecular Types

The distribution of different risk scores in age, gender, chemo\_therapy, IDH1 mutation grouping, “ferroptosis cluster,” and “Ferroptosis.gene.cluster” was further checked



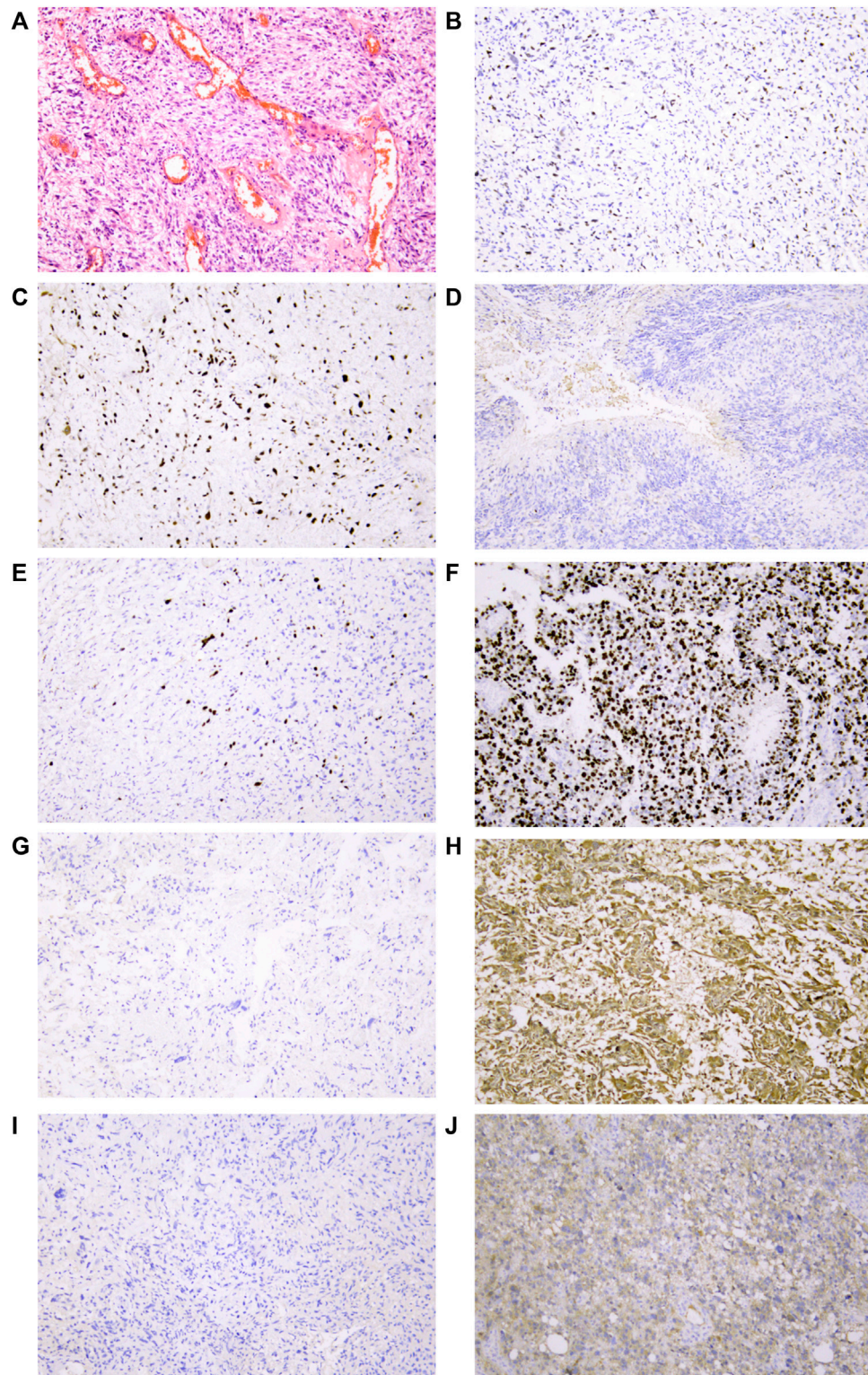


**FIGURE 6 |** Representative IHC analyses of p53/Ki-67/MGMT/IDH1R132H protein expression in cancer cells of glioblastoma patients. **(A)** Representative glioblastoma with HE staining. **(B)** Normal/wild-type p53 protein expression pattern with partly and weakly positive expression in tumor nuclei. Two patterns were identified as abnormal/mutant-staining pattern. **(C)** Abnormal overexpression of p53 protein with strong staining in nearly all tumor nuclei compared to internal control central fibroblasts. **(D)** Abnormal complete absence of p53 staining with sufficient staining of internal controls (fibroblasts, endothelial cells, or lymphocytes). **(E)** Low proportion of Ki-67 protein expression in tumor nuclei suggested that the tumor has low proliferative activity. **(F)** High proportion of Ki-67 protein expression in tumor (Continued)

**FIGURE 6** | nuclei suggested that the tumor has high proliferative activity. **(G)** Negative expression of MGMT protein in tumor nuclei might be related to MGMT methylation. **(H)** Strong positive expression of MGMT protein in tumor nuclei. **(I)** IDH1 R132H wild-type protein expression pattern with cytoplasmic negative staining of tumor cells. **(J)** IDH1 R132H mutation protein expression pattern with cytoplasmic positive staining of tumor cells. All images were taken at 10 × 10 magnification on the Leica DM2000 microscope.

and plotted as box plots. The results showed that the distributions of different risk scores in age, IDH1 mutation group, “ferroptosis cluster,” and “Ferroptosis.gene.cluster” were significantly different (Figure 5E).

### 3.15 Correlation Analyses Between Risk Score and Tumor Mutation Burden, homologous recombination deficiency, Neoantigen Load, Chromosomal Instability, and mRNAsi

The correlations between risk score and TMB, HRD, neoantigen load, chromosomal instability, and mRNAsi were calculated, and then a linear correlation graph was drawn. The results indicated that risk score had a strong correlation with mRNAsi ( $R = -0.498$ ), which was consistent with the previous report (Malta et al., 2018). In addition, similar significant correlation could also be found between the risk score and HRD, HRD\_TAI, and HRD\_LST (Supplementary Figure S5).

### 3.16 The Landscape of High- and Low-Risk Score Groups

The differences of CNV sites between the high- and low-risk score groups were checked, and it was found that the CNV sites of the two groups were similar. However, the G-score of 7p11.2 in the high-risk group was slightly higher than that of the low-risk group, indicating that the proportion of the relevant sites was higher in the high-risk group. In addition, 9p21.2 and 9p21.3 in the high-risk group also had higher G-scores, while 12q13.3 in the low-risk group had a higher G-score (Figures 5F,G).

Then, combined with risk score grouping, the genetic mutations of the two group samples would be displayed. The waterfall chart showed that both of the two risk groups had higher mutation rates. Among them, PTEN had the highest mutation rate in the high-risk group, while TP53 enjoyed a higher mutation rate in the low-risk group (Figures 5H,I).

### 3.17 Immunotherapy Analysis Results in the High- and Low-Risk Score Groups (TIDE Prediction + GDSC)

#### 3.17.1 Analysis Results of GDSC in the High- and Low-Risk Groups, Estimated by the IC<sub>50</sub> Value

The drug treatment response of the high- and low-risk group samples was further analyzed. The results indicated that the two risk groups enjoyed significant differences in the efficacy of cisplatin, vinblastine, gemcitabine, and paclitaxel. Moreover, the samples in the low-risk group were much more sensitive to cisplatin, vinblastine, gemcitabine, and paclitaxel.

After that, the TIDE score was used to predict the immunotherapy efficacy. The results indicated that the TIDE score of the high-risk group was significantly higher than that of the low-risk group, implying that the high-risk group might have a poorer immunotherapy efficacy (Supplementary Figure S6A-E).

#### 3.17.2 Expression Differences of Immune Check Sites in the High- and Low-Risk Groups

The expression of immune checkpoints in the high- and low-risk groups was checked. The results indicated that the expression of CD274, CTLA4, PDCD1, and LAG3 in the samples of the high-risk group was significantly higher than that of the low-risk group, suggesting that the high expression of relevant genes might be one of the reasons that affected GBM treatment efficacy (Supplementary Figure S6F-I).

### 3.18 Immunohistochemical Validation Results of Clinical Samples

From forty-two glioblastoma patients, including 17 females and 25 males, histopathological sections were collected. The basic characteristics of all enrolled clinical samples are summarized in Table 2. There were 15 patients with P53 gene mutation, and 27 patients were P53 wild-type. There was no significant difference in the P53 status between the two parts. IDH1 gene mutation was detected in six patients, while Ki-67 > 30% was found in 14 patients. Typical immunohistochemical staining results, including P53, Ki-67, MGMT, and IDH1, are provided in Figure 6.

## 4. DISCUSSION

The flow diagram of the study is provided in Supplementary Figure S1. Among the 257 ferroptosis-related genes with expression information, there were 239 ferroptosis-related genes whose expression was significantly different between cancer and normal samples ( $p < 0.05$ ), indicating that the expression of most ferroptosis-related genes was related to glioblastoma (Supplementary Figure S2). The results of PCA also further verified the aforementioned conclusions (Supplementary Figure S3A,B). Some of those genes, such as CDKN2A (Kraus et al., 2001; Hu et al., 2017), CA9 (Said et al., 2007), and HSPB1 (Rajesh et al., 2020), were also found in previous reports, which further confirmed the feasibility of our study design. Further analysis found that CDKN2A, TP53, IDH1, and EGFR were still the most abnormally altered genes in glioblastoma (Figure 1) (Kraus et al., 2001; Hu et al., 2017; Hu et al., 2022; Hu et al., 2018), while the most common



variation in SNP was C > T (**Figure 1C**) (McDonald et al., 2013; Mistry et al., 2018). This was similar to the mutation frequency of *TP53* and *IDH1* obtained in the immunohistochemistry of clinical samples (**Table 2; Figure 6**). PCA also showed that there were significant differences in ferroptosis-related genes between cancer and normal tissues (**Supplementary Figure S3B**). This further confirmed the important role of ferroptosis in glioblastoma.

Clustering analysis is a commonly used method for analyzing abnormal genome alterations in research (Töpfer et al., 2017; Adolfsson et al., 2019; Raymaekers and Zamar, 2020). Based on the expression information of ferroptosis-related genes in cancer samples, unsupervised clustering analysis was carried out. It was found that positive correlation was the main trend among ferroptosis-related genes (**Supplementary Figure S3C**), which was rarely mentioned in glioblastoma before. Through survival analysis of the two clusters obtained by the unsupervised clustering analysis of cancer samples, it was found that there was a statistically significant difference in the survival curve (**Supplementary Figure S3D,E**); similar differences could also be seen when GSVA, ssGSEA, and correlation analysis of clinical characteristics were completed (**Figures 2A–H**). Further analysis indicated that 12 types of immune cells had significant effects on survival (**Figure 2C**). Those would be helpful for us to use them to evaluate the clinical survival prognosis (Thomas et al., 2015; Du Four et al., 2016; Vinuesa et al., 2016; Pellegatta et al., 2018; Bayik et al., 2020; Han et al., 2020; Lupo and Matosevic, 2020; Xiong et al., 2020; Zhou et al., 2021; Campian et al., 2022).

After the differential expression analysis of ferroptosis-related genes in different ferroptosis clusters were carried out, it was found that the mutation frequency of *IDH1* in cluster 2 was significantly higher than that of cluster 1 (**Figures 2G–I**), which further explained the reason for that cluster 2 had better survival prognosis than cluster 1 (**Supplementary Figure S3E**). It also further affirmed the potential prognostic significance of *IDH1* mutation in glioblastoma (Nobusawa et al., 2009; Yan et al., 2009; Molenaar et al., 2014), which was also consistent with our focus on *IDH1* in clinical works (**Table 2; Figure 6**).

Both Gene Ontology (GO) and KEGG enrichment analyses of DEGs in ferroptosis clusters suggested that ferroptosis played an important role at a certain time in the entire process of glioblastoma (**Supplementary Figure S4**) (Ma et al., 2019; Hynes and Naba, 2012; Bryukhovetskiy et al., 2019; Kiyokawa et al., 2021). Some of them, such as ECM–receptor interaction, nicotine addiction, and complex of collagen trimers, were rarely reported in glioblastoma (Bryukhovetskiy et al., 2019), which might provide some new ideas for further research. “Ferroptosis.gene.cluster” obtained by clustering analysis based on DEGs also showed similar prognostic effect as before (**Supplementary Figure S3D,E**, and **Figure 3**). Furthermore, the differences presented between Ferroptosis.gene.cluster 1 and Ferroptosis.gene.cluster 2 in the DEG heatmap (**Figure 3A**) were much more pronounced than previous clusters (**Figure 2I**). Statistically significant expression differences could also be found in most of the “Ferroptosis.gene.cluster” groups (**Figure 3C**). This means that this kind of clustering method may be a much more better

approach to reveal abnormal information in glioblastoma. This was the basis for the subsequent construction of the risk score predictive model containing 23 genes. Therefore, we believed that the 23-gene risk scoring model (*CP*, *EMP1*, *AKR1C1*, *FMOD*, *MYBPH*, *IFI30*, *SRPX2*, *PDLIM1*, *MMP19*, *SPOCD1*, *FCGBP*, *NAMPT*, *SLC11A1*, *S100A10*, *TNC*, *CSMD3*, *ATP1A2*, *CUX2*, *GALNT9*, *TNFAIP6*, *C15orf48*, *WSCD2*, and *CBLN1*) constructed based on this might have a better prognostic prediction efficacy (Xiao et al., 2021; Yu et al., 2022), which had been verified in the subsequent analysis results (**Figures 4A–G**). Also, this prognostic prediction advantage was particularly evident when it was depicted in the form of “risk score” in the Sankey diagram (**Figure 4H**).

For those 23 genes, 3 (*CP*, *EMP1*, and *AKR1C1*) of them were found to be reported in ferroptosis-related studies (Yang et al., 2019; Huang et al., 2021; Huang et al., 2021), while 19 genes (*CP*, *EMP1*, *AKR1C1*, *FMOD*, *MYBPH*, *IFI30*, *SRPX2*, *PDLIM1*, *MMP19*, *SPOCD1*, *FCGBP*, *NAMPT*, *SLC11A1*, *S100A10*, *TNC*, *CSMD3*, *ATP1A2*, *CUX2*, and *GALNT9*) were previously reported in glioblastoma. The four tumor-related genes (*TNFAIP6*, *C15orf48*, *WSCD2*, and *CBLN1*) were neither reported in ferroptosis-related reports nor in glioblastoma-related studies (Wei et al., 2012; Su et al., 2013; Shin et al., 2020; Bushel et al., 2022), which were first found by us. While there was not necessarily a causal relationship between related things, these findings at least provided a range of options for further investigation. Therefore, the specific roles of these genes in glioblastoma still needed to be further verified by basic experiments.

We enrolled 23 genes in this risk score prediction model, which could minimize the bias in the prediction results due to the inclusion of too few predictive genes. Subsequent analysis showed that most of the pathways were negatively correlated with risk score, while these pathways were positively correlated with each other (**Figure 4I**). The risk score of related pathways in cluster 1 was significantly lower than that in cluster 2, and the survival probability of cluster 1 was lower, which was consistent with the results of risk score-related analysis results (**Supplementary Figure S3D–3E**, **Figure 2A**, **Figure 4**, **Figures 5A–D**). This further verified the consistent trend of our overall analysis results and the feasibility of the analysis method. In the follow-up analysis results, it was found that the distribution of risk score was significantly different among age, *IDH1* mutation group, “ferroptosis cluster,” and “Ferroptosis.gene.cluster” (**Figure 5E**). This will provide an important reference for comprehensively judging the prognosis of patients in our clinical work.

Through the correlation analysis between risk score and TMB, homologous recombination deficiency (HRD), neoantigen load and chromosomal instability, and mRNAsi (**Supplementary Figure S5**), we found that it had a significant correlation with HRD, HRD\_TAI, and HRD\_LST, especially with mRNAsi ( $R = -0.498$ ), which would help us apply the mRNAsi to single-cell data to reveal patterns of intratumoral molecular heterogeneity, leading to a better understanding of glioblastoma (Malta et al., 2018; Zheng et al., 2021). By analyzing the differences of CNV loci in the high- and low-risk score groups, it was found that a G-score of 12q13.3 (mainly including *OS9* gene, *CDK4* gene, and *SAS*

gene) in the low-risk group was higher (**Figures 5F,G**), which was considered to be the characteristic locus (Reifenberger et al., 1994; Rollbrocker et al., 1996). Regardless of grouping, missense mutations, including PTEN, TP53, EGFR, and TTN, consistent with former reports and clinical verification (**Table 2** and **Figure 6**), were still the predominant genomic alteration type in glioblastoma (**Figures 5H,I**) (Smith et al., 2001; Ohgaki et al., 2004; Lee et al., 2006; Binder et al., 2018). Among them, PTEN had the highest alteration rate in the high-risk score group, while TP53 had a higher alteration rate in the low-risk score group (**Figures 5H,I**).

TIDE and GDSC assays were often used to assess anti-tumor therapy responses (Wang et al., 2021; Cascio et al., 2021; Cancer Cell Line Encyclopedia Consortium, 2015). In this study, the results of these two analyses showed significant differences in different risk score subgroups (**Supplementary Figure S6A–E**), further supporting the feasibility of the risk score model to be used for the clinical prognostic assessment. Subsequent immune checkpoint analyses revealed that the expressions of CD274, CTLA4, PDCD1, and LAG3 in the high-risk group were significantly higher than those of the low-risk group, suggesting that the high expression of related genes might be one of the reasons that affected GBM treatment and prognosis (**Supplementary Figure 6F–I**), which was also consistent with previous reports on the correlation between those four genes and the glioblastoma prognosis (Andrews et al., 2020; Du et al., 2020; Yang et al., 2021; Bi et al., 2022; Preddy et al., 2022).

There were three groups of consistent clustering analyses in this study. The first was the gene clustering analysis for Ferroptosis gene; the second was the clustering analysis based on the expression of Ferroptosis gene, named “Ferroptosis.cluster”; the last was the expression of DEGs based on Ferroptosis.cluster named “Ferroptosis.gene.cluster.” The whole process of cluster analysis was also an optimization process of all the data. Therefore, the consistency of the obtained results had a better feasibility and reliability. In addition, the data size of this study was relatively sufficient, and the analysis results of the verification data were consistent from each other and had a statistical significance, which might provide a certain reference for later basic or clinical research in this field.

## 5 CONCLUSION

In glioblastoma, there were a large number of abnormal ferroptosis-related alterations, which were significant for the prognosis of patients. The risk score-predicting model

including 23 ferroptosis-related genes might have a better predictive significance.

## DATA AVAILABILITY STATEMENT

The datasets presented in this study can be found in online repositories. The names of the repository/repositories and accession number(s) can be found in the article/**Supplementary Material**.

## ETHICS STATEMENT

The studies involving human participants were reviewed and approved by the Ethics Committee of the First Affiliated Hospital of Shandong First Medical University. The patients/participants provided their written informed consent to participate in this study.

## AUTHOR CONTRIBUTIONS

The study was designed by YT and YS; the collection of clinical information was completed by TW; HL was responsible for data collection and immunohistochemical staining of clinical samples; all the data cleaning and analyses were put into practice by YT, WL, and XY; the manuscript was drafted by YT; and YT and YS reviewed the manuscript for scientific soundness. All authors reviewed the final draft and approved its submission.

## FUNDING

The sources of funding for this study are listed as follows: the Academic Promotion Program of Shandong First Medical University (2019QL025; YS), the Natural Science Foundation of Shandong Province (ZR2019MH042; YS), the Jinan Science and Technology Program (201805064; YS), and the Postdoctoral Innovation Project of Jinan (YT).

## SUPPLEMENTARY MATERIAL

The Supplementary Material for this article can be found online at: <https://www.frontiersin.org/articles/10.3389/fmolb.2022.904098/full#supplementary-material>

## REFERENCES

- Adolfsson, A., Ackerman, M., and Brownstein, N. C. (2019). To Cluster, or Not to Cluster: An Analysis of Clusterability Methods. *Pattern Recognit.* 88, 13–26. doi:10.1016/j.patcog.2018.10.026
- Andrews, L. P., Somasundaram, A., Moskovitz, J. M., Szymczak-Workman, A. L., Liu, C., Cillo, A. R., et al. (2020). Resistance to PD1 Blockade in the Absence of Metalloprotease-Mediated LAG3 Shedding. *Sci. Immunol.* 5 (49), eabc2728. doi:10.1126/sciimmunol.abc2728
- Bayik, D., Zhou, Y., Park, C., Hong, C., Vail, D., Silver, D. J., et al. (2020). Myeloid-Derived Suppressor Cell Subsets Drive Glioblastoma Growth in a Sex-specific Manner. *Cancer Discov.* 10 (8), 1210–1225. doi:10.1158/2159-8290.CD-19-1355
- Bi, Y., Wu, Z.-H., and Cao, F. (2022). Prognostic Value and Immune Relevancy of a Combined Autophagy-, Apoptosis- and Necrosis-Related Gene Signature in Glioblastoma. *BMC Cancer* 22 (1), 233. doi:10.1186/s12885-022-09328-3



- Binder, Z. A., Thorne, A. H., Bakas, S., Wileyto, E. P., Bilello, M., Akbari, H., et al. (2018). Epidermal Growth Factor Receptor Extracellular Domain Mutations in Glioblastoma Present Opportunities for Clinical Imaging and Therapeutic Development. *Cancer Cell* 34 (1), 163–177. doi:10.1016/j.ccell.2018.06.006
- Bryukhovetskiy, I. S., Khotimchenko, Y., and Shevchenko, V. (2019). Molecular Determinants of Interaction between Glioblastoma CD133+ Cancer Stem Cells and Extracellular Matrix. *Ann. Oncol.* 30, vii4. doi:10.1093/annonc/mdz413.016
- Bushel, P. R., Ward, J., Burkholder, A., Li, J., and Anchang, B. (2022). Mitochondrial-nuclear Epistasis Underlying Phenotypic Variation in Breast Cancer Pathology. *Sci. Rep.* 12 (1), 1393. doi:10.1038/s41598-022-05148-4
- Campian, J. L., Ghosh, S., Kapoor, V., Yan, R., Thotala, S., Jash, A., et al. (2022). Long-Acting Recombinant Human Interleukin-7, NT-17, Increases Cytotoxic CD8 T Cells and Enhances Survival in Mouse Glioma Models. *Clin. Cancer Res.* 28, 1229–1239. doi:10.1158/1078-0432.CCR-21-0947
- Cancer Cell Line Encyclopedia Consortium (2015). Pharmacogenomic Agreement between Two Cancer Cell Line Data Sets. *Nature* 528 (7580), 84–87. doi:10.1038/nature15736
- Cascio, S., Chandler, C., Zhang, L., Sinno, S., Gao, B., Onkar, S., et al. (2021). Cancer-associated MSC Drive Tumor Immune Exclusion and Resistance to Immunotherapy, Which Can Be Overcome by Hedgehog Inhibition. *Sci. Adv.* 7 (46), eabi5790. doi:10.1126/sciadv.abi5790
- Chen, L., Wang, C., Sun, H., Wang, J., Liang, Y., Wang, Y., et al. (2021). The Bioinformatics Toolbox for circRNA Discovery and Analysis. *Brief. Bioinform.* 22 (2), 1706–1728. doi:10.1093/bib/bbaa001
- Chen, X., Kang, R., Kroemer, G., and Tang, D. (2021). Broadening Horizons: the Role of Ferroptosis in Cancer. *Nat. Rev. Clin. Oncol.* 18 (5), 280–296. doi:10.1038/s41571-020-00462-0
- Cimino, P. J., McFerrin, L., Wirsching, H.-G., Arora, S., Bolouri, H., Rabadan, R., et al. (2018). Copy Number Profiling across Glioblastoma Populations Has Implications for Clinical Trial Design. *Neuro Oncol.* 20 (10), 1368–1373. doi:10.1093/neuonc/noy108
- Du Four, S., Maenhout, S. K., Benteyn, D., De Keersmaecker, B., Duerinck, J., Thielemans, K., et al. (2016). Disease Progression in Recurrent Glioblastoma Patients Treated with the VEGFR Inhibitor Axitinib Is Associated with Increased Regulatory T Cell Numbers and T Cell Exhaustion. *Cancer Immunol. Immunother.* 65 (6), 727–740. doi:10.1007/s00262-016-1836-3
- Du, L., Lee, J.-H., Jiang, H., Wang, C., Wang, S., Zheng, Z., et al. (2020).  $\beta$ -Catenin Induces Transcriptional Expression of PD-L1 to Promote Glioblastoma Immune Evasion. *J. Exp. Med.* 217 (11), e20191115. doi:10.1084/jem.20191115
- Han, J., Khatwani, N., Searles, T. G., Turk, M. J., and Angeles, C. V. (2020). Memory CD8+ T Cell Responses to Cancer. *Seminars Immunol.* 49, 101435. doi:10.1016/j.smim.2020.101435
- Hu, C., Leche, C. A., 2nd, Kiyatkin, A., Yu, Z., Stayrook, S. E., Ferguson, K. M., et al. (2022). Glioblastoma Mutations Alter EGFR Dimer Structure to Prevent Ligand Bias. *Nature* 602 (7897), 518–522. doi:10.1038/s41586-021-04393-3
- Hu, H., Mu, Q., Bao, Z., Chen, Y., Liu, Y., Chen, J., et al. (2018). Mutational Landscape of Secondary Glioblastoma Guides MET-Targeted Trial in Brain Tumor. *Cell* 175 (6), 1665–1678. doi:10.1016/j.cell.2018.09.038
- Hu, L. S., Ning, S., Eschbacher, J. M., Baxter, L. C., Gaw, N., Ranjbar, S., et al. (2017). Radiogenomics to Characterize Regional Genetic Heterogeneity in Glioblastoma. *Neuro Oncol.* 19 (1), 128–137. doi:10.1093/neuonc/now135
- Huang, F., Zheng, Y., Li, X., Luo, H., and Luo, L. (2021). Ferroptosis-related Gene AKR1C1 Predicts the Prognosis of Non-small Cell Lung Cancer. *Cancer Cell Int.* 21 (1), 567. doi:10.1186/s12935-021-02267-2
- Hynes, R. O., and Naba, A. (2012). Overview of the Matrisome-Aan Inventory of Extracellular Matrix Constituents and Functions. *Cold Spring Harb. Perspect. Biol.* 4 (1), a004903. doi:10.1101/cshperspect.a004903
- Jiang, X., Stockwell, B. R., and Conrad, M. (2021). Ferroptosis: Mechanisms, Biology and Role in Disease. *Nat. Rev. Mol. Cell Biol.* 22 (4), 266–282. doi:10.1038/s41580-020-00324-8
- Kiyokawa, J., Kawamura, Y., Ghouse, S. M., Acar, S., Barçın, E., Martínez-Quintanilla, J., et al. (2021). Modification of Extracellular Matrix Enhances Oncolytic Adenovirus Immunotherapy in Glioblastoma. *Clin. Cancer Res.* 27 (3), 889–902. doi:10.1158/1078-0432.CCR-20-2400
- Knijnenburg, T. A., Wang, L., Zimmermann, M. T., Chambwe, N., Gao, G. F., Cherniack, A. D., et al. (2018). Genomic and Molecular Landscape of DNA Damage Repair Deficiency across the Cancer Genome Atlas. *Cell Rep.* 23 (1), 239. doi:10.1016/j.celrep.2018.03.076
- Kraus, J. A., Lamszus, K., Glesmann, N., Beck, M., Wolter, M., Sabel, M., et al. (2001). Molecular Genetic Alterations in Glioblastomas with Oligodendroglial Component. *Acta Neuropathol.* 101 (4), 311–320. doi:10.1007/s004010000258
- Lee, H., Zandkarimi, F., Zhang, Y., Meena, J. K., Kim, J., Zhuang, L., et al. (2020). Energy-stress-mediated AMPK Activation Inhibits Ferroptosis. *Nat. Cell Biol.* 22 (2), 225–234. doi:10.1038/s41556-020-0461-8
- Lee, J. C., Vivanco, I., Beroukhi, R., Huang, J. H. Y., Feng, W. L., DeBiasi, R. M., et al. (2006). Epidermal Growth Factor Receptor Activation in Glioblastoma through Novel Missense Mutations in the Extracellular Domain. *PLoS Med.* 3 (12), e485. doi:10.1371/journal.pmed.0030485
- Liang, C., Zhang, X., Yang, M., and Dong, X. (2019). Recent Progress in Ferroptosis Inducers for Cancer Therapy. *Adv. Mat.* 31 (51), 1904197. doi:10.1002/adma.201904197
- Liang, J.-y., Wang, D.-s., Lin, H.-c., Chen, X.-x., Yang, H., Zheng, Y., et al. (2020). A Novel Ferroptosis-Related Gene Signature for Overall Survival Prediction in Patients with Hepatocellular Carcinoma. *Int. J. Biol. Sci.* 16 (13), 2430–2441. doi:10.7150/ijbs.45050
- Liu, T., Zhu, C., Chen, X., Guan, G., Zou, C., Shen, S., et al. (2022). Ferroptosis, as the Most Enriched Programmed Cell Death Process in Glioma, Induces Immunosuppression and Immunotherapy Resistance. *Neuro Oncol.* noac033. doi:10.1093/neuonc/noac033
- Lupo, K. B., and Matosevic, S. (2020). CD155 Immunoregulation as a Target for Natural Killer Cell Immunotherapy in Glioblastoma. *J. Hematol. Oncol.* 13 (1), 76. doi:10.1186/s13045-020-00913-2
- Ma, D., Liu, S., Lal, B., Wei, S., Wang, S., Zhan, D., et al. (2019). Extracellular Matrix Protein Tenascin C Increases Phagocytosis Mediated by CD47 Loss of Function in Glioblastoma. *Cancer Res.* 79 (10), 2697–2708. doi:10.1158/0008-5472.CAN-18-3125
- Malta, T. M., Sokolov, A., Gentles, A. J., Burzykowski, T., Poisson, L., Weinstein, J. N., et al. (2018). Machine Learning Identifies Stemness Features Associated with Oncogenic Dedifferentiation. *Cell* 173 (2), 338–354. doi:10.1016/j.cell.2018.03.034
- McDonald, K. L., Rapkins, R. W., Olivier, J., Zhao, L., Nozue, K., Lu, D., et al. (2013). The T Genotype of the MGMT C>T (Rs16906252) Enhancer Single-Nucleotide Polymorphism (SNP) Is Associated with Promoter Methylation and Longer Survival in Glioblastoma Patients. *Eur. J. Cancer* 49 (2), 360–368. doi:10.1016/j.ejca.2012.08.012
- Mistry, A. M., Vnencak-Jones, C. L., and Mobley, B. C. (2018). Clinical Prognostic Value of the Isocitrate Dehydrogenase 1 Single-Nucleotide Polymorphism Rs11554137 in Glioblastoma. *J. Neurooncol.* 138 (2), 307–313. doi:10.1007/s11060-018-2796-6
- Molenaar, R. J., Verbaan, D., Lamba, S., Zanon, C., Jeuken, J. W. M., Boots-Sprenger, S. H. E., et al. (2014). The Combination of IDH1 Mutations and MGMT Methylation Status Predicts Survival in Glioblastoma Better Than Either IDH1 or MGMT Alone. *Neuro Oncol.* 16 (9), 1263–1273. doi:10.1093/neuonc/nou005
- Nobusawa, S., Watanabe, T., Kleihues, P., and Ohgaki, H. (2009). IDH1 Mutations as Molecular Signature and Predictive Factor of Secondary Glioblastomas. *Clin. Cancer Res.* 15 (19), 6002–6007. doi:10.1158/1078-0432.CCR-09-0715
- Ohgaki, H., Dessen, P., Jourde, B., Horstmann, S., Nishikawa, T., Di Patre, P.-L., et al. (2004). Genetic Pathways to Glioblastoma: A Population-Based Study. *Cancer Res.* 64 (19), 6892–6899. doi:10.1158/0008-5472.CAN-04-1337
- Pellegatta, S., Eoli, M., Cuccarini, V., Anghileri, E., Pollo, B., Pessina, S., et al. (2018). Survival Gain in Glioblastoma Patients Treated with Dendritic Cell Immunotherapy Is Associated with Increased NK but Not CD8+ T Cell Activation in the Presence of Adjuvant Temozolomide. *Oncoimmunology* 7 (4), e1412901. doi:10.1080/2162402X.2017.1412901
- Predy, I., Nandoliya, K., Miska, J., and Ahmed, A. U. (2022). Checkpoint: Inspecting the Barriers in Glioblastoma Immunotherapies. *Seminars Cancer Biol.* doi:10.1016/j.semcancer.2022.02.012
- Qu, K., Garamszegi, S., Wu, F., Thorvaldsdottir, H., Liefeld, T., Ocana, M., et al. (2016). Integrative Genomic Analysis by Interoperation of Bioinformatics Tools in GenomeSpace. *Nat. Methods* 13 (3), 245–247. doi:10.1038/nmeth.3732
- Rajesh, Y., Biswas, A., Kumar, U., Banerjee, I., Das, S., Maji, S., et al. (2020). Lumefantrine, an Antimalarial Drug, Reverses Radiation and Temozolomide Resistance in Glioblastoma. *Proc. Natl. Acad. Sci. U.S.A.* 117 (22), 12324–12331. doi:10.1073/pnas.1921531117

- Raymaekers, J., and Zamar, R. H. (2020). Pooled Variable Scaling for Cluster Analysis. *Bioinformatics* 36 (12), 3849–3855. doi:10.1093/bioinformatics/btaa243
- Reifenberger, G., Reifenberger, J., Ichimura, K., Meltzer, P. S., and Collins, V. P. (1994). Amplification of Multiple Genes from Chromosomal Region 12q13-14 in Human Malignant Gliomas: Preliminary Mapping of the Amplicons Shows Preferential Involvement of CDK4, SAS, and MDM2. *Cancer Res.* 54 (16), 4299–4303.
- Rollbrocker, B., Waha, A., Louis, D. N., Wiestler, O. D., and von Deimling, A. (1996). Amplification of the Cyclin-dependent Kinase 4 ( CDK4 ) Gene Is Associated with High Cdk4 Protein Levels in Glioblastoma Multiforme. *Acta Neuropathol.* 92 (1), 70–74. doi:10.1007/s004010050491
- Rutledge, W. C., Kong, J., Gao, J., Gutman, D. A., Cooper, L. A. D., Appin, C., et al. (2013). Tumor-infiltrating Lymphocytes in Glioblastoma Are Associated with Specific Genomic Alterations and Related to Transcriptional Class. *Clin. Cancer Res.* 19 (18), 4951–4960. doi:10.1158/1078-0432.CCR-13-0551
- Said, H. M., Hagemann, C., Staab, A., Stojic, J., Kühnel, S., Vince, G. H., et al. (2013). Expression Patterns of the Hypoxia-Related Genes Osteopontin, CA9, Erythropoietin, VEGF and HIF-1 $\alpha$  in Human Glioma *In Vitro* and *In Vivo*. *Radiotherapy Oncol.* 83 (3), 398–405. doi:10.1016/j.radonc.2007.05.003
- Shen, Z., Song, J., Yung, B. C., Zhou, Z., Wu, A., and Chen, X. (2018). Emerging Strategies of Cancer Therapy Based on Ferroptosis. *Adv. Mat.* 30 (12), 1704007. doi:10.1002/adma.201704007
- Shin, S.-B., Jang, H.-R., Xu, R., Won, J.-Y., and Yim, H. (2020). Active PLK1-Driven Metastasis Is Amplified by TGF- $\beta$  Signaling that Forms a Positive Feedback Loop in Non-small Cell Lung Cancer. *Oncogene* 39 (4), 767–785. doi:10.1038/s41388-019-1023-z
- Smith, J. S., Tachibana, I., Passe, S. M., Huntley, B. K., Borell, T. J., Iturria, N., et al. (2001). PTEN Mutation, EGFR Amplification, and Outcome in Patients with Anaplastic Astrocytoma and Glioblastoma Multiforme. *JNCI J. Natl. Cancer Inst.* 93 (16), 1246–1256. doi:10.1093/jnci/93.16.1246
- Su, A., Ra, S., Li, X., Zhou, J., and Binder, S. (2013). Differentiating Cutaneous Squamous Cell Carcinoma and Pseudoepitheliomatous Hyperplasia by Multiplex qRT-PCR. *Mod. Pathol.* 26 (11), 1433–1437. doi:10.1038/modpathol.2013.82
- Thomas, A. A., Fisher, J. L., Rahme, G. J., Hampton, T. H., Baron, U., Olek, S., et al. (2015). Regulatory T Cells Are Not a Strong Predictor of Survival for Patients with Glioblastoma. *Neuro-Oncology* 17 (6), 801–809. doi:10.1093/neuonc/nou363
- Töpfer, N., Fuchs, L. M., and Aharoni, A. (2017). The PhytoClust Tool for Metabolic Gene Clusters Discovery in Plant Genomes. *Nucleic Acids Res.* 45 (12), 7049–7063. doi:10.1093/nar/gkx404
- Vinuesa, C. G., Linterman, M. A., Yu, D., and MacLennan, I. C. M. (2016). Follicular Helper T Cells. *Annu. Rev. Immunol.* 34, 335–368. doi:10.1146/annurev-immunol-041015-055605
- Wang, W., Green, M., Choi, J. E., Gijón, M., Kennedy, P. D., Johnson, J. K., et al. (2019). CD8+ T Cells Regulate Tumour Ferroptosis during Cancer Immunotherapy. *Nature* 569 (7755), 270–274. doi:10.1038/s41586-019-1170-y
- Wang, Z., Wang, Y., Yang, T., Xing, H., Wang, Y., Gao, L., et al. (2021). Machine Learning Revealed Stemness Features and a Novel Stemness-Based Classification with Appealing Implications in Discriminating the Prognosis, Immunotherapy and Temozolomide Responses of 906 Glioblastoma Patients. *Brief. Bioinform* 22 (5), bbab032. doi:10.1093/bib/bbab032
- Wei, P., Pattarini, R., Rong, Y., Guo, H., Bansal, P. K., Kusnoor, S. V., et al. (2012). The Cbln Family of Proteins Interact with Multiple Signaling Pathways. *J. Neurochem.* 121 (5), 717–729. doi:10.1111/j.1471-4159.2012.07648.x
- Wu, J., Minikes, A. M., Gao, M., Bian, H., Li, Y., Stockwell, B. R., et al. (2019). Intercellular Interaction Dictates Cancer Cell Ferroptosis via NF2-YAP Signalling. *Nature* 572 (7769), 402–406. doi:10.1038/s41586-019-1426-6
- Xiao, D., Zhou, Y., Wang, X., Zhao, H., Nie, C., and Jiang, X. (2021). A Ferroptosis-Related Prognostic Risk Score Model to Predict Clinical Significance and Immunogenic Characteristics in Glioblastoma Multiforme. *Oxidative Med. Cell. Longev.* 2021, 9107857–9107930. doi:10.1155/2021/9107857
- Xiong, Y., Xiong, Z., Cao, H., Li, C., Wanggou, S., and Li, X. (2020). Multi-dimensional Omics Characterization in Glioblastoma Identifies the Purity-Associated Pattern and Prognostic Gene Signatures. *Cancer Cell Int.* 20, 37. doi:10.1186/s12935-020-1116-3
- Yan, H., Parsons, D. W., Jin, G., McLendon, R., Rasheed, B. A., Yuan, W., et al. (2009). IDH1 and IDH2 Mutations in Gliomas. *N. Engl. J. Med.* 360 (8), 765–773. doi:10.1056/NEJMoa0808710
- Yang, F., He, Z., Duan, H., Zhang, D., Li, J., Yang, H., et al. (2021). Synergistic Immunotherapy of Glioblastoma by Dual Targeting of IL-6 and CD40. *Nat. Commun.* 12 (1), 3424. doi:10.1038/s41467-021-23832-3
- Yang, W.-H., Ding, C.-K. C., Sun, T., Rupprecht, G., Lin, C.-C., Hsu, D., et al. (2019). The Hippo Pathway Effector TAZ Regulates Ferroptosis in Renal Cell Carcinoma. *Cell Rep.* 28 (10), 2501–2508. doi:10.1016/j.celrep.2019.07.107
- Yee, P. P., Wei, Y., Kim, S.-Y., Lu, T., Chih, S. Y., Lawson, C., et al. (2020). Neutrophil-induced Ferroptosis Promotes Tumor Necrosis in Glioblastoma Progression. *Nat. Commun.* 11 (1), 5424. doi:10.1038/s41467-020-19193-y
- Yu, Z., Du, M., and Lu, L. (2022). A Novel 16-Genes Signature Scoring System as Prognostic Model to Evaluate Survival Risk in Patients with Glioblastoma. *Biomedicine* 10 (2), 317. doi:10.3390/biomedicine10020317
- Zhao, L., Zhou, X., Xie, F., Zhang, L., Yan, H., Huang, J., et al. (2022). Ferroptosis in Cancer and Cancer Immunotherapy. *Cancer Commun.* 42 (2), 88–116. doi:10.1002/cac2.12250
- Zheng, H., Song, K., Fu, Y., You, T., Yang, J., Guo, W., et al. (2021). An Absolute Human Stemness Index Associated with Oncogenic Dedifferentiation. *Brief. Bioinform* 22 (2), 2151–2160. doi:10.1093/bib/bbz174
- Zhou, B., Lawrence, T., and Liang, Y. (2021). The Role of Plasmacytoid Dendritic Cells in Cancers. *Front. Immunol.* 12, 749190. doi:10.3389/fimmu.2021.749190
- Zhuo, S., Chen, Z., Yang, Y., Zhang, J., Tang, J., and Yang, K. (2020). Clinical and Biological Significances of a Ferroptosis-Related Gene Signature in Glioma. *Front. Oncol.* 10, 590861. doi:10.3389/fonc.2020.590861

**Conflict of Interest:** The authors declare that the research was conducted in the absence of any commercial or financial relationships that could be construed as a potential conflict of interest.

**Publisher's Note:** All claims expressed in this article are solely those of the authors and do not necessarily represent those of their affiliated organizations, or those of the publisher, the editors, and the reviewers. Any product that may be evaluated in this article, or claim that may be made by its manufacturer, is not guaranteed or endorsed by the publisher.

Copyright © 2022 Tian, Liu, Zhang, Liu, Wu, Yang, Zhao and Sun. This is an open-access article distributed under the terms of the Creative Commons Attribution License (CC BY). The use, distribution or reproduction in other forums is permitted, provided the original author(s) and the copyright owner(s) are credited and that the original publication in this journal is cited, in accordance with accepted academic practice. No use, distribution or reproduction is permitted which does not comply with these terms.



# New Insights on Ferroptosis and Gynecological Malignancies

Ruiqi Fan<sup>†</sup>, Yujun Sun<sup>†</sup>, Mengxue Wang, Qian Wang, Aifang Jiang\* and Tingting Yang\*

Center of Reproductive Medicine, Affiliated Hospital of Weifang Medical University, Weifang, China

## OPEN ACCESS

### Edited by:

Xin Wang,  
National Institutes of Health (NIH),  
United States

### Reviewed by:

Yanqing Liu,  
Columbia University, United States  
Zhenyi Su,  
Columbia University, United States  
Bohao Zheng,  
Jiangnan University, China

### \*Correspondence:

Tingting Yang  
y402115432@163.com  
Aifang Jiang  
wfaj@sina.com

<sup>†</sup>These authors have contributed  
equally to this work and share first  
authorship

### Specialty section:

This article was submitted to  
Molecular Diagnostics and  
Therapeutics,  
a section of the journal  
Frontiers in Molecular Biosciences

**Received:** 15 April 2022

**Accepted:** 16 May 2022

**Published:** 14 June 2022

### Citation:

Fan R, Sun Y, Wang M, Wang Q,  
Jiang A and Yang T (2022) New  
Insights on Ferroptosis and  
Gynecological Malignancies.  
Front. Mol. Biosci. 9:921298.  
doi: 10.3389/fmolb.2022.921298

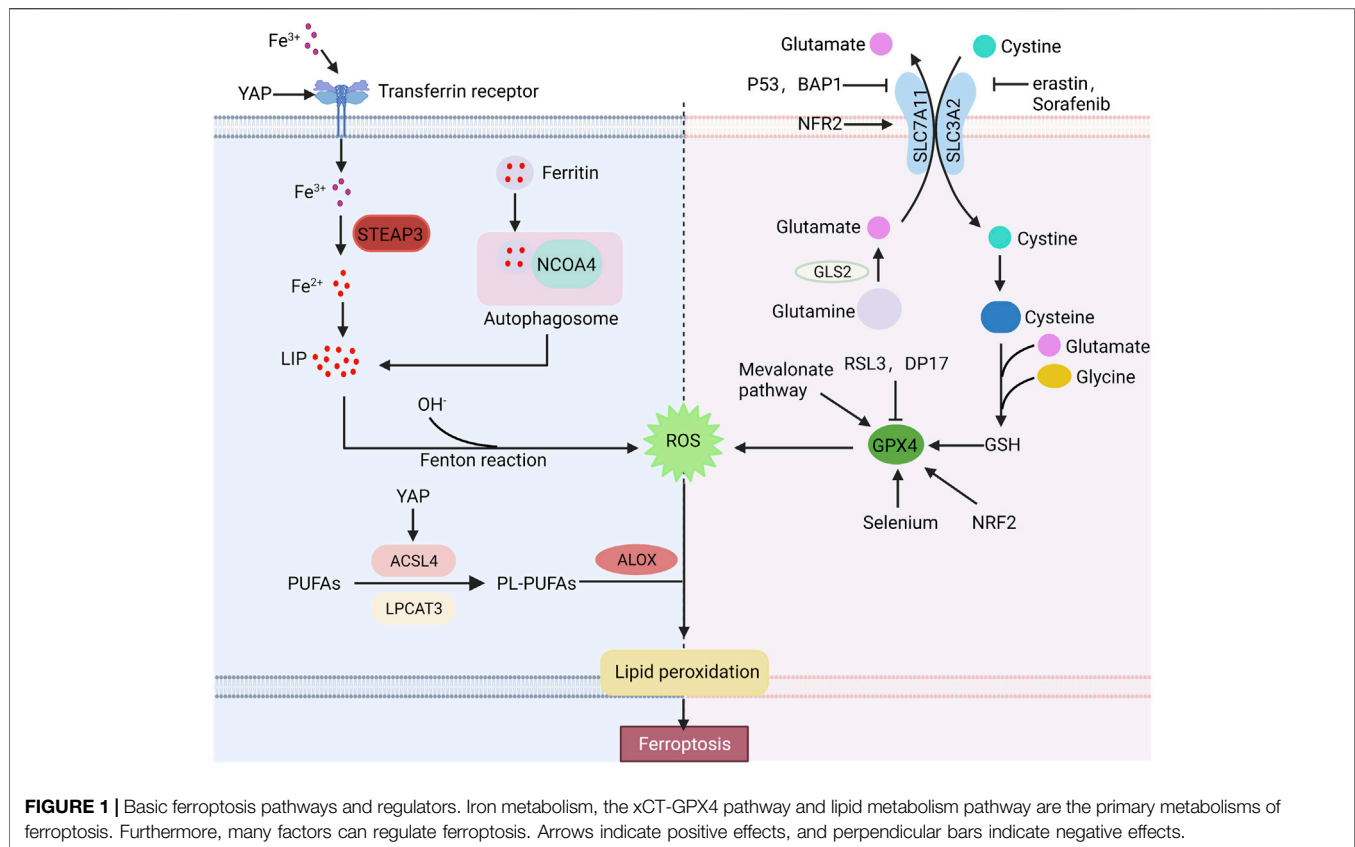
Ferroptosis is a new type of cell death different from apoptosis and necrosis, which can regulate the accumulation of lipid peroxidation through different pathways, ultimately leading to cell death. An increasing number of studies have revealed that the relationship between ferroptosis and cancer is extremely complex, which holds promise as a new treatment. In gynecological malignancies, ferroptosis has been found to have excellent antitumor activity, which can regulate the proliferation, metastasis and radiochemotherapy resistance. With the continuous progress of research, nanodrugs, gene therapy and other new therapeutic techniques for inducing ferroptosis have been proposed. However, the study of ferroptosis in gynecological malignancies is still in its infancy, and further research is needed to design safe and effective cancer therapies based on ferroptosis. This article reviews the mechanism of ferroptosis and the latest research progress and prospects in gynecological malignancies.

**Keywords:** ferroptosis, gynecological malignancies, iron metabolism, reactive oxygen species, radiochemotherapy resistance, nanotechnology

## INTRODUCTION

Ovarian, cervical and endometrial cancer are the most common malignancies and the major causes of cancer-related mortality in women (Jin et al., 2021). At present, the treatments of gynecological malignant tumors are mainly surgical treatment combined with radiotherapy and chemotherapy, but the results are still not ideal because of its recurrence and drug resistance. Therefore, it is important to investigate the underlying molecular mechanisms and potential therapeutic targets associated with such tumors.

Ferroptosis is an iron-dependent cell death proposed by Dixon et al., in 2012 (Wang H. et al., 2020), characterized by the accumulation of reactive oxygen species (ROS) and lipid peroxidation (Zuo et al., 2020). This particular cell death pattern can be suppressed by lipophilic antioxidants and iron chelators (Chen et al., 2020). Morphologically, ferroptotic cells mainly manifest as rupture of the cell membrane and mitochondrial membrane, increased mitochondrial membrane density, reduced mitochondrial size, and decreased or disappeared mitochondrial ridge. While morphological changes in the nucleus are not obvious (Li et al., 2020). Ferroptosis has been found to play an important role in the pathogenesis and treatment of many diseases including nervous system diseases, ischemia reperfusion injury, various inflammatory disorders and cancers (Qiu et al., 2020). In recent years, many studies have shown that ferroptosis can not only inhibit the proliferation of ovarian cancer cells and their diffusion in the abdominal cavity (Basuli et al., 2017) but also reverse the chemotherapy resistance of ovarian cancer (Zhou et al., 2019). In addition, ferroptosis also plays an important role in the development and treatment of cervical cancer (Zuo et al., 2020) and endometrial cancer (Wang H. et al., 2021). Therefore, in-depth study of the ferroptosis will provide new opportunities for the treatment of gynecological malignant tumors.



## MECHANISM OF FERROPTOSIS

Ferroptosis is a novel cell death mode, which requires excessive free iron and the accumulation of reactive oxygen species. Ferroptosis-inducing factors can reduce intracellular glutathione (GSH) levels and the activity of glutathione peroxidase 4 (GPX4) *via* different pathways, leading to the accumulation of ROS and ferroptosis (Figure 1).

### Iron Metabolism

The equilibrium state of iron is strictly controlled by iron metabolism in human body. Extracellular  $\text{Fe}^{2+}$  is oxidized to  $\text{Fe}^{3+}$  by ceruloplasmin, which binds to transferrin (TRF) and is transported into cells *via* transferrin receptor 1 (TFR1) (Frazer and Anderson, 2014). Then,  $\text{Fe}^{3+}$  is reduced to  $\text{Fe}^{2+}$  by six transmembrane epithelial antigen of prostate 3 (STEAP3) and stored in the unstable iron pool (LIP) or ferritin. The maladjustment of iron homeostasis may lead to ferroptosis (Bogdan et al., 2016). Excessive  $\text{Fe}^{2+}$  in cells can produce a large number of hydroxyl radical *via* the Fenton reaction. Hydroxyl radical has a strong oxidation ability to promote the accumulation of lipid peroxides, which leads to ferroptosis (Sun et al., 2021). The sensitivity of cells to ferroptosis can be influenced by regulating Fe absorption, storage and transport in human body. High TFR1 expression or increased ferritin autophagy affected by multiple factors and decreased ferritin

expression can lead to excessive intracellular iron accumulation, thus improving cell sensitivity to ferroptosis. While low expression of TFR1 or overexpression of ferritin can reduce cell sensitivity to ferroptosis. It is reported that deletion of the transferrin receptor one gene (TFR1) reduces intracellular iron accumulation, while heme oxygenase promotes ferroptosis in cells by increasing intracellular iron accumulation (Kwon et al., 2015). Overexpression of heat shock protein family B (HSPB1) can downregulate TFR1 expression and reduce the intracellular iron concentration (Sun et al., 2015). In addition, researches have shown that inhibition of iron response element binding protein 2 (IREB2) increases the expression of ferritin and decreases the intracellular free iron concentration, thus inhibiting ferroptosis (Kim et al., 2021). Thus, regulation of iron metabolism, expression of iron transporters and intracellular iron concentration are additional potential points of ferroptosis.

### xCT-Glutathione Peroxidase 4 Pathway

The xCT system is an important component of the cellular antioxidant system, which is a cystine-glutamate antiporter composed of two subunits, SLC7A11 and SLC3A2. It pumps glutamate out of cells and cystine into cells at a 1:1 ratio, and cystine is an important raw material for the synthesis of intracellular glutathione (Bridges et al., 2012; Conrad and



**TABLE 1 |** Ferroptosis and gynecological malignancies.

Tumor	Therapeutic target and drug	Mechanism of action	References
Ovarian cancer	Olaparib	Inhibit SLC7A11 expression by upregulating p53 to promote ferroptosis	Hong et al. (2021)
	SPIO	Synergize with p53 to promote ferroptosis	Zhang Y. et al. (2021)
	Erastin	Reduce the efflux transport activity of ABCB1 to reverse docetaxel resistance in ABCB1-overexpressing ovarian cancer cells	Zhou et al. (2019)
	Artesunate	Induce ROS accumulation to promote ferroptosis	(Shield et al., 2009; Greenshields et al., 2017)
	Ionizing radiation	Increase ROS accumulation and upregulate ACSL4 expression to promote ferroptosis	Zhang et al. (2022)
	Ferroptosis inducers	Inhibit SLC7A11 and GPX4 to enhance tumor cell sensitive to radiotherapy	Zhang et al. (2022)
Cervical cancer	PD-L1 inhibitors	Activate CD8 <sup>+</sup> T cells to promote ferroptosis	Author Anonymous, (2019)
	Oleanolic acid	Upregulate ACSL4 expression to promote ferroptosis	Xiaofei et al. (2021)
	Sorafenib	Increase iron concentration and ROS levels and decrease glutathione to promote ferroptosis	Wang C. et al. (2021)
	Artesunate-conjugated phosphorescence rhenium (I) complexes	Deplete glutathione, inactivate GPX4 and accumulate lipid peroxidation to promote both apoptosis and ferroptosis	Ye et al. (2021)
	Ferroptosis inducers (sulfamazine)	Inhibit SLC7A11 and GPX4 to enhance tumor cell sensitive to radiotherapy	Lei et al. (2021)
Endometrial Cancer	Quinone	Regulate heme oxygenase, transferrin, SLC7A11 to promote ferroptosis	Zhang Y.-Y. et al. (2021)
	Inhibit PTPN18	Downregulate the activity of GPX4/xCT to promote ferroptosis	Wang H. et al. (2021)

Sato, 2012; Koppula et al., 2018). Glutathione is widely present in cells and organelles. It can interact with glutathione peroxidase to eliminate lipid reactive oxygen species, thus maintaining cellular redox balance. Erastin, a small molecule of ferroptosis inducers, affects the synthesis of intracellular glutathione by inhibiting the xCT system, and decreases glutathione peroxidase activity, resulting in ROS accumulation and ultimately ferroptosis (Dixon et al., 2012). SLC7A11 is also an important regulatory site of ferroptosis. SLC7A11 overexpression enhances the antioxidant capacity of cells, thereby inhibiting erastin-induced ferroptosis (Huang et al., 2005). RSL3, a ferroptosis inducer, directly acts on GPX4 rather than the xCT system. GPX4, a member of the glutathione peroxidase family (GPXs), is a key regulator of ferroptosis. GPX4 catalyzes the reduction of lipid peroxides in complex cytomembrane environments. Researches have reported that downregulated GPX4 promotes tumor sensitive to ferroptosis, while upregulated GPX4 decreases ferroptosis sensitivity (Yang et al., 2014). In addition to inducers such as RSL3, DP17, the mevalonate pathway and selenium also act on the xCT system (Feng and Stockwell, 2018).

## Lipid Metabolism Pathway

Iron-dependent lipid peroxide accumulation is involved in all pathways of ferroptosis. Polyunsaturated fatty acids (PUFAs) in cells need to be embedded into membrane phospholipids under the catalysis of acyl-CoA synthase long chain family member 4 (ACSL4) and lysophosphatidyltransferase 3 (LPCAT3) (Lin et al., 2020). Researches indicate that knockdown of ACSL4 or LPCAT3 reduces PUFA phospholipid production to inhibit lipid peroxidation (LPO) deposition and erastin-induced ferroptosis (Nie

et al., 2022), while ACSL4 overexpression promotes ferroptosis (Qiu et al., 2020).

## Important Regulators of Ferroptosis

Early studies have shown that p53 plays an important role in tumor suppression by inducing cell cycle arrest, senescence and apoptosis (Kaiser and Attardi, 2018). Recently, p53 has been found to be involved in the regulation of ferroptosis (Liu and Gu, 2022). p53 can downregulate SLC7A11 expression and affect intracellular glutathione synthesis, resulting in the accumulation of lipid peroxidation and ferroptosis (Jiang et al., 2015). In addition to affecting glutathione synthesis, SLC7A11 can bind to arachidonate 12-lipoxygenase (ALOX12) and reduce its enzyme activity (Chu et al., 2019). p53-mediated reduction of SLC7A11 can promote the release of ALOX12, which can play the role of oxide membrane PUFAs, eventually lead to ferroptosis (Liu and Gu, 2021). Moreover, p53 can promote the decomposition of glutamine by enhancing the activity of glutaminase 2 (GLS2). A high concentration of glutamate inhibits System xCT and induces ferroptosis (Hu et al., 2010; Suzuki et al., 2010). However, in some cases, p53 can inhibit ferroptosis by inducing p21 to converse GSH against ROS-mediated damage (Maddocks et al., 2013).

Nuclear factor E2-related factor 2 (NRF2) is considered to be an important inhibitor of ferroptosis, which can regulate the level of intracellular iron, limit the production of reactive oxygen species and upregulate the expression of SLC7A11 and GPX4 (Fan et al., 2017; Zimta et al., 2019; Takahashi et al., 2020). NRF2 activity is regulated by Keap1, which binds to NRF2 and inhibits NRF2 activity under normoxic conditions. However, NRF2 dissociates from Keap1 and transferred into the nucleus during stress conditions, where it activates antioxidant response elements (AREs) to maintain redox homeostasis (Fan et al., 2017).

The E-cadherin-NF2-Hippo-YAP/TAZ pathway plays an important role in regulating ferroptosis. High-density cells are insensitive to ferroptosis resulting in cysteine deficiency and GPX4 inhibition (Wu et al., 2019). E-cadherin (ECAD) is an important mediator of cell-cell contacts in epithelial cells and is highly expressed in dense cells (van Roy and Berx, 2008). In epithelial cells, ECAD inhibits YAP activity by inducing the intracellular NF2 and Hippo signaling pathways. YAP can promote ferroptosis by upregulation of several ferroptosis targets including ACSL4 and TFRC (Wu et al., 2019).

BRCA1-associated protein 1 (BAP1) is a tumor suppressor gene that promotes ferroptosis by downregulating SLC7A11, similar to p53. BAP1 downregulates SLC7A11 by H2Aub deubiquitination on SLC7A11, inhibiting cystine uptake and leading to lipid peroxidation and ferroptosis (Zhang et al., 2018).

## FERROPTOSIS IN GYNECOLOGICAL MALIGNANCIES

Ferroptosis has been found to play an important role in the pathophysiological process of many malignant tumors. Studies confirm that inducing ferroptosis not only inhibits the growth of tumor cells but also enhances the sensitivity of tumor cells to chemoradiotherapy drugs in ovarian, cervical and endometrial cancers (Table 1).

### Ferroptosis in Ovarian Cancer

Ovarian cancer is the deadliest gynecological malignant tumor. And the effective treatment is resection of all macroscopic tumors combined with chemotherapy. Although patients initially respond well to this treatment, 50% of patients relapse and develop drug resistance within six months (Lengyel, 2010). Multidrug resistance is considered to be a main cause of chemotherapy failure and a low 5-year survival rate in ovarian cancer, so eliminating the drug resistance of tumor cells is very important. It is revealed that iron efflux pump expression is decreased and transferrin receptor 1 (TFRI) is overexpressed in both high-grade serous ovarian cancer tissues and ovarian cancer tumor initiating cells (TICs), leading to intracellular free iron concentration increased (Basuli et al., 2017). Meanwhile, decreasing intracellular iron concentrations inhibits ovarian cancer cell proliferation and intraperitoneal dissemination. These suggest that ovarian cancer cells are highly iron-dependent in their growth, invasion and metastasis. This “iron addiction” increases ovarian cancer cell sensitivity to ferroptosis inducers such as erastin. So inducing ferroptosis in ovarian cancer could be a breakthrough for inhibiting tumor cell growth and metastasis.

p53 can directly act on the xCT system and inhibit cysteine-glutamate transporters to reduce intracellular glutathione production, thus leading to the accumulation of lipid reactive oxygen and ultimately increasing cell sensitivity to ferroptosis (Wang Y. et al., 2020). Although the mechanism of p53 regulation of ferroptosis in ovarian cancer cells is not fully understood, this target provides a new research direction for ovarian cancer treatment. PARP inhibitor olaparib in BRCA-mutant ovarian cancer targets this point. Olaparib inhibits SLC7A11 expression by upregulating p53 in ovarian cancer cells, and then affects glutathione synthesis,

resulting in the accumulation of lipid peroxidation and ferroptosis (Hong et al., 2021). Ferroptosis inducers can enhance the sensitivity of BRCA-mutant ovarian cancer cells to PARP inhibitors *in vivo* and *in vitro* to inhibit the proliferation of tumor cell (Hong et al., 2021). This may provide a new strategy for the treatment of PARP inhibitors in BRCA-mutant ovarian cancer. In addition, p53-mediated ferroptosis contributes to the effects of metal-based drugs. For example, overexpression of p53 significantly promotes ferroptosis induced by superparamagnetic iron oxides (SPIO) in ovarian cancer cells, then inhibiting the growth of ovarian cancer (Zhang Y. et al., 2021). p53 mutation is associated with the clinical stage and progression of ovarian cancer. Previous studies confirmed that p53 mutation occurs in 96% of high-grade serous ovarian cancers and mutations in p53 and Kras promote ovarian cancer by transforming primary tubal epithelial cells into cancer cells in mice (Tarangelo et al., 2018). p53 mutation may promote the proliferation of ovarian cancer cells by reducing tumor sensitivity to ferroptosis.

The ferroptosis inducers erastin and sorafenib have been shown to inhibit tumor cell proliferation, metastasis and invasion in malignant tumors such as lung cancer and fibrosarcoma. The combination of ferroptosis inducers and chemotherapy drugs such as docetaxel and platinum drugs can improve the prognosis of patients by reducing chemotherapy resistance in ovarian cancer cells. ATP-binding cassette transporters subfamily B member 1 (ABCB1) is a multidrug resistance protein, overexpression of which is one of the main factors of cancer chemotherapy failure. Erastin reduces the efflux transport activity of ABCB1 to lead the accumulation of chemotherapeutic drugs in tumor cells. This reverses docetaxel resistance in ABCB1-overexpressing ovarian cancer cells (Zhou et al., 2019). Another study found that platinum-resistant ovarian cancer patients treated with sorafenib have significantly longer progression-free survival than those with placebo (Chekerov et al., 2018). However, erastin treatment over time can inhibit ferroptosis in tumor cells by upregulating cysteine biosynthesis and decreasing lipid peroxidation (Seborova et al., 2019).

Artesunate, an antimalarial drug, inhibits the proliferation of tumor cells by inducing ferroptosis accompanied by the accumulation of ROS in cells. According to research findings, artesunate can induce ROS accumulation in ovarian cancer cells *in vivo* and *in vitro*, leading to ferroptosis and eventually inhibiting the proliferation of ovarian cancer (Greenshields et al., 2017). In addition, artesunate also restrains cancer peritoneal metastasis in a mouse model of ovarian cancer by inducing ferroptosis (Shield et al., 2009). Although the mechanism of these drugs in malignant tumors is still under investigation, it provides a novel direction for ovarian cancer treatment.

### Ferroptosis in Cervical Cancer

Cervical cancer, one of the most common gynecological malignancies, is mainly caused by human papillomavirus (HPV) infection (Cruz-Gregorio et al., 2021). In recent years, the morbidity and mortality rates of cervical cancer have declined because of early screening. Nevertheless, patients with local or distant metastasis have a poor prognosis due to limited treatment options. Studies on ferroptosis in cervical cancer are limited. ACSL4 is a ligase that synthesizes polyunsaturated fatty acid-containing phospholipids in the lipid metabolic pathway of ferroptosis, the deletion of which can

inhibit ferroptosis by reducing lipid peroxidation (Kagan et al., 2017; Lei et al., 2020). In cervical cancer cells, oleanolic acid can induce ferroptosis by promoting ACSL4, while interfering with ACSL4 expression can reduce the inhibitory effect of oleanolic acid on tumor cell viability and proliferation (Xiaofei et al., 2021). Ferroptosis inducers also play an important role in cervical cancer proliferation and chemotherapy resistance. Sorafenib inhibits the growth of cervical cancer in mice by increasing iron concentration, ROS levels and decreasing glutathione (Wang C. et al., 2021). However, other research has reported that long-term using of the ferroptosis inducer erastin can promote HSPB1 expression in cervical cancer cells, which reduces lipid ROS and iron accumulation, and thus leads to erastin resistance. While inhibition of HSPB1 expression increases the anticancer activity of erastin in cervical cancer (Sun et al., 2015). In addition, researchers designed two artesunate-conjugated phosphorescence rhodium (I) complexes, which can induce both apoptosis and ferroptosis of cervical cancer cells by glutathione depletion, GPX4 inactivation and lipid peroxidation accumulation, improving the treatment efficiency (Ye et al., 2021). Further exploration of the mechanism of ferroptosis in cervical cancer may be significant for cervical cancer progression and treatment.

## Ferroptosis in Endometrial Cancer

The incidence and mortality rates of endometrial cancer have rapidly increased in recent years, and the prognosis of patients with metastasis or recurrence remains poor.

Currently, studies on ferroptosis in endometrial cancer are also increasing. Ferroptosis can be regulated by a variety of protein kinases. Protein tyrosine phosphatase nonreceptor type 18 (PTPN18) is associated with the occurrence and development of malignant tumors. PTPN18 expression is upregulated in endometrial cancer and inhibited ferroptosis by upregulating the activity of GPX4/xCT, thus promoting the growth of endometrial cancer cells (Wang H. et al., 2021). Quinones can not only lead to tumor cell death by regulating cell apoptosis and cycle arrest, but also lead to iron homeostasis imbalance by regulating iron metabolism in tumor cells. In endometrial cancer, quinone compounds inhibit endometrial cancer cell growth by inducing iron-dependent autophagy. It has been reported that quinone mediates the accumulation of free iron in endometrial cancer cells by regulating heme oxygenase, transferrin and SLC7A11, inducing ferroptosis (Zhang Y.-Y. et al., 2021). In a word, there are few studies on ferroptosis in endometrial cancer and more research is necessary. Ferroptosis plays an important role in endometrial growth and survival, and further study of its mechanism can provide new targets and strategies for the prevention and treatment of endometrial cancer.

## PROSPECTS OF FERROPTOSIS IN GYNECOLOGICAL MALIGNANCY TREATMENT

### Ferroptosis and Radiation Therapy

Radiation therapy is one of the main methods of treating gynecological malignant tumors, but radiation resistance is still

the main factor of radiotherapy failure. In malignant tumors, ferroptosis inducers increase the sensitivity of tumor cells to ionizing radiation. Studies have shown that ionizing radiation can induce ovarian cancer cell ferroptosis by increasing ROS accumulation and upregulating ACSL4 expression. Besides, ionizing radiation also upregulates SLC7A11 and GPX4 to make tumor cells surviving resistant to radiotherapy (Zhang et al., 2022). Treating radioresistant ovarian cancer cells with ferroptosis inducers that inhibit SLC7A11 and GPX4 can enhance tumor cell sensitivity to radiotherapy. This phenomenon also occurs in cervical cancer that ferroptosis inducers enhance radiation efficacy by inhibiting SLC7A11 and GPX4 in a model of cervical cancer (Lei et al., 2021). Previous study found that sulfamazine alone has a poor effect on inducing ferroptosis in tumor cells, but it is less toxic and suitable for using *in vivo*. Combined with radiotherapy, sulfamazine can enhance the sensitivity of tumor cells to radiotherapy, which is expected to be a radiotherapy sensitizer for cancer treatment (Lei et al., 2020). These studies have great significance for the development of new drugs for sensitizing tumors to radiotherapy.

### Ferroptosis and Immunotherapy

Ferroptosis is involved in T cell-mediated antitumor immunity and affects tumor immunotherapy. Activated CD8<sup>+</sup> T cells release interferon  $\gamma$  (IFN $\gamma$ ) to downregulate the expression of SLC3A2 and SLC7A11, and inhibit the uptake of cystine by tumor cells, thereby promoting lipid peroxidation and ferroptosis (Wang et al., 2019). Meanwhile, IFN- $\gamma$  can also increase cell sensitivity to ferroptosis by upregulating the level of Fe<sup>2+</sup> and downregulating the expression of GPX4 (Wei et al., 2022). Immunotherapy is used in combination with related therapies that induce ferroptosis such as targeted therapy, radiotherapy and chemotherapy, to achieve better therapeutic outcomes. A recent study showed that PD-L1 inhibitors can suppress tumor growth in ovarian cancer by activating CD8<sup>+</sup> T cells, leading to the accumulation of lipid peroxidation and ferroptosis in the cells, and the combination with cystine/cystinase showed stronger tumor inhibition (Author Anonymous, 2019).

### Ferroptosis, Nanomaterials, and Gene Technology

In recent years, some new methods, such as nanomaterials and gene technology, have been applied in malignant tumor treatments and chemotherapy resistance. Nanomaterials can use ultrasmall iron particles to release iron in malignant tumor cells, triggering the Fenton reaction to induce ferroptosis. Due to the complexity of malignant tumor treatment, the combination of multiple therapies can achieve better therapeutic effects. For example, chemotherapeutic drugs can be packed into ultrasmall particles of iron oxides to work together. A new ferroptosis inducer, sorafenib-mesoporous polydopamine-superparamagnetic iron oxide nanoparticles, which combine chemotherapy drugs, photothermal therapy and iron-based nanoparticles to inhibit the metastasis of malignant tumor cells (Guan et al., 2020). There are many similarly designed drugs, self-supplying lipid peroxidation nanoreactors that simultaneously release adriamycin, unsaturated lipids and iron,

inducing ferroptosis (Zhu et al., 2022). These treatments can not only improve the effectiveness of malignant tumor but also reduce drug toxicity. In addition, gene technology can also be applied to gynecological malignant tumor, including gene knockout and gene transfection (Shen et al., 2018). p53, CBS and GPX4 are all functional gene loci mentioned above. It is of great significance to promote these studies and clinical applications in the treatment of gynecological malignant tumors.

## CONCLUSION

Ferroptosis is a new form of cell death, the role of which in malignant tumors has attracted extensive attention. The mechanisms of ferroptosis are very complex, and there are many other pathways besides the iron metabolism pathway, xCT-GPX4 pathway and lipid metabolic pathway mentioned above. Therefore, the mechanism of ferroptosis still needs to be further studied to provide more valuable treatments for diseases. At present, some key therapeutic targets in gynecological malignant tumors have been discovered, such as p53, CBS and GPX4. A number of small-molecule drugs have been designed for these targets to induce ferroptosis, but these drugs are not yet available in humans. Ferroptosis inducers can reverse chemotherapy resistance in gynecological malignant tumors, which is very beneficial for patients with advanced and chemotherapy-resistant gynecologic malignancies.

## REFERENCES

- Author Anonymous (2019). Immunotherapy Activates Unexpected Cell Death Mechanism. *Cancer Discov.* 9 (7), OF2. doi:10.1158/2159-8290.CD-NB2019-058
- Basuli, D., Tesfay, L., Deng, Z., Paul, B., Yamamoto, Y., Ning, G., et al. (2017). Iron Addiction: A Novel Therapeutic Target in Ovarian Cancer. *Oncogene* 36 (29), 4089–4099. doi:10.1038/onc.2017.11
- Bogdan, A. R., Miyazawa, M., Hashimoto, K., and Tsuji, Y. (2016). Regulators of Iron Homeostasis: New Players in Metabolism, Cell Death, and Disease. *Trends Biochem. Sci.* 41 (3), 274–286. doi:10.1016/j.tibs.2015.11.012
- Bridges, R., Lutgen, V., Lobner, D., and Baker, D. A. (2012). Thinking outside the Cleft to Understand Synaptic Activity: Contribution of the Cystine-Glutamate Antiporter (System Xc<sup>-</sup>) to Normal and Pathological Glutamatergic Signaling. *Pharmacol. Rev.* 64 (3), 780–802. doi:10.1124/pr.110.003889
- Chekerov, R., Hilpert, F., Mahner, S., El-Balat, A., Harter, P., De Gregorio, N., et al. (2018). Sorafenib Plus Topotecan versus Placebo Plus Topotecan for Platinum-Resistant Ovarian Cancer (TRIAS): A Multicentre, Randomised, Double-Blind, Placebo-Controlled, Phase 2 Trial. *Lancet Oncol.* 19 (9), 1247–1258. doi:10.1016/S1470-2045(18)30372-3
- Chen, X., Li, J., Kang, R., Klionsky, D. J., and Tang, D. (2020). Ferroptosis: Machinery and Regulation. *Autophagy* 17, 2054–2081. doi:10.1080/15548627.2020.1810918
- Chu, B., Kon, N., Chen, D., Li, T., Liu, T., Jiang, L., et al. (2019). ALOX12 Is Required for P53-Mediated Tumour Suppression through a Distinct Ferroptosis Pathway. *Nat. Cell Biol.* 21 (5), 579–591. doi:10.1038/s41556-019-0305-6
- Conrad, M., and Sato, H. (2012). The Oxidative Stress-Inducible Cystine/glutamate Antiporter, System X C<sup>-</sup> : Cystine Supplier and beyond. *Amino Acids* 42 (1), 231–246. doi:10.1007/s00726-011-0867-5
- Cruz-Gregorio, A., Aranda-Rivera, A. K., Ortega-Lozano, A. J., Pedraza-Chaverri, J., and Mendoza-Hoffmann, F. (2021). Lipid Metabolism and
- Moreover, some less toxic ferroptosis inducers can be used as radiotherapy sensitizers, breaking the bottleneck of radiotherapy resistance. New technologies such as nanomaterials and gene technology are specific for gynecological malignant tumor treatment, but more experiments and researches are still needed. In conclusion, ferroptosis inducers are promising as emerging drugs in the treatment of gynecological malignant tumors, which are also the direction of our future research.

## AUTHOR CONTRIBUTIONS

RF and YS wrote and discussed the manuscript. MW discussed the manuscript. RF and QW designed and created figures. TY and AJ reviewed the manuscript. All authors read and approved the final manuscript.

## FUNDINGS

This research is supported by the National Natural Science Foundation of China (Nos. 81602301 and 81972489), Natural Science Foundation of Shandong Province (No. ZR2021MH235), Shandong province college science and technology plan project (No. J17KA254) and Clinical Research Center of Affiliated Hospital of Weifang Medical University (No. 2021wyfylcyj01).

- Oxidative Stress in HPV-Related Cancers. *Free Radic. Biol. Med.* 172, 226–236. doi:10.1016/j.freeradbiomed.2021.06.009
- Dixon, S. J., Lemberg, K. M., Lamprecht, M. R., Skouta, R., Zaitsev, E. M., Gleason, C. E., et al. (2012). Ferroptosis: An Iron-dependent Form of Nonapoptotic Cell Death. *Cell* 149 (5), 1060–1072. doi:10.1016/j.cell.2012.03.042
- Fan, Z., Wirth, A.-K., Chen, D., Wruck, C. J., Rauh, M., Buchfelder, M., et al. (2017). Nrf2-Keap1 Pathway Promotes Cell Proliferation and Diminishes Ferroptosis. *Oncogenesis* 6 (8), e371. doi:10.1038/oncsis.2017.65
- Feng, H., and Stockwell, B. R. (2018). Unsolved Mysteries: How Does Lipid Peroxidation Cause Ferroptosis? *PLOS Biol.* 16 (5), e2006203. doi:10.1371/journal.pbio.2006203
- Frazer, D. M., and Anderson, G. J. (2014). The Regulation of Iron Transport. *Biofactors* 40 (2), 206–214. doi:10.1002/biof.1148
- Greenshields, A. L., Shepherd, T. G., and Hoskin, D. W. (2017). Contribution of Reactive Oxygen Species to Ovarian Cancer Cell Growth Arrest and Killing by the Anti-malarial Drug Artesunate. *Mol. Carcinog.* 56 (1), 75–93. doi:10.1002/mc.22474
- Guan, Q., Guo, R., Huang, S., Zhang, F., Liu, J., Wang, Z., et al. (2020). Mesoporous Polydopamine Carrying Sorafenib and SPIO Nanoparticles for MRI-Guided Ferroptosis Cancer Therapy. *J. Control. Release* 320, 392–403. doi:10.1016/j.jconrel.2020.01.048
- Hong, T., Lei, G., Chen, X., Li, H., Zhang, X., Wu, N., et al. (2021). PARP Inhibition Promotes Ferroptosis via Repressing SLC7A11 and Synergizes with Ferroptosis Inducers in BRCA-Proficient Ovarian Cancer. *Redox Biol.* 42, 101928. doi:10.1016/j.redox.2021.101928
- Hu, W., Zhang, C., Wu, R., Sun, Y., Levine, A., and Feng, Z. (2010). Glutaminase 2, a Novel P53 Target Gene Regulating Energy Metabolism and Antioxidant Function. *Proc. Natl. Acad. Sci. U.S.A.* 107 (16), 7455–7460. doi:10.1073/pnas.1001006107
- Huang, Y., Dai, Z., Barbacioru, C., and Sadée, W. (2005). Cystine-glutamate Transporter SLC7A11 in Cancer Chemosensitivity and Chemoresistance. *Cancer Res.* 65 (16), 7446–7454. doi:10.1158/0008-5472.CAN-04-4267



- Jiang, L., Kon, N., Li, T., Wang, S.-J., Su, T., Hibshoosh, H., et al. (2015). Ferroptosis as a P53-Mediated Activity during Tumour Suppression. *Nature* 520 (7545), 57–62. doi:10.1038/nature14344
- Jin, Z., Chenghao, Y., and Cheng, P. (2021). Anticancer Effect of Tanshinones on Female Breast Cancer and Gynecological Cancer. *Front. Pharmacol.* 12, 824531. doi:10.3389/fphar.2021.824531
- Kagan, V. E., Mao, G., Qu, F., Angeli, J. P. F., Doll, S., Croix, C. S., et al. (2017). Oxidized Arachidonic and Adrenic PEs Navigate Cells to Ferroptosis. *Nat. Chem. Biol.* 13 (1), 81–90. doi:10.1038/nchembio.2238
- Kaiser, A. M., and Attardi, L. D. (2018). Deconstructing Networks of P53-Mediated Tumor Suppression *In Vivo*. *Cell Death Differ.* 25 (1), 93–103. doi:10.1038/cdd.2017.171
- Kim, M. J., Yun, G. J., and Kim, S. E. (2021). Metabolic Regulation of Ferroptosis in Cancer. *Biology* 10 (2), 83. doi:10.3390/biology10020083
- Koppula, P., Zhang, Y., Zhuang, L., and Gan, B. (2018). Amino Acid Transporter SLC7A11/xCT at the Crossroads of Regulating Redox Homeostasis and Nutrient Dependency of Cancer. *Cancer Commun.* 38 (1), 12. doi:10.1186/s40880-018-0288-x
- Kwon, M.-Y., Park, E., Lee, S.-J., and Chung, S. W. (2015). Heme Oxygenase-1 Accelerates Erastin-Induced Ferroptotic Cell Death. *Oncotarget* 6 (27), 24393–24403. doi:10.18632/oncotarget.5162
- Lei, G., Zhang, Y., Koppula, P., Liu, X., Zhang, J., Lin, S. H., et al. (2020). The Role of Ferroptosis in Ionizing Radiation-Induced Cell Death and Tumor Suppression. *Cell Res.* 30 (2), 146–162. doi:10.1038/s41422-019-0263-3
- Lei, G., Zhang, Y., Hong, T., Zhang, X., Liu, X., Mao, C., et al. (2021). Ferroptosis as a Mechanism to Mediate P53 Function in Tumor Radiosensitivity. *Oncogene* 40 (20), 3533–3547. doi:10.1038/s41388-021-01790-w
- Lengyel, E. (2010). Ovarian Cancer Development and Metastasis. *Am. J. Pathology* 177 (3), 1053–1064. doi:10.2353/ajpath.2010.100105
- Li, J., Cao, F., Yin, H.-L., Huang, Z.-J., Lin, Z.-T., Mao, N., et al. (2020). Ferroptosis: Past, Present and Future. *Cell Death Dis.* 11 (2), 88. doi:10.1038/s41419-020-2298-2
- Lin, X., Ping, J., Wen, Y., and Wu, Y. (2020). The Mechanism of Ferroptosis and Applications in Tumor Treatment. *Front. Pharmacol.* 11, 1061. doi:10.3389/fphar.2020.01061
- Liu, Y., and Gu, W. (2021). The Complexity of P53-Mediated Metabolic Regulation in Tumor Suppression. *Seminars Cancer Biol.* [Online ahead of print] S1044-579X(21) 00060-2. doi:10.1016/j.semcancer.2021.03.010
- Liu, Y., and Gu, W. (2022). p53 in Ferroptosis Regulation: The New Weapon for the Old Guardian. *Cell Death Differ.* 29, 895–910. doi:10.1038/s41418-022-00943-y
- Maddocks, O. D. K., Berkers, C. R., Mason, S. M., Zheng, L., Blyth, K., Gottlieb, E., et al. (2013). Serine Starvation Induces Stress and P53-dependent Metabolic Remodelling in Cancer Cells. *Nature* 493 (7433), 542–546. doi:10.1038/nature11743
- Nie, Q., Hu, Y., Yu, X., Li, X., and Fang, X. (2022). Induction and Application of Ferroptosis in Cancer Therapy. *Cancer Cell Int.* 22 (1), 12. doi:10.1186/s12935-021-02366-0
- Qiu, Y., Cao, Y., Cao, W., Jia, Y., and Lu, N. (2020). The Application of Ferroptosis in Diseases. *Pharmacol. Res.* 159, 104919. doi:10.1016/j.phrs.2020.104919
- Seborova, K., Vaclavikova, R., Soucek, P., Elsnerova, K., Bartakova, A., Cernaj, P., et al. (2019). Association of ABC Gene Profiles with Time to Progression and Resistance in Ovarian Cancer Revealed by Bioinformatics Analyses. *Cancer Med.* 8 (2), 606–616. doi:10.1002/cam4.1964
- Shen, Z., Song, J., Yung, B. C., Zhou, Z., Wu, A., and Chen, X. (2018). Emerging Strategies of Cancer Therapy Based on Ferroptosis. *Adv. Mat.* 30 (12), 1704007. doi:10.1002/adma.201704007
- Shield, K., Ackland, M. L., Ahmed, N., and Rice, G. E. (2009). Multicellular Spheroids in Ovarian Cancer Metastases: Biology and Pathology. *Gynecol. Oncol.* 113 (1), 143–148. doi:10.1016/j.ygyno.2008.11.032
- Sun, X., Ou, Z., Xie, M., Kang, R., Fan, Y., Niu, X., et al. (2015). HSPB1 as a Novel Regulator of Ferroptotic Cancer Cell Death. *Oncogene* 34 (45), 5617–5625. doi:10.1038/onc.2015.32
- Sun, L. L., Linghu, D. L., and Hung, M. C. (2021). Ferroptosis: A Promising Target for Cancer Immunotherapy. *Am. J. Cancer Res.* 11 (12), 5856–5863.
- Suzuki, S., Tanaka, T., Poyurovsky, M. V., Nagano, H., Mayama, T., Ohkubo, S., et al. (2010). Phosphate-activated Glutaminase (GLS2), a P53-Inducible Regulator of Glutamine Metabolism and Reactive Oxygen Species. *Proc. Natl. Acad. Sci. U.S.A.* 107 (16), 7461–7466. doi:10.1073/pnas.1002459107
- Takahashi, N., Cho, P., Selfors, L. M., Kuiken, H. J., Kaul, R., Fujiwara, T., et al. (2020). 3D Culture Models with CRISPR Screens Reveal Hyperactive NRF2 as a Prerequisite for Spheroid Formation via Regulation of Proliferation and Ferroptosis. *Mol. Cell* 80 (5), 828–844. doi:10.1016/j.molcel.2020.10.010
- Tarangelo, A., Magtanong, L., Biegging-Rolett, K. T., Li, Y., Ye, J., Attardi, L. D., et al. (2018). p53 Suppresses Metabolic Stress-Induced Ferroptosis in Cancer Cells. *Cell Rep.* 22 (3), 569–575. doi:10.1016/j.celrep.2017.12.077
- van Roy, F., and Berx, G. (2008). The Cell-Cell Adhesion Molecule E-Cadherin. *Cell. Mol. Life Sci.* 65 (23), 3756–3788. doi:10.1007/s00018-008-8281-1
- Wang, C., Zeng, J., Li, L.-J., Xue, M., and He, S.-L. (2021). Cdc25A Inhibits Autophagy-Mediated Ferroptosis by Upregulating ErbB2 through PKM2 Dephosphorylation in Cervical Cancer Cells. *Cell Death Dis.* 12 (11), 1055. doi:10.1038/s41419-021-04342-y
- Wang, W., Green, M., Choi, J. E., Gijón, M., Kennedy, P. D., Johnson, J. K., et al. (2019). CD8+ T Cells Regulate Tumour Ferroptosis during Cancer Immunotherapy. *Nature* 569 (7755), 270–274. doi:10.1038/s41586-019-1170-y
- Wang, H., Liu, C., Zhao, Y., and Gao, G. (2020). Mitochondria Regulation in Ferroptosis. *Eur. J. Cell Biol.* 99 (1), 151058. doi:10.1016/j.ejcb.2019.151058
- Wang, H., Peng, S., Cai, J., and Bao, S. (2021). Silencing of PTPN18 Induced Ferroptosis in Endometrial Cancer Cells through P-P38-Mediated GPX4/xCT Down-Regulation. *Cmar* 13, 1757–1765. doi:10.2147/CMAR.S278728
- Wang, Y., Wei, Z., Pan, K., Li, J., and Chen, Q. (2020). The Function and Mechanism of Ferroptosis in Cancer. *Apoptosis* 25 (11-12), 786–798. doi:10.1007/s10495-020-01638-w
- Wei, T. T., Zhang, M. Y., Zheng, X. H., Xie, T. H., Wang, W., Zou, J., et al. (2022). Interferon- $\gamma$  Induces Retinal Pigment Epithelial Cell Ferroptosis by a JAK1-2/STAT1/SLC7A11 Signaling Pathway in Age-related Macular Degeneration. *FEBS J.* 289 (7), 1968–1983. doi:10.1111/febs.16272
- Wu, J., Minikes, A. M., Gao, M., Bian, H., Li, Y., Stockwell, B. R., et al. (2019). Intercellular Interaction Dictates Cancer Cell Ferroptosis via NF2-YAP Signalling. *Nature* 572 (7769), 402–406. doi:10.1038/s41586-019-1426-6
- Xiaofei, J., Mingqing, S., Miao, S., Yizhen, Y., Shuang, Z., Qinhua, X., et al. (2021). Oleonic Acid Inhibits Cervical Cancer Hela Cell Proliferation through Modulation of the ACSL4 Ferroptosis Signaling Pathway. *Biochem. Biophysical Res. Commun.* 545, 81–88. doi:10.1016/j.bbrc.2021.01.028
- Yang, W. S., SriRamaratnam, R., Welsch, M. E., Shimada, K., Skouta, R., Viswanathan, V. S., et al. (2014). Regulation of Ferroptotic Cancer Cell Death by GPX4. *Cell* 156 (1-2), 317–331. doi:10.1016/j.cell.2013.12.010
- Ye, R.-R., Chen, B.-C., Lu, J.-J., Ma, X.-R., and Li, R.-T. (2021). Phosphorescent Rhenium(I) Complexes Conjugated with Artesunate: Mitochondrial Targeting and Apoptosis-Ferroptosis Dual Induction. *J. Inorg. Biochem.* 223, 111537. doi:10.1016/j.jinorgbio.2021.111537
- Zhang, Y., Shi, J., Liu, X., Feng, L., Gong, Z., Koppula, P., et al. (2018). BAP1 Links Metabolic Regulation of Ferroptosis to Tumour Suppression. *Nat. Cell Biol.* 20 (10), 1181–1192. doi:10.1038/s41556-018-0178-0
- Zhang, X., Li, X., Zheng, C., Yang, C., Zhang, R., Wang, A., et al. (2022). Ferroptosis, a New Form of Cell Death Defined after Radiation Exposure. *Int. J. Radiat. Biol.* [Online ahead of print] 1. 1–9. doi:10.1080/09553002.2022.2020358
- Zhang, Y., Xia, M., Zhou, Z., Hu, X., Wang, J., Zhang, M., et al. (2021). p53 Promoted Ferroptosis in Ovarian Cancer Cells Treated with Human Serum Incubated-Superparamagnetic Iron Oxides. *Ijn* 16, 283–296. doi:10.2147/IJN.S282489
- Zhang, Y.-Y., Ni, Z.-J., Elam, E., Zhang, F., Thakur, K., Wang, S., et al. (2021). Juglone, a Novel Activator of Ferroptosis, Induces Cell Death in

- Endometrial Carcinoma Ishikawa Cells. *Food Funct.* 12 (11), 4947–4959. doi:10.1039/d1fo00790d
- Zhou, H.-H., Chen, X., Cai, L.-Y., Nan, X.-W., Chen, J.-H., Chen, X.-X., et al. (2019). Erastin Reverses ABCB1-Mediated Docetaxel Resistance in Ovarian Cancer. *Front. Oncol.* 9, 1398. doi:10.3389/fonc.2019.01398
- Zhu, L., Wang, J., Tang, X., Zhang, C., Wang, P., Wu, L., et al. (2022). Efficient Magnetic Nanocatalyst-Induced Chemo- and Ferroptosis Synergistic Cancer Therapy in Combination with T1-T2 Dual-Mode Magnetic Resonance Imaging through Doxorubicin Delivery. *ACS Appl. Mat. Interfaces* 14 (3), 3621–3632. doi:10.1021/acsami.1c17507
- Zimta, A.-A., Cenariu, D., Irimie, A., Magdo, L., Nabavi, S. M., Atanasov, A. G., et al. (2019). The Role of Nrf2 Activity in Cancer Development and Progression. *Cancers* 11 (11), 1755. doi:10.3390/cancers11111755
- Zuo, S., Yu, J., Pan, H., and Lu, L. (2020). Novel Insights on Targeting Ferroptosis in Cancer Therapy. *Biomark. Res.* 8, 50. doi:10.1186/s40364-020-00229-w

**Conflict of Interest:** The authors declare that the research was conducted in the absence of any commercial or financial relationships that could be construed as a potential conflict of interest.

**Publisher's Note:** All claims expressed in this article are solely those of the authors and do not necessarily represent those of their affiliated organizations, or those of the publisher, the editors and the reviewers. Any product that may be evaluated in this article, or claim that may be made by its manufacturer, is not guaranteed or endorsed by the publisher.

Copyright © 2022 Fan, Sun, Wang, Wang, Jiang and Yang. This is an open-access article distributed under the terms of the Creative Commons Attribution License (CC BY). The use, distribution or reproduction in other forums is permitted, provided the original author(s) and the copyright owner(s) are credited and that the original publication in this journal is cited, in accordance with accepted academic practice. No use, distribution or reproduction is permitted which does not comply with these terms.



# Multifaceted Roles of Ferroptosis in Lung Diseases

Yi Li<sup>1,2,3†</sup>, Ying Yang<sup>1,2</sup> and Yongfeng Yang<sup>1,2,3\*†</sup>

<sup>1</sup>Institute of Respiratory Health, West China Hospital, Sichuan University, Chengdu, China, <sup>2</sup>Precision Medicine Key Laboratory, West China Hospital, Sichuan University, Chengdu, China, <sup>3</sup>Department of Respiratory and Critical Care Medicine, West China Hospital, Sichuan University, Chengdu, China

## OPEN ACCESS

### Edited by:

Xin Wang,  
National Institutes of Health (NIH),  
United States

### Reviewed by:

Xintong Yao,  
Chongqing Medical University, China  
Gang Wang,  
Weill Cornell Medicine, United States  
Qiong Meng,  
National Institutes of Health (NIH),  
United States

### \*Correspondence:

Yongfeng Yang  
yangyongfeng0523@163.com

### †ORCID:

Yi Li  
orcid.org/0000-0001-8661-4617  
Yongfeng Yang  
orcid.org/0000-0002-8109-9801

### Specialty section:

This article was submitted to  
Molecular Diagnostics and  
Therapeutics,  
a section of the journal  
Frontiers in Molecular Biosciences

**Received:** 13 April 2022

**Accepted:** 20 May 2022

**Published:** 24 June 2022

### Citation:

Li Y, Yang Y and Yang Y (2022)  
Multifaceted Roles of Ferroptosis in  
Lung Diseases.  
Front. Mol. Biosci. 9:919187.  
doi: 10.3389/fmolb.2022.919187

Ferroptosis is a distinct type of programmed cell death (PCD) that depends on iron and is characterized by the accumulation of intracellular iron, exhaustion of glutathione, deactivation of glutathione peroxidase, and promotion of lipid peroxidation. Recently, accumulated investigations have demonstrated that ferroptosis is strongly correlated with the initiation and development of many lung diseases. In this review, we summarized the contribution of ferroptosis to the pathologic process of lung diseases, namely, obstructive lung diseases (chronic obstructive pulmonary disease, asthma, and cystic fibrosis), interstitial lung diseases (pulmonary fibrosis of different causes), pulmonary diseases of vascular origin (ischemia-reperfusion injury and pulmonary hypertension), pulmonary infections (bacteria, viruses, and fungi), acute lung injury, acute respiratory distress syndrome, obstructive sleep apnea, pulmonary alveolar proteinosis, and lung cancer. We also discussed the therapeutic potential of targeting ferroptosis for these lung diseases.

**Keywords:** ferroptosis, lung disease, infection, injury, cancer

## INTRODUCTION

The term “ferroptosis” was first coined by Dixon et al. (2012) to define a previously unknown form of programmed cell death (PCD) elicited by erastin in Ras-mutant cells in 2012. It is dependent on iron and is characterized by the accumulation of intracellular iron, exhaustion of glutathione, deactivation of glutathione peroxidase, and promotion of lipid peroxidation (Figure 1). Iron can catalyze the formation of free radicals from reactive oxygen species (ROS) via the Fenton reaction, which is the reduction of H<sub>2</sub>O<sub>2</sub> by a single electron to produce a hydroxyl radical. Ferroptosis is distinct from other types of cell death, such as apoptosis, autophagy, pyroptosis, or necrosis, in morphology, genetics, metabolism, and molecular biology. The specific morphology of ferroptosis includes intact cytomembranes, cellular shrinkage, enhanced mitochondrial membrane density, reduced or absent mitochondrial cristae, crumpling of the mitochondrial membrane, rupture of the outer membrane, and regular nucleus size without concentrated chromatin (Dixon et al., 2012; Yang and Stockwell, 2016). However, apoptosis is characterized by typical apoptotic cellular bodies without rupture of cell membranes, while necrosis is characterized by the occurrence of cell swelling, nucleus concentration, fragmentation and dissolution, chromatin staining and flocculence, and organelle enlargement or fragmentation. In terms of pathological processes, cell apoptosis increases ROS, Ca<sup>2+</sup>, and pH levels, which activates cysteinyl aspartate-specific proteinase and releases cytochrome c to promote caspase-3/7. During cell necrosis, the inflammatory response is induced by the activation of several signaling pathways, namely, Toll-like receptor 4/myeloid

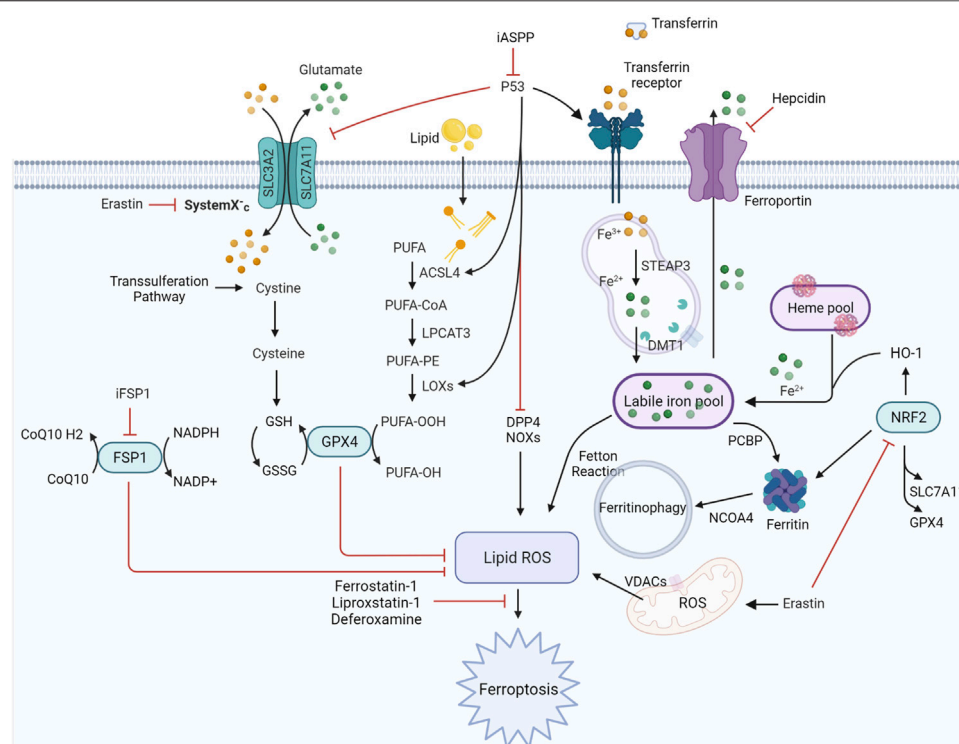


**FIGURE 1 |** Regulatory signaling pathways implicated in ferroptosis. The features of ferroptosis include the substrate of lipid peroxidation (PUFA), executor of lipid peroxidation (iron metabolism), and anti-ferroptosis systems (GPX4-centered and p53-centered systems). ACSL4, acyl-CoA synthetase long-chain family member four; DDP4, dipeptidyl peptidase-4; DMT1, divalent metal transporter 1; FSP1, ferroptosis suppressor protein 1; GPX4, glutathione peroxidase four; GSH, glutathione; HO-1, heme oxygenase 1; iASPP, inhibitor of apoptosis stimulating protein of p53; iFSP1, FSP1 inhibitor 1; LOXs, lipoxygenases; LPCAT3, lysophosphatidylcholine acyltransferase three; NRF2, nuclear factor erythroid 2-related factor 2; NCOA4, nuclear receptor coactivator four; PCBP, poly (RC)-binding proteins; PUFA, polyunsaturated fatty acid; ROS, reactive oxygen species; SLC3A2, solute carrier family three member 2; SLC7A11, solute carrier family seven member 11; STEAP3, six-transmembrane epithelial antigen of prostate three; VDACs, voltage-dependent anion channels.

differentiation primary response gene 88 (TLR4/Myd88)-dependent tumor necrosis factor (TNF) and receptor-interacting protein kinases (RIPK). Ferroptosis is regulated by glutathione peroxidase 4 (GPX4), which directly converts lipid hydroperoxides (L-OOH) to nontoxic lipid alcohols (L-OH) (Yang et al., 2014; Forcina and Dixon, 2019; and Stockwell et al., 2020). Later, a shred of evidence showed that p53 influences ferroptosis, it was reported and demonstrated that p53 is a key regulator of both classical ferroptosis pathways and noncanonical ferroptosis pathways, such as arachidonate 12-lipoxygenase (ALOX12) and iPLA2 $\beta$ . (Jiang et al., 2015a; Liu and Gu, 2021; Liu and Gu, 2022). Besides, ferroptosis is manipulated by several signaling pathways, such as p62-kelch-like ECH-associated protein (Keap1)-nuclear factor erythroid 2-related factor 2 (Nrf2)/heme oxygenase-1 (HO-1) (Sun et al., 2016; Dodson et al., 2019) and acyl-CoA synthetase long-chain family member 4 (ACSL4) (Doll et al., 2017). In addition, ferroptosis can be prevented by iron chelation or by the use of a lipophilic antioxidant but not by inhibitors of other forms of cell death. Aberrant regulation of ferroptosis has been implicated in disease pathogenesis in the heart, kidney, brain, liver, and lung (Zheng and Conrad, 2020). The

contributions of ferroptosis to the pathologic process of multiple lung diseases have been recognized. In addition, many interventions, including ferroptosis inducers and inhibitors, iron chelators, lipid peroxidation inhibitors, and antioxidants, have been introduced into ferroptosis-related lung diseases (Table 1). In this review, we will summarize the recent understanding of ferroptosis in lung diseases and provide a new angle for future research on the pathologic process and clinical treatment of lung diseases (Figure 2).

## Chronic Obstructive Pulmonary Disease

At present, chronic obstructive pulmonary disease (COPD) is the fourth leading cause of morbidity and mortality worldwide and is still increasing (Barnes et al., 2015; Barnes et al., 2019). It is characterized by chronic airway inflammation, lung destruction, and remodeling, resulting in irreversible airflow obstruction. Cigarette smoke (CS) exposure is the main risk factor for COPD due to its high concentration of ROS. The consequent cellular oxidative stress provokes inflammation, cell senescence, and death. Early studies have demonstrated that accumulated iron and ferritin and increased serum ferritin and nonheme iron were observed in lung epithelial cells and alveolar macrophages during exposure to CS (Wesselius et al., 1994; Ghio et al., 2008a).



**TABLE 1 |** Reagents and mechanisms of ferroptosis in lung diseases.

Disease	Reagent	Proposed mechanism	References
COPD	Deferoxamine	Chelate iron and block iron-dependent lipid peroxidation	Ghio et al. (2008a); Yoshida et al. (2019); Tang et al. (2021a)
	Ferrostatin-1	Inhibit lipid peroxidation	Yoshida et al. (2019); Tang et al. (2021a); Lian et al. (2021)
	NAC	Recover intracellular cysteine	Tang et al. (2021a) Liu et al. (2022a)
	Curcumin	Activate GPX4; Upregulate SLC7A11	
	Dihydroquercetin	Regulate NRF2	
Asthma	Deferoxamine	Chelate iron and block iron-dependent lipid peroxidation	Wenzel et al. (2017)
	Ferrostatin-1	Inhibit lipid peroxidation	Wenzel et al. (2017); Yang and Shang, (2022)
	3-methyladenine	Upregulate system Xc-; Activate GPX4	Yang and Shang, (2022)
	Acupuncture	Downregulate SLC3A2 and ATP1A3	Tang et al. (2021c)
	Erastin	Block cysteine import, inducing GSH depletion and GPX4 inactivation	Wu et al. (2020)
	RSL3	Covalently inhibit GPX4, causing accumulation of lipid peroxidation	Wu et al. (2020)
	Artesunate	Activate ferritinophagy to increase iron abundance	Wu et al. (2020)
Cystic fibrosis	Deferoxamine	Chelate iron and block iron-dependent lipid peroxidation	Maniam et al. (2021)
	Ferrostatin-1	Inhibit lipid peroxidation	Maniam et al. (2021)
Pulmonary fibrosis	Deferoxamine	Chelate iron and block iron-dependent lipid peroxidation	(Cheng et al., 2021; Takahashi et al., 2021)
	Lipoxstatin-1	Inhibit lipid peroxidation	He et al. (2021)
	Phytic acid	Chelate iron and block iron-dependent lipid peroxidation	
Ischemia–Reperfusion Injury	Lipoxstatin-1	Inhibit lipid peroxidation	Xu et al. (2020)
	Rosiglitazone	Inhibition of ACSL4	Xu et al. (2020)
	Irisin	Regulate Nrf2/HO-1 axis; activates GPX4; inhibition of ACSL4	Wang et al. (2022a)
	Lidocaine	Regulate the p38/MAPK; increase FTH1 and GPX4; decrease Tf	Ma et al. (2022)
	Deferoxamine	Chelate iron and block iron-dependent lipid peroxidation	Lui et al. (2013)
	Pirfenidone	Chelate iron and block iron-dependent lipid peroxidation	Liu et al. (2005)
Pulmonary hypertension	Ferrostatin-1	Inhibit lipid peroxidation	Xie et al. (2022)
	Deferoxamine	Chelate iron and block iron-dependent lipid peroxidation	Jasenosky et al. (2015)
Infection: <i>P. aeruginosa</i>	Ferrostatin-1	Inhibit lipid peroxidation	Ousingsawat et al. (2021)
	Baicalin	Suppress peroxidation of polyunsaturated fatty acids	Dar et al. (2022)
	CoQ10	Inhibit lipid peroxidation	Ousingsawat et al. (2021)
	Idebenone	Inhibit lipid peroxidation	Ousingsawat et al. (2021)
Pulmonary tuberculosis	Ferrostatin-1	Inhibit lipid peroxidation	Amaral et al. (2019)
	Glutathione	Recover intracellular cysteine	Pan et al. (2020)
	Vitamin E	Inhibit lipid peroxidation	Seyedrezazadeh et al. (2008)
Infection: Gram-negative bacteria	Lipoxstatin-1	Inhibit lipid peroxidation	Klobucar et al. (2021)
COVID-19	Vitamin C	Inhibit lipid peroxidation	Chavarria et al. (2021)
	Vitamin E	Inhibit lipid peroxidation	Chavarria et al. (2021)
	NAC	Recover intracellular cysteine	Jaiswal et al. (2020); Chavarria et al. (2021)
	Melatonin	Chelate iron and block iron-dependent lipid peroxidation	Chavarria et al. (2021)
	Deferoxamine	Chelate iron; inhibit viral replication; immunomodulation; downregulate hepcidin I	Dalamaga et al. (2020)
	Deferiprone	Chelate iron; inhibit viral replication; immunomodulation	Dalamaga et al. (2020)
	Deferasirox	Chelate iron; inhibit viral replication; immunomodulation	Dalamaga et al. (2020)
	Lactoferrin	Bind iron and inhibit viral replication	Carota et al. (2021)
	Methemoglobin reductase	Chelate iron and	Muhoberac, (2020)
	Glutathione	Recover intracellular cysteine	Silvagno et al. (2020)
Infection: Zygomycetes	Melatonin	Chelate iron; inhibit microbial activity	Sen, (2021)
	Deferoxamine	Chelate iron and block iron-dependent lipid peroxidation	Kontoghiorghe et al. (2010); Álvarez et al. (2013)

(Continued on following page)

**TABLE 1 |** (Continued) Reagents and mechanisms of ferroptosis in lung diseases.

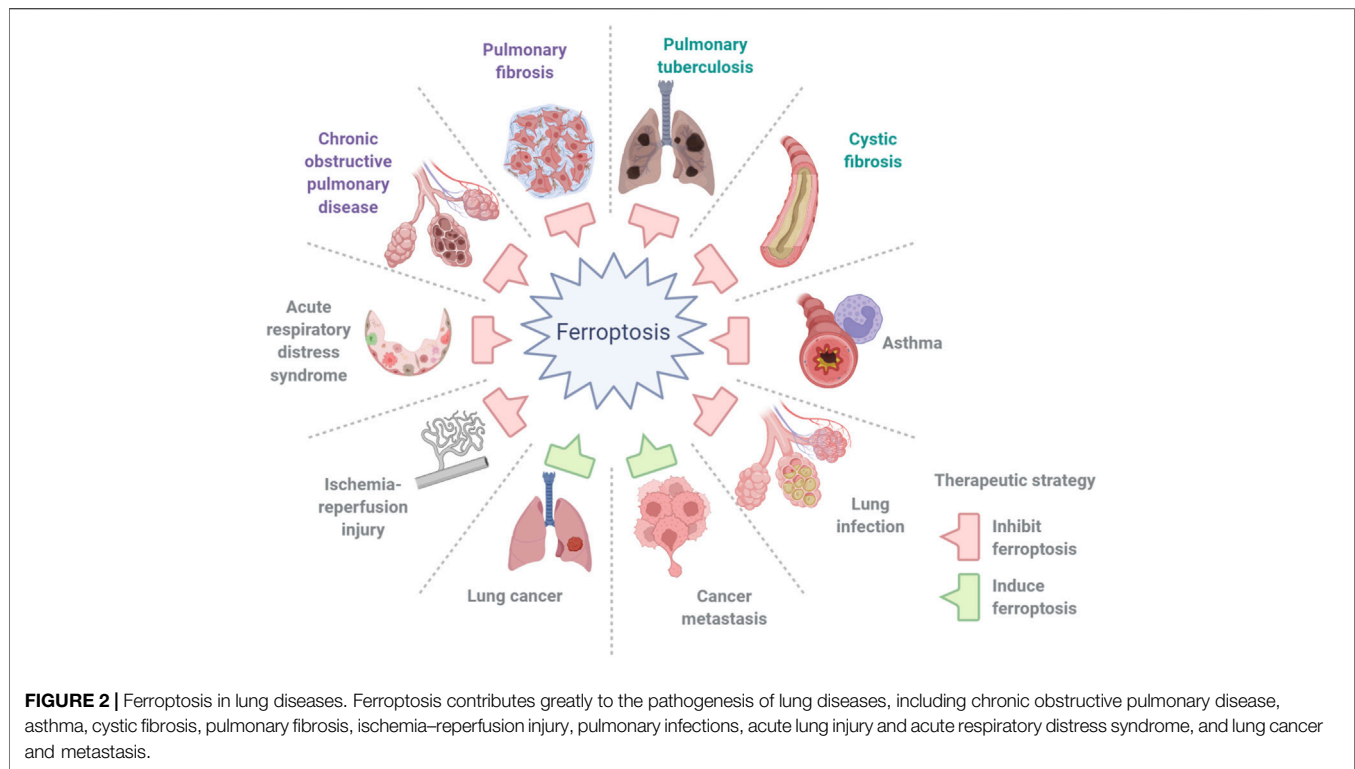
Disease	Reagent	Proposed mechanism	References
	Deferiprone	Chelate iron; inhibit microbial activity with better tissue penetration capacity	Kontoghiorghe et al. (2010); Álvarez et al. (2013)
	Deferirox	Chelate iron; inhibit microbial activity	Kontoghiorghe et al. (2010); Álvarez et al. (2013)
Infection: <i>A. Fumigatus</i>	Deferoxamine	Chelate iron and block iron-dependent lipid peroxidation	Hsu et al. (2018)
	Deferiprone	Chelate iron and block iron-dependent lipid peroxidation	Hsu et al. (2018)
	Deferirox	Chelate iron and block iron-dependent lipid peroxidation	Hsu et al. (2018)
Acute lung injury/acute respiratory distress syndrome	iASPP	Regulate p53 and NRF2	Li et al. (2020a)
	Ferrostatin-1	Inhibit lipid peroxidation	Liu et al. (2020)
	Liproxstatin-1	Inhibit lipid peroxidation	Li et al. (2020a)
	Panaxadiol	Regulate KEAP1/NRF2/HO-1 axis; activates GSH and GPX4	Li et al. (2021b)
	4-octyl itaconate	Regulate NRF2/HO-1 axis; activates GSH and GPX4	He et al. (2022b)
	Obacunone	Regulate NRF2/HO-1 axis; activates GSH and GPX4	Li et al. (2022)
	Puerarin	Activate SLC7A11, GPX4, and FTH1; inhibit NOX1 to reduce lipid ROS generation	Xu et al. (2021a)
	Acupuncture	Activate SLC7A11, GPX4, and FTH1	Zhang et al. (2022)
Lung cancer/metastasis	Erastin	Block cysteine import, inducing GSH depletion and GPX4 inactivation	Huang et al. (2018); Pan et al. (2019)
	RSL3	Covalently inhibit GPX4, causing accumulation of lipid peroxidation	Zhang et al. (2020b); Liu et al. (2021b)
	Cisplatin	Block cysteine import, inducing GSH depletion and GPX4 inactivation	Guo et al. (2018)
	PRLX9336	Regulate NRF2/HO-1 axis; GSH depletion and GPX4 inactivation	Liang et al. (2021)
	Imidazole ketone erastin	Block cysteine import, inducing GSH depletion and GPX4 inactivation	Ye et al. (2020)
	Sorafenib	Block cysteine import, inducing GSH depletion and GPX4 inactivation	Li et al. (2020b)
	Levobupivacaine	Increases iron abundance and mediate iron-dependent lipid peroxidation	Meng et al. (2021)
	BEBT-908	Regulate p53 and STAT1	Fan et al. (2021)
	iFSP1	Inhibit FSP1–CoQ10–NAD(P)H system	Doll et al. (2019)
	Eriatin	Induce GSH depletion and mediate iron-dependent lipid peroxidation	Chen et al. (2020b)
	Sanguinarine	Inhibit GSH and GPX4	Xu et al. (2022)
	Dihydroisotanshinone I	Inhibit GSH and GPX4	Wu et al. (2021)

Mitochondrial dysfunction and endoplasmic reticulum stress are usually observed in the cytoplasm, and ferroptosis occurs in bronchial epithelial cells (Park et al., 2019). The increased ferritinophagy mediated by nuclear receptor coactivator 4 (NCOA4) and reduction of glutathione peroxidase 4 (GPX4) led to the accumulation of free iron and lipid peroxidation during CS exposure. Moreover, GPX4<sup>+/-</sup> mice showed significantly higher degrees of lipid peroxidation and an enhanced COPD phenotype than wild-type mice, whereas these phenotypes could be attenuated in GPX-transgenic mice (Dowdle et al., 2014; Yoshida et al., 2019). PM2.5 is another risk factor for COPD. Increased cellular iron content and ROS production in human endothelial cells were observed after inhaling PM2.5 particles, while the levels of glutathione (GSH) and nicotinamide adenine dinucleotide phosphate (NADPH) decreased. Iron overload and redox imbalance caused by TFRC and ferritin dysregulation are the major inducers of ferroptosis (Wang and Tang, 2019). The abovementioned investigations indicated that ferroptosis is involved and plays a crucial damaging role in COPD

(Mizumura and Gon, 2021), and searching for an accurate inhibitor of ferroptosis to delay the progression and prevent the occurrence of COPD is pivotal to the forthcoming research. Experimental interventions, such as the iron chelator deferoxamine, the ferroptosis inhibitor ferrostatin-1, and suppression of lipid peroxidation by GPX4, could effectively reduce lipid peroxidation, upregulate GSH and NADPH levels, and inhibit ferroptosis (Ghio et al., 2008a; Yoshida et al., 2019; Tang et al., 2021a; and Lian et al., 2021). Moreover, recent reports revealed that antioxidants, such as N-acetyl-L-cysteine (NAC) and curcumin, could improve the reduction of GSH and reduce lipid peroxidation (Tang et al., 2021a), while dihydroquercetin could inhibit ferroptosis in lung epithelial cells by activating the Nrf2-mediated pathway (Liu et al., 2022a).

## Asthma

Asthma is a chronic inflammatory respiratory disorder that results in intermittent episodes of wheezing, breathlessness, chest stuffiness, and cough. The distinguishing features of the



disease are sporadic and reversible airway obstruction, chronic bronchial inflammation, bronchial smooth muscle cell hypertrophy and hyperreactivity, and increased mucus secretion (Papi et al., 2018). The function of type-2 helper T (Th2) cells is critical to the pathologic process of asthma. Upon activation, Th2 cells produce cytokines and active mediators, such as interleukin-4 (IL-4), which stimulate IgE secretion by B cells, IL-5 triggers eosinophils, and IL-13 arouses mucus and IgE production. Meanwhile, mast cells, macrophages, neutrophils, and T cells are activated and gather in the airways and secrete inflammatory mediators, resulting in chronic airway inflammation (Hammad and Lambrecht, 2021). Continuous studies have demonstrated that airway epithelial cells from asthmatic patients actively produced 15-lipoxygenase-1 (15-LOX1) and 15-hydroxyeicosatetraenoic acid (15-HETE). The reports demonstrated that 15LOX1-phosphatidylethanolamine-binding protein 1 (PEBP1) complex activation consistently stimulates IL-13/IL-4-mediated Th2 inflammation, including mucin 5AC (MUC5AC), periostin (POSTN), and chemokine (C-C motif) ligand 26 (CCL26). 15-LOX1-PEBP1 can activate autophagy and ferroptosis. Besides, there was a positive correlation between the colocalization of 15LOX1/PEBP1 puncta in freshly brushed airway epithelial cells and the fraction of exhaled nitric oxide (FeNO) in asthmatic patients. The ferroptosis inducer Ras-selective lethal small molecule 3 (RSL3) significantly promotes the occurrence of lipid peroxidation and ferroptosis in IL-13-treated human airway epithelial cells (Zhao et al., 2009; Zhao et al., 2011; Wenzel et al., 2017; Zhao et al., 2020a; Nagasaki et al., 2022). In an

experimental model of house dust mite-induced asthma, an association between elevated lung iron levels in airway tissue, increased ROS and lipid peroxidation and decreased GSH levels in the lungs was observed (Tang et al., 2021b), suggesting the involvement of ferroptosis in the pathogenesis of allergic asthma. These results reveal the correlation between ferroptosis and the pathobiologic pathway of asthma and the possibility of targeted inhibition of ferroptosis. Ferrostatin-1 and deferoxamine are introduced to reduce sensitivity to ferroptosis (Wenzel et al., 2017; Yang and Shang, 2022); otherwise, the 15LOX1/PEBP1 pathway is under investigation as a novel asthma therapeutic target to regulate the ferroptotic cell death (Zhao et al., 2011). On the other hand, 3-methyladenine was proven to ameliorate ferroptosis in an ovalbumin (OVA)-induced asthma model by suppressing the production of ROS and inflammatory cytokines, while upregulating superoxide dismutase (SOD) (Yang and Shang, 2022). In addition, acupuncture was reported to be effective in treating asthma by reducing solute carrier family 3 member 2 (SLC3A2) and ATPase Na<sup>+</sup>/K<sup>+</sup> transporting subunit alpha 3 (ATP1A3) expression, oxidative stress, and inflammatory cytokine levels and was recently connected with the manipulation of ferroptosis (Tang et al., 2021c).

Eosinophils are vital in allergic disorders, such as asthma, and prompting eosinophil death, which effectively weakens inflammation (Hammad and Lambrecht, 2021). The increased number and prolonged survival time of eosinophils in asthma suggest the selected targeting of ferroptosis as a promising therapeutic strategy for airway inflammation. Ferroptosis-inducing agents, namely, erastin, RSL3, and artesunate (ART),

were proven to induce eosinophil ferroptosis and collaborate with dexamethasone to promote eosinophil death. Targeted administration of eosinophil ferroptosis appeared to relieve allergic airway inflammation and might cut the dosage and reduce the side effects of glucocorticoids in an OVA-induced asthma model (Wu et al., 2020). The concept of inducing ferroptosis of specific immune cells to diminish airway inflammation and alleviate mediator production is promising but needs to be investigated for its clinical potential in future studies of asthma.

## Cystic Fibrosis

Cystic fibrosis (CF) is an autosomal recessive genetic disease that causes dysfunction of ion transport in the exocrine glands (Ratjen and Döring, 2003). It is the most common fatal genetic disorder among white populations. The disease is due to defects in the cystic fibrosis transmembrane conductance regulator (CFTR) gene, resulting in abnormalities in chloride transport in epithelial transport affecting fluid secretion in exocrine glands and respiratory, gastrointestinal, and reproductive tracts. Recurrent respiratory infection and pancreatic dysfunction are the two most important clinical symptoms (Prentice et al., 2021). In patients with CF, the excretion of chloride ions in the airway is reduced and the resorption of sodium and water is increased, which results in dehydration of mucous layer coating epithelial cells, loss of mucociliary function, mucus blockage, and mucous plugging. A recent report demonstrated that CF airway epithelial cells exposed to ferric ammonium citrate (FAC) and the ferroptosis inducer erastin are susceptible to ferroptosis compared to isogenic CFTR-corrected airway epithelial cells *in vitro* (Maniam et al., 2021). Ferrostatin-1 and deferoxamine are able to inhibit ferroptosis by alleviating iron accumulation and lipid peroxidation and thus, may be potential therapeutic interventions for CF. On the other hand, patients with CF commonly develop respiratory infections caused by *Pseudomonas aeruginosa*, *Staphylococcus aureus*, *Hemophilus influenzae*, and *Burkholderia cepacia*. Among these, *P. aeruginosa* is an important opportunistic pathogen responsible for the ferroptotic cell death in airways, as discussed later in the section on pulmonary infections.

## Obstructive Sleep Apnea

Obstructive sleep apnea (OSA) is a respiratory disease characterized by an intermittent nocturnal decrease in oxygenated hemoglobin and sleep interruption (Patel et al., 2019). The main feature of OSA is chronic intermittent hypoxia (CIH) from the view of pathophysiology. Cardiovascular diseases, liver diseases, and metabolic diseases are the major health risks to OSA patients. Although there is no report of ferroptosis caused by hypoxia-reperfusion in lung diseases, oxidative stress, and lipid peroxidation have been reported to induce liver injury in OSA (Chen et al., 2020a; Chen et al., 2021a). Both reports revealed that ferroptosis mediated liver injury induced by CIH in rodent models, as evidenced by the increase in lipid peroxidation, the decrease in GPX4 expression, and the increase in ACSL4 expression.

## Pulmonary Fibrosis

Idiopathic pulmonary fibrosis (IPF) refers to a refractory and irreversible progressive pulmonary fibrotic disorder without clear etiology. The characteristic feature of IPF is patchy but progressive bilateral interstitial fibrosis, leading to severe hypoxemia and cyanosis in advanced cases (Lederer et al., 2018). Recurrent epithelial activation and injury is the leading cause of IPF occurrence. Epithelial repair deficiency and inflammation at damage sites give rise to the vigorous proliferation of fibroblasts and myofibroblasts, resulting in typical fibroblastic foci. Ferroptosis-related genes, which includes neuroblastoma RAS viral (v-ras) oncogene homolog (NRAS) and MUC1, but not limited to them, were elevated in bronchoalveolar lavage fluid and cells in IPF patients, which suggests the participation of ferroptosis in the disease and may be used for prognostic prediction of IPF (Li et al., 2021a; He et al., 2021; He et al., 2022a).

Pulmonary fibrosis (PF) is an interstitial lung disease that derives from long-term inhalation of CS and dust, such as asbestos, silica, and coal, the use of drugs, such as bleomycin and amiodarone, accidental exposure to paraquat, or lung injury are caused by radiation therapy. A previous study showed that erastin promoted transforming growth factor  $\beta$ 1 (TGF- $\beta$ 1)-induced fibroblast-to-myofibroblast differentiation by promoting ROS and lipid peroxidation and hindering GPX4 expression, resulting in collagen accumulation and destruction of the alveolar structure, while ferrostatin-1 may inhibit this process (Gong et al., 2019). A recent report demonstrated that the upregulated long noncoding RNA (lncRNA) zinc finger antisense 1 (ZFAS1) is positively correlated with SLC38A1 expression in bleomycin-induced PF rat lung tissue and in TGF- $\beta$ 1-induced human fetal lung fibroblast cells. Experiments have shown that inhibition by knockdown or silencing of the lncRNA ZFAS1 can significantly attenuate lipid peroxidation and inflammation, thus, inhibiting ferroptosis and progression of PF induced by bleomycin (Yang et al., 2020). Another study demonstrated that SET domain bifurcated 1 (SETDB1) and H3K9me3 expression was downregulated in a bleomycin-induced PF rat model, leading to the induction of epithelial-mesenchymal transition and increased lipid ROS, ferrous ions, and ferroptosis (Liu et al., 2022b). On the other hand, inducing ferroptosis by erastin could elicit iron accumulation, ROS production, epithelial-mesenchymal transition, and autophagy in lung epithelial cell lines, as evidenced by upregulated microtubule-associated protein 1A/1B-light chain 3 (MAP1LC3) and Beclin 1 (BECN1) (Han et al., 2021; Sun et al., 2021). Links between pulmonary fibrosis and ferroptosis are complicated and still under investigation. Experimental interventions, such as deferoxamine, effectively reduced iron accumulation and lipid peroxidation, thus, inhibiting ferroptosis in a bleomycin-induced PF cell and mouse model (Cheng et al., 2021; Takahashi et al., 2021).

Asbestos is a silicate mineral containing iron, magnesium, and calcium with a core of SiO<sub>2</sub>. It has been established that asbestos fibers tend to accumulate near the mesothelial cell layer, where they produce ROS, leading to DNA damage and potential carcinogenic mutations. Workers exposed to asbestos can



develop lung cancer and malignant mesothelioma. Iron homeostasis is changed among patients with asbestosis, as evidenced by the accumulation of iron, ferritin, divalent metal transporter 1 (DMT1), and ferroportin 1 (FPN1) in the lung autopsy. Iron chelators, including deferoxamine and phytic acid, were utilized in asbestos- and silica-induced PF animal models, which shows that procollagen and inflammation could partly reversed, whereas glutathione had no effect.

Paraquat (PQ) is an economic and effective herbicide that could cause multiple organ acute injury, lung fibrosis, multiple organ failure, and death due to unintentional or intentional inhalation, ingestion, and percutaneous absorption. Evidence of the connection between PQ poisoning and ferroptosis is emerging, confirmed by the formation of high-energy oxygen free radicals and lipid peroxidation (Rashidipour et al., 2020). The hypothesis that ferroptosis inhibitors might be introduced in PQ-induced PF was raised and needs to be confirmed.

Radiation-induced lung fibrosis (RILF) is a life-threatening complication after radiotherapy of chest tumors. Collagen deposition, decreased GPX4 expression, and increased ROS were observed in the mouse model, indicating that ferroptosis was involved when exposed to radiation. The ferroptosis inhibitor liproxstatin-1 alleviated RILF by activating the Nrf2 pathway in this experimental study (Li et al., 2019). Therefore, strategies for regulating iron metabolism and controlling ferroptosis can be exploited to delay the progression of PF in future experimental and clinical practice.

## Lung Ischemia-Reperfusion Injury

An ischemia injury arises at the initial stage of vascular compromise, however, airway epithelial cells are relatively resistant to transient hypoxia. Reperfusion injury is caused by recovery of blood flow and is related to overwhelming damage. Multiple organ failure might arise in serious cases. Although the underlying mechanisms of reperfusion injury are not fully understood, they involve the production of free radicals, neutrophil infiltration, and the secretion of inflammatory mediators, namely, cytokines, chemokines, and complements. Clinical disorders associated with the development of ischemia-reperfusion include pulmonary thromboembolism and thrombolysis, lung resection and trauma, lung transplantation, and other operations. Increased iron content and lipid peroxidation accumulation, together with decreased GPX4 and elevated ACSL4 expression, were detected in ischemia-reperfusion lungs. Treatment with liproxstatin-1 to inhibit ferroptosis, administration of the ACSL4 inhibitor rosiglitazone before ischemia, and ACSL4 knockdown ameliorated lung ischemia-reperfusion injury by protecting against ferroptotic damage in animal and cell models (Xu et al., 2020). Irisin, a novel muscle-derived myokine, was reported to suppress ferroptosis in lung ischemia-reperfusion damage *in vitro* and *vivo*, as confirmed by lower ROS, malondialdehyde (MDA), and iron accumulation, along with alterations in GPX4 and ACSL4 (Wang et al., 2022a). Lidocaine attenuated inflammation, apoptosis, and ferroptosis in a lung epithelial cell line by controlling the p38/mitogen-activated protein kinase (MAPK) pathway (Ma et al., 2022).

Furthermore, there were elevated iron concentrations in alveolar fluid and tissue in human lung allografts (Baz et al., 1997), which could increase the risk of lung allografts to iron radicals, ROS, fibrosis, and chronic rejection. An early study demonstrated that HO-1 expression was elevated in human lung allografts with acute cellular rejection and obliterative bronchiolitis (Lu et al., 2002). Recipient iron overload and hyperferritinemia were also associated with poor prognosis after lung transplantation (Pugh et al., 2005). Administrations for optimizing iron homeostasis before and after lung transplantation were considered. Different iron chelators, namely, deferoxamine, were used in lung preservation and alleviated oxidative stress after transplantation (Lui et al., 2013). Pirfenidone significantly reduced the deposition of iron, increased the expression of HO-1, and alleviated fibrosis and collagen deposits (Liu et al., 2005), demonstrating anti-ferroptosis, anti-fibrotic and antioxidative properties in preventing chronic airway rejection in a rat model.

Targeted inhibition of ferroptosis may be a potential way to protect against ischemia-reperfusion injury. By reducing the oxidative stress response, the cell damage caused by ferroptosis can be avoided to reduce the occurrence of complications.

## Pulmonary Hypertension

Pulmonary hypertension (PH) is usually secondary to a decrease in vessel diameter or an increase in blood flow in the pulmonary vascular bed (Vonk Noordegraaf et al., 2016). Less commonly, PH caused by unknown causes is called primary or idiopathic PH. At present, the dysfunction of pulmonary endothelial and/or vascular smooth muscle cells is considered to be the potential basis for most forms of PH. The proliferation of endothelial and smooth muscle cells leads to thickening of the intima and media with narrowing of the lumina in the entire pulmonary arterial tree. Dysregulated iron homeostasis in the pathological mechanism of PH is not clear and fully recognized. Investigations have established that pulmonary vascular function could be affected by intracellular iron deficiency in pulmonary artery smooth muscle cells (Rhodes et al., 2011), and rats fed on an iron-deficient diet showed substantial pulmonary vascular remodeling and muscularization, medial hypertrophy, perivascular inflammatory cell infiltration strongly associated with rising pulmonary artery pressure (PAH), and right ventricular hypertrophy (Cotroneo et al., 2015), which suggests that iron metabolism participates in the homeostasis of the pulmonary vasculature and that abnormal iron metabolism takes part in the occurrence and development of PH. In contrast, iron deposition was noted in lung tissue sections and was highly correlated with advanced PH in IPF patients (Kim et al., 2010). Moreover, the administration of the iron chelator deferoxamine prevented pulmonary vascular remodeling in chronic hypoxia-induced PH rats (Wong et al., 2012). Whether iron deficiency or overload leads to PH or is merely a consequence is still under debate. Recently, bioinformatic analyses of unregulated ferroptosis-associated genes were performed, and the targets and potential drugs were predicted. However, there were contradictions between the dysregulation and function of some key genes, such as SLC7A11, in these

studies (Zhang et al., 2021; Zou et al., 2021). In another recent study, ferroptosis of pulmonary artery endothelial cells (PAECs) was reported to play a critical role in the progression of PH in a monocrotaline-induced model, proven by increased lipid peroxidation, cellular iron concentrations, mitochondrial damage, abnormal expression of GXP4, ferritin heavy chain 1 (FTH1), and NADPH oxidase 4 (NOX4), followed by activation of inflammatory factors and pulmonary artery remodeling. Ferroptosis suppression by ferrostatin-1 postponed lung vascular remodeling and protected right ventricle function in PH (Xie et al., 2022). Based on these findings, a thorough understanding of ferroptosis in PH is needed, and treating PH with medicines based on ferroptosis regulation might be promising in the future.

## Pulmonary Infections

Deaths from pulmonary infections in the form of pneumonia are not rare worldwide. The epithelial surfaces of the lung are consistently exposed to open air containing microbial contaminants, and other common lung diseases and unhealthy lifestyles, such as smoke and alcohol use, render the lung parenchyma vulnerable to virulent organisms.

Although previously discussed, *P. aeruginosa* is associated with infections in CF patients, and it is most commonly seen in the hospital environment. Based on reports, *P. aeruginosa* can express lipoxygenase (pLoxA) after infection, oxidize host arachidonoyl-phosphatidylethanolamine (ETE-PE) to pro-ferroptotic 15-hydroperoxy-arachidonoyl-PE (15-HpETE-PE), and cause ferroptosis of human bronchial epithelial cells (Dar et al., 2018). In addition, *P. aeruginosa* can degrade the host GPX4 defense by stimulating lysosomal chaperone-mediated autophagy (CMA) (Dar et al., 2021). Baicalein inhibits LOX-mediated ferroptotic pathways, which may be a possible target for the treatment of respiratory infections (Dar et al., 2022). In another study, knockdown of anoctamin 1 (ANO1 or TMEM16A), antioxidants, such as coenzyme Q10 (CoQ10) and idebenone, and ferrostatin-1 attenuated *Pseudomonas aeruginosa*-induced cell death in CF bronchial epithelial cells (Ousingsawat et al., 2021).

Pulmonary tuberculosis (TB) is the major infectious disease within the spectrum of chronic pneumonia that seriously endangers human health. The World Health Organization (WHO) estimates that TB causes 6% of the world's deaths and is now deteriorating the condition more worldwide. Immunity to tuberculosis infection is mainly driven by Th1 cells, which trigger macrophages to kill bacteria (Jasenosky et al., 2015). Re-exposure to *Mycobacterium tuberculosis* (Mtb) or reactivation of the infection in a previously sensitized host stimulates a swift defensive reaction, but hypersensitivity also increases tissue necrosis and tissue destruction. Mtb-induced macrophage death was related to a decrease in GSH and GPX4 levels and an increase in free iron, mitochondrial superoxide, and lipid peroxidation, which indicates that ferroptosis was involved in tissue necrosis in Mtb infection (Amaral et al., 2019). Mtb also increased the expression of HO-1, which may in turn facilitate Mtb survival and growth as a consequence of increased iron availability (Yang et al., 2022). The destruction of macrophages

by Mtb and bacterial load were reduced after ferrostatin-1 treatment (Amaral et al., 2019). The primary anti-tuberculosis drugs isoniazid (INH) and rifampicin (LFP) usually exhaust GSH and cause lipid peroxidation and ferroptosis of hepatocytes during liver metabolism. GSH replenishment prevented injury, while iron supplementation augmented the ferroptosis process (Pan et al., 2020). Vitamin E (vit E) was used to intervene in tuberculosis patients in clinical trials. The results showed that MDA levels were reduced, and the plasma total antioxidants were improved in tuberculosis patients after 2 months of administration (Seyedrezazadeh et al., 2008). This can be explained by the fact that vit E can reduce nonheme iron from ferric iron to ferrous iron to inhibit 15-LOX1 (Hinman et al., 2018), therefore, preventing the ferroptosis pathway regulated by 15-LOX1 (Kagan et al., 2017).

Ferroptosis inhibitors were also investigated for the treatment of resistant pathogens, such as lipoxstatin-1, which was proven to interact with lipopolysaccharide in the outer leaflet to disrupt the integrity of the outer membrane of Gram-negative bacteria and potentially serve as an outer membrane permeabilizing compound (Klobucar et al., 2021).

The coronavirus disease 2019 (COVID-19) outbreak caused by severe acute respiratory syndrome coronavirus 2 (SARS-CoV-2) is an ongoing global health emergency, and the pathologic process of the virus has not been completely elucidated. The clinical symptoms are mostly cough, fever, chest distress, muscle aches, fatigue, dyspnea, and headache (Huang et al., 2020a; Wang et al., 2020). Conditions including acute respiratory distress syndrome (ARDS), septic shock, severe metabolic acidosis, and a hypercoagulable state are life-threatening in severe cases with COVID-19, and respiratory failure is the most common cause of death. The pathological lesions include hemoglobinopathy, hypoxia, and hyperferritinemia (Zhao et al., 2020b; Cavezzi et al., 2020; and Colafrancesco et al., 2020). Cellular iron overload is believed to play a pivotal role in COVID-19 infection. Elevated serum ferritin can further aggravate systematic inflammation, which is closely related to poor prognosis (Huang et al., 2020b; Edeas et al., 2020; and Zhou et al., 2020). Considering that the expression of transferrin and the risk of severe cases in male patients were higher than those in female patients and increased with age, this relationship could explain the higher infection rate and mortality in elderly male COVID-19 patients. Transferrin could deliver iron to cells by binding the transferrin receptor and mediating endocytosis. The higher levels of the soluble transferrin receptor in COVID-19 patients confirmed this possibility (Duca et al., 2021). It remains unclear whether hyperferritinemia is a systemic marker or a key modulator in the pathogenesis of COVID-19. Iron is engaged in several biological processes involving DNA, RNA, and ATP synthesis. There is evidence that the replication of SARS-CoV-2 depends on iron-containing enzymes. Regulating host iron metabolism can play an antiviral role and prolong cell survival. Iron is also responsible for SARS-CoV-2 replication, which include key steps, such as ATP hydrolysis (Jia et al., 2019). Moreover, SOD and lipid peroxidation levels were significantly elevated in COVID-19 patients, while GSH and GPX4 levels were decreased (Silvagno et al., 2020). Changes in iron metabolism,

GSH depletion, GPX4 inactivation, and upregulation of lipid peroxidation may lead to the hypothesis that ferroptosis may be triggered after SARS-CoV-2 infection, which results in damage to multiple organs. Early treatments with the antioxidants vitamin C (Vit C), vitamin E (Vit E), N-acetylcysteine (NAC) and melatonin (MT) with pentoxifylline were reported to scavenge ROS, supply GSH, and delay the aggression and death of COVID-19 (Jaiswal et al., 2020; Chavarria et al., 2021). Iron chelators, such as deferiprone, deferasirox, deferoxamine exhibited iron chelating, antiviral, and immunomodulatory effects *in vitro* and *in vivo*. Critically ill patients can benefit from orally given deferasirox or intravenously given deferoxamine. Several mechanisms are involved in this process: a. inhibiting viral replication; b. reducing iron availability; c. upregulating B cells; d. increasing neutralizing antibody titer; e. inhibiting endothelial cell inflammation; and f. preventing lung fibrosis and pulmonary recession by reducing pulmonary iron accumulation (Cavezzi et al., 2020; Dalamaga et al., 2020). However, there have been debates on the use of deferoxamine or hepcidin antagonists, whereas it was declared that deferoxamine could also downregulate the expression of hepcidin I (Abobaker, 2021; Garrick and Ghio, 2021). Lactoferrin is a naturally occurring, nontoxic glycoprotein that contains more pertinence to binding iron than transferrin and has demonstrated antiviral efficacy against different kinds of viruses *in vitro*, including SARS-CoV, and might potentially serve as a preventative and adjunct treatment for COVID-19 (Carota et al., 2021). Theoretically, drugs, for instance, methemoglobin reductase, ascorbic acid (Vit C), and GSH were inferred to reduce ferric iron to ferrous iron in hemoglobin to restore its ability to combine with oxygen to alleviate the symptoms of hypoxia in COVID-19 patients (Muhoberac, 2020). In conclusion, reducing cellular iron and replenishing the level of reductants are the most basic treatment methods to lessen tissue injury in COVID-19 patients. These drugs also ought to be investigated in future clinical studies to confirm their safety and effectiveness.

Mucormycosis is caused by a fungus called Zygomycetes. It is a life-threatening opportunistic mycosis that is generally confined to immunocompromised patients, especially those with hematolymphoid malignancies or severe neutropenia, those receiving corticosteroids, or other immunosuppressive drugs, allogeneic stem cell transplant recipients, poorly controlled diabetes mellitus (DM), and those with an iron overload state. Evidence suggests that iron metabolism and fungal endothelial cell interactions play an important role in the pathogenesis of mucormycosis (Hamilos et al., 2011). In a recent report, both infected and recovered COVID-19 patients were promptly infected with mucormycetes (Pasrija and Naime, 2022). The reason might be that COVID-19 patients with elevated serum levels of available iron were susceptible to mucormycosis, and these infections are highly angioinvasive, since the pathogens could acquire iron from the host and interact with endothelial cells lining blood vessels (Pasrija and Naime, 2022). In addition, SARS-CoV-2 increased the susceptibility of patients to mucormycosis by augmenting the virulence factors of the Mucor species. Iron chelator therapy may be advantageous to treat the infection by correcting and inappropriately supplying

the fungus with iron. However, there was evidence that the new oral iron chelators deferiprone and deferasirox, better than deferoxamine, could deteriorate the growth of fungi both *in vitro* and in animal models. The iron liberated from deferoxamine was likely transported into the fungus by the high-affinity iron permease, thus, promoting infections. Deferiprone showed the highest antimicrobial activity and tissue penetration capacity, particularly access to the brain (Kontoghiorghes et al., 2010; Álvarez et al., 2013). Melatonin (MT) is an iron chelator, calmodulin blocker, and inhibitor of myeloperoxidase along with an inhibitor of ferroptosis and pyroptosis. By correcting MT deficiency, the enhancement of fungal virulence in COVID-19 patients was alleviated because MT could hinder the iron acquisition of Mucor species and prevent their morphological transformation from yeast to the virulent hyphal form (Sen, 2021).

*Aspergillus fumigatus* is the most common airborne fungal pathogen and is accountable for invasive aspergillosis in immunocompromised hosts. The acquisition of iron is important for the growth of *Aspergillus fumigatus*. This fungus synthesizes and secretes triacetylfusarinine C to capture iron and accumulates ferricrocin and hydroxyferricrocin to store iron for hyphae and conidia. Meanwhile, it decreased the expression of the iron importer DMT1 and the transferrin receptor and iron exporter FPN1 (Seifert et al., 2008). In lung transplant recipients, *Aspergillus fumigatus* infection can be life-threatening. The microhemorrhage-related iron content in the graft might be the main determining factor of invasion and virulence of infection, and progressive graft rejection was related to the increase in ferric iron concentration. Iron chelation, including deferiprone, deferasirox, and deferoxamine, maybe a potential therapy for *Aspergillus fumigatus* (Hsu et al., 2018), but the effects can be paradoxical, thus, chelators must be chosen carefully.

## Acute Lung Injury/Acute Respiratory Distress Syndrome

The pulmonary infiltrates in ALI are caused by damage to the alveolar-capillary membrane, consisting of the microvascular endothelium and the alveolar epithelium. The acute results of damage include increased vascular permeability and alveolar flooding, impaired diffusion capacity, and extensive surfactant abnormalities. ALI can progress to more severe diffuse alveolar damage and is known as ARDS in the setting of sepsis, severe trauma, or a diffuse lung infection. The clinical features are the emergence of life-threatening respiratory dysfunction, cyanosis, and hypoxemia that is refractory to oxygen therapy and rapidly progresses to multisystem organ failure. Neutrophils and their products, e.g., oxidants, proteases, platelet-activating factor, and leukotrienes, play a crucial role in the pathologic process of ARDS by causing damage to the alveolar-capillary membrane. On the other hand, the endogenous antiproteases, antioxidants, and anti-inflammatory cytokines that counteract the destruction and balance determine the degree of tissue injury and severity of clinical symptoms in ARDS. The characteristic finding in ARDS is the presence of hyaline membranes

consisting of fibrin-rich edema fluid admixed with remnants of necrotic epithelial cells, particularly lining the distended alveolar ducts.

In ALI mouse models induced by intestinal ischemia-reperfusion and oleic acid, mitochondrial shrinkage, and mitochondrial membrane rupture were noted in type II alveolar epithelial cells (AEC2). The characteristic indicators of ferroptosis, namely, iron overload, GSH depletion and MDA accumulation, and downregulated GPX4 and ferritin in lung tissue were also detected (Zhou et al., 2019; Dong et al., 2020). In a mouse model of ALI-induced by intestinal ischemia-reperfusion, Nrf2 expression can inhibit ferroptosis *via* modulation of telomerase reverse transcriptase (TERT), HO-1, and SLC7A11 levels (Dong et al., 2020; Dong et al., 2021). In another study, the overexpression of inhibitor of apoptosis stimulating protein of p53 (IASPP) and Nrf2 exhibited therapeutic effects. IASPP inhibited ferroptosis and alleviated tissue injury, depending on Nrf2/hypoxia-inducible factor 1 (HIF1) signal transduction (Li et al., 2020a). Nrf2 upregulation also alleviated GPX4 decreases and attenuated signal transducer and activator of transcription-3 (STAT3) phosphorylation (pSTAT3). STAT3 enhanced the antioxidant capacity through SLC7A11 activation, thereby attenuating the development of ferroptosis during the disease (Qiang et al., 2020). In lipopolysaccharide (LPS)-induced ALI animal models and bronchial epithelial cell lines, the levels of MDA, 4-hydroxynonenal (4-HNE), and total iron were dramatically increased, and the expression levels of SLC7A11 and GPX4 were decreased, indicating that ferroptosis was involved in LPS-induced ALI (Liu et al., 2020). Ferroptosis inhibitors, including ferrostatin-1 and liproxstatin-1, showed a protective effect in these ALI/ARDS models. In addition, Panaxadiol (PX) derived from Panax ginseng root was utilized in LPS-induced ALI/ARDS, and the results showed that PX lessened the pathological lesions in mouse lungs, inhibiting ferroptosis by upregulating the Kelch-like ECH-associated protein 1 (KEAP1)/Nrf2/HO-1 pathway (Li et al., 2021b). Similarly, 4-octyl itaconate (4-OI) and obacunone (OB) were reported to significantly alleviate lung injury, increase GSH and GPX4, and reduce malonaldehyde and lipid peroxidation by activating Nrf2 and HO-1 *in vivo* (He et al., 2022b; Li et al., 2022). Puerarin (PUE) (Xu et al., 2021a), silencing or knockdown of mixed lineage kinase 3 (MLK3) (Chen et al., 2022), lipocalin-2 (Wang et al., 2022b) and Jumonji domain-containing 3 (JMJD3) (Peng et al., 2021), and electroacupuncture (EA) (Zhang et al., 2022) presented novel targets for the treatment of LPS-induced ALI/ARDS. These studies preliminarily confirmed that ferroptosis is intricately connected to ALI/ARDS and that it can be a novel therapeutic target.

## Pulmonary Alveolar Proteinosis

Pulmonary alveolar proteinosis (PAP) is an infrequent disease characterized by the aggregation of surfactant and phospholipids in the distal airways and alveoli. The causative factors in primary PAP are still unknown, but it is postulated to be an autoimmune disorder since the emergence of antibodies to granulocyte-macrophage colony-stimulating factor (GM-CSF). Disturbance of iron homeostasis in epithelial cells and macrophages in the lung has been reported in idiopathic PAP patients. Several early reports demonstrated that the contents of iron, transferrin,

transferrin receptor, lactoferrin, and ferritin were remarkably elevated in lavage from PAP patients in comparison with healthy controls, while the concentrations of ascorbate, glutathione, and urate were remarkably lower. The cells of PAP patients accumulated significant iron and ferritin. Immunohistochemistry for the lung tissue revealed the accumulation of ferritin in the lower respiratory tract of PAP patients (Ghio et al., 2008b; Shimizu et al., 2011). This led to the hypothesis that ferroptosis might participate in the development of PAPs; however, there is neither direct evidence to prove the correlation between ferroptosis and PAPs nor intervention experiments to evaluate the effect of medicines based on ferroptosis regulation on PAPs.

## Lung Cancer

Lung cancer has the highest incidence rate and mortality rate in the world. Accumulated studies have found that ferroptosis has a close relationship with lung cancer and tumor metastasis, and lung cancer cells are in a state of ferroptosis inhibition.

a System Xc- (xCT) is a cystine/glutamate antiporter consisting of SLC3A2 and SLC7A11, which is accountable for exporting glutamate and importing cysteine. By upregulating SLC3A2 and SLC7A11, lung cancer cells could enhance their antioxidant effect, inhibit the occurrence of ferroptosis, and increase drug resistance to inducers of ferroptosis, such as imidazole ketone erastin (IKE) and cisplatin (DDP) (Huang et al., 2005; Ma et al., 2021; Tabnak et al., 2021; and Wang et al., 2021).

b The antioxidant enzymes GPXs, GPX8, and GPX4 in particular, have been identified to play an extensive and broad role in the pathological process of cancers (Zhang et al., 2020a). Overexpression of GPX4 promoted the proliferative capacity of lung cancer cells and inhibited ferroptosis, whereas RSL3 hindered GPX4 activity and limited the proliferation, migration, invasion, and angiogenesis of lung cancer cells (Zhang et al., 2020a; Tabnak et al., 2021). Besides, these antioxidants can protect metastasizing cancer cells in both circulations and the metastatic niche to resist ferroptosis (Liu et al., 2021a). Targeting the GPX4 pathway may provide a new strategy for treating lung cancer growth and metastasis.

c The tumor-suppressive activity of p53 has been proposed and proven after decades of intensive study. Mutation of p53 cannot repress SLC7A11 and promote ferroptosis (Jiang et al., 2015b). In addition, the p53 P47S polymorphism, commonly found in people of African descent, is also defective in promoting ferroptosis and repressing tumor development (Leu et al., 2019). Targeting p53 can potentially improve the efficiency of lung cancer treatment by mediating ferroptotic responses.

d Ferroptosis suppressor protein 1 (FSP1) is a ferroptosis inhibitor that is independent of the GPX4 pathway and could suppress ferroptosis *via* CoQ10 (Doll et al., 2019). FSP1 is decorated with cardamom acylation by regulating NADPH to reduce CoQ10, producing lipophilic free radicals to capture free antioxidants to prevent lipid



peroxidation to suppress ferroptosis (Doll et al., 2019). High expression of FSP1 could lead to increased resistance in lung cancer cells (Doll et al., 2019).

e MicroRNAs (miRNAs) are a class of noncoding RNAs (ncRNAs) with a length of 18–25 nucleotides that could impede protein translation by regulating their target mRNAs. Tumor suppressor miRNAs are negatively regulated in cancers and usually target oncogenic proteins. Downregulated tumor suppressor miRNAs that induce ferroptosis, such as miR-302a-3p and miR-324-3p, can promote survival and proliferation, and their overexpression sensitizes resistant cells to ferroptosis and increases the sensitivity of chemotherapeutic drugs (Deng et al., 2021; Wei et al., 2021).

f LncRNAs engage in the occurrence and development of non-small-cell lung cancers (NSCLCs) by mediating ferroptosis. LINC00472 (P53RRA) activates the p53 pathway by interacting with Ras GTPase-activating protein-binding protein 1 (G3BP1) and induces ferroptosis (Mao et al., 2018). P53RRA promotes erastin-induced growth inhibition and increases the cellular iron and lipid ROS concentrations in NSCLC cells (Mao et al., 2018). Low expression of P53RRA removed p53 and weakened ferroptosis in NSCLC (Mao et al., 2018). In addition, overexpressed LINC00336 acted as a crucial ferroptosis inhibitor in lung cancer by lowering cellular iron, lipid peroxidation, and mitochondrial superoxide through ELAV-like RNA-binding protein 1 (ELAVL1) interactivity, a novel regulator of ferroptosis (Wang et al., 2019). LINC00336 also served as an endogenous sponge of MIR6852 as a circulating extracellular DNA (ceRNA) to increase cystathionine- $\beta$  synthase (CBS) expression and inhibit ferroptosis in lung cancer (Wang et al., 2019). Overexpression of LINC00336 limited RSL3-induced ferroptosis in lung adenocarcinoma cells.

These studies established that resistance to ferroptosis was enhanced from multiple aspects in lung cancer and metastasis. The first thing that comes to mind is that the promising ferroptosis inducers erastin and RSL3 can inhibit the biological process of System Xc- and GPXs (Huang et al., 2018; Pan et al., 2019; Zhang et al., 2020b; Liu et al., 2021b). Other signaling pathways can be involved in these ferroptosis inducers. For example, erastin can activate the p53 signaling pathway, subsequently inhibiting the expression of SCL7A11 posttranscriptionally and subsequently inducing ferroptosis (Huang et al., 2018). DDP, a classical chemotherapeutic drug, was recently proven to trigger ferroptosis in NSCLC by inhibiting the activity of the GSH-GPX system and promoting the therapeutic effect together with erastin (Guo et al., 2018). Similarly, an analog of erastin, PRLX93936, can induce ferroptosis *via* GPX4 inhibition when combined with DDP (Liang et al., 2021). Novel ferroptosis inhibitors, such as IKE and sorafenib, can inhibit the cystine/glutamate transporter, exhaust GSH, and increase sensitivity to radiotherapy (Li et al., 2020b; Ye et al., 2020). The local anesthetic levobupivacaine could increase p53 expression, enhance ferroptosis, and inhibit tumor growth in NSCLC (Meng et al., 2021). The dual PI3K/HDAC inhibitor BEBT-908 could activate

immunogenic ferroptosis by hyperacetylating and activating p53 in lung cancer cells (Fan et al., 2021). An FSP1 inhibitor (iFSP1) could reverse FSP1-mediated drug resistance by increasing cellular sensitivity to ferroptosis and thus, promoting PCD in lung cancer cells (Doll et al., 2019). The application of erianin (Chen et al., 2020b), sanguinarine (SAG) (Xu et al., 2022), and dihydroisotanshinone I (DT) (Wu et al., 2021) also repressed tumor growth and prevented metastasis *in vivo* and *in vitro*. In addition, targeted delivery of ncRNAs is also considered a promising anticancer strategy (Tabnak et al., 2021), and the application of delicate nanotechnology has recently attracted extensive attention due to its specific physicochemical properties (Chen et al., 2021b). Follow-up research can carry out more effective and precise interventions in the above and other regulatory pathways, regulating cellular sensitivity to ferroptosis, inhibiting the growth and metastasis of lung cancer cells, and prolonging the survival of patients.

## CONCLUSION AND PERSPECTIVES

As a unique form of PCD, ferroptosis has received growing attention and interest since its first report in 2012 (Dixon et al., 2012). With the progress of ferroptosis-related research, it has been revealed that ferroptosis plays a crucial role in many pathological changes in lung diseases. Among these findings, the dysregulation of ferroptosis in lung cancer has been more widely and deeply explored (Xu et al., 2021b; Yu et al., 2021). In this review, we provide a current understanding and views of ferroptosis in lung diseases, especially beyond lung cancer, from the aspects of the molecular basis and the corresponding therapeutic significance. Impressive efforts have been made to reveal the potential pathological mechanisms of ferroptosis in diseases, such as COPD, asthma, and pulmonary fibrosis, which provide fresh thinking for the treatment of these diseases in a large number of suffering patients. However, the following questions remain to be addressed for further clinical development of ferroptosis-targeted therapies. First, are there other potential ferroptosis regulators and mechanisms? Current thinking suggests that p53 and GPX4 are two main ferroptosis-regulatory mechanisms but are not mutually exclusive. Second, what is the optimal timing, dose, and route of administration for treatment targeting ferroptosis in specific pathological lung conditions and disease stages? Persistent usage, overdose, and systemic administration of drugs that inactivate ferroptosis might theoretically increase cancer occurrence. Third, what physiological role does ferroptosis play in lung disease? Ferroptosis is involved in the occurrence of asthma and the development of inflammation, thus, some studies have shown that inhibition of ferroptosis can be developed as a therapeutic target, while ferroptosis of eosinophils could result in sensitivity to dexamethasone and relieve the symptoms of asthmatic patients. Hence, an appropriate treatment for different types of lung disease must be carefully chosen. Fourth, in treating lung cancer and metastasis, can we activate ferroptosis specifically in cancer cells without affecting healthy cells? Inhibitions of specific ferroptotic targets are better choices than targeting p53 or GPX4

to preserve their comprehensive influence on tumor suppression and antioxidation in normal cells. It is of great significance and value to further study the pathogenesis of ferroptosis in lung diseases because of insufficient understanding, to determine sensitive biological indicators, and reliable therapeutic targets. More efficient and specific regulation of cellular ferroptosis is pivotal to further investigations.

## AUTHOR CONTRIBUTIONS

YL collected and analyzed the data, conceived the study, and wrote the manuscript. YY collected and analyzed the data. Yfy

collected and analyzed the data and designed the study. All authors commented on previous versions of the manuscript, read and approved the final manuscript.

## FUNDING

The research leading to these results has received funding from Sichuan University Full-time Postdoctoral Research and Development Fund, Grant/Award Number: 2020SCU12023; Post-Doctor Research Project, West China Hospital, Sichuan University, Grant/Award Number: 2018HXBH041. The financial support were received by YL.

## REFERENCES

- Abobaker, A. (2021). Reply: Iron Chelation May Harm Patients with COVID-19. *Eur. J. Clin. Pharmacol.* 77 (2), 267–268. doi:10.1007/s00228-020-02988-9
- Álvarez, F., Fernández-Ruiz, M., and Aguado, J. M. (2013). Iron and Invasive Fungal Infection. *Rev. Iberoam. Micol.* 30 (4), 217–225.
- Amaral, E. P., Costa, D. L., Namasivayam, S., Riteau, N., Kamenyeva, O., Mittereder, L., et al. (2019). A Major Role for Ferroptosis in Mycobacterium Tuberculosis-Induced Cell Death and Tissue Necrosis. *J. Exp. Med.* 216 (3), 556–570. doi:10.1084/jem.20181776
- Barnes, P. J., Burney, P. G., Silverman, E. K., Celli, B. R., Vestbo, J., Wedzicha, J. A., et al. (2015). Chronic Obstructive Pulmonary Disease. *Nat. Rev. Dis. Prim.* 1 (1), 15076. doi:10.1038/nrdp.2015.76
- Barnes, P. J., Baker, J., and Donnelly, L. E. (2019). Cellular Senescence as a Mechanism and Target in Chronic Lung Diseases. *Am. J. Respir. Crit. Care Med.* 200 (5), 556–564. doi:10.1164/rccm.201810-1975tr
- Baz, M. A., Ghio, A. J., Roggli, V. L., Tapon, V. F., and Piantadosi, C. A. (1997). Iron Accumulation in Lung Allografts after Transplantation\*. *Chest* 112 (2), 435–439. doi:10.1378/chest.112.2.435
- Carota, G., Ronsisvalle, S., Panarello, F., Tibullo, D., Nicolosi, A., and Li Volti, G. (2021). Role of Iron Chelation and Protease Inhibition of Natural Products on COVID-19 Infection. *J. Clin. Med.* 10 (11). doi:10.3390/jcm10112306
- Cavezzi, A., Troiani, E., and Corrao, S. (2020). COVID-19: Hemoglobin, Iron, and Hypoxia beyond Inflammation. A Narrative Review. *Clin. Pract.* 10 (2), 1271. doi:10.4081/cp.2020.1271
- Chavarría, A. P., Valdez Vázquez, R. R., Domínguez Cherit, J. G., Herrera Bello, H., Castillejos Suastegui, H., Moreno-Castañeda, L., et al. (2021). Antioxidants and Pentoxifylline as Coadjuvant Measures to Standard Therapy to Improve Prognosis of Patients with Pneumonia by COVID-19. *Comput. Struct. Biotechnol. J.* 19, 1379–1390. doi:10.1016/j.csbj.2021.02.009
- Chen, K., Zhang, S., Jiao, J., and Zhao, S. (2021). Ferroptosis and its Potential Role in Lung Cancer: Updated Evidence from Pathogenesis to Therapy. *Jir Vol.* 14, 7079–7090. doi:10.2147/jir.s347955
- Chen, L.-D., Huang, Z.-W., Huang, Y.-Z., Huang, J.-F., Zhang, Z.-P., and Lin, X.-J. (2021). Untargeted Metabolomic Profiling of Liver in a Chronic Intermittent Hypoxia Mouse Model. *Front. Physiol.* 12, 701035. doi:10.3389/fphys.2021.701035
- Chen, L.-D., Wu, R.-H., Huang, Y.-Z., Chen, M.-X., Zeng, A.-M., Zhuo, G.-f., et al. (2020). The Role of Ferroptosis in Chronic Intermittent Hypoxia-Induced Liver Injury in Rats. *Sleep. Breath.* 24 (4), 1767–1773. doi:10.1007/s11325-020-02091-4
- Chen, P., Wu, Q., Feng, J., Yan, L., Sun, Y., Liu, S., et al. (2020). Erianin, a Novel Dibenzyl Compound in Dendrobium Extract, Inhibits Lung Cancer Cell Growth and Migration via Calcium/calmodulin-dependent Ferroptosis. *Sig Transduct. Target Ther.* 5 (1), 51. doi:10.1038/s41392-020-0149-3
- Chen, X., Qi, G., Fang, F., Miao, Y., and Wang, L. (2022). Silence of MLK3 Alleviates Lipopolysaccharide-Induced Lung Epithelial Cell Injury via Inhibiting P53-Mediated Ferroptosis. *J. Mol. Histol.* 53 (2), 503–510. doi:10.1007/s10735-022-10064-y
- Cheng, H., Feng, D., Li, X., Gao, L., Tang, S., Liu, W., et al. (2021). Iron Deposition-Induced Ferroptosis in Alveolar Type II Cells Promotes the Development of Pulmonary Fibrosis. *Biochimica Biophysica Acta (BBA) - Mol. Basis Dis.* 1867 (12), 166204. doi:10.1016/j.bbdis.2021.166204
- Colafrancesco, S., Alessandri, C., Conti, F., and Priori, R. (2020). COVID-19 Gone Bad: A New Character in the Spectrum of the Hyperferritinemic Syndrome? *Autoimmun. Rev.* 19 (7), 102573. doi:10.1016/j.autrev.2020.102573
- Cotroneo, E., Ashek, A., Wang, L., Wharton, J., Dubois, O., Bozorgi, S., et al. (2015). Iron Homeostasis and Pulmonary Hypertension. *Circ. Res.* 116 (10), 1680–1690. doi:10.1161/circresaha.116.305265
- Dalamaga, M., Karampela, I., and Mantzoros, C. S. (2020). Commentary: Could Iron Chelators Prove to Be Useful as an Adjunct to COVID-19 Treatment Regimens? *Metabolism* 108, 154260. doi:10.1016/j.metabol.2020.154260
- Dar, H. H., Epperly, M. W., Tyurin, V. A., Amoscato, A. A., Anthonyuthu, T. S., Souryavong, A. B., et al. (2022). *P. aeruginosa* Augments Irradiation Injury via 15-Lipoxygenase-Catalyzed Generation of 15-HpETE-PE and Induction of Theft-Ferroptosis. *JCI Insight* 7 (4). doi:10.1172/jci.insight.156013
- Dar, H. H., Anthonyuthu, T. S., Ponomareva, L. A., Souryavong, A. B., Shurin, G. V., Kapralov, A. O., et al. (2021). A New Thiol-independent Mechanism of Epithelial Host Defense against *Pseudomonas aeruginosa*: iNOS/NO Sabotage of Theft-Ferroptosis. *Redox Biol.* 45, 102045. doi:10.1016/j.redox.2021.102045
- Dar, H. H., Tyurina, Y. Y., Mikulska-Ruminska, K., Shrivastava, I., Ting, H.-C., Tyurin, V. A., et al. (2018). *Pseudomonas aeruginosa* Utilizes Host Polyunsaturated Phosphatidylethanolamines to Trigger Theft-Ferroptosis in Bronchial Epithelium. *J. Clin. Invest.* 128 (10), 4639–4653. doi:10.1172/jci99490
- Deng, S.-h., Wu, D.-m., Li, L., Liu, T., Zhang, T., Li, J., et al. (2021). miR-324-3p Reverses Cisplatin Resistance by Inducing GPX4-Mediated Ferroptosis in Lung Adenocarcinoma Cell Line A549. *Biochem. Biophysical Res. Commun.* 549, 54–60. doi:10.1016/j.bbrc.2021.02.077
- Dixon, S. J., Lemberg, K. M., Lamprecht, M. R., Skouta, R., Zaitsev, E. M., Gleason, C. E., et al. (2012). Ferroptosis: an Iron-dependent Form of Nonapoptotic Cell Death. *Cell.* 149 (5), 1060–1072. doi:10.1016/j.cell.2012.03.042
- Dodson, M., Castro-Portuguez, R., and Zhang, D. D. (2019). NRF2 Plays a Critical Role in Mitigating Lipid Peroxidation and Ferroptosis. *Redox Biol.* 23, 101107. doi:10.1016/j.redox.2019.101107
- Doll, S., Freitas, F. P., Shah, R., Aldrovandi, M., da Silva, M. C., Ingold, I., et al. (2019). FSP1 Is a Glutathione-independent Ferroptosis Suppressor. *Nature* 575 (7784), 693–698. doi:10.1038/s41586-019-1707-0
- Doll, S., Proneth, B., Tyurina, Y. Y., Panzilius, E., Kobayashi, S., Ingold, I., et al. (2017). ACSL4 Dictates Ferroptosis Sensitivity by Shaping Cellular Lipid Composition. *Nat. Chem. Biol.* 13 (1), 91–98. doi:10.1038/nchembio.2239
- Dong, H., Qiang, Z., Chai, D., Peng, J., Xia, Y., Hu, R., et al. (2020). Nrf2 Inhibits Ferroptosis and Protects against Acute Lung Injury Due to Intestinal Ischemia Reperfusion via Regulating SLC7A11 and HO-1. *Aging* 12 (13), 12943–12959. doi:10.18632/aging.103378
- Dong, H., Xia, Y., Jin, S., Xue, C., Wang, Y., Hu, R., et al. (2021). Nrf2 Attenuates Ferroptosis-Mediated IIR-ALI by Modulating TERT and SLC7A11. *Cell. Death Dis.* 12 (11), 1027. doi:10.1038/s41419-021-04307-1
- Dowdle, W. E., Nyfeler, B., Nagel, J., Elling, R. A., Liu, S., Triantafellow, E., et al. (2014). Selective VPS34 Inhibitor Blocks Autophagy and Uncovers a Role for

- NCOA4 in Ferritin Degradation and Iron Homeostasis *In Vivo*. *Nat. Cell. Biol.* 16 (11), 1069–1079. doi:10.1038/ncb3053
- Duca, L., Ottolenghi, S., Coppola, S., Rinaldo, R., Dei Cas, M., Rubino, F. M., et al. (2021). Differential Redox State and Iron Regulation in Chronic Obstructive Pulmonary Disease, Acute Respiratory Distress Syndrome and Coronavirus Disease 2019. *Antioxidants (Basel)* 10 (9). doi:10.3390/antiox10091460
- Edeas, M., Saleh, J., and Peyssonnaud, C. (2020). Iron: Innocent Bystander or Vicious Culprit in COVID-19 Pathogenesis? *Int. J. Infect. Dis.* 97, 303–305. doi:10.1016/j.ijid.2020.05.110
- Fan, F., Liu, P., Bao, R., Chen, J., Zhou, M., Mo, Z., et al. (2021). A Dual PI3K/HDAC Inhibitor Induces Immunogenic Ferroptosis to Potentiate Cancer Immune Checkpoint Therapy. *Cancer Res.* 81 (24), 6233–6245. doi:10.1158/0008-5472.can-21-1547
- Forcina, G. C., and Dixon, S. J. (2019). GPX4 at the Crossroads of Lipid Homeostasis and Ferroptosis. *Proteomics* 19 (18), 1800311. doi:10.1002/pmic.201800311
- Garrick, M. D., and Ghio, A. J. (2021). Iron Chelation May Harm Patients with COVID-19. *Eur. J. Clin. Pharmacol.* 77 (2), 265–266. doi:10.1007/s00228-020-02987-w
- Ghio, A. J., Hilborn, E. D., Stonehuerner, J. G., Dailey, L. A., Carter, J. D., Richards, J. H., et al. (2008). Particulate Matter in Cigarette Smoke Alters Iron Homeostasis to Produce a Biological Effect. *Am. J. Respir. Crit. Care Med.* 178 (11), 1130–1138. doi:10.1164/rccm.200802-334oc
- Ghio, A. J., Stonehuerner, J. G., Richards, J. H., Crissman, K. M., Roggli, V. L., Piantadosi, C. A., et al. (2008). Iron Homeostasis and Oxidative Stress in Idiopathic Pulmonary Alveolar Proteinosis: a Case-Control Study. *Respir. Res.* 9 (1), 10. doi:10.1186/1465-9921-9-10
- Gong, Y., Wang, N., Liu, N., and Dong, H. (2019). Lipid Peroxidation and GPX4 Inhibition Are Common Causes for Myofibroblast Differentiation and Ferroptosis. *DNA Cell. Biol.* 38 (7), 725–733. doi:10.1089/dna.2018.4541
- Guo, J., Xu, B., Han, Q., Zhou, H., Xia, Y., Gong, C., et al. (2018). Ferroptosis: A Novel Anti-tumor Action for Cisplatin. *Cancer Res. Treat.* 50 (2), 445–460. doi:10.4143/crt.2016.572
- Hamilos, G., Samonis, G., and Kontoyiannis, D. P. (2011). Pulmonary Mucormycosis. *Semin. Respir. Crit. Care Med.* 32 (6), 693–702. doi:10.1055/s-0031-1295717
- Hammad, H., and Lambrecht, B. N. (2021). The Basic Immunology of Asthma. *Cell.* 184 (6), 1469–1485. doi:10.1016/j.cell.2021.02.016
- Han, Y., Ye, L., Du, F., Ye, M., Li, C., Zhu, X., et al. (2021). Iron Metabolism Regulation of Epithelial-Mesenchymal Transition in Idiopathic Pulmonary Fibrosis. *Ann. Transl. Med.* 9 (24), 1755. doi:10.21037/atm-21-5404
- He, J., Li, X., and Yu, M. (2021). Bioinformatics Analysis Identifies Potential Ferroptosis Key Genes in the Pathogenesis of Pulmonary Fibrosis. *Front. Genet.* 12, 788417. doi:10.3389/fgene.2021.788417
- He, R., Liu, B., Xiong, R., Geng, B., Meng, H., Lin, W., et al. (2022). Itaconate Inhibits Ferroptosis of Macrophage via Nrf2 Pathways against Sepsis-Induced Acute Lung Injury. *Cell. Death Discov.* 8 (1), 43. doi:10.1038/s41420-021-00807-3
- He, Y., Shang, Y., Li, Y., Wang, M., Yu, D., Yang, Y., et al. (2022). An 8-Ferroptosis-Related Genes Signature from Bronchoalveolar Lavage Fluid for Prognosis in Patients with Idiopathic Pulmonary Fibrosis. *BMC Pulm. Med.* 22 (1), 15. doi:10.1186/s12890-021-01799-7
- Hinman, A., Holst, C. R., Latham, J. C., Bruegger, J. J., Ulas, G., McCusker, K. P., et al. (2018). Vitamin E Hydroquinone Is an Endogenous Regulator of Ferroptosis via Redox Control of 15-lipoxygenase. *PLoS One* 13 (8), e0201369. doi:10.1371/journal.pone.0201369
- Hsu, J. L., Manouvakova, O. V., Clemons, K. V., Inayathullah, M., Tu, A. B., Sobel, R. A., et al. (2018). Microhemorrhage-associated Tissue Iron Enhances the Risk for Aspergillus fumigatus Invasion in a Mouse Model of Airway Transplantation. *Sci. Transl. Med.* 10 (429). doi:10.1126/scitranslmed.aag2616
- Huang, C., Yang, M., Deng, J., Li, P., Su, W., and Jiang, R. (2018). Upregulation and Activation of P53 by Erastin-induced R-active O-oxygen S-species C-contribute to C-ytotoxic and C-ystatic E-effects in A549 L-ung C-ancer C-ells. *Oncol. Rep.* 40 (4), 2363–2370. doi:10.3892/or.2018.6585
- Huang, C., Wang, Y., Li, X., Ren, L., Zhao, J., Hu, Y., et al. (2020). Clinical Features of Patients Infected with 2019 Novel Coronavirus in Wuhan, China. *Lancet* 395 (10223), 497–506. doi:10.1016/s0140-6736(20)30183-5
- Huang, I., Pranata, R., Lim, M. A., Oehadian, A., and Alisjahbana, B. (2020). C-reactive Protein, Procalcitonin, D-Dimer, and Ferritin in Severe Coronavirus Disease-2019: a Meta-Analysis. *Ther. Adv. Respir. Dis.* 14, 1753466620937175. doi:10.1177/1753466620937175
- Huang, Y., Dai, Z., Barbacioru, C., and Sadée, W. (2005). Cystine-glutamate Transporter SLC7A11 in Cancer Chemoresensitivity and Chemoresistance. *Cancer Res.* 65 (16), 7446–7454. doi:10.1158/0008-5472.can-04-4267
- Jaiswal, N., Bhatnagar, M., and Shah, H. (2020). N-acetylcysteine: A Potential Therapeutic Agent in COVID-19 Infection. *Med. Hypotheses* 144, 110133. doi:10.1016/j.mehy.2020.110133
- Jasenosky, L. D., Scriba, T. J., Hanekom, W. A., and Goldfeld, A. E. (2015). T Cells and Adaptive Immunity to Mycobacterium Tuberculosis in Humans. *Immunol. Rev.* 264 (1), 74–87. doi:10.1111/imr.12274
- Jia, Z., Yan, L., Ren, Z., Wu, L., Wang, J., Guo, J., et al. (2019). Delicate Structural Coordination of the Severe Acute Respiratory Syndrome Coronavirus Nsp13 upon ATP Hydrolysis. *Nucleic Acids Res.* 47 (12), 6538–6550. doi:10.1093/nar/gkz409
- Jiang, L., Hickman, J. H., Wang, S.-J., and Gu, W. (2015). Dynamic Roles of P53-Mediated Metabolic Activities in ROS-Induced Stress Responses. *Cell. Cycle* 14 (18), 2881–2885. doi:10.1080/15384101.2015.1068479
- Jiang, L., Kon, N., Li, T., Wang, S.-J., Su, T., Hibshoosh, H., et al. (2015). Ferroptosis as a P53-Mediated Activity during Tumour Suppression. *Nature* 520 (7545), 57–62. doi:10.1038/nature14344
- Kagan, V. E., Mao, G., Qu, F., Angeli, J. P. F., Doll, S., Croix, C. S., et al. (2017). Oxidized Arachidonic and Adrenic PEs Navigate Cells to Ferroptosis. *Nat. Chem. Biol.* 13 (1), 81–90. doi:10.1038/nchembio.2238
- Kim, K.-H., Maldonado, F., Ryu, J. H., Eiken, P. W., Hartman, T. E., Bartholmai, B. J., et al. (2010). Iron Deposition and Increased Alveolar Septal Capillary Density in Nonfibrotic Lung Tissue Are Associated with Pulmonary Hypertension in Idiopathic Pulmonary Fibrosis. *Respir. Res.* 11 (1), 37. doi:10.1186/1465-9921-11-37
- Klobucar, K., Côté, J.-P., French, S., Borrillo, L., Guo, A. B. Y., Serrano-Wu, M. H., et al. (2021). Chemical Screen for Vancomycin Antagonism Uncovers Probes of the Gram-Negative Outer Membrane. *ACS Chem. Biol.* 16 (5), 929–942. doi:10.1021/acscchembio.1c00179
- Kontoghiorghes, G. J., Kolnagou, A., Skiada, A., and Petrikos, G. (2010). The Role of Iron and Chelators on Infections in Iron Overload and Non Iron Loaded Conditions: Prospects for the Design of New Antimicrobial Therapies. *Hemoglobin* 34 (3), 227–239. doi:10.3109/03630269.2010.483662
- Lederer, D. J., Martinez, F. J., and Martinez, F. J. (2018). Idiopathic Pulmonary Fibrosis. *N. Engl. J. Med.* 378 (19), 1811–1823. doi:10.1056/nejmra1705751
- Leu, J. I.-J., Murphy, M. E., and George, D. L. (2019). Mechanistic Basis for Impaired Ferroptosis in Cells Expressing the African-Centric S47 Variant of P53. *Proc. Natl. Acad. Sci. U.S.A.* 116 (17), 8390–8396. doi:10.1073/pnas.1821277116
- Li, J., Deng, S.-h., Li, J., Li, L., Zhang, F., Zou, Y., et al. (2022). Obacunone Alleviates Ferroptosis during Lipopolysaccharide-Induced Acute Lung Injury by Upregulating Nrf2-dependent Antioxidant Responses. *Cell. Mol. Biol. Lett.* 27 (1), 29. doi:10.1186/s11658-022-00318-8
- Li, J., Lu, K., Sun, F., Tan, S., Zhang, X., Sheng, W., et al. (2021). Panaxydol Attenuates Ferroptosis against LPS-Induced Acute Lung Injury in Mice by Keap1-Nrf2/HO-1 Pathway. *J. Transl. Med.* 19 (1), 96. doi:10.1186/s12967-021-02745-1
- Li, M., Wang, K., Zhang, Y., Fan, M., Li, A., Zhou, J., et al. (2021). Ferroptosis-Related Genes in Bronchoalveolar Lavage Fluid Serves as Prognostic Biomarkers for Idiopathic Pulmonary Fibrosis. *Front. Med.* 8, 693959. doi:10.3389/fmed.2021.693959
- Li, X., Duan, L., Yuan, S., Zhuang, X., Qiao, T., and He, J. (2019). Ferroptosis Inhibitor Alleviates Radiation-Induced Lung Fibrosis (RILF) via Down-Regulation of TGF-β1. *J. Inflamm.* 16, 11. doi:10.1186/s12950-019-0216-0
- Li, Y., Yan, H., Xu, X., Liu, H., Wu, C., and Zhao, L. (2020). Erastin/sorafenib Induces Cisplatin-Resistant Non-small Cell Lung Cancer Cell Ferroptosis through Inhibition of the Nrf2/xCT Pathway. *Oncol. Lett.* 19 (1), 323–333. doi:10.3892/ol.2019.11066
- Li, Y., Cao, Y., Xiao, J., Shang, J., Tan, Q., Ping, F., et al. (2020). Inhibitor of Apoptosis-Stimulating Protein of P53 Inhibits Ferroptosis and Alleviates Intestinal Ischemia/reperfusion-Induced Acute Lung Injury. *Cell. Death Differ.* 27 (9), 2635–2650. doi:10.1038/s41418-020-0528-x



- Lian, N., Zhang, Q., Chen, J., Chen, M., Huang, J., and Lin, Q. (2021). The Role of Ferroptosis in Bronchoalveolar Epithelial Cell Injury Induced by Cigarette Smoke Extract. *Front. Physiol.* 12, 751206. doi:10.3389/fphys.2021.751206
- Liang, Z., Zhao, W., Li, X., Wang, L., Meng, L., and Yu, R. (2021). Cisplatin Synergizes with PRLX93936 to Induce Ferroptosis in Non-small Cell Lung Cancer Cells. *Biochem. Biophysical Res. Commun.* 569, 79–85. doi:10.1016/j.bbrc.2021.06.088
- Liu, H., Drew, P., Cheng, Y., and Visner, G. A. (2005). Pirfenidone Inhibits Inflammatory Responses and Ameliorates Allograft Injury in a Rat Lung Transplant Model. *J. Thorac. Cardiovasc. Surg.* 130 (3), 852–858. doi:10.1016/j.jtcvs.2005.04.012
- Liu, P., Feng, Y., Li, H., Chen, X., Wang, G., Xu, S., et al. (2020). Ferrostatin-1 Alleviates Lipopolysaccharide-Induced Acute Lung Injury via Inhibiting Ferroptosis. *Cell. Mol. Biol. Lett.* 25, 10. doi:10.1186/s11658-020-00205-0
- Liu, T., Xu, P., Ke, S., Dong, H., Zhan, M., Hu, Q., et al. (2022). Histone Methyltransferase SETDB1 Inhibits TGF- $\beta$ -Induced Epithelial-Mesenchymal Transition in Pulmonary Fibrosis by Regulating SNAI1 Expression and the Ferroptosis Signaling Pathway. *Archives Biochem. Biophysics* 715, 109087. doi:10.1016/j.abb.2021.109087
- Liu, W., Zhou, Y., Duan, W., Song, J., Wei, S., Xia, S., et al. (2021). Glutathione Peroxidase 4-dependent Glutathione High-Consumption Drives Acquired Platinum Chemoresistance in Lung Cancer-Derived Brain Metastasis. *Clin. Transl. Med.* 11 (9), e517. doi:10.1002/ctm2.517
- Liu, W., Chakraborty, B., Safi, R., Kazmin, D., Chang, C.-y., and McDonnell, D. P. (2021). Dysregulated Cholesterol Homeostasis Results in Resistance to Ferroptosis Increasing Tumorigenicity and Metastasis in Cancer. *Nat. Commun.* 12 (1), 5103. doi:10.1038/s41467-021-25354-4
- Liu, X., Ma, Y., Luo, L., Zong, D., Li, H., Zeng, Z., et al. (2022). Dihydroquercetin Suppresses Cigarette Smoke Induced Ferroptosis in the Pathogenesis of Chronic Obstructive Pulmonary Disease by Activating Nrf2-Mediated Pathway. *Phytomedicine* 96, 153894. doi:10.1016/j.phymed.2021.153894
- Liu, Y., and Gu, W. (2022). p53 in Ferroptosis Regulation: the New Weapon for the Old Guardian. *Cell. Death Differ.* 29 (5), 895–910. doi:10.1038/s41418-022-00943-y
- Liu, Y., and Gu, W. (2021). The Complexity of P53-Mediated Metabolic Regulation in Tumor Suppression. *Semin. Cancer Biol.* doi:10.1016/j.semcancer.2021.03.010
- Lu, F., Zander, D. S., and Visner, G. A. (2002). Increased Expression of Heme Oxygenase-1 in Human Lung Transplantation. *J. Heart Lung Transplant.* 21 (10), 1120–1126. doi:10.1016/s1053-2498(02)00423-0
- Lui, G. Y. L., Obeidy, P., Ford, S. J., Tselepis, C., Sharp, D. M., Jansson, P. J., et al. (2013). The Iron Chelator, Deferasirox, as a Novel Strategy for Cancer Treatment: Oral Activity against Human Lung Tumor Xenografts and Molecular Mechanism of Action. *Mol. Pharmacol.* 83 (1), 179–190. doi:10.1124/mol.112.081893
- Ma, L., Zhang, X., Yu, K., Xu, X., Chen, T., Shi, Y., et al. (2021). Targeting SLC3A2 Subunit of System XC– Is Essential for m6A Reader YTHDC2 to Be an Endogenous Ferroptosis Inducer in Lung Adenocarcinoma. *Free Radic. Biol. Med.* 168, 25–43. doi:10.1016/j.freeradbiomed.2021.03.023
- Ma, X., Yan, W., and He, N. (2022). Lidocaine Attenuates Hypoxia/reoxygenation-Induced Inflammation, Apoptosis and Ferroptosis in Lung Epithelial Cells by Regulating the P38 MAPK Pathway. *Mol. Med. Rep.* 25 (5). doi:10.3892/mmr.2022.12666
- Maniam, P., Essilfie, A.-T., Kalimutho, M., Ling, D., Frazer, D. M., Phipps, S., et al. (2021). Increased Susceptibility of Cystic Fibrosis Airway Epithelial Cells to Ferroptosis. *Biol. Res.* 54 (1), 38. doi:10.1186/s40659-021-00361-3
- Mao, C., Wang, X., Liu, Y., Wang, M., Yan, B., Jiang, Y., et al. (2018). A G3BP1-Interacting lncRNA Promotes Ferroptosis and Apoptosis in Cancer via Nuclear Sequestration of P53. *Cancer Res.* 78 (13), 3484–3496. doi:10.1158/0008-5472.CAN-17-3454
- Meng, M., Huang, M., Liu, C., Wang, J., Ren, W., Cui, S., et al. (2021). Local Anesthetic Levobupivacaine Induces Ferroptosis and Inhibits Progression by Up-Regulating P53 in Non-small Cell Lung Cancer. *Aging* 13.
- Mizumura, K., and Gon, Y. (2021). Iron-Regulated Reactive Oxygen Species Production and Programmed Cell Death in Chronic Obstructive Pulmonary Disease. *Antioxidants (Basel)* 10 (10). doi:10.3390/antiox10101569
- Muhoherac, B. B. (2020). What Can Cellular Redox, Iron, and Reactive Oxygen Species Suggest about the Mechanisms and Potential Therapy of COVID-19? *Front. Cell. Infect. Microbiol.* 10, 569709. doi:10.3389/fcimb.2020.569709
- Nagasaki, T., Schuyler, A. J., Zhao, J., Samovich, S. N., Yamada, K., Deng, Y., et al. (2022). 15LO1 Dictates Glutathione Redox Changes in Asthmatic Airway Epithelium to Worsen Type 2 Inflammation. *J. Clin. Invest.* 132 (1). doi:10.1172/JCI151685
- Ousingsawat, J., Schreiber, R., Gulbins, E., Kamler, M., and Kunzelmann, K. (2021). *P. aeruginosa* Induced Lipid Peroxidation Causes Ferroptotic Cell Death in Airways. *Cell. Physiol. Biochem.* 55 (5), 590–604. doi:10.33594/000000437
- Pan, X., Lin, Z., Jiang, D., Yu, Y., Yang, D., Zhou, H., et al. (2019). Erastin Decreases Radioresistance of NSCLC Cells Partially by Inducing GPX4-Mediated Ferroptosis. *Oncol. Lett.* 17 (3), 3001–3008. doi:10.3892/ol.2019.9888
- Pan, Y., Tang, P., Cao, J., Song, Q., Zhu, L., Ma, S., et al. (2020). Lipid Peroxidation Aggravates Anti-tuberculosis Drug-Induced Liver Injury: Evidence of Ferroptosis Induction. *Biochem. Biophysical Res. Commun.* 533 (4), 1512–1518. doi:10.1016/j.bbrc.2020.09.140
- Papi, A., Brightling, C., Pedersen, S. E., and Reddel, H. K. (2018). Asthma. *Lancet* 391 (10122), 783–800. doi:10.1016/s0140-6736(17)33311-1
- Park, E.-J., Park, Y.-J., Lee, S. J., Lee, K., and Yoon, C. (2019). Whole Cigarette Smoke Condensates Induce Ferroptosis in Human Bronchial Epithelial Cells. *Toxicol. Lett.* 303, 55–66. doi:10.1016/j.toxlet.2018.12.007
- Pasirja, R., and Naime, M. (2022). Resolving the Equation between Mucormycosis and COVID-19 Disease. *Mol. Biol. Rep.* 49 (4), 3349–3356. doi:10.1007/s11033-021-07085-3
- Patel, A. R., Patel, A. R., Singh, S., Singh, S., and Khawaja, I. (2019). The Association between Obstructive Sleep Apnea and Arrhythmias. *Cureus* 11 (11), e4429–itc96. doi:10.7759/cureus.4429
- Peng, J., Fan, B., Bao, C., and Jing, C. (2021). JMJD3 Deficiency Alleviates Lipopolysaccharide-induced A-cute L-lung I-njury by I-nhibiting A-lveolar E-pithelial F-erroptosis in a Nrf2-dependent M-anner. *Mol. Med. Rep.* 24 (5). doi:10.3892/mmr.2021.12447
- Prentice, B. J., Jaffe, A., Hameed, S., Verge, C. F., Waters, S., and Widger, J. (2021). Cystic Fibrosis-Related Diabetes and Lung Disease: an Update. *Eur. Respir. Rev.* 30 (159). doi:10.1183/16000617.0293-2020
- Pugh, C., Hathwar, V., Richards, J. H., Stonehurner, J., and Ghio, A. J. (2005). Disruption of Iron Homeostasis in the Lungs of Transplant Patients. *J. Heart Lung Transplant.* 24 (11), 1821–1827. doi:10.1016/j.healun.2005.03.016
- Qiang, Z., Dong, H., Xia, Y., Chai, D., Hu, R., and Jiang, H. (2020). Nrf2 and STAT3 Alleviates Ferroptosis-Mediated IIR-ALI by Regulating SLC7A11. *Oxid. Med. Cell. Longev.* 2020, 5146982. doi:10.1155/2020/5146982
- Rashidipour, N., Karami-Mohajeri, S., Mandegary, A., Mohammadinejad, R., Wong, A., Mohit, M., et al. (2020). Where Ferroptosis Inhibitors and Paraquat Detoxification Mechanisms Intersect, Exploring Possible Treatment Strategies. *Toxicology* 433–434, 152407. doi:10.1016/j.tox.2020.152407
- Ratjen, F., and Döring, G. (2003). Cystic Fibrosis. *Lancet* 361 (9358), 681–689. doi:10.1016/s0140-6736(03)12567-6
- Rhodes, C. J., Wharton, J., Howard, L., Gibbs, J. S. R., Vonk-Noordegraaf, A., and Wilkins, M. R. (2011). Iron Deficiency in Pulmonary Arterial Hypertension: a Potential Therapeutic Target. *Eur. Respir. J.* 38 (6), 1453–1460. doi:10.1183/09031936.00037711
- Seifert, M., Nairz, M., Schroll, A., Schrettl, M., Haas, H., and Weiss, G. (2008). Effects of the *Aspergillus fumigatus* Siderophore Systems on the Regulation of Macrophage Immune Effector Pathways and Iron Homeostasis. *Immunobiology* 213 (9–10), 767–778. doi:10.1016/j.imbio.2008.07.010
- Sen, A. (2021). Deficient Synthesis of Melatonin in COVID-19 Can Impair the Resistance of Coronavirus Patients to Mucormycosis. *Med. Hypotheses* 158, 110722. doi:10.1016/j.mehy.2021.110722
- Seyedrezazadeh, E., Ostadrahimi, A., Mahboob, S., Assadi, Y., Ghaemmagami, J., and Pourmogaddam, M. (2008). Effect of Vitamin E and Selenium Supplementation on Oxidative Stress Status in Pulmonary Tuberculosis Patients. *Respirology* 13 (2), 294–298. doi:10.1111/j.1440-1843.2007.01200.x
- Shimizu, Y., Matsuzaki, S., Dobashi, K., Yanagitani, N., Satoh, T., Koka, M., et al. (2011). Elemental Analysis of Lung Tissue Particles and Intracellular Iron Content of Alveolar Macrophages in Pulmonary Alveolar Proteinosis. *Respir. Res.* 12 (1), 88. doi:10.1186/1465-9921-12-88



- Silvagno, F., Vernone, A., and Pescarmona, G. P. (2020). The Role of Glutathione in Protecting against the Severe Inflammatory Response Triggered by COVID-19. *Antioxidants (Basel)* 9 (7). doi:10.3390/antiox9070624
- Stockwell, B. R., Jiang, X., and Gu, W. (2020). Emerging Mechanisms and Disease Relevance of Ferroptosis. *Trends Cell. Biol.* 30 (6), 478–490. doi:10.1016/j.tcb.2020.02.009
- Sun, L., Dong, H., Zhang, W., Wang, N., Ni, N., Bai, X., et al. (2021). Lipid Peroxidation, GSH Depletion, and SLC7A11 Inhibition Are Common Causes of EMT and Ferroptosis in A549 Cells, but Different in Specific Mechanisms. *DNA Cell. Biol.* 40 (2), 172–183. doi:10.1089/dna.2020.5730
- Sun, X., Ou, Z., Chen, R., Niu, X., Chen, D., Kang, R., et al. (2016). Activation of the P62-Keap1-NRF2 Pathway Protects against Ferroptosis in Hepatocellular Carcinoma Cells. *Hepatology* 63 (1), 173–184. doi:10.1002/hep.28251
- Tabnak, P., HajiEsmailPoor, Z., and Sorane, S. (2021). Ferroptosis in Lung Cancer: From Molecular Mechanisms to Prognostic and Therapeutic Opportunities. *Front. Oncol.* 11, 792827. doi:10.3389/fonc.2021.792827
- Takahashi, M., Mizumura, K., Gon, Y., Shimizu, T., Kozu, Y., Shikano, S., et al. (2021). Iron-Dependent Mitochondrial Dysfunction Contributes to the Pathogenesis of Pulmonary Fibrosis. *Front. Pharmacol.* 12, 643980. doi:10.3389/fphar.2021.643980
- Tang, W., Dong, M., Teng, F., Cui, J., Zhu, X., Wang, W., et al. (2021). Environmental Allergens House Dust Mite-induced Asthma Is Associated with Ferroptosis in the Lungs. *Exp. Ther. Med.* 22 (6), 1483. doi:10.3892/etm.2021.10918
- Tang, W., Dong, M., Teng, F., Cui, J., Zhu, X., Wang, W., et al. (2021). TMT-based Quantitative Proteomics Reveals Suppression of SLC3A2 and ATP1A3 Expression Contributes to the Inhibitory Role of Acupuncture on Airway Inflammation in an OVA-Induced Mouse Asthma Model. *Biomed. Pharmacother.* 134, 111001. doi:10.1016/j.biopha.2020.111001
- Tang, X., Li, Z., Yu, Z., Li, J., Zhang, J., Wan, N., et al. (2021). Effect of Curcumin on Lung Epithelial Injury and Ferroptosis Induced by Cigarette Smoke. *Hum. Exp. Toxicol.* 40 (12 Suppl. 1), S753–S762. doi:10.1177/09603271211059497
- Vonk Noordegraaf, A., Groeneveldt, J. A., and Bogaard, H. J. (2016). Pulmonary Hypertension. *Eur. Respir. Rev.* 25 (139), 4–11. doi:10.1183/16000617.0096-2015
- Wang, C., Horby, P. W., Hayden, F. G., and Gao, G. F. (2020). A Novel Coronavirus Outbreak of Global Health Concern. *Lancet* 395 (10223), 470–473. doi:10.1016/s0140-6736(20)30185-9
- Wang, M., Mao, C., Ouyang, L., Liu, Y., Lai, W., Liu, N., et al. (2019). Long Noncoding RNA LINC00336 Inhibits Ferroptosis in Lung Cancer by Functioning as a Competing Endogenous RNA. *Cell. Death Differ.* 26 (11), 2329–2343. doi:10.1038/s41418-019-0304-y
- Wang, X., Chen, Y., Wang, X., Tian, H., Wang, Y., Jin, J., et al. (2021). Stem Cell Factor SOX2 Confers Ferroptosis Resistance in Lung Cancer via Upregulation of SLC7A11. *Cancer Res.* 81 (20), 5217–5229. doi:10.1158/0008-5472.can-21-0567
- Wang, X., Zhang, C., Zou, N., Chen, Q., Wang, C., Zhou, X., et al. (2022). Lipocalin-2 Silencing Suppresses Inflammation and Oxidative Stress of Acute Respiratory Distress Syndrome by Ferroptosis via Inhibition of MAPK/ERK Pathway in Neonatal Mice. *Bioengineered* 13 (1), 508–520. doi:10.1080/21655979.2021.2009970
- Wang, Y., Dong, Z., Zhang, Z., Wang, Y., Yang, K., and Li, X. (2022). Postconditioning with Irisin Attenuates Lung Ischemia/Reperfusion Injury by Suppressing Ferroptosis via Induction of the Nrf2/HO-1 Signal Axis. *Oxid. Med. Cell. Longev.* 2022, 9911167. doi:10.1155/2022/9911167
- Wang, Y., and Tang, M., PM2.5 Induces Ferroptosis in Human Endothelial Cells through Iron Overload and Redox Imbalance. *Environ. Pollut.*, 2019. 254(Pt A): p. 112937. doi:10.1016/j.envpol.2019.07.105
- Wei, D., Ke, Y. Q., Duan, P., Zhou, L., Wang, C. Y., and Cao, P. (2021). MicroRNA-302a-3p Induces Ferroptosis of Non-small Cell Lung Cancer Cells via Targeting Ferroportin. *Free Radic. Res.* 55 (7), 821–830. doi:10.1080/10715762.2021.1947503
- Wenzel, S. E., Tyurina, Y. Y., Zhao, J., St. Croix, C. M., Dar, H. H., Mao, G., et al. (2017). PEBP1 Wardens Ferroptosis by Enabling Lipoygenase Generation of Lipid Death Signals. *Cell.* 171 (3), 628–641.e26. doi:10.1016/j.cell.2017.09.044
- Wesselius, L. J., Nelson, M. E., and Skikne, B. S. (1994). Increased Release of Ferritin and Iron by Iron-Loaded Alveolar Macrophages in Cigarette Smokers. *Am. J. Respir. Crit. Care Med.* 150 (3), 690–695. doi:10.1164/ajrcm.150.3.8087339
- Wong, C.-M., Preston, I. R., Hill, N. S., and Suzuki, Y. J. (2012). Iron Chelation Inhibits the Development of Pulmonary Vascular Remodeling. *Free Radic. Biol. Med.* 53 (9), 1738–1747. doi:10.1016/j.freeradbiomed.2012.08.576
- Wu, C.-Y., Yang, Y.-H., Lin, Y.-S., Chang, G.-H., Tsai, M.-S., Hsu, C.-M., et al. (2021). Dihydroisotanshinone I Induced Ferroptosis and Apoptosis of Lung Cancer Cells. *Biomed. Pharmacother.* 139, 111585. doi:10.1016/j.biopha.2021.111585
- Wu, Y., Chen, H., Xuan, N., Zhou, L., Wu, Y., Zhu, C., et al. (2020). Induction of Ferroptosis-like Cell Death of Eosinophils Exerts Synergistic Effects with Glucocorticoids in Allergic Airway Inflammation. *Thorax* 75 (11), 918–927. doi:10.1136/thoraxjnl-2020-214764
- Xie, S.-S., Deng, Y., Guo, S.-L., Li, J.-q., Zhou, Y.-c., Liao, J., et al. (2022). Endothelial Cell Ferroptosis Mediates Monocrotaline-Induced Pulmonary Hypertension in Rats by Modulating NLRP3 Inflammasome Activation. *Sci. Rep.* 12 (1), 3056. doi:10.1038/s41598-022-06848-7
- Xu, B., Wang, H., and Chen, Z. (2021). Puerarin Inhibits Ferroptosis and Inflammation of Lung Injury Caused by Sepsis in LPS Induced Lung Epithelial Cells. *Front. Pediatr.* 9, 706327. doi:10.3389/fped.2021.706327
- Xu, R., Wu, J., Luo, Y., Wang, Y., Tian, J., Teng, W., et al. (2022). Sanguinarine Represses the Growth and Metastasis of Non-small Cell Lung Cancer by Facilitating Ferroptosis. *Curr. Pharm. Des.* 28 (9), 760–768. doi:10.2174/138161282866220217124542
- Xu, W., Deng, H., Hu, S., Zhang, Y., Zheng, L., Liu, M., et al. (2021). Role of Ferroptosis in Lung Diseases. *Jir Vol.* 14, 2079–2090. doi:10.2147/jir.s307081
- Xu, Y., Li, X., Cheng, Y., Yang, M., and Wang, R. (2020). Inhibition of ACSL4 Attenuates Ferroptotic Damage after Pulmonary Ischemia-reperfusion. *FASEB J.* 34 (12), 16262–16275. doi:10.1096/fj.202001758r
- Yang, N., and Shang, Y. (2022). Ferrostatin-1 and 3-Methyladenine Ameliorate Ferroptosis in OVA-Induced Asthma Model and in IL-13-Challenged BEAS-2B Cells. *Oxid. Med. Cell. Longev.* 2022, 9657933. doi:10.1155/2022/9657933
- Yang, S., Ouyang, J., Lu, Y., Harypusat, V., and Chen, Y. (2022). A Dual Role of Heme Oxygenase-1 in Tuberculosis. *Front. Immunol.* 13, 842858. doi:10.3389/fimmu.2022.842858
- Yang, W. S., SriRamaratnam, R., Welsch, M. E., Shimada, K., Skouta, R., Viswanathan, V. S., et al. (2014). Regulation of Ferroptotic Cancer Cell Death by GPX4. *Cell.* 156 (1–2), 317–331. doi:10.1016/j.cell.2013.12.010
- Yang, W. S., and Stockwell, B. R. (2016). Ferroptosis: Death by Lipid Peroxidation. *Trends Cell. Biol.* 26 (3), 165–176. doi:10.1016/j.tcb.2015.10.014
- Yang, Y., Tai, W., Lu, N., Li, T., Liu, Y., Wu, W., et al. (2020). lncRNA ZFAS1 Promotes Lung Fibroblast-To-Myofibroblast Transition and Ferroptosis via Functioning as a ceRNA through miR-150-5p/SLC38A1 axis. *Aging* 12 (10), 9085–9102. doi:10.18632/aging.103176
- Ye, L. F., Chaudhary, K. R., Zandkarimi, F., Harken, A. D., Kinslow, C. J., Upadhyayula, P. S., et al. (2020). Radiation-Induced Lipid Peroxidation Triggers Ferroptosis and Synergizes with Ferroptosis Inducers. *ACS Chem. Biol.* 15 (2), 469–484. doi:10.1021/acscchembio.9b00939
- Yoshida, M., Minagawa, S., Araya, J., Sakamoto, T., Hara, H., Tsubouchi, K., et al. (2019). Involvement of Cigarette Smoke-Induced Epithelial Cell Ferroptosis in COPD Pathogenesis. *Nat. Commun.* 10 (1), 3145. doi:10.1038/s41467-019-10991-7
- Yu, S., Jia, J., Zheng, J., Zhou, Y., Jia, D., and Wang, J. (2021). Recent Progress of Ferroptosis in Lung Diseases. *Front. Cell. Dev. Biol.* 9, 789517. doi:10.3389/fcell.2021.789517
- Zhang, F., Liu, H., and Liu, H. (2021). Identification of Ferroptosis-Associated Genes Exhibiting Altered Expression in Pulmonary Arterial Hypertension. *Mbe* 18 (6), 7619–7630. doi:10.3934/mbe.2021377
- Zhang, J., Liu, Y., Guo, Y., and Zhao, Q. (2020). GPX8 Promotes Migration and Invasion by Regulating Epithelial Characteristics in Non-small Cell Lung Cancer. *Thorac. Cancer* 11 (11), 3299–3308. doi:10.1111/1759-7714.13671
- Zhang, X., Sui, S., Wang, L., Li, H., Zhang, L., Xu, S., et al. (2020). Inhibition of Tumor Propellant Glutathione Peroxidase 4 Induces Ferroptosis in Cancer Cells and Enhances Anticancer Effect of Cisplatin. *J. Cell. Physiol.* 235 (4), 3425–3437. doi:10.1002/jcp.29232
- Zhang, Y., Zheng, L., Deng, H., Feng, D., Hu, S., Zhu, L., et al. (2022). Electroacupuncture Alleviates LPS-Induced ARDS through  $\alpha 7$  Nicotinic

- Acetylcholine Receptor-Mediated Inhibition of Ferroptosis. *Front. Immunol.* 13, 832432. doi:10.3389/fimmu.2022.832432
- Zhao, J., Dar, H. H., Deng, Y., St. Croix, C. M., Li, Z., Minami, Y., et al. (2020). PEBP1 Acts as a Rheostat between Prosurvival Autophagy and Ferroptotic Death in Asthmatic Epithelial Cells. *Proc. Natl. Acad. Sci. U.S.A.* 117 (25), 14376–14385. doi:10.1073/pnas.1921618117
- Zhao, J., Maskrey, B., Balzar, S., Chibana, K., Mustovich, A., Hu, H., et al. (2009). Interleukin-13-induced MUC5AC Is Regulated by 15-lipoxygenase 1 Pathway in Human Bronchial Epithelial Cells. *Am. J. Respir. Crit. Care Med.* 179 (9), 782–790. doi:10.1164/rccm.200811-1744oc
- Zhao, J., O'Donnell, V. B., Balzar, S., St. Croix, C. M., Trudeau, J. B., and Wenzel, S. E. (2011). 15-Lipoxygenase 1 Interacts with Phosphatidylethanolamine-Binding Protein to Regulate MAPK Signaling in Human Airway Epithelial Cells. *Proc. Natl. Acad. Sci. U.S.A.* 108 (34), 14246–14251. doi:10.1073/pnas.1018075108
- Zhao, K., Huang, J., Dai, D., Feng, Y., Liu, L., and Nie, S. (2020). Serum Iron Level as a Potential Predictor of Coronavirus Disease 2019 Severity and Mortality: A Retrospective Study. *Open Forum Infect. Dis.* 7 (7), ofaa250. doi:10.1093/ofid/ofaa250
- Zheng, J., and Conrad, M. (2020). The Metabolic Underpinnings of Ferroptosis. *Cell. Metab.* 32 (6), 920–937. doi:10.1016/j.cmet.2020.10.011
- Zhou, F., Yu, T., Du, R., Fan, G., Liu, Y., Liu, Z., et al. (2020). Clinical Course and Risk Factors for Mortality of Adult Inpatients with COVID-19 in Wuhan, China: a Retrospective Cohort Study. *Lancet* 395 (10229), 1054–1062. doi:10.1016/s0140-6736(20)30566-3
- Zhou, H., Li, F., Niu, J. Y., Zhong, W. Y., Tang, M. Y., Lin, D., et al. (2019). Ferroptosis Was Involved in the Oleic Acid-Induced Acute Lung Injury in Mice. *Sheng Li Xue Bao* 71 (5), 689–697.
- Zou, H. X., Qiu, B. Q., Lai, S. Q., Zhou, X. L., Gong, C. W., Wang, L. J., et al. (2021). Iron Metabolism and Idiopathic Pulmonary Arterial Hypertension: New Insights from Bioinformatic Analysis. *Biomed. Res. Int.* 2021, 5669412. doi:10.1155/2021/5669412

**Conflict of Interest:** The authors declare that the research was conducted in the absence of any commercial or financial relationships that could be construed as a potential conflict of interest.

**Publisher's Note:** All claims expressed in this article are solely those of the authors and do not necessarily represent those of their affiliated organizations, or those of the publisher, the editors, and the reviewers. Any product that may be evaluated in this article, or claim that may be made by its manufacturer, is not guaranteed or endorsed by the publisher.

Copyright © 2022 Li, Yang and Yang. This is an open-access article distributed under the terms of the Creative Commons Attribution License (CC BY). The use, distribution or reproduction in other forums is permitted, provided the original author(s) and the copyright owner(s) are credited and that the original publication in this journal is cited, in accordance with accepted academic practice. No use, distribution or reproduction is permitted which does not comply with these terms.



# The Role of Ferroptosis in Acute Kidney Injury

Jinshi Zhang<sup>1†</sup>, Binqi Wang<sup>2†</sup>, Shizhu Yuan<sup>1,2†</sup>, Qiang He<sup>1\*</sup> and Juan Jin<sup>1\*</sup>

<sup>1</sup>Urology & Nephrology Center, Department of Nephrology, Zhejiang Provincial People's Hospital (Affiliated People's Hospital, Hangzhou Medical College), Hangzhou, China, <sup>2</sup>Zhejiang Chinese Medical University, The Second School of Clinical Medical, Hangzhou, China

Ferroptosis is a novel cell death method discovered in recent years. It is usually accompanied by massive accumulations of iron and lipid peroxidation during cell death. Recent studies have shown that ferroptosis is closely associated with the pathophysiological processes of many diseases, such as tumors, neurological diseases, localized ischemia-reperfusion injury, kidney injury, and hematological diseases. How to intervene in the incidence and development of associated diseases by regulating the ferroptosis of cells has become a hot topic of research. This article provides a review of the role of ferroptosis in the pathogenesis and potential treatment of acute kidney injury.

**Keywords:** acute kidney injury, ferroptosis, mechanism, treatment, regulators

## OPEN ACCESS

### Edited by:

Xin Wang,  
National Institutes of Health (NIH),  
United States

### Reviewed by:

Gang Wang,  
Weill Cornell Medicine, United States  
Xintong Yao,  
Chongqing Medical University, China

### \*Correspondence:

Juan Jin  
lang\_018@163.com  
Qiang He  
qianghe1973@126.com

<sup>†</sup>These authors have contributed  
equally to this work and share first  
authorship

### Specialty section:

This article was submitted to  
Molecular Diagnostics and  
Therapeutics,  
a section of the journal  
Frontiers in Molecular Biosciences

**Received:** 23 May 2022

**Accepted:** 13 June 2022

**Published:** 30 June 2022

### Citation:

Zhang J, Wang B, Yuan S, He Q and  
Jin J (2022) The Role of Ferroptosis in  
Acute Kidney Injury.  
Front. Mol. Biosci. 9:951275.  
doi: 10.3389/fmolb.2022.951275

## INTRODUCTION

Acute kidney injury (AKI), is a disease that can have a variety of causes, including ischemia, nephrotoxic drugs, and urinary tract obstruction (Wang and Tao, 2015). AKI has high morbidity and mortality rates in hospitalized patients, and yet research on the therapeutic options for AKI prevention and treatment, other than hemodialysis, has been slow. Therefore, new therapeutic options are urgently needed to prevent AKI, as well as to promote kidney repair after AKI onset. In 2012, Dixon et al. (2012) proposed a new concept of cell death, known as ferroptosis, which was subsequently proven to be closely associated with the pathophysiological processes of many diseases (Alvarez et al., 2017; Tang et al., 2021). A recent study has shed light on the role of iron homeostasis in the pathogenesis of AKI and its therapeutic potential (Swaminathan, 2018). This article reviews the current research on the regulatory mechanisms, research progress, and therapeutic potential of ferroptosis in AKI.

## FERROPTOSIS

### Overview

As one of the most important essential trace elements, iron is involved in a wide variety of metabolic processes in the body. In 2003, Dolma et al. (Yao et al., 2021) discovered a novel erastin compound that is selectively lethal to tumor cells with the RAS gene mutation, but this causes cell death in a manner that is different from conventional apoptosis without nuclear morphological changes. Neither DNA fragmentation, cysteine-containing aspartate protein hydrolase (caspase) activation, nor caspase inhibitors inhibit this mode of cell death. Subsequently, Yang et al. (Heintzman et al., 2022) and Yagoda et al. (2007) found that this mode of cell death could be inhibited by iron chelators and discovered another compound, RSL3, which could also cause this mode of cell death. In 2012,

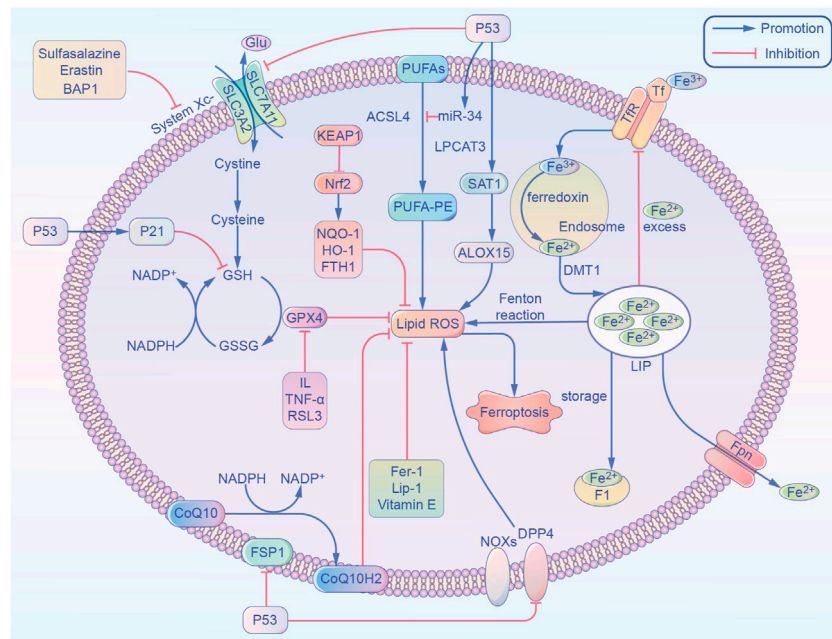


**FIGURE 1 |** Overview of the metabolic routes contributing to ferroptosis. This non-exhaustive list includes (1) iron-Fenton reaction. (2) GPX4 antioxidant activity. (3) Lipid metabolism pathway. ACSL4, acyl-coenzyme A synthetase long chain family member 4; ALOX15, arachidonate 15-lipoxygenase; BAP1, BRCA1 associated protein 1; CoQ10, coenzyme Q10; CoQ10 H2, ubiquinol; DPP4, dipeptidyl-peptidase-4; DMT1, divalent metal transporter 1; FTH1, ferritin heavy chain 1; Fer-1, ferrostatin-1; FSP1, ferroptosis suppressor protein 1; Fpn, ferroportin; GPX4, glutathione peroxidase 4; GSH, glutathione; GSSG, oxidized glutathione; Glu, glutamic acid; HO-1, heme oxygenase-1; IL, interleukin; Lip-1, liprostatin-1; LPCAT3, lysophosphatidylcholine acyltransferase 3; LIP, labile iron pool; NADPH, nicotinamide adenine dinucleotide phosphate; Nrf2, nuclear factor E2 related factor 2; NOX1, NADPH Oxidase 1; NQO-1, NAD(P)H quinone dehydrogenase 1; PUFAs, polyunsaturated fatty acids; ROS, reactive oxygen species; SAT1, spermidine/spermine N1-acetyltransferase 1; System Xc-, glutamate-cystine/antiporter; SLC7A11, solute carrier family 7 member 11; SLC3A2, solute carrier family 3 member 2; TNF- $\alpha$ , tumor necrosis factor- $\alpha$ ; TfR, transferrin receptor; Tf, transferrin.

Dixon et al. (2012) officially named this mode of cell death “ferroptosis,” or “iron death,” based on its characteristics. Unlike other regulated cell deaths like apoptosis and autophagy, ferroptosis has the following characteristics: 1) Morphologically, it is primarily characterized by cell membrane rupture and blebbing, reduction in mitochondrial volume, increase in membrane density, and reduction or even disappearance of mitochondrial cristae. It does not have the morphological features of apoptosis, such as cell shrinkage, chromatin condensation, skeleton disassembly, or apoptotic vesicle formation (Mou et al., 2019); 2) Unlike apoptosis, ferroptosis occurs without the activation of caspase 3, and the process cannot be reversed by caspase inhibitors; 3) Ferroptosis cannot be interrupted by inhibitors of apoptosis, pyroptosis, or cellular autophagy, but can be inhibited by iron chelators and antioxidants; 4) Ferroptosis can be induced or inhibited through several metabolic pathways (Figure 1), it is characterized by the aggregation of iron and reactive oxygen species (ROS), both of which are thought to be central to ferroptosis, and the inhibition of cystine/glutamate antiporter (cystine/glutamate antiporter system, or System Xc-) and glutathione peroxidase 4 (GPX4) activity, by reducing cystine uptake, depleting glutathione (GSH), and releasing molecules, such as arachidonic acid (Doll and Conrad, 2017); 5) Genetically abnormal expression of several genes can occur, especially of those related to iron metabolism, such as the transferrin receptor (TfR), divalent metal transporter

1 (DMT1), ferritin heavy chain 1 (FTH1), and nuclear receptor coactivator 4 (NCOA4) (Wang et al., 2018). Caspase activation and autophagic lysosome formation are specific markers of apoptosis and autophagy, respectively. Although there are no recognized specific markers for ferroptosis, acyl-coenzyme A synthetase long chain family member 4 (ACSL4) causes the earliest upregulation of adrenaline in non-lethal ferroptosis in various AKI models, which suggests that this molecule is a reliable biomarker for ferroptosis detection. Whether these different modes of cell death can be integrated into a complete regulatory network requires further exploration (Doll et al., 2017).

## Iron Metabolism

Iron homeostasis has an important influence on the incidence of ferroptosis, and iron is present in the circulation as the trivalent iron ( $\text{Fe}^{3+}$ ) bound to transferrin.  $\text{Fe}^{3+}$  is converted to  $\text{Fe}^{2+}$  by the membrane protein transferrin receptor 1 and divalent metal transport protein 1 and is released into the cytoplasmic labile iron pool (LIP). Excess iron is stored as ferritin, and the ferritin heavy chain (FTH1) has iron oxidase activity that catalyzes the conversion of  $\text{Fe}^{2+}$  into  $\text{Fe}^{3+}$ , allowing iron to be safely incorporated into the ferritin shell and therefore reduce free iron levels. Hydrogen peroxide reacts with  $\text{Fe}^{2+}$  to produce hydroxyl radicals with strong oxidizing properties, and this is known as the Fenton reaction. Iron overload causes abnormalities



in the mitochondrial oxidative phosphorylation pathway, producing ATP along with large amounts of ROS, oxidizing polyunsaturated fatty acids (PUFA) on cell and organelle membranes, forming lipid peroxides, and directly or indirectly disrupting cellular structure and function. In AKI due to IRI, ROS production is increased during reperfusion and induces ferroptosis in renal tubular epithelial cells. In AKI, plasma catalytic iron concentrations were significantly increased and correlated with extensive injury caused by cisplatin, ischemia-reperfusion, aminoglycosides, rhabdomyolysis, and hemoglobinuria, and both higher plasma catalytic iron levels and lower hepcidin concentrations were associated with increased mortality in patients with AKI (Leaf et al., 2019).

## Amino Acid Metabolism

The glutamate-cystine/antiporter (System Xc-) is a non-sodium-dependent cystine/glutamate reverse transporter protein encoded by the solute carrier family 7 member 11 (SLC7A11), consisting of the catalytic subunit SLC7A11 and the chaperone subunit solute carrier family 3 member 2 (SLC3A2). SLC7A11 is also commonly used to refer to the Xc- system. The Xc-system exchanges glutamate and cystine intracellularly and extracellularly in a 1:1 ratio, and the intracellular cystine is reduced to cysteine. The methionine amino acids generate S-adenosylmethionine under enzymatic action, and cysteine is also produced after demethylation and deadenylation. Cysteine binds glutamate and glycine to form GSH, which is an intracellular antioxidant that is used in intracellular enzymatic and non-enzymatic antioxidant reactions to maintain hydrogen peroxide levels within the physiological range. GPX4 is a GSH-dependent enzyme with an active center, composed of selenoproteins. Selenoproteins contain selenocysteine that reduces peroxide accumulation by reducing lipid-peroxide (L-OOH) to the corresponding harmless alcohol (L-OH) using GSH and thiol-containing compounds, thereby inhibiting lipoxygenase (LOX) activity and phospholipid/cardiolioid oxidation events. Mevalonate is used as a raw material for the synthesis of isoglutamate pyrophosphate (IPP) from acetyl coenzyme A (CoA), which is an essential signal for the maturation of selenocysteine tRNAs and the synthesis of active GPX4 (Moon et al., 2019). Erastin and sulfasalazine inhibit System Xc- function, resulting in insufficient cystine uptake, decreased intracellular antioxidant capacity, and lipid accumulation, and thereby, inducing cellular ferroptosis. AKI morbidity and mortality were significantly increased in GPX4 knockout mice, and during IRI there was a significant decrease in GSH levels, reduced GPX4 activity, increased iron accumulation and lipid peroxidation, and upregulated expression of proteins and genes associated with iron-sensitivity in kidney tissue (Ma et al., 2021).

## Lipid Metabolism

PUFA contains arachidonic acid (AA) or its derivative adrenergic acid (AdA), and the pentose phosphate pathway directly dehydrogenates and decarboxylates glucose oxidatively to produce nicotinamide adenine dinucleotide phosphate

(NADPH) as a reducing agent involved in the synthesis of fatty acids. AA and ACSL4 are esterified into phosphatidylethanolamine (PE), which in turn is formed by LOX through association with recombinant human phosphatidylethanolamine binding protein 1 to form the complex 15-LOX/phosphatidylethanolamine binding protein 1 (PEBP1). This undergoes metamorphic regulation to provide the signal sn2-15-HpETE-PE site that promotes ferroptosis and is ultimately oxidized to phospholipid hydroperoxides (PE-AA/AdA-OOH) and ROS. This is where 15-LO2 is highly expressed in renal tubular epithelial cells, and both 15-LO1 and 15-LO2 are involved in ischemic acute kidney injury (Anthonymuthu et al., 2018). ROS generate destructive hydroxyl radicals through the Fenton reaction, which react rapidly with neighboring molecules or peroxidize with cellular lipid components to generate large amounts of lipid radicals, resulting in thinning of PUFA-rich cell membranes and plasma membranes and irreversible damage to structure and function. Nuclear factor E2-related factor 2 (Nrf2) is considered an important regulator of the antioxidant system, and its downstream target genes are involved in maintaining redox homeostasis. These include GSH synthase, GPX4, and the oxidative stress sensor molecule kelch-like ECH-associated protein 1 (KEAP1), which reduces Nrf2 activity by ubiquitination. In AKI, methylpadoxolone activates Nrf2 by inhibiting KEAP1's ubiquitin activity to activate Nrf2. This results in improved glomerular filtration rate. Renal lipid peroxidation was found in FA-AKI, and mice pretreated with ferritin-1 had improved renal function and reduced tissue damage (Shimada et al., 2016).

## P53

P53 has become one of the most extensively studied genes since its discovery in 1979. (Liu and Gu, 2021). Apart from its effects on common forms of cell death, p53 is well known for its key role in ferroptosis. (Tang et al., 2019). In the first study to investigate the role of p53 in ferroptosis, we found that p53 promotes ferroptosis by decreasing the expression of SLC7A11 (Jiang et al., 2015). In addition, p53 can regulate ferroptosis and lipid peroxidation by virtue of its target gene spermidine/spermine N1-acetyltransferase (SAT1) whose effect is demonstrated by ALOX15 upregulation after SAT1 induction (Gao et al., 2015). Recently, p53 has been discovered to delay the ferroptosis by up-regulating the expression of its downstream target p21 (Tarangelo et al., 2018). Furthermore, in p53-deficient cells, the dipeptidyl-peptidase-4 (DPP4) interacts with NADPH Oxidase 1 (NOX1), thus forming a NOX1-DPP4 complex that mediates plasma membrane lipid peroxidation and ferroptosis (Gao et al., 2019). ACSL4 has been reported as both a reliable biomarker and a pivotal contributor to ferroptosis. Recent studies have confirmed that ACSL4 levels are post-transcriptionally downregulated by p53-activated miR-34 (Chang et al., 2007; Jiang et al., 2020). And there is a possibility that the p53/miR-34/ACSL4 axis represses ferroptosis by limiting lipid peroxidation. Controversial results of p53 are quite common in different ferroptosis studies, which may result from

“different cell types,” “duality of p53 functions” or “different interventions” (Liu and Gu, 2022).

## Other Mechanisms

Erastin can bind to VDAC2 and VDAC3 in the mitochondrial voltage-dependent anion channel (VDAC) to alter cell membrane permeability and ion selectivity, causing mitochondrial dysfunction and the release of oxidative substances, which ultimately lead to ferroptosis (Yagoda et al., 2007). Heme oxygenase-1 (HO-1) is an important source of intracellular iron, and Adedoyin et al. (2018) found that HO-1 can act as a protective enzyme to inhibit erastin-induced occurrence of ferroptosis in proximal tubular epithelial cells in acute kidney injury. In contrast, in fibrosarcoma cells, Kwon et al. (2015) found that inhibition of erastin-induced ferroptosis was alleviated, and this contradictory result suggests that the exact relationship between HO-1 and ferroptosis requires further exploration. Kinolfin, a class of oral, small molecule, gold-containing compounds for the treatment of RA, was recently found to cause ferroptosis through high doses of inhibition of thioredoxin reductase (TXNRD) activity, which led to lipid peroxidation and ferroptosis, and suggested that TXNRD is a key factor in ferroptosis (Yang et al., 2020). Autophagy-related protein Beclin 1 can form a complex with SLC7A11 to promote ferroptosis, and this process requires AMP-activated protein kinase (AMPK) to mediate phosphorylation of the S90/93/96 sites of Beclin 1 (BECN1) (Song et al., 2018). Bersuker et al. (2019) found that coenzyme Q10 (CoQ10) captures lipid reactive oxygen species through its reduced form, while ferroptosis suppressor protein 1 (FSP1) catalyzes the regeneration of CoQ10 *via* NADH to prevent the release of lipid peroxides, and that FSP/CoQ10 can inhibit ferroptosis independently of the glutathione peroxidase 4 (GPX4) pathway.

As the mechanism of ferroptosis is being studied, many specific ferroptosis inhibitors have been discovered, such as the novel compounds ferrostatin-1 (Fer-1), liproxstatin-1 (Lip-1), and vitamin E, in addition to iron chelators. It is important to clarify the mechanism of ferroptosis and its regulation to provide new research ideas and therapeutic options for diseases related to ferroptosis, and the inhibitors.

## FERROPTOSIS AND ACUTE KIDNEY INJURY

### Ferroptosis and Rhabdomyolysis Syndrome Resulted in Acute Kidney Injury

The etiology of rhabdomyolysis syndrome is complex, with studies pointing to more than 190 acquired causes and more than 40 genetically related causes. Common causes include strenuous exercise, direct trauma, metabolic myopathy, toxic chemicals, physical or biological agents, and genetic factors (Thévenod et al., 2020). Previous studies suggest that the main mechanisms of rhabdomyolysis-induced AKI are: 1) Accumulation of myoglobin (Mb) in the kidney after massive damage to skeletal muscles that blocks the distal renal tubules. This is the central mechanism leading to renal damage; 2)

Leakage of bodily fluids after muscle damage, insufficient blood volume, activation of renin-angiotensin, sympathetic nervous system, release of plasma antidiuretic hormone, other inflammatory mediators, such as endothelin-1 (ET1), tumor necrosis factor- $\alpha$  (TNF- $\alpha$ ), which promote vasoconstriction; 3) Nitric oxide in the renal microcirculation is scavenged by Mb resulting in insufficient vasodilator levels. Increased vasoconstrictor and decreased vasodilator levels lead to the constriction of renal arteries, causing inadequate blood supply to the kidneys. Some recent studies suggest that ferroptosis plays a more important role in Mb-induced AKI than previously thought (Tang et al., 2021). In rhabdomyolysis, Mb is released in large amounts beyond the binding capacity of  $\alpha$ 2-globulin, and Mb is filtered out of the glomerulus into the proximal tubule, where it is eventually broken down into free iron ions and ferrous hemoglobin. Transferrin receptors and divalent metal ion transporters transfer extracellular free iron ions into the cell.  $\text{Fe}^{3+}$  entering the cell is converted to  $\text{Fe}^{2+}$ , and part of  $\text{Fe}^{2+}$  is stored in ferritin, while the other part is transported extracellularly by membrane iron transport proteins to be rebound by Hb or Mb (Tang et al., 2021). If there were too much Mb in the renal tubules, it would lead to  $\text{Fe}^{2+}$  overload in the renal tubular cells in the presence of insufficient intracellular ATP, hypotension, and hypoperfusion. Overloaded  $\text{Fe}^{2+}$  will then induce direct damage to proximal tubular lipid peroxidation through the Fenton reaction, leading to acute tubular necrosis or renal failure (Bosch et al., 2009; Zeng and Tomlinson, 2021), where ferritin heavy chain 1 (FTH1) is of importance (Xie et al., 2016a). Zarjou et al. (2013) found that FTH1 knockout mice had higher mortality rates and more severe kidney injury than wild-type mice in a rhabdomyolysis-induced AKI model, which shows the protective effect of FTH1 against tubular injury and the role of iron ions in AKI. A study by Guerrero-Hue et al. (2019) found that Fer-1, a small molecule inhibitor of ferroptosis, could inhibit Mb-induced AKI, a finding that demonstrates the key role played by ferroptosis in this process. Skouta et al. (Tang et al., 2021) also found that Fer-1 effectively inhibited hydroxyquinoline and ferrous ammonium sulfate-induced cell necrosis in a rhabdomyolysis-induced *in vitro* ferroptosis model. In summary, the literature show that ferroptosis is one of the important mechanisms causing rhabdomyolysis-induced AKI.

### Ferroptosis and Acute Kidney Injury due to Ischemia Reperfusion Injury

Ferroptosis and AKI due to ischemia reperfusion injury (IRI) is a condition in which the degree of tissue damage increases rapidly after restoration of blood flow to cells that have suffered a period of ischemia, resulting in a clinical condition called reperfusion syndrome. This process exacerbates tissue injury by initiating an inflammatory cascade of responses. The cascade mainly covers ROS, cytokines, chemokines, and leukocyte activation. (Nieuwenhuijs-Moeke et al., 2020; Messerer et al., 2021). IRI is also an important factor in contributing to AKI. The main pathophysiological mechanisms of renal IRI include inflammation, oxidative stress and lipid peroxidation, mitochondrial dysfunction, and activation of the renin-

angiotensin system (Franzin et al., 2021). A recent study suggests that ferroptosis may be one of the main drivers of renal IRI (Tonnus and Linkermann, 2017). In a mouse model of IRI, application of ferroptosis small molecule inhibitors protected mice from AKI and other organ damage (Tonnus et al., 2021). In clinical practice, renal IRI is usually the leading cause of AKI after cardiac surgery. The pathogenesis of postoperative AKI in the heart is complex and multifactorial, and these mechanisms of injury might play different roles at different times and may also act synergistically, with the release of free iron being a key part (Han et al., 2021). Due to the prolonged exposure of blood cells to the mechanical extracorporeal circulation system during various manipulations, such surgical procedures may lead to the destruction of red blood cells, resulting in the entry of free Hb into the circulation (van Swelm et al., 2020). It has been shown that free Hb levels in the blood increase to several times the physiological level during extracorporeal circulation and remain so until several hours after the procedure (Lee et al., 2021). The role of Hb in the induction of AKI is similar to that of Mb, with tubular cell iron overload being the main cause of eventual acute renal failure or tubular necrosis (Tang et al., 2021); studies have shown that free Hb levels are a significant independent risk factor for renal impairment after cardiac surgery (Leaf et al., 2019). Hemodynamic instability might occur during the transition from complete extracorporeal circulatory support to the patient's own circulation, and this state of hemodynamic instability likely leads to systemic hypoperfusion, particularly ischemia and hypoxia of the kidneys (Haase et al., 2010). During ischemia, free iron levels in the kidney are increased by lower pH and dissociation of protein-bound iron. An increase in free iron might activate cellular ferroptosis, ultimately leading to tubular necrosis (van Swelm et al., 2020). Choi et al. (2019) proposed that lower intraoperative levels of iron-binding protein indirectly reflect impaired processing of catalytic iron by the body during extracorporeal circulation, leading to renal injury. This result emphasizes the importance of iron homeostasis in ischemia-reperfusion injury and suggests that iron homeostasis is a potential therapeutic target in kidney injury associated with cardiac surgery or in AKI induced by ischemia-reperfusion (Choi et al., 2019). In addition, studies have found that mechanical ventilation is an independent risk factor for the development of AKI after cardiac surgery. In an IRI mouse model, prolonged mechanical ventilation led to a gradual decrease in GPX4 levels, increased renal lipid peroxidation, and a gradual decrease in blood GSH and renal homogenate GSH levels. This suggests that prolonged mechanical ventilation leads to blood GSH depletion and induces renal ferroptosis via the GSH-GPX4 axis (Zhou et al., 2020a). In a model of hypoxic injury to renal tubular epithelial cells, application of small molecule inhibitors of ferroptosis effectively attenuated hypoxic damage to renal tubular epithelial cells, which suggests that ferroptosis may be an earlier mode of cell death in hypoxic renal tubular epithelial cells and that hypoxia plays a critical role in the development of ischemia-reperfusion AKI (Li et al., 2021a). Reperfusion injury to other organs during extracorporeal circulation may also bring additional iron to the kidney, and iron released from the upstream necrotic

kidney unit might further descend to the next kidney unit, further exacerbating oxidative stress and inducing tissue damage (Martines et al., 2013). Linkermann et al. (Tonnus et al., 2021) found that ferroptosis is a key mechanism for sequential renal tubular cell death after ischemic AKI, and that triggering ferroptosis by inhibiting the cysteine glutamate transporter and applying the ferroptosis activator erastin to reduce intracellular GSH could cause proximal tubular cell cascade cell death. The use of Fer-1 not only inhibited ferroptosis *in vitro*, but also attenuated ischemia-reperfusion injury in mouse kidneys. Therefore, it can be inferred that ferroptosis is one of the important mechanisms of ischemia-reperfusion AKI. Huang et al. (2019) inhibited the expression of augmentor of liver regeneration (ALR) in an *in vitro* model of IRI-induced AKI and found that the level of cellular ferroptosis was increased, along with an increase in ROS and significant mitochondrial damage. In addition, the inhibition of System Xc<sup>-</sup> with erastin promoted cellular ferroptosis and silenced ALR expression, which suggests that ischemia-reperfusion-induced AKI is mediated by ALR and that this process is associated with the glutathione-glutathione peroxidase (GSH-GPx) system. It was recently shown that IRI induced the upregulation of miR-182-5p and miR378a-3p and further downregulated GPX4 and SLC7A11, which also induced ferroptosis in AKI (Ding et al., 2020).

## Ferroptosis and Drug-Induced Acute Kidney Injury

Cisplatin is an important chemotherapeutic agent for the treatment of many solid tumors, but its clinical application is limited by serious adverse effects, especially nephrotoxicity. Baliga et al. (Sharma and Leaf, 2019) reported in 1998 on a cisplatin-induced cytotoxicity *in vitro* model and a cisplatin-induced acute renal failure *in vivo* model, which showed that iron was detectable in bleomycin released into the medium after exposure to cisplatin, which, a significant increase in iron that could catalyze free radical reactions. They also found that iron chelators significantly reduced cisplatin induced cytotoxicity, suggesting an important role for iron, but the exact mechanism could not be elucidated. Ferritin plays a central role in iron metabolism, and it was found that in the proximal tubule, FTH1 knockout mice had more severe renal injury after cisplatin administration than the control group, which is a finding that underscored the protective role of FTH1 in AKI (van Swelm et al., 2020). Inositol dioxygenase is a proximal renal tubular enzyme, whose overexpression was found by Deng et al. (2019) to exacerbate cisplatin-induced redox damage in cells with AKI. They also found that it promotes ferroptosis through ferritin phagocytosis and lipid peroxidation, and that it might also inhibit GPX4 activity and intracellular GSH concentration by downregulating the “ferroptosis termination system.” In rodents, folic acid could lead to the development of AKI, and certain doses of folic acid could form crystals in the kidney lumen, and high doses could also be directly toxic to the renal tubular epithelium. Martin-Sanchez et al. (2017) confirmed the presence of lipid peroxidation and GSH downregulation, which are typical

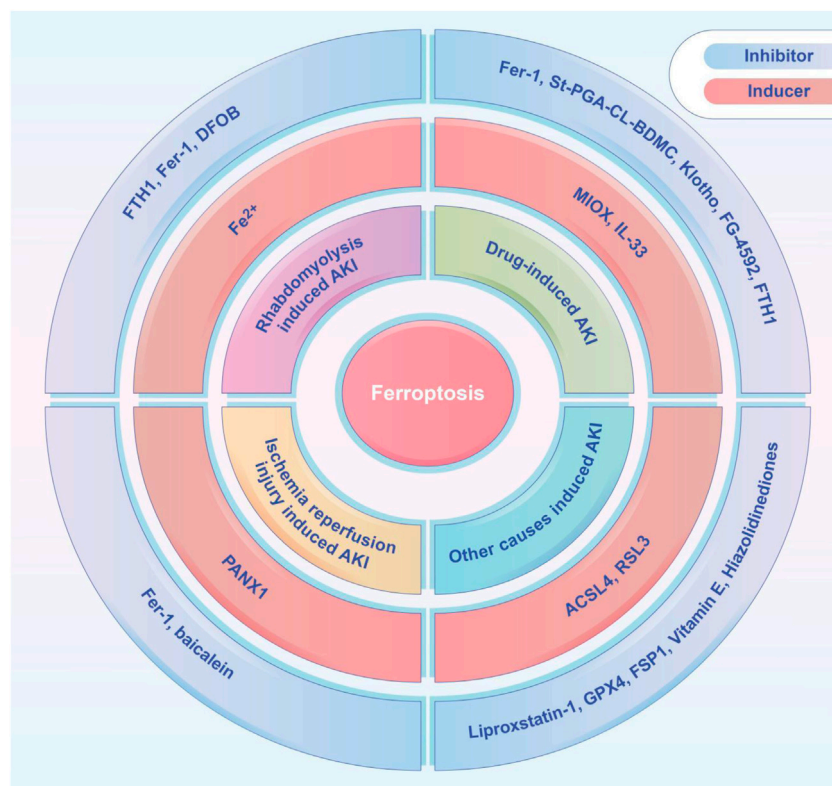


**FIGURE 2 |** The ferroptosis inducers and inhibitors tested in animal models of AKI, including rhabdomyolysis induced AKI, drug-induced AKI, ischemia-reperfusion induced AKI, and other causes induced AKI. ACSL4, acyl-coenzyme A synthetase long chain family member 4; DFOB, desferrioxamine B; FTH1, ferritin heavy chain 1; Fer-1, ferrostatin-1; FG-4592, roxadustat; FSP1, ferroptosis suppressor protein 1; GPX4, glutathione peroxidase 4; IL-33, interleukin 33; MIOX, myo-inositol oxygenase; PANX1, pannexin1; St-PGA-CL-BDMC, star-shaped polyglutamate conjugate of bisdemethoxycurcumin.

features of ferroptosis, in a folic acid-induced AKI mouse model. In addition, the ferroptosis inhibitor Fer-1 reduced oxidative stress, decreased tubular cell death, and attenuated tissue injury by inhibiting the upregulation of chemokines and cytokines, such as interleukin 33 (IL-33), and by inhibiting macrophage infiltration and downregulating the protective factor Klotho. Caspase inhibitors, however, had no nephroprotective effect (Martin-Sanchez et al., 2017). It was also found that receptor-interacting protein kinase 3 (RIPK3) and mixed lineage domain-like protein kinase (MLKL) were inhibited. However, the use of RIPK1 inhibitors or RIPK3 and MLKL gene defects did not prevent kidney injury, which suggests that ferroptosis was the predominant cell death pathway in folic acid-induced AKI (Martin-Sanchez et al., 2017). One recent study from China found that higher p53 activation in tubular cells of folic acid-induced AKI model, while A-lipoic acid (ALA) supplementation blocked the activity of p53 and inhibit ferroptosis (Li et al., 2021b). Thus, p53-mediated ferroptosis in tubular epithelial cell may be a target of treatment of AKI. FG-4592 is an inhibitor of hypoxia-inducible factor (HIF) precursor hydroxylase, and Li et al. (2020) recently found in a folic acid-induced AKI model that renal function was significantly improved in FG-4592 pretreated mice, while the levels of iron, malondialdehyde, and 4-hydroxynonenal in tissues

were reduced. In addition, there was upregulation of HIF-1 $\alpha$  expression, activation of nuclear factor E2 related factor 2 (Nrf2), and high expression of downstream proteins, including hemeoxygenase 1 (HO1), GPX4, System Xc-, and membrane iron transport protein. Further signaling pathway studies suggested that Nrf2 activation is regulated by protein kinase B/glycogen synthase kinase-3 $\beta$  (PKB/GSK-3 $\beta$ ), which suggests that PKB/GSK-3 $\beta$  is a potential therapeutic target for ferroptosis.

## Others

Increased iron accumulation and lipid peroxidation in the renal tissue of severe acute pancreatitis rats showed that these changes were accompanied by decreased GPX4 activity and up-regulation of ferroptosis-related proteins and genes. This demonstrates that ferroptosis is associated with severe acute pancreatitis-induced AKI, and lipase I (LIPI) could inhibit ferroptosis, and both reduce renal damage and improve renal function (Ma et al., 2021).

## TREATMENT OF FERROPTOSIS IN ACUTE KIDNEY INJURY

Recent studies demonstrated the importance of ferroptosis in AKI and many studies have shown that ferroptosis can be



successfully modulated in different kinds of AKI. A variety of ferroptosis inducers and inhibitors have been administrated in those studies (Figure 2). Several studies have shown that ferroptosis is a promising therapeutic target, especially in diseases dominated by tubular necrosis (Linkermann, 2016). GPX4 is an antioxidant enzyme that catalyzes the reduction of lipid peroxides at the expense of reducing GSH, and thereby preventing oxidative damage and ferroptosis. If GPX4 is absent, it will trigger the accumulation of lipid peroxidation products, which eventually leads to the death of mice due to acute renal failure (Demuyne et al., 2021). Small molecule ferroptosis inhibitors (lipoxigenases), which completely block lipid peroxidation, were able to increase the survival rate of GPX4-deficient mice by 35% (Kang et al., 2021). A novel ferroptosis inhibitor 1 that is independent of the classical GPX4 signaling pathway was also recently identified. It uses reduced NADPH to reduce CoQ10 to CoQ10 H<sub>2</sub> in the cell membrane which reducing cell membrane lipid peroxidation and thereby inhibiting ferroptosis (Bersuker et al., 2019; Doll et al., 2019). Another study found that thiazolidinediones (e.g., rosiglitazone) reduced mortality in GPX4-deficient mice by inhibiting ACSL4, and demonstrated their potential benefit for AKI (Doll et al., 2017; Kagan et al., 2017). Fer-1 can prevent membrane lipid damage through redox reactions, thereby inhibiting cellular ferroptosis (Xie et al., 2016b; Martin-Sanchez et al., 2017; Zilka et al., 2017; Zhou et al., 2020b). Linkermann et al. (Tonnus et al., 2021) found that the use of Fer-1 not only blocked erastin-induced ferroptosis *in vitro*, but also prevented renal IRI in mice. It was also found that desferrioxamine could be used to obtain the less cytotoxic compound 3-Hydroxy-Adamant-1-yl by binding to iron adamantine derivatives, which attenuated AKI-causing rhabdomyolysis in rats by inhibiting lipid peroxidation, reducing the ferrous form of Mb, and inhibiting ferroptosis (Groeblert et al., 2011; Yu et al., 2017). Pannexin1 (Panx1) is an ATP release pathway family protein. Su et al. (2019) found in a mouse model of ischemia-reperfusion-induced AKI that silencing Panx1 expression significantly attenuated lipid peroxidation and iron accumulation, mainly through mitogen-activated protein kinase/extracellular signal-regulated kinase (MAPK/ERK) signaling. MAPK/ERK signaling activated ferritin and regulated NCOA4-mediated iron phagocytosis and HO1 expression, which provided potential therapeutic targets for AKI management (Su et al., 2019). Deferiprone has been used in patients with high ferrous load from repeated transfusions, but there have been no studies related to the application of deferiprone for the prevention or treatment of AKI due to rhabdomyolysis (Szymonik et al., 2021). Baicalein, an important active ingredient in the Chinese herb *Scutellaria baicalensis*, attenuated myocardial ischemia-reperfusion-induced AKI by regulating the B-cell lymphoma-2 (BCL2), extracellular signal-regulated kinase 1/2, and BCL2 associated X (BAX) activation of protein kinase B (PKB) (Lai et al., 2016; Szymonik et al., 2021). It has been shown that baicalein can also enhance cellular resistance to ferroptosis by limiting iron accumulation and lipid peroxidation in cells, which makes it a promising therapeutic agent for ferroptosis-related tissue damage (Xie et al., 2016b).

In a mouse model of folic acid-induced AKI, Córdoba-David et al. (2020) proposed that stellate polyglutamate-curcumin coupling inhibited nuclear factor kappa B (NF- $\kappa$ B) activation and downregulated ferroptosis marker expression, while preserving the renal expression of Klotho, ultimately exerting a reno-protective effect. In addition, rhabdomyolysis-induced renal dysfunction and histological damage could also be reduced by curcumin treatment, with the involvement of HO1 (Guerrero-Hue et al., 2019). Li et al. (2021b) confirmed that ALA also could be used as an anti-ferroptosis agent to reduce iron overload in folic acid-induced AKI through upregulation of Ferritin and ferroportin (Fpn). Additionally, LA has the ability to increase the expression of system xCT, thus increasing the synthesis of GSH and enhancing the activity of GPX4. Roxadustat, an inhibitor of the hypoxia-inducible factor prolyl hydroxylase, is protective against folic acid-induced AKI, and studies have shown improved renal function, inhibition of iron accumulation and lipid peroxidation, and increased levels of antioxidant enzymes and GSH in pretreated mice as compared to untreated mice (Li et al., 2020). Mishima et al. (2020) found in a mouse model of cisplatin-induced AKI that cytochrome P450 (CYP450) substrates, such as isoproterenol and rifampin, attenuated tissue damage and cell death, by scavenging lipid peroxidation radicals. However, due to non-specific ferroptosis markers, multiple cell death pathways might exist in the injury model, and the inhibitory effect of drugs on ferroptosis was not directly confirmed. Some studies have tentatively shown that vitamin D receptor (VDR) activation is protective against cisplatin-induced AKI, and that paricalcitol reduces lipid peroxidation, 4-hydroxynonenal, and malondialdehyde, functionally and histologically attenuating cisplatin-induced AKI (Mishima et al., 2020).

## CONCLUSION

Ferroptosis is a recently discovered, iron-dependent, non-apoptotic cell death mechanism. This paper outlines the mechanisms underlying its incidence, its characteristics, and its general preliminary understanding. In AKI, it has been possible to clarify that ferroptosis is one of the important causes of cell death. The application of small molecule ferroptosis inhibitors to inhibit ferroptosis is expected to be a new strategy in the treatment of AKI. It is applied in AKI particularly in cases of rhabdomyolysis or ischemia-reperfusion AKI, which is mainly caused by heme and non-matrix iron. Although the majority of these studies targeting small molecule ferroptosis inhibitors have been conducted in mice models of AKI or *in vitro* experiments, we believe that an in-depth exploration of the role played by ferroptosis in the process of AKI and the rational use of ferroptosis in the regulation of AKI would provide new perspectives and new strategies for AKI treatment.

## AUTHOR CONTRIBUTIONS

JZ contributed to the organization of the preparation, writing, reading, correction and submission of the manuscript, as well as

to the writing of the Abstract and Chapters 1, 2, and 4; BW and SY contributed to the writing of Chapter 3 and 5; JJ and QH contributed to the editing and reading of all manuscripts.

## FUNDING

This research was supported by the Construction of Key Projects by Zhejiang Provincial Ministry (Project No. WKJ-ZJ-2017), the Zhejiang Province Chinese Medicine Modernization Program

## REFERENCES

- Adedoyin, O., Boddu, R., Traylor, A., Lever, J. M., Bolisetty, S., George, J. F., et al. (2018). Heme Oxygenase-1 Mitigates Ferroptosis in Renal Proximal Tubule Cells. *Am. J. Physiology-Renal Physiology* 314, F702–F714. doi:10.1152/ajprenal.00044.2017
- Alvarez, S. W., Sviderskiy, V. O., Terzi, E. M., Papagiannakopoulos, T., Moreira, A. L., Adams, S., et al. (2017). NFS1 Undergoes Positive Selection in Lung Tumours and Protects Cells from Ferroptosis. *Nature* 551, 639–643. doi:10.1038/nature24637
- Anthonymuthu, T. S., Kenny, E. M., Shrivastava, I., Tyurina, Y. Y., Hier, Z. E., Ting, H.-C., et al. (2018). Empowerment of 15-Lipoxygenase Catalytic Competence in Selective Oxidation of Membrane ETE-PE to Ferroptotic Death Signals, HpETE-PE. *J. Am. Chem. Soc.* 140, 17835–17839. doi:10.1021/jacs.8b09913
- Bersuker, K., Hendricks, J. M., Li, Z., Magtanong, L., Ford, B., Tang, P. H., et al. (2019). The CoQ Oxidoreductase FSP1 Acts Parallel to GPX4 to Inhibit Ferroptosis. *Nature* 575, 688–692. doi:10.1038/s41586-019-1705-2
- Bosch, X., Poch, E., and Grau, J. M. (2009). Rhabdomyolysis and Acute Kidney Injury. *N. Engl. J. Med.* 361, 62–72. doi:10.1056/nejmra0801327
- Chang, T.-C., Wentzel, E. A., Kent, O. A., Ramachandran, K., Mullendore, M., Lee, K. H., et al. (2007). Transactivation of miR-34a by P53 Broadly Influences Gene Expression and Promotes Apoptosis. *Mol. Cell* 26, 745–752. doi:10.1016/j.molcel.2007.05.010
- Choi, N., Whitlock, R., Klassen, J., Zappitelli, M., Arora, R. C., Rigatto, C., et al. (2019). Early Intraoperative Iron-Binding Proteins Are Associated with Acute Kidney Injury after Cardiac Surgery. *J. Thorac. Cardiovasc. Surg.* 157, 287–297. e2. doi:10.1016/j.jtcvs.2018.06.091
- Córdoba-David, G., Duro-Castano, A., Castelo-Branco, R. C., González-Guerrero, C., Cannata, P., Sanz, A. B., et al. (2020). Effective Nephroprotection Against Acute Kidney Injury with a Star-Shaped Polyglutamate-Curcuminoid Conjugate. *Sci. Rep.* 10, 2056. doi:10.1038/s41598-020-58974-9
- Demuyne, R., Efimova, I., Naessens, F., and Krysko, D. (2021). Immunogenic Ferroptosis and where to Find it? *J. Immunother. cancer* 9, e003430. doi:10.1136/jitc-2021-003430
- Deng, F., Sharma, I., Dai, Y., Yang, M., and Kanwar, Y. S. (2019). Myo-inositol Oxygenase Expression Profile Modulates Pathogenic Ferroptosis in the Renal Proximal Tubule. *J. Clin. investigation* 129, 5033–5049. doi:10.1172/jci129903
- Ding, C., Ding, X., Zheng, J., Wang, B., Li, Y., Xiang, H., et al. (2020). miR-182-5p and miR-378a-3p Regulate Ferroptosis in I/R-induced Renal Injury. *Cell Death Dis.* 11, 929. doi:10.1038/s41419-020-03135-z
- Dixon, S. J., Lemberg, K. M., Lamprecht, M. R., Skouta, R., Zaitsev, E. M., Gleason, C. E., et al. (2012). Ferroptosis: an Iron-dependent Form of Nonapoptotic Cell Death. *Cell* 149, 1060–1072. doi:10.1016/j.cell.2012.03.042
- Doll, S., and Conrad, M. (2017). Iron and Ferroptosis: A Still Ill-defined Liaison. *IUBMB life* 69, 423–434. doi:10.1002/iub.1616
- Doll, S., Freitas, F. P., Shah, R., Aldrovandi, M., da Silva, M. C., Ingold, I., et al. (2019). FSP1 Is a Glutathione-independent Ferroptosis Suppressor. *Nature* 575, 693–698. doi:10.1038/s41586-019-1707-0
- Doll, S., Proneth, B., Tyurina, Y. Y., Panzilius, E., Kobayashi, S., Ingold, I., et al. (2017). ACSL4 Dictates Ferroptosis Sensitivity by Shaping Cellular Lipid Composition. *Nat. Chem. Biol.* 13, 91–98. doi:10.1038/nchembio.2239
- Franzin, R., Stasi, A., Fiorentino, M., Simone, S., Oberbauer, R., Castellano, G., et al. (2021). Renal Delivery of Pharmacologic Agents During Machine Perfusion to Prevent Ischaemia-Reperfusion Injury: From Murine Model to Clinical Trials. *Front. Immunol.* 12, 673562. doi:10.3389/fimmu.2021.673562
- (Project No. 2020ZX001), the Key Project of Scientific Research Foundation of Chinese Medicine (2022ZZ002), the Key project of Zhejiang Science and Technology Department (2022C03118), the Huadong Medicine Joint Funds of the Zhejiang Provincial Natural Science Foundation of China (Grant No. LHDMZ22H050001), the Key project of Basic Scientific Research Operating Funds of Hangzhou Medical College (KYZD202002) and the Clinical and Experimental Research of YSHS Granule.
- Gao, M., Yi, J., Zhu, J., Minikes, A. M., Monian, P., Thompson, C. B., et al. (2019). Role of Mitochondria in Ferroptosis. *Mol. Cell* 73, 354–e3. doi:10.1016/j.molcel.2018.10.042
- Gao, M., Monian, P., Quadri, N., Ramasamy, R., and Jiang, X. (2015). Glutaminolysis and Transferrin Regulate Ferroptosis. *Mol. Cell* 59, 298–308. doi:10.1016/j.molcel.2015.06.011
- Groebler, L. K., Liu, J., Shanu, A., Codd, R., and Witting, P. K. (2011). Comparing the Potential Renal Protective Activity of Desferrioxamine B and the Novel Chelator Desferrioxamine B-N-(3-hydroxyadamant-1-yl)carboxamide in a Cell Model of Myoglobinuria. *Biochem. J.* 435, 669–677. doi:10.1042/bj20101728
- Guerrero-Hue, M., García-Caballero, C., Palomino-Antolín, A., Rubio-Navarro, A., Vázquez-Carballo, C., Herencia, C., et al. (2019). Curcumin Reduces Renal Damage Associated with Rhabdomyolysis by Decreasing Ferroptosis-Mediated Cell Death. *FASEB J.* 33, 8961–8975. doi:10.1096/fj.201900077R
- Haase, M., Bellomo, R., and Haase-Fielitz, A. (2010). Novel Biomarkers, Oxidative Stress, and the Role of Labile Iron Toxicity in Cardiopulmonary Bypass-Associated Acute Kidney Injury. *J. Am. Coll. Cardiol.* 55, 2024–2033. doi:10.1016/j.jacc.2009.12.046
- Han, H., Wen, Z., Wang, J., Zhang, P., Gong, Q., Ge, S., et al. (2021). Prediction of Short-Term Mortality with Renal Replacement Therapy in Patients with Cardiac Surgery-Associated Acute Kidney Injury. *Front. Cardiovasc. Med.* 8, 738947. doi:10.3389/fcvm.2021.738947
- Heintzman, D., Fisher, E., and Rathmell, J. (2022). Microenvironmental Influences on T Cell Immunity in Cancer and Inflammation. *Cell. Mol. Immunol.* 19, 316. doi:10.1038/s41423-021-00833-2
- Huang, L. L., Liao, X. h., Sun, H., Jiang, X., Liu, Q., and Zhang, L. (2019). Augmenter of Liver Regeneration Protects the Kidney from Ischaemia-reperfusion Injury in Ferroptosis. *J. Cell Mol. Med.* 23, 4153–4164. doi:10.1111/jcmm.14302
- Jiang, L., Kon, N., Li, T., Wang, S.-J., Su, T., Hibshoosh, H., et al. (2015). Ferroptosis as a P53-Mediated Activity during Tumour Suppression. *Nature* 520, 57–62. doi:10.1038/nature14344
- Jiang, X., Guo, S., Zhang, Y., Zhao, Y., Li, X., Jia, Y., et al. (2020). LncRNA NEAT1 Promotes Docetaxel Resistance in Prostate Cancer by Regulating ACSL4 via Sponging miR-34a-5p and miR-204-5p. *Cell. Signal.* 65, 109422. doi:10.1016/j.cellsig.2019.109422
- Kagan, V. E., Mao, G., Qu, F., Angeli, J. P. F., Doll, S., Croix, C. S., et al. (2017). Oxidized Arachidonic and Adrenic PEs Navigate Cells to Ferroptosis. *Nat. Chem. Biol.* 13, 81–90. doi:10.1038/nchembio.2238
- Kang, Y. P., Mockabee-Macias, A., Jiang, C., Falzone, A., Prieto-Farigua, N., Stone, E., et al. (2021). Non-canonical Glutamate-Cysteine Ligase Activity Protects against Ferroptosis. *Cell metab.* 33, 174–189. e7. doi:10.1016/j.cmet.2020.12.007
- Kwon, M.-Y., Park, E., Lee, S.-J., and Chung, S. W. (2015). Heme Oxygenase-1 Accelerates Erastin-Induced Ferroptotic Cell Death. *Oncotarget* 6, 24393–24403. doi:10.18632/oncotarget.5162
- Lai, C. C., Huang, P. H., Yang, A. H., Chiang, S. C., Tang, C. Y., Tseng, K. W., et al. (2016). Baicalein, a Component of Scutellaria Baicalensis, Attenuates Kidney Injury Induced by Myocardial Ischemia and Reperfusion. *Planta Med.* 82, 181–189. doi:10.1055/s-0035-1558114
- Leaf, D. E., Rajapurkar, M., Lele, S. S., Mukhopadhyay, B., Boerger, E. A. S., Mc Causland, F. R., et al. (2019). Iron, Hepcidin, and Death in Human AKI. *J. Am. Soc. Nephrol.* 30, 493–504. doi:10.1681/asn.2018100979
- Lee, T., Lee, C., Chen, J., Fan, P., Tu, Y., Yen, C., et al. (2021). Assessment of Cardiopulmonary Bypass Duration Improves Novel Biomarker Detection for Predicting Postoperative Acute Kidney Injury after Cardiovascular Surgery. *J. Clin. Med.* 10, 2741. doi:10.3390/jcm10132741
- Li, J.-y., Liu, S.-q., Yao, R.-q., Tian, Y.-p., and Yao, Y.-m. (2021). A Novel Insight into the Fate of Cardiomyocytes in Ischemia-Reperfusion Injury: From Iron

- Metabolism to Ferroptosis. *Front. Cell Dev. Biol.* 9, 799499. doi:10.3389/fcell.2021.799499
- Li, X., Zou, Y., Xing, J., Fu, Y. Y., Wang, K. Y., Wan, P. Z., et al. (2020). Pretreatment with Roxadustat (FG-4592) Attenuates Folic Acid-Induced Kidney Injury through Antiferroptosis via Akt/GSK-3 $\beta$ /Nrf2 Pathway. *Oxid. Med. Cell Longev.* 2020, 6286984. doi:10.1155/2020/6286984
- Li, X., Zou, Y., Fu, Y.-Y., Xing, J., Wang, K.-Y., Wan, P.-Z., et al. (2021). A-Lipoic Acid Alleviates Folic Acid-Induced Renal Damage through Inhibition of Ferroptosis. *Front. Physiol.* 12, 680544. doi:10.3389/fphys.2021.680544
- Linkermann, A. (2016). Nonapoptotic Cell Death in Acute Kidney Injury and Transplantation. *Kidney Int.* 89, 46–57. doi:10.1016/j.kint.2015.10.008
- Liu, Y., and Gu, W. (2022). p53 in Ferroptosis Regulation: the New Weapon for the Old Guardian. *Cell Death Differ.* 29, 895–910. doi:10.1038/s41418-022-00943-y
- Liu, Y., and Gu, W. (2021). The Complexity of P53-Mediated Metabolic Regulation in Tumor Suppression. *Semin. Cancer Biol.* S1044-579X (21), 00060–00062. doi:10.1016/j.semcancer.2021.03.010
- Ma, D., Li, C., Jiang, P., Jiang, Y., Wang, J., and Zhang, D. (2021). Inhibition of Ferroptosis Attenuates Acute Kidney Injury in Rats with Severe Acute Pancreatitis. *Dig. Dis. Sci.* 66, 483–492. doi:10.1007/s10620-020-06225-2
- Martin-Sanchez, D., Ruiz-Andres, O., Poveda, J., Carrasco, S., Cannata-Ortiz, P., Sanchez-Niño, M. D., et al. (2017). Ferroptosis, but Not Necroptosis, Is Important in Nephrotoxic Folic Acid-Induced AKI. *J. Am. Soc. Nephrol.* 28, 218–229. doi:10.1681/asn.2015121376
- Martines, A. M. F., Masereeuw, R., Tjalsma, H., Hoenderop, J. G., Wetzels, J. F. M., and Swinkels, D. W. (2013). Iron Metabolism in the Pathogenesis of Iron-Induced Kidney Injury. *Nat. Rev. Nephrol.* 9, 385–398. doi:10.1038/nrneph.2013.98
- Messerer, D. A. C., Halbgebauer, R., Nilsson, B., Pavenstädt, H., Radermacher, P., and Huber-Lang, M. (2021). Immunopathophysiology of Trauma-Related Acute Kidney Injury. *Nat. Rev. Nephrol.* 17, 91–111. doi:10.1038/s41581-020-00344-9
- Mishima, E., Sato, E., Ito, J., Yamada, K.-i., Suzuki, C., Oikawa, Y., et al. (2020). Drugs Repurposed as Antiferroptosis Agents Suppress Organ Damage, Including AKI, by Functioning as Lipid Peroxyl Radical Scavengers. *J. Am. Soc. Nephrol.* 31, 280–296. doi:10.1681/asn.2019060570
- Moon, S.-H., Huang, C.-H., Houlihan, S. L., Regunath, K., Freed-Pastor, W. A., Morris, J. P., et al. (2019). p53 Represses the Mevalonate Pathway to Mediate Tumor Suppression. *Cell* 176, 564–580. e19. doi:10.1016/j.cell.2018.11.011
- Mou, Y., Wang, J., Wu, J., He, D., Zhang, C., Duan, C., et al. (2019). Ferroptosis, a New Form of Cell Death: Opportunities and Challenges in Cancer. *J. Hematol. Oncol.* 12, 34. doi:10.1186/s13045-019-0720-y
- Nieuwenhuijs-Moeke, G. J., Pischke, S. E., Berger, S. P., Sanders, J. S. F., Pol, R. A., Struys, M. M. R. F., et al. (2020). Ischemia and Reperfusion Injury in Kidney Transplantation: Relevant Mechanisms in Injury and Repair. *J. Clin. Med.* 9, 253. doi:10.3390/jcm9010253
- Sharma, S., and Leaf, D. E. (2019). Iron Chelation as a Potential Therapeutic Strategy for AKI Prevention. *J. Am. Soc. Nephrol.* 30, 2060–2071. doi:10.1681/asn.2019060595
- Shimada, K., Skouta, R., Kaplan, A., Yang, W. S., Hayano, M., Dixon, S. J., et al. (2016). Global Survey of Cell Death Mechanisms Reveals Metabolic Regulation of Ferroptosis. *Nat. Chem. Biol.* 12, 497–503. doi:10.1038/nchembio.2079
- Song, X., Zhu, S., Chen, P., Hou, W., Wen, Q., Liu, J., et al. (2018). AMPK-Mediated BECN1 Phosphorylation Promotes Ferroptosis by Directly Blocking System Xc- Activity. *Curr. Biol.* 28, 2388–2399. e5. doi:10.1016/j.cub.2018.05.094
- Su, L., Jiang, X., Yang, C., Zhang, J., Chen, B., Li, Y., et al. (2019). Pannexin 1 Mediates Ferroptosis that Contributes to Renal Ischemia/reperfusion Injury. *J. Biol. Chem.* 294, 19395–19404. doi:10.1074/jbc.ra119.010949
- Swaminathan, S. (2018). Iron Homeostasis Pathways as Therapeutic Targets in Acute Kidney Injury. *Nephron* 140, 156–159. doi:10.1159/000490808
- Szymonik, J., Wala, K., Górnicki, T., Saczko, J., Pencakowski, B., and Kulbacka, J. (2021). The Impact of Iron Chelators on the Biology of Cancer Stem Cells. *Int. J. Mol. Sci.* 23, 89. doi:10.3390/ijms23010089
- Tang, C., Ma, Z., Zhu, J., Liu, Z., Liu, Y., Liu, Y., et al. (2019). P53 in Kidney Injury and Repair: Mechanism and Therapeutic Potentials. *Pharmacol. Ther.* 195, 5–12. doi:10.1016/j.pharmthera.2018.10.013
- Tang, D., Chen, X., Kang, R., and Kroemer, G. (2021). Ferroptosis: Molecular Mechanisms and Health Implications. *Cell Res.* 31, 107–125. doi:10.1038/s41422-020-00441-1
- Tarangelo, A., Magtanong, L., Bieging-Rolett, K. T., Li, Y., Ye, J., Attardi, L. D., et al. (2018). p53 Suppresses Metabolic Stress-Induced Ferroptosis in Cancer Cells. *Cell Rep.* 22, 569–575. doi:10.1016/j.celrep.2017.12.077
- Thévenod, F., Lee, W.-K., and Garrick, M. D. (2020). Iron and Cadmium Entry into Renal Mitochondria: Physiological and Toxicological Implications. *Front. Cell Dev. Biol.* 8, 848. doi:10.3389/fcell.2020.00848
- Tonnus, W., and Linkermann, A. (2017). The *In Vivo* Evidence for Regulated Necrosis. *Immunol. Rev.* 277, 128–149. doi:10.1111/imr.12551
- Tonnus, W., Meyer, C., Steinebach, C., Belavgeni, A., von Mässenhausen, A., Gonzalez, N. Z., et al. (2021). Dysfunction of the Key Ferroptosis-Surveillance Systems Hypersensitizes Mice to Tubular Necrosis during Acute Kidney Injury. *Nat. Commun.* 12, 4402. doi:10.1038/s41467-021-24712-6
- van Swelm, R. P. L., Wetzels, J. F. M., and Swinkels, D. W. (2020). The Multifaceted Role of Iron in Renal Health and Disease. *Nat. Rev. Nephrol.* 16, 77–98. doi:10.1038/s41581-019-0197-5
- Wang, S., Luo, J., Zhang, Z., Dong, D., Shen, Y., Fang, Y., et al. (2018). Iron and Magnetic: New Research Direction of the Ferroptosis-Based Cancer Therapy. *Am. J. Cancer Res.* 8, 1933–1946.
- Wang, Y., and Tao, Y. (2015). Research Progress on Regulatory T Cells in Acute Kidney Injury. *J. Immunol. Res.* 2015, 174164. doi:10.1155/2015/174164
- Xie, Y., Hou, W., Song, X., Yu, Y., Huang, J., Sun, X., et al. (2016). Ferroptosis: Process and Function. *Cell Death Differ.* 23, 369–379. doi:10.1038/cdd.2015.158
- Xie, Y., Song, X., Sun, X., Huang, J., Zhong, M., Lotze, M. T., et al. (2016). Identification of Baicalein as a Ferroptosis Inhibitor by Natural Product Library Screening. *Biochem. biophysical Res. Commun.* 473, 775–780. doi:10.1016/j.bbrc.2016.03.052
- Yagoda, N., von Rechenberg, M., Zaganjori, E., Bauer, A. J., Yang, W. S., Fridman, D. J., et al. (2007). RAS-RAF-MEK-dependent Oxidative Cell Death Involving Voltage-dependent Anion Channels. *Nature* 447, 864–868. doi:10.1038/nature05859
- Yang, L., Wang, H., Yang, X., Wu, Q., An, P., Jin, X., et al. (2020). Auranofin Mitigates Systemic Iron Overload and Induces Ferroptosis via Distinct Mechanisms. *Sig Transduct. Target Ther.* 5, 138. doi:10.1038/s41392-020-00253-0
- Yao, X., Li, W., Fang, D., Xiao, C., Wu, X., Li, M., et al. (2021). Emerging Roles of Energy Metabolism in Ferroptosis Regulation of Tumor Cells. *Adv. Sci. Wein* 8, e2100997. Baden-Württemberg, Germany. doi:10.1002/adv.202100997
- Yu, H., Guo, P., Xie, X., Wang, Y., and Chen, G. (2017). Ferroptosis, a New Form of Cell Death, and its Relationships with Tumorous Diseases. *J. Cell. Mol. Med.* 21, 648–657. doi:10.1111/jcmm.13008
- Zarjou, A., Bolisetty, S., Joseph, R., Traynor, A., Apostolov, E. O., Arosio, P., et al. (2013). Proximal Tubule H-Ferritin Mediates Iron Trafficking in Acute Kidney Injury. *J. Clin. Invest.* 123, 4423–4434. doi:10.1172/jci67867
- Zeng, W., and Tomlinson, B. (2021). Causes and Outcome of Rhabdomyolysis in Patients Admitted to Medical Wards in the Prince of Wales Hospital. *Ann. Transl. Med.* 9, 1329. doi:10.21037/atm-21-3660
- Zhou, F., Yang, Y., Luo, L., Chen, Y., Luo, Q., and Chen, J. (2020). Impact of Prolonged Mechanical Ventilation on Ferroptosis in Renal Ischemia/Reperfusion Injury in Rats. *Biomed. Res. Int.* 2020, 6097516. doi:10.1155/2020/6097516
- Zhou, R.-P., Chen, Y., Wei, X., Yu, B., Xiong, Z.-G., Lu, C., et al. (2020). Novel Insights into Ferroptosis: Implications for Age-Related Diseases. *Theranostics* 10, 11976–11997. doi:10.7150/thno.50663
- Zilka, O., Shah, R., Li, B., Friedmann Angeli, J. P., Griesser, M., Conrad, M., et al. (2017). On the Mechanism of Cytoprotection by Ferrostatin-1 and Liproxstatin-1 and the Role of Lipid Peroxidation in Ferroptotic Cell Death. *ACS Cent. Sci.* 3, 232–243. doi:10.1021/acscentsci.7b00028

**Conflict of Interest:** The authors declare that the research was conducted in the absence of any commercial or financial relationships that could be construed as a potential conflict of interest.

**Publisher's Note:** All claims expressed in this article are solely those of the authors and do not necessarily represent those of their affiliated organizations, or those of the publisher, the editors and the reviewers. Any product that may be evaluated in this article, or claim that may be made by its manufacturer, is not guaranteed or endorsed by the publisher.

Copyright © 2022 Zhang, Wang, Yuan, He and Jin. This is an open-access article distributed under the terms of the Creative Commons Attribution License (CC BY). The use, distribution or reproduction in other forums is permitted, provided the original author(s) and the copyright owner(s) are credited and that the original publication in this journal is cited, in accordance with accepted academic practice. No use, distribution or reproduction is permitted which does not comply with these terms.



# Development and Validation of a Novel Ferroptosis-Related Gene Signature for Prognosis and Immunotherapy in Hepatocellular Carcinoma

Bo Zhang<sup>1,2†</sup>, Jilong Zhao<sup>1,2†</sup>, Bing Liu<sup>1,2†</sup>, Yanan Shang<sup>1,2†</sup>, Fei Chen<sup>1,2</sup>, Sidi Zhang<sup>1,2</sup>, Jiayao He<sup>1,3</sup>, Yumei Fan<sup>1,2\*</sup> and Ke Tan<sup>1,2\*</sup>

<sup>1</sup>Key Laboratory of Molecular and Cellular Biology of Ministry of Education, College of Life Sciences, Hebei Normal University, Shijiazhuang, China, <sup>2</sup>Key Laboratory of Animal Physiology, Biochemistry and Molecular Biology of Hebei Province, College of Life Sciences, Hebei Normal University, Shijiazhuang, China, <sup>3</sup>Department of Neurosurgery, Handan Central Hospital, Hebei Medical University, Shijiazhuang, China

## OPEN ACCESS

### Edited by:

Yanqing Liu,  
Columbia University, United States

### Reviewed by:

Haiqing Zhao,  
Columbia University Irving Medical  
Center, United States  
Xiaolu Zhu,  
Columbia University, United States

### \*Correspondence:

Yumei Fan  
fanyumei@hebtu.edu.cn  
Ke Tan  
tanke@hebtu.edu.cn

<sup>†</sup>These authors have contributed  
equally to this work

### Specialty section:

This article was submitted to  
Molecular Diagnostics and  
Therapeutics,  
a section of the journal  
Frontiers in Molecular Biosciences

**Received:** 10 May 2022

**Accepted:** 07 June 2022

**Published:** 30 June 2022

### Citation:

Zhang B, Zhao J, Liu B, Shang Y,  
Chen F, Zhang S, He J, Fan Y and  
Tan K (2022) Development and  
Validation of a Novel Ferroptosis-  
Related Gene Signature for Prognosis  
and Immunotherapy in  
Hepatocellular Carcinoma.  
Front. Mol. Biosci. 9:940575.  
doi: 10.3389/fmolb.2022.940575

Hepatocellular carcinoma (HCC) is a cancer that is sensitive to ferroptosis, and immunotherapy has emerged as a promising treatment for HCC patients. However, the prognostic potential of ferroptosis-related genes (FRGs) and the effect of ferroptosis on the tumor immune microenvironment in HCC remain largely obscure. Here, we analyzed the expression pattern of FRGs using the TCGA, ICGC and GEO databases. The expression of most FRGs was upregulated in HCC tissues compared with normal liver tissues. Three independent clusters were determined by consensus clustering analysis based on FRG expression in HCC. Cluster 3 exhibited higher expression, unfavorable prognosis, and higher histological tumor stage and grade than clusters 1 and 2. CIBERSORT analysis indicated different infiltrating levels of various immune cells among the three clusters. Moreover, most immune checkpoint genes were highly expressed in cluster 3. Univariate Cox regression and LASSO regression analyses were performed to develop a five FRG-based prognostic risk model using the TCGA and ICGC datasets. Kaplan–Meier analysis and ROC curves were performed to verify the prognostic potential of the risk model. A nomogram containing independent prognostic factors was further developed. Compared with low-risk patients, high-risk HCC patients exhibited worse overall survival (OS). In addition, this risk model was significantly correlated with the infiltrating levels of six major types of immune cells in HCC. Finally, the relationships between the five FRGs and drug sensitivity were investigated. The present study suggests that the five FRGs could elucidate the molecular mechanisms of HCC and lead to a new direction for the improvement of predictive, preventive, and personalized medicine for HCC.

**Keywords:** ferroptosis, hepatocellular carcinoma, prognosis, FRG signature, immune infiltration

## INTRODUCTION

Primary liver cancer is a global, pathological and fatal malignancy, with approximately 906,000 new liver cancer cases and 830,000 deaths according to the statistics of GLOBOCAN in 2020 (Sung et al., 2021). Liver cancer is the sixth most frequently diagnosed cancer and ranks as the third leading cause of cancer-related death in the world. Hepatocellular carcinoma (HCC) is the most common



histological type of primary liver cancer, accounting for approximately 90% of cases (Forner et al., 2018). Over the decades, great progress has been achieved in multidisciplinary treatments, including surgery, liver transplantation, chemotherapy, radiotherapy, monoclonal antibody therapy and immunotherapy. However, the overall survival (OS) rate of HCC patients remains to be further improved, especially for advanced-stage HCC patients (Forner et al., 2018; Sung et al., 2021). Therefore, it is urgent to discover more effective prognostic models and therapeutic targets for HCC. The rapid development of bioinformatics has undoubtedly provided important methods and platforms for screening prognostic biomarkers in cancer patients.

Successful avoidance of programmed cell death, such as apoptosis, necrosis and autophagic cell death, is a major common feature of cancer. The discovery of a new form of regulatory cell death called ferroptosis, provides new therapeutic targets and strategies for human tumors (Dixon et al., 2012). The occurrence of ferroptosis depends on the lethal accumulation of cellular iron, the overwhelming generation of reactive oxygen species (ROS), lipid peroxidation and the unbalanced oxidative stress response (Chen J. et al., 2022). As research continues to expand and deepen, an increasing number of genes and signaling pathways that regulate ferroptosis are gradually being discovered (Chen X. et al., 2021; Li et al., 2021; Zhang et al., 2021). Accumulating evidence implies that ferroptosis is closely associated with the development and progression of diverse human cancers, including HCC (Liu et al., 2021; Lei et al., 2022). Sorafenib, a multikinase inhibitor, is the first-line drug for HCC patients that induces apoptosis, inhibits cell proliferation, and suppresses angiogenesis. Interestingly, recent studies have found that sorafenib could induce ferroptotic cell death in HCC, which adds a piece to the puzzle of its anticancer mechanisms (Gao et al., 2021; Wang Q. et al., 2021). In addition to sorafenib, an increasing number of small molecules or drugs have been identified to induce ferroptosis through different targets or signaling pathways in HCC (Nie et al., 2018). Many genes have been identified as suppressors or drivers in the development of HCC and of ferroptosis in HCC. NRF2 protects HCC cells from sorafenib- or erastin-induced ferroptosis by upregulating the expression of different antioxidants, such as NQO1, HO-1 and FTH1 (Sun et al., 2016b). Mechanistically, erastin or sorafenib treatment inhibited the degradation of NRF2, increased the nuclear translocation of NRF2 and facilitated the interaction between NRF2 and its transcriptional coactivator (Sun et al., 2016b). Metallothionein-1G is a suppressor of ferroptosis in HCC and could serve as a promising therapeutic target in sorafenib-resistant HCC cells (Sun et al., 2016a). The increased expression of metallothionein-1G could mediate GSH depletion and lipid peroxidation without affecting the intracellular iron concentrations. CDGSH iron sulfur domain 1 (CISD1) negatively modulates ferroptosis by limiting mitochondrial iron uptake and alleviating lipid peroxidation (Yuan et al., 2016). ACSL4 was identified as an important determinant of ferroptosis sensitivity (Doll et al., 2017). The ACSL4 protein level was significantly and negatively correlated

with the half-maximal inhibitory concentration (IC<sub>50</sub>) value of sorafenib in a panel of HCC cell lines (Feng et al., 2021). Silencing ACSL4 inhibited sorafenib-induced lipid peroxidation and ferroptotic cell death in HCC cells, indicating that ACSL4 may be a potential predictive biomarker of HCC. Moreover, ETS proto-oncogene 1 (EST1)-mediated upregulation of miR-23a-3p suppressed ACSL4 transcription by directly binding to the 3'-UTR of ACSL4 (Lu et al., 2022). Inhibition of miR-23a-3p triggered ferroptosis by rescuing the expression of ACSL4 in sorafenib-treated cells (Lu et al., 2022). Glycolytic enzyme enolase 1 (ENO1), acting as an RNA-binding protein, facilitates the mRNA degradation of IRP1 to mediate iron homeostasis, inhibits the expression of mitoferrin-1 (Mfrn1) and suppresses ferroptosis in HCC cells, suggesting that the ENO1-IRP1-Mfrn1 axis regulates the pathogenesis of HCC and ferroptotic cell death (Zhang et al., 2022). Copper metabolism MURR1 domain 10 (COMMD10) suppressed HIF1 $\alpha$  degradation and the nuclear translocation of HIF1 $\alpha$ , thus inhibiting the transcription of ceruloplasmin and SLC7A11 to increase ferroptosis and radiosensitivity by disrupting Cu-Fe homeostasis in HCC (Yang et al., 2022). Additionally, CRISPR-based loss-of-function genetic screens identified phosphoserine-tRNA kinase (PSTK) as a regulator of ferroptosis by inactivating GPX4 and disrupting glutathione metabolism in HCC (Chen Y. et al., 2022). Nevertheless, the relationships between ferroptosis-associated genes and the prognosis of HCC patients still need to be deeply explored.

The present study systematically examined the differential expression of ferroptosis-related genes (FRGs) in HCC and investigated the relationships between the FRG signature and the prognosis and tumor microenvironment (TME) of HCC patients. Clustering subgroups and a five-FRG model were established to optimize prognostic risk stratification. Moreover, the clinical features, risk score, immune cell infiltration, immune microenvironment and drug sensitivity of the five FRGs were thoroughly analyzed to deeply evaluate the effects of the FRGs in HCC. In conclusion, this study attempts to explore the prognostic power of FRGs and immunotherapy strategies for patients with HCC.

## MATERIALS AND METHODS

### Data Collection and Processing

The RNA sequencing (RNA-seq) data (level 3) and corresponding clinical information of HCC patients were obtained from The Cancer Genome Atlas (TCGA) database (<https://portal.gdc.cancer.gov>), including 371 HCC cancer samples and 50 normal samples. The RNA-seq data of 226 normal human liver samples were downloaded from the Genotype-Tissue Expression (GTEx) database. Moreover, the RNA-seq data and clinical information from the external validation cohort were extracted from the International Cancer Gene Consortium (ICGC) database (<https://dcc.icgc.org/releases/current/Projects>, including 240 HCC samples and 202 normal samples), GSE36376 (240 HCC samples and 193 normal liver samples) and GSE10143 (80 HCC samples and 307 normal liver samples) datasets.

## Analysis of the Expression of Ferroptosis-Related Genes

A total of 25 FRGs were obtained from a previous study to systematically analyze the aberrances and functional implications of ferroptosis in HCC (Liu et al., 2020). Differential gene expression analysis was performed by comparing HCC tissues and normal liver tissues using the R packages ggplot2 and pheatmap in the TCGA and ICGC datasets. The Wilcoxon test was used to assess the significance between two groups.

## Immunohistochemistry Analysis

The protein levels in HCC tissues and normal liver tissues from the online Human Protein Atlas (HPA) database (<https://www.proteinatlas.org/>) were obtained based on immunohistochemical (IHC) staining results.

## Analysis of the Protein–Protein Interaction Network

With the aim of analyzing the Protein–Protein Interaction (PPI) network between different genes, the STRING (<https://string-db.org/>) online platform was used to evaluate the interactions among FRGs in HCC (Fan et al., 2021). The Metascape online platform was used in the construction of a visual PPI network. Subsequently, Gene Ontology (GO) and Kyoto Encyclopedia of Genes and Genomes (KEGG) enrichment analyses of FRGs were performed using Metascape.

## Ferroptosis-Related Gene-Based Consensus Clustering Analysis

The number of unsupervised clusters and their stability in the TCGA and ICGC datasets were estimated based on the mRNA expression profiles of 25 FRGs with the consensus clustering method using the ConsensusClusterPlus package (v1.54.0). The maximum number of clusters was 6, and 80% of the total samples were drawn 100 times. The R software package pheatmap (v1.0.12) was used for clustering heatmaps. The R (v4.0.3) packages survival and survminer were used for the Kaplan–Meier survival analyses of different subtypes.

## Construction and Validation of a Prognostic Ferroptosis-Related Gene Signature

Univariate Cox analysis of the OS of HCC patients was first carried out to identify FRGs with prognostic potential in HCC with the threshold of  $p < 0.01$ . A prognostic risk signature of 5 differential FRGs was established by using least absolute shrinkage and selection operator (LASSO) regression analysis in the TCGA training and ICGC validation cohorts. The risk scores of HCC patients were calculated according to the normalized expression level of each FRG and its corresponding regression coefficient. The equation was established as follows: risk score = sum of coefficients  $\times$  prognostic FRGs expression levels. According to this equation, the risk score of each patient was separately calculated in the

TCGA training and ICGC validation cohorts. Subsequently, the patients were stratified into high- and low-risk groups, and the median value of the risk score was set as the cutoff point.

The predictive ability of the nomogram and other clinical parameters (age, sex, TNM stage and grade) for the 1-, 3- and 5-year OS of patients was investigated. Calibration curves were carried out to illustrate the uniformity between the actual outcome and the predicted outcome of the model.

## Evaluation of Immune Cell Infiltration Levels in Hepatocellular Carcinoma

Immune cell infiltration scores were calculated based on the CIBERSORT and TIMER algorithms and were compared between the two risk groups. The infiltration levels of different immune cells in each HCC sample were investigated using the R package immunedeconv. The results of the heatmap were exhibited by the R package pheatmap. The Kruskal–Wallis test was used to assess the significance of the three groups. In addition, the expression of the immune checkpoint genes in three subgroups was examined using the R packages ggplot2 and pheatmap. The expression differences of the key immune checkpoint molecules, including PD-1, CTLA-4 and PD-L1, in the high- and low-risk groups were further analyzed using the R packages ggplot2 and pheatmap. The Wilcoxon test was used to assess the significance between two groups.

## Prediction of the Immunotherapeutic Response

The Tumor Immune Dysfunction and Exclusion (TIDE) score was used to predict the potential clinical immunotherapy response of HCC patients using the R (v4.0.3) packages ggplot2 and ggpubr. TIDE is an algorithm for predicting the clinical response to immune checkpoint inhibitors using TCGA RNA-seq data and the corresponding clinical information of HCC patients.

## Genomics of Drug Sensitivity in Cancer Database

Based on Genomics of Drug Sensitivity in Cancer (GDSC) 2016 ([www.cancerrxgene.org/](http://www.cancerrxgene.org/)), the chemotherapeutic sensitivity according to the IC50 value of each HCC sample was estimated using the R package pRRophetic. We investigated the different sensitivities of common liver cancer chemotherapy drugs between the high-expression group and the low-expression group.

## Statistical Analysis

All bioinformatic statistical analyses of the present study were performed in R (v4.0.3) software. Differences between the high- and low-risk groups were compared through the Wilcoxon test. Differences in three different groups were compared through the Kruskal–Wallis test. Kaplan–Meier curve analysis was performed by the log-rank test to compare the survival of HCC patients. Pearson correlation analysis was also performed to calculate the correlation coefficient between two variables.

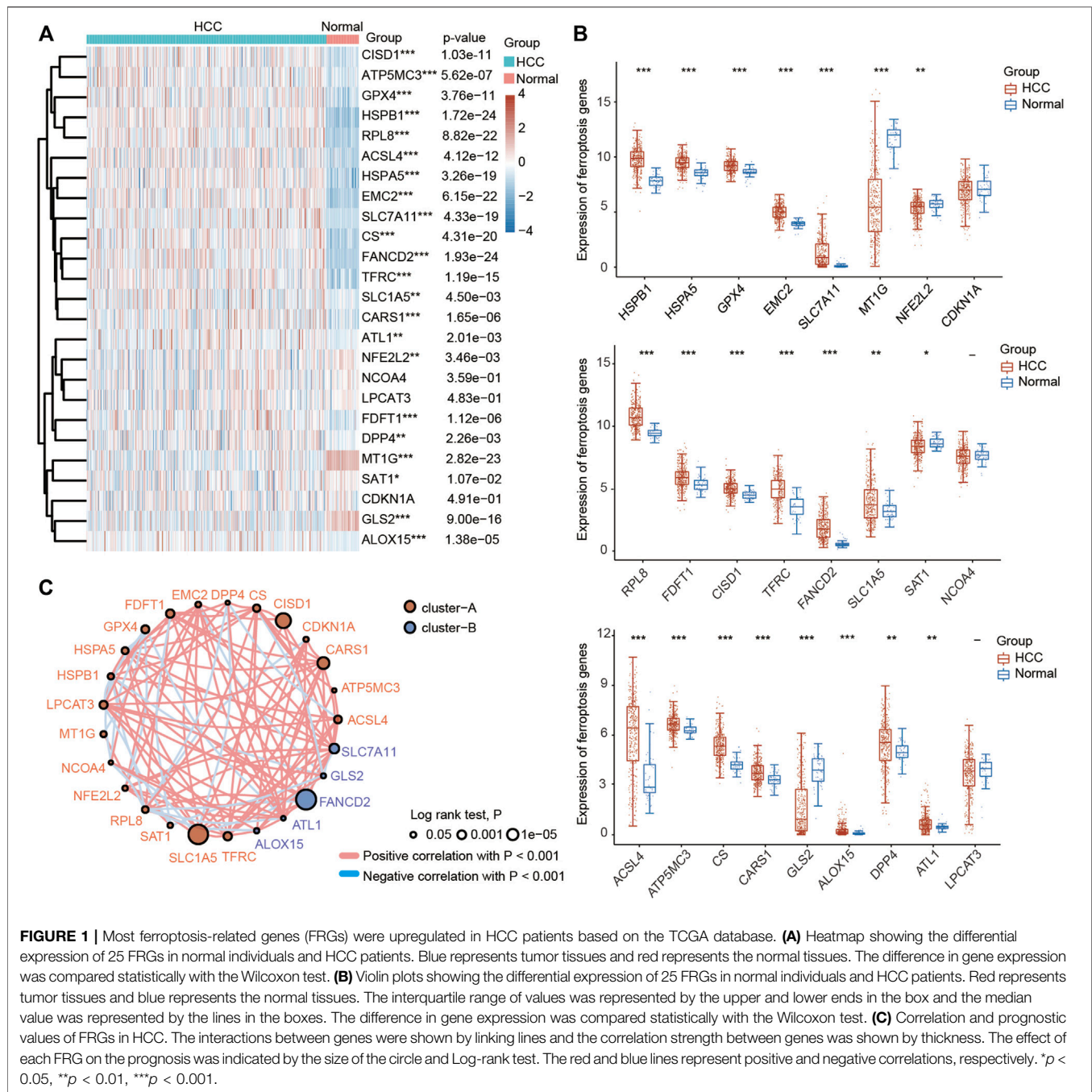


**FIGURE 1 |** Most ferroptosis-related genes (FRGs) were upregulated in HCC patients based on the TCGA database. **(A)** Heatmap showing the differential expression of 25 FRGs in normal individuals and HCC patients. Blue represents tumor tissues and red represents the normal tissues. The difference in gene expression was compared statistically with the Wilcoxon test. **(B)** Violin plots showing the differential expression of 25 FRGs in normal individuals and HCC patients. Red represents tumor tissues and blue represents the normal tissues. The interquartile range of values was represented by the upper and lower ends in the box and the median value was represented by the lines in the boxes. The difference in gene expression was compared statistically with the Wilcoxon test. **(C)** Correlation and prognostic values of FRGs in HCC. The interactions between genes were shown by linking lines and the correlation strength between genes was shown by thickness. The effect of each FRG on the prognosis was indicated by the size of the circle and Log-rank test. The red and blue lines represent positive and negative correlations, respectively. \* $p < 0.05$ , \*\* $p < 0.01$ , \*\*\* $p < 0.001$ .

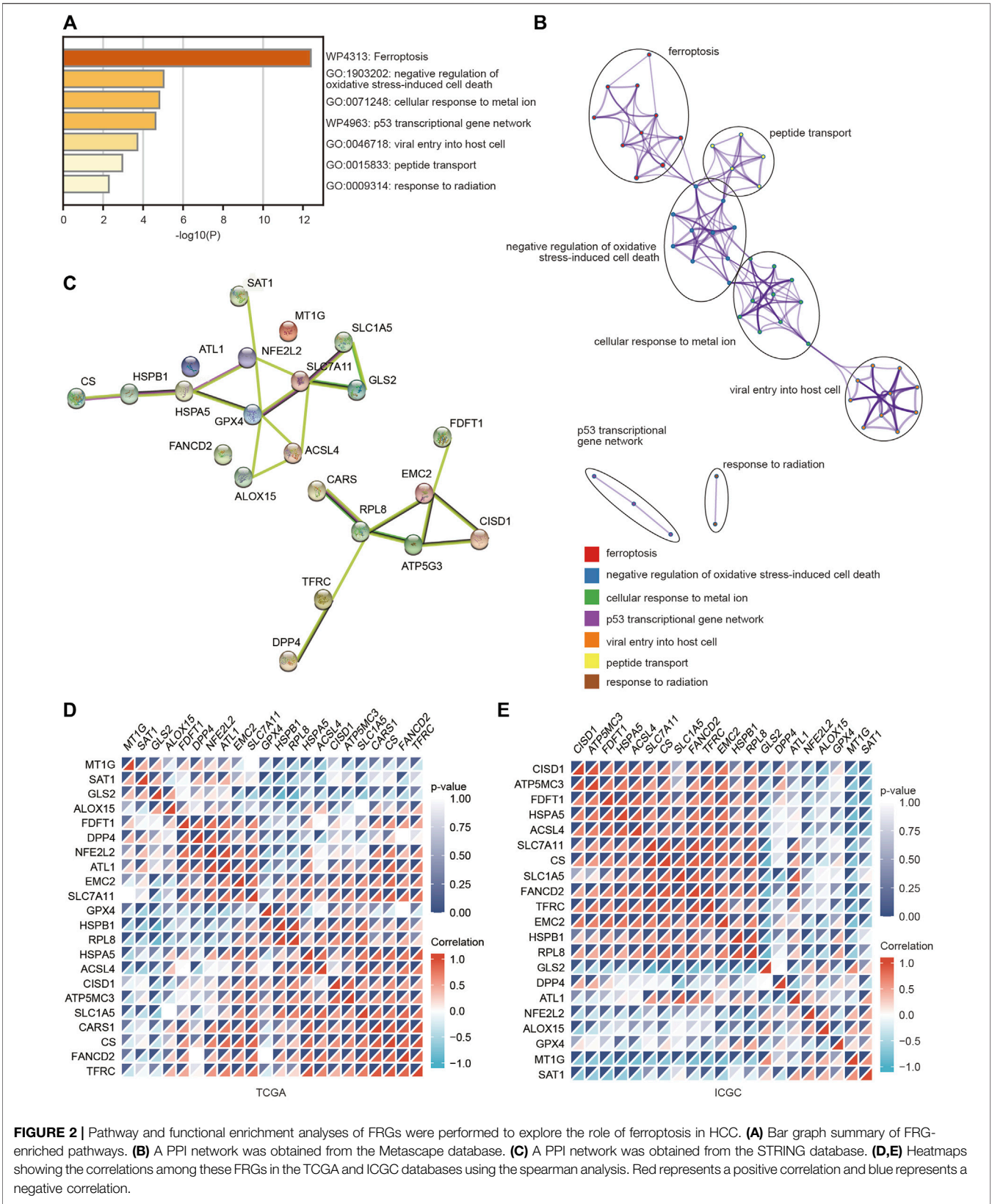
## RESULTS

### Expression of Ferroptosis-Related Genes in Hepatocellular Carcinoma in the The Cancer Genome Atlas Database

A previous study identified twenty-four genes that play important roles in modulating ferroptotic cell death (Liu et al., 2020). To explore the function of ferroptosis in HCC, we first investigated

the differential expression of these ferroptosis regulator genes in HCC tissues and normal liver tissues using the TCGA database. As shown in **Figures 1A,B**, the expression of HSPA5, EMC2, SLC7A11, HSPB1, GPX4, FANCD2, CISD1, FDFT1, SLC1A5, TFRC, RPL8, DPP4, CS, CARS1, ATP5MC3, ALOX15, ACSL4 and ATL1 was significantly increased in HCC tissues compared with normal liver tissues. In contrast, the expression of NFE2L2, MT1G, SAT1 and GLS2 was greatly decreased in HCC tissues compared with normal liver tissues. In addition, the results of the







correlation analysis combined with gene expression and prognosis indicated that most FRGs were positively associated with HCC and exhibited prognostic value in HCC (Figure 1C).

## Validation of the Changed Expression of Ferroptosis-Related Genes in the International Cancer Gene Consortium Database

To confirm the results obtained from the TCGA database, we further evaluated the expression levels of these FRGs using the ICGC database. Consistent with the results obtained from the TCGA database, we found that the expression levels of HSPA5, EMC2, SLC7A11, HSPB1, GPX4, FANCD2, C1SD1, FDFT1, SLC1A5, TFRC, RPL8, LPCAT3, DPP4, CS, CARS1, ATP5MC3, ALOX15, ACSL4 and ATL1 were higher in HCC tissues than in normal liver tissues, while the expression levels of CDKN1A, NFE2L2, MT1G, SAT1 and GLS2 were obviously lower in HCC tissues than in normal liver tissues (Supplementary Figures S1A,B). Moreover, the expression of most ferroptosis regulators was positively correlated with prognosis in HCC according to the ICGC database (Supplementary Figure S1C). In addition, the differential expression of these FRGs was further confirmed by the GSE10143 and GSE36376 datasets (Supplementary Figures 2A,B).

## Construction of an Interactive Network of Ferroptosis-Related Genes and Correlation Analysis

To deeply explore the molecular function of these FRGs with changed expression in HCC, pathway and process enrichment analyses were performed based on the Metascape online tool. As shown in Figure 2A, these genes were significantly associated with ferroptosis, negative regulation of oxidative stress-induced cell death, cellular response to metal ions, p53 transcriptional gene network, viral entry into host cells, peptide transport and response to radiation. Furthermore, the PPI network was constructed using the Metascape and STRING online databases. The protein interaction was relatively strong, and various types of interactions are shown in Figures 2B,C. We then assessed the correlations among the FRGs based on the TCGA and ICGC databases, and significant positive or negative correlations between these FRGs were observed (Figures 2D,E).

## Consensus Clustering Analysis of Ferroptosis-Related Genes in Hepatocellular Carcinoma

Based on the distinct expression level of FRGs and the proportion of ambiguous clustering measures, consensus clustering analysis was performed, and  $k$  (clustering variable) was increased from 2 to 6. We identified  $k = 3$  as the optimal clustering stability, suggesting that it was suitable to separate HCC patients into three subgroups (Figure 3A). Principal component analysis (PCA)

according to the whole transcriptome profiles of the 3 clusters was conducted (Figures 3A–C). Compared with cluster 1 and cluster 2, most FRGs were highly expressed in cluster 3 (Figure 3D). Additionally, HCC patients in cluster 3 exhibited worse OS, disease-free survival (DFS), progression-free survival (PFS) and disease-specific survival (DSS) than those in cluster 1 and cluster 2 (Figures 3E–H). Subsequently, significant differences were obtained in different characteristic groups, including T stage, TNM stage and grade groups, among the three clusters (Table 1).

## Association of Patient Clusters With Immune Cell Infiltration in Hepatocellular Carcinoma

To explore the correlation between ferroptosis and the tumor immune microenvironment (TAM), we examined the effect of FRGs on immune cell infiltration in HCC. The heatmap results demonstrated that the infiltration scores of naïve B cells, memory B cells, CD8<sup>+</sup> T cells, follicular helper T cells (T<sub>fh</sub> cells), regulatory T cells (Tregs), resting NK cells, monocytes, M0 macrophages, M1 macrophages, activated mast cells, resting mast cells and neutrophils were significantly different among the C1, C2 and C3 clusters using the CIBERSORT algorithm (Figure 4A). The percentage abundances of tumor-infiltrating immune cells in each sample, with different colors and different types of immune cells using the CIBERSORT algorithm, are shown in Figure 4B. We further evaluated the impact of FRGs on the expression of several important immune checkpoints. Higher expression of CD274 (PD-1), CTLA-4, HAVCR2, LAG3, PDCD-1 (PD-L1), PDCD1LG2 and TIGIT was found in cluster 3 than in cluster 1 and cluster 2, while the highest expression of SIGLCE15 was observed in the cluster 2 (Figure 4C).

We also examined the expression of the 24 FRGs among these three clusters and found that the expression of CDKN1A, HSPA5, EMC2, SLC7A11, NFE2L2, HSPB1, GPX4, FANCD2, C1SD1, FDFT1, SLC1A5, TFRC, RPL8, NCOA4, LPCAT3, GLS2, DPP4, CS, CARS1, ATP5MC3, ALOX15, ACSL4 and ATL1 was significantly different in these three clusters (Supplementary Figure S3A). Additionally, we examined the correlation between clusters and the response to immunotherapy to further explore the clinical application value of the model. HCC patients in cluster 3 had higher TIDE scores, suggesting a higher possibility of immune escape (Supplementary Figure S3B).

## Identification of Prognostic Ferroptosis-Related Genes in the TCGA-HCC Cohort

We then performed univariate Cox regression analysis of the differentially expressed genes in Figure 1 to select prognostic FRGs in HCC. Five genes were selected from the univariate Cox regression analysis with a cutoff of  $p < 0.01$ , including SLC7A11, SLC1A5, TFRC, RPL8 and CARS1 (Figure 5A). The Kaplan–Meier analysis results further indicated that the

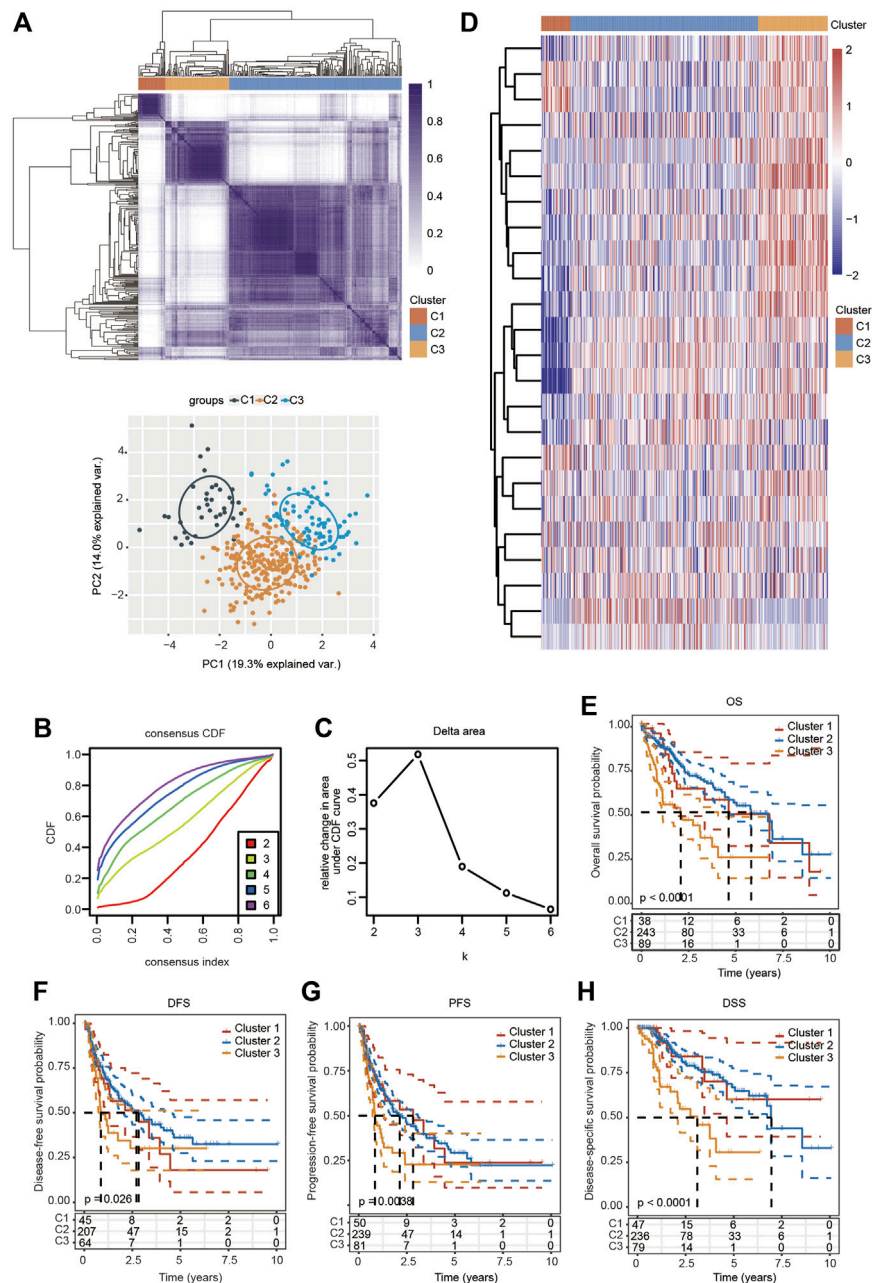


**FIGURE 3 |** Survival analysis and changed expression of FRGs in distinct HCC clusters in the TCGA cohort. **(A)** Consensus clustering matrix for  $k = 3$ . **(B,C)** Cumulative distribution function curves for  $k = 2–6$ . **(D)** Heatmap visualizing the expression patterns of FRGs in three clusters. **(E–H)** The Kaplan–Meier curves indicate the OS **(E)**, DFS **(F)**, PFS **(G)** and DSS **(H)** for three clusters of HCC patients.

increased expression of SLC7A11, SLC1A5, TFRC, RPL8 and CARS1 corresponded with unfavorable OS in HCC patients (**Figure 5B**). Thus, these five genes were selected as hub genes for further analysis.

The expression of these five genes was investigated based on the TCGA, ICGC and Gene Expression Omnibus (GEO) databases. Consistent with the results obtained from TCGA (**Figure 1**), upregulated expression of SLC7A11, SLC1A5, TFRC, RPL8 and CARS1 was observed in HCC tissues

compared with adjacent normal liver tissues according to the TCGA + GTEx and ICGC databases (**Figures 5C,D**). SLC7A11, SLC1A5, TFRC, RPL8 and CARS1 were also highly expressed in HCC tissues according to the GSE10143 and GSE36376 datasets (**Figure 5E; Supplementary Figure S4**).

We also investigated the expression of SLC7A11, SLC1A5, TFRC, RPL8 and CARS1 in HCC and normal liver tissues using single-cell RNA-seq data. Higher expression of these five genes

**TABLE 1 |** Correlations between different clinicopathological parameters and the three clusters in HCC. The p-values are shown in bold.

	Characteristic	C1	C2	C3	p_value
Status	Alive	33	167	41	<b>0.005</b>
	Dead	17	72	41	
Age	Mean (SD)	58.9 (12.8)	60 (13.7)	58.2 (13.3)	<b>0.343</b>
	Median [Min, Max]	60 [24, 80]	62 [16, 90]	60 [20, 81]	
Sex	Female	12	81	28	<b>0.377</b>
	Male	38	158	54	
Race	American Indian	1		1	<b>0.243</b>
	Asian	24	93	41	
	Black	1	13	3	
	White	20	128	36	
pT-stage	T1	28	129	24	<b>0.007</b>
	T2	16	52	24	
	T3	2	27	16	
	T3a	2	17	10	
	T3b	1	2	3	
	T4	1	8	4	
	T2b		1		
	TX		1		
	T2a			1	
pN-stage	N0	34	162	56	<b>0.906</b>
	NX	16	75	23	
	N1		2	2	
pM-stage	M0	37	167	62	<b>0.613</b>
	M1	1	3		
	MX	12	69	20	
pTNM-stage	I	28	120	23	<b>0.001</b>
	II	16	49	21	
	IIIA	3	37	25	
	IIIB	1	4	3	
	IIIC	1	4	4	
	IV	1	1		
	III		3		
	IVA		1		
	IVB		2		
Grade	G1	7	44	4	<b>0</b>
	G2	27	119	31	
	G3	13	69	40	
	G4	3	3	6	

was observed in carcinoma cells than in hepatocytes (Figures 6A–E). More importantly, the single-cell RNA-seq analysis results suggested that these genes were not only expressed in liver cells but also expressed in other types of cells, such as cancer-associated fibroblasts (CAFs), T cells and B cells (Figures 6A–E). The protein expression levels of these genes were further evaluated using the Clinical Proteomic Tumor Analysis Consortium (CPTAC) database. The protein levels of TFRC, RPL8 and SLC1A5 were higher in HCC tissues than in normal liver tissues (Figure 7A). The IHC staining results from the HPA database also provided the protein levels of four prognostic FRGs, including TFRC, RPL8, CRAS1 and SLC1A5, between HCC and adjacent normal liver tissues, which were consistent with the CPTAC data (Figure 7B).

### Construction of a Key Ferroptosis-Related Gene Prognostic Signature

We then performed LASSO Cox regression analysis to construct a gene signature based on the optimum  $\lambda$  value

(Figures 8A–C). The risk score was calculated as follows: risk score =  $(0.1668 \times \text{SLC7A11}) + (0.1507 \times \text{SLC1A5}) + (0.0221 \times \text{TFRC}) + (0.1515 \times \text{CARS1}) + (0.0234 \times \text{RPL8})$ . According to the median score calculated by the risk score formula, the HCC patients were divided into two subgroups: the low-risk subgroup and the high-risk subgroup. Importantly, HCC patients in the high-risk subgroup exhibited worse OS than those in the low-risk subgroup (Figure 8D). Receiver operating characteristic (ROC) analysis was used to assess the specificity and sensitivity of the prognostic model. The areas under the ROC curve (AUCs) were 0.764 for 1-year survival, 0.667 for 3-year survival, and 0.674 for 5-year survival (Figure 8E).

### External Validation of the 5-FRG Signature Using the International Cancer Gene Consortium Database

A total of 240 HCC patients from the ICGC database were used for the validation of the prognostic signature. We also

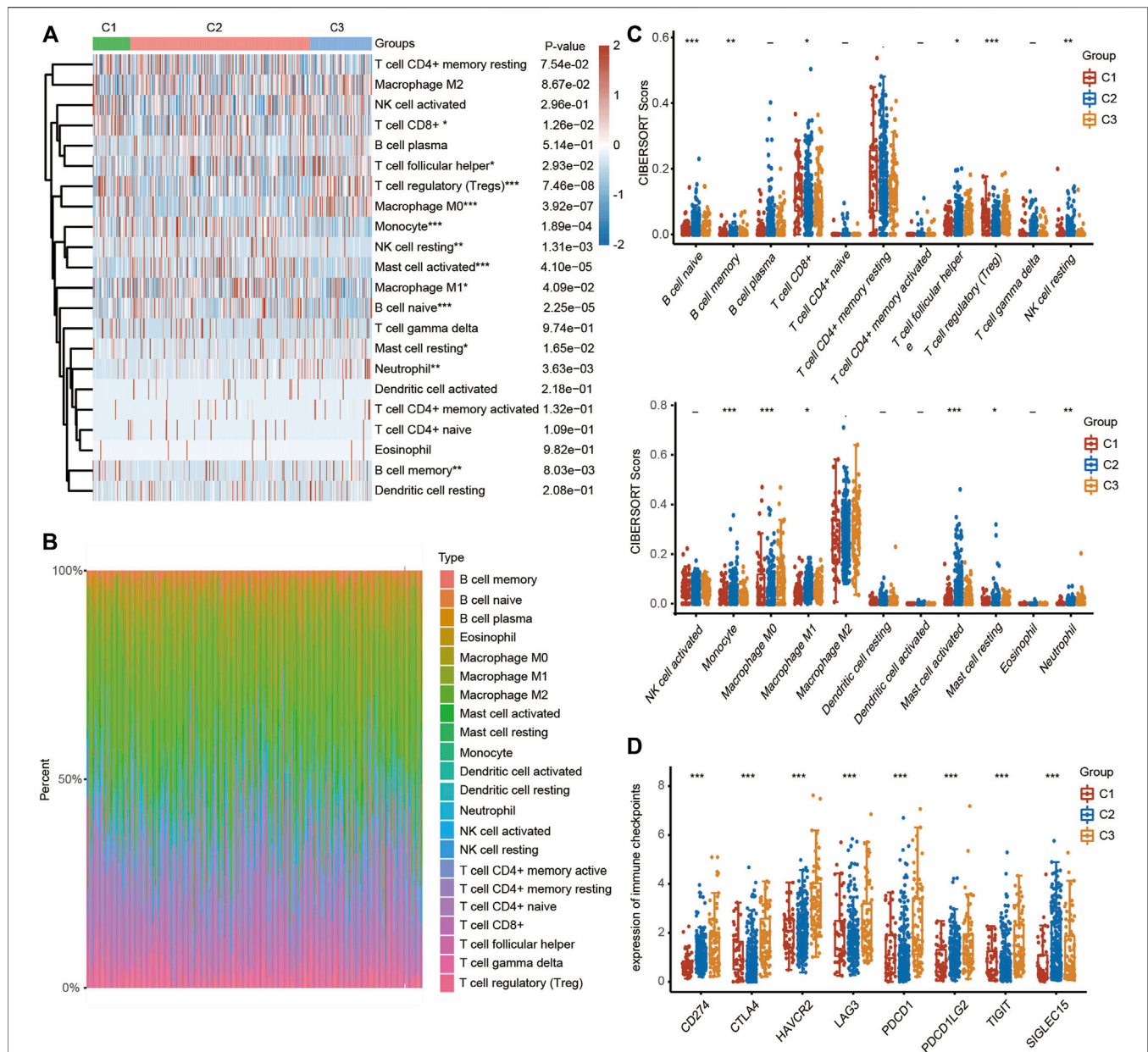


**FIGURE 4 |** TME characteristics in three different HCC clusters. (FRGs in three clusters are positively correlated with immune cell infiltration in HCC). **(A)** Heatmap showing the different infiltration levels of immune cells in the three clusters. **(B)** Bar plot showing the composition of different immune cells in each patient from the three clusters analyzed by CIBERSORT. **(C)** Violin plots showing the different infiltration levels of immune cells in the three clusters. The difference in three clusters was compared statistically with the Kruskal–Wallis test. **(D)** Violin plots showing the different expression levels of immune checkpoint genes in the three clusters. The difference in gene expression was compared statistically with the Kruskal–Wallis test. The interquartile range of values is represented by the upper and lower ends in the box and the median value is represented by the lines in the boxes. The outliers are shown as dots. \* $p < 0.05$ , \*\* $p < 0.01$ , \*\*\* $p < 0.001$ .

established a multivariate LASSO Cox regression model according to the expression information of the five hub FRGs (**Supplementary Figures S5A–C**). The ferroptosis-related signature was constructed based on the best setting for the tuning parameter  $\lambda$ . The formula for the prognostic risk assessment score was as follows: risk score =  $(0.1343 \times \text{SLC7A11} + 0.5613 \times \text{TFRC} + 0.3277 \times \text{RPL8} + 0.2725 \times \text{CARS1})$ . The HCC patients in the ICGC dataset were also

divided into high-risk and low-risk subgroups. When the risk score increased, the risk of death increased, and the survival time of HCC patients decreased (**Supplementary Figure S5C**). The patients in the high-risk group had an unfavorable prognosis compared with those in the low-risk group (**Supplementary Figure S5**). The prognostic efficiency of the five-gene signature was further evaluated by time-dependent ROC curves. The AUC values were 0.766 for 1-



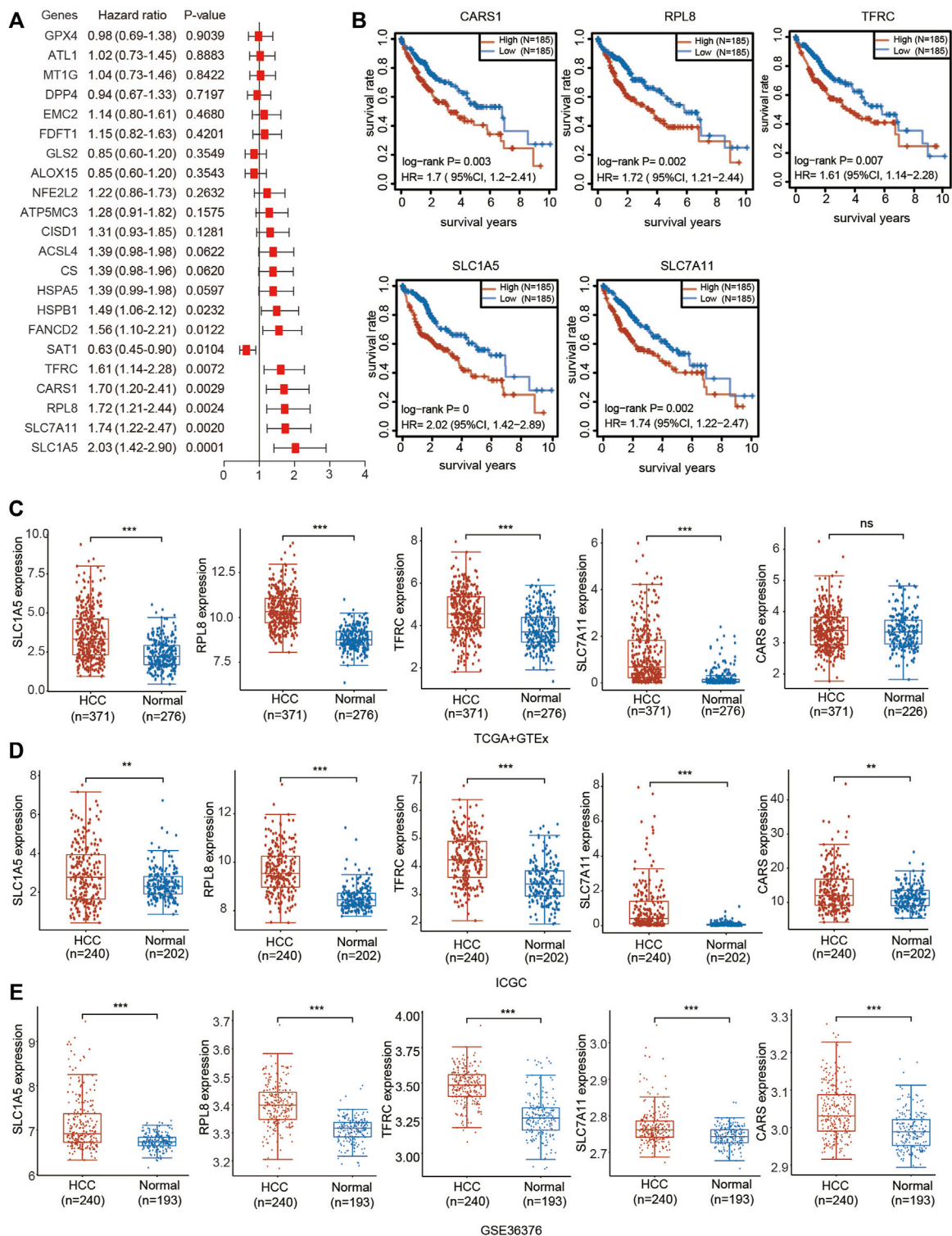
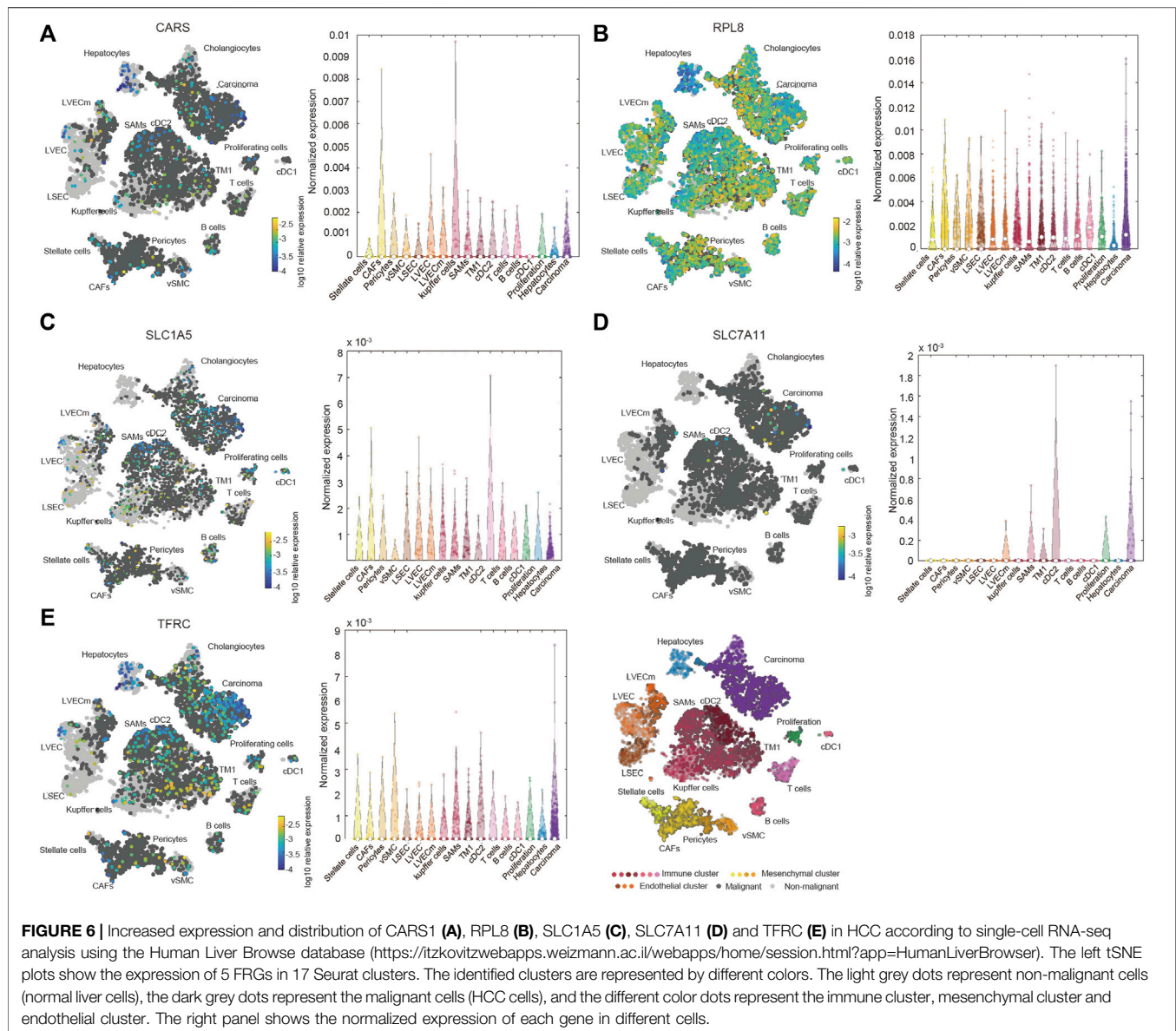


**FIGURE 5 |** Prognostic value and upregulated expression of five FRGs. **(A)** Univariate Cox regression analysis of the prognostic potential of FRGs in HCC. **(B)** The Kaplan-Meier curves indicate the prognostic values of CARS1, RPL8, TFRC, SLC1A5 and SLC7A11 ( $p < 0.05$ , Log-rank test). **(C)** Upregulated expression of CARS1, RPL8, TFRC, SLC1A5 and SLC7A11 in the TCGA combined with GTEx databases. The difference in gene expression was compared statistically with the Wilcoxon test. **(D)** Upregulated expression of CARS1, RPL8, TFRC, SLC1A5 and SLC7A11 in the ICGC databases. The difference in gene expression was compared statistically with the Wilcoxon test. **(E)** Upregulated expression of CARS1, RPL8, TFRC, SLC1A5 and SLC7A11 in GSE36376. The difference in gene expression was compared statistically with the Wilcoxon test. \* $p < 0.05$ , \*\* $p < 0.01$ , \*\*\* $p < 0.001$ .



year survival, 0.78 for 2- year survival, and 0.771 for 3-year survival (Supplementary Figure S5E).

### Independent Prognostic Value of the 5-FRG Signature Based on Different Clinicopathological Characteristics

The prognostic potential of the 5-FRG signature was further confirmed according to different clinicopathological parameters of HCC. As shown in Figure 9A, the 5-FRG signature was significantly correlated with unfavorable prognosis in young (<50 years) and old (>50 years), early grade (G1 and G2) and advanced grade (G3 + G4), early stage (T1 + T2) and advanced stage (T3 + T4), M0, N0, and

TNM stage III patients with HCC. These results imply that the 5-FRG signature according to the risk grouping can serve as a useful tool for predicting the survival of HCC patients among each stratum of age, grade and stage.

We then performed univariate and multivariate Cox regression analyses to further assess the prognostic value of the 5 FRGs in HCC patients (Figure 9B). According to the results of univariate Cox regression analysis, TFRC, SLC7A11, RPL8, CARS1, SLC1A5 and TNM stage were obviously correlated with the OS of HCC patients. According to the results of multivariate Cox regression analysis, SLC7A11, SLC1A5 and TNM stage showed significant correlations with the OS of HCC patients (Figure 9B).

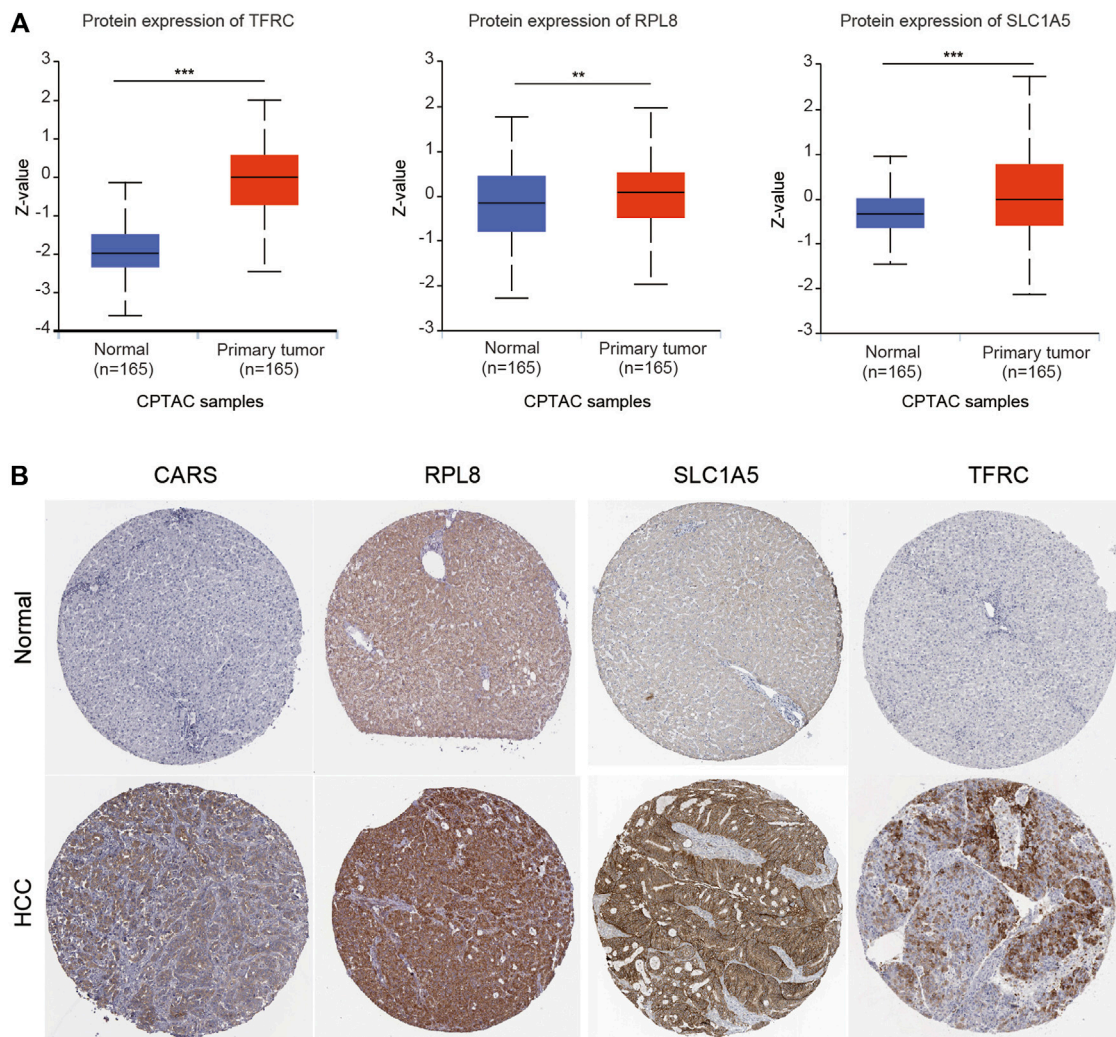


**FIGURE 7 |** Higher protein expression of FRGs in HCC tissues than in normal liver tissues. **(A)** The protein expression of TFRC, RPL8 and SLC1A5 in HCC tissues and normal tissues was investigated in the CPTAC database. Z-values represent standard deviations from the median across samples for HCC. **(B)** Immunohistochemistry analysis was used to examine the protein expression levels of SLC1A5, TFRC, RPL8 and CARS1 in the HPA database. \* $p < 0.05$ , \*\* $p < 0.01$ , \*\*\* $p < 0.001$ .

Based on the multivariate regression analysis, we constructed a novel nomogram model integrating SLC7A11, SLC1A5 and TNM stage to predict the 1-, 3- and 5-year OS rates of patients with HCC (**Figure 9C**). The C-index of the prognostic nomogram was 0.684 (**Figure 9C**). The calibration plots of the nomogram showed good agreement between the actual and nomogram-predicted 1-, 3- and 5-year survival rates (**Figure 9D**).

### Associations of the Risk Score With Immune Cell Infiltration in Hepatocellular Carcinoma

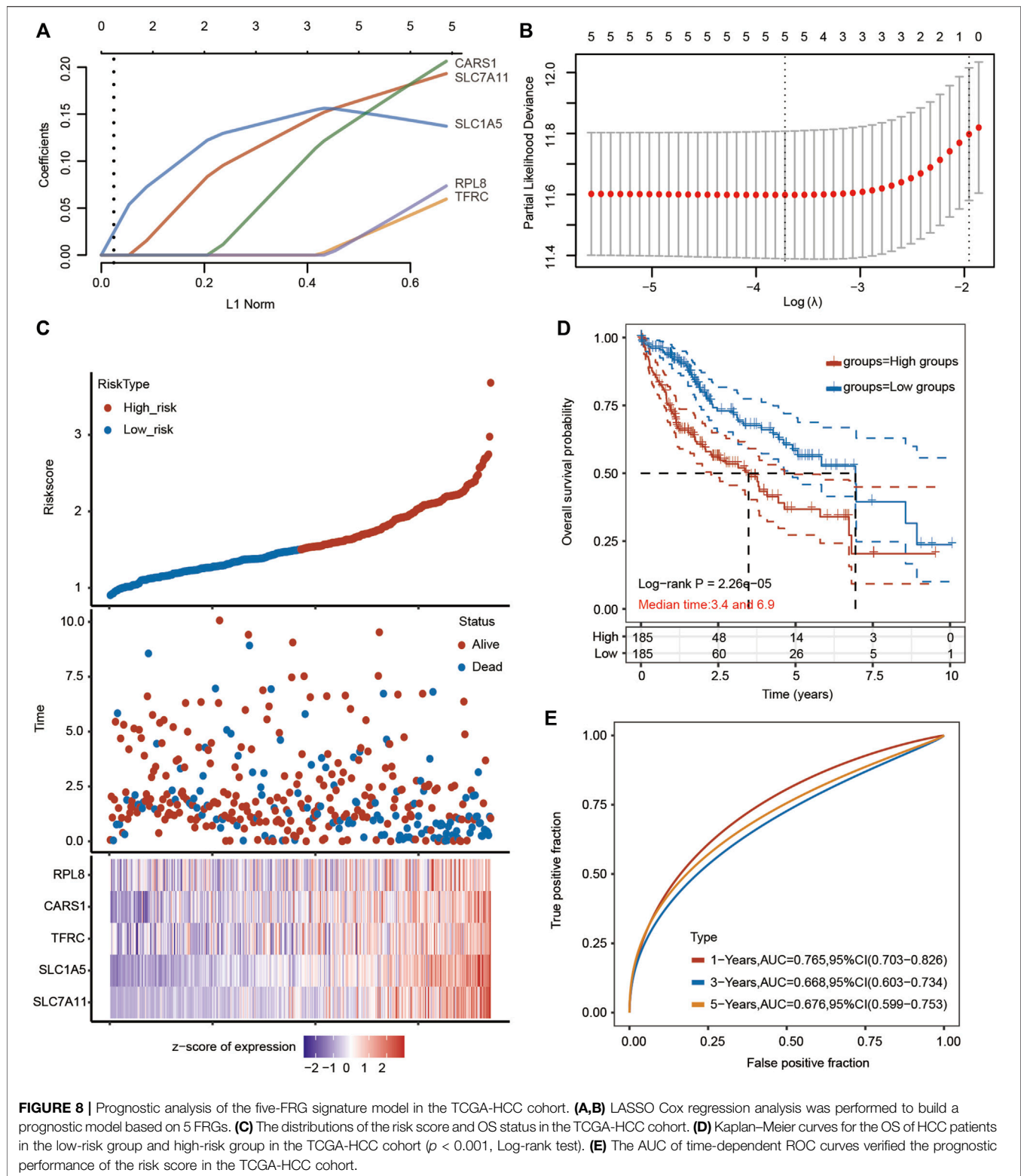
To further explore whether the risk score is correlated with the characteristics of the TME, we estimated the relationship between the infiltration level of different immune cells and the risk score using the TIMER algorithm. We observed significant and positive correlations between the ferroptosis-related risk score and the infiltration levels of

B cells, CD4+ T cells, CD8+ T cells, neutrophils, macrophages and dendritic cells (**Figure 10A**). We also found that SLC7A11, SLC1A5, CARS1 and TFRC were obviously associated with the infiltration of most types of immune cells (**Figure 10B**).

### Genetic Mutation and Drug Sensitivity of the 5 Ferroptosis-Related Genes in Hepatocellular Carcinoma

Genome-wide analysis of the genetic mutations of these five genes was explored through the cBioPortal database. The RPL8 gene exhibited the highest mutation frequency (10%), followed by TFRC (1.9%), SLC7A11 (0.8%), CARS1 (0.5%) and SLC1A5 (0.3%) (**Figure 11A**; **Supplementary Figure S6A**). The most common type of genetic alteration was amplification. We then analyzed the association between these five FRGs and common





oncogenesis-related pathways, including the apoptosis, cell cycle, DNA damage response, EMT, hormone AR, hormone ER, PI3K/AKT, RAS/MAPK, RTK and TSC/mTOR pathways. We found that the hub FRGs were significantly correlated with

the activation or inhibition of these pathways (**Figure 11B; Supplementary Figure S6B**).

Chemotherapy is still commonly used in the comprehensive treatment for HCC. We then estimated whether these 5 FRGs



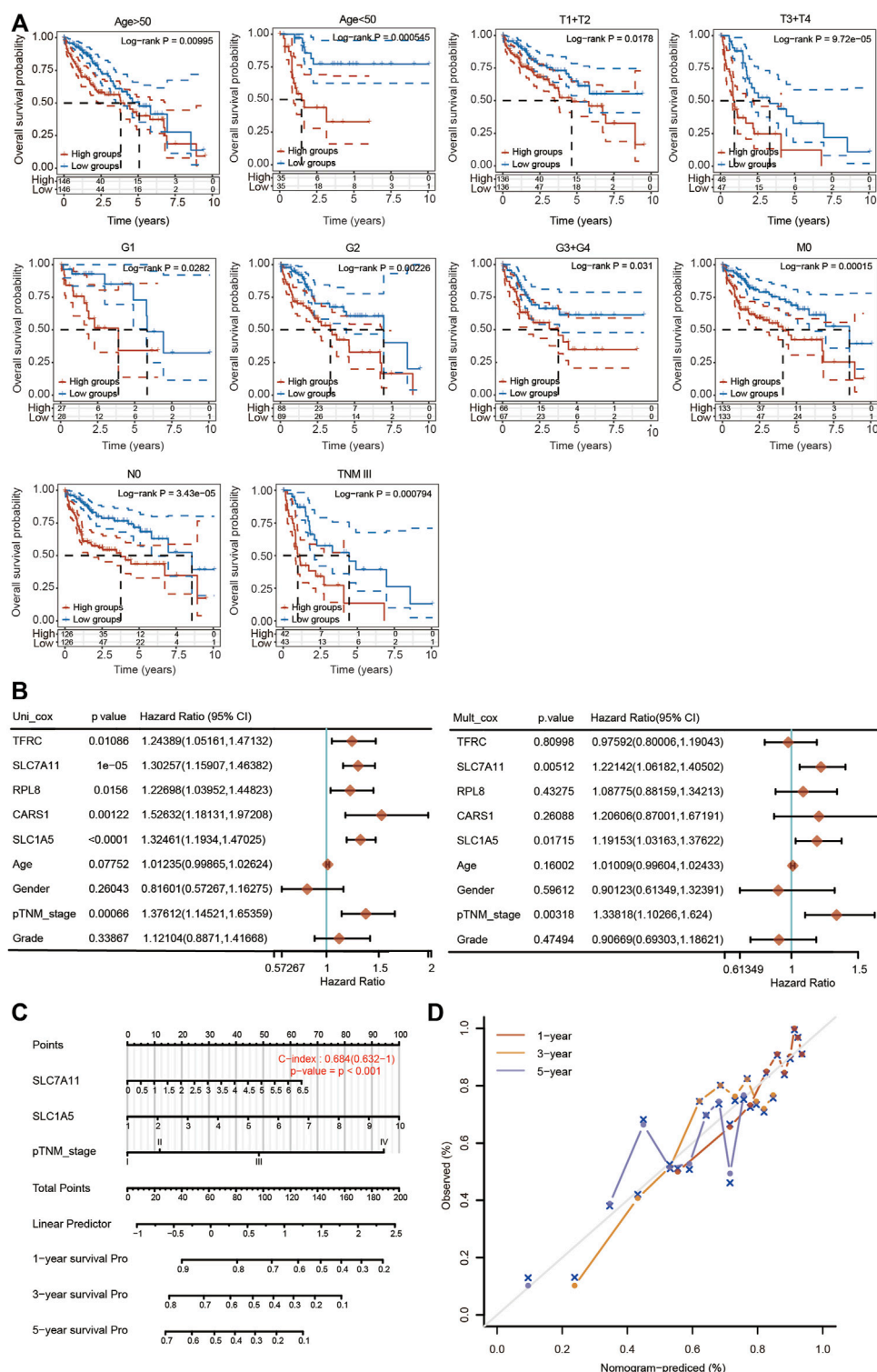


**FIGURE 9 |** Construction of a nomogram based on five FRGs and clinical factors. **(A)** Kaplan–Meier curves of OS between every two groups stratified by age < 50, age > 50, T1 + T2, T3 + T4, G1, G2, G3 + G4, N0, M0 and TNM stage III ( $p < 0.05$ , Log-rank test). **(B)** Univariate and multivariate Cox regression analyses of five FRGs and clinical factors are shown. **(C)** A stable and accurate hybrid nomogram that contains clinicopathological characteristics and the novel prognostic signature. Nomogram for predicting 1-, 3-, and 5-year OS. **(D)** Calibration curves were generated and the 1-, 3-, and 5-year predictions of the nomogram were observed to be consistent with the actual survival rates.

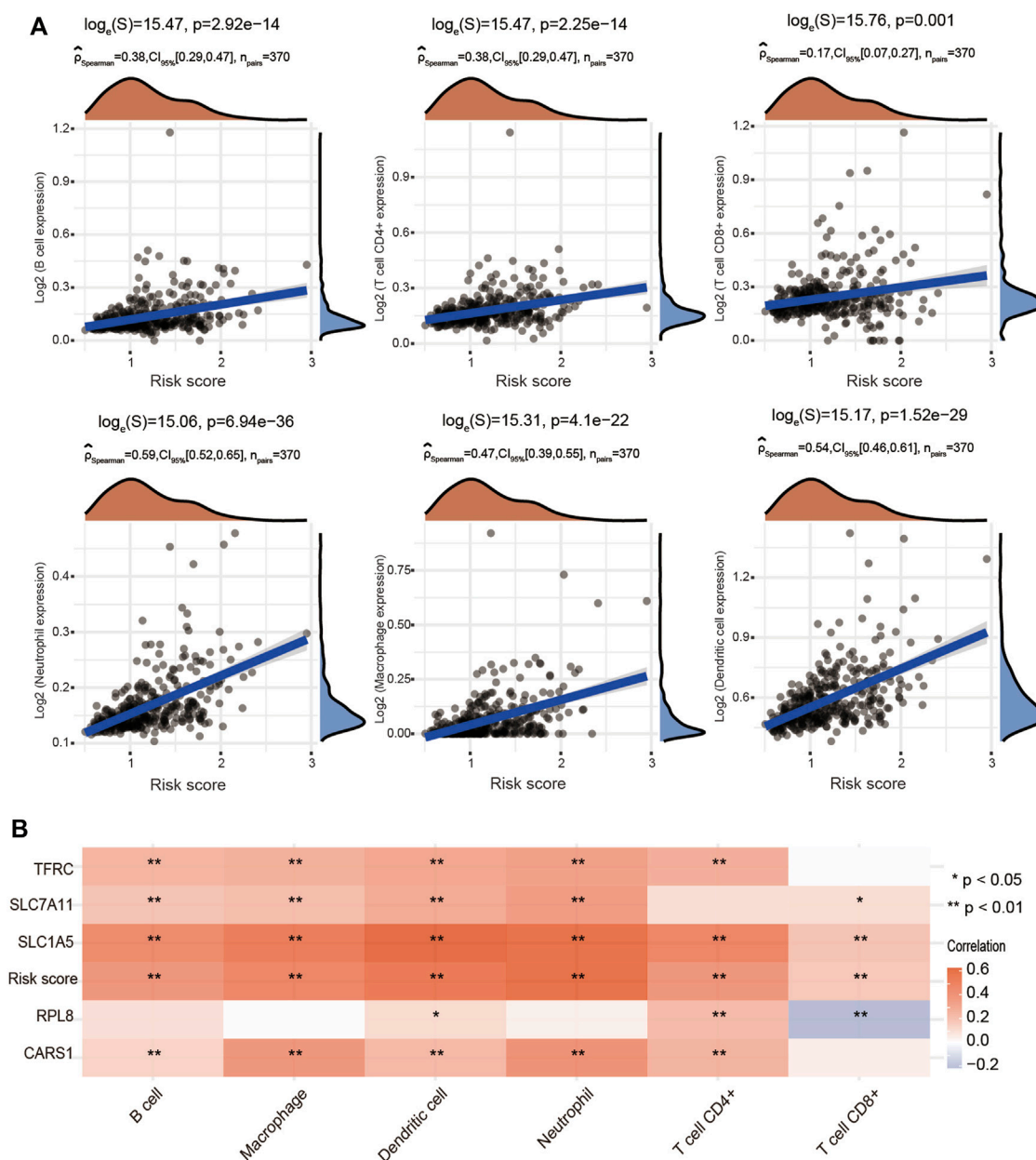


**FIGURE 10 |** Positive association of the risk score with immune cell infiltration in HCC. **(A)** Correlations between the risk score and the infiltration levels of B cells, CD4+ T cells, CD8+ T cells, macrophages, neutrophils and dendritic cells using the spearman analysis. **(B)** Heatmap showing the correlation between risk score and five ferroptosis-related genes and the infiltration levels of six major immune cells. Red represents a positive correlation and blue represents a negative correlation. \*p < 0.05, \*\*p < 0.01.

could affect the sensitivity of chemotherapeutic agents commonly used for treating HCC, including sorafenib, gefitinib, paclitaxel, 5-fluorouracil, etoposide, doxorubicin, vinblastine, docetaxel, gemcitabine, cytarabine, AKT inhibitor VIII, sunitinib and methotrexate according to the GDSC database using the R package pRRophetic. Based on the median expression level of the 5 FRGs, all of the HCC patients were divided into the high-expression group and low-expression group. We found that a significant difference in the IC<sub>50</sub> existed between the high- and

low-expression groups for all these chemotherapeutic drugs (Figure 11C; Supplementary Figure S7). HCC patients with high expression of 5 FRGs were more sensitive to these well-known chemotherapy drugs (Figure 11C; Supplementary Figure S7). These data suggest that these five genes affect the actual therapeutic effect of these drugs in HCC through ferroptosis.

Immunotherapy targeting immune checkpoints has emerged as a novel and rapidly developing therapeutic approach for the clinical treatment of multiple tumor types. The high expression of

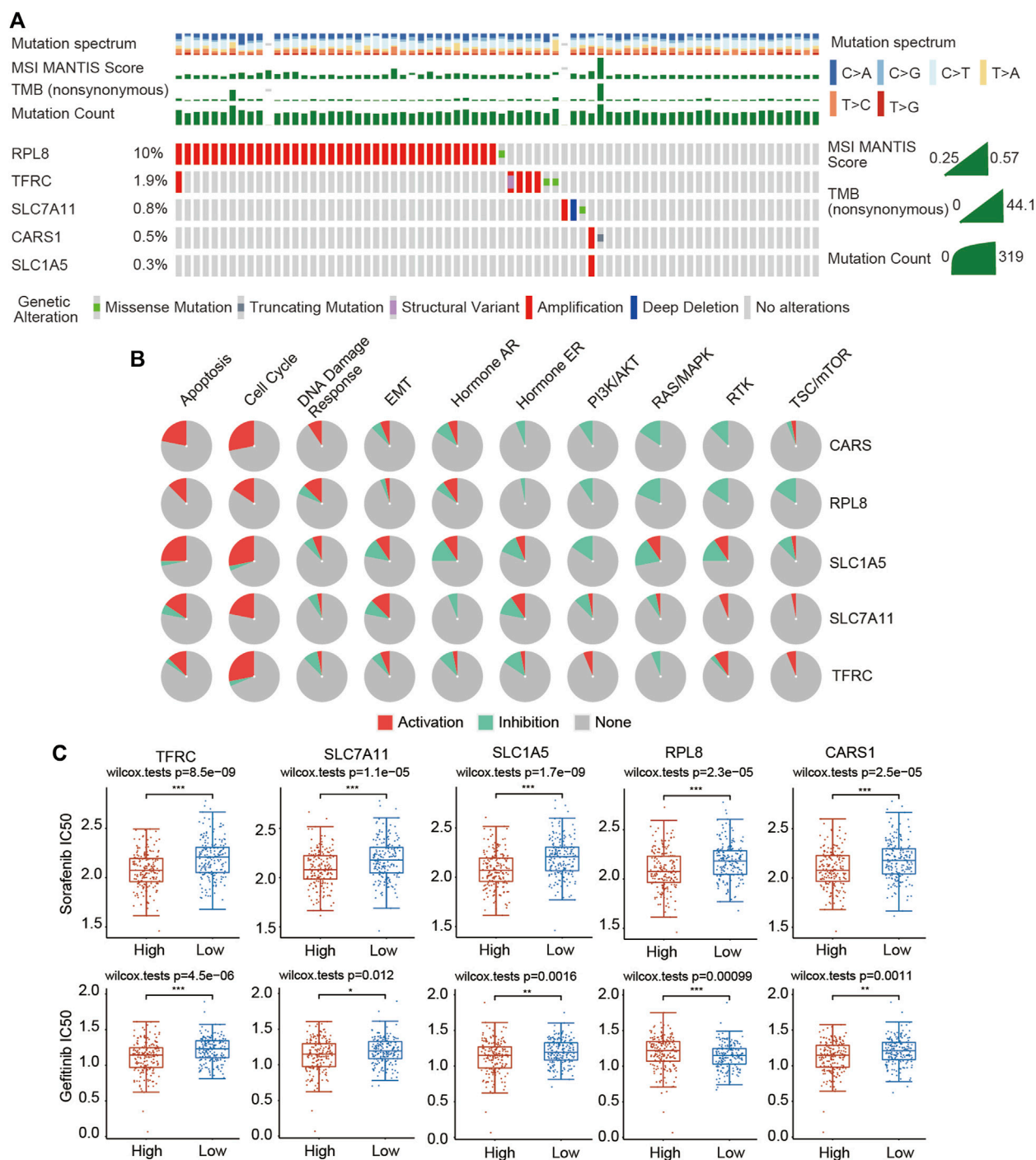
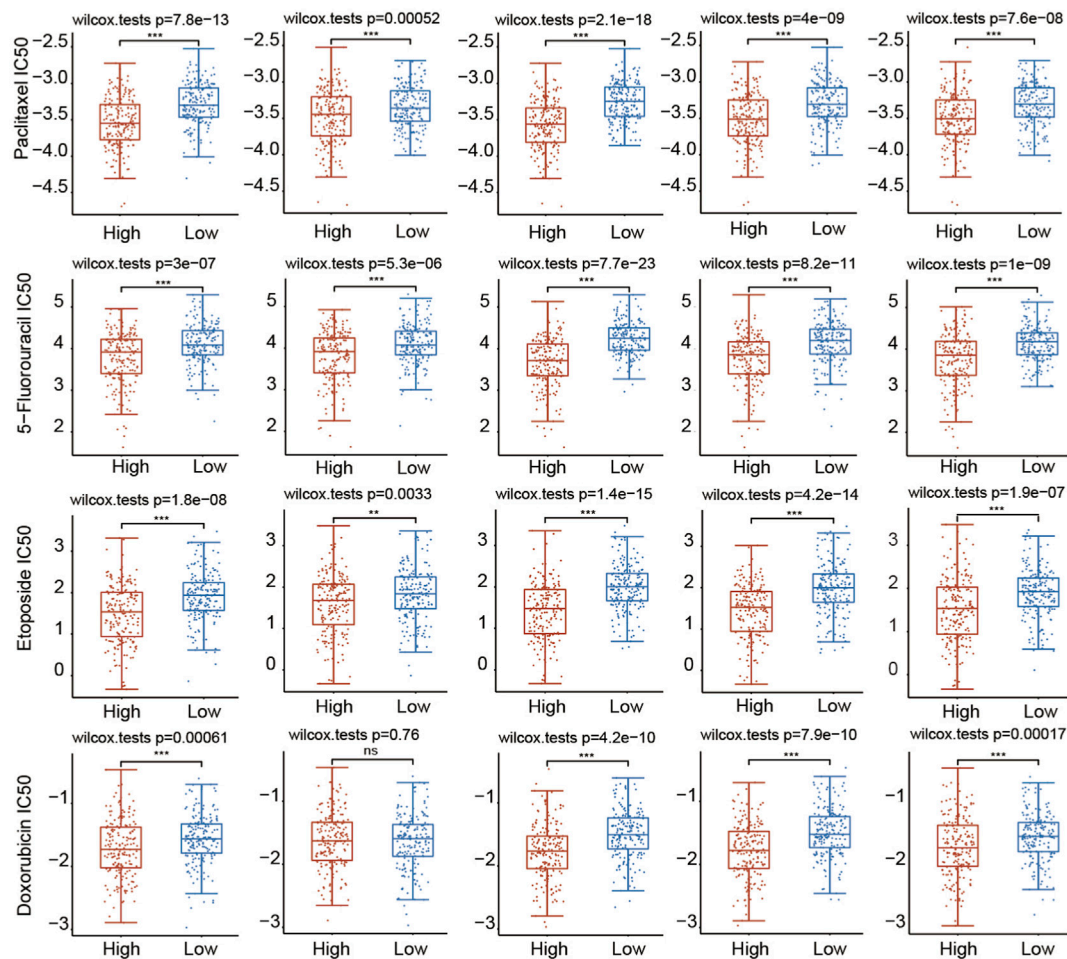


FIGURE 11 | (Continued).

the 5 FRGs was associated with high expression of most immune checkpoints, such as CTLA-4, PD-1 and PD-L1 (Supplementary Figure S8A). According to the TIDE algorithm, we found that upregulated expression of SLC1A5 and RPL8 corresponded to a high TIDE score, indicating that decreasing FRG expression may

improve the therapeutic effect of immunotherapy (Supplementary Figure S8B). Taken together, these results indicate that these 5 hub genes could serve as potential biomarkers for drug screening and provide additional targets for the immunotherapy of HCC.



**FIGURE 11 |** (Continued). Landscape of the genetic alterations of the 5 FRGs and upregulated expression of the 5 FRGs is correlated with drug sensitivity in HCC.

**(A)** The genetic alteration rates of CARS1, RPL8, TFRC, SLC1A5 and SLC7A11 in HCC were examined in the cBioPortal database. **(B)** The correlations between 5 FRGs and various cancer-related pathways were examined in the GSCALite database. **(C)** The correlations between the expression of 5 FRGs and drug sensitivity was investigated according to the GDSC database using the R package pRRophetic. Higher expression of the 5 FRGs was significantly correlated with lower IC50 values of these well-known chemotherapy drugs. The difference was compared statistically with the Wilcoxon test. \* $p < 0.05$ , \*\* $p < 0.01$ , \*\*\* $p < 0.001$ .

## DISCUSSION

Liver cancer is a commonly diagnosed malignancy worldwide and has a high mortality rate among all human tumors (Forner et al., 2018; Sung et al., 2021). Tremendous efforts have been made to develop novel strategies against liver cancer. However, the OS of HCC patients is still unsatisfactory (Sung et al., 2021). Resistance to chemotherapy has been widely recognized as an important cause of death in cancer patients. The in-depth and systematic elucidation of the underlying molecular mechanisms of liver cancer could open new horizons for its treatment. Ferroptosis, a newly identified type of programmed cell death, occurs in an iron-dependent manner, peroxidizes unsaturated phospholipids and causes the accumulation of lethal ROS (Stockwell et al., 2017). The subsequent oxidative damage and oxidative stress imbalance induced by ferroptosis contribute to cell death in multiple cancer cells (Bebber et al., 2020; Chen X. et al., 2021). In fact, initiating

ferroptosis pathways may be able to overcome existing chemotherapeutic resistance and open a new therapeutic area for cancer treatment (Zhao et al., 2022). Therefore, understanding the molecular mechanism of ferroptosis in HCC is a promising therapeutic strategy for liver cancer that selectively induces ferroptosis. Here, using data from the TCGA, ICGC and GEO datasets, we performed extensive bioinformatics analyses to build a risk model composed of five FRGs, which were significantly correlated with the prognosis of patients with HCC. The predictive significance of the constructed signature was further investigated by exploring the ferroptosis-related oncogenic roles and immunological response in HCC patients. This ferroptosis risk model may provide clinicians with more intuitive and rational information for the treatment of HCC in the future.

In the present study, three independent subtypes were comprehensively identified by consensus clustering analysis based on the expression level of 25 FRGs in HCC. There were



significant differences in terms of T stage, TNM stage and grade among these three clusters (**Figure 3**). Moreover, cluster 3 exhibited higher expression and unfavorable prognosis compared with clusters 1 and 2 (**Figure 3**). Next, prognosis-related ferroptosis regulators were selected and used to construct a novel risk signature to predict the OS of HCC patients. A risk model of 5 FRGs (SLC7A11, SLC1A5, CARS1, RPL8 and TFRC) was developed and validated on the basis of the differential FRGs among these three clusters (**Figure 5**). Patients with HCC were further divided into high-risk and low-risk groups according to the median value of the risk model. Multivariate Cox regression analysis indicated that the FRG risk model was an independent prognostic model of OS (**Figure 9**). ROC analysis further suggested the superiority of our risk model in predicting the OS of HCC patients compared with established clinicopathological characteristics. We then extended our risk model and built a nomogram to predict 1-year, 3-year and 5-year OS. The calibration curve exhibited excellent agreement between the model predictions and the actual OS (**Figure 9**). Therefore, our risk model, based on five FRGs, has a high degree of accuracy and may contribute to the search for new biomarkers of HCC.

The development of new drugs for cancer is a long and tortuous process, inevitably involving thousands of failures. Drugs that are currently available have already passed safety assessments, which means that research on these drugs to treat other cancers can save time and money. Sorafenib is a novel oral kinase inhibitor that targets various tyrosine kinases. Based on favorable data from preclinical and clinical trials, sorafenib has been approved as a first-line treatment for advanced HCC. However, it is still necessary to further understand the role of sorafenib in the treatment of HCC and to explore more effective drug combination regimens. Based on evidence that the cytotoxic effect of sorafenib on liver cancer cells Huh7 was significantly inhibited by the iron chelator deferoxamine and the ferroptosis-specific inhibitor ferrostatin-1, sorafenib was proposed as a ferroptosis-inducing agent in 2013 (Louandre et al., 2013). Subsequently, it was found that sorafenib triggers ferroptosis by inhibiting the System Xc-, while beta-mercaptoethanol ( $\beta$ -ME), deferoxamine, and ferrostatin-1 can restore sorafenib-induced cell death (Louandre et al., 2013; Sun et al., 2016b). In addition, sorafenib induces ferroptosis in renal adenocarcinoma ACHN and liver cancer HepG2 cells (Lachaier et al., 2014; Houessinon et al., 2016; Sun et al., 2016a). In addition to sorafenib, various chemotherapeutic drugs commonly used for treating liver cancer, including gefitinib, paclitaxel, 5-fluorouracil, etoposide, doxorubicin, vinblastine, docetaxel, gemcitabine, cytarabine, AKT inhibitor VIII, sunitinib and methotrexate, by blocking the cell cycle, promoting cell death, suppressing specific signaling pathways and inhibiting angiogenesis. Here, we showed that 5 FRGs were significantly associated with the sensitivity of these drugs according to the GDSC database (**Figure 11**). The GDSC database records approximately 1,000 different human cancer cell lines and screens them with more than 100 existing anticancer drugs. We found that in the high FRG expression group, the IC<sub>50</sub> values of various chemotherapeutics and small-molecule anticancer drugs

were significantly lower, demonstrating that HCC patients with high expression of 5 FRGs might obtain more therapeutic benefit from these drugs (**Figure 11C**; **Supplementary Figure S7**). These data suggest that these five genes may affect the actual therapeutic effect of these drugs in HCC through ferroptosis. In future research, the development of drugs targeting these five genes may result in a more effective treatment for liver cancer with fewer side effects.

Previous studies have suggested that ferroptosis is immunogenic and induces an inflammatory immune response (Chen X. et al., 2021; Zhao et al., 2022). Cells undergoing ferroptosis can often interact with the immune system in multiple ways through complex cellular and molecular mechanisms. For example, ferroptotic cells can release damage-associated molecular patterns (DAMPs) or lipids that act as messengers for surrounding immune cells (Friedmann Angeli et al., 2019; Chen X. et al., 2021). The signals released can be immunogenic or inflammatory, leading to the activation of various immune responses. Furthermore, danger signals in the TME may affect the function of immune cells and contribute to tumor immune escape. Interestingly, the interaction between ferroptosis and anticancer immunotherapy is multifaceted. A recent study revealed the role of ferroptosis in CD8<sup>+</sup> T cell-mediated antitumor immunity. Immune checkpoint inhibitor treatment activates CD8<sup>+</sup> T cells to produce interferon gamma (IFN $\gamma$ ) and promotes ferroptosis in tumor cells (Wang et al., 2019). The underlying mechanism of this effect is that IFN $\gamma$  is recognized by receptors on the tumor cell membrane, increasing the expression of the transcription factor STAT1, which in turn downregulates the expression of SLC7A11 and SLC3A2, resulting in the inhibition of the GSH/GPX4 axis, and finally sensitizing tumor cells to ferroptosis (Wang et al., 2019). In addition, IFN $\gamma$  secreted by CD8<sup>+</sup> T cells, which are activated by immunotherapy binds to IFNR, activates the JAK-STAT1-IRF1 signaling axis, and induces the expression of ACSL4 in tumor cells (Liao et al., 2022). Increased ACSL4 expression synergizes with arachidonic acid (AA) treatment to trigger potent ferroptosis in various cancer cell lines in an ACSL4-dependent manner (Liao et al., 2022). Thus, ferroptosis has been clearly proven to play an important role in antitumor immunity, not only participating in the elimination of tumor cells by T cells activated by immune checkpoint inhibitors, but also directly affecting the functions of various immune cells, suggesting that ferroptosis may synergize with immunotherapy to inhibit tumor development and progression. Undoubtedly, a better understanding of the interplay between ferroptosis and immunity will greatly facilitate the development of new therapeutic strategies with translational and applied potential.

Chemotherapy and immunotherapy are crucial adjunctive therapies for HCC. PD-1/PD-L1 checkpoint inhibitors have emerged as a promising therapeutic strategy for HCC. In September 2017, the anti-PD-1 antibody nivolumab (Opdivo) was approved by the FDA for the second-line treatment of sorafenib-pretreated patients with advanced liver cancer (El-Khoueiry et al., 2017). Separately, in a phase 2 study, the anti-PD-1 inhibitor pembrolizumab (Keytruda) was investigated as second-line therapy in patients with advanced HCC following sorafenib failure (Zhu et al., 2018). The results confirmed an

objective response rate of 17% in HCC patients; thus, the FDA approved pembrolizumab in November 2018 for the treatment of HCC patients who had previously received sorafenib (Zhu et al., 2018; Macek Jilkova et al., 2019). However, the harsh reality shows that only a minority of patients with liver cancer can benefit from this treatment. To enhance the efficacy of immune checkpoint inhibition in HCC patients, future strategies may require predictive factor-based selection to identify which patients may be more sensitive to immunotherapy and combination strategies to improve the antitumor efficacy and clinical success. However, very little has been described about predictive biomarkers of the response to PD-1/PD-L1 blockade in HCC (Macek Jilkova et al., 2019). To date, there are few studies on predictive biomarkers of immunotherapy response in HCC. A previous study demonstrated that deletion of SLC1A5 affects T-cell effector function, resulting in the impaired differentiation of helper T cells into Th1 and Th17 subsets (Nakaya et al., 2014). C-myc is essential for NK-cell metabolism and T-cell activation (Wang et al., 2011; Loftus et al., 2018). Glutamine is extremely important for the immune system, maturation and the differentiation of immune cells. Glutamine uptake through SLC1A5 is necessary for c-myc induction in cytokine-stimulated NK cells (Wang et al., 2011; Loftus et al., 2018). Moreover, recent studies demonstrated that SLC1A5 expression was positively and significantly associated with the abundance of tumor-infiltrating immune cells in stomach adenocarcinoma (STAD) and HCC (Zhao et al., 2021; Zhu et al., 2022). SLC1A5 expression was positively correlated with the expression of PD-1, but negatively correlated with the expression of PD-L1. Therefore, SLC1A5 may have an important role in the TME by modulating immune cell infiltration in STAD and HCC (Zhao et al., 2021; Zhu et al., 2022). In addition, a previous study suggested that enhanced expression of CARS1 was strongly correlated with unfavorable prognosis in various cancers and was associated with the expression of immune checkpoint genes, including PD-L1 (Wang S. et al., 2021). Thus, CARS1 may be a potential novel prognostic biomarker and novel target for cancer immunotherapy. A recent study demonstrated that patients and a mouse model with a homozygous mutation in *TFRC* showed combined immunodeficiency characterized by decreased proliferation of T and B cells and defective class switching (Jabara et al., 2016). *TFRC* is also associated with the formation of immunological synapses in T cells during TCR engagement. Our previous study also indicated that *TFRC* expression was closely and positively correlated with the infiltration levels of many immune cells in breast cancer (Chen F. et al., 2021). We observed that the infiltrating levels of CD8+ T cells, CD4+ T cells, neutrophils, macrophages and dendritic cells were higher in the *TFRC* high-expression group than in the *TFRC* low-expression group (Chen F. et al., 2021). Moreover, the expression of LAG3, CTLA-4, PD-L1, CD274, TIGIT, HAVCR2 and PDCD1LG2 was upregulated in the *TFRC* high-expression group compared with the *TFRC* low-expression group in breast cancer (Chen F. et al., 2021).

In the present study, CIBERSORT analysis revealed that the three clusters had different infiltrating levels of naïve B cells,

memory B cells, CD8+ T cells, Tregs, T follicular helper cells, resting NK cells, monocytes, M0 macrophages, M1 macrophages, activated mast cells, resting mast cells and neutrophils. Interestingly, we subsequently identified that cluster 3 showed higher expression of immune checkpoints, including CD274, CTLA4, HAVCR2, LAG3, PDCD1, PDCD1LG2 and TIGIT (Figure 4). More importantly, in the present study, the single-cell sequencing analysis results implied that SLC7A11, SLC1A5, CARS1, RPL8 and *TFRC* were not only upregulated in liver cancer cells but also expressed in immune cells. Moreover, the expression of the 5 FRGs was positively correlated with the expression of most immune checkpoints, including CTLA-4, PD-1 and PD-L1 (Supplementary Figure S8A). We also observed that increased expression of SLC1A5 and RPL8 corresponded to a high TIDE score based on the TIDE algorithm, suggesting that decreasing FRG expression may improve the therapeutic effect of immunotherapy (Supplementary Figure S8B). Taken together, these findings identify the essential roles of these 5 genes in regulating the immune response and immune cell infiltration in cancer.

Inevitably, there are several limitations in the present study. First, we constructed a prognostic model based on differential FRGs to predict the survival rate of patients with HCC according to retrospective data from the TCGA database. Although we validated our risk model using the ICGC cohort, more large-scale data to verify the clinical application value of our FRG-based survival model are needed. Second, although the expression levels of 5 FRGs in HCC and normal tissues were investigated using TCGA, ICGC and GEO datasets, the expression levels and scores of clinical samples are needed. Third, although the correlations between the 5 FRGs and immune cell infiltration were observed from our analyses, the correlation coefficient was not strong. Thus, the potential relationships between the prognostic signature and immune infiltration need to be experimentally validated. Fourth, when the consensus clustering analysis was performed, although we identified that  $k = 3$  as the optimal clustering stability, there was some crossover of the samples in the three clusters. Clearer cluster separation and a more satisfactory classification of HCC samples will make the conclusion more convincing.

## CONCLUSION

In the present study, we comprehensively analyzed the clustering effects of ferroptosis in patients with HCC based on the expression levels of reported FRGs. Three clusters of patients with HCC suggested a prominent prognostic difference, and a risk model of 5 FRGs was developed on the basis of the differential FRGs among the three clusters. Although similar risk models of FRGs have been established in HCC patients, our analyses provided a new method for discovering new prognosis-associated genes in HCC by differential analysis in three clusters. Our analysis results indicated that the 5 FRGs of the risk model were significantly associated with the OS of HCC patients.

## DATA AVAILABILITY STATEMENT

The datasets presented in this study can be found in online repositories. The names of the repository/repositories and accession number(s) can be found in the article/**Supplementary Material**.

## ETHICS STATEMENT

The representative IHC staining results were obtained from the HPA database. Written informed consent was obtained from the individual(s) for the publication of any potentially identifiable images or data included in this article.

## AUTHOR CONTRIBUTIONS

Study concept and design: KT. Acquisition of data: KT, YF, BZ, JZ, and BL. Analysis and interpretation of data: KT, YF, BZ, JZ, BL, YS, SZ, JH, and FC. Statistical analysis: KT, BZ, JZ, and BL. Drafting of the article: KT. Critical revision and final approval of the article: KT and YF. Obtained funding: YF and KT. Study supervision: KT. All authors contributed to the article and approved the submitted version.

## FUNDING

This research was supported by the One Hundred Person Project of Hebei Province (E2016100019), the Graduate Student Innovation Funding of Hebei Normal University (CXZZSS2022064), Key R&D Program of Hebei Province (21372602D) and Natural Science Foundation of Hebei Province (C2020205003).

## ACKNOWLEDGMENTS

We would like to thank the TCGA, GTEX, ICGC, GEO and HPA databases for the availability of the data.

## SUPPLEMENTARY MATERIAL

The Supplementary Material for this article can be found online at: <https://www.frontiersin.org/articles/10.3389/fmolb.2022.940575/full#supplementary-material>

**Supplementary Figure S1** | Confirmation of the upregulated or downregulated expression of FRGs based on the ICGC database. **(A)** Heatmap showing the differential expression of 25 FRGs in normal individuals and HCC patients. Blue

represents tumor tissues and red represents the normal tissues. The difference in gene expression was compared statistically with the Wilcoxon test. **(B)** Violin plots showing the differential expression of 25 FRGs in normal individuals and HCC patients. Red represents tumor tissues and blue represents the normal tissues. The interquartile range of values is represented by the upper and lower ends in the box and the median value is represented by the lines in the boxes. The difference in gene expression was compared statistically with the Wilcoxon test. **(C)** Correlation and prognostic values of FRGs in HCC. The interactions between genes were shown by linking lines and the correlation strength between genes was shown by thickness. The effect of each FRG on the prognosis was indicated by the size of the circle and Log-rank test. The red and blue lines represent positive and negative correlations, respectively.

**Supplementary Figure 2** | Increased or decreased expression of FRGs in HCC patients based on GEO datasets. **(A)** Violin plots showing the differential expression of FRGs in normal individuals and HCC patients in the GSE10143 dataset. **(B)** Violin plots showing the differential expression of FRGs in normal individuals and HCC patients in the GSE36376 dataset.

**Supplementary Figure 3** | **(A)** The differential expression of 24 FRGs in three clusters. The difference in gene expression is compared statistically with the Kruskal–Wallis test. The interquartile range of values is represented by the upper and lower ends in the box and the median value is represented by the lines in the boxes. The outliers are shown as dots. **(B)** Potential immunotherapy response in three clusters was predicted with the Tumor Immune Dysfunction and Exclusion (TIDE) algorithm using the R packages ggplot2 and ggpvr. The difference in TIDE scores was compared statistically with the Kruskal–Wallis test. \* $p < 0.05$ , \*\* $p < 0.01$ , \*\*\* $p < 0.001$ .

**Supplementary Figure 4** | Differential expression of CARS1, RPL8, TFRC, SLC1A5 and SLC7A11 in GSE10143. The difference in gene expression was compared statistically with the Wilcoxon test. \*\*\* $p < 0.001$ .

**Supplementary Figure 5** | Confirmation of the prognostic value of the 5 FRG signature model in the ICGC cohort. **(A,B)** LASSO Cox regression analysis was performed to build a prognostic model based on the 5 FRGs. **(C)** The distributions of the risk score and OS status in the TCGA dataset. **(D)** Kaplan–Meier curves for the OS of HCC patients in the low-risk group and high-risk group in the ICGC cohort ( $p < 0.001$ , Log-rank test). **(E)** The AUCs of time-dependent ROC curves verified the prognostic performance of the risk score in the ICGC dataset.

**Supplementary Figure 6** | Correlations between the 5 FRGs and genetic alterations and cancer pathways. **(A)** The genetic alteration rates of CARS1, RPL8, TFRC, SLC1A5 and SLC7A11 were examined in the cBioPortal database. **(B)** Pathway analysis of 5 FRGs was performed in the GSCALite database. Network diagram indicating the correlations between FRGs and multiple cancer pathways.

**Supplementary Figure 7** | Chemosensitivity difference provides potential therapeutic targets. The correlations between the expression of 5 FRGs and drug sensitivity was investigated according to the GDSC database using the R package pRRophetic. Higher expression of the 5 FRGs was significantly correlated with lower IC50 values of these well-known chemotherapy drugs. The difference was compared statistically with the Wilcoxon test. \* $p < 0.05$ , \*\* $p < 0.01$ , \*\*\* $p < 0.001$ .

**Supplementary Figure 8** | The 5 FRGs affect immune checkpoint gene expression and immunotherapy response in HCC. **(A)** The different expression levels of immune checkpoint genes in the high- or low-expression groups. The difference in gene expression was compared statistically with the Wilcoxon test. **(B)** Potential immunotherapy response in the high- or low-expression groups was predicted with the TIDE algorithm using the R packages ggplot2 and ggpvr. Upregulated expression of SLC1A5 and RPL8, but not TFRC, SLC7A11 and CARS1, corresponded to a high TIDE score. The difference of the TIDE scores was compared statistically with the Wilcoxon test. \* $p < 0.05$ , \*\* $p < 0.01$ , \*\*\* $p < 0.001$ .

## REFERENCES

Bebber, C. M., Müller, F., Prieto Clemente, L., Weber, J., and Von Karstedt, S. (2020). Ferroptosis in Cancer Cell Biology. *Cancers (Basel)* 12, 164. doi:10.3390/cancers12010164

Chen, F., Fan, Y., Hou, J., Liu, B., Zhang, B., Shang, Y., et al. (2021). Integrated Analysis Identifies Tfr1 as a Prognostic Biomarker Which Correlates with Immune Infiltration in Breast Cancer. *Aging* 13, 21671–21699. doi:10.18632/aging.203512

Chen, J., Li, X., Ge, C., Min, J., and Wang, F. (2022). The Multifaceted Role of Ferroptosis in Liver Disease. *Cell Death Differ.* 29, 467–480. doi:10.1038/s41418-022-00941-0

- Chen, X., Kang, R., Kroemer, G., and Tang, D. (2021). Broadening Horizons: the Role of Ferroptosis in Cancer. *Nat. Rev. Clin. Oncol.* 18, 280–296. doi:10.1038/s41571-020-00462-0
- Chen, Y., Li, L., Lan, J., Cui, Y., Rao, X., Zhao, J., et al. (2022). CRISPR Screens Uncover Protective Effect of PSTK as a Regulator of Chemotherapy-Induced Ferroptosis in Hepatocellular Carcinoma. *Mol. Cancer* 21, 11. doi:10.1186/s12943-021-01466-9
- Dixon, S. J., Lemberg, K. M., Lamprecht, M. R., Skouta, R., Zaitsev, E. M., Gleason, C. E., et al. (2012). Ferroptosis: an Iron-dependent Form of Nonapoptotic Cell Death. *Cell* 149, 1060–1072. doi:10.1016/j.cell.2012.03.042
- Doll, S., Proneth, B., Tyurina, Y. Y., Panzilius, E., Kobayashi, S., Ingold, I., et al. (2017). ACSL4 Dictates Ferroptosis Sensitivity by Shaping Cellular Lipid Composition. *Nat. Chem. Biol.* 13, 91–98. doi:10.1038/nchembio.2239
- El-Khoueiry, A. B., Sangro, B., Yau, T., Crocenzi, T. S., Kudo, M., Hsu, C., et al. (2017). Nivolumab in Patients with Advanced Hepatocellular Carcinoma (CheckMate 040): an Open-Label, Non-comparative, Phase 1/2 Dose Escalation and Expansion Trial. *Lancet* 389, 2492–2502. doi:10.1016/s0140-6736(17)31046-2
- Fan, Y., Liu, B., Chen, F., Song, Z., Han, B., Meng, Y., et al. (2021). Hepcidin Upregulation in Lung Cancer: A Potential Therapeutic Target Associated with Immune Infiltration. *Front. Immunol.* 12, 612144. doi:10.3389/fimmu.2021.612144
- Feng, J., Lu, P.-z., Zhu, G.-z., Hooi, S. C., Wu, Y., Huang, X.-w., et al. (2021). ACSL4 Is a Predictive Biomarker of Sorafenib Sensitivity in Hepatocellular Carcinoma. *Acta Pharmacol. Sin.* 42, 160–170. doi:10.1038/s41401-020-0439-x
- Forner, A., Reig, M., and Bruix, J. (2018). Hepatocellular Carcinoma. *Lancet* 391, 1301–1314. doi:10.1016/s0140-6736(18)30010-2
- Friedmann Angeli, J. P., Krysko, D. V., and Conrad, M. (2019). Ferroptosis at the Crossroads of Cancer-Acquired Drug Resistance and Immune Evasion. *Nat. Rev. Cancer* 19, 405–414. doi:10.1038/s41568-019-0149-1
- Gao, R., Kalathur, R. K. R., Coto-Llerena, M., Ercan, C., Buechel, D., Shuang, S., et al. (2021). YAP/TAZ and ATF4 Drive Resistance to Sorafenib in Hepatocellular Carcinoma by Preventing Ferroptosis. *EMBO Mol. Med.* 13, e14351. doi:10.15252/emmm.202114351
- Houessinon, A., François, C., Sauzay, C., Louandre, C., Mongelard, G., Godin, C., et al. (2016). Metallothionein-1 as a Biomarker of Altered Redox Metabolism in Hepatocellular Carcinoma Cells Exposed to Sorafenib. *Mol. Cancer* 15, 38. doi:10.1186/s12943-016-0526-2
- Jabara, H. H., Boyden, S. E., Chou, J., Ramesh, N., Massaad, M. J., Benson, H., et al. (2016). A Missense Mutation in TFRC, Encoding Transferrin Receptor 1, Causes Combined Immunodeficiency. *Nat. Genet.* 48, 74–78. doi:10.1038/ng.3465
- Lachaier, E., Louandre, C., Godin, C., Saidak, Z., Baert, M., Diouf, M., et al. (2014). Sorafenib Induces Ferroptosis in Human Cancer Cell Lines Originating from Different Solid Tumors. *Anticancer Res.* 34, 6417–6422.
- Lei, G., Zhuang, L., and Gan, B. (2022). Targeting Ferroptosis as a Vulnerability in Cancer. *Nat. Rev. Cancer*. doi:10.1038/s41568-022-00459-0
- Li, D., Liu, B., Fan, Y., Liu, M., Han, B., Meng, Y., et al. (2021). Nuciferine Protects against Folic Acid-Induced Acute Kidney Injury by Inhibiting Ferroptosis. *Br. J. Pharmacol.* 178, 1182–1199. doi:10.1111/bph.15364
- Liao, P., Wang, W., Wang, W., Kryczek, I., Li, X., Bian, Y., et al. (2022). CD8(+) T Cells and Fatty Acids Orchestrate Tumor Ferroptosis and Immunity via ACSL4. *Cancer Cell* 40, 365–378.e6. doi:10.1016/j.ccell.2022.02.003
- Liu, Z., Zhao, Q., Zuo, Z.-X., Yuan, S.-Q., Yu, K., Zhang, Q., et al. (2020). Systematic Analysis of the Aberrances and Functional Implications of Ferroptosis in Cancer. *iScience* 23, 101302. doi:10.1016/j.isci.2020.101302
- Liu, M., Fan, Y., Li, D., Han, B., Meng, Y., Chen, F., et al. (2021). Ferroptosis Inducer Erastin Sensitizes NSCLC Cells to Celastrol through Activation of the ROS-Mitochondrial Fission-Mitophagy axis. *Mol. Oncol.* 15, 2084–2105. doi:10.1002/1878-0261.12936
- Loftus, R. M., Assmann, N., Kedia-Mehta, N., O'Brien, K. L., Garcia, A., Gillespie, C., et al. (2018). Amino Acid-dependent cMyc Expression Is Essential for NK Cell Metabolic and Functional Responses in Mice. *Nat. Commun.* 9, 2341. doi:10.1038/s41467-018-04719-2
- Louandre, C., Ezzoukhry, Z., Godin, C., Barbare, J.-C., Mazière, J.-C., Chaffert, B., et al. (2013). Iron-dependent Cell Death of Hepatocellular Carcinoma Cells Exposed to Sorafenib. *Int. J. Cancer* 133, 1732–1742. doi:10.1002/ijc.28159
- Lu, Y., Chan, Y.-T., Tan, H.-Y., Zhang, C., Guo, W., Xu, Y., et al. (2022). Epigenetic Regulation of Ferroptosis via ETS1/miR-23a-3p/ACSL4 axis Mediates Sorafenib Resistance in Human Hepatocellular Carcinoma. *J. Exp. Clin. Cancer Res.* 41, 3. doi:10.1186/s13046-021-02208-x
- Macek Jilkova, Z., Aspord, C., and Decaens, T. (2019). Predictive Factors for Response to PD-1/PD-L1 Checkpoint Inhibition in the Field of Hepatocellular Carcinoma: Current Status and Challenges. *Cancers (Basel)* 11, 1554. doi:10.3390/cancers11101554
- Nakaya, M., Xiao, Y., Zhou, X., Chang, J.-H., Chang, M., Cheng, X., et al. (2014). Inflammatory T Cell Responses Rely on Amino Acid Transporter ASCT2 Facilitation of Glutamine Uptake and mTORC1 Kinase Activation. *Immunity* 40, 692–705. doi:10.1016/j.immuni.2014.04.007
- Nie, J., Lin, B., Zhou, M., Wu, L., and Zheng, T. (2018). Role of Ferroptosis in Hepatocellular Carcinoma. *J. Cancer Res. Clin. Oncol.* 144, 2329–2337. doi:10.1007/s00432-018-2740-3
- Stockwell, B. R., Friedmann Angeli, J. P., Bayir, H., Bush, A. L., Conrad, M., Dixon, S. J., et al. (2017). Ferroptosis: A Regulated Cell Death Nexus Linking Metabolism, Redox Biology, and Disease. *Cell* 171, 273–285. doi:10.1016/j.cell.2017.09.021
- Sun, X., Niu, X., Chen, R., He, W., Chen, D., Kang, R., et al. (2016a). Metallothionein-1G Facilitates Sorafenib Resistance through Inhibition of Ferroptosis. *Hepatology* 64, 488–500. doi:10.1002/hep.28574
- Sun, X., Ou, Z., Chen, R., Niu, X., Chen, D., Kang, R., et al. (2016b). Activation of the P62-Keap1-NRF2 Pathway Protects against Ferroptosis in Hepatocellular Carcinoma Cells. *Hepatology* 63, 173–184. doi:10.1002/hep.28251
- Sung, H., Ferlay, J., Siegel, R. L., Laversanne, M., Soerjomataram, I., Jemal, A., et al. (2021). Global Cancer Statistics 2020: GLOBOCAN Estimates of Incidence and Mortality Worldwide for 36 Cancers in 185 Countries. *CA A Cancer J. Clin.* 71, 209–249. doi:10.3322/caac.21660
- Wang, R., Dillon, C. P., Shi, L. Z., Milasta, S., Carter, R., Finkelstein, D., et al. (2011). The Transcription Factor Myc Controls Metabolic Reprogramming upon T Lymphocyte Activation. *Immunity* 35, 871–882. doi:10.1016/j.immuni.2011.09.021
- Wang, W., Green, M., Choi, J. E., Gijón, M., Kennedy, P. D., Johnson, J. K., et al. (2019). CD8(+) T Cells Regulate Tumour Ferroptosis during Cancer Immunotherapy. *Nature* 569, 270–274. doi:10.1038/s41586-019-1170-y
- Wang, Q., Bin, C., Xue, Q., Gao, Q., Huang, A., Wang, K., et al. (2021). GSTZ1 Sensitizes Hepatocellular Carcinoma Cells to Sorafenib-Induced Ferroptosis via Inhibition of NRF2/GPX4 axis. *Cell Death Dis.* 12, 426. doi:10.1038/s41419-021-03718-4
- Wang, S., Chen, S., Ying, Y., Ma, X., Shen, H., Li, J., et al. (2021). Comprehensive Analysis of Ferroptosis Regulators with Regard to PD-L1 and Immune Infiltration in Clear Cell Renal Cell Carcinoma. *Front. Cell Dev. Biol.* 9, 676142. doi:10.3389/fcell.2021.676142
- Yang, M., Wu, X., Hu, J., Wang, Y., Wang, Y., Zhang, L., et al. (2022). COMMD10 Inhibits HIF1 $\alpha$ /CP Loop to Enhance Ferroptosis and Radiosensitivity by Disrupting Cu-Fe Balance in Hepatocellular Carcinoma. *J. Hepatology* 76, 1138–1150. doi:10.1016/j.jhep.2022.01.009
- Yuan, H., Li, X., Zhang, X., Kang, R., and Tang, D. (2016). C1SD1 Inhibits Ferroptosis by Protection against Mitochondrial Lipid Peroxidation. *Biochem. Biophys. Res. Commun.* 478, 838–844. doi:10.1016/j.bbrc.2016.08.034
- Zhang, B., Fan, Y., Cao, P., and Tan, K. (2021). Multifaceted Roles of HSF1 in Cell Death: A State-Of-The-Art Review. *Biochimica Biophys. Acta (BBA) - Rev. Cancer* 1876, 188591. doi:10.1016/j.bbcan.2021.188591
- Zhang, T., Sun, L., Hao, Y., Suo, C., Shen, S., Wei, H., et al. (2022). ENO1 Suppresses Cancer Cell Ferroptosis by Degrading the mRNA of Iron



- Regulatory Protein 1. *Nat. Cancer* 3, 75–89. doi:10.1038/s43018-021-00299-1
- Zhao, J., Yang, Z., Tu, M., Meng, W., Gao, H., Li, M. D., et al. (2021). Correlation between Prognostic Biomarker SLC1A5 and Immune Infiltrates in Various Types of Cancers Including Hepatocellular Carcinoma. *Front. Oncol.* 11, 608641. doi:10.3389/fonc.2021.608641
- Zhao, L., Zhou, X., Xie, F., Zhang, L., Yan, H., Huang, J., et al. (2022). Ferroptosis in Cancer and Cancer Immunotherapy. *Cancer Commun.* 42, 88–116. doi:10.1002/cac2.12250
- Zhu, A. X., Finn, R. S., Edeline, J., Cattani, S., Ogasawara, S., Palmer, D., et al. (2018). Pembrolizumab in Patients with Advanced Hepatocellular Carcinoma Previously Treated with Sorafenib (KEYNOTE-224): a Non-randomised, Open-Label Phase 2 Trial. *Lancet Oncol.* 19, 940–952. doi:10.1016/S1470-2045(18)30351-6
- Zhu, D., Wu, S., Li, Y., Zhang, Y., Chen, J., Ma, J., et al. (2022). Ferroptosis-related Gene SLC1A5 Is a Novel Prognostic Biomarker and Correlates with Immune Infiltrates in Stomach Adenocarcinoma. *Cancer Cell Int.* 22, 124. doi:10.1186/s12935-022-02544-8

**Conflict of Interest:** The authors declare that the research was conducted in the absence of any commercial or financial relationships that could be construed as a potential conflict of interest.

**Publisher's Note:** All claims expressed in this article are solely those of the authors and do not necessarily represent those of their affiliated organizations, or those of the publisher, the editors and the reviewers. Any product that may be evaluated in this article, or claim that may be made by its manufacturer, is not guaranteed or endorsed by the publisher.

Copyright © 2022 Zhang, Zhao, Liu, Shang, Chen, Zhang, He, Fan and Tan. This is an open-access article distributed under the terms of the Creative Commons Attribution License (CC BY). The use, distribution or reproduction in other forums is permitted, provided the original author(s) and the copyright owner(s) are credited and that the original publication in this journal is cited, in accordance with accepted academic practice. No use, distribution or reproduction is permitted which does not comply with these terms.



# Ferroptosis: Opportunities and Challenges in Treating Endometrial Cancer

Jianfa Wu<sup>1,2†</sup>, Li Zhang<sup>1,2†</sup>, Suqin Wu<sup>1,2\*</sup> and Zhou Liu<sup>1,2\*</sup>

<sup>1</sup>Department of Gynecology, Shanghai University of Medicine and Health Sciences Affiliated Zhoupu Hospital, Shanghai, China,

<sup>2</sup>Department of Gynecology, Shanghai University of Medicine and Health Sciences, Shanghai, China

## OPEN ACCESS

### Edited by:

Yanqing Liu,  
Columbia University, United States

### Reviewed by:

Zhenyi Su,  
Columbia University, United States  
Qiaosi Tang,  
Calico Life Sciences LLC,  
United States  
Shuang Chen,  
Henan University of Science and  
Technology, China

### \*Correspondence:

Suqin Wu  
wu\_su\_qing@126.com  
Zhou Liu  
zpyyfc@126.com

<sup>†</sup>The authors contributed equally to  
this work

### Specialty section:

This article was submitted to  
Molecular Diagnostics and  
Therapeutics,  
a section of the journal  
Frontiers in Molecular Biosciences

**Received:** 27 April 2022

**Accepted:** 25 May 2022

**Published:** 01 July 2022

### Citation:

Wu J, Zhang L, Wu S and Liu Z (2022)  
Ferroptosis: Opportunities and  
Challenges in Treating  
Endometrial Cancer.  
Front. Mol. Biosci. 9:929832.  
doi: 10.3389/fmolb.2022.929832

Ferroptosis, a new way of cell death, is involved in many cancers. A growing number of studies have focused on the unique role of ferroptosis on endometrial cancer. In this study, we made a comprehensive review of the relevant articles published to get deep insights in the association of ferroptosis with endometrial cancer and to present a summary of the roles of different ferroptosis-associated genes. Accordingly, we made an evaluation of the relationships between the ferroptosis-associated genes and TNM stage, tumor grade, histological type, primary therapy outcome, invasion and recurrence of tumor, and accessing the different prognosis molecular typing based on ferroptosis-associated genes. In addition, we presented an introduction of the common drugs, which targeted ferroptosis in endometrial cancer. In so doing, we clarified the opportunities and challenges of ferroptosis activator application in treating endometrial cancer, with a view to provide a novel approach to the disease.

**Keywords:** ferroptosis, prognosis, progress, treatment, initiation, endometrial cancer

## INTRODUCTION

Endometrial carcinoma is one of the most common gynecological malignancies. In the United States, there were 66,570 new cases in 2021, of which, 12,940 patients died from endometrial cancer (Siegel et al., 2022). Most endometrial cancers are diagnosed at an early stage, and in most cases, the 5-year survival rate was over 80%; however, we must admit that the prognosis of those who have recurrence or distant metastasis was still not optimistic, and that the 5-year survival rate is only 17.8% (Jeppesen et al., 2016; European Commission 2020). Many signaling pathways have been considered to be involved in the development of endometrial cancer, such as mitogen activated kinase-like pathway (MAPK), DNA repair process, PI3K-Akt pathway, steroid hormone receptors-associated pathway, WNT pathways, L1 cell adhesion molecule interaction pathway (L1CAM), and ferroptosis pathway (López-Janeiro et al., 2021). Of them, targeting ferroptosis signaling pathway has been considered as a new therapeutic strategy for the treatment of endometrial cancer. However, it is still unclear how these signaling pathways, especially ferroptosis pathway, modulate the initiation, metastasis, treatment, and prognosis of endometrial cancer.

Ferroptosis, a new and iron-dependent cell death form, is different from apoptosis, autophagy, and necrosis. Mainly, ferroptosis plays an important role in amino acid metabolism, oxidative stress, and iron metabolism, which is involved in various physiological and pathological processes, such as neuronal degeneration, antiviral immune response, ischemia re-perfusion injury, and especially in tumor suppression (Chen et al., 2021a; Hoy et al., 2021; Xiong et al., 2021; Lei et al., 2022). Studies have found that ferroptosis is closely associated with liver cancer, stomach cancer, pancreatic cancer,

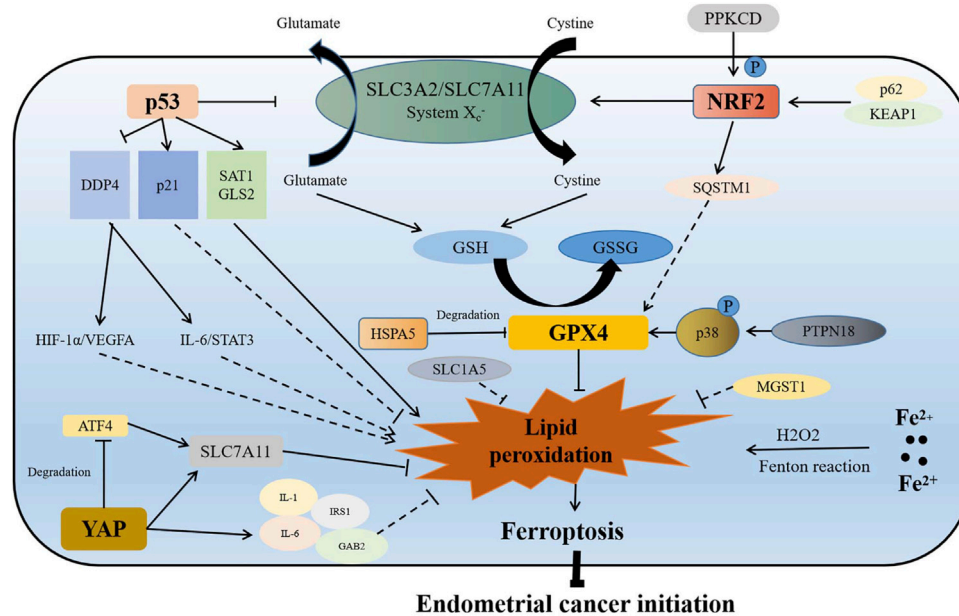


**FIGURE 1 |** Association of ferroptosis with initiation of endometrial cancer. On the one hand, p53 directly reduces the production of GSH by inhibiting the function of the SLC3A2/SLC7A11 complex, which inhibits the function of GPX4 to promote lipid peroxidation and ferroptosis. On the other hand, p53 indirectly targets p21, SAT1, GLS2, and DDP4, which may regulate ferroptosis and endometrial cancer initiation by activating the HIF-1 $\alpha$ /VEGFA and IL-6/STAT3 signaling pathways. When Nrf2 is overexpressed or phosphorylated activated by p62/KEAP1 or PPKCD, it inhibits lipid peroxidation and ferroptosis by promoting the expression of SQSTM1, and enhancing the function of SLC7A11 and GPX4. GPX4 is a ferroptosis inhibitor, which is regulated by HSPA5 and PTPN18. GPX4 plays an important role in inhibiting ferroptosis and promoting initiation of endometrial cancer. Increase of intracellular iron results in lipid peroxidation and ferroptosis by Fenton reaction. MGST1, SLC1A5, and YAP are also inhibitors of ferroptosis. YAP promotes the expression of SLC7A11 directly or through inhibiting ATF4 degradation. YAP also promotes the increase of IL-6, IL-1, IRS1, and GAB2, which may inhibit lipid peroxidation to promote endometrial cancer initiation. P in the graph represents phosphorylation.

breast cancer, stomach cancer, and ovarian cancer (Wang et al., 2021a; Jiang et al., 2021; Lin et al., 2021; López-Janeiro et al., 2021; Yang L et al., 2021; Yuan Y. et al., 2021). Ferroptosis activation has been considered to be a new approach to most tumors (Eling et al., 2015; Sun et al., 2016; Roh et al., 2017; Zhou et al., 2019; Gao et al., 2020). In particular, a growing number of studies have focused on the relationship between ferroptosis and endometrial cancer in recent years. Up to now, a large number of studies on ferroptosis *in vivo* and *in vitro* have provided new insights into the initiation, metastasis, recurrence, treatment, and prognosis of endometrial cancer.

In the current review, we systematically explored the relationship between ferroptosis and the initiation, metastasis, recurrence, treatment, and prognosis of endometrial cancer, in order to provide evidence-based guidance for the diagnosis and treatment of endometrial cancer.

## FERROPTOSIS AND INITIATION OF ENDOMETRIAL CANCER

Iron, an important component of most metabolic enzymes, is involved in mitochondrial oxidative phosphorylation, DNA synthesis, and cell cycle (Chen et al., 2017). Abnormal accumulation of intracellular iron is an important reason for ferroptosis, which has been considered to be associated with

many gynecological diseases, such as endometrial hyperplasia, endometriosis, and repeated transplantation failure (Bielfeld et al., 2019; Ng et al., 2020; Vogt et al., 2021). Similarly, ferroptosis has been found to be involved in the initiation of endometrial cancer through different pathways (Figure 1).

Nrf2 is a prerequisite for spheroid formation *via* regulation of ferroptosis in 3D culture models (Takahashi et al., 2020). Activation of antioxidant stress signaling pathway regulated by Nrf2 is an important reason for ferroptosis resistance (Chen et al., 2021a). Nrf2 inhibits ferroptosis mainly by activating iron metabolism-related genes (SLC40A1 and MT1G), GSH metabolism-related genes (SLC7A11 and GCLM), and ROS detoxification enzymes (AKR1C1 and NQO1) in many cancers (Chen et al., 2021b). As previously revealed, the p62-Keap1-Nrf2 signaling pathway played an important role in promoting estrogen-induced endometrial hyperplasia by inhibiting ferroptosis (Zhang M et al., 2021). On one hand, Nrf2 regulated the expression of glutathione-dependent lipid antioxidant (GPX4) directly or indirectly, while GPX4 overexpression resulted in ferroptosis inhibition (Fan et al., 2017); on the other hand, the overexpression of Nrf2 was found to promote the expression of solute carrier family 7 member 11 (SLC7A11) and increase the GSH level to inhibit ferroptosis (Song and Long, 2020). The phosphorylation activation of Nrf2 with protein kinase C delta (PRKCD) contributed to endometrial hyperplasia *via* promoting sequestosome 1 (SQSTM1) expression (Feng et al., 2017). All these results suggest that Nrf2, as an important inhibitor of ferroptosis,

plays an important role in the initiation of endometrial cancer. Furthermore, the positive expression rate of Nrf2 was found to be higher in endometrial serous carcinoma than in endometrioid carcinomas and clear cell carcinomas (68 vs. 6 vs. 13%) (Chen et al., 2010). In addition, Nrf2 could be used as a diagnostic marker for the different types of endometrial cancer.

Glutathione-dependent lipid antioxidant (GPX4), a member of the glutathione peroxidase family, catalyzed the reduction of hydrogen peroxide to protect cells against oxidative damage (Xu et al., 2021). GPX4, a key suppressor of the ferroptosis pathway, has been reported to be associated with many tumors (Lu Y. et al., 2021; Sha et al., 2021; Sun et al., 2021). As to endometrial cancer, proteomic analysis indicated that the expressions of GPX4, glutathione synthetase (GSS), ferroptosis suppressor protein 1 (FSP1), and transferring receptor 1 protein (TFRC) were higher in the early-stage endometrial cancer than in the normal tissues (López-Janeiro et al., 2021). Therefore, GPX4-suppressed ferroptosis can be an important reason for the initiation of endometrial cancer. Moreover, GPX4 has been recognized as a potential target for many genes; heatshock 70-kDa protein 5 (HSPA5) bound to GPX4 and inhibited its protein degradation, thus promoting the initiation of endometrial cancer (Zhu et al., 2017), and protein tyrosine phosphatase non-receptor type 18 (PTPN18) targeted and activated the p-P38-GPX4/xCT signaling pathway, which also contributed to the initiation of endometrial cancer (Wang et al., 2021a).

p53 is a double-edged sword for ferroptosis, which regulates ferroptosis through both canonical and non-canonical ferroptosis pathways (Liu and Gu 2022). However, p53 alone does not induce ferroptosis directly. p53 is an important regulator for lipid, amino acid, glucose, nucleotide, and iron metabolism (Liu and Gu et al., 2021; Liu J. et al., 2021). Based on metabolism targets, p53 contributed to ferroptosis (Liu and Gu 2022). In most cases, p53 acts as a promoter of ferroptosis. However, in some special cases, p53 can inhibit apoptosis. p53 has been identified as a central regulator of ferroptosis, which represents an independent pathway as GPX4-based ferroptosis. As an activator of ferroptosis in endometrial cancer (León-Castillo et al., 2020; Liu et al., 2020), p53 hampers SLC7A11 expression to induce ferroptosis. As an important component of cystine transport protein Xc<sup>-</sup> (system Xc<sup>-</sup>), SLC7A11 has been found to inhibit ferroptosis by promoting cystine transport, increasing the intracellular cysteine level and GSH level (Jiang et al., 2015; Koppula et al., 2021), and also SLC7A11 has been considered to be a poor prognosis factor for endometrial cancer (Martin et al., 2022). Moreover, it was another way for p53 to induce ferroptosis when spermidine/spermine N1-acetyltransferase 1 (SAT1) and glutaminase 2 (GLS2) expressions was promoted (Kang et al., 2019). As a regulator of polyamine metabolism, SAT1 acted as a target of p53, being responsible for oxidative stress (Thomas and Thomas 2003), while SAT1 deletion weakened ferroptosis induced by p53 (Ou et al., 2016). GLS2, a member of mitochondrial glutaminases, also served as a target of p53 (Hu et al., 2010). When GLS2 was knocked down, ferroptosis caused by p53 was also minimized (Gao et al., 2015). Another important role of p53 in endometrial cancer was when cyclin-dependent kinase inhibitor 1 A (CDKN1A/p21) expression was promoted by

p53. CDKN1A mutation induced microsatellite instability (MSI) via the epigenetic silencing of the mutL homolog 1 (MLH1) (Waheed et al., 2019). However, the relationship between p21 and endometrial cancer remains controversial. Some reports indicated that the growth of endometrial cancer cells was hampered when CDKN1A was upregulated, which implied that p21 inhibited the proliferation of endometrial cancer (Waheed et al., 2019; Costa et al., 2021). Nevertheless, Planagumà et al. (2006) found that the expression of p21 in endometrial cancer was higher compared to normal control, simple hyperplasia endometria, and complex hyperplasia endometria, which suggested that p21 promoted the initiation of endometrial cancer. Therefore, the relationship between p21 and initiation of endometrial cancer still needs to be verified by subsequent experiments. As an inhibitor of ferroptosis in endometrial cancer, another mechanism of ferroptosis regulation mediated by p53 was when dipeptidyl peptidase 4 (DPP4) expression was inhibited (Kang et al., 2019). DPP4, an intrinsic type II transmembrane glycoprotein, was found to be involved in insulin metabolism, immune regulation, and cancer development (Xie et al., 2017). In endometrial cancer, DPP4 is a risk factor, which promotes cancer proliferation, invasion and tumorigenesis through HIF-1a/VEGFA signaling, and IL-6/STAT3 signaling pathway. However, DPP4 inhibitor therapy has been reported to be capable of inhibiting tumor growth (Yang et al., 2017; Yang et al., 2021a).

As to iron, which is an important condition for ferroptosis, its dietary intake was positively associated with endometrial cancer risk (adjusted OR = 1.9; 95% CI = 1.4–2.7), especially in postmenopausal women (OR = 2.2; 95% CI = 1.4–3.4) and women with BMI ≥25 kg/m<sup>2</sup> (OR = 3.2; 95% CI = 1.4–7.5) (Kallianpur et al., 2010). A previous study, which enrolled 60,895 women in the Swedish mammography cohort, indicated that the higher intake of heme iron mildly increased the risk of endometrial cancer (RR: 1.24; 95% CI: 1.01–1.53; for ≥1.63 mg/d vs. <0.69 mg/d), so did the higher intake of total iron (RR: 1.31; 95% CI: 1.07–1.61; for ≥15.09 mg/d vs. <12.27 mg/d) (Genkinger et al., 2012). However, controversy still exists between dietary iron and endometrial cancer, as indicated by a large cohort study in Canada with 34,148 women enrolled and followed for a mean of 16.4 years, showing that there was no association between intake of meat or any of the dietary iron-related variables and risk of endometrial cancer. Furthermore, iron overload caused by increased iron absorption reduced iron storage and restricted iron outflow contributed to ferroptosis (Kabat et al., 2008). On one hand, increased intracellular iron promoted the increase of reactive oxygen species (ROS) through iron-dependent Fenton reaction (Chen et al., 2020). On the other hand, iron-containing lipid oxidase was activated to induce lipid peroxidation (Stockwell 2017). Nevertheless, iron-chelating agents (deferoxamine), as well as drugs which increased iron-mediated toxicity (sulfasalazine, statins, sorafenib, etc.) showed favorable effects in many cancers (Stockwell 2017). In particular, the combination of sulfasalazine and cisplatin indicated synergistic inhibitory effect on cell proliferation in uterine serous carcinoma cell lines (Sendo et al., 2022).

Other ferroptosis-associated genes have also been found to be involved in the initiation of endometrial cancer (**Supplementary**



**Table S1).** Since microsomal glutathione S-transferase 1 (MGST1) is a ferroptosis suppressor, the expression of MGST1 was higher in endometrial cancer than in the normal tissues (Yan et al., 2022). The upregulation of solute carrier family 1 member 5 (SLC1A5), a glutamine transporter, has also been observed in many cancers (Huang et al., 2014; Kaira et al., 2015; Luo et al., 2018). In endometrial cancer in comparison with the normal endometrium, highly expressed SLC1A5 was similarly found in endometrioid and serous subtypes of endometrial carcinoma (Marshall et al., 2017). As a novel ferroptosis inducer, BRCA1-associated protein 1 (BAP1) encodes a nuclear deubiquitinating enzyme. BAP1 represses SLC7A11 expression by decreasing H2Aub occupancy on the SLC7A11 promoter in many cancers (Zhang et al., 2018). Nevertheless, BAP1 was found to be rarely investigated in endometrial cancer. One case report revealed that the negative expression of BRCA1-associated protein 1 (BAP1) was observed in the peritoneal masses after endometrial cancer surgery (Makiuchi et al., 2020). As a ferroptosis suppressor, Yes1 associated transcriptional regulator (YAP) is also a downstream gene of the Hippo signaling pathway. On one hand, YAP/TAZ directly induced the expression of SLC7A11; on the other hand, it sustained the protein stability of ATF4, which synergistically induced SLC7A11 expression to inhibit ferroptosis (Gao et al., 2021). Moreover, Wu et al. (2019) reported that the NF2-YAP signaling pathway played an important role on ferroptosis suppression, while antagonizing this signaling pathway contributed to ferroptosis through upregulating expression of Acyl-CoA Synthetase long-chain family member 4 (ACSL4) and TFRC. The expression of YAP was higher in endometrial cancer than in the normal tissues and cells, which was associated with higher grade, stage, lympho-vascular space invasion, and postoperative recurrence/metastasis (Tsujiura et al., 2014; Cheng et al., 2020); the inhibition of YAP restrained proliferation, increasing therapy sensibility by reducing interleukin-6 (IL-6), IL-11, and IRS1 (Wang C. et al., 2016; Wang et al., 2019); and the knockdown of YAP and TAZ also prevented PI3K pathway activation by inhibiting the expression of GAB2 linker molecule in endometrial cancer (Wang et al., 2017).

However, most of the previous studies have been based on *in vitro* experiments or correlational studies, with a lack of large-sample clinical studies; most of the mechanism clarifications have not been sufficient enough. The underlying mechanism of ferroptosis-associated genes still needs to be further explored to better understand the initiation of endometrial cancer.

## FERROPTOSIS AND METASTASIS OR RECURRENCE OF ENDOMETRIAL CANCER

Endometrial cancers metastasize mainly through lymphatic metastasis and local invasive metastasis, but less through hematogenous metastasis. It has been reported that 71% of stage 3 patients experience distant metastasis (Tangjitgamol et al., 2004; Franchello et al., 2015), and that 15% of patients

with FIGO I and II endometrial cancer undergo recurrences, especially those who had deep myometrial invasion and lympho-vascular invasion (Fung-Kee-Fung et al., 2006; Sartori et al., 2010). Since metastasis and recurrence are closely associated with prognosis of endometrial cancer, the 5-year overall survival (OS) rates of patients with metastasis, pelvic recurrence, and extrapelvic recurrence were lower than those of the localized endometrial carcinoma (16, 55 and 17% vs. 95%) (Xu et al., 2016; National Cancer Institute Surveillance, 2017). Therefore, it is of great significance to clarify the mechanism of metastasis and recurrence of endometrial cancer, since it has not been unclear so far. Thus no effective strategy is available to improve the prognosis of endometrial cancer, especially with metastasis or recurrence.

Previous studies have found that ferroptosis is associated with metastasis and recurrence of many tumors (Ubellacker et al., 2020; Li et al., 2021; Liu W. et al., 2021; Luis et al., 2021). In endometrial cancer, actually, many ferroptosis-associated genes have been discovered to be involved in its metastasis or recurrence (Figure 2). Bioinformatics analysis showed that CDKN1A was closely related to the occurrence of type II endometrial carcinoma, which was prone to recurrence and metastasis (Zhang K. et al., 2019). More importantly, DETA/NO and progesterone-inhibited invasion of endometrial cancer by upregulating CDKN1A expression *in vitro* (Dai et al., 2002; Waheed et al., 2019). As a ferroptosis suppressor, fanconi anemia complementation group D2 (FANCD2) was involved in DNA damage repair (Song et al., 2016). According to a tissue microarray analysis, FANCD2 overexpression was associated with lympho-vascular invasion in type I endometrial cancer and recurrence in type II endometrial cancer (Mhawech-Fauceglia et al., 2014). High expression of MGST1 was also found to be associated with the high frequency of tumor invasion (Yan et al., 2022). Therefore, MGST1 can serve as a predictive factor for the prognosis of endometrial cancer.

It was revealed that DDP4 facilitated the invasion of endometrial cancer *in vitro*, while this facilitation was abrogated with the DDP4 inhibitor (Yang et al., 2017). Moreover, p53 inactivated with enhanced ubiquitination was found to be associated with the invasion or recurrence of endometrial cancer (Liu et al., 2020). As an apoptosis inducer, apoptosis-stimulating p53 protein 2 (ASPP2) suppressed cell migration and invasion by reducing the expression of phosphorylated YAP (Konno et al., 2020). Since p190A is frequently mutated in endometrial cancer, its knockout was reported to promote cell proliferation and migration *via* activation of the Hippo-YAP pathway (Wen et al., 2020). Being a molecular marker of fibrosis, fibroblast-specific protein 1 (FSP1) acts as a GPX4-independent ferroptosis inhibitor. FSP1 has been reported to inhibit ferroptosis by reducing CoQ10 to prevent lipid oxidation, while cell sensitivity to ferroptosis increased after FSP1 inhibitor (iFSP1) treatment (Bersuker et al., 2019; Doll et al., 2019). In endometrial cancer, it was revealed that TGF-beta1 stimulated cell migration and invasion by increasing FSP1 expression (Xie et al., 2009).

In addition, the drugs which target ferroptosis have shown to be capable of invasion inhibition in endometrial cancer, as in the

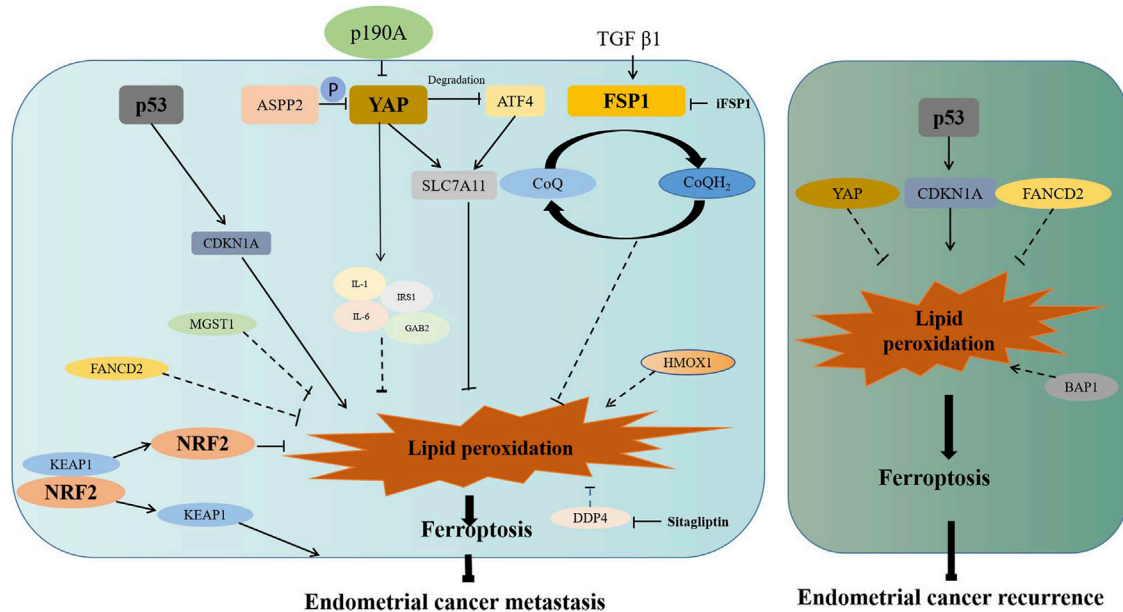


**FIGURE 2 |** Association of ferroptosis-associated genes with metastasis or recurrence of endometrial cancer. ASPP2 and p190A inhibit migration of endometrial cancer via inactivating the Hippo–YAP signaling pathway. YAP promotes the expression of SLC7A11 directly or through inhibiting ATF4 degradation. YAP also promotes the increase of IL-6, IL-1, IRS1, and GAB2, which may inhibit lipid peroxidation to promote invasion or migration. TGFβ1 promotes the expression of FSP1, which inhibit lipid peroxidation to promote invasion or migration. After Nrf2 dissociated from KEAP1, activated Nrf2 inhibits lipid peroxidation to promote invasion or migration. p53 enhances the expression of CDKN1A to promote lipid peroxidation. MGST1, FANCD2, and DDP4 may promote invasion or migration through inhibiting lipid peroxidation and ferroptosis. HMOX1 may restrain invasion or migration through promoting lipid peroxidation and ferroptosis. Moreover, increased ubiquitinated degradation of p53 results in the decreased expression of CDKN1A, which results in reduced ferroptosis and enhanced recurrence. FANCD2 and YAP may promote recurrence through inhibiting lipid peroxidation and ferroptosis. BAP1 may prevent recurrence through promoting lipid peroxidation and ferroptosis. P in the graph represents phosphorylation.

case of juglone, which promoted HMOX1 expression, thereby inhibiting the migration of endometrial cancer (Yuan Y. et al., 2021) and of simvastatin which inhibited metastasis through the modulation of the MAPK and AKT/mTOR pathways (Schointuch et al., 2014).

At present, however, the studies are still limited on the relationship between ferroptosis-associated genes and metastasis or recurrence of endometrial cancer. The previous studies are mostly based on clinical correlation analysis and *in vitro* experiments, and the mechanism of ferroptosis-associated genes has not been sufficiently clarified on the metastasis or recurrence of endometrial cancer. This, therefore, pushes us to stay at the forefront of the studies to pursue the underlying mechanism of endometrial cancer metastasis or recurrence.

## FERROPTOSIS AND TREATMENT OF ENDOMETRIAL CANCER

In general, surgery is the main approach to endometrial cancer. To prevent its metastasis and recurrence, it is important that post-surgical adjuvant chemotherapy and radiotherapy are administered (Lu et al., 2020; Concin et al., 2021); however, it is admitted that drug resistance is a significant challenge for the treatment. Drug resistance is a complex process in endometrial

cancer, which involves factors such as enhancing proliferation, reducing apoptosis, and abnormal transmembrane transport of drugs (Huang W. et al., 2021; Kong et al., 2021; Yuan S. et al., 2021). However, no good predictor is still available for drug resistance in endometrial cancer. As a newly discovered way of cell death, ferroptosis has been considered to be closely related to drug resistance in endometrial cancer (He et al., 2021). It was reported that the IC<sub>50</sub> of cisplatin and paclitaxel was higher in those who had a low score than in those who had a high score of ferroptosis, while the IC<sub>50</sub> of erlotinib, rapamycin, and temsirolimus was lower in those who had a low score than in those who had a high score of ferroptosis (Wang et al., 2021b). This suggests that those who had a low score of ferroptosis are more likely to be resistant to cisplatin and paclitaxel, while those who had a high score are more likely to be resistant to erlotinib, rapamycin, and temsirolimus. Similarly, another ferroptosis-related prognosis signature showed lower IC<sub>50</sub> of roscovitine, vinblastine, tipifarnib, lapatinib, and other twenty-two routinely administered chemotherapy drugs in the low-risk group than the high-risk group (Liu J. et al., 2021). Moreover, quite a number of ferroptosis-associated genes are responsible for chemoresistance in ovarian cancer, as indicated by the activation of the HSPA5-GPX4 pathway, which induced ferroptosis resistance, an important reason for gemcitabine resistance (Zhu et al., 2017); by the overexpression of FANCD2, which resulted in platinum resistance, while restraining FANCD2 expression with

pristimerin sensitized endometrial cancer to platinum (Bi et al., 2019), and the activation of the Nrf2 signaling pathway led to chemoresistance in endometrial cancer, while targeting Nrf2 with metformin rendered endometrial cancer more sensitive to chemotherapeutics (Wang Y. et al., 2016; Bai et al., 2018). In view of these evidence, the ferroptosis-associated genes serve as favorable predictors for chemotherapy sensitivity in clinical practice.

As indicated in **Supplementary Table S1**, targeting ferroptosis-associated genes could be an effective way for treatment in endometrial cancer. Being a natural compound, quinones are of good anti-inflammatory, antioxidant stress, and antitumor effects. Juglone and plumbagin, as natural quinones compounds, have been found to have a good therapeutic effect on endometrial carcinoma (Zhang Y. Y. et al., 2019; Zhang et al., 2020). In particular, juglone, one of the 16 organic compounds of *C. cathayensis*, induced ferroptosis by promoting intracellular iron accumulation, GSH, and MDA depletion in endometrial carcinoma (Zhang Y. Y. et al., 2021). However, the therapeutic effects of juglone and plumbagin on endometrial cancer are still limited to *in vitro* experiments. Thus, *in vivo* experiments and clinical studies are still needed to determine the therapeutic effects of juglone and plumbagin.

Known as the inducer of ferroptosis, statins target cholesterol synthesis of rate-limiting enzymes (HMG-CoA) (Schweitzer et al., 2020). FSP1-CoQ10-NAD (P) H signaling pathway acted synergistically with GPX4 and GSH to inhibit lipid peroxidation and ferroptosis (Doll et al., 2019). As a common statin, simvastatin was found to inhibit cell proliferation and induce cell death in a dose-dependent manner in endometrial cancer cell lines (Schointuch et al., 2014). Statins exerted a chemo-protective effect in endometrial cancer (Kato et al., 2010). However, there is still a lack of sufficient evidence to verify the association of statins use with prognosis improvement in endometrial cancer (Hafizz et al., 2020). Moreover, quite a number of problems and challenges are lying ahead to be addressed; this is particularly true when statins' compatible variety, optimal dose, application duration, and therapeutic effects or side effects are to be certified while they are being combined with routinely administered chemotherapy drugs.

Sorafenib, a novel oral targeted therapy, can inhibit the serine/threonine kinase activation of RAF-1 and B-Raf, as well as the tyrosine kinase activation of vGFR-2, VEGF-3, PDGF- $\beta$ , KIT, and FLT-3 receptors (Keating, 2017). Specially, it also functions as an inducer of ferroptosis to inhibit the activation of system Xc<sup>-</sup> (Gao et al., 2021). In the case of endometrial cancer, sorafenib was revealed to sensitize endometrial carcinoma cells to TRAIL- and Fas-induced apoptosis *in vitro* (Llobet et al., 2010). Moreover, sorafenib alone induced apoptosis in endometrial cancer by transcriptionally inhibiting myeloid cell leukemia 1 (MCL-1) expression and promoting its protein degradation (Sun et al., 2013), while it showed a limited effect on both uterine carcinoma and uterine carcinosarcoma in a multi-center phase II clinical study (Nimeiri et al., 2010). Sorafenib activated MAPK/JNK-dependent autophagy to enhance the antitumor activity (Eritja et al., 2017). Nevertheless, there is still a long way to go before sorafenib can be used as a routine clinical therapy for endometrial

cancer, since quite a number of problems and challenges lie ahead to be addressed in terms of clinical efficacy, adverse reaction, drug resistance and regulatory mechanisms associated with ferroptosis.

Given that the expressions of TMB and MSI in endometrial cancer are significantly correlated to the SLC7A11 level, it has been hypothesized that the use of ferroptosis inducers can have synergistic effects with immune checkpoint inhibitors (McConechy et al., 2015; Yang, 2015; Yang et al., 2019). However, this hypothesis only stays at the theoretical level, which still needs to be verified *via in vivo* and *in vitro* experiments.

In conclusion, ferroptosis inducers have shown a potential application value in the treatment of endometrial cancer, by increasing the sensitivity of cancer to the traditional medications compared to those traditional drugs such as carboplatin, paclitaxel, doxorubicin, bevacizumab, medroxyprogesterone acetate, and GnRHa. However, the application data of ferroptosis inducers is limited in clinical, especially the specific ferroptosis inducers. The efficacy and safety of ferroptosis inducers still need to be verified with further basic and clinical studies, so do the indications and applicable populations of ferroptosis inducers as well as the efficacies, drug dosages and side effects of single drug or different combination regimens. In particular, it remains unknown whether ferroptosis inducers can simultaneously induce ferroptosis of cancer cells and immune cells to comprise the body's immune function, and how ferroptosis inducers can modulate different immune cells to enhance or weaken the body's immune response.

## FERROPTOSIS AND PROGNOSIS OF ENDOMETRIAL CANCER

It is well recognized that the prognosis of endometrial cancer is related to quite a number of contributing factors such as tumor histological type, tumor stage, pathological stage, metabolism, and recurrence, which is also true of many ferroptosis-associated genes in endometrial cancer (**Figure 3**). The high expressions of CDKN1A, SLC7A11, and SAT1 were found to be linked to the low stage, grade of pTNM, and longer survival time in endometrial cancer (Qin et al., 2021). As a ferroptosis suppressor, it was revealed that FANCD2 overexpression was associated with high tumor grade, advanced tumor stage, and lympho-vascular invasion in type I endometrial cancer (Mhawech-Fauceglia et al., 2014), while in type II endometrial cancer, the patients with the positive expression of FANCD2 were found to be more likely to recur within 5 years and with poor 5-year recurrence free survival (RFS) (71.4 vs. 85.5%) and OS (68 vs. 80.3%) (Mhawech-Fauceglia et al., 2014). The expression of HSPA5 was reported to be higher in high-risk endometrial cancer than in low-risk endometrial cancer and normal endometrium, which suggested that HSPA5 was also associated with higher malignant degree and poor prognosis of endometrial cancer (Teng et al., 2013). In addition, univariate and multivariate regression analyses indicated that the high

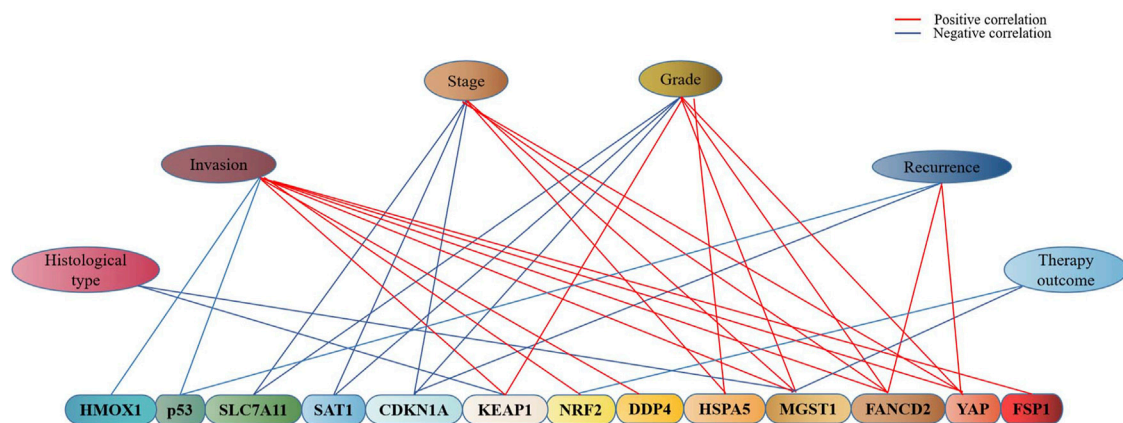


**FIGURE 3 |** Association of ferroptosis-associated genes with clinical characteristics of endometrial cancer. As indicated in the graph, there exists an association of ferroptosis-associated genes with the stage, grade, invasion, recurrence, histopathological type, and therapy outcome of endometrial cancer, blue represents the negative and red represents the positive.

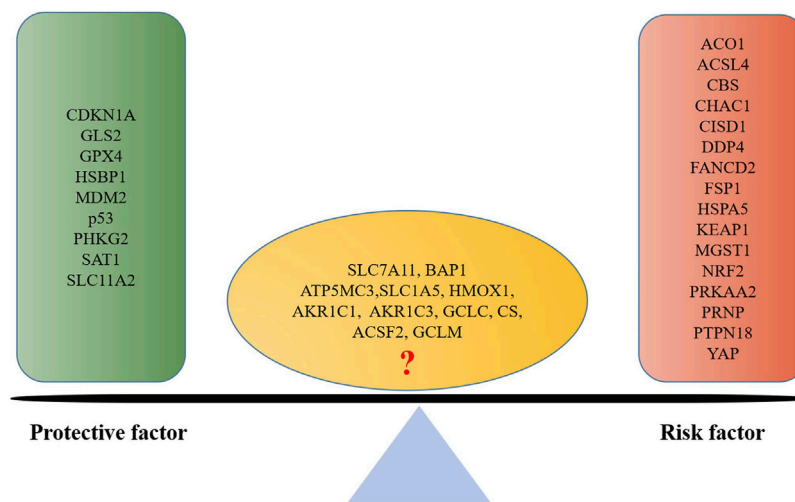


**FIGURE 4 |** Ferroptosis-associated gene-based protective factor and risk factor in endometrial cancer. A list is made of ferroptosis-associated genes involved in endometrial cancer prognosis based on the previous literature; those which are positively associated with a good prognosis are defined as protective factors, and those which are negatively associated are defined as risk factors.

expression of MGST1 was associated with the high clinical stage (TNM), poor primary therapy outcome, poor histological type, high tumor invasion, and poor histologic grade (Yan et al., 2022), hence MGST1 is regarded as a progress predictive factor for endometrial cancer.

Moreover, many other ferroptosis-associated genes were also found to be associated with prognosis of endometrial cancer *via* clinical observation or bioinformatics analysis (Figure 4). A pan-cancer analysis indicated that SLC7A11, a key gene of ferroptosis, was a risk factor for worsen OS in such cancers as adrenocortical carcinoma, bladder urothelial carcinoma, head-and-neck squamous cell carcinoma, kidney renal clear cell carcinoma, liver hepatocellular carcinoma, and

skin cutaneous melanoma, while it was a protective factor for prolonged OS for ovarian cancer and rectum adenocarcinoma (He et al., 2021). No association has been reported of SLC7A11 with endometrial cancer; however, the association of SLC7A11 with the prognosis of endometrial cancer remains controversial. Qin et al. (2021) reported that SLC7A11 was associated with prolonged survival time of endometrial cancer, which suggested a protective factor. While CDKN1A was found to be an activator of ferroptosis, which was significantly associated with better prognosis of endometrial cancer (Yamawaki et al., 2017); and ACSL4 was associated with lipid metabolism and lipid peroxidation dependent ferroptosis, while the low expression of ACSL4 was



**TABLE 1 |** Molecular typing for endometrial cancer.

Author	Article title	Date	Gene panel	Risk prediction formula	AUC
Yin Weijiao et al.	Immune infiltration and a ferroptosis-associated gene signature for predicting the prognosis of patients with endometrial cancer	2021	MDM2, GPX4, PRKAA2, PRNP, SLC11A2, ATP5MC3, PHKG2, and ACO1	Risk score = $(-0.34216 \times \text{MDM2 expression}) + (-0.08952 \times \text{GPX4 expression}) + (0.55497 \times \text{PRKAA2 expression}) + (0.08230 \times \text{PRNP expression}) + (-0.46253 \times \text{SLC11A2 expression}) + (0.41109 \times \text{ATP5MC3 expression}) + (-0.50883 \times \text{PHKG2 expression}) + (0.30930 \times \text{ACO1 expression})$	1-year: 0.676 2-year: 0.775 3-year: 0.797 5-year: 0.826
Jinhui Liu et al.	Identification of the prognostic signature associated with tumor immune microenvironment of uterine corpus endometrial carcinoma based on eroptosis-related genes	2021	HMOX1, KEAP1, HSBP1, SAT1, C1SD1, and GPX4	Risk score = $(0.002907 \times \text{HMOX1}) + (0.013486 \times \text{KEAP1}) + (-0.089640 \times \text{HSBP1}) + (-0.001665 \times \text{SAT1}) + (0.148,239 \times \text{C1SD1}) + (-0.003060 \times \text{GPX4})$	1-year: 0.705 3-year: 0.607 5-year: 0.713
L.S. E. ERIKSSON et al.	Combination of proactive molecular risk classifier for endometrial cancer (ProMisE) with sonographic and demographic characteristics in preoperative prediction of recurrence or progression of endometrial cancer	2021	ProMisE subtype, age, waist circumference, sonographic tumor extension, and size	-	3-year: 0.890
Xiao Yang et al.	A novel transcription factor-based prognostic signature in endometrial cancer: establishment and validation	2021	MSX1, HOXB9, E2F1, DLX4, BNC2, DLX2, PDX1, POU3F2, and FOXP3	Risks core = $(-0.0621 \times \text{ExpDLX2}) + (-0.2395 \times \text{ExpFOXP3}) + (0.1016 \times \text{ExpPOU3F2}) + (0.2536 \times \text{ExpPDX1}) + (0.3276 \times \text{ExpBNC2}) + (0.2091 \times \text{ExpDLX4}) + (0.0158 \times \text{ExpE2F1}) + (0.0071 \times \text{ExpHOXB9}) + (-0.0021 \times \text{ExpMSX1})$	5-year: 0.761
Xuecheng Pang et al.	Development and validation of m6A regulators' prognostic significance for endometrial cancer	2021	IGF2BP1 and YTHDF3	Risk score = $0.0904 \times \text{IGF2BP1} + 0.195 \times \text{YTHDF3}$	1-year: 0.6552 3-year: 0.6408 5-year: 0.6439
Nan Lu et al.	MiRNA-based tumor mutation burden diagnostic and prognostic prediction models for endometrial cancer	2021	hsa-miR-146a-5p, hsa-miR-708-5p, hsa-miR-4746-5p, hsa-miR-452-5p, hsa-miR-452-3p, hsa-miR-224-5p, hsa-miR-375-3p, hsa-miR-30a-5p, hsa-miR-598-3p, hsa-miR-335-3p, hsa-miR-30c-5p, hsa-miR-101-5p, hsa-miR-210-3p, hsa-miR-676-3p, hsa-miR-130a-3p, hsa-miR-1266-5p, hsa-miR-1271-5p, hsa-miR-130a-5p, hsa-miR-203b-3p, hsa-miR-3074-5p, and hsa-miR-30d-5p	Risk score = $\text{hsa-miR-146a-5p} \times 0.091672 + \text{hsa-miR-708-5p} \times (-0.01454) + \text{hsa-miR-4746-5p} \times 0.647,021 + \text{hsa-miR-452-5p} \times 0.057283 + \text{hsa-miR-452-3p} \times (-0.26965) + \text{hsa-miR-224-5p} \times 0.018647 + \text{hsa-miR-375-3p} \times 0.11641 + \text{hsa-miR-30a-5p} \times 0.328,458 + \text{hsa-miR-598-3p} \times 0.022044 + \text{hsa-miR-335-3p} \times (-0.49775) + \text{hsa-miR-30c-5p} \times (-0.63721) + \text{hsa-miR-101-5p} \times 0.021696 + \text{hsa-miR-210-3p} \times 0.571,997 + \text{hsa-miR-676-3p} \times (-0.53052) + \text{hsa-miR-130a-3p} \times 0.021182 + \text{hsa-miR-1266-5p} \times 0.346,479 + \text{hsa-miR-1271-5p} \times (-0.10099) + \text{hsa-miR-130a-5p} \times (-0.09051) + \text{hsa-miR-203b-3p} \times (-0.06494) + \text{hsa-miR-3074-5p} \times 0.432,032 + \text{hsa-miR-30d-5p} \times (-0.40024)$	1-year: 0.649 3-year: 0.602 5-year: 0.699
Ziwei Wang et al.	An immune-related long noncoding RNA signature as a prognostic biomarker for human endometrial cancer	2021	ELN-AS1, AC103563.7, PCAT19, AF131215.5, LINC01871, AC084117.1, NRAV, SCARNA9, AL049539.1, POC1B-AS1, AC108134.4, and AC019080.5	Risk Score = $(\text{ELN-AS1} \times 0.229) + (\text{AC103563.7} \times 0.313) + (\text{PCAT19} \times -0.277) + (\text{AF131215.5} \times 0.252) + (\text{LINC01871} \times -0.357) + (\text{AC084117.1} \times 0.449) + (\text{NRAV} \times -0.433) + (\text{SCARNA9} \times -0.339) + (\text{AL049539.1} \times 0.476) + (\text{POC1B-AS1} \times -0.758) + (\text{AC108134.4} \times -0.262) + (\text{AC019080.5} \times 0.899)$	3-year: 0.808 5-year: 0.831
Shijin Huang et al.	Identification of a four-gene signature with prognostic significance in endometrial cancer using weighted gene correlation network analysis	2021	BUB1B, NDC80, TPX2, and TTK	Risk Score = $0.8871 \times \text{expression of TTK} + (-0.5266 \times \text{expression of BUB1B}) + (-0.5022 \times \text{expression of NDC80}) + 0.5177 \times \text{expression of TPX2}$	2-year: 0.683 3-Year: 0.703 5-year: 0.684
Eva Coll-de la Rubia et al.	<i>In silico</i> approach for validating and unveiling new applications for prognostic biomarkers of endometrial cancer	2021	ASRGL1, ESR1, FASN, HDGF, MACC1, MCM6, MCM7, MSH2, MSH6, PTK2, and TPX2	—	4-year: 0.827

observed in endometrial cancer to be associated with better prognosis (Yu et al., 2022).

Intriguingly, quite a few research studies have probed into the regulated mechanism of ferroptosis-associated genes in endometrial cancer, as indicated by the evidence that ferroptosis-associated genes were positively related to M1 macrophages, M2 macrophages, T cell follicular helper, and B cells naive, while they were negatively related to NK cells activated, T cells regulatory (Tregs) and neutrophils (Liu W. et al., 2021); and that damage-associated molecular patterns (DAMPs) released by ferroptosis were sensed by the immune cells, thus enhancing inflammatory responses and improving the immune microenvironment in cancer was found (López-Janeiro et al., 2021). Therefore, it was thought that different patients with endometrial cancer could have different immune microenvironments to have different prognosis (Blaisdell et al., 2015; Antomarchi et al., 2019; Pan et al., 2019). An abnormal microenvironment induced by ferroptosis-associated genes can be the underlying mechanism of poor prognosis in endometrial cancer.

In fact, gene-combined panels have been used to predict the prognosis of endometrial cancer. Of them, TCGA molecular typing and ProMisE molecular typing, based on POLE gene, p53 gene, and DNA mismatch repair genes, are the most classic molecular typing of endometrial cancer (Levine et al., 2013; Eriksson et al., 2021). Definitely, these molecular typings established play an important role in predicting prognosis and guiding clinical practice; however, two of them still have shortcomings, which limits their clinical application: complicated testing processes and high testing cost, and their consistency with clinical practice still needs to be improved. Therefore, it is significant that a novel, simple, and economical molecular prognostic model be explored in predicting endometrial cancer. It is well known that abnormal ferroptosis is an important reason behind the poor prognosis of endometrial cancer, as indicated by the evidence that molecular typing based on ferroptosis-associated genes showed good prognosis predictive value: 1) the ferroptosis score, based on thirteen ferroptosis-associated genes, was established, and OS of patients with a low score of ferroptosis was superior to that of those with high score of ferroptosis (AUC = 0.726) (Wang et al., 2021b); 2) a molecular typing of endometrial cancer, based on six ferroptosis-associated genes of HMOX1, KEAP1, HSBP1, SAT1, C1SD1, and GPX4, showed good 1-, 3-, and 5-year prognostic predictive value (AUC = 0.705, 0.676, and 0.713) (Liu J. et al., 2021); 3) a ferroptosis-associated gene signature with eight genes of MDM2, GPX4, PRKAA2, PRNP, SLC11A2, ATP5MC3, PHKG2, and ACO1, showed better 1-, 3-, and 5-year prognostic predictive value (AUC = 0.676, 0.797, and 0.826) than the aforementioned two ferroptosis prognosis molecular typings (Weijiao et al., 2021). Ferroptosis prognosis molecular typing possessed a comparable or superior prognosis predictive value when compared with the previous prognosis molecular typings of endometrial cancer (Table 1) (Tang et al., 2019; Yang et al., 2021b; Coll-de la Rubia et al., 2021; Huang S. et al., 2021; Lu N. et al., 2021; Pang et al., 2021; Wang Z. et al., 2021). As

indicated by the evidence, ferroptosis-associated genes-based molecular typing can be considered as an effective method to predict the prognosis of endometrial cancer.

However, most studies on the correlation of ferroptosis-associated genes with the prognosis of endometrial cancer have been conducted based on bioinformatics analysis, lacking large, and multi-center clinical samples for prospective validation. The sensitivity, specificity, and stability of ferroptosis-associated genes-based molecular typing models still merit further investigations. The correlation of ferroptosis-associated genes with immune response, immune infiltration still remains unclear, and the previously reported studies have been performed mostly based on correlation analysis of clinical cases. Whether there is a causal or concomitant correlation between the abnormal expression of ferroptosis-associated genes with the immune response and immune infiltration in endometrial cancer still needs to be verified by a large number of experiments *in vivo* and *in vitro*. More importantly, it remains unclear whether the use of ferroptosis inducer will improve the prognosis of endometrial cancer; further research studies are needed in terms of dosage selection, application method, and therapeutic safety and effectiveness.

## FUTURE RESEARCHES

Further studies are needed on the association of ferroptosis with initiation, metastasis, recurrence, treatment, and prognosis of endometrial cancer. A focus is to be placed on the identification of the key ferroptosis-associated genes in endometrial cancer. Much importance is to be attached to the underlying mechanism of ferroptosis-associated genes in the initiation and progress of endometrial cancer, with the laboratory-derived research results shifting to the clinical investigations to determine proper ferroptosis inducers and precise dose and duration of administration. In so doing, the best treatment plan, either as combination chemotherapy or non-chemotherapy, can be developed for the patient with endometrial cancer.

## CONCLUSION

A large amount of evidence suggest that ferroptosis is involved in all aspects of endometrial cancer, including initiation, metastasis, recurrence, treatment, and prognosis. Ferroptosis-associated gene-based molecular typing model has shown a comparable prognosis predictive value than others, and many conventional drugs, which activate ferroptosis, have also shown favorable antitumor effects *in vitro*. Targeting ferroptosis has displayed a favorable role in reversing drug resistance of endometrial cancer. Therefore, it is hypothesized that targeting ferroptosis can be an underlying therapeutic approach to endometrial cancer, although the evidence is not sufficient enough at present.

## AUTHOR CONTRIBUTIONS

Study design: JW and LZ; data interpretation: JW, SW, and ZL; manuscript preparation: JW and LZ; literature search: LZ; and funds collections: JW.

## FUNDING

The study was jointly supported by the Shanghai Municipal Health Commission (Grant No. 201940222), Academic Leader

## REFERENCES

- Antomarchi, J., Ambrosetti, D., Cohen, C., Delotte, J., Chevallier, A., Karimjee-Soilihi, B., et al. (2019). Immunosuppressive Tumor Microenvironment Status and Histological Grading of Endometrial Carcinoma. *Cancer Microenviron.* 12, 169–179. doi:10.1007/s12307-019-00225-1
- Bai, M., Yang, L., Liao, H., Liang, X., Xie, B., Xiong, J., et al. (2018). Metformin Sensitizes Endometrial Cancer Cells to Chemotherapy through IDH1-Induced Nrf2 Expression via an Epigenetic Mechanism. *Oncogene* 37, 5666–5681. doi:10.1038/s41388-018-0360-7
- Bersuker, K., Hendricks, J. M., Li, Z., Magtanong, L., Ford, B., Tang, P. H., et al. (2019). The CoQ Oxidoreductase FSP1 Acts Parallel to GPX4 to Inhibit Ferroptosis. *Nature* 575, 688–692. doi:10.1038/s41586-019-1705-2
- Bi, J., Areecheewakul, S., Li, Y., Yang, S., Zhang, Y., Ebeid, K., et al. (2019). MTDH/AEG-1 Downregulation Using Pristimerin-Loaded Nanoparticles Inhibits Fanconi Anemia Proteins and Increases Sensitivity to Platinum-Based Chemotherapy. *Gynecol. Oncol.* 155, 349–358. doi:10.1016/j.ygyno.2019.08.014
- Bielfeld, A. P., Pour, S. J., Poschmann, G., Stühler, K., Krüssel, J.-S., and Baston-Büst, D. M. (2019). A Proteome Approach Reveals Differences between Fertile Women and Patients with Repeated Implantation Failure on Endometrial Level-Does hCG Render the Endometrium of RIF Patients? *Int. J. Mol. Sci.* 20, 425. doi:10.3390/ijms20020425
- Blaisdell, A., Crequer, A., Columbus, D., Daikoku, T., Mittal, K., Dey, S. K., et al. (2015). Neutrophils Oppose Uterine Epithelial Carcinogenesis via Debridement of Hypoxic Tumor Cells. *Cancer Cell* 28, 785–799. doi:10.1016/j.ccell.2015.11.005
- Chen, M.-S., Wang, S.-F., Hsu, C.-Y., Yin, P.-H., Yeh, T.-S., Lee, H.-C., et al. (2017). CHAC1 Degradation of Glutathione Enhances Cystine-Starvation-Induced Necroptosis and Ferroptosis in Human Triple Negative Breast Cancer Cells via the GCN2-eIF2 $\alpha$ -ATF4 Pathway. *Oncotarget* 8, 114588–114602. doi:10.18632/oncotarget.23055
- Chen, N., Yi, X., Abushahin, N., Pang, S., Zhang, D., Kong, B., et al. (2010). Nrf2 Expression in Endometrial Serous Carcinomas and its Precancers. *Int. J. Clin. Exp. Pathol.* 4, 85–96.
- Chen, X., Kang, R., Kroemer, G., and Tang, D. (2021b). Broadening Horizons: the Role of Ferroptosis in Cancer. *Nat. Rev. Clin. Oncol.* 18, 280–296. doi:10.1038/s41571-020-00462-0
- Chen, X., Kang, R., Kroemer, G., and Tang, D. (2021a). Ferroptosis in Infection, Inflammation, and Immunity. *J. Exp. Med.* 218, e20210518. doi:10.1084/jem.20210518
- Chen, X., Yu, C., Kang, R., and Tang, D. (2020). Iron Metabolism in Ferroptosis. *Front. Cell. Dev. Biol.* 8, 590226. doi:10.3389/fcell.2020.590226
- Cheng, Y., Huang, H., Han, Y., and Zhu, Y. (2020). Expression of YAP in Endometrial Carcinoma Tissues and its Effect on Epithelial to Mesenchymal Transition. *Transl. Cancer Res.* TCR 9, 7248–7258. doi:10.21037/tcr-20-3155
- Coll-de la Rubia, E., Martínez-García, E., Dittmar, G., Nazarov, P. V., Bebia, V., Cabrera, S., et al. (2021). In Silico Approach for Validating and Unveiling New Applications for Prognostic Biomarkers of Endometrial Cancer. *Cancers* 13, 5052. doi:10.3390/cancers13205052
- Concin, N., Matias-Guiu, X., Vergote, I., Cibula, D., Mirza, M. R., Marnitz, S., et al. (2021). ESGO/ESTRO/ESP Guidelines for the Management of Patients with Endometrial Carcinoma. *Int. J. Gynecol. Cancer.* 31, 12–39. doi:10.1136/ijgc-2020-002230
- Costa, B. P., Nassr, M. T., Diz, F. M., Fernandes, K. H. A., Antunes, G. L., Grun, L. K., et al. (2021). Methoxyeugenol Regulates the P53/p21 Pathway and Suppresses Human Endometrial Cancer Cell Proliferation. *J. Ethnopharmacol.* 267, 113645. doi:10.1016/j.jep.2020.113645
- Dai, D., Wolf, D. M., Litman, E. S., White, M. J., and Leslie, K. K. (2002). Progesterone Inhibits Human Endometrial Cancer Cell Growth and Invasiveness: Down-Regulation of Cellular Adhesion Molecules through Progesterone B Receptors. *Cancer Res.* 62, 881–886.
- Doll, S., Freitas, F. P., Shah, R., Aldrovandi, M., da Silva, M. C., Ingold, I., et al. (2019). FSP1 Is a Glutathione-independent Ferroptosis Suppressor. *Nature* 575, 693–698. doi:10.1038/s41586-019-1707-0
- Eling, N., Reuter, L., Hazin, J., Hamacher-Brady, A., and Brady, N. R. (2015). Identification of Artesunate as a Specific Activator of Ferroptosis in Pancreatic Cancer Cells. *Oncoscience* 2, 517–532. doi:10.18632/oncoscience.160
- Eriksson, L. S. E., Nastic, D., Lindqvist, P. G., Imboden, S., Järnbert-Pettersson, H., Carlson, J. W., et al. (2021). Combination of Proactive Molecular Risk Classifier for Endometrial Cancer ( ProMisE ) with Sonographic and Demographic Characteristics in Preoperative Prediction of Recurrence or Progression of Endometrial Cancer. *Ultrasound Obstet. Gynecol.* 58, 457–468. doi:10.1002/uog.23573
- Eritja, N., Chen, B.-J., Rodríguez-Barrueco, R., Santacana, M., Gatiús, S., Vidal, A., et al. (2017). Autophagy Orchestrates Adaptive Responses to Targeted Therapy in Endometrial Cancer. *Autophagy* 13, 608–624. doi:10.1080/15548627.2016.1271512
- European Commission (2020). European Cancer Information System (ECIS). Available at: <https://ecis.jrc.ec.europa.eu/> (Accessed November 15, 2020).
- Fan, Z., Wirth, A.-K., Chen, D., Wruck, C. J., Rauh, M., Buchfelder, M., et al. (2017). Nrf2-Keap1 Pathway Promotes Cell Proliferation and Diminishes Ferroptosis. *Oncogenesis* 6, e371. doi:10.1038/oncsis.2017.65
- Feng, L., Li, J., Yang, L., Zhu, L., Huang, X., Zhang, S., et al. (2017). Tamoxifen Activates Nrf2-dependent SQSTM1 Transcription to Promote Endometrial Hyperplasia. *Theranostics* 7, 1890–1900. doi:10.7150/thno.19135
- Franchello, A., Fronda, G., Deiro, G., Fiore, A., Cassine, D., Molinaro, L., et al. (2015). Unusual Presentation of Recurrent Early Stage Endometrial Carcinoma 28 Years after Primary Surgery. *Case Rep. Surg.* 2015, 1–4. doi:10.1155/2015/256838
- Fung-Kee-Fung, M., Dodge, J., Elit, L., Lukka, H., Chambers, A., Oliver, T., et al. (2006). Follow-up after Primary Therapy for Endometrial Cancer: A Systematic Review. *Gynecol. Oncol.* 101, 520–529. doi:10.1016/j.ygyno.2006.02.011
- Gao, M., Monian, P., Quadri, N., Ramasamy, R., and Jiang, X. (2015). Glutaminolysis and Transferrin Regulate Ferroptosis. *Mol. Cell* 59, 298–308. doi:10.1016/j.molcel.2015.06.011
- Gao, R., Kalathur, R. K. R., Coto-Llerena, M., Ercan, C., Buechel, D., Shuang, S., et al. (2021). YAP/TAZ and ATF4 Drive Resistance to Sorafenib in Hepatocellular Carcinoma by Preventing Ferroptosis. *EMBO Mol. Med.* 13 (12), e14351. doi:10.15252/emmm.202114351
- Gao, Z., Deng, G., Li, Y., Huang, H., Sun, X., Shi, H., et al. (2020). Actinidia Chinensis Planch Prevents Proliferation and Migration of Gastric Cancer Associated with Apoptosis, Ferroptosis Activation and Mesenchymal Phenotype Suppression. *Biomed. Pharmacother.* 126, 110092. doi:10.1016/j.biopha.2020.110092

## SUPPLEMENTARY MATERIAL

The Supplementary Material for this article can be found online at: <https://www.frontiersin.org/articles/10.3389/fmolb.2022.929832/full#supplementary-material>

- Genkinger, J. M., Friberg, E., Goldbohm, R. A., and Wolk, A. (2012). Long-term Dietary Heme Iron and Red Meat Intake in Relation to Endometrial Cancer Risk. *Am. J. Clin. Nutr.* 96, 848–854. doi:10.3945/ajcn.112.039537
- Hafizz, A. M. H. A., Zin, R. R. M., Aziz, N. H. A., Kampan, N. C., and Shafiee, M. N. (2020). Beyond Lipid-Lowering: Role of Statins in Endometrial Cancer. *Mol. Biol. Rep.* 47, 8199–8207. doi:10.1007/s11033-020-05760-5
- He, J., Ding, H., Li, H., Pan, Z., and Chen, Q. (2021). Intra-Tumoral Expression of SLC7A11 Is Associated with Immune Microenvironment, Drug Resistance, and Prognosis in Cancers: A Pan-Cancer Analysis. *Front. Genet.* 12, 770857. doi:10.3389/fgene.2021.770857
- Hoy, A. J., Nagarajan, S. R., and Butler, L. M. (2021). Tumour Fatty Acid Metabolism in the Context of Therapy Resistance and Obesity. *Nat. Rev. Cancer* 21, 753–766. doi:10.1038/s41568-021-00388-4
- Hu, W., Zhang, C., Wu, R., Sun, Y., Levine, A., and Feng, Z. (2010). Glutaminase 2, a Novel P53 Target Gene Regulating Energy Metabolism and Antioxidant Function. *Proc. Natl. Acad. Sci. U.S.A.* 107, 7455–7460. doi:10.1073/pnas.1001006107
- Huang, F., Zhao, Y., Zhao, J., Wu, S., Jiang, Y., Ma, H., et al. (2014). Upregulated SLC1A5 Promotes Cell Growth and Survival in Colorectal Cancer. *Int. J. Clin. Exp. Pathol.* 7, 6006–6014.
- Huang, S., Pang, L., and Wei, C. (2021). Identification of a Four-Gene Signature with Prognostic Significance in Endometrial Cancer Using Weighted-Gene Correlation Network Analysis. *Front. Genet.* 12, 678780. doi:10.3389/fgene.2021.678780
- Huang, W., Zhang, J., Dong, B., Chen, H., Shao, L., and Li, X. (2021). A Novel miR-98 Negatively Regulates the Resistance of Endometrial Cancer Cells to Paclitaxel by Suppressing ABCC10/MRP-7. *Front. Oncol.* 11, 809410. doi:10.3389/fonc.2021.809410
- Jeppesen, M. M., Jensen, P. T., Gilså Hansen, D., Iachina, M., and Mogensen, O. (2016). The Nature of Early-Stage Endometrial Cancer Recurrence-A National Cohort Study. *Eur. J. Cancer* 69, 51–60. doi:10.1016/j.ejca.2016.09.033
- Jiang, L., Kon, N., Li, T., Wang, S.-J., Su, T., Hibshoosh, H., et al. (2015). Ferroptosis as a P53-Mediated Activity during Tumour Suppression. *Nature* 520, 57–62. doi:10.1038/nature14344
- Jiang, P., Yang, F., Zou, C., Bao, T., Wu, M., Yang, D., et al. (2021). The Construction and Analysis of a Ferroptosis-Related Gene Prognostic Signature for Pancreatic Cancer. *Aging* 13, 10396–10414. doi:10.18632/aging.202801
- Kabat, G. C., Miller, A. B., Jain, M., and Rohan, T. E. (2008). Dietary Iron and Haem Iron Intake and Risk of Endometrial Cancer: a Prospective Cohort Study. *Br. J. Cancer* 98, 194–198. doi:10.1038/sj.bjc.6604110
- Kaira, K., Sunose, Y., Arakawa, K., Sunaga, N., Shimizu, K., Tominaga, H., et al. (2015). Clinicopathological Significance of ASC Amino Acid Transporter-2 Expression in Pancreatic Ductal Carcinoma. *Histopathology* 66, 234–243. doi:10.1111/his.12464
- Kallianpur, A. R., Lee, S.-A., Xu, W.-H., Zheng, W., Gao, Y.-T., Cai, H., et al. (2009). Dietary Iron Intake and Risk of Endometrial Cancer: a Population-Based Case-Control Study in Shanghai, China. *Nutr. Cancer* 62, 40–50. doi:10.1080/01635580903191544
- Kang, R., Kroemer, G., and Tang, D. (2019). The Tumor Suppressor Protein P53 and the Ferroptosis Network. *Free Radic. Biol. Med.* 133, 162–168. doi:10.1016/j.freeradbiomed.2018.05.074
- Kato, S., Smalley, S., Sadarangani, A., Chen-Lin, K., Oliva, B., Brañes, J., et al. (2009). Lipophilic but Not Hydrophilic Statins Selectively Induce Cell Death in Gynecological Cancers Expressing High Levels of HMGCoA Reductase. *J. Cell. Mol. Med.* 14, 1180. doi:10.1111/j.1582-4934.2009.00771.x
- Keating, G. M. (2017). Sorafenib: A Review in Hepatocellular Carcinoma. *Targ. Oncol.* 12, 243–253. doi:10.1007/s11523-017-0484-7
- Kong, C., Zhu, Z., Li, Y., Xue, P., and Chen, L. (2021). Downregulation of HOXA11 Enhances Endometrial Cancer Malignancy and Cisplatin Resistance via Activating PTEN/AKT Signaling Pathway. *Clin. Transl. Oncol.* 23, 1334–1341. doi:10.1007/s12094-020-02520-6
- Konno, T., Kohno, T., Okada, T., Shimada, H., Satohisa, S., Kikuchi, S., et al. (2020). ASPP2 Suppression Promotes Malignancy via LSR and YAP in Human Endometrial Cancer. *Histochem. Cell. Biol.* 154, 197–213. doi:10.1007/s00418-020-01876-8
- Koppula, P., Zhuang, L., and Gan, B. (2021). Cystine Transporter SLC7A11/xCT in Cancer: Ferroptosis, Nutrient Dependency, and Cancer Therapy. *Protein Cell* 12, 599–620. doi:10.1007/s13238-020-00789-5
- Lei, G., Zhuang, L., and Gan, B. (2022). Targeting Ferroptosis as a Vulnerability in Cancer. *Nat. Rev. Cancer*. doi:10.1038/s41568-022-00459-0
- León-Castillo, A., de Boer, S. M., Powell, M. E., Mileschkin, L. R., MackayMackay, H. J., Leary, A., et al. (2020). Molecular Classification of the PORTEC-3 Trial for High-Risk Endometrial Cancer: Impact on Prognosis and Benefit from Adjuvant Therapy. *J. Clin. Oncol.* 38, 3388–3397. doi:10.1200/JCO.20.00549
- Levine, D. A., Kandath, C., Schultz, N., Cherniack, A. D., Akbani, R., Liu, Y., et al. (2013). Integrated Genomic Characterization of Endometrial Carcinoma. *Nature* 497, 67–73. doi:10.1038/nature12113
- Li, L., Qiu, C., Hou, M., Wang, X., Huang, C., Zou, J., et al. (2021). Ferroptosis in Ovarian Cancer: A Novel Therapeutic Strategy. *Front. Oncol.* 11, 665945. doi:10.3389/fonc.2021.665945
- Lin, C.-C., Yang, W.-H., Lin, Y.-T., Tang, X., Chen, P.-H., Ding, C.-K. C., et al. (2021). DDR2 Upregulation Confers Ferroptosis Susceptibility of Recurrent Breast Tumors through the Hippo Pathway. *Oncogene* 40, 2018–2034. doi:10.1038/s41388-021-01676-x
- Liu, J., Wang, Y., Meng, H., Yin, Y., Zhu, H., and Ni, T. (2021). Identification of the Prognostic Signature Associated with Tumor Immune Microenvironment of Uterine Corpus Endometrial Carcinoma Based on Ferroptosis-Related Genes. *Front. Cell. Dev. Biol.* 9, 735013. doi:10.3389/fcell.2021.735013
- Liu W., W., Chakraborty, B., Safi, R., Kazmin, D., Chang, C.-y., and McDonnell, D. P. (2021). Dysregulated Cholesterol Homeostasis Results in Resistance to Ferroptosis Increasing Tumorigenicity and Metastasis in Cancer. *Nat. Commun.* 12, 5103. doi:10.1038/s41467-021-25354-4
- Liu, Y., and Gu, W. (2022). p53 in Ferroptosis Regulation: the New Weapon for the Old Guardian. *Cell. Death Differ.* 29, 895–910. doi:10.1038/s41418-022-00943-y
- Liu, Y., and Gu, W. (2021). The Complexity of P53-Mediated Metabolic Regulation in Tumor Suppression. *Seminars Cancer Biol.* 2021, S1044-579X(21)00060-00062. doi:10.1016/j.semcancer.2021.03.010
- Liu, Y., Zhao, R., Chi, S., Zhang, W., Xiao, C., Zhou, X., et al. (2020). UBE2C Is Upregulated by Estrogen and Promotes Epithelial-Mesenchymal Transition via P53 in Endometrial Cancer. *Mol. Cancer Res.* 18, 204–215. doi:10.1158/1541-7786.MCR-19-0561
- Llobet, D., Eritja, N., Yeramian, A., Pallares, J., Sorolla, A., Domingo, M., et al. (2010). The Multikinase Inhibitor Sorafenib Induces Apoptosis and Sensitises Endometrial Cancer Cells to TRAIL by Different Mechanisms. *Eur. J. Cancer* 46, 836–850. doi:10.1016/j.ejca.2009.12.025
- López-Janeiro, Á., Ruz-Caracul, I., Ramón-Patino, J. L., De Los Ríos, V., Villalba Esparza, M., Berjón, A., et al. (2021). Proteomic Analysis of Low-Grade, Early-Stage Endometrial Carcinoma Reveals New Dysregulated Pathways Associated with Cell Death and Cell Signaling. *Cancers* 13, 794. doi:10.3390/cancers13040794
- Lu, K. H., and Broadbent, R. R. (2020). Endometrial Cancer. *N. Engl. J. Med.* 383, 2053–2064. doi:10.1056/NEJMra1514010
- Lu, N., Liu, J., Ji, C., Wang, Y., Wu, Z., Yuan, S., et al. (2021). MiRNA Based Tumor Mutation Burden Diagnostic and Prognostic Prediction Models for Endometrial Cancer. *Bioengineered* 12, 3603–3620. doi:10.1080/21655979.2021.1947940
- Lu, Y., Qin, H., Jiang, B., Lu, W., Hao, J., Cao, W., et al. (2021). KLF2 Inhibits Cancer Cell Migration and Invasion by Regulating Ferroptosis through GPX4 in Clear Cell Renal Cell Carcinoma. *Cancer Lett.* 522, 1–13. doi:10.1016/j.canlet.2021.09.014
- Luis, G., Godfroid, A., Nishiumi, S., Cimino, J., Blacher, S., Maquoi, E., et al. (2021). Tumor Resistance to Ferroptosis Driven by Stearoyl-CoA Desaturase-1 (SCD1) in Cancer Cells and Fatty Acid Binding Protein-4 (FABP4) in Tumor Microenvironment Promote Tumor Recurrence. *Redox Biol.* 43, 102006. doi:10.1016/j.redox.2021.102006
- Luo, M., Wu, L., Zhang, K., Wang, H., Zhang, T., Gutierrez, L., et al. (2018). miR-137 Regulates Ferroptosis by Targeting Glutamine Transporter SLC1A5 in Melanoma. *Cell. Death Differ.* 25, 1457–1472. doi:10.1038/s41418-017-0053-8
- Makiuchi, S., Yoshida, H., Ishikawa, M., Kojima, N., Kanai, Y., and Kato, T. (2020). Primary Peritoneal Low-Grade Serous Carcinoma in a Patient with Lynch Syndrome: A Case Report. *Int. J. Gynecol. Pathol.* 39, 327–332. doi:10.1097/PGP.0000000000000622



- Marshall, A. D., van Geldermalsen, M., Otte, N. J., Lum, T., Vellozzi, M., Thoeng, A., et al. (2017). ASCT2 Regulates Glutamine Uptake and Cell Growth in Endometrial Carcinoma. *Oncogenesis* 6, e367. doi:10.1038/oncsis.2017.70
- Martin, J. H., Mohammed, R., Delforce, S. J., Skerrett-Byrne, D. A., de Meaultsart, C. C., Almazi, J. G., et al. (2022). Role of the Prorenin Receptor in Endometrial Cancer Cell Growth. *Oncotarget* 13, 587–599. doi:10.18632/oncotarget.28224
- McConechy, M. K., Talhouk, A., Li-Chang, H. H., Leung, S., Huntsman, D. G., Gilks, C. B., et al. (2015). Detection of DNA Mismatch Repair (MMR) Deficiencies by Immunohistochemistry Can Effectively Diagnose the Microsatellite Instability (MSI) Phenotype in Endometrial Carcinomas. *Gynecol. Oncol.* 137, 306–310. doi:10.1016/j.ygyno.2015.01.541
- Mhawech-Fauceglia, P., Wang, D., Kim, G., Sharifian, M., Chen, X., Liu, Q., et al. (2014). Expression of DNA Repair Proteins in Endometrial Cancer Predicts Disease Outcome. *Gynecol. Oncol.* 132, 593–598. doi:10.1016/j.ygyno.2014.02.002
- National Cancer Institute Surveillance (2017). National Cancer Institute Surveillance, Epidemiology, and Results Program. Cancer Stat Facts: Uterine Cancer. Available at: <https://seer.cancer.gov/statfacts/html/corp.html> (Accessed December 28, 2017).
- Ng, S.-W., Norwitz, S. G., Taylor, H. S., and Norwitz, E. R. (2020). Endometriosis: The Role of Iron Overload and Ferroptosis. *Reprod. Sci.* 27, 1383–1390. doi:10.1007/s43032-020-00164-z
- Nimeiri, H. S., Oza, A. M., Morgan, R. J., Huo, D., Elit, L., Knost, J. A., et al. (2010). A Phase II Study of Sorafenib in Advanced Uterine Carcinoma/carcinosarcoma: A Trial of the Chicago, PMH, and California Phase II Consortia. *Gynecol. Oncol.* 117, 37–40. doi:10.1016/j.ygyno.2010.01.013
- Ou, Y., Wang, S.-J., Li, D., Chu, B., and Gu, W. (2016). Activation of SAT1 Engages Polyamine Metabolism with P53-Mediated Ferroptotic Responses. *Proc. Natl. Acad. Sci. U.S.A.* 113, E6806–E6812. doi:10.1073/pnas.1607152113
- Pan, Y., Jia, L. P., Liu, Y., Han, Y., and Deng, Q. (2019). Alteration of Tumor Associated Neutrophils by PIK3CA Expression in Endometrial Carcinoma from TCGA Data. *J. Ovarian Res.* 12, 1–7. doi:10.1186/s13048-019-0557-6
- Pang, X., Zhang, X., Huang, Y., and Qian, S. (2021). Development and Validation of m6A Regulators' Prognostic Significance for Endometrial Cancer. *Med.* 100, e26551. doi:10.1097/MD.00000000000026551
- Planagumà, J., Gonzalez, M., Doll, A., Monge, M., Gilmoreno, A., Baró, T., et al. (2006). The Up-Regulation Profiles of p21WAF1/CIP1 and RUNX1/AML1 Correlate with Myometrial Infiltration in Endometrioid Endometrial Carcinoma. *Hum. Pathol.* 37, 1050–1057. doi:10.1016/j.humpath.2006.03.007
- Qin, J., Shao, X., Wu, L., and Du, H. (2021). Identification of the Ferroptosis-Associated Gene Signature to Predict the Prognostic Status of Endometrial Carcinoma Patients. *Comput. Math. Methods Med.* 2021, 1–23. doi:10.1155/2021/9954370
- Roh, J.-L., Kim, E. H., Jang, H., and Shin, D. (2017). Nrf2 Inhibition Reverses the Resistance of Cisplatin-Resistant Head and Neck Cancer Cells to Arsenite-Induced Ferroptosis. *Redox Biol.* 11, 254–262. doi:10.1016/j.redox.2016.12.010
- Sartori, E., Pasinetti, B., Chiudinelli, F., Gadducci, A., Landoni, F., Maggino, T., et al. (2010). Surveillance Procedures for Patients Treated for Endometrial Cancer: A Review of the Literature. *Int. J. Gynecol. Cancer* 20, 985–992. doi:10.1111/IGC.0b013e3181e2abcc
- Schointuch, M. N., Gilliam, T. P., Stine, J. E., Han, X., Zhou, C., Gehrig, P. A., et al. (2014). Simvastatin, an HMG-CoA Reductase Inhibitor, Exhibits Anti-metastatic and Anti-tumorigenic Effects in Endometrial Cancer. *Gynecol. Oncol.* 134, 346–355. doi:10.1016/j.ygyno.2014.05.015
- Schweitzer, A. M., Gingrich, M. A., HawkeHawke, T. J., and RebalkaRebalka, I. A. (2020). The Impact of Statins on Physical Activity and Exercise Capacity: an Overview of the Evidence, Mechanisms, and Recommendations. *Eur. J. Appl. Physiol.* 120, 1205–1225. doi:10.1007/s00421-020-04360-2
- Sendo, K., Seino, M., Ohta, T., and Nagase, S. (2022). Impact of the Glutathione Synthesis Pathway on Sulfasalazine-Treated Endometrial Cancer. *Oncotarget* 13, 224–236. doi:10.18632/oncotarget.28185
- Sha, R., Xu, Y., Yuan, C., Sheng, X., Wu, Z., Peng, J., et al. (2021). Predictive and Prognostic Impact of Ferroptosis-Related Genes ACSL4 and GPX4 on Breast Cancer Treated with Neoadjuvant Chemotherapy. *EBioMedicine* 71, 103560. doi:10.1016/j.ebiom.2021.103560
- Siegel, R. L., Miller, K. D., Fuchs, H. E., and Jemal, A. (2022). Cancer Statistics, 2022. *CA A Cancer J. Clin.* 72, 7–33. doi:10.3322/caac.21708
- Song, X., and Long, D. (2020). Nrf2 and Ferroptosis: a New Research Direction for Neurodegenerative Diseases. *Front. Neurosci.* 14, 267. doi:10.3389/fnins.2020.00267
- Song, X., Xie, Y., Kang, R., Hou, W., Sun, X., Epperly, M. W., et al. (2016). FANCD2 Protects against Bone Marrow Injury from Ferroptosis. *Biochem. Biophysical Res. Commun.* 480, 443–449. doi:10.1016/j.bbrc.2016.10.068
- Stockwell, B. R., Friedmann Angeli, J. P., Bayir, H., Bush, A. I., Conrad, M., Dixon, S. J., et al. (2017). Ferroptosis: a Regulated Cell Death Nexus Linking Metabolism, Redox Biology, and Disease. *Cell* 171, 273–285. doi:10.1016/j.cell.2017.09.021
- Sun, N. K., Huang, S. L., Chang, T. C., and Chao, C. C. K. (2013). Sorafenib Induces Endometrial Carcinoma Apoptosis by Inhibiting Elk-1-dependent Mcl-1 Transcription and Inducing Akt/GSK3 $\beta$ -dependent Protein Degradation. *J. Cell. Biochem.* 114, 1819–1831. doi:10.1002/jcb.24530
- Sun, X., Ou, Z., Chen, R., Niu, X., Chen, D., Kang, R., et al. (2016). Activation of the P62-Keap1-NRF2 Pathway Protects against Ferroptosis in Hepatocellular Carcinoma Cells. *Hepatology* 63, 173–184. doi:10.1002/hep.28251
- Sun, Y., Berleth, N., Wu, W., Schlütermann, D., Deitersen, J., Stuhldreier, F., et al. (2021). Fin56-induced Ferroptosis Is Supported by Autophagy-Mediated GPX4 Degradation and Functions Synergistically with mTOR Inhibition to Kill Bladder Cancer Cells. *Cell. Death Dis.* 12, 1028. doi:10.1038/s41419-021-04306-2
- Takahashi, N., Cho, P., Selfors, L. M., Kuiken, H. J., Kaul, R., Fujiwara, T., et al. (2020). 3D Culture Models with CRISPR Screens Reveal Hyperactive NRF2 as a Prerequisite for Spheroid Formation via Regulation of Proliferation and Ferroptosis. *Mol. Cell.* 80, 828–844. e6. doi:10.1016/j.molcel.2020.10.010
- Tang, F.-H., Chang, W.-A., Tsai, E.-M., Tsai, M.-J., and Kuo, P.-L. (2019). Investigating Novel Genes Potentially Involved in Endometrial Adenocarcinoma Using Next-Generation Sequencing and Bioinformatic Approaches. *Int. J. Med. Sci.* 16, 1338–1348. doi:10.7150/ijms.38219
- Tangitgamol, S., Levenback, C. F., Beller, U., and Kavanagh, J. J. (2004). Role of Surgical Resection for Lung, Liver, and Central Nervous System Metastases in Patients with Gynecological Cancer: a Literature Review. *Int. J. Gynecol. Cancer* 14, 399–422. doi:10.1111/j.1048-891x.2004.14326.x
- Teng, Y., Ai, Z., Wang, Y., Wang, J., and Luo, L. (2013). Proteomic Identification of PKM2 and HSPA5 as Potential Biomarkers for Predicting High-Risk Endometrial Carcinoma. *J. Obstet. Gynaecol. Res.* 39, 317–325. doi:10.1111/j.1447-0756.2012.01970.x
- Thomas, T., and Thomas, T. J. (2003). Polyamine Metabolism and Cancer. *J. Cell. Mol. Med.* 7, 113–126. doi:10.1111/j.1582-4934.2003.tb00210.x
- Tsujiura, M., Mazack, V., Sudol, M., Kaspar, H. G., Nash, J., Carey, D. J., et al. (2014). Yes-associated Protein (YAP) Modulates Oncogenic Features and Radiation Sensitivity in Endometrial Cancer. *PLoS One* 9, e100974. doi:10.1371/journal.pone.0100974
- Ubellacker, J. M., Tasdogan, A., Ramesh, V., Shen, B., Mitchell, E. C., Martin-Sandoval, M. S., et al. (2020). Lymph Protects Metastasizing Melanoma Cells from Ferroptosis. *Nature* 585, 113–118. doi:10.1038/s41586-020-2623-z
- Vogt, A.-C. S., Arsiwala, T., Mohsen, M., Vogel, M., Manolova, V., and Bachmann, M. F. (2021). On Iron Metabolism and its Regulation. *Ijms* 22, 4591. doi:10.3390/ijms22094591
- Waheed, S., Cheng, R. Y., Casablanca, Y., Maxwell, G. L., Wink, D. A., and Syed, V. (2019). Nitric Oxide Donor DETA/NO Inhibits the Growth of Endometrial Cancer Cells by Upregulating the Expression of RASSF1 and CDKN1A. *Molecules* 24, 3722. doi:10.3390/molecules24203722
- Wang, C., Jeong, K., Jiang, H., Guo, W., Gu, C., Lu, Y., et al. (2016). YAP/TAZ Regulates the Insulin Signaling via IRS1/2 in Endometrial Cancer. *Am. J. Cancer Res.* 6, 996–1010.
- Wang, C., Gu, C., Jeong, K. J., Zhang, D., Guo, W., Lu, Y., et al. (2017). YAP/TAZ-Mediated Upregulation of GAB2 Leads to Increased Sensitivity to Growth Factor-Induced Activation of the PI3K Pathway. *Cancer Res.* 77, 1637–1648. doi:10.1158/0008-5472.CAN-15-3084
- Wang, H., Wu, Y., Chen, S., Hou, M., Yang, Y., Xie, M., et al. (2021b). Construction and Validation of a Ferroptosis-Related Prognostic Model for Endometrial Cancer. *Front. Genet.* 12, 729046. doi:10.3389/fgene.2021.729046
- Wang, H., Peng, S., Cai, J., and Bao, S. (2021a). Silencing of PTPN18 Induced Ferroptosis in Endometrial Cancer Cells through P-P38-Mediated GPX4/xCT Down-Regulation. *Cancer Manag. Res.* 13, 1757–1765. doi:10.2147/CMAR.S278728

- Wang, J., Song, T., Zhou, S., and Kong, X. (2019). YAP Promotes the Malignancy of Endometrial Cancer Cells via Regulation of IL-6 and IL-11. *Mol. Med.* 25, 32. doi:10.1186/s10020-019-0103-4
- Wang, Y., Wang, Y., Zhang, Z., Park, J.-Y., Guo, D., Liao, H., et al. (2016). Mechanism of Progesterone Resistance in Endometrial Precancer/cancer through Nrf2-Akr1c1 Pathway. *Oncotarget* 7, 10363–10372. doi:10.18632/oncotarget.7004
- Wang, Z., Liu, Y., Zhang, J., Zhao, R., Zhou, X., and Wang, H. (2021). An Immune-Related Long Noncoding RNA Signature as a Prognostic Biomarker for Human Endometrial Cancer. *J. Oncol.* 2021, 1–14. doi:10.1155/2021/9972454
- Weijiao, Y., Fuchun, L., Mengjie, C., Xiaoqing, Q., Hao, L., Yuan, L., et al. (2021). Immune Infiltration and a Ferroptosis-Associated Gene Signature for Predicting the Prognosis of Patients with Endometrial Cancer. *Aging* 13, 16713–16732. doi:10.18632/aging.203190
- Wen, X., Wan, J., He, Q., Wang, M., Li, S., Jiang, M., et al. (2020). p190A Inactivating Mutations Cause Aberrant RhoA Activation and Promote Malignant Transformation via the Hippo-YAP Pathway in Endometrial Cancer. *Sig Transduct. Target Ther.* 5, 81. doi:10.1038/s41392-020-0170-6
- Wu, J., Minikes, A. M., Gao, M., Bian, H., Li, Y., Stockwell, B. R., et al. (2019). Intercellular Interaction Dictates Cancer Cell Ferroptosis via NF2-YAP Signaling. *Nature* 572, 402–406. doi:10.1038/s41586-019-1426-6
- Xie, R., Schlumbrecht, M. P., Shipley, G. L., Xie, S., Bassett, R. L., Jr, and Broadus, R. R. (2009). S100A4 Mediates Endometrial Cancer Invasion and Is a Target of TGF- $\beta$ 1 Signaling. *Lab. Invest.* 89, 937–947. doi:10.1038/labinvest.2009.52
- Xie, Y., Zhu, S., Song, X., Sun, X., Fan, Y., Liu, J., et al. (2017). The Tumor Suppressor P53 Limits Ferroptosis by Blocking DPP4 Activity. *Cell. Rep.* 20, 1692–1704. doi:10.1016/j.celrep.2017.07.055
- Xiong, Y., Xiao, C., Li, Z., and Yang, X. (2021). Engineering Nanomedicine for Glutathione Depletion-Augmented Cancer Therapy. *Chem. Soc. Rev.* 50, 6013–6041. doi:10.1039/d0cs00718h
- Xu, C., Sun, S., Johnson, T., Qi, R., Zhang, S., Zhang, J., et al. (2021). The Glutathione Peroxidase Gpx4 Prevents Lipid Peroxidation and Ferroptosis to Sustain Treg Cell Activation and Suppression of Antitumor Immunity. *Cell. Rep.* 35, 109235. doi:10.1016/j.celrep.2021.109235
- Xu, Y., Burmeister, C., Hanna, R. K., Munkarah, A., and Elshaikh, M. A. (2016). Predictors of Survival after Recurrence in Women with Early-Stage Endometrial Carcinoma. *Int. J. Gynecol. Cancer* 26, 1137–1142. doi:10.1097/IGC.0000000000000733
- Yamawaki, K., Ishiguro, T., Mori, Y., Yoshihara, K., Suda, K., Tamura, R., et al. (2017). Sox2-dependent Inhibition of P21 Is Associated with Poor Prognosis of Endometrial Cancer. *Cancer Sci.* 108, 632–640. doi:10.1111/cas.13196
- Yan, J., Ye, G., and Shao, Y. (2022). High Expression of the Ferroptosis-associated MGST1 Gene in Relation to Poor Outcome and Maladjusted Immune Cell Infiltration in Uterine Corpus Endometrial Carcinoma. *Clin. Lab. Anal.* 36, e24317. doi:10.1002/jcla.24317
- Yang, G., Zheng, R. Y., and Jin, Z. S. (2019). Correlations between Microsatellite Instability and the Biological Behaviour of Tumours. *J. Cancer Res. Clin. Oncol.* 145, 2891–2899. doi:10.1007/s00432-019-03053-4
- Yang, L., Tian, S., Chen, Y., Miao, C., Zhao, Y., Wang, R., et al. (2021). Ferroptosis-Related Gene Model to Predict Overall Survival of Ovarian Carcinoma. *J. Oncol.* 2021, 1–14. doi:10.1155/2021/6687391
- Yang, X., Cheng, Y., Li, X., Zhou, J., Dong, Y., Shen, B., et al. (2021a). A Novel Transcription Factor-Based Prognostic Signature in Endometrial Cancer: Establishment and Validation. *Onco Targets Ther.* 14, 2579–2598. doi:10.2147/OTT.S293085
- Yang, X., Zhang, X., Wu, R., Huang, Q., Jiang, Y., Qin, J., et al. (2017). DPPIV Promotes Endometrial Carcinoma Cell Proliferation, Invasion and Tumorigenesis. *Oncotarget* 8, 8679–8692. doi:10.18632/oncotarget.14412
- Yang, X., Zhu, Y., Shi, Q., Zhao, X., Huang, Y., Yao, F., et al. (2021b). Dipeptidyl Peptidase IV Is Required for Endometrial Carcinoma Cell Proliferation and Tumorigenesis via the IL -6/STAT3 Pathway. *J. Obstet. Gynaecol. Res.* 47, 2449–2459. doi:10.1111/jog.14788
- Yang, Y. (2015). Cancer Immunotherapy: Harnessing the Immune System to Battle Cancer. *Clin. Oncol.* 125, 3335–3337. doi:10.1172/jci83871
- Yu, Y., Sun, X., Chen, F., and Liu, M. (2022). Genetic Alteration, Prognostic and Immunological Role of Acyl-CoA Synthetase Long-Chain Family Member 4 in a Pan-Cancer Analysis. *Front. Genet.* 13, 812674. doi:10.3389/fgene.2022.812674
- Yuan, S., Zheng, P., Sun, X., Zeng, J., Cao, W., Gao, W., et al. (2021). Hsa\_Circ\_0001860 Promotes Smad7 to Enhance MPA Resistance in Endometrial Cancer via miR-520h. *Front. Cell. Dev. Biol.* 9, 738189. doi:10.3389/fcell.2021.738189
- Yuan, Y., Cao, W., Zhou, H., Qian, H., and Wang, H. (2021). CLTRN, Regulated by NRF1/RAN/DLD Protein Complex, Enhances Radiation Sensitivity of Hepatocellular Carcinoma Cells through Ferroptosis Pathway. *Int. J. Radiat. Oncol. Biol. Phys.* 110, 859–871. doi:10.1016/j.ijrobp.2020.12.062
- Zhang, K., Li, H., Yan, Y., Zang, Y., Li, K., Wang, Y., et al. (2019). Identification of Key Genes and Pathways between Type I and Type II Endometrial Cancer Using Bioinformatics Analysis. *Oncol. Lett.* 18, 2464–2476. doi:10.3892/ol.2019.10550
- Zhang, M., Zhang, T., Song, C., Qu, J., Gu, Y., Liu, S., et al. (2021). Guizhi Fuling Capsule Ameliorates Endometrial Hyperplasia through Promoting P62-Keap1-NRF2-Mediated Ferroptosis. *J. Ethnopharmacol.* 274, 114064. doi:10.1016/j.jep.2021.114064
- Zhang, X., Kan, H., Liu, Y., and Ding, W. (2021). Plumbagin Induces Ishikawa Cell Cycle Arrest, Autophagy, and Apoptosis via the PI3K/Akt Signaling Pathway in Endometrial Cancer. *Food Chem. Toxicol.* 148, 111957. doi:10.1016/j.fct.2020.111957
- Zhang, Y.-Y., Ni, Z.-J., Elam, E., Zhang, F., Thakur, K., Wang, S., et al. (2021). Juglone, a Novel Activator of Ferroptosis, Induces Cell Death in Endometrial Carcinoma Ishikawa Cells. *Food Funct.* 12, 4947–4959. doi:10.1039/d1fo00790d
- Zhang, Y., Shi, J., Liu, X., Feng, L., Gong, Z., Koppula, P., et al. (2018). BAP1 Links Metabolic Regulation of Ferroptosis to Tumour Suppression. *Nat. Cell. Biol.* 20, 1181–1192. doi:10.1038/s41556-018-0178-0
- Zhang, Y. Y., Zhang, F., Zhang, Y.-S., Thakur, K., Zhang, J.-G., Liu, Y., et al. (2019). Mechanism of Juglone-Induced Cell Cycle Arrest and Apoptosis in Ishikawa Human Endometrial Cancer Cells. *J. Agric. Food Chem.* 67, 7378–7389. doi:10.1021/acs.jafc.9b02759
- Zhou, H.-H., Chen, X., Cai, L.-Y., Nan, X.-W., Chen, J.-H., Chen, X.-X., et al. (2019). Erastin Reverses ABCB1-Mediated Docetaxel Resistance in Ovarian Cancer. *Front. Oncol.* 9, 1398. doi:10.3389/fonc.2019.01398
- Zhu, S., Zhang, Q., Sun, X., Zeh, H. J., Lotze, M. T., Kang, R., et al. (2017). HSPA5 Regulates Ferroptotic Cell Death in Cancer Cells. *Cancer Res.* 77, 2064–2077. doi:10.1158/0008-5472.CAN-16-1979

**Conflict of Interest:** The authors declare that the research was conducted in the absence of any commercial or financial relationships that could be construed as a potential conflict of interest.

**Publisher's Note:** All claims expressed in this article are solely those of the authors and do not necessarily represent those of their affiliated organizations, or those of the publisher, the editors, and the reviewers. Any product that may be evaluated in this article, or claim that may be made by its manufacturer, is not guaranteed or endorsed by the publisher.

Copyright © 2022 Wu, Zhang, Wu and Liu. This is an open-access article distributed under the terms of the Creative Commons Attribution License (CC BY). The use, distribution or reproduction in other forums is permitted, provided the original author(s) and the copyright owner(s) are credited and that the original publication in this journal is cited, in accordance with accepted academic practice. No use, distribution or reproduction is permitted which does not comply with these terms.



# Modified Iron Deposition in Nigrosomes by Pharmacotherapy for the Management of Parkinson's Disease

## OPEN ACCESS

### Edited by:

Yanqing Liu,  
Columbia University, United States

### Reviewed by:

Gang Wang,  
Weill Cornell Medicine, United States  
Xin Wang,  
National Institutes of Health (NIH),  
United States

### \*Correspondence:

Jing Wang  
mlbwj@163.com  
Qi Zheng  
13589729182@163.com  
Jinbo Chen  
chenjinbo6720@126.com  
Hongcai Wang  
whc2891@126.com

<sup>†</sup>These authors have contributed  
equally to this work

### Specialty section:

This article was submitted to  
Molecular Diagnostics and  
Therapeutics,  
a section of the journal  
Frontiers in Molecular Biosciences

**Received:** 30 March 2022

**Accepted:** 01 June 2022

**Published:** 07 July 2022

### Citation:

Wang M, Wang H, Wang J, Lu S, Li C,  
Zhong X, Wang N, Ge R, Zheng Q,  
Chen J and Wang H (2022) Modified  
Iron Deposition in Nigrosomes by  
Pharmacotherapy for the Management  
of Parkinson's Disease.  
Front. Mol. Biosci. 9:908298.  
doi: 10.3389/fmolb.2022.908298

Mengdi Wang<sup>1†</sup>, Hongxia Wang<sup>2†</sup>, Jing Wang<sup>2\*</sup>, Shujun Lu<sup>1</sup>, Chen Li<sup>3</sup>, Xiaofei Zhong<sup>2</sup>,  
Nan Wang<sup>3</sup>, Ruli Ge<sup>1</sup>, Qi Zheng<sup>1\*</sup>, Jinbo Chen<sup>1\*</sup> and Hongcai Wang<sup>1\*</sup>

<sup>1</sup>Department of Neurology, Binzhou Medical University Hospital, Binzhou, China, <sup>2</sup>Department of Radiology, Binzhou Medical University Hospital, Binzhou, China, <sup>3</sup>Medical Research Center, Binzhou Medical University Hospital, Binzhou, China

**Background:** Increased iron deposition in nigrosome as assessed by susceptibility-weighted imaging (SWI) is involved in the pathogenesis of Parkinson's disease (PD). This study investigated the effects of antiparkinson drugs on iron deposition in the nigrosome of PD patients.

**Methods:** Based on the retrospective analysis of clinical data, alterations in iron deposition in the substantia nigra were investigated in 51 PD patients across different types of therapies and in nine Parkinson-plus syndrome patients. The Movement Disorder Society revision of the Unified Parkinson's Disease Rating Scale (MDS-UPDRS) Part III/IV (UPDRS III/IV) was utilized to evaluate motor function and complications. SWI (slice = 0.6 mm) was used to detect iron deposition in the nigrosome and substantia nigra. Nigrosome loss was scored on a 1-point nigrosome visibility scale. Visual assessment of dorsolateral nigral hyperintensity (DNH) was separately performed for each side of the nigrosome with SWI.

**Results:** Increased UPDRS III scores were correlated with low nigrosome scores based on correlation analysis at a disease duration of 6–12 months ( $r = -0.8420$ ). The loss of the nigrosome on SWI was clearly inhibited in PD patients with a 3–5-year duration of administration of antiparkinson medications compared with no treatment. Decreased UPDRS III scores and increased nigrosome scores were observed in the regular treatment of PD patients with a 6–7-year disease duration. For patients with Parkinson-plus syndromes, such as multiple system atrophy, iron accumulation was apparent in the corpus striatum and substantia nigra compared with that for patients with progressive supranuclear palsy.

**Conclusions:** Early and regular treatment with antiparkinson drugs not only alleviates the chance of PD disability but also prevents the loss of DNH, namely, iron accumulation in the nigrosome.

**Keywords:** iron accumulation, nigrosome, Parkinson's disease, levodopa, dorsolateral nigral hyperintensity

## INTRODUCTION

Parkinson's disease (PD) is a progressive degenerative disorder characterized by the selective loss of dopaminergic neurons in the

substantia nigra pars compacta (SNc) (Kinoshita et al., 2015). Iron-specific accumulation in the SNc but not in other iron-rich areas is a cardinal feature of degenerating regions in a PD brain (Hare and Double, 2016; Billings et al., 2019). Susceptibility-

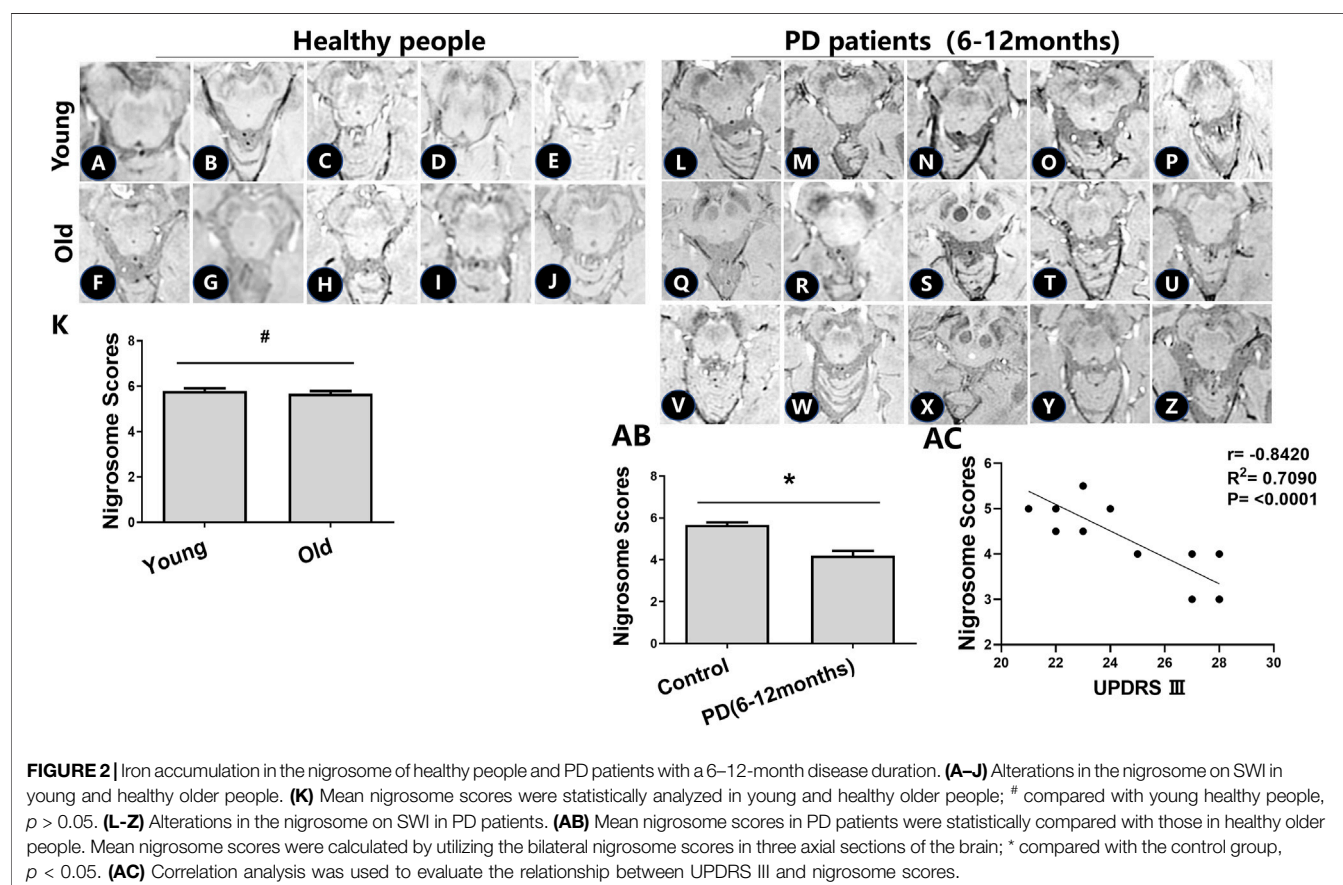
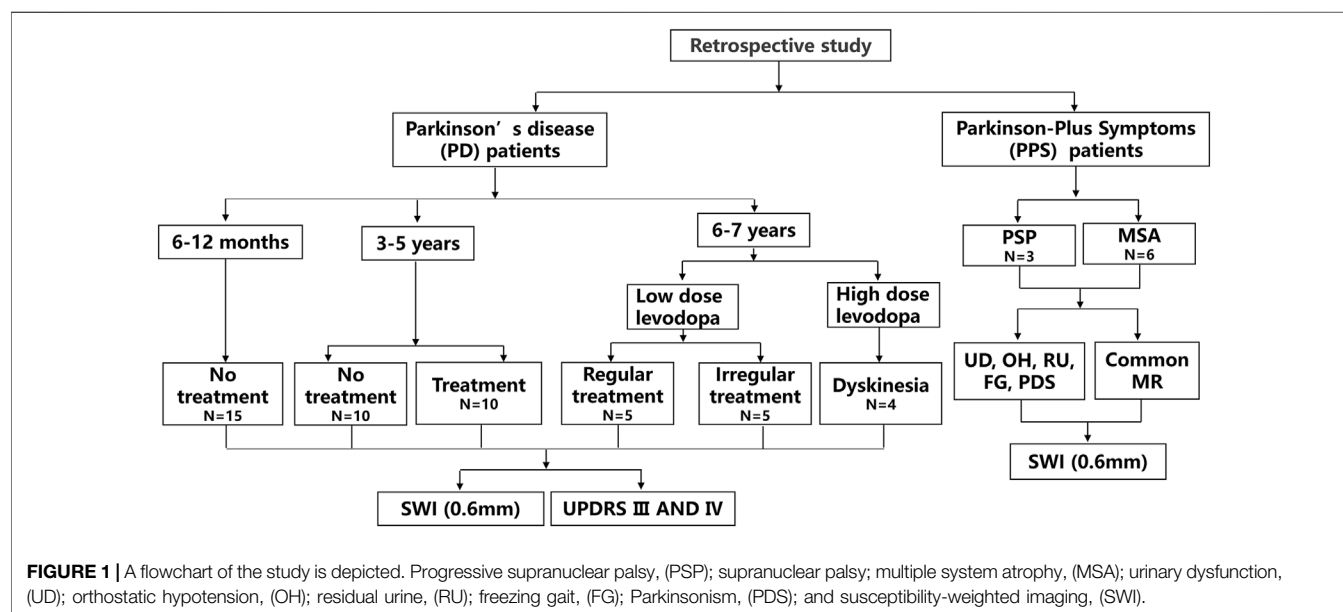




**TABLE 1** | The information of PD patients who had no drug treatment with a 6–12 month disease duration.

Patients	Gender	Age (Y)	UPDRS III	H&Y	Nigrosme scores
L	F	56	28	1	3
M	F	54	27	1	3
N	N	59	23	1	5.5
O	F	61	28	1	3
P	F	54	23	1	4.5
Q	M	52	24	1	5
R	F	56	28	1	3
S	M	61	27	1	4
T	F	62	28	1	4
U	F	59	27	1	4
V	F	54	22	1	4.5
W	F	57	21	1	5
X	F	58	25	1	4
Y	F	61	22	1	5
Z	F	51	23	1	5.5

weighted imaging (SWI) results in a high-contrast image and is sensitive to iron overload (Haller et al., 2021). The nigrosome, a dopaminergic neuron-rich region in the SNc, is the most severely affected region in PD (Kim et al., 2019). Enhanced iron content in the nigrosome leads to the loss of dorsolateral nigral

hyperintensity (DNH) on SWI (Pavese and Tai, 2018). Increased iron deposition in the SNc has been linked to the progression of motor impairment and disability in patients with PD (Huang et al., 2020). The absence of DNH on SWI may serve as a new magnetic resonance imaging (MRI) marker for the progression of PD (Pang et al., 2020). Moreover, the loss of the nigrosome on SWI helps distinguish PD from healthy controls, although this approach fails to reliably differentiate PD from atypical parkinsonism (Pavese and Tai, 2018).

Studies have reported interactions of iron and dopamine that are colocalized in dopaminergic neurons of the SNc (Billings et al., 2019). Dopamine replacement treatment, which has neuroprotective effects and prevents age-related iron accumulation in the SNc of mutant mouse models, remains the most effective symptomatic pharmacotherapy for PD (Billings et al., 2019). However, the chelation of iron by levodopa is insufficient to attenuate neuron loss (Billings et al., 2019). In *in vitro* and *in vivo* models, levodopa replacement therapy was shown to be neurotoxic, and the effect of levodopa on iron accumulation was somewhat muted (Billings et al., 2019).

Nevertheless, clinical data have indicated that levodopa either slows the progression of PD or has a long-lasting effect on the symptoms of the disease, but the potential long-term effects of levodopa on PD remain uncertain (Fahn et al., 2004). An in-

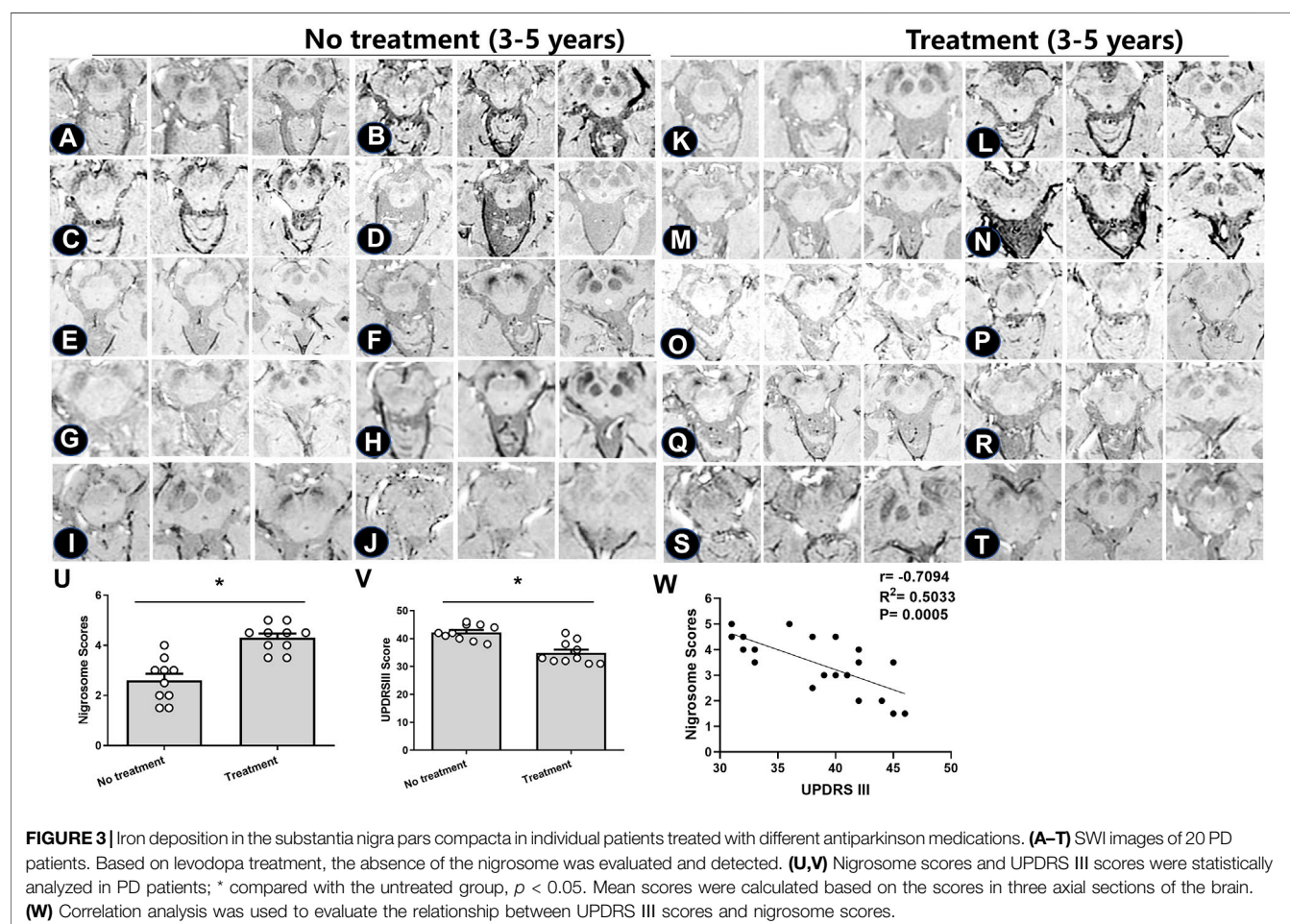


**TABLE 2 |** The information of PD patients with a 3–5 year duration between the treatment and no treatment groups.

Patients		Age(Y)	Gender	H&Y	Average age (mean $\pm$ SD)
No treatment	A	70	M	3	65.4 $\pm$ 6.7
	B	59	M	3	
	C	63	F	3	
	D	64	M	3	
	E	58	F	3	
	F	77	F	3	
	G	72	F	3	
	H	68	M	3	
	I	69	M	3	
	J	54	F	3	
Treatment	K	74	M	3	63.9 $\pm$ 8.1 <sup>#</sup>
	L	55	F	3	
	M	56	M	3	
	N	58	M	3	
	O	63	F	3	
	P	73	F	3	
	Q	65	M	3	
	R	76	M	3	
	S	67	F	3	
	T	52	F	3	

<sup>#</sup>Compared with no treatment group,  $p > 0.05$ .

depth exploration of the prolonged effects of levodopa on iron accumulation in the nigrosome might be helpful in establishing new therapeutic strategies for PD treatment. In this study, a retrospective analysis was used to explore the effects of antiparkinson medications on DNH on SWI, which represents iron accumulation in the nigrosome, in PD patients with different disease durations.

## MATERIALS AND METHODS

### Parkinson's Disease Patient Information

The neuroimaging data and medical records of 51 patients with PD, nine Parkinson-plus syndrome patients, and 30 healthy subjects were used in this study (different English letters represent the brain images from individual patients). The study was approved by the Ethics Committee of Binzhou Medical University Hospital, and all methods were performed in accordance with the relevant guidelines and regulations. Written informed consent was obtained from all subjects and their legal guardians. Research involving human participants was performed in accordance with the Declaration of Helsinki. Research on patients or healthy volunteers required the supervision of a competent and appropriately qualified physician. This research conformed to generally accepted scientific principles. The physician fully informed the subjects about which aspects of their care were related to the research. Every precaution has been taken to protect the privacy of research subjects and the confidentiality of their personal information. The refusal of a patient to participate in a study or the patient's decision to withdraw from the study never adversely affected the patient–physician relationship.

The no treatment group represented patients who were not administered antiparkinson medications. The treatment group included patients who were administered Madopar (200 mg/50 mg) and selegiline hydrochloride. This regular treatment group included patients who were regularly treated with oral Madopar and selegiline hydrochloride depending on the specialist advice (oral Madopar at fixed time intervals and with a stable oral dosage). Patients with Parkinson-plus syndromes were also treated with Madopar and selegiline hydrochloride in the early stage. A flowchart of the study is shown in **Figure 1**.

### Visualization of the Nigrosome

Visualization of the nigrosome on SWI with uniform susceptibility was carried out. According to the scores of each side of the midbrain in three cross-sectional planes, bilateral alterations in the nigrosome were evaluated. Nigrosome loss was scored on a 1-point nigrosome visibility scale (1 = unilateral side with normal brightness and present; 0.5 = slightly more difficult to see than normal/reduced size or very difficult to see but identifiable, or possibly parts of the outline are visible but not definitely identifiable; 0 = not identifiable).

### Movement of Parkinson's Disease Patients was Analyzed Using Unified Parkinson's Disease Rating Scale III/IV Motor Scores

PD was diagnosed based on the UK Parkinson's Disease Society Brain Bank diagnostic criteria. PD patients were from Binzhou Medical University Hospital. The severity of PD symptoms was assessed using the Movement Disorder Society revision of the Unified Parkinson's Disease Rating Scale (MDS-UPDRS) section III (UPDRS III), after the patient had been off levodopa for 24 h (off state). All patients underwent a thorough clinical examination. UPDRS Part IV was used to evaluate the complications of PD, including dyskinesia and dysmyotonia.

### MR Imaging and Image Processing

maging was performed using a 3T MRI device (GE 750w, Amersham, United Kingdom) with a standard body coil for transmitting and a 12-channel head coil for receiving. SWI and T2-weighted sequences were utilized. The volume of the nigrosome was assessed using SWI at 3T with a 0.6-mm slice thickness. Voxel size = 0.75 mm  $\times$  0.75 mm  $\times$  0.6 mm; field of view 240 mm  $\times$  216 mm, TR = 40.3 ms, TE = 24.1 ms, slice: 0.6 mm, Flip Angles: 15, Freq Dir: A/P, Freq. Fov: 24.0, Phase Fov: 0.90, Frequency: 320, Phase: 288, Bandwidth: 41.67. Data were analyzed by three different radiologists.

### Statistical Analysis

The descriptive statistics are presented as the mean  $\pm$  SEM. Statistical analysis was performed using GraphPad Prism 8.0 (GraphPad Software Inc., San Diego, CA, USA). Correlation analysis was used to quantify the degree to which the two variables were related, and  $p < 0.05$  was accepted as significant. Pearson correlation analysis was used to assess the relationship between UPDRS III and nigrosome scores. Student's *t* tests were used to compare the means of two groups. A *p* value of less than 0.05 implies statistical significance.

**TABLE 3 |** The information of patients with irregular and regular treatment.

Patients		Age(Y)	Gender	Duration (Y)	H&Y	UPDRS III (mean $\pm$ SD)	Nigrosome score (mean $\pm$ SD)
Irregular treatment	A	65	F	7	3	65 $\pm$ 1.4	2.1 $\pm$ 0.5
	B	68	F	6	3		
	C	66	F	6	3		
	D	72	M	6	3		
	E	75	M	7	3		
Regular treatment	F	63	M	6	3	56.2 $\pm$ 1.3	3.8 $\pm$ 0.2
	G	72	M	7	3		
	H	71	M	6	3		
	I	73	F	7	3		
	J	66	M	6	3		

## RESULTS

### Loss of Dorsolateral Nigral Hyperintensity on Susceptibility Weighted Imaging in Healthy People and Early-Stage Parkinson's Disease Patients

To determine the effects of age-related iron accumulation in the nigrosome, young (30–50 years) and old (51–80 years) healthy people without brain disease were chosen. DNH was observed in healthy people. In healthy control subjects, there was no significant difference in the nigrosome scores between young and old healthy people (Figures 2A–J).

There had been no drug treatment for PD patients with a 6–12-month disease duration who were seeking treatment for the first time. Patient information, including sex, UPDRS III scores, Hoehn and Yahr scale scores, and nigrosome scores, is recorded in Table 1. The alteration of substantia nigra hyperintensity was recorded in SWI, and nigrosome scores were calculated using the 1-point nigrosome visibility scale (Figures 2L–Z). According to the modified Hoehn and Yahr scale, the patients were classified as stage 1. The UPDRS III scores ranged from 20 to 30. The bilateral asymmetric loss of signal hyperintensity of the nigrosome was shown on SWI. There was a significant difference in the nigrosome scores between old healthy people and PD patients (Figure 2AB,  $p < 0.05$ ). Correlation analysis indicated that the UPDRS III scores negatively correlated with nigrosome scores in the patients with a 6–12-month disease duration ( $r = -0.8420$ , Figure 2AC).

### Effects of Levodopa Therapy on Dorsolateral Nigral Hyperintensity

For those with a 3–5-year duration of PD, the alterations in the nigrosome on SWI were investigated depending on the different treatments (Figures 3A–T). Patient information is recorded in Table 2. There was no significant difference in the average age of patients between the treatment and no treatment groups (Table 2). The loss of the nigrosome was statistically analyzed according to the 1-point nigrosome visibility scale on high-resolution 3T-SWI. Compared with those in untreated patients, the nigrosome scores were increased owing to early treatment with antiparkinson drugs ( $p < 0.05$ ) (Figure 3U). There is a significant

difference in UPDRS III scores between the treatment and no treatment groups (Figure 3V). Correlation analysis indicated that the UPDRS III scores negatively correlated with nigrosome scores ( $r = -0.7094$ , Figure 3W).

Subsequent analyses were performed to investigate the loss of DNH in patients with irregular and regular treatment. As shown in Table 3, the nigrosome scores were increased from 2.1  $\pm$  0.5 to 3.8  $\pm$  0.2 in those with regular oral administration of Madopar and selegiline hydrochloride compared with those with irregular treatment ( $p < 0.05$ ) (Figures 4A–K). The motor symptoms of PD were ameliorated according to UPDRS III scores from 65  $\pm$  1.4 to 56.2  $\pm$  1.3 owing to regular treatment. UPDRS III scores were negatively correlated with nigrosome scores ( $r = -0.9338$ ) (Figure 4L).

After administration of levodopa for 10 months, the alterations in iron deposition in the nigrosome were different in two of the patients (Figures 5A,B). For patient case 76 receiving regular oral Madopar and selegiline hydrochloride, increased nigrosome scores and unchanged UPDRS III scores were detected. For patient case 77, compared with pretreatment scores, decreased nigrosome scores and increased UPDRS III scores were observed owing to irregular treatment.

### Loss of Dorsolateral Nigral Hyperintensity was Prevented in Patients with a High Dose of Levodopa

UPDRS IV scores were used to evaluate the motor complications induced by levodopa (Figure 6). In one patient treated with high-dose levodopa for 7–8 years, there was no apparent loss of DNH on SWI, as shown in Figure 6A (black arrow). Four of the PD patients had peak-dose dyskinesia or biphasic dyskinesia. A greater severity of dyskinesia with a high UPDRS IV score and higher nigrosome scores was revealed in patient A than in patients B–D (Figure 6, black arrow).

### The Early Levodopa Treatment for the Alteration of Iron Deposition in Parkinson-Plus Symptoms

To further investigate iron accumulation in those with Parkinson-plus syndrome, alterations in signal hyperintensity in the nigrosome in nine patients were examined. As Figure 7 indicates, patients A–F were diagnosed with multiple system



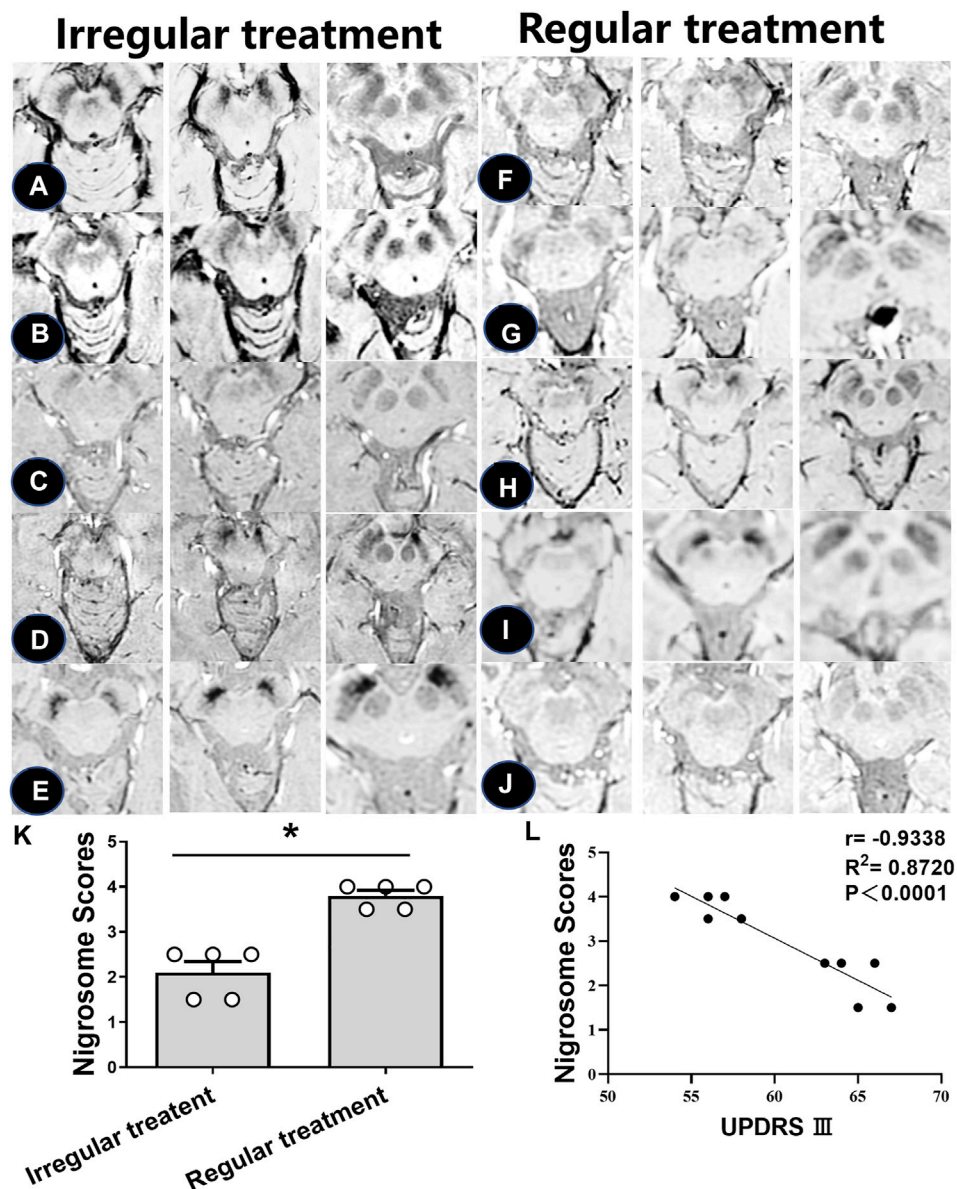


**FIGURE 4 |** Iron accumulation in the nigrosome with regular and irregular treatments. **(A–J)** SWI images of 10 PD patients receiving irregular or regular levodopa treatment. **(K)** Mean scores of the nigrosome was increased with regular treatment compared with irregular treatment; \* compared with irregular treatment,  $p < 0.05$ . **(L)** Correlation analysis was used to reveal the relationship between UPDRS III scores and nigrosome scores.

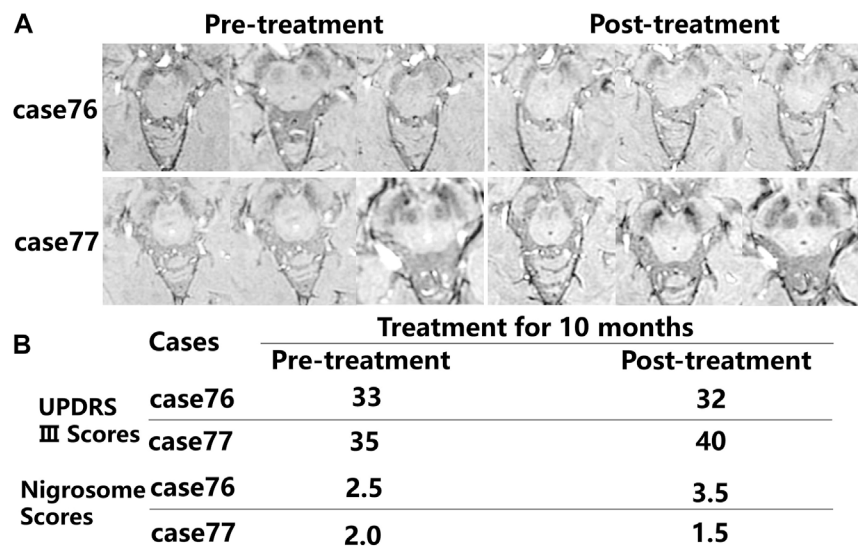
atrophy (MSA) depending on clinical evidence of urinary dysfunction (UD), orthostatic hypotension (OH), residual urine (RU), freezing gait (FG), parkinsonism (PDS), and ataxia and on neuroimaging evidence including a hot cross bun sign in the pons on a 3T MRI (Figure 7B, white arrow). As Figure 7 shows, hypointensity increased in the substantia nigra and corpus striatum of patients on SWI. Figures 8A–C indicates hypointensity in the corpus striatum of patients diagnosed with probable progressive supranuclear palsy (PSP). The hummingbird sign was seen on sagittal T1WI of the brain in patients A and B (Figures 8A,B, white arrow).

## DISCUSSION

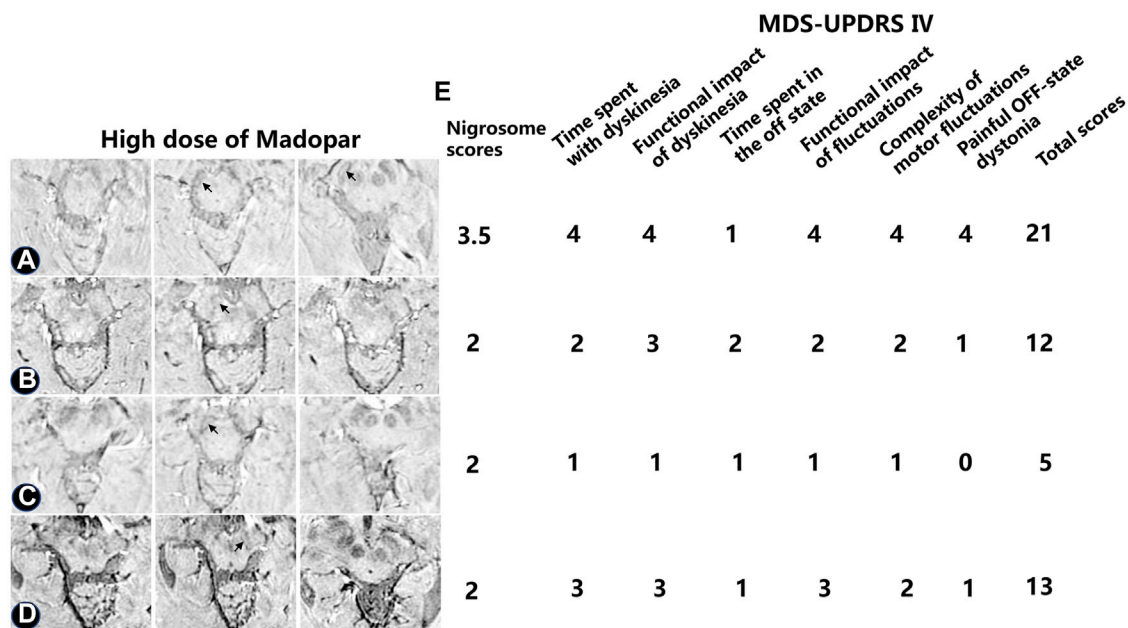
In this study, the retrospective data suggested that the clinical symptoms of PD with no drug treatment quickly progressed and resulted in physiological deformities. Nevertheless, early and regular treatment with levodopa decreased UPDRS III motor scores and the loss of DNH. The rational administration of levodopa not only delayed the progression of PD but also affected iron deposition in the nigrosome.

The imaging of nigrosome loss has been recognized as a biomarker of the pathogenesis of PD (Sung et al., 2021).





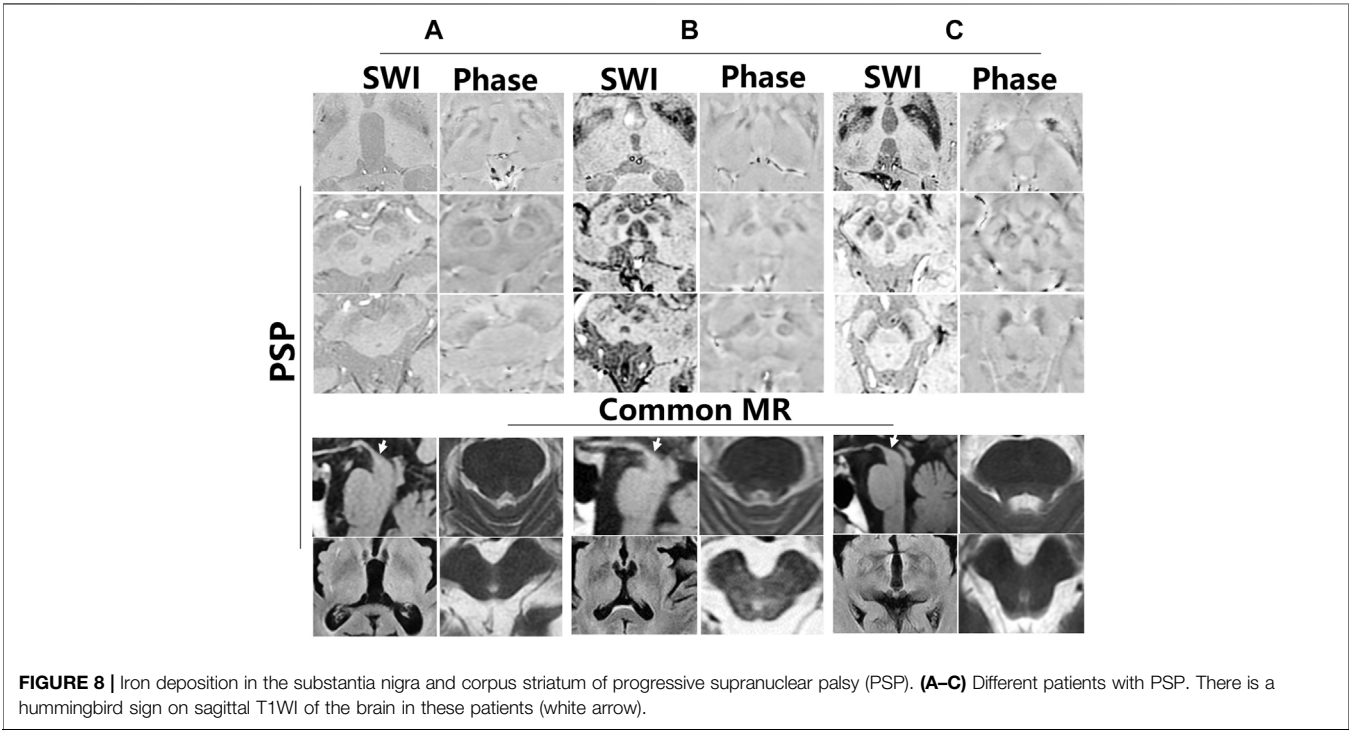
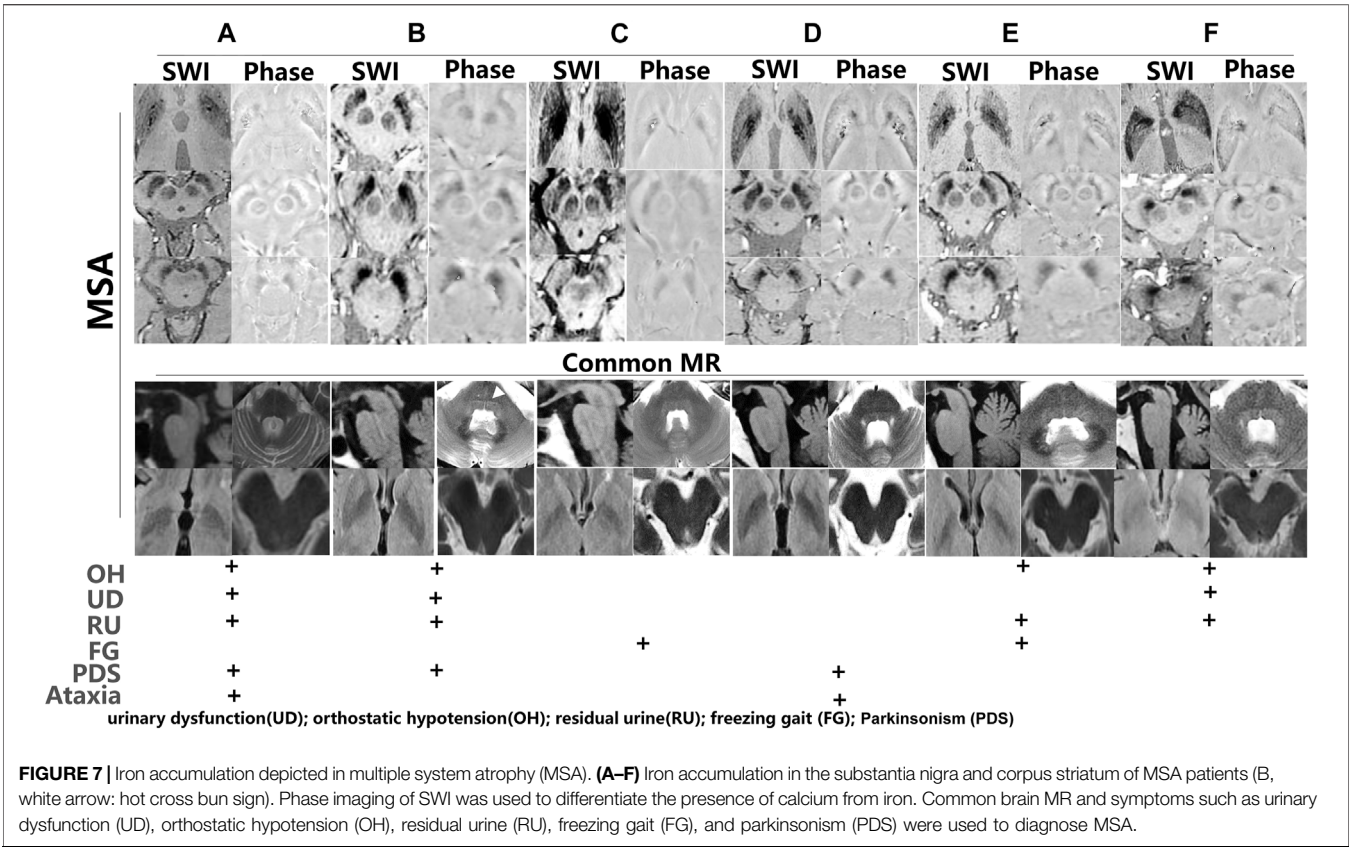
**FIGURE 5** | Comparison in the alterations in iron accumulation in the nigrosome in the pretreatment and posttreatment groups. **(A)** The alterations in iron deposition in the nigrosome were evaluated in two of the patients after treatment for 10 months. **(B)** Nigrosome scores and UPDRS III scores were observed after receiving pharmacological treatment.

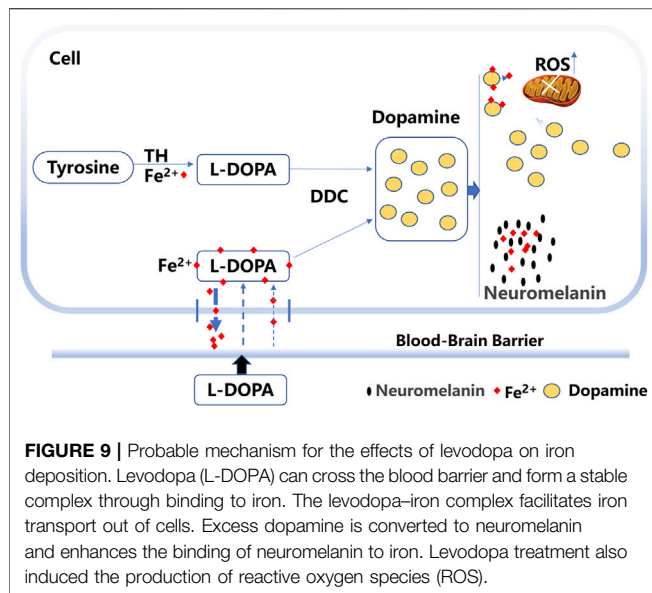


**FIGURE 6** | Alterations in iron aggregation in the substantia nigra in four PD patients treated with high-dose levodopa with peak-dose dyskinesia or biphasic dyskinesia. The nigrosome was visible as a bright area **(A–D)** The nigrosome was visible (black arrow) as a bright area. **(E)** The dyskinesia was evaluated by utilizing the UPDRS IV.

Additional evidence suggested that poor visualization of the nigrosome in PD provides diagnostic evidence of the disease (Billings et al., 2019). The loss of the nigrosome was significantly associated with higher motor asymmetry on the contralateral side in subjects (Billings et al., 2019). In our study, all PD patients had

different degrees of nigrosome volume loss compared with healthy people. Although some studies have suggested that the nigrosome had the typical “swallow tail” appearance (Lee et al., 2021), a greater volume of the nigrosome was observed in the SNc by using SWI with different susceptibilities. Moreover, SWI





measures iron accumulation with a semiquantitative pattern and can be used to track iron accumulation in PD (Weinreb et al., 2013; Takahashi et al., 2018). In our study, SWI at 3T was adequate for showing the alteration of iron accumulation in the nigrosome.

Some studies have indicated that in the SNc, metabolic disturbances associated with levodopa are related to iron accumulation (Billings et al., 2019). Iron is essential for many biological functions, including neurotransmitter synthesis, where the metal is a cofactor of tyrosine, which converts tyrosine to dopamine (Zucca et al., 2008). In previous studies, only dopamine but not tyrosine or norepinephrine interfered with cellular iron homeostasis and promoted cellular iron accumulation (Dichtl et al., 2018). Furthermore, increases in intracellular iron with dopamine therapy result in the production of reactive oxygen species (ROS) and neurodegeneration (Dichtl et al., 2018). Targeting iron and dopamine interactions may be an effective way to modify neuronal vulnerability and thus slow neuronal loss (Hare and Double, 2016). In another study, levodopa was shown to be neuroprotective and to prevent age-related iron accumulation in the substantia nigra (Beard, 2001; Fahn et al., 2004). Our retrospective study indicated that early and regular treatment with levodopa prevented the loss of DNH and alleviated the symptoms of PD. A recent study suggested that the nigral iron deposition was associated with levodopa-induced dyskinesia (Song et al., 2021). However, in our study, decreased loss of DNH was observed in one patient with more severe dyskinesia.

Studies have indicated that levodopa binding to iron forms a stable complex (Alhassen et al., 2022). The levodopa molecule is known to contain a domain with iron-chelating properties or the ability to prevent iron deposition and the toxic effects of extra free iron (Billings

et al., 2019; Alhassen et al., 2022). Iron transport is regulated by the hepcidin-ferroportin system to control iron release into the plasma (Wu et al., 2021). Hepcidin expression is principally regulated by plasma iron in a feedback loop (Zucca et al., 2017). In our study, excess extracellular levodopa binds iron, which reduces the plasma iron level and regulates hepcidin expression, which might subsequently facilitate iron transport out of cells and decrease iron deposition (Figure 9).

In addition, excess dopamine is converted to neuromelanin, and iron binds to neuromelanin in the human SNc (Zucca et al., 2017). Neuromelanin was shown to be markedly decreased in the SNc of PD patients, and neuromelanin represented the major iron storage capacity in substantia nigra neurons (Zucca et al., 2001; Nagatsu et al., 2022). Neuromelanin serves to trap iron, which results in a high load of iron in the brain (Zucca et al., 2017). After binding to neuromelanin, iron changes its location or state (Zucca et al., 2017). The accumulation of neuromelanin increases the free  $\text{Fe}^{2+}$  form in the SNc of patients with PD (Faucheux et al., 2003). Whether neuromelanin enhances the binding activity to iron with long-term levodopa treatment remains to be elucidated. Thus, iron bound to neuromelanin might be another mechanism for decreased iron levels (Figure 9).

Previous evidence has suggested that MSA and PSP patients have obvious iron accumulation in different brain regions (Lee and Lee, 2019). Histopathological studies in MSA patients revealed that iron deposition in the putamen was a hallmark of the disease (Kaindlstorfer et al., 2018). Similarly, our study showed the enhancement of hypointensity in the substantia nigra and corpus striatum on SWI in MSA patients. The PSP group had significantly increased iron content in the globus pallidus and caudate nucleus (Lee et al., 2013). In our study, increased hypointensity in the globus pallidus and putamen was observed in PSP patients.

In our study, by comparing the effects of different treatments on the loss of DNH, the view that proper treatment with levodopa prevented iron deposition in the nigrosome was validated. Nigrosome scores were calculated objectively using the 1-point nigrosome visibility scale. However, a small sample size can also lead to the introduction of bias and cannot exclude the influence of individual differences in iron content in the nigrosome. The genuine effects of levodopa treatment on iron deposition need more clinical evidence. In future studies, we will investigate alterations in iron accumulation in the nigrosome between patients from pretreatment to posttreatment. In summary, early rational pharmacotherapy might prevent iron accumulation in the nigrosome and ameliorate motor symptoms.

## DATA AVAILABILITY STATEMENT

The original contributions presented in the study are included in the article/Supplementary Material, and further inquiries can be directed to the corresponding authors.

## ETHICS STATEMENT

The studies involving human participants were reviewed and approved by the Ethics Committee of Binzhou Medical University Hospital. The patients/participants provided their written informed consent to participate in this study.

## AUTHOR CONTRIBUTIONS

MW and HW designed the experiments; JW, SL, XZ, CL, and NW collected the data and analyzed results; RG, QZ, and JC gave suggestions in the study; MW and HW prepared the manuscript; and HW critically revised the manuscript. All authors read and agreed to submit for publication.

## REFERENCES

- Alhassen, S., Senel, M., and Alachkar, A. (2022). Surface Plasmon Resonance Identifies High-Affinity Binding of L-DOPA to Siderocalin/Lipocalin-2 through Iron-Siderophore Action: Implications for Parkinson's Disease Treatment. *ACS Chem. Neurosci.* 13, 158–165. doi:10.1021/acchemneuro.1c00693
- Beard, J. L. (2001). Iron Biology in Immune Function, Muscle Metabolism and Neuronal Functioning. *J. Nutr.* 131, 568S–580S. doi:10.1093/jn/131.2.568S
- Billings, J. L., Gordon, S. L., Rawling, T., Doble, P. A., Bush, A. I., Adlard, P. A., et al. (2019). 1-3,4-dihydroxyphenylalanine (L-DOPA) Modulates Brain Iron, Dopaminergic Neurodegeneration and Motor Dysfunction in Iron Overload and Mutant Alpha-synuclein Mouse Models of Parkinson's Disease. *J. Neurochem.* 150, 88–106. doi:10.1111/jnc.14676
- Dichtl, S., Haschka, D., Nairz, M., Seifert, M., Volani, C., Lutz, O., et al. (2018). Dopamine Promotes Cellular Iron Accumulation and Oxidative Stress Responses in Macrophages. *Biochem. Pharmacol.* 148, 193–201. doi:10.1016/j.bcp.2017.12.001
- Fahn, S., Oakes, D., Shoulson, I., Kieburtz, K., Rudolph, A., Lang, A., et al. (2004). Levodopa and the Progression of Parkinson's Disease. *N. Engl. J. Med.* 351, 2498–2508. doi:10.1056/NEJMoa033447
- Faucheux, B. A., Martin, M.-E., Beaumont, C., Hauw, J.-J., Agid, Y., and Hirsch, E. C. (2003). Neuromelanin Associated Redox-Active Iron Is Increased in the Substantia Nigra of Patients with Parkinson's Disease. *J. Neurochem.* 86, 1142–1148. doi:10.1046/j.1471-4159.2003.01923.x
- Haller, S., Haacke, E. M., Thurnher, M. M., and Barkhof, F. (2021). Susceptibility-weighted Imaging: Technical Essentials and Clinical Neurologic Applications. *Radiology* 299, 3–26. doi:10.1148/radiol.2021203071
- Hare, D. J., and Double, K. L. (2016). Iron and Dopamine: a Toxic Couple. *Brain* 139, 1026–1035. doi:10.1093/brain/aww022
- Huang, W., Ogbuji, R., Zhou, L., Guo, L., Wang, Y., and Kopell, B. H. (2020). Motoric Impairment versus Iron Deposition Gradient in the Subthalamic Nucleus in Parkinson's Disease. *J. Neurosurg.* 135, 284–290. doi:10.3171/2020.5.JNS201163
- Kaandstorfer, C., Jellinger, K. A., Eschlöböck, S., Stefanova, N., Weiss, G., and Wenning, G. K. (2018). The Relevance of Iron in the Pathogenesis of Multiple System Atrophy: A Viewpoint. *Jad* 61, 1253–1273. doi:10.3233/JAD-170601
- Kim, E. Y., Sung, Y. H., and Lee, J. (2019). Nigrosome 1 Imaging: Technical Considerations and Clinical Applications. *Bjr* 92, 20180842. doi:10.1259/bjr.20180842
- Kinoshita, K.-i., Tada, Y., Muroi, Y., Unno, T., and Ishii, T. (2015). Selective Loss of Dopaminergic Neurons in the Substantia Nigra Pars Compacta after Systemic Administration of MPTP Facilitates Extinction Learning. *Life Sci.* 137, 28–36. doi:10.1016/j.lfs.2015.07.017
- Lee, J.-H., Han, Y.-H., Kang, B.-M., Mun, C.-W., Lee, S.-J., and Baik, S.-K. (2013). Quantitative Assessment of Subcortical Atrophy and Iron Content in Progressive Supranuclear Palsy and Parkinsonian Variant of Multiple System Atrophy. *J. Neurol.* 260, 2094–2101. doi:10.1007/s00415-013-6951-x
- Lee, J.-H., and Lee, M.-S. (2019). Brain Iron Accumulation in Atypical Parkinsonian Syndromes: In Vivo MRI Evidences for Distinctive Patterns. *Front. Neurol.* 10, 74. doi:10.3389/fneur.2019.00074
- Lee, T.-W., Chen, C.-Y., Chen, K., Tso, C.-W., Lin, H.-H., Lai, Y.-L. L., et al. (2021). Evaluation of the Swallow-Tail Sign and Correlations of Neuromelanin Signal with Susceptibility and Relaxations. *Tomography* 7, 107–119. doi:10.3390/tomography7020010
- Nagatsu, T., Nakashima, A., Watanabe, H., Ito, S., and Wakamatsu, K. (2022). Neuromelanin in Parkinson's Disease: Tyrosine Hydroxylase and Tyrosinase. *Ijms* 23, 4176. doi:10.3390/ijms23084176
- Pang, H., Yu, Z., Li, R., Yang, H., and Fan, G. (2020). MRI-Based Radiomics of Basal Nuclei in Differentiating Idiopathic Parkinson's Disease from Parkinsonian Variants of Multiple System Atrophy: A Susceptibility-Weighted Imaging Study. *Front. Aging Neurosci.* 12, 587250. doi:10.3389/fnagi.2020.587250
- Pavese, N., and Tai, Y. F. (2018). Nigrosome Imaging and Neuromelanin Sensitive MRI in Diagnostic Evaluation of Parkinsonism. *Mov. Disord. Clin. Pract.* 5, 131–140. doi:10.1002/mdc3.12590
- Song, T., Li, J., Mei, S., Jia, X., Yang, H., Ye, Y., et al. (2021). Nigral Iron Deposition Is Associated with Levodopa-Induced Dyskinesia in Parkinson's Disease. *Front. Neurosci.* 15, 647168. doi:10.3389/fnins.2021.647168
- Sung, Y. H., Noh, Y., and Kim, E. Y. (2021). Early-stage Parkinson's Disease: Abnormal Nigrosome 1 and 2 Revealed by a Voxelwise Analysis of Neuromelanin-sensitive MRI. *Hum. Brain Mapp.* 42, 2823–2832. doi:10.1002/hbm.25406
- Takahashi, H., Watanabe, Y., Tanaka, H., Mihara, M., Mochizuki, H., Liu, T., et al. (2018). Quantifying Changes in Nigrosomes Using Quantitative Susceptibility Mapping and Neuromelanin Imaging for the Diagnosis of Early-Stage Parkinson's Disease. *Bjr* 91, 20180037. doi:10.1259/bjr.20180037
- Weinreb, O., Mandel, S., Youdim, M. B. H., and Amit, T. (2013). Targeting Dysregulation of Brain Iron Homeostasis in Parkinson's Disease by Iron Chelators. *Free Radic. Biol. Med.* 62, 52–64. doi:10.1016/j.freeradbiomed.2013.01.017
- Wu, L., Liu, M., Liang, J., Li, N., Yang, D., Cai, J., et al. (2021). Ferroptosis as a New Mechanism in Parkinson's Disease Therapy Using Traditional Chinese Medicine. *Front. Pharmacol.* 12, 659584. doi:10.3389/fphar.2021.659584
- Zecca, L., Casella, L., Albertini, A., Bellei, C., Zucca, F. A., Engelen, M., et al. (2008). Neuromelanin Can Protect against Iron Mediated Oxidative Damage in System Modeling Iron Overload of Brain Aging and Parkinson's Disease. *J. Neurochem.* 106, 1866–1875. doi:10.1111/j.1471-4159.2008.05541.x
- Zecca, L., Gallorini, M., Schünemann, V., Trautwein, A. X., Gerlach, M., Riederer, P., et al. (2001). Iron, Neuromelanin and Ferritin Content in the Substantia Nigra of Normal Subjects at Different Ages: Consequences for Iron Storage and Neurodegenerative Processes. *J. Neurochem.* 76, 1766–1773. doi:10.1046/j.1471-4159.2001.00186.x

## FUNDING

This work was supported by grants from the National Natural Science Foundation of China (NSFC) (81601108 and 81700472) and the Natural Science Foundation of Shandong Province of China (ZR2016HQ14 and ZR2021MH135).

## SUPPLEMENTARY MATERIAL

The Supplementary Material for this article can be found online at: <https://www.frontiersin.org/articles/10.3389/fmolb.2022.908298/full#supplementary-material>



Zucca, F. A., Segura-Aguilar, J., Ferrari, E., Muñoz, P., Paris, I., Sulzer, D., et al. (2017). Interactions of Iron, Dopamine and Neuromelanin Pathways in Brain Aging and Parkinson's Disease. *Prog. Neurobiol.* 155, 96–119. doi:10.1016/j.pneurobio.2015.09.012

**Conflict of Interest:** The authors declare that the research was conducted in the absence of any commercial or financial relationships that could be construed as a potential conflict of interest.

**Publisher's Note:** All claims expressed in this article are solely those of the authors and do not necessarily represent those of their affiliated organizations or those of

the publisher, the editors, and the reviewers. Any product that may be evaluated in this article, or claim that may be made by its manufacturer, is not guaranteed or endorsed by the publisher.

Copyright © 2022 Wang, Wang, Wang, Lu, Li, Zhong, Wang, Ge, Zheng, Chen and Wang. This is an open-access article distributed under the terms of the Creative Commons Attribution License (CC BY). The use, distribution or reproduction in other forums is permitted, provided the original author(s) and the copyright owner(s) are credited and that the original publication in this journal is cited, in accordance with accepted academic practice. No use, distribution or reproduction is permitted which does not comply with these terms.



# Screening for Potential Therapeutic Agents for Non-Small Cell Lung Cancer by Targeting Ferroptosis

Xin Zhao<sup>1</sup>, Lijuan Cui<sup>1</sup>, Yushan Zhang<sup>1</sup>, Chao Guo<sup>1</sup>, Lijiao Deng<sup>1</sup>, Zhitong Wen<sup>1</sup>, Zhihong Lu<sup>1,2</sup>, Xiaoyuan Shi<sup>1</sup>, Haojie Xing<sup>1</sup>, Yunfeng Liu<sup>2\*†</sup> and Yi Zhang<sup>1\*†</sup>

<sup>1</sup>Department of Pharmacology, Shanxi Medical University, Taiyuan, China, <sup>2</sup>Department of Endocrinology, First Hospital of Shanxi Medical University, Shanxi Medical University, Taiyuan, China

## OPEN ACCESS

### Edited by:

Yanqing Liu,  
Columbia University, United States

### Reviewed by:

Yili Chen,  
Sun Yat-sen University, China  
Yixuan Guo,  
The University of Utah, United States

### \*Correspondence:

Yunfeng Liu  
nectarliu@163.com  
Yi Zhang  
yizhang@sxmu.edu.cn  
orcid.org/0000-0003-0305-3127

<sup>†</sup>These authors have contributed  
equally to this work

### Specialty section:

This article was submitted to  
Molecular Diagnostics and  
Therapeutics,  
a section of the journal  
Frontiers in Molecular Biosciences

**Received:** 11 April 2022

**Accepted:** 23 June 2022

**Published:** 14 July 2022

### Citation:

Zhao X, Cui L, Zhang Y, Guo C,  
Deng L, Wen Z, Lu Z, Shi X, Xing H,  
Liu Y and Zhang Y (2022) Screening for  
Potential Therapeutic Agents for Non-  
Small Cell Lung Cancer by  
Targeting Ferroptosis.  
Front. Mol. Biosci. 9:917602.  
doi: 10.3389/fmolb.2022.917602

Ferroptosis is a form of non-apoptotic and iron-dependent cell death originally identified in cancer cells. Recently, emerging evidence showed that ferroptosis-targeting therapy could be a novel promising anti-tumour treatment. However, systematic analyses of ferroptosis-related genes for the prognosis of non-small cell lung cancer (NSCLC) and the development of antitumor drugs exploiting the ferroptosis process remain rare. This study aimed to identify genes related to ferroptosis and NSCLC and to initially screen lead compounds that induce ferroptosis in tumor cells. We downloaded mRNA expression profiles and NSCLC clinical data from The Cancer Genome Atlas database to explore the prognostic role of ferroptosis-related genes. Four prognosis-associated ferroptosis-related genes were screened using univariate Cox regression analysis and the lasso Cox regression analysis, which could divide patients with NSCLC into high- and low-risk groups. Then, based on differentially expressed risk- and ferroptosis-related genes, the negatively correlated lead compound flufenamic acid (FFA) was screened through the Connective Map database. This project confirmed that FFA induced ferroptosis in A549 cells and inhibited growth and migration in a dose-dependent manner through CCK-8, scratch, and immunofluorescence assays. In conclusion, targeting ferroptosis might be a therapeutic alternative for NSCLC.

**Keywords:** ferroptosis, prognostic, non-small cell lung cancer, CMap database, antitumor drug

## INTRODUCTION

Lung cancer is one of the most common malignant tumors in China and the world. Non-small cell lung cancer (NSCLC) accounts for 85% of all lung cancers and is the main cause of cancer-related deaths worldwide (Liu et al., 2017). NSCLC, including adenocarcinoma, squamous cell carcinoma, and large cell carcinoma, is a heterogeneous group of diseases that is frequently diagnosed at advanced or metastatic stages (Best and Sutherland, 2018; La Montagna et al., 2020). It is well known that various prognostic factors based on clinical and pathological characteristics determine the

**Abbreviations:** AUC, area under the curve; BMSCs, bone marrow stromal cells; CCK-8, cell counting kit-8; COX-2, cyclooxygenase-2; CMap database, connective map database; DEGs, differentially expressed genes; ESCC, esophageal squamous cell carcinoma; FFA, flufenamic acid; Fer-1, Ferrostatin-1; GPX4, glutathione peroxidase 4; GSH, Glutathione; HR, hazard ratio; NC, negative control group; NGS, next-generation sequencing technology; NSCLC, non-small cell lung cancer; ROC, receiver operating characteristic; R&D, research and development; ROS, reactive oxygen species; TCGA, the cancer genome atlas.

overall prognosis of patients, and the most important prognostic factors remain the stage and presentation of the disease at the time of diagnosis (Gadgeel and Thakur, 2016). The lack of obvious symptoms in the early stages of disease progression and late diagnosis might explain the observed poor prognosis (Liu et al., 2017). Han K and Wang Y et al. demonstrated that ferroptosis-related genes are closely associated with the prognosis of NSCLC patients, which will allow for the effective treatment of patients (Han et al., 2021; Wang et al., 2022).

Ferroptosis is an iron-dependent, non-apoptotic mode of programmed cell death that is driven by the lethal accumulation of lipid peroxides (Liang et al., 2020; Li Y. et al., 2020). Previous studies have reported that ferroptosis plays a vital role in NSCLC, and certain genes, such as SLC7A11 (Ji et al., 2018; Kang et al., 2019) and GPX4 (Lai et al., 2019), are known to negatively regulate ferroptosis; moreover, NFS1, a ferroptosis-related gene, is most highly expressed in well-differentiated lung adenocarcinomas and protect cells from ferroptosis (Alvarez et al., 2017). The activation of ferroptosis by several small molecules and FDA-approved clinical drugs in cancer cells and the efficacy of tumor suppression with ferroptosis inducers in various experimental cancer models underline the potential of ferroptosis to be targeted as a novel anti-cancer therapy (Stockwell et al., 2017). Therefore, this study intended to screen out new lead compounds for the treatment of NSCLC based on the induction of ferroptosis in NSCLC cells using bioinformatics theory.

In this study, we used mRNA expression data from NSCLC patients in The Cancer Genome Atlas (TCGA) database to construct a prognostic multigene signature with ferroptosis-related differentially expressed genes (DEGs). These ferroptosis-related risk signatures could independently and effectively classify patients with NSCLC with a high risk of unfavorable outcomes. Finally, we preliminarily screened and proved that the lead compound, flufenamic acid, could induce ferroptosis with anticancer effects by using biological experiments and bioinformatics analysis. These results provide a new strategy for the treatment of NSCLC, help to reveal the association between ferroptosis-related genes and patient prognosis, and also offer basic research data for targeting ferroptosis in the treatment of NSCLC.

## Materials and Methods

### Reagents

The Cell Counting Kit-8 (CCK-8, C0005) and flufenamic acid (FFA, T0858) were purchased from Taoshu Biotechnology Co., Ltd. Ferrostatin-1 (Fer-1, HY-100579) was purchased from MedChemExpress Company. Rabbit anti-human glutathione peroxidase 4 (GPX4, A1933) monoclonal antibody was received from ABclonal Technology Co., Ltd. The Goat Anti-Rabbit IgG H&L/FITC antibody (bs-0295G-FITC) was acquired from Beijing Boasens Biotechnology Co., Ltd. Glutathione (GSH, A126-1-1) detection kits was purchased from Nanjing Jiancheng Bioengineering Institute.

### Downloading mRNA Expression Profiles and Clinical Information

The RNA sequencing data of HTSeq-FPKM and relevant clinical information from the NSCLC cohort were downloaded from

TCGA database (<https://portal.gdc.cancer.gov/repository>). RNA-seq data and clinical information from 228 tumor samples were obtained from the GEO database (GSE 37745, GSE102287, <https://www.ncbi.nlm.nih.gov/geo>).

### Extraction of Ferroptosis-Related Genes From TCGA and GEO Databases

60 ferroptosis-related genes were retrieved from previous literature (Stockwell et al., 2017; Bersuker et al., 2019; Hassannia et al., 2019) and are provided in **Supplementary Table S1**. The R package “limma” and “sva” were used to extract mRNA expression levels of ferroptosis-related genes in TCGA and GEO databases.

### Identification of Differentially Expressed Ferroptosis-Related Genes in the TCGA Cohort

DEGs related to ferroptosis were screened using the R package “limma” (Ritchie et al., 2015). The expression of candidate ferroptosis-related genes in the TCGA cohort was used to identify the DEGs between tumor tissues and adjacent nontumorous tissues. The screening criteria were set as a  $p$ -value < 0.05 and false discovery rate (FDR) < 0.05.

### Identification of Prognosis-Associated Ferroptosis-Related Genes in TCGA Cohort

Univariate Cox analysis regression was performed to evaluate the association between DGEs and patient survival time in TCGA cohort using the R package “survival”, and to obtain the corresponding  $p$ -value and hazard ratio (HR) for each differential gene. When the  $p$ -value was <0.05, it was considered that the ferroptosis-related gene was connected with patient prognosis. The higher the HR, the higher the risk of the disease.

### Construction of a Multigene Signature by Lasso Cox Regression Analysis

The R package “glmnet” was used to perform lasso regression analysis. The candidate ferroptosis-related genes were subjected to univariate Cox linear regression analysis using the R package “survival”. The candidate ferroptosis-related gene was taken as the included signature variable, and the variables were added or deleted until the optimum multigene signature to evaluate the overall survival (OS) outcome was found. The formula for the risk score was as follows: risk score = the sum of each coefficient of mRNA multiple for the expression of each mRNA.

### Survival Analysis Based on the Stratification of Low- and High-Risk Scores

Patients were divided into high and low-risk groups based on the median risk score of TCGA cohort. The R package “survival” and “survminer” was used to perform Kaplan–Meier survival analysis and log-rank tests, which were used to evaluate the OS difference between high- and low-risk groups. A  $p$ -value of the log-rank test was less than 0.05 indicated a statistically significant difference in survival between the two groups. To validate the survival analysis of TCGA cohort, the Kaplan–Meier method was performed on

the GEO cohort to evaluate the OS difference between high- and low-risk groups.

### Validation of Risk Score by Univariate and Multivariate Cox Analyses

The patient risk scores and clinicopathological characteristics such as age, sex, tumor stage, and grade were taken as variables, and the corresponding survival status was taken as dependent variables. Univariate and multivariate Cox regression analyses were conducted to obtain the risk ratio HR and seek factors that could independently be used to evaluate a patient's risk of developing the disease. A factor was used as an independent risk factor when the  $p$ -value was  $<0.05$ .

### Validation of Risk Score by Generating Receiver Operating Characteristic Curve

The R package “survivalROC” was used to generate a receiver operating characteristic curve (ROC curve), which was used to evaluate the specificity and sensitivity of the risk score for patient survival prediction and the diagnostic score for the prediction of patient diagnosis. The robustness of the risk score was evaluated by comparing the area under the curve (AUC) of the ROC curves for different factors.

### Preliminary Screening of Therapeutic Drugs for NSCLC Using the Connective Map Database

The differential genes related to ferroptosis and those of high- and low-risk patients were entered into the CMap (<https://clue.io/query>) database in Grp form. With this comparison, related small molecule compounds or drugs were obtained. Taking  $p < 0.05$  and enrichment  $<0$  as the screening conditions, the potential small molecule lead compounds for the treatment of NSCLC were screened after the intersection of the two groups of screened drugs.

### Assessment of Cell Migration and Activity

A549 cells were routinely cultured with 1,640 medium containing 10% fetal bovine serum, digested and passaged, inoculated into a 6-well plate according to  $5 \times 10^6$  cells/well, or inoculated into a 96-well plate with  $1 \times 10^4$  cells/well. The cells were cultured in a 5% carbon dioxide incubator for 24 h. After 24 h of drug treatment, the activity in each group of cells was detected using a CCK-8 kit. The cells were incubated in a 96-well plate, 10  $\mu$ L of CCK-8 solution was added to each well, and the culture was continued at 37°C for 4 h. Absorbance was measured at 450 nm. The formula to calculate cell viability was as follows: cell viability (%) =  $[A(\text{treatment}) - A(\text{blank})] / [A(\text{control}) - A(\text{blank})]$ . The cell wound healing assay was performed according to Li's research (Li Z.-Y. et al., 2020).

### Detection of Cellular GSH and GPX4 Levels

A549 cells were divided into a negative control group (NC), FFA-treated group (FFA), and ferrostatin-1 (Fer-1) and combined treatment groups (Fer-1+FFA). After 24 h of drug treatment, the CCK-8 kit was utilized as described. GSH detection kits was used to evaluate the contents of GSH in the cells of each group. The operation steps were performed according to the instructions.

Immunofluorescence staining was performed according to Yang's instructions (Yang et al., 2019). The primary antibody was a rabbit anti-human GPX4 monoclonal antibody, dilution 1:200.

### Statistical Methods

Spss26.0, Prism 8.0, Image J, SigmaPlot 14, and R software were used for statistical analysis of results (Student's  $t$ -test or one-way ANOVA tests). Data were presented as mean  $\pm$  standard error of the mean. The Kaplan-Meier method and log-rank tests were used to evaluate the predictive power of the prognostic model. Univariate Cox regression and multivariate Cox regression were used to identify whether the model could be used as an independent prognostic factor.  $p < 0.05$  was considered statistically significant.

## RESULTS

### Profile of the NSCLC Dataset From TCGA and GEO

In this study, 551 cases were obtained from TCGA database, including 54 normal datasets and 497 tumor datasets. A total of 316 cases with clinical characteristics met the inclusion criteria by removing cases with survival periods of less than 30 days with incomplete clinical information. We downloaded a total of 228 cases from the GEO database, including 161 cases with researchable clinical information. The detailed clinical characteristics of these patients, such as age, gender, survival time, and survival status, are summarized in **Table 1**.

### Identification of Differentially Expressed Ferroptosis-Related Genes in TCGA Cohort

Sixty ferroptosis-related genes were extracted from TCGA cohort. A nonparametric rank-sum test was performed on 497 patients with tumor tissues and 54 patients with normal lung tissues, and a total of 43 ferroptosis-related genes met the screening criteria of  $p$ -value  $< 0.05$  and FDR  $< 0.05$ , including 29 upregulated and 14 downregulated ferroptosis-related genes. These genes were clustered and presented as heatmaps. A heatmap of these differentially expressed ferroptosis-related genes is shown in **Figure 1**.

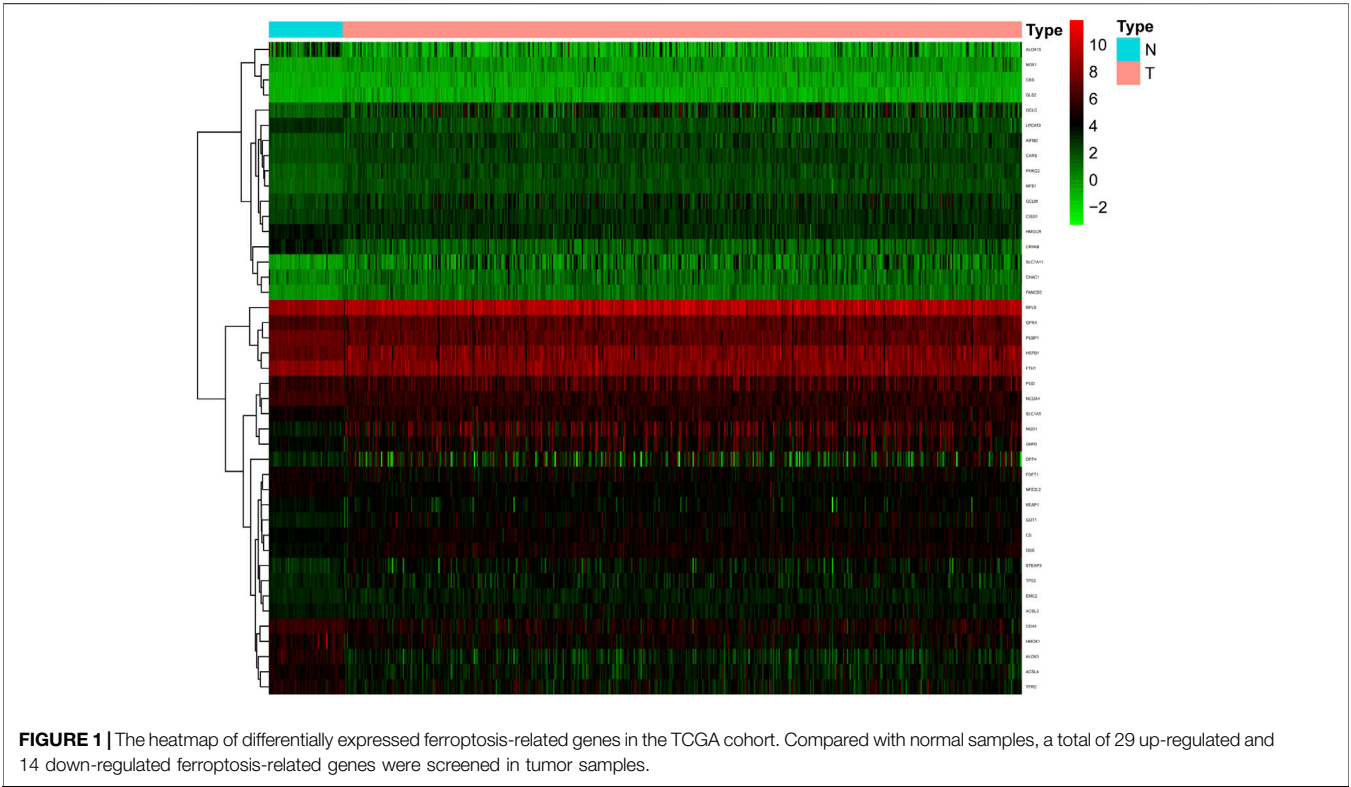
### Identification of Prognostic Ferroptosis-Related DEGs in TCGA Cohort

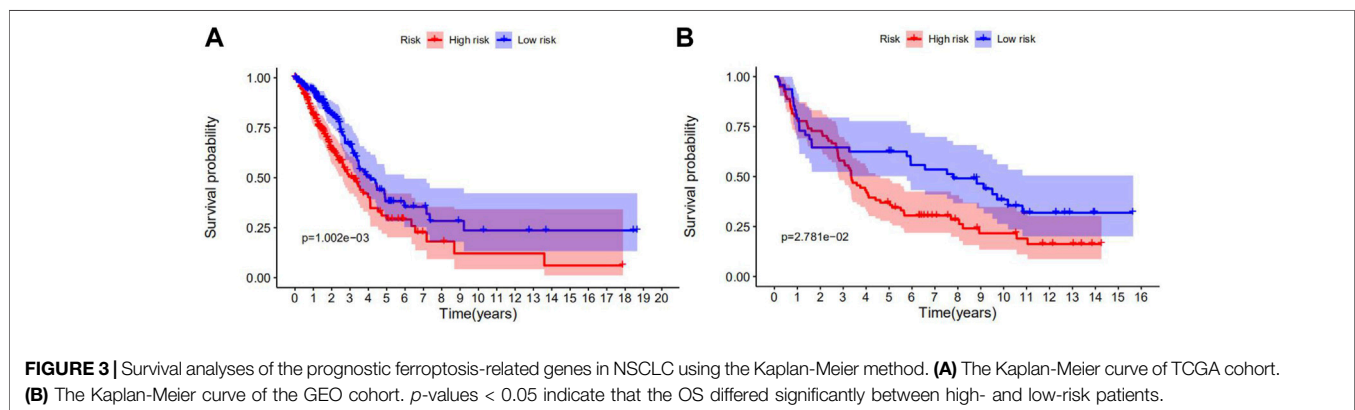
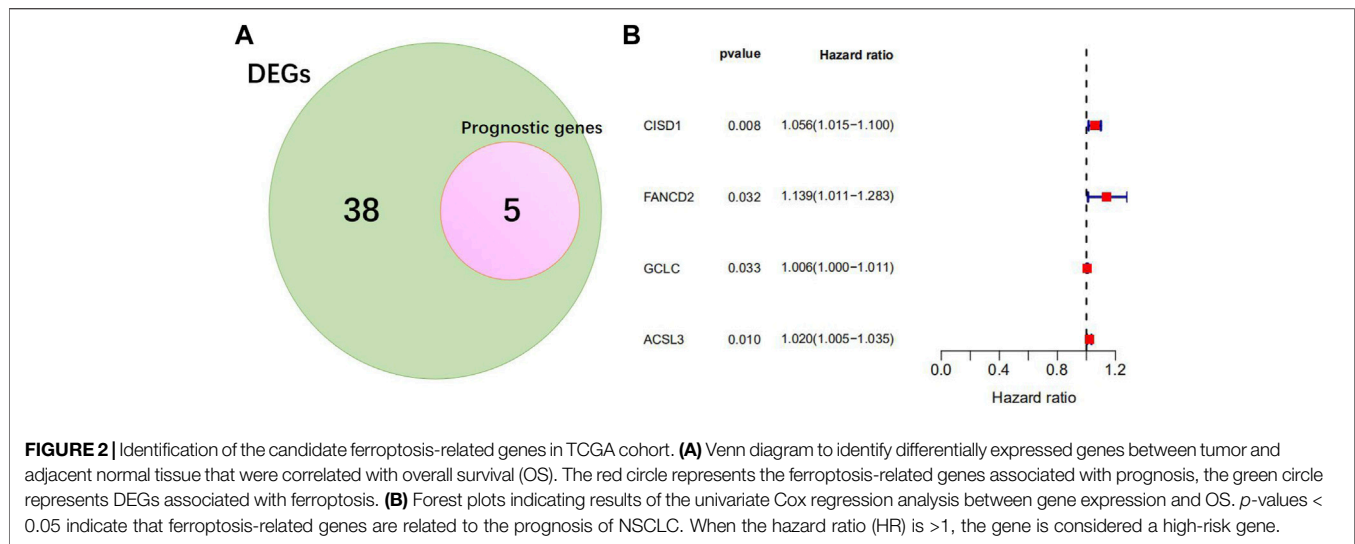
In view of the above differentially expressed ferroptosis-related genes, combined with the clinical information on survival status and OS days patients in the TCGA cohort, five ferroptosis-related genes related to the prognosis of NSCLC were preliminarily screened using univariate Cox analysis (**Figure 2A**). Irrationally, *PHKG2* was excluded from further studies, as its expression in univariate Cox regression analysis predicted it to be a low-risk gene with an excellent prognosis. Four prognostic ferroptosis-related DEGs were identified as key genes using lasso regression analysis and preserved (**Figure 2B**).



**TABLE 1 |** Clinical characteristics of the NSCLC patients used in this study.

Variables	TCGA cohort (n = 316)	GEO cohort (n = 161)
Age, n (%)		
<65 years	137 (43.35)	88 (54.66)
≥65 years	179 (56.65)	73 (45.34)
Gender, n (%)		
Female	163 (51.58)	88 (54.66)
Male	153 (48.42)	73 (45.34)
Overall survival days, (25%-75%)	596.00 (362.00–947.75)	1366.00 (451.00–2877.00)
Survival status, n (%)		
Alive	203 (64.24)	51 (31.68)
Dead	113 (35.76)	110 (68.32)
Stage, n (%)		
Stage I	164 (51.90)	106 (65.84)
Stage II	76 (24.05)	29 (18.01)
Stage III	56 (17.72)	22 (13.66)
Stage IV	20 (6.33)	4 (2.49)
T, n (%)		
T1	97 (30.70)	NA
T2	178 (56.33)	
T3	24 (7.59)	
T4	17 (5.38)	
M, n (%)		
M0	296 (93.67)	NA
M1	20 (6.33)	
N, n (%)		
N0	200 (63.29)	NA
N1	67 (21.20)	
N2	48 (15.20)	
N3	1 (0.31)	





## Construction of a Risk Score in TCGA Cohort

Based on the four ferroptosis-related genes identified using lasso regression analysis, the prognostic risk score of each patient was calculated using the risk score expression described above. The risk score =  $0.0415124361172914 \times \text{expression of } CISD1 + 0.0643218824479954 \times \text{expression of } FANCD2 + 0.0018714013929312 \times \text{expression of } GCLC + 0.0139528364527794 \times \text{expression of } ACSL3$ . All patients were divided into high-risk and low-risk groups according to the median risk score of TCGA cohort.

## Validation of Survival Analysis of TCGA Cohort by Utilizing Data From the GEO Cohort

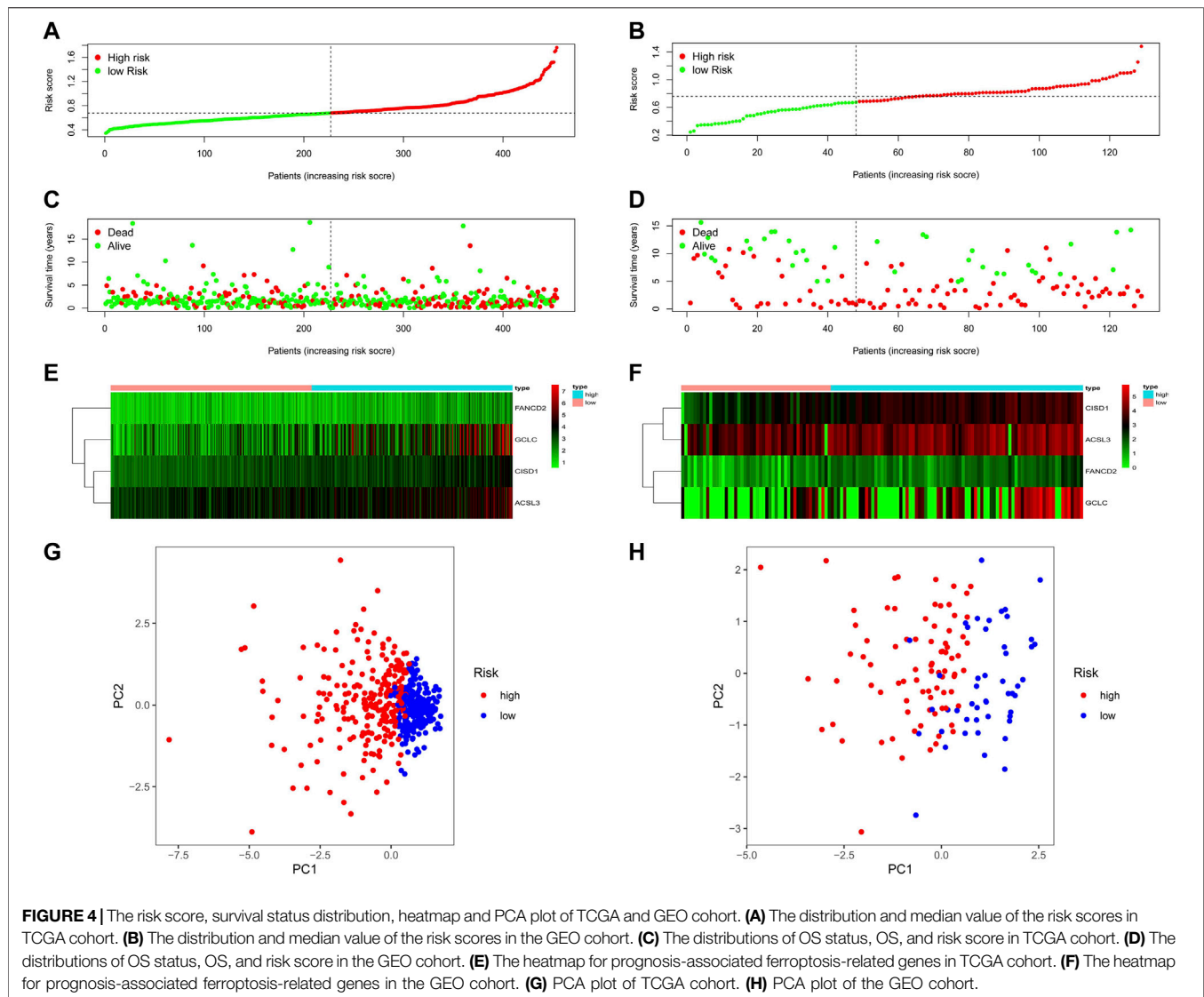
Kaplan-Meier survival analysis showed that the OS of the low-risk group was higher than that of the high-risk group in both TCGA (Figure 3A) and GEO cohorts (Figure 3B). *p*-values < 0.05 indicate that the difference in OS curves between high-risk and low-risk groups is considered statistically significant.

## Validation of Risk Score, Survival Status Distribution, and Heatmap of TCGA Cohort Utilizing Data From the GEO Cohort

The patients were separated into high- or low-risk groups based on the median cut-off value (Figures 4A,B). In both TCGA and GEO cohorts, the risk score increased from left to right. The distribution of the survival status demonstrated that the number of deaths increased gradually with the increase in risk value. High-risk patients displayed shorter OS days and a higher probability of early death compared to low-risk patients (Figures 4C,D). Further, the heat maps clearly indicated that the expression of *CISD1*, *FANCD2*, *GCLC*, and *ACSL3* were added in the wake of the increase in risk value in both TCGA and GEO cohorts (Figures 4E,F). Based on the expression of this four potential risk genes, we classified patients with NSCLC into high- and low-risk groups. PCA analysis clearly indicated that patients in different risk groups were distributed in two directions (Figures 4G,H).

## Univariate and Multivariate Cox Analysis

Univariate and multivariate Cox regression analyses were used to examine whether the predicted risk incidence of the risk score was



independent of clinical data in both TCGA and GEO cohorts. The risk score was significantly correlated with OS in both TCGA and GEO cohorts in univariate Cox regression analyses (HR = 2.918,  $p < 0.001$ ; HR = 2.632,  $p = 0.040$ , respectively). Surprisingly, in TCGA cohort, stage is considered interrelated to OS, but cannot be verified in the GEO cohort (Figures 5A,B). The risk of poor survival outcomes increased with an increase in the risk score. After adjusting for other intricate factors, multivariate Cox regression analysis demonstrated that the risk score remained an independent predictor of OS in NSCLC patients (HR = 2.407,  $p = 0.009$ ; HR = 3.900,  $p = 0.005$ , respectively, Figures 5C,D.)

## Receiver Operating Characteristic Curve Analysis

Receiver operating characteristic (ROC) analysis, which is a method combining sensitivity and specificity, was performed to comprehensively evaluate the multivariate Cox regression analysis for long-term survival prediction (7 years). The area under the curve

(AUC) of the risk score in TCGA cohorts was 0.611 (Figure 6A) and the area under the curve (AUC) of the risk score in GEO cohorts was 0.651 (Figure 6B), making it clear that the predictive model possessed powerful prognostic capability in forecasting overall survival.

## Screening Potential Therapeutic Agents to Induce Ferroptosis in High-Risk Groups Using the CMap Database

Based on the query results of the CMap database, the partial potential lead compounds for the treatment of high-risk NSCLC patients are listed in Figure 7A, and the partial potential lead compounds that might trigger ferroptosis in NSCLC are listed in Figure 7B. After the intersection of the two groups of screened drugs, we believed the small molecule compound, FFA, was a therapeutic agent to induce ferroptosis in NSCLC. Previous studies have found that FFA exerts antitumor effects (Matsumoto et al., 2016; Li Z.-Y. et al., 2020), suggesting that our screening strategy and results possess preferable credibility.

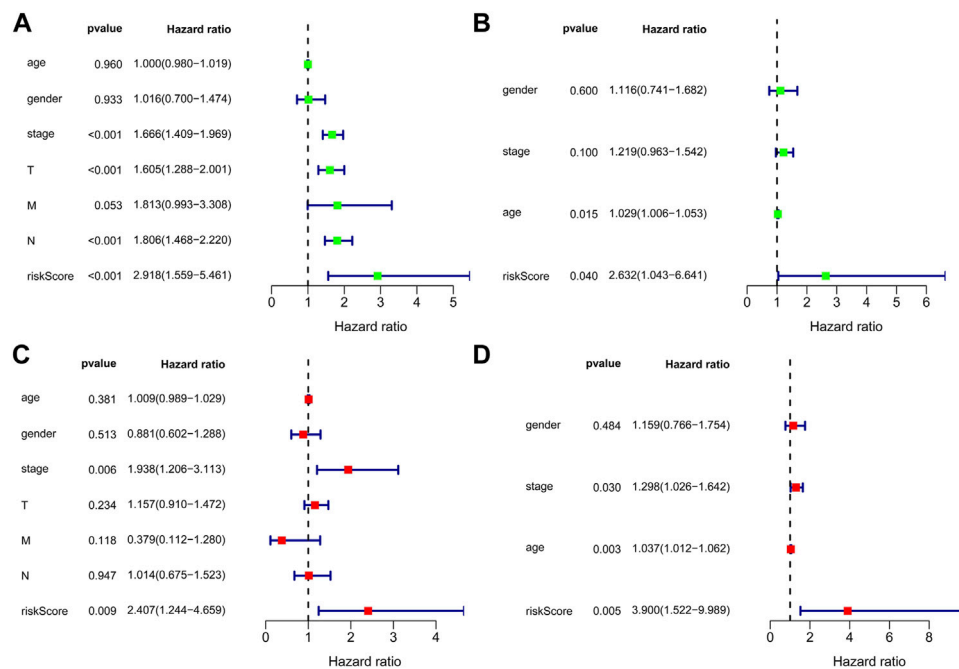


**FIGURE 5 |** Forest plot of the univariate and multivariate Cox regression analyses in NSCLC. Forest plot of the univariate Cox regression analysis of TCGA cohort (A) and GEO cohort (B). Forest plot of the multivariate Cox regression analysis of TCGA cohort (C) and GEO cohort (D).

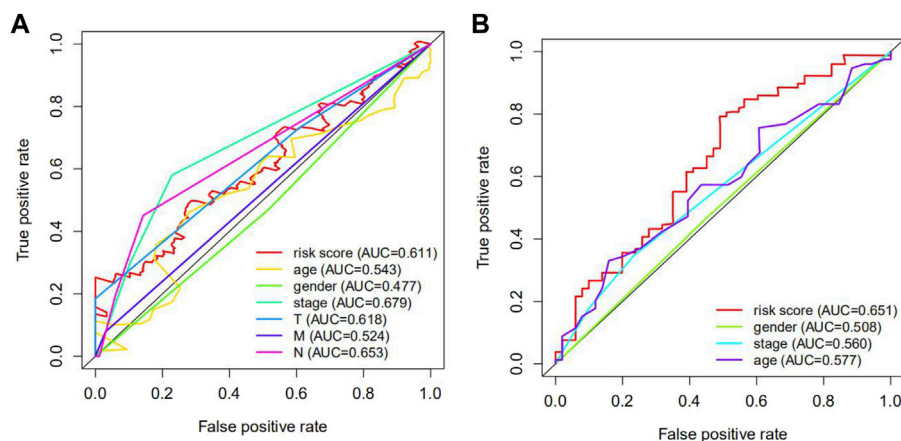


**FIGURE 6 |** The receiver operating characteristic (ROC) curve of TCGA and GEO cohorts. (A) the ROC curve of TCGA cohorts. (B) the ROC curve of GEO cohorts. The AUC of the ROC curve was more than 0.5, which signified that the predictive model possessed extraordinary diagnosis and prediction values.

## FFA Decreases the Viability and Migration of A549 Cells

After exposing cells to different concentrations of FFA (50, 100, 150, 200  $\mu\text{mol/L}$ ) for 24 h, as shown in **Figure 8A**, cell viability was reduced with an increase in the FFA concentration. Cell migration into the wound was measured according to the distance between the wound edges before and after FFA treatment. We found that FFA significantly impaired cell migration into the wound (**Figures 8B,C**). As shown in **Figures 8A,D,E**, low doses

of FFA (50 and 100  $\mu\text{mol/L}$ ) had a negligible effect on the growth of normal lung cells (BEAS-2B).

## FFA Partially Induces Ferroptosis in A549 Cells by Repressing the GSH-dependent GPX4 Signaling Pathway

It is well known that the GSH depletion caused by cysteine deficiency directly inactivates glutathione peroxidase 4 (GPX4)



A				B			
number	cmap name	enrichment	p-value	number	cmap name	enrichment	p-value
1	phenoxybenzamine	-0.964	0	1	sirolimus	-0.44	0
2	medrysone	-0.883	0	2	mepyramine	-0.91	0.0001
3	trichostatin A	-0.19	0	3	practolol	-0.856	0.00078
4	apigenin	-0.929	0.00002	4	metacycline	-0.832	0.00145
5	0175029-0000	-0.83	0.00006	5	ethotoin	-0.698	0.00179
6	phthalylsulfathiazole	-0.805	0.00064	6	wortmannin	-0.422	0.00241
7	alsterpaullone	-0.923	0.00076	7	doxylamine	-0.726	0.00328
8	camptothecin	-0.902	0.0018	8	Prestwick-689	-0.775	0.00527
9	daunorubicin	-0.821	0.00193	9	vigabatrin	-0.847	0.00717
10	levonorgestrel	-0.693	0.00201	10	anisomycin	-0.749	0.00794
11	GW-8510	-0.804	0.00282	11	lycorine	-0.674	0.00867
12	thioguanosine	-0.801	0.00306	12	sulfathiazole	-0.672	0.00887
13	cycloserine	-0.799	0.00318	13	nicergoline	-0.671	0.00891
14	pyrvinium	-0.674	0.00326	14	sulfadoxine	-0.832	0.00953
15	flufenamic acid	-0.556	0.02894	15	flufenamic acid	-0.542	0.03653

**FIGURE 7 |** Partial analysis results from CMap database. **(A)** Prediction results from cMap for the differential gene profiles of high- and low-risk groups. **(B)** Prediction results from cMap for the differential gene profiles of DEGs related to ferroptosis.

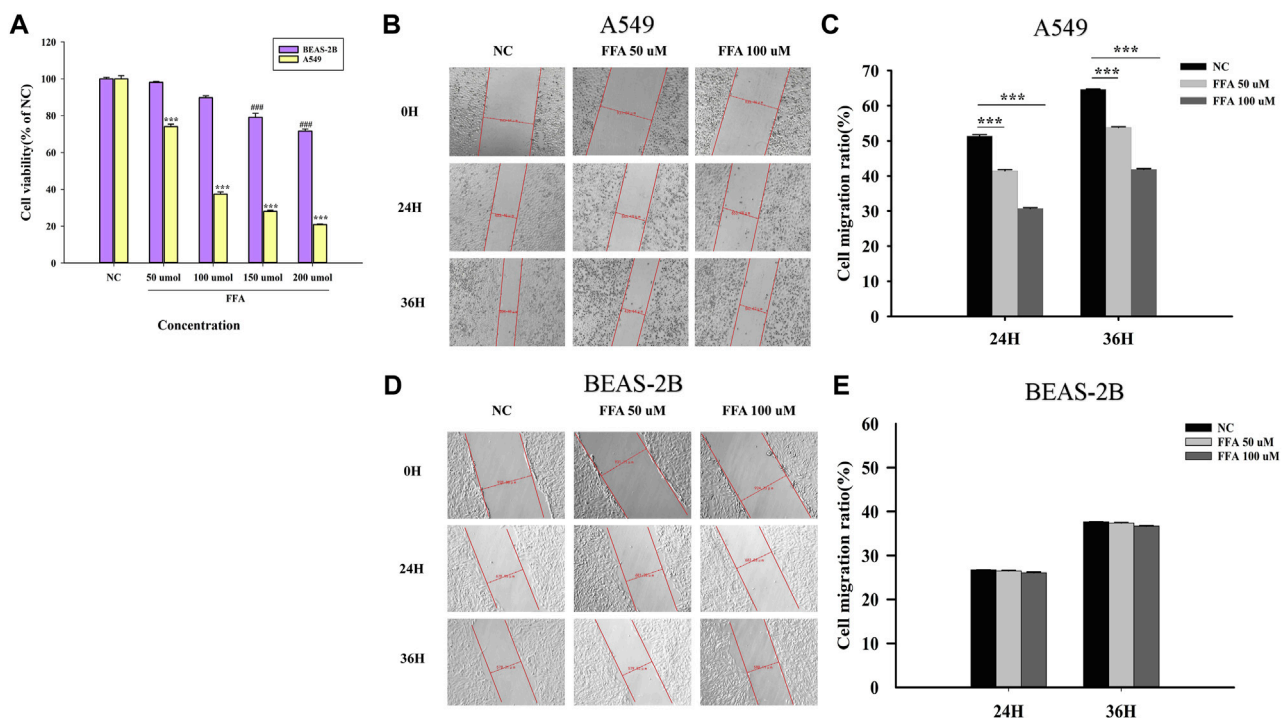


**FIGURE 8 |** Flufenamic acid inhibits cell viability and migration in A549 cells. **(A)** Effects of different concentrations of flufenamic acid on the cellular activity in A549 cells and BEAS-2B cells ( $n = 5$ ). \*\*\* $p < 0.001$  vs. NC of A549 cells. ### $p < 0.001$  vs. NC of BEAS-2B cells. **(B)** The scratch healing of A549 cells in different time periods. The scale bar is 50  $\mu$ m. **(C)** Statistical chart of cell migration ratio in A549 cells ( $n = 3$ ). \*\*\* $p < 0.001$  vs. NC. **(D)** The scratch healing of BEAS-2B cells in different time periods. The scale bar is 50  $\mu$ m. **(E)** Statistical chart of cell migration ratio in BEAS-2B cells ( $n = 3$ ). NC, negative control group.

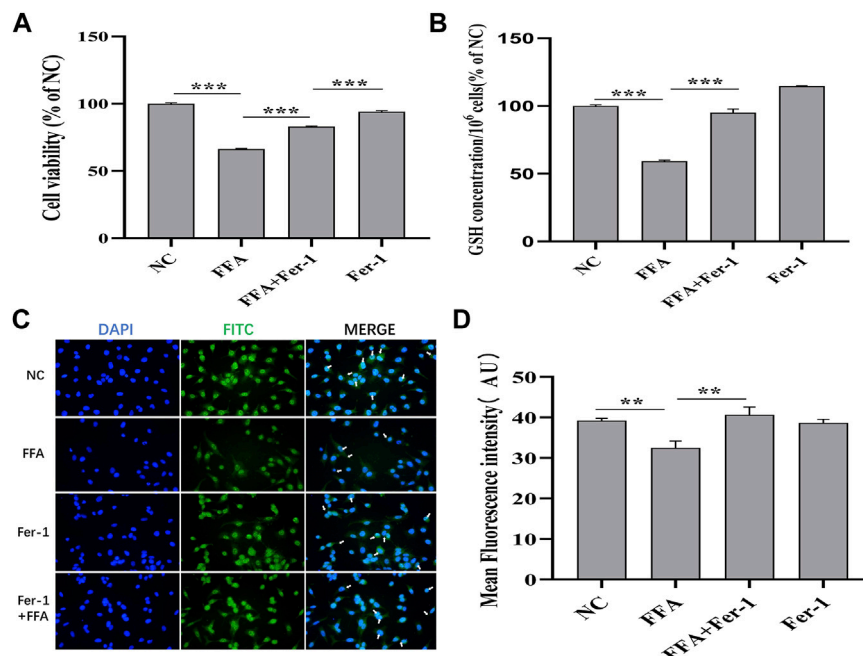


**FIGURE 9** | Flufenamic acid(FFA) partially induces ferroptosis in A549 cells by repressing GSH-dependent GPX4 signaling pathway. **(A)** Effect of Ferrostatin-1(Fer-1) on flufenamic acid-restrained cellular activity in A549 cells ( $n = 5$ ). **(B)** Fer-1 reverses the reduced levels of GSH by FFA in A549 cells ( $n = 3$ ). **(C)** Observation of GPX4 immunofluorescence staining in each group ( $\times 400$ ). **(D)** Statistical diagram of the average fluorescence intensity of cells in each group ( $n = 6$ ). NC, negative control group. \*\* $p < 0.01$  and \*\*\* $p < 0.001$ .

and leads to subsequent ferroptosis (He et al., 2022). Our results showed that FFA remarkably reduced the expression of GSH and GPX4 in A549 cells, whereas Fer-1, an inhibitor of ferroptosis, significantly reversed this trend (Figures 9B–D). The A549 cell activity reduced by FFA could not completely reversed by Fer-1, indicating that the antitumor effect of FFA was not only mediated by ferroptosis (Figure 9A). Therefore, we concluded that FFA partially induced ferroptosis in NSCLC cells by repressing GSH-dependent GPX4 signaling.

## DISCUSSION

### Ferroptosis-Related Genes Could Be Used as Prognostic Markers of NSCLC

Lung cancer is one of the most common malignancies and accounts for nearly one quarter of cancer deaths worldwide (Siegel et al., 2021). The most representative histological type of lung cancer is NSCLC, which is generally diagnosed at an advanced stage owing to finite symptoms at the early stage and the restriction of proteome biomarkers (Wu et al., 2021). Patients with lung cancer generally experience tumor recurrence and metastasis, leading to a comparatively poor OS rate (Zhou et al., 2020). Therefore, there is an urgent need to conduct more in-depth research on the identification of novel diagnostic or prognostic markers and potential drug targets to promote prognosis and personalized treatment. With the innovative development of gene chips and next-generation sequencing technology (NGS), gene signatures based on

abnormal mRNA have shown the ability to predict the OS outcomes for malignant tumors (Njoku et al., 2020; Tan et al., 2020). Utilizing genomics and/or transcriptome analysis of neoplasm biopsy samples to infer disease severity is relatively fast and inexpensive. Doctors can use NGS to analyze multiple genes associated with an increased cancer risk at one time (Judkins et al., 2015; Fazio et al., 2020). According to NGS, doctors can accurately obtain the genetic variation information of patients, select potential targeted drugs for patients, evaluate the prognosis of patients, design drug-resistance treatment regimens, and realize individualized treatment (Van Allen et al., 2014; Hagemann et al., 2015; Forschner et al., 2021; Grobbel et al., 2021). In recent years, ferroptosis has attracted much attention because it plays a significant role in the occurrence, development, and multidrug resistance of tumors (Liang et al., 2019; Xia et al., 2019). Convincing evidence suggests that ferroptosis can inhibit tumorigenesis (Mou et al., 2019). Moreover, the genes associated with ferroptosis can be used as candidate biomarkers for tumor therapy (Zhuo et al., 2020). Hence, based on RNA sequencing data from TCGA and GEO, we evaluated the relationship between the expression profile of ferroptosis-related genes and the prognosis of patients with NSCLC. In this study, more than two-thirds of ferroptosis-related genes were differentially expressed between tumor and adjacent normal tissues, indicating that there is an association between ferroptosis and NSCLC. Four prognosis-associated ferroptosis-related genes (*FANCD2*, *ACSL3*, *GCLC*, and *CISD1*) were identified using univariate Cox regression analysis and a lasso Cox regression analysis. Our study

indicated that the OS outcome was worse for patients with high risk score ( $p < 0.05$ ) in Kaplan-Meier analysis. Analyses such as survival status distribution and PCA showed that the prognostic multigene signature notably divided high- and low-risk patients into two categories. In brief, a prognostic multigene signature could not only be used for risk assessment and the identification of high-risk patients but also to ameliorate nursing care by changing treatment schemes (Judkins et al., 2015), promote individualized treatment, and improve cancer treatment efficiency.

## Prognosis-Associated Ferroptosis-Related Genes Provide Opportunities for Neoplastic Therapeutic Approaches

These four prognosis-associated ferroptosis-related genes were up-regulated in NSCLC cancerous tissues and associated with poor prognosis, which are also different from the findings of Han et al. (Lai et al., 2019). Our results further broadened the prognosis-associated ferroptosis-related gene signatures for NSCLC. *FANCD2* overexpression increases the risk of metastasis in esophageal squamous cell carcinoma (ESCC) by activating DNA replication and regulating cell cycle progression, which is associated with the negative prognosis of ESCC (Lei et al., 2020). Bone marrow stromal cells (BMSCs) lacking *FANCD2* exhibit iron overload and lipid peroxidation with erastin (inducing ferroptosis to selectively kill NSCLC cells) (Song et al., 2016; Gai et al., 2020). Monounsaturated fatty acids activated by *ACSL3* can protect cells against ferroptosis (Magtanong et al., 2019). High levels of *ACSL3* are frequently positively associated with poor clinical outcomes in patients with advanced NSCLC (Fernández et al., 2020). High mRNA expression of *GCLC* in tumor tissue significantly shortens the postoperative recurrence survival period of patients, and potentially can predict cisplatin resistance in patients with lung adenocarcinoma (Hiyama et al., 2018). *GCLC* promotes the ferroptosis-resistant state of NSCLC cells by preserving the glutamate balance (Kang et al., 2021). *CISD1*, also known as mitoNEET, is instrumental for the proliferation, migration, and invasion of tumor cells and accelerates the occurrence of malignant tumors (Mittler et al., 2019). Genetic inhibition of *CISD1* induces iron-mediated lipid peroxidation in the mitochondria, which intensifies the strength of erastin-induced ferroptosis (Yuan et al., 2016). Unfortunately, whether *CISD1* has a marked effect on the prognosis of malignant tumors has not been reported. Based on these results, we speculated whether the high-risk ferroptosis-related genes could be genetically suppressed to induce NSCLC cell death. We went a step further by investigating the lead compound with potential therapeutic effects in NSCLC.

## FFA Suppresses Tumor Development by Partially Inducing Ferroptosis in NSCLC Cells

At present, the research and development (R&D) costs of new molecular entity drugs have increased significantly, and the R&D

cycle appears to be lengthy (Yildirim et al., 2016). Drug repurposing, that is, a novel drug development strategy to discover new drug indications based on drugs already on the market or in the clinical research stage, can mitigate a variety of costs including time, manpower, and material resources (Parvathaneni et al., 2019). Application of the CMap database can reveal drug-gene associations and identify possible therapeutic effects of compounds (Shi et al., 2016; Li H. et al., 2020). Based on gene chip technology and the CMap database for drug repositioning, we identified the potential candidate lead compound FFA to induce ferroptosis in NSCLC cells and cure this disease. We then used biological techniques to investigate whether FFA plays an important role in inhibiting the growth and metastasis of NSCLC. As expected, the results of CCK-8 and scratch experiments found that FFA dramatically induced cell death and suppressed proliferation in A549 cells. The small-molecule lead compound FFA is thus expected to be an effective drug for the treatment of NSCLC.

Ferroptosis is a novel mode of regulated cell death mediated by the iron-dependent accumulation of lipid peroxides and lipid reactive oxygen species (ROS). Tumor suppression can be mediated by iron inducers in various experimental cancer models, underscoring the potential of ferroptosis inducers as a new anticancer therapy (Hassannia et al., 2019; Yu et al., 2019; Badgley et al., 2020; Liao et al., 2020). Regulation of the classic ferroptosis-repressed GSH-dependent GPX4 signaling pathway is the dominating mechanism for causing ferroptosis in NSCLC (Shui et al., 2021; Zou et al., 2021). GSH was suggested to be a pivotal factor in maintaining GPX4 activity (Yan et al., 2021). The function of GPX4 is to prevent cells from amassing lipid hydroperoxides and avoid cellular ferroptosis. Studies clearly show that the inhibitor of GPX4 induces ferroptosis in not only cultured cancer cells but also tumor xenografts implanted in mice (Pu et al., 2020; Wang et al., 2020). *In vitro* experiments have shown that ferroptosis can be detected via multifarious methods involving the measurement of cell activity, GPX4, GSH, malondialdehyde, and ROS levels (Hu et al., 2020; Pu et al., 2020; Huang et al., 2022). Our study found that FFA decreased the levels of GSH and GPX4 in A549 cells, which was reversed by Fer-1, confirming that FFA caused ferroptosis in NSCLC cells. However, the A549 cell activity reduced by FFA could not completely reversed by Fer-1, suggesting that FFA suppresses tumor development partially by ferroptosis pathway in NSCLC cells.

Tumor-associated inflammation appears to be a new hallmark of cancer therapy (Li Z.-Y. et al., 2020). It has been widely noticed that FFA is an inhibitor of cyclooxygenase-2 (COX-2) (Pal et al., 2021). COX-2, an important inflammatory factor, is considered a key factor in tumorigenesis and might as a potential marker of poor prognosis in NSCLC (Castelao et al., 2003; Sandler and Dubinett, 2004; Liu et al., 2015). Inhibiting the excessive expression of COX-2 suppresses tumor growth and metastasis (Xu, 2002). Vainio H et al. also concluded that evidence for a cancer-preventive effect of COX-2 inhibitors has also been found in a variety of animal models (Vainio, 2001). Therefore, we speculated that the inhibitory effect of FFA on NSCLC may also be related to the improvement of COX-2-associated inflammation (Gridelli et al., 2002). Regrettably, the role of

COX-2 in the treatment of NSCLC with FFA was not investigated in this study. In the future, further experiments will be performed to explore the relationship between COX-2 and FFA-suppressed NSCLC growth. In conclusion, these experimental results confirm the feasibility of targeting ferroptosis for the treatment of NSCLC and further verify that our screening strategy.

## CONCLUSION

In summary, we analyzed and verified the ferroptosis-related genes for the prognosis of NSCLC, which can be used as a novel biomarker for targeting ferroptosis in the individualized treatment of NSCLC patients. Further, the potential lead compound FFA for the treatment of NSCLC were detected based on the above screening of high-risk ferroptosis-related genes. We also confirmed that FFA induced ferroptosis in A549 cells and inhibited growth and migration in a dose-dependent manner. Our findings also developed a new strategy for the antitumor drugs exploiting the ferroptosis process.

## DATA AVAILABILITY STATEMENT

The original contributions presented in the study are included in the article/**Supplementary Material**, further inquiries can be directed to the corresponding authors.

## REFERENCES

- Alvarez, S. W., Sviderskiy, V. O., Terzi, E. M., Papagiannakopoulos, T., Moreira, A. L., Adams, S., et al. (2017). NFS1 Undergoes Positive Selection in Lung Tumours and Protects Cells from Ferroptosis. *Nature* 551 (7682), 639–643. doi:10.1038/nature24637
- Badgley, M. A., Kremer, D. M., Maurer, H. C., DelGiorno, K. E., Lee, H.-J., Purohit, V., et al. (2020). Cysteine Depletion Induces Pancreatic Tumor Ferroptosis in Mice. *Science* 368 (6486), 85–89. doi:10.1126/science.aaw9872
- Bersuker, K., Hendricks, J. M., Li, Z., Magtanong, L., Ford, B., Tang, P. H., et al. (2019). The CoQ Oxidoreductase FSP1 Acts Parallel to GPX4 to Inhibit Ferroptosis. *Nature* 575 (7784), 688–692. doi:10.1038/s41586-019-1705-2
- Best, S. A., and Sutherland, K. D. (2018). "Keaping" a Lid on Lung Cancer: The Keap1-Nrf2 Pathway. *Cell Cycle* 17 (14), 1696–1707. doi:10.1080/15384101.2018.1496756
- Castelao, J. E., Bart, R. D., 3rd, DiPerna, C. A., Sievers, E. M., and Bremner, R. M. (2003). Lung Cancer and Cyclooxygenase-2. *Ann. Thorac. Surg.* 76 (4), 1327–1335. doi:10.1016/s0003-4975(03)00334-5
- Fazio, M., Ablain, J., Chuan, Y., Langenau, D. M., and Zon, L. I. (2020). Zebrafish Patient Avatars in Cancer Biology and Precision Cancer Therapy. *Nat. Rev. Cancer* 20 (5), 263–273. doi:10.1038/s41568-020-0252-3
- Fernández, L. P., Merino, M., Colmenarejo, G., Moreno-Rubio, J., Sánchez-Martínez, R., Quijada-Freire, A., et al. (2020). Metabolic Enzyme ACSL3 is a Prognostic Biomarker and Correlates with Anticancer Effectiveness of Statins in Non-Small Cell Lung Cancer. *Mol. Oncol.* 14 (12), 3135–3152. doi:10.1002/1878-0261.12816
- Forschner, A., Sinnberg, T., Mroz, G., Schroeder, C., Reinert, C. P., Gatidis, S., et al. (2021). Case Report: Combined CDK4/6 and MEK Inhibition in Refractory CDKN2A and NRAS Mutant Melanoma. *Front. Oncol.* 11, 643156. doi:10.3389/fonc.2021.643156
- Gadgeel, S., and Thakur, M. (2016). Predictive and Prognostic Biomarkers in Non-Small Cell Lung Cancer. *Semin. Respir. Crit. Care Med.* 37 (5), 760–770. doi:10.1055/s-0036-1592337

## AUTHOR CONTRIBUTIONS

XZ and LC mainly wrote and revised the manuscripts, and constructed the framework of the manuscript. YuZ and CG provided constructive opinions on the formation of the manuscript. LD, ZW, ZL, XS, and HX participated in the drawing of manuscript pictures and the investigation and sorting of documents. YL and YiZ participated in topic design, manuscript writing, manuscript editing and providing instructional support. All authors approved the final version of the article.

## FUNDING

This work was supported by NSFC (81973378, 82073909), Natural Science Basic Research Plan in Shanxi Province of China (20210302124584, 202103021223233), and Postgraduate Innovation Project in Shanxi Province of China (2021Y408). This research project was supported by FSKSC and 1331KSC.

## SUPPLEMENTARY MATERIAL

The Supplementary Material for this article can be found online at: <https://www.frontiersin.org/articles/10.3389/fmolb.2022.917602/full#supplementary-material>

- Gai, C., Liu, C., Wu, X., Yu, M., Zheng, J., Zhang, W., et al. (2020). MT1DP Loaded by Folate-Modified Liposomes Sensitizes Erastin-Induced Ferroptosis via Regulating miR-365a-3p/NRF2 axis in Non-Small Cell Lung Cancer Cells. *Cell Death Dis.* 11 (9), 751. doi:10.1038/s41419-020-02939-3
- Gridelli, C., Maione, P., Airoma, G., and Rossi, A. (2002). Selective Cyclooxygenase-2 Inhibitors and Non-Small Cell Lung Cancer. *Curr. Med. Chem.* 9 (21), 1851–1858. doi:10.2174/0929867023368863
- Grobbe, H.-P., Merker, M., Köhler, N., Andres, S., Hoffmann, H., Heyckendorf, J., et al. (2021). Design of Multidrug-Resistant Tuberculosis Treatment Regimens Based on DNA Sequencing. *Clin. Infect. Dis.* 73 (7), 1194–1202. doi:10.1093/cid/ciab359
- Hagemann, I. S., Devarakonda, S., Lockwood, C. M., Spencer, D. H., Guebert, K., Bredemeyer, A. J., et al. (2015). Clinical Next-Generation Sequencing in Patients with Non-Small Cell Lung Cancer. *Cancer* 121 (4), 631–639. doi:10.1002/cncr.29089
- Han, K., Wang, J., Qian, K., Zhao, T., Liu, X., and Zhang, Y. (2021). Construction of a Prognostic Model for Non-Small-Cell Lung Cancer Based on Ferroptosis-Related Genes. *Biosci. Rep.* 41 (5), BSR20210527. doi:10.1042/BSR20210527
- Hassannia, B., Vandenabeele, P., and Vanden Berghe, T. (2019). Targeting Ferroptosis to Iron Out Cancer. *Cancer Cell* 35 (6), 830–849. doi:10.1016/j.ccell.2019.04.002
- He, R., Liu, B., Xiong, R., Geng, B., Meng, H., Lin, W., et al. (2022). Itaconate Inhibits Ferroptosis of Macrophage via Nrf2 Pathways against Sepsis-Induced Acute Lung Injury. *Cell Death Discov.* 8 (1), 43. doi:10.1038/s41420-021-00807-3
- Hiyama, N., Ando, T., Maemura, K., Sakatani, T., Amano, Y., Watanabe, K., et al. (2018). Glutamate-Cysteine Ligase Catalytic Subunit is Associated with Cisplatin Resistance in Lung Adenocarcinoma. *Jpn. J. Clin. Oncol.* 48 (4), 303–307. doi:10.1093/jjco/hyy013
- Hu, J.-C., Zhu, T.-P., Gui, Y.-C., Tan, Z.-B., Wei, R.-Q., Hu, B.-L., et al. (2020). miR-28-5p Inhibits Carcinogenesis in Colon Cancer Cells and Is Necessary for Erastin-Induced Ferroptosis. *Transl. Cancer Res. TCR* 9 (4), 2931–2940. doi:10.21037/tcr-20-1809



- Huang, J., Chen, G., Wang, J., Liu, S., and Su, J. (2022). Platycodin D Regulates High Glucose-Induced Ferroptosis of HK-2 Cells through Glutathione Peroxidase 4 (GPX4). *Bioengineered* 13 (3), 6627–6637. doi:10.1080/21655979.2022.2045834
- Ji, X., Qian, J., Rahman, S. M. J., Siska, P. J., Zou, Y., Harris, B. K., et al. (2018). xCT (SLC7A11)-Mediated Metabolic Reprogramming Promotes Non-Small Cell Lung Cancer Progression. *Oncogene* 37 (36), 5007–5019. doi:10.1038/s41388-018-0307-z
- Judkins, T., Leclair, B., Bowles, K., Gutin, N., Trost, J., McCulloch, J., et al. (2015). Development and Analytical Validation of a 25-Gene Next Generation Sequencing Panel that Includes the BRCA1 and BRCA2 Genes to Assess Hereditary Cancer Risk. *BMC Cancer* 15, 215. doi:10.1186/s12885-015-1224-y
- Kang, R., Kroemer, G., and Tang, D. (2019). The Tumor Suppressor Protein P53 and the Ferroptosis Network. *Free Radic. Biol. Med.* 133, 162–168. doi:10.1016/j.freeradbiomed.2018.05.074
- Kang, Y. P., Mockabee-Macias, A., Jiang, C., Falzone, A., Prieto-Farigua, N., Stone, E., et al. (2021). Non-Canonical Glutamate-Cysteine Ligase Activity Protects against Ferroptosis. *Cell Metab.* 33 (1), 174–189. doi:10.1016/j.cmet.2020.12.007
- La Montagna, M., Ginn, L., and Garofalo, M. (2020). Mechanisms of Drug Resistance Mediated by Long Non-Coding RNAs in Non-Small-Cell Lung Cancer. *Cancer Gene Ther.* 28, 175–187. doi:10.1038/s41417-020-00214-3
- Lai, Y., Zhang, Z., Li, J., Li, W., Huang, Z., Zhang, C., et al. (2019). STYK1/NOK Correlates with Ferroptosis in Non-small Cell Lung Carcinoma. *Biochem. Biophys. Res. Commun.* 519 (4), 659–666. doi:10.1016/j.bbrc.2019.09.032
- Lei, L. C., Yu, V. Z., Ko, J. M. Y., Ning, L., and Lung, M. L. (2020). FANCD2 Confers a Malignant Phenotype in Esophageal Squamous Cell Carcinoma by Regulating Cell Cycle Progression. *Cancers* 12 (9), 2545. doi:10.3390/cancers12092545
- Li, Y., Yan, H., Xu, X., Liu, H., Wu, C., and Zhao, L. (2020). Erastin/Sorafenib Induces Cisplatin-Resistant Non-Small Cell Lung Cancer Cell Ferroptosis through Inhibition of the Nrf2/xCT Pathway. *Oncol. Lett.* 19 (1), 323–333. doi:10.3892/ol.2019.11066
- Li, Z.-Y., Yin, Y.-F., Guo, Y., Li, H., Xu, M.-Q., Liu, M., et al. (2020). Enhancing Anti-Tumor Activity of Sorafenib Mesoporous Silica Nanomatrix in Metastatic Breast Tumor and Hepatocellular Carcinoma via the Co-Administration with Flufenamic Acid. *Int. J. Nanomedicine* 15, 1809–1821. doi:10.2147/IJN.S240436
- Li, H., Shi, X., Jiang, H., Kang, J., Yu, M., Li, Q., et al. (2020). CMap Analysis Identifies Atractyloside as a Potential Drug Candidate for Type 2 Diabetes Based on Integration of Metabolomics and Transcriptomics. *J. Cell Mol. Med.* 24 (13), 7417–7426. doi:10.1111/jcmm.15357
- Liang, C., Zhang, X., Yang, M., and Dong, X. (2019). Recent Progress in Ferroptosis Inducers for Cancer Therapy. *Adv. Mat.* 31 (51), e1904197. doi:10.1002/adma.201904197
- Liang, J.-Y., Wang, D.-S., Lin, H.-C., Chen, X.-X., Yang, H., Zheng, Y., et al. (2020). A Novel Ferroptosis-Related Gene Signature for Overall Survival Prediction in Patients with Hepatocellular Carcinoma. *Int. J. Biol. Sci.* 16 (13), 2430–2441. doi:10.7150/ijbs.45050
- Liao, D., Yang, G., Yang, Y., Tang, X., Huang, H., Shao, J., et al. (2020). Identification of Pannexin 2 as a Novel Marker Correlating with Ferroptosis and Malignant Phenotypes of Prostate Cancer Cells. *Onco. Targets Ther.* 13, 4411–4421. doi:10.2147/OTT.S249752
- Liu, R., Xu, K.-P., and Tan, G.-S. (2015). Cyclooxygenase-2 Inhibitors in Lung Cancer Treatment: Bench to Bed. *Eur. J. Pharmacol.* 769, 127–133. doi:10.1016/j.ejphar.2015.11.007
- Liu, G., Pei, F., Yang, F., Li, L., Amin, A., Liu, S., et al. (2017). Role of Autophagy and Apoptosis in Non-Small-Cell Lung Cancer. *Int. J. Mol. Sci.* 18 (2), 367. doi:10.3390/ijms18020367
- Magtanong, L., Ko, P.-J., To, M., Cao, J. Y., Forcina, G. C., Tarangelo, A., et al. (2019). Exogenous Monounsaturated Fatty Acids Promote a Ferroptosis-Resistant Cell State. *Cell Chem. Biol.* 26 (3), 420–432. doi:10.1016/j.chembiol.2018.11.016
- Matsumoto, R., Tsuda, M., Yoshida, K., Tanino, M., Kimura, T., Nishihara, H., et al. (2016). Aldo-keto Reductase 1C1 Induced by Interleukin-1 $\beta$  Mediates the Invasive Potential and Drug Resistance of Metastatic Bladder Cancer Cells. *Sci. Rep.* 6, 34625. doi:10.1038/srep34625
- Mittler, R., Darash-Yahana, M., Sohn, Y. S., Bai, F., Song, L., Cabantchik, I. Z., et al. (2019). NEET Proteins: A New Link between Iron Metabolism, Reactive Oxygen Species, and Cancer. *Antioxidants Redox Signal.* 30 (8), 1083–1095. doi:10.1089/ars.2018.7502
- Mou, Y., Wang, J., Wu, J., He, D., Zhang, C., Duan, C., et al. (2019). Ferroptosis, a New Form of Cell Death: Opportunities and Challenges in Cancer. *J. Hematol. Oncol.* 12 (1), 34. doi:10.1186/s13045-019-0720-y
- Njoku, K., Sutton, C. J. J., Whetton, A. D., and Crosbie, E. J. (2020). Metabolomic Biomarkers for Detection, Prognosis and Identifying Recurrence in Endometrial Cancer. *Metabolites* 10 (8), 314. doi:10.3390/metabo10080314
- Pal, R., Kumar, A., and Misra, G. (2021). Exploring TEAD2 as a Drug Target for Therapeutic Intervention of Cancer: A Multi-Computational Case Study. *Brief. Bioinform.* 22 (5), bbab007. doi:10.1093/bib/bbab007
- Parvathaneni, V., Kulkarni, N. S., Muth, A., and Gupta, V. (2019). Drug Repurposing: A Promising Tool to Accelerate the Drug Discovery Process. *Drug Discov. Today* 24 (10), 2076–2085. doi:10.1016/j.drudis.2019.06.014
- Pu, F., Chen, F., Zhang, Z., Shi, D., Zhong, B., Lv, X., et al. (2020). Ferroptosis as a Novel Form of Regulated Cell Death: Implications in the Pathogenesis, Oncometabolism and Treatment of Human Cancer. *Genes Dis.* 9 (2), 347–357. doi:10.1016/j.gendis.2020.11.019
- Ritchie, M. E., Phipson, B., Wu, D., Hu, Y., Law, C. W., Shi, W., et al. (2015). Limma Powers Differential Expression Analyses for RNA-Sequencing and Microarray Studies. *Nucleic Acids Res.* 43 (7), e47. doi:10.1093/nar/gkv007
- Sandler, A. B., and Dubinett, S. M. (2004). COX-2 Inhibition and Lung Cancer. *Seminars Oncol.* 31 (2 Suppl. 7), 45–52. doi:10.1053/j.seminoncol.2004.03.045
- Shi, J., Jiang, S., Qiu, D., Le, W., Wang, X., Lu, Y., et al. (2016). Rapid Identification of Potential Drugs for Diabetic Nephropathy Using Whole-Genome Expression Profiles of Glomeruli. *BioMed Res. Int.* 2016, 1634730. doi:10.1155/2016/1634730
- Shui, S., Zhao, Z., Wang, H., Conrad, M., and Liu, G. (2021). Non-Enzymatic Lipid Peroxidation Initiated by Photodynamic Therapy Drives a Distinct Ferroptosis-Like Cell Death Pathway. *Redox Biol.* 45, 102056. doi:10.1016/j.redox.2021.102056
- Siegel, R. L., Miller, K. D., Fuchs, H. E., and Jemal, A. (2021). Cancer Statistics, 2021. *CA A Cancer J. Clin.* 71 (1), 7–33. doi:10.3322/caac.21654
- Song, X., Xie, Y., Kang, R., Hou, W., Sun, X., Epperly, M. W., et al. (2016). FANCD2 Protects against Bone Marrow Injury from Ferroptosis. *Biochem. Biophys. Res. Commun.* 480 (3), 443–449. doi:10.1016/j.bbrc.2016.10.068
- Stockwell, B. R., Friedmann Angeli, J. P., Bayir, H., Bush, A. I., Conrad, M., Dixon, S. J., et al. (2017). Ferroptosis: A Regulated Cell Death Nexus Linking Metabolism, Redox Biology, and Disease. *Cell* 171 (2), 273–285. doi:10.1016/j.cell.2017.09.021
- Tan, Z., Lei, Y., Xu, J., Shi, S., Hua, J., Zhang, B., et al. (2020). The Value of a Metabolic Reprogramming-Related Gene Signature for Pancreatic Adenocarcinoma Prognosis Prediction. *Aging* 12 (23), 24228–24241. doi:10.18632/aging.104134
- Vainio, H. (2001). Is COX-2 Inhibition a Panacea for Cancer Prevention? *Int. J. Cancer* 94 (5), 613–614. doi:10.1002/ijc.1518
- Van Allen, E. M., Wagle, N., Stojanov, P., Perrin, D. L., Cibulskis, K., Marlow, S., et al. (2014). Whole-Exome Sequencing and Clinical Interpretation of Formalin-Fixed, Paraffin-Embedded Tumor Samples to Guide Precision Cancer Medicine. *Nat. Med.* 20 (6), 682–688. doi:10.1038/nm.3559
- Wang, L., Chen, X., and Yan, C. (2020). Ferroptosis: An Emerging Therapeutic Opportunity for Cancer. *Genes Dis.* 9 (2), 334–346. doi:10.1016/j.gendis.2020.09.005
- Wang, Y., Pan, Y., Wu, J., Luo, Y., Fang, Z., Xu, R., et al. (2022). A Novel Predictive Model Incorporating Ferroptosis-Related Gene Signatures for Overall Survival in Patients with Lung Adenocarcinoma. *Med. Sci. Monit.* 27, e934050. doi:10.12659/MSM.934050
- Wu, W., Yu, X., Wu, J., Wu, T., Fan, Y., Chen, W., et al. (2021). Surface Plasmon Resonance Imaging-Based Biosensor for Multiplex and Ultrasensitive Detection of NSCLC-Associated Exosomal miRNAs Using DNA Programmed Heterostructure of Au-On-Ag. *Biosens. Bioelectron.* 175, 112835. doi:10.1016/j.bios.2020.112835
- Xia, X., Fan, X., Zhao, M., and Zhu, P. (2019). The Relationship between Ferroptosis and Tumors: A Novel Landscape for Therapeutic Approach. *Curr. Gene Ther.* 19 (2), 117–124. doi:10.2174/1566523219666190628152137
- Xu, X.-C. (2002). COX-2 Inhibitors in Cancer Treatment and Prevention, a Recent Development. *Anti-Cancer Drugs* 13 (2), 127–137. doi:10.1097/00001813-200202000-00003
- Yan, H.-F., Zou, T., Tuo, Q.-Z., Xu, S., Li, H., Belaidi, A. A., et al. (2021). Ferroptosis: Mechanisms and Links with Diseases. *Sig Transduct. Target Ther.* 6 (1), 49. doi:10.1038/s41392-020-00428-9

- Yang, W.-Z., Yu, W.-Y., Chen, T., Wang, X.-F., Dong, F., Xie, M.-E., et al. (2019). A Single-Cell Immunofluorescence Method for the Division Patterns Research of Mouse Bone Marrow-Derived Hematopoietic Stem Cells. *Stem Cells Dev.* 28 (14), 954–960. doi:10.1089/scd.2018.0239
- Yildirim, O., Gottwald, M., Schüler, P., and Michel, M. C. (2016). Opportunities and Challenges for Drug Development: Public-Private Partnerships, Adaptive Designs and Big Data. *Front. Pharmacol.* 7, 461. doi:10.3389/fphar.2016.00461
- Yu, M., Gai, C., Li, Z., Ding, D., Zheng, J., Zhang, W., et al. (2019). Targeted Exosome-Encapsulated Erastin Induced Ferroptosis in Triple Negative Breast Cancer Cells. *Cancer Sci.* 110 (10), 3173–3182. doi:10.1111/cas.14181
- Yuan, H., Li, X., Zhang, X., Kang, R., and Tang, D. (2016). C1SD1 Inhibits Ferroptosis by Protection against Mitochondrial Lipid Peroxidation. *Biochem. Biophys. Res. Commun.* 478 (2), 838–844. doi:10.1016/j.bbrc.2016.08.034
- Zhou, Y., Guo, D., and Zhang, Y. (2020). Association of MicroRNA-21 with P53 at Mutant Sites R175H and R248Q, Clinicopathological Features, and Prognosis of NSCLC. *Mol. Ther. Oncolytics* 19, 208–217. doi:10.1016/j.omto.2020.10.005
- Zhuo, S., Chen, Z., Yang, Y., Zhang, J., Tang, J., and Yang, K. (2020). Clinical and Biological Significances of a Ferroptosis-Related Gene Signature in Glioma. *Front. Oncol.* 10, 590861. doi:10.3389/fonc.2020.590861
- Zou, J., Wang, L., Tang, H., Liu, X., Peng, F., and Peng, C. (2021). Ferroptosis in Non-Small Cell Lung Cancer: Progression and Therapeutic Potential on it. *Int. J. Mol. Sci.* 22 (24), 13335. doi:10.3390/ijms222413335

**Conflict of Interest:** The authors declare that the research was conducted in the absence of any commercial or financial relationships that could be construed as a potential conflict of interest.

**Publisher's Note:** All claims expressed in this article are solely those of the authors and do not necessarily represent those of their affiliated organizations, or those of the publisher, the editors and the reviewers. Any product that may be evaluated in this article, or claim that may be made by its manufacturer, is not guaranteed or endorsed by the publisher.

Copyright © 2022 Zhao, Cui, Zhang, Guo, Deng, Wen, Lu, Shi, Xing, Liu and Zhang. This is an open-access article distributed under the terms of the Creative Commons Attribution License (CC BY). The use, distribution or reproduction in other forums is permitted, provided the original author(s) and the copyright owner(s) are credited and that the original publication in this journal is cited, in accordance with accepted academic practice. No use, distribution or reproduction is permitted which does not comply with these terms.



# The Mechanisms of Ferroptosis and the Applications in Tumor Treatment: Enemies or Friends?

Shuzheng Tan<sup>1,2†</sup>, Ying Kong<sup>3†</sup>, Yongtong Xian<sup>4†</sup>, Pengbo Gao<sup>4</sup>, Yue Xu<sup>4</sup>, Chuzhong Wei<sup>4</sup>, Peixu Lin<sup>4</sup>, Weilong Ye<sup>4</sup>, Zesong Li<sup>5\*</sup> and Xiao Zhu<sup>1\*</sup>

<sup>1</sup>School of Laboratory Medicine and Biological Engineering, Hangzhou Medical College, Hangzhou, China, <sup>2</sup>Department of Dermatology, The First Affiliated Hospital of Guangzhou Medical University, Guangzhou, China, <sup>3</sup>Department of Clinical Laboratory, Hubei No.3 People's Hospital of Jiangnan University, Wuhan, China, <sup>4</sup>Computational Oncology Laboratory, Guangdong Medical University, Zhanjiang, China, <sup>5</sup>Guangdong Provincial Key Laboratory of Systems Biology and Synthetic Biology for Urogenital Tumors, Shenzhen Key Laboratory of Genitourinary Tumor, Department of Urology, The First Affiliated Hospital of Shenzhen University, Shenzhen Second People's Hospital (Shenzhen Institute of Translational Medicine), Shenzhen, China

## OPEN ACCESS

### Edited by:

Guo Chen,  
Jinan University, China

### Reviewed by:

Shuguang Zuo,  
Chifeng Municipal Hospital, China  
Yun-Jiu Cheng,  
Sun Yat-sen University, China

### \*Correspondence:

Zesong Li  
lzssc@email.szu.edu.cn  
Xiao Zhu  
biozhu@yahoo.com

<sup>†</sup>These authors have contributed  
equally to this work

### Specialty section:

This article was submitted to  
Molecular Diagnostics and  
Therapeutics,  
a section of the journal  
Frontiers in Molecular Biosciences

**Received:** 07 May 2022

**Accepted:** 20 June 2022

**Published:** 15 July 2022

### Citation:

Tan S, Kong Y, Xian Y, Gao P, Xu Y,  
Wei C, Lin P, Ye W, Li Z and Zhu X  
(2022) The Mechanisms of Ferroptosis  
and the Applications in Tumor  
Treatment: Enemies or Friends?  
Front. Mol. Biosci. 9:938677.  
doi: 10.3389/fmolb.2022.938677

Ferroptosis, as a newly discovered non-apoptotic cell death mode, is beginning to be explored in different cancer. The particularity of ferroptosis lies in the accumulation of iron dependence and lipid peroxides, and it is different from the classical cell death modes such as apoptosis and necrosis in terms of action mode, biochemical characteristics, and genetics. The mechanism of ferroptosis can be divided into many different pathways, so it is particularly important to identify the key sites of ferroptosis in the disease. Herein, based on ferroptosis, we analyze the main pathways in detail. More importantly, ferroptosis is linked to the development of different systems of the tumor, providing personalized plans for the examination, treatment, and prognosis of cancer patients. Although some mechanisms and side effects of ferroptosis still need to be studied, it is still a promising method for cancer treatment.

**Keywords:** ferroptosis, immunotherapy, iron overload, lipid peroxidation, mitochondria

## INTRODUCTION

Ferroptosis is a kind of iron-dependent programmed cell death, which is different from traditional cell necrosis, apoptosis, and autophagy in morphology, biochemistry, and genetics. It is a new type of programmed cell death. In a word, the mode of cell death in which extensive lipid peroxidation occurs is called ferroptosis (Chen et al., 2021b; Ding et al., 2021).

When Erastin is used to selectively act on the RAL gene in human cancer cells, it is found that lots of iron ions and lipid oxidizing substances were produced in the cells and iron ions catalyzed the oxidation of lipids. Abnormal metabolism of substances leads to cell death on account of destroying the normal redox environment in the cell. Therefore, the essence of ferroptosis is the oxidative death of cells caused by the accumulation of several iron ions. Biologically, the pivotal feature of the ferroptosis is the iron-dependent lipid reactive oxygen accumulation and the activation of the mitogen-activated protein kinase system (Dixon et al., 2012). Morphologically, once ferroptosis occurs, the nucleus is normal in size but lacks chromatin agglutination. At the same time, the mitochondria shrink and the mitochondrial ridges are reduced or even disappear. The outer membrane is broken, and the bilateral membrane density increases in the mitochondria. The application of iron chelating agents and antioxidants can effectively play inhibitory effects on the

occurrence of ferroptosis. On the contrary, the supplementation of iron will aggravate this process. Genetically, ferroptosis is primarily regulated by iron response element-binding protein (IREB2), citrate synthase (CS), and ATP synthase F0 complex subunit C3 (ATP5G3). Immunologically, inflammatory mediators released by DAMPs, such as high mobility group protein b1, cause both innate and adaptive immune responses.

Ferroptosis was initially discovered and established only in tumor cells, but as research continues to deepen, ferroptosis is shown to play a vital role in pathological processes such as tumors, neurodegenerative diseases, and tissue ischemia-reperfusion injury (Stockwell et al., 2017).

## BIOLOGICAL CHARACTERISTICS OF FERROPTOSIS

### Iron Overload

Excessive accumulation of iron is the necessary condition and main characteristic of ferroptosis.  $\text{Fe}^{2+}$ , whose quantity is the kernel to the formation of PL-OOH, serves as the dominating form of iron in the intracellular labile iron pool (LIP). LIP is regulated by intracellular iron homeostasis. Accumulation of PL-OOH is a sign of ferroptosis. The free radicals and hyperoxides generated after the redox reaction of  $\text{Fe}^{2+}$  and  $\text{Fe}^{3+}$  can react with Polyunsaturated fatty acids (PUFAs) containing phospholipids (PLs) in the cell membrane to facilitate the spread of lipid peroxidation on the cell membrane. This process produces lots of ROS and induces cell ferroptosis (Doll and Conrad, 2017; Ruiz-de-Angulo et al., 2020; Nieto-Garai et al., 2022). In addition, iron-dependent lipid peroxidation can be attenuated by GPX4, radical trapping protein removal, ferroptosis-specific inhibitors, and iron chelation. William et al. lately found that if iron chelation, such as Deferoxamine (DFO), is added to cells, the occurrence of ferroptosis could be inhibited. In contrast, iron supplements intensify the process (Abrams et al., 2016). This discovery fully reveals that ferroptosis is dependent on iron.

### Lipid Peroxidation

Cell peroxidation caused by lipid reactive oxygen accumulation is the direct cause of ferroptosis (Chu et al., 2019), among which the key lipid is sn2-15-HPET-PE (Anthonymuthu et al., 2018). When lipid antioxidants are applied to cell membranes, lipid degradation could significantly reduce the occurrence of cell ferroptosis (Yang et al., 2016; Doll et al., 2019; Lin Z. et al., 2021). In brief, lipid metabolism is an important process of ferroptosis. Researchers discovered that in addition to long-chain polyunsaturated fatty acid, long-chain saturated fatty acid can potentiate ferroptosis through peroxisome-driven ether phospholipid biosynthesis (Hwang et al., 2021). FAR1 and 1-hexadecanol (1-HE) remarkably accelerate ferroptosis in tumor cells. Moreover, TMEM189 can replace the role of the FAR1-alkyl-ether lipids axis in inducing ferroptosis, which lays the ground for becoming a target of a new generation of anticancer drugs (Cui et al., 2021).

The enzymes that stimulate ferroptosis are the oxidoreductases POR and CYB5R1 located on the endoplasmic reticulum. It was found that phospholipids containing long-chain

unsaturated fatty acids are catalyzed by POR and CYB5R1 to produce lipid peroxidation, resulting in oxidative damage of liposome membranes. This process revealed the biochemical mechanism of cell membrane oxidative damage during ferroptosis (Yan et al., 2021). In addition, MDM2 and MDMX promote ferroptosis by regulating PPAR $\alpha$ -mediated lipid homeostasis, which is independent of P53. Therefore, MDM2 and MDMX inhibitors can be used to treat diseases associated with ferroptosis (Venkatesh et al., 2020).

## The Role of Mitochondria

Iron and cysteine are involved in the regulation of one of the mechanisms of ferroptosis. Cysteine deficiency results in mitochondrial membrane potential hyperpolarization and lipid peroxides accumulation. But when cysteine is deficient, serum transferrin and glutamine are requisite for ferroptosis. Also, Mitochondria are of the essence in regulating cysteine deprivation-induced (CDI) ferroptosis, including the mitochondrial TCA cycle and mitochondrial electron transport chain (Jiang X. et al., 2021; Wei et al., 2022). In the mitochondrial TCA cycle, the breakdown of glutamine produces  $\alpha$ -ketoglutarate to provide energy, thus improving mitochondrial respiration rate and promoting ROS production. Conversely, loss of function of fumarate hydratase (FH), a mitochondrial tumor suppressor, causes kidney cancer cells to resist ferroptosis. Moreover, The hyperpolarization of mitochondrial membrane potential promotes lipid accumulation (Gao et al., 2019). When Erastin was applied to treat voltage-dependent anion channels (VDACs), mitochondrial function was disrupted so that oxidative substances were released, leading to oxidative death (Yagoda et al., 2007). Furthermore, Dihydroorotate Dehydrogenase (DHODH) is of great importance. In tumor cells with low GPX4 expression, DHODH activity is significantly reduced or even inactivated, which gives rise to mitochondrial lipid peroxidation accumulation and activates ferroptosis, thereby inhibiting tumor growth (Mao et al., 2021). Whereas mitochondria and glutamine come into no effect in inhibiting the GPX4-mediated pathway that boosts ferroptosis. Whether to remove the mitochondria, add electron transfer chain (ETC) inhibitors, or remove glutamine, RSL3 can inhibit GPX4-induced ferroptosis (Gaschler et al., 2018). Mitochondrial ferritin is also worth our attention. It not only inhibits oxidative stress-dependent neuronal cell damage, but also has a protective effect on Erastin-induced ferroptosis (Wang et al., 2016).

## THE MECHANISM OF FERROPTOSIS

The mechanism of ferroptosis is that under the action of iron or ester oxygenase, it catalyzes the lipid peroxidation of a great deal of unsaturated fatty acids on the cell membrane. Finally, ferroptosis causes the accumulation of ROS and induces cell death (Dixon et al., 2012; Stockwell et al., 2017) (**Figure 1**).

### Glutathione Peroxidase (GPX4)

GPX is an indispensable peroxidase that exists widely in the body (Han et al., 2013). In the GPXs family, GPX4 takes a crucial effect on the ferroptosis regulatory pathway (Ingold et al., 2018). Its



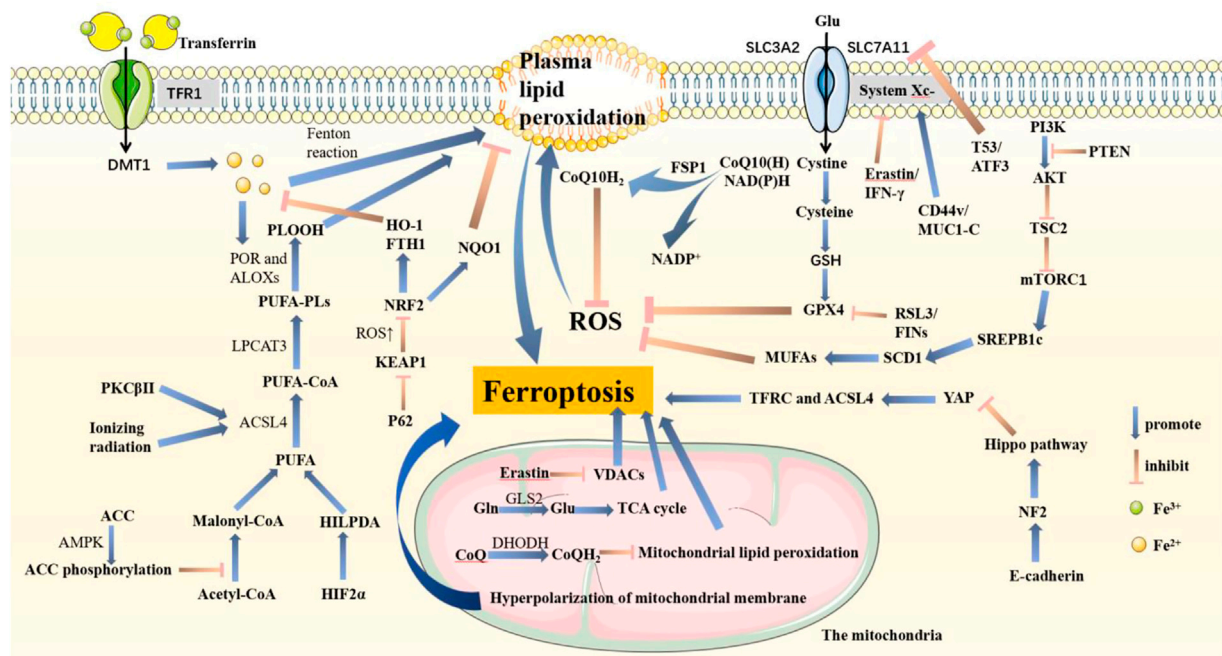


**FIGURE 1 |** Pathways associated with ferroptosis in cells. PTEN promotes lipid peroxidation and ferroptosis by inhibiting the PI3K-AKT-mTOR pathway. System Xc<sup>-</sup>, composed of SLC3A2 and SLC7A11, is an important structure that helps synthesize GSH. GSH promotes GPX4 to inhibit ferroptosis. In this pathway, T53 and ATF3 acting on SLC7A11, RSL3 and FINs acting on GPX4, and Erastin and IFN- $\gamma$  acting on System Xc<sup>-</sup> are important inhibitors that are conducive to ferroptosis. Also, CD44v and MUC1-C acting on System Xc<sup>-</sup> promote GPX4 synthesis. P62-KEAP1-NRF2 goes against ferroptosis by increasing NQO1, HO-1, and FTH1. Fe<sup>3+</sup> binds to transferrin and enters cells through TFR1, which is reduced to Fe<sup>2+</sup> and released from DMT1-mediated endosomes. Plasma lipid peroxidation is induced by the Fenton reaction process. PUFA is activated by ACSL4 and LPCAT3 and catalyzed by POR and ALOXs to promote ROS accumulation. The HIF2 $\alpha$ -HILPDA axis, PKC $\beta$  II, and ionizing radiation both positively regulate ferroptosis, in which PKC $\beta$  II and ionizing radiation acted on ACSL4. AMPK fights ferroptosis by promoting ACC phosphorylation. E-cadherin activates the NF2-Hippo pathway and then inhibits YAP expression. Therefore, TFRC and ACSL4 are also inhibited, resulting in tumor cells growing and metastasizing more quickly. FSP1 inhibits ferroptosis by reducing CoQ10. In mitochondria, Erastin induces lipid peroxidation in both VDACs and mitochondrial potential hyperpolarization. GLS2 helps Gln transform into Glu, which enters the TCA cycle to promote ROS production. Besides, DHODH inhibits ferroptosis.

function is generally responsible for catalyzing the degradation of lipid peroxides, specifically in reducing lipid peroxides to non-toxic lipid alcohols. When the activity of GPX4 is inhibited or the amount of GPX4 is decreased, it will increase the iron-dependent reactive oxygen species in the cell, destroy the membrane structure, and induce ferroptosis (Yang et al., 2014; Seibt et al., 2019). Studies have found that GSH, in the form of reactants, participates in the process of GPX4 catalyzing the degradation of lipid peroxides (Zheng and Conrad, 2020). Accordingly, the GSH deficiency can lead to a decrease in the activity of GPX4, which in turn leads to ferroptosis. The ferroptosis inducer RL3 can also inhibit GPX4 activity by covalently binding with GPX4. The Berghe team found that through chemical proteomics experiments, RSL3 covalently binds to the active site-containing selenocysteine of GPX4. Hence RSL3 can not only directly inhibit the phospholipid peroxidase activity of GPX4, but lead to the accumulation of superoxide. At last, ferroptosis is triggered (Fang et al., 2019). It is noteworthy that GPX4 may produce unnecessary targeting effects on CD8<sup>+</sup>T cells in the anti-tumor process, leading to adverse reactions.

## Glutamate-Cystine Transporter

The glutamate-cystine transporter (system Xc<sup>-</sup>) is a heterodimer composed of SLC7A11 and SLC3A2. Cystine enters the cell via system Xc<sup>-</sup>, then GSH and GPX4 can be synthesized in the cell (Yang et al., 2014). GPX4 requires the participation of GSH in the catalytic reduction of lipid peroxides to alcohols, so inhibiting cystine uptake by cells can induce ferroptosis. Wang et al. (Wang L. et al., 2020) demonstrated that activating transcription factor 3 (ATF3) inhibits system Xc<sup>-</sup> by inhibiting the expression of SLC7A11, thereby promoting ferroptosis induced by Erastin. In addition, it is shown that pancreatic cancer cells need to take in exogenous cystine through system Xc<sup>-</sup> to prevent ferroptosis. Knockout of SLC7A11 can result in massive death of pancreatic cancer cells (Badgley et al., 2020). Lei, G. et al. revealed that ionizing radiation (IR) induces SLC7A11 and GPX4 expression as an adaptive response, which inhibits ferroptosis and enhances radiation resistance. The use of FINs, a ferroptosis inducer, restored IR sensitivity in radiation-resistant cancer cells and xenograft cells (Lei et al., 2020).

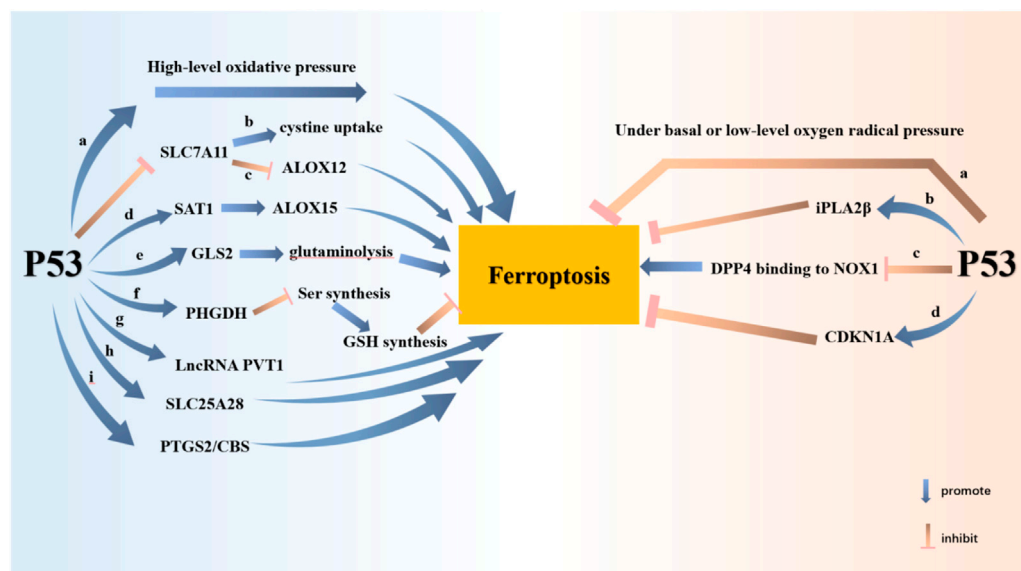


**FIGURE 2 |** P53 potentiates ferroptosis through nine pathways and attenuates ferroptosis through three pathways. P53 promotes ferroptosis at high levels of oxidative stress. Ferroptosis is promoted by P53 inhibition of SLC7A11 expression. The consequent inhibition of cystine uptake and the release of ALOX12 contribute to ferroptosis. P53 inhibits tumor cell growth by promoting SAT1-ALOX15 and GLS-glutaminolysis axes, respectively. P53 inhibits GSH synthesis through PHGDH. P53 also promotes ferroptosis by enhancing the expression of LncRNA PVT1, SLC25A28, PTGS2 and CBS. Nevertheless, P53 inhibits ferroptosis at basal or low levels of oxygen radical pressure. P53 inhibits ferroptosis by raising the expression of iPLA2 $\beta$  and CDKN1A. P53 protects cells from ferroptosis by inhibiting DPP4 binding to NOX1.

## p53

p53 is an important and key tumor suppressor gene in humans, which induces cell senescence or apoptosis by regulating cell cycle arrest. Tumor suppressor activity is regulated by the classical function of p53 (Cordani et al., 2016). What's more, p53 is capable of controlling the redox state of cells through non-classical functions. p53 regulates ferroptosis in tumor cells in a manner independent of GPX4 at high ROS levels (Chen D. et al., 2021). According to the cell environment and state, p53 has the dual effect of promoting and inhibiting ferroptosis (Hassannia et al., 2019; Sun et al., 2022; Yuan et al., 2022) (Figure 2)

### 1) p53 can promote ferroptosis.

- p53 has the effect of promoting ferroptosis under high-level oxidative pressure (Kruiswijk et al., 2015).
- p53 inhibits SLC7A11 transcription, then attenuates cystine uptake, and finally facilitates ferroptosis (Jiang et al., 2015).
- p53 acts in a GSH-independent manner. SLC7A11 is downregulated while ALOX12 is released. ALOX12 is not only a key regulator of p53-dependent ferroptosis but can be directly bound and inhibited by SLC7A11 (Chu et al., 2019).
- p53 can potentiate tumor ferroptosis by inducing SAT1 expression and promoting ALOX15 work (Ou et al., 2016).
- GLS2, the target gene of p53, catalyzes the process of Glutaminolysis to promote ferroptosis (Gao et al., 2019).
- p53 inhibits Ser synthesis by regulating PHGDH, thus inhibiting GSH synthesis and promoting ferroptosis.

- LncRNA PVT1 potentiates ferroptosis through the expression of TFR1 and p53 (Lu et al., 2020).
  - p53 binds to the mitochondrial transporter SLC25A28 to facilitate ferroptosis (Zhang Z. et al., 2020).
  - PTGS2 and CBS are both target genes of p53 and markers of ferroptosis.
- 2) p53 also negatively regulates ferroptosis in other cells or under certain conditions.
- p53 has the effect of inhibiting ferroptosis under basal or low-level oxygen radical pressure (Kruiswijk et al., 2015).
  - iPLA2 $\beta$  mediates lipid peroxide detoxification to inhibit ROS-induced p53-driven ferroptosis in a GPX4-independent manner (Chen D. et al., 2021).
  - In colorectal cancer, p53 directly binds DPP4 and inhibits DPP4 binding to NOX1 in the cytoplasm, resulting in inhibition of lipid peroxidation and ferroptosis in cancer cells (Xie et al., 2017).
  - In fibrosarcoma cells, p53 induces CDKN1A expression to limit ferroptosis (Hassannia et al., 2019).

## NF2

Normal NF2 genes express ECAD, LATS1, and LATS2, which can confer resistance to ferroptosis. It is found that E-cadherin-mediated activation of intercellular NF2 and Hippo signaling pathways inhibits proto-oncogene transcription coactivator YAP. Ferroptosis is thus suppressed. This pathway is the main pathway through which cell density affects ferroptosis. If this signaling pathway is inhibited, YAP promotes cellular ferroptosis by elevating ferroptosis regulators of ACSL4 and TFRC. It is noteworthy that NF2 inhibits ferroptosis by inhibiting YAP

activity, although cells expressing YAP are more sensitive to ferroptosis. As a result, malignant mutations in E-cadherin-NF2-Hippo-YAP signaling, used as biomarkers, predict the therapeutic response to ferroptosis induced in cancer (Wu et al., 2019).

The study found that silencing of NF2 activates ferroptosis-related pathways in GPX4-knockout tumor mice. NF2-silenced tumor cells grow faster without GPX4 knockout. This is because NF2 knockout facilitates tumor cell metastasis, which GPX4 knockout inhibits. These results indicated that NF2 also depended on GPX4 to regulate ferroptosis.

## FSP1 (AIFM2)

FSP1, formerly known as AIFM2, is a biomarker of ferroptosis resistance in many different cancers, protecting GPX4-deficient cells from ferroptosis. FSP1 is a key component of the non-mitochondrial coenzyme Q antioxidant system, whose inhibition of ferroptosis is mediated by ubiquinone (CoQ10) (Doll et al., 2019; Stockwell, 2019). FSP1 reduces CoQ10 to inhibit ferroptosis. Reductive CoQ is an antioxidant that traps free radicals with the ability to inhibit the propagation of lipid peroxides and prevent lipid damage. The NAD(P)H-FSP1-CoQ10 pathway is independent of the GPX4 pathway of glutathione, which synergistically inhibits phospholipid peroxidation (PLPO) and ferroptosis. Now it has been found that FSP1 is resistant to ferroptosis only when modified by cardamomylation. Cardamomylation mediates the recruitment of FSP1 into lipid droplets and the plasma membrane, where NADH-dependent CoQ is reduced (Bersuker et al., 2019). The expression of FSP1 provides a strategy for predicting the sensitivity and efficacy of cancer cells to ferroptosis-inducing chemotherapies, as well as directions for developing FSP1 inhibitors to treat cancer and overcome ferroptosis resistance in many cancers.

## AMPK

AMP-activated protein kinase (AMPK) is a crucial substance that senses and regulates the balance of cellular energy metabolism. When glucose is deficient, insufficient intracellular energy metabolism gives rise to a decrease in ATP content, which further leads to an increase in AMP/ATP ratio and activation of AMPK (Hardie et al., 2012). AMPK, which acts as the primary signaling hub to trigger energy stress, ultimately combats ferroptosis. It has been found that AMPK can block PUFAs biosynthesis regulated by Acetyl CoA carboxylase (ACC), resulting in significant inhibition of ferroptosis. As a result, on the one side, ACC phosphorylation is instrumental to regulate ferroptosis (Lee et al., 2020). On the other side, it has also been suggested that AMPK can mediate phosphorylation of Beclin 1, thereby inhibiting GSH production and promoting ferroptosis (Chen et al., 2021b).

## PI3K

The PI3K-AKT-mTOR signaling pathway, one of the most frequently mutated pathways in human cancer, prevents cancer cells from oxidative stress and ferroptosis through SREBP1/SCD1-mediated adipogenesis during carcinogenic

activation (Fruman et al., 2017; Zhang et al., 2017; Zou et al., 2020). When mTORC1 activation is raised, SREBP1 can be upregulated and confer activation to SCD1 (Saxton and Sabatini, 2017). Inhibition of mTORC1 or ablation of SREBP1/SCD1 plays a protective role in ferroptosis in cancer cells with mutations in the PI3K-AKT-mTOR pathway, as well as enhances the effect of ferroptosis-induced cancer therapy. A research team discovered that drugs that block the PI3K-AKT-mTOR pathway, in combination with drugs that induce ferroptosis, evidently destroy and clear tumors (Yi J. et al., 2020).

Since both the PI3K pathway and the HDAC pathway are vital signaling pathways of malignant tumors (Li and Seto, 2016), the combination of inhibitors of the two can achieve good antitumor effects and overcome the problem of drug resistance of single drug use. A research team developed the PI3K/HDAC dual inhibitor BEBT-908, which is capable of distinctly inhibiting PI3K kinase, HDAC1, HDAC2, HDAC3, HDAC10, and HDAC11, thus delaying tumor cell growth and giving promotion cell ferroptosis. When used in association with immune checkpoint inhibitors, such as an anti-PD-1 antibody, BEBT-908 can also enhance immunotherapy efficacy and generate antitumor immune memory (Fan et al., 2021; Wang et al., 2021).

## HIF2 $\alpha$

Hypoxia dramatically enhances HIF2 $\alpha$  -dependent cancer cell death and facilitates cancer cell sensitivity to ferroptosis. HIF2 $\alpha$  inhibits GPX4 expression and drives PUFA remodeling by activating hypoxia-induced lipid droplet-associated (HILPDA), causing cancer cells to be highly sensitive to ferroptosis. As HIF2 $\alpha$  is absent, cancer cells develop tolerance to GPX4 inhibitors and reduce the occurrence of ferroptosis. Therefore, the mechanism of cell ferroptosis driven by the HIF2 $\alpha$  -HILPDA signaling pathway is expected to be applied in the clinic, especially in the treatment of colorectal cancer and renal clear cell carcinoma (Zou et al., 2019; Singhal et al., 2021).

# FERROPTOSIS AND CANCER

## Overview of Ferroptosis and Tumors

Ferroptosis is a form of cell death caused by the accumulation of iron and ROS (Dixon et al., 2012). Tumors refer to neoplasms formed by the excessive proliferation of local cells under the action of various tumor-causing factors. Normally, benign tumors can be removed by surgery, and malignant tumors require radiation therapy and chemotherapy in addition to removal. Unfortunately, some tumors are highly malignant with strong drug resistance and radiation resistance. However, recent studies have found that with the deepening of research, the relationship between the proliferation of tumor cells and iron metabolism is getting closer and closer. Tumor cells cause ferroptosis through different pathways leading to their growth inhibition or death (Torti and Torti, 2020). Further investigation of ferroptosis is expected to solve the problems of cancer cell treatment resistance and drug insensitivity. Here we will systematically show the research progress of ferroptosis in

cancer of different systems, providing a groundbreaking perspective for clinical treatment to inhibit and kill cancer cells.

## Ferroptosis and Respiratory Tumors

Lung cancer, the most common cancer in humans, originates in the epithelium or glands of the lungs (Berns, 2005). Mature tumor cells usually exhibit NSF1 gene dependence under circumstances of high oxygen. NSF1 maintains an iron-sulfur cluster in proteins, which are essential for tumor cells to perform basic functions. Sequentially, NSF1 protects cancer cells from oxidative damage and prevents ferroptosis. Conversely, if NSF1 and iron-sulfur clusters are inactivated, iron starvation response and ferroptosis sensitive pathways of lung cancer cells will be activated, which will induce cell ferroptosis (Nurtjahja-Tjendraputra et al., 2007; Alvarez et al., 2017). The synthesis of iron-sulfur clusters and NSF1 inhibitors may be a new method for lung cancer treatment in the future (Mao et al., 2018).

The KEAP1/NRF2 genes are highly mutated in non-small cell lung cancer (NSCLC) and tend to be found in heavy smokers. Abnormal activation of KEAP1/NRF2 can prevent cancer cells from being harmed by oxidative stress and improve the survival chance of cancer cells (Kang et al., 2021). Now Telaglenastat, a drug targeting KEAP1/NRF2 mutations, is available, offering hope for patients with NSCLC.

Furthermore, acetaminophen has been shown to induce ferroptosis by modulating the NRF2-heme oxygenase-1 signaling pathway in NSCLC (Gai et al., 2020). lncRNA P53RRA can inhibit the G1-S phase of lung cancer cells, promoting cell apoptosis and ferroptosis. By contrast, knockdown of GPX4 reverses the inhibition of ferroptosis caused by overexpression of serine/threonine/tyrosine kinase 1 and GPX4 in NSCLC (Lai et al., 2021).

## Ferroptosis and Urinary System Tumors

Ferroptosis, one of the main pathways of cell carcinoma death, has also been seen in urinary system tumors. With the interest of in-depth research on the mechanism of ferroptosis, it has the chance to be combined with targeted therapy and immunotherapy shortly, improving the success rate of urinary system tumor treatment.

Clear cell renal cell carcinoma (ccRCC) is a kind of malignant and common metastatic cancer marked by clear cytoplasm. We demonstrate that the HIF2 $\alpha$ -HILPDA signaling pathway is the main pathway to activate ccRCC, and HIF2 $\alpha$  strongly inhibits GPX4 expression by activating downstream proteins (Zou et al., 2019; Courtney et al., 2020; Hoefflin et al., 2020). On account of ccRCC being exceedingly sensitive to the absence of GPX4, GPX4 inhibitors can show high selective destruction (Yang and Stockwell, 2016). Not only so, the protein-modifying gene KDM5C significantly synergizes Erastin-induced lipid peroxidation and inhibits glucose to the pentose-phosphate pathway (PPP) flow and glycolysis in ccRCC. Ultimately ferroptosis is promoted while tumorigenicity is inhibited (Zheng et al., 2021). In the future, glycogen metabolism will hopefully be one of the therapeutic targets for ccRCC. Some further researches reveal that there are two new approaches for the treatment of ccRCC, which are the

inhibition of glutathione synthesis and the use of fumarate hydratase, inducing ferroptosis in renal tumor cells (Kerins et al., 2018; Miess et al., 2018).

Prostate tumor is one of the most common tumors of the urinary system. For the above reason, research on the treatment of prostate cancer has been the talk of the world. Some studies have found that with the increased expression of heat shock protein (HSPB1) and ZNF217, ferroptosis of prostate cancer cells is restrained and the growth of tumor cells is synergized (Sun et al., 2015). Fe<sub>3</sub>O<sub>4</sub> nanoparticles are surprisingly detected to trigger ferroptosis in prostate cells while avoiding damage to normal tissue. In addition, acsbg1 is a key factor regulating the transition of different modes of death, which provides new enlightenment and methods for the treatment of prostate tumors (Xie et al., 2021).

## Ferroptosis and Digestive System Tumors

The P62-KEAP1-NRF2 signaling pathway exists in hepatocellular carcinoma cells, among which NRF2 is the core transcription factor. Target genes, such as quinone oxidoreductase 1 (NQO1), heme oxygenase 1, HO-1 and ferritin heavy chain-1 (FTH1), involved in iron and ROS metabolism are up-regulated when this pathway is activated (Zhu et al., 2010; Zhu et al., 2011; Liao et al., 2013; Sun et al., 2016b). Metallothionein-1G (MT-1G) is also regulated and significantly expressed (Sun et al., 2016a). Ultimately, ferroptosis is undermined. Also, resistance to Erastin and Sorafenib in hepatocellular carcinoma is intensified. Louandre, C. et al. strongly suggested that tumor suppressor gene Rb can achieve a tumor-suppressive effect by increasing mitochondrial ROS level and ferroptosis toxicity (Louandre et al., 2015).

Pancreatic ductal adenocarcinoma (PDAC) stops ferroptosis by extracellular cysteine input despite a high concentration of lipid peroxides in cells. Cysteine outside PDAC synthesizes glutathione and CoA through the transporter SLC7A11, which counteracts the excess lipid peroxides. In contrast, when cysteine depletion occurs, intracellular autophagy promotes the degradation of the nuclear receptor Coactivator 4 (NCOA4) in PDAC. Lysosomal function and autophagy flux are impaired, thus in turn affecting cell iron overload and lipid peroxide production (Hou et al., 2016; Song et al., 2018). In other words, ferroptosis is facilitated when PDAC lacks exogenous cysteine or knocks out the cysteine transporter (SLC7A11). To our excitement, the combination of GSH and CoA, as well as metabolic disorders, that synergizes ferroptosis to treat PDAC is promising clinical option (Badgley et al., 2020). Dai, E. et al. found that a high iron diet and consumption of GPX4 can activate the TMEM173/STING-dependent DNA sensor pathway, leading to macrophages entering and activating KRAS-driven PDAC, which can significantly be inhibited by Liproxstatin -1 (Dai et al., 2020). Chen, X. et al. considered that the blockade of NUPR1, LCN2, or MGST1-mediated ALOX5 will also be a feasible strategy for the treatment of PUAC. At present, what also manifests obvious anticancer activity and promising clinical application is the combination of the antimalarial drug Artesunate and the anti-HIV1 drug Zalcitabine (Chen et al., 2021a).



In colorectal cancer, P53 not only directly inhibits DPP4 binding to NOX1 but also mediates SLC7A11, reducing the anticancer activity of Erastin *in vivo*. Whether Kras gene mutations or bromelain can stimulate ACSL4 expression, contributes to ferroptosis, and circumvents the development of colorectal cancer. With *Betula etnensis* Raf stimulates colorectal cancer cells, heme oxygenase (HO-1) overexpression increases intracellular iron content and redox balance was broken, followed by ferroptosis and cancer cell death (Malfa et al., 2019).

Zhang, H. et al. revealed that when processing cancer-associated fibroblasts (CAFs) of gastric cancer cells with cisplatin and paclitaxel, the USP7/hnRNPA1 axis is activated, through which miR-522 secretion is promoted. Then, the level of ferroptosis in cancer cells was downregulated in the wake of the targeted inhibition of ALOX15, and lipid peroxidation was reduced (Zhang H. et al., 2020). In other words, high levels of ALOX15 play a critical role in mediating tumor lipid peroxidation and improving overall survival in patients. Ying Liu et al. demonstrated that Jiyuan oridonin A (JDA) derivative a2 has the effect of inducing ferroptosis and anti-tumor proliferation by down-regulating GPX4 and causing iron ion accumulation. Gastric cancer drugs targeting a2 will be a hot topic in the future (Liu Y. et al., 2021). Of note, stearoyl-CoA desaturase (SCD1), perilipin2 (PLN2), and SLC7A11 can exert ferroptosis resistance in gastric cancer cells, which will be an effective target for early diagnosis, treatment, and prognosis of gastric cancer (Wang C. et al., 2020; Sun et al., 2020).

## Ferroptosis and Reproductive System Tumors

Triple-negative breast cancer (TNBC), which is famous for its high aggressiveness, high metastasis rate and high mortality, has always been the goal and direction of human efforts to explore the target of its early diagnosis and effective treatment. In TNBC, holo-lactoferrin (Holo-Lf) has been shown to inhibit MDAMB-231 cell viability while enhancing the ability of Erastin-induced cell ferroptosis. Of course, it also has an undeniable significance in improving the sensitivity of cells to radiotherapy (Zhang et al., 2021). Current studies have fully demonstrated that when MUC1-C, SREBP1, SCD1, KLF4, CD44variant, DKK1, and Cysteine are expressed in TNBC, they inhibit the occurrence of ferroptosis, resulting in high proliferation and high invasive activity (Hasegawa et al., 2016; Yi J. et al., 2020; Luis et al., 2021). MUC1-C, CD44variant, and KLF4, as negative regulators, up-regulate xCT expression and GSH level to reduce the sensitivity of tumor cells to ferroptosis (Lee et al., 2021; Zhou et al., 2021). Moreover, DKK1 regulates tumor stem cells to protect lung metastases from ferroptosis (Wu et al., 2022). Conversely, as TNBC expresses ACSL4, GPX4, DDR2, miR-324-3p, miR-3825p, and miR-5096, the imbalance of GSH levels enhances the probability of ferroptosis in cells (Lin C.-C. et al., 2021; Hou et al., 2021; Sun et al., 2021; Yadav et al., 2021). Surprisingly, the ACSL4 level can be an independent predictor of complete response and tumor-free survival after TNBC neoadjuvant chemotherapy (Dinarvand et al., 2020; Sha et al., 2021). These aforementioned proteins or genes not only have the chance to

serve as novel biomarkers to predict efficacy and prognosis but are expected to become potential treatment methods for TNBC, reducing the proliferation, migration, and invasion ability of TNBC.

## Ferroptosis and Neurological System Tumors

Ferroptosis plays an incomparable key role in the characteristics and biological behavior of nervous system tumors, especially gliomas and neuroblastoma. In other words, the mechanism of ferroptosis in gliomas and neuroblastoma deserves further exploration.

One study, through analyzing 19 ferroptosis-associated genes in gliomas, found that they are closely associated with the malignancy, immunity, migration, progression, and death of gliomas. This also indicates that they are potential prognostic markers and therapeutic targets for glioma, which have a milestone significance for predicting overall survival in glioma patients and understanding the underlying mechanisms of ferroptosis (Liu et al., 2020). Chen, D. et al. manifested that in glioma, with the increase of ATF4 expression, the expression of xCT is up-regulated, resulting in three major effects. First, normal nerve cells die at an increased rate. Second, tumor cells become less sensitive to ferroptosis. Third, tumor angiogenesis and vascular structure were enhanced (Chen et al., 2017a; Chen et al., 2017b). Similarly, overexpression of NRF2 can change the tumor microenvironment, reducing the sensitivity of the tumors to ferroptosis and ferroptosis inducers and promoting tumor proliferation and migration. Concerning the glioma treatment process with Dihydroartemisinin (DHA), the PERK-ATF4 negative feedback pathway is activated. HSPA5 and GPX4 are induced to express. Most importantly, the possibility of ferroptosis of glioma cells is largely avoided. As a result, inhibition of the PERK-ATF4 pathway has a chance to significantly improve the efficiency of DHA in treating glioma (Chen et al., 2019; Yi R. et al., 2020).

Neuroblastoma, as MYC gene-driven tumors, is mainly characterized by malignancy, which is highly metastatic and prone to recurrence. Studies have shown that neuroblastoma with high expression of MYCN gene is highly dependent on cysteine and sensitive to ferroptosis. Thus, neuroblastoma can trigger ferroptosis due to cysteine deficiency and inhibition of ferroptosis by blocking cysteine uptake, transsulfuration, and inhibition of GPX4. This suggests that simultaneous targeting of multiple ferroptosis-related targets has the potential to be an effective treatment for MYCN-driven tumor therapy (Alborzinia et al., 2022).

## Ferroptosis and Melanoma

Although targeted therapy and immunotherapy have greatly improved the survival rate of melanoma patients, there are still cases of relapse and treatment failure. The discovery of ferroptosis offers hope of solving the problem. Luo, M. et al. showed that miR-137 knockdown can target SLC1A5, reducing glutamine uptake and malondialdehyde (MDA) accumulation. Finally, melanoma cells are killed by drugs due to increased

**TABLE 1 |** Introduction of the more innovative methods and their respective advantages and disadvantages.

Approaches	Characteristics	Advantages	Disadvantages
Aniline-derived Probe	Lipid-derived electrophiles (LDEs) produced by Ferroptosis can influence the protein function in the manner of covalently modifying the protein. Aniline-derived probe can detect protein carbonylations and novel cysteine sites in the process of cell ferroptosis.	<ol style="list-style-type: none"> <li>1. This is a commercial compound that is cheap and easy to obtain</li> <li>2. Compared with classic hydrazine and hydroxylamine probes, it has higher sensitivity and is very suitable for studying endogenous carbonylation modifications with weak signals</li> <li>3. The chemical properties of the adduct of the aniline probe and the peptide are very stable, which can avoid fragmentation during sample preparation and computer application.</li> </ol>	—
Arginine-rich manganese silicate nanobubbles (AMSNs)	AMSNs is a novel tumor targeted nanoparticle that inhibits the growth of cancer cells by effectively consuming glutathione and synergistic chemotherapy drugs. During this process, the ferroptosis pathway is activated.	<ol style="list-style-type: none"> <li>1. The particle size of nanobubbles is about 6.2 nm, and the potential is -17.6mv. It has a high specific surface area, porosity, colloidal stability, long half-life (4.07 h) and tumor targeting recognition function. Its lethal effect is significantly lower than that of cancer cells</li> <li>2. AMSNs have better degradability than solid nanomaterials (such as MnO). In the process of consuming GSH, the color of AMSNs solution gradually becomes lighter, while the color of solid nanomaterials changes less, indicating that manganese ions in AMSNs are released faster and more easily degraded</li> <li>3. AMSNs, as a contrast agent for NMR, are easily degraded in the microenvironment of tumor cells (weak acid and high GSH concentration) and produce Mn (II) to help enhance the contrast effect of NMR T1-weighted imaging. AMSNs can be used as anti-cancer drug carriers or anti-cancer agents, effectively inhibiting the growth of cancer cells</li> </ol>	<ol style="list-style-type: none"> <li>1. There is still a challenge to kill cancer by consuming GSH because of the low consumption rate of GSH.</li> </ol>
Covalent inhibitor that selectively targets GPX4	The author synthesized a series of GPX4 covalent inhibitors containing electrophilic warhead and nitrile oxidation to selectively inhibit GPX4 activity and induce ferroptosis in drug-resistant tumor cells. This is a novel highly selective probe molecule for GPX4-mediated detection, providing a strategy for broadening the selection of covalent inhibitor warheads.	<ol style="list-style-type: none"> <li>1. Compared with the previous covalent inhibitor-containing chloroacetamide, it has significantly superior pharmacokinetic properties</li> <li>2. It can more specifically induce cell ferroptosis through GPX4, and the signal pathway is single and clear. It is more suitable as a probe to study related pathways</li> </ol>	<ol style="list-style-type: none"> <li>1. JKE-1674, the intermediate of ML-210, will decompose when stored in DMSO for a long time.</li> </ol>
Dual-function fluorescent probe (H-V)	The H-V probe can be used to detect the cytoplasmic Viscosity and OH changes during ferroptosis with a typical molecular rotor structure. With the increase of microenvironmental viscosity, the fluorescence of the probe was enhanced.	<ol style="list-style-type: none"> <li>1. The unique hydroxylation of OH on aromatic compounds results in high selectivity</li> <li>2. A strong electron-donating methoxy group is added to enhance the H-V probe's capture ability of OH, thereby improving the detection sensitivity</li> <li>3. The probe can work more effectively in the cytoplasm. The probe can detect viscosity and OH in two independent channels</li> <li>4. It has good biocompatibility</li> </ol>	—
SRF@FeIIITA nanoparticles	SRF@FeIIITA nanoparticles are formed by the self-assembly of iron ions ( $\text{Fe}^{3+}$ ) and tannic acid (TA) on the surface of sorafenib nanocrystals. SRF inhibits GPX4 to induce ferroptosis. The $\text{Fe}^{2+}$ sustainably reduced from TA was toxic to cancer cells. The photosensitizers assist in photodynamic therapy in conjunction with ferroptosis.	<ol style="list-style-type: none"> <li>1. The prepared nanomedicine selectively causes ferroptosis of tumor cells, which is low cytotoxicity</li> <li>2. Many functional substances can adhere to the surface of polyphenols to facilitate the expansion of deep applications based on ferroptosis treatment methods</li> </ol>	—
Hypoxia-responsive micelles	Hypoxia-responsive micelles, acting as ferroptosis inducers, promote ferroptosis against solid tumors by reducing glutathione and thioredoxin in hypoxia.	<ol style="list-style-type: none"> <li>1. Compared with other chemotherapeutic drugs (including procaspase-3 agonist, PAC-1, 1541B, nucleoside analog gemcitabine, 5-F, etc.), the median lifetimewas found to be short</li> <li>2. The same dose of these compounds showed better than RSL3 and Erastin in inhibiting the proliferation of HCT116 and A549 cancer cells</li> <li>3. These compounds exert their ability to inhibit tumor proliferation by inducing ferroptosis in tumor cells.</li> <li>4. Novel structure and excellent activity.</li> </ol>	—

sensitivity to Erastin and RSL3-induced ferroptosis (Luo et al., 2018). When melanoma cells express ACSL3, the protective effect of oleic acid on Erastin-induced ferroptosis is restored. In other words, the protection of oleic acid on tumor cells depends on ACSL3. In addition, the lymphatic environment also contributes to inhibiting ferroptosis and improves the survival of tumor cells, making it easier for tumors to metastasize distally (Ubellacker et al., 2020). Tsoi, J. et al. suggested that dedifferentiated melanoma cells are extraordinarily sensitive to ferroptosis inducers despite their obvious resistance to mitogen-activated protein kinase pathway inhibitors. Melanoma can be effectively treated with a combination of anti-melanoma drugs and ferroptosis inducers (Tsoi et al., 2018).

## FERROPTOSIS AND TUMOR IMMUNOTHERAPY

Tumor immunotherapy is an incredibly innovative treatment for cancer today, which has the advantages of stronger targeting and fewer side effects (Li et al., 2020; Lin et al., 2020; Tan et al., 2020; Xu et al., 2020; Wu et al., 2021; Xu et al., 2022). Although it has incomparable advantages compared with other traditional therapies, there are still problems of poor efficacy and drug resistance (Liu X. et al., 2021; Dey et al., 2021; Repellin et al., 2021; Xiong et al., 2021). As research progresses, it is revealed that immunotherapy combined with therapies that activate ferroptosis will kill tumor cells more efficiently and quickly.

- 1) Zhang, H.L. et al. found that PKC $\beta$ II, a sensory molecule of lipid peroxidation, promotes PUFA-phospholipid peroxide accumulation by activating ACSL4, initiating the process of inducing tumor ferroptosis. After the continuous operation of the lipid peroxide-PKC $\beta$ II-ACSL4 positive feedback axis, tumor sensitivity to PD-1 antibody is significantly increased and the efficacy of immunotherapy is enhanced (Zhang et al., 2022).
- 2) Wang, W. et al. demonstrated that the number of CD8 (+) T cells and IFN- $\gamma$  expression are positively correlated with the treatment prognosis of cancer patients. IFN- $\gamma$  released by CD8 (+) T cells inhibits the expression of system Xc-, SLC3A2 and SLC7A11, thus blocking the uptake of cystine by tumor cells. This pathway enhances lipid peroxidation and promotes ferroptosis. The combination of anti-PD-L1 immunotherapy and cyst(e)kinase can effectively achieve anti-tumor immunity (Wang et al., 2019).
- 3) Other studies have shown that high expression and phosphorylation of TYRO3 are significantly associated with resistance to immune checkpoint inhibitors and the creation of an anti-inflammatory tumor microenvironment. TYRO3 protects tumor cells from ferroptosis through the AKT-NRF2 pathway and leads to a poor prognosis for various cancers. The combination of TYRO3-targeted drugs and anti-PD-1 drugs can not only overcome drug resistance but also reduce the therapeutic toxicity and improve the therapeutic efficacy of patients (Jiang Z. et al., 2021; Deng et al., 2022).

- 4) It was found that radiotherapy enhances the sensitivity of lipid peroxidation and ferroptosis by down-regulating SLC7A11 and up-regulating ACSL4 (Lang et al., 2019). In brief, radiotherapy combined with immunotherapy is conducive to treat cancer effectively (Lei et al., 2021).
- 5) Ma, X. et al. found that CD8 (+) T cells induce lipid peroxidation and ferroptosis mediated by CD36, resulting in reduced production of cytotoxic factors and antitumor ability of CD8 (+) T cells. Targeting CD36 restores the ability of CD8 (+) T cells to participate in tumor immunotherapy (Ma et al., 2021; Aksoylar and Patsoukis, 2022; Zhu et al., 2022).

In conclusion, the combination of immunotherapy and ferroptosis inducer has opened up a new way of thinking and strategy for cancer treatment, which will be a milestone in the improvement of cancer treatment.

## OTHER NOVEL TREATMENT ASSOCIATED WITH FERROPTOSIS

In addition to immunotherapy, many other advanced therapies conduce to induce ferroptosis and promote tumor cell development, deserving our understanding and attention. Currently, the preparation of probes and nanomedicine particles has helped to locate and observe ferroptosis and target tumor cells with precision therapy. Aniline-derived probe (Chen et al., 2018) and H-V probe (Li et al., 2019) can observe the changes of ferroptosis on cancer cells. Arginine-rich manganese silicate nanobubbles (AMSNs) (Wang et al., 2018), GPX4 covalent inhibitors (Eaton et al., 2020), SRF@FeIITA nanoparticles (Liu et al., 2018) and hypoxia-responsive micelles (Guo et al., 2020) achieve the purpose of precise treatment of tumors. There is no doubt that, compared with the previous methods, they have their advantages and disadvantages (Table 1).

## CONCLUSION AND OUTLOOK

In summary, the discovery of ferroptosis is of epoch-making significance as it participates in the regulation of cancer in various systems through its complex mechanism (Xie et al., 2016). Researchers have developed novel therapeutic modalities based on key targets of ferroptosis pathways that complement traditional therapies and have achieved impressive results in improving treatment success, survival, and anti-tumor drug resistance in cancer patients (Chen et al., 2021b). However, ferroptosis still needs a lot of further research, especially the physiological and pathological effects, gene expression, and regulation involved in ferroptosis. First, in addition to the currently known pathway of ferroptosis, some other factors or pathways mediate ferroptosis and tumor metabolism. Second, whether there is some connection between ferroptosis and other cell death modes, such as autophagy and programmed cell death, to mediate the

occurrence and development of tumors and other diseases. Third, further identification of ferroptosis-related biomarkers will contribute greatly to applying ferroptosis-based therapies to clinical cancer patients as soon as possible, as well as making precise and personalized treatment plans. Fourth, it is high time that there is a need to explore ferroptosis in association with other therapies to broaden tumor treatment regimens and slow disease progressions, such as immunotherapy, chemotherapy, and radiotherapy. Whether additional toxicity, drug resistance, and adaptation are generated during combination therapy is of public and scientific concern. The link between ferroptosis and cancer is a burgeoning area that still needs to be detected, and we still have a long way to go in the future (Wang et al., 2022).

## REFERENCES

- Abrams, R. P., Carroll, W. L., and Woerpel, K. A. (2016). Five-Membered Ring Peroxide Selectively Initiates Ferroptosis in Cancer Cells. *ACS Chem. Biol.* 11, 1305–1312. doi:10.1021/acschembio.5b00900
- Aksoylar, H. I., and Patsoukis, N. (2022). Treatment with Exogenously Added Catalase Alters CD8 T Cell Memory Differentiation and Function. *Adv. Biol. (Weinh)* [Online ahead of print], e2101320. doi:10.1002/adbi.202101320
- Alborzinia, H., Flórez, A. F., Kreth, S., Brückner, L. M., Yildiz, U., Gartlgruber, M., et al. (2022). MYCN Mediates Cysteine Addiction and Sensitizes Neuroblastoma to Ferroptosis. *Nat. Cancer* 3, 471–485. doi:10.1038/s43018-022-00355-4
- Alvarez, S. W., Sviderskiy, V. O., Terzi, E. M., Papagiannakopoulos, T., Moreira, A. L., Adams, S., et al. (2017). NFS1 Undergoes Positive Selection in Lung Tumours and Protects Cells from Ferroptosis. *Nature* 551, 639–643. doi:10.1038/nature24637
- Anthonyamuthu, T. S., Kenny, E. M., Shrivastava, I., Tyurina, Y. Y., Hier, Z. E., Ting, H.-C., et al. (2018). Empowerment of 15-Lipoxygenase Catalytic Competence in Selective Oxidation of Membrane ETE-PE to Ferroptotic Death Signals, HpETE-PE. *J. Am. Chem. Soc.* 140, 17835–17839. doi:10.1021/jacs.8b09913
- Badgley, M. A., Kremer, D. M., Maurer, H. C., DelGiorno, K. E., Lee, H.-J., Purohit, V., et al. (2020). Cysteine Depletion Induces Pancreatic Tumor Ferroptosis in Mice. *Science* 368, 85–89. doi:10.1126/science.aaw9872
- Berns, A. (2005). Stem Cells for Lung Cancer? *Cell* 121, 811–813. doi:10.1016/j.cell.2005.06.004
- Bersuker, K., Hendricks, J. M., Li, Z., Magtanong, L., Ford, B., Tang, P. H., et al. (2019). The CoQ Oxidoreductase FSP1 Acts Parallel to GPX4 to Inhibit Ferroptosis. *Nature* 575, 688–692. doi:10.1038/s41586-019-1705-2
- Chen, D., Chu, B., Yang, X., Liu, Z., Jin, Y., Kon, N., et al. (2021). iPLA2 $\beta$ -mediated Lipid Detoxification Controls P53-Driven Ferroptosis Independent of GPX4. *Nat. Commun.* 12, 3644. doi:10.1038/s41467-021-23902-6
- Chen, X., Kang, R., Kroemer, G., and Tang, D. (2021a). Broadening Horizons: the Role of Ferroptosis in Cancer. *Nat. Rev. Clin. Oncol.* 18, 280–296. doi:10.1038/s41571-020-00462-0
- Chen, X., Kang, R., Kroemer, G., and Tang, D. (2021b). Targeting Ferroptosis in Pancreatic Cancer: a Double-Edged Sword. *Trends Cancer* 7, 891–901. doi:10.1016/j.trecan.2021.04.005
- Chen, D., Fan, Z., Rauh, M., Buchfelder, M., Eyupoglu, I. Y., and Savaskan, N. (2017a). ATF4 Promotes Angiogenesis and Neuronal Cell Death and Confers Ferroptosis in a xCT-dependent Manner. *Oncogene* 36, 5593–5608. doi:10.1038/onc.2017.146
- Chen, D., Rauh, M., Buchfelder, M., Eyupoglu, I. Y., and Savaskan, N. (2017b). The Oxido-Metabolic Driver ATF4 Enhances Temozolamide Chemo-Resistance in Human Gliomas. *Oncotarget* 8, 51164–51176. doi:10.18632/oncotarget.17737
- Chen, Y., Liu, Y., Lan, T., Qin, W., Zhu, Y., Qin, K., et al. (2018). Quantitative Profiling of Protein Carbonylations in Ferroptosis by an Aniline-Derived Probe. *J. Am. Chem. Soc.* 140, 4712–4720. doi:10.1021/jacs.8b01462
- Chen, Y., Mi, Y., Zhang, X., Ma, Q., Song, Y., Zhang, L., et al. (2019). Dihydroartemisinin-induced Unfolded Protein Response Feedback Attenuates Ferroptosis via PERK/ATF4/HSPA5 Pathway in Glioma Cells. *J. Exp. Clin. Cancer Res.* 38, 402. doi:10.1186/s13046-019-1413-7
- Chu, B., Kon, N., Chen, D., Li, T., Liu, T., Jiang, L., et al. (2019). ALOX12 Is Required for P53-Mediated Tumour Suppression through a Distinct Ferroptosis Pathway. *Nat. Cell Biol.* 21, 579–591. doi:10.1038/s41556-019-0305-6
- Cordani, M., Oppici, E., Dando, I., Butturini, E., Dalla Pozza, E., Nadal-Serrano, M., et al. (2016). Mutant P53 Proteins Counteract Autophagic Mechanism Sensitizing Cancer Cells to mTOR Inhibition. *Mol. Oncol.* 10, 1008–1029. doi:10.1016/j.molonc.2016.04.001
- Courtney, K. D., Ma, Y., Diaz de Leon, A., Christie, A., Xie, Z., Woolford, L., et al. (2020). HIF-2 Complex Dissociation, Target Inhibition, and Acquired Resistance with PT2385, a First-In-Class HIF-2 Inhibitor, in Patients with Clear Cell Renal Cell Carcinoma. *Clin. Cancer Res.* 26, 793–803. doi:10.1158/1078-0432.ccr-19-1459
- Cui, W., Liu, D., Gu, W., and Chu, B. (2021). Peroxisome-driven Ether-Linked Phospholipids Biosynthesis Is Essential for Ferroptosis. *Cell Death Differ.* 28, 2536–2551. doi:10.1038/s41418-021-00769-0
- Dai, E., Han, L., Liu, J., Xie, Y., Zeh, H. J., Kang, R., et al. (2020). Ferroptotic Damage Promotes Pancreatic Tumorigenesis through a TMEM173/STING-dependent DNA Sensor Pathway. *Nat. Commun.* 11, 6339. doi:10.1038/s41467-020-20154-8
- Deng, J., Zhou, M., Liao, T., Kuang, W., Xia, H., Yin, Z., et al. (2022). Targeting Cancer Cell Ferroptosis to Reverse Immune Checkpoint Inhibitor Therapy Resistance. *Front. Cell Dev. Biol.* 10, 818453. doi:10.3389/fcell.2022.818453
- Dey, M., Ayan, B., Yurieva, M., Unutmaz, D., and Ozbolat, I. T. (2021). Studying Tumor Angiogenesis and Cancer Invasion in a Three-Dimensional Vascularized Breast Cancer Micro-Environment. *Adv. Biol. (Weinh)* 5, e2100090. doi:10.1002/adbi.202100090
- Dinarvand, N., Khanahmad, H., Hakimian, S. M., Sheikhi, A., Rashidi, B., and Pourfarzam, M. (2020). Evaluation of Long-Chain Acyl-Coenzyme A Synthetase 4 (ACSL4) Expression in Human Breast Cancer. *Res. Pharm. Sci.* 15, 48–56. doi:10.4103/1735-5362.278714
- Ding, H., Chen, S., Pan, X., Dai, X., Pan, G., Li, Z., et al. (2021). Transferrin Receptor 1 Ablation in Satellite Cells Impedes Skeletal Muscle Regeneration through Activation of Ferroptosis. *J. Cachexia Sarcopenia Muscle* 12, 746–768. doi:10.1002/jcsm.12700
- Dixon, S. J., Lemberg, K. M., Lamprecht, M. R., Skouta, R., Zaitsev, E. M., Gleason, C. E., et al. (2012). Ferroptosis: an Iron-dependent Form of Nonapoptotic Cell Death. *Cell* 149, 1060–1072. doi:10.1016/j.cell.2012.03.042
- Doll, S., and Conrad, M. (2017). Iron and Ferroptosis: A Still Ill-Defined Liaison. *IUBMB Life* 69, 423–434. doi:10.1002/iub.1616
- Doll, S., Freitas, F. P., Shah, R., Aldrovandi, M., da Silva, M. C., Ingold, I., et al. (2019). FSP1 Is a Glutathione-independent Ferroptosis Suppressor. *Nature* 575, 693–698. doi:10.1038/s41586-019-1707-0

## AUTHOR CONTRIBUTIONS

XZ and ZL designed this study and supervised the research. ST wrote the manuscript. YK, YXi, PG, YXu, CW, PL, WY, and XZ discussed the manuscript. ST, YK and XZ edited the manuscript. All authors read and approved the final manuscript.

## FUNDING

The National Natural Science Foundation of China (81972366); Guangdong Key Laboratory funds of Systems Biology and Synthetic Biology for Urogenital Tumors (2017B030301015 and 2020B030301015-3).



- Eaton, J. K., Furst, L., Cai, L. L., Viswanathan, V. S., and Schreiber, S. L. (2020). Structure-Activity Relationships of GPX4 Inhibitor Warheads. *Bioorg. Med. Chem. Lett.* 30, 127538. doi:10.1016/j.bmcl.2020.127538
- Fan, F., Liu, P., Bao, R., Chen, J., Zhou, M., Mo, Z., et al. (2021). A Dual PI3K/HDAC Inhibitor Induces Immunogenic Ferroptosis to Potentiate Cancer Immune Checkpoint Therapy. *Cancer Res.* 81, 6233–6245. doi:10.1158/0008-5472.can-21-1547
- Fang, X., Wang, H., Han, D., Xie, E., Yang, X., Wei, J., et al. (2019). Ferroptosis as a Target for Protection against Cardiomyopathy. *Proc. Natl. Acad. Sci. U.S.A.* 116, 2672–2680. doi:10.1073/pnas.1821022116
- Fruman, D. A., Chiu, H., Hopkins, B. D., Bagrodia, S., Cantley, L. C., and Abraham, R. T. (2017). The PI3K Pathway in Human Disease. *Cell* 170, 605–635. doi:10.1016/j.cell.2017.07.029
- Gai, C., Yu, M., Li, Z., Wang, Y., Ding, D., Zheng, J., et al. (2020). Acetaminophen Sensitizing Erastin-Induced Ferroptosis via Modulation of Nrf2/Heme Oxygenase-1 Signaling Pathway in Non-Small-Cell Lung Cancer. *J. Cell Physiol.* 235, 3329–3339. doi:10.1002/jcp.29221
- Gao, M., Yi, J., Zhu, J., Minikes, A. M., Monian, P., Thompson, C. B., et al. (2019). Role of Mitochondria in Ferroptosis. *Mol. Cell* 73, 354–363. doi:10.1016/j.molcel.2018.10.042
- Gaschler, M. M., Hu, F., Feng, H., Linkermann, A., Min, W., and Stockwell, B. R. (2018). Determination of the Subcellular Localization and Mechanism of Action of Ferrostatins in Suppressing Ferroptosis. *ACS Chem. Biol.* 13, 1013–1020. doi:10.1021/acscmbio.8b00199
- Guo, X., Liu, F., Deng, J., Dai, P., Qin, Y., Li, Z., et al. (2020). Electron-Accepting Micelles Deplete Reduced Nicotinamide Adenine Dinucleotide Phosphate and Impair Two Antioxidant Cascades for Ferroptosis-Induced Tumor Eradication. *ACS Nano* 14, 14715–14730. doi:10.1021/acsnano.0c00764
- Han, X., Fan, Z., Yu, Y., Liu, S., Hao, Y., Huo, R., et al. (2013). Expression and Characterization of Recombinant Human Phospholipid Hydroperoxide Glutathione Peroxidase. *IUBMB Life* 65, 951–956. doi:10.1002/iub.1220
- Hardie, D. G., Ross, F. A., and Hawley, S. A. (2012). AMPK: a Nutrient and Energy Sensor that Maintains Energy Homeostasis. *Nat. Rev. Mol. Cell Biol.* 13, 251–262. doi:10.1038/nrm3311
- Hasegawa, M., Takahashi, H., Rajabi, H., Alam, M., Suzuki, Y., Yin, L., et al. (2016). Functional Interactions of the Cystine/Glutamate Antiporter, CD44v and MUC1-C Oncoprotein in Triple-Negative Breast Cancer Cells. *Oncotarget* 7, 11756–11769. doi:10.18632/oncotarget.7598
- Hassannia, B., Vandenabeele, P., and Vanden Berghe, T. (2019). Targeting Ferroptosis to Iron Out Cancer. *Cancer Cell* 35, 830–849. doi:10.1016/j.ccell.2019.04.002
- Hoefflin, R., Harlander, S., Schäfer, S., Metzger, P., Kuo, F., Schönerberger, D., et al. (2020). HIF-1 $\alpha$  and HIF-2 $\alpha$  Differently Regulate Tumour Development and Inflammation of Clear Cell Renal Cell Carcinoma in Mice. *Nat. Commun.* 11, 4111. doi:10.1038/s41467-020-17873-3
- Hou, W., Xie, Y., Song, X., Sun, X., Lotze, M. T., Zeh, H. J., 3rd, et al. (2016). Autophagy Promotes Ferroptosis by Degradation of Ferritin. *Autophagy* 12, 1425–1428. doi:10.1080/15548627.2016.1187366
- Hou, Y., Cai, S., Yu, S., and Lin, H. (2021). Metformin Induces Ferroptosis by Targeting miR-324-3p/GPX4 axis in Breast Cancer. *Acta Biochim. Biophys. Sin. (Shanghai)* 53, 333–341. doi:10.1093/abbs/gmaa180
- Hwang, J. S., Kim, E., Lee, H. G., Lee, W. J., Won, J. P., Hur, J., et al. (2021). Peroxisome Proliferator-Activated Receptor  $\delta$  Rescues xCT-Deficient Cells from Ferroptosis by Targeting Peroxisomes. *Biomed. Pharmacother.* 143, 112223. doi:10.1016/j.biopha.2021.112223
- Ingold, I., Berndt, C., Schmitt, S., Doll, S., Poschmann, G., Buday, K., et al. (2018). Selenium Utilization by GPX4 Is Required to Prevent Hydroperoxide-Induced Ferroptosis. *Cell* 172, 409–422. doi:10.1016/j.cell.2017.11.048
- Jiang, L., Kon, N., Li, T., Wang, S.-J., Su, T., Hibshoosh, H., et al. (2015). Ferroptosis as a P53-Mediated Activity during Tumour Suppression. *Nature* 520, 57–62. doi:10.1038/nature14344
- Jiang, X., Stockwell, B. R., and Conrad, M. (2021). Ferroptosis: Mechanisms, Biology and Role in Disease. *Nat. Rev. Mol. Cell Biol.* 22, 266–282. doi:10.1038/s41580-020-00324-8
- Jiang, X., Lim, S. O., Yan, M., Hsu, J. L., Yao, J., Wei, Y., et al. (2021). TYRO3 Induces Anti-PD-1/pd-L1 Therapy Resistance by Limiting Innate Immunity and Tumoral Ferroptosis. *J. Clin. Invest.* 131, e139434. doi:10.1172/jci139434
- Kang, Y. P., Mockabee-Macias, A., Jiang, C., Falzone, A., Prieto-Farigua, N., Stone, E., et al. (2021). Non-canonical Glutamate-Cysteine Ligase Activity Protects against Ferroptosis. *Cell Metab.* 33, 174–189. doi:10.1016/j.cmet.2020.12.007
- Kerins, M. J., Milligan, J., Wohlschlegel, J. A., and Ooi, A. (2018). Fumarate Hydratase Inactivation in Hereditary Leiomyomatosis and Renal Cell Cancer Is Synthetic Lethal with Ferroptosis Induction. *Cancer Sci.* 109, 2757–2766. doi:10.1111/cas.13701
- Kruiswijk, F., Labuschagne, C. F., and Voudsen, K. H. (2015). p53 in Survival, Death and Metabolic Health: a Lifeguard with a Licence to Kill. *Nat. Rev. Mol. Cell Biol.* 16, 393–405. doi:10.1038/nrm4007
- Lai, Y., Lin, F., Wang, X., Zhang, J., Xia, J., Sun, Y., et al. (2021). STYK1/NOK Promotes Metastasis and Epithelial-Mesenchymal Transition in Non-small Cell Lung Cancer by Suppressing FoxO1 Signaling. *Front. Cell Dev. Biol.* 9, 621147. doi:10.3389/fcell.2021.621147
- Lang, X., Green, M. D., Wang, W., Yu, J., Choi, J. E., Jiang, L., et al. (2019). Radiotherapy and Immunotherapy Promote Tumoral Lipid Oxidation and Ferroptosis via Synergistic Repression of SLC7A11. *Cancer Discov.* 9, 1673–1685. doi:10.1158/2159-8290.cd-19-0338
- Lee, H., Zandkarimi, F., Zhang, Y., Meena, J. K., Kim, J., Zhuang, L., et al. (2020). Energy-Stress-Mediated AMPK Activation Inhibits Ferroptosis. *Nat. Cell Biol.* 22, 225–234. doi:10.1038/s41556-020-0461-8
- Lee, N., Carlisle, A. E., Peppers, A., Park, S. J., Doshi, M. B., Spears, M. E., et al. (2021). xCT-Driven Expression of GPX4 Determines Sensitivity of Breast Cancer Cells to Ferroptosis Inducers. *Antioxidants (Basel)* 10, 317. doi:10.3390/antiox10020317
- Lei, G., Mao, C., Yan, Y., Zhuang, L., and Gan, B. (2021). Ferroptosis, Radiotherapy, and Combination Therapeutic Strategies. *Protein Cell* 12, 836–857. doi:10.1007/s13238-021-00841-y
- Lei, G., Zhang, Y., Koppula, P., Liu, X., Zhang, J., Lin, S. H., et al. (2020). The Role of Ferroptosis in Ionizing Radiation-Induced Cell Death and Tumor Suppression. *Cell Res.* 30, 146–162. doi:10.1038/s41422-019-0263-3
- Li, H., Shi, W., Li, X., Hu, Y., Fang, Y., and Ma, H. (2019). Ferroptosis Accompanied by  $\bullet$ OH Generation and Cytoplasmic Viscosity Increase Revealed via Dual-Functional Fluorescence Probe. *J. Am. Chem. Soc.* 141, 18301–18307. doi:10.1021/jacs.9b09722
- Li, S., Zhang, Z., Lai, W.-F., Cui, L., and Zhu, X. (2020). How to Overcome the Side Effects of Tumor Immunotherapy. *Biomed. Pharmacother.* 130, 110639. doi:10.1016/j.biopha.2020.110639
- Li, Y., and Seto, E. (2016). HDACs and HDAC Inhibitors in Cancer Development and Therapy. *Cold Spring Harb. Perspect. Med.* 6, a026831. doi:10.1101/cshperspect.a026831
- Liao, Y.-F., Zhu, W., Li, D. P., and Zhu, X. (2013). Heme Oxygenase-1 and Gut Ischemia/Reperfusion Injury: A Short Review. *World J. Gastroenterol.* 19, 3555–3561. doi:10.3748/wjg.v19.i23.3555
- Lin, B., Du, L., Li, H., Zhu, X., Cui, L., and Li, X. (2020). Tumor-infiltrating Lymphocytes: Warriors Fight against Tumors Powerfully. *Biomed. Pharmacother.* 132, 110873. doi:10.1016/j.biopha.2020.110873
- Lin, C.-C., Yang, W.-H., Lin, Y.-T., Tang, X., Chen, P.-H., Ding, C.-K. C., et al. (2021). DDR2 Upregulation Confers Ferroptosis Susceptibility of Recurrent Breast Tumors through the Hippo Pathway. *Oncogene* 40, 2018–2034. doi:10.1038/s41388-021-01676-x
- Lin, Z., Liu, J., Kang, R., Yang, M., and Tang, D. (2021). Lipid Metabolism in Ferroptosis. *Adv. Biol. (Weinh)* 5, e2100396. doi:10.1002/adbi.202100396
- Liu, H.-j., Hu, H.-m., Li, G.-z., Zhang, Y., Wu, F., Liu, X., et al. (2020). Ferroptosis-Related Gene Signature Predicts Glioma Cell Death and Glioma Patient Progression. *Front. Cell Dev. Biol.* 8, 538. doi:10.3389/fcell.2020.00538
- Liu, T., Liu, W., Zhang, M., Yu, W., Gao, F., Li, C., et al. (2018). Ferrous-Supply-Regeneration Nanoengineering for Cancer-cell-specific Ferroptosis in Combination with Imaging-Guided Photodynamic Therapy. *ACS Nano* 12, 12181–12192. doi:10.1021/acsnano.8b05860
- Liu, X., Li, Z., and Wang, Y. (2021). Advances in Targeted Therapy and Immunotherapy for Pancreatic Cancer. *Adv. Biol. (Weinh)* 5, e1900236. doi:10.1002/adbi.201900236
- Liu, Y., Song, Z., Liu, Y., Ma, X., Wang, W., Ke, Y., et al. (2021). Identification of Ferroptosis as a Novel Mechanism for Antitumor Activity of Natural Product Derivative A2 in Gastric Cancer. *Acta Pharm. Sin. B* 11, 1513–1525. doi:10.1016/j.apsb.2021.05.006

- Louandre, C., Marcq, I., Bouhlal, H., Lachaier, E., Godin, C., Saidak, Z., et al. (2015). The Retinoblastoma (Rb) Protein Regulates Ferroptosis Induced by Sorafenib in Human Hepatocellular Carcinoma Cells. *Cancer Lett.* 356, 971–977. doi:10.1016/j.canlet.2014.11.014
- Lu, J., Xu, F., and Lu, H. (2020). lncRNA PVT1 Regulates Ferroptosis through miR-214-Mediated TFR1 and P53. *Life Sci.* 260, 118305. doi:10.1016/j.lfs.2020.118305
- Luis, G., Godfroid, A., Nishiumi, S., Cimino, J., Blacher, S., Maquoi, E., et al. (2021). Tumor Resistance to Ferroptosis Driven by Stearoyl-CoA Desaturase-1 (SCD1) in Cancer Cells and Fatty Acid Binding Protein-4 (FABP4) in Tumor Microenvironment Promote Tumor Recurrence. *Redox Biol.* 43, 102006. doi:10.1016/j.redox.2021.102006
- Luo, M., Wu, L., Zhang, K., Wang, H., Zhang, T., Gutierrez, L., et al. (2018). miR-137 Regulates Ferroptosis by Targeting Glutamine Transporter SLC1A5 in Melanoma. *Cell Death Differ.* 25, 1457–1472. doi:10.1038/s41418-017-0053-8
- Ma, X., Xiao, L., Liu, L., Ye, L., Su, P., Bi, E., et al. (2021). CD36-mediated Ferroptosis Dampens Intratumoral CD8<sup>+</sup> T Cell Effector Function and Impairs Their Antitumor Ability. *Cell Metab.* 33, 1001–1012. doi:10.1016/j.cmet.2021.02.015
- Malfa, G. A., Tomasello, B., Acquaviva, R., Genovese, C., La Mantia, A., Cammarata, F. P., et al. (2019). Betula Etnensis Raf. (Betulaceae) Extract Induced HO-1 Expression and Ferroptosis Cell Death in Human Colon Cancer Cells. *Int. J. Mol. Sci.* 20, 2723. doi:10.3390/ijms20112723
- Mao, C., Liu, X., Zhang, Y., Lei, G., Yan, Y., Lee, H., et al. (2021). DHODH-Mediated Ferroptosis Defence Is a Targetable Vulnerability in Cancer. *Nature* 593, 586–590. doi:10.1038/s41586-021-03539-7
- Mao, C., Wang, X., Liu, Y., Wang, M., Yan, B., Jiang, Y., et al. (2018). A G3BP1-Interacting lncRNA Promotes Ferroptosis and Apoptosis in Cancer via Nuclear Sequestration of P53. *Cancer Res.* 78, 3484–3496. doi:10.1158/0008-5472.can-17-3454
- Miess, H., Dankworth, B., Gouw, A. M., Rosenfeldt, M., Schmitz, W., Jiang, M., et al. (2018). The Glutathione Redox System Is Essential to Prevent Ferroptosis Caused by Impaired Lipid Metabolism in Clear Cell Renal Cell Carcinoma. *Oncogene* 37, 5435–5450. doi:10.1038/s41388-018-0315-z
- Nieto-Garai, J. A., Contreras, F. X., Arbolea, A., and Lorizate, M. (2022). Role of Protein-Lipid Interactions in Viral Entry. *Adv. Biol. (Weinh)* 6, e2101264. doi:10.1002/adbi.202101264
- Nurtjahja-Tjendraputra, E., Fu, D., Phang, J. M., and Richardson, D. R. (2007). Iron Chelation Regulates Cyclin D1 Expression via the Proteasome: a Link to Iron Deficiency-Mediated Growth Suppression. *Blood* 109, 4045–4054. doi:10.1182/blood-2006-10-047753
- Ou, Y., Wang, S. J., Li, D., Chu, B., and Gu, W. (2016). Activation of SAT1 Engages Polyamine Metabolism with P53-Mediated Ferroptotic Responses. *Proc. Natl. Acad. Sci. U. S. A.* 113, E6806–E6812. doi:10.1073/pnas.1607152113
- Repellin, C. E., Ssemadaali, M. A., Newmyer, S., Radhakrishnan, H., Javitz, H. S., and Bhatnagar, P. (2021). NK-cell Biofactory as an Off-The-Shelf Cell-Based Vector for Targeted *In Situ* Synthesis of Engineered Proteins. *Adv. Biol. (Weinh)* 5, e2000298. doi:10.1002/adbi.202000298
- Ruiz-de-Angulo, A., Bilbao-Asensio, M., Cronin, J., Evans, S. J., Clift, M. J. D., Llop, J., et al. (2020). Chemically Programmed Vaccines: Iron Catalysis in Nanoparticles Enhances Combination Immunotherapy and Immunotherapy-Promoted Tumor Ferroptosis. *iScience* 23, 101499. doi:10.1016/j.isci.2020.101499
- Saxton, R. A., and Sabatini, D. M. (2017). mTOR Signaling in Growth, Metabolism, and Disease. *Cell* 169, 361–371. doi:10.1016/j.cell.2017.03.035
- Seibt, T. M., Proneth, B., and Conrad, M. (2019). Role of GPX4 in Ferroptosis and its Pharmacological Implication. *Free Radic. Biol. Med.* 133, 144–152. doi:10.1016/j.freeradbiomed.2018.09.014
- Sha, R., Xu, Y., Yuan, C., Sheng, X., Wu, Z., Peng, J., et al. (2021). Predictive and Prognostic Impact of Ferroptosis-Related Genes ACSL4 and GPX4 on Breast Cancer Treated with Neoadjuvant Chemotherapy. *EBioMedicine* 71, 103560. doi:10.1016/j.ebiom.2021.103560
- Singhal, R., Mitta, S. R., Das, N. K., Kerk, S. A., Sajjakulnukit, P., Solanki, S., et al. (2021). HIF-2 $\alpha$  Activation Potentiates Oxidative Cell Death in Colorectal Cancers by Increasing Cellular Iron. *J. Clin. Invest* 131, e143691. doi:10.1172/JCI143691
- Song, X., Zhu, S., Chen, P., Hou, W., Wen, Q., Liu, J., et al. (2018). AMPK-Mediated BECN1 Phosphorylation Promotes Ferroptosis by Directly Blocking System X<sub>c</sub><sup>-</sup> Activity. *Curr. Biol.* 28, 2388–2399. e2385. doi:10.1016/j.cub.2018.05.094
- Stockwell, B. R. (2019). A Powerful Cell-Protection System Prevents Cell Death by Ferroptosis. *Nature* 575, 597–598. doi:10.1038/d41586-019-03145-8
- Stockwell, B. R., Friedmann Angeli, J. P., Bayir, H., Bush, A. I., Conrad, M., Dixon, S. J., et al. (2017). Ferroptosis: A Regulated Cell Death Nexus Linking Metabolism, Redox Biology, and Disease. *Cell* 171, 273–285. doi:10.1016/j.cell.2017.09.021
- Sun, D., Li, Y.-C., and Zhang, X.-Y. (2021). Lidocaine Promoted Ferroptosis by Targeting miR-382-5p/SLC7A11 Axis in Ovarian and Breast Cancer. *Front. Pharmacol.* 12, 681223. doi:10.3389/fphar.2021.681223
- Sun, Q., Xu, Y., Yuan, F. e., Qi, Y., Wang, Y., Chen, Q., et al. (2022). Rho Family GTPase 1 (RND1), a Novel Regulator of P53, Enhances Ferroptosis in Glioblastoma. *Cell Biosci.* 12, 53. doi:10.1186/s13578-022-00791-w
- Sun, X., Niu, X., Chen, R., He, W., Chen, D., Kang, R., et al. (2016a). Metallothionein-1G Facilitates Sorafenib Resistance through Inhibition of Ferroptosis. *Hepatology* 64, 488–500. doi:10.1002/hep.28574
- Sun, X., Ou, Z., Chen, R., Niu, X., Chen, D., Kang, R., et al. (2016b). Inactivation of the P62-Keap1-NRF2 Pathway Protects against Ferroptosis in Hepatocellular Carcinoma Cells. *Hepatology* 63, 173–184. doi:10.1002/hep.28251
- Sun, X., Ou, Z., Xie, M., Kang, R., Fan, Y., Niu, X., et al. (2015). HSPB1 as a Novel Regulator of Ferroptotic Cancer Cell Death. *Oncogene* 34, 5617–5625. doi:10.1038/onc.2015.32
- Sun, X., Yang, S., Feng, X., Zheng, Y., Zhou, J., Wang, H., et al. (2020). The Modification of Ferroptosis and Abnormal Lipometabolism through Overexpression and Knockdown of Potential Prognostic Biomarker Perilipin2 in Gastric Carcinoma. *Gastric Cancer* 23, 241–259. doi:10.1007/s10120-019-01004-z
- Tan, S., Li, D., and Zhu, X. (2020). Cancer Immunotherapy: Pros, Cons and beyond. *Biomed. Pharmacother.* 124, 109821. doi:10.1016/j.biopha.2020.109821
- Torti, S. V., and Torti, F. M. (2020). Iron: The Cancer Connection. *Mol. Aspects Med.* 75, 100860. doi:10.1016/j.mam.2020.100860
- Tsoi, J., Robert, L., Paraiso, K., Galvan, C., Sheu, K. M., Lay, J., et al. (2018). Multi-stage Differentiation Defines Melanoma Subtypes with Differential Vulnerability to Drug-Induced Iron-Dependent Oxidative Stress. *Cancer Cell* 33, 890–904. doi:10.1016/j.ccell.2018.03.017
- Ubellacker, J. M., Tasdogan, A., Ramesh, V., Shen, B., Mitchell, E. C., Martin-Sandoval, M. S., et al. (2020). Lymph Protects Metastasizing Melanoma Cells from Ferroptosis. *Nature* 585, 113–118. doi:10.1038/s41586-020-2623-z
- Venkatesh, D., O'Brien, N. A., Zandkarimi, F., Tong, D. R., Stokes, M. E., Dunn, D. E., et al. (2020). MDM2 and MDMX Promote Ferroptosis by PPAR $\alpha$ -Mediated Lipid Remodeling. *Genes Dev.* 34, 526–543. doi:10.1101/gad.334219.119
- Wang, C., Shi, M., Ji, J., Cai, Q., Zhao, Q., Jiang, J., et al. (2020). Stearoyl-CoA Desaturase 1 (SCD1) Facilitates the Growth and Anti-ferroptosis of Gastric Cancer Cells and Predicts Poor Prognosis of Gastric Cancer. *Aging* 12, 15374–15391. doi:10.18632/aging.103598
- Wang, L., Liu, Y., Du, T., Yang, H., Lei, L., Guo, M., et al. (2020). ATF3 Promotes Erastin-Induced Ferroptosis by Suppressing System X<sub>c</sub><sup>-</sup>. *Cell Death Differ.* 27, 662–675. doi:10.1038/s41418-019-0380-z
- Wang, H.-T., Ju, J., Wang, S.-C., Zhang, Y.-H., Liu, C.-Y., Wang, T., et al. (2022). Insights into Ferroptosis, a Novel Target for the Therapy of Cancer. *Front. Oncol.* 12, 812534. doi:10.3389/fonc.2022.812534
- Wang, Q., Bardhan, K., Boussiotis, V. A., and Patsoukis, N. (2021). The PD-1 Interactome. *Adv. Biol. (Weinh)* 5, e2100758. doi:10.1002/adbi.202100758
- Wang, S., Li, F., Qiao, R., Hu, X., Liao, H., Chen, L., et al. (2018). Arginine-Rich Manganese Silicate Nanobubbles as a Ferroptosis-Inducing Agent for Tumor-Targeted Theranostics. *ACS Nano* 12, 12380–12392. doi:10.1021/acsnano.8b06399
- Wang, W., Green, M., Choi, J. E., Gijón, M., Kennedy, P. D., Johnson, J. K., et al. (2019). CD8<sup>+</sup> T Cells Regulate Tumour Ferroptosis during Cancer Immunotherapy. *Nature* 569, 270–274. doi:10.1038/s41586-019-1170-y
- Wang, Y.-Q., Chang, S.-Y., Wu, Q., Gou, Y.-J., Jia, L., Cui, Y.-M., et al. (2016). The Protective Role of Mitochondrial Ferritin on Erastin-Induced Ferroptosis. *Front. Aging Neurosci.* 8, 308. doi:10.3389/fnagi.2016.00308
- Wei, C., Li, M., Li, X., Lyu, J., and Zhu, X. (2022). Phase Separation: "The Master Key" to Deciphering the Physiological and Pathological Functions of Cells. *Adv. Biol. (Weinh)*, e2200006. doi:10.1002/adbi.202200006
- Wu, J., Minikes, A. M., Gao, M., Bian, H., Li, Y., Stockwell, B. R., et al. (2019). Intercellular Interaction Dictates Cancer Cell Ferroptosis via NF2-YAP Signalling. *Nature* 572, 402–406. doi:10.1038/s41586-019-1426-6

- Wu, M., Zhang, X., Zhang, W., Chiou, Y. S., Qian, W., Liu, X., et al. (2022). Cancer Stem Cell Regulated Phenotypic Plasticity Protects Metastasized Cancer Cells from Ferroptosis. *Nat. Commun.* 13, 1371. doi:10.1038/s41467-022-29018-9
- Wu, Z., Li, S., and Zhu, X. (2021). The Mechanism of Stimulating and Mobilizing the Immune System Enhancing the Anti-tumor Immunity. *Front. Immunol.* 12, 682435. doi:10.3389/fimmu.2021.682435
- Xie, S., Sun, W., Zhang, C., Dong, B., Yang, J., Hou, M., et al. (2021). Metabolic Control by Heat Stress Determining Cell Fate to Ferroptosis for Effective Cancer Therapy. *ACS Nano* 15, 7179–7194. doi:10.1021/acsnano.1c00380
- Xie, Y., Hou, W., Song, X., Yu, Y., Huang, J., Sun, X., et al. (2016). Ferroptosis: Process and Function. *Cell Death Differ.* 23, 369–379. doi:10.1038/cdd.2015.158
- Xie, Y., Zhu, S., Song, X., Sun, X., Fan, Y., Liu, J., et al. (2017). The Tumor Suppressor P53 Limits Ferroptosis by Blocking DPP4 Activity. *Cell Rep.* 20, 1692–1704. doi:10.1016/j.celrep.2017.07.055
- Xiong, J., Wang, H., and Wang, Q. (2021). Suppressive Myeloid Cells Shape the Tumor Immune Microenvironment. *Adv. Biol. (Weinh)* 5, e1900311. doi:10.1002/adbi.201900311
- Xu, J., Li, X., and Du, Y. (2022). Antibody-Pattern Recognition Receptor Agonist Conjugates: A Promising Therapeutic Strategy for Cancer. *Adv. Biol. (Weinh)* 6, e2101065. doi:10.1002/adbi.202101065
- Xu, P., Luo, H., Kong, Y., Lai, W.-F., Cui, L., and Zhu, X. (2020). Cancer Neoantigen: Boosting Immunotherapy. *Biomed. Pharmacother.* 131, 110640. doi:10.1016/j.biopha.2020.110640
- Yadav, P., Sharma, P., Sundaram, S., Venkatraman, G., Bera, A. K., and Karunakaran, D. (2021). SLC7A11/xCT Is a Target of miR-5096 and its Restoration Partially Rescues miR-5096-Mediated Ferroptosis and Anti-tumor Effects in Human Breast Cancer Cells. *Cancer Lett.* 522, 211–224. doi:10.1016/j.canlet.2021.09.033
- Yagoda, N., von Rechenberg, M., Zaganjor, E., Bauer, A. J., Yang, W. S., Fridman, D. J., et al. (2007). RAS-RAF-MEK-dependent Oxidative Cell Death Involving Voltage-dependent Anion Channels. *Nature* 447, 864–868. doi:10.1038/nature05859
- Yan, B., Ai, Y., Sun, Q., Ma, Y., Cao, Y., Wang, J., et al. (2021). Membrane Damage during Ferroptosis Is Caused by Oxidation of Phospholipids Catalyzed by the Oxidoreductases POR and CYB5R1. *Mol. Cell* 81, 355–369. doi:10.1016/j.molcel.2020.11.024
- Yang, W. S., Kim, K. J., Gaschler, M. M., Patel, M., Shchepinov, M. S., and Stockwell, B. R. (2016). Peroxidation of Polyunsaturated Fatty Acids by Lipoxygenases Drives Ferroptosis. *Proc. Natl. Acad. Sci. U. S. A.* 113, E4966–E4975. doi:10.1073/pnas.1603244113
- Yang, W. S., SriRamaratnam, R., Welsch, M. E., Shimada, K., Skouta, R., Viswanathan, V. S., et al. (2014). Regulation of Ferroptotic Cancer Cell Death by GPX4. *Cell* 156, 317–331. doi:10.1016/j.cell.2013.12.010
- Yang, W. S., and Stockwell, B. R. (2016). Ferroptosis: Death by Lipid Peroxidation. *Trends Cell Biol.* 26, 165–176. doi:10.1016/j.tcb.2015.10.014
- Yi, J., Zhu, J., Wu, J., Thompson, C. B., and Jiang, X. (2020). Oncogenic Activation of PI3K-AKT-mTOR Signaling Suppresses Ferroptosis via SREBP-Mediated Lipogenesis. *Proc. Natl. Acad. Sci. U.S.A.* 117, 31189–31197. doi:10.1073/pnas.2017152117
- Yi, R., Wang, H., Deng, C., Wang, X., Yao, L., Niu, W., et al. (2020). Dihydroartemisinin Initiates Ferroptosis in Glioblastoma through GPX4 Inhibition. *Biosci. Rep.* 40. doi:10.1042/BSR20193314
- Yuan, F., Sun, Q., Zhang, S., Ye, L., Xu, Y., Deng, G., et al. (2022). The Dual Role of P62 in Ferroptosis of Glioblastoma According to P53 Status. *Cell Biosci.* 12, 20. doi:10.1186/s13578-022-00764-z
- Zhang, H.-L., Hu, B.-X., Li, Z.-L., Du, T., Shan, J.-L., Ye, Z.-P., et al. (2022). PKC $\beta$ II Phosphorylates ACSL4 to Amplify Lipid Peroxidation to Induce Ferroptosis. *Nat. Cell Biol.* 24, 88–98. doi:10.1038/s41556-021-00818-3
- Zhang, H., Deng, T., Liu, R., Ning, T., Yang, H., Liu, D., et al. (2020). CAF Secreted miR-522 Suppresses Ferroptosis and Promotes Acquired Chemo-Resistance in Gastric Cancer. *Mol. Cancer* 19, 43. doi:10.1186/s12943-020-01168-8
- Zhang, Z., Guo, M., Shen, M., Kong, D., Zhang, F., Shao, J., et al. (2020). The BRD7-P53-Slc25a28 axis Regulates Ferroptosis in Hepatic Stellate Cells. *Redox Biol.* 36, 101619. doi:10.1016/j.redox.2020.101619
- Zhang, Y., Kwok-Shing Ng, P., Kucherlapati, M., Chen, F., Liu, Y., Tsang, Y. H., et al. (2017). A Pan-Cancer Proteogenomic Atlas of PI3K/AKT/mTOR Pathway Alterations. *Cancer Cell* 31, 820–832. e823. doi:10.1016/j.ccell.2017.04.013
- Zhang, Z., Lu, M., Chen, C., Tong, X., Li, Y., Yang, K., et al. (2021). Holo-lactoferrin: the Link between Ferroptosis and Radiotherapy in Triple-Negative Breast Cancer. *Theranostics* 11, 3167–3182. doi:10.7150/thno.52028
- Zheng, J., and Conrad, M. (2020). The Metabolic Underpinnings of Ferroptosis. *Cell Metab.* 32, 920–937. doi:10.1016/j.cmet.2020.10.011
- Zheng, Q., Li, P., Zhou, X., Qiang, Y., Fan, J., Lin, Y., et al. (2021). Deficiency of the X-Inactivation Escaping Gene KDM5C in Clear Cell Renal Cell Carcinoma Promotes Tumorigenicity by Reprogramming Glycogen Metabolism and Inhibiting Ferroptosis. *Theranostics* 11, 8674–8691. doi:10.7150/thno.60233
- Zhou, Y., Yang, J., Chen, C., Li, Z., Chen, Y., Zhang, X., et al. (2021). Polyphyllin III-Induced Ferroptosis in MDA-MB-231 Triple-Negative Breast Cancer Cells Can Be Protected against by KLF4-Mediated Upregulation of xCT. *Front. Pharmacol.* 12, 670224. doi:10.3389/fphar.2021.670224
- Zhu, M., Zhang, H., Pedersen, K. S., Foster, N. R., Jaszewski, B. L., Liu, X., et al. (2022). Understanding Suboptimal Response to Immune Checkpoint Inhibitors. *Adv. Biol. (Weinh)*, e2101319. doi:10.1002/adbi.202101319
- Zhu, X., Fan, W. G., Li, D. P., Kung, H., and Lin, M. C. (2011). Heme Oxygenase-1 System and Gastrointestinal Inflammation: a Short Review. *World J Gastroenterol* 17, 4283–4288. doi:10.3748/wjg.v17.i38.4283
- Zhu, X., Fan, W. G., Li, D. P., Lin, M. C., and Kung, H. (2010). Heme Oxygenase-1 System and Gastrointestinal Tumors. *Wjg* 16, 2633–2637. doi:10.3748/wjg.v16.i21.2633
- Zou, Y., Palte, M. J., Deik, A. A., Li, H., Eaton, J. K., Wang, W., et al. (2019). A GPX4-dependent Cancer Cell State Underlies the Clear-Cell Morphology and Confers Sensitivity to Ferroptosis. *Nat. Commun.* 10, 1617. doi:10.1038/s41467-019-09277-9
- Zou, Z., Tao, T., Li, H., and Zhu, X. (2020). mTOR Signaling Pathway and mTOR Inhibitors in Cancer: Progress and Challenges. *Cell Biosci.* 10, 31. doi:10.1186/s13578-020-00396-1

**Conflict of Interest:** The authors declare that the research was conducted in the absence of any commercial or financial relationships that could be construed as a potential conflict of interest.

**Publisher's Note:** All claims expressed in this article are solely those of the authors and do not necessarily represent those of their affiliated organizations, or those of the publisher, the editors and the reviewers. Any product that may be evaluated in this article, or claim that may be made by its manufacturer, is not guaranteed or endorsed by the publisher.

Copyright © 2022 Tan, Kong, Xian, Gao, Xu, Wei, Lin, Ye, Li and Zhu. This is an open-access article distributed under the terms of the Creative Commons Attribution License (CC BY). The use, distribution or reproduction in other forums is permitted, provided the original author(s) and the copyright owner(s) are credited and that the original publication in this journal is cited, in accordance with accepted academic practice. No use, distribution or reproduction is permitted which does not comply with these terms.



# Hydrogen Sulfide Inhibits Ferroptosis in Cardiomyocytes to Protect Cardiac Function in Aging Rats

Zihui Liang<sup>1</sup>, Yuxin Miao<sup>1</sup>, Xu Teng<sup>1</sup>, Lin Xiao<sup>1</sup>, Qi Guo<sup>1</sup>, Hongmei Xue<sup>1</sup>, Danyang Tian<sup>1</sup>, Sheng Jin<sup>1\*</sup> and Yuming Wu<sup>1,2\*</sup>

<sup>1</sup>Department of Physiology, Hebei Medical University, Shijiazhuang, China, <sup>2</sup>Hebei Collaborative Innovation Center for Cardio-Cerebrovascular Disease, Shijiazhuang, China

## OPEN ACCESS

### Edited by:

Xin Wang,  
National Institutes of Health (NIH),  
United States

### Reviewed by:

Qiong Meng,  
National Institutes of Health (NIH),  
United States  
Xiaolu Zhu,  
Columbia University, United States  
Jia-Hua Qu,  
University of California, San Francisco,  
United States

### \*Correspondence:

Sheng Jin  
jinshengsheng@126.com  
Yuming Wu  
wuyum@yahoo.com

### Specialty section:

This article was submitted to  
Molecular Diagnostics and  
Therapeutics,  
a section of the journal  
Frontiers in Molecular Biosciences

**Received:** 19 May 2022

**Accepted:** 22 June 2022

**Published:** 22 July 2022

### Citation:

Liang Z, Miao Y, Teng X, Xiao L, Guo Q,  
Xue H, Tian D, Jin S and Wu Y (2022)  
Hydrogen Sulfide Inhibits Ferroptosis in  
Cardiomyocytes to Protect Cardiac  
Function in Aging Rats.  
Front. Mol. Biosci. 9:947778.  
doi: 10.3389/fmolb.2022.947778

Aging contributes significantly to cardiovascular diseases and cardiac dysfunction. To explore the reasons for the decline in cardiac function in the elderly, we collected clinical data and blood samples from 231 individuals. Our results indicated that aging was accompanied by a decline in cardiac function and remodeling of the left ventricle, and cardiac function was negatively correlated with age. Serum hydrogen sulfide (H<sub>2</sub>S) decreased, while serum malondialdehyde (MDA) and iron increased with aging in healthy individuals. A rat model of aging and iron overload was constructed for *in vivo* research. In the animal model, we found that the expression of endogenous H<sub>2</sub>S-producing enzymes decreased, and endogenous H<sub>2</sub>S levels decreased, while oxidative stress levels rose. The regulation of iron metabolism and the maintenance of iron homeostasis declined. The accumulation of MDA and iron led to ferroptotic cell death and subsequent myocardial injury and deterioration. A high-iron diet accelerated the aging process and death in rats. The decline of cardiac function in aging rats and iron-overload rats may be caused by cardiomyocyte ferroptosis. Exogenous H<sub>2</sub>S enhanced the expression of endogenous H<sub>2</sub>S synthase, promoted endogenous H<sub>2</sub>S production, regulated iron metabolism, and reduced oxidative stress levels. The protective effects of H<sub>2</sub>S on cardiac function in aging rats and iron-overload rats may be partly due to the inhibition of cardiomyocyte ferroptosis. We demonstrated that cardiac dysfunction associated with aging was closely related to decreased endogenous H<sub>2</sub>S levels and cardiomyocyte ferroptosis. H<sub>2</sub>S-regulated iron metabolism reduced oxidative stress levels in cardiomyocytes, inhibited cardiomyocyte ferroptosis, and protected cardiac function in aging rats.

**Keywords:** aging, ferroptosis, cardiac dysfunction, hydrogen sulfide, iron metabolism

## INTRODUCTION

Aging is a dominant risk factor for cardiovascular diseases, including hypertension, cardiac hypertrophy, and heart failure, which ultimately lead to increased mortality (Timmers et al., 2020). Aging hearts exhibit unique histological and physical features, including increased cell death, increased cardiomyocyte volume, and collagen fiber accumulation (Julian et al., 2019). Given the dramatically aging population, age-related cardiac dysfunction represents one of the greatest challenges confronting global healthcare today.



The main reason for cardiac dysfunction due to aging is cardiomyocyte death. At least 12 forms of regulated cell death have been described, of which seven have been implicated in the cardiovascular system, including apoptosis, mitochondrial-permeability-transition-driven necrosis, necroptosis, pyroptosis, parthanatos, autophagy-mediated cell death, and ferroptosis (Galluzzi et al., 2015; Galluzzi et al., 2018). Ferroptosis is an iron-dependent form of regulated cell death characterized by the accumulation of lipid peroxide to lethal levels, resulting in oxidative damage to cell membranes. Ferroptosis differs from apoptosis, necroptosis, and autophagy in several aspects (Dixon et al., 2012; Stockwell et al., 2017). Ferroptosis plays critical roles in cardiomyopathy, myocardial infarction, ischemia/reperfusion injury, and heart failure (Park et al., 2019; Tang et al., 2021; Tian et al., 2021; Zheng et al., 2021; Lin et al., 2022).

Ferroptosis triggered by excess iron causes cardiomyocyte death by regulating iron metabolism. Understanding the signaling pathways preventing iron-mediated cell death will provide new approaches for treating patients with acute myocardial infarctions (Baba et al., 2018). Therefore, the ability of H<sub>2</sub>S to regulate iron metabolism and homeostasis deserves our attention (Zhang et al., 2019). H<sub>2</sub>S is an important gaseous signaling molecule. H<sub>2</sub>S exerts protective effects, including vasoactive effects and anti-inflammatory and antioxidant properties (Perna et al., 2010). H<sub>2</sub>S contributes to ischemic postconditioning-induced cardioprotection in aging hearts and cardiomyocytes (Li et al., 2016a). Our research group demonstrated that exogenous H<sub>2</sub>S restored the diurnal variations in cardiac function in aging mice (Zhang et al., 2021). Decreased antioxidative stress capabilities can cause ferroptosis in cardiomyocytes, and decreasing iron accumulation and/or inhibiting lipid peroxidation is cardioprotective during both acute and chronic cardiac ischemia/reperfusion-induced cardiomyopathy (Fang et al., 2019). Thus, regulating the expression of antioxidative stress-related proteins, such as NRF2 and GPX4, can inhibit cardiomyocyte ferroptosis (Bai et al., 2018). These findings indicate that ferroptosis is a potential target for protection against cardiomyopathy. Therefore, the impact of H<sub>2</sub>S on iron accumulation and the antioxidative stress characteristics contributing to decreased cardiomyocyte ferroptosis are worth exploring.

The specific form of cell death in cardiomyocytes associated with aging in humans remains unclear. Furthermore, the different effects of aging on human cardiac function during health and disease have not been elucidated. The world's population is aging, highlighting the need to understand the impact of aging on cardiac function. However, the occurrence of cardiomyocyte ferroptosis in healthy individuals and the effects of endogenous H<sub>2</sub>S levels on cardiac aging and ferroptosis in cardiomyocytes are not clear. With this in mind, the aim of the present research was to investigate whether cardiac dysfunction caused by aging is related to cardiomyocyte ferroptosis and changes in endogenous H<sub>2</sub>S levels. Potential mechanisms will be explored.

## MATERIALS AND METHODS

### Clinical Sample Data and Blood Sample Collection

Clinical data and blood samples were collected from 231 individuals undergoing medical examination at The Third Hospital of Shijiazhuang

in China from July 2021 to October 2021. Participants were aged 20–75 years and included 135 males and 96 females. Participants were divided into the following age groups: 20–29 years, 30–39 years, 40–49 years, 50–59 years, and 60 + years. The inclusion criteria were as follows: 1) denial of a medical history of coronary heart disease, cerebral infarction, cerebral hemorrhage, hypertension, or diabetes; 2) denial of a medical history of hepatitis or tuberculosis; and 3) denial of a medical history of surgery and blood transfusion. The general condition and medical history of all participants were recorded. Blood samples were prospectively obtained from participants at admission. After centrifugation for 10 min at 3,500 rpm, the supernatants were frozen at –80°C. All participants provided written informed consent prior to the study. The protocol was approved by the Ethics Committee of the Hebei Medical University (Shijiazhuang, China) and performed in accordance with all applicable laws, regulations, and guidelines in China (including good clinical practice guidelines), which are related to the protection of human subjects as volunteers. The study was conducted according to the published regulations of the Declaration of Helsinki.

### Animals and Experimental Protocol

The animal study was reviewed and approved by the Animal Management Rule of the Ministry of Health, People's Republic of China (documentation number 5, 2001) and the Animal Care Committee of Hebei Medical University. The protocols and procedures performed were in compliance with the Guide for the Care and Use of Laboratory Animals (NIH Publication No. 85–23, revised 2011). Animals were obtained from the Animal Center of Hebei Medical University (Shijiazhuang, China) and housed in plastic cages in a room with a controlled humidity of 50–65%, at a temperature of 20–25°C and on a regular 12 h light and dark cycle (lights on from 8:00 to 20:00). They were fed on standard rat chow and tap water *ad libitum*.

### Rat Model of Aging

Twenty-four Sprague–Dawley (SD) rats were divided into three groups ( $n = 8/\text{group}$ ): an old group, an old + NaHS group, and a young group. The old groups were composed of 15-month-old male SD rats randomly divided into treated and untreated groups (+/–NaHS), and the young group was composed of 8-week-old male SD rats. The old + NaHS group received NaHS (100 μmol/kg, i.p./d) for 3 months. The young and untreated old groups received an equal volume of saline (i.p./d) for 3 months.

### High-Iron Diet Aging Rat Model

Thirty-six 15-month-old male SD rats were randomly divided into three groups ( $n = 12/\text{group}$ ): an old + normal-iron diet (NID) group, an old + HID group, and an old + HID + NaHS group. The old + NID group received an NID for 3 months, and the old + HID groups received an HID for 3 months. The old + HID + NaHS group received the HID and NaHS (100 μmol/kg, i.p./d) for 3 months.

### HID Young Rat Model

Twenty-four 8-week-old male SD rats were randomly divided into three groups ( $n = 8/\text{group}$ ): an NID group, an HID group,

and an HID + NaHS group. The NID group received NID for 3 months, and the HID group received HID for 3 months. The HID + NaHS group received HID and NaHS (100  $\mu\text{mol/kg}$ , i. p./d) for 3 months.

At the end of the study protocol, cardiac function was determined by echocardiography, and hemodynamic parameters were measured using the Power Lab (ML4818) Data Acquisition System (ADInstruments, Australia). Blood samples were collected, immediately centrifuged for 10 min at 3,500 rpm, and frozen at  $-80^{\circ}\text{C}$ . The heart was rapidly removed and frozen at  $-80^{\circ}\text{C}$ .

## HID Preparation

A chow diet containing 0.241% elemental iron (Research Diets, D08080405, Beijing KeAoXieLi Feed Co., Ltd., China) was prepared. In brief, 1 kg of a chow diet was ground and combined with 2.41 g of carbonyl iron. Then, 1.2 L of deionized water was added to the HID. After mixing, the iron loading diet was molded and baked at  $80^{\circ}\text{C}$  for 24 h in a hot air oven.

## Echocardiographic Assessment

The participants took the supine position, and after an appropriate amount of couplant was applied to the precordial area, the participants were examined with an M-mode ultrasound. Cardiac functional parameters were evaluated, including left ventricular ejection fraction (LVEF), left ventricular fractional shortening (LVFS), stroke volume (SV), left ventricular internal dimension (LVID), interventricular septum (IVS), left ventricular anterior wall (LVAW), left ventricular posterior wall (LVPW), left atrial volume, maximum flow velocity of the mitral valve in early diastole ( $E'$  wave), maximum flow velocity of the mitral valve in late diastole ( $A'$  wave), mean diastolic velocity of mitral annulus in diastole ( $e'$ ), and heart beats per minute (BPM). The cardiac output (CO), cardiac index (CI),  $E'$  wave/ $A'$  wave ( $E/A$ ),  $E/e'$ , and left atrial volume index (LAVI) were calculated from the measured cardiac parameters from five consecutive cardiac cycles and averaged.

Rats were anesthetized with 2–3% inhaled isoflurane (RWD Life Science Co., Ltd., Shenzhen) and immobilized on the operating table. To evaluate the cardiac function, mouse two-dimensional echocardiography was performed using a Vevo 2,100 ultrasound device (FUJIFILM Visual Sonics Inc., Toronto, Canada). Parasternal long axis and short axis images were obtained in two-dimensional and M-modes for quantification. Left ventricular anterior wall diastole (LVAW' d) and left ventricular posterior wall diastole (LVPW' d) were measured on the parasternal left ventricular long axis view. Using the PW-Doppler mode,  $E'$  wave and  $A'$  wave were measured. LVEF, LVFS, and CO were calculated using computer algorithms. Measurements were averaged over five consecutive cardiac cycles in a blinded manner.

## Hemodynamics Evaluation

Rats were anesthetized with pentobarbital sodium (30 mg/kg, i. p.), and the carotid artery was catheterized. A pressure transducer (ML4818) connected to the Power Lab apparatus (AD

Instruments, Australia) was used to measure blood pressure and cardiac function. A polyethylene catheter was introduced from the right carotid artery, and a catheter (retrograde) was introduced through the aortic valve to reach the left ventricular (LV) cavity. LV pressure was recorded for 15–30 min. All data were recorded and analyzed by Lab Chart 7 software. The maximum rates of the left ventricular pressure rise and fall ( $+dp/dt_{\text{max}}$  and  $-dp/dt_{\text{max}}$ ) and left ventricular end diastolic pressure (LVEDP) were acquired from the pressure waves. The rats were euthanized after determining pressure, and blood and heart tissues were collected and stored.

## Blood Analysis

Serum creatinine (CRE), blood urea nitrogen (BUN), alanine aminotransferase (ALT), and aspartate aminotransferase (AST) levels were measured in participants. Plasma lactate dehydrogenase (LDH), creatine kinase (CK), and CK-myocardial band (CK-MB) levels were measured in rats. The blood parameters were determined using an automatic biochemical analyzer (AU5800, Beckman, United States).

## Measurement of $\text{H}_2\text{S}$ Levels

Serum and plasma  $\text{H}_2\text{S}$  concentrations were detected by liquid chromatography-tandem mass spectrometry. The blood samples were centrifuged at 3,500 rpm for 15 min, and the serum was tested. The frozen heart tissue samples were thawed on ice and weighed. Saline was added to the heart tissue at a ratio of weight (g): volume (ml) = 1:9, and the tissue was mechanically homogenized on ice. The homogenized tissue was centrifuged at 2,500 rpm for 10 min, and the supernatant was collected.  $\text{Na}_2\text{S}$  at different concentrations (0.00, 0.08, 0.16, 0.31, 0.63, 1.25, 2.50, 5.00, 10.00, 20.00, and 40.00  $\mu\text{mol}$ ) were used to generate a standard curve. Samples (60  $\mu\text{L}$ ) were added to the EP pipe filled with nitrogen, and 140  $\mu\text{L}$  of tris HCl buffer solution (pH = 10.1) and 60  $\mu\text{L}$  of MBB derivatization reagent were added. After 120 min of light-shielded reaction at  $50^{\circ}\text{C}$ , 100  $\mu\text{L}$  of SSA solution was added to terminate. The precipitated protein was centrifuged at 12,000 rpm at  $4^{\circ}\text{C}$  for 10 min, and the supernatant was collected and filtered through a 0.22- $\mu\text{m}$  filter membrane. The filtered solution was injected into the sample injection bottle and put it into the automatic sample injector for sample injection detection. The  $\text{Na}_2\text{S}$  standard curve was used to calculate the  $\text{H}_2\text{S}$  concentration in serum (unit:  $\mu\text{mol/L}$ ), plasma (unit:  $\mu\text{mol/L}$ ), and cardiac tissues (unit:  $\mu\text{mol/g}$  protein).

## Measurement of MDA, Iron, and GSH Levels

The levels of MDA in the serum, plasma, and cardiac tissues were measured using a malondialdehyde (MDA) Assay Kit (A003-2-2, JianCheng, Nanjing, China). Frozen serum, plasma, and heart samples were thawed on ice. The heart tissue was weighed, and normal saline was added at a ratio of weight (g): volume (ml) = 1:9. After mechanical homogenization on ice, the sample was centrifuged at 500 rpm for 10 min. The protein concentration in the supernatant was determined using the BCA assay. The reagents were prepared according to the MDA kit instructions and kept on ice away from light. The sample (0.2 ml), reagent 1 (0.2 ml), reagent 2 (3 ml), and reagent 3 (1 ml) were combined in

the sample test samples, and standard (0.2 ml), reagent 1 (0.2 ml), reagent 2 (3 ml), and reagent 3 (1 ml) were added to the standard test tubes. Absolute ethanol (0.2 ml), reagent 1 (0.2 ml), reagent 2 (3 ml), and reagent 3 (1 ml) were combined in the blank tube, and sample (0.2 ml), reagent 1 (0.2 ml), reagent 2 (3 ml), and 50% glacial acetic acid (1 ml) were added to the control tube. After mixing, the samples and controls were boiled for 40 min and then cooled. After centrifuging at 3,500 rpm for 20 min, the absorbance of the supernatant (1 ml) was measured at 532 nm. MDA levels of each sample were calculated according to the formula from the manufacturer.

The levels of iron in the serum, plasma, and cardiac tissues were measured using Iron Assay Kits (A039-1-1 and A039-2-1, respectively, Jiancheng, Nanjing, China). The frozen samples were thawed on ice. The heart tissue was weighed, and normal saline was added at a ratio of weight (g): volume (ml) = 1:9. After mechanical homogenization on ice, the samples were centrifuged at 2,500 rpm for 10 min. The protein concentration in the supernatant was determined using the BCA assay. The reagents were prepared according to the instructions of the iron determination kits. Samples were boiled for 5 min, cooled, and centrifuged at 3,500 rpm for 20 min. The absorbance of supernatants (1 ml) was measured at 520 nm. Iron levels were calculated according to the formula from the kit.

The levels of GSH in cardiac tissues were measured using a GSH Assay Kit (A006-1-1, Jiancheng, Nanjing, China) according to the manufacturer's instructions. The frozen heart tissue was thawed on ice. The heart tissue was weighed, and normal saline was added at a ratio of weight (g): volume (ml) = 1: 9. After mechanical homogenization on ice, the samples were centrifuged at 2,500 rpm for 10 min. The protein concentration in the supernatant was determined using the BCA assay. The reagents were prepared according to the instructions of the GSA Assay Kit. The absorbance of each sample was measured at 420 nm, and GSH levels were calculated according to the formula in the instructions of the kit.

## Measurement of the Reactive Oxygen Species Level

ROS levels in cardiac tissues were measured by staining the fresh frozen sections with DHE. Fresh cardiac tissues were mounted using Tissue-Tek O.C.T. Blocks were sectioned into 5- $\mu$ m thick slices, washed twice with phosphate-buffered saline, and incubated for 30 min with DHE (10  $\mu$ mol/L). The resulting color reaction was immediately measured with a fluorescence microscope (Leica, Germany).

## Histopathological Analysis

Cardiac tissues were collected from five mice in each group. The tissue was fixed in 10% neutral buffered formalin, embedded in paraffin, and then sectioned at 4- $\mu$ m thickness. Cardiac sections were deparaffinized at 60°C for 1 h and hydrated in distilled water. After hematoxylin and eosin (HE) staining, the tissue sections were examined using an optical microscope (OLYMPUS) at  $\times$ 200 magnification. The proportion of inflammatory cells was determined as the percentage of

inflammatory cells to the total cardiomyocytes. To evaluate myocardial fibrosis, the tissue sections were stained using a Masson's trichrome staining kit (BASO, BA-4079). Tissue sections were examined using an optical microscope (OLYMPUS) at  $\times$ 100 magnification. The myocardium was stained red, the nucleus was stained black, and collagen fibers were stained blue. The collagen volume fraction was determined as the percentage of collagen (blue-stained area) to the total cardiac tissue area. Using Prussian blue iron staining, iron accumulation in cardiac tissues was evaluated, and equal volumes of potassium ferrocyanide solution and hydrochloric acid solution were mixed to make a working iron stain solution. The cardiac tissues were then incubated with the working solution for 3 min. The tissue sections were examined using an optical microscope (OLYMPUS) at  $\times$ 400 magnification. The cardiac iron density was determined as the percentage of blue-stained cells to the total cardiomyocytes. All data were processed and analyzed by ImageJ software (1.52, NIH, United States).

## Electron Microscopy

To detect changes in the mitochondrial morphology of cardiomyocytes during aging, electron microscopy was conducted. Cardiac tissues were fixed at 4°C with 2% glutaraldehyde in a 0.1 M sodium cacodylate buffer and post-fixed for 1 h on ice with 1% osmium tetroxide. The slices were stained with uranyl acetate and observed under an electron microscope.

## Western Blotting

Frozen heart tissues were lysed mechanically in cold RIPA buffer. Proteins were extracted and quantified using a BCA protein assay kit (Best Bio, Shanghai, China). The proteins were electrophoretically separated using SDS-PAGE and transferred to a polyvinylidene difluoride membranes (Millipore, United States). The membranes were blocked with 3% BSA for 1.5 h at room temperature, and antigens were detected using the following antibodies at 4°C overnight, CSE (1:1,000, Proteintech, United States), CBS (1:1,000, Proteintech, United States), 3-MST (1:5,000, SantaCruz, United States), P53 (1:2,000, Proteintech, United States), P21 (1:2,000, Proteintech, United States), NRF2 (1:2,000, Proteintech, United States), SLC7A11 (1:2,000, Proteintech, United States), ACSL4 (1:2,000, Abcam, United States), GPX4 (1:2,000, Proteintech, United States), FPN1 (1:1,000, Proteintech, United States), FTH (1:1,000, Immunoway, United States), TRF1 (1:1,000, Abcam, United States), and GAPDH (1:5,000, Proteintech, United States). The blots were incubated with a horseradish peroxidase-conjugated anti-rabbit (Proteintech, United States) or anti-mouse (Proteintech, United States) secondary antibody at room temperature for 1.5 h. All antibodies were diluted with TBST. Blot bands were visualized by enhanced chemiluminescence and detected by ImageJ software (1.52, NIH, United States).

## Statistical Analyses

Statistical analyses were performed by SPSS 21 software (SPSS Inc., Chicago, IL, United States). Data are presented as the mean  $\pm$

**TABLE 1** | Characteristics of 231 healthy participants.

Group	20–29 (n = 39)	30–39 (n = 56)	40–49 (n = 47)	50–59 (n = 42)	60+ (n = 47)	p
Gender, male (%)	25 (64.10)	29 (51.79)	30 (63.83)	23 (54.76)	28 (59.57)	NS
Height mean ± SD (cm)	171.03 ± 9.09	169.71 ± 9.15	169.34 ± 7.92	167.81 ± 8.49	165.26 ± 9.64	0.028
Weight mean ± SD (kg)	67.51 ± 11.74	69.91 ± 13.73	72.15 ± 11.70	73.55 ± 12.27	70.96 ± 10.75	NS
SBP mean ± SD (mmHg)	114.92 ± 15.37	116.54 ± 16.46	119.68 ± 14.33	117.50 ± 14.86	116.19 ± 14.53	NS
DBP mean ± SD (mmHg)	76.95 ± 13.12	80.63 ± 12.37	78.60 ± 13.50	80.50 ± 11.31	78.15 ± 11.70	NS
GLU mean ± SD (mmol/L)	5.06 ± 0.66	5.09 ± 0.64	5.02 ± 0.69	4.99 ± 0.69	4.94 ± 0.67	NS
CHO mean ± SD (mmol/L)	3.92 ± 0.72	4.15 ± 0.66	3.91 ± 0.68	3.86 ± 0.69	3.96 ± 0.65	NS
CRE mean ± SD (mmol/L)	76.49 ± 13.90	83.89 ± 15.77	81.89 ± 14.53	76.60 ± 15.84	81.66 ± 15.63	NS
BUN mean ± SD (mmol/L)	4.80 ± 1.08	5.06 ± 1.11	4.88 ± 1.06	5.06 ± 1.46	4.74 ± 1.48	NS
ALT mean ± SD (U/L)	30.44 ± 13.93	29.71 ± 15.14	29.36 ± 11.97	30.71 ± 11.95	30.09 ± 15.62	NS
AST mean ± SD (U/L)	30.15 ± 13.36	27.27 ± 10.60	29.28 ± 8.95	30.10 ± 8.05	29.96 ± 11.84	NS

standard error of the mean, and independent t-tests were used to compare two groups. The results of more than three groups were compared using a one-way analysis of variance followed by the LSD test. Spearman correlation analysis was performed.  $p < 0.05$  was considered statistically significant.

## RESULTS

### Cardiac Function Negatively Correlates With Age in Healthy Participants

The characteristics of the 231 healthy participants are shown in **Table 1**. No significant differences in general characteristics were detected between the five groups. According to the echocardiographic measurements, the values of EF%, FS%, and SV did not decrease with aging (**Supplementary Figures S1A–C**), but the BPM decreased with the progress of aging, indicating that the BPM negatively correlated with age (**Figure 1A**). The CO and CI decreased with the progress of aging, indicating that the cardiac systolic function negatively correlated with age (**Figures 1B,C**). The values of E/A, E/e', e', and LAVI were statistically different between the 60+ age group and the 20–29 age groups, indicating that the cardiac diastolic function negatively correlated with age (**Figures 1D–G**). LVID of healthy participants expanded with aging, and the IVS, LVAW, and LVPW thickened, indicating the left ventricle remodeling with the progress of aging (**Figures 1H–K**).

### Serum H<sub>2</sub>S, Iron, and MDA Levels Change With Aging in Healthy Participants

Serum H<sub>2</sub>S levels in healthy participants decreased with aging and peaked in the 30–39 age groups, indicating that serum H<sub>2</sub>S negatively correlated with age (**Figures 2A,D**). Serum iron levels increased with aging, indicating that serum iron positively correlated with age (**Figures 2B,E**). Serum MDA increased with aging, indicating that serum MDA positively correlated with age (**Figures 2C,F**). Serum iron levels increased when serum H<sub>2</sub>S levels decreased, indicating a negative correlation between serum iron and the H<sub>2</sub>S level (**Figures 2G,H**).

### Exogenous H<sub>2</sub>S Enhanced H<sub>2</sub>S Synthase Expression in the Myocardial Tissue of Aging Rats

H<sub>2</sub>S in the plasma and myocardial tissue of aging rats decreased compared with that of young rats. Treatment with NaHS increased the endogenous H<sub>2</sub>S levels (**Figures 3A,B**). The expression of endogenous H<sub>2</sub>S synthase CSE and 3-MST decreased in the myocardial tissue of aging rats. Treatment with NaHS enhanced the expression of endogenous H<sub>2</sub>S synthase CSE and 3-MST, but no significant differences in CBS expression were detected (**Figures 3C–F**).

### H<sub>2</sub>S Improved Cardiac Function in Aging Rats

According to the echocardiography results, the E' wave was higher than A' wave in young rats, and the E' wave was lower than A' wave in aging rats (**Figure 4A**). The E' wave/A' wave ratio was lower in aging rats (**Figure 4B**). Treatment with NaHS increased the E' wave/A' wave ratio in aging rats (**Figures 4A,B**). CO decreased in aging rats compared with that in young rats, and treatment with NaHS increased CO in aging rats (**Figure 4C**). The hemodynamics evaluation of +dp/dt<sub>max</sub> and -dp/dt<sub>max</sub> was lower, and LVEDP was higher in aging rats, indicating that the cardiac function significantly decreased in aging rats compared with that in young rats. Treatment with NaHS increased + dp/dt<sub>max</sub> and -dp/dt<sub>max</sub> and lowered LVEDP in aging rats (**Figures 4D–F**).

### H<sub>2</sub>S Alleviated Myocardial Injury in Aging Rats

Serum myocardial injury markers, including elevated LDH, CK, and CK-MB levels decreased significantly in response to NaHS treatment in aging rats (**Figures 5A–C**). The HE staining showed that the myocardial tissue structure in young rats was dense, and the myocardial fibers were intact. The number of inflammatory cells in the myocardial interstitium was significantly lower in young rats than the number in aging rats. The myocardial tissue in aging rats exhibited severe cell alignment disorders and more cardiomyocyte inflammatory infiltration and death. Treatment



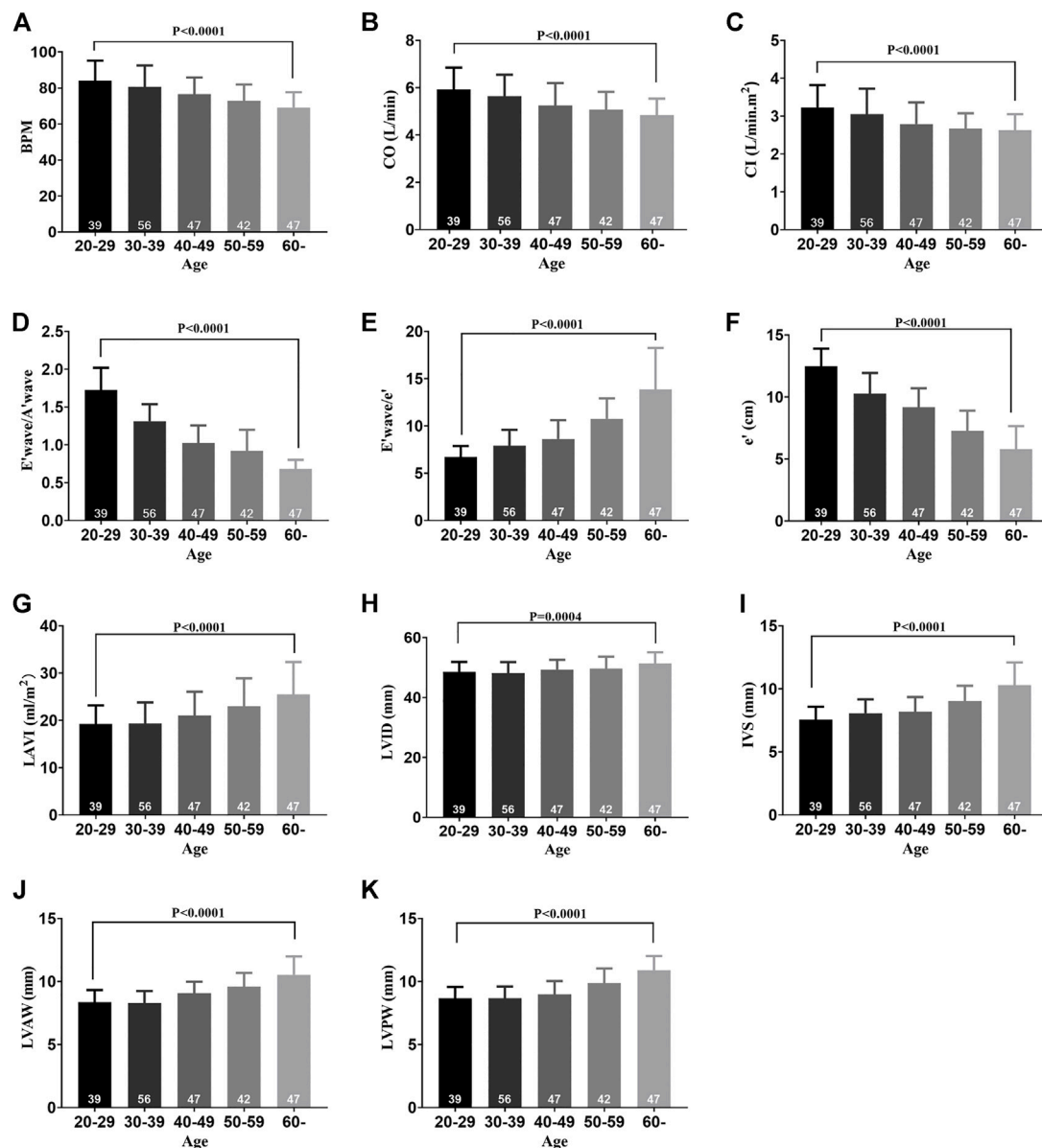


**FIGURE 1 |** Cardiac function decline and left ventricle remodeling with aging in healthy participants. **(A)** BPM of five groups. **(B)** CO of five groups. **(C)** CI of five groups. **(D)** E' wave/A' wave ratios of five groups. **(E)** E' wave/e' ratios of five groups. **(F)** e' of five groups. **(G)** LAVI of five groups. **(H)** LVID of five groups. **(I)** IVS of five groups. **(J)** LVAW of five groups. **(K)** LVPW of five groups. Results are means  $\pm$  SEM. A  $p$ -value of  $<0.05$  was considered significant. BPM: beat per minute. CO: cardiac output. CI: cardiac index. E' wave: maximum flow velocity of mitral valve in early diastole. A' wave: maximum flow velocity of mitral valve in late diastole. e': mean diastolic velocity of mitral annulus in diastole. LAVI: left atrial volume index. LVID: left ventricular internal dimension. IVS: interventricular septum. LVAW: left ventricular anterior wall. LVPW: left ventricular posterior wall.

with NaHS significantly decreased the number of inflammatory cells in the myocardial interstitium and inhibited cardiomyocyte death in aging rats compared with the myocardium of untreated aging rats (Figure 5D).

The Masson staining showed that myocardial fibrosis increased in aging rats compared with that in young rats, and treatment with NaHS reduced myocardial fibrosis in aging rats (Figure 5E). The HW/BW ratio of aging rats increased, and M-mode images by echocardiography showed

that the values of LVAW'd and LVPW'd increased compared with these parameters in young rats. Treatment with NaHS lowered the HW/BW ratio and inhibited LV remodeling in aging rats compared with that in untreated aging rats (Figures 5F–I).

Western blot analysis showed that treatment with NaHS reduced the protein expressions of p53 and p21 in myocardial tissue of aging rats and reduced the cardiac senescence phenomenon of aging rats (Figures 5J–L).

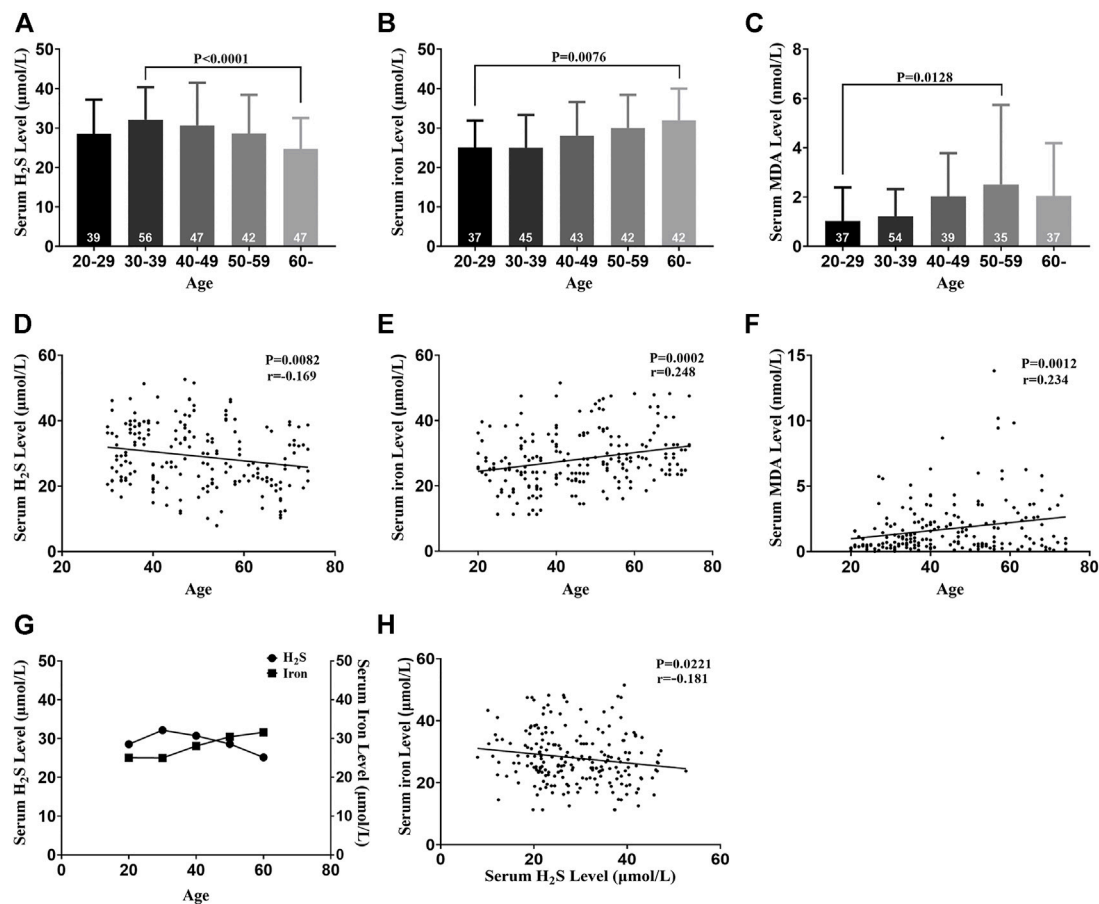


**FIGURE 2 |** Serum H<sub>2</sub>S, iron, and MDA levels change with aging in healthy participants. **(A)** Serum H<sub>2</sub>S levels of five groups. **(B)** Serum iron levels of five groups. **(C)** Serum MDA levels of five groups. **(D)** Serum H<sub>2</sub>S level was negatively correlated with age. **(E)** Serum iron level was positively correlated with age. **(F)** Serum MDA level was positively correlated with age. **(G)** Serum iron and H<sub>2</sub>S levels changed with aging. **(H)** Serum iron level was negatively correlated with the serum H<sub>2</sub>S level. Results are means  $\pm$  SEM. A  $p$ -value of  $<0.05$  was considered significant. MDA: malondialdehyde.

## H<sub>2</sub>S Inhibited Cardiomyocyte Ferroptosis in Aging Rats

Iron levels in the plasma and myocardial tissue of aging rats increased compared with those of young rats. The proportion of Prussian blue iron-stained cells in the myocardial tissue increased in aging rats. Treatment with NaHS reduced iron levels in the plasma and myocardial tissue and the proportion of Prussian blue iron-stained cells in the myocardial tissue of aging rats (**Figures 6A–D**). Western blot analyses showed that compared with young rats, the expressions of TFR1, FPN1, and FTH in the myocardial tissue of aging rats were attenuated compared with those of young rats. Treatment with NaHS partially enhanced the expression of iron metabolism regulatory proteins (**Figures 6E–H**).

Compared with young rats, the levels of MDA in plasma and myocardial tissue of aging rats increased, and the fluorescence intensity of DHE in the myocardial tissue increased. NaHS treatment lowered the levels of MDA in plasma and myocardial tissue and reduced the fluorescence intensity of DHE (**Figures 7A–D**). The GSH level in the myocardial tissue of aging rats was lower than the GSH levels in young rats, and treatment with NaHS promoted the

generation of GSH (**Figure 7E**); Western blot analyses showed that SLC7A11 and GPX4 expressions decreased, and the ACSL4 expression was enhanced in the myocardial tissue of aging rats compared with the expression in young rats. Treatment with NaHS enhanced NRF2 SLC7A11 and GPX4 protein expressions and attenuated the expression of ACSL4 (**Figures 7F–J**). Electron microscopy of cardiomyocytes showed that compared with young rats, the density of mitochondrial membranes increased, the mitochondrial cristae decreased or disappeared, the outer membranes of mitochondria were broken, and mitochondria edema was observed in aging rats compared with that in young rats. Treatment with NaHS inhibited the abnormal changes in cardiomyocyte mitochondria (**Figure 7K**). Based on these findings, we cautiously surmised that H<sub>2</sub>S inhibited cardiomyocyte ferroptosis.

## H<sub>2</sub>S Alleviated Myocardial Injury and Improved Cardiac Function in Rats Fed With a HID

To verify whether H<sub>2</sub>S could regulate iron metabolism, we used a HID to induce iron-overload cardiomyopathy in rats. Aging rats

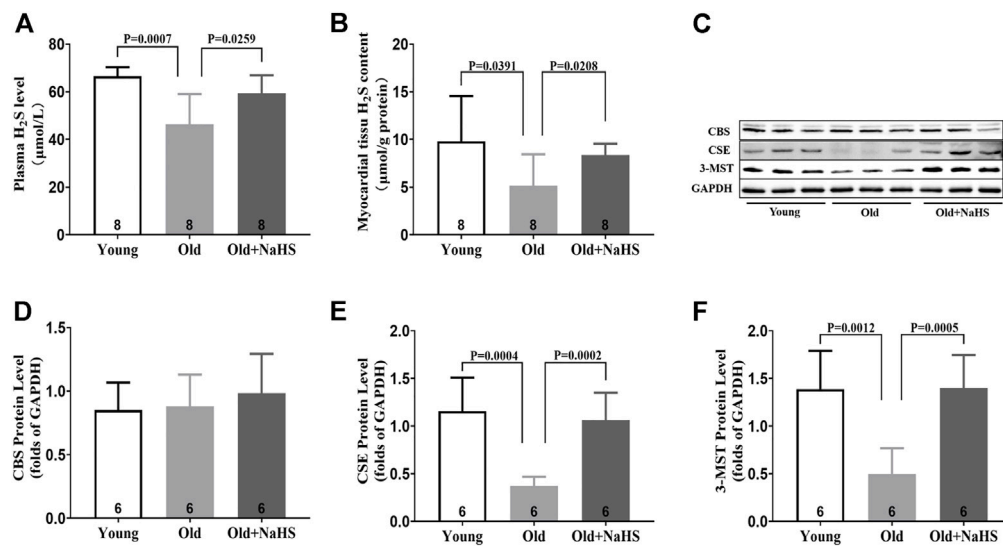


**FIGURE 3 |** Exogenous H<sub>2</sub>S enhanced H<sub>2</sub>S synthase expression in the myocardial tissue of aging rats. **(A)** H<sub>2</sub>S levels in the plasma of aging rats. **(B)** H<sub>2</sub>S levels in the myocardial tissue of aging rats. **(C)** Representative Western blots for CBS, CSE, and 3-MST expressions in myocardial tissues of aging rats. GAPDH was used as the internal control. **(D)** Quantitative analysis for CBS expression in the myocardial tissue of aging rats. **(E)** Quantitative analysis for the CSE expression in the myocardial tissue of aging rats. **(F)** Quantitative analysis for the 3-MST expression in the myocardial tissue of aging rats. Results are means ± SEM. A *p*-value of <0.05 was considered significant.

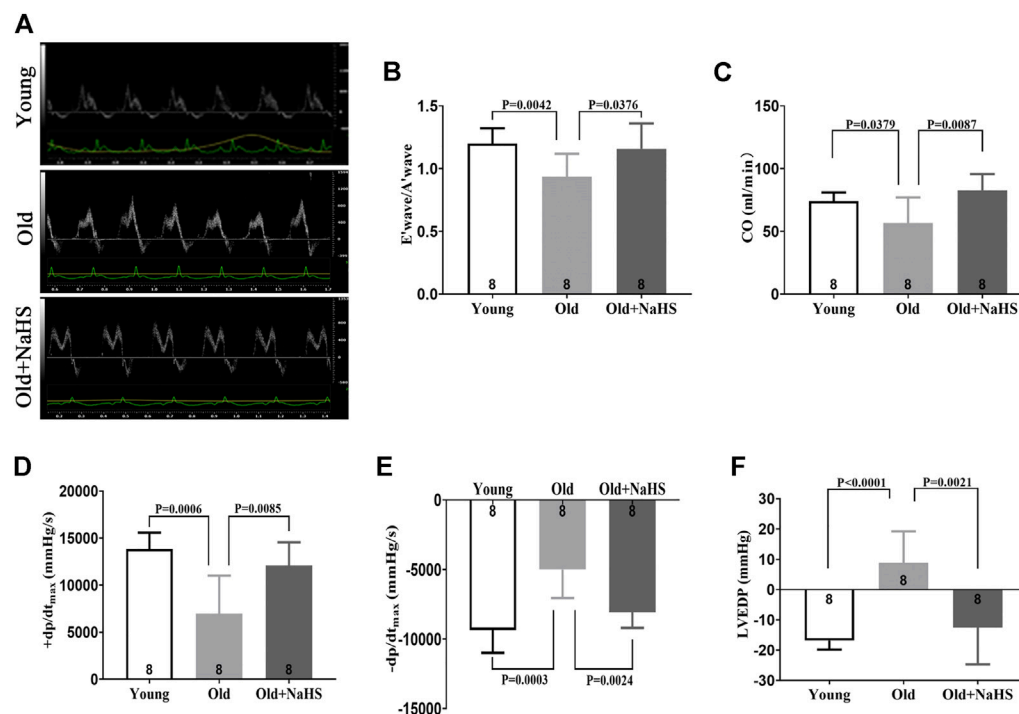


**FIGURE 4 |** H<sub>2</sub>S improved cardiac function in aging rats. **(A)** Representative images of the PW Doppler-mode by echocardiography indicated E' wave and A' wave in aging rats. **(B)** E' wave/A' wave ratios in aging rats. **(C)** Values of CO in aging rats. **(D)** Values of +dp/dt<sub>max</sub> in aging rats. **(E)** Values of -dp/dt<sub>max</sub> in aging rats. **(F)** Values of LVEDP in aging rats. Results are means ± SEM. A *p*-value of <0.05 was considered significant. +dp/dt<sub>max</sub>: the maximum rate of left ventricular pressure rise. -dp/dt<sub>max</sub>: the maximum rate of left ventricular pressure fall. LVEDP: left ventricular end diastolic pressure.

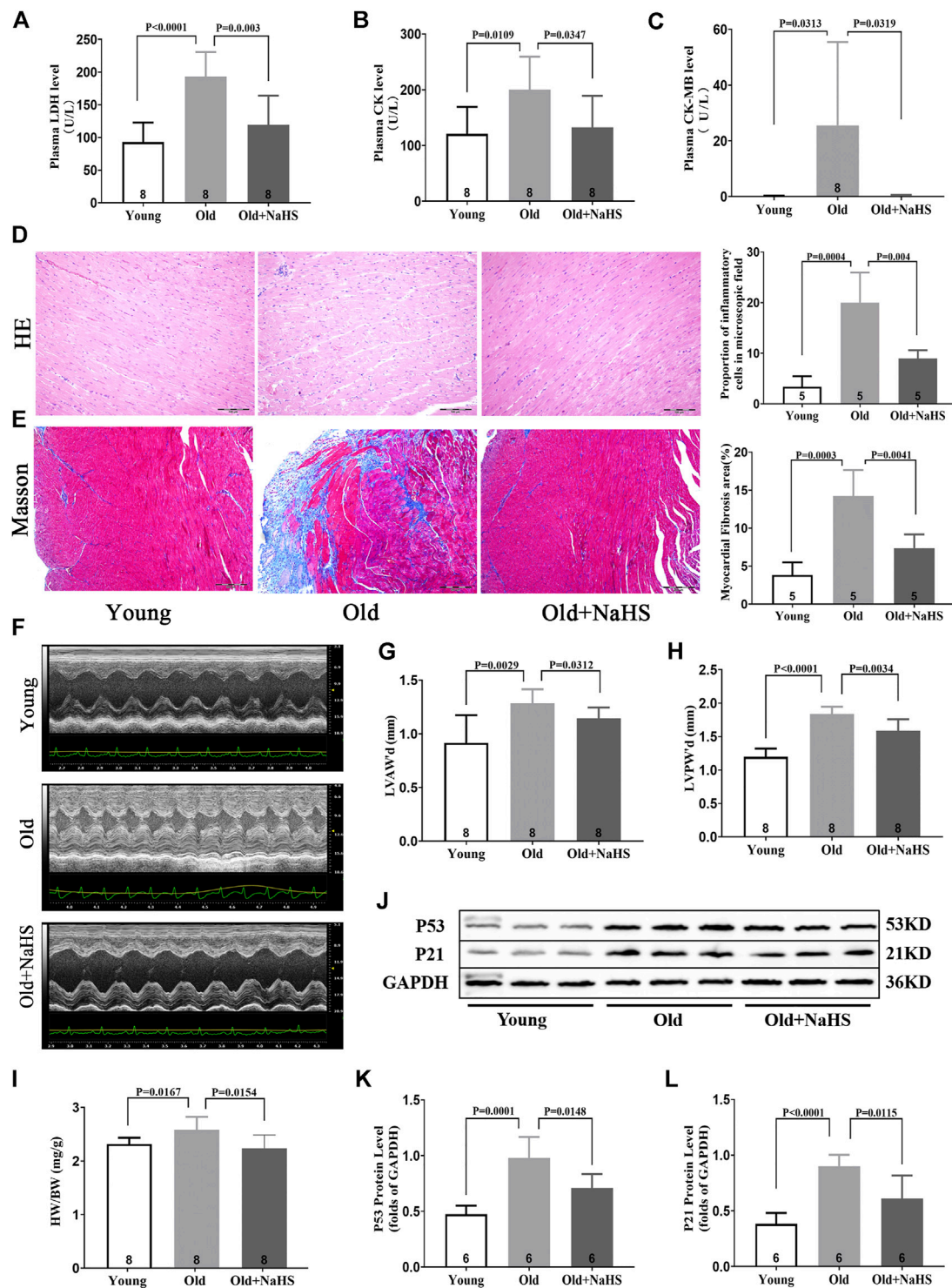


**FIGURE 5 |** H<sub>2</sub>S alleviated myocardial injury in aging rats. **(A)** Levels of plasma LDH in aging rats. **(B)** Levels of plasma CK in aging rats. **(C)** Levels of plasma CK-MB in aging rats. **(D)** Representative HE-stained myocardial sections in aging rats and quantitative data on inflammatory or death cells in microscopic field (%). **(E)** Representative Masson-stained myocardial sections in aging rats and quantitative data on myocardial fibrosis (%). **(F)** Representative images of M-mode by echocardiography indicated LVAW and LVPW in aging rats. **(G)** Values of LVAW'd in aging rats. **(H)** Values of LVPW'd in aging rats. **(I)** HW/BW ratios in aging rats. **(J)** Representative Western blots for P53 and P21 expressions in myocardial tissues of aging rats. GAPDH was used as the internal control. **(K)** Quantitative analysis for the P53 expression in the myocardial tissue of aging rats. **(L)** Quantitative analysis for the P21 expression in the myocardial tissue of aging rats. Results are means  $\pm$  SEM. A *p*-value of <0.05 was considered significant. LDH: lactate dehydrogenase, CK: creatine kinase, CK-MB: creatine kinase isoenzyme-MB, HW/BW: heart weight/body weight ratios.



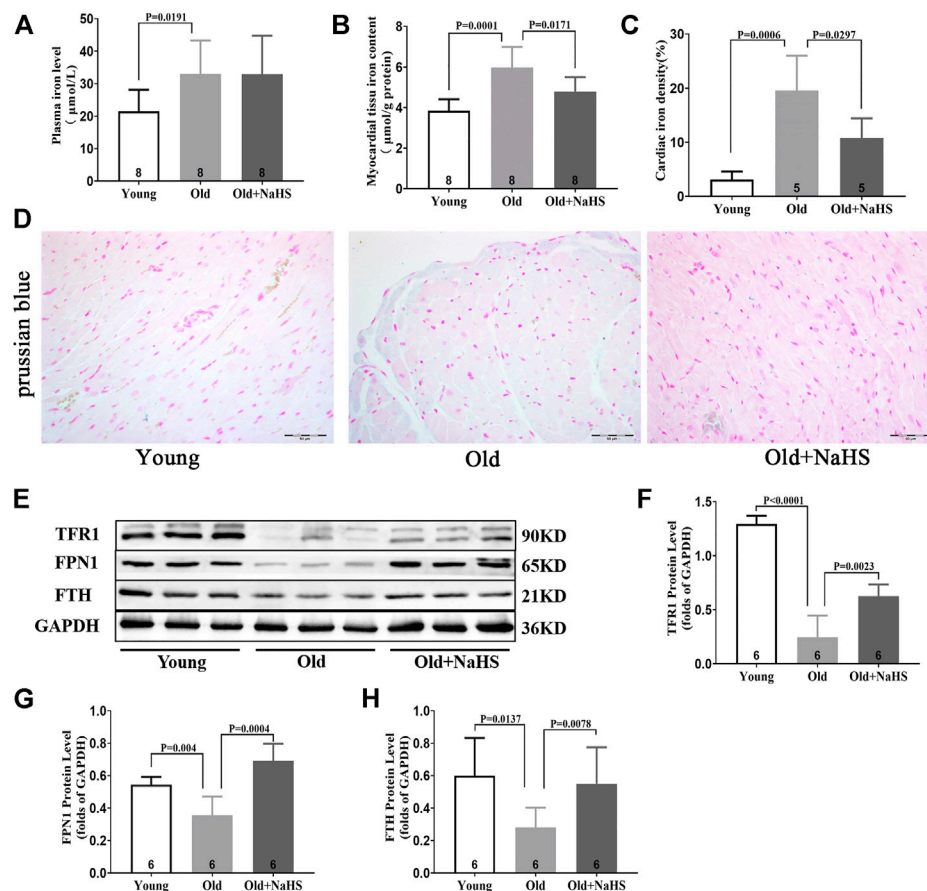


**FIGURE 6 |**  $\text{H}_2\text{S}$  regulated iron metabolism and reduced iron accumulation in aging rats. **(A)** Iron levels in the plasma of aging rats. **(B)** Iron levels in the myocardial tissue of aging rats. **(C)** Quantitative data on the Prussian-blue-iron-stained in aging rats. **(D)** Representative Prussian-blue-iron-stained in myocardial tissue sections of aging rats. **(E)** Representative Western blots for TFR1, FPN1, and FTH expressions in myocardial tissues. GAPDH was used as the internal control. **(F)** Quantitative analysis for the TFR1 expression in the myocardial tissue of aging rats. **(G)** Quantitative analysis for the FPN1 expression in the myocardial tissue of aging rats. **(H)** Quantitative analysis for the FTH expression in the myocardial tissue of aging rats. Results are means  $\pm$  SEM. A  $p$ -value of  $<0.05$  was considered significant.

began to die on the eighth of HID feeding. By the 10th week, all 12 aging rats on the HID died. Meanwhile, seven aging rats in the old + HID + NaHS group died and five survived, with a mortality rate of 58.3%. Three aging rats in the old + NID group died, and nine survived, with a mortality rate of 25%. These findings indicated that HID accelerated the death of aging rats (Supplementary Figures S2A,B).

HID did not affect  $\text{H}_2\text{S}$  levels in the plasma and myocardial tissue of young rats, and no significant differences in the expression of endogenous  $\text{H}_2\text{S}$  synthase CSE, CBS, and 3-MST were detected in the myocardial tissue. However, treatment with NaHS enhanced the expression of endogenous  $\text{H}_2\text{S}$  synthase CSE, CBS, and 3-MST in the myocardial tissue of young rats fed with HID and increased  $\text{H}_2\text{S}$  levels in plasma and myocardial tissue compared with the  $\text{H}_2\text{S}$  levels in untreated rats fed with a HID (Supplementary Figures S3A–F).

Feeding HID reduced the cardiac function in young rats, which was mainly manifested by the decrease in EF%, FS%,  $+\text{dp}/\text{dt}_{\text{max}}$ , and  $-\text{dp}/\text{dt}_{\text{max}}$  and increased LVEDP. Treatment

with NaHS restored EF%, FS%,  $+\text{dp}/\text{dt}_{\text{max}}$ , and  $-\text{dp}/\text{dt}_{\text{max}}$  and reduced LVEDP (Figures 8A–F).

Serum LDH and CK increased in rats fed with HID, and treatment with NaHS significantly reduced the levels of serum myocardial injury biomarkers (Figures 8G,H). HE staining showed that cardiomyocytes in rats fed with NID were dense, and the number of inflammatory cells in the myocardial interstitium was significantly lower than rats fed with HID. Treatment with NaHS decreased the number of inflammatory cells in the myocardial interstitium (Figures 8I,J). However, no significant differences in the area of myocardial fibrosis were detected between the groups (Supplementary Figure S4). Western blot analysis showed that HID enhanced the expression of senescence marker proteins p53 and P21, indicating that the cardiac senescence increased and accelerated the aging process in rats. Treatment with NaHS reduced the protein expression of p53 in the myocardial tissue of rats fed with a HID, indicating that cardiac senescence was reduced (Figures 8K–M).

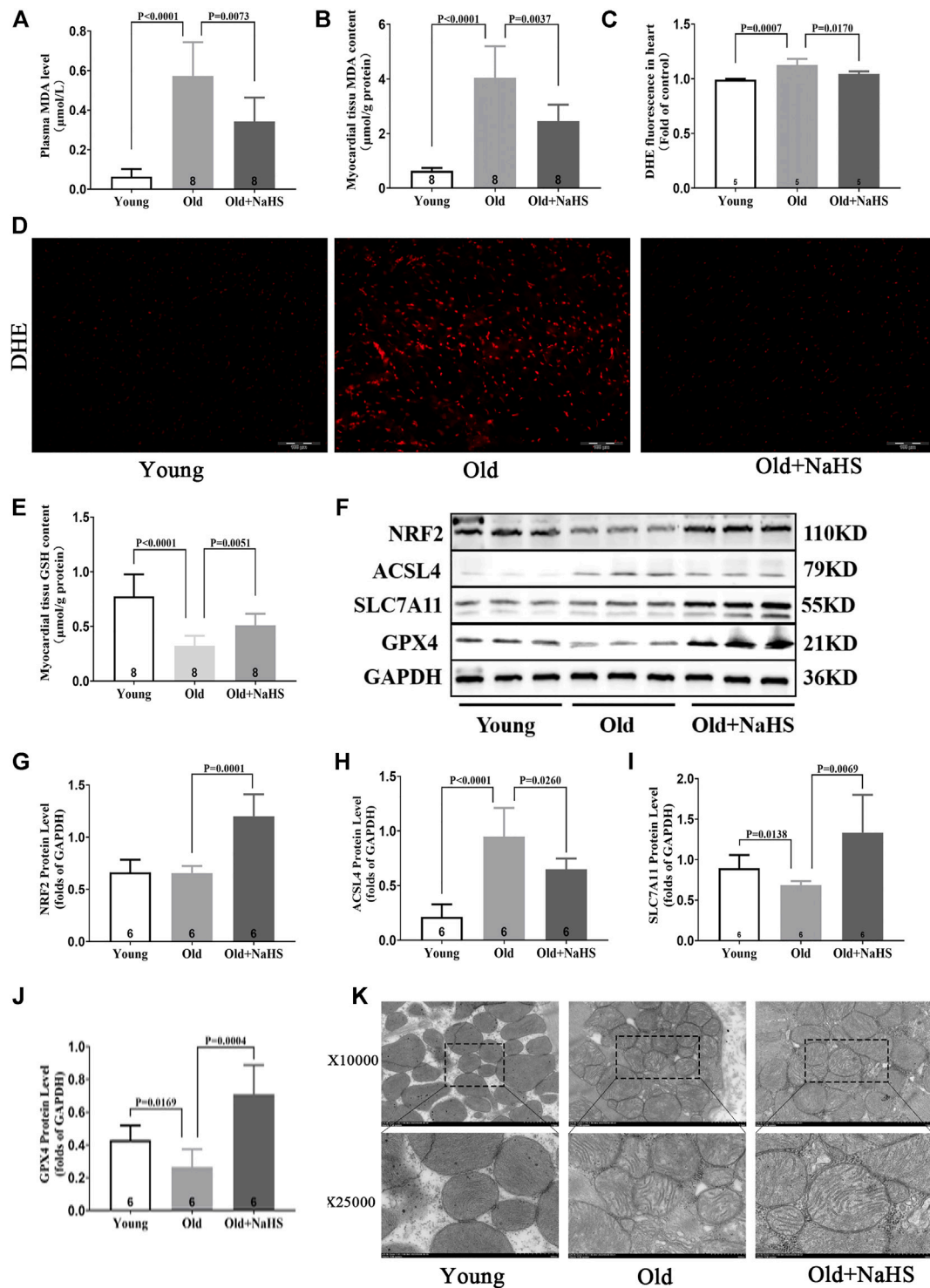


**FIGURE 7 |**  $\text{H}_2\text{S}$  inhibited cardiomyocyte ferroptosis in aging rats. **(A)** MDA levels in the plasma of aging rats. **(B)** MDA levels in the myocardial tissue of aging rats. **(C)** Quantitative data on DHE-fluorescence in aging rats. **(D)** Representative DHE-fluorescence in the myocardial tissue sections of aging rats. **(E)** GSH levels in the myocardial tissue of aging rats. **(F)** Representative Western blots for NRF2, ACSL4, SLC7A11, and GPX4 expressions in the myocardial tissues of aging rats. GAPDH was used as the internal control. **(G)** The quantitative analysis for NRF2 expression in the myocardial tissue of aging rats. **(H)** Quantitative analysis for ACSL4 expression in the myocardial tissue of aging rats. **(I)** Quantitative analysis for the SLC7A11 expression in the myocardial tissue of aging rats. **(J)** Quantitative analysis for the GPX4 expression in the myocardial tissue of aging rats. **(K)** Representative images of transmission electron microscopy for mitochondria in the cardiomyocyte of aging rats. Results are means  $\pm$  SEM. A  $p$ -value of  $<0.05$  was considered significant.

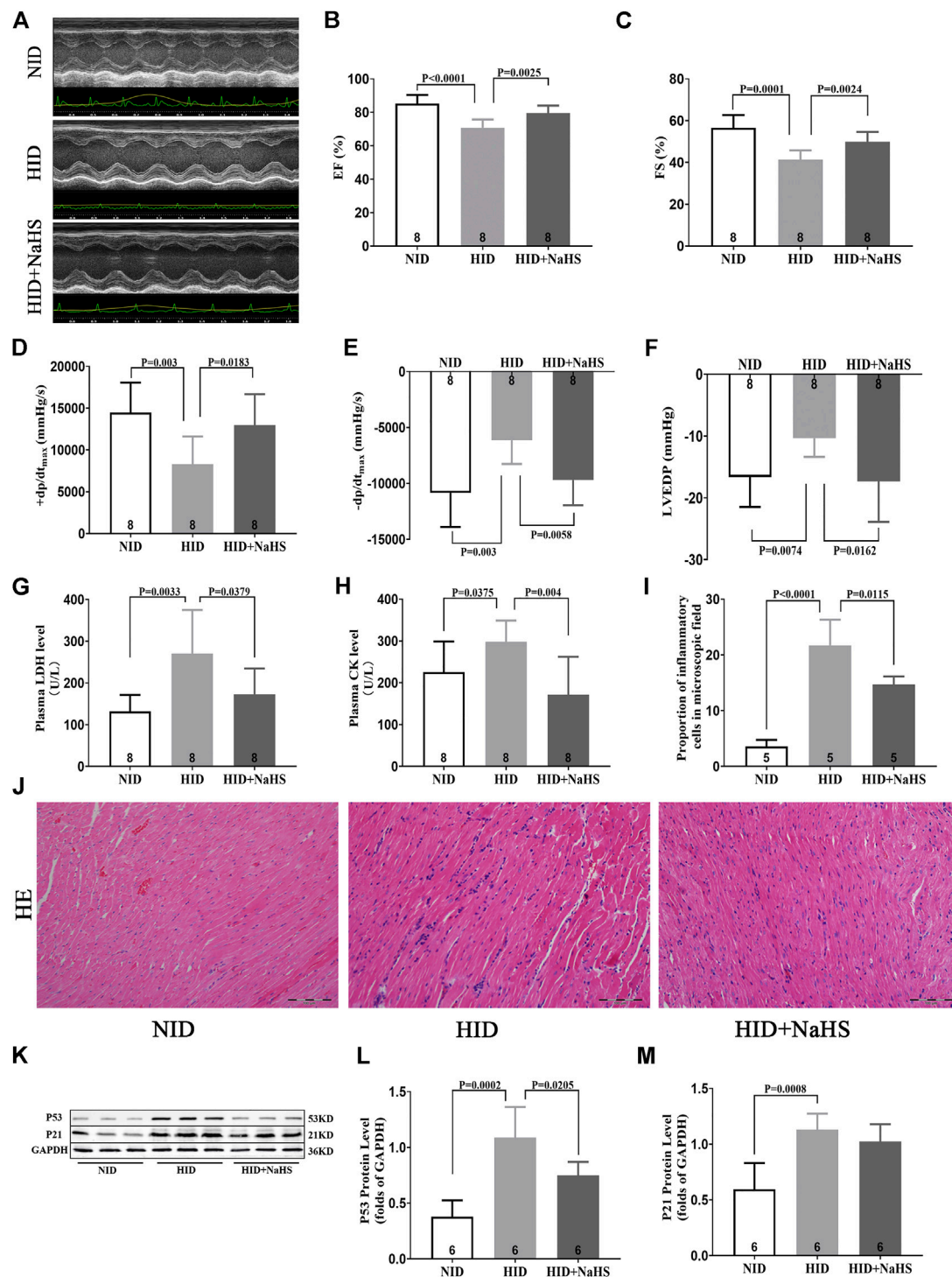


**FIGURE 8** |  $H_2S$  alleviated myocardial injury and improved cardiac function in rats fed with HID. **(A)** Representative images of M-mode by echocardiography in HID rats. **(B)** Values of EF (%) in HID rats. **(C)** Values of FS (%) in HID rats. **(D)** Values of  $+dp/dt_{max}$  in HID rats. **(E)** Values of  $-dp/dt_{max}$  in HID rats. **(F)** Values of LVEDP in HID rats. **(G)** Levels of plasma LDH in HID rats. **(H)** Levels of plasma CK in HID rats. **(I)** Quantitative data on inflammatory cells in the microscopic field (%) of HID rats. **(J)** Representative HE-stained myocardial sections of HID rats. **(K)** Representative Western blots for P53 and P21 expressions in myocardial tissues of HID rats. GAPDH was used as the internal control. **(L)** Quantitative analysis for the P53 expression in the myocardial tissue of HID rats. **(M)** Quantitative analysis for the P21 expression in the myocardial tissue of HID rats. Results are means  $\pm$  SEM. A  $p$ -value of  $<0.05$  was considered significant.

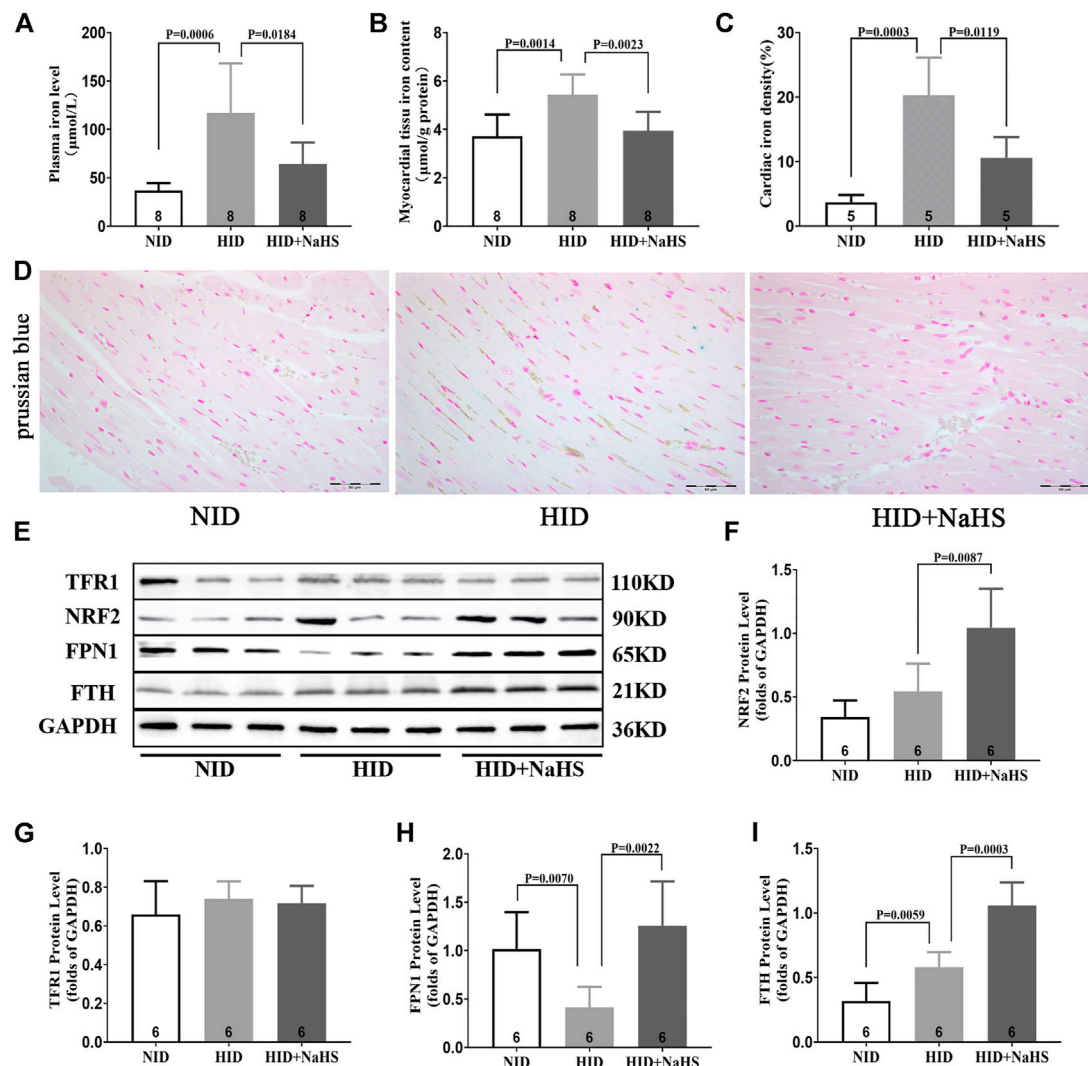


**FIGURE 9** |  $\text{H}_2\text{S}$  regulated cardiomyocyte iron metabolism in rats fed with HID. **(A)** Iron levels in the plasma of HID rats. **(B)** Iron levels in the myocardial tissue of HID rats. **(C)** Quantitative data on Prussian-blue staining in HID rats. **(D)** Representative Prussian-blue staining in myocardial tissue sections of HID rats. **(E)** Representative Western blots for TFR1, NRF2, FPN1, and FTH expressions in the myocardial tissues of HID rats. GAPDH was used as the internal control. **(F)** Quantitative analysis for NRF2 expression in the myocardial tissue of HID rats. **(G)** Quantitative analysis for the TFR1 expression in the myocardial tissue of HID rats. **(H)** Quantitative analysis for the FPN1 expression in the myocardial tissue of HID rats. **(I)** Quantitative analysis for the FTH expression in the myocardial tissue of HID rats. Results are means  $\pm$  SEM. A  $p$ -value of  $<0.05$  was considered significant.

Iron levels in the plasma and myocardial tissue and the proportion of iron-stained cells in the myocardial tissue of rats fed with a HID increased. Treatment with NaHS lowered the levels of iron in plasma and myocardial tissue and reduced the proportion of iron-stained cells in the myocardial tissue (**Figures 9A–D**). Western blot analysis showed that NaHS enhanced the expressions of NRF2, FPN1, and FTH in the myocardial tissue of rats fed with HID, but no significant differences in the expression of TFR1 were detected (**Figures 9E–I**).

## DISCUSSION

Age is a major risk factor for cardiac dysfunction and overall cardiovascular disease. Greater time for exposure to injurious

stimuli, such as hypertension, metabolic stress, or ischemic injury, clearly contributes to cardiac dysfunction with aging. The aging heart has limited endogenous capacity for repair or regeneration. Thus, aging impairs cardiac reserves and elevates the risk of cardiac dysfunction.

In our clinical experiments, echocardiographic measurements indicated that structural and functional changes contributing to cardiac dysfunction occurred in the aging heart, even in the absence of overt injury or disease. Normal aging is generally accompanied by thickening and stiffening of the LV walls and the interventricular septum. In addition, the LV diameter and cardiac fibrosis increase. These findings are consistent with previous studies (Fleg et al., 2015). However, our study also demonstrates that the abnormal cardiac diastolic function



usually occurred before changes in the cardiac systolic function during aging. This may be due to the slow degeneration and death of cardiomyocytes in the aging process. Compensatory mechanisms cause fibrosis-like changes in the ventricular wall, specifically manifested as increased ventricular stiffness, limited ventricular diastolic capacity, insufficient filling times, and cardiac dysfunction. Thus, although EF%, FS%, and SV did not change, E/A, E/e', E', and LAVI, which measured cardiac diastolic function, were abnormal. This “diastolic heart failure” with preserved cardiac systolic function (Francesco et al., 2013) was verified in aging rats (**Figures 4A,B**). At the same time, centripetal hypertrophy of the left ventricle occurred, resulting in LV lumen stenosis (**Figures 5F–I**). Limited filling of the heart during diastole leads to less effective circulating blood, cardiac dysfunction, and even fatal heart failure.

Iron is an essential element and is fundamental to many biological processes, including oxygen transport and storage and oxidative phosphorylation and redox reactions due to its ability to transport oxygen and electrons (Coffey and Ganz, 2017). Therefore, iron metabolism disorders, especially iron excess, result in abnormal oxidation–reduction reactions, which contribute to organ dysfunction *via* the accumulation of ROS (Gudjoncik et al., 2014). Our results showed that serum iron and MDA increased with aging and with decreased serum H<sub>2</sub>S levels. Thus, serum iron and MDA negatively correlated with the level of serum H<sub>2</sub>S in healthy individuals. The decrease in endogenous H<sub>2</sub>S levels aggravates the progress of cardiovascular diseases (Testai et al., 2021). However, the relationship between endogenous H<sub>2</sub>S, aging, and cardiac dysfunction in healthy individuals has not been reported yet. For the first time, we found that endogenous H<sub>2</sub>S levels decreased with aging in healthy individuals, and the decreased H<sub>2</sub>S was accompanied by cardiac dysfunction.

The animal experiments were consistent with the clinical experiments. In aging rats, endogenous H<sub>2</sub>S levels decreased, oxidative stress increased, iron accumulated, myocardial injury and myocardial fibrous tissue hyperplasia increased, and cardiac function declined. After treatment with exogenous H<sub>2</sub>S, H<sub>2</sub>S in plasma and myocardial tissue increased, the expression of endogenous H<sub>2</sub>S synthase was enhanced in the myocardial tissue, the levels of oxidative stress and iron in plasma and myocardial tissue decreased, myocardial injury was attenuated, and cardiac function improved. The mechanism for the enhanced endogenous H<sub>2</sub>S by exogenous H<sub>2</sub>S supplementation seems to be the enhanced CSE expression at a certain range of H<sub>2</sub>S concentration, and the appropriate concentration of exogenous H<sub>2</sub>S affects CSE transcription and translation (Yan, 2004; Wang, 2013). The increased expression of mitochondrial 3-MST in response to exogenous H<sub>2</sub>S supplementation may be *via* the reduction in mitochondrial damage in cardiomyocytes (Li et al., 2016b). The heart contains several kinds of cells, and H<sub>2</sub>S can be synthesized by cells other than cardiomyocytes; thus, CBS is also expressed in the myocardial tissue. The appropriate concentration of exogenous H<sub>2</sub>S supplementation can promote the expression of CBS in myocardial tissue (Shyam Sundar Nandi, 2017). However, the expression of endogenous H<sub>2</sub>S synthase in the two animal models constructed in our study

was slightly different, which conflicted with previous conclusions. These differences may be due to the different animal species and animal model conditions.

Cardiac dysfunction was caused by iron accumulation in aging and HID animal models, consistent with several previous studies. However, the previous studies focused on the increased oxidative stress induced by iron accumulation and the effects of iron accumulation on cardiac electrophysiological conduction (Wongjaikam et al., 2016; Wongjaikam and Kumfu, 2017). Our study demonstrated that iron accumulation increased oxidative stress levels and caused cardiac dysfunction, which may be partly caused by cardiomyocyte ferroptosis and aggravated by cardiac senescence. Iron metabolism in cardiomyocytes is mainly regulated by FPN1, TFR1, and FTH (Muckenthaler et al., 2017). We found that the expressions of TFR1, FTH, and FPN1 were lower in myocardial cells of aging rats than the expression in young rats. These effects in aging rats may be caused by the decreased ability to regulate iron metabolism and maintain iron homeostasis. In aged cardiomyocytes, increases in autophagic flow and autocrine effects of hepcidin promote the degradation of FPN1 and FTH, therefore reducing the expression of these two proteins (Gao et al., 2016; Hou et al., 2016; Zhang et al., 2019). In most types of cells, the control of TFR1 expression is mediated by IRP1 *via* interactions with iron-responsive elements (Muckenthaler et al., 2017). The reduced expression of FPN1 leads to decreased iron release out of the cells, and autophagy of FTH increases intracellular iron, leading to the accumulation of iron inside of the cells. These can downregulate IRP1 expression, resulting in decreased TFR1 expression.

Exogenous H<sub>2</sub>S supplementation affected the expression of several key iron metabolism regulatory proteins and reduced cardiac senescence similar to previous studies (Wang et al., 2021). However, our study also demonstrated the effects of H<sub>2</sub>S on the expressions of FTH and FPN1 in cardiomyocytes. FPN1 is the only known mammalian iron export protein, and FTH is the main iron storage protein in cells (Tian et al., 2021; Wang et al., 2022). Increasing FPN1 expression and inhibiting the degradation of FTH reduce intracellular iron accumulation (Gao et al., 2016; Hou et al., 2016). H<sub>2</sub>S inhibits ferritinophagy signaling by activating NRF2 and PPAR- $\gamma$ , which suppress ferroptosis (Wang et al., 2021; Wang et al., 2022). In our study, the NRF2 protein expression also changed when the expressions of FTH and FPN1 were enhanced after exogenous H<sub>2</sub>S supplementation. The NRF2/FTH and NRF2/FPN1 axes have already confirmed (Liu et al., 2020; Han et al., 2021). Thus, we speculated that the factors led to altered FTH and FPN1 expressions. Changes in the TFR1 expression may be due to a decreased intracellular iron accumulation. Decreased FPN1 in HID-fed rats may be related to the increased autocrine function of hepcidin caused by the increased expression of p53 in myocardial tissue (Wang et al., 2019; Zhang et al., 2019), while the increased expression of FTH in HID-fed rats may be a positive feedback effect caused by cellular iron accumulation. However, further research is needed to explore the specific mechanisms and causal relationships.

Apart from iron-mediated oxidative stress, cells must also cope with a variety of ROS. The NRF2 pathway regulates not only several genes involved in iron metabolism but also the cellular antioxidant responses. H<sub>2</sub>S stabilizes NRF2 and induces NRF2 target genes through antioxidant/electrophilic response

elements. The ability of H<sub>2</sub>S antioxidant stress to inhibit cell death is dependent on NRF2 (Hourihan, 2013). In aging rats, cardiac dysfunction was accompanied by decreased levels of H<sub>2</sub>S in plasma and myocardial tissue and elevated oxidative stress levels. In addition, the GSH level in myocardial tissue decreased, and GSH is synthesized by glutamate, glycine, and cysteine. Cysteine comes from the transformation of cystine, which is transported from the extracellular place into cells by system<sup>XC-</sup> (Lin et al., 2015). The transmembrane transporter SLC7A11 is an important component of system<sup>XC-</sup>, and the expression of SLC7A11 is regulated by the upstream NRF2 pathway (Kimura et al., 2010). Pathways related to H<sub>2</sub>S antioxidant stress include the activation of the NRF2 pathway (Calvert et al., 2009). H<sub>2</sub>S also induces the reduction of cystine to cysteine, increases the intracellular content of cysteine as the substrate of GSH synthesis, and enhances the transport of cysteine (Kimura et al., 2010). Our findings indicated that exogenous H<sub>2</sub>S treatment in aging rats enhanced the expressions of NRF2, SLC7A11, and GPX4 and elevated GSH levels in myocardial tissue. GSH is a necessary substrate for GPX4 to exert antioxidant effects. These combined effects reduced oxidative stress levels, reduced myocardial injury, and improved cardiac function.

Ferroptosis is an iron-dependent cell death form and is triggered by the excessive accumulation of lipid peroxide (Dixon et al., 2012). The phenomena we observed in the aging rat model, including the accumulation of iron and the increase in the lipid metabolite MDA, were consistent with the characteristics of ferroptosis. ACSL4 plays an important role in the occurrence and development of ferroptosis by promoting the synthesis of lipid peroxide. Of note, ACSL4 can be used as an indicator of the ferroptosis program (Proneth et al., 2017; Stockwell et al., 2017). The expression of ACSL4 increased in both myocardial injury and aging organisms, which aggravated the accumulation of lipid peroxides (Proneth et al., 2017; Wang et al., 2021; Zhou et al., 2022). Exogenous H<sub>2</sub>S supplementation may inhibit the expression of ACSL4 by reducing myocardial injury and consequently inhibiting the synthesis of polyunsaturated fatty acids. GPX4 is a selenoprotein and is a unique intracellular antioxidant enzyme that can directly quench the metabolites of lipid peroxide in cell membranes (Shah et al., 2018; Li et al., 2020). Therefore, decreased GPX4 activity leads to ferroptosis. In our current research, the ACSL4 expression increased, and the expression of GPX4 decreased in the myocardial tissue of aging rats. The main subcellular organ attacked by ROS is mitochondria, and the abnormal changes in mitochondria showed by electron microscopy were consistent with the characteristics of ferroptosis. After treatment with exogenous H<sub>2</sub>S, the expression of GPX4 increased, the expression of ACSL4 decreased, and the abnormal changes in mitochondria were suppressed. Therefore, we speculate that the decline in endogenous H<sub>2</sub>S levels and the cardiomyocyte ferroptosis may be involved in the cardiac dysfunction of aging, and the decline in endogenous H<sub>2</sub>S levels aggravates cardiomyocyte ferroptosis.

We have only preliminarily confirmed that aging involves elevated oxidative stress levels, iron accumulation, and decreased endogenous H<sub>2</sub>S levels, accompanied by cardiac dysfunction and

cardiac remodeling. The cardiac dysfunction and cardiac remodeling associated with aging are closely related to the decreased endogenous H<sub>2</sub>S levels, and ferroptosis participates in the pathological process of cardiac dysfunction and cardiac remodeling. However, H<sub>2</sub>S and ferroptosis agonists and inhibitors are not used *in vivo*. Therefore, the specific process of ferroptosis leading to cardiac dysfunction and the protective mechanism of H<sub>2</sub>S will be further studied.

We speculate that H<sub>2</sub>S may inhibit cardiomyocyte ferroptosis by reducing iron accumulation and the oxidative stress level to reduce the impact of aging on cardiac function. Targeted intervention in the endogenous H<sub>2</sub>S levels may protect cardiac function and reduce the risk of cardiovascular diseases in aging.

## DATA AVAILABILITY STATEMENT

The original contributions presented in the study are included in the article/**Supplementary Material**; further inquiries can be directed to the corresponding authors.

## ETHICS STATEMENT

The studies involving human participants were reviewed and approved by the Ethics Committee of the Hebei Medical University (Shijiazhuang, China). The patients/participants provided their written informed consent to participate in this study. The animal study was reviewed and approved by all animal procedures and were approved by the Animal Management Rule of the Ministry of Health, People's Republic of China (documentation number 5,2001) and the Animal Care Committee of Hebei Medical University. The protocols and procedures performed were in compliance with the Guide for the Care and Use of Laboratory Animals (NIH Publication No. 85-23, revised 2011). Written informed consent was obtained from the individual(s) for the publication of any potentially identifiable images or data included in this article.

## AUTHOR CONTRIBUTIONS

ZL, YM, XT, LX, QG, HX, and DT acquired, analyzed, and interpreted the data and drafted the manuscript. YW and SJ designed the studies. All authors revised the manuscript critically for important intellectual content. All authors have approved the final version of the manuscript and agree to be accountable for all aspects of the work.

## FUNDING

This study was supported by the National Natural Science Foundation of China (91849120, 31871154, and 31671185), the Natural Science Foundation of Hebei Province of China (C2020206025 and H2020206417), and the Key R &D Project of Hebei Province (20277735D).

## ACKNOWLEDGMENTS

The authors thank Huaxing Zhang (Hebei Medical University Core Facilities and Centers, Shijiazhuang, Hebei, China) for his technical assistance.

## REFERENCES

- Baba, Yuichi, Higa, Jason K., Matsui, Takashi, Marh, Karra S., Kitaoka, Hiroaki, Matsui, Takashi, et al. (2018). Protective Effects of the Mechanistic Target of Rapamycin 1 against Excess Iron and Ferroptosis in Cardiomyocytes. *Articles. Am. J. Physiol. Heart Circ. Physiol.* 314 (3), H659–H668. doi:10.1152/ajpheart.00452.2017
- Bai, Yu-Ting, Chang, Rong, Wang, Li-Sheng, Xiao, Feng-Jun, Ge, Ri-Li, Wang, Li-Sheng, et al. (2018). ENPP2 Protects Cardiomyocytes from Erastin-Induced Ferroptosis. *Biochem. Biophysical Res. Commun.* 499 (1), 44–51. doi:10.1016/j.bbrc.2018.03.113
- Calvert, J. W., Elrod, J. W., Ramachandran, A., Pattillo, Christopher B., Kevil, Christopher G., Lefer, David J., et al. (2009). Hydrogen Sulfide Mediates Cardioprotection through Nrf2 Signaling. *Circ. Res.* 105, 365–374. doi:10.1161/circresaha.109.199919
- Coffey, R., and Ganz, T. (2017). Iron Homeostasis: an Anthropocentric Perspective. *J. Biol. Chem.* 292, 12727–12734. doi:10.1074/jbc.R117.781823
- Dixon, S. J., Lemberg, K. M., Skouta, R., Andras, J. B., Alexandra, M. C., Wan Seok, Y., et al. (2012). Ferroptosis: an Iron-dependent Form of Nonapoptotic Cell Death. *Cell* 149 (5), 1060–1072. doi:10.1016/j.cell.2012.03.042
- Fang, Xuexian, Min, Junxia, Wang, Fudi, Gu, W., Min, J., Wang, F., et al. (2019). Ferroptosis as a Target for Protection against Cardiomyopathy. *Proc. Natl. Acad. Sci.* 116 (7), 2672–2680. doi:10.1073/pnas.1821022116
- Fleg, J. L., Cooper, L. S., Blood Institute Working, G., Piña, Ileana L., Poole, David C., Reeves, Gordon R., et al. (2015). Exercise Training as Therapy for Heart Failure: Current Status and Future Directions. *Circ. Heart Fail.* 1, 209–220. doi:10.1161/circheartfailure.113.001420
- Francesco, S. L., Matthew, L. S., Steven, M. J., Joseph, G., James, R. P., Pratyusha, Y., et al. (2013). Growth Differentiation Factor 11 Is a Circulating Factor that Reverses Age-Related Cardiac Hypertrophy. *Cell* 153 (4), 828–839. doi:10.1016/j.cell.2013.04.015
- Galluzzi, L., M Bravo-San Pedro, J., Vitale, I., Yuan, J., Zakeri, Z., Zhivotovsky, B., et al. (2015). Essential versus Accessory Aspects of Cell Death: Recommendations of the NCCD 2015. *Cell Death Differ.* 22 (1), 58–73. doi:10.1038/cdd.2014.137
- Galluzzi, L., Vitale, I., S Alnemri, E., Alnemri, E. S., Altucci, L., Amelio, I., et al. (2018). Molecular Mechanisms of Cell Death: Recommendations of the Nomenclature Committee on Cell Death 2018. *Cell Death Differ.* 25 (3), 486–541. doi:10.1038/s41418-017-0012-4
- Gao, Minghui, Monian, Prashant, Jiang, Xuejun, Zhang, Wei, Xiang, Jenny, Jiang, Xuejun, et al. (2016). Ferroptosis Is an Autophagic Cell Death Process. *Cell Res.* 9, 1021–1032. doi:10.1038/cr.2016.95
- Gudjoncik, A., Guenancia, C., Zeller, M., Cottin, Y., Vergely, C., and Rochette, L. (2014). Iron, Oxidative Stress, and Redox Signaling in the Cardiovascular System. *Mol. Nutr. Food Res.* 58, 1721–1738. doi:10.1002/mnfr.201400036
- Han, Kang, Jin, Xiaofang, Chang, Yan-Zhong, Tian, Siyu, Song, Yiming, Zuo, Yuanyuan, et al. (2021). Nrf2 Knockout Altered Brain Iron Deposition and Mitigated Age-Related Motor Dysfunction in Aging Mice. *Free Radic. Biol. Med.* 162, 592–602. doi:10.1016/j.freeradbiomed.2020.11.019
- Hou, Wen, Xie, YangChun, Tang, DaoLin, Sun, Xiaofang, Lotze, Michael T., Zeh, Herbert J., et al. (2016). Autophagy Promotes Ferroptosis by Degradation of Ferritin. *Autophagy* 8, 1425–1428. doi:10.1080/15548627.2016.1187366
- Hourihan, John M. (2013). J Gerry Kenna, John D Hayes. The Gasotransmitter Hydrogen Sulfide Induces Nrf2-Target Genes by Inactivating the Keap1 Ubiquitin Ligase Substrate Adaptor through Formation of a Disulfide Bond between Cys-226 and Cys-613. *Antioxid. Redox Signal* 5, 465–481. doi:10.1089/ars.2012.4944
- Julian, U., Wagner, G., and Dimmeler, S. (2019). Cellular Cross-Talks in the Diseased and Aging Heart. *J. Mol. Cell Cardiol.* 2020 Jan. 138, 136–146. doi:10.1016/j.yjmcc.2019.11.152
- Kimura, Y., Goto, Y., and Kimura, H. (2010). Hydrogen Sulfide Increases Glutathione Production and Suppresses Oxidative Stress in Mitochondria. *Antioxid. Redox Signal* 12, 1–13. doi:10.1089/ars.2008.2282
- Li, Lina, Li, Meixiu, Xu, Changing, Sun, Weiming, Wang, Yuehong, Bai, Shuzhi, et al. (2016). Exogenous H<sub>2</sub>S Contributes to Recovery of Ischemic Post-conditioning-induced Cardioprotection by Decrease of ROS Level via Down-Regulation of NF-Kb and JAK2-STAT3 Pathways in the Aging Cardiomyocytes. *Cell Biosci.* 6, 26. doi:10.1186/s13578-016-0090-x
- Li, M., He, X., Guo, W., Li, N., Nie, Xiaoqun, Li, Yu, et al. (2020). Aldolase B Suppresses Hepatocellular Carcinogenesis by Inhibiting G6PD and Pentose Phosphate Pathways. *Nat. Cancer* 7, 735–747. doi:10.1038/s43018-020-0086-7
- Li, Na, Wang, Ming-Jie, Zhu, Yi-Chun, Hou, Cui-Lan, Ma, Fen-Fen, Li, Xing-Hui, et al. (2016). The H<sub>2</sub>S Donor NaHS Changes the Expression Pattern of H<sub>2</sub>S-Producing Enzymes after Myocardial Infarction. *Oxid. Med. Cell Longev.* 2016, 6492469. doi:10.1155/2016/6492469
- Lin, C. H., Lin, P. P., Lin, C. Y., Lin, C-H., Huang, Chiung-Hsien, Huang, Yu-Jhen, et al. (2015). Decreased mRNA Expression for the Two Subunits of System X<sup>cc</sup>, SLC3A2 and SLC7A11, in WBC in Patients with Schizophrenia: Evidence in Support of the Hypo-Glutamatergic Hypothesis of Schizophrenia. *Psy Chiatres.* 72, 58–63. doi:10.1016/j.jpsychires.2015.10.007
- Lin, Jian-Hong, Yang, Kun-Ta, Chang, Jui-Chih, Ting, Pei-Ching, Luo, Yu-Po, Ding, Jyun, et al. (2022). Xanthohumol Protects the Rat Myocardium against Ischemia/Reperfusion Injury-Induced Ferroptosis. *Oxid. Med. Cell Longev.* 17 (2022), 9523491. doi:10.1155/2022/9523491
- Liu, Zixuan, Lv, Xuying, and Song, Yang (2020). Fostered Nrf2 Expression Antagonizes Iron Overload and Glutathione Depletion to Promote Resistance of Neuron-like Cells to Ferroptosis. *Toxicol. Appl. Pharmacol.* 407, 115241. doi:10.1016/j.taap.2020.115241
- Muckenthaler, M. U., Rivella, S., and Hentze, M. W. (2017). A Red Carpet for Iron Metabolism. *Cell* 168, 344–361. doi:10.1016/j.cell.2016.12.034
- Park, Tae-Jun, Hyoung Park, Jei, Chul Lee, Sang, Kim, Min Wook, Kim, Yong Sook, Kim, Jeong-Yoon, et al. (2019). Quantitative Proteomic Analyses Reveal that GPX4 Downregulation during Myocardial Infarction Contributes to Ferroptosis in Cardiomyocytes. *Cell Death Dis.* 10 (11), 835. doi:10.1038/s41419-019-2061-8
- Perna, A. F., Luciano, M. G., Pulzella, P., Violetti, E., Capasso, Rosanna, Lombardi, Cinzia, et al. (2010). Hydrogen Sulfide, the Third Gaseous Signaling Molecule with Cardiovascular Properties, Is Decreased in Hemodialysis Patients. *J. Ren. NutrSuppl.* S11–S14. doi:10.1053/j.jrn.2010.05.004
- Proneth, B. S., Tyurina, Y. Y., Conrad, M., Beckers, Johannes, Aichler, Michaela, Walch, Axel, et al. (2017). ACSL4 Dictates Ferroptosis Sensitivity by Shaping Cellular Lipid Composition. *Nat. Chem. Biol.* 13, 91–98. doi:10.1038/nchembio.2239
- Shah, R., Shchepinov, M. S., and Pratt, D. A. (2018). Resolving the Role of Lipoxygenases in the Initiation and Execution of Ferroptosis. *ACS Cent. Sci.* 4, 387–396. doi:10.1021/acscentsci.7b00589
- Shyam Sundar Nandi (2017). Paras Kumar Mishra. H<sub>2</sub>S and Homocysteine Control a Novel Feedback Regulation of Cystathionine Beta Synthase and Cystathionine Gamma Lyase in Cardiomyocytes. *Sci. Rep.* 7 (1), 3639. doi:10.1038/s41598-017-03776-9
- Stockwell, B. R., Bush, A. I., Dixon, S. J., Ashley, I. B., Marcus, C., Scott, J. D., et al. (2017). Ferroptosis: A Regulated Cell Death Nexus Linking Metabolism, Redox Biology, and Disease. *Cell* 171 (2), 273–285. doi:10.1016/j.cell.2017.09.021
- Tang, L-J., Zhou, Y-J., Xiong, X-M., Li, N-S., Zhang, J-J., Luo, X-J., et al. (2021). Ubiquitin-specific Protease 7 Promotes Ferroptosis via Activation of the p53/TfR1 Pathway in the Rat Hearts after Ischemia/reperfusion. *Free Radic. Biol. Med.* 162, 339–352. doi:10.1016/j.freeradbiomed.2020.10.307

## SUPPLEMENTARY MATERIAL

The Supplementary Material for this article can be found online at: <https://www.frontiersin.org/articles/10.3389/fmolb.2022.947778/full#supplementary-material>

- Testai, L., Brancaleone, V., Flori, L., Montanaro, R., and Calderone, V. (2021). Modulation of EndMT by Hydrogen Sulfide in the Prevention of Cardiovascular Fibrosis. *Antioxidants (Basel)* 10 (6), 910. doi:10.3390/antiox10060910
- Tian, H., Xiong, Y., and Zhang, Y. (2021). Activation of NRF2 FPN1 Pathway Attenuates Myocardial Ischemia-Reperfusion Injury in Diabetic Rats by Regulating Iron Homeostasis and Ferroptosis. *Cell Stress Chaperones* 27 (2), 149–164. doi:10.1007/s12192-022-01257-1
- Timmers, P. R. H. J., Wilson, J. F., Joshi, P. K., and Deelen, J. (2020). Multivariate Genomic Scan Implicates Novel Loci and Haem Metabolism in Human Ageing. *Nat. Commun.* 11 (1), 3570. doi:10.1038/s41467-020-17312-3
- Wang, Maoxian (2013). Zhanyun Guo, Shilong Wang. The Effect of Certain Conditions in the Regulation of Cystathionine  $\gamma$ -lyase by Exogenous Hydrogen Sulfide in Mammalian Cells. *Biochem. Genet.* 1 (7–8), 503–513. doi:10.1007/s10528-013-9581-1
- Wang, Minjun, Xin, Hong, and Zhun Zh, Yi (2019). S-Propargyl-Cysteine, a Novel Hydrogen Sulfide Donor, Inhibits Inflammatory Hepcidin and Relieves Anemia of Inflammation by Inhibiting IL-6/STAT3 Pathway. *J. Cell Physiol.* 234 (4), 3158–3169. doi:10.1002/jcp.27431
- Wang, Ying, Liao, Sha, Chen, Yahong, Mad, S., TongLiu, C., Zhang, J., et al. (2022). Hydrogen Sulfide Alleviates Particulate Matter-Induced Emphysema and Airway Inflammation by Suppressing Ferroptosis. *Free Radic. Biol. Med.* 86, 1–16. doi:10.1016/j.freeradbiomed.2022.04.014
- Wang, Yuehong, Yu, Ruihuan, and Yang, Guangdong (2021). Hydrogen Sulfide Guards Myoblasts from Ferroptosis by Inhibiting ALOX12 Acetylation. *Cell Signal* 78, 1098–1110. doi:10.1016/j.cellsig.2020.109870
- Wongjaikam, S., Kumfu, S., Khamsekaew, J., Fucharoen, S., Chattipakorn, Siriporn C., Chattipakorn, Nipon, et al. (2016). Combined Iron Chelator and Antioxidant Exerted Greater Efficacy on Cardioprotection Than Monotherapy in Iron-Overloaded Rats. *PLoS One* 11, e0159414. doi:10.1371/journal.pone.0159414
- Wongjaikam, S., and Kumfu, S., Chattipakorn N. (2017). Restoring the Impaired Cardiac Calcium Homeostasis and Cardiac Function in Iron Overload Rats by the Combined Deferiprone and N-Acetyl Cysteine. *Sci. Rep.* 7, 44460. doi:10.1038/srep44460
- Yan, Hui (2004). Junbao Du, Chaoshu Tang. The Possible Role of Hydrogen Sulfide on the Pathogenesis of Spontaneous Hypertension in Rats. *Biochem. Biophys. Res. Commun.* 313 (1), 22–27. doi:10.1016/j.bbrc.2003.11.081
- Zhang, Huaxing, Sheng, Jin, Yuming, Wu, Teng, Xu, Jin, Sheng, Wu, Yuming, et al. (2021). Hydrogen Sulfide Restored the Diurnal Variation in Cardiac Function of Aging Mice. *Oxid. Med. Cell Longev.* 2 (2021), 8841575. doi:10.1155/2021/8841575
- Zhang, M., Qian, C., Qian, Z., Mu, M-D., Ke, Ya, Qian, Zhong-Ming, et al. (2019). Regulating Ferroportin-1 and Transferrin Receptor-1 Expression: A Novel Function of Hydrogen Sulfide. *J. Cell Physiol.* 4, 3158–3169. doi:10.1002/jcp.27431
- Zheng, H., Shi, L., Tong, C., Liu, Y., and Hou, M. (2021). CircSnx12 Is Involved in Ferroptosis during Heart Failure by Targeting miR-224-5p. *Front. Cardiovasc Med.* 8, 656093. doi:10.3389/fcvm.2021.656093
- Zhou, Bin, Zhang, Jing, Yu, Shuchun, Liu, Yang, Tang, Xiaoyi, Xia, Panpan, et al. (2022). Puerarin Protects against Sepsis-Induced Myocardial Injury through AMPK-Mediated Ferroptosis Signaling. *Aging (Albany NY)* 8, 3617–3632. doi:10.18632/aging.204033

**Conflict of Interest:** The authors declare that the research was conducted in the absence of any commercial or financial relationships that could be construed as a potential conflict of interest.

**Publisher's Note:** All claims expressed in this article are solely those of the authors and do not necessarily represent those of their affiliated organizations, or those of the publisher, the editors, and the reviewers. Any product that may be evaluated in this article, or claim that may be made by its manufacturer, is not guaranteed or endorsed by the publisher.

Copyright © 2022 Liang, Miao, Teng, Xiao, Guo, Xue, Tian, Jin and Wu. This is an open-access article distributed under the terms of the Creative Commons Attribution License (CC BY). The use, distribution or reproduction in other forums is permitted, provided the original author(s) and the copyright owner(s) are credited and that the original publication in this journal is cited, in accordance with accepted academic practice. No use, distribution or reproduction is permitted which does not comply with these terms.





# NPC1 Deficiency Contributes to Autophagy-Dependent Ferritinophagy in HEI-OC1 Auditory Cells

Lihong Liang<sup>1†</sup>, Hongshun Wang<sup>1†</sup>, Jun Yao<sup>1,2</sup>, Qinjun Wei<sup>1,2</sup>, Yajie Lu<sup>1</sup>, Tianming Wang<sup>3\*</sup> and Xin Cao<sup>1,2\*</sup>

<sup>1</sup>Department of Medical Genetics, School of Basic Medical Science, Nanjing Medical University, Nanjing, China, <sup>2</sup>Jiangsu Key Laboratory of Xenotransplantation, Nanjing Medical University, Nanjing, China, <sup>3</sup>Central Laboratory, Translational Medicine Research Center, The Affiliated Jiangning Hospital with Nanjing Medical University, Nanjing, China

## OPEN ACCESS

### Edited by:

Yanqing Liu,  
Columbia University, United States

### Reviewed by:

Tiancheng Fang,  
University of California, United States  
Yi Wang,  
Sichuan Academy of Medical  
Sciences and Sichuan Provincial  
People's Hospital, China

### \*Correspondence:

Tianming Wang  
wangtianming@njmu.edu.cn  
Xin Cao  
caoxin@njmu.edu.cn

<sup>†</sup>These authors have contributed  
equally to this work

### Specialty section:

This article was submitted to  
Molecular Diagnostics and  
Therapeutics,  
a section of the journal  
Frontiers in Molecular Biosciences

**Received:** 25 May 2022

**Accepted:** 21 June 2022

**Published:** 22 July 2022

### Citation:

Liang L, Wang H, Yao J, Wei Q, Lu Y,  
Wang T and Cao X (2022)  
NPC1 Deficiency Contributes to  
Autophagy-Dependent Ferritinophagy  
in HEI-OC1 Auditory Cells.  
Front. Mol. Biosci. 9:952608.  
doi: 10.3389/fmolb.2022.952608

Niemann–Pick type C disease (NPCD) is a rare genetic syndrome characterized by cholesterol accumulation in multiple organelles. NPCD is mainly caused by gene deficiency of NPC intracellular cholesterol transporter 1 (NPC1). It has been reported that some of the NPCD patients exhibit clinical features of progressive hearing loss at high frequency and iron disorder, but the underlying relationship is unknown. A recent study has reported that ferroptosis contributes to the impairment of cochlear hair cells that are related to sensory hearing. In this study, we generated NPC1-deficient HEI-OC1 cells to show the effect of NPC1 deficiency on cochlear outer hair cells. We found that NPC1 deficiency enhances autophagy-dependent ferritinophagy to release Fe (II). Our work provides important insights into the effect of NPC1 deficiency in auditory cells, indicating that it induces ferroptosis and results in hearing loss.

**Keywords:** Niemann–Pick type C disease, NPC1 deficiency, hearing loss, NCOA4, ferroptosis

## INTRODUCTION

Niemann–Pick type C disease (NPCD) is a genetic syndrome with a wide range of clinical features from rapidly fatal disorders in neonates to the onset of chronic neurodegenerative diseases in adults, affecting about 1/120,000 live births (Vanier, 2010). NPCD is mainly characterized by cholesterol accumulation, and it affects multiple organelles such as the central nervous system (CNS), visceral organelles, and auditory system (King, 2014a; Wheeler and Sillence, 2020). Current research shows more interests on the former (Vanier, 2010; Santos-Lozano et al., 2015; Balboa et al., 2021; Van Hoecke et al., 2021), but fewer studies have focused on the effect of NPCD related to genetic hearing loss and the molecular mechanism has not been fully understood to date.

The gene deficiency of NPC intracellular cholesterol transporter 1 (NPC1) mainly contributes to NPCD, accounting for approximately 95% of the NPCD family (Vanier et al., 1996; Higgins et al., 1999). NPC1 is a multiple transmembrane protein, consisting of 3 large luminal domains (NTD, MLD, and CTD) and 13 transmembrane domains (TM), located on the late-endosomal/lysosomal (LE/L) membrane and functions as a cholesterol transporter from the lumen to the membrane of late endosomes/lysosomes (Gong et al., 2016; Qian et al., 2020). Besides the role in cholesterol regulation, NPC1 deficiency has also been reported to lead to the dyshomeostasis of multiple metals (Hung et al., 2014) and even cause a deficient immunoreactivity of ferritin (a protein for iron storage) in the liver and spleen (Christomanou et al., 1995; Christomanou and Harzer, 1996), suggesting an important role of NPC1 in iron regulation. Ferroptosis is a type of regulated cell death (RCD) driven by iron-dependent lipid peroxidation through inducing ROS generation by the Fenton reaction (Mou et al.,

2019; Qu et al., 2022). Among the ferroptosis pathways, ferritinophagy is an autophagy-dependent process leading to ferritin-iron release (Gryzik et al., 2021). Recent studies have reported that ferroptosis contributes to the impairment of cochlear hair cells that relate to sensory hearing (Hu et al., 2020; Zheng et al., 2020). Moreover, some previous studies of NPCD have reported that NPC1 deficiency leads to metal dyshomeostasis (Hung et al., 2014) and lysosome dysfunction (Pluvinaige et al., 2021; Roney et al., 2021) in multiple organelles. We thus hypothesize a possible mechanism of genetic hearing loss related to NPCD, that is, NPC1 deficiency causes outer hair cells (OHCs) loss or damage in the cochlea by inducing ferroptosis.

Here, we generated the NPC1<sup>-/-</sup> HEI-OC1 cell line to simulate the auditory cells of NPCD patients. In this study, we found an altered autophagy flux in NPC1<sup>-/-</sup> HEI-OC1 cells with increased autophagy synthesis and blocked autophagy degradation. We also found enhanced ferritin degradation and dysregulation of iron homeostasis in NPC1<sup>-/-</sup> HEI-OC1 cells, which promote ferroptosis. Our study provides a novel insight into NPC1 function for further diagnosis and treatment of NPCD.

## MATERIAL AND METHOD

### Cell Culture

HEI-OC1 and HeLa cells were preserved in our lab. HEI-OC1 cells were cultured in Dulbecco's Modified Eagle's Medium (DMEM, Gibco, United States) supplemented with 10% fetal bovine serum (#FSP500, ExCell Bio, China) in the cell incubator containing 10% CO<sub>2</sub> at 33°C, and HeLa cells were cultured in DMEM supplemented with 10% fetal bovine serum, 100 U/mL penicillin, and 100 µg/ml streptomycin (#15140122, Gibco, United States) in the cell incubator containing 5% CO<sub>2</sub> at 37°C.

### Chemical Compounds

Chloroquine (CQ, HY-17589A, 100 µM), wortmannin (#HY-10197, 1 µM), Mg132 (HY-13259, 10 µM), ferric ammonium citrate (FAC, #HY-B1645, 10 µg/ml), deferoxamine mesylate (DFOM, #HY-B0988, 100 µM), and Rapamycin (#HY-10219, 10 µM) were purchased from MCE (China).

### Generation of Stable NPC1-Deficient HEI-OC1 Cell Lines

The single-guide RNAs (sgRNAs) targeting the fifth exon of the mouse NPC1 gene (**Supplementary Table S1**) were designed on the CHOPCHOP website (<http://chopchop.cbu.uib.no/>) and ligated to digested PX330 plasmid containing the Cas9 backbone with T4 DNA ligase (Vazyme, China). The recombinant plasmids were transfected into HEI-OC1 cells by nucleofection (LONZA) with Amaxa™ Basic Nucleofector™ Kit, and the viable monoclonal cell colonies were obtained by G418 (#A1720, Sigma, Germany) screening and subjected to genotyping *via* direct PCR-based sequencing (**Supplementary Table S2**). The effectiveness of the NPC1-deficient cell lines was analyzed by the level of NPC1 protein and the expression of NPC1 mRNA.

### Total RNA Isolation and Quantitative Real-Time Polymerase Chain Reaction

Total RNA was extracted from the HEI-OC1 cells by the phenol chloroform extracting method, and cDNA was synthesized from 1 µg of the total RNA with the HiScript II One Step RT-PCR kit (Vazyme, China). Real-time PCR was performed using ChamQ SYBR qPCR Master Mix (Vazyme, China) on a Step One Plus Real-Time PCR System (Applied Biosystems, United States). The qRT-PCR primers are listed in **Supplementary Table S3**. Each sample was tested in triplicate, and the relative gene expression was obtained by the comparative CT method (2<sup>-ΔΔCT</sup>). The GAPDH served as the internal control.

### Western Blotting Analysis

The total protein obtained from the cells lysed with RIPA buffer (Beyotime, China) was separated by polyacrylamide gel electrophoresis (SDS-PAGE, Bio-Rad, United States) and then transferred onto polyvinylidene fluoride (PVDF) membranes (Merck, Germany). Blots were incubated in blocking buffer [5% skim milk powder (BD, United States) in PBS-T] for 2 h followed by incubation with the primary antibodies overnight at 4°C on a shaker. The membranes were probed with HRP-conjugated AffiniPure goat anti-mouse IgG (H+L) (1:5000, #SA00001-1, Proteintech, China) or HRP-conjugated AffiniPure goat anti-rabbit IgG (H+L) (1:5000, #SA00001-2, Proteintech, China) secondary antibodies for 2 h at room temperature, and the blot signals were visualized with a molecular imager ChemiDoc XRS+ imaging system (Bio-Rad) by supersensitive ECL chemiluminescent substrate (#BL520B-1, Biosharp, China).

### Filipin Staining

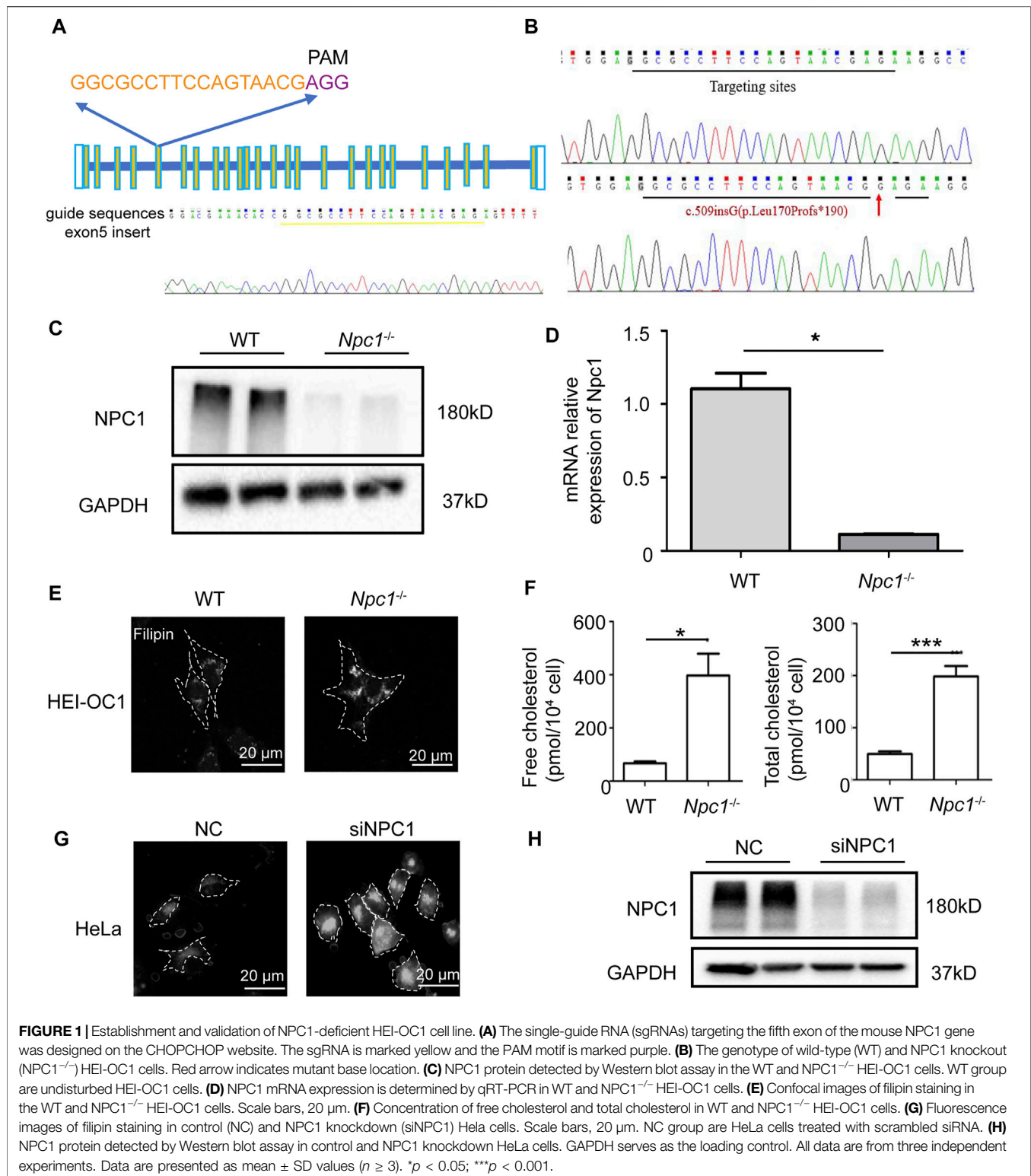
Cells were fixed with 4% paraformaldehyde for 15 min and then incubated with 1.5 mg/ml glycine for 10 min. After that, the cells were incubated in 50 µg/ml (PBS diluted) Filipin III ready-made solution (#SAE0087, Merck, Germany) for 2 h at room temperature. Images were acquired by laser confocal microscopy (LSM710, Zeiss) using 405 nm excitation wavelength.

### Free Cholesterol Content Assay

Free cholesterol content in HEI-OC1 cells was detected with the free cholesterol content assay kit (#BC 1890, Solarbio, China) according to the manufacturer's instructions, as follows. The HEI-OC1 cells (5 × 10<sup>6</sup>) were harvested, and then 1 ml of ethanol was added. After ultrasonication and centrifugation, the supernatant was used as the solution to detect the free cholesterol content. The content of free cholesterol was calculated according to the formula given.

### Total Cholesterol Content Assay

The total cholesterol content in HEI-OC1 cells was detected with a total cholesterol content assay kit (#BC 1985, Solarbio, China) according to the manufacturer's instructions, as follows. First, 1 ml of isopropanol was added into 5 × 10<sup>6</sup> HEI-OC1 cells, and after ultrasonication and centrifugation, the supernatant was



taken for detection. After incubation at 37°C for 15 min, the absorbance value at 500 nm was measured with a microplate reader. The absorbance value was then interpolated on a standard

curve to obtain x value (standard curve:  $y = 0.5098x - 0.0445$ ). The total cholesterol content was calculated according to the formula given. TC ( $\mu$ mol/10000 cell) = 0.002x.

## Immunofluorescence Staining

Cells grown on the coverslips were fixed with 4% PFA for 15 min, then permeabilized with 0.1% Triton X-100 (Sigma-Aldrich, United States) for 10 min. After blocking with 10% goat serum for 60 min, the primary antibodies LC3A/B (1:200, #4108S, CST, United States), FTH1 (1:200, #4393S, CST, United States), FLAG (1:200, AE005, ABclonal, China), or HA (1:200, #5017S, CST, United States) was added to incubate with the cells overnight at 4°C, and the corresponding secondary antibodies—donkey anti-rabbit IgG Alexa Fluor 546 (1:1000, #A-21202, Thermo Fisher) and donkey anti-mouse IgG Alexa Fluor 488 (1:1000, #A10040, Thermo Fisher) for 2 h at room temperature. The nuclei were stained with DAPI (#F6057, Sigma). Images were acquired by laser confocal microscopy (LSM710, Zeiss).

## Electron Microscopy Analysis

Cells were collected and fixed with glutaraldehyde and osmic acid and dyed with 2% uranyl acetate aqueous solution for 2 h. After gradient dehydration of alcohol, the cells were permeated with a mixture of acetone and embedding (1:1) for 2 h and then transferred to a pure embedding agent overnight. After embedding and polymerization, the cells were cut into sections at a thickness setting of 50 nm and stained with uranyl acetate and lead citrate, and photographed with an AMT CCD camera.

## Fe (II) Content Analysis

FerroOrange (#F374, Dojindo, Japan), a ferrous ion fluorescent probe, was used to detect intracellular ferrous ions. Cells were grown on the laser confocal dish or 24-well cell culture plates, were washed thrice with HBSS, and incubated with 1 μmol/l FerroOrange working solution for 30 min. Images were acquired by laser confocal microscopy or fluorescence microscope using 514 nm excitation wavelength.

## Intracellular Reactive Oxygen Species Level

The ROS detection kit (#KGT010-1, KeyGEN Biotech) was used for quantitative determination of intracellular reactive oxygen species levels based on the fluorescence intensity changes of DCFH-DA. The HEI-OC1 cells ( $5 \times 10^5$ ) were seeded in a six-well plate and cultured overnight. DCFH-DA was diluted with DMEM at 1:1000 to reach a final concentration of 10 μM, then added into cells to incubate for 30 min in the dark. After washing thrice with DMEM, the cells were harvested and detected by flow cytometry using 488 nm wavelength. The ROSUP solution (50 μg/ml, 30 min) was used for the positive control.

## Construction of Overexpression Vector Plasmids

The cDNA extracted from the HEI-OC1 cells was used as a template for PCR amplification with KOD FX Neo (TOYOBO, Japan). The products were cloned into PXJ40-FLAG and PXJ40-HA, and renamed as FLAG-Fth1 and HA-NCOA4, respectively (Supplementary Table S4).

## Co-Immunoprecipitation

WT and NPC1<sup>-/-</sup> HEI-OC1 cells were transfected with equal amounts of FLAG-Fth1 and HA-NCOA4 plasmids with lipofectamine 3000 reagent (#L3000150, Thermo Fisher) for 48 h. After the cells were lysed on ice with IP lysis buffer (Beyotime, China) and centrifuged, 20 μl of ANTI-FLAG® M2 Affinity Gel (#A2220, Sigma, United States) was added into the supernatant for immunoprecipitation at 4°C overnight on a shaker. After washing five times with IP lysis buffer, the immunoprecipitated materials were eluted with 20 μl of the protein loading buffer (6×), boiled for 10 min, and subjected to immunoblot analysis. The empty FLAG vector was used as the control.

## Cell Proliferation Assay

The CCK8 assay was used to determine the proliferation of HEI-OC1 cells. About 2000 cells were seeded in a 96-well plate and cultured overnight. Then 10 μl of the CCK8 reagent (#K1018, ApexBio) was added into the cells at the indicated time point, and the cells continued to be incubated for 2 h. The absorbance at 450 nm was then measured using a microplate reader. The OD values were used to plot the cell proliferation curve.

## Apoptosis Analysis

The HEI-OC1 cells were detected with the Annexin V-FITC/PI Apoptosis Detection Kit (#A211-01, Vazyme, China) to evaluate apoptosis levels. CCCP (#C2759, Sigma) was used to induce apoptosis. The detailed procedure is as follows: about  $5 \times 10^5$  cells were harvested by cell dissociation with EDTA-free trypsin, then the cells were washed twice with precooled PBS and followed by a resuspension with 100 μl of binding buffer (1×). After that, 5 μl Annexin V-FITC and 5 μl PI staining solution were added and incubation for 10 min in the dark. Next, 400 μl binding buffer (1×) was added in the end, and the samples were detected by flow cytometry within 1 h, with Ex: 488 nm.

## Intracellular Lipid Peroxides Detection

Liperfluo (#L248, Dojindo, Japan), a lipid fluorescent peroxide probe, was used to detect intracellular lipid peroxides. The cells in the six-well plate were washed with HBSS, and the final concentration of 5 μM Liperfluo working solution (DMEM diluted) was added into the cells. After incubation for 30 min, the cells were washed twice with HBSS and detected by flow cytometry, with Ex: 488 nm.

## Malondialdehyde Detection

Malondialdehyde, one of the lipid peroxide metabolites was detected by the malondialdehyde (MDA) colorimetric test kit (#E-BC-K028-M, Elabscience, China) according to instructions. The total protein concentration was determined using a BCA assay (#P0012S, Beyotime), and the MDA content was calculated by the given formula.  $MDA (nmol/mgprot) = \Delta A1 / \Delta A2 \times 10 nmol/mL \times f \div Cpr$ , where  $\Delta A1$  = OD value of sample - OD value of blank tube,  $\Delta A2$  = OD value of standard substance - OD value of



blank tube,  $f$  is dilution ratio, and  $C_{pr}$  is protein concentration of sample (mgprot/mL).

## Statistical Analysis

All data are presented as mean  $\pm$  SD. Student's  $t$ -test was used for comparisons between two independent sample groups, one-way analysis of variance (ANOVA) was used for single-factor comparisons among multiple groups, and two-way ANOVA was used for two-factor comparisons among multiple groups;  $p < 0.05$  was regarded as significant.

## RESULTS

### Cholesterol Accumulated in NPC1-Deficient HEI-OC1 Auditory Cells

Besides CNS and visceral symptoms disorders, most NPCD patients exhibit a progressive high frequency hearing loss. The cochlea's OHCs are essential sensory receptor cells and are important for hearing in the organ of Corti, especially at high frequencies (Basch et al., 2016).

To explore the effect of NPC1 deficiency in the auditory system, we thus generated NPC1-deficient HEI-OC1 auditory cells using the CRISPR-Cas9 gene-editing technique to truncate and alter amino acid sequences (Figures 1A–D). The single-guide RNA (sgRNA) targeting the fifth exon of the mouse NPC1 gene was designed and synthesized, then ligated to the PX330 vector plasmid with Cas9 skeleton protein (Figure 1A). The recombinant plasmid together with tdTomato was transfected into the HEI-OC1 cells by electroporation, and the viable monoclonal strains were screened by G418 prior to sequencing. The transfected cells underwent different degrees of gene editions, mainly manifested as changes in the number of bases which caused frameshift mutation and premature termination of protein translation (Figure 1B). The Western blot analysis results showed that the NPC1 band almost completely disappeared in the NPC1<sup>-/-</sup> cells when compared with the wild-type (WT) cells (Figure 1C). The RT-PCR analysis results also showed that the NPC1 was significantly decreased in the NPC1<sup>-/-</sup> cells when compared with the WT cells (Figure 1D).

Because cholesterol accumulation is the main feature of NPC1 deficiency previously reported in many other cell types, we first detected the cholesterol level in NPC1-deficient HEI-OC1 auditory cells. The cholesterol detection results showed that the cholesterol level in NPC1<sup>-/-</sup> HEI-OC1 cells was much higher than in the WT cells, and the filipin staining images also showed cholesterol accumulation in NPC1<sup>-/-</sup> HEI-OC1 cells (Figures 1E,F), which is similar to the results shown in the NPC1 knockdown HeLa cells (Figures 1G,H). We also found that transfecting NPC1 plasmid in NPC1<sup>-/-</sup> HEI-OC1 cells could rescue the phenotype of cholesterol accumulation, while increasing NPC1 in the WT cells had no significant effect (Supplementary Figures S1A,B).

Our results show that we had generated NPC1<sup>-/-</sup> HEI-OC1 cells successfully and also obtained a similar phenotype of cholesterol accumulation both in NPC1<sup>-/-</sup> HEI-OC1 and NPC1 knockdown HeLa cells, indicating that the function of

NPC1 had a good commonality between hearing cells and other cells in cholesterol regulation.

### NPC1 Deficiency Changed Autophagy Flux in HEI-OC1 Cells

Autophagy is a conserved catabolic process which plays an important role in cell fate determination and cell homeostasis under stress (Dikic and Elazar, 2018). It has been reported that high cholesterol stimulation induces autophagy (Li J, 2020), and autophagy also regulates cholesterol efflux (Ouimet et al., 2011).

Due to the phenotype of cholesterol accumulation in NPC1-deficient HEI-OC1 cells shown earlier, we first detected the intracellular autophagy levels to confirm whether NPC1 deficiency induces autophagy in hearing cells. The immunofluorescent staining and Western blot results showed that the microtubule-associated protein 1 light-chain 3 (LC3II) expression level (an autophagy marker) was higher in NPC1-deficient HEI-OC1 cells than in WT cells, indicating an increase of autophagosomes in the NPC1-deficient HEI-OC1 cells (Figures 2A,B). We also observed increased LC3II levels in NPC1 knockdown HeLa cells (Figures 2C,D). By using the transmission electron microscope (TEM), we found more autophagosomes in NPC1<sup>-/-</sup> HEI-OC1 cells (Figure 2E). Then, we transfected the NPC1 plasmid in the WT and NPC1<sup>-/-</sup> HEI-OC1 cells to find out whether it could affect autophagy. We found that transfecting with NPC1 plasmid in NPC1<sup>-/-</sup> HEI-OC1 cells could reduce LC3II, indicating an important role of NPC1 in autophagy (Supplementary Figure S1C).

We further evaluated the effect of NPC1 deficiency on autophagosome synthesis and degradation by treating the HEI-OC1 cells with autophagy inhibitors. To block the autophagosome degradation, we treated the HEI-OC1 cells with chloroquine (a late autophagy inhibitor) and found that the LC3II levels were increased and more pronounced in the NPC1<sup>-/-</sup> HEI-OC1 cells, suggesting that NPC1 deficiency increased autophagy synthesis (Figures 2F–G). We next treated HEI-OC1 cells with wortmannin, another autophagy inhibitor, to determine the effect of NPC1 deficiency in autophagy degradation. As shown in Figures 2F,G, the wortmannin treatment significantly reduced the LC3II level in the NPC1<sup>-/-</sup> HEI-OC1 cells, however, the LC3II levels in the NPC1<sup>-/-</sup> HEI-OC1 cells were also higher than those found in the WT cells. A similar result was found in the NPC1 knockdown HeLa cells under the same treatment condition (Figure 2H).

Our data suggest that NPC1 deficiency changed autophagy flux by increasing autophagosome synthesis and blocking autophagosome degradation in HEI-OC1 cells.

### Abnormal Autophagy Causes Fe (II) Accumulation in NPC1-Deficient HEI-OC1 Cells

Iron is an important trace element that when present either in abnormal distribution or content can break redox

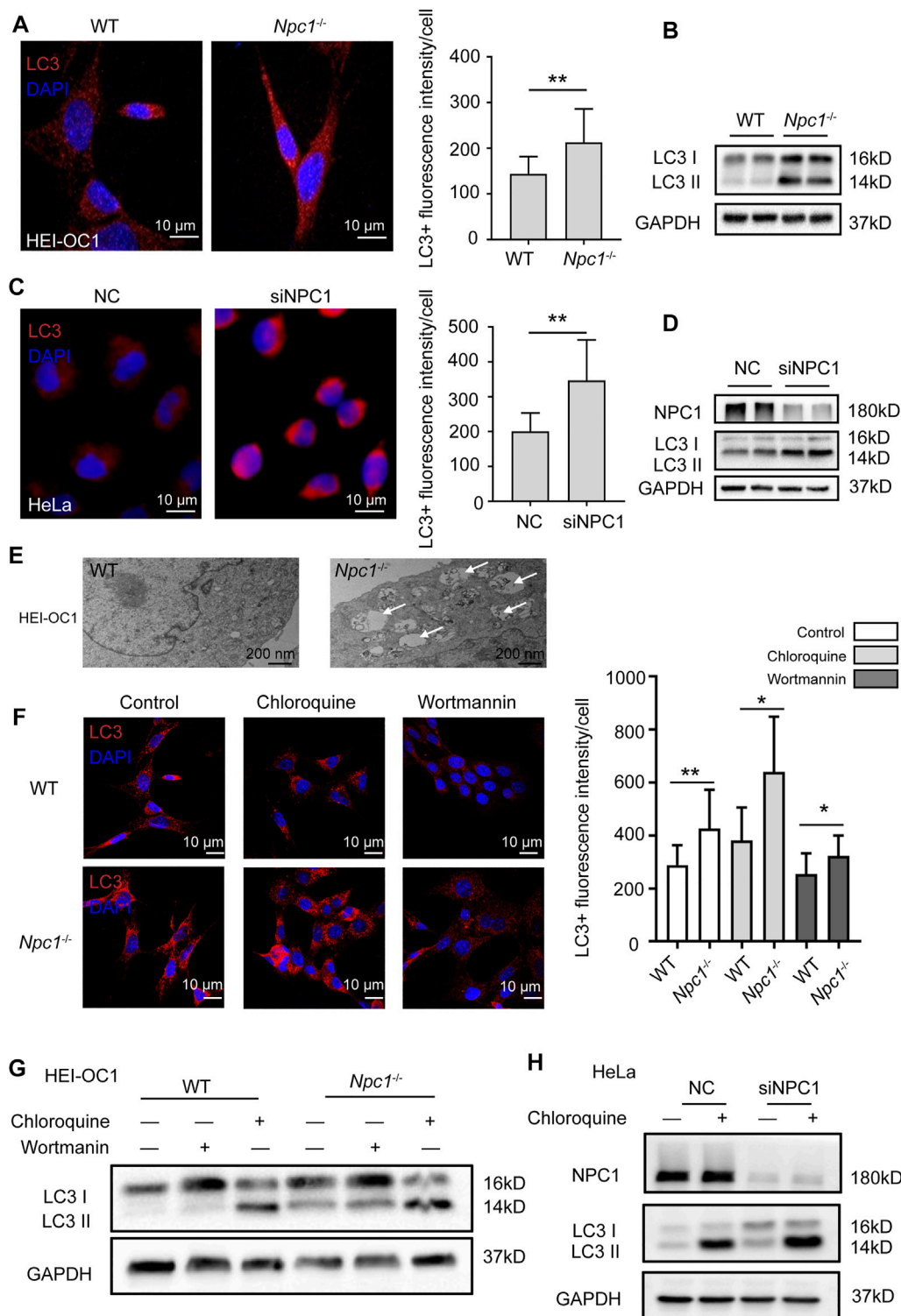
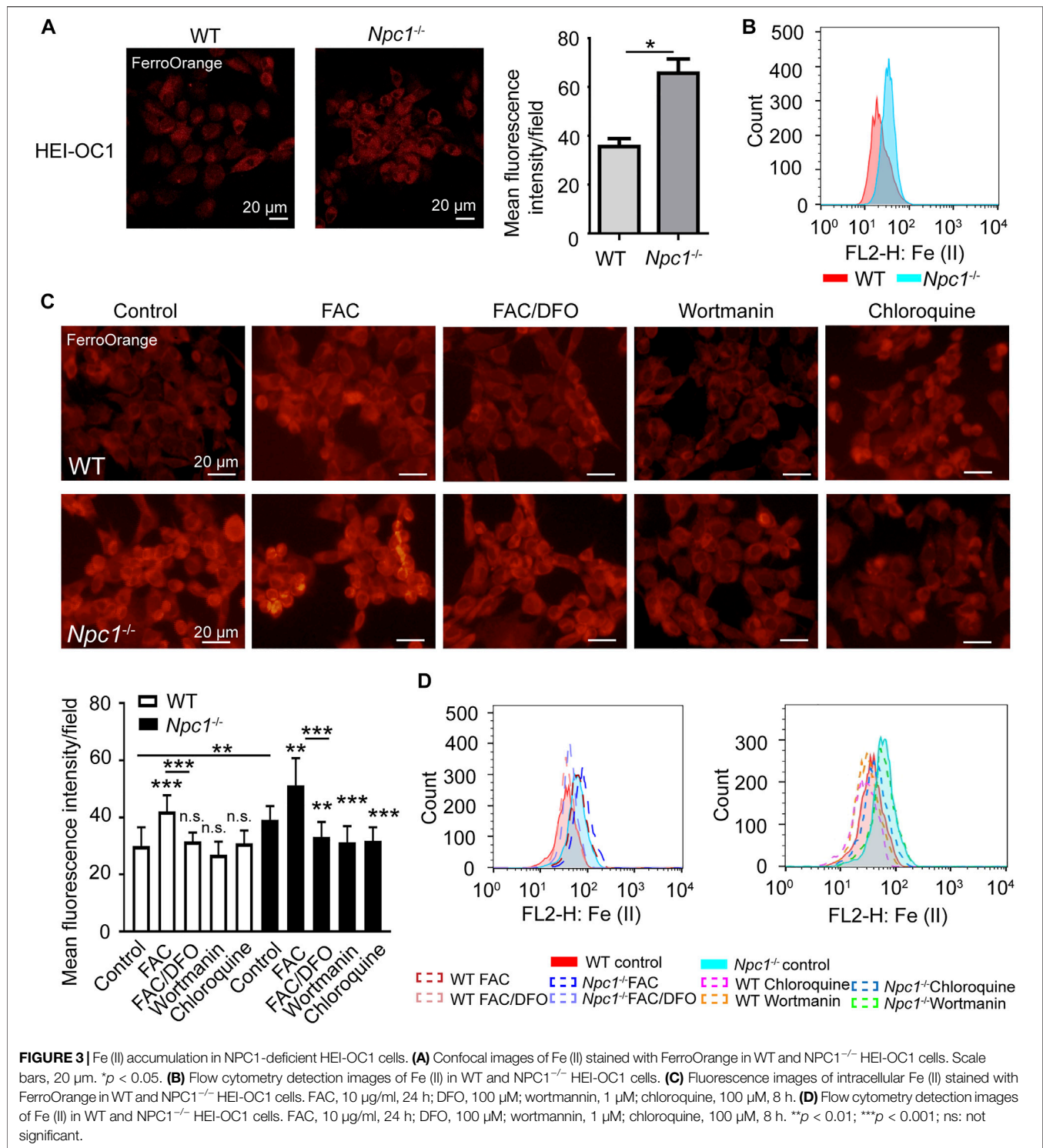


**FIGURE 2 |** NPC1 deficiency enhanced autophagy flux. **(A)** Confocal images of immunofluorescence staining with anti-LC3 antibody in WT and NPC1<sup>-/-</sup> HEI-OC1 cells. DAPI-labeled nucleus. Scale bars, 10  $\mu$ m. **(B)** LC3 protein level detected by Western blot using the anti-LC3 antibody in WT and NPC1<sup>-/-</sup> HEI-OC1 cells. GAPDH serves as the loading control. **(C)** Immunofluorescence images of control and NPC1 knockdown HeLa cells with anti-LC3 antibody. DAPI-labeled nucleus. Scale bars, 10  $\mu$ m. **(D)** LC3 protein level detected in the control and NPC1 knockdown HeLa cells. GAPDH serves as the loading control. **(E)** TEM images of the WT and NPC1<sup>-/-</sup> HEI-OC1 cells. Scale bars, 200 nm. White arrows indicate autophagosomes. **(F)** Immunofluorescence images of WT and NPC1<sup>-/-</sup> HEI-OC1 cells with anti-LC3 antibody; chloroquine: 100  $\mu$ M, 8 h; wortmannin: 1  $\mu$ M, 8 h. Scale bars, 10  $\mu$ m. **(G)** LC3 protein level detected by Western blot in WT and NPC1<sup>-/-</sup> HEI-OC1 cells after the addition of chloroquine, 100  $\mu$ M, 8 h or wortmannin, 1  $\mu$ M, 8 h. GAPDH serves as the loading control. **(H)** LC3 protein level in control and NPC1 knockdown HeLa cells under the condition of chloroquine (10  $\mu$ M). GAPDH serves as the loading control. Data are presented as mean  $\pm$  SD values ( $n \geq 3$ ). \* $p < 0.05$ ; \*\* $p < 0.01$ .



homeostasis and affect normal physiological processes by generating toxic reactive oxygen species (ROS) through the Fenton reaction (Li K, 2020).

A previous study had reported the failure of metal homeostasis in the liver and spleen from a mouse model of NPCD (Hung et al.,

2014), and there have been many evidence about autophagy regulating iron content (Park and Chung, 2019), and we thus wondered whether NPC1 deficiency induced iron metabolic disorder in auditory cells through autophagy. We found out by fluorescence staining and flow cytometry detection that Fe

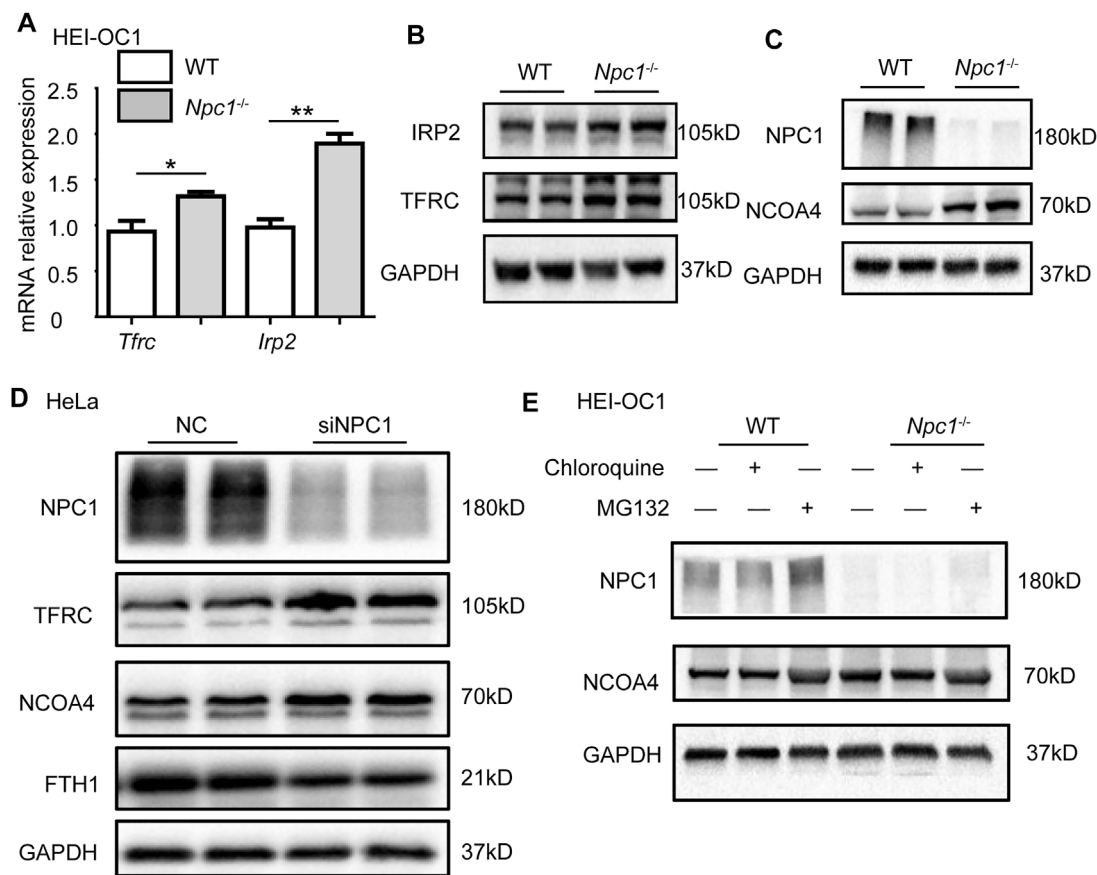


**FIGURE 4 |** Abnormal iron flux in NPC1-deficient HEI-OC1 cells. **(A)** mRNA expression levels were determined by qRT-PCR in WT and NPC1<sup>-/-</sup> HEI-OC1 cells. **(B,C)** The protein levels were detected by Western blot using antibodies to TFRC, IRP2, NPC1, NCOA4, and GAPDH in WT and NPC1<sup>-/-</sup> HEI-OC1 cells. **(D)** HeLa cells transfected with control siRNA or siRNAs to NPC1 for 48 h, and the lysates subjected to immunoblotting using antibodies to NCOA4, TFRC, and FTH1. GAPDH serves as the loading control. **(E)** The NCOA4 protein level detected by Western blot under the condition of MG132 (10  $\mu$ M, 8 h) or chloroquine (100  $\mu$ M, 8 h) treatment in WT and NPC1<sup>-/-</sup> HEI-OC1 cells using anti-NCOA4 antibody. Data are presented as mean  $\pm$  SD values ( $n \geq 3$ ). \* $p < 0.05$ ; \*\* $p < 0.01$ .

(II) was increased in the NPC1<sup>-/-</sup> HEI-OC1 cells (Figures 3A,B), indicating that NPC1 deficiency altered iron homeostasis in auditory cells. We also found that Fe (II) was not changed in the WT HEI-OC1 cells with NPC1 overexpression (Supplementary Figure S1D). Furthermore, we found that the Fe (II) fluorescence intensity level in the NPC1<sup>-/-</sup> HEI-OC1 cells was higher than that in the WT cells with or without ferric ammonium citrate (FAC) treatment, while deferoxamine mesylate (DFO) could reduce the ferrous iron concentration in the HEI-OC1 cells (Figure 3C). In addition, we confirmed that Fe (II) was significantly reduced when the NPC1<sup>-/-</sup> HEI-OC1 cells were treated with wortmannin or chloroquine (Figure 3C), suggesting that inhibiting autophagy by either repressing autophagosome synthesis or blocking autophagosome degradation could relieve the NPC1 deficiency-induced iron metabolic disorders.

Our results indicated that autophagy was involved in NPC1 deficiency-induced iron metabolic disorders.

## NPC1 Deficiency Promotes Ferritinophagy in HEI-OC1 Cells

The aforementioned data show that NPC1 deficiency increased Fe (II) in HEI-OC1 cells, and this alteration was regulated through an autophagy-dependent manner, and we thus focused on the underlying targets of autophagy in regulating Fe (II) content.

To confirm whether NPC1 deficiency affected iron intake, we first detected the expression levels of transferrin receptor protein 1 (TFRC) which plays an important role in iron intake and intracellular transport, and iron-responsive element-binding protein 2 (IRP2) which is an indicator of cellular iron



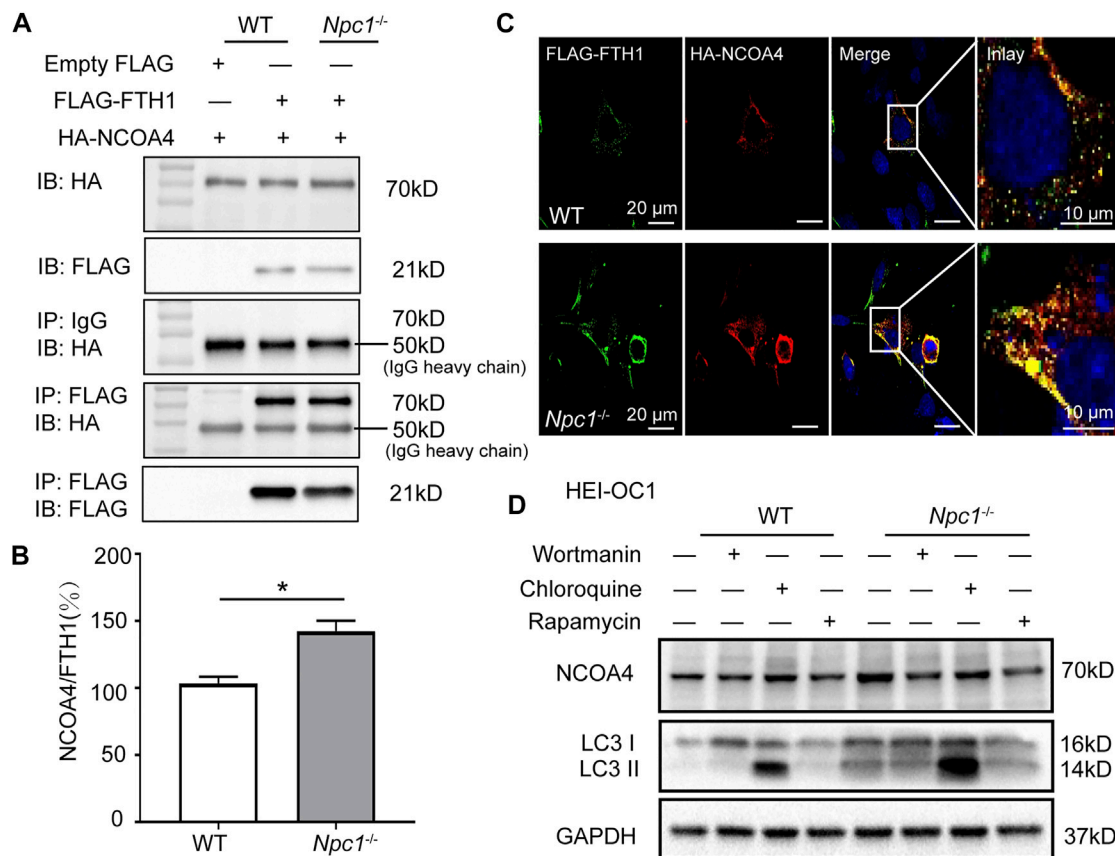


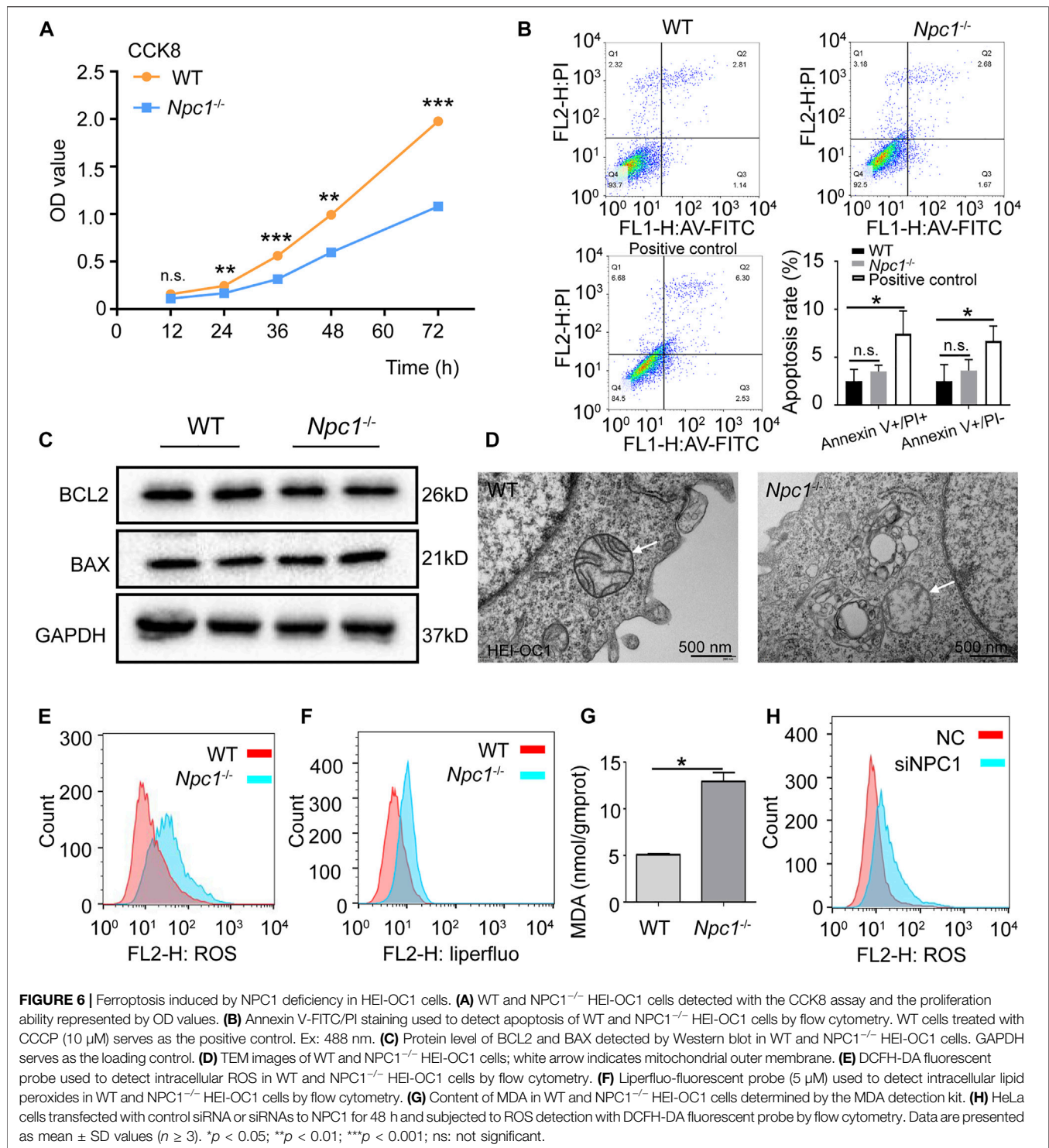
**FIGURE 5 |** Enhanced ferritinophagy in NPC1-deficient HEI-OC1 cells. **(A)** Immunoblotting analysis performed to detect protein binding ability of FTH1 and NCOA4 in WT and NPC1<sup>-/-</sup> HEI-OC1 cells. WT and NPC1<sup>-/-</sup> HEI-OC1 cells transfected with equal amounts of FLAG-tagged Fth1 and HA-tagged NCOA4 plasmids for 48 h; samples then lysed and immunoprecipitated with anti-FLAG beads or anti-normal IgG. Inputs and immunoprecipitated fractions are detected by immunoblotting analysis with anti-FLAG and HA. The empty vector of the FLAG plasmid serves as the negative control. HA-NCOA4 serves as the loading control. **(B)** The protein binding ability normalized as the gray value ratio of HA to FLAG in **(A)**. **(C)** Confocal images of immunofluorescence staining with anti-FLAG and HA antibodies showing the colocalization of FTH1 and NCOA4 in WT and NPC1<sup>-/-</sup> HEI-OC1 cells. Scale bar, 10 μm. **(D)** Immunoblotting analysis with anti-NCOA4 and anti-LC3 antibodies in WT and NPC1<sup>-/-</sup> HEI-OC1 cells with or without treatment of wortmannin (1 μM, 8 h), chloroquine (100 μM, 8 h), or Rapamycin (10 μM, 8 h). GAPDH serves as the loading control. Data are presented as mean ± SD values ( $n \geq 3$ ). \* $p < 0.05$ .

bioavailability. We found that both TFRC and IRP2 were increased slightly in NPC1<sup>-/-</sup> HEI-OC1 cells (Figures 4A,B), indicating that the iron intake and intracellular transport were slightly increased. To study the effect of NPC1 deficiency in iron release, we next detected the expression level of nuclear receptor coactivator 4 (NCOA4) which delivers ferritin heavy chain (FTH1) to the lysosome for iron release and is also considered to be a ferritinophagy marker. We found a significant increase in the NCOA4 expression level in NPC1<sup>-/-</sup> HEI-OC1 cells (Figure 4C), indicating that NPC1 deficiency promotes iron release. A similar result was found in NPC1 knockdown HeLa cells, and we also found that FTH1, which is used for iron storage, was decreased (Figure 4D). The aforementioned results suggest that NPC1 deficiency promotes iron intake and iron release.

We next studied whether NPC1 deficiency contributed to autophagy-dependent ferritinophagy in the hearing sensory receptor cells. We found that repressing autophagy decreased the NCOA4 level, by treating the NPC1<sup>-/-</sup> HEI-OC1 cells with

chloroquine (Figure 4E). In addition, we found that MG132 (a reversible proteasome inhibitor) increased NCOA4 protein levels in both WT and NPC1<sup>-/-</sup> HEI-OC1 cells, suggesting that the ubiquitin-proteasome degradation pathway was not influenced by NPC1 deficiency (Figure 4E). The aforementioned results suggest that the increased expression of NCOA4 induced by NPC1 deficiency was regulated through autophagy.

We next transfected FLAG-tagged FTH1 plasmid and HA-tagged NCOA4 plasmid in HEI-OC1 cells to confirm whether NPC1 deficiency could promote NCOA4 to bind FTH1. The co-immunoprecipitation (co-IP) results showed that NCOA4 was increased in NPC1<sup>-/-</sup> HEI-OC1 cells, suggesting that more NCOA4 bound to FTH1 in NPC1<sup>-/-</sup> HEI-OC1 cells than they did in WT cells (Figures 5A,B). Furthermore, the immunofluorescent staining results showed an increase in colocalization between NCOA4 and FTH1 in NPC1<sup>-/-</sup> HEI-OC1 cells (Figure 5C), supporting the aforementioned results, and we found that by treating the cells with either wortmannin or



chloroquine to inhibit autophagy reduced NCOA4 expression levels (Figure 5D). However, inducing autophagy by treating the HEI-OC1 cells with Rapamycin, an autophagy inducer through inhibition of the mTOR pathway, did not reverse ferritinophagy in the NPC1<sup>-/-</sup> HEI-OC1 cells, maybe due to the impaired

function of the lysosome's outer membrane caused by NPC1 deficiency.

Taken together, our results show that NPC1 deficiency promoted autophagy-dependent ferritinophagy by enhancing the binding of NCOA4 to FTH1 and promoting it to release Fe (II).

## Enhanced Ferritinophagy Induces Ferroptosis in NPC1-Deficient HEI-OC1 Cells

Some previous studies have reported that inducing ferroptosis can inhibit HEI-OC1 cell proliferation, while treating the cells with a selective ferroptosis inhibitor liproxstatin-1 (Lip-1) could recover HEI-OC1 cell viability (Zheng et al., 2020).

We next confirmed whether ferritinophagy induced by NPC1 deficiency impacted the viability of auditory cells. The results of **Figure 6A** show that the proliferation of NPC1<sup>-/-</sup> HEI-OC1 cells was inhibited and detected with the CCK8 assay. Inhibition of autophagy with chloroquine, but not wortmannin, could reverse the viability decrease seen in NPC1<sup>-/-</sup> HEI-OC1 cells (**Supplementary Figures S2A,B**). To further confirm whether apoptosis contributed to cell damage, Annexin V/PI detection was performed with flow cytometry. We found that there was no significant difference between the WT and NPC1<sup>-/-</sup> HEI-OC1 cells (**Figure 6B**). Moreover, the Western blot results showed that there was no significant difference between the WT and NPC1<sup>-/-</sup> HEI-OC1 cells in BCL2 and BAX expressions (two apoptosis indicators) (**Figure 6C**), suggesting that the impaired proliferation of the NPC1<sup>-/-</sup> HEI-OC1 cells was not caused through the apoptosis pathway.

To further confirm whether NPC1 deficiency induced ferroptosis in auditory cells, the TEM was used to observe the mitochondrial structure. We found reduced mitochondrial cristae and impaired outer mitochondrial membranes in the NPC1<sup>-/-</sup> HEI-OC1 cells (**Figure 6D**), which are similar to the ferroptosis feature (Dixon et al., 2012). We also observed an accumulation of intracellular ROS in the NPC1<sup>-/-</sup> HEI-OC1 cells (**Figure 6E**). In addition, lipid peroxides, an indicator of ferroptosis, were found increased in the NPC1<sup>-/-</sup> HEI-OC1 cells, and MDA, which is one of the major metabolites of lipid peroxide, was increased in the NPC1<sup>-/-</sup> HEI-OC1 cells (**Figures 6F,G**). We also found a similar trend of ROS in NPC1 knockdown HeLa cells (**Figure 6H**). All these results suggest that NPC1 deficiency induced ferroptosis in HEI-OC1 cells.

Taken together, our data show that 1) NPC1 deficiency changes autophagy flux by both increasing autophagosome synthesis and inhibiting autophagosome degradation; 2) abnormal autophagy induces ferritinophagy by promoting NCOA4 to deliver FTH1 to the lysosomes; 3) ferritinophagy promotes FTH1 to release Fe (II) and this is followed by an increase of lipid peroxide that induces ferroptosis in HEI-OC1 cells.

## DISCUSSION

The mutation or absence of NPC1 is considered to be the main reason for NPCD occurrence, which is characterized as a lipid storage disorder with a high level of cholesterol that affects multiple organs and the CNS (Wheeler and Sillence, 2020). NPC1 deficiency is not only involved in CNS and visceral diseases but also in genetic hearing loss. The OHCs are

important hearing sensory receptor cells in the auditory system and they convert the mechanical cilia swing caused by sound waves into electrical signals. Therefore, any loss or damage to the OHCs with their inability to regenerate thereby results in hearing loss (HL) (Kwan et al., 2009). In this study, we state a novel molecular mechanism of NPCD in causing genetic hearing loss, that is, NPC1 deficiency induces ferroptosis in auditory cells through an autophagy-dependent ferritinophagy manner.

The effect of NPC1 deficiency on autophagy flux provides a clue for follow-up research on ferritinophagy. Autophagy is associated with cholesterol regulation in many cell types. It is reported that high cholesterol induces autophagy in tendon-derived stem cells *via* the AKT/FOXO1 pathway (Li et al., 2020). In macrophage foam cells, autophagy mediates the generation of free cholesterol for ABCA1-dependent efflux (Ouimet et al., 2011). As an important cholesterol transporter, the studies of NPC1 related to autophagy have been previously reported in many cell types and mouse models. In primary human fibroblasts, NPC1 deficiency is reported to promote LC3II expression, which is to show an increase in active autophagy (Pacheco et al., 2007). In human dermal fibroblasts, the NPC1 deficiency impairs the clearance of autophagosomes induced by stored lipids (Elrick et al., 2012). In our data, we found that autophagosome synthesis was increased and degradation of autophagosomes was decreased in NPC1-deficient HEI-OC1 cells, which resulted in an altered autophagy flux in the auditory cells.

In this study, we further found that NPC1 deficiency increased Fe (II) content in auditory cells by enhancing the interaction between NCOA4 and FTH1, indicating the underlying molecular mechanism by which NPC1 regulates autophagy-dependent ferritinophagy. To date, there are only a few studies on NPC1 in the auditory system, and studies about the relationships in between NPC1, autophagy, and iron homeostasis are even fewer. Autophagy plays an important role in iron homeostasis, and it also induces ferritinophagy (Hou et al., 2016; Liu et al., 2020). It has been reported in lung fibroblastic cells that autophagy functions to promote the degradation of ferritin and TFRC expression to regulate iron content (Park and Chung, 2019). Nuclear receptor coactivator 4 (NCOA4) is crucial for ferritin-iron release by delivering ferritin for lysosomal degradation in ferritinophagy (Hou et al., 2016; Gryzik et al., 2021). A recent study has proved that disrupting the NCOA4-FTH1 protein-protein interaction by using compound 9a reduces intracellular Fe (II) and inhibits ferroptosis (Fang et al., 2021). In our results, we found that the expression levels of NCOA4 and TFRC were both increased, and NCOA4-FTH1 interaction was also enhanced in NPC1-deficient HEI-OC1 cells. Moreover, we found Fe (II) content and NCOA4 expression were regulated by autophagy, suggesting that NPC1 deficiency may cause autophagy-dependent ferritinophagy in auditory cells.

In addition, we found ferroptosis rather than apoptosis in NPC1-deficient HEI-OC1 cells. As we know, features of ferroptosis are different from those of apoptosis, with significant increase of Fe (II) content and exceeding lipid peroxide levels which are harmful to the mitochondria (Dixon et al., 2012; Wang et al., 2022). There have been some studies of NPCD on the effect of NPC1 deficiency and mental disorders. In a previous study of



NPCD, it was reported that multiple metals such as Cu and Fe were found altered in the cerebellum and cerebrum of NPC1<sup>-/-</sup> mouse (Hung et al., 2014). Recent research has also proven that iron content was increased in the brain of mice in an NPCD model (Hung et al., 2020). Besides the Fe (II) content, we also found that NPC1 deficiency changed cellular metabolic productions such as ROS, lipid peroxide, and MDA in HEI-OC1 cells. In addition, some researchers have shown progressive high frequency HL in NPC1 mutant mice (King, 2014b; Wheeler and Silience, 2020), while others have also provided evidence of OHC loss in the basal region of the cochlea (Zhou et al., 2018). In our data, we have shown TEM images of the impaired mitochondrial membrane and provided evidence of the inhibited proliferation of NPC1<sup>-/-</sup> HEI-OC1 cells, suggesting that NPC1 deficiency may impair auditory cells by ferroptosis.

Overall, this work reveals an underlying molecular mechanism by which NPC1 deficiency causes ferroptosis in auditory cells through the autophagy-dependent ferritinophagy pathway. This article presents a novel insight into the effect of NPC1 deficiency which may provide the potential target and therapeutic approach in the treatment of genetic hearing loss related to NPCD.

## REFERENCES

- Balboa, E., Marín, T., Oyarzún, J. E., Contreras, P. S., Hardt, R., van den Bosch, T., et al. (2021). Proteomic Analysis of Niemann-Pick Type C Hepatocytes Reveals Potential Therapeutic Targets for Liver Damage. *Cells* 10 (8), 2159. doi:10.3390/cells10082159
- Basch, M. L., Brown, R. M., 2nd, Jen, H. I., and Groves, A. K. (2016). Where Hearing Starts: the Development of the Mammalian Cochlea. *J. Anat.* 228 (2), 233–254. doi:10.1111/joa.12314
- Christomanou, H., and Harzer, K. (1996). Ouchterlony Double Immunodiffusion Method Demonstrates Absence of Ferritin Immunoreactivity in Visceral Organs from Nine Patients with Niemann-Pick Disease Type C. *Biochem. Mol. Med.* 58 (2), 176–183. doi:10.1006/bmme.1996.0046
- Christomanou, H., Kellermann, J., Link, R. P., and Harzer, K. (1995). Deficient Ferritin Immunoreactivity in Visceral Organs from Four Patients with Niemann-Pick Disease Type C. *Biochem. Mol. Med.* 55 (2), 105–115. doi:10.1006/bmme.1995.1040
- Dikic, I., and Elazar, Z. (2018). Mechanism and Medical Implications of Mammalian Autophagy. *Nat. Rev. Mol. Cell. Biol.* 19 (6), 349–364. doi:10.1038/s41580-018-0003-4
- Dixon, S. J., Lemberg, K. M., Lamprecht, M. R., Skouta, R., Zaitsev, E. M., Gleason, C. E., et al. (2012). Ferroptosis: an Iron-dependent Form of Nonapoptotic Cell Death. *Cell* 149 (5), 1060–1072. doi:10.1016/j.cell.2012.03.042
- Elrick, M. J., Yu, T., Chung, C., and Lieberman, A. P. (2012). Impaired Proteolysis Underlies Autophagic Dysfunction in Niemann-Pick Type C Disease. *Hum. Mol. Genet.* 21 (22), 4876–4887. doi:10.1093/hmg/dds324
- Fang, Y., Chen, X., Tan, Q., Zhou, H., Xu, J., and Gu, Q. (2021). Inhibiting Ferroptosis through Disrupting the NCOA4-FTH1 Interaction: A New Mechanism of Action. *ACS Cent. Sci.* 7 (6), 980–989. doi:10.1021/acscentsci.0c01592
- Gong, X., Qian, H., Zhou, X., Wu, J., Wan, T., Cao, P., et al. (2016). Structural Insights into the Niemann-Pick C1 (NPC1)-Mediated Cholesterol Transfer and Ebola Infection. *Cell* 165 (6), 1467–1478. doi:10.1016/j.cell.2016.05.022
- Gryzik, M., Asperti, M., Denardo, A., Arosio, P., and Poli, M. (2021). NCOA4-mediated Ferritinophagy Promotes Ferroptosis Induced by Erastin, but Not by RSL3 in HeLa Cells. *Biochimica Biophysica Acta (BBA) - Mol. Cell. Res.* 1868 (2), 118913. doi:10.1016/j.bbamcr.2020.118913
- Higgins, M. E., Davies, J. P., Chen, F. W., and Ioannou, Y. A. (1999). Niemann-Pick C1 Is a Late Endosome-Resident Protein that Transiently Associates with

## DATA AVAILABILITY STATEMENT

The raw data supporting the conclusions of this article will be made available by the authors, without undue reservation.

## AUTHOR CONTRIBUTIONS

TW and XC: conceptualization, resources, and writing—review and editing. LL, HW, and JY: methodology and validation. LL, HW, and QW: software and formal analysis. HW, JY, QW, and YL: investigation and data curation. TW, LL, and HW: writing—original draft. TW and XC: project administration. All authors have contributed to the article and approved the submitted version.

## SUPPLEMENTARY MATERIAL

The Supplementary Material for this article can be found online at: <https://www.frontiersin.org/articles/10.3389/fmolb.2022.952608/full#supplementary-material>

- Lysosomes and the Trans-golgi Network. *Mol. Genet. metabolism* 68 (1), 1–13. doi:10.1006/mgme.1999.2882
- Hou, W., Xie, Y., Song, X., Sun, X., Lotze, M. T., Zeh, H. J., et al. (2016). Autophagy Promotes Ferroptosis by Degradation of Ferritin. *Autophagy* 12 (8), 1425–1428. doi:10.1080/15548627.2016.1187366
- Hu, B., Liu, Y., Chen, X., Zhao, J., Han, J., Dong, H., et al. (2020). Ferrostatin-1 Protects Auditory Hair Cells from Cisplatin-Induced Ototoxicity *In Vitro* and *In Vivo*. *Biochem. biophysical Res. Commun.* 533 (4), 1442–1448. doi:10.1016/j.bbrc.2020.10.019
- Hung, Y. H., Faux, N. G., Killilea, D. W., Yanjanin, N., Firnkjes, S., Volitakis, I., et al. (2014). Altered Transition Metal Homeostasis in Niemann-Pick Disease, Type C1. *Metallomics* 6 (3), 542–553. doi:10.1039/c3mt00308f
- Hung, Y. H., Lotan, A., Yeshurun, S., Schroeder, A., and Bush, A. I. (2020). Iron Chelation by Deferiprone Does Not Rescue the Niemann-Pick Disease Type C1 Mouse Model. *Biomaterials* 33 (2–3), 87–95. doi:10.1007/s10534-020-00233-5
- King, K. A., Gordon-Salant, S., Pawlowski, K. S., Taylor, A. M., Griffith, A. J., Houser, A., et al. (2014b). Hearing Loss Is an Early Consequence of Npc1 Gene Deletion in the Mouse Model of Niemann-Pick Disease, Type C. *Jaro* 15 (4), 529–541. doi:10.1007/s10162-014-0459-7
- King, K. A., Gordon-Salant, S., Yanjanin, N., Zalewski, C., Houser, A., Porter, F. D., et al. (2014a). Auditory Phenotype of Niemann-Pick Disease, Type C1. *Ear Hear.* 35 (1), 110–117. doi:10.1097/AUD.0b013e3182a362b8
- Kwan, T., White, P. M., and Segil, N. (2009). Development and Regeneration of the Inner Ear. *Ann. N. Y. Acad. Sci.* 1170, 28–33. doi:10.1111/j.1749-6632.2009.04484.x
- Li, J., Cao, F., Yin, H. L., Huang, Z.-j., Lin, Z.-t., Mao, N., et al. (2020). Ferroptosis: Past, Present and Future. *Cell. Death Dis.* 11 (2), 88. doi:10.1038/s41419-020-2298-2
- Li, K., Deng, Y., Deng, G., Chen, P., Wang, Y., Wu, H., et al. (2020). High Cholesterol Induces Apoptosis and Autophagy through the ROS-Activated AKT/FOXO1 Pathway in Tendon-Derived Stem Cells. *Stem Cell. Res. Ther.* 11 (1), 131. doi:10.1186/s13287-020-01643-5
- Liu, J., Kuang, F., Kroemer, G., Klionsky, D. J., Kang, R., and Tang, D. (2020). Autophagy-Dependent Ferroptosis: Machinery and Regulation. *Cell. Chem. Biol.* 27 (4), 420–435. doi:10.1016/j.chembiol.2020.02.005
- Mou, Y., Wang, J., Wu, J., He, D., Zhang, C., Duan, C., et al. (2019). Ferroptosis, a New Form of Cell Death: Opportunities and Challenges in Cancer. *J. Hematol. Oncol.* 12 (1), 34. doi:10.1186/s13045-019-0720-y
- Ouimet, M., Franklin, V., Mak, E., Liao, X., Tabas, I., and Marcel, Y. L. (2011). Autophagy Regulates Cholesterol Efflux from Macrophage Foam Cells via



- Lysosomal Acid Lipase. *Cell. metab.* 13 (6), 655–667. doi:10.1016/j.cmet.2011.03.023
- Pacheco, C. D., Kunkel, R., and Lieberman, A. P. (2007). Autophagy in Niemann-Pick C Disease Is Dependent upon Beclin-1 and Responsive to Lipid Trafficking Defects. *Hum. Mol. Genet.* 16 (12), 1495–1503. doi:10.1093/hmg/ddm100
- Park, E., and Chung, S. W. (2019). ROS-Mediated Autophagy Increases Intracellular Iron Levels and Ferroptosis by Ferritin and Transferrin Receptor Regulation. *Cell. Death Dis.* 10 (11), 822. doi:10.1038/s41419-019-2064-5
- Pluvinage, J. V., Sun, J., Claes, C., Flynn, R. A., Haney, M. S., Iram, T., et al. (2021). The CD22-Igf2r Interaction Is a Therapeutic Target for Microglial Lysosome Dysfunction in Niemann-Pick Type C. *Sci. Transl. Med.* 13 (622), eabg2919. doi:10.1126/scitranslmed.abg2919
- Qian, H., Wu, X., Du, X., Yao, X., Zhao, X., Lee, J., et al. (2020). Structural Basis of Low-pH-dependent Lysosomal Cholesterol Egress by NPC1 and NPC2. *Cell.* 182 (1), 98–111. doi:10.1016/j.cell.2020.05.020
- Qu, C., Peng, Y., and Liu, S. (2022). Ferroptosis Biology and Implication in Cancers. *Front. Mol. Biosci.* 9, 892957. doi:10.3389/fmolb.2022.892957
- Roney, J. C., Li, S., Farfel-Becker, T., Huang, N., Sun, T., Xie, Y., et al. (2021). Lipid-mediated Motor-Adaptor Sequestration Impairs Axonal Lysosome Delivery Leading to Autophagic Stress and Dystrophy in Niemann-Pick Type C. *Dev. Cell* 56 (10), 1452–1468. e8. doi:10.1016/j.devcel.2021.03.032
- Santos-Lozano, A., Villamandos García, D., Sanchis-Gomar, F., Fiuza-Luces, C., Pareja-Galeano, H., Garatachea, N., et al. (2015). Niemann-Pick Disease Treatment: a Systematic Review of Clinical Trials. *Ann. Transl. Med.* 3 (22), 360. doi:10.3978/j.issn.2305-5839.2015.12.04
- Van Hoecke, L., Van Cauwenberghe, C., Dominko, K., Van Imschoot, G., Van Wouterghem, E., Castelein, J., et al. (2021). Involvement of the Choroid Plexus in the Pathogenesis of Niemann-Pick Disease Type C. *Front. Cell. Neurosci.* 15, 757482. doi:10.3389/fncel.2021.757482
- Vanier, M. T., Duthel, S., Rodriguez-Lafrasse, C., Pentchev, P., and Carstea, E. D. (1996). Genetic Heterogeneity in Niemann-Pick C Disease: a Study Using Somatic Cell Hybridization and Linkage Analysis. *Am. J. Hum. Genet.* 58 (1), 118–125.
- Vanier, M. T. (2010). Maladie de Niemann-Pick type C : aspects historiques et actuels, diagnostic biochimique et génétique. *Arch. Pédiatrie* 17 (Suppl. 2), S41–S44. doi:10.1016/S0929-693X(10)70010-5
- Wang, T., Gong, M., Cao, Y., Zhao, C., Lu, Y., Zhou, Y., et al. (2022). Persistent Ferroptosis Promotes Cervical Squamous Intraepithelial Lesion Development and Oncogenesis by Regulating KRAS Expression in Patients with High Risk-HPV Infection. *Cell. Death Discov.* 8 (1), 201. doi:10.1038/s41420-022-01013-5
- Wheeler, S., and Sillence, D. J. (2020). Niemann-Pick Type C Disease: Cellular Pathology and Pharmacotherapy. *J. Neurochem.* 153 (6), 674–692. doi:10.1111/jnc.14895
- Zheng, Z., Tang, D., Zhao, L., LiHanHu, et al. Liproxstatin-1 Protects Hair Cell-like HEI-OC1 Cells and Cochlear Hair Cells against Neomycin Ototoxicity. *Oxidative Med. Cell. Longev.* 2020;2020, 15doi:doi:10.1155/2020/1782659
- Zhou, Y., Takahashi, S., Homma, K., Duan, C., Zheng, J., Cheatham, M. A., et al. (2018). The Susceptibility of Cochlear Outer Hair Cells to Cyclodextrin Is Not Related to Their Electromotile Activity. *acta neuropathol. Commun.* 6 (1), 98. doi:10.1186/s40478-018-0599-9

**Conflict of Interest:** The authors declare that the research was conducted in the absence of any commercial or financial relationships that could be construed as a potential conflict of interest.

**Publisher's Note:** All claims expressed in this article are solely those of the authors and do not necessarily represent those of their affiliated organizations, or those of the publisher, the editors, and the reviewers. Any product that may be evaluated in this article, or claim that may be made by its manufacturer, is not guaranteed or endorsed by the publisher.

Copyright © 2022 Liang, Wang, Yao, Wei, Lu, Wang and Cao. This is an open-access article distributed under the terms of the Creative Commons Attribution License (CC BY). The use, distribution or reproduction in other forums is permitted, provided the original author(s) and the copyright owner(s) are credited and that the original publication in this journal is cited, in accordance with accepted academic practice. No use, distribution or reproduction is permitted which does not comply with these terms.



## OPEN ACCESS

## EDITED BY

Yanqing Liu,  
Columbia University, United States

## REVIEWED BY

Yi Wang,  
Sichuan Academy of Medical Sciences  
and Sichuan Provincial People's  
Hospital, China  
Anqi Li,  
The Ohio State University, United States

## \*CORRESPONDENCE

Jinbo Sun,  
sjbzjy@163.com  
Yanfei Jia,  
jiayanfei\_@126.com

## SPECIALTY SECTION

This article was submitted to Molecular  
Diagnostics and Therapeutics,  
a section of the journal  
Frontiers in Molecular Biosciences

RECEIVED 10 June 2022

ACCEPTED 04 July 2022

PUBLISHED 25 July 2022

## CITATION

Zhang L, Lu Y, Ma X, Xing Y, Sun J and  
Jia Y (2022), The potential interplay  
between G-quadruplex and p53: their  
roles in regulation of ferroptosis  
in cancer.  
*Front. Mol. Biosci.* 9:965924.  
doi: 10.3389/fmolb.2022.965924

## COPYRIGHT

© 2022 Zhang, Lu, Ma, Xing, Sun and Jia.  
This is an open-access article  
distributed under the terms of the  
Creative Commons Attribution License  
(CC BY). The use, distribution or  
reproduction in other forums is  
permitted, provided the original  
author(s) and the copyright owner(s) are  
credited and that the original  
publication in this journal is cited, in  
accordance with accepted academic  
practice. No use, distribution or  
reproduction is permitted which does  
not comply with these terms.

# The potential interplay between G-quadruplex and p53: their roles in regulation of ferroptosis in cancer

Lulu Zhang<sup>1,2</sup>, Yi Lu<sup>1</sup>, Xiaoli Ma<sup>1,2</sup>, Yuanxin Xing<sup>1,2</sup>, Jinbo Sun<sup>3\*</sup>  
and Yanfei Jia<sup>1,2\*</sup>

<sup>1</sup>Research Center of Basic Medicine, Jinan Central Hospital, Shandong First Medical University, Jinan, China, <sup>2</sup>Research Center of Basic Medicine, Jinan Central Hospital, Shandong University, Jinan, China, <sup>3</sup>Department of Neurology, Jinan Central Hospital, Shandong University, Jinan, China

Ferroptosis is a novel form of regulated cell death triggered by various biological processes, and p53 is involved in different ferroptosis regulations and functions as a crucial regulator. Both DNA and RNA can fold into G-quadruplex in GC-rich regions and increasing shreds of evidence demonstrate that G-quadruplexes have been associated with some important cellular events. Investigation of G-quadruplexes is thus vital to revealing their biological functions. Specific G-quadruplexes are investigated to discover new effective anticancer drugs. Multiple modulations have been discovered between the secondary structure G-quadruplex and p53, probably further influencing the ferroptosis in cancer. G-quadruplex binds to ferric iron-related structures directly and may affect the p53 pathways as well as ferroptosis in cancer. In addition, G-quadruplex also interacts with p53 indirectly, including iron-sulfur cluster metabolism, telomere homeostasis, lipid peroxidation, and glycolysis. In this review, we summarized the latent interplay between G-quadruplex and p53 which focused mainly on ferroptosis in cancer to provide the potential understanding and encourage future studies.

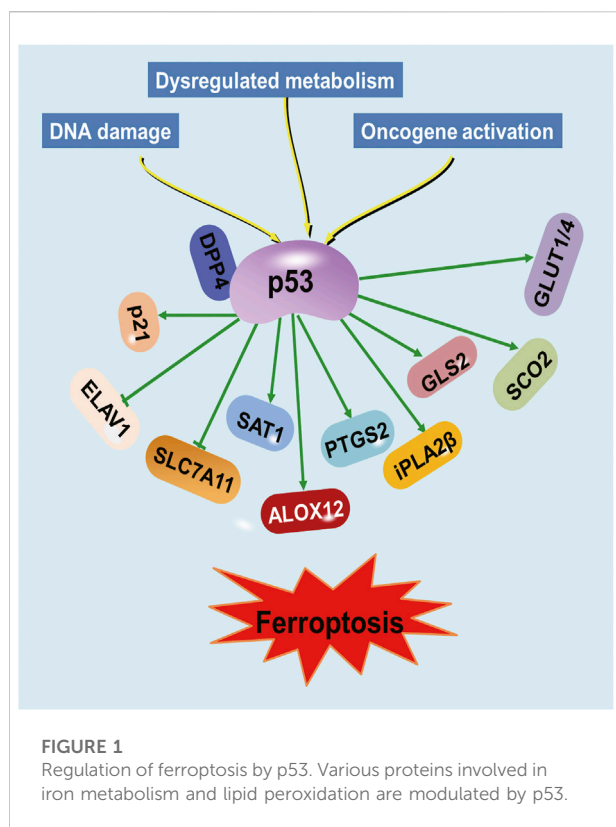
## KEYWORDS

G-quadruplex, p53, ferroptosis, cancer, biological activities

## Introduction

Ferroptosis is a newly identified type of regulated cell death that has attracted considerable attention in explaining the signaling pathways and defined effector mechanisms. Triggering cell death is one of the principal approaches to killing cancer cells. Emerging evidence shows cancer cells exhibit an increased iron demand compared with normal, non-cancer cells. This iron dependency can make cancer cells more vulnerable to ferroptosis. Therefore, exploiting how the ferroptosis are modulated could open new therapeutic avenues for eliminating cancer cells.

Although the precise molecular mechanism of ferroptosis has not been fully understood, many different genes involved in iron metabolism and lipid peroxidation,

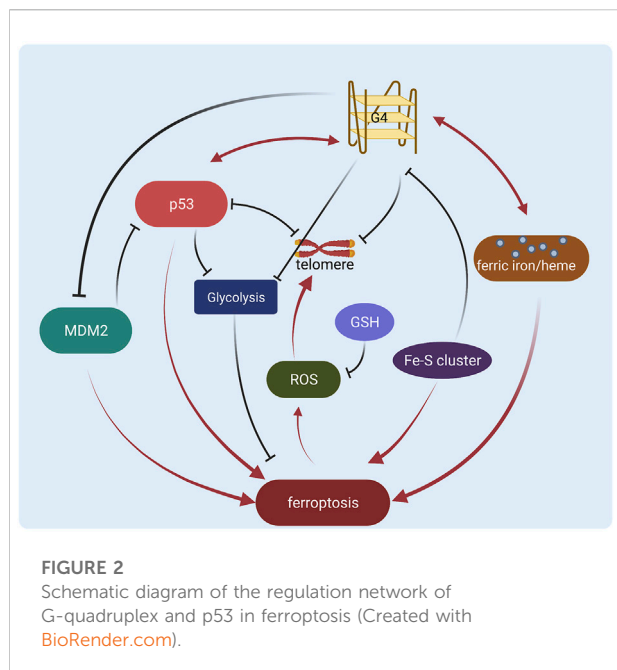


such as GSH peroxidase 4 (GPX4) and solute carrier family 7 member 11 (SLC7A11), have been shown to be the key regulators in ferroptosis (Chen X. et al., 2021). Recently, studies have demonstrated that p53 regulates ferroptosis through transcription-dependent and -independent mechanisms (Kang et al., 2019; Liu et al., 2019; Liu J. et al., 2020; Liu and Gu, 2022). P53 was discovered to bind to the promoter region of SLC7A11 to repress its expression (Jiang et al., 2015; Ou et al., 2016). The binding of p53 to dipeptidyl-peptidase-4 (DPP4) protein decreased lipid peroxidation and ferroptosis (Xie et al., 2017). PTGS2 expression was demonstrated to be upregulated by ferroptosis in a p53-dependent manner (Jiang et al., 2015). Conversely, p53 acts as a positive regulator of ferroptosis via regulation of cytochrome c oxidase 2 (SCO2), glucose transporter (GLUT)1, GLUT4 and glutaminase 2 (GLS2) (Schwartzberg-Bar-Yoseph et al., 2004; Zhang et al., 2018). Besides, p53 suppresses the expression of RNA-binding protein ELAV-like RNA-binding protein 1 (ELAVL1), leading to impaired ELAVL1-LINC00336 interaction and further promoting ferroptosis (Wang et al., 2019).

Furthermore, p53's role in the regulation of genes involved in metabolism has been implicated in its ability to regulate ferroptosis (Tarangelo et al., 2018; Liu and Gu, 2021; Yu et al., 2021). Arachidonate 12-lipoxygenase (ALOX12), a member of the lipoxygenase family that oxygenates

polyunsaturated fatty acids (PUFAs), was identified as an important positive regulator for p53-mediated ferroptosis (Chu et al., 2019). The p53 suppresses ferroptosis through the induction of cyclin-dependent kinase inhibitor 1A (CDKN1A/p21) expression by suppressing the metabolic stress-induced ferroptosis (Tarangelo et al., 2018). The iPLA2 $\beta$  controls p53-driven ferroptosis by mediation detoxification of peroxidized lipids (Chen D. et al., 2021). Spermidine/spermine N1-acetyltransferase (SAT1) was also a direct p53 target that induced lipid peroxidation and sensitizes cells to undergo ferroptosis (Ou et al., 2016). Therefore, p53 represents a novel regulator of ferroptosis, an iron-catalyzed form of regulated necrosis that occurs through excessive peroxidation of PUFAs (Dixon et al., 2012) (Figure 1). An improved understanding of the molecular mechanisms and cellular factors of p53 in ferroptosis regulation will yield new therapeutic strategies for cancer.

Four guanines bind together through eight Hoogsteen hydrogen bonds to form G-quartet, and two or more G-quartets stack to become G-quadruplex (Yuan et al., 2011). Both DNA and RNA can fold into G-quadruplex in GC-rich regions, such as protomer regions, telomere regions, or UTR regions, and increasing shreds of evidence demonstrate the involvement of G-quadruplexes in different biological pathways (Spiegel et al., 2020; Varshney et al., 2020). The correction between G-quadruplex and cancer can be mainly described in the following three aspects. First, the promoter regions contain numerous G-rich sequences which can form G-quadruplexes (Shen et al., 2021). The G-quadruplex on the coding strand blocks the transcription complex and inhibits transcription, while the G-quadruplex on the non-coding strand helps to unwind the duplex and facilitate the transcription (Hänsel-Hertsch et al., 2016), hence the G-quadruplex functions in oncogene promoters have been well studied as well as ligands investigation (Siddiqui-Jain et al., 2002; Nasiri et al., 2014; Zhang et al., 2017). Second, as nucleoprotein complexes at the ends of chromosomes, the telomere is essential for chromosome stability and genome integrity. The repetitive G-rich sequences in telomere fold into G-quadruplex and block the telomeric elongation in cancer cells, thus the G-quadruplex is an effective target for tumor suppression and different G-quadruplex ligands are being developed to inhibit telomerase activity in cancer (Tauchi et al., 2003; Zhu et al., 2012; Beniaminov et al., 2016). Third, the genome instability is regulated by G-quadruplex through DNA replication (Rhodes and Lipps, 2015), leading to apoptosis and autophagy of cancer cells, and the ligand study in this area has been well-developed (Bywater et al., 2012; Xu et al., 2017; Beauvarlet et al., 2019). All these regulations support G-quadruplex as the anti-cancer target using G-quadruplex binding ligands as a tool. Although the primary sequences of G-quadruplexes are all G-riched with similar lengths, the secondary structures in three-dimensional reveal diverse topologies, providing possibilities for targeting.



The p53 has been found to bind telomeric G-quadruplex directly through DNA binding domains (Adámik et al., 2016). Both full-length and C-terminal regions of p53 display strong binding with myc G-quadruplex in the NHEIII<sub>1</sub> region (Petr et al., 2016). The binding between p53 and G-quadruplex participates in gene regulation, in addition, the G-quadruplex can in return modulate the p53 function. The p53 RNA G-quadruplex structure close to the poly(A) site recruits DHX36, RNA helicase maintaining pre-mRNA 3'-end processing after UV damage (Newman et al., 2017), and the G-quadruplex structures formed in the GC-riched region of p53 intron 3 can regulate the splicing of p53 intron 2 (Marcel et al., 2010). Moreover, as part of the non-B DNA structure suppression system, the defection of p53 promotes the influence of genetic instability by G-quadruplex and i-motif (AMPARO et al., 2020), and the G-quadruplex structure impairs the transactivation of the target genes of p53α isoform (Porubiaková et al., 2019). The regulation network of p53 and G-quadruplex suggests potential modulation in more fields and this paper summarized their roles in the regulation of ferroptosis in cancer (Table 1).

## G-quadruplex interacts with ferric iron or heme

A mononuclear Fe (III) complex stabilizes G-quadruplex through  $\pi$ - $\pi$  stacking and inhibits DNA amplification (Ebrahimi et al., 2015). As an essential regulatory factor, heme is originally considered as ferric ions storage and release pool (Daher et al.,

2017; Fiorito et al., 2020), and in recent decades more studies display the heme function in cancer area (Gamage et al., 2021). Tumor cells employ heme to promote mitochondrial oxidative phosphorylation (OXPHOS) through the electron transport chain (ETC) (Hooda et al., 2013; Sugiyama et al., 2014; Alam et al., 2016; Fukuda et al., 2017; Ghosh et al., 2020). Heme binds to almost all parallel G-quadruplex structures to form a stable heme-G-quadruplex complex (Nakajima et al., 2022). Labile heme binds to the G-quadruplex in the myc promoter region and blocks the transcription, as well as the expression of myc downstream genes (Canesin et al., 2020). The G-quadruplexes formed in human ribosomes regulate heme bioavailability through binding to heme or releasing heme through a competitive ligand, PhenDC3 (Mestre-Fos et al., 2020), and further regulating genes related to ferroptosis (Gray et al., 2019). Moreover, G-quadruplex displays the function to be the labile heme pool *in vivo* (Kawai et al., 2022). Through dye-loaded hemin/G-quadruplex modification, the UiO-66 metal-organic framework nanoparticles can be used to detect microRNAs or genes including p53 and BRCA1 (Zhang et al., 2021). An extension of this study is the detection of more genes or RNAs based on sequence specificity. In brief, the G-quadruplex exhibits regulatory function through direct interaction with ferric ion or heme.

## G-quadruplex and p53 in ferroptosis

### G-quadruplex and iron-sulfur cluster biosynthesis in p53-regulated ferroptosis

The p53 participates in iron metabolism by regulating the transcriptional process of iron-sulfur cluster assembly enzyme (ISCU), and ISCU is critical for the biogenesis of iron-sulfur (Fe-S) cluster (Funauchi et al., 2015). The structure of the Fe-S cluster is first determined in the last century (Iwata et al., 1996) and it plays important role in cancer. In lung cancer, the overexpression of NFS1, one kind of iron-sulfur cluster biosynthetic enzyme, will sustain the iron-sulfur cluster expression, and inhibition of NFS1 leads to iron starvation and result in ferroptosis (Alvarez et al., 2017). In addition, sulfur transfer pathways also participate in the occurrence of ferroptosis (Yu et al., 2017). Fe-S cluster is involved in intracellular reduction/oxidation (REDOX) processes, FANCI is one of the Fe-S cluster helicases, and the conserved Fe-S domain containing four cysteine residues is important for the cluster regulation (Bharti et al., 2013). Mutations in this FANCI Fe-S domain would influence the cancer susceptibility (Paulo et al., 2018).

FANCI is likely to be the only Fe-S cluster helicase to open the G-quadruplex structures to this day (Bharti et al., 2013). Human cells with FANCI defection exhibit increased sensitivity to the G-quadruplex specific ligand (Wu et al., 2008), and FANCI mutated cells derived from patients enrich in genome regions



TABLE 1 The regulation and mechanism in ferroptosis related to G-quadruplex and p53.

Process	Regulator	Targets	Mechanism	Reference
G-quadruplex-heme interaction	labile heme	G-quadruplex in myc promoter region	Labile heme binds to the G-quadruplex in the myc promoter region and blocks the transcription	Canesin et al. (2020)
	G-quadruplex	heme	G-quadruplex could bind or release heme in different conditions	Mestre-Fos et al. (2020); Gray et al. (2019)
iron-sulfur cluster biosynthesis	p53	iron-sulfur cluster assembly enzyme (ISCU)	P53 regulates ISCU and affects the biosynthesis of Fe-S cluster	Funauchi et al. (2015)
	Fe-S cluster helicase FANCJ	G-quadruplex	FANCJ unwinds G-quadruplex through Fe-S domain	Wu et al. (2008); London et al. (2008); Odermatt et al. (2020)
telomere homeostasis	telomere	p53	Telomere inactivation could activate p53	Sahin et al. (2011)
	p53	telomere	P53–p21–DREAM–E2F/CHR pathway down-regulates telomere maintenance	Engeland (2018); Vodicka et al. (2021)
	ROS	G-quadruplex	ROS in ferroptosis destroys G-quadruplex and affect telomere homeostasis	Ko et al. (2018); Kordowitzki (2021)
lipid peroxidation	MDM2	p53, PPARα	MDM2 promotes ferroptosis by p53 degradation and PPARα-mediated lipid remodeling	Bykov et al. (2018); Venkatesh et al. (2020)
	G-quadruplex	MDM2	G-quadruplex suppresses MDM2 transcription	Lago et al. (2021)
Glycolysis	p53	GLUT1, GLUT4, GLUT12	P53 inhibits the transcription of GLUT family, and imposes ferroptosis	Schwartzberg-Bar-Yoseph et al. (2004); Zawacka-Pankau et al. (2011); Yokoyama et al. (2014)
	G-quadruplex	AMPK/SnRK, Nrf2-related, and hypoxia-responsive transcription factors	G-quadruplex regulates transcription of target genes	Belmonte-Reche et al. (2022); Andorf et al. (2014)

along with G-quadruplex structures (London et al., 2008). A series of mutation designs demonstrate that FANCJ unwinds G-quadruplex in the genome through the Fe-S domain, correlating with the ability of ferric iron incorporation and metabolism. Therefore, based on ferric iron regulation and ferroptosis, drugs targeting G-quadruplexes should be reconsidered in clinical use in cancer patients with FANCJ deficiency (Odermatt et al., 2020).

In a word, the Fe-S cluster helicase FANCJ utilizes the Fe-S domain to regulate G-quadruplex and likely further influence p53-related iron metabolism and ferroptosis, as well as affect genomic instability by unwinding G-quadruplexes in cancer.

The p53-regulated telomere and the G-quadruplex function in ferroptosis

The regulatory relationship between telomere and p53 is complex. For example, telomere inactivation can activate p53, which leads to DNA damage and DNA repair at the end of chromosomes (Sahin et al., 2011), meanwhile, the p53–p21–DREAM–E2F/CHR pathway, in turn, down-regulates telomere maintenance and influence telomere homeostasis in cancer (Engeland, 2018; Vodicka et al., 2021).

As a signature of ferroptosis, ROS plays a crucial role in cancer. ROS could generate 8-oxoguanine through *in situ*

oxidation of guanine in telomere, and this oxidative telomeric DNA damage, as well as the increased TERT expression, appears to be one of the most important causes of telomere shortening, resulting in increased mortality and cancer recurrence (Ko et al., 2018; Kordowitzki, 2021). RSL3-mediated oxidative stress in ferroptosis drives a series of histone modifications, and H3K79me3/H2A.Z could regulate the telomeric regions (Logie et al., 2021). Telomerase reverse transcriptase (TERT) is involved in ferroptosis-related differential expression genes, indicating potential regulation between telomere and ferroptosis (Liu H.-J. et al., 2020).

Telomeres are found to form G-quadruplex structures to inhibit DNA repair and sustain genome integrity. The ROS in ferroptosis will cause the replacement of guanine by 8-oxoguanine and destroy the G-quadruplex structure, influencing genome instability and telomere homeostasis in cancer, which is also regulated by p53 pathways.

G-quadruplex and lipid peroxidation in the p53-regulated ferroptosis

Accumulated iron triggers ferroptosis by producing excessive ROS and inducing lipid peroxidation (Liu et al., 2022; Ou et al., 2022; Qiao et al., 2022). As a critical component of the cellular antioxidant defense system, glutathione (GSH) prevents the accumulation of

ROS and constitutes the major cellular defense mechanism against ferroptosis. GSH is synthesized from L-cysteine, L-glutamate, and glycine; therefore, the cellular availability of these amino acids could directly affect the concentration of GSH. Several studies have developed a strategy based on G-quadruplex formation for the detection of glutathione and cysteine in the biological sample (Leung et al., 2013; Zhao et al., 2013). These methods were developed to investigate G-quadruplex prevalence in human cells and to study their biological functions, presenting the next key challenges that need to be addressed to fully unravel their biology and therapeutic potential. MDM2 can target and degrade p53, while oncogene activation could prevent MDM2 from binding to p53 and stimulate the p53 acetylation (Bykov et al., 2018). MDM2 also can promote ferroptosis by PPAR $\alpha$ -mediated lipid remodeling (Venkatesh et al., 2020). G-quadruplex structures are present in the MDM2 promoter and G-quadruplex ligands inhibit MDM2 expression and p53 degradation in the liposarcoma (Lago et al., 2021). Based on these published data, we have reasons to believe that G-quadruplex could be exploited to detect and modulate lipid peroxidation, probably reconstituting the p53-regulated ferroptosis signal.

## G-quadruplex involved in p53-regulated glycolysis and ferroptosis

Under most circumstances, p53 inhibits glucose uptake via direct attenuating glucose transporters glucose transporter 1 (GLUT1), GLUT4, and GLUT12 gene transcription and then drives glycolysis inhibition (Schwartzberg-Bar-Yoseph et al., 2004; Zawacka-Pankau et al., 2011; Yokoyama et al., 2014). Glucose-metabolism imbalance would activate the LKB1/AMPK regulatory axis to cause the phosphorylation of acetyl-CoA carboxylase (ACC) to inhibit its activity and impose a regulatory effect on tumor cell ferroptosis (Lee et al., 2020; Li et al., 2020). Glycosyl conjugation to drugs is a strategy being used to take advantage of GLUT overexpression in cancer cells in comparison with non-cancerous cells. Efres *et al.* have synthesized thiosugar naphthalene diimide conjugates as G-quadruplex ligand and proved their antiproliferative activity in colon cancer cells (Belmonte-Reche et al., 2022). Furthermore, G-quadruplex motifs are found in numerous genes encoding members of the AMPK/SnRK, NrF2-related, and hypoxia-responsive transcription factors (Andorf et al., 2014). Collectively, G-quadruplex may aid in energy status gene responses and provide a mechanistic basis for linking Glycolysis signals to ferroptosis.

## Conclusion and perspectives

Ferroptosis is a new regulated cell death form and the mechanisms in cancer are still under exploration. As important regulatory elements, both G-quadruplex and

p53 are involved in various ferroptosis-related processes, and the potential diversified interplay provides more understanding of ferric ion/heme, Fe-S cluster biosynthesis, telomere homeostasis, lipid peroxidation, and glucose metabolism.

The classic regulatory mode of p53 contains stabilization, antirepression, and promoter-specific activation (Kruse and Gu, 2009), and recent research has highlighted the importance of the posttranslational modifications (Liu et al., 2019; Zhang L. et al., 2022). The p53 participates in regulating iron-sulfur cluster assembly enzyme activity, interacts with telomere, is involved in lipid peroxidation, and regulates glycolysis. The complicated models are tightly involved in p53-mediated ferroptosis. Targeting p53 pathways is a promising strategy for anticancer therapy, and various inhibitors are being developed, including ZNF498 (Zhang X. et al., 2022), and Eupaformosanin (Wei et al., 2022).

G-quadruplex acts as a vital regulator for gene activity based on its biological function thus attracting great enthusiasm from researchers in the field of drug discovery. G-quadruplex binding ligands, mostly small molecules, change the stabilization of this kind of secondary structure and further affect the gene activity, telomeric function, and genome instability in multiple cancers. Many small molecules have been discovered and several molecules have progressed to clinical trials, such as Quarfloxin/CX-3534 (Phase I/II) targeting different cancers (NCT00780663, NCT00955786) (Papadopoulos et al., 2007; Drygin et al., 2009), and CX-5461 (Phase I) targeting BRCA1/2 deficient cancer (NCT02719977) (Xu et al., 2017; Khot et al., 2019; Hilton et al., 2022).

However, the G-quadruplex regulation in cancer still remains unsolved problems. Many G-quadruplex ligands don't exhibit selectivity between different G-quadruplexes (Chen J. et al., 2021; Galati et al., 2021), generating potential side effects or low efficiency. The binding affinity of some ligands still needs to be improved (Kosiol et al., 2021) to benefit clinical usage. The regulation of G-quadruplex and ligand function in cancer is yet not clear. Therefore it is necessary to explore new modulations, such as the direct/indirect interactions with p53 in ferroptosis regulation. Here we show that p53 might be an important regulator or target of the G-quadruplex, especially in ferroptosis of cancer research (Figure 2). It is still a challenge to figure out how p53 and G-quadruplex interplay in more stages such as posttranslational modifications or DNA binding, and if the crosstalk functions in other processes like cell cycle/apoptosis. More potential interactions need to be characterized with high resolution, thus methodologies including computational simulation and experimental tools are also required for robust molecular exploration. In addition, it will be interesting and crucial to study the direct interactions between p53 and G-quadruplex in the regulation of ferroptosis in cancer to achieve a clearer mechanism. Besides, diverse studies regarding p53 and G-quadruplex in ferroptosis are operated *in vitro*, and more *in vivo* validations are essential for future therapeutic investigations. Furthermore, more specific targeting strategies are required to evolve based on the potential interplay between p53 and G-quadruplex.

In conclusion, the G-quadruplex and p53 regulation network might be a potential target for cancer research in the future and the mechanisms will be better understood as the research attention increases, hopefully benefiting the clinical cancer treatment.

## Author contributions

LZ: Conceptualization, Writing-Original Draft. YJ: Conceptualization, Supervision, Writing-Review and Editing. JS: Supervision, Writing-Review and Editing. YL, XM, and YX: Review and Editing. All authors contributed to the article and approved the submitted version.

## Funding

This research was supported by the National Natural Science Foundation of China (Nos. 31671468 and 31970728), the Shandong Provincial Natural Science Foundation of China (Nos. ZR2020LZL005 and ZR2020MH050), and the

Academic Promotion Program of Shandong First Medical University (No. 2019QL024). Jinan Technological Innovation and Development Plan (No.202019019).

## Conflict of interest

The authors declare that the research was conducted in the absence of any commercial or financial relationships that could be construed as a potential conflict of interest.

## Publisher's note

All claims expressed in this article are solely those of the authors and do not necessarily represent those of their affiliated organizations, or those of the publisher, the editors and the reviewers. Any product that may be evaluated in this article, or claim that may be made by its manufacturer, is not guaranteed or endorsed by the publisher.

## References

- Adámik, M., Kejnovská, I., Bažantová, P., Petr, M., Renčíuk, D., Vorlíčková, M., et al. (2016). p53 binds human telomeric G-quadruplex *in vitro*. *Biochimie* 128–129, 83–91. doi:10.1016/j.biochi.2016.07.004
- Alam, M. M., Lal, S., FitzGerald, K. E., and Zhang, L. (2016). A holistic view of cancer bioenergetics: Mitochondrial function and respiration play fundamental roles in the development and progression of diverse tumors. *Clin. Transl. Med.* 5 (1), 3. doi:10.1186/s40169-016-0082-9
- Alvarez, S. W., Sviderskiy, V. O., Terzi, E. M., Papagiannakopoulos, T., Moreira, A. L., Adams, S., et al. (2017). NFS1 undergoes positive selection in lung tumours and protects cells from ferroptosis. *Nature* 551 (7682), 639–643. doi:10.1038/nature24637
- Amparo, C., Clark, J., Bedell, V., Murata-Collins, J. L., Martella, M., Pichiorri, F., et al. (2020). Duplex DNA from sites of helicase-polymerase Uncoupling Links non-B DNA structure formation to replicative stress. *Cancer Genomics Proteomics* 17 (2), 101–115. doi:10.21873/cgp.20171
- Andorf, C. M., Kopylov, M., Dobbs, D., Koch, K. E., Stroupe, M. E., Lawrence, C. J., et al. (2014). G-quadruplex (G4) motifs in the maize (*Zea mays* L.) genome are enriched at specific Locations in Thousands of genes Coupled to energy status, hypoxia, low sugar, and Nutrient Deprivation. *J. Genet. Genomics* 41 (12), 627–647. doi:10.1016/j.jgg.2014.10.004
- Beniaminov, A. D., Novikov, R. A., Mamaeva, O. K., Mitkevich, V. A., Smirnov, I. P., Livshits, M. A., et al. (2016). Light-induced oxidation of the telomeric G4 DNA in complex with Zn(II) tetracarboxymethyl porphyrin. *Nucleic Acids Res.* 44 (21), 10031–10041. doi:10.1093/nar/gkw947
- Beauvarlet, J., Bensadoun, P., Darbo, E., Labrunie, G., Rousseau, B., Richard, E., et al. (2019). Modulation of the ATM/autophagy pathway by a G-quadruplex ligand tips the balance between senescence and apoptosis in cancer cells. *Nucleic Acids Res.* 47 (6), 2739–2756. doi:10.1093/nar/gkz095
- Belmonte-Reche, E., Benassi, A., Peñalver, P., Cucchiari, A., Guédin, A., Mergny, J. L., et al. (2022). Thiosugar naphthalene diimide conjugates: G-Quadruplex ligands with antiparasitic and anticancer activity. *Eur. J. Med. Chem.* 232, 114183. doi:10.1016/j.ejmech.2022.114183
- Bharti, S. K., Sommers, J. A., George, F., Kuper, J., Hamon, F., Shin-ya, K., et al. (2013). Specialization among iron-sulfur cluster helicases to resolve G-quadruplex DNA structures that threaten genomic stability. *J. Biol. Chem.* 288 (39), 28217–28229. doi:10.1074/jbc.M113.496463
- Bykov, V. J. N., Eriksson, S. E., Bianchi, J., and Wiman, K. G. (2018). Targeting mutant p53 for efficient cancer therapy. *Nat. Rev. Cancer* 18 (2), 89–102. doi:10.1038/nrc.2017.109
- Bywater, M. J., Poortinga, G., Sanij, E., Hein, N., Peck, A., Cullinane, C., et al. (2012). Inhibition of RNA polymerase I as a therapeutic strategy to promote cancer-specific activation of p53. *Cancer Cell* 22 (1), 51–65. doi:10.1016/j.ccr.2012.05.019
- Canesin, G., Di Ruscio, A., Li, M., Umarmarino, S., Hedblom, A., Choudhury, R., et al. (2020). Scavenging of labile heme by Hemopexin is a key Checkpoint in cancer Growth and Metastases. *Cell Rep.* 32 (12), 108181. doi:10.1016/j.celrep.2020.108181
- Chen, D., Chu, B., Yang, X., Liu, Z., Jin, Y., Kon, N., et al. (2021a). iPLA2 $\beta$ -mediated lipid detoxification controls p53-driven ferroptosis independent of GPX4. *Nat. Commun.* 12 (1), 3644. doi:10.1038/s41467-021-23902-6
- Chen, J., Jin, X., Mei, Y., Shen, Z., Zhu, J., Shi, H., et al. (2021b). The different biological effects of TMPyP4 and cisplatin in the inflammatory microenvironment of osteosarcoma are attributed to G-quadruplex. *Cell Prolif.* 54 (9), e13101. doi:10.1111/cpr.13101
- Chen, X., Kang, R., Kroemer, G., and Tang, D. (2021c). Broadening horizons: The role of ferroptosis in cancer. *Nat. Rev. Clin. Oncol.* 18 (5), 280–296. doi:10.1038/s41571-020-00462-0
- Chu, B., Kon, N., Chen, D., Li, T., Liu, T., Jiang, L., et al. (2019). ALOX12 is required for p53-mediated tumour suppression through a distinct ferroptosis pathway. *Nat. Cell Biol.* 21 (5), 579–591. doi:10.1038/s41556-019-0305-6
- Daher, R., Manceau, H., and Karim, Z. (2017). Iron metabolism and the role of the iron-regulating hormone hepcidin in health and disease. *Presse Med.* 46 (12 Pt 2), e272–e278. doi:10.1016/j.jlpm.2017.10.006
- Dixon, S. J., Lemberg, K. M., Lamprecht, M. R., Skouta, R., Zaitsev, E. M., Gleason, C. E., et al. (2012). Ferroptosis: An iron-dependent form of nonapoptotic cell death. *Cell* 149 (5), 1060–1072. doi:10.1016/j.cell.2012.03.042
- Drygin, D., Siddiqui-Jain, A., O'Brien, S., Schwabe, M., Lin, A., Bliesath, J., et al. (2009). Anticancer activity of CX-3543: A direct inhibitor of rRNA biogenesis. *Cancer Res.* 69 (19), 7653–7661. doi:10.1158/0008-5472.Can-09-1304
- Ebrahimi, M., Khayamian, T., Hadadzadeh, H., Sayed Tabatabaei, B. E., Jannesari, Z., Khaksar, G., et al. (2015). Spectroscopic, biological, and molecular modeling studies on the interactions of [Fe(III)-meloxicam] with G-quadruplex DNA and investigation of its release from bovine serum albumin (BSA) nanoparticles. *J. Biomol. Struct. Dyn.* 33 (11), 2316–2329. doi:10.1080/07391102.2014.1003195
- Engeland, K. (2018). Cell cycle arrest through indirect transcriptional repression by p53: I have a DREAM. *Cell Death Differ.* 25 (1), 114–132. doi:10.1038/cdd.2017.172

- Fiorito, V., Chiabrando, D., Petrillo, S., Bertino, F., and Tolosano, E. (2020). The Multifaceted role of heme in cancer. *Front. Oncol.* 9, 1540. doi:10.3389/fonc.2019.01540
- Fukuda, Y., Wang, Y., Lian, S., Lynch, J., Nagai, S., Fanshawe, B., et al. (2017). Upregulated heme biosynthesis, an exploitable vulnerability in MYCN-driven leukemogenesis. *JCI Insight* 2 (15), 92409. doi:10.1172/jci.insight.92409
- Funauchi, Y., Tanikawa, C., Yi Lo, P. H., Mori, J., Daigo, Y., Takano, A., et al. (2015). Regulation of iron homeostasis by the p53-ISCU pathway. *Sci. Rep.* 5, 16497. doi:10.1038/srep16497
- Galati, E., Bosio, M. C., Novarina, D., Chiara, M., Bernini, G. M., Mozzarelli, A. M., et al. (2021). VID22 counteracts G-quadruplex-induced genome instability. *Nucleic Acids Res.* 49 (22), 12785–12804. doi:10.1093/nar/gkab1156
- Gamage, S. M. K., Lee, K. T. W., Dissabandara, D. L. O., Lam, A. K., and Gopalan, V. (2021). Dual role of heme iron in cancer; promotor of carcinogenesis and an inducer of tumour suppression. *Exp. Mol. Pathol.* 120, 104642. doi:10.1016/j.yexmp.2021.104642
- Ghosh, P., Vidal, C., Dey, S., and Zhang, L. (2020). Mitochondria targeting as an effective strategy for cancer therapy. *Int. J. Mol. Sci.* 21 (9), 3363. doi:10.3390/ijms21093363
- Gray, L. T., Puig Lombardi, E., Verga, D., Nicolas, A., Teulade-Fichou, M. P., Londoño-Vallejo, A., et al. (2019). G-Quadruplexes Sequester free heme in Living cells. *Cell Chem. Biol.* 26 (12), 1681–1691. e1685. doi:10.1016/j.chembiol.2019.10.003
- Hänsel-Hertsch, R., Beraldi, D., Lensing, S. V., Marsico, G., Zyner, K., Parry, A., et al. (2016). G-quadruplex structures mark human regulatory chromatin. *Nat. Genet.* 48 (10), 1267–1272. doi:10.1038/ng.3662
- Hilton, J., Gelmon, K., Bedard, P. L., Tu, D., Xu, H., Tinker, A. V., et al. (2022). Results of the phase I CCTG IND.231 trial of CX-5461 in patients with advanced solid tumors enriched for DNA-repair deficiencies. *Nat. Commun.* 13 (1), 3607. doi:10.1038/s41467-022-31199-2
- Hooda, J., Cadinu, D., Alam, M. M., Shah, A., Cao, T. M., Sullivan, L. A., et al. (2013). Enhanced heme function and mitochondrial respiration promote the progression of lung cancer cells. *PLoS One* 8 (5), e63402. doi:10.1371/journal.pone.0063402
- Iwata, S., Saynovits, M., Link, T. A., and Michel, H. (1996). Structure of a water soluble fragment of the 'Rieske' iron-sulfur protein of the bovine heart mitochondrial cytochrome bc1 complex determined by MAD phasing at 1.5 Å resolution. *Structure* 4 (5), 567–579. doi:10.1016/s0969-2126(96)00062-7
- Jiang, L., Kon, N., Li, T., Wang, S. J., Su, T., Hibshoosh, H., et al. (2015). Ferroptosis as a p53-mediated activity during tumour suppression. *Nature* 520 (7545), 57–62. doi:10.1038/nature14344
- Kang, R., Kroemer, G., and Tang, D. (2019). The tumor suppressor protein p53 and the ferroptosis network. *Free Radic. Biol. Med.* 133, 162–168. doi:10.1016/j.freeradbiomed.2018.05.074
- Kawai, K., Hirayama, T., Imai, H., Murakami, T., Inden, M., Hozumi, I., et al. (2022). Molecular Imaging of labile heme in Living cells using a small molecule fluorescent probe. *J. Am. Chem. Soc.* 144 (9), 3793–3803. doi:10.1021/jacs.1c08485
- Khot, A., Brajanovski, N., Cameron, D. P., Hein, N., MacLachlan, K. H., Sanij, E., et al. (2019). First-in-Human RNA polymerase I transcription inhibitor CX-5461 in patients with advanced Hematologic cancers: Results of a phase I Dose-Escalation study. *Cancer Discov.* 9 (8), 1036–1049. doi:10.1158/2159-8290.Cd-18-1455
- Ko, E., Seo, H.-W., and Jung, G. (2018). Telomere length and reactive oxygen species levels are positively associated with a high risk of mortality and recurrence in hepatocellular carcinoma. *Hepatology* 67 (4), 1378–1391. doi:10.1002/hep.29604
- Kordowitzki, P. (2021). Oxidative stress induces telomere dysfunction and shortening in human Oocytes of advanced Age Donors. *Cells* 10 (8), 1866. doi:10.3390/cells10081866
- Kosiol, N., Juranek, S., Brossart, P., Heine, A., and Paeschke, K. (2021). G-Quadruplexes: A promising target for cancer therapy. *Mol. Cancer* 20 (1), 40. doi:10.1186/s12943-021-01328-4
- Kruse, J. P., and Gu, W. (2009). Modes of p53 regulation. *Cell* 137 (4), 609–622. doi:10.1016/j.cell.2009.04.050
- Lago, S., Nadai, M., Ruggiero, E., Tassinari, M., Marušić, M., Tosoni, B., et al. (2021). The MDM2 inducible promoter folds into four-tetrad antiparallel G-quadruplexes targetable to fight malignant liposarcoma. *Nucleic Acids Res.* 49 (2), 847–863. doi:10.1093/nar/gkaa1273
- Lee, H., Zhuang, L., and Gan, B. (2020). Energy stress inhibits ferroptosis via AMPK. *Mol. Cell. Oncol.* 7 (4), 1761242. doi:10.1080/23723556.2020.1761242
- Leung, K. H., He, H. Z., Ma, V. P., Chan, D. S., Leung, C. H., Ma, D. L., et al. (2013). A luminescent G-quadruplex switch-on probe for the highly selective and tunable detection of cysteine and glutathione. *Chem. Commun.* 49 (8), 771–773. doi:10.1039/c2cc37710a
- Li, C., Dong, X., Du, W., Shi, X., Chen, K., Zhang, W., et al. (2020). LKB1-AMPK axis negatively regulates ferroptosis by inhibiting fatty acid synthesis. *Signal Transduct. Target. Ther.* 5 (1), 187. doi:10.1038/s41392-020-00297-2
- Liu, H.-J., Hu, H.-M., Li, G.-Z., Zhang, Y., Wu, F., Liu, X., et al. (2020a). Ferroptosis-related gene signature Predicts Glioma cell death and Glioma patient progression. *Front. Cell Dev. Biol.* 8, 538. doi:10.3389/fcell.2020.00538
- Liu, J., Zhang, C., Wang, J., Hu, W., and Feng, Z. (2020b). The regulation of ferroptosis by tumor suppressor p53 and its pathway. *Int. J. Mol. Sci.* 21 (21), E8387. doi:10.3390/ijms21218387
- Liu, M., Kong, X. Y., Yao, Y., Wang, X. A., Yang, W., Wu, H., et al. (2022). The critical role and molecular mechanisms of ferroptosis in antioxidant systems: A narrative review. *Ann. Transl. Med.* 10 (6), 368. doi:10.21037/atm-21-6942
- Liu, Y., and Gu, W. (2022). p53 in ferroptosis regulation: the new weapon for the old guardian. *Cell Death Differ.* 29 (5), 895–910. doi:10.1038/s41418-022-00943-y
- Liu, Y., and Gu, W. (2021). The complexity of p53-mediated metabolic regulation in tumor suppression. *Semin. Cancer Biol.* doi:10.1016/j.semcancer.2021.03.010
- Liu, Y., Tavana, O., and Gu, W. (2019). p53 modifications: exquisite decorations of the powerful guardian. *J. Mol. Cell Biol.* 11 (7), 564–577. doi:10.1093/jmcb/mjz060
- Logie, E., Van Puyvelde, B., Cuypers, B., Schepers, A., Berghmans, H., Verdonck, J., et al. (2021). Ferroptosis induction in multiple Myeloma cells triggers DNA Methylation and histone modification changes associated with cellular senescence. *Int. J. Mol. Sci.* 22 (22), 12234. doi:10.3390/ijms222212234
- London, T. B., Barber, L. J., Mosedale, G., Kelly, G. P., Balasubramanian, S., Hickson, I. D., et al. (2008). FANCI is a structure-specific DNA helicase associated with the maintenance of genomic G/C tracts. *J. Biol. Chem.* 283 (52), 36132–36139. doi:10.1074/jbc.M808152200
- Marcel, V., Tran, P. L. T., Sagne, C., Martel-Planche, G., Vaslin, L., Teulade-Fichou, M.-P., et al. (2010). G-Quadruplex structures in TP53 intron 3: Role in alternative splicing and in production of p53 mRNA isoforms. *Carcinogenesis* 32 (3), 271–278. doi:10.1093/carcin/bgq253
- Mestre-Fos, S., Ito, C., Moore, C. M., Reddi, A. R., and Williams, L. D. (2020). Human ribosomal G-quadruplexes regulate heme bioavailability. *J. Biol. Chem.* 295 (44), 14855–14865. doi:10.1074/jbc.RA120.014332
- Nakajima, Y., Momotake, A., Suzuki, A., Neya, S., and Yamamoto, Y. (2022). Nature of a H<sub>2</sub>O molecule Confined in the Hydrophobic Interface between the heme and G-quartet Planes in a heme-DNA complex. *Biochemistry* 61 (7), 523–534. doi:10.1021/acs.biochem.1c00751
- Nasiri, H. R., Bell, N. M., McLuckie, K. I., Husby, J., Abell, C., Neidle, S., et al. (2014). Targeting a c-MYC G-quadruplex DNA with a fragment library. *Chem. Commun.* 50 (14), 1704–1707. doi:10.1039/c3cc48390h
- Newman, M., Sfaki, R., Saha, A., Monchaud, D., Teulade-Fichou, M. P., Vagner, S., et al. (2017). The G-quadruplex-specific RNA helicase DHX36 regulates p53 pre-mRNA 3'-end processing following UV-induced DNA damage. *J. Mol. Biol.* 429 (21), 3121–3131. doi:10.1016/j.jmb.2016.11.033
- Odermatt, D. C., Lee, W. T. C., Wild, S., Jozwiakowski, S. K., Rothenberg, E., Gari, K., et al. (2020). Cancer-associated mutations in the iron-sulfur domain of FANCI affect G-quadruplex metabolism. *PLoS Genet.* 16 (6), e1008740. doi:10.1371/journal.pgen.1008740
- Ou, M., Jiang, Y., Ji, Y., Zhou, Q., Du, Z., Zhu, H., et al. (2022). Role and mechanism of ferroptosis in neurological diseases. *Mol. Metab.* 61, 101502. doi:10.1016/j.molmet.2022.101502
- Ou, Y., Wang, S. J., Li, D., Chu, B., and Gu, W. (2016). Activation of SAT1 engages polyamine metabolism with p53-mediated ferroptotic responses. *Proc. Natl. Acad. Sci. U. S. A.* 113 (44), E6806–E6812. doi:10.1073/pnas.1607152113
- Papadopoulos, K., Mita, A., Ricart, A., Hufnagel, D., Northfelt, D., Von Hoff, D., et al. (2007). Pharmacokinetic findings from the phase I study of Quarfloxin (CX-3543): A protein-rDNA quadruplex inhibitor, in patients with advanced solid tumors. *Mol. Cancer Ther.* 6 (11\_Suppl. ment), B93.
- Paulo, P., Maia, S., Pinto, C., Pinto, P., Monteiro, A., Peixoto, A., et al. (2018). Targeted next generation sequencing identifies functionally deleterious germline mutations in novel genes in early-onset/familial prostate cancer. *PLoS Genet.* 14 (4), e1007355. doi:10.1371/journal.pgen.1007355
- Petr, M., Helma, R., Polášková, A., Krejčí, A., Dvořáková, Z., Kejnovská, I., et al. (2016). Wild-type p53 binds to MYC promoter G-quadruplex. *Biosci. Rep.* 36 (5), e00397. doi:10.1042/BSR20160232
- Porubíková, O., Bohálová, N., Inga, A., Vadovičová, N., Coufal, J., Fojta, M., et al. (2019). The influence of quadruplex structure in Proximity to P53 target sequences on the transactivation potential of P53 Alpha isoforms. *Int. J. Mol. Sci.* 21 (1), 127. doi:10.3390/ijms21010127



- Qiao, G., Zhang, W., and Dong, K. (2022). Regulation of ferroptosis by noncoding RNAs: A novel promise treatment in esophageal squamous cell carcinoma. *Mol. Cell. Biochem.* doi:10.1007/s11010-022-04441-0
- Rhodes, D., and Lipps, H. J. (2015). G-quadruplexes and their regulatory roles in biology. *Nucleic Acids Res.* 43 (18), 8627–8637. doi:10.1093/nar/gkv862
- Sahin, E., Colla, S., Liesa, M., Moslehi, J., Müller, F. L., Guo, M., et al. (2011). Telomere dysfunction induces metabolic and mitochondrial compromise. *Nature* 470 (7334), 359–365. doi:10.1038/nature09787
- Schwartzberg-Bar-Yoseph, F., Armoni, M., and Karnieli, E. (2004). The tumor suppressor p53 down-regulates glucose transporters GLUT1 and GLUT4 gene expression. *Cancer Res.* 64 (7), 2627–2633. doi:10.1158/0008-5472.can-03-0846
- Shen, J., Varshney, D., Simeone, A., Zhang, X., Adhikari, S., Tannahill, D., et al. (2021). Promoter G-quadruplex folding precedes transcription and is controlled by chromatin. *Genome Biol.* 22 (1), 143. doi:10.1186/s13059-021-02346-7
- Siddiqui-Jain, A., Grand, C. L., Bearss, D. J., and Hurley, L. H. (2002). Direct evidence for a G-quadruplex in a promoter region and its targeting with a small molecule to repress c-MYC transcription. *Proc. Natl. Acad. Sci. U. S. A.* 99 (18), 11593–11598. doi:10.1073/pnas.182256799
- Spiegel, J., Adhikari, S., and Balasubramanian, S. (2020). The structure and function of DNA G-quadruplexes. *Trends Chem.* 2 (2), 123–136. doi:10.1016/j.trechm.2019.07.002
- Sugiyama, Y., Hagiya, Y., Nakajima, M., Ishizuka, M., Tanaka, T., Ogura, S., et al. (2014). The heme precursor 5-aminolevulinic acid disrupts the Warburg effect in tumor cells and induces caspase-dependent apoptosis. *Oncol. Rep.* 31 (3), 1282–1286. doi:10.3892/or.2013.2945
- Tarangelo, A., Magtanong, L., Biegling-Rolett, K. T., Li, Y., Ye, J., Attardi, L. D., et al. (2018). p53 suppresses metabolic stress-induced ferroptosis in cancer cells. *Cell Rep.* 22 (3), 569–575. doi:10.1016/j.celrep.2017.12.077
- Tauchi, T., Shin-Ya, K., Sashida, G., Sumi, M., Nakajima, A., Shimamoto, T., et al. (2003). Activity of a novel G-quadruplex-interactive telomerase inhibitor, telomestatin (SOT-095), against human leukemia cells: Involvement of ATM-dependent DNA damage response pathways. *Oncogene* 22 (34), 5338–5347. doi:10.1038/sj.onc.1206833
- Varshney, D., Spiegel, J., Zyner, K., Tannahill, D., and Balasubramanian, S. (2020). The regulation and functions of DNA and RNA G-quadruplexes. *Nat. Rev. Mol. Cell Biol.* 21 (8), 459–474. doi:10.1038/s41580-020-0236-x
- Venkatesh, D., O'Brien, N. A., Zandkarimi, F., Tong, D. R., Stokes, M. E., Dunn, D. E., et al. (2020). MDM2 and MDMX promote ferroptosis by PPAR $\alpha$ -mediated lipid remodeling. *Genes Dev.* 34 (7–8), 526–543. doi:10.1101/gad.334219.119
- Vodicka, P., Andera, L., Opatova, A., and Vodickova, L. (2021). The interactions of DNA repair, telomere homeostasis, and p53 mutational status in solid cancers: Risk, Prognosis, and Prediction. *Cancers (Basel)* 13 (3), 479. doi:10.3390/cancers13030479
- Wang, M., Mao, C., Ouyang, L., Liu, Y., Lai, W., Liu, N., et al. (2019). Long noncoding RNA LINC00336 inhibits ferroptosis in lung cancer by functioning as a competing endogenous RNA. *Cell Death Differ.* 26 (11), 2329–2343. doi:10.1038/s41418-019-0304-y
- Wei, Y., Zhu, Z., Hu, H., Guan, J., Yang, B., Zhao, H., et al. (2022). Eupaformosanin induces apoptosis and ferroptosis through ubiquitination of mutant p53 in triple-negative breast cancer. *Eur. J. Pharmacol.* 924, 174970. doi:10.1016/j.ejphar.2022.174970
- Wu, Y., Shin-ya, K., and Brosh, R. M., Jr. (2008). FANCD1 helicase defective in Fanconi anemia and breast cancer unwinds G-quadruplex DNA to defend genomic stability. *Mol. Cell. Biol.* 28 (12), 4116–4128. doi:10.1128/mcb.02210-07
- Xie, Y., Zhu, S., Song, X., Sun, X., Fan, Y., Liu, J., et al. (2017). The tumor suppressor p53 Limits ferroptosis by blocking DPP4 activity. *Cell Rep.* 20 (7), 1692–1704. doi:10.1016/j.celrep.2017.07.055
- Xu, H., Di Antonio, M., McKinney, S., Mathew, V., Ho, B., O'Neil, N. J., et al. (2017). CX-5461 is a DNA G-quadruplex stabilizer with selective lethality in BRCA1/2 deficient tumours. *Nat. Commun.* 8, 14432. doi:10.1038/ncomms14432
- Yokoyama, M., Okada, S., Nakagomi, A., Moriya, J., Shimizu, I., Nojima, A., et al. (2014). Inhibition of endothelial p53 improves metabolic abnormalities related to dietary obesity. *Cell Rep.* 7 (5), 1691–1703. doi:10.1016/j.celrep.2014.04.046
- Yu, H., Guo, P., Xie, X., Wang, Y., and Chen, G. (2017). Ferroptosis, a new form of cell death, and its relationships with tumourous diseases. *J. Cell. Mol. Med.* 21 (4), 648–657. doi:10.1111/jcmm.13008
- Yu, L., Wu, M., Zhu, G., and Xu, Y. (2021). Emerging roles of the tumor suppressor p53 in metabolism. *Front. Cell Dev. Biol.* 9, 762742. doi:10.3389/fcell.2021.762742
- Yuan, G., Zhang, Q., Zhou, J., and Li, H. (2011). Mass spectrometry of G-quadruplex DNA: Formation, recognition, property, conversion, and conformation. *Mass Spectrom. Rev.* 30 (6), 1121–1142. doi:10.1002/mas.20315
- Zawacka-Pankau, J., Grinkevich, V. V., Hüntner, S., Nikulenkov, F., Gluch, A., Li, H., et al. (2011). Inhibition of glycolytic enzymes mediated by pharmacologically activated p53: Targeting Warburg effect to fight cancer. *J. Biol. Chem.* 286 (48), 41600–41615. doi:10.1074/jbc.M111.240812
- Zhang, L., Hou, N., Chen, B., Kan, C., Han, F., Zhang, J., et al. (2022a). Post-translational modifications of p53 in ferroptosis: Novel Pharmacological targets for cancer therapy. *Front. Pharmacol.* 13, 908772. doi:10.3389/fphar.2022.908772
- Zhang, L., Tan, W., Zhou, J., Xu, M., and Yuan, G. (2017). Investigation of G-quadruplex formation in the FGFR2 promoter region and its transcriptional regulation by liensinine. *Biochim. Biophys. Acta. Gen. Subj.* 1861 (4), 884–891. doi:10.1016/j.bbagen.2017.01.028
- Zhang, P., Ouyang, Y., and Willner, I. (2021). Multiplexed and amplified chemiluminescence resonance energy transfer (CRET) detection of genes and microRNAs using dye-loaded hemin/G-quadruplex-modified UiO-66 metal-organic framework nanoparticles. *Chem. Sci.* 12 (13), 4810–4818. doi:10.1039/d0sc06744j
- Zhang, W., Gai, C., Ding, D., Wang, F., and Li, W. (2018). Targeted p53 on small-molecules-induced ferroptosis in cancers. *Front. Oncol.* 8, 507. doi:10.3389/fonc.2018.00507
- Zhang, X., Zheng, Q., Yue, X., Yuan, Z., Ling, J., Yuan, Y., et al. (2022b). ZNF498 promotes hepatocellular carcinogenesis by suppressing p53-mediated apoptosis and ferroptosis via the attenuation of p53 Ser46 phosphorylation. *J. Exp. Clin. Cancer Res.* 41 (1), 79. doi:10.1186/s13046-022-02288-3
- Zhao, J., Chen, C., Zhang, L., Jiang, J., Shen, G., Yu, R., et al. (2013). A Hg(2+)-mediated label-free fluorescent sensing strategy based on G-quadruplex formation for selective detection of glutathione and cysteine. *Analyst* 138 (6), 1713–1718. doi:10.1039/c3an36657j
- Zhu, L. N., Zhao, S. J., Wu, B., Li, X. Z., and Kong, D. M. (2012). A new cationic porphyrin derivative (TMPipEOPP) with large side arm substituents: A highly selective G-quadruplex optical probe. *PLoS One* 7 (5), e35586. doi:10.1371/journal.pone.0035586



## OPEN ACCESS

## EDITED BY

Yanqing Liu,  
Columbia University, United States

## REVIEWED BY

Qian Wang,  
College of Staten Island, United States  
Zhicheng Peng,  
University of Pennsylvania, United States

## \*CORRESPONDENCE

Siying Ren,  
610909857@qq.com  
Guofeng Wu,  
wuguofeng3013@sina.com

<sup>†</sup>These authors have contributed equally to this work and share first authorship

## SPECIALTY SECTION

This article was submitted to Molecular Diagnostics and Therapeutics, a section of the journal Frontiers in Molecular Biosciences

RECEIVED 11 June 2022

ACCEPTED 12 July 2022

PUBLISHED 05 August 2022

## CITATION

Ren S, Chen Y, Wang L and Wu G (2022), Neuronal ferroptosis after intracerebral hemorrhage. *Front. Mol. Biosci.* 9:966478. doi: 10.3389/fmolb.2022.966478

## COPYRIGHT

© 2022 Ren, Chen, Wang and Wu. This is an open-access article distributed under the terms of the [Creative Commons Attribution License \(CC BY\)](#). The use, distribution or reproduction in other forums is permitted, provided the original author(s) and the copyright owner(s) are credited and that the original publication in this journal is cited, in accordance with accepted academic practice. No use, distribution or reproduction is permitted which does not comply with these terms.

# Neuronal ferroptosis after intracerebral hemorrhage

Siying Ren<sup>1\*†</sup>, Yue Chen<sup>2†</sup>, Likun Wang<sup>1</sup> and Guofeng Wu<sup>1\*</sup>

<sup>1</sup>Department of Emergency, Affiliated Hospital of Guizhou Medical University, Guiyang, China,

<sup>2</sup>Graduate School of Guizhou Medical University, Guiyang, China

Intracerebral hemorrhage (ICH) is a devastating form of stroke with high rates of morbidity, mortality, and disability. It induces cell death that is responsible for the secondary brain injury (SBI). The underlying mechanism of SBI after ICH is still unclear, and whether it is related to iron overload is worthy to be discussed. Ferroptosis is an iron-dependent non-apoptotic modes of cell death and plays a particularly important role in the occurrence and progression of ICH. Many ICH-induced regulators and signalling pathways of ferroptosis have been reported as promising targets for treating ICH. In this article, we review the definition, characteristics, and inhibition methods of neuronal ferroptosis caused by iron deposition after ICH, and review the biomarkers for ferroptosis.

## KEYWORDS

intracerebral hemorrhage, secondary brain injury, cell death, ferroptosis, iron overload, oxidative damage, reactive oxygen species

## 1 Introduction

Intracerebral hemorrhage (ICH) is a subtype of stroke with the highest morbidity, mortality, and disability (van Asch et al., 2010). After ICH occurs, in addition to the primary brain injury caused by the hematoma compressing the surrounding brain tissue, blood components, haemoglobin (Hb), iron, and other neurotoxic substances released by the hematoma also contribute to neuroinflammation and oxidative stress, increase the synthesis of reactive oxygen species (ROS), resulting in secondary brain injury (SBI) (Xi et al., 2006; Wang, 2010). Both the primary and SBI trigger significant cell death and loss of neurological functions. In consideration of the physical compression of the hematoma, many studies have explored the effect of surgical removal of hematoma; however, no significant benefits have been found for patients with ICH (Xi et al., 2014). Similarly, there are limited medical therapy available to alleviate SBI effectively (Bai et al., 2020).

The mechanism of SBI after ICH is complex and remains unclear. Modes of cell death which ICH-induced including necroptosis, pyroptosis, ferroptosis, autophagy, and parthanatos (Zhang et al., 2022). These models of cell death may be associated with SBI after ICH simultaneously. Thus, a better understanding of the modes of cell death in ICH should provide new insights to counter the pathology of ICH. It could result in more effective and targeted neuroprotective or neurorestorative therapeutic strategies (Guo et al., 2020; Zhang et al., 2022).

Studies have shown that excess Hb and iron ions released from hematomas accumulate in the brain parenchyma, causing neurotoxicity and accelerating neurodegeneration (Zecca et al., 2004; Wang et al., 2002). Iron-dependent non-

apoptotic cell death, namely, ferroptosis, has been identified as a potential therapeutic target for ICH (Dixon et al., 2012). Neuronal ferroptosis plays key roles in SBI caused by ICH (Xu et al., 2018). Limiting ferroptosis caused by ferrotoxicity and excess accumulation of ROS reduces brain damage and improves the clinical outcomes of patients with ICH (Wang, 2010; Wu L et al., 2012). Therefore, we review the research progress of neuronal ferroptosis, and provide new ideas for treating SBI following ICH.

## 2 Definition and characteristics of ferroptosis

ICH refers to blood entering into the brain parenchyma, ventricle system, or subarachnoid space from a fracturing intracerebral vessel. The mortality rate in ICH patients is 50% approximately, while most of the survivors lose the capability of living independently (Gross et al., 2019). Especially, SBI, which refers to oxidative stress (Yao et al., 2021), inflammation (Xue and Yong, 2020), blood-brain barrier (BBB) hyperpermeability (Keep et al., 2018), and cerebral vasospasm (Athiraman and Zipfel, 2021), further drives brain cell death. Iron is a major product of lysed erythrocytes in hematoma. It can form highly toxic hydroxyl radicals to attack DNA, proteins, and lipid membranes, thereby disrupting cellular functions and causing neuronal death. Iron released from haemoglobin triggers ROS formation, which also induced ferroptosis (Magtanong and Dixon, 2018; Zhang et al., 2022) and is required for the accumulation of lipid peroxides and the execution of ferroptosis (Stockwell et al., 2017). Ferroptosis is iron-dependent non-apoptotic cell death and may play an important role in the development of SBI following ICH.

### 2.1 Definition of ferroptosis

Ferroptosis, a newly identified regulated cell death (RCD) type. More and more researches in this field have revealed the potential roles of ferroptosis in development, immune system regulation, ischemia-reperfusion injury, and tumor suppression (Stockwell et al., 2017). Ferroptosis was first discovered and reported by Dixon et al. in 2012 (Dixon et al., 2012). Ferroptosis is an iron-dependent non-apoptotic form of cell death, which occurs through excessive accumulation of ROS when glutathione (GSH) peroxidase 4 (GPX4), a lipid peroxide reduction system, is dysregulated or relatively insufficient. The Nomenclature Committee on Cell Death (NCCD) defined ferroptosis as “a form of RCD initiated by oxidative perturbations of the intracellular microenvironment that is under constitutive control by GPX4 and can be inhibited by iron chelators and lipophilic antioxidants” (Galluzzi et al., 2018). Iron, lipid, and ROS are three core components of ferroptosis.

Metabolic dysregulation of any one of them may influence ferroptotic cell death. Any molecular change or pharmacological intervention that regulates any of these elements may affect the final consequences of ferroptosis (Liu and Gu, 2022).

### 2.2 Characteristics of ferroptosis

Ferroptosis is distinct from apoptosis, necrosis, and autophagy in terms of morphological, biochemical, and genetic properties (Dixon et al., 2012). Electron microscopy has shown that the morphological characteristics of ferroptosis include an obvious reduction in mitochondrial volume, increased density of the mitochondrial double membrane structure, reduced or disappeared cristae formed by the inner membrane, and a near absence of other obvious morphological changes before cell death, particularly the intact nuclei (Yu et al., 2017). The biochemical characteristics of ferroptosis include excessive ROS accumulation, which is dependent on iron ions (Dixon et al., 2012). During the oxidative phosphorylation of mitochondria, cells generate a certain amount of ROS and adenosine triphosphate (ATP). However, a level of ROS that exceeds the antioxidant capacity of cells leads to an enhanced oxidative stress response, which directly or indirectly damages proteins, nucleic acids, lipids, and other macromolecular substances, leading to cell damage or cell death (Abrams et al., 2016). The genetic characteristics of ferroptosis are regulated by a unique set of genes, mainly including ribosomal protein L8 (*RPL8*), ATP synthase  $F_0$  complex subunit C3 (*ATP5G3*), iron response element binding protein 2 (*IREB2*), citrate synthase (*CS*), tetratricopeptide repeat domain 35 (*TTC35*), and acyl-CoA synthetase family member 2 (*ACSF2*) genes (Dixon et al., 2012).

### 2.3 Autophagy promotes ferroptosis

Ferroptosis is caused by dysregulated cell metabolism, including iron, lipid, amino acids, and ROS metabolism (Liu and Gu, 2022). Gao et al. showed that autophagy promotes ferroptosis by regulating intracellular iron homeostasis and ROS synthesis (Gao et al., 2016). *In vitro* experiments showed that the application of Erastin, a synthetic small-molecule compound, which induces ferroptosis and activates autophagy, led to intracellular ferritin degradation to further increase the level of intracellular iron ions through autophagy, resulting in rapid accumulation of intracellular ROS, which promote ferroptosis. Hou et al. also demonstrated that the activation of autophagy further promoted ferroptosis by degrading ferritin in tumor cells (Hou et al., 2016).

### 3 Discovery of neuronal ferroptosis after ICH

Li et al. used a collagenase-induced ICH mouse model to observe morphological changes and showed that the proportion of shrunken mitochondria in the cytoplasm and axon of neurons around the hematoma increased, which strongly confirmed the occurrence of ferroptosis and was the earliest report of neuronal ferroptosis after ICH. They also applied ferrostatin-1 (Fer-1), a specific ferroptosis inhibitor after acute ICH and showed that Fer-1 improved the neurological functions of the mice (Li et al., 2017a). In the same year, Zille et al. showed that the ICH model pretreated with Hb had increased levels of phosphorylated extracellular regulated protein kinases (ERK1/2) (Zille et al., 2017). As ERK1/2 is an important signaling molecule in the RAS-RAF-MEK pathway in the process of ferroptosis induced by the small-molecule Erastin, the finding of Zille et al. further prove from a molecular viewpoint that neurons undergo ferroptosis after ICH. In 2018, Li et al. used transmission electron microscopy (TEM) to monitor the ultra-micromorphological changes of neurons in a collagenase-induced ICH animal model and showed that on the third and sixth day after ICH, both the soma and axon of neurons had an increased proportion of shrunken mitochondria (Li et al., 2018), providing sufficient evidence for the occurrence of neuronal ferroptosis after ICH. Recently, an increasing number of researchers have investigated neuronal ferroptosis after ICH, with the aim to identify new directions and targets for treating SBI after ICH.

### 4 Biomarkers for neuronal ferroptosis after ICH

Observations of morphological changes by TEM or pharmacological and molecular characteristics are the most common approaches to identify neuronal ferroptosis. Although these are relatively complicated processes, the identification of biomarkers of ferroptosis will bring great convenience to the determination of ferroptosis in the future. Li et al. used Hb to stimulate hippocampal tissue slice culture *in vitro* and showed high expression of prostaglandin endoperoxide synthase 2 (PTGS2), but no significant changes in the mRNA levels of *IREB2*, *CS*, *RPL8*, and *ATP5G3* (Li et al., 2017b). PTGS2 encodes cyclooxygenase-2 (COX-2), which is a key enzyme in prostaglandin biosynthesis. Studies have confirmed that ferroptosis is regulated by PTGS2, a unique and potentially direct downstream gene that induces ferroptosis. COX-2 is highly expressed after ICH and its inhibition alleviates the SBI caused by ICH, suggesting that COX-2 may be a biomarker for neuronal ferroptosis after ICH. However, existing research is limited to the Hb-induced ICH mouse model, and further research is needed to confirm the sensitivity, representativeness, and reproducibility of using COX-

2 as a biomarker for neuronal ferroptosis after ICH (Chen et al., 2019).

### 5 Mechanism of neuronal ferroptosis after ICH

#### 5.1 Intracellular iron overload

Iron ions are essential for the occurrence of ferroptosis. However, the specific mechanism by which iron ions promote ferroptosis is not yet fully understood (Cao and Dixon, 2016). After ICH, the excess ferric ions from the red blood cells (RBC) lysis combine with transferrin (TF) in the serum to transport iron ions into cells through receptor-mediated effects (Andrews, 2000). Ferric ions are reduced to ferrous ions by divalent metal transporter 1 (DMT1) and accumulate in neurons, where ferrous ions induce excessive generation of lethal ROS and lipid peroxides (Figure 1). A previous study of the ICH mouse model showed that two iron chelators, deferoxamine (DFX) and VK-28 (5-[4-(2-hydroxyethyl) piperazine-1-ylmethyl]-quinoline-8-ol), reduced neuronal death, ROS synthesis, accumulation of iron ions around the hematoma, activation of microglia, and improved the neurological function of the mouse model (Li et al., 2017a). Wu et al. demonstrated that fat-soluble iron chelator, 2,2'-dipyridyl (DP), reduced iron deposition around the hematoma and ROS synthesis, improving the neuronal function and reducing the neuronal death of the ICH mouse model (Wu L et al., 2012). Pyridoxal isonicotinoyl hydrazine (PIH), a lipophilic iron-chelating agent, has been reported to reduce excess iron-induced cytotoxicity following ICH, which was associated with mitigation of inflammation and ferroptosis (Zhang H et al., 2021). The effect of iron ion chelators on the improvement of neuronal function in mice after ICH indicated that the occurrence of ferroptosis was inseparable from the effect of iron ions (Figure 1). Nevertheless, the specific mechanism still needs further exploration.

#### 5.2 Inhibiting the cystine/glutamate antiporter

Studies have confirmed an increased level of glutamate (Glu) in the brain tissue surrounding the hematoma after ICH in mice, rabbits, and patients with ICH (Li et al., 2017b; Wu et al., 2013; Castillo et al., 2002). The addition of Glu to the culture medium of HT22 hippocampal neurons led to a significant increase in cell death, and the application of the 5-lipoxygenase (5-LOX) inhibitor Zileuton suppressed 5-LOX to reduce lipid peroxide production, which inhibits ferroptosis and thereby protects neurons (Liu et al., 2015). Li et al. observed an increase in the level of Glu around the hematoma of the ICH mouse model and



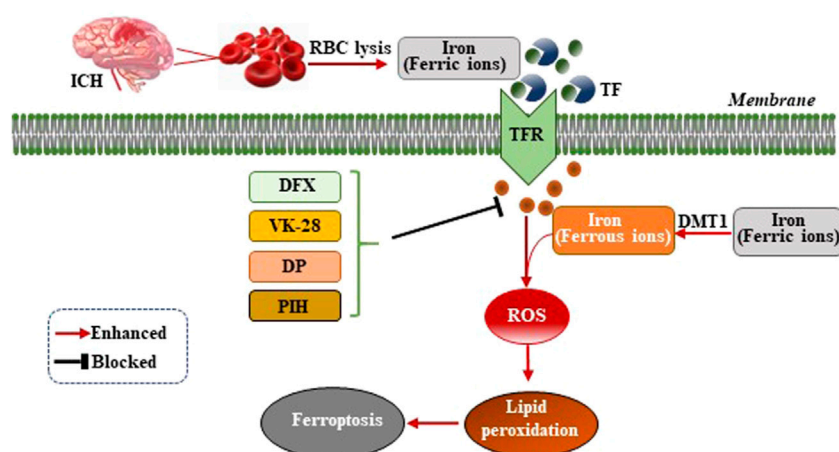


FIGURE 1

Mechanism of ferroptosis following ICH by intracellular iron overload. After ICH occurs, the hematoma releases iron ions from RBC lysis, the concentration of iron ions increase around neurons and combine with transferrin (TF) to transport iron ions into cells through TF receptor (TFR)-mediated effects. Ferric ions are reduced to ferrous ions by divalent metal transporter 1 (DMT1) and accumulate in neurons, where ferrous ions induce excessive generation of lethal ROS and lipid peroxides, therefore, resulting in ferroptosis. Iron chelators (DFX, VK-28, DP, and PIH) form a chelating ferric amine with iron ions to prevent iron ions from donating electrons to oxygen to form ROS.

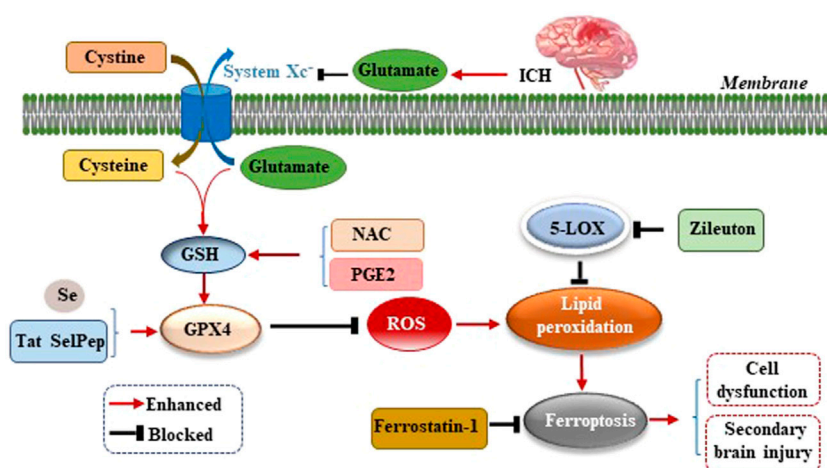


FIGURE 2

Mechanism of ferroptosis following ICH by inhibiting cystine/glutamate antiporter (System Xc<sup>-</sup>). After ICH occurs, excessive glutamate (Glu) around neurons inhibits the activity of System Xc<sup>-</sup> and the transfer of cysteine (Cys), leading to reduction of glutathione (GSH) synthesis, which reduces the activity of glutathione peroxidase 4 (GPX4), resulting in excessive reactive oxygen species (ROS) and lipid peroxide levels which cannot be scavenged, thereby leading to neuronal ferroptosis, cell dysfunction, and secondary brain injury (SBI) caused by ICH.

used the glutaminase inhibitor 968 to inhibit the decomposition of glutamine into Glu to significantly reduce the number of degenerated neurons around the hematoma, suggesting that the breakdown of glutamine led to neuronal ferroptosis after ICH *in vivo* (Li et al., 2017a). The reason for this finding may be that excessive Glu around neurons inhibits the activity of cystine/

glutamate antiporter (System Xc<sup>-</sup>) and the transfer of cysteine (Cys). As Cys is the raw material for GSH synthesis, the reduction of Cys leads to a further reduction of GSH synthesis, which reduces the activity of GPX4 (Figure 2). This, results in excessive ROS and lipid peroxide levels which cannot be scavenged, thereby leading to neuronal ferroptosis and aggravating the

dysfunction, cerebral edema, oxidative stress, BBB damage, and inflammatory response caused by ICH (Gao et al., 2015). Up-regulating the expression of GPX4 in ICH model can inhibit ferroptosis and treat ICH (Peng et al., 2022).

### 5.3 P53 in ferroptosis regulation

The tumor suppressor p53 as a master regulator of ferroptosis, has been among the most extensively studied genes since its discovery in 1979. A major function of p53 is mediating cellular and systematic metabolism. Interestingly, p53 is tightly associated with all key metabolic pathways involved in ferroptosis. Unlike apoptotic cell death, activation of p53 solely is not sufficient to induce ferroptosis directly; instead, through its metabolic targets, p53 is able to modulate the ferroptosis response in the presence of ferroptosis inducers such as GPX4 inhibitors or high levels of ROS. More and more studies to this day have been revealed that p53 is a key regulator of both canonical and non-canonical ferroptosis pathways via a variety of mechanisms. In most cases, p53 promotes ferroptosis. However, under a certain context, p53 can inhibit ferroptosis (Liu and Gu, 2022).

#### 5.3.1 P53 modulates GPX4-dependent ferroptosis pathways

p53 was shown to promote ferroptosis via its capacity to inhibit the import of cystine into target cells. Mechanistically, p53 was found to suppress the transcription of SLC7A11 solute carrier family 7 member 11 (SLC7A11), which is a core subunit of the System Xc<sup>-</sup>. The activity of System Xc<sup>-</sup> is mainly determined by SLC7A11. SLC7A11 was first identified as a direct target gene suppressed by p53 (Jiang et al., 2015). SLC7A11 mediates cellular uptake of extracellular cystine in exchange for intracellular Glu. Interference of cystine absorption reduces downstream GSH biosynthesis and thus decreases GPX4's ability to antagonize ferroptosis. p53 also promotes ferroptosis through regulating other metabolic pathways. Spermidine/spermine N1-acetyltransferase 1 (SAT1) is a rate-limiting enzyme in polyamine catabolism. p53 can transactivate SAT1. SAT1 induction leads to lipid peroxidation and ferroptosis. This effect is due to arachidonate-15-lipoxygenase (ALOX15) upregulation after SAT1 induction. Therefore, the p53/SAT1/ALOX15 axis partially contributes to p53-mediated ferroptosis. p53 enhances the activity of SLC25A28 solute carrier family 25 member 28 (SLC25A28), a protein coding gene that causes abnormal accumulation of redox-active iron and promotes ferroptosis (Zhang et al., 2020). p53 can inhibit the serine synthesis pathway and transsulfuration pathway by suppressing phosphoglycerate dehydrogenase (PHGDH) and cystathionine  $\beta$ -synthase (CBS) respectively, limiting GSH production (Ou et al., 2015; Wang et al., 2019). In summary, p53 promotes ferroptosis through its multipotent roles in

regulating cellular metabolism, particularly lipid, iron, ROS, and amino acid metabolism (Liu and Gu, 2021). Mechanistically, dipeptidyl peptidase 4 (DPP4) promotes ferroptosis in p53-deficient cells by binding nicotinamide adenine dinucleotide phosphate (NADPH) oxidase 1 (NOX1) and boosting the production of ROS resulting in lipid peroxidation and ferroptosis (Gao et al., 2019). p21 is a target gene of p53 (Hong et al., 2010), and p21 induction redistributes the serine usage from nucleotide biogenesis to GSH synthesis, and GSH is an inhibitor of ROS and ferroptosis (Tarangelo et al., 2018; Mattocks et al., 2013). p53 modulates GPX4-dependent ferroptosis pathways as is shown in the Figure 3.

#### 5.3.2 P53 modulates GPX4-independent ferroptosis pathways

It is well established that ferroptosis is controlled by GPX4 primarily. Amazingly, Chu et al. observed that p53 modulates ferroptosis without apparent effects on GPX4. By screening the ALOX arachidonate lipoxygenase family to identify potential contributors to p53-mediated ferroptosis, founding that ALOX12 is a critical candidate (Chu et al., 2019). p53 promotes the activity of ALOX12 via inhibiting SLC7A11 which binds and sequesters ALOX12 from its substrate, polyunsaturated fatty acid (PUFA), including those esterified in membranes. When p53 downregulates SLC7A11, ALOX12 is released and subsequently oxidizes membrane PUFAs and initiates ferroptosis. Therefore, the p53/SLC7A11/ALOX12 axis is independent of the reduce in GSH and GPX4 activity, and is a mechanism underlying different than the p53/SLC7A11/GPX4 pathway. In a recent study, Yang et al. reported that another ALOX family member, ALOXE3, acts in a similar way to ALOX12 in generating ferroptosis (Yang et al., 2021). SLC7A11 also binds and sequesters ALOXE3 from its substrate. p53/SLC7A11/ALOXE3-mediated ferroptosis is independent of long-chain acyl-CoA synthetases 4 (ACSL4). In consideration of that ALOXE3 is downstream of ALOX12, the p53/SLC7A11/ALOX12 and p53/SLC7A11/ALOXE3 axes can both collaboratively and independently in modulating ferroptosis. Phospholipase A2 group VI (iPLA2 $\beta$ ) is a calcium-independent phospholipase that gaps acyl tails from the glycerol backbone of lipids and releases oxidized fatty acids, which can be further detoxified by the antioxidants in the cytoplasm (Malley et al., 2018). iPLA2 $\beta$ -mediated detoxification of peroxidated membrane lipids is adequate to inhibit p53/ALOX12-driven ferroptosis in a GPX4-independent pattern (Liu and Gu, 2022). P53 modulates GPX4-independent ferroptosis pathways as is shown in the Figure 4.

#### 5.3.3 p53 modulates ferroptosis in ICH

Kuang et al. observed ferroptosis characteristics in the cerebral cortex of rats with subarachnoid hemorrhage (SAH) after 24 h, and could be alleviated by Fer-1 treatment. Fer-1 could increase SLC7A11 and GPX4. Similarly, BBB impairment, brain

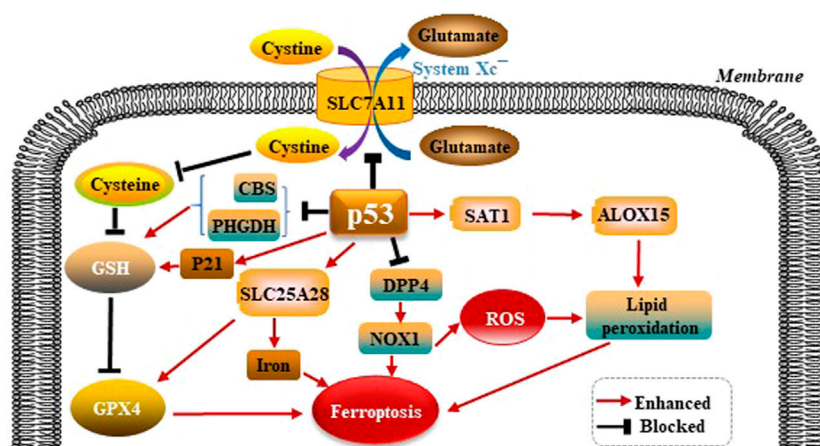


FIGURE 3

p53 modulates GPX4-dependent ferroptosis pathways. p53 suppresses the transcription of SLC7A11, which is a core subunit of the System Xc<sup>-</sup>. SLC7A11 mediates cellular uptake of extracellular cystine in exchange for intracellular Glu, reduces downstream GSH and GPX4 biosynthesis, thus leading to ferroptosis. p53 also promotes ferroptosis through regulating other metabolic pathways. p53 can upregulate ALOX15 via SAT1-mediated, leads to lipid peroxidation and ferroptosis. p53 enhances the activity of SLC25A28, causes abnormal accumulation of redox-active iron and promotes ferroptosis. p53 also can suppress PHGDH and CBS respectively, limiting GSH production. p53 inhibits DPP4 by binding NOX1, boosting the production of ROS, and resulting in lipid peroxidation and ferroptosis. p21 is a target gene of p53. p21 suppresses GSH synthesis, and promotes ferroptosis.

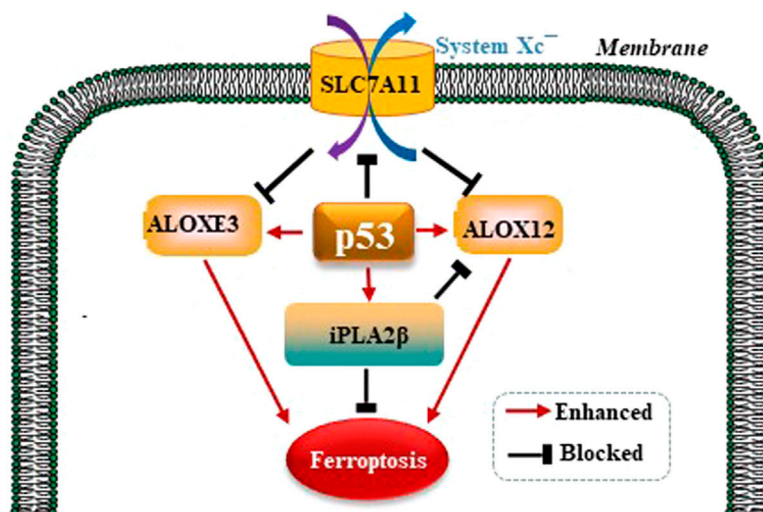


FIGURE 4

p53 modulates GPX4-independent ferroptosis pathways. p53/SLC7A11/ALOX12 and p53/SLC7A11/ALOX15 axes can both collaboratively and independently in modulating ferroptosis in a GPX4-independent manner. iPLA2β-mediated detoxification of peroxidized membrane lipids is adequate to inhibit p53/ALOX12-driven ferroptosis also in a GPX4-independent pattern.

edema, behavioral deficits and neuronal damage were relieved by inhibiting ferroptosis. Moreover, the p53 inhibitor Pifithrin-α could block cortical SAH-induced ferroptosis. These results indicated that ferroptosis aggravated SBI after SAH was partly dependent on p53, and inhibiting ferroptosis might be an

effective therapeutic target for SBI (Kuang et al., 2021). Zhang et al. used ICH rats model to explore the mechanism of Ubiquitin-specific protease 11(USP11) regulating neuroinflammation in ICH. It was showed in microglial cells that USP11 stabilized p53 by deubiquitination and p53 targeted

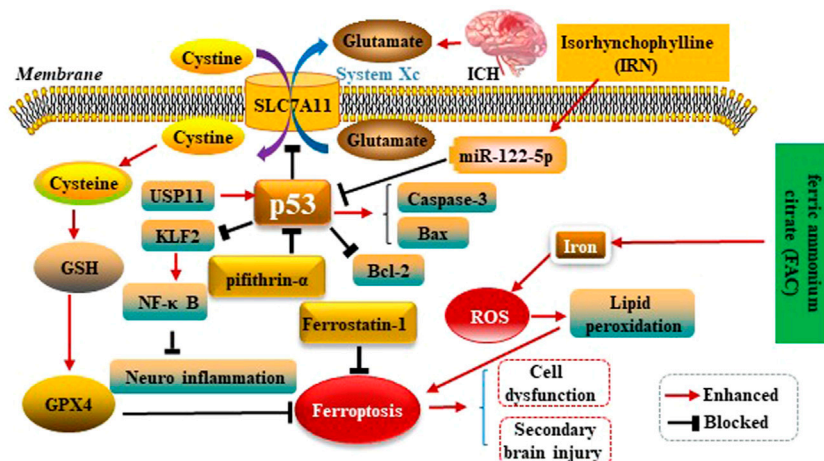


FIGURE 5

p53 modulates ferroptosis in ICH. p53 inhibits SLC7A11 resulting in dysfunction of the cystine/glutamate antiporter (System Xc<sup>-</sup>) after ICH, leading to decreased synthesis of glutathione (GSH) and activity of glutathione peroxidase 4 (GPX4). p53 could increase Caspase-3 as well as Bax expressions, and decrease Bcl-2 expression conversely. Therefore, p53 plays key roles in SBI caused by ICH. IRN suppressed the p53 expression to anti-ferroptosis via miR-122-5p/p53/SLC7A11 pathway. Ubiquitin-specific protease 11(USP11) stabilized p53 by deubiquitination and p53 targeted Krüppel like factor 2 (KLF2) promoter to repress KLF2 transcription, thereby activating the nuclear factor-kappa B (NF-κB) pathway to anti-ferroptosis. Ferric ammonium citrate (FAC) could be a source of iron to induce iron overload, thus leading to ferroptosis.

Krüppel like factor 2(KLF2) promoter to repress KLF2 transcription, thereby activating the nuclear factor-kappa B (NF-κB) pathway. Further, rescue experiments were conducted *in vivo* to make sure the function of USP11/p53/KLF2/NF-κB axis in ICH-induced inflammation, which confirmed that USP11 silencing inhibited the release of pro-inflammatory cytokines following ICH by downregulating p53, thus protecting against neurological deficit. (Zhang X et al., 2021). Xu et al. first reported p53 could increase apoptosis-associated protein cysteine aspartate protease-3 (Caspase-3) as well as Bcl-2 associated X protein (Bax) expressions, and decrease B-celllymphoma-2 (Bcl-2) expression conversely. Therefore, p53 plays key roles in SBI caused by ICH (Xu et al., 2018). Isorhynchophylline (IRN), a component of traditional Chinese herb *Uncaria rhynchophylla*, possesses strong antioxidant activity. A present study showed IRN exhibited neuroprotective effects *in vivo* and *in vitro* by inhibiting ferroptosis. In particular, IRN suppressed the p53 expression to promote the transcription of SLC7A11 by upregulating the miR-122-5p expression, thus exerting its anti-ferroptosis activity. The findings reveal that IRN protects neurocyte from ferric ammonium citrate (FAC)-induced ferroptosis via miR-122-5p/p53/SLC7A11 pathway, which may provide a potential therapeutic mechanism for ICH (Zhao et al., 2021). p53 modulates ferroptosis in ICH as is shown in the Figure 5.

In conclusion, how can p53 enhance or block ferroptosis are developing, and many problems remain unknown. Emerging research results have increasingly advanced our knowledge of

p53. p53 and ferroptosis fields need much more research to obtain more achievements.

## 6 Inhibition of neuronal ferroptosis after ICH

### 6.1 Ferroptosis inhibitor (Fer-1)

Fer-1 is a specific ferroptosis inhibitor. Dixon et al. showed that Fer-1 inhibited Hb-induced cell death in hippocampal slice culture, confirming that Fer-1 reduced iron ion-induced cell death and the release of lactate dehydrogenase (LDH) induced by Hb and ferrous ions. Additionally, the content of ROS in the cultured hippocampal slices in the experimental group with Fer-1 intervention was significantly lower than that in the control group (Dixon et al., 2012). Zhang et al. (Zhang et al., 2018) also confirmed that Fer-1 significantly reduced the levels of interleukin-1 beta (IL-1β) and tumor necrosis factor-alpha (TNF-α) in the serum and cerebrospinal fluid, which in turn alleviated the inflammatory response of rats after ICH, reduced albumin extravasation and BBB damage, and alleviated SBI after ICH. Generally, the *in vivo* and *in vitro* experiments have confirmed that the application of Fer-1 inhibits the occurrence of ferroptosis, thereby alleviating the SBI after ICH and providing a theoretical basis for further clinical application of Fer-1. Fer-1 is listed in Supplementary Table S1 which summarize the potential inhibition methods of ferroptosis following ICH.



## 6.2 Iron chelator (DFX, VK-28, DP and PIH)

The iron chelator DFX reduces brain edema, neurological deficit, and brain atrophy in rats after ICH (Okauchi et al., 2010). The sustained release of iron ions from the hematoma after ICH activates local microglia and causes secondary brain damage. DFX forms a chelating ferric amine with iron ions in the brain tissue around the hematoma to prevent iron ions from donating electrons to oxygen to form ROS and inhibits the hyperactivation of microglia (Li et al., 2017b; Dixon and Stockwell, 2014), which is the most important mechanism of neuronal ferroptosis. Another study showed that the application of DFX or VK-28 6 h after ICH in mice effectively reduced ROS synthesis by approximately 50%, thereby reducing neuronal cell death after ICH and improving secondary neuronal damage. Compared to DFX, the iron chelator VK-28 had a greater advantage of penetrating the intact BBB, while DFX failed to do so. Thus, VK-28 may act in the brain at a relatively low concentration, which is more suitable for clinical application (Li et al., 2017a). Generally, iron chelators further inhibit the occurrence of ferroptosis by forming chelating ferric amines with iron ions in the brain tissue around hematoma. VK-28 is more effective and safer than DFX in inhibiting ferroptosis. Additionally, a previous study showed that fat-soluble iron chelator, 2,2'-dipyridy (DP), reduced iron deposition around the hematoma and ROS synthesis, improving the neuronal function and reducing the neuronal death of the ICH mouse model (Wu H et al., 2012).

Pyridoxal isonicotinoyl hydrazine (PIH), a lipophilic iron-chelating agent, has been reported to reduce excess iron-induced cytotoxicity after ICH, which was associated with mitigation of inflammation and ferroptosis (Zhang H et al., 2021). Iron chelators (DFX, VK-28, DP and PIH) are listed in [Supplementary Table S1](#) which summarize the potential inhibition methods of ferroptosis following ICH.

## 6.3 DMT1 inhibitor (Ebselen)

DMT1 is involved in iron ionization in cells and is the only protein that transports iron ions into cells (Gao et al., 2015). After ICH, the expression of DMT1 is significantly increased, and ferric ions are reduced to ferrous ions under the action of DMT1. Ferrous ions induce excessive ROS and lipid peroxide production and are important factors causing neuronal ferroptosis (Xie et al., 2012). Pretreatment with Ebselen, a DMT1 inhibitor, significantly reduces the iron ion transport activity of DMT1 and suppresses ROS synthesis (Wang et al., 2016). A previous study from China showed that Ebselen further reduced neuronal ferroptosis after subarachnoid hemorrhage in rats by inhibiting DMT1 (Zhang et al., 2017). Hence, it is necessary to further strengthen the research on Ebselen in the context of ICH. Ebselen is listed in [Supplementary Table S1](#)

which summarize the potential inhibition methods of ferroptosis following ICH.

## 6.4 Flavanol compound (epicatechin)

Epicatechin (EC) is a flavanol compound present in natural plants (e.g., fruits, vegetables, and green tea). EC activates NF-E2-related factor (Nrf2) signaling to scavenge oxidants and free radicals. Existing reports have shown that the application of EC reduced the volume of brain damage and brain edema, improved neurological function and prognosis, and significantly reduced *IREB2* mRNA expression in the early stage of ICH in mice. *IREB2* is involved in encoding iron-ion regulators and inhibits neuronal ferroptosis by further regulating the intracellular iron-ion metabolism (Chang et al., 2014). After ICH, the neuronal cell viability of *IREB2*-knockout mice was higher than that of the mice in the *IREB2*-non-knockout group, showing a relatively strong resistance to Hb toxicity (Regan et al., 2008). Importantly, EC passes through the BBB and is convenient to use (Wu L et al., 2012). Hence, EC has promising clinical research value for inhibiting neuronal ferroptosis and SBI after ICH. EC is listed in [Supplementary Table S1](#) which summarize the potential inhibition methods of ferroptosis following ICH.

## 6.5 Combined application of n-acetyl-l-cys and prostaglandin E2

NAC is a Cys precursor approved by the Food and Drug Administration of the United States for clinical use for treating paracetamol-induced liver failure (Green et al., 2013). Much preclinical data are available to support the use of NAC in acute and chronic neurological and psychiatric disorders (Ansari et al., 2019; De Rosa et al., 2015; Monti et al., 2016). Cys, as a component of the cellular reducing agent GSH, is necessary to maintain cellular redox homeostasis; hence, Cys deficiency further depletes intracellular GSH, thereby increasing ROS synthesis and inducing ferroptosis. Under these circumstances, supplementation with another biosynthetic precursor of GSH, i.e., NAC, can effectively prevent cells from undergoing ferroptosis (Liu et al., 2015). A study by Zille et al. on ICH in male mice showed that NAC inhibited neuronal ferroptosis *in vitro* (Zille et al., 2017). Moreover, Karuppagounder et al. confirmed that NAC prevented heme oxygenase-1 induction by neutralizing toxic lipids produced by arachidonic acid-dependent 5-LOX 7 days after ICH, resulting in reduced neuronal cell death after ICH and improved functional recovery. The application of PGE2 combined with NAC may have a synergistic effect and reduce the NAC administration dosage required for the protection and functional recovery of brain tissue. Nevertheless, the application of NAC may cause serious adverse reactions. Thus, further research should focus on

controlling NAC dosage and its adverse reactions (Karuppagounder et al., 2018). Combined NAC and PGE2 are listed in **Supplementary Table S1** which summarize the potential inhibition methods of ferroptosis following ICH.

## 6.6 Supplementation with selenium

Ingold et al. reported that Se effectively inhibited GPX4-dependent ferroptosis and synergistically activated transcription factor activator protein 2C (TFAP2C) and transcription factor Sp1 (TSFP1), which further activated GPX4 transcription (Ingold et al., 2018). Another study confirmed that an intraventricular injection of sodium selenite promoted the expression of TSFP1 and GPX4 in neurons of the ICH mouse model, significantly reducing the neuronal death rate and promoting the recovery of nerve function in the mice (Alim et al., 2019). However, intraventricular injection requires the insertion of a catheter or needle into the brain tissue, which is invasive and carries the risk of developing intracranial infection and exacerbating the disease (Alim et al., 2019; Ding et al., 2015). Additionally, Se has a narrow therapeutic window and causes neurotoxicity if the dose is not titrated within an appropriate range (Fam et al., 2017). To overcome this problem, Alim et al. developed a Se-containing Cys polypeptide, Tat SelPep, to not only penetrate the BBB in a broad therapeutic window, but also to induce high GPX4 expression in various organs including the brain, heart, and liver. Se and its related new drugs provide additional potential treatment options for diseases related to GPX4 deficiency, including ICH. Se or Tat SelPep is listed in **Supplementary Table S1** which summarize the potential inhibition methods of ferroptosis following ICH.

## 7 Summary and outlook

ICH is the stroke subtype with the highest mortality rate of acute cerebrovascular disease, accounting for 15–20% of all strokes, with no effective treatments currently available (Feigin et al., 2009; Keep et al., 2012). Neuronal cell death after ICH includes necroptosis, pyroptosis, ferroptosis, autophagy, and parthanatos (Zhang et al., 2022). Ferroptosis may play an important role in the development of SBI after ICH. Recently, research on ferroptosis has become popular, and new mechanisms of ferroptosis and its potential clinical functions are still emerging, which are of great significance for exploring the therapeutic directions and intervention targets after ICH. This review article presents the definition of ferroptosis, the discovery of neuronal ferroptosis after ICH, the mechanism of ferroptosis, and the ways in which ferroptosis can be suppressed. Generally, the occurrence of ferroptosis is closely related to the content of intracellular iron ions, GSH, lipid peroxidases. Fer-1, iron-ion chelators, Ebselen, EC, NAC, PGE2, Se, and others,

which may suppress ferroptosis after ICH, providing a new direction for the clinical treatment of ICH. However, more in-depth studies are necessary to determine how to best apply the above substances in clinical practice and reduce their related adverse reactions.

## Author contributions

SR and YC drafted the manuscript. LW and GW revised the manuscript for content. All authors approved the final manuscript.

## Funding

This work was supported by grants from the Science and Technology Foundation of Guizhou Province (No. Qiankehe Foundation (2020) 1Y316), the Cultivation Fund of the Affiliated Hospital of Guizhou Medical University for National Natural Science Foundation of China (No. gyfynsfc (2020)-11), and the Doctoral Research Start-up Fund of the Affiliated Hospital of Guizhou Medical University (No. gyfysky-2021-30).

## Acknowledgments

We thank LetPub ([www.letpub.com](http://www.letpub.com)) for its linguistic assistance during the preparation of this manuscript.

## Conflict of interest

The authors declare that the research was conducted in the absence of any commercial or financial relationships that could be construed as a potential conflict of interest.

## Publisher's note

All claims expressed in this article are solely those of the authors and do not necessarily represent those of their affiliated organizations, or those of the publisher, the editors and the reviewers. Any product that may be evaluated in this article, or claim that may be made by its manufacturer, is not guaranteed or endorsed by the publisher.

## Supplementary material

The Supplementary Material for this article can be found online at: <https://www.frontiersin.org/articles/10.3389/fmolb.2022.966478/full#supplementary-material>

## References

- Abrams, R. P., Carroll, W. L., and Woerpel, K. A. (2016). Five-membered ring peroxide selectively initiates ferroptosis in cancer cells. *ACS Chem. Biol.* 11, 1305–1312. doi:10.1021/acschembio.5b00900
- Alim, I., Caulfield, J. T., Chen, Y., Swarup, V., Geschwind, D. H., Ivanova, E., et al. (2019). Selenium drives a transcriptional adaptive program to block ferroptosis and treat stroke. *Cell* 177, 1262–1279. doi:10.1016/j.cell.2019.03.032
- Andrews, N. C. (2000). Iron homeostasis: Insights from genetics and animal models. *Nat. Rev. Genet.* 1, 208–217. doi:10.1038/35042073
- Ansari, S. F., Memon, M., Brohi, N., and Tahir, A. (2019). N-Acetylcysteine in the management of acute exacerbation of chronic obstructive pulmonary disease. *Cureus* 11, e6073. doi:10.7759/cureus.6073
- Athiraman, U., and Zipfel, G. J. (2021). Role of anesthetics and their adjuvants in neurovascular protection in secondary brain injury after aneurysmal subarachnoid hemorrhage. *Int. J. Mol. Sci.* 22, 6550. doi:10.3390/ijms22126550
- Bai, Q., Sheng, Z., Liu, Y., Zhang, R., Yong, V. W., and Xue, M. (2020). Intracerebral haemorrhage: from clinical settings to animal models. *Stroke Vasc. Neurol.* 5, 388–395. doi:10.1136/svn-2020-000334
- Cao, J., and Dixon, S. J. (2016). Mechanisms of ferroptosis. *Cell. Mol. Life Sci.* 73, 2195–2209. doi:10.1007/s00018-016-2194-1
- Castillo, J., Dávalos, A., Álvarez-Sabín, J., Pumar, J. M., Leira, R., Silva, Y., et al. (2002). Molecular signatures of brain injury after intracerebral hemorrhage. *Neurology* 58, 624–629. doi:10.1212/WNL.58.4.624
- Chang, C., Cho, S., and Wang, J. (2014). (-)-Epicatechin protects hemorrhagic brain via synergistic Nrf2 pathways. *Ann. Clin. Transl. Neurol.* 1, 258–271. doi:10.1002/acn3.54
- Chen, B., Chen, Z., Liu, M., Gao, X., Cheng, Y., Wei, Y., et al. (2019). Inhibition of neuronal ferroptosis in the acute phase of intracerebral hemorrhage shows long-term cerebroprotective effects. *Brain Res. Bull.* 153, 122–132. doi:10.1016/j.brainresbull.2019.08.013
- Chu, B., Kon, N., Chen, D., Li, T., Liu, T., Jiang, L., et al. (2019). ALOX12 is required for p53-mediated tumour suppression through a distinct ferroptosis pathway. *Nat. Cell Biol.* 21, 579–591. doi:10.1038/s41556-019-0305-6
- De Rosa, S. C., Zaretsky, M. D., Dubs, J. G., Roederer, M., Green, A., Mitra, D., et al. (2015). N-acetylcysteine replenishes glutathione in HIV infection. *Eur. J. Clin. Invest.* 30, 915–929. doi:10.1046/j.1365-2362.2000.00736.x
- Ding, D., Przybylowski, C. J., Starke, R. M., Street, R. S., Tyree, A. E., Crowley, R. W., et al. (2015). A minimally invasive anterior skull base approach for evacuation of a basal ganglia hemorrhage. *J. Clin. Neurosci.* 22, 1816–1819. doi:10.1016/j.jocn.2015.03.052
- Dixon, S. J., Lemberg, K. M., Lamprecht, M. R., Skouta, R., Zaitsev, E. M., Gleason, C. E., et al. (2012). Ferroptosis: An iron-dependent form of nonapoptotic cell death. *Cell* 149, 1060–1072. doi:10.1016/j.cell.2012.03.042
- Dixon, S. J., and Stockwell, B. R. (2014). The role of iron and reactive oxygen species in cell death. *Nat. Chem. Biol.* 10, 9–17. doi:10.1038/nchembio.1416
- Fam, M. D., Hanley, D., Stadnik, A., Zeineddine, H. A., Girard, R., Jesselson, M., et al. (2017). Surgical performance in minimally invasive surgery plus recombinant tissue plasminogen activator for intracerebral hemorrhage evacuation phase III clinical trial. *Neurosurgery* 81, 860–866. doi:10.1093/neuros/nyx123
- Feigin, V. L., Lawes, C. M. M., Bennett, D. A., Barker-Collo, S. L., and Parag, V. (2009). Worldwide stroke incidence and early case fatality reported in 56 population-based studies: A systematic review. *Lancet. Neurol.* 8, 355–369. doi:10.1016/s1474-4422(09)70025-0
- Galluzzi, L., Vitale, I., Aaronson, S. A., Abrams, J. M., Adam, D., Agostinis, P., et al. (2018). Molecular mechanisms of cell death: Recommendations of the nomenclature committee on cell death 2018. *Cell Death Differ.* 25, 486–541. doi:10.1038/s41418-017-0012-4
- Gao, M., Monian, P., Pan, Q., Zhang, W., Xiang, J., and Jiang, X. (2016). Ferroptosis is an autophagic cell death process. *Cell Res.* 26, 1021–1032. doi:10.1038/cr.2016.95
- Gao, M., Monian, P., Quadri, N., Ramasamy, R., and Jiang, X. (2015). Glutaminolysis and trans-ferritin regulate ferroptosis. *Mol. Cell* 59, 298–308. doi:10.1016/j.molcel.2015.06.011
- Gao, M., Yi, J., Zhu, J., Minikes, A. M., Monian, P., Thompson, C. B., et al. (2019). Role of mitochondria in ferroptosis. *Mol. Cell* 73, 354–363. e3. doi:10.1016/j.molcel.2018.10.042
- Green, J. L., Heard, K. J., Reynolds, K. M., and Albert, D. (2013). Oral and intravenous acetylcysteine for treatment of acetaminophen toxicity: A systematic review and meta-analysis. *West. J. Emerg. Med.* 14, 218–226. doi:10.5811/westjem.2012.4.6885
- Gross, B. A., Jankowitz, B. T., and Friedlander, R. M. (2019). Cerebral intraparenchymal hemorrhage: A review. *JAMA* 321, 1295–1303. doi:10.1001/jama.2019.2413
- Guo, X., Xue, Q., Zhao, J., Yang, Y., Yu, Y., Liu, D., et al. (2020). Clinical diagnostic and therapeutic guidelines of stroke neurorestoration (2020 China Version). *J. Neurorestoratol.* 8, 241–251. doi:10.26599/JNR.2020.9040026
- Hong, L., Zhao, X., and Zhang, H. (2010). p53-mediated neuronal cell death in ischemic brain injury. *Neurosci. Bull.* 26, 232–240. doi:10.1007/s12264-010-1111-0
- Hou, W., Xie, Y., Song, X., Sun, X., Lotze, M. T., Zeh, H. J., 3rd, et al. (2016). Autophagy promotes ferroptosis by degradation of ferritin. *Autophagy* 12, 1425–1428. doi:10.1080/15548627.2016.1187366
- Ingold, I., Berndt, C., Schmitt, S., Doll, S., Poschmann, G., Buday, K., et al. (2018). Selenium utilization by GPX4 is required to prevent hydrogen peroxide-induced ferroptosis. *Cell* 172, 409–422. e21. doi:10.1016/j.cell.2017.11.048
- Jiang, L., Kon, N., Li, T., Wang, S., Su, T., Hibshoosh, H., et al. (2015). Ferroptosis as a p53-mediated activity during tumour suppression. *Nature* 520, 57–62. doi:10.1038/nature14344
- Karuppagounder, S. S., Alin, L., Chen, Y., Brand, D., Bourassa, M. W., Dietrich, K., et al. (2018). N-acetylcysteine targets 5 lipoxygenase-derived, toxic lipids and can synergize with prostaglandin E2 to inhibit ferroptosis and improve outcomes following hemorrhagic stroke in mice. *Ann. Neurol.* 84, 854–872. doi:10.1002/ana.25356
- Keep, R. F., Andjelkovic, A. V., Xiang, J., Stamatovic, S. M., Antonetti, D. A., Hua, Y., et al. (2018). Brain endothelial cell junctions after cerebral hemorrhage: Changes, mechanisms and therapeutic targets. *J. Cereb. Blood Flow. Metab.* 38, 1255–1275. doi:10.1177/0271678X18774666
- Keep, R. F., Hua, Y., and Xi, G. (2012). Intracerebral haemorrhage: Mechanisms of injury and therapeutic targets. *Lancet. Neurol.* 11, 720–731. doi:10.1016/S1474-4422(12)70104-7
- Kuang, H., Wang, T., Liu, L., Tang, C., Li, T., Liu, M., et al. (2021). Treatment of early brain injury after subarachnoid hemorrhage in the rat model by inhibiting p53-induced ferroptosis. *Neurosci. Lett.* 762, 136134. doi:10.1016/j.neulet.2021.136134
- Li, Q., Han, X., Lan, X., Gao, Y., Wan, J., Durham, F., et al. (2017a). Inhibition of neuronal ferroptosis protects Hemorrhagic brain. *JCI Insight* 2, e90777. doi:10.1172/jci.insight.90777
- Li, Q., Wan, J., Lan, X., Han, X., Wang, Z., and Wang, J. (2017b). Neuroprotection of brain-permeable iron chelator VK-28 against intracerebral hemorrhage in mice. *J. Cereb. Blood Flow. Metab.* 37, 3110–3123. doi:10.1177/0271678X17709186
- Li, Q., Weiland, A., Chen, X., Lan, X., Han, X., Durham, F., et al. (2018). Ultrastructural characteristics of neuronal death and white matter injury in mouse brain tissues after intracerebral hemorrhage: Coexistence of ferroptosis, autophagy, and necrosis. *Front. Neurol.* 9, 581. doi:10.3389/fneur.2018.00581
- Liu, Y., and Gu, W. (2022). p53 in ferroptosis regulation: the new weapon for the old guardian. *Cell Death Differ.* 29, 895–910. doi:10.1038/s41418-022-00943-y
- Liu, Y., and Gu, W. (2021). The complexity of p53-mediated metabolic regulation in tumor suppression. *Semin. Cancer Biol.* S1044-579X (21), 00060–00062. doi:10.1016/j.semcancer.2021.03.010
- Liu, Y., Wang, W., Li, Y., Xiao, Y., Cheng, J., and Jia, J. (2015). The 5-lipoxygenase inhibitor zileuton confers neuroprotection against glutamate oxidative damage by inhibiting ferroptosis. *Biol. Pharm. Bull.* 38, 1234–1239. doi:10.1248/bpb.b15-00048
- Magtanong, L., and Dixon, S. J. (2018). Ferroptosis and brain injury. *Dev. Neurosci.* 40, 382–395. doi:10.1159/000496922
- Malley, K. R., Koroleva, O., Miller, I., Sanishvili, R., Jenkins, C. M., Gross, R. W., et al. (2018). The structure of iPLA2 $\beta$  reveals dimeric active sites and suggests mechanisms of regulation and localization. *Nat. Commun.* 9, 765. doi:10.1038/s41467-018-03193-0
- Mattocks, O. D., Berkers, C. R., Mason, S. M., Zheng, L., Blyth, K., Gottlieb, E., et al. (2013). Serine starvation induces stress and p53-dependent metabolic remodelling in cancer cells. *Nature* 493, 542–546. doi:10.1038/nature11743
- Monti, D. A., George, Z., Daniel, K., Liang, T., Wintering, N. A., Cai, J., et al. (2016). N-acetyl cysteine may support dopamine neurons in Parkinson's disease: Preliminary clinical and cell line data. *PLoS One* 11, e0157602. doi:10.1371/journal.pone.0157602
- Okauchi, M., Hua, Y., Keep, R. F., Morgenstern, L. B., Schallert, T., Xi, G., et al. (2010). Deferoxamine treatment for intracerebral hemorrhage in aged rats: Therapeutic time window and optimal duration. *Stroke* 41, 375–382. doi:10.1161/STRO-KEAHA.109.569830

- Ou, Y., Wang, S., Jiang, L., Zheng, B., and Gu, W. (2015). p53 Protein-mediated regulation of phosphoglycerate dehydrogenase (PHGDH) is crucial for the apoptotic response upon serine starvation. *J. Biol. Chem.* 290, 457–466. doi:10.1074/jbc.M114.616359
- Peng, C., Fu, X., Wang, K., Chen, L., Luo, B., Huang, N., et al. (2022). Dauricine alleviated secondary brain injury after intracerebral hemorrhage by upregulating GPX4 expression and inhibiting ferroptosis of nerve cells. *Eur. J. Pharmacol.* 914, 174461. doi:10.1016/j.ejphar.2021.174461
- Regan, R. F., Chen, M., Li, Z., Zhang, X., Benveniste-Zarom, L., and Chen-Roetling, J. (2008). Neurons lacking iron regulatory protein-2 are highly resistant to the toxicity of hemoglobin. *Neurobiol. Dis.* 31, 242–249. doi:10.1016/j.nbd.2008.04.008
- Stockwell, B. R., Friedmann, A. J., Bayir, H., Bush, A. I., Conrad, M., Dixon, S. J., et al. (2017). Ferroptosis: A regulated cell death nexus linking metabolism, redox biology, and disease. *Cell* 171, 273–285. doi:10.1016/j.cell.2017.09.021
- Tarangelo, A., Magtanong, L., Biegling-Rolett, K. T., Li, Y., Ye, J., Attardi, L. D., et al. (2018). p53 suppresses metabolic stress-induced ferroptosis in cancer cells. *Cell Rep.* 22, 569–575. doi:10.1016/j.celrep.2017.12.077
- van Asch, C. J., Luitse, M. J., Rinkel, G. J., van der Tweel, I., Algra, A., and Klijn, C. J. (2010). Incidence, case fatality, and functional outcome of intracerebral haemorrhage over time, according to age, sex, and ethnic origin: A systematic review and meta-analysis. *Lancet. Neurol.* 9, 167–176. doi:10.1016/S1474-4422(09)70340-0
- Wang, G., Hu, W., Tang, Q., Wang, L., Sun, X., Chen, Y., et al. (2016). Effect comparison of both iron chelators on outcomes, iron deposit, and iron transporters after intracerebral hemorrhage in rats. *Mol. Neurobiol.* 53, 3576–3585. doi:10.1007/s12035-015-9302-3
- Wang, J. (2010). Preclinical and clinical research on inflammation after intracerebral hemorrhage. *Prog. Neurobiol.* 92, 463–477. doi:10.1016/j.pneurobio.2010.08.001
- Wang, M., Mao, C., Ouyang, L., Liu, Y., Lai, W., Liu, N., et al. (2019). Long noncoding RNA LINC00336 inhibits ferroptosis in lung cancer by functioning as a competing endogenous RNA. *Cell Death Differ.* 26, 2329–2343. doi:10.1038/s41418-019-0304-y
- Wang, X., Mori, T., Sumii, T., and Lo, E. H. (2002). Hemoglobin-induced cytotoxicity in rat cerebral cortical neurons: Caspase activation and oxidative stress. *Stroke* 33, 1882–1888. doi:10.1161/01.str.0000020121.41527.5d
- Wu, G., Sun, S., Sheng, F., Wang, L., and Wang, F. (2013). Perihematomal glutamate level is associated with the blood–brain barrier disruption in a rabbit model of intracerebral hemorrhage. *Springerplus* 2, 358. doi:10.1186/2193-1801-2-358
- Wu, H., Wu, T., Li, M., and Wang, J. (2012). Efficacy of the lipid-soluble iron chelator 2, 2'-dipyridyl against hemorrhagic brain injury. *Neurobiol. Dis.* 45, 388–394. doi:10.1016/j.nbd.2011.08.028
- Wu, L., Zhang, Q., Zhang, X., Lv, C., Li, J., Yuan, Y., et al. (2012). Pharmacokinetics and blood-brain barrier penetration of (+)-catechin and (-)-epicatechin in rats by microdialysis sampling coupled to high-performance liquid chromatography with chemiluminescence detection. *J. Agric. Food Chem.* 60, 9377–9383. doi:10.1021/jf301787f
- Xi, G., Keep, R. F., and Hoff, J. T. (2006). Mechanisms of brain injury after intracerebral haemorrhage. *Lancet. Neurol.* 5, 53–63. doi:10.1016/S1474-4422(05)70283-0
- Xi, G., Strahle, J., Hua, Y., and Keep, R. F. (2014). Progress in translational research on intra-cerebral hemorrhage: Is there an end in sight? *Prog. Neurobiol.* 115, 45–63. doi:10.1016/j.pneurobio.2013.09.007
- Xie, L., Zheng, W., Xin, N., Xie, J., Wang, T., and Wang, Z. (2012). Ebselen inhibits iron-induced tau phosphorylation by attenuating DMT1 up-regulation and cellular iron uptake. *Neurochem. Int.* 61, 334–340. doi:10.1016/j.neuint.2012.05.016
- Xu, W., Gao, L., Li, T., Zheng, J., and Shao, A. (2018). Mesencephalic astrocyte-derived neuro-trophic factor (MANF) protects against neuronal apoptosis via activation of akt/MDM2/p53 signaling pathway in a rat model of intracerebral hemorrhage. *Front. Mol. Neurosci.* 11, 176. doi:10.3389/fnmol.2018.00176
- Xue, M., and Yong, V. W. (2020). Neuroinflammation in intracerebral haemorrhage: Immunotherapies with potential for translation. *Lancet. Neurol.* 19, 1023–1032. doi:10.1016/S1474-4422(20)30364-1
- Yang, X., Liu, J., Wang, C., Cheng, K., Xu, H., Li, Q., et al. (2021). miR-18a promotes glioblastoma development by down-regulating ALOXE3-mediated ferroptotic and anti-migration activities. *Oncogenesis* 10, 15. doi:10.1038/s41389-021-00304-3
- Yao, Z., Bai, Q., and Wang, G. (2021). Mechanisms of oxidative stress and therapeutic targets following intracerebral hemorrhage. *Oxid. Med. Cell. Longev.* 2021, 8815441. doi:10.1155/2021/8815441
- Yu, H., Guo, P., Xie, X., Wang, Y., and Chen, G. (2017). Ferroptosis, a new form of cell death, and its relationships with tumorous diseases. *J. Cell. Mol. Med.* 21, 648–657. doi:10.1111/jcmm.13008
- Zecca, L., Youdim, M. B. H., Riederer, P., Connor, J. R., and Crichton, R. R. (2004). Iron, brain ageing and neurodegenerative disorders. *Nat. Rev. Neurosci.* 5, 863–873. doi:10.1038/nrn1537
- Zhang, H., Jiang, D., Che, X., Zhao, Q., Zhao, J., Xiang, J., et al. (2017). Ebselen relieves ferroptosis induced by divalent metal transporter 1 in rats with subarachnoid hemorrhage. *Acta. Acad. med.mil.ter.* 39, 1618–1624. (in Chinese). doi:10.16016/j.1000-5404.201701128
- Zhang, H., Wen, M., Chen, J., Yao, C., Lin, X., Lin, Z., et al. (2021). Pyridoxal isonicotinoyl hydrazone improves neurological recovery by attenuating ferroptosis and inflammation in cerebral hemorrhagic mice. *Biomed. Res. Int.* 2021, 9916328. doi:10.1155/2021/9916328
- Zhang, X., Liu, T., Xu, S., Gao, P., Dong, W., Liu, W., et al. (2021). A pro-inflammatory mediator USP11 enhances the stability of p53 and inhibits KLF2 in intracerebral hemorrhage. *Mol. Ther. Methods Clin. Dev.* 21, 681–692. doi:10.1016/j.omtm.2021.01.015
- Zhang, Y., Khan, S., Liu, Y., Zhang, R., Li, H., Wu, G., et al. (2022). Modes of brain cell death following intracerebral hemorrhage. *Front. Cell. Neurosci.* 16, 799753. doi:10.3389/fncel.2022.799753
- Zhang, Z., Guo, M., Shen, M., Kong, D., Zhang, F., Shao, J., et al. (2020). The BRD7-P53-SLC25A28 axis regulates ferroptosis in hepatic stellate cells. *Redox Biol.* 36, 101619. doi:10.1016/j.redox.2020.101619
- Zhang, Z., Wu, Y., Yuan, S., Zhang, P., Zhang, J., Li, H., et al. (2018). Glutathione peroxidase 4 participates in secondary brain injury through mediating ferroptosis in a rat model of intra-cerebral hemorrhage. *Brain Res.* 1701, 112–125. doi:10.1016/j.brainres.2018.09.012
- Zhao, H., Li, X., Yang, L., Zhang, L., Jiang, X., Gao, W., et al. (2021). Isorhynchophylline relieves ferroptosis-induced nerve damage after intracerebral hemorrhage via miR-122-5p/TP53/SLC7A11 pathway. *Neurochem. Res.* 46, 1981–1994. doi:10.1007/s11064-021-03320-2
- Zille, M., Karuppagounder, S. S., Chen, Y., Gough, P. J., Bertin, J., Finger, J., et al. (2017). Neuronal death after hemorrhagic stroke *in vitro* and *in vivo* shares features of ferroptosis and necroptosis. *Stroke* 48, 1033–1043. doi:10.1161/STROKEAHA.116.015609



## Glossary

<b>ATP</b> adenosine triphosphate	<b>5-LOX</b> 5-lipoxygenase
<b>ATP5G3</b> ATP synthase F0 complex subunit C3	<b>Nrf2</b> NF-E2-related factor
<b>ACSF2</b> acyl-CoA synthetase family member 2	<b>NAC</b> N-Acetyl-L-Cys
<b>ALOX15</b> arachidonate-15-lipoxygenase	<b>NOX1</b> NADPH oxidase 1
<b>BBB</b> blood-brain barrier	<b>NCCD</b> The Nomenclature Committee on Cell Death
<b>Bax</b> Bcl-2 associated X protein	<b>NADPH</b> nicotinamide adenine dinucleotide phosphate
<b>Bcl-2</b> B-cell lymphoma-2	<b>NF-<math>\kappa</math>B</b> nuclear factor-kappa B
<b>Caspase-3</b> Cysteine aspartate protease-3	<b>PTGS2</b> prostaglandin endoperoxide synthase 2
<b>CS</b> citrate synthase	<b>PGE2</b> prostaglandin E2
<b>COX-2</b> cyclooxygenase-2	<b>PIH</b> pyridoxal isonicotinoyl hydrazine
<b>Cys</b> cysteine	<b>PHGDH</b> phosphoglycerate dehydrogenase phosphoglycerate dehydrogenase
<b>CBS</b> cystathionine $\beta$ -synthase	<b>PUFA</b> polyunsaturated fatty acid
<b>DMT1</b> divalent metal transporter 1	<b>ROS</b> reactive oxygen species
<b>DFX</b> deferoxamine	<b>RPL8</b> ribosomal protein L8
<b>DP</b> 2,2'-dipyridy	<b>RCD</b> regulated cell death
<b>DPP4</b> dipeptidyl peptidase 4	<b>SBI</b> secondary brain injury
<b>EC</b> Epicatechin	<b>SLC7A11</b> solute carrier family 7 member 11
<b>ERK1/2</b> extracellular regulated protein kinases	<b>SLC25A28</b> olute carrier family 25 member 28
<b>Fer-1</b> ferrostatin-1	<b>System Xc-</b> cystine/glutamate antiporter
<b>FXDR</b> ferredoxin reductase	<b>SAT1</b> spermidine/spermine N1- acetyltransferase 1
<b>FAC</b> ferric ammonium citrate	<b>Se</b> selenium
<b>Glu</b> glutamate	<b>SAH</b> subarachnoid haemorrhage
<b>GSH</b> glutathione	<b>TF</b> transferrin
<b>GPX4</b> glutathione peroxidase 4	<b>TFR</b> transferrin receptor
<b>HB</b> hemoglobin	<b>TTC35</b> tetratricopeptide repeat domain 35
<b>IREB2</b> Iron response element binding protein 2	<b>TEM</b> transmission electron microscopy
<b>ICH</b> intracerebral haemorrhage	<b>TNF-<math>\alpha</math></b> tumor necrosis factor-alpha
<b>IL-1<math>\beta</math></b> interleukin-1 beta	<b>TSFP1</b> transcription factor Sp1
<b>iPLA2<math>\beta</math></b> Phospholipase A2 group VI	<b>TFAP2C</b> transcription factor activator protein 2C
<b>IRN</b> isorhynchophylline	<b>Tat SelPep</b> Se-containing Cys polypeptide
<b>KLF2</b> Krüppel like factor 2	<b>USP11</b> Ubiquitin-specific protease 11
<b>LDH</b> dehydrogenase	



## OPEN ACCESS

## EDITED BY

Yanqing Liu,  
Columbia University, United States

## REVIEWED BY

Di Shen,  
NovaRock Biotherapeutics Ltd.,  
United States  
Yixuan Guo,  
The University of Utah, United States  
Sachchida Nand Rai,  
University of Allahabad, India

## \*CORRESPONDENCE

Rong Tang,  
Rssilverbullet@126.com  
Dongqing Zhang,  
zhangdq2001@sina.com

<sup>†</sup>These authors share first authorship

## SPECIALTY SECTION

This article was submitted to Molecular  
Diagnostics and Therapeutics,  
a section of the journal  
Frontiers in Molecular Biosciences

RECEIVED 04 June 2022

ACCEPTED 04 July 2022

PUBLISHED 05 August 2022

## CITATION

He J, Liu D, Liu M, Tang R and Zhang D  
(2022), Characterizing the role of  
SLC3A2 in the molecular landscape and  
immune microenvironment across  
human tumors.  
*Front. Mol. Biosci.* 9:961410.  
doi: 10.3389/fmolb.2022.961410

## COPYRIGHT

© 2022 He, Liu, Liu, Tang and Zhang.  
This is an open-access article  
distributed under the terms of the  
[Creative Commons Attribution License  
\(CC BY\)](#). The use, distribution or  
reproduction in other forums is  
permitted, provided the original  
author(s) and the copyright owner(s) are  
credited and that the original  
publication in this journal is cited, in  
accordance with accepted academic  
practice. No use, distribution or  
reproduction is permitted which does  
not comply with these terms.

# Characterizing the role of SLC3A2 in the molecular landscape and immune microenvironment across human tumors

Jiajun He<sup>1†</sup>, Dong Liu<sup>2†</sup>, Mei Liu<sup>1</sup>, Rong Tang<sup>3\*</sup> and  
Dongqing Zhang<sup>1\*</sup>

<sup>1</sup>Minhang Hospital, Fudan University, Shanghai, China, <sup>2</sup>The First Affiliated Hospital of Soochow University, Suzhou, China, <sup>3</sup>Shanghai Medical College, Fudan University, Shanghai, China

**Background:** Inducing ferroptosis in human tumors has become a potential strategy to improve the prognosis of patients, even in those with chemotherapeutic resistance. The xCT complex is a major target for ferroptosis induction, constituted by SLC7A11 and SLC3A2. The role of SLC7A11 in cancer has been widely studied in recent years. However, related research studies for its partner SLC3A2 are still rare.

**Methods:** Bulk transcriptome, single-cell sequencing, and immunohistochemical staining were analyzed to explore the expression distribution of SLC3A2. Clinical outcomes were referred to uncover the relationship between SLC3A2 expression and patients' prognosis. Immune cell infiltration was estimated by multiple deconvolution algorithms. The effect of SLC3A2 on the proliferation and drug resistance of cancer cell lines was evaluated by DEPMAP.

**Results:** Upregulated SLC3A2 may have an adverse effect on the survival of multiple cancers such as lower-grade glioma and acute myeloid leukemia. SLC3A2 expression is indispensable for multiple cell lines' proliferation, especially for ESO51 (a cell line for esophageal cancer). In addition, SLC3A2 expression level was related to the remodeling of the immune microenvironment in cancers and some immune checkpoints such as PD-1 and PD-L1, which were potential therapeutic targets in many distinct cancers.

**Conclusion:** Our study systematically elucidated the role of SLC3A2 in the survival of cancer patients and the potential immunotherapeutic response. Few molecular mechanisms by which SLC3A2 regulates anti-tumor immunity have been clarified in the present study, which is the main limitation. Future research into the biological mechanism could further help with targeted treatment for cancer patients.

## KEYWORDS

SLC3A2, cancer, ferroptosis, immune microenvironment, pan-cancer

## Introduction

Cancer is a leading cause of death worldwide and afflicts millions of people (Bray et al., 2018). Multimodal therapies, such as chemotherapy and immunotherapy, have been applied to improve overall survival to some extent, which is the final goal of any cancer-directed treatment (Chen et al., 2017; Riley et al., 2019). Despite the significant advances in cancer treatments, the management of patients faced with chemotherapeutic resistance remains dramatically tough. Ferroptosis is a novel cell death mechanism characterized by excessively accumulated lipid peroxidation, that has been reported to be effective in curing tumors with chemotherapeutic resistance (Hassannia et al., 2019). Targeting ferroptosis is expected to benefit numerous patients with cancer.

Cystine/glutamate exchanger (xCT) is an important molecule mediating ferroptosis resistance in cancer cells, which is comprised of SLC7A11 and SLC3A2. While the role of SLC7A11 in cancer biology has been studied widely in recent years, few studies have focused on the effect of SLC3A2 during tumorigenesis and its association with patients' prognosis. Sun et al. have reported that overexpression of SLC3A2 on cell membrane contributed to the accelerated proliferation of oral squamous cancer cells, while knockdown of SLC3A2 could counteract tumor cell invasion and migration (Liang and Sun, 2021). Mechanistically, SLC3A2 promoted the aggressive phenotype by facilitating the expression of several mucin genes in gastric cancer (Wang et al., 2017). The intra-cellular level of SLC3A2 could be regulated by post-transcription modification like m6A-dependent degradation (Ma et al., 2021). Overall, these *in vitro* studies preliminarily suggest that SLC3A2 may be significant in tumor initiation and progression. Nonetheless, a comprehensive analysis of the role of SLC3A2 in cancers based on human genetic resources was still lacking, which may hinder further in-depth translational research.

Here, we conducted a pan-cancer level study to systematically analyze the role of SLC3A2 in patients with cancer. First, the association between SLC3A2 expression and patients' prognosis was analyzed. Then, the disturbance of molecules and microenvironment associated with the SLC3A2 level was revealed. Moreover, SLC3A2 expression and the intra-tumoral mutation landscape were also investigated in the present study.

## Materials and methods

### The source of genome sequencing, bulk and single-cell transcriptome, clinical information, and gene effect for cell-line proliferation

The bulk transcriptome data of 33 cancers, including adrenocortical carcinoma (ACC), bladder urothelial carcinoma

(BLCA), breast invasive carcinoma (BRCA), cholangiocarcinoma (CHOL), colon adenocarcinoma (COAD), cervical squamous cell carcinoma and endocervical adenocarcinoma (CSEA), lymphoid neoplasm diffuse large B cell lymphoma (DLBC), esophageal carcinoma (ESCA), glioblastoma multiforme (GBM), head and neck squamous cell carcinoma (HNSC), kidney chromophore (KICH), kidney renal clear cell carcinoma (KIRC), kidney renal papillary cell carcinoma (KIRP), acute myeloid leukemia (LAML), brain lower grade glioma (LGG), liver hepatocellular carcinoma (LIHC), lung squamous cell carcinoma (LUSC), lung adenocarcinoma (LUAD), mesothelioma (MESO), ovarian serous cystadenocarcinoma (OV), pheochromocytoma and paraganglioma (PCPG), pancreatic adenocarcinoma (PAAD), prostate adenocarcinoma (PRAD), rectum adenocarcinoma (READ), sarcoma (SARC), skin cutaneous melanoma (SKCM), testicular germ cell tumors (TGCT), thyroid carcinoma (THCA), stomach adenocarcinoma (STAD), thymoma (THYM), and uterine corpus endometrial carcinoma (UCEC), uterine carcinosarcoma (UCS), uveal melanoma (UVM), were all downloaded from The Cancer Genome Atlas (TCGA) database. Due to the lack of normal samples in TCGA, we also included the transcriptome data from the Genotype-Tissue Expression (GTEx) (<https://www.gtexportal.org/home/index.html>), which is a comprehensive public resource to study tissue-specific gene expression. In addition, the expression level of SLC3A2 is also evaluated in distinct cancer cell-lines through the Cancer Cell Line Encyclopedia (CCLE) (<https://portals.broadinstitute.org/ccle/data>). We selected fragments per kilobase million (FPKM) as the data format for the following calculation. The patients' clinical features containing overall survival (OS), disease-specific survival (DSS), disease-free interval (DFI), and progression-free interval (PFI) were also downloaded from the TCGA database and matched to transcriptome data.

## Differential expression analysis

A unified standardized pan-cancer dataset integrating the TCGA and GTEx databases were downloaded from UCSC (<https://xenabrowser.net/>). Wilcoxon Rank Sum and Signed Rank Tests were used to evaluate the statistical significance of the differential expression of SLC3A2 between tumor and normal tissue. Given all transcriptome data experienced a  $\log_2(x + 1)$  transformation, *p* values less than 0.05 of the Wilcoxon test was seen to be significant for differentially expressed SLC3A2.

## Immunohistochemical staining

The IHC data were collected from the human protein atlas (<https://www.proteinatlas.org/>). The antibody CAB010455 was chosen for further analysis.

## Prognostic relevance

A univariate Cox regression analysis was used to identify the relationship between SLC3A2 expression level and OS, DSS, DFI, and PFI across 33 cancers. Furthermore, hazard rate (HR) was applied to evaluate the magnitude of association with the “survival” package in R software (version: 3.1–8). Kaplan-Meier survival curve was depicted to visualize the associations with statistical significance. The R package “maxstat” (version:0.7-25) was used to determine the optimal cut-off value for the distinguishment of high- and low-risk groups.

## Immune infiltration estimation

The R package “Estimate” (version: 1.013) was used to estimate the proportion of immune and stromal cells in malignant tumor tissues from transcriptome data according to “immune score”. The estimate score equals to the sum of immune and stromal scores. Pearson correlation coefficient ( $r$ ) was applied to access the strength of the association between SLC3A2 expression level and immune/stromal/estimate scores. The expression level of 150 immunostimulatory genes and 60 immune check-point genes were extracted from the transcriptome data of each cancer. The co-expression association was also calculated using the Pearson correlation coefficient and visualized as a heatmap.

The infiltration of six common immune cells, including CD8<sup>+</sup> T cells, CD4<sup>+</sup> T cells, B cells, macrophages, neutrophils, and dendritic cells, was evaluated using the Tumor Immune Estimation Resource (TIMER) database. Other algorithms including CIBERSORT, QUANTISEQ, XCELL, EPIC, MCPOUNTER, and IPS were also performed according to respective guidance (Newman et al., 2015; Becht et al., 2016; Aran et al., 2017; Charoentong et al., 2017; Li et al., 2017; Racle et al., 2017).

To investigate the single-cell transcriptomic expression of SLC3A2, we applied the TISCH method to analyze the expression pattern of SLC3A2 in different types of cells in the tumor microenvironment (<http://tisch.comp-genomics.org/>).

To further study the relationship between SLC3A2 expression and T-cell dysfunction and immunotherapeutic response, we turned to the TIDE algorithm and performed relevant analysis (<http://tide.dfci.harvard.edu/>).

## Genome analysis

Tumor mutant burden (TMB) is defined as the total number of somatic gene coding errors, base substitutions, and gene insertions or deletions detected per million bases.

We calculated the TMB of each cancer sample based on the exome sequencing data from the TCGA database (VarScan2) using the maftools package. MSI, which stands for microsatellite instability, refers to the occurrence of new microsatellite alleles due to any change in the length of a microsatellite or due to the insertion or deletion of duplicate units in a tumor as compared to normal tissue. We referred to previous studies for summarized MSI data across distinct cancers. Neoantigens are encoded by mutated genes of tumor cells, which are mainly abnormal proteins produced by gene point mutation, deletion mutation, and gene fusion that are different from those expressed by normal cells. The function “inferHeterogeneity” was used to calculate mutant-allele tumor heterogeneity. The HRD, LOH, and ploidy for each sample were downloaded from a previous study (Thorsson et al., 2018). We analyzed the level of neoantigen through TCGA exome sequencing data.

## Methylation regulators and SLC3A2 expression

Transcriptome data of 44 methylation regulators were extracted from the RNA sequencing data of each cancer (m1A (10), m5C (13), m6A (21)). The correlation between these genes and SLC3A2 was evaluated by Pearson correlation.

## Cell culture and viability detection

HCT116 and Panc-01 cell lines were cultured in DMEM or RPMI-1640 (Gibco, United States) supplemented with 10% fetal bovine serum (Gibco, United States) and 1% antibiotics (penicillin 10,000 U/ml, streptomycin 100 mg/ml) (Solarbio, China). The cells were maintained at 37°C in a humidified atmosphere of 5% CO<sub>2</sub>.

Cells were seeded in 96-well plates in a 100 µL medium and treated with erastin (0–10 µM) (MCE, China). 10 µL Cell counting kit-8 solution (Bimake, China) was added to each well and incubated at 37°C for 2 h. The absorbance at 490 or 450 nm was measured on a spectrophotometer.

## RNA interfering and qRT-PCR

The sequence of siRNA used to interfere SLC3A2 was 5'-AGAUG AAGAUAGUCAAGAA-3' (forward), and 5'-UUCUUGACUAUCUUAUCU-3' (reverse). Lipofectamine 3000 (Thermo Fisher Scientific) was used for siRNA transfection according to the manufacturer's guidelines. Briefly, when the cells reached around 70% confluence at the time of transfection, the DNA-lipid complex was added to the cells using serum-free Opti-MEM medium. After



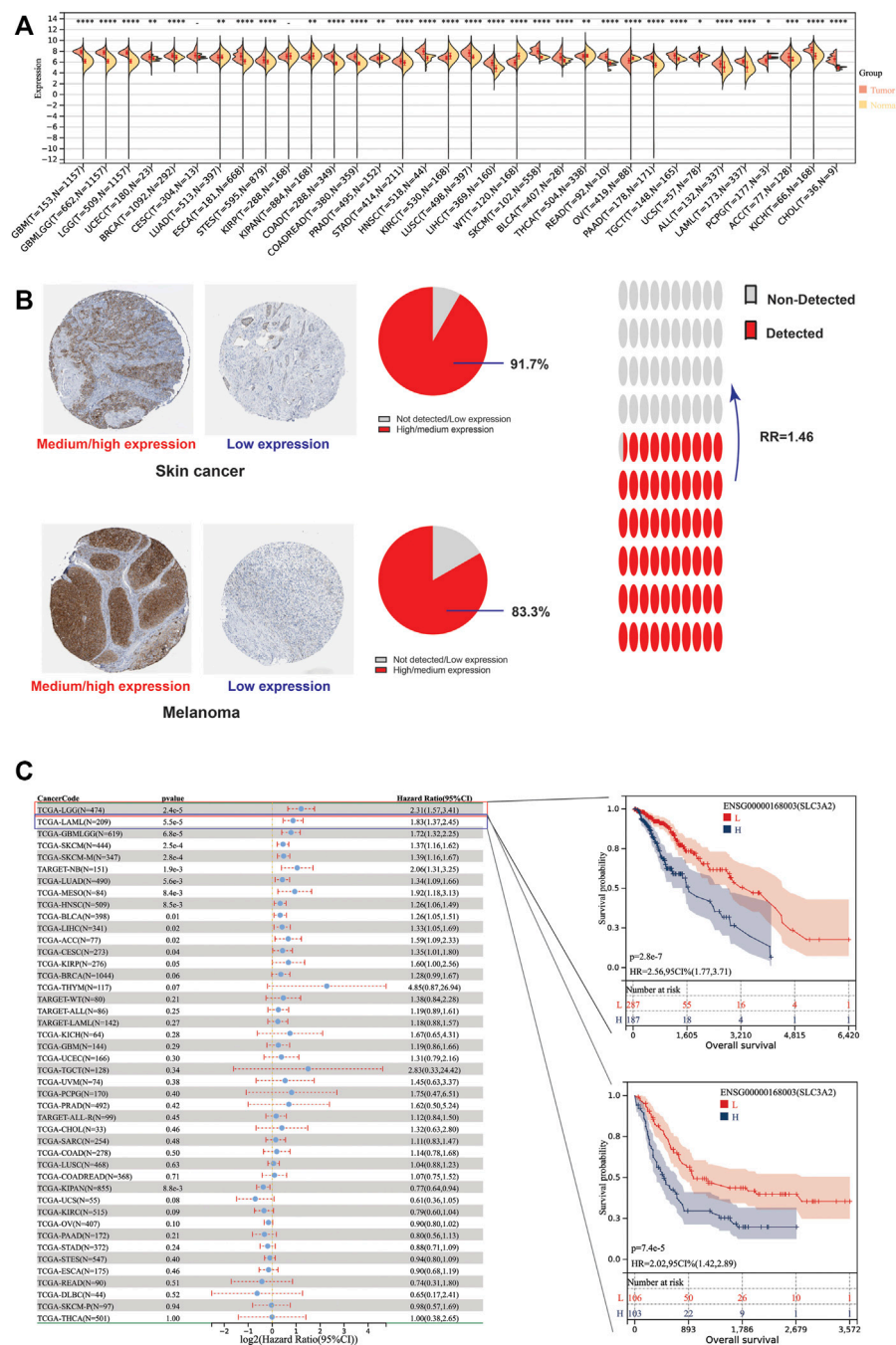


FIGURE 1

Differential expression level and prognostic implications of SLC3A2 among 34 cancers. (A) Differential expression of SLC3A2 between tumor and normal tissue. (B) Immunohistochemical staining showed higher SLC3A2 expression in cancers. (C) Correlation between SLC3A2 expression and OS of patients with cancer.

48–72 h of transfection, the efficiency of RNAi was detected by qRT-PCR.

The information of the primer sequences used was described as follows: ACCCTGTGTTTCAGCTACGG (forward) and GGTC TTCCTCTGGCCCTTC (reverse);  $\beta$ -actin: TTGTTACAGGAA

GTCCCTTGCC (forward) and ATGCTA TCACCTCCCCTGTGTG (reverse). Total RNA was extracted from HCT116 or panc-01 cells with TRIzol Reagent (Invitrogen, United States) in line with the manufacturer's instructions. The CT values were further analyzed to evaluate the knockdown efficiency of siRNA.

## Gene effect on cell-line proliferation and drug sensitivity

CRISPR-based screening of genes which is significant for cancer cell-lines' proliferation was analyzed using the DepMap database (<https://depmap.org/>). Meanwhile, we also evaluated the correlation between SLC3A2 expression and drug sensitivity using the Sanger GDSC2 database.

## Results

### The differential distribution of SLC3A2 expression in bulk and single-cell transcriptome analysis

Due to the lack of normal samples in the TCGA cohort, we first integrated tumor samples in TCGA and normal tissues in the GTEx database, which made it more reliable to explore the differential expression of SLC3A2. The results showed SLC3A2 is upregulated in 67.6% (23/34) cancers, such as LGG, GBM, and UCEC (Figure 1A). In addition, we analyzed the protein level of SLC3A2 in tumor slices using immunohistochemical staining. For some cancers, SLC3A2 showed increased expression in cancer regions compared with normal tissues. Notably, 91.7% of SKCM showed upregulated SLC3A2 expression and 16.7% melanoma did not express SLC3A2 or showed a low expression level (Figure 1B). Overall, the ratio between high/medium expression and low expression/not detected was 1.46, which revealed that SLC3A2 may play a pivotal role in tumorigenesis.

Pan-cancer single cell analysis revealed that SLC3A2 was most abundant in malignant cells (Supplementary Figure S1A), for example in HNSC and SKCM. However, SLC3A2 was also enriched in immune cells as in glioma, which suggested that SLC3A2 may be involved in some molecular function in immune cells. In detail, SLC3A2 showed a high abundance in mononuclear macrophages and AC-like malignant cells (Supplementary Figure S1B). However, SLC3A2 was also expressed highly in fibroblasts and T cells in BRCA and NSCLC, respectively (Supplementary Figures S1C,D).

### The association between intra-tumoral SLC3A2 expression level and patient prognosis

To explore whether SLC3A2 exerted an effect on the survival interval of patients with cancer, we correlated SLC3A2 expression with patients' OS, DSS, and DFI. Samples with a follow-up time less than 30 days were excluded from the analysis. Among the cancer types analyzed, SLC3A2 was

associated with prognosis in 15 cancers, where in 93.3% (14/15) of the cases, SLC3A2 over expression was correlated with poor OS (Figure 1C). Similarly, SLC3A2 correlated with shorter DSS in 9 cancers, while only in KIRC it was associated with prolonged DSS. Notably, SLC3A2 was simultaneously related to poor OS, DSS, and DFI in ACC (Supplementary Figures S2A,B). In addition, SLC3A2 expressed the highest level in the 4<sup>th</sup> grade of HNSC, which means SLC3A2 may play an important role in terminal HNSC (Supplementary Figures S3A). Likewise, for patients with LIHC, SLC3A2 had the highest expression level in the T4 stage (Figure 2A). When it comes to N stage, we found that SLC3A2 had the highest expression in N3 stage in LIHC, STAD, STES, and THYM (Figure 2B). In metastatic HNSC, SLC3A2 had higher expression compared with those that did not disseminate (Figure 2C). For stage IV UVM, SLC3A2 expressed the highest level relatively to other stages (Figure 2D). SLC3A2 also increased in the elderly patients with KIRP, KIRC, and KIPAN (Supplementary Figures S3B). These results suggest that SLC3A2 expression may be related to patients' post-operative survival. Aberrant methylation modification either in DNA or RNA contributes to the malignant behavior of cancer cells. We also found that SLC3A2 expression was widely associated with essential regulators for various methylation modifications (m6A, m5C, and m1A) (Supplementary Figures S4A). SLC3A2 was negatively associated with the expression level of an eraser (FTO), but significantly correlated with higher expression of METTL3 and some m6A readers, which suggests SLC3A2 may be involved with enhanced m6A modification in KIPAN (Supplementary Figures S4B–E).

Given both malignant phenotype of cancer cell and tumor microenvironment could affect the clinical outcomes, we further investigated the potential role of SLC3A2 in these aspects.

### SLC3A2 is indispensable for the proliferation in multiple cancers

Given that SLC3A2 is associated with patients' prognoses in multiple cancer types, we questioned whether SLC3A2 directly affects cell proliferation ability. We analyzed the CRISPR-based experimental data using DepMap and found that SLC3A2 could affect cell proliferation in the majority of tumor cell-lines (Figures 3A,B). Approximately 95% cell-lines decreased proliferative phenotypes after SLC3A2 was knocked out. Further analysis showed cell-lines derived from metastasis loci were more dependent on SLC3A2 (Figure 3C). Meanwhile, compared with other locations, cell-lines derived from the digestive system manifested more dependence on SLC3A2 expression (Figure 3D). 5-fluorouracil was a classic chemotherapy drug that was widely applied in post-operative adjuvant treatment. Interestingly, the SLC3A2 gene effect was mildly correlated

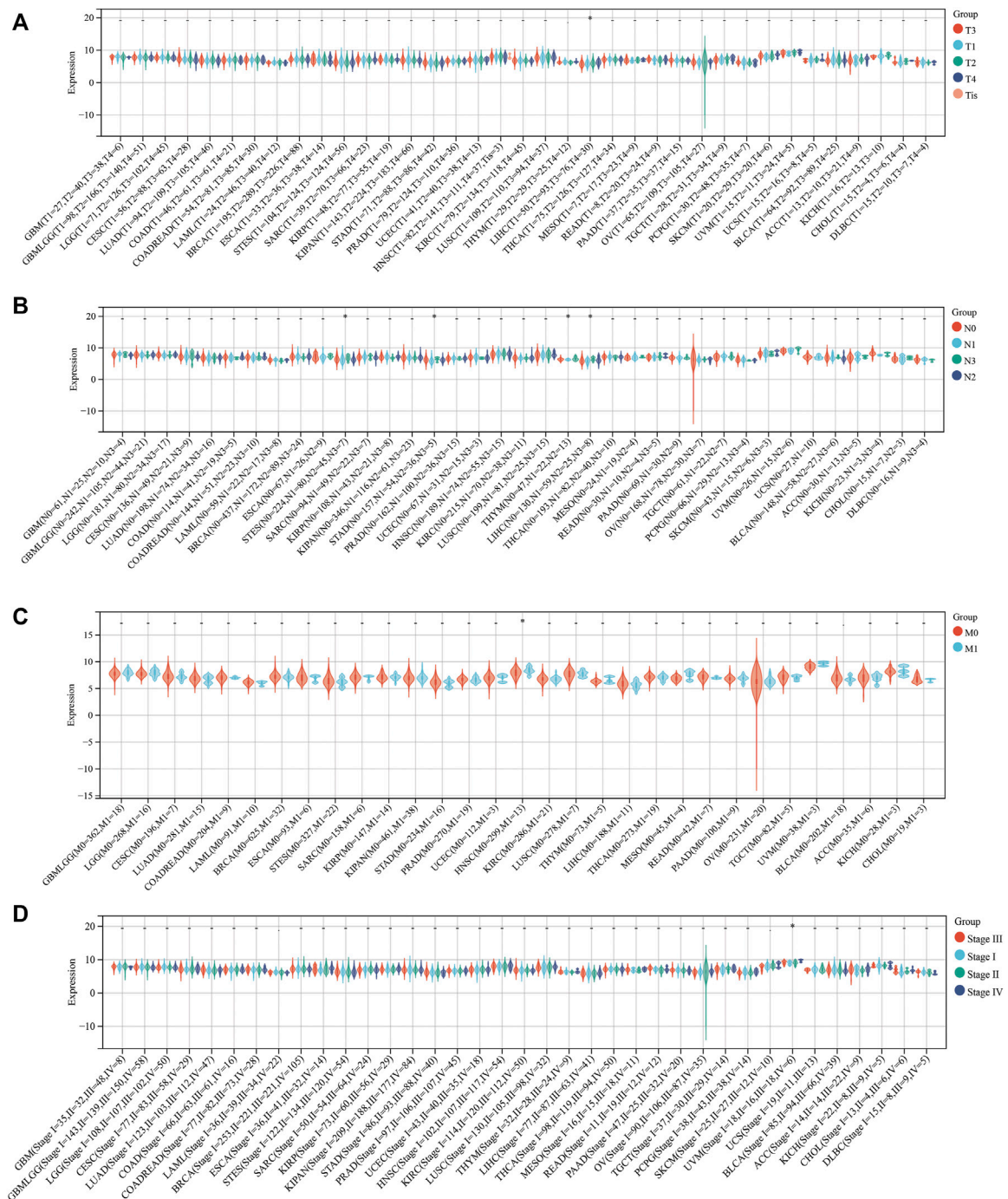


FIGURE 2

Relationship between the expression of SLC3A2 and patients' clinical parameters. (A) T stage. (B) N stage. (C) M stage. (D) Stage.

with 5-fluorouracil resistance, which indicated that the dependence on SLC3A2 was increased in 5-fluorouracil-resistant tumors (Figure 3E). We performed *in vitro* experiments to validate that SLC3A2 knockdown could improve the sensitivity to ferroptosis in a colorectal cancer cell-line and a pancreatic cancer cell-line (Figures 3F,G).

## The association between SLC3A2 expression level and tumor microenvironment remodeling

Recently, ferroptosis has been recently reported as a potential immunogenic cell death mechanism. In this

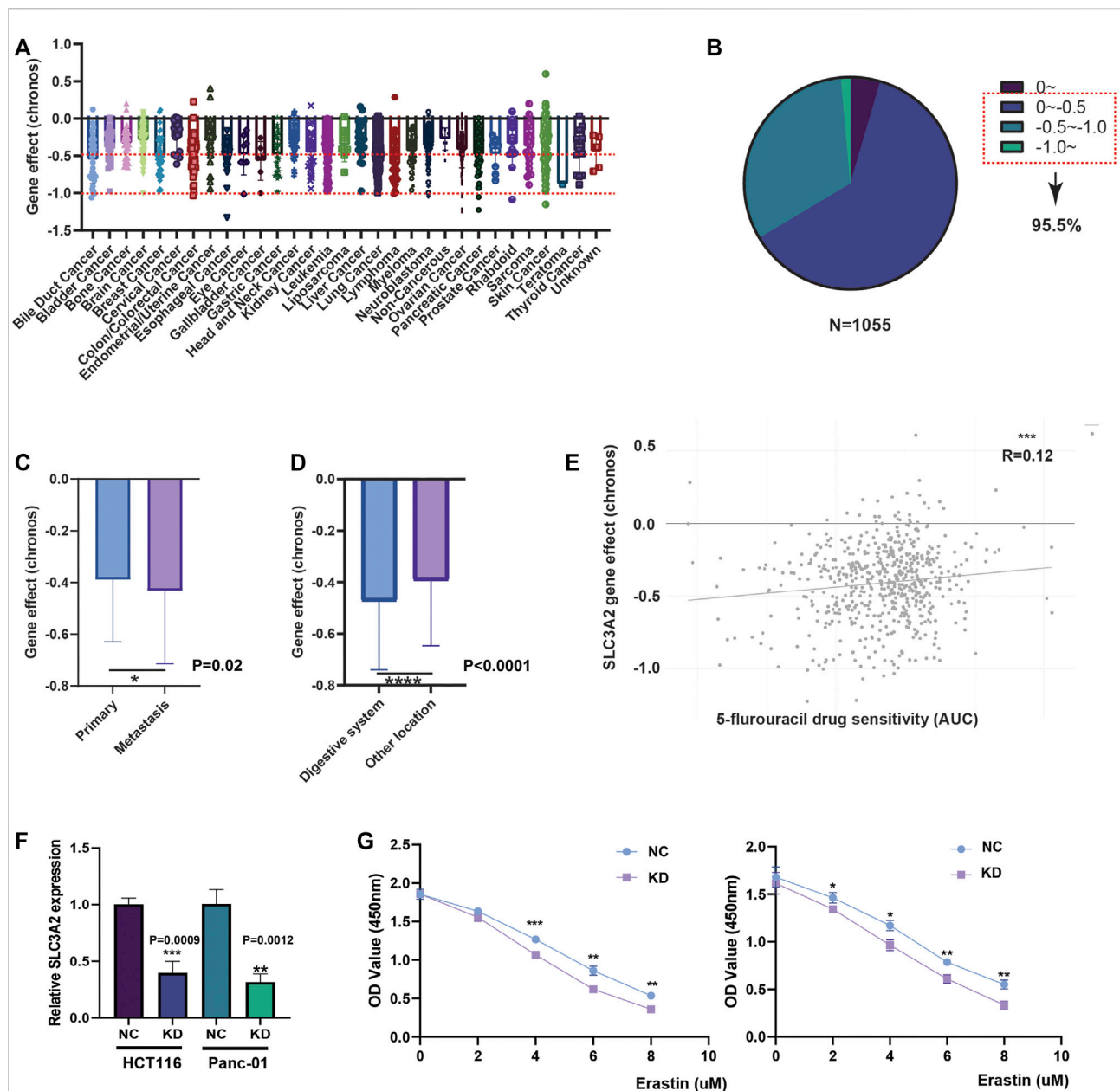


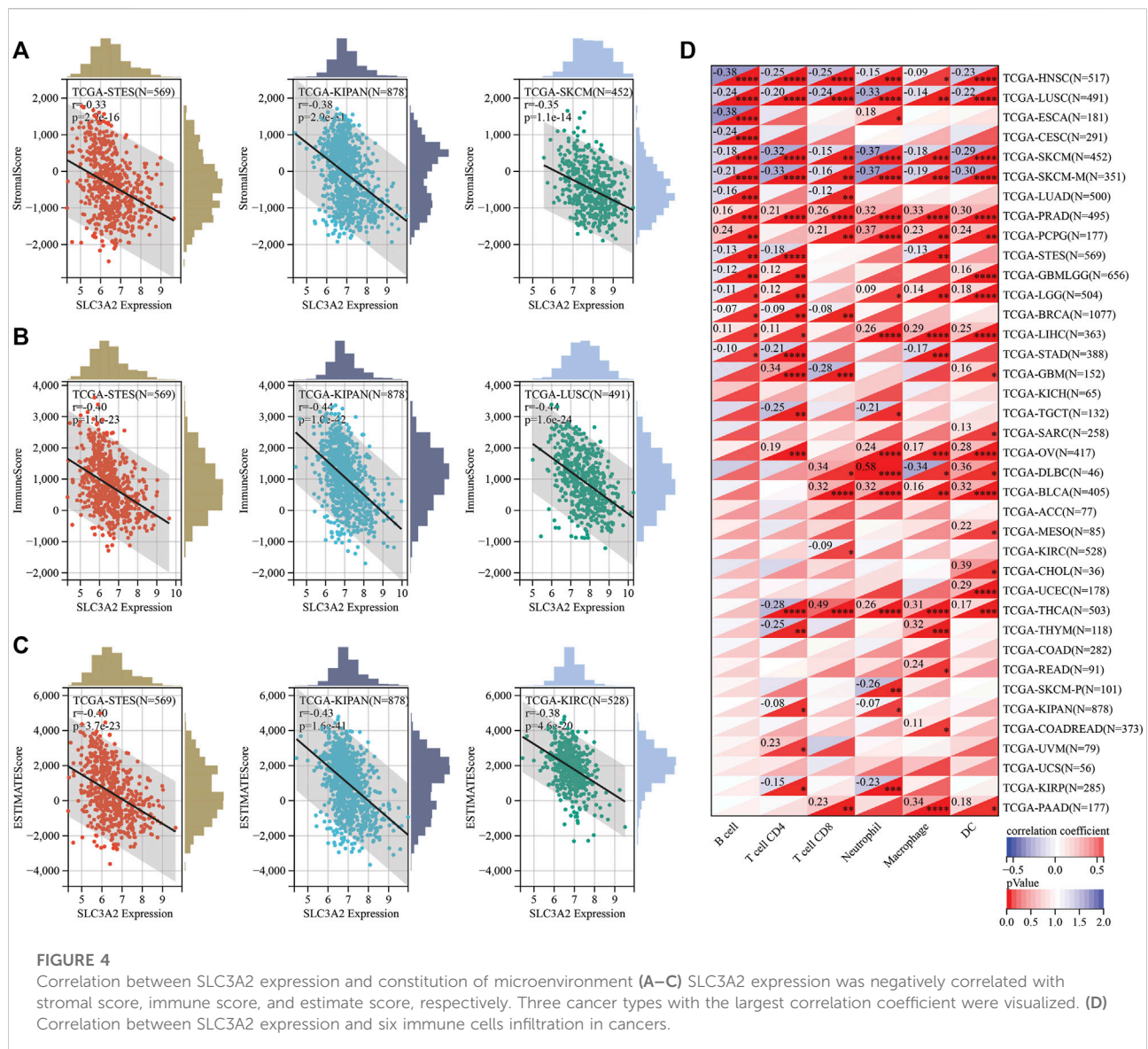
FIGURE 3

Effect of SLC3A2 on cell-proliferation and drug sensitivity in tumor cell-lines. (A) Gene effect of SLC3A2 in all cell-lines. (B) Stratification and proportion of cell-lines with different gene effect. (C) Metastatic cell-lines depends more on SLC3A2 expression to sustain rapid proliferation. (D) Digestive cell-lines depends more on SLC3A2 expression to sustain rapid proliferation. (E) SLC3A2 gene effect was mildly correlated with 5-FU sensitivity. (F) RNAi efficiency of SLC3A2 knockdown. (G) SLC3A2 knockdown improved sensitivity to ferroptosis in both HCT116 and Panc-01 cell-lines.

context, SLC3A2 expression level may be associated with the remodeling of microenvironment in cancers. We analyzed the correlation between SLC3A2 and stromal, immune, and estimation scores for every cancer. Notably, SLC3A2 was negatively associated with these microenvironment parameters in multiple cancers, which suggested that SLC3A2 might be a culprit for the formation of “cold”

tumors (Figures 4A–C). Furthermore, we evaluated the association between SLC3A2 and immune cell infiltration using different algorithms. In HNSC, LUSC, and SKCM, SLC3A2 was negatively associated with all kinds of infiltrated immune cells. On the contrary, SLC3A2 was positively correlated with immune infiltrates in PRAD and PCPG, which suggested that SLC3A2 may play distinct roles

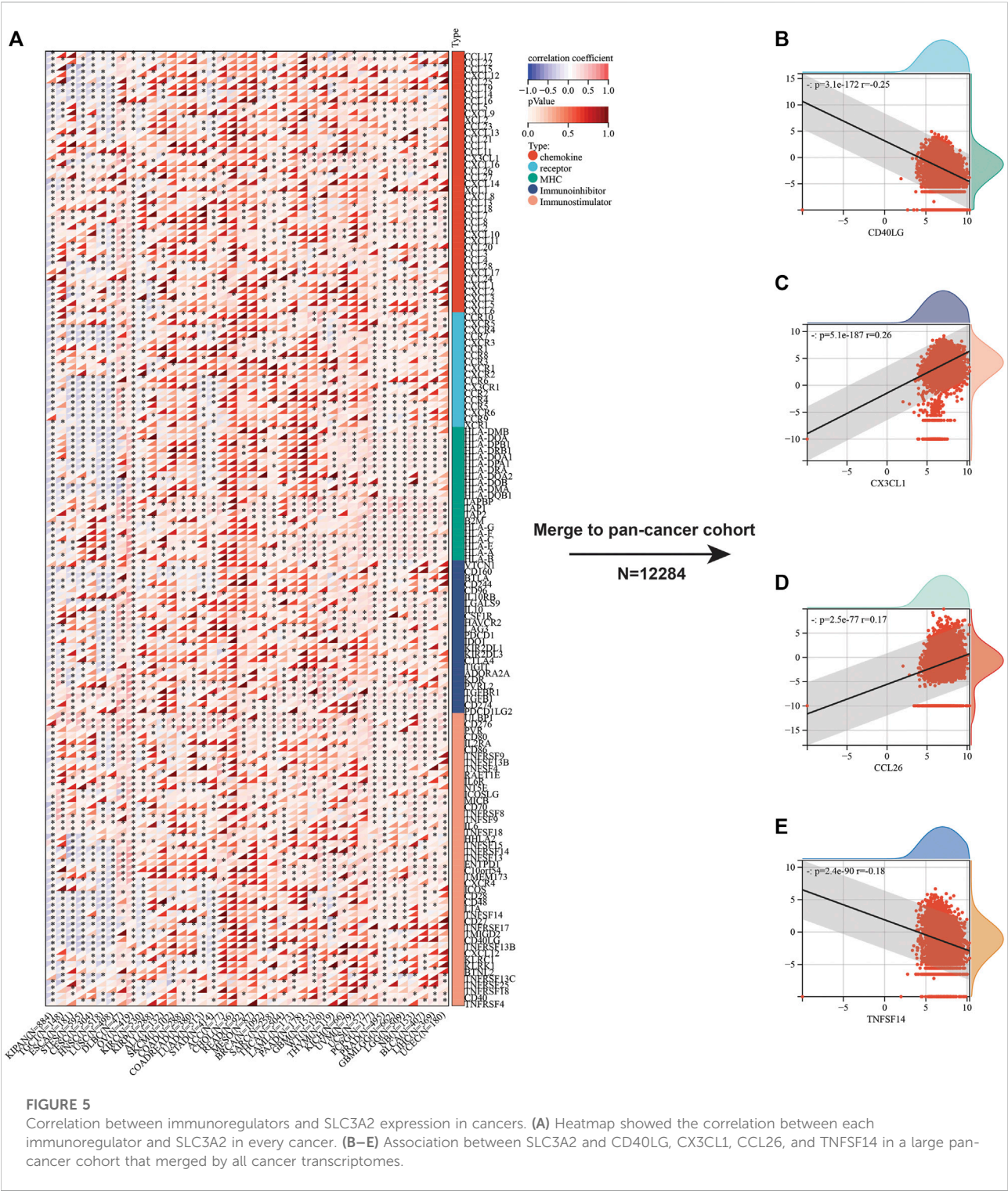




in different cancer types in terms of immune cell recruitment (Figure 4D). Notably, SLC3A2 may have different correlation among distinct immune cells. For example, SLC3A2 was positively correlated with more infiltration of CD4<sup>+</sup>T cells and dendritic cells. However, it was negatively associated with CD8<sup>+</sup> T cell infiltration in GBM (Supplementary Figures S5A–C). It was validated using both the Xcell and quantiseq algorithms to show the negative correlation between CD8<sup>+</sup> T cells and SLC3A2 expression (Supplementary Figures S5D). Moreover, we also found that SLC3A2 was negatively associated with the M1 signature, which was also an essential player in anti-tumor immunity (Supplementary Figures S5D). In this case, despite sufficient co-stimulatory factors and antigen-presentation in the microenvironment, anti-tumor immunity failed because of decrease in CD8<sup>+</sup>

T cells as the weapon to kill cancer cells. Cancer associated fibroblast (CAF) was also regarded as an important factor mediating the immune evasion in tumors. Interestingly, SLC3A2 was stringently associated with infiltrated CAFs in DLBC ( $r = 0.41$ ,  $p < 0.01$ ), suggesting that SLC3A2 could be a factor for fibrosis in DLBC microenvironment (Supplementary Figures S5A,B). In addition, SLC3A2 predicted decreased CD8<sup>+</sup> T cells and cytotoxic lymphocytes. However, it was related to more abundant neutrophils in KIRC (Supplementary Figures S5B), which implied an immunosuppressive role of SLC3A2 in these patients.

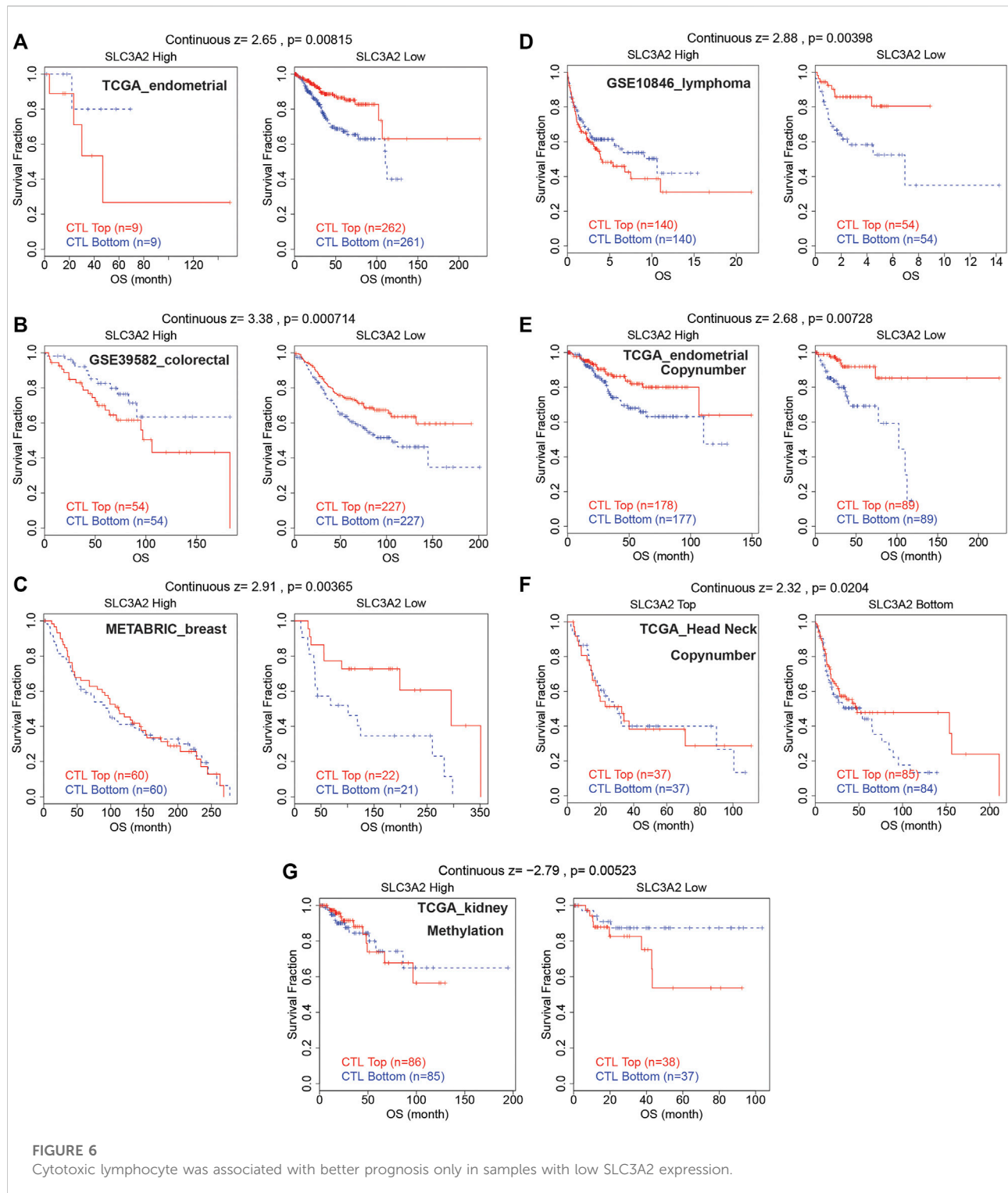
Beyond immune cell infiltrates, we also focused on the relation between immunoregulatory molecules and SLC3A2 expression. Initially, we analyzed the relationship



between 150 immunoregulatory factors and SLC3A2 in each cancer type (Figure 5A). These factors comprised of five categories, including 41 chemokines, 18 receptors, 21 MHC, 24 immunoinhibitors, and 36 immunostimulators. In most cancers, as classical immunostimulators, CD40LG and

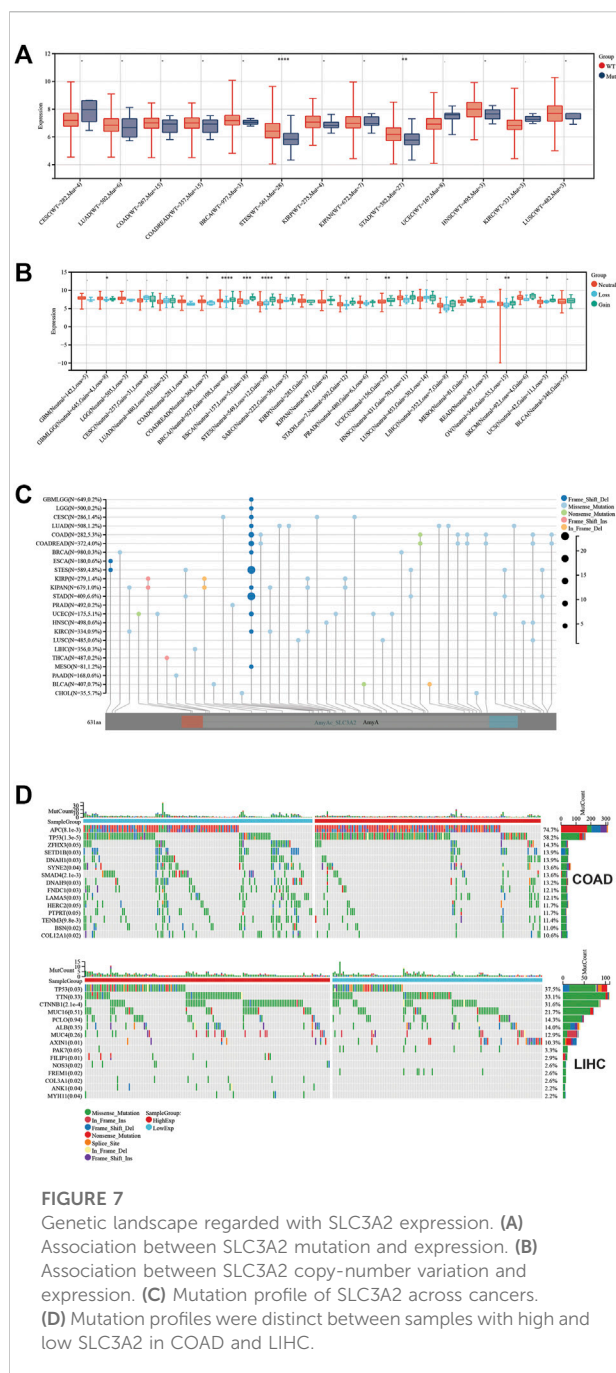
TNFSF14 were negatively associated with SLC3A2. On the contrary, SLC3A2 was positively correlated with CX3CL1, which was a metastasis-related chemokine ligand. Similarly, CCL26 also showed a moderate correlation with higher SLC3A2 expression across cancer types, which has been





reported to be a key element in tumor invasion and chemoresistance. These results were validated in a merged pan-cancer cohort (Figures 5B–E). Then, we analyzed the correlation between SLC3A2 expression and 60 immune check-point genes (Supplementary Figure S6A), of which

24 were stimulatory, like ICOS and CD28, while the other 36 genes were inhibitory for anti-tumor immunity, such as PD1 and PDL1 (CD274). The results demonstrated that SLC3A2 was significantly associated with PDL1 overexpression in most cancers, even in the merged



cohort ( $r = 0.21$ ,  $p < 0.0001$ ). Similarly, SLC3A2 expression was correlated with elevated VEGFB and CD276, which were notorious targets mediating immune evasion. By contrast, in the merged pan-cancer cohort, SLC3A2 expression was significantly correlated with lower levels of GZMA and INFγ, which were cytotoxic molecules that matter in anti-tumor responses (Supplementary Figures S6B–F). These findings pointed SLC3A2 as an immunosuppressive factor from a pan-cancer vision.

## The role of SLC3A2 in T-cell dysfunction and potential responses to immunotherapy

The abovementioned findings suggested that SLC3A2 might be associated with alterations in the immune microenvironment. Then, we further explored whether SLC3A2 was associated with T cell dysfunction and immunotherapeutic efficacy. Using the TIDE algorithm, we found that SLC3A2 overexpression was associated with obvious T cell dysfunction. In detail, in independent cohorts for endometrial cancer, lymphoma, colorectal cancer, and breast cancer, cytotoxic T lymphocyte was associated with better overall survival only in samples with lower SLC3A2 expression (Figures 6A–D). Similarly, the copy number amplification of SLC3A2 also predicted T cell dysfunction in two independent cohorts (Figures 6E,F). By contrast, excessive methylation of SLC3A2, which reflected suppressed transcription, was associated with poor T cell function in a kidney cancer cohort (Figure 6G).

## The association between SLC3A2 and genetic parameters

To explore the relevance between SLC3A2 and the genetic landscape in each cancer, we first investigated whether the SLC3A2 mutation itself could affect its mRNA expression. Intriguingly, only in STES and STAD, SLC3A2 mutations corresponded to reduced transcriptomic levels, which was possibly attributed to the low mutated rate in other types of cancer (Figure 7A). The copy number variation well reflected the transcriptomic level of SLC3A2 in most cancer types. In brief, higher expression of SLC3A2 was expected to appear in samples with gain variation compared to loss variation or wild type. It indicated that SLC3A2 was not influenced dramatically by post-transcriptomic regulation (Figure 7B). The total mutation rate of SLC3A2 ranged from 0.7 to 6.6%, in which missense variation was the most common variation of SLC3A2 across cancers (Figures 7C,D).

Furthermore, we calculated the mutant-allele tumor heterogeneity (MATH), landscape of microsatellite instability (MSI), tumor mutation burden (TMB), neoantigen, purity, ploidy, homologous recombination deficiency (HRD), and loss of heterozygosity (LOH) for each sample across cancers. Then, correlation analysis was performed in terms of these parameters and SLC3A2 expression (Figures 8A–H). Notably, SLC3A2 was significantly associated with higher TMB, MSI, and neoantigen in THYM, which meant more events of immunosurveillance would appear in this type of cancer. In addition, SLC3A2 was positively associated with HRD in multiple cancers, especially in ACC. In this context, SLC3A2 targeting could be considered when applying PARP inhibitors. Overall, the landscape of gene



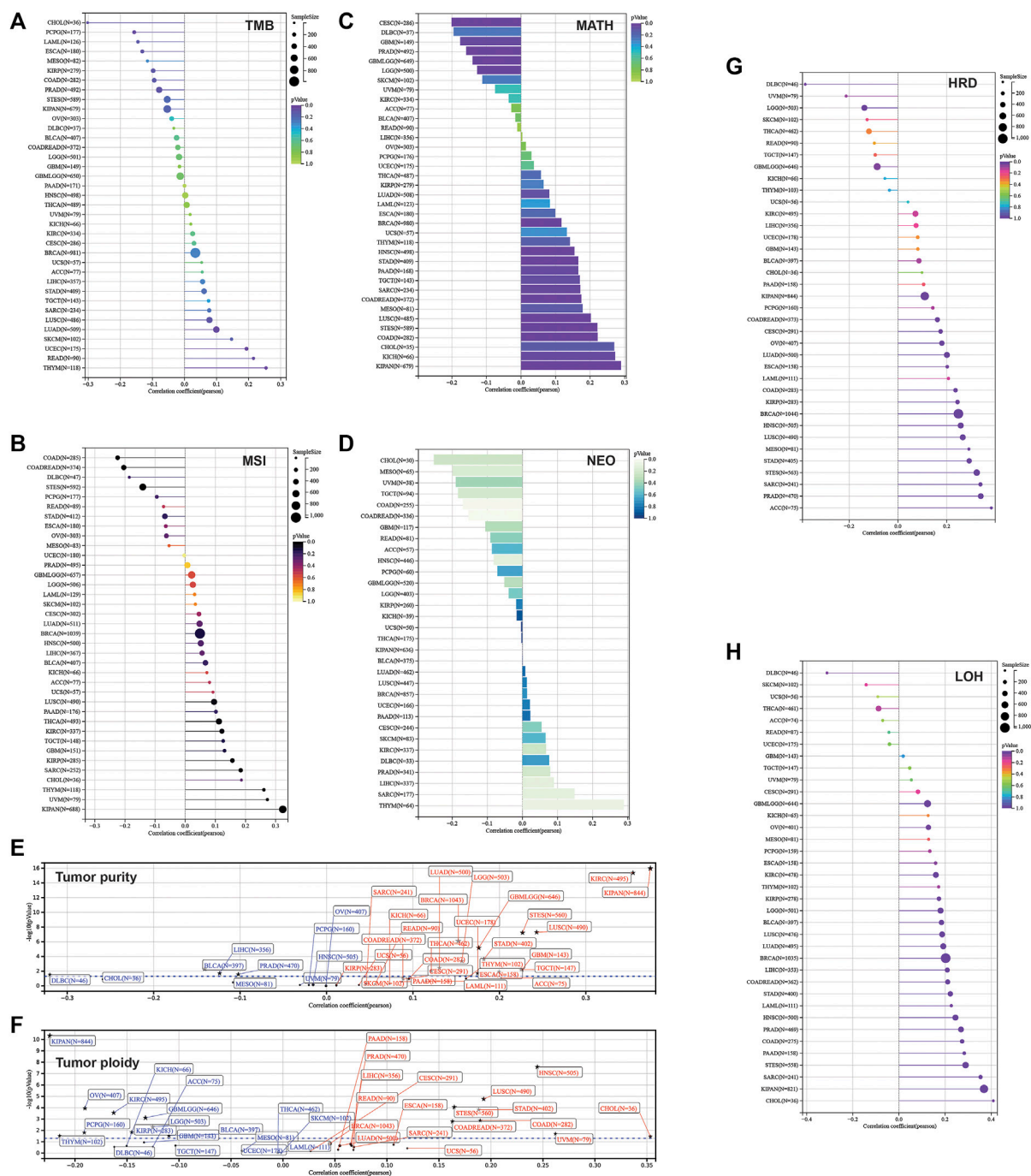


**FIGURE 8**  
Correlation between parameters of genetic instability and SLC3A2 expression. (A) TMB. (B) MSI. (C) MATH. (D) NEOANTIGEN. (E) Tumor purity. (F) Tumor ploidy. (G) HRD. (H) LOH.

mutation in samples with high and low SLC3A2 expression was different, which may be explained by distinct drive genes for each cancer. However, some genes had a higher mutation rate in SLC3A2-high samples. For example, TP53 mutation appeared more in samples with higher SLC3A2 expression in COAD and LIHC.

## Discussion

The xCT complex is a major target for ferroptosis inducers and is elevated in cancer cells. Ferroptosis inducer “erastin” targets the xCT complex to trigger ferroptosis *in vitro* and *in vivo* (Zhao et al., 2020; Koppula et al., 2021; Liu et al., 2022; Wiernicki et al., 2022).

This complex is comprised of two units, which are SLC7A11 and SLC3A2 (Koppula et al., 2021). Among them, numerous studies have uncovered the role of SLC7A11 in cancer development. However, less attention has been paid to the latter.

Only few studies initially revealed that SLC3A2 contributes to initiation and development in carcinogenesis. It is necessary to explore the function of SLC3A2 in patients' tumor samples. Therefore, it is imperative to explore the expression and clinical relevance of SLC3A2 in different cancer types. In this study, we found that SLC3A2 predicted worse prognosis in multiple cancers, which was consistent with previous studies. For example, we revealed a worse prognosis associated with SLC3A2 in LUAD and LIHC, which was consistent with some previous reports (Shin et al., 2018; Li et al., 2019; Ma et al., 2021). While Zhu et al. revealed that SLC3A2 was upregulated in human osteosarcoma and promoted disease progression *via* the PI3K/Akt signaling pathway (Zhu et al., 2017), our study did not find SLC3A2 could reflect a better survival interval for patients with SARC. To validate the effect of SLC3A2 on cell proliferation, we analyzed the results from a large-scaled CRISPR-based screening in DepMap and found that the growth of around 95% cell-lines was partially dependent on SLC3A2 (Liu et al., 2022; Wiernicki et al., 2022), which supported the essential role of SLC3A2 in fueling cancer cell proliferation. Indeed, SLC3A2 was involved in the transportation of cysteine and glutamate, which maintained the resistance to ferroptosis. It was assumed that tumor cells faced a lot of pressure from ferroptosis induction *in vivo*, such as chemotherapy (Zhang et al., 2020), radiotherapy, and immune cell killing (Lang et al., 2019). In this context, it is plausible for SLC3A2 to maintain the proliferative phenotype of cancer cells *in vivo*. However, it could not explain why SLC3A2 could promote the proliferation of cell-lines *in vitro*, which implied another mechanism by which SLC3A2 activated the proliferative ability beyond ferroptosis pathways.

Immunotherapy has recently emerged as a very effective new therapy and has become a powerful clinical strategy for treating cancer (Lu and Robbins, 2016; Marabelle et al., 2017; Riley et al., 2019). The number of immunotherapy drug approvals has been increasing, with numerous treatments in clinical and preclinical development (Ngwa et al., 2018; Liu et al., 2019). Despite this success, immunotherapy only works in a subset of cancers, and only a fraction of patients with cancer respond to immunotherapy. Therefore, it is important to consider the role of SLC3A2 in immunotherapy in distinct cancer types. Few studies have researched the role of SLC3A2 in anti-tumor immunity. Ikeda et al. reported that SLC3A2 was essential for the functioning of regulator T cells, although it did not yield from cancer research, but it could be estimated that SLC3A2 expressed on Tregs could facilitate its immunosuppressive function and promote immune evasion (Ikeda et al., 2017). In addition, SLC3A2 could also serve as a target for CAR-T therapy given its overexpression on the membrane of cancer cells (Pellizzari et al., 2021).

Here, we conducted a bioinformatic study at pan-cancer level to systematically explore whether the intra-tumoral expression of SLC3A2 is associated with patients' survival and its potential value in immunotherapy. This study has several strengths to declare. First, SLC3A2 is a promising anti-cancer target in the future. Our study was the first to comprehensively analyze the role of SLC3A2 at pan-cancer level, which provided many valuable and integrated advice for the selection of appropriate cancer types. Second, analysis based on human samples made our results more credible compared with previous studies that explored the SLC3A2 function at cell or animal levels. Third, we explored the association between SLC3A2 expression and potential response to immunotherapy at a pan-cancer level, which has an important reference value in judging patients' condition, estimating prognosis, directing treatment, and evaluating the curative effect. Certainly, this study has some limitations. On one hand, the present study lacks pathological samples for validation. However, as a pan-cancer study, it is difficult to validate the findings using tumor tissues of all origins. The dataset we used in the present study was well-designed and widely tested, which supported the reliability of our study. On the other hand, whether SLC3A2 expressed in tumors affects the tumor microenvironment was clarified in the present study. Future studies are encouraged to explore the underlying mechanism by which SLC3A2 affects anti-tumor immunity.

In conclusion, this pan-cancer level bioinformatic study systematically elucidated the role of intra-tumoral expression of SLC3A2 in the survival of cancer patients and potential immunotherapeutic response. Our results helped in identifying a new biomarker for detection and monitoring of cancer. Future research into the biological mechanism could further help with targeted treatment for cancer patients.

## Data availability statement

The original contributions presented in the study are included in the article/Supplementary Material; further inquiries can be directed to the corresponding authors.

## Author contributions

JH wrote the manuscript. JH, DL, and ML performed bioinformatic analysis. RT and DZ designed the study.

## Funding

This work was supported the Open Fund of the Minhang District Health Committee Scientific Research Project Plan, Shanghai, China (2021MW67).

## Conflict of interest

The authors declare that the research was conducted in the absence of any commercial or financial relationships that could be construed as a potential conflict of interest.

## Publisher's note

All claims expressed in this article are solely those of the authors and do not necessarily represent those of their affiliated

organizations, or those of the publisher, the editors, and the reviewers. Any product that may be evaluated in this article, or claim that may be made by its manufacturer, is not guaranteed or endorsed by the publisher.

## Supplementary material

The Supplementary Material for this article can be found online at: <https://www.frontiersin.org/articles/10.3389/fmolb.2022.961410/full#supplementary-material>

## References

- Aran, D., Hu, Z., and Butte, A. J. (2017). xCell: digitally portraying the tissue cellular heterogeneity landscape. *Genome Biol.* 18, 220. doi:10.1186/s13059-017-1349-1
- Becht, E., Giraldo, N. A., Lacroix, L., Buttard, B., Elarouci, N., Petitprez, F., et al. (2016). Estimating the population abundance of tissue-infiltrating immune and stromal cell populations using gene expression. *Genome Biol.* 17, 218. doi:10.1186/s13059-016-1070-5
- Bray, F., Ferlay, J., Soerjomataram, I., Siegel, R. L., Torre, L. A., Jemal, A., et al. (2018). Global cancer statistics 2018: GLOBOCAN estimates of incidence and mortality worldwide for 36 cancers in 185 countries. *Ca. Cancer J. Clin.* 68, 394–424. doi:10.3322/caac.21492
- Charoentong, P., Finotello, F., Angelova, M., Mayer, C., Efremova, M., Rieder, D., et al. (2017). Pan-cancer immunogenomic analyses reveal genotype-immunophenotype relationships and predictors of response to checkpoint blockade. *Cell Rep.* 18, 248–262. doi:10.1016/j.celrep.2016.12.019
- Chen, Y. L., Chang, M. C., and Cheng, W. F. (2017). Metronomic chemotherapy and immunotherapy in cancer treatment. *Cancer Lett.* 400, 282–292. doi:10.1016/j.canlet.2017.01.040
- Hassannia, B., Vandenabeele, P., and Vanden Berghe, T. (2019). Targeting ferroptosis to iron out cancer. *Cancer Cell.* 35, 830–849. doi:10.1016/j.ccell.2019.04.002
- Ikeda, K., Kinoshita, M., Kayama, H., Nagamori, S., Kongpracha, P., Umemoto, E., et al. (2017). Slc3a2 mediates branched-chain amino-acid-dependent maintenance of regulatory T cells. *Cell Rep.* 21, 1824–1838. doi:10.1016/j.celrep.2017.10.082
- Koppula, P., Zhuang, L., and Gan, B. (2021). Cystine transporter slc7a11/xCT in cancer: Ferroptosis, nutrient dependency, and cancer therapy. *Protein Cell.* 12, 599–620. doi:10.1007/s13238-020-00789-5
- Lang, X., Green, M. D., Wang, W., Yu, J., Choi, J. E., Jiang, L., et al. (2019). Radiotherapy and immunotherapy promote tumoral lipid oxidation and ferroptosis via synergistic repression of SLC7A11. *Cancer Discov.* 9, 1673–1685. doi:10.1158/2159-8290.CD-19-0338
- Li, T., Fan, J., Wang, B., Traugh, N., Chen, Q., Liu, J. S., et al. (2017). TIMER: A web server for comprehensive analysis of tumor-infiltrating immune cells. *Cancer Res.* 77, e108–e110. doi:10.1158/0008-5472.CAN-17-0307
- Li, W., Dong, X., He, C., Tan, G., Li, Z., Zhai, B., et al. (2019). LncRNA SNHG1 contributes to sorafenib resistance by activating the Akt pathway and is positively regulated by miR-21 in hepatocellular carcinoma cells. *J. Exp. Clin. Cancer Res.* 38, 183. doi:10.1186/s13046-019-1177-0
- Liang, J., and Sun, Z. (2021). Overexpression of membranous SLC3A2 regulates the proliferation of oral squamous cancer cells and affects the prognosis of oral cancer patients. *J. Oral Pathol. Med.* 50, 371–377. doi:10.1111/jop.13132
- Liu, M., Song, W., and Huang, L. (2019). Drug delivery systems targeting tumor-associated fibroblasts for cancer immunotherapy. *Cancer Lett.* 448, 31–39. doi:10.1016/j.canlet.2019.01.032
- Liu, X., Chen, C., Han, D., Zhou, W., Cui, Y., Tang, X., et al. (2022). SLC7A11/GPX4 inactivation-mediated ferroptosis contributes to the pathogenesis of triptolide-induced cardiotoxicity. *Oxidative Med. Cell. Longev.* 2022, 1–16. doi:10.1155/2022/3192607
- Lu, Y. C., and Robbins, P. F. (2016). Cancer immunotherapy targeting neoantigens. *Semin. Immunol.* 28, 22–27. doi:10.1016/j.smim.2015.11.002
- Ma, L., Zhang, X., Yu, K., Xu, X., Chen, T., Shi, Y., et al. (2021). Targeting SLC3A2 subunit of system X(C)(-) is essential for m(6)A reader YTHDC2 to be an endogenous ferroptosis inducer in lung adenocarcinoma. *Free Radic. Biol. Med.* 168, 25–43. doi:10.1016/j.freeradbiomed.2021.03.023
- Marabelle, A., Tselikas, L., de Baere, T., and Houot, R. (2017). Intratumoral immunotherapy: Using the tumor as the remedy. *Ann. Oncol.* 28, xii33–xii43. doi:10.1093/annonc/mdx683
- Newman, A. M., Liu, C. L., Green, M. R., Gentles, A. J., Feng, W., Xu, Y., et al. (2015). Robust enumeration of cell subsets from tissue expression profiles. *Nat. Methods* 12, 453–457. doi:10.1038/nmeth.3337
- Ngwa, W., Irabor, O. C., Schoenfeld, J. D., Hesser, J., Demaria, S., Formenti, S. C., et al. (2018). Using immunotherapy to boost the abscopal effect. *Nat. Rev. Cancer* 18, 313–322. doi:10.1038/nrc.2018.6
- Pellizzari, G., Martinez, O., Crescioli, S., Page, R., Di Meo, A., Mele, S., et al. (2021). Immunotherapy using IgE or CAR T cells for cancers expressing the tumor antigen SLC3A2. *J. Immunother. Cancer* 9, e002140. doi:10.1136/jitc-2020-002140
- Racle, J., de Jonge, K., Baumgaertner, P., Speiser, D. E., and Gfeller, D. (2017). Simultaneous enumeration of cancer and immune cell types from bulk tumor gene expression data. *eLife* 6, e26476. doi:10.7554/eLife.26476
- Riley, R. S., June, C. H., Langer, R., and Mitchell, M. J. (2019). Delivery technologies for cancer immunotherapy. *Nat. Rev. Drug Discov.* 18, 175–196. doi:10.1038/s41573-018-0006-z
- Shin, D. H., Jo, J. Y., and Han, J. Y. (2018). Dual targeting of ERBB2/ERBB3 for the treatment of slc3a2-NRG1-mediated lung cancer. *Mol. Cancer Ther.* 17, 2024–2033. doi:10.1158/1535-7163.MCT-17-1178
- Thorsson, V., Gibbs, D. L., Brown, S. D., Wolf, D., Bortone, D. S., Ou Yang, T. H., et al. (2018). The immune landscape of cancer. *Immunity* 48, 812–830. e14. doi:10.1016/j.immuni.2018.03.023
- Wang, S., Han, H., Hu, Y., Yang, W., Lv, Y., Wang, L., et al. (2017). SLC3A2, antigen of mAb 3G9, promotes migration and invasion by upregulating of mucins in gastric cancer. *Oncotarget* 8, 88586–88598. doi:10.18632/oncotarget.19529
- Wiernicki, B., Maschalidi, S., Pinney, J., Adjemian, S., Vanden Berghe, T., Ravichandran, K. S., et al. (2022). Cancer cells dying from ferroptosis impede dendritic cell-mediated anti-tumor immunity. *Nat. Commun.* 13, 3676. doi:10.1038/s41467-022-31218-2
- Zhang, H., Deng, T., Liu, R., Ning, T., Yang, H., Liu, D., et al. (2020). CAF secreted miR-522 suppresses ferroptosis and promotes acquired chemo-resistance in gastric cancer. *Mol. Cancer* 19, 43. doi:10.1186/s12943-020-01168-8
- Zhao, Y., Li, Y., Zhang, R., Wang, F., Wang, T., Jiao, Y., et al. (2020). The role of erastin in ferroptosis and its prospects in cancer therapy. *Onco. Targets. Ther.* 13, 5429–5441. doi:10.2147/OTT.S254995
- Zhu, B., Cheng, D., Hou, L., Zhou, S., Ying, T., Yang, Q., et al. (2017). SLC3A2 is upregulated in human osteosarcoma and promotes tumor growth through the PI3K/Akt signaling pathway. *Oncol. Rep.* 37, 2575–2582. doi:10.3892/or.2017.5530



## OPEN ACCESS

## EDITED BY

Xin Wang,  
National Institutes of Health (NIH),  
United States

## REVIEWED BY

Shuai Zhang,  
Tianjin University of Traditional Chinese  
Medicine, China  
Yuliang Feng,  
University of Oxford, United Kingdom  
Weiwei Qi,  
Zhongshan School of Medicine, Sun  
Yat-sen University, China

## \*CORRESPONDENCE

Zhao Yin,  
zhaoyin@stu2014.jnu.edu.cn  
Jingjun He,  
hjjs2@126.com  
Junzhang Tian,  
jz.tian@163.com

<sup>†</sup>These authors have contributed equally  
to this work

## SPECIALTY SECTION

This article was submitted to Molecular  
Diagnostics and Therapeutics,  
a section of the journal  
Frontiers in Molecular Biosciences

RECEIVED 06 June 2022

ACCEPTED 08 July 2022

PUBLISHED 08 August 2022

## CITATION

Liu F, Tang L, Li Q, Chen L, Pan Y, Yin Z,  
He J and Tian J (2022), Single-cell  
transcriptomics uncover the key  
ferroptosis regulators contribute to  
cancer progression in head and neck  
squamous cell carcinoma.  
*Front. Mol. Biosci.* 9:962742.  
doi: 10.3389/fmolb.2022.962742

## COPYRIGHT

© 2022 Liu, Tang, Li, Chen, Pan, Yin, He  
and Tian. This is an open-access article  
distributed under the terms of the  
[Creative Commons Attribution License](#)  
(CC BY). The use, distribution or  
reproduction in other forums is  
permitted, provided the original  
author(s) and the copyright owner(s) are  
credited and that the original  
publication in this journal is cited, in  
accordance with accepted academic  
practice. No use, distribution or  
reproduction is permitted which does  
not comply with these terms.

# Single-cell transcriptomics uncover the key ferroptosis regulators contribute to cancer progression in head and neck squamous cell carcinoma

Fei Liu<sup>1†</sup>, Lindong Tang<sup>2†</sup>, Qing Li<sup>3†</sup>, Leihui Chen<sup>3</sup>, Yuyue Pan<sup>3</sup>,  
Zhao Yin<sup>4\*</sup>, Jingjun He<sup>1\*</sup> and Junzhang Tian<sup>1\*</sup>

<sup>1</sup>Cancer Screening Center, Department of Health Management, Guangdong Second Provincial General Hospital, Guangdong, China, <sup>2</sup>Institute of Hematology School of Medicine Jinan University, Guangdong, China, <sup>3</sup>Department of Stomatology Guangdong Second Provincial General Hospital, Guangdong, China, <sup>4</sup>Department of Hematology Guangdong Second Provincial General Hospital, Guangdong, China

The mechanism underlying the association between the development of head and neck squamous cell carcinoma (HNSCC) and ferroptosis is unclear. We analyzed the transcriptomes of 5902 single cells from a single-cell RNA-sequencing (scRNA-seq) dataset. They then aggregate into B cells, epithelial cells, fibroblasts, germ cells, mesenchymal cells, cancer stem cells, stem cells, T cells and endometrial cells, respectively. Our study shows that multiple pathways are significantly enriched in HNSCC development including extracellular matrix structural components, humoral immune responses, and muscle contraction. Differentially expressed genes analysis in Pseudotime analysis, pathway and biological function indicated that there was a significant correlation in the ferroptosis pathway. Furthermore, higher ferroptosis potential index (FPI) scores were significantly associated with worse overall survival prognosis in HNSCC patients. Pseudo-temporal, survival analyses and immunohistochemistry identified multiple central genes in HNSCC development, including ACSL1, SLC39A14, TFRC, and PRNP genes, and indicated associated ferroptosis. Overall, our study detected ferroptosis-related features is closely correlated with HNSCC prognosis and development, and deserved candidates suitable for immunotherapy treatment strategies determination for HNSCC patients.

## KEYWORDS

head and neck squamous cell carcinoma, cell heterogeneity, ferroptosis, prognostic, single cell RNA sequencing



## Introduction

Head and neck squamous cell carcinoma (HNSCC), which is frequently encountered in the clinical setting, is the seventh leading cause of cancer-related death worldwide: approximately 700,000 new cases and 350,000 deaths were reported worldwide in 2018 (Membreno et al., 2021; Sacco et al., 2021). HNSCC mainly includes cancers of the nasal cavity, paranasal sinus, oral cavity, pharynx, and throat, and over 90% of these cancers are squamous cell carcinomas (Jing et al., 2021; Membreno et al., 2021). Although there have been continuous advances in the field of comprehensive surgery, radiotherapy, and chemotherapy in recent years, the 5-year survival rate of HNSCC has not significantly improved, and 30–40% of patients are likely to develop distant metastasis within 5 years (Membreno et al., 2021). Moreover, 58% of patients may have advanced disease (stage III to IV) when they are first diagnosed, and this is a great challenge to treatment (Hamman et al., 2021). In order to improve the diagnosis and treatment of this cancer, it is important to understand the cellular mechanisms involved in its progression and metastasis (Hamman et al., 2021; Membreno et al., 2021).

Ferroptosis is a newly discovered form of programmed cell death characterized by iron-dependent lethal accumulation of lipid peroxides (lipid reactive oxygen species or lipid ROS) that was recently identified as one of the mechanisms of cancer cell death in several cancers, including liver cancer, kidney cancer, bone cancer, and lung cancer (Chen et al., 2022; Peng et al., 2023). Ferroptosis occurs when the levels of lipid ROS exceed the cellular antioxidative threshold and oxidative stress overload is induced in cells (Zhang et al., 2022). Excess oxidative stress causes damage to large molecules such as proteins, nucleic acids, and lipids, and eventually leads to cell injury or death (Zhai et al., 2022). With regard to cellular morphology, ferroptosis is characterized by loss of membrane integrity with morphologically normal nuclei and shrunken mitochondria as well as thickening of the mitochondrial double membranes and rupture of the outer mitochondrial membrane (Zhang et al., 2022).

Ferroptosis was first discovered in the study of the lethal mechanisms of the small molecule drug erastin against tumor cells carrying a mutation of the oncogene RAS (Liang et al., 2019). Erastin can bind to voltage-dependent anion channel-2/3 of mitochondria to induce ferroptosis of cancer cells. Erastin can also inhibit the function of the cystine/glutamate antiporter system to reduce intracellular glutathione levels, resulting in the accumulation of lipid ROS to induce ferroptosis. In addition, a series of artificial compounds, such as RSL3, DPI7, DPI10, DPI12, and DPI13, can inhibit glutathione peroxidase-4, and thereby increase the levels of peroxides in cancer cells, leading to Fe<sup>2+</sup>-dependent metabolic abnormalities (Yang and Stockwell, 2016). Translational research has shown that the chemotherapeutic drug sorafenib can also suppress the cystine/glutamate antiporter system to trigger cell ferroptosis in several cancers (Cao and Dixon, 2016). Furthermore, low-dose sorafenib can induce ferroptosis, but high-dose sorafenib can induce not only ferroptosis, but also other forms of programmed

cell death (Peng et al., 2023). Xie et al. (2022), investigating the transcriptome data of TCGA and Chinese Glioma Genome Atlas (CGGA) database, and thus identifying 36 radiosensitivity- and 19 ferroptosis associated differentially expressed genes with a prognostic value. In results, they also revealed that the radiosensitivity- and ferroptosis-associated biomarkers, includes HSPB1, STAT3, CA9, MAP1LC3A, MAPK1, ZEB1, and TNFAIP3, with a prognostic value for gliomas patients. Huang et al. (2022), found that the ferroptosis therapy can be a effectively approach to trigger the cancer cell death, and thus activating the cell oxidative phosphorylates and promoting cell oxidative damage. Magesh and Cai (Forthcoming 2022), revealed that the ferritin play an important susceptor for abnormal mitochondrial function, metabolism and oxidative phosphorylation in tumor cells, and also a target for tumor therapy.

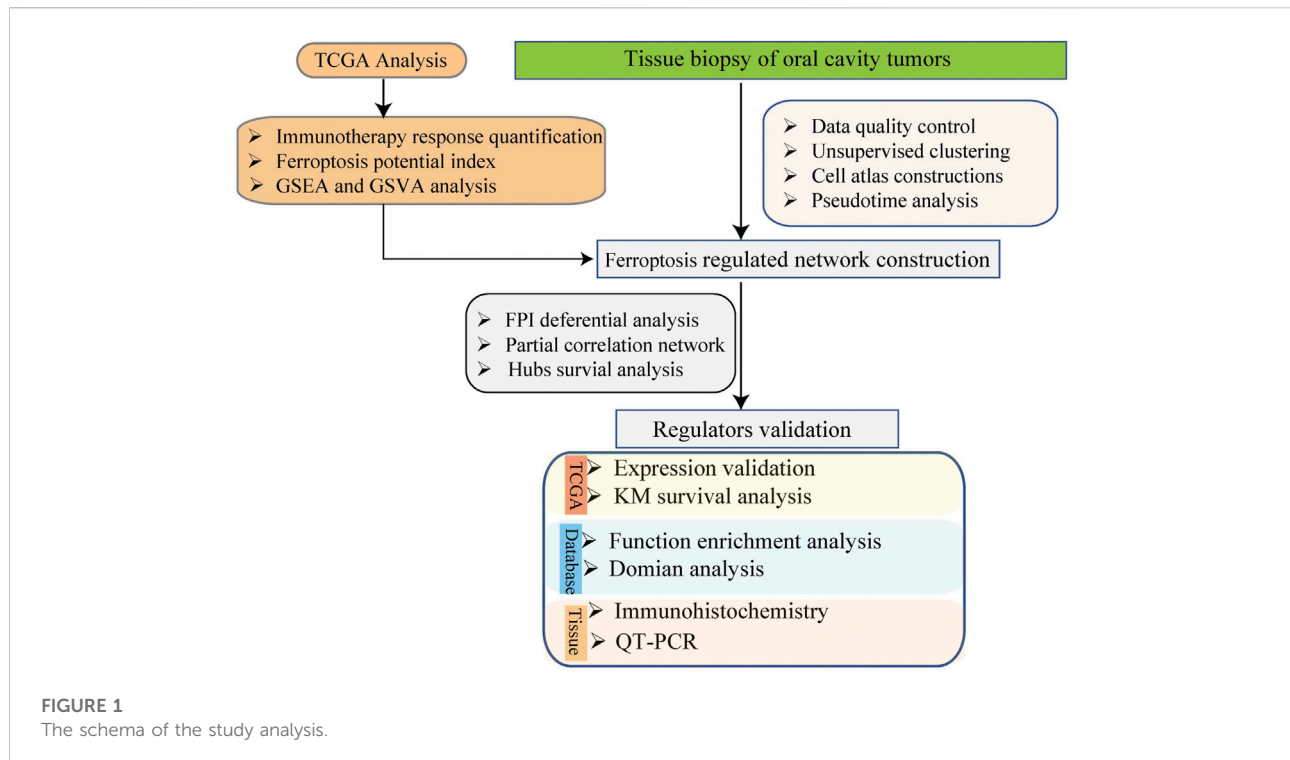
As explained above, there is evidence to demonstrate the role and mechanisms of ferroptosis in several cancers, but the mechanism of the association among HNSCC development and ferroptosis is unclear. In this article, we integrated the single-cell sequencing data and TCGA transcriptome data of HNSCC in order to systematically analyze the relationship between ferroptosis and the prognosis of HNSCC, as well as the related molecular mechanism networks and regulatory molecules, in order to identify markers for targeted treatment of HNSCC.

## Materials and methods

### Single-cell RNA sequencing analysis

The expression profiling data of 5902 single cells from the tumors of 18 patients with oral cavity tumors were downloaded from the Gene Expression Omnibus database (accession number GSE103322) (Puram et al., 2017). The expression was analyzed with single-cell RNA sequencing (scRNA-seq) using the high-throughput sequencing method Smart-Seq2. The data analysis process is described below. The flow chart of this study analysis shown in Figure 1.

- 1) Quality control of data: The following data filtering parameters were set: minimum number of cells = 3; minimum number of features = 200; mitochondrial gene proportion <0.05; gene count = 200–20,000 (Aran et al., 2019; Kobak and Berens, 2019).
- 2) Unsupervised clustering and construction of a cell Atlas: 1) normalization of the data; 2) screening of genes with high expression variation based on the mean value algorithm; 3) assessment of batch effects across samples by principal component analysis; 4) use of random sampling to construct the background distribution of correlation values between feature genes and principal components in Seurat, and use of the Jackstraw algorithm to select suitable principal components for subsequent cell cluster analysis; 5) use of the k-nearest neighbors algorithm to transform the expression



profiles of cells into highly related cell clusters and identify the clusters (resolution = 0.6); 6) selection of genes that exhibit certain log-fold changes and can be used as markers in most cells based on the following criteria: min.pct = 0.25, logfc.threshold = 0.25 (Kobak and Berens, 2019).

- 3) Cell cluster definition: SingleR and scCATCH were used to annotate cell clusters (Aran et al., 2019).

## Pseudotime analysis

The Monocle algorithm was used to perform developmental trajectory analysis based on highly variable gene sets, and genes with high expression variation in the trajectory were selected for subsequent analysis. The criteria settings were as follows: status = ok; family = tobit; q-value < 0.05; ordering = true (Qiu et al., 2017).

## The quantification of immunotherapy response

To calculate the immunophenotypes of tumor-immune cell interactions and the cancer antigenomes, and thus predict the tumor immunotherapy response, the algorithm of Immunophenoscore was used. Here, basing the Immunophenogram algorithm, the weighted averaged Z score were identified, and shown a good predictor of response to immunotherapy, includes anti-cytotoxic T lymphocyte antigen-4

(CTLA-4) and anti-programmed cell death protein 1 (anti-PD-1) antibodies. In addition, the sum of Immunophenoscore (IPS) were calculated by histocompatibility complex (MHC)-related molecules, checkpoints or immunomodulators, effector cells, and suppressor cells (Charoentong et al., 2017).

## Correlation analysis of ferroptosis and immunotherapy response

In order to identify the immunotherapy response that were closely associated with ferroptosis, the normalized GSVA scores for ferroptosis and IPS were computed and subjected to Spearman correlation analysis to detect unsupervised clustering (Liberzon et al., 2011; Hänzelmann et al., 2013; Ferreira et al., 2021).

## TCGA analysis

The RNA-seq Recompute TPM data, clinical data, and survival data of the GDC TCGA-HNSCC datasets were downloaded from the Xena database at <https://xenabrowser.net/datapages/>. The DESeq algorithm was used to normalize gene expression profiles and filter out low-expression genes. The criteria for selecting differentially expressed genes were as follows: log<sub>2</sub> |fold change| ≥ 1.0; Benjamini-Hochberg (B-H) adjusted *p*-value < 0.05 (Anders and Huber, 2010). While the multiple comparisons were tested by one-way ANOVA,

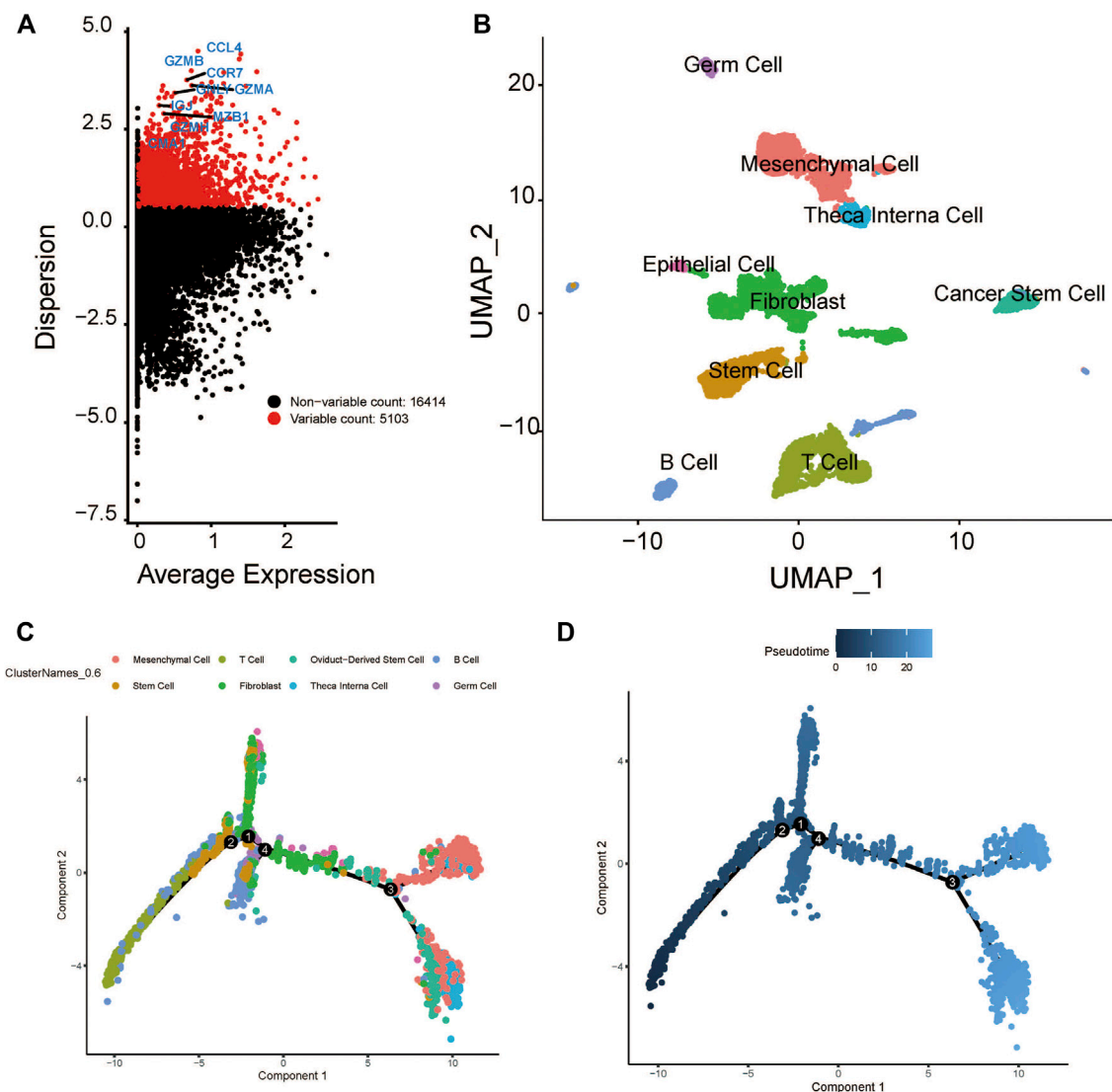


FIGURE 2

Cluster identification and pseudotime analysis of the HNSCC scRNA dataset. (A) Gene variation plot of the dataset, where each dot is a gene and the red dots represent genes with variable expression. (B) UMAP plot of HNSCC cell clusters, which are annotated as B cells, epithelial cells, fibroblast, germ cells, mesenchymal cells, cancer stem cells, stem cells, T cells, and theca interna cells. (C) Trajectory plot of the dataset, where each cluster (represented by each of the dots) is indicated by a different color. (D) Trajectory plot of the dataset, where the color of the dot indicates the differentiation state. The darker dot indicate a lower level of differential expression.

and the Bonferroni adjusted  $p$ -value  $< 0.05$  was considered as significant.

## Hub gene identification and functional enrichment analysis

Hub genes were identified based on the intersection of pseudotime analysis-derived differential genes, TCGA-derived differential genes, and ferroptosis pathway genes. Next, functional enrichment analysis and binding protein prediction

were performed on the identified hub genes that were deposited in the Toppgene database at <https://toppgene.cchmc.org/>. The filtering criterion was a false discovery rate-adjusted  $p$ -value of  $< 0.05$  (Chen et al., 2009; Liberzon et al., 2011).

## Calculation of ferroptosis potential index and survival analysis

Based on Liu et al.'s research, 24 ferroptosis regulator genes were selected and were classified into 1) positive regulators

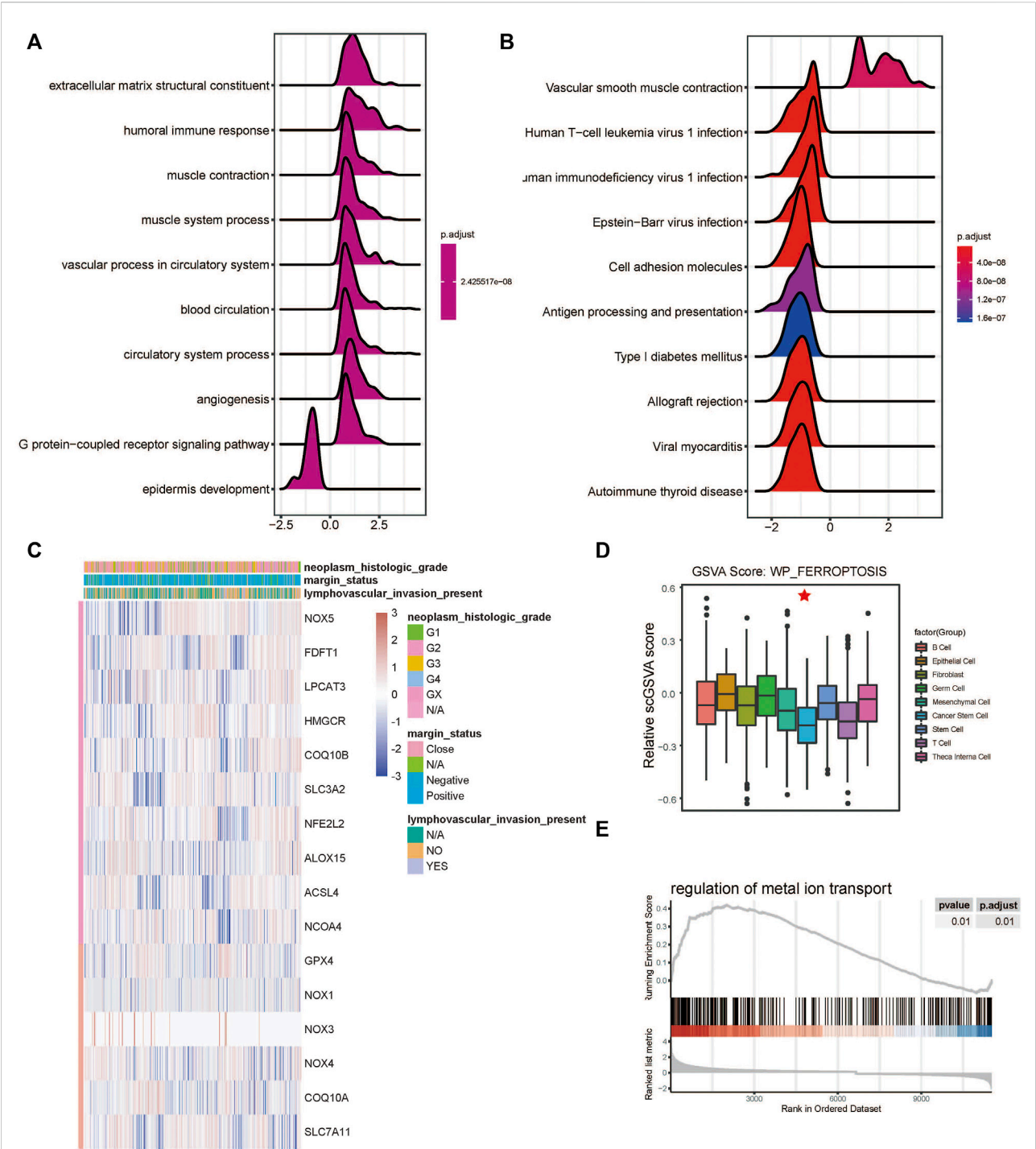


**FIGURE 3** Ferroptosis-related cell cluster and pathway analysis in HNSCC. **(A)** GO and **(B)** KEGG pathway enrichment analyses of differential gene clusters from the scRNA dataset: the abscissa represents the normalized enrichment score, and the adjusted *p*-value is represented by the colored areas of the graph. **(C)** Unsupervised clustering of expression level of genes of WP-FERROPTOSIS pathway. **(D)** Distribution of WP-FERROPTOSIS score in HNSCC cell clusters. **(E)** Significant enrichment of regulation of the metal ion transport pathway in the differentially expressed genes of the cancer stem cell cluster.



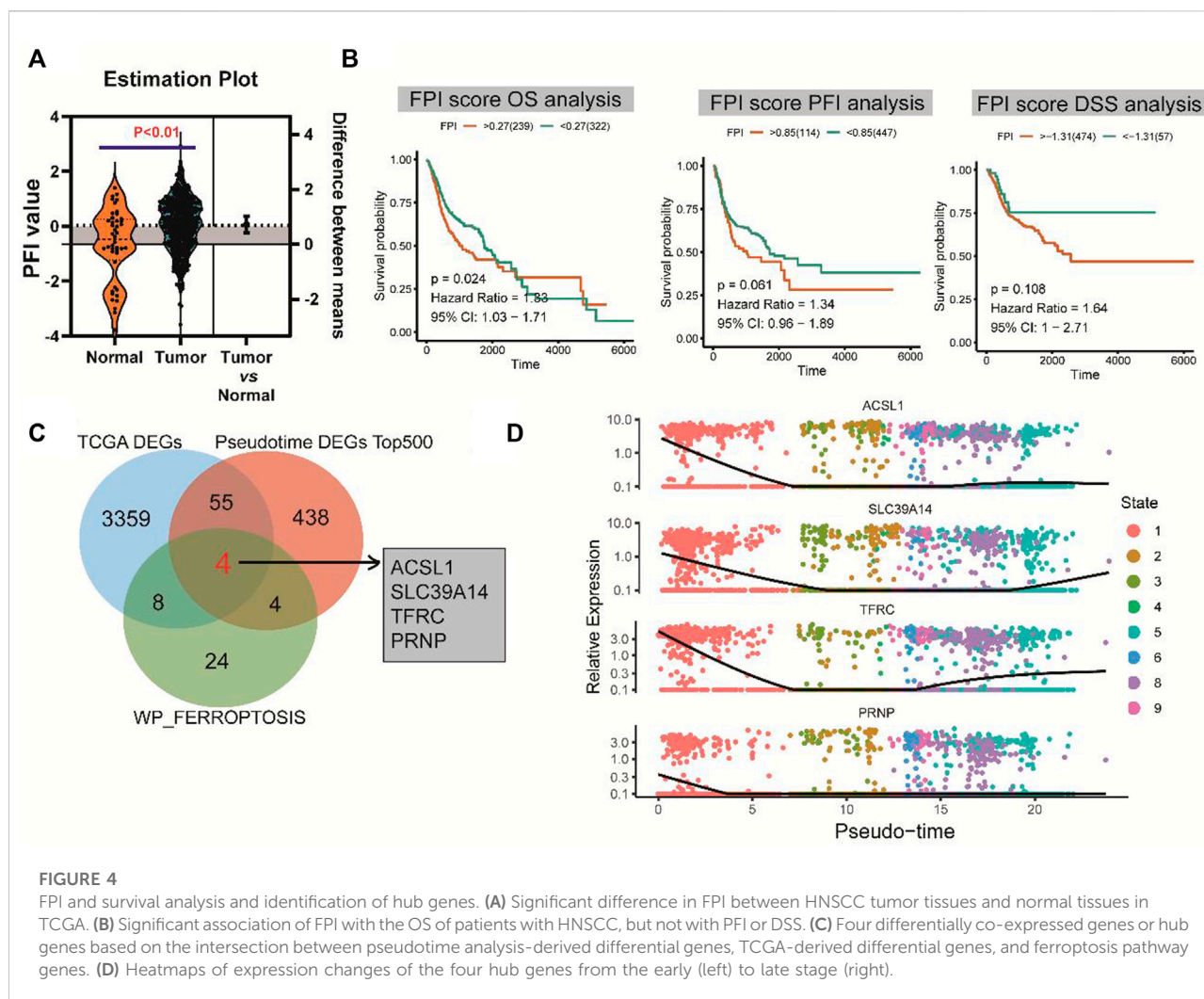


FIGURE 4

FPI and survival analysis and identification of hub genes. (A) Significant difference in FPI between HNSCC tumor tissues and normal tissues in TCGA. (B) Significant association of FPI with the OS of patients with HNSCC, but not with PFI or DSS. (C) Four differentially co-expressed genes or hub genes based on the intersection between pseudotime analysis-derived differential genes, TCGA-derived differential genes, and ferroptosis pathway genes. (D) Heatmaps of expression changes of the four hub genes from the early (left) to late stage (right).

(LPCAT3, ACSL4, NCOA4, ALOX15, NFE2L2, NOX1, NOX3, NOX4, NOX5, GPX4, SLC3A2, and SLC7A11) and 2) negative regulators (FDFT1, HMGCR, COQ10A, and COQ10B) Liu et al. (2020). The enrichment score (ES) for the positive regulators and the negative regulators was calculated by single-sample gene set enrichment analysis (ssGSEA) in the GSVA package, and ferroptosis potential index (FPI) was calculated as the difference between the two scores. In addition, the survminer package was employed to analyze the relationship of FPI with overall survival (OS), progression-free interval (PFI), and disease-specific survival (DSS).

## Pathway enrichment analysis and GSVA

The clusterProfiler package was used to perform gene ontology (GO) analysis, Kyoto Encyclopedia of Genes and Genomes (KEGG) pathway analysis, and reactome pathway analysis on the differentially expressed genes and hub genes

that were identified through pseudotime analysis. B-H adjustment (adjusted  $p$ -value,  $< 0.05$ ) was applied to differential pathways. In addition, C2 (curated gene sets), C5 (ontology gene sets), and H (hallmark gene sets) were downloaded from MSigDB at <https://www.gsea-msigdb.org/gsea/msigdb/>, and the GSVA and the GSEABase packages were used for standardized scoring of the gene sets for each cell (Liberzon et al., 2011). The B-H adjusted  $p$ -value  $< 0.05$  were considered as significant terms in GSVA analysis.

## Immunohistochemical staining

All three HNSCC samples and paired non-neoplastic tissues used in immunohistochemical were retrieved from the Department of Pathology, Guangdong Second Provincial General Hospital, China. Before they were used, all cases were diagnosed by three certificated pathologists without discrepancy. This research was conducted under the

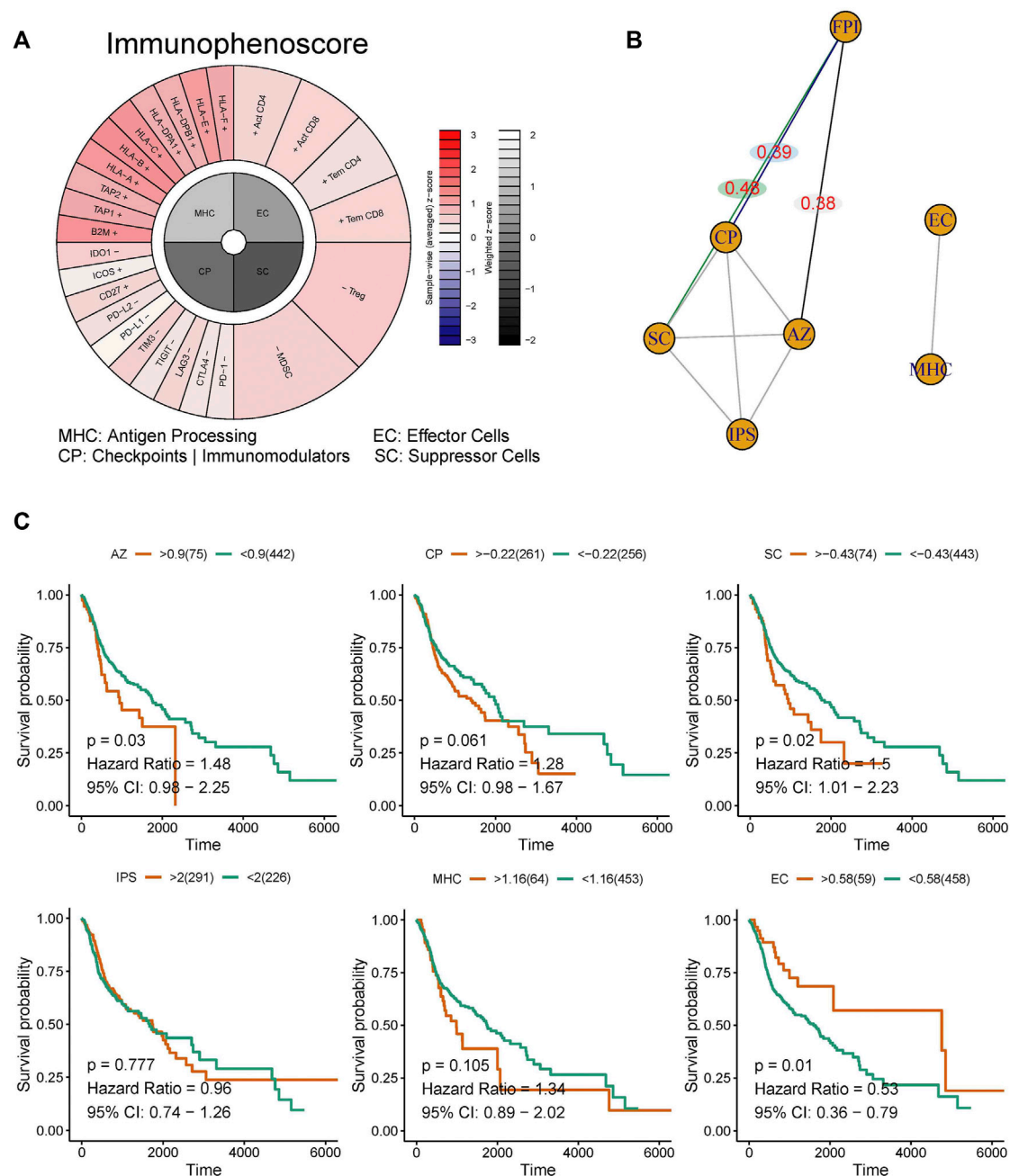


FIGURE 5

Correlation analysis among the ferroptosis pathway and immunotherapy response. (A) The immunophenotypes of tumor-immune landscape were calculated by Immunophenogram algorithm. Significant difference in FPI between HNSCC tumor tissues and normal tissues in TCGA. (B) The partial correlations based on spearman analysis were identified. (C) Survival analysis showed that AZ, SC, and EC were significantly associated with the OS of patients with HNSCC, but not with CP, MHC, and IPS.

approval and supervision of the Ethics Committee of Guangdong Second Provincial General Hospital. Subsequently, deparaffinized sections were treated with 3% H<sub>2</sub>O<sub>2</sub> and subjected to antigen retrieval by citric acid (pH6.0). After overnight incubation with primary antibody

(anti-ACSL1, anti-SLC39A14, anti-TFRC and PRNP antibody (Proteintech Group, China) by 1:200 at 4°C, sections were incubated for 15 min at room temperature with horseradish peroxidase-labeled polymer conjugated with secondary antibody (MaxVision Kits) and incubated for 1 min with

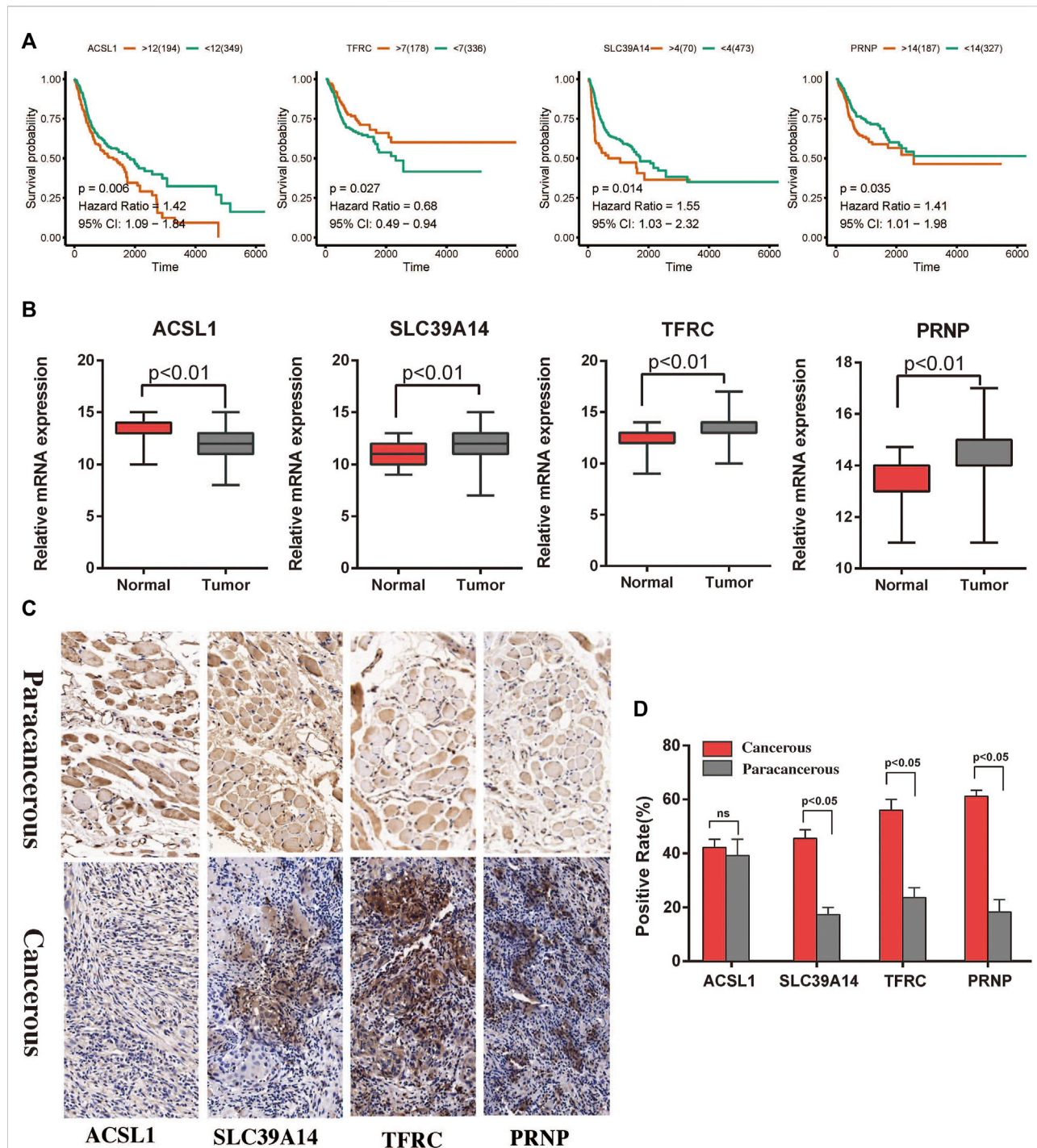


FIGURE 6

Survival analysis and immunohistochemistry to detect differential expression analysis of the hub genes. **(A)** Associations of the *ACSL1*, *SLC39A14*, *TFRC*, and *PRNP* genes with the survival of patients with HNSCC in TCGA. **(B)** Differential expression of the *ACSL1*, *SLC39A14*, *TFRC*, and *PRNP* genes between cancerous and paracancerous tissues in TCGA. **(C,D)** Expression of ferroptosis related proteins between the cancerous and paracancerous tissues (x400).

diaminobenzidine. The sections were then lightly counterstained with hematoxylin. The sections without primary antibody were served as negative controls.

Expression area of ACSL1, SLC39A14, TFRC and PRNP was determined according to the Image J (<https://imagej.net/software/fiji/downloads>; Life-Line versions).



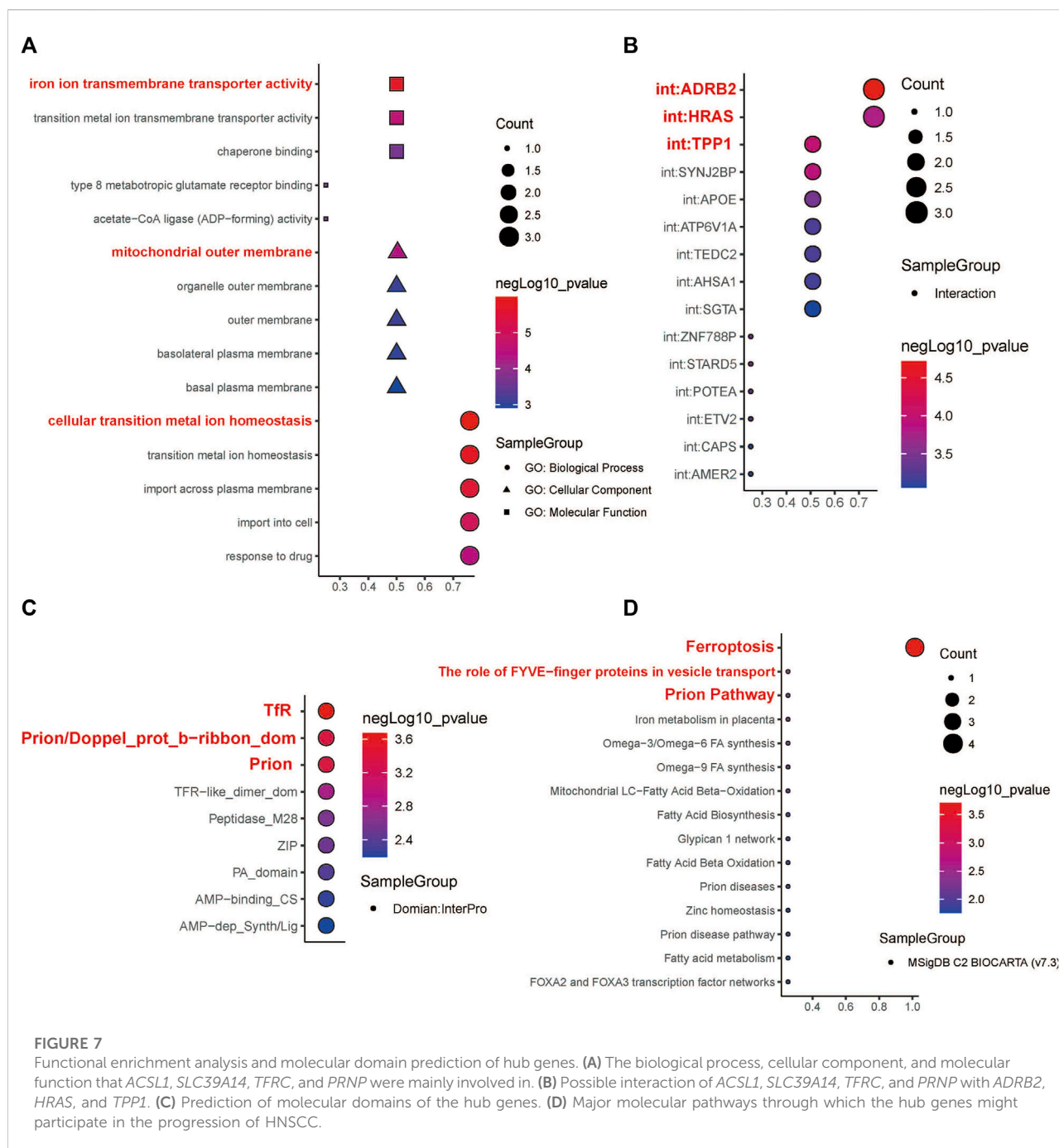


FIGURE 7

Functional enrichment analysis and molecular domain prediction of hub genes. (A) The biological process, cellular component, and molecular function that *ACSL1*, *SLC39A14*, *TFRC*, and *PRNP* were mainly involved in. (B) Possible interaction of *ACSL1*, *SLC39A14*, *TFRC*, and *PRNP* with *ADRB2*, *HRAS*, and *TPP1*. (C) Prediction of molecular domains of the hub genes. (D) Major molecular pathways through which the hub genes might participate in the progression of HNSCC.

## Results

### Single-cell RNA-sequencing analysis

After quality control, the single-cell transcriptomic data of 5902 cells from 18 patients with oral cavity tumors were obtained. Unsupervised clustering was performed on merged datasets after normalization and correction. Cells were annotated with marker genes of known cell types. A

total of 5103 genes with variable expression were identified, including *GZMB*, *GNLY*, *MZB1*, *CCR7*, and *CCL4* (Figure 2A). Using t-distributed stochastic neighbor embedding and uniform manifold approximation and projection for dimension reduction, 5902 cell clusters were identified, including B cells, epithelial cells, fibroblasts, germ cells, mesenchymal cells, cancer stem cells, stem cells, T cells, and theca interna cells. The distribution of cells was plotted in a two-dimensional space (Figure 2B).



## Pseudotime analysis and enrichment analysis

The expression profiles of cells were projected onto a low-dimensional space to construct a differentiation trajectory of cells, wherein cells of similar states were aggregated together. There were four branching points along the differentiation trajectory of HNSCC that represented potential decision points of the cellular biological process (Figures 2C,D).

The developmental trajectory analysis was performed on highly variable gene sets. Following log normalization and dimension reduction using the DDRTree algorithm, differentially regulated genes, after B-H adjustment in the pseudotime analysis, were selected for subsequent functional enrichment analyses. GO analysis showed that the following pathways were associated with the differentiation and progression of HNSCC: extracellular matrix structural constituent (ES = 0.56, normalized ES [NES] = 2.61, P.adjust = 1.00E-10), humoral immune response (ES = 0.54, NES = 2.71, P.adjust = 1.00E-10), and muscle contraction (ES = 0.51, NES = 2.69, P.adjust = 1.00E-10) (Figure 3A). KEGG analysis revealed that the following pathways were significantly enriched: vascular smooth muscle contraction (ES = 0.55, NES = 2.58, P.adjust = 1.44E-9), human T-cell leukemia virus one infection (ES = -0.34, NES = -2.52, P.adjust = 1.00E-10), and human immunodeficiency virus one infection (ES = -0.35, NES = -2.64, P.adjust = 1.00E-10) (Figure 3B). In addition, we draw a heatmap prototype for showing the expression level of genes in ferroptosis pathway (Figure 3C). Among all the cell clusters of HNSCC, the cancer stem cell cluster showed the lowest expression and highest variation in the FERROPTOSIS pathway and, therefore, was considered as the FERROPTOSIS-related core cell cluster (Figure 2D). Further, the regulation of the metal ion transport pathway was significantly enriched in the differentially expressed genes of the cancer stem cell cluster (ES = 0.42, NES = 2.24, P.adjust = 5.97E-10) (Figure 3E).

## Ferroptosis potential index and survival analysis and identification of hub genes

FPI was calculated for each HNSCC sample in the TCGA database based on the method described by Liu et al. (2022). There was a significant difference in FPI between HNSCC tumor tissues and normal tissues ( $p < 0.01$ ) (Figure 4A). With the survminer package and survival R package, patients with HNSCC were divided into high and low expression groups. Survival analysis showed that FPI was significantly associated with the OS of patients with HNSCC [ $p = 0.024$ , hazard ratio = 1.33, 95% confidence interval (CI) = 1.03–1.71], but not with PFI ( $p = 0.061$ ,

hazard ratio = 1.34, 95% CI = 0.96–1.89), or DSS ( $p = 0.108$ , hazard ratio = 1.64, 95% CI = 1–2.71) (Figure 4B).

A total of four differentially co-expressed genes, or hub genes, were identified based on the intersection of pseudotime analysis-derived differentially expressed genes, TCGA-derived differentially expressed genes, and FERROPTOSIS pathway genes: ACSL1, SLC39A14, TFRC, and PRNP (Figure 4C). The results of pseudotime analysis indicated that these four hub genes exhibited consistent expression changes in the differentiation process of HNSCC (Figure 4D).

## Correlation between the ferroptosis pathway and immunotherapy response

The scores for WP-FERROPTOSIS and IPS were quantified (Figure 5A). Unsupervised clustering based on the correlation coefficients according to Spearman correlation analysis revealed close correlations between WP-FERROPTOSIS and antigen processing of MHC, effector cells (EC), immunomodulators of checkpoints (CP, correlation coefficient = 0.39,  $p = 0.04$ ), suppressor cells (SC, correlation coefficient = 0.48,  $p = 0.03$ ), and averaged Z (AZ, correlation coefficient = 0.38,  $p = 0.04$ ) score (Figure 5B). Survival analysis showed that AZ [ $p = 0.03$ , hazard ratio = 1.48, 95% confidence interval (CI) = 0.98–2.25], SC ( $p = 0.02$ , hazard ratio = 1.50, 95% CI = 1.01–2.23), and EC ( $p = 0.01$ , hazard ratio = 0.53, 95% CI = 0.36–0.79) were significantly associated with the OS of patients with HNSCC, but not with CP ( $p = 0.06$ , hazard ratio = 1.28, 95% CI = 0.98–1.67), MHC ( $p = 0.11$ , hazard ratio = 1.34, 95% CI = 0.89–2.02), and IPS ( $p = 0.78$ , hazard ratio = 0.96, 95% CI = 0.74–1.26) (Figure 5C).

## Survival analysis and functional enrichment analysis of the hub genes

The expression levels of the four hub genes were significantly associated with the survival of patients with HNSCC (Figure 6A). They also showed significantly different expression levels between the cancer tissues and the para-cancerous tissues of patients with HNSCC (Figure 6B). Our results indicated that SLC39A14, TFRC and PRNP are up-regulated in most HNSCC patients. However, there was no significant difference in the expression of ACSL1 (Figures 6C,D). The iron ion transmembrane transporter activity, mitochondrial outer membrane, and cellular transition metal ion homeostasis pathways were significantly enriched in the four hub genes (Figure 7A). Further, exploration of the biological mechanisms indicated that the hub genes may exert their effects in HNSCC through interactions with the ADRB2, HRAS, and TPPI genes (Figure 7B).

## Hub gene interaction and molecular domain prediction

According to the InterPro database, Tfr, Prion/Doppel\_prot\_b-ribbon\_dom, and Prion are likely to be the molecular domains of the four hub genes (Figure 7C). The four hub genes were mainly enriched in the following Biocarta pathways: Ferroptosis, The role of FYVE-finger proteins in vesicle transport, and Prion Pathway (Figure 7D).

## Discussion

The current study explores the role and mechanisms of the ferroptosis pathway in HNSCC, as ferroptosis is an important inhibitory mechanism in tumor cells. We believe that the findings shed light on the underlying ferroptosis-related mechanisms of HNSCC and can help in the identification of molecular markers that could accurately predict the outcome of HNSCC. These findings could eventually have immense clinical value for the treatment and prognosis of HNSCC.

Our results indicate that the ferroptosis pathway is closely associated with the overall survival of patients with HNSCC, and it is mainly involved in the regulation of extracellular matrix structure, humoral immune response, and vascular smooth muscle contraction. Additionally, it was found that ferroptosis pathway changes mainly occur in cancer stem cells, in comparison to other cell types; additionally, changes in the metal ion transport pathway were also significant in cancer cells. The latter finding supports the role of ferroptosis in HNSCC, as ferroptosis is induced by lipid ROS, which are largely generated by enzymes that contain iron or iron derivatives such as ferroheme and heme oxygenase-1.

According to the present findings, the expression levels of four genes, namely, *ACSL1*, *SLC39A14*, *TFRC*, and *PRNP*, were closely linked with ferroptosis, the occurrence of HNSCC, and the long-term outcome of patients. These genes are, therefore, potential targets for the development, progression, and treatment of HNSCC. Zhang et al. (2021) found that the higher expression level of *ACSL1* could activate fatty-acid (FA) metabolic reprogramming during ovarian cancer metastasis and convert the lipid profile via AMP-activated protein kinase and Src pathways. Guo et al. (2020), demonstrated that the Acyl-CoA synthetase long-chain family member 1 (*ACSL1*) is an oncogene in thyroid cancers, and the higher expression level of *ACSL1* led to a suppression of cancer cell progression and migration. Thomas et al. (2019), the activity of *ACSL1* could convert the TNF $\alpha$  mediates inflammatory responses via attenuates the phosphorylation of p38 MAPK, ERK1/2, and NF- $\kappa$ B in breast cancer. Thorsen et al. (2011), illustrated that the alternative splicing of *SLC39A14* is significantly difference among the adenomas and cancers, especially in the mutation of exclusive exons 4A, 4B, and the exon 4A/4B ratio. Wang et al. (2018),

found that the expression level of *SLC39A14* significantly correlated with the weightlessness of skeletal muscle mass and cachexia via regulated with zinc uptake in muscle progenitor cells. Xu et al. (2016), demonstrated that the lower expression level of *SLC39A14* protein may significantly correlated with a higher Gleason score, advanced clinical stage, presence of metastasis, and prostate-specific antigen failure in human prostate cancer. Wu et al. (2019), reported that *TFRC* play a key role in cancer cellular metabolism and proto-oncogenic transcription via regulated by NF2-YAP signaling axis. *TFRC* regard as the key transporter in the intracellular iron, and the higher expression level of increased *TFRC* was associated with a worse prognosis for epithelial ovarian cancer patients (Huang et al., 2020). Stewart et al. (2019), shown that the expression level of TP63, PSAT1, and *TFRC* may correlated with the function of oxidation-reduction and glutathione in squamous cell lung cancer. Santos et al. (2021), found that the expression level of *PRNP* may significantly correlated with lymph node metastasis progression and worse prognosis for patients with head and neck squamous cell carcinoma. López-Cortés et al. (2020), demonstrated that the protein of *PRNP*, S100A9, DDA1, TXN, RPS27, S100A14, S100A7, MAPK1, AGR3 and NDUFA13 were considered as the best ranked metastasis driver proteins. AS an evolutionarily conserved cell surface protein, the higher expression level of *PRNP* closely related with the acquisition of malignant feature of cancer stem cells of multiple cancers, includes glioblastoma multiforme, breast cancer, and gastric cancer (Ryskalin et al., 2019).

In this study, the GSVA score for the ferroptosis pathway was closely correlated with the OS of patients with HNSCC, had a potential correlation with the PFI, and had no significant correlation with DSS. These findings indicate that HNSCC cells might escape ferroptosis through a balance of iron and thiol redox signaling. However, more research is required in the future to clarify the relationship between iron pathways, ferroptosis, and the origin of HNSCC.

## Conclusion

In summary, the ferroptosis pathway is closely associated with the development and progression of HNSCC, possibly through regulation of cancer stem cell proliferation. The *ACSL1*, *SLC39A14*, *TFRC*, and *PRNP* genes may be critical for ferroptosis-related development and progression of HNSCC, and may serve as potential treatment targets. These informative protein domains might be used in novel strategies for developing effective therapies targeting HNSCC. These findings also allow a better understanding of the molecular mechanisms involved in HNSCC development, thereby enabling the exploration of ferroptosis-related pathophysiology from a new perspective, and thus may raise current therapies to a new standard. Although these results are encouraging, we

currently do not understand how hub regulators contributing to HNSCC development or which regulators with clinical transformation value, that improved prognostic outcomes. Thus, the further confirmed is required and necessary, based on animal models and large sample clinical verification, for the above analysis results.

## Data availability statement

The datasets presented in this study can be found in online repositories. The names of the repository/repositories and accession number(s) can be found below: GEO with accession GSE103322.

## Ethics statement

The studies involving human participants were reviewed and approved by The Ethics Committee of Guangdong Second Provincial General Hospital. The patients/participants provided their written informed consent to participate in this study.

## Author contributions

FL conceived and conceptualized the project, acquired data, and wrote the draft manuscript. LT and QL were responsible for

methodology and software. JT, JH, and ZY were responsible for writing, reviewing and editing. All authors read, edited several draft versions, and approved the final manuscript.

## Funding

This research was supported financially by the Doctoral workstation foundation of Guangdong Second Provincial General hospital (No. 2021BSH001); Funding by Science and Technology Projects in Guangzhou (No. 20212020298).

## Conflict of interest

The authors declare that the research was conducted in the absence of any commercial or financial relationships that could be construed as a potential conflict of interest.

## Publisher's note

All claims expressed in this article are solely those of the authors and do not necessarily represent those of their affiliated organizations, or those of the publisher, the editors and the reviewers. Any product that may be evaluated in this article, or claim that may be made by its manufacturer, is not guaranteed or endorsed by the publisher.

## References

- Anders, S., and Huber, W. (2010). Differential expression analysis for sequence count data. *Genome Biol.* 11 (10), R106. doi:10.1186/gb-2010-11-10-r106
- Aran, D., Looney, A. P., Liu, L., Wu, E., Fong, V., Hsu, A., et al. (2019). Reference-based analysis of lung single-cell sequencing reveals a transitional profibrotic macrophage. *Nat. Immunol.* 20 (2), 163–172. doi:10.1038/s41590-018-0276-y
- Cao, J. Y., and Dixon, S. J. (2016). Mechanisms of ferroptosis. *Cell. Mol. Life Sci.* 73 (11–12), 2195–2209. doi:10.1007/s00018-016-2194-1
- Chen, J., Bardes, E. E., Aronow, B. J., and Jegga, A. G. (2009). ToppGene Suite for gene list enrichment analysis and candidate gene prioritization. *Nucleic Acids Res.* 37, W305–W311. Web Server issue. doi:10.1093/nar/gkp427
- Chen, Z., Li, Z., Li, C., Huang, H., Ren, Y., Li, Z., et al. (2022). Manganese-containing polydopamine nanoparticles as theranostic agents for magnetic resonance imaging and photothermal/chemodynamic combined ferroptosis therapy treating gastric cancer. *Drug Deliv.* 29 (1), 1201–1211. doi:10.1080/10717544.2022.2059124
- Ferreira, M. R., Santos, G. A., Biagi, C. A., Silva Junior, W. A., and Zambuzzi, W. F. (2021). GSVA score reveals molecular signatures from transcriptomes for biomaterials comparison. *J. Biomed. Mat. Res. A* 109 (6), 1004–1014. doi:10.1002/jbma.a.37090
- Guo, L., Lu, J., Gao, J., Li, M., Wang, H., Zhan, X., et al. (2020). The function of SNHG7/miR-449a/ACSL1 axis in thyroid cancer. *J. Cell. Biochem.* 121 (10), 4034–4042. doi:10.1002/jcb.29569
- Hamman, J., Howe, C. L., Borgstrom, M., Baker, A., Wang, S. J., Bearely, S., et al. (2021). Impact of close margins in head and neck mucosal squamous cell carcinoma: A systematic review. *Laryngoscope* 132, 307–321. doi:10.1002/lary.29690
- Hänzelmann, S., Castelo, R., and Guinney, J. (2013). Gsva: gene set variation analysis for microarray and RNA-seq data. *BMC Bioinforma.* 14, 7. doi:10.1186/1471-2105-14-7
- Huang, S., Le, H., Hong, G., Chen, G., Zhang, F., Lu, L., et al. (2022). An all-in-one biomimetic iron-small interfering RNA nanoplateform induces ferroptosis for cancer therapy. *Acta Biomater.* S1742-7061, 00357–00359. doi:10.1016/j.actbio.2022.06.017
- Huang, Y., Huang, J., Huang, Y., Gan, L., Long, L., Pu, A., et al. (2020). TFRC promotes epithelial ovarian cancer cell proliferation and metastasis via up-regulation of AXIN2 expression. *Am. J. Cancer Res.* 10 (1), 131–147.
- Jing, F. Y., Zhou, L. M., Ning, Y. J., Wang, X. J., and Zhu, Y. M. (2021). The biological function, mechanism, and clinical significance of m6A RNA modifications in head and neck carcinoma: A systematic review. *Front. Cell Dev. Biol.* 9, 683254. doi:10.3389/fcell.2021.683254
- Kobak, D., and Berens, P. (2019). The art of using t-SNE for single-cell transcriptomics. *Nat. Commun.* 10 (1), 5416. doi:10.1038/s41467-019-13056-x
- Liang, C., Zhang, X., Yang, M., and Dong, X. (2019). Recent progress in ferroptosis inducers for cancer therapy. *Adv. Mat.* 31 (51), e1904197. doi:10.1002/adma.201904197
- Liberzon, A., Subramanian, A., Pinchback, R., Thorvaldsdóttir, H., Tamayo, P., Mesirov, J. P., et al. (2011). Molecular signatures database (MSigDB) 3.0. *Bioinformatics* 27 (12), 1739–1740. doi:10.1093/bioinformatics/btr260
- Liu, Z., Zhao, Q., Zuo, Z. X., Yuan, S. Q., Yu, K., Zhang, Q., et al. (2020). Systematic analysis of the aberrances and functional implications of ferroptosis in cancer. *iScience* 23 (7), 101302. doi:10.1016/j.isci.2020.101302
- López-Cortés, A., Cabrera-Andrade, A., Vázquez-Naya, J. M., Pazos, A., González-Díaz, H., Paz, Y. M. C., et al. (2020). Prediction of breast cancer proteins involved in immunotherapy, metastasis, and RNA-binding using molecular descriptors and artificial neural networks. *Sci. Rep.* 10 (1), 8515. doi:10.1038/s41598-020-65584-y

- Magesh, S., and Cai, D. (Forthcoming 2022). Roles of YAP/TAZ in ferroptosis. *Trends Cell Biol.* S0962-8924, 00136–142. doi:10.1016/j.tcb.2022.05.005
- Membreno, P. V., Luttrell, J. B., Mamidala, M. P., Schwartz, D. L., Hayes, D. N., Gleysteen, J. P., et al. (2021). Outcomes of primary radiotherapy with or without chemotherapy for advanced oral cavity squamous cell carcinoma: Systematic review. *Head. Neck* 43, 3165–3176. doi:10.1002/hed.26779
- Peng, H., Zhang, X., Yang, P., Zhao, J., Zhang, W., Feng, N., et al. (2023). Defect self-assembly of metal-organic framework triggers ferroptosis to overcome resistance. *Bioact. Mat.* 19, 1–11. doi:10.1016/j.bioactmat.2021.12.018
- Puram, S. V., Tirosh, I., Parikh, A. S., Patel, A. P., Yizhak, K., Gillespie, S., et al. (2017). Single-cell transcriptomic analysis of primary and metastatic tumor ecosystems in head and neck cancer. *Cell* 171 (7), 1611–1624. e1624. doi:10.1016/j.cell.2017.10.044
- Qiu, X., Mao, Q., Tang, Y., Wang, L., Chawla, R., Pliner, H. A., et al. (2017). Reversed graph embedding resolves complex single-cell trajectories. *Nat. Methods* 14 (10), 979–982. doi:10.1038/nmeth.4402
- Ryskalin, L., Busceti, C. L., Biagioni, F., Limanaqi, F., Familiari, P., Frati, A., et al. (2019). Prion protein in glioblastoma multiforme. *Int. J. Mol. Sci.* 20 (20), E5107. doi:10.3390/ijms20205107
- Sacco, A. G., Chen, R., Worden, F. P., Wong, D. J. L., Adkins, D., Swiecicki, P., et al. (2021). Pembrolizumab plus cetuximab in patients with recurrent or metastatic head and neck squamous cell carcinoma: An open-label, multi-arm, non-randomised, multicentre, phase 2 trial. *Lancet. Oncol.* 22 (6), 883–892. doi:10.1016/s1470-2045(21)00136-4
- Santos, E. M., Fraga, C. A. C., Xavier, A., Xavier, M. A. S., Souza, M. G., Jesus, S. F., et al. (2021). Prion protein is associated with a worse prognosis of head and neck squamous cell carcinoma. *J. Oral Pathol. Med.* 50, 985–994. doi:10.1111/jop.13188
- Stewart, P. A., Welsh, E. A., Slebos, R. J. C., Fang, B., Izumi, V., Chambers, M., et al. (2019). Proteogenomic landscape of squamous cell lung cancer. *Nat. Commun.* 10 (1), 3578. doi:10.1038/s41467-019-11452-x
- Thomas, R., Al-Rashed, F., Akhter, N., Al-Mulla, F., and Ahmad, R. (2019). ACSL1 regulates tnfa-induced GM-CSF production by breast cancer MDA-MB-231 cells. *Biomolecules* 9 (10), E555. doi:10.3390/biom9100555
- Thorsen, K., Mansilla, F., Schepeler, T., Øster, B., Rasmussen, M. H., Dyrskjøl, L., et al. (2011). Alternative splicing of SLC39A14 in colorectal cancer is regulated by the Wnt pathway. *Mol. Cell. Proteomics* 10 (1), M110002998. doi:10.1074/mcp.M110.002998
- Wang, G., Biswas, A. K., Ma, W., Kandpal, M., Coker, C., Grandgenett, P. M., et al. (2018). Metastatic cancers promote cachexia through ZIP14 upregulation in skeletal muscle. *Nat. Med.* 24 (6), 770–781. doi:10.1038/s41591-018-0054-2
- Wu, J., Minikes, A. M., Gao, M., Bian, H., Li, Y., Stockwell, B. R., et al. (2019). Intercellular interaction dictates cancer cell ferroptosis via NF2-YAP signalling. *Nature* 572 (7769), 402–406. doi:10.1038/s41586-019-1426-6
- Xie, Y., Xiao, Y., Liu, Y., Lu, X., Wang, Z., Sun, S., et al. (2022). Construction of a novel radiosensitivity- and ferroptosis-associated gene signature for prognosis prediction in gliomas. *J. Cancer* 13 (8), 2683–2693. doi:10.7150/jca.72893
- Xu, X. M., Wang, C. G., Zhu, Y. D., Chen, W. H., Shao, S. L., Jiang, F. N., et al. (2016). Decreased expression of SLC 39A14 is associated with tumor aggressiveness and biochemical recurrence of human prostate cancer. *Onco. Targets. Ther.* 9, 4197–4205. doi:10.2147/ott.S103640
- Yang, W. S., and Stockwell, B. R. (2016). Ferroptosis: Death by lipid peroxidation. *Trends Cell Biol.* 26 (3), 165–176. doi:10.1016/j.tcb.2015.10.014
- Zhai, F. G., Liang, Q. C., Wu, Y. Y., Liu, J. Q., and Liu, J. W. (2022). Red ginseng polysaccharide exhibits anticancer activity through GPX4 downregulation-induced ferroptosis. *Pharm. Biol.* 60 (1), 909–914. doi:10.1080/13880209.2022.2066139
- Zhang, H., Zhuo, Y., Li, D., Zhang, L., Gao, Q., Yang, L., et al. (2022). Dihydroartemisinin inhibits the growth of pancreatic cells by inducing ferroptosis and activating antitumor immunity. *Eur. J. Pharmacol.* 926, 175028. doi:10.1016/j.ejphar.2022.175028
- Zhang, Q., Zhou, W., Yu, S., Ju, Y., To, S. K. Y., Wong, A. S. T., et al. (2021). Metabolic reprogramming of ovarian cancer involves ACSL1-mediated metastasis stimulation through upregulated protein myristoylation. *Oncogene* 40 (1), 97–111. doi:10.1038/s41388-020-01516-4





## OPEN ACCESS

EDITED BY  
Guo Chen,  
Jinan University, China

REVIEWED BY  
Yue Sun,  
Stanford University, United States  
Yi Wang,  
Sichuan Academy of Medical Sciences  
and Sichuan Provincial People's  
Hospital, China  
Jie Xu,  
Northwestern University, United States

\*CORRESPONDENCE  
Hua You,  
youhua307@163.com

<sup>†</sup>These authors have contributed equally to this work

SPECIALTY SECTION  
This article was submitted to Molecular  
Diagnostics and Therapeutics,  
a section of the journal  
Frontiers in Molecular Biosciences

RECEIVED 27 May 2022  
ACCEPTED 08 July 2022  
PUBLISHED 11 August 2022

CITATION  
Tao Y, Wei L and You H (2022),  
Ferroptosis-related gene signature  
predicts the clinical outcome in  
pediatric acute myeloid leukemia  
patients and refines the 2017 ELN  
classification system.  
*Front. Mol. Biosci.* 9:954524.  
doi: 10.3389/fmolb.2022.954524

COPYRIGHT  
© 2022 Tao, Wei and You. This is an  
open-access article distributed under  
the terms of the [Creative Commons  
Attribution License \(CC BY\)](#). The use,  
distribution or reproduction in other  
forums is permitted, provided the  
original author(s) and the copyright  
owner(s) are credited and that the  
original publication in this journal is  
cited, in accordance with accepted  
academic practice. No use, distribution  
or reproduction is permitted which does  
not comply with these terms.

# Ferroptosis-related gene signature predicts the clinical outcome in pediatric acute myeloid leukemia patients and refines the 2017 ELN classification system

Yu Tao<sup>1†</sup>, Li Wei<sup>2†</sup> and Hua You<sup>1\*</sup>

<sup>1</sup>Department of Oncology, Affiliated Cancer Hospital & Institute of Guangzhou Medical University, Guangzhou, China, <sup>2</sup>NHC Key Laboratory of Birth Defects and Reproductive Health, Chongqing Population and Family Planning Science and Technology Research Institute, Chongqing, China

**Background:** The prognostic roles of ferroptosis-related mRNAs (FG) and lncRNAs (FL) in pediatric acute myeloid leukemia (P-AML) patients remain unclear.

**Methods:** RNA-seq and clinical data of P-AML patients were downloaded from the TARGET project. Cox and LASSO regression analyses were performed to identify FG, FL, and FGL (combination of FG and FL) prognostic models, and their performances were compared. Tumor microenvironment, functional enrichment, mutation landscape, and anticancer drug sensitivity were analyzed.

**Results:** An FGL model of 22 ferroptosis-related signatures was identified as an independent parameter, and it showed performance better than FG, FL, and four additional public prognostic models. The FGL model divided patients in the discovery cohort ( $N = 145$ ), validation cohort ( $N = 111$ ), combination cohort ( $N = 256$ ), and intermediate-risk group ( $N = 103$ ) defined by the 2017 European LeukemiaNet (ELN) classification system into two groups with distinct survival. The high-risk group was enriched in apoptosis, hypoxia, TNFA signaling via NFkB, reactive oxygen species pathway, oxidative phosphorylation, and p53 pathway and associated with low immunity, while patients in the low-risk group may benefit from anti-TIM3 antibodies. In addition, patients within the FGL high-risk group might benefit from treatment using SB505124\_1194 and JAK\_8517\_1739.

**Conclusion:** Our established FGL model may refine and provide a reference for clinical prognosis judgment and immunotherapies for P-AML patients.

## KEYWORDS

ferroptosis, prognostic model, pediatric acute myeloid leukemia, immune infiltration, immune checkpoint (ICP)

## Introduction

Acute myeloid leukemia (AML) encompasses a high heterogeneity hematologic malignancy, characterized by uncontrolled proliferation of myeloid blasts or progranulocytes, leading to suppression of the normal hematopoietic function of bone marrow (Newell and Cook, 2021). Its heterogeneity is related to clinical behavior, morphology, immunophenotyping, germline and somatic genetic abnormalities, and epigenetic anomalies, as well as patient outcomes (Creutzig et al., 2012).

The 2017 European LeukemiaNet (ELN) classification system integrated karyotypic abnormalities and genetic mutations to classify AML patients into three genetic risk groups: favorable, intermediate, and adverse, and subsequently found widespread adoption in clinical practice (Döhner et al., 2017). However, around 50% of AML patients are still classified as the intermediate-risk subgroup, and their survival is highly heterogeneous (Wang et al., 2017), implying the need for integrating additional prognostic factors to improve risk stratification power.

Pediatric acute myeloid leukemia (P-AML), despite constant treatment improvements over the past decades, remains a catastrophic disease with 3-year relapse rates up to 30% and 5-year survival rates below 75% (Unis et al., 2021). Since most of the genetic investigations are based on adult AML patients, distinct molecular genetic landscapes have been mapped out between pediatric and adult AML patients (Bolouri et al., 2018; Marceau-Renaut et al., 2018). It is important to define a better description of the pattern of molecular aberrations in P-AML in order to refine prognostication and develop age-specific therapies in such patients.

Ferroptosis is a new mode of regulated cell death, which is usually accompanied by iron accumulation and lipid peroxidation during the cell death process and is involved in the development of many critical diseases, such as tumors, ischemic tissue damage, kidney injury, neurodegeneration, and blood diseases (Li et al., 2020), especially recent research has shown that ferroptosis-inducing agents and genetic modulators of ferroptosis resulted in a synergistic effect on the promotion of early death of AML cells and increasing the sensitivity of leukemia cells to chemotherapeutic agents (Yu et al., 2015; Birsan et al., 2021). Thus, we reasonably hypothesize that ferroptosis is involved in the pathobiology of AML including pediatric patients. In addition, emerging evidence has proven that high-complexity links between N6-methyladenosine (m6A) and different types of programmed cell death pathways might be closely associated with the initiation, progression, and resistance of cancer (Liu et al., 2022). An intriguing study investigated the mechanisms underlying the oncogenic role of m6A demethylase FTO in AML and found that a bio-imprinted nanoplatform targeting the FTO/m6A pathway can selectively target leukemic stem cells (LSCs) and induce ferroptosis (Cao et al., 2022),

implying the clinical potential of targeting “m6A modification-ferroptosis axis” as a treatment strategy against AML.

Currently, a few studies indicated that abnormalities in mRNAs or long non-coding RNAs (lncRNAs) of ferroptosis were closely correlated with cancer patient outcomes (Lelièvre et al., 2020). However, no study has been performed to discover ferroptosis-related prognostic signatures and predict P-AML outcomes.

Here, the main aim of the present study was to explore the prognostic roles of ferroptosis-related mRNAs and lncRNAs for P-AML patients, construct three prognostic models based on the RNA sequencing data of pediatric samples from the TARGET AML cohort (Downing et al., 2012), compare their predictive efficiency among three models to obtain the best one, and investigate the potential benefits of immune therapy. Second, we explored whether the incorporation of the best ferroptosis-related signatures could further improve the prognostic prediction for the intermediate-risk subgroup of the 2017 ELN risk classification system.

## Materials and methods

### Samples and datasets

RNA-seq data and clinical information of 256 P-AML samples were collected at the first presentation/diagnosis from the Therapeutically Applicable Research to Generate Effective Treatment (TARGET) AML program and were available from NCI's data portal (collected on 18/September/2021). Out of these 256 samples, 145 have been harmonized by the NCI's Genomic Data Commons (GDC) (Zhang et al., 2021). Raw expression counts of these 145 AML patients were extracted TARGET-AML program of GDC (collected on 18/August/2021), as the TARGET-discovery cohort. The remaining 111 cases were used as a validation cohort and raw expression counts were gathered from the (NCI)'s data portal (TARGET-validation cohort). For model validation in the adult AML cohort, RNA-Sequencing data of 151 adult patients with AML and the corresponding clinical information were extracted from the The Cancer Genome Atlas (TCGA)-LAML program of GDC. The “DESeq2” package based on the negative binomial distribution was used to normalize the raw count expression data (Love et al., 2014). Detailed clinical information about the data cohorts is provided in Table 1, and the workflow is briefly depicted in Figure 1.

### Ferroptosis-related mRNAs and lncRNAs

We obtained 259 ferroptosis-related genes from the FerrDb database (<http://www.zhounan.org/ferrdb>, collected on 16/

TABLE 1 Summary of P-AML patient clinical information from TARGET-Discovery and validation databases.

	TARGET-GDC	TARGET-111	TAREGT-combined	<i>p</i> -value
Patients, <i>n</i>	145	111	256	
Gender				0.62
Female	71 (48.97%)	50 (45.05%)	121 (47.27%)	
Male	74 (51.03%)	61 (54.95%)	135 (52.73%)	
Age at diagnosis in days				
Mean $\pm$ SD	3,364.50 $\pm$ 2,210.76	3,776.92 $\pm$ 1980.25	3,543.32 $\pm$ 2,119.79	0.12
Median [min-max]	3,438.00 [137.00,8231.00]	4,183.00 [10.00,7442.00]	3,831.00 [10.00,8231.00]	
Cytogenetic abnormality, carriers (%)				
t (8; 21)	21 (14.48%)	23 (20.72%)	44 (17.19%)	0.42
t (6; 9)	1 (0.69%)	2 (1.80%)	3 (1.17%)	0.71
t (3; 5) (q25; q34)	2 (1.38%)	1 (0.90%)	3 (1.17%)	0.92
t (6; 11) (q27; q23)	2 (1.38%)	2 (1.80%)	4 (1.56%)	0.95
t (9; 11) (p22; q23)	13 (8.97%)	5 (4.50%)	18 (7.03%)	0.37
t (10; 11) (p11.2; q23)	4 (2.76%)	2 (1.80%)	6 (2.34%)	0.86
t (11;19) (q23;p13.1)	5 (3.45%)	0	5 (1.95%)	0.14
inv (16)	28 (19.31%)	14 (12.61%)	42 (16.41%)	0.34
del5q	1 (0.69%)	0	1 (0.39%)	0.67
del7q	4 (2.76%)	5 (4.50%)	9 (3.52%)	0.75
del9q	5 (3.45%)	5 (4.50%)	10 (3.91%)	0.90
trisomy 8	9 (6.21%)	9 (8.11%)	18 (7.03%)	0.83
trisomy 21	4 (2.76%)	1 (0.90%)	5 (1.95%)	0.21
Minus Y	6 (4.14%)	5 (4.50%)	11 (4.30%)	0.97
Minus X	6 (4.14%)	4 (3.60%)	10 (3.91%)	0.96
FLT3_ITD_positive	11 (7.59%)	29 (26.13%)	40 (15.63%)	<0.001
AML with biallelic mutations of CEBPA	7 (4.86%)	9 (8.33%)	16 (6.25%)	0.41
AML with mutated WT1	8 (5.67%)	9 (8.33%)	17 (6.64%)	0.83
AML with mutated NPM1	5 (3.45%)	13 (12.26%)	18 (7.03%)	0.07
Median WBC count (range), $3 \times 10^9/L$	45.30 [1.30,519.00]	42.80 [0.90,432.00]	44.75 [0.90,519.00]	0.36
Median percentage of BM blasts (range)	74.80 [14.00,100.00]	72.00 [25.00,98.00]	73.00 [14.00,100.00]	0.41
Median percentage of PB (range)	61.00 [0.0e+0,97.00]	61.00 [0.0e+0,97.00]	61.00 [0.0e+0,97.00]	0.28
2017 ELN classification system, <i>n</i> (%)				<0.001
Favorable	60 (41.38%)	52 (46.85%)	112 (43.75%)	
Intermediate	69 (47.59%)	34 (30.63%)	103 (40.23%)	
Adverse	8 (5.52%)	20 (18.02%)	28 (10.94%)	
Unknown	8 (5.52%)	5 (4.50%)	13 (5.08%)	
FAB subtype				0.15
M0	3 (2.07%)		3 (1.17%)	
M1	17 (11.72%)	16 (14.41%)	33 (12.89%)	
M2	35 (24.14%)	31 (27.93%)	66 (25.78%)	
M4	36 (24.83%)	26 (23.42%)	62 (24.22%)	
M5	30 (20.69%)	19 (17.12%)	49 (19.14%)	
M6	2 (1.38%)	1 (0.90%)	3 (1.17%)	
M7	7 (4.83%)	6 (5.41%)	7 (2.73%)	
NOS	8 (5.52%)	12 (10.81%)	14 (5.47%)	
Unknown	7 (4.83%)	16 (14.41%)	19 (7.42%)	
CNS disease				0.70
No	135 (93.10%)	101 (90.99%)	236 (92.19%)	
Yes	10 (6.90%)	10 (9.01%)	20 (7.81%)	

(Continued on following page)

TABLE 1 (Continued) Summary of P-AML patient clinical information from TARGET-Discovery and validation databases.

	TARGET-GDC	TARGET-111	TAREGT-combined	<i>p</i> -value
Chloroma				<b>0.03</b>
No	134 (93.06%)	92 (82.88%)	226 (88.28%)	
Yes	10 (6.94%)	19 (17.12%)	29 (11.33%)	
Unknown	1 (0.69%)		1 (0.39%)	
MRD at the end of course 1				0.14
No	83 (75.45%)	52 (46.85%)	135 (52.73%)	
Yes	27 (24.55%)	20 (18.02%)	47 (18.36%)	
Unknown	35 (13.67%)	39 (35.13%)	74 (28.91%)	
HSCT, <i>n</i>				0.06
No	131 (90.34%)	89 (80.18%)	220 (85.94%)	
Yes	13 (8.97%)	19 (17.11%)	32 (12.50%)	
Yes	1 (0.69%)	3 (2.71%)	4 (1.56%)	
Event-free survival time in days				0.41
Mean ± SD	954.70 ± 972.36	1,058.67 ± 1,022.27	999.78 ± 993.67	
Median [min-max]	458.00 [77.00,3630.00]	506.00 [2.00,4037.00]	461.00 [2.00,4037.00]	
Overall Survival Time in days				0.32
Mean ± SD	1,577.18 ± 1,064.78	1,446.80 ± 1,008.87	1,520.65 ± 1,040.91	
Median [min-max]	1,464.00 [112.00,4022.00]	1,532.00 [2.00,4037.00]	1,523.50 [2.00,4037.00]	
Vital Status				0.24
Alive	77 (53.10%)	68 (61.26%)	145 (56.64%)	
Dead	68 (46.90%)	43 (38.74%)	111 (43.36%)	

Notes: WBC, white blood cell; BM, bone marrow; PB, peripheral blast; ELN, European LeukemiaNet; FAB, French–American–British; NOS, not otherwise specified; CNS, central nervous system; MRD, measurable residual disease; HSCT, hematopoietic stem-cell transplantation; SD, standard deviation.

November/2021), the first manually curated resource for regulators and markers of ferroptosis, which was released in January 2020 (Zhou and Bao, 2020) (Supplementary Table S1). lncRNAs were extracted by the GENCODE v20 annotation (<http://www.genencodegenes.org>) (Derrien et al., 2012). Ferroptosis-related lncRNAs co-expressed with ferroptosis-related genes were identified according to Pearson's correlation analysis by the correlation test function of R (correlation coefficient  $Cor > 0.8$ ,  $p < 0.001$ ).

## Prognostic model construction and validation

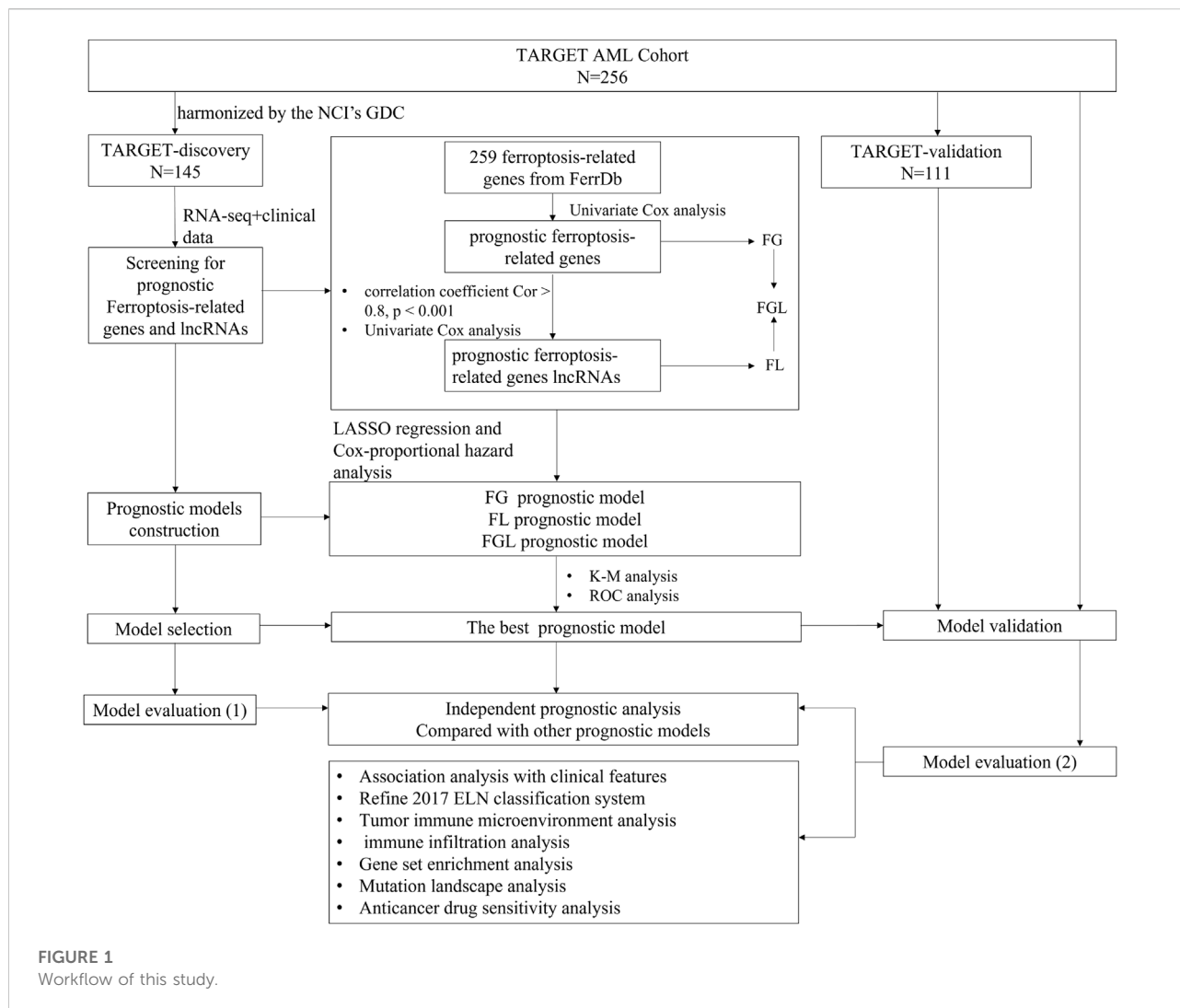
Univariate Cox regression was applied to screen prognosis-related mRNAs and lncRNAs in the discovery cohort, using  $p < 0.05$  as the cutoff. Then, model-making procedures were conducted for three lists of prognostic ferroptosis-related signatures separately, ferroptosis-related mRNA genes (FG), ferroptosis-related lncRNAs (FL), and ferroptosis-related mRNA genes combined with ferroptosis-related lncRNAs (FGL), and consisted of the following steps. Step 1, the least absolute shrinkage and selection operator (LASSO) Cox regression analysis was conducted on the prognosis-related signatures, and the optimal penalty parameter “ $\lambda$ ” was selected by the 10-fold cross-validation method. Step 2, the

prognostic risk score formula was established as follows: risk score = expression of gene 1  $\times$  *Coef*<sub>1</sub> + expression of gene 2  $\times$  *Coef*<sub>2</sub> + ... + expression of gene *n*  $\times$  *Coef*<sub>*n*</sub>. *Coef* indicates the regression coefficients of each signature selected from the LASSO regression analysis. According to the risk model, samples in the discovery cohort were given a risk score and then divided into high- and low-risk groups using the median score as the cutoff. The survival curves of the patients in the high- and low-risk groups were drawn with the R-package “Survival,” and the survival time of the two groups was compared by log-rank test. The receiver operating characteristic (ROC) curves were drawn using the R package “survival ROC” for validation of the risk model and the AUC values of 1-, 3-, and 5-year survival were calculated. The best prognostic model identified with prognostic significance was selected for further analysis and the same algorithm was performed in the TARGET-validation cohort, TARGET-combined cohort, and TCGA-LAML cohort (151 adult patients), with the same coefficients derived for the discovery dataset.

## Tumor immune microenvironment analysis

Tumor microenvironment, immune, and stroma scores were calculated based on the gene expression data using ESTIMATE





(Yoshihara et al., 2013) and xCell (<https://xcell.ucsf.edu>) tool (Aran et al., 2017). Estimating the proportion of immune and cancer cells (EPIC) was applied to estimate the infiltration ratio of eight types of immune cells (Racle et al., 2017). Furthermore, based on the review of relevant literature (Gong et al., 2018; Rowshanravan et al., 2018; Qin et al., 2019; Wang et al., 2020), we explored the difference in the expression of 10 potential immune checkpoint genes between the groups. Detailed information is provided in [Supplementary Note S1](#).

## Functional and pathway enrichment analysis

Gene set enrichment analysis (GSEA) on the 50 hallmark gene sets was used to identify the potential molecular mechanisms or potential functional pathways that involve the prognostic model (Liberzon et al., 2015). Significant gene sets

were based on the following parameters: normalized enrichment score (NES)  $| > 1$ , nominal  $p$ -value  $< 0.05$ , and false discovery rate (FDR)  $q$ -value  $< 0.05$ . Furthermore, 19 m6A-related genes and regulators based on Juan Xu's research (Li et al., 2019) were further screened and investigated in high- and low-risk groups.

## Sensitivity analysis of common chemotherapeutic drugs

To evaluate the potential of FGL models in clinical practice for P-AML treatment, the half-maximal inhibitory concentration ( $IC_{50}$ ) of commonly administered chemotherapeutic drugs in the TARGET-combined cohort was calculated using the algorithm R package "oncoPredict" (Maeser et al., 2021). The algorithm predicts the clinical drug response value ( $IC_{50}$ ) in patients based on gene expression data in tumor, which is derived from the ridge regression model based on drug sensitivity

data from the Genomics of Drug Sensitivity in Cancer (GDSC) database.

## Statistical analysis

Kaplan–Meier curves were plotted to estimate overall survival (OS) time and event-free survival (EFS) time, and the data were statistically compared with the log-rank test. Univariate and multivariate analyses were performed by the Cox proportional hazard model. The ROC curve was established, and the area under the curve (AUC) was calculated to determine the predictive value of the prognostic model. Five-fold cross-validation was applied for model evaluation (Supplementary Note S2). All statistical analyses were carried out using R (3.5.2) software and  $p < 0.05$  was taken as being statistically significant. The Wilcoxon test was used to compare the immune scores, immune infiltrate, and expression of genes between groups.

## Results

### Prognostic ferroptosis-related signatures are identified

Normalized gene expression data of the TARGET-discovery cohort included 244 ferroptosis-related genes. Univariate Cox regression analysis revealed 39 ferroptosis-related genes with significant prognostic value for P-AML ( $p < 0.05$ ) (Supplementary Table S2). By ferroptosis-related lncRNA co-expression analysis and univariate Cox regression analysis, we identified 8 prognostic ferroptosis-related lncRNAs out of 2,734 co-expressed lncRNAs (Supplementary Table S2). These 39 ferroptosis-related genes and 8 lncRNAs and merged lists were served as candidate lists for LASSO Cox regression analysis, respectively. After optimal parameter (lambda) selection in the LASSO regression, three prognostic ferroptosis-related signature models with 20 FG components, 6 FL components, and 22 FGL components were built, respectively (Supplementary Figure S1; Supplementary Table S3). The expression level of each gene and LASSO regression coefficient ( $\beta$ ) were integrated to calculate the FG, FL, and FGL risk score for each patient (Supplementary Table S4).

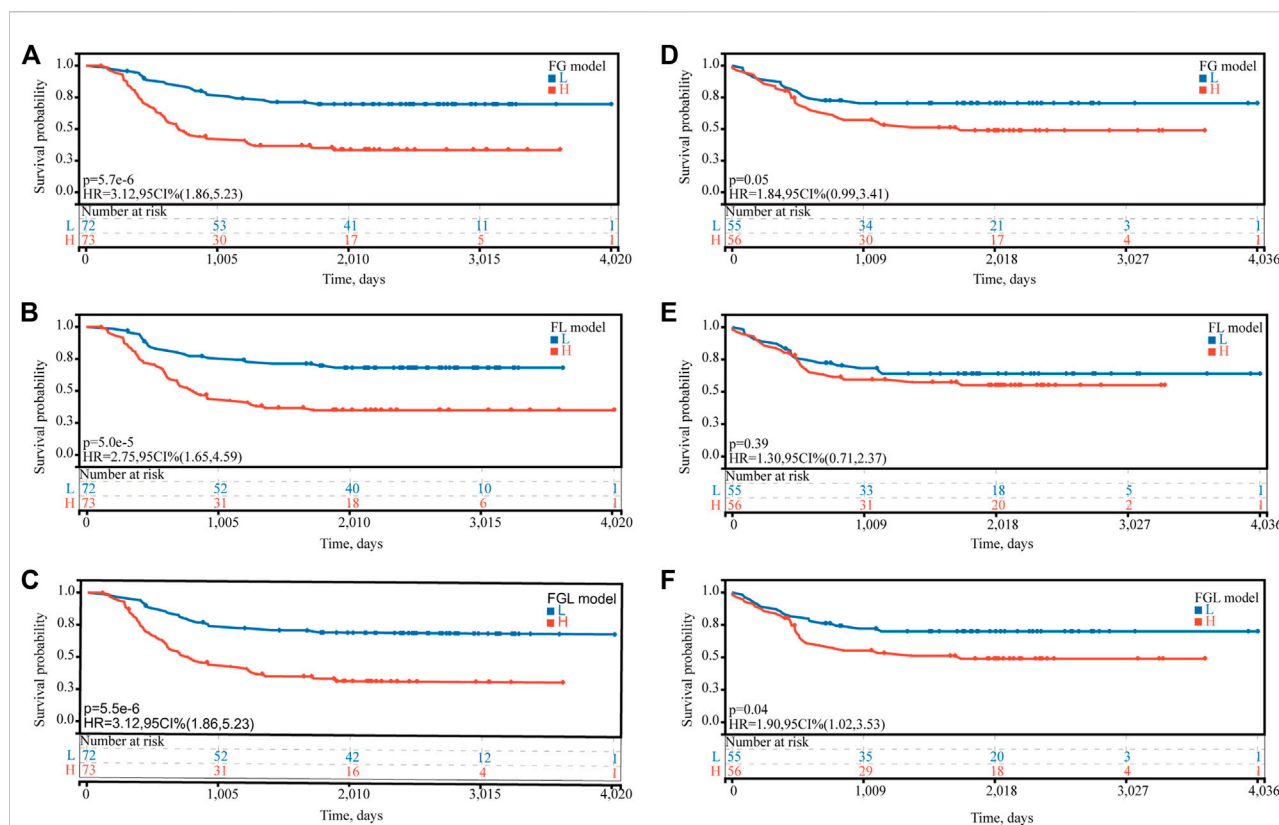
### Prognostic ferroptosis-related models are established and optimized

In the TARGET-discovery cohort, patients were stratified into high- and low-risk groups using the median risk score as the cutoff value. Statistical differences in overall-survival probability have been identified for the patient groups stratified by the cutoff

point of FG, FL, and FGL risk scores, and the survival rate of P-AML patients in the low-risk group of the three models was significantly higher than that in the high-risk group (all  $p < 0.05$ ) (Figures 2A–C). However, only the FGL model was validated in both the TARGET-validation cohort ( $p = 0.04$ , Figures 2D–F) and the TARGET-combined cohort ( $p < 0.001$ , Figure 3A), with significant differences in the survival rate between the two risk groups. The same results have been found for the event-free survival rate (EFS) (Supplementary Figure S2). Thus, the FGL risk score was selected for all subsequent analyses. The distribution and status of OS of the TARGET-combined cohort were then analyzed by ranking the risk scores (Figure 3B). The results showed that patients with higher FGL risk scores had a worse prognosis. Expression profiles of the 22 ferroptosis-related signatures are listed in the heatmap of Figure 3B. The AUC corresponding to 1-, 3- and 5-year OS in the TARGET-combined cohort were 0.70, 0.68, and 0.70, respectively, indicating that the predictive efficiency of the model was good (Figure 3C).

### Increasing FGL risk score is an independent predictor for poorer OS

FLT3\_ITD\_positive, WT1 mutation, 2017 ELN classification system, and FGL risk score were considered significant risk parameters in the univariate analysis ( $p < 0.05$ ) (Figure 4A), and further multivariate Cox analysis indicated that the FGL risk score was the only independent risk parameter in the discovery cohort (HR = 3.772, 95% CI = 2.529–5.625) (Figure 4B). In the TARGET-combined cohort, the results indicated that the higher FGL risk score was also the only independent poor prognosticator for OS (HR = 1.515, 95% CI = 1.344–1.708) (Figures 4C,D). Several prognostic models have been established or validated in the TARGET cohort recently: LSC17 (Duployez et al., 2019), LSC6 (Elsayed et al., 2020), yang\_10\_genes (Yang et al., 2020), docking\_16\_genes (Docking et al., 2021), and cai\_3\_genes (Cai et al., 2021). Risk scores were further calculated based on the coefficient defined in these studies and used further for correlation analysis with FGL risk score. FGL risk score was negatively correlated with LSC17 risk score and positively correlated with the docking\_16\_genes model and cai\_3\_genes model (Figures 5A,B). FGL risk model demonstrated the best predictive performance compared with previous prognostic models, 2017 ELN classification system, and other prognostic molecular characteristics in TARGET-discovery and -combined cohort, respectively (Figures 5C,D). The five-fold cross-validation method was applied to give a robust estimation of the performance of the FGL model. As shown in Supplementary Table S5, in the testing stage, the AUC of the FGL model ranged from 0.693 to 0.741 in the TARGET-discovery cohort and 0.693 to 0.741 in the combined cohort.

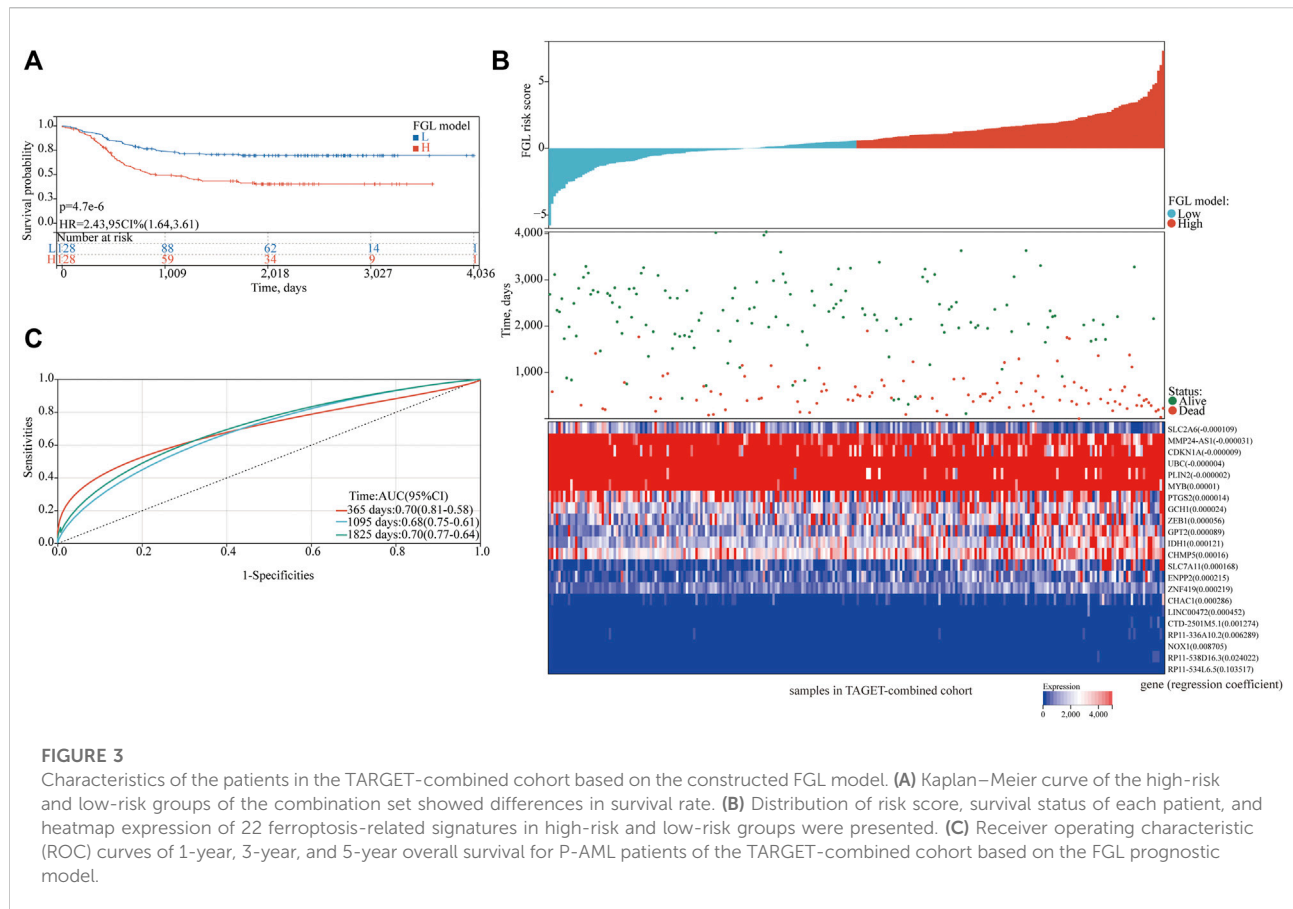


Collectively, the risk score calculated according to the 22 ferroptosis-related signatures could serve as an independent and stable prognostic parameter for P-AML patients. However, we further explored the predictive ability of the FGL prognostic model for prognosis in adult AML patients. OS was not significantly different in the high-risk and low-risk groups of the TCGA-LAML cohort ( $p = 0.37$ , [Supplementary Figure S3](#)).

## Evaluation of the relationship between clinicopathological and molecular characteristics and the ferroptosis-related signature

We next investigated the clinical, molecular, and immune features of the low- and high-risk groups in the TARGET-combined cohort, considering the sample size. The results identified a significant difference between the two groups with respect to the distribution of *inv* (16) mutation, WT1 mutation, 2017 ELN classification system, and FAB subtype (all  $p < 0.05$ , [Table 2](#)). Of the 42 patients with *inv*

(16), 7.14% (3/42) were in the high-risk group and 92.86% (39/42) were in the low-risk group ( $p < 0.001$ ) ([Figure 6A](#)); WT1 mutation occurs in 6.85% (17/256) of AML patients and 13 of them were in the high-risk group ( $p = 0.04$ ) ([Figure 6A](#)). Consistent with expectations, the number of people identified as adverse-risk by the 2017 ELN classification system was significantly higher in the high-risk group than that of the low-risk group (14.06 vs. 7.81%), while the number of people identified as favorable-risk was on the contrary (27.34 vs. 60.16%). The morphological subtypes in order of frequency among P-AML cases were M2 (66/256, 25.78%), M4 (62/256, 24.22%), M5 (49/256, 19.14%), M1 (33/256, 12.89%), M7 (7/256, 2.73%), and M0 and M6 (3/256 and 1.17%). No M3 case was identified in the present study. M4 subtype was more common in the low-risk group than in the high-risk group (35.16 vs. 13.28%) ([Figure 6B](#)). The mutation landscapes in the FGL high- and low-risk groups showed top mutated genes with a frequency above 5%, and NARS mutation was the predominant alteration in both the high- and low-risk groups. The second highest mutation rate (30.49%) was found for KIT in the high-risk group, while



the mutation rate is 5.19% in the low-risk group ( $p < 0.001$ ) (Figures 6C,D).

## Association of FGL risk score with the intermediate-risk subgroup of 2017 ELN is defined

We identified 112 (43.75%), 103 (40.23%), and 28 (10.94%) patients in the TARGET-combined cohort classified as favorable-, intermediate-, and adverse-risk groups, respectively, according to the 2017 ELN classification system. Our results validated the prognostic significance of the revised 2017 ELN classification system in the TARGET-combined cohort ( $p < 0.001$ ) (Figures 7A,B). Individuals in the favorable group defined by the 2017 ELN classification system had significantly better OS. However, no significant prognostic difference between the intermediate and adverse groups was found ( $p = 0.76$  for OS;  $p = 0.96$  for EFS). Then, in the 2017 ELN intermediate-risk subgroup of the TARGET-combined cohort ( $N = 103$ ), we found 70 patients grouped with a high FGL risk score and 33 patients grouped with a low FGL risk score, which could be well risk-stratified by the FGL scoring system ( $p = 0.003$  for OS;  $p = 0.0047$  for EFS, Figures 7C,D).

## Functional analysis and immune characteristics of high-risk and low-risk groups

Examining the molecular trends of divergence across two risk groups using GSEA revealed 8 hallmark gene sets significantly perturbed (Figure 8A, and detailed results for 50 hallmark gene sets are shown in Supplementary Table S6). Six tumor-related hallmarks, apoptosis, hypoxia, TNFA signaling *via* NFKB, reactive oxygen species pathway, oxidative phosphorylation, and *p53* pathway, were significantly enriched in the low-risk group, while bile acid (BA) metabolism pathway and spermatogenesis were found significantly enriched in the high-risk group.

To determine whether the FGL risk score was related to tumor immunity, we next evaluated the correlation between FGL risk and immune score and immune cell infiltration. We observed significantly higher immune score, microenvironment score, stromal score, and ESTIMATE score in the low-risk group (Figure 8B and Figure 8C; all  $p < 0.05$ ). Strong relationship between infiltration levels of several immune cells and FGL risk score has also been established. As shown in Figure 8D, infiltration levels of cancer-associated fibroblasts (CAFs), CD4<sup>+</sup> T cells, and endothelial were significantly



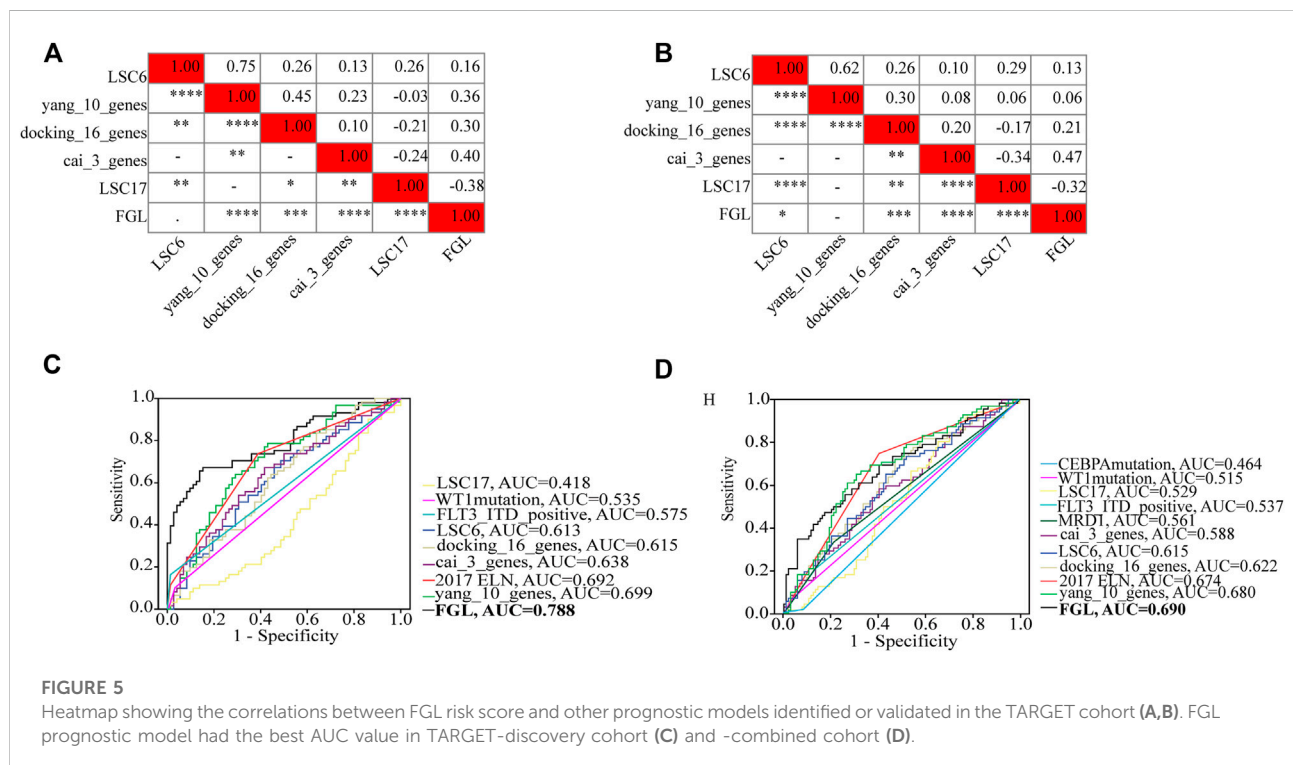
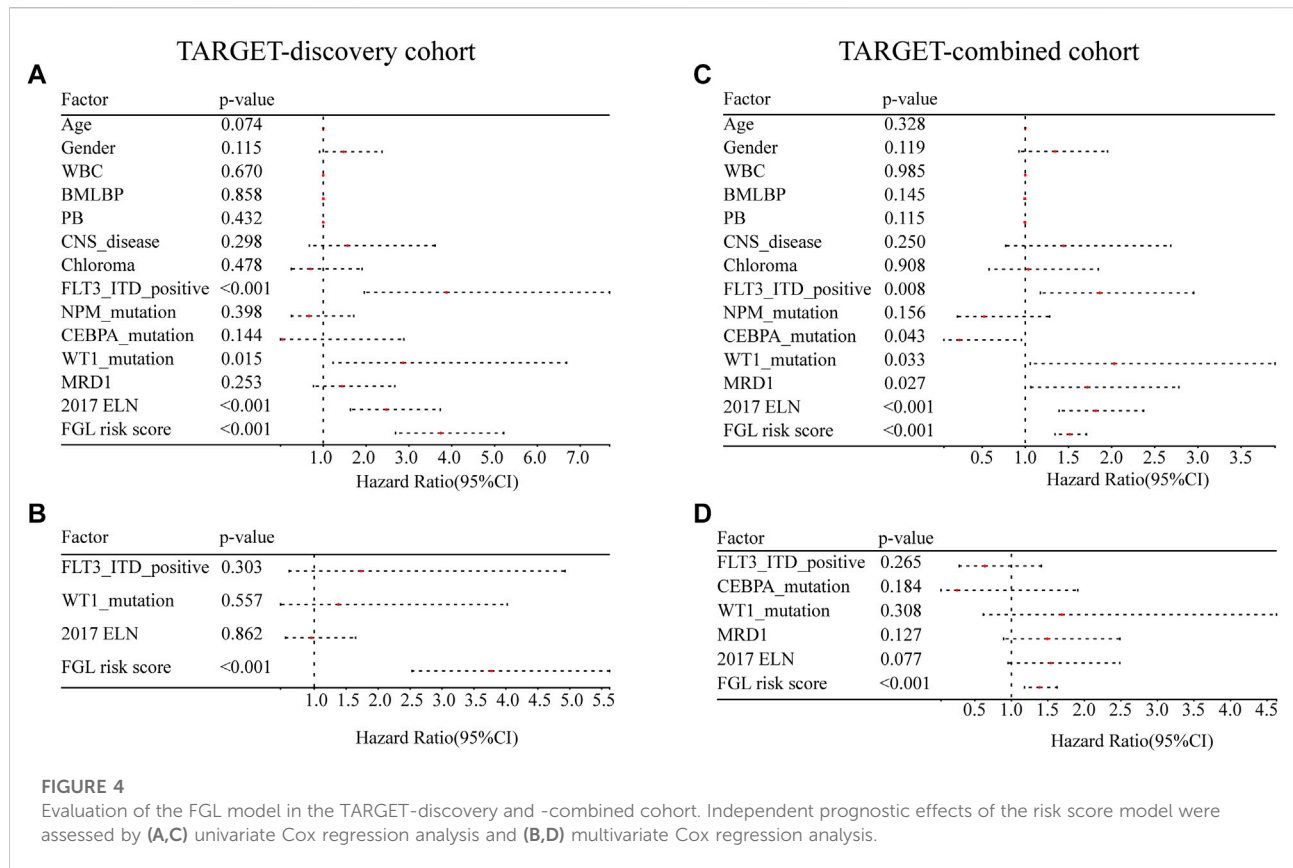


TABLE 2 Clinicopathological Characteristics for high and low FGL risk score subgroups.

	High-risk group	Low-risk group	TAREGT-combined	<i>p</i> -value
Patients, <i>n</i>	128	128	256	
Gender				0.620
Female	63 (49.22%)	58 (45.31%)	121 (47.27%)	
Male	65 (50.78%)	70 (54.69%)	135 (52.73%)	
Age at diagnosis in days				0.882
Mean $\pm$ SD	3,563.05 $\pm$ 2094.95	3,523.59 $\pm$ 2,152.39	3,543.32 $\pm$ 2,119.79	
Median [min-max]	3,810.50 [10.00,7442.00]	3,871.50 [113.00,8231.00]	3,831.00 [10.00,8231.00]	
Cytogenetic abnormality				
t (8; 21) carriers (%)	17 (13.28%)	27 (21.09%)	44 (17.19%)	0.16
t (6; 9)	3 (2.34%)	0	3 (1.17%)	0.17
t (3; 5) (q25; q34)	3 (2.34%)	0	3 (1.17%)	0.17
t (6; 11) (q27; q23)	3 (2.34%)	1 (0.78%)	4 (1.56%)	0.46
t (9; 11) (p22; q23)	10 (7.81%)	8 (6.25%)	18 (7.03%)	0.70
t (10; 11) (p11.2; q23)	4 (3.13%)	2 (1.56%)	6 (2.34%)	0.55
t (11;19) (q23;p13.1)	4 (3.13%)	1 (0.78%)	5 (1.95%)	0.31
inv (16)	3 (2.34%)	39 (30.47%)	42 (16.41%)	<0.001
del5q	1 (0.78%)	0	1 (0.39%)	0.46
del7q	3 (2.34%)	6 (4.69%)	9 (3.52%)	0.43
del9q	4 (3.13%)	6 (4.69%)	10 (3.91%)	0.59
trisomy 8	12 (9.38%)	6 (4.69%)	18 (7.03%)	0.28
trisomy 21	5 (3.91%)	0	5 (1.95%)	0.06
Minus Y	3 (2.34%)	8 (6.25%)	11 (4.30%)	0.21
Minus X	5 (3.91%)	5 (3.91%)	10 (3.91%)	0.75
FLT3_ITD_positive	25 (19.53%)	15 (11.72%)	40 (15.63%)	0.12
AML with biallelic mutations of CEBPA	8 (6.40%)	8 (6.25%)	16 (6.35%)	1.00
AML with mutated WT1	13 (10.57%)	4 (3.20%)	17 (6.85%)	0.04
AML with mutated NPM1	11 (9.02%)	7 (5.65%)	18 (7.32%)	0.44
Median WBC count (range), $3 \times 10^9/L$	30.25 [0.90,519.00]	56.45 [1.60,405.50]	44.75 [0.90,519.00]	0.24
Median percentage of BM blasts (range)	72.00 [14.00,100.00]	74.30 [21.00,100.00]	73.00 [14.00,100.00]	0.38
Median percentage of PB (range)	61.00 [0.0e+0,97.00]	61.00 [0.0e+0,97.00]	61.00 [0.0e+0,97.00]	0.06
2017 ELN classification system, <i>n</i> (%)				<0.001
Favorable	35 (27.34%)	77 (60.16%)	112 (43.75%)	
Intermediate	70 (54.69%)	33 (25.78%)	103 (40.23%)	
Adverse	18 (14.06%)	10 (7.81%)	28 (10.94%)	
Unknown	5 (3.91%)	8 (6.25%)	13 (5.08%)	
FAB subtype				<0.001
M0	3 (2.34%)	0	3 (1.17%)	
M1	23 (17.97%)	10 (7.81%)	33 (12.89%)	
M2	33 (25.78%)	33 (25.78%)	66 (25.78%)	
M4	17 (13.28%)	45 (35.16%)	62 (24.22%)	
M5	27 (21.09%)	22 (17.19%)	49 (19.14%)	
M6	2 (1.56%)	1 (0.78%)	3 (1.17%)	
M7	7 (5.47%)	0	7 (2.73%)	
NOS	6 (4.69%)	8 (6.25%)	14 (5.47%)	
Unknown	10 (7.81%)	9 (7.03%)	19 (7.42%)	
CNS disease				0.10
No	122 (95.31%)	114 (89.06%)	236 (92.19%)	
Yes	6 (4.69%)	14 (10.94%)	20 (7.81%)	

(Continued on following page)

TABLE 2 (Continued) Clinicopathological Characteristics for high and low FGL risk score subgroups.

	High-risk group	Low-risk group	TAREGT-combined	<i>p</i> -value
Chloroma				0.71
No	114 (89.76%)	112 (87.50%)	226 (88.63%)	
Yes	13 (10.24%)	16 (12.50%)	29 (11.37%)	
Unknown			1 (0.39%)	
MRD				0.11
No	63 (49.22%)	72 (56.25%)	135 (52.73%)	
Yes	30 (23.44%)	17 (13.28%)	47 (18.36%)	
Unknown	35 (27.34%)	39 (30.47%)	74 (28.91%)	
HSCT, <i>n</i>				0.11
No	110 (85.94%)	110 (85.94%)	220 (85.94%)	
Yes	14 (10.94%)	18 (14.06%)	32 (12.50%)	
Unknown	4 (3.13%)	0	4 (1.56%)	
Event-free survival time in days				<b>0.001</b>
Mean ± SD	800.63 ± 895.12	1,198.93 ± 1,049.46	999.78 ± 993.67	
Median [min-max]	379.50 [2.00,3632.00]	653.00 [80.00,4037.00]	461.00 [2.00,4037.00]	
Overall survival time in days				<b>&lt;0.001</b>
Mean ± SD	1,228.48 ± 962.09	1812.81 ± 1,038.19	1,520.65 ± 1,040.91	
Median [min-max]	824.50 [2.00,3632.00]	1940.00 [80.00,4037.00]	1,523.50 [2.00,4037.00]	
Vital status				<b>&lt;0.001</b>
Alive	55 (42.97%)	90 (70.31%)	145 (56.64%)	
Dead	73 (57.03%)	38 (29.69%)	111 (43.36%)	
FG risk score				<b>&lt;0.001</b>
Mean ± SD	1.91 ± 1.20	-0.57 ± 1.10	0.67 ± 1.69	
Median [min-max]	1.64 [0.59,7.31]	-0.21 [-5.77,0.59]	0.59 [-5.77,7.31]	

Notes: WBC, white blood cell; BM, bone marrow; PB, peripheral blast; ELN, European LeukemiaNet; FAB, French–American–British; NOS, not otherwise specified; CNS, central nervous system; MRD, measurable residual disease; HSCT, hematopoietic stem-cell transplantation; SD, standard deviation.

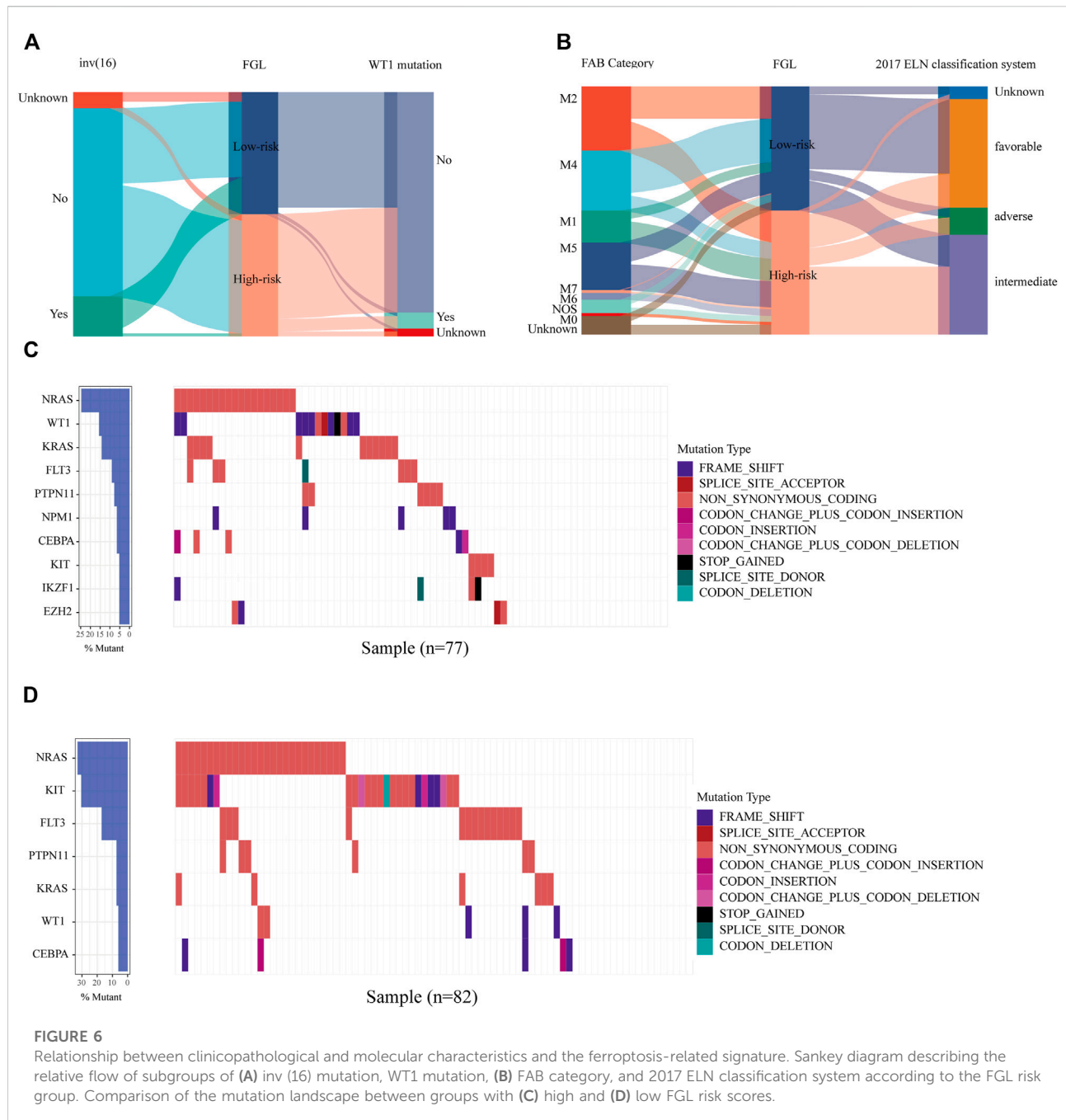
upregulated in the high-risk group, while infiltration levels of B cells, macrophages, and other cells were significantly upregulated in the low-risk group (all  $p < 0.05$ ). Notably, we observed a statistically significant difference between the two groups in terms of the expression of several important immune checkpoint genes. The expression of *PDL1*, *CTLA4*, *TIGIT*, and *PDL2* were more highly expressed in the high-risk group (all  $p < 0.05$ ). However, a substantial increase in the expression of *TIM3* was found in the low-risk group ( $p < 0.0001$ ) (Figure 8E).

In addition, we investigated the expression of m6A-related genes between the two risk groups, and the results showed that most of them were more highly expressed in the high-risk group (all  $p < 0.05$ ) (Figure 8F). Significant correlations were also identified for the expression levels of the 22 ferroptosis-related signatures and m6A-related genes (Supplementary Figure S4). According to m6A2Target, a comprehensive database for the target gene of writers, erasers, and readers (WERs) of m6A modification in a cancer cell line (Deng et al., 2021), 13 out of the 22 ferroptosis-related signatures in the FGL model were

potential target genes of WERs of m6A modification in the leukemia cell line (Supplementary Table S7).

## Anticancer drug sensitivity analysis

Sensitivity to 198 anticancer drugs was compared between the high- and low-risk groups to provide potential treatment guidance for P-AML patients. The results for 153 drugs were not considered for differences analysis because more than 20% of the samples were missing from the predicted IC<sub>50</sub> values. Since the predicted values of the samples differ significantly, differences analysis was applied after the removal of potential outliers (extremely high IC<sub>50</sub> values). ROUT method was used for outlier identification (setting Q to 5%) (Motulsky and Brown, 2006). The results demonstrated that the IC<sub>50</sub> values of SB505124\_1194 and JAK\_8517\_1739 were significantly lower in patients within the FGL high-risk group, which implies that patients within the FGL high-risk group might benefit from



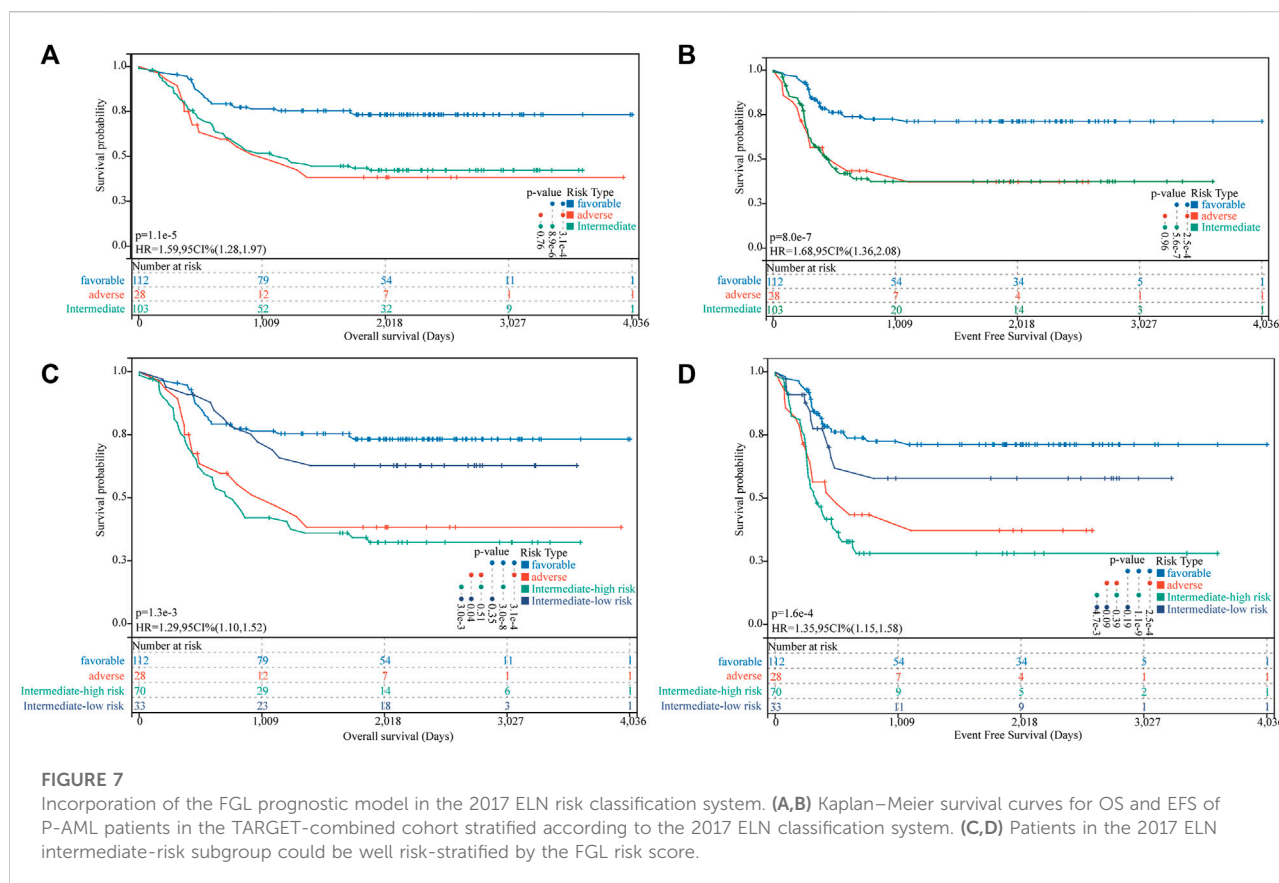
treatment using SB505124\_1194 and JAK\_8517\_1739 (Figure 8G).

## Discussion

Development of a reliable and applicable prognostic model for long-term survival prediction, risk stratification, and helping with therapeutic decision-making in AML is a far-reaching event, especially for pediatric AML patients.

In our study, we explored the role of ferroptosis-related signatures, which includes ferroptosis-related mRNAs and correlated lncRNAs in P-AML. A new model for prognosis prediction of P-AML was established with 22 signatures associated with ferroptosis in the discovery cohort of the TARGET AML program and further validated in the validation cohort and TARGET-combined cohort (all  $p < 0.05$ ). Additionally, the FGL prognostic model was identified as the only independent prognostic factor for P-AML, irrespective of the well-known 2017 ELN classification system



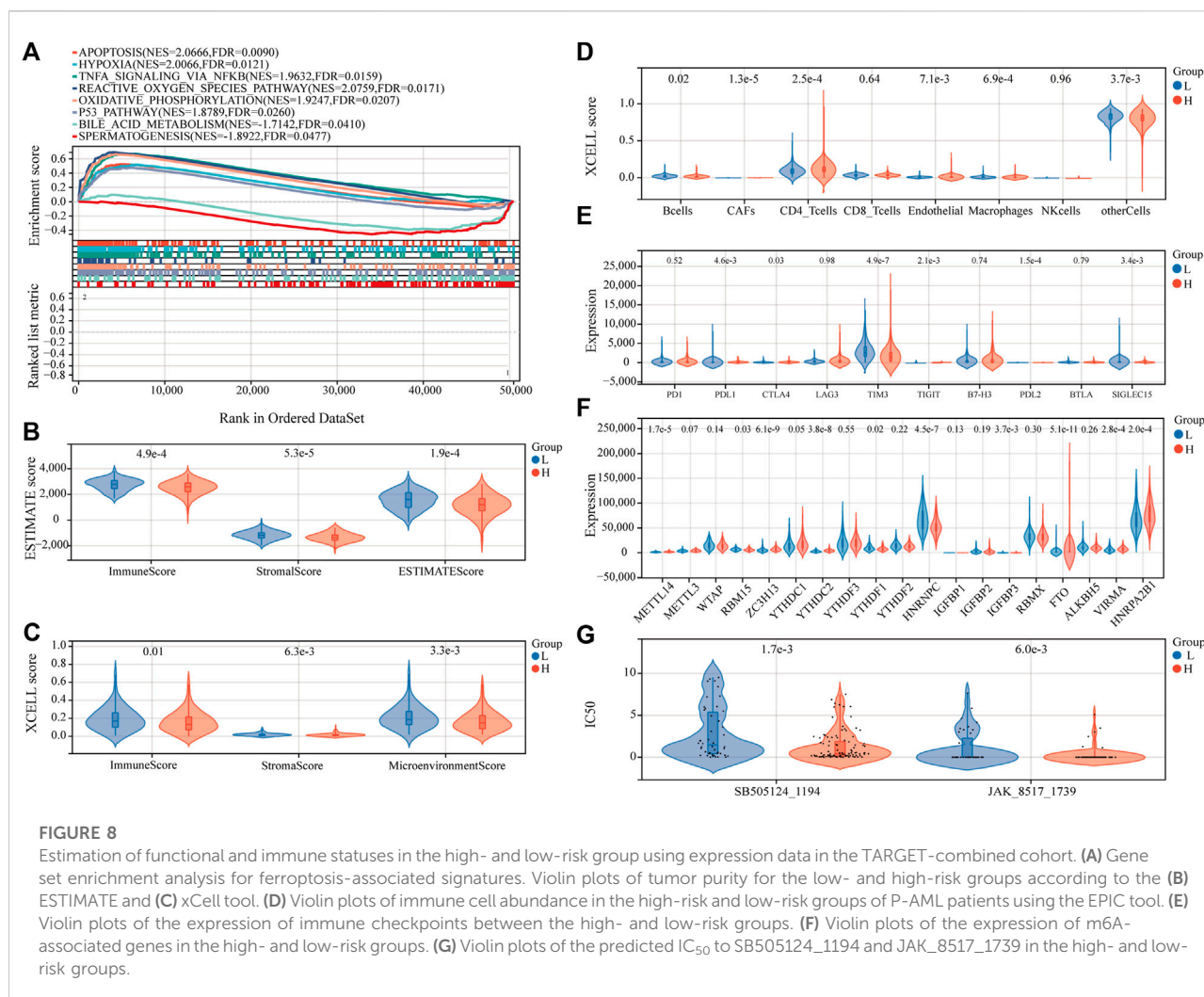


and other AML-related cytogenetic changes and gene mutations. Furthermore, substantial differences in the TME, functionally enriched pathways, expression profiles of immune checkpoint genes, and m6A-associated genes were identified between the low- and high-risk groups. To our knowledge, this is the first study to elucidate the prognostic impact of ferroptosis-related signatures on pediatric AML patients and suggest the great potential roles of ferroptosis in P-AML.

A question that cannot be ignored now is whether this FGL risk model provides additional prognosis value, or it contradicts the existing molecular risk factor or risk classification system. We found that low-risk factors (*inv* (16) mutation, FAB M4 subtype, and favorable subtype of the 2017 ELN classification system) (Thomas et al., 2009) were associated with low FGL risk, and similarly, high-risk factors (*WT1* mutation, adverse subtype of the 2017 ELN classification system) (Rampal and Figueroa, 2016) were associated with high-risk scores. In our study, 2017 ELN classification system showed great prognostic significance in pediatric patients with AML and assigned 40.23% of individuals to the intermediate-risk group, consistent with the previously reported number of 50% (Grimwade et al., 2010; Wang et al., 2017), further supporting the need for subsequent stratification for this subgroup. The novelty introduced by our work is that the FGL prognostic model

could well dichotomize the 2017 ELN intermediate-risk subgroup into two groups with distinct prognoses. At the same time, our model presented with the highest AUC value compared with other prognostic models established or validated in the TARGET cohort. Collectively, our FGL risk model had greater prognostic value and could be an important supplement to the application of the 2017 ELN classification system in P-AML.

There are also numerous existing models for adult AML early prediction or risk stratification, which have been compared to the FGL model corresponding to different aspects of modeling (Supplementary Table S8). For the immune risk score model proposed for adult AML (Wang Y. et al., 2021), we did not succeed in validating it in the TARGET dataset (data not shown). The inconsistency might be induced by the differences in the immune microenvironment of AML tumors between adults and children. A gene mutation-based model proposed additional genetic markers that might refine the current ELN classification (Eisfeld et al., 2020), which was quite promising since somatic mutations are more stable relative to RNA levels. We expect to see further internal and external validation of this model. Two outstanding models were also presented in 2018 for early prediction of AML, which had fundamental clinical prevention value for predicting AML in healthy people over



65 (Abelson et al., 2018). Considering the low prevalence of AML in children (Puumala et al., 2013), risk prediction might be more important than disease prediction for P-AML patients.

Recent results reveal that the immune system may function in part through ferroptosis to prevent tumorigenesis (Wang et al., 2019). According to the immune score analysis, the low-risk group was consistent with a longer OS rate and higher immune score, suggesting that high immune-related activity might result in a better prognosis in P-AML. This finding is consistent with a previous study on adult AML (Zeng et al., 2021). CD4<sub>T</sub> cells can differentiate into a multitude of effector cells depending on the antigens present within the microenvironment (Zhu et al., 2010). CD4<sub>T</sub> regulatory cells (Tregs) are a major subset of CD4<sub>T</sub> cells, which have been reported to suppress anti-tumor immune effector responses in the TME and may be recruited and exploited by leukemic cells to evade immune surveillance (Ustun et al., 2011; Tay et al., 2021). Immune infiltration analysis indicated the high-risk group expressed significant enrichment of CD4<sub>T</sub> cells. It provides further

evidence that an immune suppressive environment presenting with a low immune score might correlate with poor prognosis in the high-risk group.

In the past few years, major efforts have been made to develop immune therapies for the treatment of AML patients. Several clinical trials with the aim to improve the survival of AML patients are ongoing, with immune-based therapeutic modalities such as monoclonal antibodies, T cell engagers, adoptive T-cell therapy, adoptive-NK therapy, checkpoint blockade via PD-1/PD-L1, CTLA4, and newer target such as TIM3 (Isidori et al., 2021). Considering the inhibition of the PD-1/PD-L1 axis demonstrated antileukemic activity and wide-spread expression of *PDL1* (Giannopoulos, 2019), patients in the high-risk group with higher levels of *PDL1*, *PDL2*, and *TIGIT* might be more suitable for treatment using anti-PD-L1 immune checkpoint inhibitor (ICI) approved in multiple solid tumors, Avelumab for example (Saxena et al., 2021). *TIM3* (T cell immunoglobulin and mucin domain-3) is an ideal target for selectively killing LSCs but not normal hematopoietic stem cells

(HSCs) in most human AML cells, and it was significantly upregulated in the low-risk group, suggesting that patients in the low-risk group might benefit from anti-TIM3 antibodies (Wang Z. et al., 2021). In addition, providing potential immune therapy guidance, we also identified the correlation relationship between FGL risk score and anticancer drug sensitivity. However, the present finding was based on the predicted algorithm in cell lines, further validation with preclinical studies is warranted. In our study, the expression of identified FGL-related signatures was found significantly correlated with many m6A-regulator genes, and 13 out of them were identified as potential target genes of WERs of m6A modification in a leukemia cell line, this is in line with previous analysis showing that a wide-ranging connection was found between m6A methylation and ferroptosis using 31 cancer type-specific datasets in TCGA (Zhang, 2021). Moreover, the majority of m6A-regulator genes were found with higher expression in the high-risk group than those in the low-risk group, implying that a combination strategy of RNA epigenetics and ferroptosis therapies might benefit more with comprehensive consideration of the expression pattern of the specific m6A-regulator.

GSEA analysis indicated that the low-risk group might be protected from a high level of ferroptosis, or apoptosis-induced cancer cell death or through the function of *NOX1* and *ZEB1* in the *p53* and ROS pathway. Bile acids (BAs) are well known as chemical chaperones to reduce endoplasmic reticulum stress in hematopoietic stem cells (Oguro, 2019). Recently, BA was reported to play a key role in the reconstitution of hematopoiesis and BA levels in the blood of pediatric cancer patients and mice treated with chemotherapeutic agents were increased in synchrony with an early proliferation of bone marrow cells and recovery from myelosuppression (Sigurdsson et al., 2020). BA metabolism pathway was found significantly enriched in the high-risk group, proving further evidence that dysregulated cholesterol homeostasis might result in ferroptosis resistance and promote tumorigenicity and metastasis in cancer (Liu et al., 2021).

Furthermore, several limitations of the FGL prognostic model need to be noticed. This model is generated from bioinformatics analysis and has been validated by limited additional cohorts. Furthermore, external validations with a large patient population are certainly warranted in the near future. *SLC7A11* (solute carrier family 7 member 11) gene in the model was found as the direct protein target of ferroptosis agonists (erastin) according to experimental evidence from The Cancer Therapeutics Response Portal (CTRP) database (<http://portals.broadinstitute.org/ctrp/>) (Rees et al., 2016). However, molecular mechanisms and potential for therapeutic targets of the ferroptosis-related signatures on P-AML need further study.

In conclusion, we established a concise prognostic model composed of 22 ferroptosis-related signatures for predicting the prognosis of P-AML patients. The high-risk score was an

independent poor prognostic parameter and influences the immune status, expression level of immune checkpoint genes, and enriched tumor-related pathways, thereby providing new evidence for immune therapy for P-AML. Furthermore, the FGL risk score further refines the predicted clinical outcomes of the 2017 ELN risk system by sub-dividing the intermediate-risk patients.

## Data availability statement

The original contributions presented in the study are included in the article/Supplementary Material; further inquiries can be directed to the corresponding author.

## Author contributions

YT and LW designed the study, collected the datasets, and wrote the manuscript. YT performed the bioinformatics analysis. HY directed the project, supervised the analysis, and revised the manuscript.

## Funding

All sources of funding received for the research have been submitted. The research activities are supported by the National Natural Science Foundation of China (81911530169).

## Conflict of interest

The authors declare that the research was conducted in the absence of any commercial or financial relationships that could be construed as a potential conflict of interest.

## Publisher's note

All claims expressed in this article are solely those of the authors and do not necessarily represent those of their affiliated organizations, or those of the publisher, the editors, and the reviewers. Any product that may be evaluated in this article, or claim that may be made by its manufacturer, is not guaranteed or endorsed by the publisher.

## Supplementary material

The Supplementary Material for this article can be found online at: <https://www.frontiersin.org/articles/10.3389/fmolb.2022.954524/full#supplementary-material>

## References

- Abelson, S., Collord, G., Ng, S. W. K., Weissbrod, O., Mendelson Cohen, N., Niemeyer, E., et al. (2018). Prediction of acute myeloid leukaemia risk in healthy individuals. *Nature* 559, 400–404. doi:10.1038/s41586-018-0317-6
- Aran, D., Hu, Z., and Butte, A. J. (2017). xCell: digitally portraying the tissue cellular heterogeneity landscape. *Genome Biol.* 18, 220. doi:10.1186/s13059-017-1349-1
- Birsén, R., Larrue, C., Decroocq, J., Johnson, N., Guiraud, N., Gotanegre, M., et al. (2021). APR-246 induces early cell death by ferroptosis in acute myeloid leukemia. *Haematologica* 107, 403–416. doi:10.3324/haematol.2020.259531
- Bolouri, H., Farrar, J. E., Triche, T., Ries, R. E., Lim, E. L., Alonzo, T. A., et al. (2018). The molecular landscape of pediatric acute myeloid leukemia reveals recurrent structural alterations and age-specific mutational interactions. *Nat. Med.* 24, 103–112. doi:10.1038/nm.4439
- Cai, Z., Wu, Y., Zhang, F., and Wu, H. (2021). A three-gene signature and clinical outcome in pediatric acute myeloid leukemia. *Clin. Transl. Oncol.* 23, 866–873. doi:10.1007/s12094-020-02480-x
- Cao, K., Du, Y., Bao, X., Han, M., Su, R., Pang, J., et al. (2022). Glutathione-bioimprinted nanoparticles targeting of N6-methyladenosine FTO demethylase as a strategy against leukemic stem cells. *Small* 18, e2106558. doi:10.1002/sml.202106558
- Creutzig, U., Van Den Heuvel-Eibrink, M. M., Gibson, B., Dworzak, M. N., Adachi, S., De Bont, E., et al. (2012). Diagnosis and management of acute myeloid leukemia in children and adolescents: Recommendations from an international expert panel. *Blood* 120, 3187–3205. doi:10.1182/blood-2012-03-362608
- Deng, S., Zhang, H., Zhu, K., Li, X., Ye, Y., Li, R., et al. (2021). *M6A2Target: a comprehensive database for targets of m6A writers, erasers and readers*, 22, bbaa055. doi:10.1093/bib/bbaa055 *Brief. Bioinform*
- Derrien, T., Johnson, R., Bussotti, G., Tanzer, A., Djebali, S., Tilgner, H., et al. (2012). The GENCODE v7 catalog of human long noncoding RNAs: Analysis of their gene structure, evolution, and expression. *Genome Res.* 22, 1775–1789. doi:10.1101/gr.132159.111
- Docking, T. R., Parker, J. D. K., JäDERSTEN, M., Duns, G., Chang, L., Jiang, J., et al. (2021). A clinical transcriptome approach to patient stratification and therapy selection in acute myeloid leukemia. *Nat. Commun.* 12, 2474. doi:10.1038/s41467-021-22625-y
- Döhner, H., Estey, E., Grimwade, D., Amadori, S., Appelbaum, F. R., BüCHNER, T., et al. (2017). Diagnosis and management of AML in adults: 2017 ELN recommendations from an international expert panel. *Blood* 129, 424–447. doi:10.1182/blood-2016-08-733196
- Downing, J. R., Wilson, R. K., Zhang, J., Mardis, E. R., Pui, C. H., Ding, L., et al. (2012). The pediatric cancer Genome project. *Nat. Genet.* 44, 619–622. doi:10.1038/ng.2287
- Duployez, N., Marceau-Renaut, A., Villenet, C., Petit, A., Rousseau, A., Ng, S. W. K., et al. (2019). The stem cell-associated gene expression signature allows risk stratification in pediatric acute myeloid leukemia. *Leukemia* 33, 348–357. doi:10.1038/s41375-018-0227-5
- Eisfeld, A. K., Kohlschmidt, J., Mims, A., Nicolet, D., Walker, C. J., Blachly, J. S., et al. (2020). Additional gene mutations may refine the 2017 European LeukemiaNet classification in adult patients with de novo acute myeloid leukemia aged <60 years. *Leukemia* 34, 3215–3227. doi:10.1038/s41375-020-0872-3
- Elsayed, A. H., Rafiee, R., Cao, X., Raimondi, S., Downing, J. R., Ribeiro, R., et al. (2020). A six-gene leukemic stem cell score identifies high risk pediatric acute myeloid leukemia. *Leukemia* 34, 735–745. doi:10.1038/s41375-019-0604-8
- Giannopoulos, K. (2019). Targeting immune signaling checkpoints in acute myeloid leukemia. *J. Clin. Med.* 8, 236. doi:10.3390/jcm8020236
- Gong, J., Chehrizi-Raffle, A., Reddi, S., and Salgia, R. (2018). Development of PD-1 and PD-L1 inhibitors as a form of cancer immunotherapy: A comprehensive review of registration trials and future considerations. *J. Immunother. Cancer* 6, 8. doi:10.1186/s40425-018-0316-z
- Grimwade, D., Hills, R. K., Moorman, A. V., Walker, H., Chatters, S., Goldstone, A. H., et al. (2010). Refinement of cytogenetic classification in acute myeloid leukemia: Determination of prognostic significance of rare recurring chromosomal abnormalities among 5876 younger adult patients treated in the United Kingdom medical research council trials. *Blood* 116, 354–365. doi:10.1182/blood-2009-11-254441
- Isidori, A., Cerchione, C., Daver, N., Dinardo, C., Garcia-Manero, G., Konopleva, M., et al. (2021). Immunotherapy in acute myeloid leukemia: Where we stand. *Front. Oncol.* 11, 656218. doi:10.3389/fonc.2021.656218
- Lelièvre, P., Sancey, L., Coll, J., Deniaud, A., and Busser, B. (2020). Iron dysregulation in human cancer: Altered metabolism, biomarkers for diagnosis, prognosis, monitoring and rationale for therapy. *Cancers* 12, E3524. doi:10.3390/cancers12123524
- Li, J., Cao, F., Yin, H.-L., Huang, Z.-J., Lin, Z.-T., Mao, N., et al. (2020). Ferroptosis: Past, present and future. *Cell Death Dis.* 11, 88. doi:10.1038/s41419-020-2298-2
- Li, Y., Xiao, J., Bai, J., Tian, Y., Qu, Y., Chen, X., et al. (2019). Molecular characterization and clinical relevance of m6A regulators across 33 cancer types. *Mol. Cancer* 18, 137. doi:10.1186/s12943-019-1066-3
- Liberzon, A., Birger, C., THORVALDSDÓTTIR, H., Ghandi, M., Mesirov, J. P., Tamayo, P., et al. (2015). The Molecular Signatures Database (MSigDB) hallmark gene set collection. *Cell Syst.* 1, 417–425. doi:10.1016/j.cels.2015.12.004
- Liu, L., Li, H., Hu, D., Wang, Y., Shao, W., Zhong, J., et al. (2022). Insights into N6-methyladenosine and programmed cell death in cancer. *Mol. Cancer* 21, 32. doi:10.1186/s12943-022-01508-w
- Liu, W., Chakraborty, B., Safi, R., Kazmin, D., Chang, C.-Y., McDonnell, D. P., et al. (2021). Dysregulated cholesterol homeostasis results in resistance to ferroptosis increasing tumorigenicity and metastasis in cancer. *Nat. Commun.* 12, 5103. doi:10.1038/s41467-021-25354-4
- Love, M. I., Huber, W., and Anders, S. (2014). Moderated estimation of fold change and dispersion for RNA-seq data with DESeq2. *Genome Biol.* 15, 550. doi:10.1186/s13059-014-0550-8
- Maeser, D., Gruener, R. F., and Huang, R. S. (2021). oncoPredict: an R package for predicting *in vivo* or cancer patient drug response and biomarkers from cell line screening data. *Brief. Bioinform.* 22, bbab260. doi:10.1093/bib/bbab260
- Marceau-Renaut, A., Duployez, N., Ducourneau, B., Labopin, M., Petit, A., Rousseau, A., et al. (2018). Molecular profiling defines distinct prognostic subgroups in childhood AML: A report from the French ELAM02 study group. *Hemisphere* 2, e31. doi:10.1097/HS9.0000000000000031
- Motulsky, H. J., and Brown, R. E. (2006). Detecting outliers when fitting data with nonlinear regression - a new method based on robust nonlinear regression and the false discovery rate. *BMC Bioinform.* 7, 123. doi:10.1186/1471-2105-7-123
- Newell, L., and Cook, R. (2021). Advances in acute myeloid leukemia. *BMJ Clin. Res. ed.* 375, n2026. doi:10.1136/bmj.n2026
- Oguro, H. (2019). The roles of cholesterol and its metabolites in normal and malignant hematopoiesis. *Front. Endocrinol.* 10, 204. doi:10.3389/fendo.2019.00204
- Puumala, S. E., Ross, J. A., Aplenc, R., and Spector, L. G. (2013). Epidemiology of childhood acute myeloid leukemia. *Pediatr. Blood Cancer* 60, 728–733. doi:10.1002/pbc.24464
- Qin, S., Xu, L., Yi, M., Yu, S., Wu, K., Luo, S., et al. (2019). Novel immune checkpoint targets: Moving beyond PD-1 and CTLA-4. *Mol. Cancer* 18, 155. doi:10.1186/s12943-019-1091-2
- Racle, J., De Jonge, K., Baumgaertner, P., Speiser, D. E., and Gfeller, D. (2017). Simultaneous enumeration of cancer and immune cell types from bulk tumor gene expression data. *Elife* 6, e26476. doi:10.7554/eLife.26476
- Rampal, R., and Figueroa, M. E. (2016). Wilms tumor 1 mutations in the pathogenesis of acute myeloid leukemia. *Haematologica* 101, 672–679. doi:10.3324/haematol.2015.141796
- Rees, M. G., Seashore-Ludlow, B., Cheah, J. H., Adams, D. J., Price, E. V., Gill, S., et al. (2016). Correlating chemical sensitivity and basal gene expression reveals mechanism of action. *Nat. Chem. Biol.* 12, 109–116. doi:10.1038/nchembio.1986
- Rowshanravan, B., Halliday, N., and Sansom, D. M. (2018). CTLA-4: A moving target in immunotherapy. *Blood* 131, 58–67. doi:10.1182/blood-2017-06-741033
- Saxena, K., Herbrich, S. M., Pemmaraju, N., Kadia, T. M., Dinardo, C. D., Borthakur, G., et al. (2021). A phase 1b/2 study of azacitidine with PD-L1 antibody avelumab in relapsed/refractory acute myeloid leukemia. *Cancer* 127, 3761–3771. doi:10.1002/cncr.33690
- Sigurdsson, V., Haga, Y., Takei, H., Mansell, E., Okamatsu-Haga, C., Suzuki, M., et al. (2020). Induction of blood-circulating bile acids supports recovery from myelosuppressive chemotherapy. *Blood Adv.* 4, 1833–1843. doi:10.1182/bloodadvances.2019000133
- Tay, R. E., Richardson, E. K., and Toh, H. C. (2021). Revisiting the role of CD4+ T cells in cancer immunotherapy—New insights into old paradigms. *Cancer Gene Ther.* 28, 5–17. doi:10.1038/s41417-020-0183-x
- Thomas, C., Aline, R., Marion, V., Claude, G., Charikleia, K., GENEVIÈVE, L., et al. (2009). Slow relapse in acute myeloid leukemia with inv(16) or t(16;16). *Haematologica* 94, 1466–1468. doi:10.3324/haematol.2009.010702



- Unis, G. D., Vanderveen, N., Fletcher, M., and Vasquez, R. J. (2021). Very late relapse in pediatric acute myeloid leukemia: A case report and brief literature review. *J. Pediatr. Hematol. Oncol.* 43, 236–239. doi:10.1097/MPH.0000000000001989
- Ustun, C., Miller, J. S., Munn, D. H., Weisdorf, D. J., and Blazar, B. R. (2011). Regulatory T cells in acute myelogenous leukemia: Is it time for immunomodulation? *Blood* 118, 5084–5095. doi:10.1182/blood-2011-07-365817
- Wang, J.-B., Li, P., Liu, X.-L., Zheng, Q.-L., Ma, Y.-B., Zhao, Y.-J., et al. (2020). An immune checkpoint score system for prognostic evaluation and adjuvant chemotherapy selection in gastric cancer. *Nat. Commun.* 11, 6352. doi:10.1038/s41467-020-20260-7
- Wang, M., Lindberg, J., Klevebring, D., Nilsson, C., Mer, A. S., Rantalainen, M., et al. (2017). Validation of risk stratification models in acute myeloid leukemia using sequencing-based molecular profiling. *Leukemia* 31, 2029–2036. doi:10.1038/leu.2017.48
- Wang, W., Green, M., Choi, J. E., Gijón, M., Kennedy, P. D., Johnson, J. K., et al. (2019). CD8(+) T cells regulate tumour ferroptosis during cancer immunotherapy. *Nature* 569, 270–274. doi:10.1038/s41586-019-1170-y
- Wang, Y., Cai, Y. Y., Herold, T., Nie, R. C., Zhang, Y., Gale, R. P., et al. (2021a). An immune risk score predicts survival of patients with acute myeloid leukemia receiving chemotherapy. *Clin. Cancer Res.* 27, 255–266. doi:10.1158/1078-0432.CCR-20-3417
- Wang, Z., Chen, J., Wang, M., Zhang, L., and Yu, L. (2021b). One stone, two birds: The roles of tim-3 in acute myeloid leukemia. *Front. Immunol.* 12, 618710. doi:10.3389/fimmu.2021.618710
- Yang, Z., Shang, J., Li, N., Zhang, L., Tang, T., Tian, G., et al. (2020). Development and validation of a 10-gene prognostic signature for acute myeloid leukaemia. *J. Cell. Mol. Med.* 24, 4510–4523. doi:10.1111/jcmm.15109
- Yoshihara, K., Shahmoradgoli, M., Martínez, E., Vegesna, R., Kim, H., Torres-Garcia, W., et al. (2013). Inferring tumour purity and stromal and immune cell admixture from expression data. *Nat. Commun.* 4, 2612. doi:10.1038/ncomms3612
- Yu, Y., Xie, Y., Cao, L., Yang, L., Yang, M., Lotze, M. T., et al. (2015). The ferroptosis inducer erastin enhances sensitivity of acute myeloid leukemia cells to chemotherapeutic agents. *Mol. Cell. Oncol.* 2, e1054549. doi:10.1080/23723556.2015.1054549
- Zeng, T., Cui, L., Huang, W., Liu, Y., Si, C., Qian, T., et al. (2021). The establishment of a prognostic scoring model based on the new tumor immune microenvironment classification in acute myeloid leukemia. *BMC Med.* 19, 176. doi:10.1186/s12916-021-02047-9
- Zhang, Y. (2021)., 2021. Research Square. Identification of cross-talk between m6A/m5C regulators and ferroptosis associated with immune infiltration and prognosis in pan-cancer
- Zhang, Z., Hernandez, K., Savage, J., Li, S., Miller, D., Agrawal, S., et al. (2021). Uniform genomic data analysis in the NCI genomic data commons. *Nat. Commun.* 12, 1226. doi:10.1038/s41467-021-21254-9
- Zhou, N., and Bao, J. (2020). FerrDb: A manually curated resource for regulators and markers of ferroptosis and ferroptosis-disease associations. *Database* 2020, baaa021. doi:10.1093/database/baaa021
- Zhu, J., Yamane, H., and Paul, W. E. (2010). Differentiation of effector CD4 T cell populations (\*). *Annu. Rev. Immunol.* 28, 445–489. doi:10.1146/annurev-immunol-030409-101212



## OPEN ACCESS

EDITED BY  
Guo Chen,  
Jinan University, China

REVIEWED BY  
Guangchao Li,  
Guangzhou Bio-gene Technology Co.,  
Ltd., China  
Maoxiao Feng,  
Shandong University, China

\*CORRESPONDENCE  
Ruiming Ou,  
ouruiming@126.com  
Yangmin Zhu,  
zhuyangmin2005@163.com  
Qing Zhang,  
zhqing@vip.163.com  
Shuang Liu,  
liush@gd2h.org.cn

†These authors share first authorship

SPECIALTY SECTION  
This article was submitted to Molecular  
Diagnostics and Therapeutics,  
a section of the journal  
Frontiers in Molecular Biosciences

RECEIVED 02 June 2022  
ACCEPTED 30 June 2022  
PUBLISHED 15 August 2022

CITATION  
Yin Z, Li F, Zhou Q, Zhu J, Liu Z, Huang J,  
Shen H, Ou R, Zhu Y, Zhang Q and Liu S  
(2022), A ferroptosis-related gene  
signature and immune infiltration  
patterns predict the overall survival in  
acute myeloid leukemia patients.  
*Front. Mol. Biosci.* 9:959738.  
doi: 10.3389/fmolb.2022.959738

COPYRIGHT  
© 2022 Yin, Li, Zhou, Zhu, Liu, Huang,  
Shen, Ou, Zhu, Zhang and Liu. This is an  
open-access article distributed under  
the terms of the [Creative Commons  
Attribution License \(CC BY\)](#). The use,  
distribution or reproduction in other  
forums is permitted, provided the  
original author(s) and the copyright  
owner(s) are credited and that the  
original publication in this journal is  
cited, in accordance with accepted  
academic practice. No use, distribution  
or reproduction is permitted which does  
not comply with these terms.

# A ferroptosis-related gene signature and immune infiltration patterns predict the overall survival in acute myeloid leukemia patients

Zhao Yin<sup>†</sup>, Fang Li<sup>†</sup>, Qijun Zhou<sup>†</sup>, Jianfang Zhu<sup>†</sup>, Zhi Liu,  
Jing Huang, Huijuan Shen, Ruiming Ou\*, Yangmin Zhu\*,  
Qing Zhang\* and Shuang Liu\*

Department of Hematology, Guangdong Second Provincial General Hospital, Guangzhou, China

Targeted therapy for acute myeloid leukemia (AML) is an effective strategy, but currently, there are very limited therapeutic targets for AML treatment. Ferroptosis is strongly related to drug resistance and carcinogenesis. However, there are few reports about ferroptosis in AML. This article explores the relationship between ferroptosis-related gene (FRG) expression and prognosis in AML patients from the FerrDb and the Cancer Genome Atlas (TCGA) databases. The ferroptosis-related gene ARNTL was observed to have high expression and poor prognosis in AML. Receiver operating characteristic curve (ROC) analysis revealed the predictive accuracy of the signature. The area under the time-dependent ROC curve (AUC) was 0.533 at one year, 0.619 at two years, and 0.622 at three years within the training cohort. Moreover, we found that the ARNTL expression is closely associated with tumor-infiltrating immune cells like the macrophages and NK cells. Inhibiting the ARNTL expression suppressed colony formation and induced ferroptosis in AML cells. Overall, the survival prediction model constructed based on ARNTL accurately predicted the survival in AML patients, which could be a potential candidate for diagnosing and treating AML.

## KEYWORDS

ferroptosis, AML, ARNTL, immune cell infiltration, overall survival (OS)

**Abbreviation:** AML, acute myeloid leukemia; FRG, ferroptosis-related gene; TCGA, the Cancer Genome Atlas; ROC, receiver operating characteristic curve; lipid-ROS, lipid reactive oxygen species; DEGs, differentially expressed genes; K-M, Kaplan–Meier; MDA, malondialdehyde; GPX4, glutathione peroxidase 4; ACSL4, acyl-CoA synthetase long-chain family member 4; CCLE, cancer cell line encyclopedia.

## Introduction

Acute myeloid leukemia (AML) is a complex hematological neoplasm with a poor prognosis (Willier et al., 2021). This disease is the most frequent type of malignant myeloid disorder in adults with an incidence of approximately 2–4/100,000 per year (<http://seer.cancer.gov/>). Moreover, patients older than 60 years are not able to withstand induction chemotherapy and have an even worse median survival of 5–10 months, and their 5-year overall survival (OS) is as low as 5% (Lai et al., 2019). Therefore, it is necessary to explore more effective AML therapeutic strategies.

Ferroptosis is an iron-dependent cell death type, which accumulates lipid reactive oxygen species (lipid-ROS) (Dixon et al., 2012). Ferroptosis plays an essential role in regulating cancer development and can be used in antitumor treatment and predicting prognosis (Jiang et al., 2021; Zhang et al., 2022). The induction of ferroptosis becomes a candidate strategy for inducing tumor cell death, particularly in treating resistant cancers (Hassannia et al., 2019; Lei et al., 2022). Studies have shown that some genes, such as Aldh3a2 (Yusuf et al., 2020), p53 (Birsan et al., 2021), and GPX1 (Wei et al., 2020), regulated ferroptosis in cancer cells and affected AML prognosis. Combining chemotherapeutics with erastin, the ferroptosis activator, is suggested to enhance drug efficacy in AML (Yu et al., 2015). Therefore, ferroptosis has a critical effect on AML. Numerous studies have indicated that such abnormally expressed proteins can be adopted as biomarkers to predict cancer prognosis (Wang et al., 2021). Nevertheless, the relationship of such FRGs with AML survival is still unknown.

To the best of our knowledge, in this present study, we comprehensively analyzed the ARNTL expression and correlation with the prognosis of AML patients in databases such as the TCGA and Kaplan–Meier plotter. Moreover, we investigated the correlation of ARNTL with tumor-infiltrating immune cells in the different tumor microenvironments. These findings provide a promising prognostic gene for AML that was developed based on ferroptosis-associated differentially expressed genes that could be used for prognosis prediction and selection of patients for immunotherapies.

## Materials and methods

### Data collection

We downloaded clinical and RNA-seq expression profiles of 173 cancer patients and 70 healthy subjects from the TCGA website. Later, the “limma” function of the R package was utilized to normalize RNA-seq expression patterns.

We also obtained FRGs from the FerrDb database (<http://www.zhounan.org/ferrdb/>) containing the ferroptosis markers and regulators.

The GeneCards database included integrated information regarding the annotated and predicted human genes. In addition, the ferroptosis-related genes can be downloaded from this database.

The cell line mRNA expression matrix of tumors was obtained from the CCLE dataset (<https://portals.broadinstitute.org/ccle>).

### Establishment and verification of the FRG-based prognosis model

We adopted the “limma” function from the R package for identifying differentially expressed genes (DEGs) in AML samples compared with healthy controls upon the thresholds of  $\log_2[\text{fold change (FC)}] > 1$  and false discovery rate (FDR) < 0.05 based on the TCGA cohort.

### Kaplan–Meier (K–M) and ROC analyses on the prognosis model

We conducted the K–M analysis for determining the difference in OS between high- and low-expression groups for evaluating the prognosis prediction accuracy of our constructed FRG model using the log-rank test with R package “survminer” and “survival” functions (Kassambara et al., 2018). In addition, time-dependent ROC (t-ROC) curves were plotted using the “survival” and “timeROC” of the R package for assessing the accuracy of our prognosis model.

### Cell culture and siRNA silencing

We acquired human AML cells (Molm-13) from Keygentec (Jiangsu, China). Moreover, we obtained ARNTL siRNA from Ribio (Guangzhou, China). Later, Molm-13 cells were cultivated within RPMI-1640 (Gibco, Grand Island, NY, United States) containing 10% fetal bovine serum (FBS) under 5% CO<sub>2</sub> and 37°C temperature conditions. Later, Lipofectamine 2000 (Invitrogen, Carlsbad, CA, United States) was used to transfect siRNAs (target sequence: GTGGAATCCTGGGCC TTCATT, 100 nmol/L) in cells.

### Lipid ROS assay using flow cytometer

Lipid ROS levels were determined using BODIPY-C11 dye (Invitrogen, cat# D3861). The intensely fluorescent BODIPY (4,4-difluoro-3a, 4a-diaza-s-indacene) fluorophore is intrinsically lipophilic, unlike most other long wavelength dyes. The binding of BODIPY fatty acids to bovine serum albumin can be monitored by the accompanying fluorescence

quenching caused by charge–transfer interactions with aromatic amino acid residues. BODIPY 581/591C 11 can be used to measure antioxidant activity in lipid environments by exploiting its loss of fluorescence upon interaction with peroxy radicals. In brief, we inoculated cells ( $2 \times 10^4$ /well) into the six-well plates, followed by 48 h transfection with siRNAs (100 nmol/L) using the Lipofectamine 2000. Before the end of time, culture media were replaced with 1 ml media containing 5  $\mu$ M of BODIPY-C11 dye for 60 min. Cells were harvested and washed twice with PBS, followed by resuspending in 500  $\mu$ L of PBS, and subjected to the flow cytometry analysis to examine the amount of ROS within cells (Yin et al., 2020a).

## Clone-forming assays

Molm-13 cells were transfected with 100 nmol/L siRNAs for 48 h and then collected. The cells ( $1 \times 10^3$ /well) were inoculated into a 10-cm dish with soft agar culture for two weeks to conduct a clone-forming assay with the monolayer cultures. Later, clones were fixed, stained, counted, and photographed (Yin et al., 2020b).

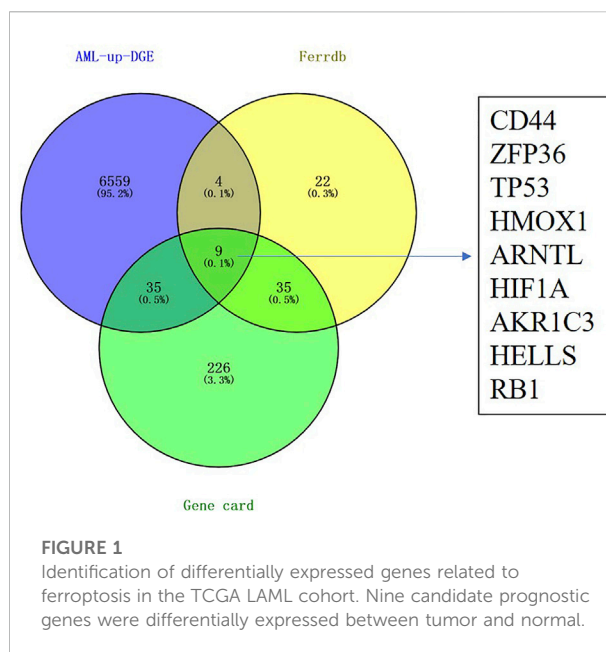
## Malondialdehyde (MDA) assay

MDA accounts for the critical factor indicating lipid peroxidation. Therefore, the MDA levels (S0131S, Beyotime, Shanghai, China) were measured and normalized to protein content according to specific protocols in this study. In brief, cells were harvested and cellular extracts were prepared by sonication in the ice-cold buffer. After sonication, lysed cells were centrifuged at  $10,000 \times g$  for 20 min to remove debris. The supernatant was subjected to the measurement of MDA levels and the protein contents. We used a BCA kit (BL521A, Biosharp, Anhui, China) to quantify protein concentration. MDA levels were then normalized to milligram protein. We used the same procedure to lyse the cells and determine the protein contents in the following assays unless otherwise indicated.

## RNA isolation and real-time PCR (RT-PCR)

We utilized the Trizol reagent (Takara) for extracting total RNA in cells transfected with siARNTL (Liu et al., 2021). Then, we incorporated PrimeScript™ RT Master Mix (HY-K0510, MCE, United States) to synthesize cDNA from total RNA (1  $\mu$ g) following the specific protocols. Using the SYBR-Green kit (B21202, Biomake, Shanghai, China), we measured the ferroptosis marker expression using RT-PCR, including ACSL4 and GPX4, and human  $\beta$ -actin as the reference. All the primers utilized in RT-PCR were purchased from Sangon Biotech and included.

GPX4-Forward (5'-3'): ATGGTTAACCTGGACAAG TACC.



ACSL4-Forward (5'-3'): ACCAGGGAAATCCTAAGT GAAG.

GPX4-Reverse (5'-3'): GACGAGCTGAGTGTAGTTTACT.

ACLS4-Reverse (5'-3'): GGTGTTCTTTGGTTTATGTC

$\beta$ -Actin-Forward (5'-3'):

CCTTCCTGGGCATGGAGTC

$\beta$ -Actin-Reverse (5'-3'):

TGATCTTCATTGTGCTGGGTG.

## Western blot assay

Molm-13 cells were collected and lysed with RIPA buffer (BL504A, Biosharp, China) for 30 min on ice. Then, the protein (50  $\mu$ g) from each sample was separated by 10% tris-acrylamide gel electrophoresis and transferred onto the PVDF membrane. After blocking with 5% skim milk for 1 h at room temperature, primary antibodies against GPX4 (DF6701, Affinity, United States), ACSL4 (DF12141, Affinity, United States), and GAPDH (AF7021, Affinity, United States) were used and incubated at 4°C overnight on a rotary shaker. After washing with TBST 5 times, the membrane was probed with goat anti-rabbit IgG highly cross-adsorbed secondary antibody (1:10,000) for 1 h at room temperature. Then, the membrane was washed 3 times with TBST and developed with an ECL reagent.

## Statistical analysis

R version 3.6.1 was used for statistical analyses. One-way ANOVA was used to analyze the FRG expression between cancer and non-cancer samples. The K–M method was used to generate



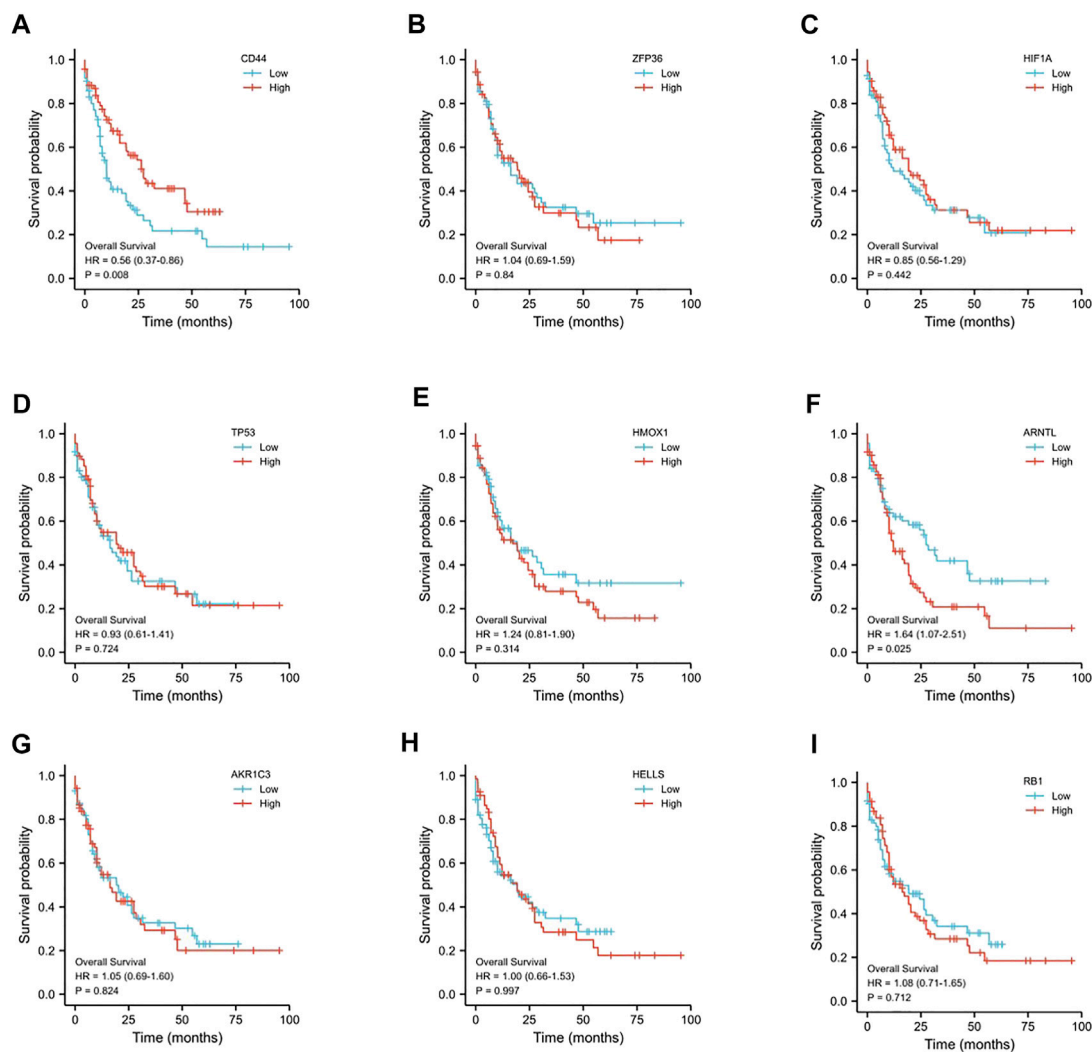


**FIGURE 2**

Prognostic value of the 9-ferroptosis-related-gene signature in AML patients. (A) Kaplan–Meier curves for the overall survival of high- and low-CD44 expression AML patients; (B) Kaplan–Meier curves for the overall survival of high- and low-ZFP36 expression AML patients; (C) Kaplan–Meier curves for the overall survival of high- and low-HIF1A expression AML patients; (D) Kaplan–Meier curves for the overall survival of high- and low-TP53 expression AML patients; (E) Kaplan–Meier curves for the overall survival of high- and low-HMOX1 expression AML patients; (F) Kaplan–Meier curves for the overall survival of high- and low-ARNTL expression AML patients; (G) Kaplan–Meier curves for the overall survival of high- and low-AKR1C3 expression AML patients; (H) Kaplan–Meier curves for the overall survival of high- and low-HELLS expression AML patients; (I) Kaplan–Meier curves for the overall survival of high- and low-RB1 expression AML patients.  $p < 0.05$  is considered as significant.

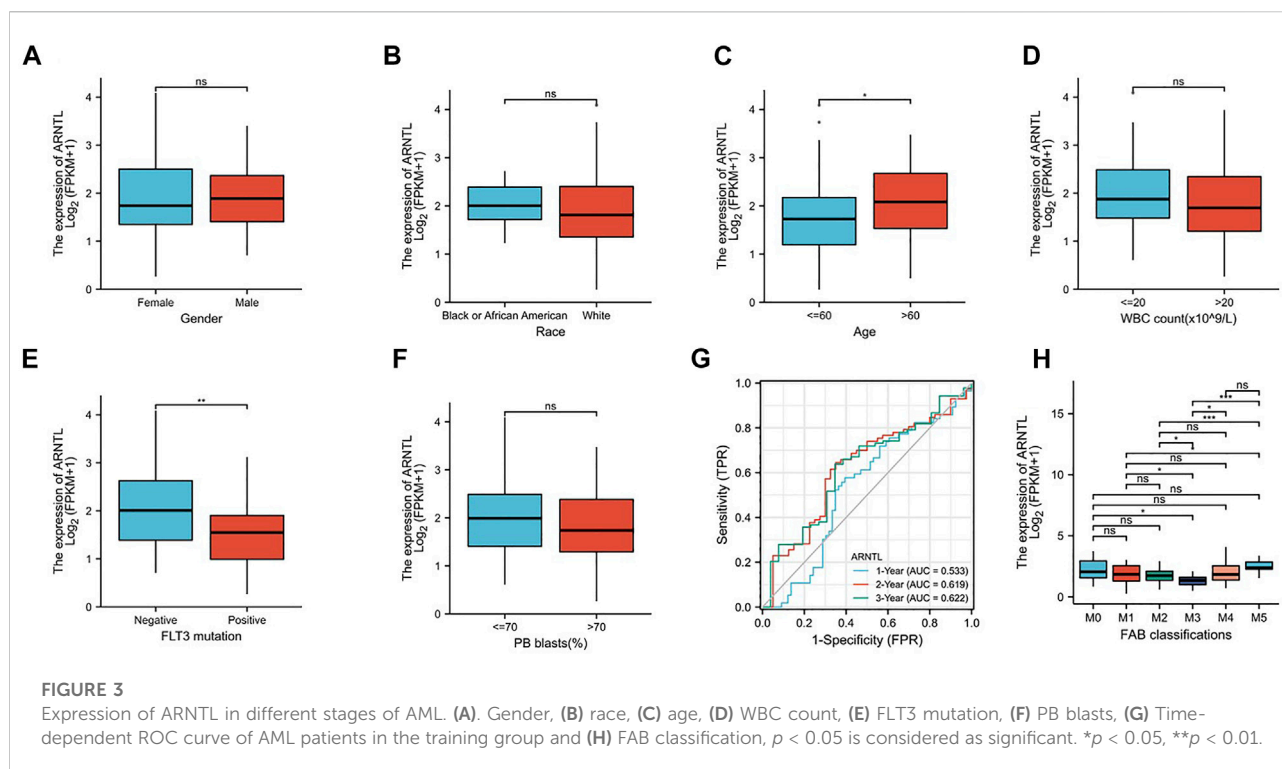
survival curves, while the log-rank test was used to compare differences.  $p < 0.05$  indicated statistical significance (two-sided).

## Results

### Identification of ferroptosis-related genes (FRGs) in AML

We extracted the RNA-Seq data of DEGs from AML patients in the TCGA database using the Gene Expression Profiling

Interactive Analysis (GEPIA2) (Tang et al., 2019) to reveal the ferroptosis-related genes in AML. We also collected the ferroptosis-related genes from the FerrDb database. We speculated that activating ferroptosis signaling pathways could inhibit AML, so we focus on the ferroptosis suppression gene and its overexpression in AML patients. As shown in Figure 1, we observed that nine genes were involved in the DEGs of AML overexpression, ferroptosis-suppression genes, and ferroptosis-related genes obtained from the GeneCards database (CD44, ZFP36, TP53, HMOX1, ARNTL, HIF1A, AKR1C3, HELLS, and RB1).



## Identification of ferroptosis-related genes associated with OS in AML

We examined OS for AML cases according to FRG levels based on the GEPIA database to determine whether our FRG-based prognosis nomogram was accurate. A threshold of 50% was accepted for dividing low and high values, with  $p < 0.05$  indicating statistical significance (Figure 2). ARNTL showed significant relation to OS for AML ( $p = 0.025$ , Figure 2F), which was identified as a risk factor. Then, we analyzed the expression of ARNTL in pan-cancer, and we found only higher expression of ARNTL in CESC, GBM, HNSC, KIRC, LAML, and THCA (Supplementary Figure S1). According to the timeROC curve analysis (Figure 3G), ARNTL significantly predicted the survival of AML (1-, 2-, and 3-year AUC of 0.533, 0.619, and 0.622, respectively).

## Ferroptosis-related gene signature is related to clinicopathological features

To explore the relationship between the constructed nomogram and clinicopathological features, we analyzed the FRG levels among diverse subgroups that were divided based on gender (Figure 3A), race (Figure 3B), age (Figure 3C), WBC count (Figure 3D), FLT3 mutation (Figure 3E), PB blast (Figure 3F), and FAB classification (Figure 3H). As a result, we found that ARNTL is the lower expression in M3 AML and higher in M5 AML.

When the age of patients was greater than 60, ARNTL had significantly higher expression. However, with the BM blast higher than 20, the ARNTL expression was substantially lower. Interestingly, the FLT3-positive mutation patients have lower ARNTL than those with negative expression.

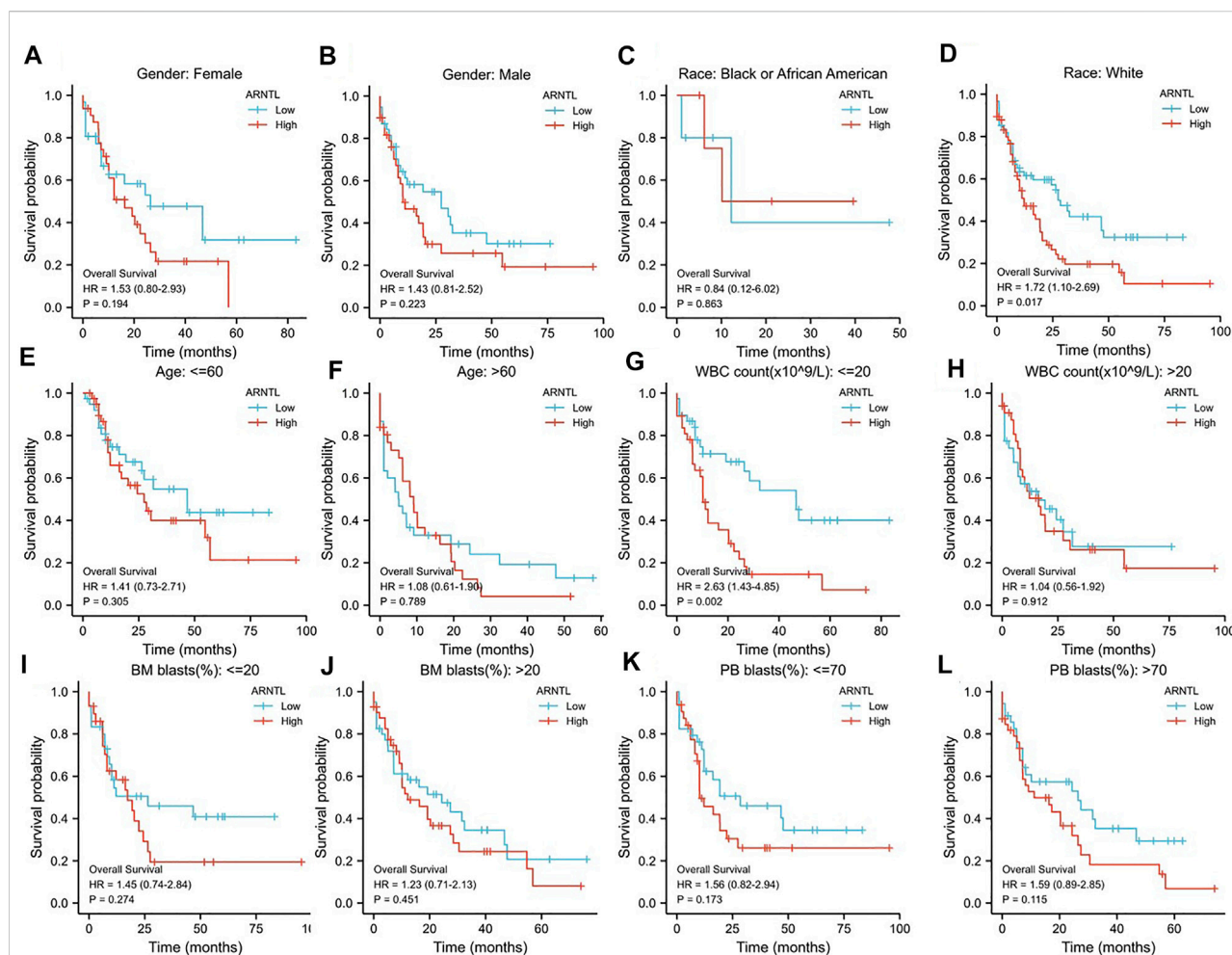
## Identification of ARNTL associated with clinicopathological features in AML

To explore the relationship of OS between ARNTL and clinicopathological features, we analyzed the ARNTL among diverse subgroups that were divided based on gender (Figures 4A,B), race (Figures 4C,D), age (Figures 4E,F), WBC count (Figures 4G,H), BM blast (Figures 4I,J), and PB blast (Figures 4K,L).

We found that ARNTL was identified as a risk factor in weight race human ( $p = 0.017$ ). When the WBC count was  $<20$ , ARNTL overexpression predicted a poor prognosis ( $p = 0.002$ ).

## The correlation of ARNTL and immune cell infiltration

We assessed the correlation between the ARNTL expression and 8 kinds of immune cells within the immune infiltration microenvironment in AML. The function of the immune cell infiltration has a significant relationship with the tumor



microenvironment (TME). The results showed total NK cells (Figure 5B), NK cd56dim cells (Figure 5C), macrophages (Figure 5E), CD8<sup>+</sup> T cells (Figure 5G), and B cells (Figure 5H) were correlated with the ARNTL expression. On the other hand, T cells (Figure 5A), NK cd56bright (Figure 5D), and DC cells (Figure 5F) were not related with the ARNTL expression.

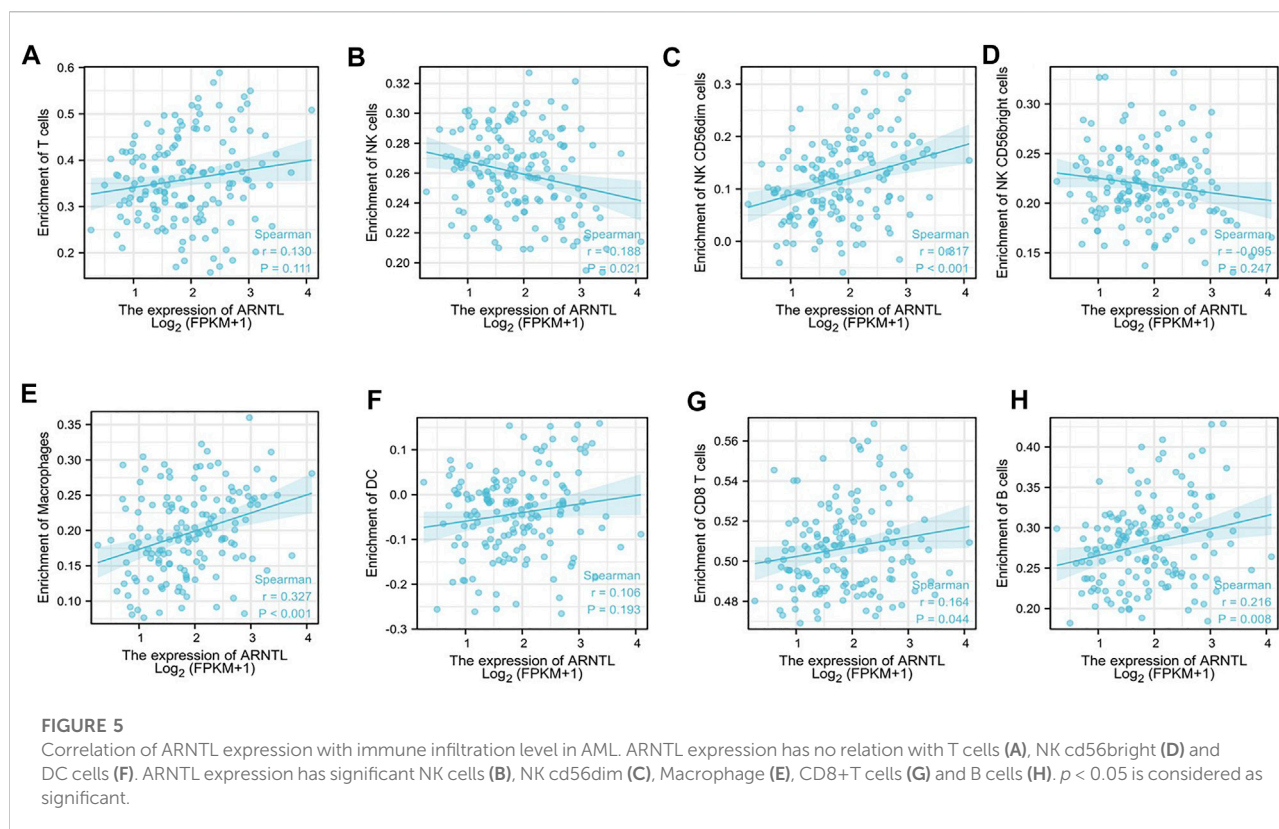
## Targeting inhibition of ARNTL suppresses the malignant progression of AML

We attempted to determine whether reducing ARNTL levels through the siARNTL treatment could attenuate the AML malignant behavior. We observed the expression of ARNTL in a different type of AML cell lines from the CCLE database (Supplementary Figure S2), and we found in Molm-13 cells that ARNTL had higher expression than other cell lines, so

we chose it to make further research. After ARNTL siRNA transfection, there was a substantial decrease in the clone-forming ability of Molm-13 cells relative to NC-transfected cells (Figure 6A). Therefore, these results indicate the ARNTL expression levels within malignant phenotypes in Molm-13 cells.

## ARNTL siRNA promotes lipid peroxidation levels in Molm-13 cells

Our results showed that ARNTL siRNA increased intracellular lipid-ROS. Accordingly, a substantial increase in the lipid-ROS was found after transfecting with ARNTL siRNA, indicating the increased oxidation status (Figure 6B). In addition, MDA is a lipid peroxidation marker, so the Molm-13 cell MDA levels were assayed after the ARNTL siRNA treatment. The results showed that the average level of MDA in the treated



group was  $3.75 \pm 0.50$  mmol/g, while that in the control group was  $2.12 \pm 0.24$  mmol/g, as shown in Figure 6E. These results suggested that ARNTL siRNA induced significant lipid peroxidation in Molm-13 cells. Therefore, targeted inhibition of ARNTL in AML cells could induce ferroptosis.

## ARNTL siRNA inhibited GPX4 and promoted ACSL4 expression in Molm-13 cells

We transfected the ARNTL siRNA in Molm-13 cells, the transfection efficiency was measured by RT-qPCR, and about 50% of ARNTL was inhibited in Molm-13 cells. Then, the mRNA and protein levels of GPX4 and ACSL4 were analyzed. Our results revealed that the mRNA and protein expression of GPX4 were decreased (Figures 6C,D). In contrast, the ACSL4 expression was increased after ARNTL siRNA transfection (Figures 6C,D). These results further confirmed the inhibition of ARNTL-induced ferroptosis in AML cells.

## Discussion

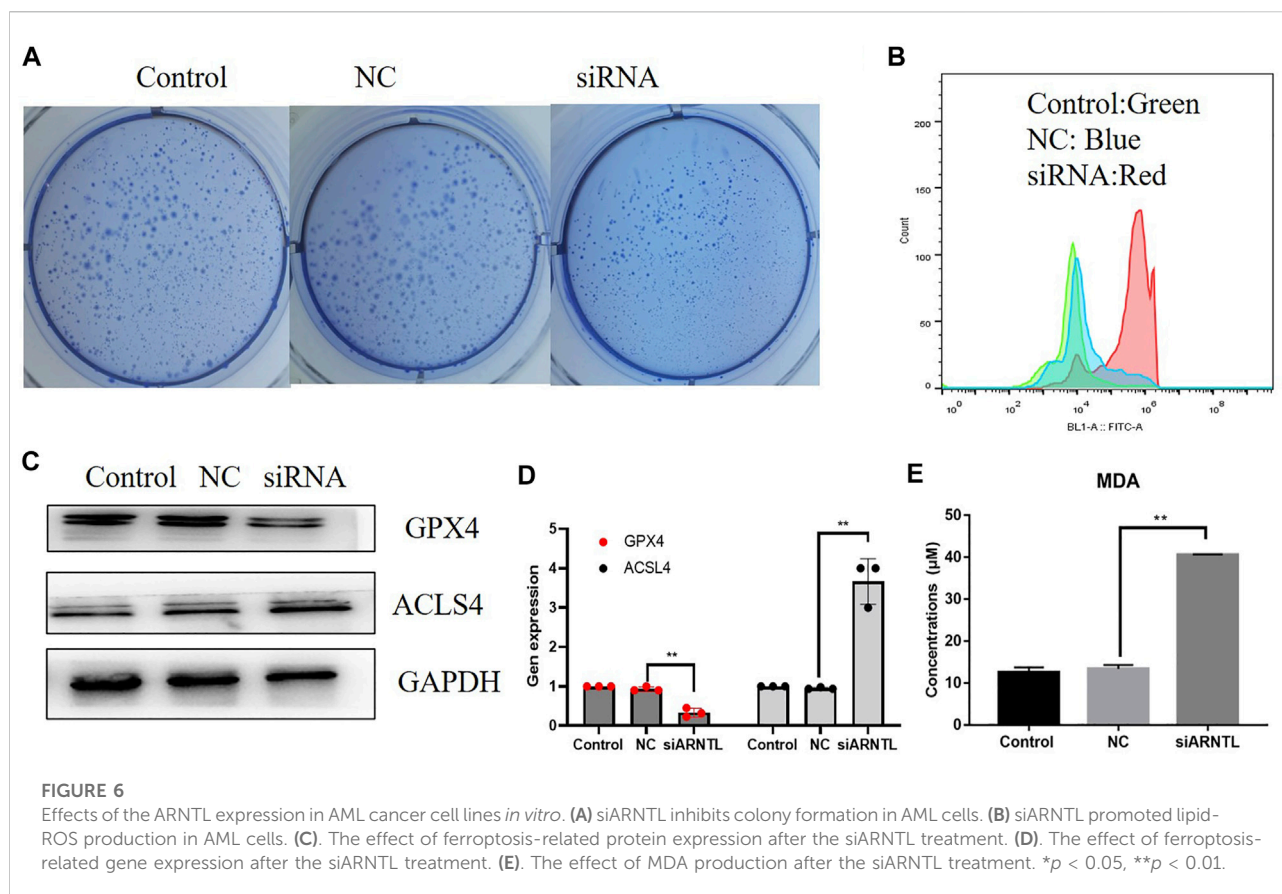
AML is one of the most common lethal hematologic malignancies (Falini et al., 2021). The genetic and molecular

features of AML have been extensively explored, and targeted anti-AML therapy can significantly improve the disease prognosis (Reville and Kadia, 2020). Therefore, it is necessary to diagnose, treat, and explore the pathogenic mechanism behind AML. Moreover, identifying efficient treatments for preventing AML development is required to reduce the significant mortality. Ferroptosis has recently been implicated as an iron-dependent form of programmed cell death in cancers (Liang et al., 2019). Its occurrence is due to lipid ROS accumulation resulting from the excessive iron content in cells (Ghoochani et al., 2021). Therefore, ferroptosis activators have been established as novel targets for therapeutics against advanced diseases (Chen et al., 2021). In this study, we observed a ferroptosis suppression gene ARNTL with significant high expression and correlated with a bad prognosis in AML. Moreover, targeted inhibition of ARNTL induced AML ferroptosis. Therefore, ARNTL could be an essential biomarker gene in AML.

Ferroptosis is caused by the loss of GPX4 (the enzyme for lipid repair) activity and lipid-ROS accumulation (Ding et al., 2021). Targeting ferroptosis is known to facilitate the ATPR-mediated AML differentiation through the ROS-autophagy-lysosomal pathway (Du et al., 2020). In AML, APR-246 can trigger early ferroptosis (Birsan et al., 2021), providing a novel strategy to cure AML.

ARNTL, belonging to the bHLH-PAS transcription factor family, can modulate the cellular circadian rhythm. The





hypermethylation of the ARNTL promoter can be detected in blood cancers (Taniguchi et al., 2009). In our study, ARNTL mRNA levels increased markedly among the AML cases. Silencing of ARNTL could suppress the proliferation and colony-forming ability of AML cells. These findings suggest that ARNTL serves as a tumor stimulate gene in AML, which is inconsistent with its role in other malignancies. In many cancers, ARNTL acts as a tumor suppressor gene [24, 25]. Furthermore, ARNTL acts as a ferroptosis suppressor factor by repressing Egln2 transcription (Yang et al., 2019). Moreover, autophagic degradation of ARNTL promotes ferroptosis (Liu et al., 2019). We also found that the inhibition of ARNTL by siRNA promotes lipid ROS production and lipid peroxidation in AML cells. Meanwhile, the ferroptosis marker protein GPX4 was inhibited, while ACSL4 was increased by siARNTL. These results also found that ARNTL promotes ferroptosis in AML cells, consistent with other research (Zhang et al., 2021).

Glutathione peroxidase 4 (GPX4) plays a vital role in regulating ferroptosis. It also catalyzes the reduction of hydrogen peroxide, lipid hydro-peroxide, and organic hydroperoxides, thereby resisting cellular oxidative damage. In addition, GPX4, an antioxidant enzyme, functions to repair lipid peroxides and regulate cytokine

signaling (Bersuker et al., 2019; Dong et al., 2021). Acyl-CoA synthetase long-chain family member 4 (ACSL4) substantially modulates lipid components and helps execute ferroptosis (Li et al., 2019). Our study found that GPX4 expression was inhibited, and ACSL4 was elevated with ARNTL inhibition. It further revealed that ARNTL acts as a ferroptosis suppressor in AML.

According to Figure 2, we observed that ARNTL expression was correlated with poor prognosis in AML. The clinical characteristics of AML patients are closely related to prognosis. The ROC curve was used to evaluate the discriminating ability of the ARNTL expression (Zhao et al., 2021). In predicting the 1-year, 2-year, and 3-year survival of AML patients in TCGA, the AUC was 0.533, 0.619, and 0.622, respectively. Therefore, the model has an excellent discrimination ability to predict survival.

The ferroptosis-related mechanism within AML is widely investigated. However, the relation of ARNTL levels with immune infiltration remains unclear. The AML immune subtypes indicated that time affected patient survival. We found macrophage, Tgd, neutrophils, cytotoxic cells, and NK CD56 bright cells have a positive correction with ARNTL. Our results revealed that the ARNTL has a tremendous immune ability to kill tumor cells.

Collectively, this work was responsible for constructing the ARNTL-based prognosis nomogram, which was accurate in discriminating and calibrating TCGA-AML patients. ARNTL could be a potential candidate for diagnosing and treating AML.

## Data Availability Statement

The datasets presented in this study can be found in online repositories. The names of the repository/repositories and accession number(s) can be found in the article/[Supplementary Material](#).

## Author Contributions

ZY: formal analysis, funding acquisition, investigation, and writing—original draft. SL: funding acquisition, project administration, data curation, and investigation. FL: conceptualization, resources, supervision, and writing—review and editing. QZ: supervision and writing—review and editing. JZ: investigation. ZL and JH: writing—review and editing. RO and QZ: supervision, visualization, writing—original draft, and writing—review and editing. All authors read and approved the final manuscript.

## Funding

This study was supported by the Guangzhou Science and Technology Plan Project (Nos. 202002030404 and 202102020423), the Foundation of Guangdong Second Provincial General Hospital (Nos. 3DB2020014, 3DA2021004, YQ 2020-002, 2021018, and TJGC-2021011), the Doctoral

Workstation Foundation of Guangdong Second Provincial General Hospital (Nos. 2019BSGZ008, 2020BSGZ048, and 2021BSGZ017), Guangdong Medical Scientific Research (No. B2020092), the Natural Science Foundation of Guangdong Province (No. 2021A1515012329), the Foundation of Deyang People's Hospital (No. FHT202004), the Guangdong Basic and Applied Basic Research Foundation (Nos. 2020A1515010002 and 2021A1515110430), and the Science and Technology Planning Project of Guangdong Province of China (Nos. 2017B030303001 and 2021B1212030008).

## Conflict of Interest

The authors declare that the research was conducted in the absence of any commercial or financial relationships that could be construed as a potential conflict of interest.

## Publisher's Note

All claims expressed in this article are solely those of the authors and do not necessarily represent those of their affiliated organizations, or those of the publisher, the editors, and the reviewers. Any product that may be evaluated in this article, or claim that may be made by its manufacturer, is not guaranteed or endorsed by the publisher.

## Supplementary material

The Supplementary Material for this article can be found online at: <https://www.frontiersin.org/articles/10.3389/fmolb.2022.959738/full#supplementary-material>

## References

- Bersuker, K., Hendricks, J. M., Li, Z., Magtanong, L., Ford, B., Tang, P. H., et al. (2019). The CoQ oxidoreductase FSP1 acts parallel to GPX4 to inhibit ferroptosis. *Nature* 575 (7784), 688–692. doi:10.1038/s41586-019-1705-2
- Birsén, R., Larrue, C., Decroocq, J., Johnson, N., Guiraud, N., Gotanegre, M., et al. (2021). APR-246 induces early cell death by ferroptosis in acute myeloid leukemia. *Haematologica* 107, 403–416. doi:10.3324/haematol.2020.259531
- Chen, X., Kang, R., Kroemer, G., and Tang, D. (2021). Broadening horizons: The role of ferroptosis in cancer. *Nat. Rev. Clin. Oncol.* 18 (5), 280–296. doi:10.1038/s41571-020-00462-0
- Ding, Y., Chen, X., Liu, C., Ge, W., Wang, Q., Hao, X., et al. (2021). Identification of a small molecule as inducer of ferroptosis and apoptosis through ubiquitination of GPX4 in triple negative breast cancer cells. *J. Hematol. Oncol.* 14 (1), 19. doi:10.1186/s13045-020-01016-8
- Dixon, S. J., Lemberg, K. M., Lamprecht, M. R., Skouta, R., Zaitsev, E. M., Gleason, C. E., et al. (2012). Ferroptosis: An iron-dependent form of nonapoptotic cell death. *Cell* 149 (5), 1060–1072. doi:10.1016/j.cell.2012.03.042
- Dong, L. H., Huang, J. J., Zu, P., Liu, J., Gao, X., Du, J. W., et al. (2021). CircKDM4C upregulates P53 by sponging hsa-let-7b-5p to induce ferroptosis in acute myeloid leukemia. *Environ. Toxicol.* 36 (7), 1288–1302. doi:10.1002/tox.23126
- Du, Y., Bao, J., Zhang, M. J., Li, L. L., Xu, X. L., Chen, H., et al. (2020). Targeting ferroptosis contributes to ATRP-induced AML differentiation via ROS-autophagy-lysosomal pathway. *Gene* 755, 144889. doi:10.1016/j.gene.2020.144889
- Falini, B., Brunetti, L., and Martelli, M. P. (2021). How I diagnose and treat NPM1-mutated AML. *Blood* 137 (5), 589–599. doi:10.1182/blood.2020008211
- Ghoochani, A., Hsu, E. C., Aslan, M., Rice, M. A., Nguyen, H. M., Brooks, J. D., et al. (2021). Ferroptosis inducers are a novel therapeutic approach for advanced prostate cancer. *Cancer Res.* 81 (6), 1583–1594. doi:10.1158/0008-5472.Can-20-3477
- Hassannia, B., Vandenabeele, P., and Vanden Berghe, T. (2019). Targeting ferroptosis to iron out cancer. *Cancer Cell* 35 (6), 830–849. doi:10.1016/j.ccell.2019.04.002
- Jiang, X., Stockwell, B. R., and Conrad, M. (2021). Ferroptosis: Mechanisms, biology and role in disease. *Nat. Rev. Mol. Cell Biol.* 22 (4), 266–282. doi:10.1038/s41580-020-00324-8
- Kassambara, A., Kosinski, M., Biecek, P., and Fabian, S.: Data from: survminer: Drawing Survival Curves using 'ggplot2'. R package version 0.4. 3. In: Google Scholar, (2018)
- Lai, C., Doucette, K., and Norsworthy, K. (2019). Recent drug approvals for acute myeloid leukemia. *J. Hematol. Oncol.* 12 (1), 100. doi:10.1186/s13045-019-0774-x

- Lei, G., Zhuang, L., and Gan, B. (2022). Targeting ferroptosis as a vulnerability in cancer. *Nat. Rev. Cancer* 22, 381–396. doi:10.1038/s41568-022-00459-0
- Li, Y., Feng, D., Wang, Z., Zhao, Y., Sun, R., Tian, D., et al. (2019). Ischemia-induced ACSL4 activation contributes to ferroptosis-mediated tissue injury in intestinal ischemia/reperfusion. *Cell Death Differ.* 26 (11), 2284–2299. doi:10.1038/s41418-019-0299-4
- Liang, C., Zhang, X., Yang, M., and Dong, X. (2019). Recent progress in ferroptosis inducers for cancer therapy. *Adv. Mat.* 31 (51), e1904197. doi:10.1002/adma.201904197
- Liu, J., Yang, M., Kang, R., Klionsky, D. J., and Tang, D. (2019). Autophagic degradation of the circadian clock regulator promotes ferroptosis. *Autophagy* 15 (11), 2033–2035. doi:10.1080/15548627.2019.1659623
- Liu, Y., Li, C., Su, R., Yin, Z., Huang, G., Yang, J., et al. (2021). Targeting SOS1 overcomes imatinib resistance with BCR-ABL independence through uptake transporter SLC22A4 in CML. *Mol. Ther. Oncolytics* 23, 560–570. doi:10.1016/j.omto.2021.11.010
- Reville, P. K., and Kadia, T. M. (2020). Maintenance therapy in AML. *Front. Oncol.* 10, 619085. doi:10.3389/fonc.2020.619085
- Tang, Z., Kang, B., Li, C., Chen, T., and Zhang, Z. (2019). GEPIA2: An enhanced web server for large-scale expression profiling and interactive analysis. *Nucleic Acids Res.* 47 (W1), W556–W560. doi:10.1093/nar/gkz430
- Taniguchi, H., Fernández, A. F., Setién, F., Ropero, S., Ballestar, E., Villanueva, A., et al. (2009). Epigenetic inactivation of the circadian clock gene BMAL1 in hematologic malignancies. *Cancer Res.* 69 (21), 8447–8454. doi:10.1158/0008-5472.Can-09-0551
- Wang, H., Cheng, Y., Mao, C., Liu, S., Xiao, D., Huang, J., et al. (2021). Emerging mechanisms and targeted therapy of ferroptosis in cancer. *Mol. Ther.* 29 (7), 2185–2208. doi:10.1016/j.ymthe.2021.03.022
- Wei, R., Qiu, H., Xu, J., Mo, J., Liu, Y., Gui, Y., et al. (2020). Expression and prognostic potential of GPX1 in human cancers based on data mining. *Ann. Transl. Med.* 8 (4), 124. doi:10.21037/atm.2020.02.36
- Willier, S., Rothämel, P., Hastreiter, M., Wilhelm, J., Stenger, D., Blaesckhe, F., et al. (2021). CLEC12A and CD33 coexpression as a preferential target for pediatric AML combinatorial immunotherapy. *Blood* 137 (8), 1037–1049. doi:10.1182/blood.202006921
- Yang, M., Chen, P., Liu, J., Zhu, S., Kroemer, G., Klionsky, D. J., et al. (2019). Clockophagy is a novel selective autophagy process favoring ferroptosis. *Sci. Adv.* 5 (7), eaaw2238. doi:10.1126/sciadv.aaw2238
- Yin, Z., Huang, G., Gu, C., Liu, Y., Yang, J., Fei, J., et al. (2020). Discovery of berberine that targetedly induces autophagic degradation of both BCR-ABL and BCR-ABL T3151 through recruiting LRSAM1 for overcoming imatinib resistance. *Clin. Cancer Res.* 26 (15), 4040–4053. doi:10.1158/1078-0432.Ccr-19-2460
- Yin, Z., Jiang, K., Shi, L., Fei, J., Zheng, J., Ou, S., et al. (2020). Formation of di-cysteine acrolein adduct decreases cytotoxicity of acrolein by ROS alleviation and apoptosis intervention. *J. Hazard. Mat.* 387, 121686. doi:10.1016/j.jhazmat.2019.121686
- Yu, Y., Xie, Y., Cao, L., Yang, L., Yang, M., Lotze, M. T., et al. (2015). The ferroptosis inducer erastin enhances sensitivity of acute myeloid leukemia cells to chemotherapeutic agents. *Mol. Cell. Oncol.* 2 (4), e1054549. doi:10.1080/23723556.2015.1054549
- Yusuf, R. Z., Saez, B., Sharda, A., van Gastel, N., Yu, V. W. C., Baryawno, N., et al. (2020). Aldehyde dehydrogenase 3a2 protects AML cells from oxidative death and the synthetic lethality of ferroptosis inducers. *Blood* 136 (11), 1303–1316. doi:10.1182/blood.2019001808
- Zhang, A., Yang, J., Ma, C., Li, F., and Luo, H. (2021). Development and validation of a robust ferroptosis-related prognostic signature in lung adenocarcinoma. *Front. Cell Dev. Biol.* 9, 616271. doi:10.3389/fcell.2021.616271
- Zhang, C., Liu, X., Jin, S., Chen, Y., and Guo, R. (2022). Ferroptosis in cancer therapy: A novel approach to reversing drug resistance. *Mol. Cancer* 21 (1), 47. doi:10.1186/s12943-022-01530-y
- Zhao, C., Wang, Y., Tu, F., Zhao, S., Ye, X., Liu, J., et al. (2021). A prognostic autophagy-related long non-coding RNA (ARLncRNA) signature in acute myeloid leukemia (AML). *Front. Genet.* 12, 681867. doi:10.3389/fgene.2021.681867



## OPEN ACCESS

## EDITED BY

Yanqing Liu,  
Columbia University, United States

## REVIEWED BY

Muhammad Farrukh Nisar,  
Cholistan University of Veterinary and  
Animal Sciences, Pakistan  
Jie Li,  
University of South Florida,  
United States

## \*CORRESPONDENCE

Xiaoqiang Wang,  
shachengren111@163.com  
Kang Xu,  
kangxu05@hbtcn.edu.cn

<sup>†</sup>These authors have contributed equally  
to this work

## SPECIALTY SECTION

This article was submitted to Molecular  
Diagnostics and Therapeutics,  
a section of the journal  
Frontiers in Molecular Biosciences

RECEIVED 18 May 2022

ACCEPTED 14 July 2022

PUBLISHED 16 August 2022

## CITATION

Li L, Wang X, Xu H, Liu X and Xu K (2022),  
Perspectives and mechanisms for  
targeting ferroptosis in the treatment of  
hepatocellular carcinoma.  
*Front. Mol. Biosci.* 9:947208.  
doi: 10.3389/fmolb.2022.947208

## COPYRIGHT

© 2022 Li, Wang, Xu, Liu and Xu. This is  
an open-access article distributed  
under the terms of the [Creative  
Commons Attribution License \(CC BY\)](#).  
The use, distribution or reproduction in  
other forums is permitted, provided the  
original author(s) and the copyright  
owner(s) are credited and that the  
original publication in this journal is  
cited, in accordance with accepted  
academic practice. No use, distribution  
or reproduction is permitted which does  
not comply with these terms.

# Perspectives and mechanisms for targeting ferroptosis in the treatment of hepatocellular carcinoma

Lanqing Li<sup>1,2†</sup>, Xiaoqiang Wang<sup>1\*†</sup>, Haiying Xu<sup>2</sup>, Xianqiong Liu<sup>2</sup>  
and Kang Xu<sup>2\*</sup>

<sup>1</sup>Department of Otolaryngology-Head and Neck Surgery, The First Affiliated Hospital of Chongqing Medical University, Chongqing, China, <sup>2</sup>Hubei Engineering Technology Research Center of Chinese Materia Medica Processing, College of Pharmacy, Hubei University of Chinese Medicine, Wuhan, China

Ferroptosis is a novel process of regulated cell death discovered in recent years, mainly caused by intracellular lipid peroxidation. It is morphologically manifested as shrinking of mitochondria, swelling of cytoplasm and organelles, rupture of plasma membrane, and formation of double-membrane vesicles. Work done in the past 5 years indicates that induction of ferroptosis is a promising strategy in the treatment of hepatocellular carcinoma (HCC). *System xc<sup>-</sup>/GSH/GPX4*, iron metabolism, p53 and lipid peroxidation pathways are the main focus areas in ferroptosis research. In this paper, we analyze the ferroptosis-inducing drugs and experimental agents that have been used in the last 5 years in the treatment of HCC. We summarize four different key molecular mechanisms that induce ferroptosis, i.e., *system xc<sup>-</sup>/GSH/GPX4*, iron metabolism, p53 and lipid peroxidation. Finally, we outline the prognostic analysis associated with ferroptosis in HCC. The findings summarized suggest that ferroptosis induction can serve as a promising new therapeutic approach for HCC and can provide a basis for clinical diagnosis and prevention of this disease.

## KEYWORDS

ferroptosis, hepatocellular carcinoma, cell death, molecular signaling, targeted therapy

**Abbreviations:** HCC, HCC; GSH, Glutathione; ACD, Accidental cell death; RCD, Regulated cell death; RR, Ribonucleotide reductase; FUF, Ferroptosis upregulation factor; FDF, Ferroptosis downregulation factor; System xc<sup>-</sup>, Cystine/Glutamate transporter; x CT, SLC7A11; TRIB2, Tribbles homolog 2; CP, Copper cyanidin; PUFAs, Polyunsaturated fatty acids; G6PD, Glucose-6-phosphate dehydrogenase; SOR, Sorafenib; FTH1, Heavy chain ferritin; HMOX1, Heme oxygenase 1; ROS, Reactive oxygen species; MT1, Metallothionein-1; GSTZ1, Glutathione S-transferase zeta 1; Rb, Retinoblastoma; DHA, Dihydroartemisinin; FC, Formosanin C.



## Introduction

Cell death is important for maintaining homeostasis and cellular functions. Cell death is classified into two types: accidental cell death (ACD) and regulated cell death (RCD) (Fuchs and Steller, 2011). Of these, RCD is further divided into apoptosis, necroptosis, pyroptosis, and ferroptosis in the early stage (Grootjans et al., 2017; Tang D et al., 2019). Different types of cell death have different morphological characteristics and response mechanisms with distinct molecular mechanisms and regulatory factors. Ferroptosis as a mechanism of cell death was first proposed in 2012. It is an iron-dependent form of RCD that, unlike apoptosis, is not dependent on caspases or the BCL-2 family. It is mainly characterized by accumulation of ferrous ions and unrestricted lipid peroxidation leading to plasma membrane rupture (Dixon et al., 2012; Stockwell et al., 2017).

Liver diseases are the leading cause of death worldwide (Asrani et al., 2019; Fu et al., 2022). Liver is the metabolic center for absorption of glucose, amino acids, and other nutrients (Feng F et al., 2021; Pan et al., 2021; Li L et al., 2022; Pan et al., 2022). Therefore, dysregulation of liver function may lead to oxidative stress, potentially causing a series of liver diseases. Ferroptosis plays an important role in liver metabolic pathways such as regulation of NADPH levels, GSH levels, and fatty acid metabolism (Chen et al., 2022). In addition, iron metabolism, which induces ferroptosis, is also mainly regulated by the liver. Ferroptosis-induced cell death plays an important role in the development of liver diseases such as hemochromatosis, alcohol-associated liver disease (ALD), hepatitis C virus (HCV) infection, non-alcoholic steatohepatitis (NASH), and hepatocellular carcinoma (HCC) (Nie et al., 2018; Shojaie et al., 2020).

The latest cancer statistics released in 2020 in the Global Cancer Statistics Report show that primary liver cancer is the sixth most common cancer and the third most deadly cancer worldwide (Sung et al., 2021). HCC ranks fifth in global incidence and places a significant economic burden on the world's public health systems. Owing to the rapid growth and migration of HCC, it is often difficult to control its development with existing treatment modalities, ultimately leading to a lower survival rate (Chen et al., 2021b; Li L et al., 2022). Modern HCC treatment include both surgical and non-surgical treatments. The proportion of patients that can be treated surgically is less than 30% (Zhou et al., 2016). Furthermore, surgical treatment is associated with a 40% recurrence rate (Ryerson et al., 2016). Non-surgical treatments include targeted drug therapy (Liu Z et al., 2019; Song et al., 2019), chemotherapy (Goyal et al., 2019), radiotherapy (Zaheer et al., 2019), and Chinese medicine (Yang et al., 2020b). These treatment strategies are aimed at selective killing of cancer cells without affecting normal

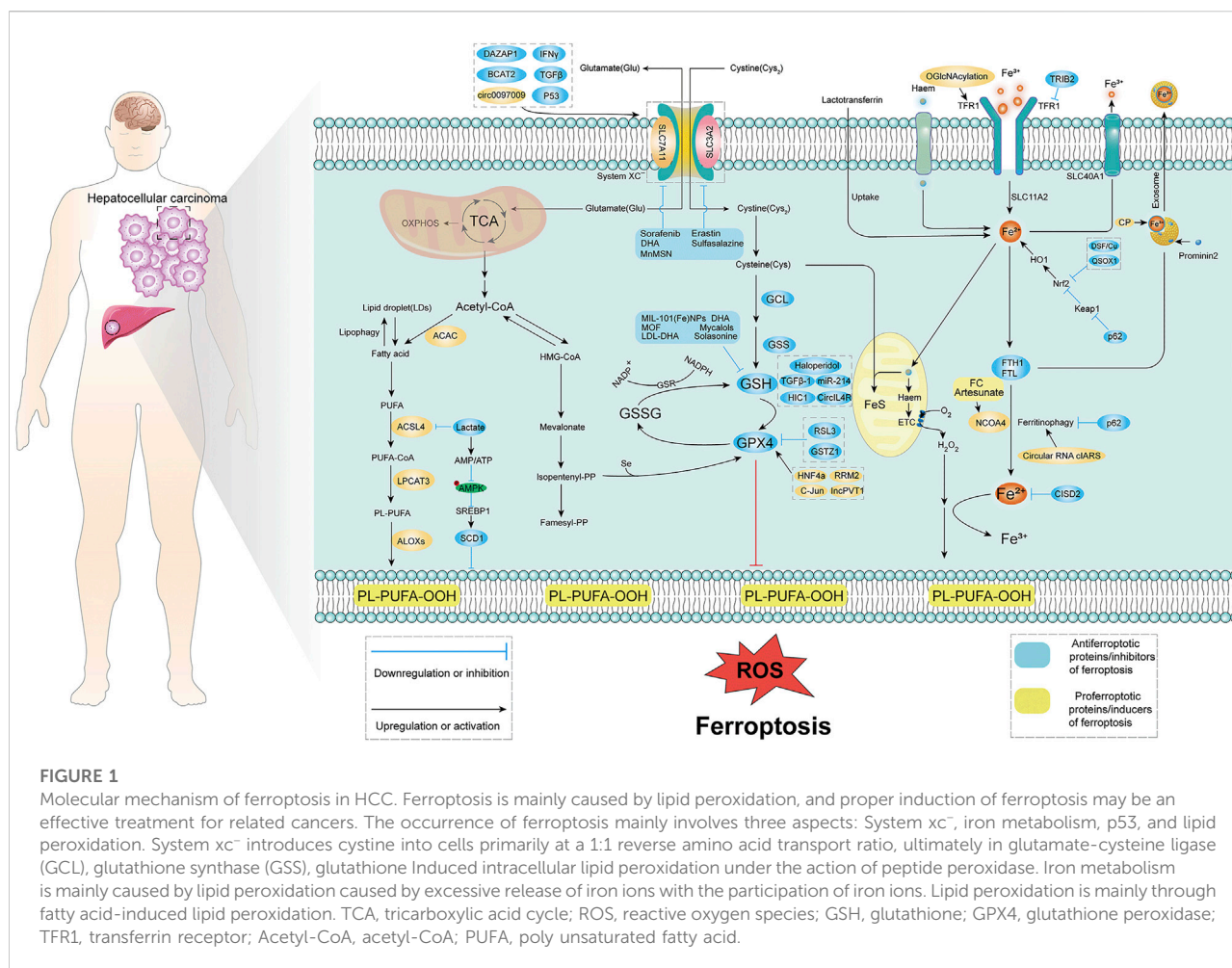
cells. Despite this, existing treatments often have the disadvantages of also causing normal cell death along with incomplete killing of cancer cells. In recent years, a major breakthrough has been made in inhibiting the growth of HCC by selective induction of cell death.

Recent studies have shown that the tumor microenvironment plays a complex and multifaceted role in the induction of cancer cell ferroptosis. For example, immune cells such as neutrophils and macrophages can be recruited into cancer tissue through chemokines released from cancer cells and cancer-associated stromal cells. These are then directed by proteins, metabolites, etc., to perform pro- or anti-tumor functions, thus affecting the regulation of iron metabolism in cancer cells (Liang and Ferrara, 2020). In addition, substantial progress has been made in the treatment of HCC *via* targeted regulation of ferroptosis. The classical method of induction of ferroptosis is by blocking intracellular glutathione peroxidase GPX4 through the inhibition of cystine/glutamate transporter (system xc<sup>-</sup>), thus resulting in inhibition of HCC cell proliferation (Yang et al., 2014). Modern drugs used to induce the onset of ferroptosis in liver cancer cells are erastin and sorafenib, which target the RCD process and may provide a new effective therapeutic measure to inhibit HCC.

In this paper, we present a systematic summary of the mechanisms of ferroptosis, including System xc<sup>-</sup>, iron metabolism, p53, and lipid peroxidation. We also enumerate the drugs and novel technologies used to target ferroptosis in recent years and discuss how ferroptosis can be used as a target in liver cancer treatment. Finally, we highlight several key questions and challenges for future research.

## Ferroptosis overview

Ferroptosis, a unique Fe-dependent cell death mechanism, was first proposed in 2012. Cells undergoing ferroptosis exhibit distinct morphological features such as shrunken mitochondria and reduced number of mitochondrial ridges. It is mainly characterized by an excessive accumulation of lipid peroxide leading to impaired cell membrane function (Dixon et al., 2012; Stockwell et al., 2017) (Figure 1). Ferroptosis can be induced by inhibition of cell membrane transport proteins through an exogenous pathway or by blocking the activation of intracellular antioxidant enzymes (Tang and Kroemer, 2020). Ferroptosis induces a unique form of cell death that offers a potential for developing novel drugs for cancers that are difficult to treat with conventional therapies. Induction of ferroptosis in HCC is an attractive alternative novel therapeutic approach for liver cancer. We have compiled relevant physiological studies describing ferroptosis in HCC and describe the relevant targets of action and mechanisms (Table 1).



## Hepatocellular carcinoma- related pathways in ferroptosis

### System xc<sup>-</sup>/GSH/GPX4

The System xc<sup>-</sup>/GSH/GPX4 axis plays a crucial role in promoting lipid peroxidation in the induction of ferroptosis (Galadari et al., 2017). System xc<sup>-</sup> acts as a cystine and glutamate transporter in the cell and promotes intracellular GSH synthesis by simultaneously transporting cystine into and glutamate outside the cell (Capelletti et al., 2020). GSH is mainly composed of glutamate, cysteine, and glycine. These amino acids contain sulfhydryl structures that can be oxidized, allowing GSH to protect cells from oxidative stress damage. As GSH serves as a cofactor for the selenoenzyme GPX4, inhibiting the *de novo* GSH synthesis induces ferroptosis by inactivating GPX4 (Ingold et al., 2018).

System xc<sup>-</sup> is a reverse transporter protein located on the plasma membrane and consists of a light chain subunit SLC7A11 (x CT) and a heavy chain subunit SLC3A2 (CD98hc or 4F2hc)

linked by a covalent disulfide bond. Of these, SLC7A11 is highly specific for cystine and glutamate. SLC3A2 is a chaperone protein that helps to enhance the stability of SLC7A11 and participates in regulating the transport of SLC7A11 to the plasma membrane (Koppula et al., 2018; Lin W et al., 2020). Inhibition of System xc<sup>-</sup> can effectively downregulate GSH/GPX4 expression, thereby inducing cancer cell ferroptosis. DAZAP1 is an RBP that was initially found to be abundantly expressed in the liver, heart and brain (Dai et al., 2001). Recent studies have shown that inhibition of DAZAP1 expression can significantly destabilize SLC7A11 (Choudhury et al., 2014; Chen et al., 2020; Wang et al., 2021d). Another recent study showed that downregulation of SLC7A11 expression both at mRNA and protein levels was effective in promoting ferroptosis. IFN $\gamma$  is a glycosylated protein that can induce apoptosis or autophagy in tumor cells *via* immune cells along with other molecules (Castro et al., 2018; Alspach et al., 2019). IFN $\gamma$  was able to sensitize HCC cells to ferroptosis by activating the JAK/STAT pathway in HCC, downregulating the mRNA and protein levels of SLC7A11 and SLC3A2, eventually inhibiting System xc<sup>-</sup>

TABLE 1 Pathways and targets of ferroptosis in HCC.

Target	Effector/reagent	Proposed mechanism	References
SLC7A11	Inhibition of DAZAP1	Destabilization of SLC7A11	Choudhury et al. (2014); Chen et al. (2020); Wang et al. (2021d)
	Knock down circ0097009	Downregulation of SLC7A11 expression	Lyu et al. (2021)
SLC7A11 and SLC3A2	IFN $\gamma$	IFN $\gamma$ activates JAK/STAT and downregulates SLC7A11 and SLC3A2 expression	Kong et al. (2021)
System Xc <sup>-</sup>	Inhibition of BCAT	Reduces glutamate synthesis and affects System x <sup>c-</sup>	Wang et al. (2021c)
	TGF $\beta$ -1	Inhibition of System x <sup>c-</sup> , reduction of GSH and GPX4 by Smad3	Dituri et al. (2019); Kim et al. (2020)
GSH	Inhibition of C-Jun	Inhibition of GSH expression level	Vogt (2002); Chen Y et al. (2019)
	Inhibition of RRM2		Duxbury et al. (2004); Duxbury and Whang (2007)
	Inhibition of PSAT1		Tang H et al. (2019)
GPX4	Knockdown CircIL4R	Inhibition of GPX4 expression levels	Yao et al. (2019); Xu et al. (2020)
ferroptosis	Upward HBA1	Direct induction of ferroptosis	Tang H et al. (2019)
	HNF4a	HNF5a upregulates STMN1 to directly inhibit ferroptosis	
TFRC	OGlcNAcylation	Enhancement of YAP transcriptional activity and upregulation of TFRC	Zhu et al. (2021)
	TRIB2	Inhibition of TRIB2 and upregulation of TFRC	Guo et al. (2021)
LIP	RSL3	Upregulation of LIP	Asperti et al. (2021)
Iron ions	CP	CP-FPN system causes iron ion efflux and inhibits ferroptosis	Shang et al. (2020)
Ferritin autophagy	Circular RNA cIARS	Negative regulation of ALKBH5	Liu et al. (2020)
SREBP1 and SCD1	Lactate	Inhibition of HCAR1/MCT1 was able to block ATP production, which initiated AMPK phosphorylation, inhibited the expression of downstream SREBP1 and SCD1, and suppressed ferroptosis	Zhao et al. (2020)
ACSL4	Lactate	Inhibition of ACSL4, inhibition of ferroptosis	Zhao et al. (2020)
POR	G6PD	Positive regulation	Yang et al. (2019); Koppula et al. (2021)

activity (Kong et al., 2021). BCAT2 is a transaminase that mediates sulfur amino acid metabolism whose inhibition can reduce glutamate *de novo* synthesis, affect the conversion of System x<sup>c-</sup> cystine to glutamate, and inhibit cystine uptake, thus inducing ferroptosis (Wang et al., 2021c). Transforming growth factor beta (TGF $\beta$ -1) can regulate cell growth and differentiation, and has inhibitory effects on cancer cells. TGF $\beta$ -1 can inhibit xCT through Smad3 and reduce the expression of GSH and GPX4 (Dituri et al., 2019; Kim et al., 2020). Finally, Circular RNAs (circRNAs) are a class of non-coding RNAs that can inhibit the growth, migration, and invasion of HCC (Yao et al., 2017). Indeed, knockdown of circ0097009 was found to enhance the sensitivity of HCC cells to ferroptosis through miR-1261 downregulation of SLC7A11 expression (Lyu et al., 2021).

GSH is a scavenger of free radicals and is the main cofactor involved in lipid peroxide reduction by GPX4. It has an important role in cellular defense against oxidative stress. Several studies have shown that inhibition of GSH/GPX4 can increase ferroptosis. Inhibition of O-GlcNAcylated c-Jun, the first oncogenic factor identified, can inhibit GSH synthesis by suppressing PSAT1 and CBS transcription (Vogt, 2002; Chen Y et al., 2019). Ribonucleotide reductase (RR) is essential during

DNA replication and repair, and consists of two subunits (RRM1 and RRM2). RRM2 plays an important role in tumor development (Duxbury et al., 2004; Duxbury and Whang, 2007). RRM2 expression was significantly elevated in HCC, and its inhibition induced ferroptosis through GSS inhibition of GSH synthesis (Yang et al., 2020a). Ferroptosis upregulation factor (FUF) and ferroptosis downregulation factor (FDF) are regulated by transcription factors HIC1 and HNF4a respectively. HIC1 induces ferroptosis directly through upregulation of HBA1 or by suppressing the expression of PSAT1 leading to downregulation of GSH. HNF4a on the other hand inhibits ferroptosis through upregulation of STMN1 or by upregulation of PSAT1 leading to upregulation of GSH. By controlling HIC1 and HNF4a expression, it is possible to selectively inhibit GSH expression (Tang H et al., 2019). Non-coding RNAs have also been reported to be involved in tumor suppression (Liu et al., 2016). CircIL4R was shown to be significantly upregulated in HCC tissues and circIL4R knockdown was able to inhibit GPX4 activity *via* mir-541-3p (Yao et al., 2019; Xu et al., 2020). Taken together, these studies suggest that HCC can be effectively inhibited by inhibiting the System x<sup>c-</sup>/GSH/GPX4 axis. However, some cancer cells remain

resistant to ferroptosis even after GPX4 inhibition, indicating the existence of additional ferroptosis defense mechanisms that deserve further investigation.

## TP53

As one of the “star molecules” in antitumor research, p53 has attracted the attention of researchers around the world. Its functions and post-translational modifications have highlighted the diversity and complexity of this protein (Liu Y et al., 2019). Studies have shown that deletion or mutation of the p53 gene leads to loss of wild-type p53 activity and malignant transformation of tumors (Bykov et al., 2018; Levine, 2020). Approximately 50% of patients with HCC have p53 gene deletion in their tumor cells (Aning and Cheok, 2019). Traditionally, it was thought that p53 mainly induces cell cycle arrest, senescence or apoptosis (Brady et al., 2011; Li et al., 2012; Liu and Gu, 2022). However, in recent years, it has been found that p53 can have oncogenic functions even with loss of function mutations (Liu and Gu, 2021). Several studies have shown that p53 plays a crucial role in regulating tumor metabolic activities (including glucose metabolism, oxidative phosphorylation, and lipid metabolism) (Schwartzberg-Bar-Yoseph et al., 2004; Contractor and Harris, 2012; Liu and Gu, 2021). TP53 is also involved in regulating ferroptosis. On the one hand, p53 is able to inhibit SLC7A11 expression at the transcriptional level, increasing the likelihood of ferroptosis through GSH-dependent versus non-dependent (P53/SLC7A11/ALOX12) forms (Jiang et al., 2015; Ou et al., 2016; Venkatesh et al., 2020). On the other hand, p53 is also able to inhibit ferroptosis. For example, p53 inhibits ferroptosis by activating iPLA2 $\beta$  but promotes ferroptosis when external stimuli exceed a certain threshold (Chen et al., 2021a). Notably, although p53 has also been widely explored in HCC, there are very few reports highlighting its role in inducing ferroptosis in HCC. Therefore, how p53 induces or inhibits ferroptosis in HCC is a topic that needs further investigation.

## Iron metabolism

Iron is indispensable for maintaining normal life activities of organisms. Iron metabolism plays an important role in the process of ferroptosis, in which extracellular Fe<sup>3+</sup> is transported to the cell and reduced to Fe<sup>2+</sup> through transferrin on the cell membrane. Fe<sup>2+</sup> accumulates with excess intracellular H<sub>2</sub>O<sub>2</sub> through the Fenton reaction leading to ROS, which promotes intracellular lipid peroxide (LPO) production and triggers ferroptosis (Stockwell et al., 2017).

Ferritin is an important site for intracellular Fe<sup>2+</sup> storage. Release of sufficient Fe<sup>2+</sup> through autophagy induces ferroptosis. Transferrin receptor (TFRC) is a protein located on the

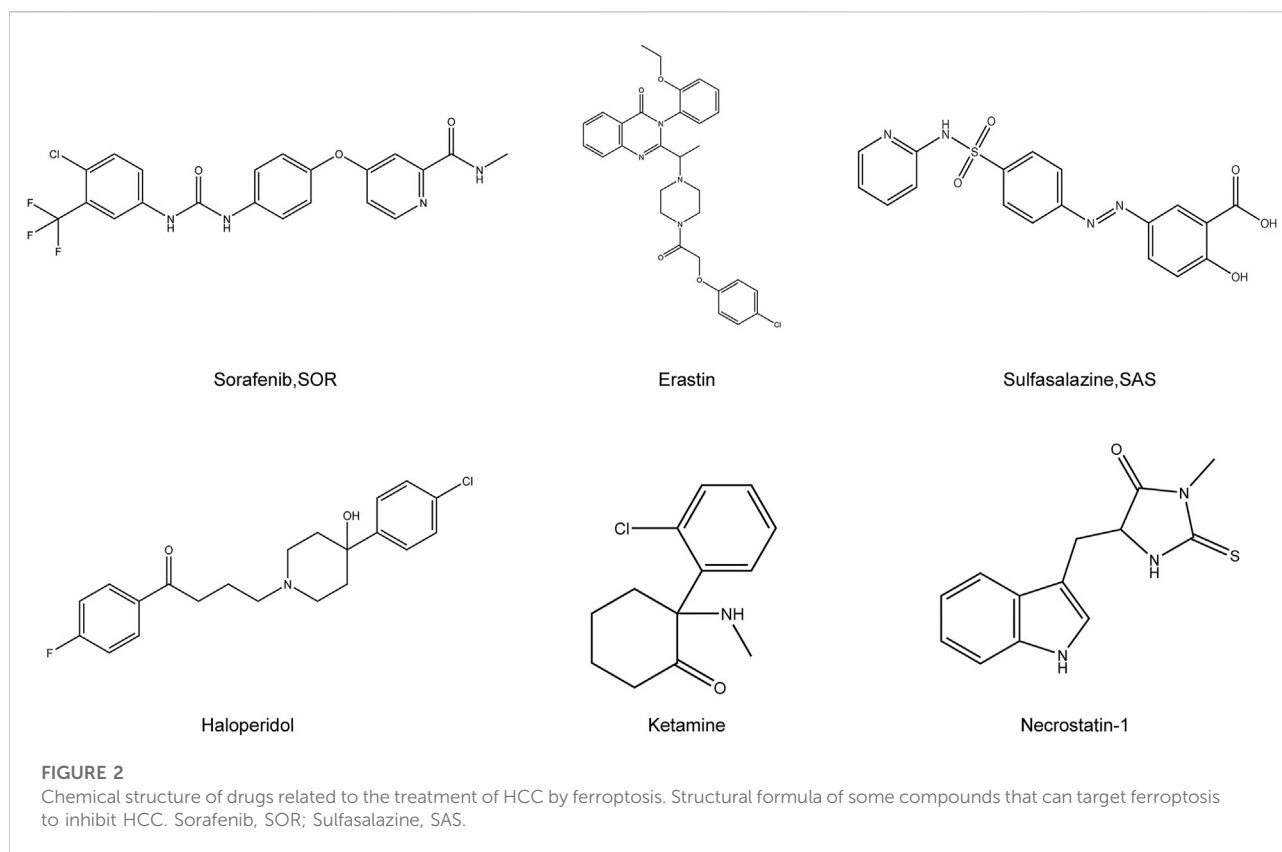
membrane whose expression correlates with tumor stage or cancer progression. Early targeted regulation of TFRC expression has been reported as an effective strategy for the treatment of various cancers (Horonchik and Wessling-Resnick, 2008; Daniels et al., 2012). For example, O-GlcNAcylation, a reversible post-translational modification catalyzed by O-GlcNAc transferase (OGT), significantly enhances YAP transcriptional activity, which leads to increased TFRC expression. TFRC overexpression enhances cellular iron uptake and enhances ferroptosis (Zhu et al., 2021). Another study indicated that Tribbles homolog 2 (TRIB2), which is highly expressed in HCC, suppresses TFRC expression, thereby inhibiting Fe<sup>3+</sup> uptake and reducing ferroptosis (Guo et al., 2021). Iron ions exist in the form of divalent ions in the cytoplasm, and formation of the cytoplasmic unstable iron pool (LIP) is key to ferroptosis induction. In well-differentiated HepG2 cells, GSH peroxidase 4 inhibitor (RSL3, (1S,3R)-RSL3) treatment can upregulate LIP levels, while the levels of transferrin receptor 1 (TFR1), membrane iron transport protein 1 (FPN1), and ferritin, related proteins involved in ferroptosis, were reduced (Asperti et al., 2021). Copper cyanidin (CP) is a copper-containing glycoprotein, mainly synthesized by the liver and present in large amounts in human plasma, which can assist FPN to export iron ions and regulate iron metabolism. The CP-FPN system causes iron ion efflux and inhibits ferroptosis. Thus, downregulation of CP can induce ferroptosis (Shang et al., 2020). Circular RNAs also play a key role in iron metabolism. It was reported that the circular RNA ciARS can negatively regulate ALKBH5 (demethylase, an autophagy inhibitor) to induce ferritin autophagy and release ferric ions thereby enhancing the effect of SOR treatment-induced ferroptosis (Liu et al., 2020). Thus, iron metabolism can increase ferroptosis sensitivity by multiple mechanisms.

## Lipid peroxidation

Fatty acid components of the mevalonate pathway and membrane phospholipids are involved in ferroptosis. The mevalonate pathway is mainly dominated by Acetyl Coenzyme A (CoA), while the fatty acids of membrane phospholipids are mainly involved in polyunsaturated fatty acids (PUFA). Polyunsaturated fatty acids (PUFAs) are susceptible to oxidation in ferroptosis, leading to disruption of the lipid bilayer and affecting cell membrane function. The biosynthesis and maintenance of normal physiological functions of polyunsaturated fatty acids in cell membranes requires a series of enzymes, such as ACSL4 and LPCAT3, to ensure that the cell membrane is not disrupted.

In cancerous cells, sugar metabolism is at the core of energy generation, and its metabolic characteristics are distinct from normal cells. Tumor cells mainly use glycolysis as the mode of energy production, i.e., Warburg effect (Hanahan and Weinberg,





2011). Lactate is a more involved product in Glucose metabolism, and studies have shown that lactate uptake by cancer cells is mainly achieved through the transporter protein MCT1, whose expression level is regulated by HCARI (Roland et al., 2014; Khan et al., 2020; Tasdogan et al., 2020). Excess lactate is able to support ATP production through the tricarboxylic acid cycle (TCA), and by inhibiting HCARI/MCT1 is able to hinder ATP production. This initiates AMPK phosphorylation, inhibits downstream SREBP1 and SCD1 expression, and induces ferroptosis. In addition, lactate inhibits the expression of ACSL4 and thus protects HCC cells from ferroptosis. Therefore, blocking lactate uptake may also induce ferroptosis and inhibit HCC (Zhao et al., 2020).

Glucose-6-phosphate dehydrogenase (G6PD) was shown to be a key enzyme in the pentose phosphate pathway (PPP) and plays a critical role in the production of NADPH. G6PD positively regulates ferroptosis by regulating POR (Cao et al., 2021). Cytochrome P450 oxidoreductase (POR) increases ferroptosis by upregulating peroxidation of membrane polyunsaturated phospholipids (Yang et al., 2019; Koppula et al., 2021). In conclusion, metabolic pathways are able to participate in the induction of ferroptosis in cancer cells to varying degrees. However, HCC is not well studied in the context of lipid peroxidation-induced ferroptosis, a potential pathway to induce ferroptosis in HCC.

## Current stage of pharmacological study of ferroptosis in hepatocellular carcinoma

The recent discovery of ferroptosis has led to its application in the inhibition of liver tumors. Use of ferroptosis inducers and emerging technologies offers new possibilities for treating patients with HCC with potentially reduced side effects (Figure 2). In the next few sections, we describe the signals associated with ferroptosis in HCC and highlight the potential therapeutic agents for clinical translation (Table 2).

### Sorafenib

Sorafenib (SOR) is the first multi-tyrosine kinase inhibitor approved for the treatment of patients with unresectable HCC, advanced kidney cancer, and differentiated thyroid cancer (Kim and Park, 2011; Zhu et al., 2017). The main feature of this compound is its ability to not only directly inhibit tumor cell proliferation but also indirectly inhibit tumor angiogenesis. Although several cancer-associated protein kinase targets have been identified for SOR in HCC, the underlying mechanism of its action remains unclear. Despite its potential, clinical SOR use is associated with

side effects. These include worsening liver dysfunction and reduced survival benefit in SOR-treated patients with advanced cirrhosis of Child-Pugh class B or C (Pinter et al., 2009; Wörns et al., 2009). Although SOR has been consistently reported to cause ferroptosis *via* system xc<sup>-</sup>, its mechanism was unlike the homologous system xc<sup>-</sup> inhibitors sulphasalazine and elastin. Therefore, SOR is not exclusively

responsible for HCC cell death *via* system xc<sup>-</sup> induced ferroptosis in different HCC cell lines (Zheng et al., 2021).

It was shown that the anticancer activity of SOR *via* ferroptosis induction relies mainly on the inhibition of System xc<sup>-</sup> (Dixon et al., 2014). Therefore, we will discuss the specific mechanism of SOR-mediated induction of ferroptosis in HCC. SOR-mediated inhibition of liver cancer cell growth is not *via* a

TABLE 2 Drugs and pathways of action related to ferroptosis in HCC.

Target	Remarks	Action mechanism	References
SOR		Disruption of mitochondrial morphology and reduction of ATP synthesis	Li Y et al. (2021)
		GSH consumption	
	Knockdown MT1G	Increase GSH consumption	Houessinon et al. (2016); Sun et al. (2016a)
	SPARC overexpression	Promotes LDH release and enhances the toxic effects of SOR	Hua et al. (2021)
	Joint use of RSL3	Inhibition of GSTZ1 increases the effect of SOR on the induction of ferroptosis	Wang K et al. (2021)
	Downward adjustment of Rb	Increased SOR-induced mortality in HCC cells	Louandre et al. (2015)
	Knock down C1SD2	Increase ROS,MDA levels and promote SOR-induced ferroptosis	Li B et al. (2021)
	Reduce P62, NRF2	Promote SOR-induced ferroptosis	Ichimura and Komatsu (2018)
	DSF/Cu,NRF2	Promote SOR-induced ferroptosis	Ren et al. (2021)
	QSOX1,NRF2	Promote SOR-induced ferroptosis	Sun et al. (2021)
Natural Products	Formosanin C	Downregulation of ferritin heavy chain polypeptide 1 (FTH1) and upregulation of NCOA4	Lin P. L et al. (2020)
	Heteronemin	Induction of ROS formation	Chang et al. (2021)
	Mycalols	Decrease the expression of GPX4 and increase the expression of NCOA4	Riccio et al. (2021)
	Solasonine	Inhibition of Gpx4 and GSS	Jin et al. (2020)
	Artesunate	Promotes lysosomal histone B/L activation, ferritin autophagy, and lipid peroxidation	Li Z. J et al. (2021)
	DHA	Increased expression of ROS, MDA and decreased activity of glutathione (GSH), GPX4, solute carrier family (SLC) SLC7A11, SLC3A2	Wang Z et al. (2021)
	<i>S. barbata</i>	Decreased GPX4 and SLC7A11, increased IREB2, ACSL4 expression	Li Y et al. (2022)
	Atractylodin	Decrease GPX4,FTL levels and increase ACSL4,TFR1 levels	He et al. (2021)
	MnMSN(FaPEG-MnMSN@SFB)	Depletion of HSG, suppression of System xc <sup>-</sup>	Tang H et al. (2019); Tang H et al. (2020)
	HKUST-1	Integrates cyclooxygenase 2 (COX-2), which depletes GSH and inhibits GPX4 activity; induces PINK1/Parkin-mediated mitochondrial autophagy	Gu et al. (2011); Tian et al. (2022)
Novel Drug Technologies	MIL-101(Fe)@sor NPs	Increased lipid peroxidation and MDA levels, decreased GSH and GPX4	Liu et al. (2021)
	Cas13a or microRNA combined with iron nanoparticles	Induce ferroptosis	Sun et al. (2021)
	LDL-DHA	GSH depletion and inhibition of GPX4	Ou et al. (2017)
	Exosomes (ExosCD47)	Bypassing the phagocytic effects of MPS, chemophotodynamic therapy targets the induction of ferroptosis	Chen R et al. (2019); Du et al. (2021)
	MicroRNA-214-3p (miR-214) combined with Erastin	Increased MDA, ROS expression levels, upregulated iron ion concentration, and decreased GSH levels	Bai et al. (2020)
	Ketamine	Inhibits GPX4 expression	Zhu et al. (2021)
	Haloperidol	Downregulation of S1R, downregulation of GSH levels and upregulation of lipid peroxidation in liver cancer cells	Wang et al. (2015); Bai et al. (2019)
	Nucleoprotein 1 (NUPR1) inhibitor ZZW-115	Disruption of mitochondrial morphology and metabolic function	Huang et al. (2021)
	YAP/TAZ	Induces the expression of SLC7A11 and inhibits ferroptosis	Gao et al. (2021)
	Necrostatin-1	Induces the expression of SLC7A11 and inhibits ferroptosis	Yuk et al. (2021)
Others			

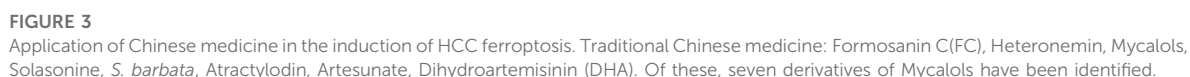
TABLE 3 Seven derivatives of Mycalols.

Mycalol-550	$R_1 = C_5H_{11}$	$R_2 = Ac$
Mycalol-522	$R_1 = C_3H_7$	$R_2 = Ac$
Mycalol-578	$R_1 = C_7H_{15}$	$R_2 = Ac$
Mycalol-594	$R_1 = C_5H_{11}$	$R_2 = (3S)-3HB$
Mycalol-622	$R_1 = C_7H_{15}$	$R_2 = (3S)-3HB$
Mycalol-636	$R_1 = C_8H_{17}$	$R_2 = (3S)-3HB$
Mycalol-650	$R_1 = C_9H_{19}$	$R_2 = (3S)-3HB$

single apoptotic process. Studies have revealed that blocking apoptosis does not prevent the iron-dependent cytotoxicity of SOR. In contrast, iron chelation did not prevent the toxic effects of SOR on HCC cells under pro-apoptotic conditions. These results suggest that SOR may be a better inducer of ferroptosis in cultured liver cancer cells (Louandre et al., 2013). Treatment of HCC cells with SOR for different times produced different levels of phosphorylation in HCC cells. E3 ubiquitin protein ligase MDM2 (Q00987) is involved in p53 regulation. The phosphosite pSer166 (FC = 0.16,  $p = 0.022$ ) on MDM2 is a key residue in this regulation. Sorafenib treatment resulted in sixfold reduction of pSer166 levels, while pSer315 (FC = 0.25,  $p = 0.019$ ) and pSer392 (FC = 0.02,  $p = 0.027$ ) sites on p53 decreased significantly by 4-fold and 50-fold, respectively. By 60 min, significant changes were observed in p53 (P04637), CAD protein (P27708), and iron homeostasis important proteins such as heavy chain ferritin FTH1, heme oxygenase 1 (HMOX1; P09601), and PCBP1 (Q15365). These key targets are largely correlated with ferroptosis, suggesting a possible involvement of phosphorus-regulated signaling during SOR-induced ferroptosis (Werth et al., 2020). In addition, ferroptosis manifests morphologically as disrupted mitochondrial morphology. SOR is thus able to disrupt the mitochondrial morphology of HCC cells accompanied with decreased oxidative phosphorylation activity, mitochondrial membrane potential and ATP synthesis, and subsequent cell death *via* ferroptosis. In addition, depletion of glutathione through cysteine deprivation or cysteinase inhibition exacerbates SOR-induced ferroptosis and lipid peroxide production, enhances oxidative stress and mitochondrial ROS accumulation, and induces ferroptosis (Li Y et al., 2021). However, SOR resistance is a potential problem in the treatment of patients with HCC. New findings suggest that NRF2 activation upregulates the expression of MT1G mRNA of the metallothionein-1 (MT1) family during SOR treatment. Knockdown of MT1G increases glutathione (GSH) depletion and lipid peroxidation, thus inducing ferroptosis. Therefore, MT1G may be a key regulator to target in tackling drug resistance during SOR chemotherapy (Sun et al., 2016a; Houessinon et al., 2016).

In HCC, there are some regulators can synergize or antagonize SOR action. For instance, overexpression of

cysteine-rich secretory acidic protein (SPARC) induces oxidative stress, which induces ferroptosis. This promotes the release of lactate dehydrogenase (LDH), disrupts the expression of proteins associated with ferroptosis, and enhances the toxic effects of SOR in Hep3B and HepG2 cells (Hua et al., 2021). Glutathione s-transferase (GSTZ1), an enzyme involved in phenylalanine metabolism, is significantly downregulated in SOR-resistant HCC cells. Downregulation of GSTZ1 leads to activation of the NRF2 pathway, which upregulates glutathione peroxidase (GPX4) and inhibits ferroptosis. The GPX4 inhibitor RSL3 significantly inhibits GSTZ1 and promotes ferroptosis. Thus, the use of RSL3 may provide a new therapeutic strategy for HCC (Wang K et al., 2021). Loss of function of the Retinoblastoma (Rb) protein has an important effect on hepatocarcinogenesis. Thus, by downregulating Rb levels, the mortality rate in SOR-exposed HCC cells is two to three times higher than with SOR alone (Louandre et al., 2015). The mitochondrial outer membrane protein CDGSH iron-sulfur cluster structural domain 2 (CISD2) is highly expressed in HCC cells. Knocking down CISD2 expression can increase ROS, MDA, and iron ion levels, which can promote SOR-induced ferroptosis in HCC resistant cells. Thus, SOR combined with CISD2 inhibition has therapeutic potential in HCC (Li B et al., 2021). Several other studies have shown that NRF2 plays a key role in enhancing SOR-induced ferroptosis in Iron metabolism. The autophagy receptor protein p62 was found to initiate autophagy *via* the Keap1-Nrf2 signaling pathway (Ichimura and Komatsu, 2018). p62 competes with Nrf2 to bind Keap1, leading to dissociation of Nrf2 from Keap1. Thus, when p62 expression increases, Keap1 can no longer bind to Nrf2, leading to increased Nrf2 signaling and inhibition of ferritin autophagy. The expression of FTH1, HO-1, etc., is upregulated and ROS production is inhibited, thus protecting cells from ferroptosis. Therefore, inhibition of NRF2 expression or activity increases the anticancer activity of erastin and SOR *in vitro* and *in vivo* (Sun et al., 2016b). Disulfiram (DSF) is a divalent metal ion chelator that binds metal ions *in vivo* and inhibits acetaldehyde dehydrogenase activity (ALDH). Recent studies have shown DSF to possess antitumor activity, which can be enhanced in combination with Cu plasma (Skrott et al., 2017). DSF/Cu can inhibit nuclear translocation of Nrf2 and enhance SOR-induced ferroptosis to inhibit HCC cell proliferation (Ren et al., 2021). Resting sulfhydryl oxidase-1 (QSOX1) promotes the formation of disulfide bonds in peptides and proteins and also the oxidation of reduced molecules to generate hydrogen peroxide. QSOX1 is highly expressed in a variety of cancer tissues (Lake and Faigel, 2014) and studies have pointed to QSOX1 as a potential oncogene in HCC (Zhang et al., 2019). However, its expression varies in different tumor environments. QSOX1 inhibits EGF-induced EGFR activation by promoting ubiquitination-mediated EGFR degradation and accelerating its intracellular endosomal transport, resulting in reduced NRF2 activity. In addition, QSOX1 enhances sorafenib-



Natural plant (Fueki et al., 2022; Huang et al., 2022; Otsuki et al., 2022) extracts and plant monomers occupy a significant proportion of the research on anti-HCC compounds. Of these, herbal medicine is a focus of research (Wang et al., 2020; Wang



et al., 2021a; Wang et al., 2021b) involving extracts and compounds implicated in the induction of ferroptosis to inhibit HCC (Figure 3). Several studies have shown that plant extracts and compounds are able to induce intracellular ROS production and increase susceptibility of cells to ferroptosis. For example, Formosanin C (FC), a natural compound that induces autophagic flux, inhibits HCC growth by downregulating ferritin heavy chain polypeptide 1 (FTH1), and upregulating NCOA4 expression. This causes increased ferritin autophagy, leading to increased intracellular ferric ion levels, thus increasing reactive oxygen species (ROS) levels and inducing ferroptosis (Lin P. L. et al., 2020). Heteronemin is a marine natural product isolated from the sponge *Hyrtios* sp. Heteronemin induces ROS formation and leads to p38/jnk activation and caspase-related apoptosis and ferroptosis, thereby inducing death in liver cancer cells (Chang et al., 2021). Mycalols, polyoxyglycerol alkyl ethers are mainly isolated from the Antarctic sponge *M. (Oxymycale) acerata*. Mycalol can reduce the expression level of GPX4 and increase the expression of NCOA4 (Table 3). Enhanced NCOA4 expression induces ferroptosis, which may be directly related to the inhibition of liver cancer cell growth by mycalol (Riccio et al., 2021). Solasonine, a compound isolated from *Solanum melongena*, has anti-infective and neurogenesis-promoting effects. Metabolomics analysis showed that Solasonine increases lipid ROS levels in HepG2 cells by inhibiting Gpx4 and GSS. Solasonine also promotes ferroptosis in HCC cells through Gpx4-induced disruption of the glutathione redox system (Jin et al., 2020). In addition, numerous Chinese herbs also possess anti-hepatocellular carcinogenic ability. For example, Semen (*Scutellaria barbata*) can increase the expression of iron peroxidation-related genes IREB2 and ACSL4 by significantly reducing the expression levels of GPX4 and SLC7A11 in nude mice. It also promotes iron peroxidation and lipid ROS metabolism to induce ferroptosis in HCC cells (Li Y et al., 2022). Atractylodin decreases GPX4 and FTL protein expression, upregulates ACSL4 and TFR1 protein expression, and increases ROS levels in liver cancer cells (He et al., 2021). In recent years, several studies have reported that active components of *Artemisia annua* can induce ferroptosis and inhibit HCC. Of these, artesunate, a semisynthetic derivative of artemisinin, has earlier been reported to have anticancer activity (Efferth et al., 2001). Newer studies have shown that artesunate-induced lysosomal activation synergizes with sorafenib-mediated pro-oxidation by promoting lysosomal histone protease B/L activation, ferritin autophagy, lipid peroxidation, and subsequent ferroptosis. A series of responses were significantly exacerbated by combining Artesunate and sorafenib treatments in the inhibition of HCC (Li Z. J et al., 2021). Another study showed that the artemisinin derivative dihydroartemisinin (DHA) can increase the expression of ROS, MDA, decrease the activity of glutathione (GSH), GPX4, solute carrier family (SLC) SLC7A11, SLC3A2, reduce their expression and induce ferroptosis. In addition, this study also found that

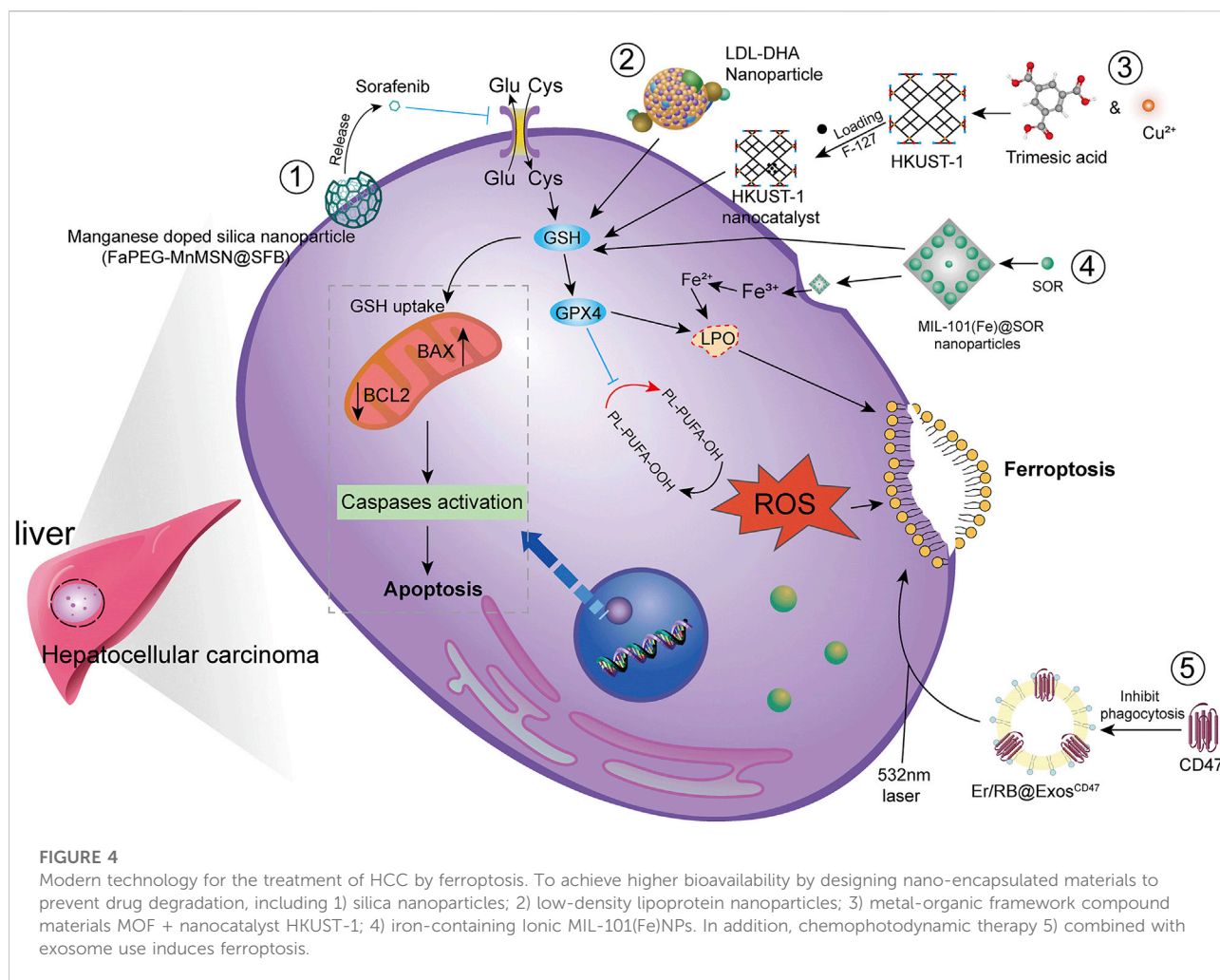
DHA was able to enhance the activity of GSH degrading cation transporter-like protein 1 (CHAC1) promoter. This enhanced activity was found to influence the unfolded protein response (UPR) resulting in reduced GSH activity and inducing ferroptosis (Wang Z et al., 2021).

## Novel drug technologies

HCC is difficult to detect in the early stages and is often transformed into advanced HCC when diagnosed clinically. Since advanced HCC often has strong resistance to chemotherapy, the efficacy of common chemotherapeutic drugs is not satisfactory. Additionally, clinical application is somewhat limited due to poor solubility, low bioavailability, and rapid metabolism of many drugs. Therefore, there is an urgent need to develop new technologies to improve bioavailability of drugs and to achieve better therapeutic outcomes (Figure 4).

Studies have shown that new technologies such as designed nanoparticles and chemical photodynamic therapy can induce ferroptosis to inhibit HCC. Biodegradable silica nanoparticles are inorganic nanoparticles that can be renally cleared and have features such as reduced toxic accumulation *in vivo* along with the advantage of facilitated drug delivery and controlled release. It was found that GSH can be depleted by developing manganese doped silica nanoparticles (MnMSN). Targeted SFB loaded MnMSN (FaPEG-MnMSN@SFB) can deplete GSH on one hand and inhibit System xc<sup>-</sup> on the other hand to achieve dual inhibition of GSH and thus induce ferroptosis (Tang H et al., 2019; Tang H et al., 2020). Metal-organic framework compound material (MOF) is a highly crystalline inorganic-organic hybrid porous material. HKUST-1 nanocatalyst is a type of MOF with large surface area, high porosity, and uniform pore size (Gu et al., 2011). By integrating cyclooxygenase 2 (COX-2), inhibitor was able to deplete GSH, inhibit GPX4 activity, and trigger chemodynamic therapy (CDT) mediated ROS accumulation lipid peroxides (LPO) induced ferroptosis. In addition, COX-2 downregulation can also induce PINK1/Parkin mediated mitochondrial autophagy synergizing with SOR to achieve a dual ability to inhibit HCC activity (Tian et al., 2022). Metal-organic framework compounds MIL-101(Fe) NPs are capable of drug loading, controlled release, peroxidase activity, biocompatibility, and T2 magnetic resonance imaging. MIL-101(Fe)@sor NPs can increase lipid peroxidation and MDA levels, decrease GSH and GPX4, and inhibit tumor progression through ferroptosis (Liu et al., 2021). The NF-κB-specific promoter Cas13a or microRNA can selectively downregulate genes related to iron metabolism, fpn or lcn2. This in combination with iron nanoparticles can significantly induce ferroptosis (Sun et al., 2021).

It has also been shown that LDL nanoparticles and exosomes play a key role in the induction of ferroptosis to inhibit the



growth of liver cancer cells. For example, LDL nanoparticles reconstituted from (LDL-DHA) natural omega-3 fatty acid, docosahexaenoic acid, significantly induce lipid peroxidation, GSH depletion, and inhibition of GPX4 activity. A study showed no association with apoptosis, necrosis or autophagy pathways from human HCC cell results. *In vivo*, elevated levels of lipid peroxidation and inhibition of GPX4 expression were found in liver tumor tissues, verifying the induction of ferroptosis by LDL-DHA (Ou et al., 2017). Exosomes are small membrane vesicles containing complex RNA and proteins. Small nanocapsules are novel communication and drug delivery mediators that can transport biologically active molecules between cells *via* a variety of biomolecules (e.g., proteins, nucleic acids) and regulate the cellular microenvironment and immune system (Chen R et al., 2019). Since exosomes are susceptible to phagocytosis by the monocyte phagocytic system (MPS), functionalization of CD47 on exosomes (ExosCD47) effectively avoids the phagocytic effect of MPS. This facilitates loading of Erastin and photosensitizer (Rose Bengal, RB) into exosomes to inhibit HCC viability by targeting induction of

ferroptosis through chemophotodynamic therapy (Du et al., 2021). In summary, novel technologies such as nanotechnology and chemophotodynamic therapy have the potential to target and improve HCC treatment, enhance the ability of drugs to induce ferroptosis, and provide new possibilities for development of new drug treatment vectors.

## Others

In addition to the above related drug studies, there is clear evidence that Erastin, sulfasalazine (SAS) can also inhibit HCC activity by inducing ferroptosis. For example, microRNA-214-3p (miR-214) further increases MDA and ROS expression levels, upregulates  $\text{Fe}^{2+}$  concentration and decreases GSH levels when combined with Erastin. This is mainly due to Erastin mediated upregulation of activating transcription factor (ATF4). miR-214 ameliorates this upregulation, and the combination reduces the ability of ATF4 to inhibit ferroptosis, thus upregulating ferroptosis (Bai et al., 2020). Ketamine (a derivative of

phencyclidine) inhibits GPX4 expression by reducing plasmacytoma variable translocation gene 1 (lncPVT1), and lncPVT1 promotes GPX4 expression by adsorbing miR-214-3p. The lncPVT1/miR-214-3p axis is one of the potential mechanisms by which ketamine regulates GPX4 expression to modulate iron sagging in HCC cells (Zhu et al., 2021). Haloperidol (Haloperidol), a typical butylphenyl antipsychotic, has been reported in recent years to have a high affinity for Sigma-1 (S1R) (Rousseaux and Greene, 2016). Downregulation of S1R can generate oxidative stress (Wang et al., 2015; Bai et al., 2019). Haloperidol treatment significantly downregulates GSH levels and upregulates lipid peroxidation levels in HCC cells (Bai et al., 2017). The nuclear protein 1 (NUPR1) inhibitor ZZW-115 is able to disrupt mitochondrial morphology and metabolic function by inhibiting the expression of mitochondrial transcription factor A (TFAM). This leads to accumulation of lipid peroxidation, thus inducing ferroptosis (Huang et al., 2021).

Additional partial studies that blocked ferroptosis in HCC enabled a better reverse understanding of the underlying mechanisms of escape resistance in cancer. For example, YAP/TAZ induces the expression of SLC7A11 in a TEAD-dependent manner. By maintaining the protein stability, nuclear localization and transcriptional activity of the transcriptional activator factor (ATF4), HCC cells inhibit SOR-induced ferroptosis (Gao et al., 2021). In addition, Necrostatin-1 inhibits System xc<sup>-</sup> mediated ferroptosis in Huh7 and SK-HEP-1 cells probably by inducing xCT expression (Yuk et al., 2021).

In conclusion, the inhibition of ferroptosis in HCC has great therapeutic potential. Such inhibition involves direct inducers of ferroptosis such as SOR, Erastin, SAS, etc., which can act synergistically or antagonistically to ferroptosis inducers by inducing or inhibiting the activity of related targets. The above also describes the role of natural products in the induction of ferroptosis inhibitory activity in HCC in recent years, revealing the potential value of natural products in the inhibition of HCC. In addition, rapid development of new technologies such as nano- and exosomes have a high potential in facilitating inhibition of HCC. The review of modern drug-induced ferroptosis inhibition of HCC viability can be a guide for subsequent research and development targeting ferroptosis inhibition of HCC.

## Prognosis of ferroptosis in hepatocellular carcinoma

Prognostic analysis can be clinically important in predicting the progression of disease after onset. Prognostic analysis of HCC and ferroptosis will provide further insight into the induction of ferroptosis to inhibit HCC. Numerous studies have shown that

ACSL4,SL7A11,SLC3A2, and G6PD are major regulators in ferroptosis. ACSL4 (Du and Zhang, 2020; Feng J et al., 2021), SL7A11 (Tang B et al., 2020; Zhang et al., 2021), SLC3A2, and G6PD (Dai et al., 2021) are genes associated with ferroptosis in HCC with clear prognostic significance. ABCB6 (Zhang et al., 2020), UBA1 (Shan et al., 2020) etc., have good predictive ability in HCC and ferroptosis by affecting HO-1, FTH1, FTL to regulate iron metabolism and induce ferroptosis. Some long-stranded non-coding RNAs (lncRNAs) also have good predictive ability in ferroptosis-induced HCC (Chen Z. A et al., 2021; Xu et al., 2021). In summary, modern prognostic analysis in ferroptosis of HCC using bioinformatics tools is important for finding key targets for treatment.

## Conclusion

Ferroptosis is an important form of regulatory cell necrosis. Proper induction or inhibition of cellular ferroptosis can help improve and treat a variety of diseases. Ferroptosis plays a very important role in HCC. Currently, the main drugs that induce ferroptosis in HCC are SOR, SAS, etc., Natural product extracts and monomers including Chinese herbs also provide new strategies for HCC treatment. To further improve drug resistance, nanotechnology, and drug combination therapy in the induction of HCC ferroptosis is a promising research hotspot. Ferroptosis-targeting drugs, drug combination applications, nanotechnology, etc., act to induce ferroptosis in HCC mainly through System xc<sup>-</sup>/GSH/GPX4, iron metabolism, p53, and lipid peroxidation pathways. These signaling pathways intersect with each other and exert combined effects. A large number of bioinformatics studies for prognostic analysis of induced HCC ferroptosis provide information not only for the study of new targets in HCC but also to support better clinical treatment.

Not surprisingly, the role of ferroptosis in HCC has attracted the interest of clinical researchers. Ferroptosis has a complex interdependent role in liver tumor prevention, diagnosis, prognosis, and treatment. These aspects will require extensive and ongoing research to better understand the regulatory mechanisms and signaling pathways of ferroptosis in HCC. In recent years, TCM has emerged to have a clear role in suppressing liver tumors. The TCM system is huge, but there are a few reports on induction of ferroptosis to inhibit HCC by TCM, which holds great promise in future HCC research. Solving the global problem of liver cancer patients through TCM alone or in combination with clinical western drugs to induce ferroptosis is a challenge. Therefore, we believe that induction of ferroptosis in HCC either by TCM alone or

in combination with modern techniques will provide a better strategy to improve the treatment and prognosis of HCC.

## Author contributions

LL wrote this manuscript, XW provided financial support, HX collected relevant materials, XW, XL, and KX directed and improved the content of this manuscript.

## Funding

This work was supported by Hubei University of Chinese Medicine “Young Crops Program” Project (2021ZZX003). Natural Science Foundation of Hubei Province, China (Grant No. 2021CFB227), Hubei Provincial Central Government Guided Local Science and Technology Development Special Project “Traditional Chinese Herbal Medicine Properties and Quality Evaluation Platform” (2020ZYD030). This work was

supported by the Chongqing Natural Science Foundation (Grant number: cstc2019jcyj-msxmX0862).

## Conflict of interest

The authors declare that the research was conducted in the absence of any commercial or financial relationships that could be construed as a potential conflict of interest.

## Publisher's note

All claims expressed in this article are solely those of the authors and do not necessarily represent those of their affiliated organizations, or those of the publisher, the editors and the reviewers. Any product that may be evaluated in this article, or claim that may be made by its manufacturer, is not guaranteed or endorsed by the publisher.

## References

- Aspach, E., Lussier, D. M., and Schreiber, R. D. (2019). Interferon  $\gamma$  and its important roles in promoting and inhibiting spontaneous and therapeutic cancer immunity. *Cold Spring Harb. Perspect. Biol.* 11, a028480. doi:10.1101/cshperspect.a028480
- Aning, O. A., and Cheok, C. F. (2019). Drugging in the absence of p53. *J. Mol. Cell Biol.* 11, 255–264. doi:10.1093/jmcb/mjz012
- Asperti, M., Bellini, S., Grillo, E., Gryzik, M., Cantamessa, L., Ronca, R., et al. (2021). H-ferritin suppression and pronounced mitochondrial respiration make Hepatocellular Carcinoma cells sensitive to RSL3-induced ferroptosis. *Free Radic. Biol. Med.* 169, 294–303. doi:10.1016/j.freeradbiomed.2021.04.024
- Asrani, S. K., Devarbhavi, H., Eaton, J., and Kamath, P. S. (2019). Burden of liver diseases in the world. *J. Hepatol.* 70, 151–171. doi:10.1016/j.jhep.2018.09.014
- Bai, T., Lei, P., Zhou, H., Liang, R., Zhu, R., Wang, W., et al. (2019). Sigma-1 receptor protects against ferroptosis in hepatocellular carcinoma cells. *J. Cell. Mol. Med.* 23, 7349–7359. doi:10.1111/jcmm.14594
- Bai, T., Liang, R., Zhu, R., Wang, W., Zhou, L., Sun, Y., et al. (2020). MicroRNA-214-3p enhances erastin-induced ferroptosis by targeting ATF4 in hepatoma cells. *J. Cell. Physiol.* 235, 5637–5648. doi:10.1002/jcp.29496
- Bai, T., Wang, S., Zhao, Y., Zhu, R., Wang, W., Sun, Y., et al. (2017). Haloperidol, a sigma receptor 1 antagonist, promotes ferroptosis in hepatocellular carcinoma cells. *Biochem. Biophys. Res. Commun.* 491, 919–925. doi:10.1016/j.bbrc.2017.07.136
- Brady, C. A., Jiang, D., Mello, S. S., Johnson, T. M., Jarvis, L. A., Kozak, M. M., et al. (2011). Distinct p53 transcriptional programs dictate acute DNA-damage responses and tumor suppression. *Cell* 145, 571–583. doi:10.1016/j.cell.2011.03.035
- Bykov, V. J. N., Eriksson, S. E., Bianchi, J., and Wiman, K. G. (2018). Targeting mutant p53 for efficient cancer therapy. *Nat. Rev. Cancer* 18, 89–102. doi:10.1038/nrc.2017.109
- Cao, F., Luo, A., and Yang, C. (2021). G6PD inhibits ferroptosis in hepatocellular carcinoma by targeting cytochrome P450 oxidoreductase. *Cell. Signal.* 87, 110098. doi:10.1016/j.cellsig.2021.110098
- Capelletti, M. M., Manceau, H., Puy, H., and Peoc'h, K. (2020). Ferroptosis in liver diseases: an overview. *Int. J. Mol. Sci.* 21, E4908. doi:10.3390/ijms21144908
- Castro, F., Cardoso, A. P., Gonçalves, R. M., Serre, K., and Oliveira, M. J. (2018). Interferon-gamma at the crossroads of tumor immune surveillance or evasion. *Front. Immunol.* 9, 847. doi:10.3389/fimmu.2018.00847
- Chang, W. T., Bow, Y. D., Fu, P. J., Li, C. Y., Wu, C. Y., Chang, Y. H., et al. (2021). A marine terpenoid, heteronemin, induces both the apoptosis and ferroptosis of hepatocellular carcinoma cells and involves the ROS and MAPK pathways. *Oxid. Med. Cell. Longev.* 2021, 7689045. doi:10.1155/2021/7689045
- Chen, D., Chu, B., Yang, X., Liu, Z., Jin, Y., Kon, N., et al. (2021a). iPLA2 $\beta$ -mediated lipid detoxification controls p53-driven ferroptosis independent of GPX4. *Nat. Commun.* 12, 3644. doi:10.1038/s41467-021-23902-6
- Chen, D., Zhao, Z., Chen, L., Li, Q., Zou, J., Liu, S., et al. (2021b). PPM1G promotes the progression of hepatocellular carcinoma via phosphorylation regulation of alternative splicing protein SRSF3. *Cell Death Dis.* 12, 722. doi:10.1038/s41419-021-04013-y
- Chen, J., Li, X., Ge, C., Min, J., and Wang, F. (2022). The multifaceted role of ferroptosis in liver disease. *Cell Death Differ.* 29, 467–480. doi:10.1038/s41418-022-00941-0
- Chen, R., Xu, X., Tao, Y., Qian, Z., and Yu, Y. (2019). Exosomes in hepatocellular carcinoma: a new horizon. *Cell Commun. Signal.* 17, 1. doi:10.1186/s12964-018-0315-1
- Chen, Y., Lu, Y., Ren, Y., Yuan, J., Zhang, N., Kimball, H., et al. (2020). Starvation-induced suppression of DAZAP1 by miR-10b integrates splicing control into TSC2-regulated oncogenic autophagy in esophageal squamous cell carcinoma. *Theranostics* 10, 4983–4996. doi:10.7150/thno.43046
- Chen, Y., Zhu, G., Liu, Y., Wu, Q., Zhang, X., Bian, Z., et al. (2019). O-GlcNAcylated c-Jun antagonizes ferroptosis via inhibiting GSH synthesis in liver cancer. *Cell. Signal.* 63, 109384. doi:10.1016/j.cellsig.2019.109384
- Chen, Z. A., Tian, H., Yao, D. M., Zhang, Y., Feng, Z. J., Yang, C. J., et al. (2021). Identification of a ferroptosis-related signature model including mRNAs and lncRNAs for predicting prognosis and immune activity in hepatocellular carcinoma. *Front. Oncol.* 11, 738477. doi:10.3389/fonc.2021.738477
- Choudhury, R., Roy, S. G., Tsai, Y. S., Tripathy, A., Graves, L. M., Wang, Z., et al. (2014). The splicing activator DAZAP1 integrates splicing control into MEK/Erk-regulated cell proliferation and migration. *Nat. Commun.* 5, 3078. doi:10.1038/ncomms4078
- Contractor, T., and Harris, C. R. (2012). p53 negatively regulates transcription of the pyruvate dehydrogenase kinase Pdk2. *Cancer Res.* 72, 560–567. doi:10.1158/0008-5472.Can-11-1215
- Dai, T., Li, J., Lu, X., Ye, L., Yu, H., Zhang, L., et al. (2021). Prognostic role and potential mechanisms of the ferroptosis-related metabolic gene signature in hepatocellular carcinoma. *Pharmacogenomics Pers. Med.* 14, 927–945. doi:10.2147/pgpm.S319524
- Dai, T., Vera, Y., Salido, E. C., and Yen, P. H. (2001). Characterization of the mouse Dazap1 gene encoding an RNA-binding protein that interacts with infertility factors DAZ and DAZL. *BMC Genomics* 2, 6. doi:10.1186/1471-2164-2-6



- Daniels, T. R., Bernabeu, E., Rodríguez, J. A., Patel, S., Kozman, M., Chiappetta, D. A., et al. (2012). The transferrin receptor in HCC progression: signaling, EMT, immune microenvironment, and novel therapeutic perspectives. *Biochim. Biophys. Acta* 1820, 291–317. doi:10.1016/j.bbagen.2011.07.016
- Dituri, F., Mancarella, S., Cigliano, A., Chieti, A., and Giannelli, G. (2019). TGF- $\beta$  as multifaceted orchestrator in HCC progression: signaling, EMT, immune microenvironment, and novel therapeutic perspectives. *Semin. Liver Dis.* 39, 53–69. doi:10.1055/s-0038-1676121
- Dixon, S. J., Lemberg, K. M., Lamprecht, M. R., Skouta, R., Zaitsev, E. M., Gleason, C. E., et al. (2012). Ferroptosis: an iron-dependent form of nonapoptotic cell death. *Cell* 149, 1060–1072. doi:10.1016/j.cell.2012.03.042
- Dixon, S. J., Patel, D. N., Welsch, M., Skouta, R., Lee, E. D., Hayano, M., et al. (2014). Pharmacological inhibition of cystine-glutamate exchange induces endoplasmic reticulum stress and ferroptosis. *Elife* 3, e02523. doi:10.7554/eLife.02523
- Du, J., Wan, Z., Wang, C., Lu, F., Wei, M., Wang, D., et al. (2021). Designer exosomes for targeted and efficient ferroptosis induction in cancer via chemophotodynamic therapy. *Theranostics* 11, 8185–8196. doi:10.7150/thno.59121
- Du, X., and Zhang, Y. (2020). Integrated analysis of immunity- and ferroptosis-related biomarker signatures to improve the prognosis prediction of hepatocellular carcinoma. *Front. Genet.* 11, 614888. doi:10.3389/fgene.2020.614888
- Duxbury, M. S., Ito, H., Zinner, M. J., Ashley, S. W., and Whang, E. E. (2004). RNA interference targeting the M2 subunit of ribonucleotide reductase enhances pancreatic adenocarcinoma chemosensitivity to gemcitabine. *Oncogene* 23, 1539–1548. doi:10.1038/sj.onc.1207272
- Duxbury, M. S., and Whang, E. E. (2007). RRM2 induces NF- $\kappa$ B-dependent MMP-9 activation and enhances cellular invasiveness. *Biochem. Biophys. Res. Commun.* 354, 190–196. doi:10.1016/j.bbrc.2006.12.177
- Effertth, T., Dunstan, H., Sauerbrey, A., Miyachi, H., and Chitambar, C. R. (2001). The anti-malarial artesunate is also active against cancer. *Int. J. Oncol.* 18, 767–773. doi:10.3892/ijo.18.4.767
- Feng, F., Pan, L., Wu, J., Li, L., Xu, H., Yang, L., et al. (2021). Cepharanthine inhibits hepatocellular carcinoma cell growth and proliferation by regulating amino acid metabolism and suppresses tumorigenesis *in vivo*. *Int. J. Biol. Sci.* 17, 4340–4352. doi:10.7150/ijbs.64675
- Feng, J., Lu, P. Z., Zhu, G. Z., Hooi, S. C., Wu, Y., Huang, X. W., et al. (2021). ACSL4 is a predictive biomarker of sorafenib sensitivity in hepatocellular carcinoma. *Acta Pharmacol. Sin.* 42, 160–170. doi:10.1038/s41401-020-0439-x
- Fu, M., Liu, Y., Cheng, H., Xu, K., and Wang, G. (2022). Coptis chinensis and dried ginger herb combination inhibits gastric tumor growth by interfering with glucose metabolism via LDHA and SLC2A1. *J. Ethnopharmacol.* 284, 114771. doi:10.1016/j.jep.2021.114771
- Fuchs, Y., and Steller, H. (2011). Programmed cell death in animal development and disease. *Cell* 147, 742–758. doi:10.1016/j.cell.2011.10.033
- Fueki, T., Nose, I., Liu, Y., Tanaka, K., Namiki, T., Makino, T., et al. (2022). Oxalic acid in ginger specifically denatures the acrid raphides in the unprocessed dried tuber of *Pinellia ternata*. *Acupunct. Herb. Med.* 2 (1), 33–40. doi:10.1097/HM9.0000000000000025
- Galadari, S., Rahman, A., Pallichankandy, S., and Thayyullathil, F. (2017). Reactive oxygen species and cancer paradox: to promote or to suppress? *Free Radic. Biol. Med.* 104, 144–164. doi:10.1016/j.freeradbiomed.2017.01.004
- Gao, R., Kalathur, R. K. R., Coto-Llerena, M., Ercan, C., Buechel, D., Shuang, S., et al. (2021). YAP/TAZ and ATF4 drive resistance to Sorafenib in hepatocellular carcinoma by preventing ferroptosis. *EMBO Mol. Med.* 13, e14351. doi:10.15252/emmm.202114351
- Goyal, L., Zheng, H., Abrams, T. A., Miksad, R., Bullock, A. J., Allen, J. N., et al. (2019). A phase II and biomarker study of sorafenib combined with modified FOLFOX in patients with advanced hepatocellular carcinoma. *Clin. Cancer Res.* 25, 80–89. doi:10.1158/1078-0432.Ccr-18-0847
- Grootjans, S., Vanden Berghe, T., and Vandenabeele, P. (2017). Initiation and execution mechanisms of necroptosis: an overview. *Cell Death Differ.* 24, 1184–1195. doi:10.1038/cdd.2017.65
- Gu, Z. Y., Chen, Y. J., Jiang, J. Q., and Yan, X. P. (2011). Metal-organic frameworks for efficient enrichment of peptides with simultaneous exclusion of proteins from complex biological samples. *Chem. Commun.* 47, 4787–4789. doi:10.1039/c1cc10579e
- Guo, S., Chen, Y., Xue, X., Yang, Y., Wang, Y., Qiu, S., et al. (2021). TRIB2 desensitizes ferroptosis via  $\beta$ TrCP-mediated TFRC ubiquitination in liver cancer cells. *Cell Death Discov.* 7, 196. doi:10.1038/s41420-021-00574-1
- Hanahan, D., and Weinberg, R. A. (2011). Hallmarks of cancer: the next generation. *Cell* 144, 646–674. doi:10.1016/j.cell.2011.02.013
- He, Y., Fang, D., Liang, T., Pang, H., Nong, Y., Tang, L., et al. (2021). Atractylodin may induce ferroptosis of human hepatocellular carcinoma cells. *Ann. Transl. Med.* 9, 1535. doi:10.21037/atm-21-4386
- Horonchik, L., and Wessling-Resnick, M. (2008). The small-molecule iron transport inhibitor ferristatin/NSC306711 promotes degradation of the transferrin receptor. *Chem. Biol.* 15, 647–653. doi:10.1016/j.chembiol.2008.05.011
- Houessinon, A., François, C., Sauzay, C., Louandre, C., Mongelard, G., Godin, C., et al. (2016). Metallothionein-1 as a biomarker of altered redox metabolism in hepatocellular carcinoma cells exposed to sorafenib. *Mol. Cancer* 15, 38. doi:10.1186/s12943-016-0526-2
- Hua, H. W., Jiang, H. S., Jia, L., Jia, Y. P., Yao, Y. L., Chen, Y. W., et al. (2021). SPARC regulates ferroptosis induced by sorafenib in human hepatocellular carcinoma. *Cancer Biomark.* 32, 425–433. doi:10.3233/cbm-200101
- Huang, C., Santofimia-Castaño, P., Liu, X., Xia, Y., Peng, L., Gotorbe, C., et al. (2021). NUPR1 inhibitor ZZW-115 induces ferroptosis in a mitochondria-dependent manner. *Cell Death Discov.* 7, 269. doi:10.1038/s41420-021-00662-2
- Huang, M. L., Yu, S. J., Shao, Q., Liu, H., Wang, Y., Chen, H., et al. (2022). Comprehensive profiling of Lingzhihuang capsule by liquid chromatography coupled with mass spectrometry-based molecular networking and target prediction. *Acupunct. Herb. Med.* 2 (1), 58–67. doi:10.1097/HM9.0000000000000012
- Ichimura, Y., and Komatsu, M. (2018). Activation of p62/SQSTM1-keap1-nuclear factor erythroid 2-related factor 2 pathway in cancer. *Front. Oncol.* 8, 210. doi:10.3389/fonc.2018.00210
- Ingold, I., Berndt, C., Schmitt, S., Doll, S., Poschmann, G., Buday, K., et al. (2018). Selenium utilization by GPX4 is required to prevent hydrogen peroxide-induced ferroptosis. *Cell* 172, 409. doi:10.1016/j.cell.2017.11.048
- Jiang, L., Kon, N., Li, T., Wang, S. J., Su, T., Hibshoosh, H., et al. (2015). Ferroptosis as a p53-mediated activity during tumour suppression. *Nature* 520, 57–62. doi:10.1038/nature14344
- Jin, M., Shi, C., Li, T., Wu, Y., Hu, C., Huang, G., et al. (2020). Solasonine promotes ferroptosis of hepatoma carcinoma cells via glutathione peroxidase 4-induced destruction of the glutathione redox system. *Biomed. Pharmacother.* 129, 110282. doi:10.1016/j.biopha.2020.110282
- Khan, A., Valli, E., Lam, H., Scott, D. A., Murray, J., Hanssen, K. M., et al. (2020). Targeting metabolic activity in high-risk neuroblastoma through Monocarboxylate Transporter 1 (MCT1) inhibition. *Oncogene* 39, 3555–3570. doi:10.1038/s41388-020-1235-2
- Kim, D. H., Kim, W. D., Kim, S. K., Moon, D. H., and Lee, S. J. (2020). TGF- $\beta$ 1-mediated repression of SLC7A11 drives vulnerability to GPX4 inhibition in hepatocellular carcinoma cells. *Cell Death Dis.* 11, 406. doi:10.1038/s41419-020-2618-6
- Kim, H. Y., and Park, J. W. (2011). Molecularly targeted therapies for hepatocellular carcinoma: sorafenib as a stepping stone. *Dig. Dis.* 29, 303–309. doi:10.1159/000327563
- Kong, R., Wang, N., Han, W., Bao, W., and Lu, J. (2021). IFN $\gamma$ -mediated repression of system xc(-) drives vulnerability to induced ferroptosis in hepatocellular carcinoma cells. *J. Leukoc. Biol.* 110, 301–314. doi:10.1002/jlb.3ma1220-815rrr
- Koppula, P., Zhang, Y., Zhuang, L., and Gan, B. (2018). Amino acid transporter SLC7A11/xCT at the crossroads of regulating redox homeostasis and nutrient dependency of cancer. *Cancer Commun.* 38, 12. doi:10.1186/s40880-018-0288-x
- Koppula, P., Zhuang, L., and Gan, B. (2021). Cytochrome P450 reductase (POR) as a ferroptosis fuel. *Protein Cell* 12, 675–679. doi:10.1007/s13238-021-00823-0
- Lake, D. F., and Faigel, D. O. (2014). The emerging role of QSOX1 in cancer. *Antioxid. Redox Signal.* 21, 485–496. doi:10.1089/ars.2013.5572
- Levine, A. J. (2020). p53: 800 million years of evolution and 40 years of discovery. *Nat. Rev. Cancer* 20, 471–480. doi:10.1038/s41568-020-0262-1
- Li, B., Wei, S., Yang, L., Peng, X., Ma, Y., Wu, B., et al. (2021). C1SD2 promotes resistance to sorafenib-induced ferroptosis by regulating autophagy in hepatocellular carcinoma. *Front. Oncol.* 11, 657723. doi:10.3389/fonc.2021.657723
- Li, L., Xu, H., Qu, L., Xu, K., and Liu, X. (2022). Daidzin inhibits hepatocellular carcinoma survival by interfering with the glycolytic/gluconeogenic pathway through downregulation of TP11. *Biofactors*. [Online ahead of print]. doi:10.1002/biof.1826
- Li, T., Kon, N., Jiang, L., Tan, M., Ludwig, T., Zhao, Y., et al. (2012). Tumor suppression in the absence of p53-mediated cell-cycle arrest, apoptosis, and senescence. *Cell* 149, 1269–1283. doi:10.1016/j.cell.2012.04.026
- Li, Y., Xia, J., Shao, F., Zhou, Y., Yu, J., Wu, H., et al. (2021). Sorafenib induces mitochondrial dysfunction and exhibits synergistic effect with cysteine depletion by promoting HCC cells ferroptosis. *Biochem. Biophys. Res. Commun.* 534, 877–884. doi:10.1016/j.bbrc.2020.10.083

- Li, Y., Zhang, J., Zhang, K., Chen, Y., Wang, W., Chen, H., et al. (2022). Scutellaria barbata inhibits hepatocellular carcinoma tumorigenicity by inducing ferroptosis of hepatocellular carcinoma cells. *Front. Oncol.* 12, 693395. doi:10.3389/fonc.2022.693395
- Li, Z. J., Dai, H. Q., Huang, X. W., Feng, J., Deng, J. H., Wang, Z. X., et al. (2021). Artesunate synergizes with sorafenib to induce ferroptosis in hepatocellular carcinoma. *Acta Pharmacol. Sin.* 42, 301–310. doi:10.1038/s41401-020-0478-3
- Liang, W., and Ferrara, N. (2020). Iron metabolism in the tumor microenvironment: contributions of innate immune cells. *Front. Immunol.* 11, 626812. doi:10.3389/fimmu.2020.626812
- Lin, P. L., Tang, H. H., Wu, S. Y., Shaw, N. S., and Su, C. L. (2020). Saponin formosanin C-induced ferritinophagy and ferroptosis in human hepatocellular carcinoma cells. *Antioxidants (Basel)* 9, 682. doi:10.3390/antiox9080682
- Lin, W., Wang, C., Liu, G., Bi, C., Wang, X., Zhou, Q., et al. (2020). SLC7A11/xCT in cancer: biological functions and therapeutic implications. *Am. J. Cancer Res.* 10, 3106–3126.
- Liu, X., Zhu, X., Qi, X., Meng, X., and Xu, K. (2021). Co-administration of iRGD with sorafenib-loaded iron-based metal-organic framework as a targeted ferroptosis agent for liver cancer therapy. *Int. J. Nanomedicine* 16, 1037–1050. doi:10.2147/ijn.S292528
- Liu, Y., and Gu, W. (2022). p53 in ferroptosis regulation: the new weapon for the old guardian. *Cell Death Differ.* 29, 895–910. doi:10.1038/s41418-022-00943-y
- Liu, Y., and Gu, W. (2021). The complexity of p53-mediated metabolic regulation in tumor suppression. *Semin. Cancer Biol.* doi:10.1016/j.semcancer.2021.03.010
- Liu, Y., Tavana, O., and Gu, W. (2019). p53 modifications: exquisite decorations of the powerful guardian. *J. Mol. Cell Biol.* 11, 564–577. doi:10.1093/jmcb/mjz060
- Liu, Y., Uzair Ur, R., Guo, Y., Liang, H., Cheng, R., Yang, F., et al. (2016). miR-181b functions as an oncomiR in colorectal cancer by targeting PDCD4. *Protein Cell* 7, 722–734. doi:10.1007/s13238-016-0313-2
- Liu, Z., Lin, Y., Zhang, J., Zhang, Y., Li, Y., Liu, Z., et al. (2019). Molecular targeted and immune checkpoint therapy for advanced hepatocellular carcinoma. *J. Exp. Clin. Cancer Res.* 38, 447. doi:10.1186/s13046-019-1412-8
- Liu, Z., Wang, Q., Wang, X., Xu, Z., Wei, X., Li, J., et al. (2020). Circular RNA clARS regulates ferroptosis in HCC cells through interacting with RNA binding protein ALKBH5. *Cell Death Discov.* 6, 72. doi:10.1038/s41420-020-00306-x
- Louandre, C., Ezzoukhy, Z., Godin, C., Barbare, J. C., Mazière, J. C., Chaffert, B., et al. (2013). Iron-dependent cell death of hepatocellular carcinoma cells exposed to sorafenib. *Int. J. Cancer* 133, 1732–1742. doi:10.1002/ijc.28159
- Louandre, C., Marcq, I., Bouhlal, H., Lachaier, E., Godin, C., Saidak, Z., et al. (2015). The retinoblastoma (Rb) protein regulates ferroptosis induced by sorafenib in human hepatocellular carcinoma cells. *Cancer Lett.* 356, 971–977. doi:10.1016/j.canlet.2014.11.014
- Lyu, N., Zeng, Y., Kong, Y., Chen, Q., Deng, H., Ou, S., et al. (2021). Ferroptosis is involved in the progression of hepatocellular carcinoma through the circ0097009/miR-1261/SLC7A11 axis. *Ann. Transl. Med.* 9, 675. doi:10.21037/atm-21-997
- Nie, J., Lin, B., Zhou, M., Wu, L., and Zheng, T. (2018). Role of ferroptosis in hepatocellular carcinoma. *J. Cancer Res. Clin. Oncol.* 144, 2329–2337. doi:10.1007/s00432-018-2740-3
- Otsuki, K., Zhang, M., and Li, W. (2021). Natural products against HIV latency. *Acupunct. Herb. Med.* 1 (1), 10–21. doi:10.1097/HM9.000000000000004
- Ou, W., Mulik, R. S., Anwar, A., McDonald, J. G., He, X., Corbin, I. R., et al. (2017). Low-density lipoprotein docosahexaenoic acid nanoparticles induce ferroptotic cell death in hepatocellular carcinoma. *Free Radic. Biol. Med.* 112, 597–607. doi:10.1016/j.freeradbiomed.2017.09.002
- Ou, Y., Wang, S. J., Li, D., Chu, B., and Gu, W. (2016). Activation of SAT1 engages polyamine metabolism with p53-mediated ferroptotic responses. *Proc. Natl. Acad. Sci. U. S. A.* 113, E6806–E6812. doi:10.1073/pnas.1607152113
- Pan, L., Feng, F., Wu, J., Fan, S., Han, J., Wang, S., et al. (2022). Demethylzeylasteral targets lactate by inhibiting histone lactylation to suppress the tumorigenicity of liver cancer stem cells. *Pharmacol. Res.* 181, 106270. doi:10.1016/j.phrs.2022.106270
- Pan, L., Feng, F., Wu, J., Li, L., Xu, H., Yang, L., et al. (2021). Diosmetin inhibits cell growth and proliferation by regulating the cell cycle and lipid metabolism pathway in hepatocellular carcinoma. *Food Funct.* 12, 12036–12046. doi:10.1039/d1fo02111g
- Pinter, M., Sieghart, W., Graziadei, I., Vogel, W., Maieron, A., Königsberg, R., et al. (2009). Sorafenib in unresectable hepatocellular carcinoma from mild to advanced stage liver cirrhosis. *Oncologist* 14, 70–76. doi:10.1634/theoncologist.2008-0191
- Ren, X., Li, Y., Zhou, Y., Hu, W., Yang, C., Jing, Q., et al. (2021). Overcoming the compensatory elevation of NRF2 renders hepatocellular carcinoma cells more vulnerable to disulfiram/copper-induced ferroptosis. *Redox Biol.* 46, 102122. doi:10.1016/j.redox.2021.102122
- Riccio, G., Nuzzo, G., Zazo, G., Coppola, D., Senese, G., Romano, L., et al. (2021). Bioactivity screening of antarctic sponges reveals anticancer activity and potential cell death via ferroptosis by mycalols. *Mar. Drugs* 19, 459. doi:10.3390/md19080459
- Roland, C. L., Arumugam, T., Deng, D., Liu, S. H., Philip, B., Gomez, S., et al. (2014). Cell surface lactate receptor GPR81 is crucial for cancer cell survival. *Cancer Res.* 74, 5301–5310. doi:10.1158/0008-5472.Can-14-0319
- Rousseaux, C. G., and Greene, S. F. (2016). Sigma receptors [ $\sigma$ R]: biology in normal and diseased states. *J. Recept. Signal Transduct. Res.* 36, 327–388. doi:10.3109/10799893.2015.1015737
- Ryerson, A. B., Ehemann, C. R., Altekruze, S. F., Ward, J. W., Jemal, A., Sherman, R. L., et al. (2016). Annual Report to the Nation on the Status of Cancer, 1975–2012, featuring the increasing incidence of liver cancer. *Cancer* 122, 1312–1337. doi:10.1002/cncr.29936
- Schwartzberg-Bar-Yoseph, F., Armoni, M., and Karnieli, E. (2004). The tumor suppressor p53 down-regulates glucose transporters GLUT1 and GLUT4 gene expression. *Cancer Res.* 64, 2627–2633. doi:10.1158/0008-5472.can-03-0846
- Shan, Y., Yang, G., Huang, H., Zhou, Y., Hu, X., Lu, Q., et al. (2020). Ubiquitin-like modifier activating enzyme 1 as a novel diagnostic and prognostic indicator that correlates with ferroptosis and the malignant phenotypes of liver cancer cells. *Front. Oncol.* 10, 592413. doi:10.3389/fonc.2020.592413
- Shang, Y., Luo, M., Yao, F., Wang, S., Yuan, Z., Yang, Y., et al. (2020). Ceruloplasmin suppresses ferroptosis by regulating iron homeostasis in hepatocellular carcinoma cells. *Cell. Signal.* 72, 109633. doi:10.1016/j.cellsig.2020.109633
- Shojaie, L., Iorga, A., and Dara, L. (2020). Cell death in liver diseases: a review. *Int. J. Mol. Sci.* 21, E9682. doi:10.3390/ijms21249682
- Skrott, Z., Mistrik, M., Andersen, K. K., Friis, S., Majera, D., Gursky, J., et al. (2017). Alcohol-abuse drug disulfiram targets cancer via p97 segregase adaptor NPL4. *Nature* 552, 194–199. doi:10.1038/nature25016
- Song, Z., Liu, T., Chen, J., Ge, C., Zhao, F., Zhu, M., et al. (2019). HIF-1 $\alpha$ -induced RIT1 promotes liver cancer growth and metastasis and its deficiency increases sensitivity to sorafenib. *Cancer Lett.* 460, 96–107. doi:10.1016/j.canlet.2019.06.016
- Stockwell, B. R., Friedmann Angeli, J. P., Bayir, H., Bush, A. I., Conrad, M., Dixon, S. J., et al. (2017). Ferroptosis: a regulated cell death nexus linking metabolism, redox biology, and disease. *Cell* 171, 273–285. doi:10.1016/j.cell.2017.09.021
- Sun, J., Zhou, C., Zhao, Y., Zhang, X., Chen, W., Zhou, Q., et al. (2021). Quiescin sulfhydryl oxidase 1 promotes sorafenib-induced ferroptosis in hepatocellular carcinoma by driving EGFR endosomal trafficking and inhibiting NRF2 activation. *Redox Biol.* 41, 101942. doi:10.1016/j.redox.2021.101942
- Sun, X., Niu, X., Chen, R., He, W., Chen, D., Kang, R., et al. (2016a). Metallothionein-1G facilitates sorafenib resistance through inhibition of ferroptosis. *Hepatology* 64, 488–500. doi:10.1002/hep.28574
- Sun, X., Ou, Z., Chen, R., Niu, X., Chen, D., Kang, R., et al. (2016b). Activation of the p62-Keap1-NRF2 pathway protects against ferroptosis in hepatocellular carcinoma cells. *Hepatology* 63, 173–184. doi:10.1002/hep.28251
- Sung, H., Ferlay, J., Siegel, R. L., Laversanne, M., Soerjomataram, I., Jemal, A., et al. (2021). Global cancer statistics 2020: GLOBOCAN estimates of incidence and mortality worldwide for 36 cancers in 185 countries. *Ca. Cancer J. Clin.* 71, 209–249. doi:10.3322/caac.21660
- Tang, B., Zhu, J., Li, J., Fan, K., Gao, Y., Cheng, S., et al. (2020). The ferroptosis and iron-metabolism signature robustly predicts clinical diagnosis, prognosis and immune microenvironment for hepatocellular carcinoma. *Cell Commun. Signal.* 18, 174. doi:10.1186/s12964-020-00663-1
- Tang, D., Kang, R., Berghe, T. V., Vandenabeele, P., and Kroemer, G. (2019). The molecular machinery of regulated cell death. *Cell Res.* 29, 347–364. doi:10.1038/s41422-019-0164-5
- Tang, D., and Kroemer, G. (2020). Ferroptosis. *Curr. Biol.* 30, R1292–R1297. doi:10.1016/j.cub.2020.09.068
- Tang, H., Chen, D., Li, C., Zheng, C., Wu, X., Zhang, Y., et al. (2019). Dual GSH-exhausting sorafenib loaded manganese-silica nanodrugs for inducing the ferroptosis of hepatocellular carcinoma cells. *Int. J. Pharm.* 572, 118782. doi:10.1016/j.jipharm.2019.118782
- Tang, H., Li, C., Zhang, Y., Zheng, H., Cheng, Y., Zhu, J., et al. (2020). Targeted Manganese doped silica nano GSH-cleaner for treatment of Liver Cancer by destroying the intracellular redox homeostasis. *Theranostics* 10, 9865–9887. doi:10.1016/j.thno.2020.04.077
- Tasdogan, A., Faubert, B., Ramesh, V., Ubellacker, J. M., Shen, B., Solmonson, A., et al. (2020). Metabolic heterogeneity confers differences in melanoma metastatic potential. *Nature* 577, 115–120. doi:10.1038/s41586-019-1847-2

- Tian, H., Zhao, S., Nice, E. C., Huang, C., He, W., Zou, B., et al. (2022). A cascaded copper-based nanocatalyst by modulating glutathione and cyclooxygenase-2 for hepatocellular carcinoma therapy. *J. Colloid Interface Sci.* 607, 1516–1526. doi:10.1016/j.jcis.2021.09.049
- Venkatesh, D., O'Brien, N. A., Zandkarimi, F., Tong, D. R., Stokes, M. E., Dunn, D. E., et al. (2020). MDM2 and MDMX promote ferroptosis by PPAR $\alpha$ -mediated lipid remodeling. *Genes Dev.* 34, 526–543. doi:10.1101/gad.334219.119
- Vogt, P. K. (2002). Fortuitous convergences: the beginnings of JUN. *Nat. Rev. Cancer* 2, 465–469. doi:10.1038/nrc818
- Wang, C., Gao, Y., Zhang, Z., Chi, Q., Liu, Y., Yang, L., et al. (2020). Safflower yellow alleviates osteoarthritis and prevents inflammation by inhibiting PGE2 release and regulating NF- $\kappa$ B/SIRT1/AMPK signaling pathways. *Phytomedicine* 78, 153305. doi:10.1016/j.phymed.2020.153305
- Wang, C., Huang, Y., Liu, X., Li, L., Xu, H., Dong, N., et al. (2021a). Andrographolide ameliorates aortic valve calcification by regulation of lipid biosynthesis and glycerolipid metabolism targeting MGLL expression *in vitro* and *in vivo*. *Cell Calcium* 100, 102495. doi:10.1016/j.ceca.2021.102495
- Wang, C., Xia, Y., Qu, L., Liu, Y., Liu, X., Xu, K., et al. (2021b). Cardamonin inhibits osteogenic differentiation of human valve interstitial cells and ameliorates aortic valve calcification via interfering in the NF- $\kappa$ B/NLRP3 inflammasome pathway. *Food Funct.* 12, 11808–11818. doi:10.1039/d1fo00813g
- Wang, J., Shanmugam, A., Markand, S., Zorrilla, E., Ganapathy, V., Smith, S. B., et al. (2015). Sigma 1 receptor regulates the oxidative stress response in primary retinal Müller glial cells via NRF2 signaling and system xc<sup>-</sup>, the Na<sup>+</sup>-independent glutamate-cystine exchanger. *Free Radic. Biol. Med.* 86, 25–36. doi:10.1016/j.freeradbiomed.2015.04.009
- Wang, K., Zhang, Z., Tsai, H. I., Liu, Y., Gao, J., Wang, M., et al. (2021). Branched-chain amino acid aminotransferase 2 regulates ferroptotic cell death in cancer cells. *Cell Death Differ.* 28, 1222–1236. doi:10.1038/s41418-020-00644-4
- Wang, Q., Bin, C., Xue, Q., Gao, Q., Huang, A., Wang, K., et al. (2021c). GSTZ1 sensitizes hepatocellular carcinoma cells to sorafenib-induced ferroptosis via inhibition of NRF2/GPX4 axis. *Cell Death Dis.* 12, 426. doi:10.1038/s41419-021-03718-4
- Wang, Q., Guo, Y., Wang, W., Liu, B., Yang, G., Xu, Z., et al. (2021d). RNA binding protein DAZAP1 promotes HCC progression and regulates ferroptosis by interacting with SLC7A11 mRNA. *Exp. Cell Res.* 399, 112453. doi:10.1016/j.yexcr.2020.112453
- Wang, Z., Li, M., Liu, Y., Qiao, Z., Bai, T., Yang, L., et al. (2021). Dihydroartemisinin triggers ferroptosis in primary liver cancer cells by promoting and unfolded protein response-induced upregulation of CHAC1 expression. *Oncol. Rep.* 46, 240. doi:10.3892/or.2021.8191
- Werth, E. G., Rajbhandari, P., Stockwell, B. R., and Brown, L. M. (2020). Time course of changes in sorafenib-treated hepatocellular carcinoma cells suggests involvement of phospho-regulated signaling in ferroptosis induction. *Proteomics* 20, e2000006. doi:10.1002/pmic.202000006
- Wörns, M. A., Weinmann, A., Pflingst, K., Schulte-Sasse, C., Messow, C. M., Schulze-Bergkamen, H., et al. (2009). Safety and efficacy of sorafenib in patients with advanced hepatocellular carcinoma in consideration of concomitant stage of liver cirrhosis. *J. Clin. Gastroenterol.* 43, 489–495. doi:10.1097/MCG.0b013e31818ddfc6
- Xu, Q., Zhou, L., Yang, G., Meng, F., Wan, Y., Wang, L., et al. (2020). CircIL4R facilitates the tumorigenesis and inhibits ferroptosis in hepatocellular carcinoma by regulating the miR-541-3p/GPX4 axis. *Cell Biol. Int.* 44, 2344–2356. doi:10.1002/cbin.11444
- Xu, Z., Peng, B., Liang, Q., Chen, X., Cai, Y., Zeng, S., et al. (2021). Construction of a ferroptosis-related nine-lncRNA signature for predicting prognosis and immune response in hepatocellular carcinoma. *Front. Immunol.* 12, 719175. doi:10.3389/fimmu.2021.719175
- Yang, H. C., Wu, Y. H., Yen, W. C., Liu, H. Y., Hwang, T. L., Stern, A., et al. (2019). The redox role of G6PD in cell growth, cell death, and cancer. *Cells* 8, 1055. doi:10.3390/cells8091055
- Yang, W. S., Sriramaratnam, R., Welsch, M. E., Shimada, K., Skouta, R., Viswanathan, V. S., et al. (2014). Regulation of ferroptotic cancer cell death by GPX4. *Cell* 156, 317–331. doi:10.1016/j.cell.2013.12.010
- Yang, Y., Lin, J., Guo, S., Xue, X., Wang, Y., Qiu, S., et al. (2020a). RRM2 protects against ferroptosis and is a tumor biomarker for liver cancer. *Cancer Cell Int.* 20, 587. doi:10.1186/s12935-020-01689-8
- Yang, Y., Sun, M., Yao, W., Wang, F., Li, X., Wang, W., et al. (2020b). Compound kushen injection relieves tumor-associated macrophage-mediated immunosuppression through TNFR1 and sensitizes hepatocellular carcinoma to sorafenib. *J. Immunother. Cancer* 8, e000317. doi:10.1136/jitc-2019-000317
- Yao, Z., Luo, J., Hu, K., Lin, J., Huang, H., Wang, Q., et al. (2017). ZKSCAN1 gene and its related circular RNA (circZKSCAN1) both inhibit hepatocellular carcinoma cell growth, migration, and invasion but through different signaling pathways. *Mol. Oncol.* 11, 422–437. doi:10.1002/1878-0261.12045
- Yao, Z., Xu, R., Yuan, L., Xu, M., Zhuang, H., Li, Y., et al. (2019). Circ\_0001955 facilitates hepatocellular carcinoma (HCC) tumorigenesis by sponging miR-516a-5p to release TRAF6 and MAPK11. *Cell Death Dis.* 10, 945. doi:10.1038/s41419-019-2176-y
- Yuk, H., Abdullah, M., Kim, D. H., Lee, H., and Lee, S. J. (2021). Necrostatin-1 prevents ferroptosis in a RIPK1- and Ido-independent manner in hepatocellular carcinoma. *Antioxidants (Basel)* 10, 1347. doi:10.3390/antiox10091347
- Zaheer, J., Kim, H., Lee, Y. J., Kim, J. S., and Lim, S. M. (2019). Combination radioimmunotherapy strategies for solid tumors. *Int. J. Mol. Sci.* 20, E5579. doi:10.3390/ijms20225579
- Zhang, H., Liu, R., Sun, L., Guo, W., and Hu, X. (2021). The effect of ferroptosis-related genes on prognosis and tumor mutational burden in hepatocellular carcinoma. *J. Oncol.* 2021, 7391560. doi:10.1155/2021/7391560
- Zhang, J., Zhang, X., Li, J., and Song, Z. (2020). Systematic analysis of the ABC transporter family in hepatocellular carcinoma reveals the importance of ABCB6 in regulating ferroptosis. *Life Sci.* 257, 118131. doi:10.1016/j.lfs.2020.118131
- Zhang, X. F., Wang, J., Jia, H. L., Zhu, W. W., Lu, L., Ye, Q. H., et al. (2019). Core fucosylated glycan-dependent inhibitory effect of QSOX1-S on invasion and metastasis of hepatocellular carcinoma. *Cell Death Discov.* 5, 84. doi:10.1038/s41420-019-0164-8
- Zhao, Y., Li, M., Yao, X., Fei, Y., Lin, Z., Li, Z., et al. (2020). HCARI1/MCT1 regulates tumor ferroptosis through the lactate-mediated AMPK-SCD1 activity and its therapeutic implications. *Cell Rep.* 33, 108487. doi:10.1016/j.celrep.2020.108487
- Zheng, J., Sato, M., Mishima, E., Sato, H., Proneth, B., Conrad, M., et al. (2021). Sorafenib fails to trigger ferroptosis across a wide range of cancer cell lines. *Cell Death Dis.* 12, 698. doi:10.1038/s41419-021-03998-w
- Zhou, J., Li, L. U., Fang, L. I., Xie, H., Yao, W., Zhou, X., et al. (2016). Quercetin reduces cyclin D1 activity and induces G1 phase arrest in HepG2 cells. *Oncol. Lett.* 12, 516–522. doi:10.3892/ol.2016.4639
- Zhu, G., Murshed, A., Li, H., Ma, J., Zhen, N., Ding, M., et al. (2021). O-GlcNAcylation enhances sensitivity to RSL3-induced ferroptosis via the YAP/TFRC pathway in liver cancer. *Cell Death Discov.* 7, 83. doi:10.1038/s41420-021-00468-2
- Zhu, Y. J., Zheng, B., Wang, H. Y., and Chen, L. (2017). New knowledge of the mechanisms of sorafenib resistance in liver cancer. *Acta Pharmacol. Sin.* 38, 614–622. doi:10.1038/aps.2017.5



## OPEN ACCESS

## EDITED BY

Xin Wang,  
National Institutes of Health (NIH),  
United States

## REVIEWED BY

Archita Venugopal Menon,  
Northeastern University, United States  
Xin Yang,  
Columbia University, United States  
Aayushi Mahajan,  
Columbia University, United States

## \*CORRESPONDENCE

Kun Yang,  
chbyk1379@163.com  
Zhenzhong Gao,  
wuque123@hainmc.edu.cn  
Jigao Feng,  
fengjigao@hainmc.edu.cn

<sup>†</sup>These authors have contributed equally  
to this work

## SPECIALTY SECTION

This article was submitted to Molecular  
Diagnostics and Therapeutics,  
a section of the journal  
Frontiers in Molecular Biosciences

RECEIVED 20 June 2022

ACCEPTED 22 July 2022

PUBLISHED 17 August 2022

## CITATION

Zhuo S, He G, Chen T, Li X, Liang Y,  
Wu W, Weng L, Feng J, Gao Z and Yang K  
(2022), Emerging role of ferroptosis in  
glioblastoma: Therapeutic  
opportunities and challenges.  
*Front. Mol. Biosci.* 9:974156.  
doi: 10.3389/fmolb.2022.974156

## COPYRIGHT

© 2022 Zhuo, He, Chen, Li, Liang, Wu,  
Weng, Feng, Gao and Yang. This is an  
open-access article distributed under  
the terms of the [Creative Commons  
Attribution License \(CC BY\)](#). The use,  
distribution or reproduction in other  
forums is permitted, provided the  
original author(s) and the copyright  
owner(s) are credited and that the  
original publication in this journal is  
cited, in accordance with accepted  
academic practice. No use, distribution  
or reproduction is permitted which does  
not comply with these terms.

# Emerging role of ferroptosis in glioblastoma: Therapeutic opportunities and challenges

Shenghua Zhuo<sup>1†</sup>, Guiying He<sup>2†</sup>, Taixue Chen<sup>1†</sup>, Xiang Li<sup>2</sup>,  
Yunheng Liang<sup>1</sup>, Wenkai Wu<sup>1</sup>, Lingxiao Weng<sup>1</sup>, Jigao Feng<sup>3\*</sup>,  
Zhenzhong Gao<sup>1\*</sup> and Kun Yang<sup>1\*</sup>

<sup>1</sup>Department of Neurosurgery, First Affiliated Hospital of Hainan Medical University, Haikou, China, <sup>2</sup>Department of Neurology, Shenzhen Sixth People's Hospital, Huazhong University of Science and Technology Union Shenzhen Hospital, Shenzhen, China, <sup>3</sup>Department of Neurosurgery, Second Affiliated Hospital of Hainan Medical University, Haikou, China

Glioblastoma (GBM) is the most common malignant craniocerebral tumor. The treatment of this cancer is difficult due to its high heterogeneity and immunosuppressive microenvironment. Ferroptosis is a newly found non-apoptotic regulatory cell death process that plays a vital role in a variety of brain diseases, including cerebral hemorrhage, neurodegenerative diseases, and primary or metastatic brain tumors. Recent studies have shown that targeting ferroptosis can be an effective strategy to overcome resistance to tumor therapy and immune escape mechanisms. This suggests that combining ferroptosis-based therapies with other treatments may be an effective strategy to improve the treatment of GBM. Here, we critically reviewed existing studies on the effect of ferroptosis on GBM therapies such as chemotherapy, radiotherapy, immunotherapy, and targeted therapy. In particular, this review discussed the potential of ferroptosis inducers to reverse drug resistance and enhance the sensitivity of conventional cancer therapy in combination with ferroptosis. Finally, we highlighted the therapeutic opportunities and challenges facing the clinical application of ferroptosis-based therapies in GBM. The data generated here provide new insights and directions for future research on the significance of ferroptosis-based therapies in GBM.

## KEYWORDS

glioblastoma, ferroptosis, cancer therapy, therapy resistance, immunotherapy

## 1 Introduction

Glioblastoma (GBM) is the most prevalent malignant tumor of the central nervous system, accounting for 54% of adult malignant cases (Miller et al., 2021). In the past 4 decades, limited significant strides have been made in its prevention, early detection, and treatment (Miller et al., 2021). Although several therapies have been developed for the treatment of GBM including surgery, radiation, and chemotherapy, patients with GBM have a poor prognosis, only 5.5% of patients survived 5 years post-diagnosis (Ostrom et al., 2016). GBM treatment faces significant challenges, such as blood-brain barrier (Xie



et al., 2021), high intra-tumoral or inter-tumoral heterogeneity (Patel et al., 2014; Jacob et al., 2020), and immunosuppressive microenvironment (Fu et al., 2020). Nonetheless, an increasing understanding of the complex and interrelated tumor microenvironment (TME) has expanded the range of therapeutic strategies (Fu et al., 2020). So far, the outcomes of monotherapy have been disappointing therefore, combination therapy is required to achieve a broad and lasting anti-tumor response. Therefore, the present study focuses on the development of effective molecular targeted therapy, immunotherapy, gene therapy, and novel drug delivery technology.

Tumor cells resist cell death and evade immune destruction, which is different from normal tissue cells. Regulatory cell death (RCD) is a type of death initiated by gene regulation that originates from the intracellular or extracellular microenvironment when other adaptive responses cannot restore cell homeostasis. RCD can be subdivided into necroptosis, pyroptosis, ferroptosis, and other types of cell death as per its mechanism (Galluzzi et al., 2018). In 2012, researchers found lethal compounds responsible for ferroptosis, a new model of cell death. Ferroptosis is morphologically, genetically, and biochemically distinct from necrosis, apoptosis, and autophagy; it is characterized by iron dependence and reactive oxygen species (ROS) accumulation (Dixon et al., 2012). Cell morphological changes include rupture and blistering of the cell membrane; contraction and increase of membrane density; decrease or disappearance of the mitochondrial ridge; rupture of the mitochondrial outer membrane and normal size nucleus without chromatin agglutination. Under the induction of iron ions, ROS accumulation causes an imbalance of redox in cells, resulting in the occurrence of ferroptosis (Dixon et al., 2012). Iron-dependent tumor cells are vulnerable to ferroptosis inducers (FINs). Ferroptosis influences the efficacy of chemotherapy, radiotherapy, and immunotherapy, hence drug combination targeting ferroptosis signals improves the current efficacy of these treatments (Sato et al., 2018; Lang et al., 2019). Therefore, drug combination with drugs targeting the pathways of ferroptosis is a novel therapeutic strategy.

Ferroptosis is closely associated with cerebral ischemia-reperfusion injury (Tuo et al., 2022), neurodegenerative diseases (Park et al., 2021), and tumors (Dixon et al., 2012). Besides its role in acquired drug resistance and cancer immunosuppression, ferroptosis is involved in metabolic reprogramming, providing a novel opportunity for drug-resistant tumors (Tarangelo et al., 2018). Noteworthy, GBM cells have strong anti-apoptosis capacity and inhibitory tumor immune microenvironment (TIME) as an immune-desert tumor, resulting in a poor response to immunotherapy. T cells showed particularly severe exhaustion signature in GBM (Woroniecka et al., 2018). At present, GBM treatments transform “cold” tumors into “hot” tumors, hence stimulating

the immune system to fight tumors (Zhang J. et al., 2021). Studies indicate that ROS levels significantly increase after anti-PD-L1 treatment, hence decreasing the sensitivity of immunotherapy after suppressing ferroptosis (Wang W. et al., 2019). Therefore, therapeutic approaches targeting ferroptosis may provide a novel and promising approach for killing GBM cells.

Recent bioinformatics studies have shown that ferroptosis-related genes (FRGs) can be used to predict the treatment response in GBM (Zhuo et al., 2020; Xiao et al., 2021; Dong et al., 2022; Tian et al., 2022; Zhang et al., 2022). Therefore, ferroptosis plays an important role in GBM. Evasion of ferroptosis may increase GBM invasiveness and development of drug resistance. Previous review has indicated that alterations in glucose, lipid, glutamine, and iron metabolism in GBM may increase sensitivity to ferroptosis due to the enhanced reliance on the antioxidant system and iron ions (Huang et al., 2021). Thus, targeting ferroptosis can be a potential treatment for GBM. This review describes the role of ferroptosis in GBM treatment, including chemotherapy, radiotherapy, immunotherapy, and targeted therapy, as well as its opportunities and challenges.

## 2 Molecular mechanisms of ferroptosis

### 2.1 Drivers of ferroptosis

Ferroptosis is driven by lethal phospholipid peroxidation resulting from imbalanced redox homeostasis and cellular metabolism. This RCD process relies on phospholipids containing polyunsaturated fatty acid chains (PUFA-PLs), transition metal iron and ROS (Figure 1). This paragraph discusses mechanisms of liposynthesis, storage, utilization, and peroxidation during ferroptosis modulation. As a key metabolic substrate for fatty acid synthesis, acetyl-CoA is mainly converted from mitochondria-derived citrate through the action of ATP citrate lyase (ACLY) (Wei et al., 2020). The rate-limiting step in fatty acid synthesis is the synthesis of malonyl-CoA from acetyl-CoA by acetyl-CoA carboxylase (ACC) (Wang et al., 2022). Then malonyl-CoA and acetyl-CoA are catalyzed and condensed by fatty acid synthase (FASN) to form 16-carbon fatty acid palmitate. After palmitate is elongated by ELOVL fatty acid elongase (ELOVL), the initial product of fatty acid synthesis is further desaturated by fatty acid desaturases. Among them, delta-5 desaturase (D5D) and delta-6 desaturase (D6D) are rate-limiting enzymes for PUFAs conversion and are considered to be the main determinants of PUFA levels (Tosi et al., 2014), whereas Stearoyl-CoA Desaturase (SCD) catalyzes the formation of monounsaturated fatty acids (MUFAs) (Ntambi, 2004). Exogenous MUFAs induce

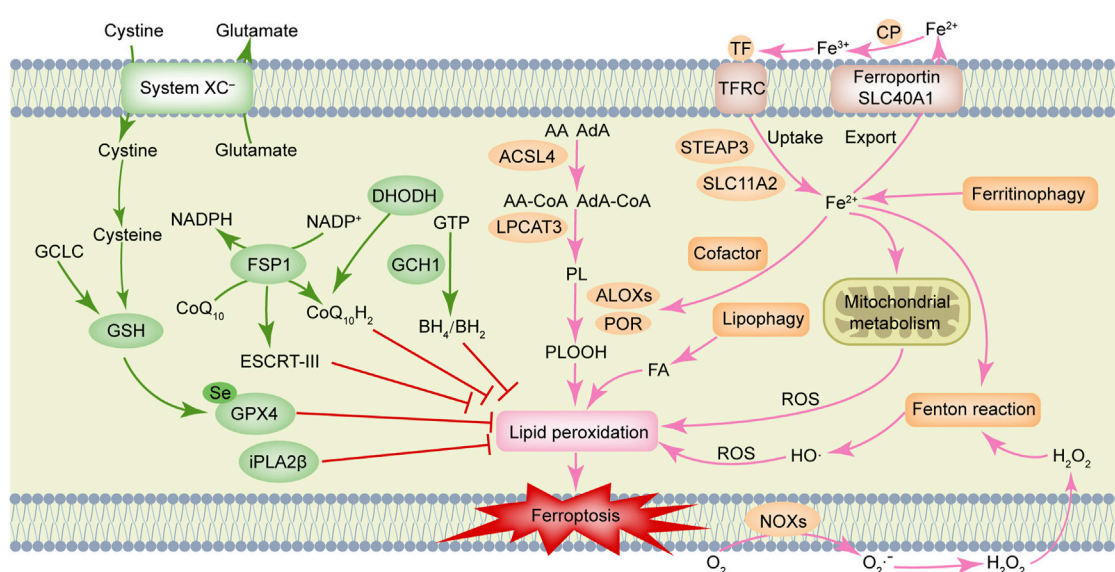


FIGURE 1

Molecular mechanisms of ferroptosis. Ferroptosis is driven by accumulation of polyunsaturated fatty acid-containing phospholipids (PUFA-PLs), transition metal iron and reactive oxygen species (ROS). Ferroptosis defense systems include cyst(e)ine/GSH/GPX4 axis, NAD(P)H/FSP1/CoQ<sub>10</sub> axis, DHODH/CoQ<sub>10</sub> axis, GCH1/BH<sub>4</sub> axis, and iPLA2 $\beta$ , etc. AA, arachidonic acid; ACSL4, Acyl-coenzyme A synthetase long-chain family member 4; AdA, adrenic acid; ALOXs, arachidonate lipoxygenases; BH<sub>2</sub>, dihydrobiopterin; BH<sub>4</sub>, tetrahydrobiopterin; CoQ<sub>10</sub>, ubiquinol; CoQ<sub>10</sub>H<sub>2</sub>, ubiquinol; CP, ceruloplasmin; DHODH, dihydroorotate dehydrogenase; ESCRT-III, endosomal sorting complex required for transport-III; FA, fatty acid; FSP1, ferroptosis suppressor protein 1; GCH1, GTP cyclohydrolase 1; GCLC, glutamate-cysteine ligase catalytic subunit; GPX4, glutathione peroxidase 4; GSH, glutathione; GTP, guanosine triphosphate; H<sub>2</sub>O<sub>2</sub>, hydrogen peroxide; iPLA2 $\beta$ , calcium-independent phospholipase A2 $\beta$ ; LPCAT3, lysophosphatidylcholine acyltransferase 3; NOXs, NADPH oxidases; PL, phospholipids; POR, cytochrome P450 oxidoreductase; SLC11A2, solute carrier family 11 member 2; SLC40A1, solute carrier family 40 member 1; STEAP3, STEAP family member 3, metalloredutase; TF, transferrin; TFRC, transferrin receptor.

a ferroptosis-resistant cell state by decreasing levels of oxidizable PUFAs and suppressing the accumulation of lipid peroxides (Magtanong et al., 2019). Lipid droplets can buffer and store excess lipids. Increased lipid droplet degradation promotes ferroptosis (Bai et al., 2019). Fatty acids are catabolized by fatty acid  $\beta$ -oxidation (FAO) in mitochondria through a series of reactions that shorten them. Carnitine palmitoyltransferase 1 (CPT1) present in mitochondrial outer membrane can catalyze carnitine esters from acyl-CoA as a rate-limiting step of FAO (van der Leij et al., 1999). Lipid peroxidation is a process in which carbon-carbon double bonds of lipids (especially PUFAs) are attacked by oxidants (such as free radicals). Two membrane remodeling enzymes, an Acyl-CoA synthetase long-chain family member 4 (ACSL4) and lysophosphatidylcholine acyltransferase 3 (LPCAT3), are key drivers of iron ptosis, as revealed by genome-wide haploid and CRISPR-Cas9 screening (Dixon et al., 2015; Doll et al., 2017). ACSL4 can catalyze the connection between CoA and long-chain PUFAs (including arachidonic acid (AA) and adrenic acid (AdA)). LPCAT3 will re-esterify these products into phospholipids (PL), increasing the cellular incorporation of long-chain PUFAs into membranes and lipids. It has been found that

some arachidonate lipoxygenases (ALOXs) have the capability of directly oxygenating PUFAs and PUFA-containing lipids within biological membranes, promoting the production of phospholipid hydroperoxides (PLOOHs), a lipid-based form of ROS, thereby mediating ferroptosis (Yang et al., 2016). Furthermore, cytochrome P450 oxidoreductase (POR) (Zou et al., 2020) and NADPH oxidases (NOXs) (Dixon et al., 2012) play a role in lipid peroxidation and contribute to ferroptosis.

Iron homeostasis is an important factor that determines ferroptosis sensitivity. It has been described in detail in a prior review that ferroptosis is tightly controlled by processes associated with iron metabolism including iron uptake, storage, utilization, and efflux (Chen X. et al., 2020). Besides initiating the non-enzymatic Fenton reaction to peroxidize PUFA-PLs, iron also acts as an essential cofactor for enzymes involved in lipid peroxidation, such as POR and ALOXs, which in turn also regulate ferroptosis. Ferroptosis susceptibility can be affected by cellular labile iron content. Ferroptosis, for instance, is triggered by increased cellular iron availability as a result of autophagic degradation of ferritin, the iron storage protein (Hou et al., 2016). Similarly, transferrin receptor and glutaminolysis also contribute to ferroptosis (Gao et al., 2015).

## 2.2 Ferroptosis defense systems

Reports have been made of multiple ferroptosis defense systems (Figure 1). Among them, cyst(e)ine/GSH/GPX4 axis is the primary regulator of ferroptosis. The cystine/glutamate reverse transporter (system  $\text{XC}^-$ ), is composed of a heavy chain solute carrier family 3 members 2 (SLC3A2) and a light chain solute carrier family 7 member 11 (SLC7A11), plays a role in cysteine synthesis (Koppula et al., 2021). Cysteine is converted into glutathione (GSH) with the help of gamma-glutamylcysteine synthetase and GSH synthetase. Glutathione Peroxidase 4 (GPX4) acts as a phospholipid hydroperoxidase to convert PLOOH into phospholipid alcohol (PLOH), preventing ferroptosis from occurring (Yang et al., 2014). Inhibition of SLC7A11 prevents glutamate/cystine exchange and reduces intracellular GSH synthesis, which further inhibits the activity of GPX4, impairs intracellular antioxidant system, and triggers ferroptosis (Koppula et al., 2021). Notably, erastin (SLC7A11 inhibitor) and RSL3 (GPX4 inhibitor) can induce ferroptosis (Dixon et al., 2012; Yang et al., 2014). The ubiquinone ( $\text{CoQ}_{10}$ ) oxidoreductase ferroptosis suppressor protein 1 (FSP1) is a glutathione-independent ferroptosis suppressor. FSP1 can directly reduce lipid radicals and terminate lipid peroxidation by reducing  $\text{CoQ}_{10}$  to ubiquinol ( $\text{CoQ}_{10}\text{H}_2$ , the reduced and active antioxidant form of  $\text{CoQ}_{10}$ ) and/or regenerating oxidized  $\alpha$ -tocopherol radical (vitamin E) to its non-radical form (Bersuker et al., 2019; Doll et al., 2019). In some cases, the membrane repair mechanisms of ESCRT-III (a protein complex) may also allow FSP1 to inhibit ferroptosis in a pathway parallel to that of  $\text{CoQ}_{10}\text{H}_2$  (Dai et al., 2020). Further, a recent study revealed that dihydroorotate dehydrogenase (DHODH) is located in the inner mitochondrial membrane and operates in parallel with mitochondrial GPX4 (but independent of cytosolic FSP1 or GPX4) to inhibit ferroptosis by reducing  $\text{CoQ}_{10}$  to  $\text{CoQ}_{10}\text{H}_2$  (Mao et al., 2021).

In another study, it was reported the metabolic products tetrahydrobiopterin ( $\text{BH}_4$ ) and dihydrobiopterin ( $\text{BH}_2$ ) derived by GTP cyclohydrolase 1 (GCH1) were shown to protect against ferroptosis by acting as a direct radical-trapping antioxidant and being involved in  $\text{CoQ}_{10}$  synthesis (Kraft et al., 2020). Recent studies indicated that calcium-independent phospholipase  $\text{A}_2\beta$  ( $\text{iPLA}_2\beta$ ) preferentially hydrolyzes peroxidized PUFA-PLs and that it represses ferroptosis induced by p53 in a GPX4-independent manner (Chen D. et al., 2021; Sun et al., 2021). As summarized in the previous review, oxidative-stress-responsive transcription factor nuclear factor erythroid 2-related factor 2 (NRF2) can mitigate ferroptosis by stimulating the expression of many of its canonical target genes (Anandhan et al., 2020). Additionally, the accumulation of squalene (a metabolite of the cholesterol pathway) has been reported to have anti-ferroptotic effects in cholesterol auxotrophic lymphoma cell lines and primary tumors (Garcia-Bermudez et al., 2019).

## 3 The role of ferroptosis in GBM treatment

### 3.1 Chemotherapy

One of the major reasons for cancer treatment failure is the resistance of malignant tumor cells to chemotherapeutic drugs. Unlike apoptosis, ferroptosis, a special cell death process resolves the inefficiency of apoptosis-inducing drugs. The use of FINs provides a new approach to addressing drug resistance to tumor chemotherapeutic drugs. The integrated use of FINs and chemotherapy yields a synergistic response and improves cancer sensitivity to chemotherapeutic drugs. For instance, the combination of cisplatin and erastin significantly improves anti-tumor activity, indicating the significance of ferroptosis in tumor treatment (Sato et al., 2018). Additionally, GPX4 inhibitors show a certain degree of lethality in drug-resistant cells via ferroptosis, and targeting GPX4 could be a therapeutic approach, preventing acquired drug resistance (Hangauer et al., 2017).

Recent studies have shown that the balance of oxidation and antioxidation, including ROS and GSH, is linked to its resistance to temozolomide (TMZ) treatment for GBM (Zhu et al., 2018; Wu et al., 2020). High expression of SLC7A11, a subunit of the glutamate/cystine transporter is related to poor GBM prognosis (Robert et al., 2015). TMZ increases GSH synthesis and decreases ROS levels by improving SLC7A11 expression. The combination therapy of TMZ and SLC7A11 inhibitor erastin are potentially effective GBM treatments (Chen et al., 2015). Sulfasalazine (SAS), another SLC7A11 inhibitor causes ferroptosis in GBM cells (Sehm et al., 2016). The effect of SAS on the survival of glioma cells does not seem to depend on significant changes in autophagy, different from the cell death pathway induced by TMZ (Sehm et al., 2016). This indicates that their combination has a synergistic effect. Induction of ferroptosis is potentially one of the promising therapies against TMZ resistance. One study revealed that inhibiting autophagy causes ferroptosis and improves the sensitivity of glioblastoma stem cells (GSCs) to TMZ (Buccarelli et al., 2018). Elsewhere, GPX4 is significant in tumor resistance. One previous study reported that highly mesenchymal therapy-resistant cancer cells depend on GPX4 for survival and GPX4 function loss causes ferroptosis in these cells. This suggests that targeting GPX4 induce ferroptosis in drug-resistant cells, thereby improving their sensitivity to chemotherapy medication (Hangauer et al., 2017). Considering that RSL3 inhibits GPX4 activity, the use of RSL3 improves ferroptosis in GBM cells (Fan et al., 2017; Li et al., 2021). The CRISPR-based genome-wide genetic screening and microarray analysis of ferroptosis-resistant cell lines revealed that ACSL4 dictates ferroptosis sensitivity as an essential component of ferroptosis execution by shaping cellular lipid composition (Doll et al., 2017). Additionally, ACSL4 is linked to sorafenib resistance in liver cancer (Lu et al., 2022). ACSL4 suppresses glioma cell proliferation by activating

ferroptosis (Cheng et al., 2020). Moreover, ACSL4 is linked to TMZ chemosensitivity in GBM cells (Bao et al., 2021). Furthermore, NRF2 (Fan et al., 2017; Zhang and Wang, 2017) and oxidative metabolism driver activating transcription factor 4 (ATF4) (Chen et al., 2017a; Chen et al., 2017b; Gao et al., 2021) and tumor protein P53 (P53) (Blough et al., 2011; Jiang et al., 2015; Tarangelo et al., 2018) are associated with ferroptosis and TMZ resistance. Therefore, ferroptosis is closely correlated to GBM chemotherapy and significantly promotes TMZ resistance. A better understanding of the ferroptotic mechanism in TMZ resistance may provide new insights and targets in the clinical reversal of GBM.

### 3.2 Radiotherapy

Recent studies have found that radiotherapy directly causes ferroptosis in cancer cells (Lang et al., 2019; Lei et al., 2020). Cells exposed to ionizing radiation (IR) activate ROS-generating oxidases, regulate antioxidants, and disrupt metabolic activity in response to oxidative damage, thereby influencing mitochondrial function (Yang P. et al., 2021). A previous review summarized that during radiation exposure and tumor microenvironment, different types of cell death occur in irradiated tumor cells due to several factors, including cell type, oxygen tension, DNA repair capacity, P53 status, radiation dose, quality, and cell cycle stage (Sia et al., 2020). Mechanistically, IR promotes ferroptosis by generating excess ROS to induce lipid peroxidation, and ACSL4 expression to promote PUFAs biosynthesis. Ferroptosis inhibitors, including GPX4 and SLC7A11, are expressed as an adaptive response to IR (Lei et al., 2020). Moreover, ataxia telangiectasia mutated (ATM) kinase acts upstream of p53 and regulates the DNA damage response (DDR) pathway, which is critical in resolving double-strand DNA breaks (Matsuoka et al., 2007). The expression level of SLC7A11 is lowered by IR in an ATM-dependent manner and promotes ferroptosis by suppressing SLC7A11-mediated cystine uptake and GSH synthesis (Lang et al., 2019). Since SLC7A11 expression is antagonized by radiotherapy-mediated P53 activation, GSH synthesis is inhibited, hence promoting radiotherapy-induced lipid peroxidation and ferroptosis (Lei et al., 2021). Many studies have shown that ferroptosis improves the sensitivity of multiple tumor cells to radiotherapy (Lei et al., 2020; Zhang Z. et al., 2021; Feng et al., 2021; Yuan et al., 2021). Targeting GPX4 or SLC7A11 is a ferroptosis-inducing radiosensitizing approach that improves radiotherapy-induced lipid peroxidation and ferroptosis. For instance, radiotherapy-induced GPX4 and SLC7A11 expression and ACSL4 deficiency or low expression trigger radioresistance (Lei et al., 2020; Feng et al., 2021). These studies reveal a synergy between radiotherapy and ferroptosis. Induction of ferroptosis improves radiotherapy efficacy, while its inhibition reduces radiotherapy toxicity.

Radioresistance in GBM is associated with hypoxia (Marampon et al., 2014), DDR (Carruthers et al., 2018), GSCs (Osuka et al., 2021), and fatty acid oxidation (Jiang et al., 2022). Previous research has shown that doranidazole as a radiosensitizer improves radiation-induced DDR in hypoxic GSCs in a mouse model of GBM and confers survival benefits to GSC-derived tumor-bearing mice. Meanwhile, doranidazole also causes mitochondrial dysfunction and ROS accumulation in GSCs, resulting in ferroptosis (Koike et al., 2020). Radiation-induced lipid peroxidation triggers ferroptosis, which synergistically acts with FINs in GBM (Ye et al., 2020). The system XC<sup>-</sup> inhibitor SAS improves radiation therapy efficacy in glioma; SAS and radiation synergistically increase DNA double-strand breaks and glioma cell death. Meanwhile, SAS integrated with gamma knife radiosurgery provides a survival benefit in human GBM xenografted rats. Thus, SAS potentially acts as a radiosensitizer to improve radiotherapy efficacy in glioma patients (Sleire et al., 2015). SAS has been clinically used as a monotherapy for GBM (NCT01577966) (Robert et al., 2015) and in combination with radiosurgery (NCT04205357). Thus, these findings indicate that exploring the integrated therapeutic approach of radiotherapy and targeting ferroptosis will resolve the radiation resistance in GBM.

### 3.3 Immunotherapy

Immunogenic cell death (ICD), a cell death process that induces an immune response, allows the release or exposure of intracellular molecules from dead or dying cells and stimulates adaptive immunity, which promotes immune responses against intracellular pathogens and tumor-associated antigens (Galluzzi et al., 2018). Cell death is an integral component of an immune response, and the type and activity of damage-associated molecular patterns (DAMPs) released during ICD elicit an immune response (Galluzzi et al., 2018). A previous review noted that cell death including necroptosis, pyroptosis, and ferroptosis causes the release of DAMPs and these 3 cell death forms are potentially new mechanisms of ICD; there is an interplay between antitumor immune activation (Tang et al., 2020). As a DAMP, high mobility group box 1 protein (HMGB1) is a crucial protein necessary for the immunogenicity of cancer cells. HMGB1 binds to toll-like receptor 4 (TLR4) on DC cells, accelerating phagocytosis of DC cells as well as process and promoting antigen presentation to T cells (Yamazaki et al., 2014). FINs cause HMGB1 release in cancer cells and non-cancer cells (Wen et al., 2019). The cell death stage is crucial in the immunogenicity of ferroptotic cancer cells, and early ferroptotic cancer cells undergo ICD, accompanied by adenosine triphosphate and HMGB1 release, which stimulates bone marrow-derived dendritic cell maturation to exert anti-tumor immunity (Efimova et al., 2020). These results have narrowed the distance between ferroptosis and anti-tumor



immunotherapy, laying a theoretical reference for the synergistic treatment of malignant tumors with ferroptosis and immunotherapy.

Tumor cells evade immune surveillance through various strategies, and the primary obstacle to effective antitumor immunity is highly heterogeneous, immunosuppressive, and metabolically stressful TME. Understanding the dynamic functional interactions in this intricate microenvironmental system comprising multiple immune cells, stromal cells, vascular networks, and acellular components provides vital insights into the design of precise anticancer combinatorial strategies. The capacity of iron to regulate antitumor immune response is closely linked to its significant role in tumor development (Sottile et al., 2019; Song et al., 2021). Ferroptosis modulate immune cells in the TME and in crosstalk between tumor and immune cells, which are new insights into targeting ferroptosis in cancer immunotherapy (Wang W. et al., 2019; Lang et al., 2019; Ma et al., 2021). Interferon Gamma (IFN- $\gamma$ ) secreted by cytotoxic CD8<sup>+</sup> T cells downregulates the expression of system XC<sup>-</sup>, sensitizing cancer cells to ferroptosis. PD-L1 antibodies and FINs synergistically suppress tumor growth *in vitro* and *in vivo*, and melanoma patients with clinical benefit from immunotherapy express a genetic signature of T-cell-induced ferroptosis, highlighting the potential of targeting the ferroptosis pathway to improve cancer immunotherapy (Wang W. et al., 2019). IFN- $\gamma$  derived from immunotherapy-activated CD8<sup>+</sup> T cells synergizes with radiotherapy-activated ATM to cause ferroptosis in cancer cells (Lang et al., 2019). Importantly, CD36 mediates fatty acid uptake by CD8<sup>+</sup> T cells, causes lipid peroxidation and ferroptosis, and reduces cytotoxic factor production, impairing CD8<sup>+</sup> T antitumor function (Ma et al., 2021). Targeting CD36 or inducing ferroptosis improves CD8<sup>+</sup> T efficacy of cellular and immune checkpoint blockade-based tumor immunotherapy (Ma et al., 2021). Conditional deletion of Gpx4 induces ferroptosis in T cells by lipid peroxidation in mice (Matsushita et al., 2015). The fate of tumor cells appears to be determined by whether tumor cells and tumor suppressor immune cells coexist, as well as the sequence of ferroptosis. On the one hand, ferroptosis of tumor cells produce DAMPs and promote an immune response. Conversely, tumor-suppressing immune cells undergo ferroptosis, whereas tumor cells escape death. Therefore, in-depth studies of these crosstalk relationships are necessary to elucidate the role of ferroptosis as an ICD or inhibition of tumor suppressor immune cells in inducing or inhibiting immune responses.

As a low-immunogenic tumor, GBM has numerous immunosuppressive mechanisms such as low mutational burden (Hodges et al., 2017) and immunosuppressive microenvironment (Fu et al., 2020). In mouse glioma cells, ferroptosis inhibitors target photodynamic therapy-induced ICD (Turubanova et al., 2019). Relevant studies based on public databases indicate that risk scores based on the

ferroptosis-related genes predict prognosis and immunotherapy response in GBM (Zhuo et al., 2020; Xiao et al., 2021). Stimulator of interferon genes (STING) is crucial for promoting anti-tumor immune responses against cancer (Mender et al., 2020). GPX4 promotes STING activation by maintaining lipid redox homeostasis (Jia et al., 2020). STING promotes anti-glioma immunity by causing type I IFN signaling (Ohkuri et al., 2014). RSL3 exerts antitumor effects via NF- $\kappa$ B pathway activation and GPX4 depletion driving ferroptosis in GBM (Li et al., 2021). These findings indicate that GPX4, a key ferroptotic gene, is closely related to an immune response in the TME, and its role in GBM antitumor immunotherapy remains uninvestigated.

In the initial GBM microenvironment, glioma-associated microglia/macrophages (GAMs) account for 59% of the total TME cells (Fu et al., 2020). Through symbiosis with GBM cells, GAMs regulate GSCs stemness (Shi et al., 2017), angiogenesis (Wei et al., 2021), and T cell activity (Takenaka et al., 2019). ICD is caused by ferroptosis, which polarizes tumor-promoting M2 type tumor-associated macrophages (TAMs) into anti-tumor M1 type TAMs, changes the immunosuppressive microenvironment, and enables synergistic effects of ferroptosis and immune regulation (Li and Rong, 2020; Wan et al., 2020). Elsewhere, one study revealed that ferroptosis, a predominant type of programmed cell death in gliomas, is linked to poor prognosis and immunosuppression in gliomas. Ferroptosis promotes the recruitment and polarization of TAMs to an M2-like phenotype, whereas inhibition of ferroptosis improves the sensitivity of mouse GBM to anti-PD1/L1 immunotherapy (Liu et al., 2022). A previous review summarized that cancer-associated fibroblasts (CAFs), as a vital component of TME stromal cells, modulate solid tumor growth, metastasis, immunosuppression, and drug resistance, and are linked to poor prognosis (Chen and Song, 2019). In gliomas, high expression of CAFs is linked to poor prognosis, and a risk model constructed by CAFs-related genes predicts immunotherapy response (Chen Z. et al., 2021). Exosome-like nanovesicle tumor vaccines (eNVs) targeting fibroblast activation protein- $\alpha$  (FAP)-positive CAFs cause-specific cytotoxic T lymphocyte immune responses that release IFN- $\gamma$  and deplete FAP<sup>+</sup> CAF to promote tumor ferroptosis. RSL3 improves eNVs-FAP-induced antitumor effects (Hu et al., 2021). Extensive tumor necrosis predicts a poor prognosis in GBM, and neutrophils trigger ferroptosis in GBM cells by transferring myeloperoxidase, thereby resulting in further necrosis and malignant progression of GBM (Yee et al., 2020).

In summary, the different compositions between tumor cells and immune cells in the TME could exert a certain effect on the response to immunotherapy. The relationship between ferroptosis and TIME in GBM is complex, rather than resulting in outright positive or negative effects. Furthermore, ICDs should have a balanced combination of adjuvant (DAMP-related effects) and antigenic (mainly due to tumor antigens) to

induce effective antitumor immunity. In highly heterogeneous GBM, ferroptotic cells could exhibit different roles by releasing different “find me” and “eat me” signals. Therefore, investigating the molecular mechanism of ferroptosis to improve the efficacy of GBM immunotherapy is problematic.

### 3.4 Targeted therapy

The WHO 2021 classification of the central nervous system (CNS) tumors highlights the role of molecular features in the diagnosis of adult diffuse gliomas, which are important for individualized treatment and clinical prognosis of gliomas. These molecular features include isocitrate dehydrogenase (IDH) mutation status, 1p/19q co-deletion, O-6-Methylguanine-DNA Methyltransferase (MGMT) promoter methylation status, telomerase reverse transcriptase (TERT) promoter mutation, and epidermal growth factor receptor (EGFR) amplification, among others (Louis et al., 2021). A clear path to precise glioma-targeted therapy can be found by combining WHO grading, histology, and molecular characterization. Nonetheless, as a result of complex regulatory networks, classical targets such as EGFR gene alteration have failed (NCT01480479) (Weller et al., 2017). The mechanism of making targeted therapy an ideal weapon for personalized and precision medicine for GBM patients is a matter of concern. Studies indicate that targeting truncal alterations/mutations in GBM provide the greatest efficacy, providing new information for selecting GBM-targeted therapy (Lee et al., 2017). Cancer cells are therapeutically vulnerable to ferroptosis due to altered metabolic profiles, genetic mutations, and an imbalance in the ferroptotic defense system (Dixon et al., 2012). A previous review concluded that targeting ferroptosis as an anticancer strategy was effective and potential, as demonstrated by several clinical trials and preclinical drugs (Wang et al., 2021). Additionally, the mechanism of action of various targeted drugs is linked to ferroptosis, such as sorafenib (Lu et al., 2022), neratinib (Nagpal et al., 2019), and APR-246 (Birsan et al., 2022). This section describes the relationship of ferroptosis to classical therapeutic targets in GBM, including EGFR and IDH mutations.

GBM is characterized by a high frequency of EGFR amplification and/or mutation and EGFRvIII mutation is the most common extracellular region mutation. In contrast with wild-type EGFR, EGFRvIII is a more stable constitutively activated receptor (Brennan et al., 2013). EGFR/EGFRvIII regulates the occurrence and development of GBM by activating downstream signaling pathways, affecting GBM invasion (Micallef et al., 2009) and angiogenesis (Bonavia et al., 2012). A recent study discovered that EGFR mutants in GBM alter its function of distinguishing between different ligands and transducing biased signals by changing the extracellular structure, suggesting a new direction for the

development of EGFR inhibitors (Hu C. et al., 2022). EGFRvIII GBM growth is dependent on lipogenesis (Guo et al., 2011). The use of fatty acid synthase inhibitors targets *in vivo* tumor growth in EGFRvIII GBM (Guo et al., 2009b). Additionally, the AMP-activated protein kinase (AMPK) regulates cellular energy metabolism, linking growth factor receptor signaling to cellular energy status; its activation inhibits the growth of EGFRvIII-expressing GBMs by targeting adipogenesis (Guo et al., 2009a). EGFR-mutated cancer cells, on the other hand, are cystine-dependent, and ferroptosis can be induced in EGFR-mutated human breast epithelial cells and non-small cell lung cancer cells after cystine deprivation (Poursaitidis et al., 2017). EGFR inhibitors including gefitinib (Song et al., 2020), erlotinib (You et al., 2021), and imatinib (Ishida et al., 2021), are associated with ferroptosis. Additionally, cetuximab, an IgG1-type human/mouse chimeric monoclonal antibody targeting the extracellular region of EGFR is closely associated with ferroptosis (Chen P. et al., 2020; Yang J. et al., 2021). Transcriptomic and genomic analyses in GBM cells with mutated activating EGFR demonstrate a range of novel resistance mechanisms, including ferroptosis and oxidative stress (Kadioglu et al., 2021). These findings suggest that treatment with ferroptosis may be more effective in overcoming the current therapeutic dilemma in GBM with EGFR amplification/mutation activation, particularly EGFRvIII.

IDH mutation status is a critical diagnostic marker for adult diffuse glioma (Louis et al., 2021). Targeting IDH mutations has certain therapeutic potential in IDH-mutant gliomas or other tumors, and various IDH mutation inhibitors have been developed. Among them, the FDA has approved enasidenib and ivosidenib (Karpel-Massler et al., 2019). Based on a previous review, multiple clinical trials have demonstrated that the IDH1-mutant small molecule inhibitor ivosidenib is biologically active and well-tolerated in patients with hematological and solid IDH1-mutant malignancies (Zarei et al., 2022). Also, the application of ivosidenib demonstrated a therapeutic effect in IDH1-mutant low-grade glioma and recurrent GBM (Mellinghoff et al., 2020; Tejera et al., 2020). A drug-transcriptome-based analysis reveals a signature of ferroptotic genes enriched in IDH-mutated brain tumors, indicating that IDH-mutated brain tumors may be uniquely vulnerable to FINs (Yang et al., 2020). IDH1 mutation improves erastin-induced lipid ROS accumulation and glutathione depletion, and its metabolite 2-Hydroxyglutarate (2-HG) sensitizes cells to ferroptosis (Wang T. X. et al., 2019). In IDH1-mutant gliomas, 2-HG inhibits glutamate levels, rendering GSH synthesis more dependent on glutaminase; suppressing glutaminase specifically improves the response of IDH-mutant glioma cells to oxidative stress and radiation sensitivity (McBrayer et al., 2018). Collectively, these studies suggest that targeting IDH mutations and inducing ferroptosis could be an effective therapeutic strategy.

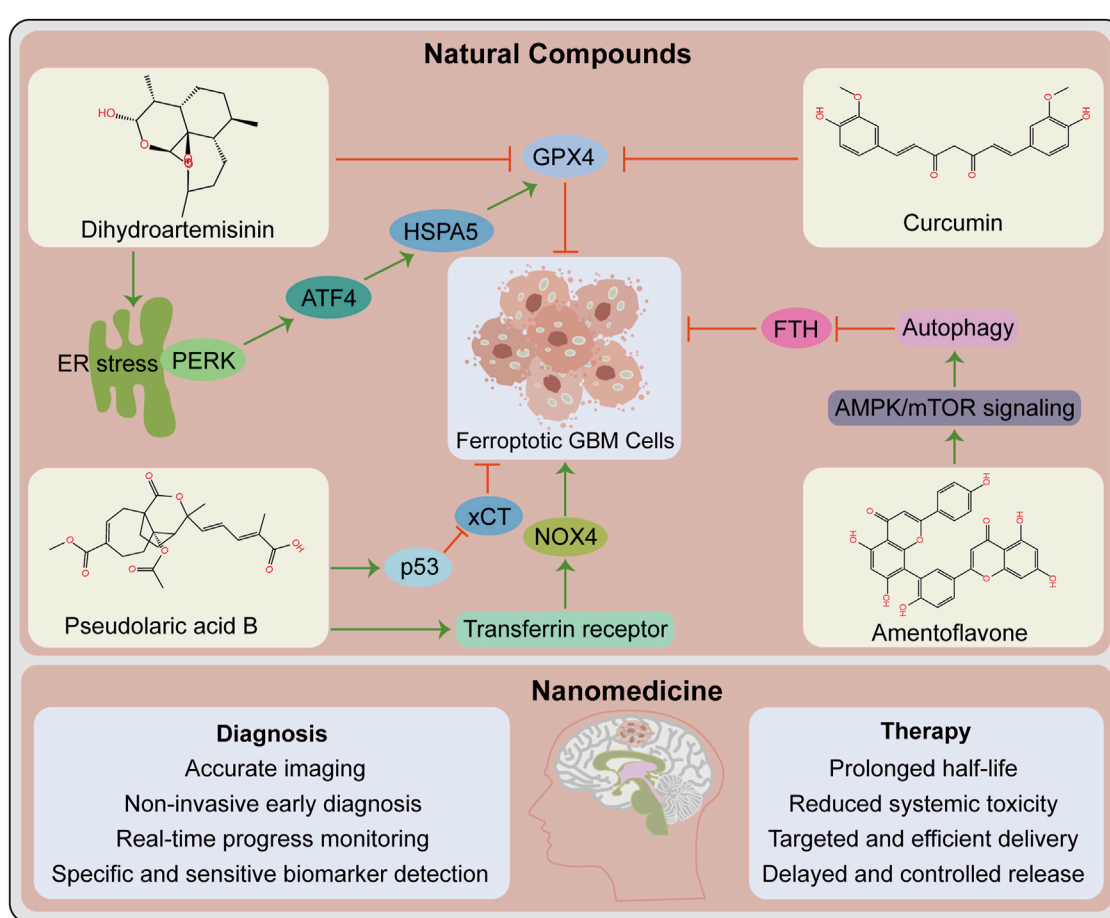


FIGURE 2

Opportunities for ferroptosis in glioblastoma therapy. Contribution of natural compounds to the treatment of glioblastoma such as dihydroartemisinin, curcumin, pseudolaric acid B and amentoflavone. The upper box shows the chemical structures of these four compounds and the associated mechanisms that regulate ferroptosis in glioblastoma. The below box lists the potential advantages of nanomedicine in the diagnosis and therapy of glioblastoma. ATF4, activating transcription factor 4; ER, endoplasmic reticulum; FTH, ferritin heavy chain. GPX4, glutathione peroxidase 4; HSPA5, heat shock protein family A (Hsp70) member 5; NOX4, NADPH oxidase 4; PERK, protein kinase R-like ER kinase; xCT, SLC7A11, solute carrier family 7 member 11.

## 4 Opportunities for ferroptosis in GBM treatment

### 4.1 The therapeutic potential of ferroptosis modulated by natural compounds

With the advancement of research on ferroptosis-related drugs, various natural compounds have been discovered to induce ferroptosis. Some review articles summarize the roles of various natural compounds in the regulation of ferroptosis (Zhang S. et al., 2021; Ge et al., 2022). Artemisinin and its derivatives extracted from *Artemisia annua* are terpenoids that cause ferroptosis in cancer patients via various mechanisms including iron-related gene expression regulation, increased intracellular iron levels, promotion of ROS production,

and intracellular GSH depletion (Ooko et al., 2015; Efferth, 2017; Hu Y. et al., 2022). Interestingly, the artemisinin derivative dihydroartemisinin causes ferroptosis in GBM cells (Chen et al., 2019; Yi et al., 2020). The phenolic compound curcumin has antioxidant and antitumor properties, exerting anti-ferroptotic or pro-ferroptotic activity in different diseases or conditions (Zhang S. et al., 2021). The curcumin analog ALZ003 induces ferroptosis in GBM cells by disrupting GPX4-mediated redox homeostasis (Chen T. C. et al., 2020). Additionally, pseudolaric acid B (diterpene acid from Cortex Pseudolaricis) (Wang et al., 2018) and amentoflavone (Chen Y. et al., 2020) (a polyphenol from Selaginella) have been confirmed *in vitro* and *in vivo* to cause ferroptosis in GBM and suppress tumor growth (Figure 2). These natural compounds have demonstrated significant therapeutic potential by causing ferroptosis in GBM. Future studies should investigate whether

these natural compounds synergize with chemoradiotherapy and overcome resistance. Whether they also promote the effect of immunotherapy and targeted therapy warrants additional investigation. It is undeniable that these natural compounds may act via other pathways than ferroptosis in the treatment of GBM.

## 4.2 Application of nanomedicine in ferroptosis detection and treatment

The current traditional treatment methods have certain shortcomings in cancer treatment. With the advancement of science and technology, nanomedicine has enabled precise cancer treatment. Nanomedicine and delivery systems based on nanotechnology have numerous benefits, including high targeting efficiency, low systemic toxicity, and long half-life (Klochov et al., 2021). Many antitumor nano-drug delivery systems have recently been developed, including strategies for causing ferroptosis and eliciting effective antitumor responses (Fu et al., 2021; Gu et al., 2021). For instance, nanoformulations combined with ferroptosis drive many pro-inflammatory signaling pathways to activate TAMs to antitumor M1 phenotype, thereby improving antitumor capacities (Gu et al., 2021). Nanotechnology-based theranostics can simultaneously diagnose and treat patients, combining different treatment modalities to improve efficacy and safety, with a wide range of applications in GBM diagnosis, drug delivery, and treatment (Tang et al., 2019) (Figure 2). Several nanotechnology-based strategies for targeting ferroptosis have been developed in GBM and have shown significant antitumor effects (Zhang et al., 2020; Zhang Y. et al., 2021). This provides additional options for preclinical research, including nanotechnology application in developing strategies for ferroptosis combined with immunotherapy that prevent off-target effects, thereby increasing the possibility of ferroptosis in GBM treatment.

## 5 Challenges of ferroptosis in GBM treatment

### 5.1 Tumor heterogeneity and stem cell characteristics

Broad tumor heterogeneity is a feature of GBM, including genetic, epigenetic, and environmental heterogeneity. Besides inter-tumoral heterogeneity, there is spatial and temporal intra-tumoral heterogeneity, which is considered a key determinant of GBM treatment failure (Patel et al., 2014; Jacob et al., 2020). Furthermore, the presence of GSCs contributes to treatment failure and disease progression for this lethal tumor (Osuka et al., 2021). Meanwhile, these two

factors, along with angiogenesis and the hypoxic niche, contribute to treatment resistance (Cheng et al., 2013; Hubert et al., 2016) (Figure 3). Nevertheless, ferroptosis studies based on 2-D cell culture using only a few classical GBM cell lines do not sufficiently reflect the complex tumor heterogeneity and stem cell characteristics. In this regard, induction or inhibition of ferroptosis can hinder GBM growth; however, this is a one-sided argument. In the future, additional studies should be performed under the premise of fully understanding tumor heterogeneity and stem cell characteristics. Novel therapeutic strategies for “State Selective Lethality”, as proposed by James G et al. (Nicholson and Fine, 2021), could provide an opportunity to address this issue. This strategy could render drug discovery and precision therapy that target ferroptosis in GBM more feasible, by inducing or inhibiting ferroptosis in GBM cells to “trap” them in a state that increases their susceptibility to specific treatments.

### 5.2 The complex tumor immune microenvironment

Ferroptosis appears to play a dual role in the TME, causing changes in the function and viability of immune infiltrating cells. The resulting balance between immune evasion and immune elimination directly affects the efficacy of immunotherapy (Xu H. et al., 2021). Differential responses of antitumor T cells to ferroptosis (Drijvers et al., 2021; Ma et al., 2021), GPX4 protects Treg cell survival (Xu C. et al., 2021), differential resistance to ferroptosis of M1 and M2 macrophages and changes in their polarization state (Kapralov et al., 2020; Li and Rong, 2020; Wan et al., 2020), additionally including myeloid-derived suppressor cells (MDSCs) (Zhu et al., 2021), natural killer (NK) cells (Poznanski et al., 2021), dendritic cells (Han et al., 2021), and B cells (Muri et al., 2019) are withal linked to ferroptosis (Figure 3). These current findings demonstrate complex and variable ferroptosis-based crosstalk among individual cells in the TME. In GBM, tumor cells cooperate with peritumoral cells to promote angiogenesis, tumor proliferation, immunosuppression, and brain invasion via multiple communication modes, thereby forming an immune microenvironment conducive to aggressive tumor growth (Broekman et al., 2018). Interactions between immune cells and cancer cells drive GBM transition to a mesenchymal-like state (Hara et al., 2021). As previously mentioned, various immune cells in GBM are involved in the regulation of ferroptosis (Yee et al., 2020; Liu et al., 2022). Nonetheless, the relationship between various immune cells and ferroptosis in their TME remains unknown. Future research should investigate the complex TME cell-to-cell interactions based on ferroptosis and develop strategies to exploit the immunogenic potential of ferroptosis with respect to FINs or inhibitors. Besides, GBM type sensitive to combined



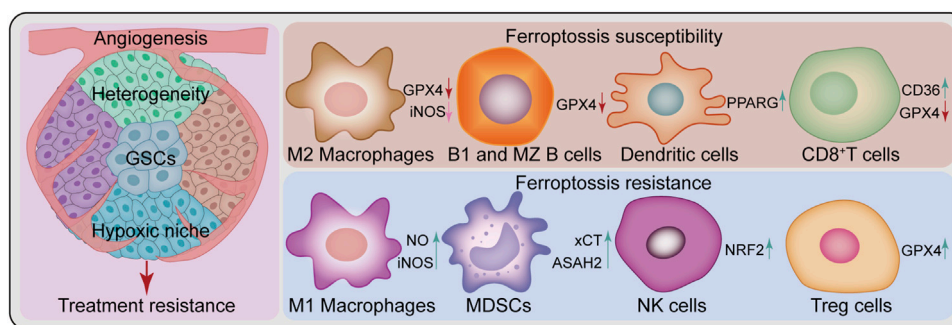


**FIGURE 3**

Challenges of ferroptosis in GBM treatment. Ferroptosis in glioblastoma treatment faces several challenges, such as heterogeneity, glioblastoma stem cells (GSCs), angiogenesis, hypoxic niche and a complex immune microenvironment composed of various immune cells. Peritumoral immune cells can be either sensitive or resistant to ferroptosis. Some cell types are sensitive to ferroptosis, such as M2 Macrophages, B1 and marginal zone (MZ) B cells, dendritic cells, and CD8<sup>+</sup>T cells, while others show resistance, such as M1 Macrophages, myeloid-derived suppressor cells (MDSCs), natural killer cells and Treg cells. ASAH2, N-Acylsphingosine Amidohydrolase 2; CD36, CD36 molecule; GPX4, glutathione peroxidase 4; iNOS, inducible nitric oxide (NO) synthase; NRF2, nuclear factor E2-related factor 2; PPARG, peroxisome proliferator-activated receptor gamma; xCT, SLC7A11, solute carrier family 7 member 11.

ferroptosis modulation and immunotherapy should be identified for effective individualized treatment.

of therapeutic necrosis remains a mystery. Therefore, additional studies are urgently required to address these unanswered questions.

### 5.3 Toxic side effects of ferroptosis

The toxic side effects of ferroptosis are another significant hurdle. Ferroptotic-induced neuronal death and the associated side effects of peripheral nervous system disease, neurodegeneration, and cognitive impairment have been described in a previous review study (Dahlmanns et al., 2021). In addition to chronic injury, acute toxic side effects caused by ferroptosis deserve high attention, including causing brain cytokine storm and necroinflammation, eventually resulting in irreversible brain edema, brain dysfunction, and death. Necrosis is one of the primary manifestations of poor prognosis in GBM and is closely related to thrombosis, hypoxia, and GSCs (Tehrani et al., 2008; Papale et al., 2020). Previous review has highlighted that the effect of treatment-induced necrosis on the CNS is a major clinical challenge in neuro-oncology (Winter et al., 2019). There is a strong relationship between ferroptosis and necroinflammation or neuroinflammation (Friedmann Angeli et al., 2014; Ingold et al., 2018). It should be noted that some subtypes of GBMs possess ferroptosis features. Necrosis in GBM was previously associated with neutrophil-triggered ferroptosis. Moreover, intratumoral GPX4 overexpression or ACSL4 depletion reduced tumor necrosis and invasiveness (Yee et al., 2020). Following the principle of fundamental importance, it is worth considering whether inhibiting ferroptosis prevents tumor necrosis from causing a cascade of irreversible toxic and side effects, thereby benefiting GBM patients. Whether certain methods (such as avoiding thrombosis and improving hypoxia, etc.) can effectively treat GBM by promoting ferroptosis while reducing the occurrence

### 6 Conclusions and perspectives

Accumulating evidence suggests that ferroptosis plays a pivotal role in tumor biology and therapy. Moreover, its role is complex and highly context-dependent. Over the past decade, several studies have investigated the role of ferroptosis in cancer. It is expected that further research will unravel deeper regulatory mechanisms of ferroptosis and provide ideas for developing ferroptosis-based strategies for the prevention, diagnosis, and treatment of cancer. Here, we comprehensively describe the role of ferroptosis in the treatment of GBM. The opportunities and challenges facing its clinical application. The data presented here lays the foundation for future basic and clinical research on ferroptosis in GBM. This review focused on ferroptosis peroxidation pathway in GBM therapy. Given the important role of iron homeostasis in ferroptosis and cancer therapy (Brown et al., 2019; Chen G. Q. et al., 2020), this pathway should be considered when targeting ferroptosis in GBM.

Other factors influence the role of ferroptosis. As ferroptosis is inherently compatible with synthetic lethal strategies (Kinowaki et al., 2021), their relationship should be fully considered in the development of anti-tumor drugs. Another factor affecting the effects of ferroptosis is epigenetic regulation. Some epigenetic modulators have been shown to exert anti-cancer effects by targeting ferroptosis. For example, inhibitors of class I histone deacetylases (HDACs) were found to promote ferroptosis in fibrosarcoma cells and prevent ferroptosis in neurons (Zille et al., 2019). A clinical trial (NCT03127514) revealed that HDAC inhibitor sodium phenylbutyrate combined with taurursodiol induced

amyotrophic lateral sclerosis in patients (Paganoni et al., 2020). This suggests that HDACs inhibitors may induce ferroptosis in GBM without causing neurotoxic side effects. However, this needs to be clarified experimentally in future studies.

Overall, ferroptosis-based therapy is an emerging clinical intervention with the potential to overcome resistance to currently used treatments such as immunotherapy. Considering that evidence supporting the clinical benefit of ferroptosis-based therapy has been generated from preclinical studies, there is a need for clinical trials to test efficacy and safety of such therapy in GBM patients. Future studies should incorporate organoid model systems, nanotechnology, single-cell sequencing, and spatial transcriptome sequencing to fully exploit the therapeutic potential of ferroptosis in GBM.

## Author contributions

KY, ZG, and JF conceived and designed the study. SZ, GH, and TC provided equal contributions to paper writing and illustration drawing. XL, YL, WW, and LW revised the manuscript. The final manuscript has been read and approved by all authors.

## Funding

This work was supported by the Finance science and technology project of Hainan province (Grant No.

ZDYF2022SHFZ088, ZDYF2019129), the National Nature Science Foundation of China (Grant No. 82060456), the Innovative Research Project of Hainan Graduate Students (Grant No. Qhyb 2021-58) and project supported by Hainan Province Clinical Medical Center.

## Acknowledgments

The authors sincerely thank Jeremiah Machuki (Home for Researchers editorial team) for the language polishment.

## Conflict of interest

The authors declare that the research was conducted in the absence of any commercial or financial relationships that could be construed as a potential conflict of interest.

## Publisher's note

All claims expressed in this article are solely those of the authors and do not necessarily represent those of their affiliated organizations, or those of the publisher, the editors and the reviewers. Any product that may be evaluated in this article, or claim that may be made by its manufacturer, is not guaranteed or endorsed by the publisher.

## References

- Anandhan, A., Dodson, M., Schmidlin, C. J., Liu, P., and Zhang, D. D. (2020). Breakdown of an ironclad defense system: The critical role of NRF2 in mediating ferroptosis. *Cell Chem. Biol.* 27 (4), 436–447. doi:10.1016/j.chembiol.2020.03.011
- Bai, Y., Meng, L., Han, L., Jia, Y., Zhao, Y., and Gao, H. (2019). Lipid storage and lipophagy regulates ferroptosis. *Biochem. Biophys. Res. Commun.* 508 (4), 997–1003. doi:10.1016/j.bbrc.2018.12.039
- Bao, C., Zhang, J., Xian, S. Y., and Chen, F. (2021). MicroRNA-670-3p suppresses ferroptosis of human glioblastoma cells through targeting ACSL4. *Free Radic. Res.* 55 (7), 853–864. doi:10.1080/10715762.2021.1962009
- Bersuker, K., Hendricks, J. M., Li, Z., Magtanong, L., Ford, B., Tang, P. H., et al. (2019). The CoQ oxidoreductase FSP1 acts parallel to GPX4 to inhibit ferroptosis. *Nature* 575 (7784), 688–692. doi:10.1038/s41586-019-1705-2
- Birsén, R., Larue, C., Decroocq, J., Johnson, N., Guiraud, N., Gotanegre, M., et al. (2022). APR-246 induces early cell death by ferroptosis in acute myeloid leukemia. *Haematologica* 107 (2), 403–416. doi:10.3324/haematol.2020.259531
- Blough, M. D., Beauchamp, D. C., Westgate, M. R., Kelly, J. J., and Cairncross, J. G. (2011). Effect of aberrant p53 function on temozolomide sensitivity of glioma cell lines and brain tumor initiating cells from glioblastoma. *J. Neurooncol* 102 (1), 1–7. doi:10.1007/s11060-010-0283-9
- Bonavia, R., Inda, M. M., Vandenberg, S., Cheng, S. Y., Nagane, M., Hadwiger, P., et al. (2012). EGFRvIII promotes glioma angiogenesis and growth through the NF- $\kappa$ B, interleukin-8 pathway. *Oncogene* 31 (36), 4054–4066. doi:10.1038/onc.2011.563
- Brennan, C. W., Verhaak, R. G., McKenna, A., Campos, B., Nushmeh, H., Salama, S. R., et al. (2013). The somatic genomic landscape of glioblastoma. *Cell* 155 (2), 462–477. doi:10.1016/j.cell.2013.09.034
- Broekman, M. L., Maas, S. L. N., Abels, E. R., Mempel, T. R., Krichevsky, A. M., and Breakefield, X. O. (2018). Multidimensional communication in the microenvirons of glioblastoma. *Nat. Rev. Neurol.* 14 (8), 482–495. doi:10.1038/s41582-018-0025-8
- Brown, C. W., Amante, J. J., Chhoy, P., Elaimy, A. L., Liu, H., Zhu, L. J., et al. (2019). Prominin2 drives ferroptosis resistance by stimulating iron export. *Dev. Cell* 51 (5), 575–586. e574. doi:10.1016/j.devcel.2019.10.007
- Buccarelli, M., Marconi, M., Pacioni, S., De Pascalis, I., D'alessandris, Q. G., Martini, M., et al. (2018). Inhibition of autophagy increases susceptibility of glioblastoma stem cells to temozolomide by igniting ferroptosis. *Cell Death Dis.* 9 (8), 841. doi:10.1038/s41419-018-0864-7
- Carruthers, R. D., Ahmed, S. U., Ramachandran, S., Strathdee, K., Kurian, K. M., Hedley, A., et al. (2018). Replication stress drives constitutive activation of the DNA damage response and radioresistance in glioblastoma stem-like cells. *Cancer Res.* 78 (17), 5060–5071. doi:10.1158/0008-5472.Can-18-0569
- Chen, D., Chu, B., Yang, X., Liu, Z., Jin, Y., Kon, N., et al. (2021a). iPLA2beta-mediated lipid detoxification controls p53-driven ferroptosis independent of GPX4. *Nat. Commun.* 12 (1), 3644. doi:10.1038/s41467-021-23902-6
- Chen, D., Fan, Z., Rauh, M., Buchfelder, M., Eyupoglu, I. Y., and Savaskan, N. (2017a). ATF4 promotes angiogenesis and neuronal cell death and confers ferroptosis in a xCT-dependent manner. *Oncogene* 36 (40), 5593–5608. doi:10.1038/onc.2017.146
- Chen, D., Rauh, M., Buchfelder, M., Eyupoglu, I., and Savaskan, N. J. O. (2017b). The oxido-metabolic driver ATF4 enhances temozolomide chemo-resistance in human gliomas. *oncotarget* 8 (31), 51164–51176. doi:10.18632/oncotarget.17737
- Chen, G. Q., Benthani, F. A., Wu, J., Liang, D., Bian, Z. X., and Jiang, X. (2020a). Artemisinin compounds sensitize cancer cells to ferroptosis by regulating iron homeostasis. *Cell Death Differ.* 27 (1), 242–254. doi:10.1038/s41418-019-0352-3

- Chen, L., Li, X., Liu, L., Yu, B., Xue, Y., and Liu, Y. (2015). Erastin sensitizes glioblastoma cells to temozolomide by restraining xCT and cystathionine-γ-lyase function. *Oncol. Rep.* 33 (3), 1465–1474. doi:10.3892/or.2015.3712
- Chen, P., Li, X., Zhang, R., Liu, S., Xiang, Y., Zhang, M., et al. (2020b). Combinative treatment of beta-elemene and cetuximab is sensitive to KRAS mutant colorectal cancer cells by inducing ferroptosis and inhibiting epithelial-mesenchymal transformation. *Theranostics* 10 (11), 5107–5119. doi:10.7150/thno.44705
- Chen, T. C., Chuang, J. Y., Ko, C. Y., Kao, T. J., Yang, P. Y., Yu, C. H., et al. (2020c). AR ubiquitination induced by the curcumin analog suppresses growth of temozolomide-resistant glioblastoma through disrupting GPX4-Mediated redox homeostasis. *Redox Biol.* 30, 101413. doi:10.1016/j.redox.2019.101413
- Chen, X., and Song, E. (2019). Turning foes to friends: Targeting cancer-associated fibroblasts. *Nat. Rev. Drug Discov.* 18 (2), 99–115. doi:10.1038/s41573-018-0004-1
- Chen, X., Yu, C., Kang, R., and Tang, D. (2020d). Iron metabolism in ferroptosis. *Front. Cell Dev. Biol.* 8, 590226. doi:10.3389/fcell.2020.590226
- Chen, Y., Li, N., Wang, H., Wang, N., Peng, H., Wang, J., et al. (2020e). Amentoflavone suppresses cell proliferation and induces cell death through triggering autophagy-dependent ferroptosis in human glioma. *Life Sci.* 247, 117425. doi:10.1016/j.lfs.2020.117425
- Chen, Y., Mi, Y., Zhang, X., Ma, Q., Song, Y., Zhang, L., et al. (2019). Dihydroartemisinin-induced unfolded protein response feedback attenuates ferroptosis via PERK/ATF4/HSPA5 pathway in glioma cells. *J. Exp. Clin. Cancer Res.* 38 (1), 402. doi:10.1186/s13046-019-1413-7
- Chen, Z., Zhao, S., He, G., Tang, J., Hao, W., Gao, W. Q., et al. (2021b). Prognosis and immunotherapy significances of a cancer-associated fibroblasts-related gene signature in gliomas. *Front. Cell Dev. Biol.* 9, 721897. doi:10.3389/fcell.2021.721897
- Cheng, J., Fan, Y. Q., Liu, B. H., Zhou, H., Wang, J. M., and Chen, Q. X. (2020). ACSL4 suppresses glioma cells proliferation via activating ferroptosis. *Oncol. Rep.* 43 (1), 147–158. doi:10.3892/or.2019.7419
- Cheng, L., Huang, Z., Zhou, W., Wu, Q., Donnelly, S., Liu, J. K., et al. (2013). Glioblastoma stem cells generate vascular pericytes to support vessel function and tumor growth. *Cell* 153 (1), 139–152. doi:10.1016/j.cell.2013.02.021
- Dahlmann, M., Yakubov, E., and Dahlmann, J. K. (2021). Genetic profiles of ferroptosis in malignant brain tumors and off-target effects of ferroptosis induction. *Front. Oncol.* 11, 783067. doi:10.3389/fonc.2021.783067
- Dai, E., Zhang, W., Cong, D., Kang, R., Wang, J., and Tang, D. (2020). AIFM2 blocks ferroptosis independent of ubiquinol metabolism. *Biochem. Biophys. Res. Commun.* 523 (4), 966–971. doi:10.1016/j.bbrc.2020.01.066
- Dixon, S. J., Lemberg, K. M., Lamprecht, M. R., Skouta, R., Zaitsev, E. M., Gleason, C. E., et al. (2012). Ferroptosis: An iron-dependent form of nonapoptotic cell death. *Cell* 149 (5), 1060–1072. doi:10.1016/j.cell.2012.03.042
- Dixon, S. J., Winter, G. E., Musavi, L. S., Lee, E. D., Snijder, B., Rebsamen, M., et al. (2015). Human haploid cell genetics reveals roles for lipid metabolism genes in nonapoptotic cell death. *ACS Chem. Biol.* 10 (7), 1604–1609. doi:10.1021/acschembio.5b00245
- Doll, S., Freitas, F. P., Shah, R., Aldrovandi, M., Da Silva, M. C., Ingold, I., et al. (2019). FSP1 is a glutathione-independent ferroptosis suppressor. *Nature* 575 (7784), 693–698. doi:10.1038/s41586-019-1707-0
- Doll, S., Proneth, B., Tyurina, Y. Y., Panzilius, E., Kobayashi, S., Ingold, I., et al. (2017). ACSL4 dictates ferroptosis sensitivity by shaping cellular lipid composition. *Nat. Chem. Biol.* 13 (1), 91–98. doi:10.1038/nchembio.2239
- Dong, J., Zhao, H., Wang, F., Jin, J., Ji, H., Yan, X., et al. (2022). Ferroptosis-related gene contributes to immunity, stemness and predicts prognosis in glioblastoma multiforme. *Front. Neurol.* 13, 829926. doi:10.3389/fneur.2022.829926
- Drijvers, J. M., Gillis, J. E., Muijls, T., Nguyen, T. H., Gaudiano, E. F., Harris, I. S., et al. (2021). Pharmacologic screening identifies metabolic vulnerabilities of CD8(+) T cells. *Cancer Immunol. Res.* 9 (2), 184–199. doi:10.1158/2326-6066.CIR-20-0384
- Efferth, T. (2017). From ancient herb to modern drug: Artemisia annua and artemisinin for cancer therapy. *Semin. Cancer Biol.* 46, 65–83. doi:10.1016/j.semcancer.2017.02.009
- Efimova, I., Catanzaro, E., Van Der Meeren, L., Turubanova, V. D., Hammad, H., Mishchenko, T. A., et al. (2020). Vaccination with early ferroptotic cancer cells induces efficient antitumor immunity. *J. Immunother. Cancer* 8 (2), e001369. doi:10.1136/jitc-2020-001369
- Fan, Z., Wirth, A. K., Chen, D., Wruck, C. J., Rauh, M., Buchfelder, M., et al. (2017). Nrf2-Keap1 pathway promotes cell proliferation and diminishes ferroptosis. *Oncogenesis* 6 (8), e371. doi:10.1038/oncsis.2017.65
- Feng, L., Zhao, K., Sun, L., Yin, X., Zhang, J., Liu, C., et al. (2021). SLC7A11 regulated by NRF2 modulates esophageal squamous cell carcinoma radiosensitivity by inhibiting ferroptosis. *J. Transl. Med.* 19 (1), 367. doi:10.1186/s12967-021-03042-7
- Friedmann Angeli, J. P., Schneider, M., Proneth, B., Tyurina, Y. Y., Tyurin, V. A., Hammond, V. J., et al. (2014). Inactivation of the ferroptosis regulator Gpx4 triggers acute renal failure in mice. *Nat. Cell Biol.* 16 (12), 1180–1191. doi:10.1038/ncb3064
- Fu, J., Li, T., Yang, Y., Jiang, L., Wang, W., Fu, L., et al. (2021). Activatable nanomedicine for overcoming hypoxia-induced resistance to chemotherapy and inhibiting tumor growth by inducing collaborative apoptosis and ferroptosis in solid tumors. *Biomaterials* 268, 120537. doi:10.1016/j.biomaterials.2020.120537
- Fu, W., Wang, W., Li, H., Jiao, Y., Huo, R., Yan, Z., et al. (2020). Single-cell atlas reveals complexity of the immunosuppressive microenvironment of initial and recurrent glioblastoma. *Front. Immunol.* 11, 835. doi:10.3389/fimmu.2020.00835
- Galluzzi, L., Vitale, I., Aaronson, S. A., Abrams, J. M., Adam, D., Agostinis, P., et al. (2018). Molecular mechanisms of cell death: Recommendations of the nomenclature committee on cell death 2018. *Cell Death Differ.* 25 (3), 486–541. doi:10.1038/s41418-017-0012-4
- Gao, M., Monian, P., Quadri, N., Ramasamy, R., and Jiang, X. (2015). Glutaminolysis and transferrin regulate ferroptosis. *Mol. Cell* 59 (2), 298–308. doi:10.1016/j.molcel.2015.06.011
- Gao, R., Kalathur, R. K. R., Coto-Llerena, M., Ercan, C., Buechel, D., Shuang, S., et al. (2021). YAP/TAZ and ATF4 drive resistance to Sorafenib in hepatocellular carcinoma by preventing ferroptosis. *EMBO Mol. Med.* 13 (12), e14351. doi:10.15252/emmm.202114351
- Garcia-Bermudez, J., Baudrier, L., Bayraktar, E. C., Shen, Y., La, K., Guarecuco, R., et al. (2019). Squalene accumulation in cholesterol auxotrophic lymphomas prevents oxidative cell death. *Nature* 567 (7746), 118–122. doi:10.1038/s41586-019-0945-5
- Ge, C., Zhang, S., Mu, H., Zheng, S., Tan, Z., Huang, X., et al. (2022). Emerging mechanisms and disease implications of ferroptosis: Potential applications of natural products. *Front. Cell Dev. Biol.* 9, 774957. doi:10.3389/fcell.2021.774957
- Gu, Z., Liu, T., Liu, C., Yang, Y., Tang, J., Song, H., et al. (2021). Ferroptosis-strengthened metabolic and inflammatory regulation of tumor-associated macrophages provokes potent tumoricidal activities. *Nano Lett.* 21 (15), 6471–6479. doi:10.1021/acs.nanolett.1c01401
- Guo, D., Hildebrandt, I. J., Prins, R. M., Soto, H., Mazzotta, M. M., Dang, J., et al. (2009a). The AMPK agonist AICAR inhibits the growth of EGFRvIII-expressing glioblastomas by inhibiting lipogenesis. *Proc. Natl. Acad. Sci. U. S. A.* 106 (31), 12932–12937. doi:10.1073/pnas.0906606106
- Guo, D., Prins, R. M., Dang, J., Kuga, D., Iwanami, A., Soto, H., et al. (2009b). EGFR signaling through an Akt-SREBP-1-dependent, rapamycin-resistant pathway sensitizes glioblastomas to antilipogenic therapy. *Sci. Signal* 2 (101), ra82. doi:10.1126/scisignal.2000446
- Guo, D., Reinitz, F., Youssef, M., Hong, C., Nathanson, D., Akhavan, D., et al. (2011). An LXR agonist promotes glioblastoma cell death through inhibition of an EGFR/AKT/SREBP-1/LDLR-dependent pathway. *Cancer Discov.* 1 (5), 442–456. doi:10.1158/2159-8290.CD-11-0102
- Han, L., Bai, L., Qu, C., Dai, E., Liu, J., Kang, R., et al. (2021). PPARG-mediated ferroptosis in dendritic cells limits antitumor immunity. *Biochem. Biophys. Res. Commun.* 576, 33–39. doi:10.1016/j.bbrc.2021.08.082
- Hangauer, M. J., Viswanathan, V. S., Ryan, M. J., Bole, D., Eaton, J. K., Matov, A., et al. (2017). Drug-tolerant persister cancer cells are vulnerable to GPX4 inhibition. *Nature* 551 (7679), 247–250. doi:10.1038/nature24297
- Hara, T., Chanoch-Myers, R., Mathewson, N. D., Myskiw, C., Atta, L., Bussema, L., et al. (2021). Interactions between cancer cells and immune cells drive transitions to mesenchymal-like states in glioblastoma. *Cancer Cell* 39 (6), 779–792. e711. doi:10.1016/j.ccell.2021.05.002
- Hodges, T. R., Ott, M., Xiu, J., Gatalica, Z., Swensen, J., Zhou, S., et al. (2017). Mutational burden, immune checkpoint expression, and mismatch repair in glioma: Implications for immune checkpoint immunotherapy. *Neuro Oncol.* 19 (8), 1047–1057. doi:10.1093/neuonc/now026
- Hou, W., Xie, Y., Song, X., Sun, X., Lotze, M. T., Zeh, H. J., 3rd, et al. (2016). Autophagy promotes ferroptosis by degradation of ferritin. *Autophagy* 12 (8), 1425–1428. doi:10.1080/15548627.2016.1187366
- Hu, C., Leche, C. A., Kiyatkin, A., Yu, Z., Staybrook, S. E., Ferguson, K. M., et al. (2022a). Glioblastoma mutations alter EGFR dimer structure to prevent ligand bias. *Nature* 602 (7897), 518–522. doi:10.1038/s41586-021-04393-3
- Hu, S., Ma, J., Su, C., Chen, Y., Shu, Y., Qi, Z., et al. (2021). Engineered exosome-like nanovesicles suppress tumor growth by reprogramming tumor microenvironment and promoting tumor ferroptosis. *Acta Biomater.* 135, 567–581. doi:10.1016/j.actbio.2021.09.003
- Hu, Y., Guo, N., Yang, T., Yan, J., Wang, W., and Li, X. (2022b). The potential mechanisms by which artemisinin and its derivatives induce ferroptosis in the

treatment of cancer. *Oxid. Med. Cell Longev.* 2022, 1458143. doi:10.1155/2022/1458143

Huang, R., Dong, R., Wang, N., He, Y., Zhu, P., Wang, C., et al. (2021). Adaptive changes allow targeting of ferroptosis for glioma treatment. *Cell Mol. Neurobiol.* doi:10.1007/s10571-021-01092-5

Hubert, C. G., Rivera, M., Spangler, L. C., Wu, Q., Mack, S. C., Prager, B. C., et al. (2016). A three-dimensional organoid culture system derived from human glioblastomas recapitulates the hypoxic gradients and cancer stem cell heterogeneity of tumors found *in vivo*. *Cancer Res.* 76 (8), 2465–2477. doi:10.1158/0008-5472.Can-15-2402

Ingold, I., Berndt, C., Schmitt, S., Doll, S., Poschmann, G., Buday, K., et al. (2018). Selenium utilization by GPX4 is required to prevent hydroperoxide-induced ferroptosis. *Cell* 172 (3), 409–422. e421. doi:10.1016/j.cell.2017.11.048

Ishida, T., Takahashi, T., Kurokawa, Y., Nishida, T., Hirota, S., Serada, S., et al. (2021). Targeted therapy for drug-tolerant persister cells after imatinib treatment for gastrointestinal stromal tumours. *Br. J. Cancer* 125 (11), 1511–1522. doi:10.1038/s41416-021-01566-9

Jacob, F., Salinas, R. D., Zhang, D. Y., Nguyen, P. T. T., Schnoll, J. G., Wong, S. Z. H., et al. (2020). A patient-derived glioblastoma organoid model and biobank recapitulates inter- and intra-tumoral heterogeneity. *Cell* 180 (1), 188–204. e122. doi:10.1016/j.cell.2019.11.036

Jia, M., Qin, D., Zhao, C., Chai, L., Yu, Z., Wang, W., et al. (2020). Redox homeostasis maintained by GPX4 facilitates STING activation. *Nat. Immunol.* 21 (7), 727–735. doi:10.1038/s41590-020-0699-0

Jiang, L., Kon, N., Li, T., Wang, S. J., Su, T., Hibshoosh, H., et al. (2015). Ferroptosis as a p53-mediated activity during tumour suppression. *Nature* 520 (7545), 57–62. doi:10.1038/nature14344

Jiang, N., Xie, B., Xiao, W., Fan, M., Xu, S., Duan, Y., et al. (2022). Fatty acid oxidation fuels glioblastoma radioresistance with CD47-mediated immune evasion. *Nat. Commun.* 13 (1), 1511. doi:10.1038/s41467-022-29137-3

Kadioglu, O., Saeed, M. E. M., Mahmoud, N., Azawi, S., Mrasek, K., Liehr, T., et al. (2021). Identification of novel drug resistance mechanisms by genomic and transcriptomic profiling of glioblastoma cells with mutation-activated EGFR. *Life Sci.* 284, 119601. doi:10.1016/j.lfs.2021.119601

Kapralov, A. A., Yang, Q., Dar, H. H., Tyurina, Y. Y., Anthonymuthu, T. S., Kim, R., et al. (2020). Redox lipid reprogramming commands susceptibility of macrophages and microglia to ferroptotic death. *Nat. Chem. Biol.* 16 (3), 278–290. doi:10.1038/s41589-019-0462-8

Karpel-Massler, G., Nguyen, T. T. T., Shang, E., and Siegelin, M. D. (2019). Novel IDH1-targeted glioma therapies. *CNS Drugs* 33 (12), 1155–1166. doi:10.1007/s40263-019-00684-6

Kinowaki, Y., Taguchi, T., Onishi, I., Kirimura, S., Kitagawa, M., and Yamamoto, K. (2021). Overview of ferroptosis and synthetic lethality strategies. *Int. J. Mol. Sci.* 22 (17), 9271. doi:10.3390/ijms22179271

Klochov, S. G., Neganova, M. E., Nikolenko, V. N., Chen, K., Somasundaram, S. G., Kirkland, C. E., et al. (2021). Implications of nanotechnology for the treatment of cancer: Recent advances. *Semin. Cancer Biol.* 69, 190–199. doi:10.1016/j.semcancer.2019.08.028

Koike, N., Kota, R., Naito, Y., Hayakawa, N., Matsuura, T., Hishiki, T., et al. (2020). 2-Nitroimidazoles induce mitochondrial stress and ferroptosis in glioma stem cells residing in a hypoxic niche. *Commun. Biol.* 3 (1), 450. doi:10.1038/s42003-020-01165-z

Koppula, P., Zhuang, L., and Gan, B. (2021). Cystine transporter slc7a11/xCT in cancer: Ferroptosis, nutrient dependency, and cancer therapy. *Protein Cell* 12 (8), 599–620. doi:10.1007/s13238-020-00789-5

Kraft, V. A. N., Bezjian, C. T., Pfeiffer, S., Ringelstetter, L., Muller, C., Zandkarimi, F., et al. (2020). GTP cyclohydrolase 1/tetrahydrobiopterin counteract ferroptosis through lipid remodeling. *ACS Cent. Sci.* 6 (1), 41–53. doi:10.1021/acscentsci.9b01063

Lang, X., Green, M. D., Wang, W., Yu, J., Choi, J. E., Jiang, L., et al. (2019). Radiotherapy and immunotherapy promote tumoral lipid oxidation and ferroptosis via synergistic repression of SLC7A11. *Cancer Discov.* 9 (12), 1673–1685. doi:10.1158/2159-8290.CD-19-0338

Lee, J. K., Wang, J., Sa, J. K., Ladewig, E., Lee, H. O., Lee, I. H., et al. (2017). Spatiotemporal genomic architecture informs precision oncology in glioblastoma. *Nat. Genet.* 49 (4), 594–599. doi:10.1038/ng.3806

Lei, G., Zhang, Y., Hong, T., Zhang, X., Liu, X., Mao, C., et al. (2021). Ferroptosis as a mechanism to mediate p53 function in tumor radiosensitivity. *Oncogene* 40 (20), 3533–3547. doi:10.1038/s41388-021-01790-w

Lei, G., Zhang, Y., Koppula, P., Liu, X., Zhang, J., Lin, S. H., et al. (2020). The role of ferroptosis in ionizing radiation-induced cell death and tumor suppression. *Cell Res.* 30 (2), 146–162. doi:10.1038/s41422-019-0263-3

Li, S., He, Y., Chen, K., Sun, J., Zhang, L., He, Y., et al. (2021). RSL3 drives ferroptosis through NF-kappaB pathway activation and GPX4 depletion in glioblastoma. *Oxid. Med. Cell Longev.* 2021, 2915019. doi:10.1155/2021/2915019

Li, Z., and Rong, L. (2020). Cascade reaction-mediated efficient ferroptosis synergizes with immunomodulation for high-performance cancer therapy. *Biomater. Sci.* 8 (22), 6272–6285. doi:10.1039/d0bm01168a

Liu, T., Zhu, C., Chen, X., Guan, G., Zou, C., Shen, S., et al. (2022). Ferroptosis, as the most enriched programmed cell death process in glioma, induces immunosuppression and immunotherapy resistance. *Neuro Oncol.* 24 (7), 1113–1125. doi:10.1093/neuonc/noac033

Louis, D. N., Perry, A., Wesseling, P., Brat, D. J., Cree, I. A., Figarella-Branger, D., et al. (2021). The 2021 WHO classification of tumors of the central nervous system: A summary. *Neuro Oncol.* 23 (8), 1231–1251. doi:10.1093/neuonc/noab106

Lu, Y., Chan, Y. T., Tan, H. Y., Zhang, C., Guo, W., Xu, Y., et al. (2022). Epigenetic regulation of ferroptosis via ETS1/miR-23a-3p/ACSL4 axis mediates sorafenib resistance in human hepatocellular carcinoma. *J. Exp. Clin. Cancer Res.* 41 (1), 3. doi:10.1186/s13046-021-02208-x

Ma, X., Xiao, L., Liu, L., Ye, L., Su, P., Bi, E., et al. (2021). CD36-mediated ferroptosis dampens intratumoral CD8+ T cell effector function and impairs their antitumor ability. *Cell Metab.* 33 (5), 1001e1005–1012. doi:10.1016/j.cmet.2021.02.015

Magtanong, L., Ko, P. J., To, M., Cao, J. Y., Forcina, G. C., Tarangelo, A., et al. (2019). Exogenous monounsaturated fatty acids promote a ferroptosis-resistant cell state. *Cell Chem. Biol.* 26 (3), 420–432. e429. doi:10.1016/j.chembiol.2018.11.016

Mao, C., Liu, X., Zhang, Y., Lei, G., Yan, Y., Lee, H., et al. (2021). DHODH-mediated ferroptosis defence is a targetable vulnerability in cancer. *Nature* 593 (7860), 586–590. doi:10.1038/s41586-021-03539-7

Marampon, F., Gravina, G. L., Zani, B. M., Popov, V. M., Fratticci, A., Cerasani, M., et al. (2014). Hypoxia sustains glioblastoma radioresistance through ERKs/DNA-PKcs/HIF-1α functional interplay. *Int. J. Oncol.* 44 (6), 2121–2131. doi:10.3892/ijo.2014.2358

Matsuoka, S., Ballif, B. A., Smogorzewska, A., McDonald, E. R., 3rd, Hurov, K. E., Luo, J., et al. (2007). ATM and ATR substrate analysis reveals extensive protein networks responsive to DNA damage. *Science* 316 (5828), 1160–1166. doi:10.1126/science.1140321

Matsushita, M., Freigang, S., Schneider, C., Conrad, M., Bornkamm, G. W., and Kopf, M. (2015). T cell lipid peroxidation induces ferroptosis and prevents immunity to infection. *J. Exp. Med.* 212 (4), 555–568. doi:10.1084/jem.20140857

Mcbrayer, S. K., Mayers, J. R., Dinatale, G. J., Shi, D. D., Khanal, J., Chakraborty, A. A., et al. (2018). Transaminase inhibition by 2-hydroxyglutarate impairs glutamate biosynthesis and redox homeostasis in glioma. *Cell* 175 (1), 101–116. e125. doi:10.1016/j.cell.2018.08.038

Mellinghoff, I. K., Ellingson, B. M., Touat, M., Maher, E., De La Fuente, M. I., Holdhoff, M., et al. (2020). Ivosidenib in isocitrate dehydrogenase 1-mutated advanced glioma. *J. Clin. Oncol.* 38 (29), 3398–3406. doi:10.1200/jco.19.03327

Mender, I., Zhang, A., Ren, Z., Han, C., Deng, Y., Siteni, S., et al. (2020). Telomere stress potentiates STING-dependent anti-tumor immunity. *Cancer Cell* 38 (3), 400–411. e406. doi:10.1016/j.ccell.2020.05.020

Micallef, J., Taccone, M., Mukherjee, J., Croul, S., Busby, J., Moran, M. F., et al. (2009). Epidermal growth factor receptor variant III-induced glioma invasion is mediated through myristoylated alanine-rich protein kinase C substrate overexpression. *Cancer Res.* 69 (19), 7548–7556. doi:10.1158/0008-5472.Can-08-4783

Miller, K. D., Ostrom, Q. T., Kruchko, C., Patil, N., Tihan, T., Cioffi, G., et al. (2021). Brain and other central nervous system tumor statistics, 2021. *CA Cancer J. Clin.* 71 (5), 381–406. doi:10.3322/caac.21693

Muri, J., Thut, H., Bornkamm, G. W., and Kopf, M. (2019). B1 and marginal zone B cells but not follicular B2 cells require Gpx4 to prevent lipid peroxidation and ferroptosis. *Cell Rep.* 29 (9), 2731e2734–2744. doi:10.1016/j.celrep.2019.10.070

Nagpal, A., Redvers, R. P., Ling, X., Ayton, S., Fuentes, M., Tavancheh, E., et al. (2019). Neoadjuvant neratinib promotes ferroptosis and inhibits brain metastasis in a novel syngeneic model of spontaneous HER2(+ve) breast cancer metastasis. *Breast Cancer Res.* 21 (1), 94. doi:10.1186/s13058-019-1177-1

Nicholson, J. G., and Fine, H. A. (2021). Diffuse glioma heterogeneity and its therapeutic implications. *Cancer Discov.* 11 (3), 575–590. doi:10.1158/2159-8290.CD-20-1474

Ntambi, J. M. (2004). Regulation of stearoyl-CoA desaturases and role in metabolism. *Prog. Lipid Res.* 43 (2), 91–104. doi:10.1016/s0163-7827(03)00039-0

Ohkuri, T., Ghosh, A., Kosaka, A., Zhu, J., Ikeura, M., David, M., et al. (2014). STING contributes to antiglioma immunity via triggering type I IFN signals in the tumor microenvironment. *Cancer Immunol. Res.* 2 (12), 1199–1208. doi:10.1158/2326-6066.CIR-14-0099



- Ooko, E., Saeed, M. E., Kadioglu, O., Sarvi, S., Colak, M., Elmasaoudi, K., et al. (2015). Artemisinin derivatives induce iron-dependent cell death (ferroptosis) in tumor cells. *Phytomedicine* 22 (11), 1045–1054. doi:10.1016/j.phymed.2015.08.002
- Ostrom, Q. T., Gittleman, H., Xu, J., Kromer, C., Wolinsky, Y., Kruchko, C., et al. (2016). CBTRUS statistical report: Primary brain and other central nervous system tumors diagnosed in the United States in 2009–2013. *Neuro Oncol.* 18, v1–v75. (suppl\_5). doi:10.1093/neuonc/now207
- Osuka, S., Zhu, D., Zhang, Z., Li, C., Stackhouse, C. T., Sampetean, O., et al. (2021). N-cadherin upregulation mediates adaptive radioresistance in glioblastoma. *J. Clin. Invest.* 131 (6), e136098. doi:10.1172/jci136098
- Paganoni, S., Macklin, E. A., Hendrix, S., Berry, J. D., Elliott, M. A., Maser, S., et al. (2020). Trial of sodium phenylbutyrate-taurursodiol for amyotrophic lateral sclerosis. *N. Engl. J. Med.* 383 (10), 919–930. doi:10.1056/NEJMoa1916945
- Papale, M., Buccarelli, M., Mollinari, C., Russo, M. A., Pallini, R., Ricci-Vitiani, L., et al. (2020). Hypoxia, inflammation and necrosis as determinants of glioblastoma cancer stem cells progression. *Int. J. Mol. Sci.* 21 (8), 2660. doi:10.3390/ijms21082660
- Park, M. W., Cha, H. W., Kim, J., Kim, J. H., Yang, H., Yoon, S., et al. (2021). NOX4 promotes ferroptosis of astrocytes by oxidative stress-induced lipid peroxidation via the impairment of mitochondrial metabolism in Alzheimer's diseases. *Redox Biol.* 41, 101947. doi:10.1016/j.redox.2021.101947
- Patel, A. P., Tirosh, I., Trombetta, J. J., Shalek, A. K., Gillespie, S. M., Wakimoto, H., et al. (2014). Single-cell RNA-seq highlights intratumoral heterogeneity in primary glioblastoma. *Science* 344 (6190), 1396–1401. doi:10.1126/science.1254257
- Poursaitidis, I., Wang, X., Crighton, T., Labuschagne, C., Mason, D., Cramer, S. L., et al. (2020). Oncogene-selective sensitivity to synchronous cell death following modulation of the amino acid nutrient cystine. *Cell Rep.* 18 (11), 2547–2556. doi:10.1016/j.celrep.2017.02.054
- Poznanski, S. M., Singh, K., Ritchie, T. M., Aguiar, J. A., Fan, I. Y., Portillo, A. L., et al. (2021). Metabolic flexibility determines human NK cell functional fate in the tumor microenvironment. *Cell Metab.* 33 (6), 1205–1220. doi:10.1016/j.cmet.2021.03.023
- Robert, S. M., Buckingham, S. C., Campbell, S. L., Robel, S., Holt, K. T., Ogunrinu-Babarinde, T., et al. (2015). SLC7A11 expression is associated with seizures and predicts poor survival in patients with malignant glioma. *Sci. Transl. Med.* 7 (289), 289ra286. doi:10.1126/scitranslmed.aaa8103
- Sato, M., Kusumi, R., Hamashima, S., Kobayashi, S., Sasaki, S., Komiya, Y., et al. (2018). The ferroptosis inducer erastin irreversibly inhibits system xc- and synergizes with cisplatin to increase cisplatin's cytotoxicity in cancer cells. *Sci. Rep.* 8 (1), 968. doi:10.1038/s41598-018-19213-4
- Sehm, T., Fan, Z., Ghoochani, A., Rauh, M., Engelhorn, T., Minakaki, G., et al. (2016). Sulfasalazine impacts on ferroptotic cell death and alleviates the tumor microenvironment and glioma-induced brain edema. *Oncotarget* 7 (24), 36021–36033. doi:10.18632/oncotarget.8651
- Shi, Y., Ping, Y. F., Zhou, W., He, Z. C., Chen, C., Bian, B. S., et al. (2017). Tumour-associated macrophages secrete pleiotrophin to promote PTPRZ1 signalling in glioblastoma stem cells for tumour growth. *Nat. Commun.* 8, 15080. doi:10.1038/ncomms15080
- Sia, J., Szmyd, R., Hau, E., and Gee, H. E. (2020). Molecular mechanisms of radiation-induced cancer cell death: A primer. *Front. Cell Dev. Biol.* 8, 41. doi:10.3389/fcell.2020.00041
- Sleire, L., Skeie, B. S., Netland, I. A., Forde, H. E., Dodoo, E., Selheim, F., et al. (2015). Drug repurposing: Sulfasalazine sensitizes gliomas to gamma knife radiosurgery by blocking cystine uptake through system xc-, leading to glutathione depletion. *Oncogene* 34 (49), 5951–5959. doi:10.1038/nc.2015.60
- Song, J., Liu, T., Yin, Y., Zhao, W., Lin, Z., Yin, Y., et al. (2021). The deubiquitinase OTUD1 enhances iron transport and potentiates host antitumor immunity. *EMBO Rep.* 22 (2), e51162. doi:10.15252/embr.202051162
- Song, X., Wang, X., Liu, Z., and Yu, Z. (2020). Role of GPX4-mediated ferroptosis in the sensitivity of triple negative breast cancer cells to gefitinib. *Front. Oncol.* 10, 597434. doi:10.3389/fonc.2020.597434
- Sottile, R., Federico, G., Garofalo, C., Talerico, R., Faniello, M. C., Quaresima, B., et al. (2019). Iron and ferritin modulate MHC class I expression and NK cell recognition. *Front. Immunol.* 10, 224. doi:10.3389/fimmu.2019.00224
- Sun, W. Y., Tyurin, V. A., Mikulska-Ruminska, K., Shrivastava, I. H., Anthony-muthu, T. S., Zhai, Y. J., et al. (2021). Phospholipase iPLA2 $\beta$  averts ferroptosis by eliminating a redox lipid death signal. *Nat. Chem. Biol.* 17 (4), 465–476. doi:10.1038/s41589-020-00734-x
- Takenaka, M. C., Gabrieli, G., Rothhammer, V., Mascaroni, I. D., Wheeler, M. A., Chao, C. C., et al. (2019). Control of tumor-associated macrophages and T cells in glioblastoma via AHR and CD39. *Nat. Neurosci.* 22 (5), 729–740. doi:10.1038/s41593-019-0370-y
- Tang, R., Xu, J., Zhang, B., Liu, J., Liang, C., Hua, J., et al. (2020). Ferroptosis, necroptosis, and pyroptosis in anticancer immunity. *J. Hematol. Oncol.* 13 (1), 110. doi:10.1186/s13045-020-00946-7
- Tang, W., Fan, W., Lau, J., Deng, L., Shen, Z., and Chen, X. (2019). Emerging blood-brain-barrier-crossing nanotechnology for brain cancer theranostics. *Chem. Soc. Rev.* 48 (11), 2967–3014. doi:10.1039/c8cs00805a
- Tarangelo, A., Magtanong, L., Bieging-Rolett, K. T., Li, Y., Ye, J., Attardi, L. D., et al. (2018). p53 suppresses metabolic stress-induced ferroptosis in cancer cells. *Cell Rep.* 22 (3), 569–575. doi:10.1016/j.celrep.2017.12.077
- Tehrani, M., Friedman, T. M., Olson, J. J., and Brat, D. J. (2008). Intravascular thrombosis in central nervous system malignancies: A potential role in astrocytoma progression to glioblastoma. *Brain Pathol.* 18 (2), 164–171. doi:10.1111/j.1750-3639.2007.00108.x
- Tejera, D., Kushnirsky, M., Gultekin, S. H., Lu, M., Steelman, L., and De La Fuente, M. I. (2020). Ivosidenib, an IDH1 inhibitor, in a patient with recurrent, IDH1-mutant glioblastoma: A case report from a phase I study. *CNS Oncol.* 9 (3), Cns62. doi:10.2217/cns-2020-0014
- Tian, Y., Liu, H., Zhang, C., Liu, W., Wu, T., Yang, X., et al. (2022). Comprehensive analyses of ferroptosis-related alterations and their prognostic significance in glioblastoma. *Front. Mol. Biosci.* 9, 904098. doi:10.3389/fmolb.2022.904098
- Tosi, F., Sartori, F., Guarini, P., Olivieri, O., and Martinelli, N. (2014). Delta-5 and delta-6 desaturases: Crucial enzymes in polyunsaturated fatty acid-related pathways with pleiotropic influences in health and disease. *Adv. Exp. Med. Biol.* 824, 61–81. doi:10.1007/978-3-319-07320-0\_7
- Tuo, Q. Z., Liu, Y., Xiang, Z., Yan, H. F., Zou, T., Shu, Y., et al. (2022). Thrombin induces ACSL4-dependent ferroptosis during cerebral ischemia/reperfusion. *Signal Transduct. Target Ther.* 7 (1), 59. doi:10.1038/s41392-022-00917-z
- Turubanova, V. D., Balalaeva, I. V., Mishchenko, T. A., Catanzaro, E., Alzeibak, R., Peskova, N. N., et al. (2019). Immunogenic cell death induced by a new photodynamic therapy based on photosens and photodithazine. *J. Immunother. Cancer* 7 (1), 350. doi:10.1186/s40425-019-0826-3
- Van Der Leij, F. R., Kram, A. M., Bartelds, B., Roelofsen, H., Smid, G. B., Takens, J., et al. (1999). Cytological evidence that the C-terminus of carnitine palmitoyltransferase I is on the cytosolic face of the mitochondrial outer membrane. *Biochem. J.* 341 (3), 777–784. doi:10.1042/0264-6021:3410777
- Wan, C., Sun, Y., Tian, Y., Lu, L., Dai, X., Meng, J., et al. (2020). Irradiated tumor cell-derived microparticles mediate tumor eradication via cell killing and immune reprogramming. *Sci. Adv.* 6 (13), eaay9789. doi:10.1126/sciadv.aay9789
- Wang, H., Cheng, Y., Mao, C., Liu, S., Xiao, D., Huang, J., et al. (2021). Emerging mechanisms and targeted therapy of ferroptosis in cancer. *Mol. Ther.* 29 (7), 2185–2208. doi:10.1016/j.ymthe.2021.03.022
- Wang, T. X., Liang, J. Y., Zhang, C., Xiong, Y., Guan, K. L., and Yuan, H. X. (2019a). The oncometabolite 2-hydroxyglutarate produced by mutant IDH1 sensitizes cells to ferroptosis. *Cell Death Dis.* 10 (10), 755. doi:10.1038/s41419-019-1984-4
- Wang, W., Green, M., Choi, J. E., Gijon, M., Kennedy, P. D., Johnson, J. K., et al. (2019b). CD8(+) T cells regulate tumour ferroptosis during cancer immunotherapy. *Nature* 569 (7755), 270–274. doi:10.1038/s41586-019-1170-y
- Wang, Y., Yu, W., Li, S., Guo, D., He, J., and Wang, Y. (2022). Acetyl-CoA carboxylases and diseases. *Front. Oncol.* 12, 836058. doi:10.3389/fonc.2022.836058
- Wang, Z., Ding, Y., Wang, X., Lu, S., Wang, C., He, C., et al. (2018). Pseudolactic acid B triggers ferroptosis in glioma cells via activation of Nox4 and inhibition of xCT. *Cancer Lett.* 428, 21–33. doi:10.1016/j.canlet.2018.04.021
- Wei, Q., Singh, O., Ekinici, C., Gill, J., Li, M., Mamatjan, Y., et al. (2021). TNF $\alpha$  secreted by glioma associated macrophages promotes endothelial activation and resistance against anti-angiogenic therapy. *Acta Neuropathol. Commun.* 9 (1), 67. doi:10.1186/s40478-021-01163-0
- Wei, X., Schultz, K., Bazilevsky, G. A., Vogt, A., and Marmorstein, R. (2020). Molecular basis for acetyl-CoA production by ATP-citrate lyase. *Nat. Struct. Mol. Biol.* 27 (1), 33–41. doi:10.1038/s41594-019-0351-6
- Weller, M., Butowski, N., Tran, D. D., Recht, L. D., Lim, M., Hirte, H., et al. (2017). Rindopepimut with temozolomide for patients with newly diagnosed, EGFRvIII-expressing glioblastoma (ACT IV): A randomised, double-blind, international phase 3 trial. *Lancet Oncol.* 18 (10), 1373–1385. doi:10.1016/s1470-2045(17)30517-x
- Wen, Q., Liu, J., Kang, R., Zhou, B., and Tang, D. (2019). The release and activity of HMGB1 in ferroptosis. *Biochem. Biophys. Res. Commun.* 510 (2), 278–283. doi:10.1016/j.bbrc.2019.01.090
- Winter, S. F., Loebel, F., Loeffler, J., Batchelor, T. T., Martinez-Lage, M., Vajkoczy, P., et al. (2019). Treatment-induced brain tissue necrosis: A clinical challenge in neuro-oncology. *Neuro Oncol.* 21 (9), 1118–1130. doi:10.1093/neuonc/noz048

- Woroniecka, K., Chongsathidkiet, P., Rhodin, K., Kemeny, H., Dechant, C., Farber, S. H., et al. (2018). T-cell exhaustion signatures vary with tumor type and are severe in glioblastoma. *Clin. Cancer Res.* 24 (17), 4175–4186. doi:10.1158/1078-0432.Ccr-17-1846
- Wu, W., Wu, Y., Mayer, K., Von Rosenstiel, C., Schecker, J., Baur, S., et al. (2020). Lipid peroxidation plays an important role in chemotherapeutic effects of temozolomide and the development of therapy resistance in human glioblastoma. *Transl. Oncol.* 13 (3), 100748. doi:10.1016/j.tranon.2020.100748
- Xiao, D., Zhou, Y., Wang, X., Zhao, H., Nie, C., and Jiang, X. (2021). A ferroptosis-related prognostic risk score model to predict clinical significance and immunogenic characteristics in glioblastoma multiforme. *Oxid. Med. Cell Longev.* 2021, 9107857. doi:10.1155/2021/9107857
- Xie, Y., He, L., Lugano, R., Zhang, Y., Cao, H., He, Q., et al. (2021). Key molecular alterations in endothelial cells in human glioblastoma uncovered through single-cell RNA sequencing. *JCI Insight* 6 (15), e150861. doi:10.1172/jci.insight.150861
- Xu, C., Sun, S., Johnson, T., Qi, R., Zhang, S., Zhang, J., et al. (2021a). The glutathione peroxidase Gpx4 prevents lipid peroxidation and ferroptosis to sustain Treg cell activation and suppression of antitumor immunity. *Cell Rep.* 35 (11), 109235. doi:10.1016/j.celrep.2021.109235
- Xu, H., Ye, D., Ren, M., Zhang, H., and Bi, F. (2021b). Ferroptosis in the tumor microenvironment: Perspectives for immunotherapy. *Trends Mol. Med.* 27 (9), 856–867. doi:10.1016/j.molmed.2021.06.014
- Yamazaki, T., Hannani, D., Poirier-Colame, V., Ladoire, S., Locher, C., Sistigu, A., et al. (2014). Defective immunogenic cell death of HMGB1-deficient tumors: Compensatory therapy with TLR4 agonists. *Cell Death Differ.* 21 (1), 69–78. doi:10.1038/cdd.2013.72
- Yang, H., Zhao, L., Gao, Y., Yao, F., Marti, T. M., Schmid, R. A., et al. (2020). Pharmacotranscriptomic analysis reveals novel drugs and gene networks regulating ferroptosis in cancer. *Cancers (Basel)* 12 (11), 3273. doi:10.3390/cancers12113273
- Yang, J., Mo, J., Dai, J., Ye, C., Cen, W., Zheng, X., et al. (2021a). Cetuximab promotes RSL3-induced ferroptosis by suppressing the Nrf2/HO-1 signalling pathway in KRAS mutant colorectal cancer. *Cell Death Dis.* 12 (11), 1079. doi:10.1038/s41419-021-04367-3
- Yang, P., Luo, X., Li, J., Zhang, T., Gao, X., Hua, J., et al. (2021b). Ionizing radiation upregulates glutamine metabolism and induces cell death via accumulation of reactive oxygen species. *Oxid. Med. Cell Longev.* 2021, 5826932. doi:10.1155/2021/5826932
- Yang, W. S., Kim, K. J., Gaschler, M. M., Patel, M., Shchepinov, M. S., and Stockwell, B. R. (2016). Peroxidation of polyunsaturated fatty acids by lipoxygenases drives ferroptosis. *Proc. Natl. Acad. Sci. U. S. A.* 113 (34), E4966–E4975. doi:10.1073/pnas.1603244113
- Yang, W. S., Sriramaratnam, R., Welsch, M. E., Shimada, K., Skouta, R., Viswanathan, V. S., et al. (2014). Regulation of ferroptotic cancer cell death by GPX4. *Cell* 156 (1–2), 317–331. doi:10.1016/j.cell.2013.12.010
- Ye, L. F., Chaudhary, K. R., Zandkarimi, F., Harken, A. D., Kinslow, C. J., Upadhyayula, P. S., et al. (2020). Radiation-induced lipid peroxidation triggers ferroptosis and synergizes with ferroptosis inducers. *ACS Chem. Biol.* 15 (2), 469–484. doi:10.1021/acscchembio.9b00939
- Yee, P. P., Wei, Y., Kim, S. Y., Lu, T., Chih, S. Y., Lawson, C., et al. (2020). Neutrophil-induced ferroptosis promotes tumor necrosis in glioblastoma progression. *Nat. Commun.* 11 (1), 5424. doi:10.1038/s41467-020-19193-y
- Yi, R., Wang, H., Deng, C., Wang, X., Yao, L., Niu, W., et al. (2020). Dihydroartemisinin initiates ferroptosis in glioblastoma through GPX4 inhibition. *Biosci. Rep.* 40 (6), BSR20193314. doi:10.1042/BSR20193314
- You, J. H., Lee, J., and Roh, J. L. (2021). Mitochondrial pyruvate carrier 1 regulates ferroptosis in drug-tolerant persister head and neck cancer cells via epithelial-mesenchymal transition. *Cancer Lett.* 507, 40–54. doi:10.1016/j.canlet.2021.03.013
- Yuan, Y., Cao, W., Zhou, H., Qian, H., and Wang, H. (2021). CLTRN, regulated by NRF1/RAN/DLD protein complex, enhances radiation sensitivity of hepatocellular carcinoma cells through ferroptosis pathway. *Int. J. Radiat. Oncol. Biol. Phys.* 110 (3), 859–871. doi:10.1016/j.ijrobp.2020.12.062
- Zarei, M., Hue, J. J., Hajihassani, O., Graor, H. J., Katayama, E. S., Loftus, A. W., et al. (2022). Clinical development of IDH1 inhibitors for cancer therapy. *Cancer Treat. Rev.* 103, 102334. doi:10.1016/j.ctrv.2021.102334
- Zhang, J., Chen, C., Li, A., Jing, W., Sun, P., Huang, X., et al. (2021a). Immunostimulant hydrogel for the inhibition of malignant glioma relapse post-resection. *Nat. Nanotechnol.* 16 (5), 538–548. doi:10.1038/s41565-020-00843-7
- Zhang, L., and Wang, H. (2017). FTY720 inhibits the Nrf2/ARE pathway in human glioblastoma cell lines and sensitizes glioblastoma cells to temozolomide. *Pharmacol. Rep.* 69 (6), 1186–1193. doi:10.1016/j.pharep.2017.07.003
- Zhang, S., Hu, R., Geng, Y., Chen, K., Wang, L., and Imam, M. U. (2021b). The regulatory effects and the signaling pathways of natural bioactive compounds on ferroptosis. *Foods* 10 (12), 2952. doi:10.3390/foods10122952
- Zhang, X., Jin, S., Shi, X., Liu, S., Li, K., Liu, G., et al. (2022). Modulation of tumor immune microenvironment and prognostic value of ferroptosis-related genes, and candidate target drugs in glioblastoma multiforme. *Front. Pharmacol.* 13, 898679. doi:10.3389/fphar.2022.898679
- Zhang, Y., Fu, X., Jia, J., Wikerholmen, T., Xi, K., Kong, Y., et al. (2020). Glioblastoma therapy using codelivery of cisplatin and glutathione peroxidase targeting siRNA from iron oxide nanoparticles. *ACS Appl. Mater. Interfaces* 12 (39), 43408–43421. doi:10.1021/acsami.0c12042
- Zhang, Y., Xi, K., Fu, X., Sun, H., Wang, H., Yu, D., et al. (2021c). Versatile metal-phenolic network nanoparticles for multitargeted combination therapy and magnetic resonance tracing in glioblastoma. *Biomaterials* 278, 121163. doi:10.1016/j.biomaterials.2021.121163
- Zhang, Z., Lu, M., Chen, C., Tong, X., Li, Y., Yang, K., et al. (2021d). Holo-lactoferrin: The link between ferroptosis and radiotherapy in triple-negative breast cancer. *Theranostics* 11 (7), 3167–3182. doi:10.7150/thno.52028
- Zhu, H., Klement, J. D., Lu, C., Redd, P. S., Yang, D., Smith, A. D., et al. (2021). Asah2 represses the p53-hmox1 Axis to protect myeloid-derived suppressor cells from ferroptosis. *J. Immunol.* 206 (6), 1395–1404. doi:10.4049/jimmunol.2000500
- Zhu, Z., Du, S., Du, Y., Ren, J., Ying, G., and Yan, Z. (2018). Glutathione reductase mediates drug resistance in glioblastoma cells by regulating redox homeostasis. *J. Neurochem.* 144 (1), 93–104. doi:10.1111/jnc.14250
- Zhuo, S., Chen, Z., Yang, Y., Zhang, J., Tang, J., and Yang, K. (2020). Clinical and biological significances of a ferroptosis-related gene signature in glioma. *Front. Oncol.* 10, 590861. doi:10.3389/fonc.2020.590861
- Zille, M., Kumar, A., Kundu, N., Bourassa, M. W., Wong, V. S. C., Willis, D., et al. (2019). Ferroptosis in neurons and cancer cells is similar but differentially regulated by histone deacetylase inhibitors. *eNeuro* 6 (1), 0263–0218. doi:10.1523/ENEURO.0263-18.2019
- Zou, Y., Li, H., Graham, E. T., Deik, A. A., Eaton, J. K., Wang, W., et al. (2020). Cytochrome P450 oxidoreductase contributes to phospholipid peroxidation in ferroptosis. *Nat. Chem. Biol.* 16 (3), 302–309. doi:10.1038/s41589-020-0472-6



## OPEN ACCESS

## EDITED BY

Yanqing Liu,  
Columbia University, United States

## REVIEWED BY

Yi Wang,  
Sichuan Academy of Medical Sciences  
and Sichuan Provincial People's  
Hospital, China  
Zhe Wang,  
Columbia University, United States

## \*CORRESPONDENCE

Luqian Zhou,  
zhlx09@163.com

## SPECIALTY SECTION

This article was submitted to Molecular  
Diagnostics and Therapeutics,  
a section of the journal  
Frontiers in Molecular Biosciences

RECEIVED 04 July 2022

ACCEPTED 21 July 2022

PUBLISHED 17 August 2022

## CITATION

Lin Z, Yang X, Guan L, Qin L, Ding J and  
Zhou L (2022), The link between  
ferroptosis and airway inflammatory  
diseases: A novel target for treatment.  
*Front. Mol. Biosci.* 9:985571.  
doi: 10.3389/fmolb.2022.985571

## COPYRIGHT

© 2022 Lin, Yang, Guan, Qin, Ding and  
Zhou. This is an open-access article  
distributed under the terms of the  
[Creative Commons Attribution License](#)  
(CC BY). The use, distribution or  
reproduction in other forums is  
permitted, provided the original  
author(s) and the copyright owner(s) are  
credited and that the original  
publication in this journal is cited, in  
accordance with accepted academic  
practice. No use, distribution or  
reproduction is permitted which does  
not comply with these terms.

# The link between ferroptosis and airway inflammatory diseases: A novel target for treatment

Zhiwei Lin, Xiaojing Yang, Lili Guan, Lijie Qin, Jiabin Ding and  
Luqian Zhou\*

State Key Laboratory of Respiratory Disease, National Clinical Research Center for Respiratory Disease,  
Guangzhou Institute of Respiratory Health, First Affiliated Hospital of Guangzhou Medical University,  
Guangzhou, China

Ferroptosis is an iron-dependent mode of cell death characterized by intracellular lipid peroxide accumulation and a redox reaction imbalance. Compared with other modes of cell death, ferroptosis has specific biological and morphological features. The iron-dependent lipid peroxidation accumulation is manifested explicitly in the abnormal metabolism of intracellular lipid oxides catalyzed by excessive iron ions with the production of many reactive oxygen species and over-oxidization of polyunsaturated fatty acids. Recent studies have shown that various diseases, which include intestinal diseases and cancer, are associated with ferroptosis, but few studies are related to airway inflammatory diseases. This review provides a comprehensive analysis of the primary damage mechanisms of ferroptosis and summarizes the relationship between ferroptosis and airway inflammatory diseases. In addition to common acute and chronic airway inflammatory diseases, we also focus on the progress of research on COVID-19 in relation to ferroptosis. New therapeutic approaches and current issues to be addressed in the treatment of inflammatory airway diseases using ferroptosis are further proposed.

## KEYWORDS

ferroptosis, metabolic networks and pathways, lung diseases, cell death, COVID-19

## 1 Introduction

Ferroptosis is a novel regulated cell death pathway discovered by Dixon et al. (Dixon et al., 2012) in 2012. Compared with other modes of cell death, such as apoptosis, necrosis, and autophagy, ferroptosis is mainly characterized by the accumulation of iron-dependent lipid peroxidation with specific features of abnormal metabolism of intracellular lipid oxides catalyzed by excess iron ions, reactive oxygen species (ROS) production, and regulatory cell death mediated by excessive oxidation of polyunsaturated fatty acids (PUFAs). The development and progression of many human diseases are related to ferroptosis (Fuchs and Steller, 2011), such as intestinal diseases (Xu et al., 2021) and tumor cell death (Xu et al., 2019).

Today there is growing evidence that ferroptosis is closely linked to inflammatory diseases (Mao et al., 2020). Airway inflammation is the body's natural response to injury and it serves to remove harmful stimuli such as pathogens, irritants and damaged cells, and to initiate the healing process (Ahmed, 2011). The main airway inflammatory diseases are acute or chronic airway inflammation and infectious inflammatory diseases (Aghasafari et al., 2019). The main acute airway inflammatory diseases are acute lung injury and acute respiratory distress syndrome, while the main chronic airway inflammatory diseases are chronic obstructive pulmonary disease (COPD) and asthma (Racanelli et al., 2018; Aghasafari et al., 2019). In addition to these, there are also infectious airway inflammatory diseases of the airways such as *Pseudomonas aeruginosa* infection, *Mycobacterium tuberculosis* infection, acute bronchiolitis and the current epidemic of COVID-19 (Dorhoi and Kaufmann, 2014; Jartti et al., 2019; Berlin et al., 2020; Garcia-Clemente et al., 2020). To date, convincing evidence suggests that ferroptosis plays an important role in inflammation and a number of antioxidants that act as inhibitors of ferroptosis have been shown to exert anti-inflammatory effects in experimental models of certain diseases (Sun et al., 2020). However, the underlying mechanisms of ferroptosis in airway inflammatory diseases have not been fully elucidated and summarized. However, the underlying mechanisms have not been elucidated fully. This review systematically summarizes the latest progress in ferroptosis research and discusses the research progress of the relationship between ferroptosis and airway inflammatory diseases, which suggests new therapeutic approaches for airway inflammatory diseases.

## 2 Overview of ferroptosis

### 2.1 Iron balance and ferroptosis

Iron is a minor element required for the proper functioning of many physiological functions and is involved in the synthesis of many substances in the human body, such as hemoglobin, which transports oxygen from the lungs to other organs. Additionally, iron is a component of many enzymes and immune system compounds. The body obtains the most required iron from food and maintains the balance of iron metabolism. Iron in food exists mainly as trivalent iron ions that are reduced to ferrous ions by gastric acid, then form complexes with certain sugars, amino acids, and vitamin C in the gastrointestinal tract, which are absorbed in the duodenum and jejunum. In the average human body, iron is in a stable balance. Iron obtained from food can not only supplement the amount needed for human growth and development, but also make up for the amount lost in normal iron metabolism (Anderson et al., 2009; Lizarraga et al., 2009; Elsenhans et al., 2011).

Previous studies have shown that various mechanisms, such as necrosis, apoptosis, and autophagy, jointly regulate and control the death of all mammalian cells. However, in 2003, Sonam, DeHart, et al. (Dolma et al., 2003; DeHart et al., 2018) indicated that the anti-tumor drug erastin induces tumor cells to die uniquely. Further found under light microscopy, this novel manner of cell death exhibited a classical necrotic morphology accompanied by reduced or absent intracellular mitochondrial cristae and ruptured outer membranes with smaller intracellular mitochondria, an increased density of bilayer membranes. Furthermore, none of the characteristic changes expected of cell death, such as cytoplasmic swelling, rupture, chromatin condensation, and margination, were present. Nicholas Yagoda (Yagoda et al., 2007) in 2007 and Yang et al. (Yang and Stockwell, 2008) in 2008 found that the novel cell death described above was inhibited by iron chelators and accompanied by increased levels of reactive oxygen species. In 2012, Dixon et al. (Dixon et al., 2012) officially named it "ferroptosis" which is a non-apoptotic, iron-dependent mode of cell death mainly characterized by accumulation of intracellular reactive oxygen species.

The primary mechanism of ferroptosis is dependent on iron, which causes lipid peroxidation of cell membranes by disrupting the antioxidant system that consists of glutathione (GSH) and glutathione peroxidase (GPx) 4. The normal structural integrity of cells is disrupted and cell death occurs as the result. It is unknown whether ferroptosis is involved in the development of various diseases. However, some research suggested that ferroptosis is a physiological process that occurs widely in mammals rather than a pathological or organ-specific process (Linkermann et al., 2014; Zille et al., 2017). Unlike other forms of cell death, ferroptosis shares some features with several types of regulated cell death (RCD).

### 2.2 Mechanism and regulation of ferroptosis damage

#### 2.2.1 System Xc<sup>-</sup> pathway

Ferroptosis is a regulated cell death due to excess iron aggregation, which leads to an explosion of intracellular lipid-based reactive oxygen species. Simultaneously, it disrupts the antioxidant mechanism in the organism and large amounts of reactive oxygen species cause further lipid peroxidation and eventually cell death (Le et al., 2021). Cystine/glutamate transporter (system Xc<sup>-</sup>), a transmembrane amino acid transporter on the cell surface, consists of a heterodimer of two amino acid chains: the SLC3A2 heavy chain and SLC7A11 light chain, which transports cystine into the cell. Glutathione is an essential cofactor for glutathione peroxidases (GPxs) and glutathione peroxidases catalyze degradation of hydrogen peroxide (H<sub>2</sub>O<sub>2</sub>) with peroxides and inhibit lipid-based reactive oxygen species production (Bridges et al.,



2012). Therefore, inhibiting cystine-glutamate transporter receptor and affecting glutathione production reduce glutathione peroxidases activity, which decreases the cellular antioxidant capacity as well as leading to lipid-based reactive oxygen species accumulation and causes cellular ferroptosis. Moreover, SLC7A11 directly promotes translational expression of glutathione peroxidase 4 protein through cystine and demonstrated that mTORC1 positively regulates the translational expression of glutathione peroxidase 4 protein by sensing cystine levels through the small G protein Rag and relies on phosphorylation to inhibit 4EBP (Zhang et al., 2021).

### 2.2.2 GPx4 pathway

GPx4 is a member of the glutathione peroxidase family and plays a crucial role in maintaining intracellular redox homeostasis. GPx4 catabolizes certain lipid peroxides and small molecule peroxides, which inhibits lipid peroxidation (Imai et al., 2017). Cells with reduced GPx4 expression have increased sensitivity to ferroptosis (Yang et al., 2014). Thus, inhibition of GPx4 expression causes cellular ferroptosis. GPx4 contains eight nucleophilic amino acids. Selenocysteine is an amino acid in the active center of GPx4. Inserting selenocysteine into GPx4 requires a special transporter, selenocysteine tRNA (Yang et al., 2016; Kagan et al., 2017). Maturation of selenocysteine tRNA requires isopentenyl transferase to transfer the isopentenyl group from isopentenyl pyrophosphate (IPP) to the selenocysteine tRNA precursor. isopentenyl pyrophosphate is the product of the mevalonate pathway, which acts on GPx4 by regulating the maturation of selenocysteine tRNA (Warner et al., 2000). Therefore, inactivation or deletion of GPx4 leads to the accumulation of lipid peroxides and causes ferroptosis in cells.

### 2.2.3 p53 pathway

Jiang et al. first revealed that p53 can promote ferroptosis in cells by the mechanism that p53 can transcriptionally repress SLC7A11 expression (Jiang et al., 2015). Further studies have shown that acetylation of p53 K101 is of importance for p53 to inhibit SLC7A11 (Jiang et al., 2015). p53<sup>3KR</sup> is an acetylation-deficient mutant form of p53 protein that does not induce cell cycle arrest, senescence and apoptotic processes, but fully retains the ability to regulate SLC7A11 expression and can contribute to cellular ferroptosis processes in a ROS-induced stress state (Jiang et al., 2015). The p53-SLC7A11 axis can also promote ferroptosis in a glutathione-independent manner. In one study, p53 was found to induce the expression of SAT1, which promotes the function of ALOX15, a member of the ALOX family, to enhance cellular ferroptosis (Ou et al., 2016). The ALOX12 is a key regulator of p53-dependent ferroptosis, and SLC7A11 can bind ALOX12 directly to limit its function, thus releasing ALOX12 when p53 inhibits SLC7A11 (Chu et al., 2019). Free ALOX12 can oxidize the polyunsaturated fatty acid chains of cell membrane phospholipids, leading to ferroptosis (Chu et al.,

2019). In addition, the target gene of p53, GLS2, catalyzes the process of glutaminolysis (Suzuki et al., 2010), and glutaminolysis can promote the occurrence of ferroptosis (Yang et al., 2014). Meanwhile, p53 is able to regulate PHGDH to inhibit serine synthesis and may be able to influence glutathione synthesis to promote ferroptosis (Ou et al., 2015). In addition to the above, there are many other factors that can regulate p53 and further promote or inhibit ferroptosis. In conclusion, p53 is an important ferroptosis regulator with a broad and complex role (Liu and Gu, 2021; Liu and Gu, 2022).

### 2.2.4 GCH1-BH4 pathway

Tetrahydrobiopterin (BH4) is a redox-active cofactor involved in the production of nitric oxide, neurotransmitters, and aromatic amino acids (Cronin et al., 2018). GTP cyclohydrolase-1- (GCH1-) 6-pyruoyltetrahydropterin synthase- (PTS-) sepiapterin reductase (SPR) pathway catalyzes the conversion of GTP to BH4, and GCH1 is the rate-limiting enzyme in BH4 synthesis (Latremoliere and Costigan, 2011). BH4 exhibits antioxidant properties *in vitro* (Kim and Han, 2020). Kraft et al. identified GCH1 and its metabolic derivative BH4 as potent endogenous ferroptosis inhibitors that act independently of GPX4 pathway through a CRISPR activation screen (Kraft et al., 2020). GCH1 overexpression is resistant to RSL3-induced ferroptosis and gene ablation-induced ferroptosis by GPX4, but does not protect cells from apoptosis inducers, and had only a weak effect on necrotic death, suggesting that GCH1 selectively resists cells from undergoing ferroptosis (Kraft et al., 2020). Soula et al. (2020) demonstrated that deletion of GCH1 or SPR, as well as inhibition of SPR with QM385, sensitized cells to RSL3 but not to Erastin treatment in Jurkat cells. Treatment of cells with BH2 or BH4 together with ferroptosis inducers saved cells from ferroptosis (Kraft et al., 2020; Soula et al., 2020). Although BH4 can act as a cofactor for several biosynthetic enzymes, both groups found this function of BH4 to be independent of its protective effect against ferroptosis (Kraft et al., 2020; Soula et al., 2020). The results of both studies suggest that the GCH1-BH4 pathway acts as an endogenous antioxidant pathway to inhibit ferroptosis by acting independently of the GPX4/glutathione mechanism. However, the role of BH4 in ferroptosis still needs to be further confirmed under pathological conditions.

### 2.2.5 Methionine pathway

Under oxidative stress conditions, the sulfur transfer pathway transfers sulfur atoms from methionine to serine to produce cysteine. Cysteine is then used as a substrate to bind glutamate and glycine to synthesize glutathione, thereby synthesizing glutathione peroxidases to maintain intracellular redox homeostasis and prevent oxidative damage. Therefore, this pathway inhibits the occurrence of ferroptosis (McBean, 2012).

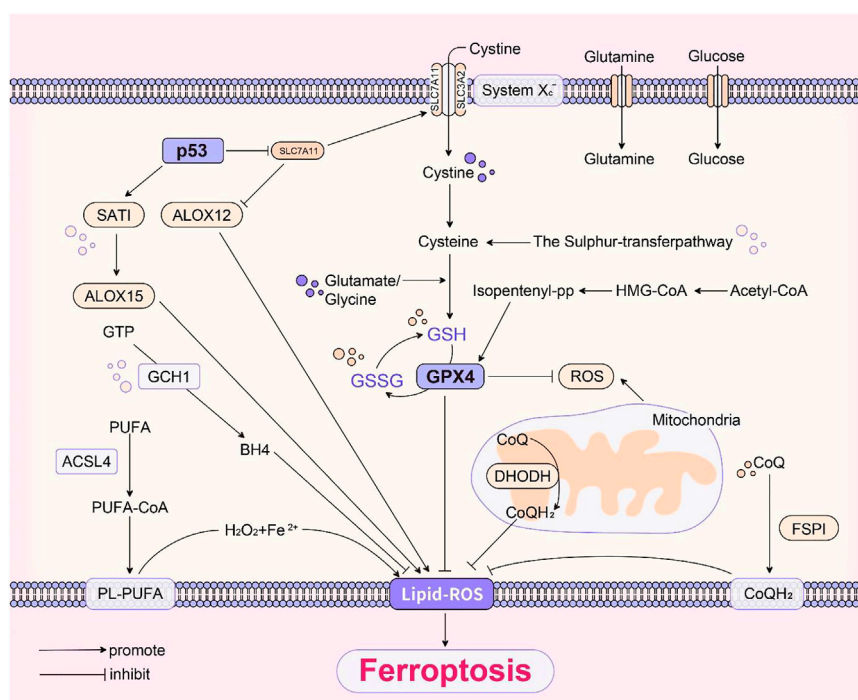


**FIGURE 1**  
(The basic pathways of ferroptosis).

### 2.2.6 Other pathways

A mixture of hydrogen peroxide and divalent iron ions is strongly oxidizing and its main oxidizing component is hydroxyl radicals ( $\text{OH}\cdot$ ) (Winterbourn, 1995). When excessive iron ions were enriched in an organism, the circulating non-transferrin-bound iron (NTBI) content increased, which reacted with hydrogen peroxide to induce the Fenton reaction, accumulate reactive oxygen species and a large amount of hydroxyl radicals, and oxidize polyunsaturated fatty acids on the cell membrane to lipid hydroperoxide (LPO) (Pignatello et al., 2006). Lipid hydroperoxide forms toxic lipid radicals, such as alkoxy radicals, which damage the structural stability of cell membranes and attack intracellular DNA and proteins to cause ferroptosis in cells. Additionally, these radicals transfer protons from neighboring polyunsaturated fatty acids, which initiates a new round of lipid oxidation reactions and further transmits oxidative damage (Shah et al., 2018).

Voltage-dependent anion channels (VDACs) are ion channels located on the outer mitochondrial membrane, which mediate and control the exchange of molecules and ions between mitochondria and the cytoplasm (Mazure, 2017; Becker and Wagner, 2018). VDACs permeability can be altered by drugs, which disrupts mitochondrial metabolism, generates

large amounts of reactive oxygen species, and leads to cellular ferroptosis (Maldonado, 2017).

Ferroptosis is inhibited by FSP1 overexpression, but when CoQ10 is simultaneously deficient, the ability of cells to inhibit ferroptosis disappears. FSP1 prevents lipid oxidation by reducing CoQ10 (Doll et al., 2019). Another study (Bersuker et al., 2019) also showed that FSP1 inhibits ferroptosis through reducing CoQ10 by mutating the conserved glutamate bound by cofactors in FSP1, which was independent of the classical GPX4 signaling pathway. The most recent study (Mao et al., 2021) found that DHODH is an enzyme located on the outer surface of the mitochondrial intima, which inhibits ferroptosis by reducing CoQ to  $\text{CoQH}_2$ , and further proposed a defense mechanism of DHODH-mediated mitochondrial ferroptosis.

Based on all the above mechanisms, Figure 1 summarised the basic pathways of ferroptosis.

## 3 Ferroptosis and acute airway inflammatory diseases

Acute lung injury (ALI) and the more severe acute respiratory distress syndrome are pulmonary manifestations of

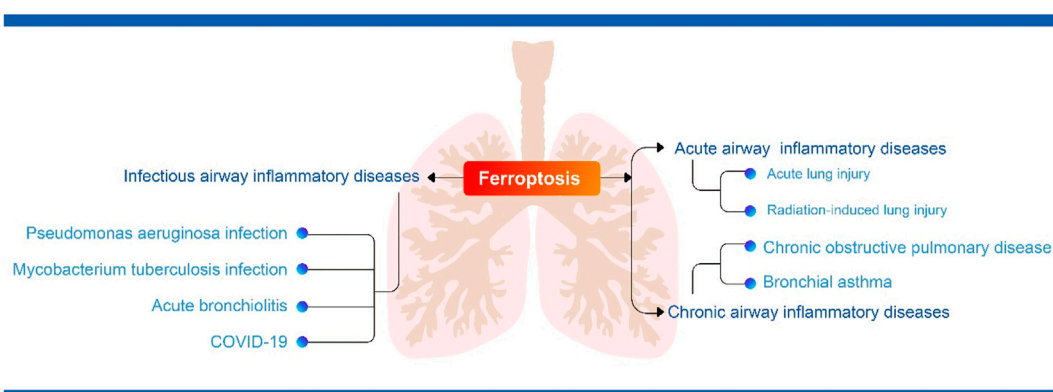


FIGURE 2

(The relationship between ferroptosis and airway inflammatory diseases).

an imperative systemic inflammatory process with clinical presentations of pulmonary infiltration, diffuse alveolar injury, hypoxemia, and pulmonary edema formation (Butt et al., 2016).

In an oleic acid (OA)-induced acute lung injury mouse model, the lung histopathological score, lung dry weight ratio, and protein content were elevated in the bronchoalveolar lavage fluid (BALF) of the oleic acid group compared with the control group, and mitochondrial contraction and mitochondrial membrane rupture were seen in lung cells. Moreover, there was iron overload, glutathione depletion, accumulation of malondialdehyde (MDA), downregulation of protein expression levels of GPx4 and ferritin in lung tissue, and 7-fold higher expression levels of PTGS2 mRNA in the oleic acid group than in the control group. These results suggest that ferroptosis plays an essential role in the pathogenesis of acute lung injury (Zhou et al., 2019). *In vivo* and *in vitro* that lipopolysaccharide (LPS) reduces SLC7A11 and GPx4 with elevated levels of malondialdehyde, 4-hydroxynonenal (4-HNE), and total iron in human bronchial epithelial cell line BEAS-2B, thereby causing ferroptosis in these cells. Ferrostatin-1 effectively alleviates the decrease in BEAS-2B cell activity caused by lipopolysaccharide and reduces lung inflammation by inhibiting ferroptosis (Liu et al., 2020). Therefore, ferroptosis may be a new therapeutic target for acute lung injury and more suitable ferroptosis inhibitors can be investigated to alleviate the progression of inflammation in acute lung injury.

Characteristic mitochondrial morphological changes caused by ferroptosis in type II alveolar epithelial cells of an intestinal ischemia/reperfusion-induced acute lung injury (IIR-ALI) model in Nrf2 gene knockout C57BL/6 mice. After treating the mice with Fe and ferrostatin-1, the former significantly aggravated pathological damage, pulmonary edema, lipid peroxidation, and promoted cell death. The latter had the opposite effects (Dong et al., 2020). In the oxygen-glucose deprivation and reoxygenation (OGD/R) model, MLE12 and BEAS-2B cells

increase expression levels of Nrf2, SLC7A11, and heme oxygenase-1 (HO-1) proteins. After treating mice with Fe and ferrostatin-1, The results also showed that the former promoted the occurrence of ferroptosis, while the latter inhibited it (Lee et al., 2014; Dong et al., 2020). Knockdown of Nrf2 significantly inhibits the expression of SLC7A11 and Heme oxygenase-1 (Dong et al., 2020). Thus, Nrf2 inhibits ferroptosis in alveolar epithelial cells by regulating SLC7A11 and heme oxygenase-1, which provides a potential therapeutic strategy for intestinal ischemia/reperfusion-induced acute lung injury. Nrf2 mitigates the progression of intestinal ischemia/reperfusion-induced acute lung injury by mediating STAT3 activation in an oxygen-glucose deprivation and reoxygenation model established with MLE12 cells (Qiang et al., 2020). Lung ischemia-reperfusion (Lung-IR) increases tissue iron content and lipid peroxidation accumulation during reperfusion and increases the expression of essential proteins (GPx4 and ACSL4). In animal and cellular models, pretreatment with liproxstatin-1 inhibits ferroptosis and ameliorates lung damage caused by lung ischemia-reperfusion. Additionally, preischemic administration of the ACSL4 inhibitor rosiglitazone attenuates the occurrence of ferroptosis in lung tissue with ischemia-reperfusion, which is consistent with the protective effect of ACSL4 knockdown on lung epithelial cells that have experienced hypoxia/reoxygenation (Xu et al., 2020). Thus, ACSL4 is associated with ferroptosis in lung tissue induced by ischemia-reperfusion.

Reactive oxygen species levels in the lung and serum levels of inflammatory cytokines (TNF- $\alpha$ , IL-6, IL-10, and TGF- $\beta$ 1) were significantly reduced in mice treated with ferroptosis inhibitors after acute radiation-induced lung injury (RILI) (Li et al., 2019). This suggests that radiation-induced reactive oxygen species is the initial trigger of ferroptosis in acute radiation-induced lung injury and that ferroptosis may also be important in affecting inflammatory cytokine levels in acute radiation-induced lung injury. Sevoflurane protected mice from LPS-induced lung

injury, which included reductions in lung histological damage, pulmonary edema, and pulmonary vascular permeability, and inflammatory factors in bronchoalveolar lavage fluid as well as improving the survival of acute lung injury mice, which are consistent with the action of the ferroptosis inhibitor ferrostatin-1 (Liu et al., 2021). Further experiments revealed that Sevoflurane alleviates LPS-induced acute lung injury by upregulating heme oxygenase-1 expression to inhibit ferroptosis.

## 4 Ferroptosis and chronic airway inflammatory diseases

Studies of ferroptosis in chronic airway inflammatory diseases have focused on chronic obstructive pulmonary disease and bronchial asthma. However, systematic and comprehensive studies have not been conducted in detail.

### 4.1 Ferroptosis and chronic obstructive pulmonary disease

The pathogenesis of the chronic obstructive pulmonary disease (COPD) is associated with disturbances in iron homeostasis, which lead to excessive oxidative stress (Yoshida et al., 2019). Further studies showed that ferroptosis is related to chronic obstructive pulmonary disease pathogenesis. *In vivo* and *ex vivo* models (Gao et al., 2016; Hou et al., 2016) have shown that cigarette smoke (CS) exposure enhances unstable iron accumulation and lipid peroxidation in human bronchial epithelial cells (HBECs). Moreover, the cells initiate NCOA4-mediated ferritinophagy in response to CS-induced ferritin degradation, which increases free iron content and promotes ferroptosis in cells. In a cigarette smoke exposure model, chronic obstructive pulmonary disease mice with GPx4 knockout showed an increase in the lipid peroxide level. Additionally, they had an increase in small airway thickness compared with normal mice with corresponding symptoms detected in the lung tissue of smokers. In addition to causing cellular ferroptosis, damage-associated molecular patterns (DAMPs) and proinflammatory cytokine release from lung epithelial cells were also detected in the above mouse model, which exacerbates the degree of peripheral inflammation. This study further suggested that the decrease in GPx4 and its substrate glutathione may be related to the inadequate antioxidant stress response of human bronchial epithelial cells to cigarette smoke, which leads to ferroptosis. NCOA4 expression levels are significantly higher in lung homogenates from chronic obstructive pulmonary disease patients than non-smokers and non-chronic obstructive pulmonary disease smokers. Immunohistochemistry of lung tissue also showed enhanced expression of NCOA4 in bronchial epithelial cells of chronic obstructive pulmonary disease patients. Taken together, these findings support the

role of CS-induced ferroptosis in the pathogenesis of chronic obstructive pulmonary disease. Particulate matter 2.5 (PM<sub>2.5</sub>) also causes chronic airway inflammation because of ferroptosis in endothelial cells, which is similar to what occurs after cigarette smoke exposure (Wang and Tang, 2019). Thus, new therapeutic ideas can be explored to alleviate chronic obstructive pulmonary disease symptoms by regulating unstable iron content and the lipid peroxidation response in human bronchial epithelial cells.

In healthy airways, alveolar macrophages (AMs) are relatively quiescent. However, in chronic obstructive pulmonary disease, various etiologies induce increased activation and numbers of alveolar macrophages that produce proinflammatory mediators to induce neutrophils, monocytes, and T cells to enter the lungs and exacerbate lung tissue injury and inflammation (Christenson, 2017). Iron overload-induced macrophages undergo ferroptosis, iron citrate induces ferroptosis in bone marrow-derived macrophages, and SLC7A11 gene deletion promotes iron overload-induced ferroptosis in macrophages (Wang et al., 2017). Additionally, macrophages recognize oxidized phospholipids on the surface of iron-dead cells through the membrane receptor toll-like receptor 2, which mediates phagocytic clearance of ferroptotic cells (Luo et al., 2021). Therefore, ferroptosis may be induced in cells and thus reduce airway inflammation, which requires further investigation.

### 4.2 Ferroptosis and bronchial asthma

Reactive oxygen species production in peripheral blood eosinophils is significantly higher in asthmatic patients than in healthy subjects and that reactive oxygen species production is further increased dramatically after excitation (Frossi et al., 2008). On the other hand, inflammation in asthma may also be associated with damage-associated molecular patterns. Tissues with ferroptosis suggest significant activation of macrophages and release of pro-inflammatory substances, which triggers a series of inflammatory responses. Additionally, there are inflammatory mediators produced by the metabolism of peroxides and arachidonic acid in ferroptosis tissues (Shah et al., 2018). As a critical lipid peroxidase in arachidonic acid metabolism, lipoxygenase is not only involved in the inflammatory and immune responses of the body but also catalyzes the oxidation of polyunsaturated fatty acids to lipid peroxides, which forms toxic lipid free radicals that damage the structural stability of cell membranes and attack intracellular DNA and proteins, thereby causing ferroptosis in cells. Furthermore, these free radicals transfer protons from neighboring PUFAs, initiate a new round of lipid oxidation reactions and impart further oxidative damage.

Establishing a mouse ovalbumin asthma model and performed experiments using ferroptosis inducers (FINs) *in vivo* and *in vitro* to detect the survival of eosinophils and the



level of inflammation in lungs, which found that ferroptosis inducers mediate eosinophil ferroptosis through a non-classical pathway (cytoplasmic reactive oxygen species accumulation), thereby effectively alleviating asthma with eosinophilic airway inflammation. Furthermore, antioxidants glutathione and N-acetylcysteine significantly attenuated FIN-induced cell death and reduced eosinophilic airway inflammation in mice. There was also a significant synergistic effect between ferroptosis of eosinophils induced by ferroptosis inducers and apoptosis of eosinophils induced by glucocorticoids (Wu et al., 2020). Thus, their combined use can further induce the death of eosinophils, reduce the application of hormones, and further protect asthmatic airways. Thus, eosinophil apoptosis may provide a new target for treating eosinophilic airway inflammation and a new therapeutic option for clinically hormone-tolerant or refractory asthma patients, which requires further investigation.

PEBP1 is essential for the dynamic balance between the ferroptosis program and cellular autophagy in asthmatic airway epithelial cells and activation of autophagy protects cells from ferroptosis and mitochondrial DNA release. Similar findings were observed in type 2 high phenotype asthma epithelial cells. The finding that the 15-lipoxygenase-1-PEBP1 (15LO1-PEBP1) complex and its phospholipid hydroperoxide are accompanied by ferroptosis and autophagy activation revealed a pathobiological pathway associated with asthma (Zhao et al., 2020). Therefore, ferroptosis is closely related to the mechanism of bronchial asthma exacerbation, which provides new ideas to improve the prognosis of asthma.

## 5 Ferroptosis and infectious airway inflammatory diseases

### 5.1 Ferroptosis and *P. aeruginosa* infection

*P. aeruginosa* expresses lipoxygenase (pLoxA) that selectively oxidizes arachidonic acid-phosphatidyl ethanolamine (AA-PE) to produce 15-hydroperoxy-AA-PE (15-HO-AA-PE). The accumulation of 15-HOO-AA-PE among other molecules causes cellular ferroptosis as a ferroptosis inducer. Although *P. aeruginosa* itself has no AA-PE on its cell membrane, the synthesized lipoxygenase can target the transformation of arachidonic acid in the cell membrane of host cells, which is similar to the body's mechanism and causes the onset of ferroptosis in host cells. In the clinic, high expression of lipoxygenase causes ferroptosis in bronchial epithelial cells with *P. aeruginosa* colonization. Conversely, mutant bacteria that lack lipoxygenase do not cause ferroptosis in human bronchial epithelial cells (Dar et al., 2018). Thus, isolation of *P. aeruginosa* in patients with chronic lower respiratory tract infections depends on the expression level and enzymatic activity of lipoxygenase. On the basis of these findings, the development of specific lipoxygenase inhibitors

may be a novel therapy for chronic lower respiratory tract infections by *P. aeruginosa*.

*P. aeruginosa* degrades host GPx4 defenses by activating lysosomal chaperon-mediated autophagy (CMA). In response, the host stimulates the iNOS/NO<sup>•</sup> driven anti-ferroptotic mechanism to prevent lipid peroxidation and protect GPx4/GSH-deficient cells. Macrophage production of NO<sup>•</sup> as an inter-cellular mechanism was found to prevent PA-stimulated ferroptosis in epithelial cells at a distance using a co-culture model system. The inhibitory effect of NO<sup>•</sup> on ferroptosis in epithelial cells was inhibited by inhibiting phospholipid peroxidation, especially the production of pro-ferroptotic 15-hydroperoxy- arachidonyl-PE (15-hPET-PE) signals. The pharmacological targeting of iNOS weakens its anti-ferroptosis function (Dar et al., 2021). Based on these studies, this could lead to new therapeutic strategies against ferroptosis induced by *P. aeruginosa*.

### 5.2 Ferroptosis and *M. tuberculosis* infection

*M. tuberculosis* (Mtb) infection increases the expression of heme oxygenase-1 that degrades heme to free iron (Andrade et al., 2013; Costa et al., 2016). Free iron levels are associated with an increased tuberculosis (TB) risk in patients. Additionally, elevated iron levels exacerbate lung inflammation and increase bacterial load in patients and animals with *M. tuberculosis* infection (Schaible et al., 2002; Boelaert et al., 2007). Mtb-induced macrophage death is associated with decreased glutathione and GPx4 levels and increased free iron, mitochondrial superoxide, and lipid peroxide, which are markers of ferroptosis. However, macrophage death after *M. tuberculosis* infection can be alleviated by ferrostatin-1 or iron chelators, which effectively reduces bacterial load and lung inflammation (Amaral et al., 2019). Therefore, appropriate treatments can be explored to inhibit host cell ferroptosis and thus alleviate tuberculosis. Of note during the COVID-19 epidemic is that human immune function can be temporarily suppressed due to the effects of SARS-CoV-2 and possibly immunosuppressive drugs, leading to reactivation of *M. tuberculosis* or infection causing active TB disease. We should be sensitive to the short-term increase in TB prevalence after the end of the COVID-19 pandemic. This requires not only the implementation of TB prevention and control, but also appropriate measures to enhance TB prevention, control and management (Yang and Lu, 2020).

### 5.3 Ferroptosis and acute bronchiolitis

Acute bronchiolitis is an acute infection of the lower respiratory tract resulting in obstruction or dyspnea, with

major symptoms including cough, runny nose, paroxysmal wheezing, and in severe cases, hypoxemia, which affects infants and children worldwide (Dalziel et al., 2022). It is most often caused by human respiratory syncytial virus (RSV) and the lung epithelium and alveolar macrophages are the first cells to be infected during RSV infection (Blanco et al., 2002). It has been shown that RSV causes more than 30 million cases of lower respiratory tract infections in children under 5 years of age each year, with 32 million hospitalizations and 200,000 deaths worldwide each year (Bohmwald et al., 2016). Bronchiolitis is one of the main reasons of consultations in pediatric emergency department (Redant et al., 2021). Vahid Salimi et al. showed that RSV increases 12/15-LOX expression and mitochondrial iron content through experiments in mice (Salimi et al., 2017). Lipoxygenases (LOX) are a family of enzymes capable of binding oxygen to unsaturated fatty acids (Rossaint et al., 2012). The mechanism is that 12/15 LOX inhibits C1SD1 (Wang M. P. et al., 2021), an iron-containing mitochondrial outer membrane protein that negatively regulates ferroptosis (Yuan et al., 2016). Knockdown of C1SD1 by RNAi increases mitochondrial Fe<sup>2+</sup> accumulation, which subsequently causes lipid peroxidation of mitochondrial membranes induced by Fe<sup>2+</sup>-mediated Fenton reaction, thus promoting ferroptosis (Yuan et al., 2016). Therefore, the 12/15-LOX/C1SD1 pathway may be a candidate target for the prevention and treatment of RSV infection through ferroptosis, and other possible mechanisms for the interaction between the 12/15-LOX pathway and RSV pathogenesis need to be discussed, which requires further targeted studies.

## 5.4 Ferroptosis and COVID-19

COVID-19 is a global pandemic with SARS-CoV-2 as the causative agent, manifesting itself as a severe inflammatory response characterised by a cytokine storm that has now caused widespread loss of life (Yi et al., 2020). SARS-CoV-2 targets the respiratory system and is transmitted from potentially symptomatic or asymptomatic infected individuals through contact droplets and contaminants. During the incubation period, the virus triggers a slow response in the lungs. SARS-CoV-2 invades mainly alveolar epithelial cells, causing respiratory symptoms (Yi et al., 2020). Although many patients are asymptomatic or have mild symptoms such as fever, fatigue and dry cough, a few cases progress to more severe forms of the disease such as ARDS, mainly in older men with comorbidities (Borges do Nascimento et al., 2020). Despite the amount of time scientists around the world have spent studying COVID-19, there is still no way to control the widespread spread of the epidemic. Studies have shown that isolation of infected cases can be effective in controlling the spread of the disease (Wang et al., 2020).

There is now growing evidence that ferroptosis is involved in the pathogenesis of COVID-19 (Li et al., 2022). Ferroptosis has been detected in human heart (Jacobs et al., 2020) and hamster lung (Han et al., 2022) samples infected with SARS-CoV-2. A study showed that changes in markers of iron metabolism in blood samples, such as decreased serum iron and increased ferritin, were associated with severe COVID-19 (Zhou et al., 2020). Inflammatory manifestations following SARS-CoV-2 infection can highly induce IL-6 secretion. Previous studies have demonstrated the effect of IL-6 on iron metabolism. On the one hand, IL-6 directly promotes transferrin uptake and ferritin expression (Kobune et al., 1994); on the other hand, IL-6 can induce the synthesis of ferroregulin (Nemeth et al., 2004), an inhibitor of iron transport proteins, which leads to cellular iron accumulation. Studies have shown that an increase in serum ferroregulin correlates with the severity of COVID-19 (Nai et al., 2021). In addition, scRNA-seq data from PBMC, T cells and B cells from COVID-19 patients showed that ferroptosis-related genes (including GPX4, FTH1, FTL and SAT1) were increased in the acute phase and decreased in the recovery phase (Huang et al., 2021). In addition, SARS-CoV-2 infection may lead to tissue depletion of selenium and transcriptional inactivation of GPX4, which synergistically disrupts GPX defences and induces the onset of ferroptosis (Wang Y. et al., 2021). In response to the ferroptosis manifestation of COVID-19, it has been suggested that drugs that enhance the GPX4-GSH axis, induce RTA and ACSL4 activity and ultimately lead to iron depletion in the unstable pool may be candidates for COVID-19 treatment (Fratta Pasini et al., 2021). In addition, the fact that Nrf2 directly or indirectly regulates antioxidant capacity and the HO-1-iron regulation-related axis suggests that NRF2 activators may be a new approach for the treatment of COVID-19 organ damage (Fratta Pasini et al., 2021). One study also identified iron chelators as useful adjunctive therapies in the treatment of COVID-19, such as deferasirox, desferrioxamine and deferiprone, as well as the naturally occurring iron chelator lactoferrin, which may be beneficial in combating COVID-19 disease progression (Perricone et al., 2020). Studies have shown that iron chelators not only chelate iron and reduce inflammation, but also prevent coronaviruses from binding to the receptors they use to enter host cells (Chang et al., 2020). To date, however, it has not been clinically established whether inhibition of ferroptosis is useful in the treatment of inflammatory storms and organ damage caused by SARS-CoV-2 infection, and more in-depth studies are needed to show the way forward. Figure 2 summarised the relationship between ferroptosis and airway inflammatory diseases.

## 6 Summary and future perspectives

The airway is a vital organ for oxygen entry into the body, and excessive inflammation can be life-threatening (Lumb, 2016). The

delicate balance between inflammation and anti-inflammation is critical for airway homeostasis. Airway inflammation is usually caused by pathogens or exposure to toxins, pollutants, irritants and allergens (Lumb, 2016). Inflammatory target proteins that cause airway inflammation are diverse, such as matrix metalloproteinase-9 (MMP-9), intercellular adhesion molecule-1 (ICAM-1), vascular cell adhesion molecule-1 (VCAM-1), cyclooxygenase-2 (COX)-2 and cytoplasmic phospholipase A2 (cPLA2) (Lee and Yang, 2013), making airway inflammatory diseases diverse and complex. As a newly discovered programmed cell death pathway, ferroptosis has morphological and biochemical characteristics that are different from other cell death pathways such as apoptosis, necrosis and autophagy, and the specific mechanisms, related pathways and drug targets of ferroptosis for the development of airway inflammatory diseases still need to be further explored and studied. This review summarizes the recent progress of ferroptosis research and highlights that in addition to GPX4-dependent ferroptosis, the non-GPX4-dependent p53 regulatory network is also crucial for the regulation of ferroptosis. Furthermore, we comprehensively discuss the role of ferroptosis in various airway inflammatory diseases, including acute airway inflammatory diseases (acute lung injury), chronic airway inflammatory diseases (COPD, asthma) and infectious airway inflammatory diseases (*p. aeruginosa* infection, *M. tuberculosis* infection, acute bronchiolitis and COVID-19), to provide a new way of thinking for the treatment of airway inflammatory diseases.

Although various related studies are emerging, there are still many issues that need to be addressed before we can turn ferroptosis to relevant clinical applications. First, almost all current studies of airway inflammatory diseases only examine ferroptosis in cellular and animal models, and there is a lack of validated human evidence. Therefore, the design of clinical trials related to ferroptosis plays a decisive role. Second, the toxicological effects of inhibitors or inducers of ferroptosis on human organs are almost unknown. How can ferroptosis therapies be developed with higher efficacy and targeting, thus reducing overall systemic toxicity and improving safety? This remains to be addressed. Ferroptosis has two-sided effects in different diseases, with some diseases in which inhibition of ferroptosis can delay disease progression, such as COPD (Yoshida et al., 2019; Lin et al., 2022), while in tumors promoting ferroptosis can inhibit disease progression (Yan et al., 2021). We need to weigh this issue when using ferroptosis reagents in patients with multiple diseases at the same time in clinical practice. In the meantime, a large number of clinical studies are still needed to investigate the administration routes to be sure. Finally, there is crosstalk between ferroptosis and other cell death, such as cuproptosis, which has been widely debated recently (Tsvetkov et al., 2022). Further elucidation of the interrelationship between different cell death modalities is also necessary to explore the mechanisms involved and to develop therapeutic approaches.

In conclusion, ferroptosis, as a new mode of cell death, has considerable potential for research in airway inflammatory diseases, and with more in-depth exploration, it will certainly bring new strategies for the diagnosis and treatment of the disease. Given the complex pathology of various types of airway inflammatory diseases, although many preclinical studies have shown ferroptosis to be a promising drug target, the potential molecular signaling pathways and networks in various types of target cells in these diseases remain to be explored in depth.

## Author contributions

LZ contributed to determining the outline and content of the review. ZL, XY, LG, LQ, and JD contributed to retrieving literature and writing a draft of this manuscript. All authors contributed to revising the draft critically for important intellectual content, providing final confirmation of the revised version, and being responsible for all aspects of the work. The authors read and approved the final manuscript.

## Funding

This work was supported by the Basic Research Program of Guangzhou (No. 202102010224), 2021 Characteristic innovation projects of colleges and universities in Guangdong Province (No. 2021KTSCX089), 2022 Guangzhou Medical University Student Innovation Ability Improvement Program project (No. 2022), 2021 Industry-University Cooperative Education Program of Higher Education Department (No. 202102557013) and the grant of State Key Laboratory of Respiratory Disease (No. SKLRD-Z-202203), Clinical Transformation Program of the First Affiliated Hospital of Guangzhou Medical University (Nos. ZH201802 and ZH201914) and Natural Science Foundation of Guangdong Province (No. 2018A030310172).

## Acknowledgments

We thank Yaqin Li (Guangdong University of Foreign Studies) for her help in the production of the figures in the manuscript.

## Conflict of interest

The authors declare that the research was conducted in the absence of any commercial or financial relationships that could be construed as a potential conflict of interest.

## Publisher's note

All claims expressed in this article are solely those of the authors and do not necessarily represent those of their affiliated

## References

- Aghasafari, P., George, U., and Pidaparti, R. (2019). A review of inflammatory mechanism in airway diseases. *Inflamm. Res.* 68 (1), 59–74. Epub 2018 Oct 10. PMID: 30306206. doi:10.1007/s00011-018-1191-2
- Ahmed, A. U. (2011). An overview of inflammation: mechanism and consequences. *Front. Biol. (Beijing)*. 6 (4), 274–281. doi:10.1007/s11515-011-1123-9
- Amaral, E. P., Costa, D. L., Namasivayam, S., Riteau, N., Kamenyeva, O., Mittereder, L., et al. (2019). A major role for ferroptosis in *Mycobacterium tuberculosis*-induced cell death and tissue necrosis. *J. Exp. Med.* 216 (3), 556–570. doi:10.1084/jem.20181776
- Anderson, G. J., Frazer, D. M., and McLaren, G. D. (2009). Iron absorption and metabolism. *Curr. Opin. Gastroenterol.* 25 (2), 129–135. doi:10.1097/MOG.0b013e32831ef1f7
- Andrade, B. B., Pavan Kumar, N., Mayer-Barber, K. D., Barber, D. L., Sridhar, R., Rekha, V. V. B., et al. (2013). Plasma heme oxygenase-1 levels distinguish latent or successfully treated human tuberculosis from active disease. *PLoS one* 8 (5), e62618. doi:10.1371/journal.pone.0062618
- Becker, T., and Wagner, R. (2018). Mitochondrial outer membrane channels: emerging diversity in transport processes. *Bioessays*. 40 (7), e1800013. doi:10.1002/bies.201800013
- Berlin, D. A., Gulick, R. M., and Martinez, F. J. (2020). Severe covid-19. *N. Engl. J. Med. Overseas. Ed.* 383 (25), 2451–2460. PMID: 32412710. doi:10.1056/nejmcp2009575
- Bersuker, K., Hendricks, J. M., Li, Z., Magtanong, L., Ford, B., Tang, P. H., et al. (2019). The CoQ oxidoreductase FSP1 acts parallel to GPX4 to inhibit ferroptosis. *Nature* 575 (7784), 688–692. doi:10.1038/s41586-019-1705-2
- Blanco, J. C., Richardson, J. Y., Darnell, M. E., Rowzee, A., Pletneva, L., Porter, D. D., et al. (2002). Cytokine and chemokine gene expression after primary and secondary respiratory syncytial virus infection in cotton rats. *J. Infect. Dis.* 185 (12), 1780–1785. PMID: 12085325. doi:10.1086/340823
- Boelaert, J. R., Vandecasteele, S. J., Appelberg, R., and Gordeuk, V. R. (2007). The effect of the host's iron status on tuberculosis. *J. Infect. Dis.* 195 (12), 1745–1753. doi:10.1086/518040
- Bohmwald, K., Espinoza, J. A., Rey-Jurado, E., Gómez, R. S., González, P. A., Bueno, S. M., et al. (2016). Human respiratory syncytial virus: Infection and Pathology. *Semin. Respir. Crit. Care Med.* 37 (4), 522–537. Epub 2016 Aug 3. PMID: 27486734; PMCID: PMC17171722. doi:10.1055/s-0036-1584799
- Borges do Nascimento, I. J., Cacic, N., Abdulaezem, H. M., von Groote, T. C., Jayarajah, U., Weerasekara, I., et al. (2020). Novel Coronavirus infection (COVID-19) in humans: a scoping review and meta-analysis. *J. Clin. Med.* 9 (4), 941. PMID: 32235486; PMCID: PMC7230636. doi:10.3390/jcm9040941
- Bridges, R. J., Natale, N. R., and Patel, S. A. (2012). System xc<sup>-</sup> cystine/glutamate antiporter: An update on molecular pharmacology and roles within the CNS. *Br. J. Pharmacol.* 165 (1), 20–34. doi:10.1111/j.1476-5381.2011.01480.x
- Butt, Y., Kurdowska, A., and Allen, T. C. (2016). Acute lung injury: a clinical and molecular review. *Arch. Pathol. Lab. Med.* 140 (4), 345–350. doi:10.5858/arpa.2015-0519-RA
- Chang, R., Ng, T. B., and Sun, W. Z. (2020). Lactoferrin as potential preventative and adjunct treatment for COVID-19. *Int. J. Antimicrob. Agents* 56 (3), 106118. Epub 2020 Jul 30. PMID: 32738305; PMCID: PMC7390755. doi:10.1016/j.ijantimicag.2020.106118
- Christenson, S. A. (2017). Flipping the kill switch. *Sci. Transl. Med.* 9 (395), ean6192. doi:10.1126/scitranslmed.aan6192
- Chu, B., Kon, N., Chen, D., Li, T., Liu, T., Jiang, L., et al. (2019). ALOX12 is required for p53-mediated tumour suppression through a distinct ferroptosis pathway. *Nat. Cell Biol.* 21 (5), 579–591. Epub 2019 Apr 8. PMID: 30962574; PMCID: PMC6624840. doi:10.1038/s41556-019-0305-6
- Costa, D. L., Namasivayam, S., Amaral, E. P., Arora, K., Chao, A., Mittereder, L. R., et al. (2016). Pharmacological inhibition of host heme Oxygenase-1 suppresses organizations, or those of the publisher, the editors and the reviewers. Any product that may be evaluated in this article, or claim that may be made by its manufacturer, is not guaranteed or endorsed by the publisher.
- Mycobacterium tuberculosis* infection in vivo by a Mechanism dependent on T lymphocytes. *mBio* 7 (5), e01675-16. doi:10.1128/mBio.01675-16
- Cronin, S. J. F., Seehus, C., Weidinger, A., Talbot, S., Reissig, S., Seifert, M., et al. (2018). The metabolite BH4 controls T cell proliferation in autoimmunity and cancer. *Nature* 563 (7732), 564–568. Epub 2018 Nov 7. Erratum in: *Nature*. 2019 Aug;572(7769):E18. PMID: 30405245; PMCID: PMC6438708. doi:10.1038/s41586-018-0701-2
- Dalziel, S. R., Haskell, L., O'Brien, S., Borland, M. L., Plint, A. C., Babl, F. E., et al. (2022). Bronchiolitis. *Lancet*. S0140-6736 (22), 01016–01019. Epub ahead of print. PMID: 35785792. doi:10.1016/S0140-6736(22)01016-9
- Dar, H. H., Anthonyamuthu, T. S., Ponomareva, L. A., Souravong, A. B., Shurin, G. V., Kapralov, A. O., et al. (2021). A new thiol-independent mechanism of epithelial host defense against *Pseudomonas aeruginosa*: iNOS/NO sabotage of theft-ferroptosis. *Redox Biol.* 45, 102045. doi:10.1016/j.redox.2021.102045
- Dar, H. H., Tyurina, Y. Y., Mikulska-Ruminska, K., Shrivastava, L., Ting, H.-C., Tyurin, V. A., et al. (2018). *Pseudomonas aeruginosa* utilizes host polyunsaturated phosphatidylethanolamines to trigger theft-ferroptosis in bronchial epithelium. *J. Clin. Invest.* 128 (10), 4639–4653. doi:10.1172/JCI99490
- DeHart, D. N., Fang, D., Heslop, K., Li, L., Lemasters, J. J., and Maldonado, E. N. (2018). Opening of voltage dependent anion channels promotes reactive oxygen species generation, mitochondrial dysfunction and cell death in cancer cells. *Biochem. Pharmacol.* 148, 155–162. doi:10.1016/j.bcp.2017.12.022
- Dixon, S. J., Lemberg, K. M., Lamprecht, M. R., Skouta, R., Zaitsev, E. M., Gleason, C. E., et al. (2012). Ferroptosis: An iron-dependent form of nonapoptotic cell death. *Cell* 149 (5), 1060–1072. doi:10.1016/j.cell.2012.03.042
- Doll, S., Freitas, F. P., Shah, R., Aldrovandi, M., da Silva, M. C., Ingold, I., et al. (2019). FSP1 is a glutathione-independent ferroptosis suppressor. *Nature* 575 (7784), 693–698. doi:10.1038/s41586-019-1707-0
- Dolma, S., Lessnick, S. L., Hahn, W. C., and Stockwell, B. R. (2003). Identification of genotype-selective antitumor agents using synthetic lethal chemical screening in engineered human tumor cells. *Cancer Cell* 3 (3), 285–296. doi:10.1016/s1535-6108(03)00050-3
- Dong, H., Qiang, Z., Chai, D., Peng, J., Xia, Y., Hu, R., et al. (2020). Nrf2 inhibits ferroptosis and protects against acute lung injury due to intestinal ischemia reperfusion via regulating SLC7A11 and HO-1. *Aging* 12 (13), 12943–12959. doi:10.18632/aging.103378
- Dorhoi, A., and Kaufmann, S. H. (2014). Perspectives on host adaptation in response to *Mycobacterium tuberculosis*: modulation of inflammation. *Semin. Immunol.* 26 (6), 533–542. Epub 2014 Oct 25. PMID: 25453228. doi:10.1016/j.smim.2014.10.002
- Elsenhans, B., Janser, H., Windisch, W., and Schumann, K. (2011). Does lead use the intestinal absorptive pathways of iron? Impact of iron status on murine <sup>210</sup>Pb and <sup>59</sup>Fe absorption in duodenum and ileum in vivo. *Toxicology* 284 (1-3), 7–11. doi:10.1016/j.tox.2011.03.005
- Fratta Pasini, A. M., Stranieri, C., Girelli, D., Busti, F., and Cominacini, L. (2021). Is ferroptosis a key Component of the Process leading to multiorgan damage in COVID-19? *Antioxidants (Basel)* 10 (11), 1677. PMID: 34829548; PMCID: PMC8615234. doi:10.3390/antiox10111677
- Frossi, B., De Carli, M., Piemonte, M., and Pucillo, C. (2008). Oxidative microenvironment exerts an opposite regulatory effect on cytokine production by Th1 and Th2 cells. *Mol. Immunol.* 45 (1), 58–64. doi:10.1016/j.molimm.2007.05.008
- Fuchs, Y., and Steller, H. (2011). Programmed cell death in animal development and disease. *Cell* 147 (4), 742–758. doi:10.1016/j.cell.2011.10.033
- Gao, M., Monian, P., Pan, Q., Zhang, W., Xiang, J., and Jiang, X. (2016). Ferroptosis is an autophagic cell death process. *Cell Res.* 26 (9), 1021–1032. doi:10.1038/cr.2016.95
- García-Clemente, M., de la Rosa, D., Máiz, L., Girón, R., Blanco, M., Oliveira, C., et al. (2020). Impact of *Pseudomonas aeruginosa* infection on Patients with Chronic inflammatory airway diseases. *J. Clin. Med.*, 9, 3800. doi:10.3390/jcm9123800



- Han, Y., Zhu, J., Yang, L., Nilsson-Payant, B. E., Hurtado, R., Lacko, L. A., et al. (2022). SARS-CoV-2 infection induces ferroptosis of sinoatrial node pacemaker cells. *Circ. Res.* 130 (7), 963–977. Epub 2022 Mar 8. PMID: 35255712; PMCID: PMC8963443. doi:10.1161/CIRCRESAHA.121.320518
- Hou, W., Xie, Y., Song, X., Sun, X., Lotze, M. T., Zeh, H. J., et al. (2016). Autophagy promotes ferroptosis by degradation of ferritin. *Autophagy* 12 (8), 1425–1428. doi:10.1080/15548627.2016.1187366
- Huang, L., Shi, Y., Gong, B., Jiang, L., Zhang, Z., Liu, X., et al. (2021). Dynamic blood single-cell immune responses in patients with COVID-19. *Signal Transduct. Target. Ther.* 6 (1), 110. PMID: 33677468; PMCID: PMC7936231. doi:10.1038/s41392-021-00526-2
- Imai, H., Matsuoka, M., Kumagai, T., Sakamoto, T., and Koumura, T. (2017). Lipid Peroxidation-dependent Cell death regulated by GPx4 and ferroptosis. *Curr. Top. Microbiol. Immunol.* 403, 143–170. doi:10.1007/82\_2016\_508
- Jacobs, W., Lammens, M., Kerckhofs, A., Voets, E., Van San, E., Van Coillie, S., et al. (2020). Fatal lymphocytic cardiac damage in coronavirus disease 2019 (COVID-19): autopsy reveals a ferroptosis signature. *Esc. Heart Fail.* 7 (6), 3772–3781. Epub ahead of print. PMID: 32959998; PMCID: PMC7607145. doi:10.1002/ehf2.12958
- Jartti, T., Smits, H. H., Bønnelykke, K., Bircan, O., Elenius, V., Konradsen, J. R., et al. (2019). EAACI task force on Clinical practice recommendations on preschool wheeze. Bronchiolitis needs a revisit: Distinguishing between virus entities and their treatments. *Allergy* 74 (1), 40–52. Epub 2018 Nov 25. PMID: 30276826; PMCID: PMC6587559. doi:10.1111/all.13624
- Jiang, L., Kon, N., Li, T., Wang, S. J., Su, T., Hibshoosh, H., et al. (2015). Ferroptosis as a p53-mediated activity during tumour suppression. *Nature* 520 (7545), 57–62. Epub 2015 Mar 18. PMID: 25799988; PMCID: PMC4455927. doi:10.1038/nature14344
- Kagan, V. E., Mao, G., Qu, F., Angeli, J. P. F., Doll, S., Croix, C. S., et al. (2017). Oxidized arachidonic and adrenic PEs navigate cells to ferroptosis. *Nat. Chem. Biol.* 13 (1), 81–90. doi:10.1038/nchembio.2238
- Kim, H. K., and Han, J. (2020). Tetrahydrobiopterin in energy metabolism and metabolic diseases. *Pharmacol. Res.* 157, 104827. Epub 2020 Apr 26. PMID: 32348841. doi:10.1016/j.phrs.2020.104827
- Kobune, M., Kohgo, Y., Kato, J., Miyazaki, E., and Niitsu, Y. (1994). Interleukin-6 enhances hepatic transferrin uptake and ferritin expression in rats. *Hepatology* 19 (6), 1468–1475. PMID: 8188178. doi:10.1002/hep.1840190623
- Kraft, V. A. N., Bezjian, C. T., Pfeiffer, S., Ringelstetter, L., Müller, C., Zandkarimi, F., et al. (2020). GTP Cyclohydrolase 1/tetrahydrobiopterin counteract ferroptosis through lipid remodeling. *ACS Cent. Sci.* 6 (1), 41–53. Epub 2019 Dec 27. PMID: 31989025; PMCID: PMC6978838. doi:10.1021/acscentsci.9b01063
- Latremoliere, A., and Costigan, M. (2011). GCH1, BH4 and pain. *Curr. Pharm. Biotechnol.* 12 (10), 1728–1741. PMID: 21466440; PMCID: PMC4469332. doi:10.2174/138920111798357393
- Le, Y., Zhang, Z., Wang, C., and Lu, D. (2021). Ferroptotic cell death: new regulatory mechanisms for metabolic diseases. *Endocr. Metab. Immune Disord. Drug Targets* 21 (5), 785–800. doi:10.2174/187153032066200731175328
- Lee, H., Ko, E. H., Lai, M., Wei, N., Balroop, J., Kashem, Z., et al. (2014). Delineating the relationships among the formation of reactive oxygen species, cell membrane instability and innate autoimmunity in intestinal reperfusion injury. *Mol. Immunol.* 58 (2), 151–159. Epub 2013 Dec 22. PMID: 24365749; PMCID: PMC3924562. doi:10.1016/j.molimm.2013.11.012
- Lee, I. T., and Yang, C. M. (2013). Inflammatory signalings involved in airway and pulmonary diseases. *Mediat. Inflamm.* 2013, 791231. Epub 2013 Apr 4. PMID: 23690670; PMCID: PMC3649692. doi:10.1155/2013/791231
- Li, X., Zhang, Z., Wang, Z., Gutiérrez-Castrellón, P., and Shi, H. (2022). Cell deaths: Involvement in the pathogenesis and intervention therapy of COVID-19. *Signal Transduct. Target. Ther.* 7 (1), 186. PMID: 35697684; PMCID: PMC9189267. doi:10.1038/s41392-022-01043-6
- Li, X., Zhuang, X., and Qiao, T. (2019). Role of ferroptosis in the process of acute radiation-induced lung injury in mice. *Biochem. Biophys. Res. Commun.* 519 (2), 240–245. doi:10.1016/j.bbrc.2019.08.165
- Lin, Z., Xu, Y., Guan, L., Qin, L., Ding, J., Zhang, Q., et al. (2022). Seven ferroptosis-specific expressed genes are considered as potential biomarkers for the diagnosis and treatment of cigarette smoke-induced chronic obstructive pulmonary disease. *Ann. Transl. Med.* 10 (6), 331. PMID: 35433978; PMCID: PMC9011264. doi:10.21037/atm-22-1009
- Linkermann, A., Skouta, R., Himmerkus, N., Mulay, S. R., Dewitz, C., De Zen, F., et al. (2014). Synchronized renal tubular cell death involves ferroptosis. *Proc. Natl. Acad. Sci. U. S. A.* 111 (47), 16836–16841. doi:10.1073/pnas.1415518111
- Liu, P., Feng, Y., Li, H., Chen, X., Wang, G., Xu, S., et al. (2020). Ferrostatin-1 alleviates lipopolysaccharide-induced acute lung injury via inhibiting ferroptosis. *Cell. Mol. Biol. Lett.* 25, 10. doi:10.1186/s11658-020-00205-0
- Liu, X., Wang, L., Xing, Q., Li, K., Si, J., Ma, X., et al. (2021). Sevoflurane inhibits ferroptosis: A new mechanism to explain its protective role against lipopolysaccharide-induced acute lung injury. *Life Sci.* 275, 119391. doi:10.1016/j.lfs.2021.119391
- Liu, Y., and Gu, W. (2022). p53 in ferroptosis regulation: the new weapon for the old guardian. *Cell Death Differ.* 29 (5), 895–910. Epub 2022 Jan 27. PMID: 35087226; PMCID: PMC9091200. doi:10.1038/s41418-022-00943-y
- Liu, Y., and Gu, W. (2021). The complexity of p53-mediated metabolic regulation in tumor suppression. *Semin. Cancer Biol.* S1044–579X (21), 00060–00062. Epub ahead of print. PMID: 33785447; PMCID: PMC8473587. doi:10.1016/j.semcancer.2021.03.010
- Lizarraga, A., Cuerda, C., Junca, E., Bretón, I., Cambor, M., Velasco, C., et al. (2009). Atrophy of the intestinal villi in a post-gastrectomy patient with severe iron deficiency anemia. *Nutr. Hosp.* 24 (5), 618–621.
- Lumb, A. B. (2016). *Nunn's applied respiratory physiology eBook*. Amsterdam: Elsevier Health Sciences.
- Luo, X., Gong, H.-B., Gao, H.-Y., Wu, Y.-P., Sun, W.-Y., Li, Z.-Q., et al. (2021). Oxygenated phosphatidylethanolamine navigates phagocytosis of ferroptotic cells by interacting with TLR2. *Cell death Differ.* 28, 1971–1989. doi:10.1038/s41418-020-00719-2
- Maldonado, E. N. (2017). VDAC-Tubulin, an anti-warburg Pro-oxidant switch. *Front. Oncol.* 7, 4. doi:10.3389/fonc.2017.00004
- Mao, C., Liu, X., Zhang, Y., Lei, G., Yan, Y., Lee, H., et al. (2021). DHODH-mediated ferroptosis defence is a targetable vulnerability in cancer. *Nature* 593 (7860), 586–590. doi:10.1038/s41586-021-03539-7
- Mao, H., Zhao, Y., Li, H., and Lei, L. (2020). Ferroptosis as an emerging target in inflammatory diseases. *Prog. Biophys. Mol. Biol.* 155, 20–28. Epub 2020 Apr 18. PMID: 32311424. doi:10.1016/j.pbiomolbio.2020.04.001
- Mazure, N. M. (2017). VDAC in cancer. *Biochim. Biophys. Acta. Bioenerg.* 1858 (8), 665–673. doi:10.1016/j.bbabi.2017.03.002
- McBean, G. J. (2012). The transsulfuration pathway: A source of cysteine for glutathione in astrocytes. *Amino acids* 42 (1), 199–205. doi:10.1007/s00726-011-0864-8
- Nai, A., Lorè, N. I., Pagani, A., De Lorenzo, R., Di Modica, S., Salvi, F., et al. (2021). Hepcidin levels predict Covid-19 severity and mortality in a cohort of hospitalized Italian patients. *Am. J. Hematol.* 96 (1), E32–E35. Epub 2020 Nov 3. PMID: 33075189. doi:10.1002/ajh.26027
- Nemeth, E., Rivera, S., Gabayan, V., Keller, C., Taudorf, S., Pedersen, B. K., et al. (2004). IL-6 mediates hypoferrremia of inflammation by inducing the synthesis of the iron regulatory hormone hepcidin. *J. Clin. Invest.* 113 (9), 1271–1276. PMID: 15124018; PMCID: PMC398432. doi:10.1172/JCI20945
- Ou, Y., Wang, S. J., Jiang, L., Zheng, B., and Gu, W. (2015). p53 Protein-mediated regulation of phosphoglycerate dehydrogenase (PHGDH) is crucial for the apoptotic response upon serine starvation. *J. Biol. Chem.* 290 (1), 457–466. Epub 2014 Nov 17. PMID: 25404730; PMCID: PMC4281747. doi:10.1074/jbc.M114.616359
- Ou, Y., Wang, S. J., Li, D., Chu, B., and Gu, W. (2016). Activation of SAT1 engages polyamine metabolism with p53-mediated ferroptotic responses. *Proc. Natl. Acad. Sci. U. S. A.* 113 (44), E6806–E6812. Epub 2016 Oct 3. PMID: 27698118; PMCID: PMC5098629. doi:10.1073/pnas.1607152113
- Perricone, C., Bartoloni, E., Bursi, R., Cafaro, G., Guidelli, G. M., Shoenfeld, Y., et al. (2020). COVID-19 as part of the hyperferritinemic syndromes: the role of iron depletion therapy. *Immunol. Res.* 68 (4), 213–224. PMID: 32681497; PMCID: PMC7366458. doi:10.1007/s12026-020-09145-5
- Pignatello, J. J., Oliveros, E., and MacKay, A. (2006). Advanced Oxidation Processes for Organic contaminant destruction based on the Fenton reaction and related chemistry. *Crit. Rev. Environ. Sci. Technol.* 36 (1), 1–84. doi:10.1080/10643380500326564
- Qiang, Z., Dong, H., Xia, Y., Chai, D., Hu, R., and Jiang, H. (2020). Nrf2 and STAT3 alleviates ferroptosis-Mediated IIR-ALI by regulating SLC7A11. *Oxid. Med. Cell. Longev.* 2020, 5146982. doi:10.1155/2020/5146982
- Racanelli, A. C., Kikkers, S. A., Choi, A. M. K., and Cloonan, S. M. (2018). Autophagy and inflammation in chronic respiratory disease. *Autophagy* 14 (2), 221–232. Epub 2018 Feb 8. PMID: 29130366; PMCID: PMC5902194. doi:10.1080/15548627.2017.1389823
- Redant, S., Nehar-Stern, N., Honoré, P. M., Attou, R., Haggenmacher, C., Tolwani, A., et al. (2021). Acute bronchiolitis: Why put an IV line? *J. Transl. Int. Med.* 9 (3), 185–189. PMID: 34900629; PMCID: PMC8629411. doi:10.2478/jtim-2021-0013

- Rossaint, J., Nadler, J. L., Ley, K., and Zarbock, A. (2012). Eliminating or blocking 12/15-lipoxygenase reduces neutrophil recruitment in mouse models of acute lung injury. *Crit. Care* 16 (5), R166. PMID: 22973824; PMCID: PMC3682261. doi:10.1186/cc11518
- Salimi, V., Ramezani, A., Mirzaei, H., Tahamtan, A., Faghihloo, E., Rezaei, F., et al. (2017). Evaluation of the expression level of 12/15 lipoxygenase and the related inflammatory factors (CCL5, CCL3) in respiratory syncytial virus infection in mice model. *Microb. Pathog.* 109, 209–213. Epub 2017 Jun 1. PMID: 28579398. doi:10.1016/j.micpath.2017.05.045
- Schaible, U. E., Collins, H. L., Priem, F., and Kaufmann, S. H. E. (2002). Correction of the iron overload defect in beta-2-microglobulin knockout mice by lactoferrin abolishes their increased susceptibility to tuberculosis. *J. Exp. Med.* 196 (11), 1507–1513. doi:10.1084/jem.20020897
- Shah, R., Shchepinov, M. S., and Pratt, D. A. (2018). Resolving the role of lipoxygenases in the initiation and execution of ferroptosis. *ACS Cent. Sci.* 4 (3), 387–396. doi:10.1021/acscentsci.7b00589
- Soula, M., Weber, R. A., Zilka, O., Alwaseem, H., La, K., Yen, F., et al. (2020). Metabolic determinants of cancer cell sensitivity to canonical ferroptosis inducers. *Nat. Chem. Biol.* 16 (12), 1351–1360. Epub 2020 Aug 10. PMID: 32778843; PMCID: PMC8299533. doi:10.1038/s41589-020-0613-y
- Sun, Y., Chen, P., Zhai, B., Zhang, M., Xiang, Y., Fang, J., et al. (2020). The emerging role of ferroptosis in inflammation. *Biomed. Pharmacother.* 127, 110108. Epub 2020 Mar 29. PMID: 32234642. doi:10.1016/j.biopha.2020.110108
- Suzuki, S., Tanaka, T., Poyurovsky, M. V., Nagano, H., Mayama, T., Ohkubo, S., et al. (2010). Phosphate-activated glutaminase (GLS2), a p53-inducible regulator of glutamine metabolism and reactive oxygen species. *Proc. Natl. Acad. Sci. U. S. A.* 107 (16), 7461–7466. Epub 2010 Mar 29. PMID: 20351271; PMCID: PMC2867754. doi:10.1073/pnas.1002459107
- Tsvetkov, P., Coy, S., Petrova, B., Dreishpoon, M., Verma, A., Abdusamad, M., et al. (2022). Copper induces cell death by targeting lipoylated TCA cycle proteins. *Science* 375 (6586), 1254–1261. Epub 2022 Mar 17. Erratum in: *Science*. 2022 Apr 22;376(6591):eabq4855. PMID: 35298263; PMCID: PMC9273333. doi:10.1126/science.abf0529
- Wang, H., An, P., Xie, E., Wu, Q., Fang, X., Gao, H., et al. (2017). Characterization of ferroptosis in murine models of hemochromatosis. *Hepatology* 66 (2), 449–465. doi:10.1002/hep.29117
- Wang, J., Wang, L., Li, L., Xu, J., Xu, C., Li, X., et al. (2020). Enlightenments of asymptomatic Cases of SARS-CoV-2 infection. *J. Transl. Int. Med.* 8 (2), 112–114. PMID: 32983934; PMCID: PMC7500117. doi:10.2478/jtim-2020-0017
- Wang, M. P., Joshua, B., Jin, N. Y., Du, S. W., and Li, C. (2021). Ferroptosis in viral infection: the unexplored possibility. *Acta Pharmacol. Sin.*, 1–11. Epub ahead of print. PMID: 34873317; PMCID: PMC8646346. doi:10.1038/s41401-021-00814-1
- Wang, Y., Huang, J., Sun, Y., Stubbs, D., He, J., Li, W., et al. (2021). SARS-CoV-2 suppresses mRNA expression of selenoproteins associated with ferroptosis, endoplasmic reticulum stress and DNA synthesis. *Food Chem. Toxicol.* 153, 112286. Epub 2021 May 21. PMID: 34023458; PMCID: PMC8139185. doi:10.1016/j.fct.2021.112286
- Wang, Y., and Tang, M. (2019). PM2.5 induces ferroptosis in human endothelial cells through iron overload and redox imbalance. *Environ. Pollut.* 254, 112937. doi:10.1016/j.envpol.2019.07.105
- Warner, G. J., Berry, M. J., Moustafa, M. E., Carlson, B. A., Hatfield, D. L., and Faust, J. R. (2000). Inhibition of selenoprotein synthesis by selenocysteine tRNA [Ser]Sec lacking isopentenyladenosine. *J. Biol. Chem.* 275 (36), 28110–28119. doi:10.1074/jbc.M001280200
- Winterbourn, C. C. (1995). Toxicity of iron and hydrogen peroxide: the Fenton reaction. *Toxicol. Lett.* 82–83, 969–974. doi:10.1016/0378-4274(95)03532-x
- Wu, Y., Chen, H., Xuan, N., Zhou, L., Wu, Y., Zhu, C., et al. (2020). Induction of ferroptosis-like cell death of eosinophils exerts synergistic effects with glucocorticoids in allergic airway inflammation. *Thorax* 75 (11), 918–927. doi:10.1136/thoraxjnl-2020-214764
- Xu, S., He, Y., Lin, L., Chen, P., Chen, M., and Zhang, S. (2021). The emerging role of ferroptosis in intestinal disease. *Cell Death Dis.* 12 (4), 289. doi:10.1038/s41419-021-03559-1
- Xu, T., Ding, W., Ji, X., Ao, X., Liu, Y., Yu, W., et al. (2019). Molecular mechanisms of ferroptosis and its role in cancer therapy. *J. Cell. Mol. Med.* 23 (8), 4900–4912. doi:10.1111/jcmm.14511
- Xu, Y., Li, X., Cheng, Y., Yang, M., and Wang, R. (2020). Inhibition of ACSL4 attenuates ferroptotic damage after pulmonary ischemia-reperfusion. *FASEB J. official Publ. Fed. Am. Soc. Exp. Biol.* 34 (12), 16262–16275. doi:10.1096/fj.202001758R
- Yagoda, N., von Rechenberg, M., Zaganjori, E., Bauer, A. J., Yang, W. S., Fridman, D. J., et al. (2007). RAS-RAF-MEK-dependent oxidative cell death involving voltage-dependent anion channels. *Nature* 447 (7146), 864–868. doi:10.1038/nature05859
- Yan, H. F., Zou, T., Tuo, Q. Z., Xu, S., Li, H., Belaidi, A. A., et al. (2021). Ferroptosis: mechanisms and links with diseases. *Signal Transduct. Target Ther.* 6 (1), 49. PMID: 33536413; PMCID: PMC7858612. doi:10.1038/s41392-020-00428-9
- Yang, H., and Lu, S. (2020). COVID-19 and Tuberculosis. *J. Transl. Int. Med.* 8 (2), 59–65. PMID: 32983927; PMCID: PMC7500119. doi:10.2478/jtim-2020-0010
- Yang, W. S., Kim, K. J., Gaschler, M. M., Patel, M., Shchepinov, M. S., and Stockwell, B. R. (2016). Peroxidation of polyunsaturated fatty acids by lipoxygenases drives ferroptosis. *Proc. Natl. Acad. Sci. U. S. A.* 113 (34), E4966–E4975. doi:10.1073/pnas.1603244113
- Yang, W. S., SriRamaratnam, R., Welsch, M. E., Shimada, K., Skouta, R., Viswanathan, V. S., et al. (2014). Regulation of ferroptotic cancer cell death by GPX4. *Cell* 156 (1–2), 317–331. doi:10.1016/j.cell.2013.12.010
- Yang, W. S., and Stockwell, B. R. (2008). Synthetic lethal screening identifies compounds activating iron-dependent, nonapoptotic cell death in oncogenic-RAS-harboring cancer cells. *Chem. Biol.* 15 (3), 234–245. doi:10.1016/j.chembiol.2008.02.010
- Yi, Y., Lagniton, P. N. P., Ye, S., Li, E., and Xu, R. H. (2020). COVID-19: what has been learned and to be learned about the novel coronavirus disease. *Int. J. Biol. Sci.* 16 (10), 1753–1766. PMID: 32226295; PMCID: PMC7098028. doi:10.7150/ijbs.45134
- Yoshida, M., Minagawa, S., Araya, J., Sakamoto, T., Hara, H., Tsubouchi, K., et al. (2019). Involvement of cigarette smoke-induced epithelial cell ferroptosis in COPD pathogenesis. *Nat. Commun.* 10 (1), 3145. doi:10.1038/s41467-019-10991-7
- Yuan, H., Li, X., Zhang, X., Kang, R., and Tang, D. (2016). Cisd1 inhibits ferroptosis by protection against mitochondrial lipid peroxidation. *Biochem. Biophys. Res. Commun.* 478 (2), 838–844. Epub 2016 Aug 7. PMID: 27510639. doi:10.1016/j.bbrc.2016.08.034
- Zhang, Y., Swanda, R. V., Nie, L., Liu, X., Wang, C., Lee, H., et al. (2021). mTORC1 couples cyst(e)ine availability with GPX4 protein synthesis and ferroptosis regulation. *Nat. Commun.* 12 (1), 1589. doi:10.1038/s41467-021-21841-w
- Zhao, J., Dar, H. H., Deng, Y., St Croix, C. M., Li, Z., Minami, Y., et al. (2020). PEBP1 acts as a rheostat between prosurvival autophagy and ferroptotic death in asthmatic epithelial cells. *Proc. Natl. Acad. Sci. U. S. A.* 117 (25), 14376–14385. doi:10.1073/pnas.1921618117
- Zhou, C., Chen, Y., Ji, Y., He, X., and Xue, D. (2020). Increased serum levels of hepcidin and ferritin are associated with severity of COVID-19. *Med. Sci. Monit.* 26, e926178. PMID: 32978363; PMCID: PMC7526336. doi:10.12659/MSM.926178
- Zhou, H., Li, F., Niu, J.-Y., Zhong, W.-Y., Tang, M.-Y., Lin, D., et al. (2019). Ferroptosis was involved in the oleic acid-induced acute lung injury in mice. *Sheng Li Xue Bao* 71 (5), 689–697.
- Zille, M., Karuppagounder, S. S., Chen, Y., Gough, P. J., Bertin, J., Finger, J., et al. (2017). Neuronal death after hemorrhagic stroke *in vitro* and *in vivo* shares features of ferroptosis and necroptosis. *Stroke* 48 (4), 1033–1043. doi:10.1161/STROKEAHA.116.015609

## Glossary

<b>ROS</b> Reactive oxygen species	<b>IIR-ALI</b> Intestinal ischemia/reperfusion-induced acute lung injury
<b>PUFAs</b> Polyunsaturated fatty acids	<b>OGD/R</b> Oxygen-glucose deprivation and reoxygenation
<b>GSH</b> Glutathione	<b>HO-1</b> Heme oxygenase-1
<b>GPx</b> Glutathione peroxidase	<b>Lung-IR</b> Lung ischemia-reperfusion
<b>RCD</b> Regulated cell death	<b>RILI</b> Radiation-induced lung injury
<b>System Xc-</b> Cystine/glutamate transporter	<b>pLoxA</b> Lipoxygenase
<b>GPxs</b> Glutathione peroxidases	<b>AA-PE</b> Arachidonic acid-phosphatidyl ethanolamine
<b>H<sub>2</sub>O<sub>2</sub></b> Hydrogen peroxide	<b>15-HO-AA-PE</b> 15-hydroperoxy-AA-PE
<b>IPP</b> Isopentenyl pyrophosphate	<b>CMA</b> Chaperon-mediated autophagy
<b>VDACs</b> Voltage-dependent anion channels	<b>15-hPET-PE</b> 15-hydroperoxy- arachidonyl-PE
<b>OH</b> Hydroxyl radicals	<b>Mtb</b> Mycobacterium tuberculosis
<b>NTBI</b> Non-transferrin-bound iron	<b>TB</b> Tuberculosis
<b>LPO</b> Lipid hydroperoxide	<b>COPD</b> Chronic obstructive pulmonary disease
<b>ALI</b> Acute lung injury	<b>CS</b> Cigarette smoke
<b>OA</b> Oleic acid	<b>HBECs</b> Human bronchial epithelial cells
<b>BALF</b> Bronchoalveolar lavage fluid	<b>DAMPs</b> Damage-associated molecular patterns
<b>MDA</b> Malondialdehyde	<b>PM<sub>2.5</sub></b> Particulate matter 2.5
<b>LPS</b> Lipopolysaccharide	<b>AMs</b> Alveolar macrophages
<b>4-HNE</b> 4-hydroxynonenal	<b>FINs</b> Ferroptosis inducers
	<b>15LO1-PEBP1</b> 15-lipoxygenase-1-PEBP1



## OPEN ACCESS

## EDITED BY

Guo Chen,  
China Pharmaceutical University, China

## REVIEWED BY

Yi Wang,  
Sichuan Academy of Medical Sciences  
and Sichuan Provincial People's  
Hospital, China  
Xin Wang,  
National Institutes of Health (NIH),  
United States

## \*CORRESPONDENCE

Yanqin Guo,  
yanqinguo@sina.com  
Luxin Li,  
liluxin@mdjmu.edu.cn

## SPECIALTY SECTION

This article was submitted to Molecular  
Diagnostics and Therapeutics,  
a section of the journal  
Frontiers in Molecular Biosciences

RECEIVED 09 June 2022

ACCEPTED 25 July 2022

PUBLISHED 26 August 2022

## CITATION

Ma H, Dong Y, Chu Y, Guo Y and Li L  
(2022), The mechanisms of ferroptosis  
and its role in alzheimer's disease.  
*Front. Mol. Biosci.* 9:965064.  
doi: 10.3389/fmolb.2022.965064

## COPYRIGHT

© 2022 Ma, Dong, Chu, Guo and Li. This  
is an open-access article distributed  
under the terms of the [Creative  
Commons Attribution License \(CC BY\)](#).  
The use, distribution or reproduction in  
other forums is permitted, provided the  
original author(s) and the copyright  
owner(s) are credited and that the  
original publication in this journal is  
cited, in accordance with accepted  
academic practice. No use, distribution  
or reproduction is permitted which does  
not comply with these terms.

# The mechanisms of ferroptosis and its role in alzheimer's disease

Hongyue Ma<sup>1</sup>, Yan Dong<sup>1</sup>, Yanhui Chu<sup>2,3</sup>, Yanqin Guo<sup>1,3\*</sup> and  
Luxin Li<sup>2,3\*</sup>

<sup>1</sup>Department of Neurology, Hongqi Hospital of Mudanjiang Medical University, Mudanjiang, China,

<sup>2</sup>College of Life Sciences, Mudanjiang Medical University, Mudanjiang, China, <sup>3</sup>Heilongjiang Key  
Laboratory of Tissue Damage and Repair, Mudanjiang Medical University, Mudanjiang, China

Alzheimer's disease (AD) accounts for two-thirds of all dementia cases, affecting 50 million people worldwide. Only four of the more than 100 AD drugs developed thus far have successfully improved AD symptoms. Furthermore, these improvements are only temporary, as no treatment can stop or reverse AD progression. A growing number of recent studies have demonstrated that iron-dependent programmed cell death, known as ferroptosis, contributes to AD-mediated nerve cell death. The ferroptosis pathways within nerve cells include iron homeostasis regulation, cystine/glutamate (Glu) reverse transporter (system xc<sup>-</sup>), glutathione (GSH)/glutathione peroxidase 4 (GPX4), and lipid peroxidation. In the regulation pathway of AD iron homeostasis, abnormal iron uptake, excretion and storage in nerve cells lead to increased intracellular free iron and Fenton reactions. Furthermore, decreased Glu transporter expression leads to Glu accumulation outside nerve cells, resulting in the inhibition of the system xc<sup>-</sup> pathway. GSH depletion causes abnormalities in GPX4, leading to excessive accumulation of lipid peroxides. Alterations in these specific pathways and amino acid metabolism eventually lead to ferroptosis. This review explores the connection between AD and the ferroptosis signaling pathways and amino acid metabolism, potentially informing future AD diagnosis and treatment methodologies.

## KEYWORDS

Alzheimer's disease, ferroptosis, oxidative stress, p53, lipid peroxidation

## Introduction

Programmed cell death occurs by apoptosis, necroptosis, pyroptosis, ferroptosis, and cell death associated with autophagy and unprogrammed necrosis (Moujalled et al., 2021). In 2003, Dolma et al. (2003) revealed that the compound erastin could kill tumor cells *via* an RAS oncogene mutation, but cell death was not involved in changing the nucleus and caspase-3 activation. Yang et al. expanded on these results, discovering RAS-selective lethal compound 3, later shown to be the inducer of ferroptosis (Zhang et al., 2004; Yang and Stockwell, 2008). In 2012, Dixon et al. were the first to report ferroptosis as a type of cell death (Dixon et al., 2012). The occurrence of ferroptosis is related to the metabolism of iron, amino acids, GSH, reactive oxygen species (ROS), and lipid peroxides (LPOs). Fe<sup>3+</sup> in the extracellular fluid is transported to cells *via* transferrin (Tf) and subsequently



reduced to  $\text{Fe}^{2+}$ . Excessive  $\text{H}_2\text{O}_2$  reacts with the  $\text{Fe}^{2+}$  in cells to generate a large number of ROS through Fenton reactions, which promote the generation of intracellular LPOs and trigger ferroptosis. Electron microscope examination of cellular morphology during ferroptosis showed that the membrane ruptures, bubbles develop within mitochondria, which then atrophy, the mitochondrial cristae shrink or disappear, and the membrane density increases. Furthermore, although the nuclear shape appears normal, condensed chromatin is lacking (Xia et al., 2021; Ou et al., 2022). Biological activity is also altered. ROS and iron ions aggregate, the mitogen-activated protein kinase (MAPK) system is activated, cystine uptake is reduced, GSH is depleted, and system  $\text{xc}^-$  is inhibited (Shin et al., 2018). A recent study found reduced iron accumulation, lipid peroxidation, and GSH and GPX4 in patients with neurodegenerative diseases. Magnetic resonance imaging showed that iron deposition is correlated with cognitive impairment, and this deposition is mainly observed in the hippocampus, cortex, and basal ganglia, where brain cells experience oxidative stress, lipid peroxidation, and increased cystine/Glu transporter expression, iron metabolism, and balance (Ghadery et al., 2015; Masaldan et al., 2019). Iron is deposited in the brain cells of AD patients, and excessive iron will exacerbate oxidative damage and cognitive deficits (Bao et al., 2021). Given this evidence an in-depth understanding of ferroptosis mechanisms involved in the occurrence and development of AD is needed to facilitate timely diagnosis and treatment before major brain damage occurs, improving the survival rate and quality of life of AD patients. The purpose of the present review is to summarize the mechanism of ferroptosis in nerve cells and further analyze the possible pathway of ferroptosis involved in AD, summarize the relationship between ferroptosis-related drugs and AD, and propose methods for future clinical practice.

## Mechanisms of ferroptosis

### Iron homeostasis and ferroptosis

The maintenance of iron homeostasis is essential for normal physiological function. There are two forms of iron in cells:  $\text{Fe}^{3+}$  and  $\text{Fe}^{2+}$ . As a storage and transportation form of iron,  $\text{Fe}^{3+}$  is relatively stable.  $\text{Fe}^{2+}$  can transfer electrons, participate in various oxidation-reduction reactions and act as a reaction catalyst. An imbalance in iron homeostasis can result in lipid peroxidation and cellular oxidative stress, ultimately leading to ferroptosis. Therefore, the transfer in, transfer out, storage, and turnover of iron play important roles in the ferroptosis process.

Iron is transported by cells in two forms, Tf bound and non-Tf-bound iron. Tf is the primary protein responsible for iron transport. Under physiological conditions,  $\text{Fe}^{3+}$  is transferred into brain microvascular endothelial cells through endocytosis

mediated by transferrin receptor 1 (TfR1) and Tf on the luminal side of the cells (Masaldan et al., 2019). In the acidic environment of the endosome,  $\text{Fe}^{3+}$  is reduced to  $\text{Fe}^{2+}$  by the six-transmembrane epithelial antigen of prostate 3 (Derry et al., 2020; Li et al., 2020; Reichert et al., 2020; Jia et al., 2021). The divalent metal transporter 1 or zinc-iron regulatory protein family 8/14 can assist in moving the iron into the labile iron pool (LIP) (Derry et al., 2020; Li et al., 2020; Reichert et al., 2020; Jia et al., 2021; Qu et al., 2022). Under normal physiological conditions, oxidation–reduction activity of  $\text{Fe}^{2+}$  in the form of LIP is maintained at a low concentration (approximately 0.2–0.5  $\mu\text{M}$ ) to meet metabolic requirements (Petrat et al., 1999).

GSH has a high affinity with  $\text{Fe}^{2+}$  and the major component of LIP in the cytosol is presented as the GSH- $\text{Fe}^{2+}$  conjugates (Lv and Shang, 2018). A decrease in intracellular GSH, increases the concentration of  $\text{Fe}^{2+}$  facilitating the Fenton reaction. The storage of labile iron in ferritin serves to circumvent its high reactivity, avoiding the generation of reactive species (Reichert et al., 2020). Ferritin is an intracellular complex of 24 subunits (composed of heavy and light ferritin chains) that stores up to 4,500 iron atoms in an inactive oxidized and reduced forms to protect cells and tissues from oxidative damage (De Domenico et al., 2009). The primary function of ferritin is to maintain the equilibrium between the reduced ( $\text{Fe}^{2+}$ ) and oxidized states ( $\text{Fe}^{3+}$ ) (Reichert et al., 2020). Ferritin can catalyze excessive intracellular  $\text{Fe}^{2+}$  into non-toxic  $\text{Fe}^{3+}$  in the presence of proteins related to iron metabolism, which are closely bound and stored in the ferritin complex to maintain iron homeostasis (Reichert et al., 2020). An iron metabolism imbalance—caused by abnormal ferritin—will induce ferroptosis (Mancias et al., 2015; Tang et al., 2018). Nuclear receptor coactivator 4 (NCOA4) is a selective carrier receptor that can perform selective autophagy of ferritin (ferritinophagy) when intracellular iron levels are low so that iron is released (Ling et al., 2017). Arginine on the surface of the heavy ferritin chain FTH1 binds to a C-terminal domain of NCOA4 when iron levels are low, thereby promoting the transfer of autophagosomes to lysosomes (Mancias et al., 2015; Tang et al., 2018; Cheng et al., 2021). Mancias et al. (2015) demonstrated that the amount of NCOA4 depends on whether it interacts with the HERC2 protein. NCOA4 on the autophagosome targets the HERC2 protein when intracellular iron levels are high and is degraded by the proteasome. NCOA4 degradation ultimately reduces the breakdown of ferritin. NCOA4-mediated ferritinophagy participates in some physiological processes associated with iron metabolism in the cell, including erythropoiesis. Recent evidence suggests that autophagy is a conserved catabolic cellular pathway. Moreover, the loss of HERC2 causes severe neurodevelopmental abnormalities, contributing to neurogenetic diseases (Morice-Picard et al., 2016; Tang et al., 2018). Therefore, it is thought that HERC2 deficiency would

result in a malfunctioning response to elevated iron levels, resulting in ferritinophagy, free iron release, and neuronal cell damage.

Studies have shown that the intracellular LIP level is regulated by ferritin (Reichert et al., 2020), and in ferroptosis, ferritinophagy increases LIP (Dixon and Stockwell, 2014), which can activate the Fenton and Haber–Weiss reactions to generate ROS (Lane et al., 2018). Specifically, the ROS  $H_2O_2$  oxidizes  $Fe^{2+}$  to  $Fe^{3+}$  via the Fenton reaction, forming the highly active hydroxyl radical ( $\cdot OH$ ), inducing oxidative stress and leading to ferroptosis, the accumulation of lipid-OOH, and the oxidation of polyunsaturated fatty acids (PUFAs) (Kehrer, 2000; Qi et al., 2020).

To date, ferroportin 1 (FPN1, also known as solute carrier family 40 member 1) is the only nonheme cellular iron exporter identified in mammals. It transports iron from iron storage cells into the blood to optimize systemic iron homeostasis. In the central nervous system, FPN1 is distributed in most cell types, including neurons, astrocytes, oligodendrocytes, and brain microvascular endothelial cells (Bao et al., 2021). In neurons, amyloid precursor protein (APP) connects to FPN1 and stabilizes the expression level of FPN1. APP is also an iron oxidase that can oxidize  $Fe^{2+}$  to  $Fe^{3+}$  and transfer it out of cells (Duce et al., 2010). FPN1 is essential to embryonic development: mice with a global FPN1 deletion are embryonically lethal (Drakesmith et al., 2015).

## Cystine/glutamate reverse transport system, GPX4 and ferroptosis

System  $x_c^-$  is a heterodimer composed of two solute carriers, solute carrier family 3A2 (SLC3A2) and solute carrier family 7A11 (SLC7A11). Through system  $x_c^-$ , Glu and cystine enter and leave the cell in equal amounts. Cystine, which is ingested, is then reduced to gamma-glutamylcystine ( $\gamma$ -Glu-Cys) in the cell, which is involved in the synthesis of GSH. The excitatory amino acid Glu can induce the death of nerve cells, which is iron-dependent. It is speculated that Glu-induced death and ferroptosis may share the same signaling pathway. Studies have shown that system  $x_c^-$  is inhibited by ferroptosis (Sato et al., 2018; Li et al., 2020). Specifically, system  $x_c^-$  is inhibited by high extracellular Glu concentration, and decreasing intracellular GSH leads to peroxidase 4 (GPX4) inhibition and lipoxygenase (LOX) activation. Eventually, lipid peroxidation and cellular oxidative stress are generated, resulting in cell ferroptosis (Huang et al., 2020).

p53 plays a role in regulating ferroptosis via SLC7A11. The p53 tumor suppressor is “the guardian of the genome” that participates in the control of cell survival and division under various stresses. Beyond its effects on apoptosis, autophagy, and the cell cycle, p53 also regulates ferroptosis through a transcriptional or posttranslational mechanism. p53 can enhance ferroptosis by inhibiting the expression of SLC7A11 (Kang et al., 2019). A complete transactivation domain is

necessary for p53 to regulate SLC7A11 and ferroptosis. Although mutant p53 inhibits the expression of SLC7A11, thereby promoting ferroptosis (Jiang et al., 2015a; Latunde-Dada, 2017). p53 mutants do not inhibit SLC7A11 (Jiang et al., 2015b; Liu and Gu, 2022). Recent reports indicate a more complex mechanism in which wild-type p53 may enhance survival advantage by promoting antioxidation in some cases, and p53-mediated activation of p21 (encoded by CDKN1a) inhibits phospholipid oxidation by protecting intracellular mercaptans (including GSH) (Tarangelo et al., 2018; Hu et al., 2020; Tang et al., 2021). In addition, p53 plays a crucial role in regulating dynamic ROS. Jiang et al. found that p53 regulates antioxidant response under short-term stress, assisting cell recovery. However, continued activation of p53 triggers a pro-oxidation reaction that induces cell death. An ROS increase in the late stage of p53 activation is partly due to the inhibition of SLC7A11 (Jiang et al., 2015b). Chu et al. showed that p53 could indirectly trigger arachidonate 12-lipoxygenase (ALOX12) function through transcriptional inhibition of SLC7A11, thus leading to ALOX12-dependent ferroptosis resulting from ROS stress (Chu et al., 2019).

Cells have several death escape mechanisms. In the ferroptotic process, one of the most important and most studied mechanisms involves the enzyme glutathione peroxidase 4 (GPX4) (Reichert et al., 2020). In mammals, the GPX family consists of eight members. GPX1–GPX4 are selenoproteins that contain selenocysteine in the catalytic center. GPX4 is the only enzyme known to reduce complex phospholipid hydroperoxides directly (Xia et al., 2021). Hydroperoxides can activate catalytic reactions in the presence of transition metals such as iron, which eventually leads to ferroptosis. Therefore, GPX4 is key to cell survival (Friedmann Angeli et al., 2019). GSH is part of an intracellular antioxidant system that plays an important role in free radical scavenging, anti-aging and antioxidation activities, and other major physiological functions. In ferroptosis, GPX4 uses GSH as a substrate to mediate the lipid-OOH conversion to lipid-OH, and the sulfhydryl group in GSH reduction is readily dehydrogenated to form oxidized glutathione disulfide (GSSG), which plays an antioxidant role. GSSG is reduced to GSH by GSH reductase in NADPH-participating reactions (Qiu et al., 2020; Lei et al., 2021). GSH is continuously produced by glutamate cysteine ligase (GCL) and glutathione synthetase (GSS), and GCL activity is the rate-limiting step in GSH synthesis (Thompson et al., 2009; Parpura et al., 2017; Stockwell et al., 2017; Abdalkader et al., 2018; Shi et al., 2021; Yan et al., 2021). When reduced GCL and GSS activity limits the synthesis of GSH, GPX4 is eventually inactivated, resulting in the accumulation of lipid peroxidation, further ROS production, and ultimately, ferroptosis.

## Lipid metabolism and ferroptosis

Initiation of lipid peroxidation requires the removal of a bis-allylic hydrogen atom (located between two carbon–carbon

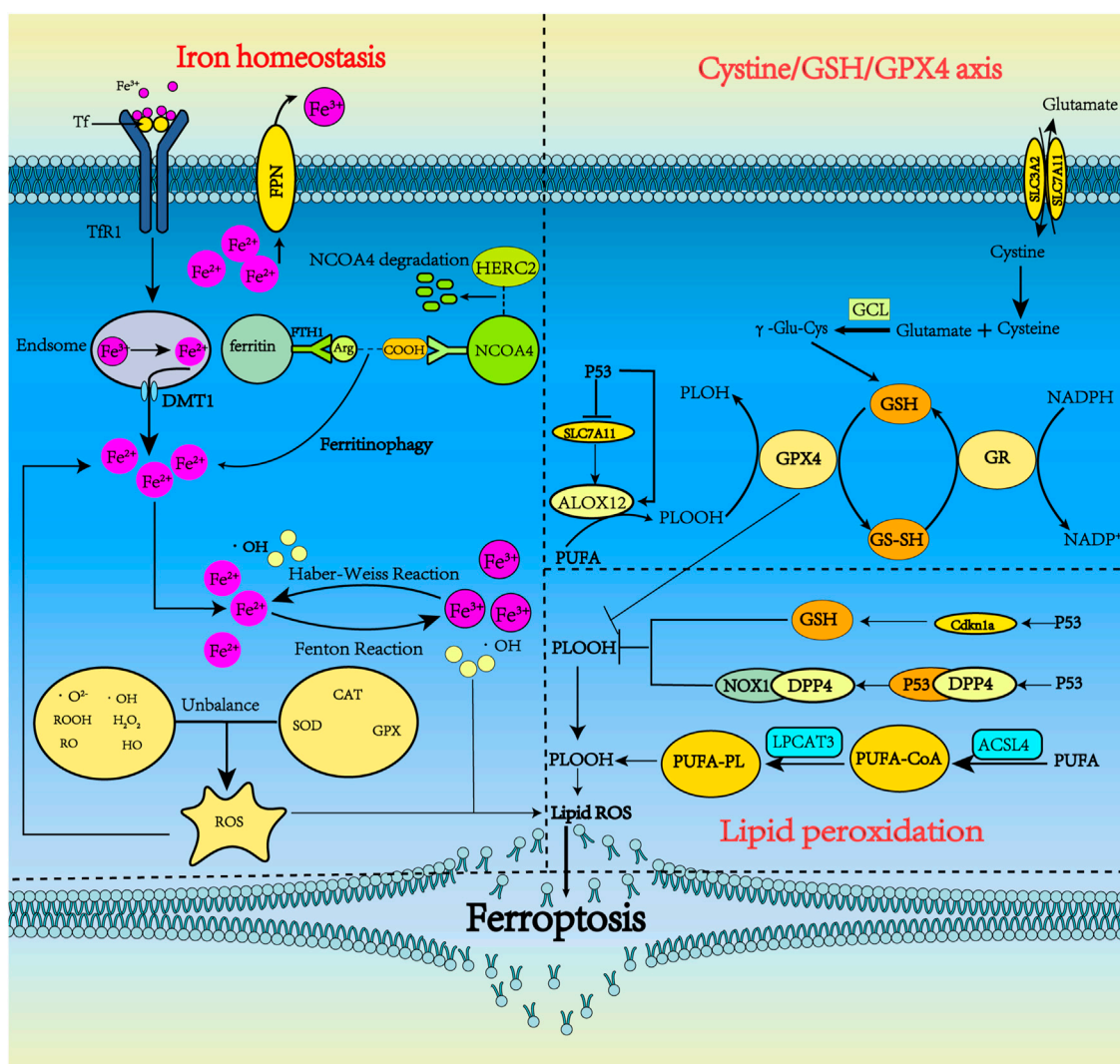


FIGURE 1

The metabolism pathways for ferroptosis. Ferroptosis can occur through three major pathways, iron homeostasis, the cystine/GSH/GPX4 axis, and lipid peroxidation. 1) Iron homeostasis. Tf carrying  $\text{Fe}^{3+}$  forms a complex with TFR1 and enters neurons via clathrin-mediated endocytosis.  $\text{Fe}^{3+}$  detaches from Tf and then is reduced by STEAP3.  $\text{Fe}^{2+}$  is pumped into the cytoplasm by DMT1 and is stored in ferritin in the form of  $\text{Fe}^{3+}$  when overloaded. Under some conditions, ferritin undergoes autophagy by binding with NCOA4, releasing iron, which subsequently leads to lethal iron levels and ferroptosis. NCOA4 can interact with HERC2, leading to NCOA4 degradation. Ferritinophagy increases LIP, which can activate the Fenton and Haber-Weiss reactions to generate ROS. 2) Cystine/GSH/GPX4 axis. System  $\text{xc}^-$  includes two chains: a specific light chain, SLC7A11, and a heavy chain, SLC3A2. Through system  $\text{xc}^-$ , Glu and cystine enter and leave the cell in equal amounts. Cystine, which is ingested, is then reduced to  $\gamma$ -Glu-Cys in the cell and becomes involved in the synthesis of GSH. GSH is continuously produced by GCL and GSS. In ferroptosis, GPX4 uses GSH as a substrate to mediate the lipid-OOH conversion to lipid-OH, and the sulfhydryl group in GSH reduction is readily dehydrogenated to form oxidized glutathione disulfide (GSSG), which plays an antioxidant role. P53 could indirectly trigger arachidonate 12-lipoxygenase (ALOX12) function through transcriptional inhibition of SLC7A11, thus leading to ALOX12-dependent ferroptosis resulting from ROS stress. 3) Lipid peroxidation. PUFA produces a large amount of lipid ROS through the continuous action of ACSL4 and LPCAT3. p53 can inhibit ferroptosis by inhibiting DPP4 activity or inducing CDKN1A expression.

double bonds) from polyunsaturated fatty acyl moieties in phospholipids (PUFA-PLs) incorporated into lipid bilayers. This process leads to the formation of a carbon-centered phospholipid radical ( $\text{PL}^\bullet$ ) and subsequent reaction with molecular oxygen to yield a phospholipid peroxy radical

( $\text{PLOO}^\bullet$ ), which removes hydrogen from another PUFA, forming PLOOH. If not converted to the corresponding alcohol (PLOH) by GPX4, PLOOH and lipid free radicals—in particular,  $\text{PLOO}^\bullet$  and alkoxyl phospholipid radicals ( $\text{PLO}^\bullet$ )—will react with PUFA-PLs to propagate PLOOH production by

removing more hydrogen atoms and reacting with molecular oxygen. This reaction eventually leads to the formation of lipid peroxide breakdown products. A consequence of this chain reaction is the eventual deterioration of membrane integrity and, ultimately, destabilization of organelles or cell membranes. Therefore, membranes with a high PUFA-PL content would be especially susceptible to peroxidation, as has been shown to occur in neurons (Jiang et al., 2021). Acyl-CoA synthetase long-chain family member 4 (ACSL4) determines a cell's sensitivity to ferroptosis (Shin et al., 2018). Responsible for the esterification of PUFA into acyl-CoA, ACSL4 promotes PUFA fatty acid activation. Activated the fatty acids under the action of Lysophosphatidylcholine Acyltransferase 3 (LPCAT3) transferred to inside and outside the cell membrane and esterification; the substrates can undergo peroxidation resulting in the formation of arachidonoyl (AA) and adrenoyl (AdA) acids. During this process, many LPOs and lipid ROS are formed, aggravating oxidative stress and contributing to ferroptosis (Friedmann Angeli et al., 2019; Reichert et al., 2020; Jia et al., 2021).

p53 also plays a role in lipid peroxidation. Cell membrane PUFAs can undergo peroxidation reactions *via* LOXs, iron-containing enzymes that also induce cell ferroptosis. p53 activates the LOX enzyme ALOX12 to induce ferroptosis in cells independent of GPX4 activity (Chu et al., 2019; Li and Li, 2020). Inhibition or knockdown of ALOX12 may be a new approach to interrupt ferroptosis (Ou et al., 2016). In contrast, loss of p53 prevents the accumulation of dipeptidyl-peptidase-4 (DPP4) in the nucleus, triggering membrane-associated DPP4-mediated lipid peroxidation. This peroxidation promotes the interaction between DPP4 and nicotinamide adenine dinucleotide phosphate oxidase 1 (NOX1), resulting in the formation of the NOX1-DPP4 complex, which mediates plasma membrane lipid peroxidation and ferroptosis (Xie et al., 2017; Li and Li, 2020). p53 inhibits ferroptosis by reducing the accumulation of toxic lipid ROS and inducing the expression of cyclin-dependent kinase inhibitor 1A (CDKN1A/p21) (Figure 1) (Li and Li, 2020; Song and Long, 2020).

## Glutamate-storage, uptake and recycling

Glu, glutamine (Gln) and cysteine play vital roles in ferroptosis. The GSH molecule consists of glutamic acid, cysteine, and glycine (Gly), with cysteine being the limiting substrate in its formation. GSH plays an important role in cells and is the main low molecular weight antioxidant, regulating various important functions. Furthermore, Glu is not only one of the major excitatory amino acids in the brain, but also participates in the Glu-Gln cycle, which links glucose and amino acid metabolism to synaptic transmission, cellular homeostasis, and cellular energy metabolism (Figure 1).

Therefore, Glu storage, synthesis, receptor signaling and transport, uptake and recycling are closely related to brain energy metabolism.

Glu transporters are mainly distributed in astrocyte synapses. The Glu bind to transporters which move it to the astrocyte cytoplasm. Glu transporters are co-transported into astrocytes by Na<sup>+</sup> and Glu, and Na<sup>+</sup> is transported to the extracellular space by Na<sup>+</sup>-K<sup>+</sup>-ATPase. Glu reacts with Gln synthetase (GS) to produce Gln; the ATP consumed in this process may be supplied by glycolysis, in which GS is only expressed in astrocytes (Parpura et al., 2017). Therefore, the Glu/Gln cycle plays a key role in maintaining Glu levels in the central nervous system (Andersen et al., 2021). The resulting Gln is released into the neuron, entering through the SLC1A5 receptor. The Gln absorbed by the neuron is converted into Glu under the action of glutaminase. GABA can also be produced by the action of Glu decarboxylase. In addition, Glu can be converted to  $\alpha$ -ketoglutarate by Glu dehydrogenase or aminotransferase, then participate in the tricarboxylic acid (TCA) cycle, which provides citrate and oxaloacetate for lipid synthesis and converts Glu to aspartate (Haddad et al., 2021). Glu can be introduced into the TCA cycle when glucose supply is limited. p53 promotes Glu decomposition by up-regulating the expression of glutaminase 2 (Figure 2) (Liu and Gu, 2021).

Glu receptors are roughly divided into ionic and metabolic types. Ionic Glu receptors include those of N-methyl-D-aspartate (NMDA), among the most important postsynaptic Glu receptors. Mediating the flow of Ca<sup>2+</sup> (Liu et al., 2021), the NMDA receptor is a heterotetramer calcium channel, mainly composed of two NR1 subunits and two NR2 subunits (Furukawa et al., 2005). In the hippocampus, the NR2 subunit is mainly expressed as NR2A and NR2B. The synaptic NMDA receptors rich in NR2A subunits are primarily activated by the cAMP response element-binding protein, and brain-derived neurotrophic factor (BDNF) gene expression induces cell survival events (Leveille et al., 2008). BDNF is an important neurotrophic factor expressed in many brain regions such as the hypothalamus, cortex, brainstem and hippocampus. It plays a key role in the survival, differentiation, and growth of neuronal dendrites and axons, and the regulation of synaptic plasticity. Vesicular Glu transporters (VGLUT1) are located in the glutamatergic presynaptic vesicle plasma membrane, controlling Glu transport into the synaptic vesicle. The VGLUT1 quantity and the extracellular Glu concentration determine the speed and efficiency of transport (Chen et al., 2011).

The tripeptide GSH is the most abundant endogenous antioxidant in the body, removing free radicals and maintaining balance in the oxidative defense system. Several studies have shown that the first step in GSH synthesis involves the formation of  $\gamma$ -Glu-Cys in an ATP-dependent reaction



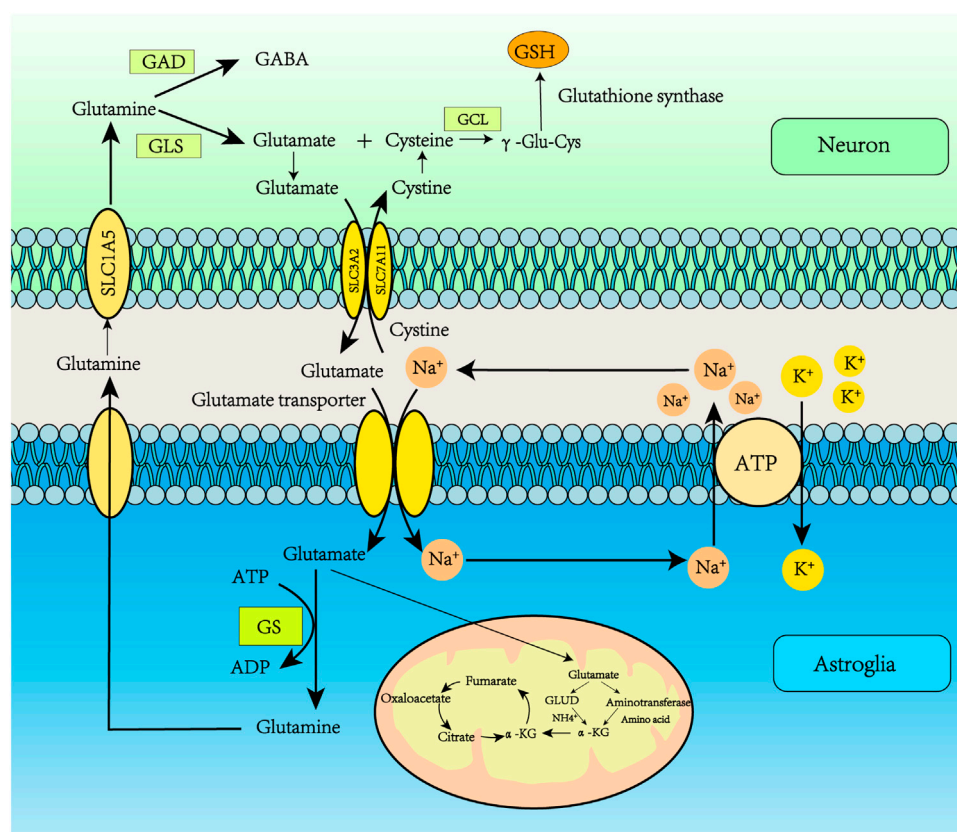


FIGURE 2

Glutamate recycling via the glutamate-glutamine cycle. Glu transporters are mainly distributed in astrocyte synapses. Glu binds to transporters which deliver it to the astrocyte cytoplasm. Glu transporters are co-transported into astrocytes by Na<sup>+</sup> and Glu, and Na<sup>+</sup> is transported to the extracellular space by Na<sup>+</sup>/K<sup>+</sup>-ATPase. Glu reacts with GS to produce Gln, and the ATP consumed in this process may be supplied by glycolysis. The resulting Gln is released into the neuron, and then Gln enters the neuron through the SLC1A5 receptor. The Gln absorbed by the neuron is converted into Glu under the action of glutaminase. GABA can also be produced by the action of Glu decarboxylase. In addition, Glu can be converted to  $\alpha$ -ketoglutarate by Glu dehydrogenase or aminotransferase, participating in the tricarboxylic acid (TCA) cycle, which provides citrate and oxaloacetate for lipid synthesis and converts Glu to aspartate.

catalyzed by GCL, which requires Mg<sup>2+</sup> or Mn<sup>2+</sup> as cofactors (Liu et al., 2021).  $\gamma$ -Glu-Cys can significantly increase GSH and the GSH/GSSG ratio (Liu et al., 2021). This step is rate-limiting because it depends on cysteine bioavailability and GCL activity. In the second step,  $\gamma$ -Glu-Cys and Gly form GSH via GSS activity (Stockwell et al., 2017). The cell's ability to biosynthesize GSH is controlled by various factors, including intracellular substrate utilization (L-cysteine), GCL activity, rate-limiting enzymes in GSH synthesis, and GSH feedback inhibition of GCL (Haddad et al., 2021).

The most significant difference between ferroptosis and other types of programmed cell death is the change in mitochondrial morphology (Luo et al., 2021). Ferroptotic mitochondria are smaller with increased membrane density (Bao et al., 2021) and elevated cytoplasmic and lipid ROS radicals (Dixon et al., 2012; Johnson et al., 2021). ROS are partially reduced oxygen-containing molecules, including

superoxide (O<sub>2</sub>•<sup>-</sup>), peroxides (H<sub>2</sub>O<sub>2</sub> and ROOH), and free radicals (HO• and RO•) (Latunde-Dada, 2017; Chen et al., 2020; Foret et al., 2020). Superoxide is the most important free radical (Serviddio et al., 2015). Excessive ROS can be detoxified by antioxidants (enzymes and non-enzymes) and in reactions catalyzed by superoxide dismutase (Cu-SOD, Zn-SOD, and Mn-SOD), GPX and catalase. ROS are produced by glucose and glutamine (Gln) metabolism, which reduces GSH and GPX4 levels (Chen et al., 2020). An imbalance in ROS production and detoxification rates leads to oxidative stress, and the subsequent radicals generate damage DNA, proteins, and lipids (Chen et al., 2020). Under oxidative stress, high levels of superoxide can induce compounds including iron (4Fe-4S) clusters, heme, and ferritin to release Fe<sup>2+</sup>, which causes ferroptosis through Fenton and Haber-Weiss reactions. In ferroptosis, SLC7A11 and GSH depletion lead to iron-dependent ROS accumulation (Dixon and Stockwell, 2014).

## Ferroptosis and alzheimer's disease

### Iron homeostasis and alzheimer's disease

Regulation of iron homeostasis is important for maintaining normal brain function, and dysregulation of iron homeostasis in the brain can lead to oxidative stress and inflammatory responses, resulting in cell damage and ultimately neurodegenerative diseases. Typical neuropathological features of AD include the deposition of beta-amyloid (A $\beta$ ) into neuroinflammatory plaques, intracellular aggregates of Tau protein in neurofibrillary tangles, synaptic loss, neuroinflammation, and neuronal death. In addition to these typical pathologies, MRI data of AD patients have shown iron deposition in the hippocampus, cortex, and basal ganglia (Ghadery et al., 2015; Masaldan et al., 2019). Subsequent studies revealed increased iron, Tf, and ferritin in the brain (Ashraf et al., 2020; Bao et al., 2021). These findings suggest that neuronal cells in AD disease upregulate ferritin and downregulate FPN expression, increasing iron intake and reducing iron excretion. This process leads to increased free Fe<sup>2+</sup> in cells and increased ferritin, manifested by iron deposition in the brain.

In AD, cytotoxicity induced by A $\beta$ 1-42 directly induces down-regulation of FPN in primary neurons and the hippocampus. Abnormal phosphorylation of the tau protein can lead to increased APP (Bao et al., 2021), a precursor of A $\beta$  production and aggregation (Derry et al., 2020). APP is first broken down by either  $\alpha$ -secretase or  $\beta$ -secretase and then by  $\gamma$ -secretase. In the physiological state,  $\alpha$ -secretase is the first to cleave APP for the non-amyloidosis pathway. However, if APP is first cleaved by  $\beta$ -secretase, neurotoxic A $\beta$  is produced (Tsatsanis et al., 2020). The protein furin plays a critical role in regulating the rate of proteolytic activation of  $\alpha$ -secretase and  $\beta$ -secretase. Furin concentration is positively correlated with  $\alpha$ -secretase activity but negatively correlated with  $\beta$ -secretase activity. Iron deposition results in reduced furin transcription and translation, thereby enhancing  $\beta$ -secretase activity by reducing furin protein expression. Enhanced  $\beta$ -secretase activity increases A $\beta$  production through the amyloidosis pathway (Ward et al., 2014). The damaging cycle then continues with A $\beta$ -induced downregulation of FPN and iron accumulation. Generally, the tau protein can mediate APP's interaction with FPN on the cell surface to promote iron excretion. However, reduced tau protein is associated with AD, affecting FPN's ability to excrete iron (Wang and Mandelkow, 2016; Ayton et al., 2020; Derry et al., 2020). Furthermore, increased FTH levels in AD are associated with lower FPN levels (Ashraf et al., 2020). Everett et al. found that amyloid plaques reduced Fe<sup>3+</sup> to Fe<sup>2+</sup> (Everett et al., 2014a), and A $\beta$  could transform Fe<sup>3+</sup> stored as ferrihydrite into redox-active biological substances containing Fe<sup>2+</sup> (Everett et al., 2014b; Derry et al., 2020).

Due to increased iron intake and decreased iron excretion, increased intracellular liberation of Fe<sup>2+</sup> activates the ferroptosis pathway. First, excessive Fe<sup>2+</sup> enhances the Fenton reaction and produces oxhydroyl radicals. Second, it promotes lipid peroxide production, which ultimately triggers ferroptosis.

### GPX4 and alzheimer's disease

GPX4, an antioxidant enzyme, is highly expressed in NCOA4 deficient mice (Bellelli et al., 2016). Yoo et al. found that GPX4 deletion in adult mice leads to mitochondrial damage, neurodegeneration in the hippocampus, and astrocyte proliferation (Yoo et al., 2012). Moreover, Hambright et al. (2017) found significant neurological deficits and cognitive impairment in GPX4-deficient mice. When Bao et al. (2021) injected A $\beta$  into the brain of mice, they found elevated levels of iron and ferritin in the hippocampus and decreased levels of GPX4, suggesting that A $\beta$  directly affects ferroptosis in neurons. Thus, GPX4 inhibition in ferroptosis offers protection against neurodegeneration (Cardoso et al., 2017). As a substrate of GPX4, GSH plays an antioxidant role. Studies have shown that  $\gamma$ -Glu-Cys can significantly increase GSH, increase the GSH/GSSG ratio, and decrease the generation of A $\beta$  and oxidative stress (Liu et al., 2021). In AD patients, the GSH content is reduced (Ashraf et al., 2020), so effectively preventing GSH decrease is a promising new treatment strategy for AD occurrence and development.

### Lipid metabolism and alzheimer's disease

Recent studies have shown that lipid ROS in ferroptosis may cause AD. Although the highest PUFA content is found in adipose tissue, PUFA in brain tissue accounts for 30%–35% of the total fatty acid content, so the central nervous system is very vulnerable to lipid peroxidation (Peng et al., 2021). ACSL4 plays an important role in PUFA activation and determines ferroptosis sensitivity (Shin et al., 2018). Yan et al. (2022) analyzed the hippocampal transcriptome of the APP/PS1 mouse model and found elevated expression of ACSL4. Unfortunately, it is not known whether ACSL4 expression or activity is modified by A $\beta$ O.

Dietary arachidonic acid (ARA) is the second most common type of PUFA in meninges phospholipids, where lipid peroxidation readily occurs, leading to lipid bilayer damage. Recent research shows that increased ARA intake induces cognitive alteration and increases the neurotoxicity of amyloid- $\beta$  peptide (A $\beta$ ) (Thomas et al., 2017), which leads to AD. In addition to its involvement in synaptic plasticity and transmission, free ARA plays a crucial role in neuroinflammation through its conversion into various eicosanoids by cyclooxygenases, prostaglandin synthases, and lipoxygenases,

the activities of which have been associated with neurodegenerative diseases (Czapski et al., 2016). As the brain's consumption and metabolism of ARA are up-regulated in AD patients, suggesting that ARA is involved in the pathomechanism of this disease (Esposito et al., 2008), ARA consumption could constitute a risk factor for AD in humans and should be considered in future preventive strategies. ARA is specifically released from membrane phospholipids by cytosolic phospholipase A2 (cPLA2), which is translocated to the membranes in a cytosolic calcium-dependent manner after its phosphorylation on Ser505 by MAPK. cPLA2 is activated by A $\beta$  oligomers. Its pharmacological inhibition or the suppression of its expression protects neuronal cells against the neurotoxicity of A $\beta$  oligomers and preserves cognitive abilities (Czapski et al., 2016). The ARA released *via* cPLA2 induction can be metabolized by COX or LOXs (Chuang et al., 2015). Among LOX alterations, those of LOX12/15 can lead to oxidative stress, resulting in free radical-dependent DNA damage and poly (ADP-ribose) polymerase-1 overactivation, neuronal degeneration and death (Czapski et al., 2013). Therefore, treating AD with LOX has broad prospects.

## Amino acid metabolism and alzheimer's disease

Amino acids play an important role in the occurrence and development of AD. Glu is an important excitatory neurotransmitter in the body, helping to transmit information between nerve cells. During post-translational modification, many proteins undergo glycation reactions between their free reducing sugars and free amino groups. Some studies have shown increased levels of advanced glycation end-products (AGEs) in the brains of AD patients, suggesting that AGEs play an important role in activating microglia and A $\beta$  deposition in AD (Byun et al., 2012). AGEs are irreversible adducts of the Maillard reaction that accumulate in the brain as we age. Glyoxal or methylglyoxal (MG) can contribute to AGE production (Currais and Maher, 2013). MG is primarily removed *via* the glyoxalase system, composed of Glo-1 and Glo-2. Glo-1 is the rate-limiting enzyme for the system and is dependent on GSH (Bijnen et al., 2018). Glo-1 activity also depends on the cellular redox state and the GSH/GSSG ratio (Haddad et al., 2021). AGE binding to albumin secreted by microglia results in toxicity and subsequent A $\beta$  aggregation. A $\beta$  can promote the release of Glu from vesicles into the synaptic cleft, leading to the activation of extrasynaptic N-methyl-D-aspartate receptors (NMDARs). Over-activation of NMDARs leads to calcium overload of postsynaptic neurons, inducing excitatory toxicity, neuronal apoptosis, and neurodegeneration. Kashani et al. (2008) found decreased Glu transporter expression in the cerebral cortex in patients with AD. VGLUT1 is significantly decreased, possibly resulting in poor clearance of glutamic acid in the

synaptic cleft, leading to excitatory toxicity. Furthermore, high extracellular Glu will inhibit system xc<sup>-</sup>, leading to ferroptosis.

The presence of amyloid oligomers (A $\beta$ O) is closely correlated to the incidence of AD. Soluble A $\beta$ O is currently considered the main source of brain neuron injury and central nervous system degeneration (Reiss et al., 2018). As an intermediate product of A $\beta$  fibrosis, A $\beta$ O is significantly more toxic than monomers and fibers. A $\beta$ O can be classified as low molecular weight (<50 kDa) and high molecular weight (>50 kDa), and different sizes and morphologies of oligomers may produce different pathological effects. For example, in a mouse model, low molecular weight A $\beta$ O (e.g., dimer and trimer) can significantly inhibit the long-term enhancement of hippocampal neurons and damage the spatial memory function. In contrast, high molecular weight soluble A $\beta$  aggregates are more likely to induce microglial activation, resulting in neuroinflammatory responses (Figueiredo et al., 2013). A $\beta$ O can interact with metabolic Glu receptor 5 to promote long-term depression and inhibit long-term potentiation in the hippocampus, leading to downstream responses and kinases activation. For example, p38-MAPK, the end of Jun N-terminal kinase (JNK), and cell-cycle dependent kinase affect the plasticity of gene transcription (Ittner et al., 2010). Furthermore, p38MAPK and JNK have been associated with AD-like lesions caused by diabetes mellitus (Kim and Song, 2020). Hyperphosphorylation of the tau protein can be mediated by activation of the p38MAPK/p53 signaling pathway (Sun et al., 2017). In addition, increased p53 expression inhibits the expression of the system xc<sup>-</sup> SLC7A11, resulting in reduced uptake of cystine, decreased GSH peroxidase activity, reduced cell antioxidant capacity, and increased sensitivity of cells to ferroptosis (Kang et al., 2019).

Neuropathological AD changes have been associated with impaired cerebral insulin signaling (Takeda et al., 2010; Martinez-Valbuena et al., 2019), and decreased insulin signaling in the brain can inhibit phosphatidylinositol 3-kinase/Akt and activate GSK-3 $\beta$  (Ma et al., 2015). Excessive iron in neurons can lead to tau hyperphosphorylation and NFT formation through the CDK5/P25 complex and GSK-3 $\beta$  kinase pathway (Yan and Zhang, 2019). GSK-3 $\beta$  phosphorylates Nrf2, leading to Nrf2 degradation (Chen et al., 2020; Qu et al., 2020). Kanninen et al. reviewed the neuroprotective role of Nrf2 in AD, with special emphasis on the role of GSK-3 $\beta$  in the Nrf2 pathway (Kanninen et al., 2011). Moreover, it was reported that GSK-3 $\beta$  inhibition in SAMP8 mice results in increased nuclear Nrf2 and total GST in the cortex (Farr et al., 2014; Qu et al., 2020). The complex roles played by ferroptosis in AD regulation are shown in Figure 3.

## Ferroptosis inhibitors and clinical application

Ferroptosis inhibitors eliminate free radicals, inhibiting enzymes that produce lipids or LPOs and reducing free iron. Iron inhibitors

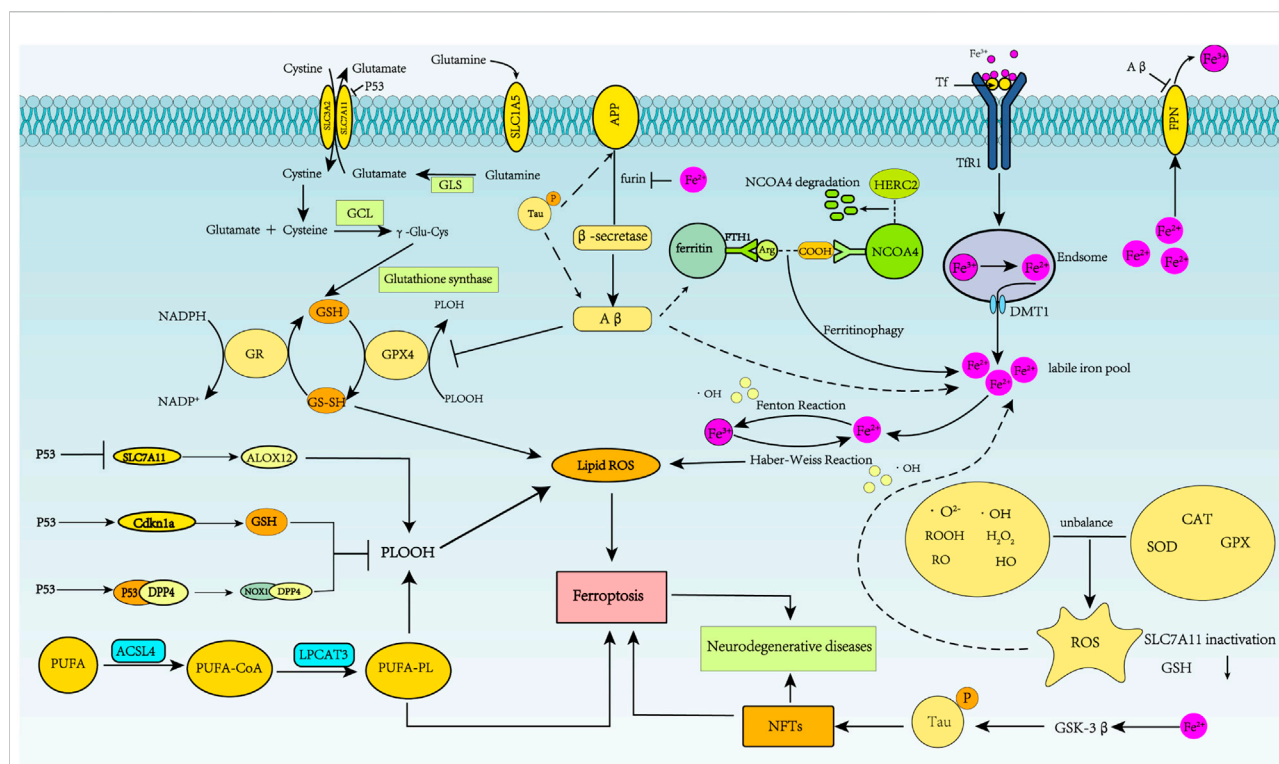


FIGURE 3

Schematic representation of ferroptosis regulation of Alzheimer's disease. In AD, APP is first cleaved by  $\beta$ -secretase, and neurotoxic A $\beta$  is produced. Abnormal phosphorylation of the tau protein can lead to increased APP and A $\beta$ 40 aggregation.  $\text{Fe}^{2+}$  enhances  $\beta$ -secretase activity by reducing furin protein expression, thereby increasing A $\beta$  production through the amyloidosis pathway. A $\beta$ 1-42 directly induces down-regulation of FPN. Increased intracellular liberation of  $\text{Fe}^{2+}$  activates the ferroptosis pathway. A $\beta$  can decrease levels of GPX4 and elevate levels of ferritin. Excessive iron in neurons can lead to tau hyperphosphorylation and NFT formation through the GSK-3 $\beta$  kinase pathway.

are classified as aromatic amine antioxidants,  $\alpha$ -tocopherol, nitroxides, natural polyphenol compounds, ACSL4 inhibitors, LOX inhibitors, or other types (Table 1). As patients with AD have iron deposits in their brain cells, and excess iron can exacerbate oxidative damage and cognitive deficits, ferroptosis inhibitors offer broad prospects for treating AD.

## Aromatic amine antioxidants

Ferostatin-1 (Fer-1) and lipoxstatin-1 (Lip-1), aromatic amine antioxidants, are free radical scavengers that block ROS production and lipid peroxidation.

Fer-1 inhibits ferroptosis much more efficiently than phenolic antioxidants. The anti-ferroptotic activity of Fer-1 is due to the scavenging of initiating alkoxyl radicals produced, with other rearrangement products, by ferrous iron from lipid hydroperoxides. Fer-1 forms a complex with iron, confirmed in cells by calcein fluorescence which indicates decreased labile iron in the presence of Fer-1 (Miotto et al., 2020). In addition, Fer-1 significantly inhibits the production of cytoplasmic and lipid

ROS and reverses Glu-induced suppression of GSH and Gpx in HT-22 cells, suggesting that Fer-1 protects HT-22 cells by blocking oxidative toxicity. Therefore, Nrf2 and Gpx4 up-regulation may be the basis of the cytoprotective mechanism of Fer-1 (Chu et al., 2020).

The aromatic amine Lip-1 is the foundation for the antioxidant activity of lipoxstatin-1 analogs. It is an excellent radical-trapping antioxidant in phospholipid bilayers, using the bilayers of unilamellar liposomes originating from egg phosphatidylcholine. Lip-1 readily penetrates and remains within the lipid bilayer, permitting its active site to remain in close directional contact with the lipid peroxidation site and initiating the  $\text{CH}_3\text{OO}\bullet$  extraction of hydrogen atoms from aromatic amine sites (Sheng et al., 2017). Moreover, Lip-1 prevents BODIPY 581/591 C11 oxidation in Gpx4 $^{-/-}$  cells but does not interfere with other classical types of cell death, such as TNF $\alpha$ -induced apoptosis and  $\text{H}_2\text{O}_2$ -induced necrosis (Friedmann Angeli et al., 2014).

Studies have shown that memory improves in A $\beta$ -induced AD mice when Fer-1 and Lip-1 are administered, and Lip-1 has a more significant effect on memory (Bao et al., 2021). Therefore, aromatic amine antioxidants may offer significant AD treatment options.



TABLE 1 Summary of the available ferroptosis Inhibitors in Alzheimer disease.

Sort	Inhibitors	Mechanism of action	Experimental models	Effector cell	References
Aromatic amine antioxidants	Ferrostatin-1	Block ROS production and lipid peroxidation	A $\beta$ induced C57 mice	Primary hippocampal neurons	Bao et al. (2021)
	liproxstatin-1	Inhibit lipid peroxidation and up-regulate GPX4 expression	A $\beta$ induced C57 mice	Primary hippocampal neurons	Li et al. (2019); Bao et al. (2021)
$\alpha$ -tocopherol	Vitamin E	Inhibit lipid peroxidation and maintain the integrity of cell membrane	Ttpa <sup>-/-</sup> mice, Ttpa <sup>-/-</sup> APPsw mice	Cerebellum cortex hippocampus Purkinje neurons	Boccardi et al. (2016); Gugliandolo et al. (2017); Kryscio et al. (2017)
Nitroxides		Participate in Fenton reaction, inhibit the production of hydroxyl radical	—	—	Shi et al. (2017)
Natural polyphenol compounds	Baicalein	Inhibits GSH depletion, GPX4 degradation and lipid peroxidation, increases Nrf2, and inhibits 12/15-LOX	APP/PS1 mice, C57/BL6 mice, HT22 cells	Hippocampus	Xie et al. (2016); Li et al. (2019); Yuan et al. (2020)
	Curcumin	Chelates iron, reduces iron accumulation, inhibits A $\beta$ aggregation, and reduces the effects of P-tau protein	SH-SY5Y cells, APP/PS1 mice, 5 $\times$ -familial AD (5XFAD)	Hippocampal CA1 area	Tang and Taghibiglou, (2017); Reddy et al. (2018); Ege, (2021)
	EGCG	Antioxidant anti-inflammatory and neuroprotective effects; reduces A $\beta$ production	APP/PS1 mice	Primary cortical neurons	Cascella et al. (2017); Plascencia-Villa and Perry, (2021)
	Melatonin	Reduce oxidative stress and stimulate the synthesis of antioxidant enzymes (SOD, GPX, and glutathione reductase) and GSH production	APP/PS1 mice, N2a/APP cells, APP 695 transgenic mice	Neuron (mitochondria endoplasmic reticulum)	Balmik and Chinnathambi, (2018)
	Ginkgo biloba	Inhibit lipid peroxidation	Wistar rats	Hippocampus, striatum and substantia nigra	Bridi et al. (2001); Plascencia-Villa and Perry, (2021)
	CMS121	Regulates lipid metabolism, reduces inflammation and lipid peroxidation	APP <sup>sw</sup> /PS1 $\Delta$ E9 transgenic mice, HT22 neuronal cell, BV2 microglial cells, C65 cells	Hippocampus	Ates et al. (2020)
LOX inhibitors	Zileuton	Decreased $\gamma$ -secretase, A $\beta$ and Tau	3xTg mice model	—	Di Meco et al. (2014)
Other inhibitors	Vitamin C	Promote the production of endogenous antioxidants (GSH, catalase, vitamin E); Decrease the production of A $\beta$	APP/PSEN1 mice	Brain cortex	Monacelli et al. (2017)
	Vitamin B	Ameliorate cognitive decline by lowering serum homocysteine levels	—	Hippocampus parahippocampal gyrus, inferior parietal lobule and retrosplenial cortex	Douaud et al. (2013); Kennedy, (2016)
	Deferoxamine	Chelate iron to reduce iron accumulation	APP/PS1 mice	Microglial activation	Feng et al. (2020); Mao et al. (2020); Moreau et al. (2018)
Other inhibitors	NQO1	Antioxidant stress and lipid peroxidation; Reductase that protects the antioxidant forms of CoQ10, $\alpha$ -tocopherol, and ascorbic acid	—	—	Ross and Siegel, (2021)

(Continued on following page)

TABLE 1 (Continued) Summary of the available ferroptosis Inhibitors in Alzheimer disease.

Sort	Inhibitors	Mechanism of action	Experimental models	Effector cell	References
	ESP1	The FSP1-CoQ10-NAD(P)H pathway, together with GPX4 and GSH, inhibits phospholipid peroxidation	HT1080 cells	—	Doll et al. (2019); Chen et al. (2020); Reichert et al. (2020); Stockwell et al. (2020); Yan et al. (2021)
	CoQ10	Inhibit lipid peroxidation	Older mice	Hippocampal striatal cortical function neocortex	Shetty et al. (2013); Yan et al. (2021)
	LA	Blocking tau-induced iron overload, lipid peroxidation and inflammation related to ferroptosis	P301S Tau transgenic mice	Hippocampus and the cortex	Zhang et al. (2018); Song and Long, (2020)

α-Tocopherol

α-Tocopherol, the main type of Vitamin E in tissues, exerts its antioxidant capacity mainly by destroying the chain reaction of automatic oxidation (Zilka et al., 2017). α-Tocopherol transfer protein (TTP) is highly expressed in the brain and regulates the level and distribution of α-tocopherol. Vitamin E and TTP deficiency can lead to oxidative stress in the brain. It has been demonstrated that AD patients have low Vitamin E in the plasma, serum, and cerebrospinal fluid (Ashraf and So, 2020). Moreover, AD patients receiving vitamin E treatment experience slower declines in cognitive function and lower oxidative stress levels than patients receiving the placebo (Boccardi et al., 2016; Gugliandolo et al., 2017; Kryscio et al., 2017).

Nitroxides

Nitroxides can permeate the cell membranes and cross the blood–brain barrier (BBB). Fe<sup>2+</sup> is the form of iron found in the LIP *in vivo*. The involvement of the iron (II)-citrate complex in Fenton-like reactions with H<sub>2</sub>O<sub>2</sub> is considered an *in vivo* mechanism of the LIP that induces oxidative stress and many pathological conditions. The nitroxide Tempo combines with Fe<sup>2+</sup>-citrate to form a Tempo-Fe<sup>2+</sup>-citrate complex, which can effectively inhibit OH production. Nitroxides have significant therapeutic potential as antioxidants in oxidative stress-related diseases (Shi et al., 2017).

Natural polyphenol compounds

Baicalein is a natural polyphenol compound that inhibits LOXs by reducing oxidative stress and acts as an anti-inflammatory and neuroprotective agent. It inhibits GSH depletion, GPX4 degradation and lipid peroxidation, increases Nrf2, and inhibits 12/15-LOX (Xie et al., 2016; Li et al., 2019; Yuan et al., 2020). Activation of Nrf2 increases iron storage, reduces iron uptake by cells, and limits lipid ROS production (Hassannia et al., 2019; Xu et al., 2021). Baicalein-fed APP/PS1 mice show decreased BACE1 activity, decreased Aβ and p-tau levels, and superior behavioral test results. Another polyphenolic compound, curcumin chelates iron, reduces iron accumulation, scavenges ROS, increases the levels of SOD, Na<sup>+</sup>-K<sup>+</sup>-ATPase, catalase, GSH and mitochondrial complex enzyme (Ege, 2021), inhibits Aβ aggregation, and reduces the effects of P-tau protein. However, curcumin has poor water solubility and has demonstrated inadequate bioavailability in clinical trials. As a result, its application in the clinical treatment of AD is limited (Tang and Taghibiglou, 2017; Reddy et al., 2018; Ege, 2021).

Epigallocatechin gallate (EGCG) is another key polyphenol compound. Found in green tea, it has antioxidant, anti-inflammatory and neuroprotective effects (Plascencia-Villa and Perry, 2021). Treatment of AD mice with EGCG demonstrated that it exerted its protective effects by decreasing the expression of APP and A $\beta$  in the hippocampus. Preclinical studies showed that EGCG has anti-inflammatory and neuroprotective effects against neuron injury and cerebral edema (Casella et al., 2017).

Decreased melatonin, associated with decreased accumulation of polyphenols, is closely related to AD occurrence. As people age, the pineal gland calcifies, and melatonin secretion gradually decreases (Luo et al., 2020). AD patients experience decreased melatonin synthesis and secretion and abnormal secretion rhythms. Melatonin can reduce oxidative stress and stimulate the synthesis of antioxidant enzymes (SOD, GPX, and glutathione reductase) and GSH production (Balmik and Chinnathambi, 2018). A $\beta$  plasma levels and deposition were found to be significantly reduced in APP/PS1 mice after 12 months of melatonin supplementation. However, clinical trials using melatonin (50–100 mg/day) for 10 days to 24 weeks showed that melatonin is safe but does not improve the cognitive ability of AD patients, only their sleep quality (Plascencia-Villa and Perry, 2021).

The ginkgo biloba tree (*Ginkgo biloba*) also produces polyphenols with antioxidant effects. After rats were injected with a standardized extract of ginkgo biloba, catalase and superoxide dismutase activities in the hippocampus, striatum, and substantia nigra were increased, lipid peroxidation decreased, and overall oxidative damage was reduced (Plascencia-Villa and Perry, 2021). Finally, the polyphenol derivative CMS121 acts as an antioxidant and inhibits fatty acid synthase to regulate lipid peroxidation levels. CMS121 was shown to improve memory, and cognitive function in APPswe/PS1  $\delta$  E9 double transgenic mice (Ates et al., 2020).

## LOX inhibitors

5-Lipoxygenase (5LO) is widely expressed in central nervous system neurons, and its levels increase in an age-dependent manner in the hippocampus and cortex, two brain regions prone to neurodegenerative damage. Studies have shown that 5LO is up-regulated in AD. Zileuton, an anti-inflammatory compound, inhibits LOX5 and decreases  $\gamma$ -secretase, A $\beta$ , and tau after three months of treatment in a 3xTg mouse AD model (Di Meco et al., 2014), demonstrating its broad prospects for clinical use.

## Other inhibitors

APP/PS1 mice treated with the iron chelator deferoxamine demonstrate reduced A $\beta$  and improved memory, but no significant improvement in cognition and memory is observed in AD patients (Feng et al., 2020). Furthermore, patients experience side effects such as loss of appetite and

weight. NQO1, a reductase that can maintain antioxidant forms of CoQ10,  $\alpha$ -tocopherol and ascorbic acid, plays an important role in maintaining antioxidant protection and inhibiting lipid peroxidation. It has long been associated with the early pathological changes of AD. However, NQO1 increases in the AD brain are limited to brain regions affected by AD pathology. Furthermore, NQO1 production is generally considered a protective response to oxidative stress, which has potential clinical significance in treating AD (Ross and Siegel, 2021).

The inhibition of ferroptosis by ferroptosis suppressor protein 1 (FSP1) is mediated by ubiquinone, also known as coenzyme Q10. Ubiquinone is converted on the cell membrane into its reduced prototype ubiquinol, which inhibits the peroxide reaction and prevents ferroptosis (Tang et al., 2021). FSP1 catalyzes the regeneration of CoQ10 through NAD(P)H, and the FSP1-CoQ10-NAD(P)H pathway, together with GPX4 and GSH, inhibits phospholipid peroxidation and ferroptosis, offering broad prospects for the treatment of degenerative diseases caused by ferroptosis (Doll et al., 2019; Chen et al., 2020; Mao et al., 2020; Reichert et al., 2020; Stockwell et al., 2020; Yan et al., 2021). GSH is a major antioxidant, combating oxidative stress. One study demonstrated that GSH levels in the hippocampus and cortex are significantly reduced in patients with mild cognitive impairment (MCI) and AD. Although GSH supplementation has been proposed as a therapeutic strategy for MCI and AD, it has not been evaluated in patients in clinical trials (Plascencia-Villa and Perry, 2021).

Vitamin C (ascorbic acid, AA) can increase GSH metabolism and improve cellular oxidative stress. Treatment with high concentrations of AA reduces amyloid plaque formation in the 5XFAD mouse model (Monacelli et al., 2017). Homocysteine is an important intermediate in methionine, folate, and onecarbon metabolism, and elevated homocysteine increases the risk of stroke, age-associated cognitive impairment, and AD. Randomized controlled trials and meta-analyses have indicated that homocysteine-lowering treatments may be recommended to prevent AD. Elevated homocysteine might promote post-stroke cognitive impairment (PSCI) through small vessel disease or AD pathology, which may explain our finding that homocysteine levels are associated with long-term incidence of PSCI (Li et al., 2021). Vitamin B can reduce cognitive decline by lowering serum homocysteine levels. Vitamins B1/B6/B9/B12 were found to improve brain metabolism, oxidative stress, inflammation, and cognition in patients with AD, and folic acid (1.25 mg/day, six months) reduces A $\beta$  and inflammatory biomarkers (TNF $\alpha$ , IL6). Notably, high doses of Vitamin B (folic acid 0.8 mg, Vitamin B6 20 mg, Vitamin B12 0.5 mg) for 2 years was shown to slow the progression of brain atrophy significantly (Donnelly et al., 2008). Another antioxidant,  $\alpha$ -lipoic acid, has been found to improve the cognitive function of AD patients by blocking tau-induced iron overload, lipid

peroxidation and inflammation related to ferroptosis (Song and Long, 2020).

## Targeted ferroptosis therapy for alzheimer's disease

The endothelial cells of the BBB are essential in regulating brain iron uptake, and the Tf/TfR1 pathway is the major route for iron absorption in the brain (Yan and Zhang, 2019). However, the BBB presents challenges for the passage of some drug therapies into the brain. Therefore, developing effective nanomaterial carriers is crucial to improving drug delivery, release, and targeting efficiency. Nanomaterials that deliver drugs targeting ferroptosis have been extensively examined in recent years. Studies have shown that transferrin nanomaterials can penetrate the BBB and deliver drug molecules to the central nervous system (Luo et al., 2021; Zheng et al., 2021), thus providing new AD therapeutic options.

GSH levels decrease with age and possible development of AD. Few studies have focused on exploring the role of exosomes in the metastasis of GSH or its precursors to enhance and supplement intracellular GSH, especially in neuronal cells. More research is needed to understand the potential role of exosomes in oxidative stress and neuroprotection, including GSH transfer. GSH may also be used as a targeted ligand for translocation across the BBB *via* nanocarriers to treat various brain dysfunctions (Haddad et al., 2021). Moreover, therapy targeted to GSH degradation can effectively treat ferroptosis-mediated organ injury (Jiang et al., 2020).

Autophagosome accumulation is a significant feature in human AD patients and animal model neurons. Increased production and accumulation of A $\beta$  in lysosomes has been observed in autophagy-deficient cells, suggesting that the turnover portion of A $\beta$  is regulated by autophagy. As autophagy-related genes are highly expressed in early AD, enhanced autophagy may be a promising research area for achieving neuroprotection in AD patients (Moujalled et al., 2021).

Nrf2 target genes have been shown to be involved in GPX4 synthesis and function, intracellular iron homeostasis, and lipid peroxidation clearance. The Nrf2 protein regulates GSH and thioredoxin-based antioxidant systems (e.g., TXN1, TXNRD1). Targeting the antioxidant transcription factor Nrf2 to inhibit ferroptosis is a promising new option for neurodegenerative control and significant in the study of human nervous system diseases and aging, especially neurodegenerative diseases such as Parkinson's disease, AD, and Huntington's disease (Song and Long, 2020).

The tau protein plays an important role in stabilizing microtubules. In AD pathology, if the protein is over-phosphorylated, it will separate from microtubules, leading to axonal microtubule disintegration (Wang and Mandelkow, 2016). Where microtubules are destroyed, and tau oligomers (tauO) are pathological, p53 cannot enter the nucleus. Over time, p53 outside the nucleus may become unstable and start to aggregate, and tauO near the nucleus interacts with p53 to form a p53 oligomer. Cell cycle arrest, DNA damage repair, apoptosis,

and other crucial functions can be compromised when p53 is not allowed to enter the nucleus. Since the cell cannot be repaired and cell death cannot be controlled, conditions inside the cell will continue to deteriorate, promoting the accumulation of other disordered proteins. Targeting pathological tau proteins, especially tauO, may prevent p53 aggregation and destruction (Farmer et al., 2020). Since p53 controls many cellular functions, affecting this key transcription factor may lead to irreversible AD pathology. A deeper understanding of p53's role in AD lesions is therefore warranted.

## Conclusion

Compared with other tissues and organs of the human body, brain tissue is rich in PUFA and iron. It consumes substantial oxygen, so it is prone to lipid peroxidation, poor antioxidant capacity, and higher ferroptosis sensitivity. The occurrence of ferroptosis is closely related to the regulation of iron homeostasis, the ferroptosis signal pathway, and amino acid metabolism. AGEs are highly detectable in the blood and cerebrospinal fluid of patients with neurodegenerative diseases such as AD (Bär et al., 2003). As an important part of the ferroptosis antioxidant system, GSH helps eliminate AGEs, so increasing the level of GSH in the brain is a new strategy for treating AD. GCL is the rate-limiting enzyme of GSH synthesis, and when its activity decreases, GSH content can be reduced and GPX4 inactivated, leading to the accumulation of lipid peroxidation. This accumulation will further increase ROS and ultimately lead to ferroptosis. Therefore, the effective synthesis of GSH is a new direction for AD treatment. Mitochondria are the main source of ROS. When antioxidant factors are unbalanced within mitochondria, oxidative stress will lead to the release of Glu in neurons. High extracellular Glu will inhibit system xc<sup>-</sup>, resulting in ferroptosis. Moreover, Glu transporter expression in the cerebral cortex of AD patients and VGLUT1 significantly decreased, possibly resulting in poor clearance of glutamic acid in the synaptic cleft, leading to excitatory toxicity. Research on targeted therapy to reduce excitatory toxicity of Glu is promising for future AD treatment.

The mechanism of AD-mediated ferroptosis is gradually being clarified, and iron inhibitors have permitted some progress in AD treatment. This progress notwithstanding, the regulatory factors that regulate the ferroptosis signaling pathway vary and are dependent upon the AD stage. Therefore, the inducing factors and specific mechanisms of ferroptosis in AD remain to be elucidated and should be the focus of next studies. AD is a complex and multifactorial chronic disease. The clinical benefits of ferroptosis inhibitors in AD and their effects on other tissues are the focus of much current research. Whether a single drug or intervention targeting iron death can avoid, reduce or reverse AD requires substantial analysis. In-depth research on the different stages of AD involved in ferroptosis will help us develop a more comprehensive understanding of the AD onset and progression mechanisms and provide a more rigorous theoretical basis for prevention and treatment.



## Author contributions

Conceptualization, LL and HM; original draft preparation, HM and YD; review and editing, LL and YG; supervision, YC.

## Funding

This work was supported by Local Colleges and Universities Talent Development Funding from Heilongjiang Provincial Department of Finance (No. 2020GSP09), the Natural Science Foundation of Heilongjiang Province (No. H2017077), the Basic Scientific Research Project of University belongs to Heilongjiang (No. 2021-KYYWF-0519) and the Science and Technology Plan Project of Mudanjiang (No. HT2020JG070).

## References

- Abdalkader, M., Lampinen, R., Kanninen, K. M., Malm, T. M., and Liddell, J. R. (2018). Targeting Nrf2 to suppress ferroptosis and mitochondrial dysfunction in neurodegeneration. *Front. Neurosci.* 12, 466. doi:10.3389/fnins.2018.00466
- Andersen, J. V., Markussen, K. H., Jakobsen, E., Schousboe, A., Waagepetersen, H. S., Rosenberg, P. A., et al. (2021). Glutamate metabolism and recycling at the excitatory synapse in health and neurodegeneration. *Neuropharmacology* 196, 108719. doi:10.1016/j.neuropharm.2021.108719
- Ashraf, A., Jeandriens, J., Parkes, H. G., and So, P. W. (2020). Iron dyshomeostasis, lipid peroxidation and perturbed expression of cystine/glutamate antiporter in Alzheimer's disease: Evidence of ferroptosis. *Redox Biol.* 32, 101494. doi:10.1016/j.redox.2020.101494
- Ashraf, A., and So, P. W. (2020). Spotlight on ferroptosis: Iron-dependent cell death in Alzheimer's disease. *Front. Aging Neurosci.* 12, 196. doi:10.3389/fnagi.2020.00196
- Ates, G., Goldberg, J., Currais, A., and Maher, P. (2020). CMS121, a fatty acid synthase inhibitor, protects against excess lipid peroxidation and inflammation and alleviates cognitive loss in a transgenic mouse model of Alzheimer's disease. *Redox Biol.* 36, 101648. doi:10.1016/j.redox.2020.101648
- Ayton, S., Wang, Y., Diouf, I., Schneider, J. A., Brockman, J., Morris, M. C., et al. (2020). Brain iron is associated with accelerated cognitive decline in people with Alzheimer pathology. *Mol. Psychiatry* 25 (11), 2932–2941. doi:10.1038/s41380-019-0375-7
- Balmik, A. A., and Chinnathambi, S. (2018). Multi-faceted role of melatonin in neuroprotection and amelioration of tau aggregates in Alzheimer's disease. *J. Alzheimers Dis.* 62 (4), 1481–1493. doi:10.3233/JAD-170900
- Bao, W. D., Pang, P., Zhou, X. T., Hu, F., Xiong, W., Chen, K., et al. (2021). Loss of ferroportin induces memory impairment by promoting ferroptosis in Alzheimer's disease. *Cell. Death Differ.* 28 (5), 1548–1562. doi:10.1038/s41418-020-00685-9
- Bär, K. J., Franke, S., Wenda, B., Muller, S., Kientsch-Engel, R., Stein, G., et al. (2003). Pentosidine and N(epsilon)-(carboxymethyl)-lysine in Alzheimer's disease and vascular dementia. *Neurobiol. Aging* 24 (2), 333–338. doi:10.1016/s0197-4580(02)00086-6
- Bellelli, R., Federico, G., Matte', A., Colecchia, D., Iolascon, A., Chiariello, M., et al. (2016). NCOA4 deficiency impairs systemic iron homeostasis. *Cell. Rep.* 14 (3), 411–421. doi:10.1016/j.celrep.2015.12.065
- Bijnen, M., Beelen, N., Wetzels, S., Gaar, J. v. d., Vroomen, M., Wijnands, E., et al. (2018). RAGE deficiency does not affect non-alcoholic steatohepatitis and atherosclerosis in Western type diet-fed Ldlr-/- mice. *Sci. Rep.* 8 (1), 15256. doi:10.1038/s41598-018-33661-y
- Boccardi, V., Baroni, M., Mangialasche, F., and Mecocci, P. (2016). Vitamin E family: Role in the pathogenesis and treatment of Alzheimer's disease. *Alzheimers Dement.* 2 (3), 182–191. doi:10.1016/j.trci.2016.08.002
- Bridi, R., Crossetti, F. P., Steffen, V. M., and Henriques, A. T. (2001). The antioxidant activity of standardized extract of Ginkgo biloba (EGb 761) in rats. *Phytother. Res.* 15 (5), 449–451. doi:10.1002/ptr.814
- Byun, K., Bayarsaikhan, E., Kim, D., Kim, C. Y., Mook-Jung, I., Paek, S. H., et al. (2012). Induction of neuronal death by microglial AGE-albumin: Implications for Alzheimer's disease. *PLoS One* 7 (5), e37917. doi:10.1371/journal.pone.0037917
- Cardoso, B. R., Hare, D. J., Bush, A. I., and Roberts, B. R. (2017). Glutathione peroxidase 4: A new player in neurodegeneration? *Mol. Psychiatry* 22 (3), 328–335. doi:10.1038/mp.2016.196
- Cascella, M., Bimonte, S., Muzio, M. R., Schiavone, V., and Cuomo, A. (2017). The efficacy of epigallocatechin-3-gallate (green tea) in the treatment of Alzheimer's disease: An overview of pre-clinical studies and translational perspectives in clinical practice. *Infect. Agent. Cancer* 12, 36. doi:10.1186/s13027-017-0145-6
- Chen, J., Wang, Y., Wu, J., Yang, J., Li, M., and Chen, Q. (2020). The potential value of targeting ferroptosis in early brain injury after acute CNS disease. *Front. Mol. Neurosci.* 13, 110. doi:10.3389/fnmol.2020.00110
- Chen, K. H., Reese, E. A., Kim, H. W., Rapoport, S. I., and Rao, J. S. (2011). Disturbed neurotransmitter transporter expression in Alzheimer's disease brain. *J. Alzheimers Dis.* 26 (4), 755–766. doi:10.3233/JAD-2011-110002
- Cheng, Y., Xie, Y., Chen, Y., and Liu, X. (2021). Epigenetic regulation and nonepigenetic mechanisms of ferroptosis drive emerging nanotherapeutics in tumor. *Oxid. Med. Cell. Longev.* 2021, 8854790. doi:10.1155/2021/8854790
- Chu, B., Kon, N., Chen, D., Li, T., Liu, T., Jiang, L., et al. (2019). ALOX12 is required for p53-mediated tumour suppression through a distinct ferroptosis pathway. *Nat. Cell. Biol.* 21 (5), 579–591. doi:10.1038/s41556-019-0305-6
- Chu, J., Liu, C. X., Song, R., and Li, Q. L. (2020). Ferrostatin-1 protects HT-22 cells from oxidative toxicity. *Neural Regen. Res.* 15 (3), 528–536. doi:10.4103/1673-5374.266060
- Chuang, D. Y., Simonyi, A., Kotzbauer, P. T., Gu, Z., and Sun, G. Y. (2015). Cytosolic phospholipase A2 plays a crucial role in ROS/NO signaling during microglial activation through the lipoxygenase pathway. *J. Neuroinflammation* 12, 199. doi:10.1186/s12974-015-0419-0
- Currais, A., and Maher, P. (2013). Functional consequences of age-dependent changes in glutathione status in the brain. *Antioxid. Redox Signal.* 19 (8), 813–822. doi:10.1089/ars.2012.4996
- Czapski, G. A., Adamczyk, A., Strosznajder, R. P., and Strosznajder, J. B. (2013). Expression and activity of PARP family members in the hippocampus during systemic inflammation: Their role in the regulation of prooxidative genes. *Neurochem. Int.* 62 (5), 664–673. doi:10.1016/j.neuint.2013.01.020
- Czapski, G. A., Czubowicz, K., Strosznajder, J. B., and Strosznajder, R. P. (2016). The lipoxygenases: Their regulation and implication in Alzheimer's disease. *Neurochem. Res.* 41 (1-2), 243–257. doi:10.1007/s11064-015-1776-x
- De Domenico, I., Ward, D. M., and Kaplan, J. (2009). Specific iron chelators determine the route of ferritin degradation. *Blood* 114 (20), 4546–4551. doi:10.1182/blood-2009-05-224188
- Derry, P. J., Hegde, M. L., Jackson, G. R., Kaye, R., Tour, J. M., Tsai, A. L., et al. (2020). Revisiting the intersection of amyloid, pathologically modified tau and iron in Alzheimer's disease from a ferroptosis perspective. *Prog. Neurobiol.* 184, 101716. doi:10.1016/j.pneurobio.2019.101716

## Conflict of interest

The authors declare that the research was conducted in the absence of any commercial or financial relationships that could be construed as a potential conflict of interest.

## Publisher's note

All claims expressed in this article are solely those of the authors and do not necessarily represent those of their affiliated organizations, or those of the publisher, the editors and the reviewers. Any product that may be evaluated in this article, or claim that may be made by its manufacturer, is not guaranteed or endorsed by the publisher.

- Di Meco, A., Lauretti, E., Vagnozzi, A. N., and Pratico, D. (2014). Zileuton restores memory impairments and reverses amyloid and tau pathology in aged Alzheimer's disease mice. *Neurobiol. Aging* 35 (11), 2458–2464. doi:10.1016/j.neurobiolaging.2014.05.016
- Dixon, S. J., Lemberg, K. M., Lamprecht, M. R., Skouta, R., Zaitsev, E. M., Gleason, C. E., et al. (2012). Ferroptosis: An iron-dependent form of nonapoptotic cell death. *Cell* 149 (5), 1060–1072. doi:10.1016/j.cell.2012.03.042
- Dixon, S. J., and Stockwell, B. R. (2014). The role of iron and reactive oxygen species in cell death. *Nat. Chem. Biol.* 10 (1), 9–17. doi:10.1038/nchembio.1416
- Doll, S., Freitas, F. P., Shah, R., Aldrovandi, M., da Silva, M. C., Ingold, I., et al. (2019). FSP1 is a glutathione-independent ferroptosis suppressor. *Nature* 575 (7784), 693–698. doi:10.1038/s41586-019-1707-0
- Dolma, S., Lessnick, S. L., Hahn, W. C., and Stockwell, B. R. (2003). Identification of genotype-selective antitumor agents using synthetic lethal chemical screening in engineered human tumor cells. *Cancer Cell* 3 (3), 285–296. doi:10.1016/s1535-6108(03)00050-3
- Donnelly, P. S., Caragounis, A., Du, T., Laughton, K. M., Volitakis, I., Cherny, R. A., et al. (2008). Selective intracellular release of copper and zinc ions from bis(thiosemicarbazone) complexes reduces levels of Alzheimer disease amyloid-beta peptide. *J. Biol. Chem.* 283 (8), 4568–4577. doi:10.1074/jbc.M705957200
- Douaud, G., Refsum, H., de Jager, C. A., Jacoby, R., Nichols, T. E., Smith, S. M., et al. (2013). Preventing Alzheimer's disease-related gray matter atrophy by B-vitamin treatment. *Proc. Natl. Acad. Sci. U. S. A.* 110 (23), 9523–9528. doi:10.1073/pnas.1301816110
- Drakesmith, H., Nemeth, E., and Ganz, T. (2015). Ironing out ferroportin. *Cell. Metab.* 22 (5), 777–787. doi:10.1016/j.cmet.2015.09.006
- Duce, J. A., Tsatsanis, A., Cater, M. A., James, S. A., Robb, E., Wikke, K., et al. (2010). Iron-export ferroxidase activity of beta-amyloid precursor protein is inhibited by zinc in Alzheimer's disease. *Cell* 142 (6), 857–867. doi:10.1016/j.cell.2010.08.014
- Ege, D. (2021). Action mechanisms of curcumin in Alzheimer's disease and its brain targeted delivery. *Mater. (Basel)* 14 (12), 3332. doi:10.3390/ma14123332
- Espósito, G., Giovacchini, G., Liow, J. S., Bhattacharjee, A. K., Greenstein, D., Schapiro, M., et al. (2008). Imaging neuroinflammation in Alzheimer's disease with radiolabeled arachidonic acid and PET. *J. Nucl. Med.* 49 (9), 1414–1421. doi:10.2967/jnumed.107.049619
- Everett, J., Cespedes, E., Shelford, L. R., Exley, C., Collingwood, J. F., Dobson, J., et al. (2014). Evidence of redox-active iron formation following aggregation of ferrihydrite and the Alzheimer's disease peptide beta-amyloid. *Inorg. Chem.* 53 (6), 2803–2809. doi:10.1021/ic402406g
- Everett, J., Cespedes, E., Shelford, L. R., Exley, C., Collingwood, J. F., Dobson, J., et al. (2014). Ferrous iron formation following the co-aggregation of ferric iron and the Alzheimer's disease peptide beta-amyloid (1–42). *J. R. Soc. Interface* 11 (95), 20140165. doi:10.1098/rsif.2014.0165
- Farmer, K. M., Ghag, G., Puangmalai, N., Montalbano, M., Bhatt, N., and Kaye, R. (2020). p53 aggregation, interactions with tau, and impaired DNA damage response in Alzheimer's disease. *Acta Neuropathol. Commun.* 8 (1), 132. doi:10.1186/s40478-020-01012-6
- Farr, S. A., Ripley, J. L., Sultana, R., Zhang, Z., Niehoff, M. L., Platt, T. L., et al. (2014). Antisense oligonucleotide against GSK-3 $\beta$  in brain of SAMP8 mice improves learning and memory and decreases oxidative stress: Involvement of transcription factor Nrf2 and implications for Alzheimer disease. *Free Radic. Biol. Med.* 67, 387–395. doi:10.1016/j.freeradbiomed.2013.11.014
- Feng, H., Schorpp, K., Jin, J., Yozwiak, C. E., Hoffstrom, B. G., Decker, A. M., et al. (2020). Transferrin receptor is a specific ferroptosis marker. *Cell. Rep.* 30 (10), 3411–3423. doi:10.1016/j.celrep.2020.02.049
- Figueiredo, C. P., Clarke, J. R., Ledo, J. H., Ribeiro, F. C., Costa, C. V., Melo, H. M., et al. (2013). Memantine rescues transient cognitive impairment caused by high-molecular-weight A $\beta$  oligomers but not the persistent impairment induced by low-molecular-weight oligomers. *J. Neurosci.* 33 (23), 9626–9634. doi:10.1523/JNEUROSCI.0482-13.2013
- Foret, M. K., Lincoln, R., Do Carmo, S., Cuervo, A. C., and Cosa, G. (2020). Connecting the "dots": From free radical lipid autoxidation to cell pathology and disease. *Chem. Rev.* 120 (23), 12757–12787. doi:10.1021/acs.chemrev.0c00761
- Friedmann Angeli, J. P., Krysko, D. V., and Conrad, M. (2019). Ferroptosis at the crossroads of cancer-acquired drug resistance and immune evasion. *Nat. Rev. Cancer* 19 (7), 405–414. doi:10.1038/s41568-019-0149-1
- Friedmann Angeli, J. P., Schneider, M., Proneth, B., Tyurina, Y. Y., Tyurin, V. A., Hammond, V. J., et al. (2014). Inactivation of the ferroptosis regulator Gpx4 triggers acute renal failure in mice. *Nat. Cell. Biol.* 16 (12), 1180–1191. doi:10.1038/ncb3064
- Furukawa, H., Singh, S. K., Mancusso, R., and Gouaux, E. (2005). Subunit arrangement and function in NMDA receptors. *Nature* 438 (7065), 185–192. doi:10.1038/nature04089
- Ghadery, C., Pirpamer, L., Hofer, E., Langkammer, C., Petrovic, K., Loitfelder, M., et al. (2015). R2\* mapping for brain iron: Associations with cognition in normal aging. *Neurobiol. Aging* 36 (2), 925–932. doi:10.1016/j.neurobiolaging.2014.09.013
- Gugliandolo, A., Bramanti, P., and Mazzon, E. (2017). Role of vitamin E in the treatment of Alzheimer's disease: Evidence from animal models. *Int. J. Mol. Sci.* 18 (12), E2504. doi:10.3390/ijms18122504
- Haddad, M., Herve, V., Ben Khedher, M. R., Rabanel, J. M., and Ramassamy, C. (2021). Glutathione: An old and small molecule with great functions and new applications in the brain and in Alzheimer's disease. *Antioxid. Redox Signal.* 35 (4), 270–292. doi:10.1089/ars.2020.8129
- Hambright, W. S., Fonseca, R. S., Chen, L., Na, R., and Ran, Q. (2017). Ablation of ferroptosis regulator glutathione peroxidase 4 in forebrain neurons promotes cognitive impairment and neurodegeneration. *Redox Biol.* 12, 8–17. doi:10.1016/j.redox.2017.01.021
- Hassannia, B., Vandenabeele, P., and Vanden Berghe, T. (2019). Targeting ferroptosis to iron out cancer. *Cancer Cell* 35 (6), 830–849. doi:10.1016/j.ccell.2019.04.002
- Hu, Z., Mi, Y., Qian, H., Guo, N., Yan, A., Zhang, Y., et al. (2020). A potential mechanism of temozolomide resistance in glioma-ferroptosis. *Front. Oncol.* 10, 897. doi:10.3389/fonc.2020.00897
- Huang, L., McClatchy, D. B., Maher, P., Liang, Z., Diedrich, J. K., Soriano-Castell, D., et al. (2020). Intracellular amyloid toxicity induces oxytosis/ferroptosis regulated cell death. *Cell. Death Dis.* 11 (10), 828. doi:10.1038/s41419-020-03020-9
- Ittner, L. M., Ke, Y. D., Delerue, F., Bi, M., Gladbach, A., van Eersel, J., et al. (2010). Dendritic function of tau mediates amyloid-beta toxicity in Alzheimer's disease mouse models. *Cell* 142 (3), 387–397. doi:10.1016/j.cell.2010.06.036
- Jia, M., Zhang, H., Qin, Q., Hou, Y., Zhang, X., Chen, D., et al. (2021). Ferroptosis as a new therapeutic opportunity for nonviral liver disease. *Eur. J. Pharmacol.* 908, 174319. doi:10.1016/j.ejphar.2021.174319
- Jiang, L., Hickman, J. H., Wang, S. J., and Gu, W. (2015). Dynamic roles of p53-mediated metabolic activities in ROS-induced stress responses. *Cell. Cycle* 14 (18), 2881–2885. doi:10.1080/15384101.2015.1068479
- Jiang, L., Kon, N., Li, T., Wang, S. J., Su, T., Hibshoosh, H., et al. (2015). Ferroptosis as a p53-mediated activity during tumour suppression. *Nature* 520 (7545), 57–62. doi:10.1038/nature14344
- Jiang, M., Qiao, M., Zhao, C., Deng, J., Li, X., and Zhou, C. (2020). Targeting ferroptosis for cancer therapy: Exploring novel strategies from its mechanisms and role in cancers. *Transl. Lung Cancer Res.* 9 (4), 1569–1584. doi:10.21037/tlcr-20-341
- Jiang, X., Stockwell, B. R., and Conrad, M. (2021). Ferroptosis: Mechanisms, biology and role in disease. *Nat. Rev. Mol. Cell. Biol.* 22 (4), 266–282. doi:10.1038/s41580-020-00324-8
- Johnson, J., Mercado-Ayon, E., Mercado-Ayon, Y., Dong, Y. N., Halawani, S., Ngaba, L., et al. (2021). Mitochondrial dysfunction in the development and progression of neurodegenerative diseases. *Arch. Biochem. Biophys.* 702, 108698. doi:10.1016/j.abb.2020.108698
- Kang, R., Kroemer, G., and Tang, D. (2019). The tumor suppressor protein p53 and the ferroptosis network. *Free Radic. Biol. Med.* 133, 162–168. doi:10.1016/j.freeradbiomed.2018.05.074
- Kanninen, K., White, A. R., Koistinaho, J., and Malm, T. (2011). Targeting glycogen synthase kinase-3 $\beta$  for therapeutic benefit against oxidative stress in Alzheimer's disease: Involvement of the nrf2-ARE pathway. *Int. J. Alzheimers Dis.* 2011, 985085. doi:10.4061/2011/985085
- Kashani, A., Lepicard, E., Poirel, O., Videau, C., David, J. P., Fallet-Bianco, C., et al. (2008). Loss of VGLUT1 and VGLUT2 in the prefrontal cortex is correlated with cognitive decline in Alzheimer disease. *Neurobiol. Aging* 29 (11), 1619–1630. doi:10.1016/j.neurobiolaging.2007.04.010
- Kehr, J. P. J. T. (2000). The Haber–Weiss reaction and mechanisms of toxicity. *Toxicology* 149 (1), 43–50. doi:10.1016/s0300-483x(00)00231-6
- Kennedy, D. O. (2016). B vitamins and the brain: Mechanisms, dose and efficacy—A review. *Nutrients* 8 (2), 68. doi:10.3390/nu8020068
- Kim, O. Y., and Song, J. (2020). The importance of BDNF and RAGE in diabetes-induced dementia. *Pharmacol. Res.* 160, 105083. doi:10.1016/j.phrs.2020.105083
- Krscio, R. J., Abner, E. L., Caban-Holt, A., Lovell, M., Goodman, P., Darke, A. K., et al. (2017). Association of antioxidant supplement use and dementia in the prevention of Alzheimer's disease by vitamin E and selenium trial (PREADViSE). *JAMA Neurol.* 74 (5), 567–573. doi:10.1001/jamaneurol.2016.5778

- Lane, D. J. R., Ayton, S., and Bush, A. I. (2018). Iron and Alzheimer's disease: An update on emerging mechanisms. *J. Alzheimers Dis.* 64 (1), S379–S395. doi:10.3233/JAD-179944
- Latunde-Dada, G. O. (2017). Ferroptosis: Role of lipid peroxidation, iron and ferritinophagy. *Biochim. Biophys. Acta. Gen. Subj.* 1861 (8), 1893–1900. doi:10.1016/j.bbagen.2017.05.019
- Lei, P., Ayton, S., and Bush, A. I. (2021). The essential elements of Alzheimer's disease. *J. Biol. Chem.* 296, 100105. doi:10.1074/jbc.REV120.008207
- Leveille, F., El Gaamouch, F., Gouix, E., Lecocq, M., Lobner, D., NicOle, O., et al. (2008). Neuronal viability is controlled by a functional relation between synaptic and extrasynaptic NMDA receptors. *FASEB J.* 22 (12), 4258–4271. doi:10.1096/fj.08-107268
- Li, D., and Li, Y. (2020). The interaction between ferroptosis and lipid metabolism in cancer. *Signal Transduct. Target. Ther.* 5 (1), 108. doi:10.1038/s41392-020-00216-5
- Li, J., Cao, F., Yin, H. L., Huang, Z. J., Lin, Z. T., Mao, N., et al. (2020). Ferroptosis: Past, present and future. *Cell. Death Dis.* 11 (2), 88. doi:10.1038/s41419-020-2298-2
- Li, Q., Li, Q. Q., Jia, J. N., Sun, Q. Y., Zhou, H. H., Jin, W. L., et al. (2019). Baicalein exerts neuroprotective effects in FeCl<sub>3</sub>-induced posttraumatic epileptic seizures via suppressing ferroptosis. *Front. Pharmacol.* 10, 638. doi:10.3389/fphar.2019.00638
- Li, R., Weng, H., Pan, Y., Meng, X., Liao, X., Wang, M., et al. (2021). Relationship between homocysteine levels and post-stroke cognitive impairment in female and male population: From a prospective multicenter study. *J. Transl. Int. Med.* 9 (4), 264–272. doi:10.2478/jtim-2021-0035
- Ling, Z., Kang, R., Zhu, S., Wang, X., Cao, L., Wang, H., et al. (2017). ALK is a therapeutic target for lethal sepsis. *Sci. Transl. Med.* 9 (412), ean5689. doi:10.1126/scitranslmed.aan5689
- Liu, Y., Chen, Z., Li, B., Yao, H., Zarka, M., Welch, J., et al. (2021). Supplementation with gamma-glutamylcysteine (gamma-GC) lessens oxidative stress, brain inflammation and amyloid pathology and improves spatial memory in a murine model of AD. *Neurochem. Int.* 144, 104931. doi:10.1016/j.neuint.2020.104931
- Liu, Y., and Gu, W. (2022). p53 in ferroptosis regulation: the new weapon for the old guardian. *Cell. Death Differ.* 29 (5), 895–910. doi:10.1038/s41418-022-00943-y
- Liu, Y., and Gu, W. (2021). The complexity of p53-mediated metabolic regulation in tumor suppression. *Semin. Cancer Biol.* doi:10.1016/j.semcancer.2021.03.010
- Luo, F., Sandhu, A. F., Rungtananawanich, W., Williams, G. E., Akbar, M., Zhou, S., et al. (2020). Melatonin and autophagy in aging-related neurodegenerative diseases. *Int. J. Mol. Sci.* 21 (19), E7174. doi:10.3390/ijms21197174
- Luo, L., Wang, H., Tian, W., Li, X., Zhu, Z., Huang, R., et al. (2021). Targeting ferroptosis-based cancer therapy using nanomaterials: Strategies and applications. *Theranostics* 11 (20), 9937–9952. doi:10.7150/thno.65480
- Lv, H., and Shang, P. (2018). The significance, trafficking and determination of labile iron in cytosol, mitochondria and lysosomes. *Metalomics* 10 (7), 899–916. doi:10.1039/c8mt00048d
- Ma, D. L., Chen, F. Q., Xu, W. J., Yue, W. Z., Yuan, G., and Yang, Y. (2015). Early intervention with glucagon-like peptide 1 analog liraglutide prevents tau hyperphosphorylation in diabetic db/db mice. *J. Neurochem.* 135 (2), 301–308. doi:10.1111/jnc.13248
- Mancias, J. D., Pontano Vaite, L., Nissim, S., Biancur, D. E., Kim, A. J., Wang, X., et al. (2015). Ferritinophagy via NCOA4 is required for erythropoiesis and is regulated by iron dependent HERC2-mediated proteolysis. *Elife* 4. doi:10.7554/eLife.10308
- Mao, H., Zhao, Y., Li, H., and Lei, L. (2020). Ferroptosis as an emerging target in inflammatory diseases. *Prog. Biophys. Mol. Biol.* 155, 20–28. doi:10.1016/j.pbiomolbio.2020.04.001
- Martinez-Valbuena, I., Valenti-Azcarate, R., Amat-Villegas, I., Riverol, M., Marcilla, I., de Andrea, C. E., et al. (2019). Amylin as a potential link between type 2 diabetes and alzheimer disease. *Ann. Neurol.* 86 (4), 539–551. doi:10.1002/ana.25570
- Masaldan, S., Bush, A. I., Devos, D., Rolland, A. S., and Moreau, C. (2019). Striking while the iron is hot: Iron metabolism and ferroptosis in neurodegeneration. *Free Radic. Biol. Med.* 133, 221–233. doi:10.1016/j.freeradbiomed.2018.09.033
- Miotto, G., Rossetto, M., Di Paolo, M. L., Orian, L., Venerando, R., Roveri, A., et al. (2020). Insight into the mechanism of ferroptosis inhibition by ferrostatin-1. *Redox Biol.* 28, 101328. doi:10.1016/j.redox.2019.101328
- Monacelli, F., Acquarone, E., Giannotti, C., Borghi, R., and Nencioni, A. (2017). Vitamin C, aging and Alzheimer's disease. *Nutrients* 9 (7), E670. doi:10.3390/nu9070670
- Moreau, C., Danel, V., Devedjian, J. C., Grolez, G., Timmerman, K., Laloux, C., et al. (2018). Could conservative iron chelation lead to neuroprotection in amyotrophic lateral sclerosis? *Antioxid. Redox Signal.* 29 (8), 742–748. doi:10.1089/ars.2017.7493
- Morice-Picard, F., Benard, G., Rezvani, H. R., Lasseaux, E., Simon, D., Moutton, S., et al. (2016). Complete loss of function of the ubiquitin ligase HERC2 causes a severe neurodevelopmental phenotype. *Eur. J. Hum. Genet.* 25 (1), 52–58. doi:10.1038/ejhg.2016.139
- Moujalled, D., Strasser, A., and Liddell, J. R. (2021). Molecular mechanisms of cell death in neurological diseases. *Cell. Death Differ.* 28 (7), 2029–2044. doi:10.1038/s41418-021-00814-y
- Ou, M., Jiang, Y., Ji, Y., Zhou, Q., Du, Z., Zhu, H., et al. (2022). Role and mechanism of ferroptosis in neurological diseases. *Mol. Metab.* 61, 101502. doi:10.1016/j.molmet.2022.101502
- Ou, Y., Wang, S. J., Li, D., Chu, B., and Gu, W. (2016). Activation of SAT1 engages polyamine metabolism with p53-mediated ferroptotic responses. *Proc. Natl. Acad. Sci. U. S. A.* 113 (44), E6806–E6812. doi:10.1073/pnas.1607152113
- Parpura, V., Fisher, E. S., Lechleiter, J. D., Schousboe, A., Waagepetersen, H. S., Brunet, S., et al. (2017). Glutamate and ATP at the interface between signaling and metabolism in astroglia: Examples from pathology. *Neurochem. Res.* 42 (1), 19–34. doi:10.1007/s11064-016-1848-6
- Peng, W., Zhu, Z., Yang, Y., Hou, J., Lu, J., Chen, C., et al. (2021). N2L, a novel lipoic acid-niacin dimer, attenuates ferroptosis and decreases lipid peroxidation in HT22 cells. *Brain Res. Bull.* 174, 250–259. doi:10.1016/j.brainresbull.2021.06.014
- Petrat, F., Rauen, U., and Groot, H. D. J. H. (1999). *Determ. chelatable iron pool Isol. rat hepatocytes by digital Fluoresc. Microsc. using Fluoresc. probe, phen green SK 29* (4).
- Plascencia-Villa, G., and Perry, G. (2021). Preventive and therapeutic strategies in Alzheimer's disease: Focus on oxidative stress, redox metals, and ferroptosis. *Antioxid. Redox Signal.* 34 (8), 591–610. doi:10.1089/ars.2020.8134
- Qi, X., Zhang, Y., Guo, H., Hai, Y., Luo, Y., and Yue, T. (2020). Mechanism and intervention measures of iron side effects on the intestine. *Crit. Rev. Food Sci. Nutr.* 60 (12), 2113–2125. doi:10.1080/10408398.2019.1630599
- Qiu, Y., Cao, Y., Cao, W., Jia, Y., and Lu, N. (2020). The application of ferroptosis in diseases. *Pharmacol. Res.* 159, 104919. doi:10.1016/j.phrs.2020.104919
- Qu, C., Peng, Y., and Liu, S. (2022). Ferroptosis biology and implication in cancers. *Front. Mol. Biosci.* 9, 892957. doi:10.3389/fmolb.2022.892957
- Qu, Z., Sun, J., Zhang, W., Yu, J., and Zhuang, C. (2020). Transcription factor NRF2 as a promising therapeutic target for Alzheimer's disease. *Free Radic. Biol. Med.* 159, 87–102. doi:10.1016/j.freeradbiomed.2020.06.028
- Reddy, P. H., Manczak, M., Yin, X., Grady, M. C., Mitchell, A., Tonk, S., et al. (2018). Protective effects of Indian spice curcumin against amyloid-beta in Alzheimer's disease. *J. Alzheimers Dis.* 61 (3), 843–866. doi:10.3233/JAD-170512
- Reichert, C. O., de Freitas, F. A., Sampaio-Silva, J., Rokita-Rosa, L., Barros, P. d. L., Levy, D., et al. (2020). Ferroptosis mechanisms involved in neurodegenerative diseases. *Int. J. Mol. Sci.* 21 (22), E8765. doi:10.3390/ijms21228765
- Reiss, A. B., Arain, H. A., Stecker, M. M., Siegert, N. M., and Kasselmann, L. J. (2018). Amyloid toxicity in Alzheimer's disease. *Rev. Neurosci.* 29 (6), 613–627. doi:10.1515/revneuro-2017-0063
- Ross, D., and Siegel, D. (2021). The diverse functionality of NQO1 and its roles in redox control. *Redox Biol.* 41, 101950. doi:10.1016/j.redox.2021.101950
- Sato, M., Kusumi, R., Hamashima, S., Kobayashi, S., Sasaki, S., Komiyama, Y., et al. (2018). The ferroptosis inducer erastin irreversibly inhibits system xc- and synergizes with cisplatin to increase cisplatin's cytotoxicity in cancer cells. *Sci. Rep.* 8 (1), 968. doi:10.1038/s41598-018-19213-4
- Serviddio, G., Cassano, T., Pace, L., Bede, G., Michele Lavecchia, A., De Marco, F., et al. (2015). Glutamate and mitochondria: Two prominent players in the oxidative stress-induced neurodegeneration. *Curr Alzheimer Res.* 13 (2), 185–97. doi:10.2174/1567205013666151218132725
- Sheng, X., Shan, C., Liu, J., Yang, J., Sun, B., and Chen, D. (2017). Theoretical insights into the mechanism of ferroptosis suppression via inactivation of a lipid peroxide radical by liproxstatin-1. *Phys. Chem. Chem. Phys.* 19 (20), 13153–13159. doi:10.1039/c7cp00804j
- Shetty, R. A., Forster, M. J., and Sumien, N. (2013). Coenzyme Q(10) supplementation reverses age-related impairments in spatial learning and lowers protein oxidation. *Age (Dordr)* 35 (5), 1821–1834. doi:10.1007/s11357-012-9484-9
- Shi, F., Zhang, P., Mao, Y., Wang, C., Zheng, M., and Zhao, Z. (2017). The nitroxide Tempo inhibits hydroxyl radical production from the Fenton-like reaction of iron(II)-citrate with hydrogen peroxide. *Biochem. Biophys. Res. Commun.* 483 (1), 159–164. doi:10.1016/j.bbrc.2016.12.174

- Shi, Z., Zhang, L., Zheng, J., Sun, H., and Shao, C. (2021). Ferroptosis: Biochemistry and biology in cancers. *Front. Oncol.* 11, 579286. doi:10.3389/fonc.2021.579286
- Shin, D., Kim, E. H., Lee, J., and Roh, J. L. (2018). Nrf2 inhibition reverses resistance to GPX4 inhibitor-induced ferroptosis in head and neck cancer. *Free Radic. Biol. Med.* 129, 454–462. doi:10.1016/j.freeradbiomed.2018.10.426
- Song, X., and Long, D. (2020). Nrf2 and ferroptosis: A new research direction for neurodegenerative diseases. *Front. Neurosci.* 14, 267. doi:10.3389/fnins.2020.00267
- Stockwell, B. R., Friedmann Angeli, J. P., Bayir, H., Bush, A. I., Conrad, M., Dixon, S. J., et al. (2017). Ferroptosis: A regulated cell death nexus linking metabolism, redox biology, and disease. *Cell* 171 (2), 273–285. doi:10.1016/j.cell.2017.09.021
- Stockwell, B. R., Jiang, X., and Gu, W. (2020). Emerging mechanisms and disease relevance of ferroptosis. *Trends Cell. Biol.* 30 (6), 478–490. doi:10.1016/j.tcb.2020.02.009
- Sun, Y., Xiao, Q., Luo, C., Zhao, Y., Pu, D., Zhao, K., et al. (2017). High-glucose induces tau hyperphosphorylation through activation of TLR9-P38MAPK pathway. *Exp. Cell. Res.* 359 (2), 312–318. doi:10.1016/j.yexcr.2017.07.032
- Takeda, S., Sato, N., Uchio-Yamada, K., Sawada, K., Kunieda, T., Takeuchi, D., et al. (2010). Diabetes-accelerated memory dysfunction via cerebrovascular inflammation and Abeta deposition in an Alzheimer mouse model with diabetes. *Proc. Natl. Acad. Sci. U. S. A.* 107 (15), 7036–7041. doi:10.1073/pnas.1000645107
- Tang, M., Chen, Z., Wu, D., and Chen, L. (2018). Ferritinophagy/ferroptosis: Iron-related newcomers in human diseases. *J. Cell. Physiol.* 233 (12), 9179–9190. doi:10.1002/jcp.26954
- Tang, M., and Taghibiglou, C. (2017). The mechanisms of action of curcumin in Alzheimer's disease. *J. Alzheimers Dis.* 58 (4), 1003–1016. doi:10.3233/JAD-170188
- Tang, Z., Huang, Z., Huang, Y., Chen, Y., Huang, M., Liu, H., et al. (2021). Ferroptosis: The silver lining of cancer therapy. *Front. Cell. Dev. Biol.* 9, 765859. doi:10.3389/fcell.2021.765859
- Tarangelo, A., Magtanong, L., Biegging-Rolett, K. T., Li, Y., Ye, J., Attardi, L. D., et al. (2018). p53 suppresses metabolic stress-induced ferroptosis in cancer cells. *Cell. Rep.* 22 (3), 569–575. doi:10.1016/j.celrep.2017.12.077
- Thomas, M. H., Paris, C., Magnien, M., Colin, J., Pelleieux, S., Coste, F., et al. (2017). Dietary arachidonic acid increases deleterious effects of amyloid-beta oligomers on learning abilities and expression of AMPA receptors: Putative role of the ACSLA-cPLA2 balance. *Alzheimers Res. Ther.* 9 (1), 69. doi:10.1186/s13195-017-0295-1
- Thompson, J. A., White, C. C., Cox, D. P., Chan, J. Y., Kavanagh, T. J., Fausto, N., et al. (2009). Distinct Nrf1/2-independent mechanisms mediate as 3+-induced glutamate-cysteine ligase subunit gene expression in murine hepatocytes. *Free Radic. Biol. Med.* 46 (12), 1614–1625. doi:10.1016/j.freeradbiomed.2009.03.016
- Tsatsanis, A., Wong, B. X., Gunn, A. P., Ayton, S., Bush, A. I., Devos, D., et al. (2020). Amyloidogenic processing of Alzheimer's disease beta-amyloid precursor protein induces cellular iron retention. *Mol. Psychiatry* 25 (9), 1958–1966. doi:10.1038/s41380-020-0762-0
- Wang, Y., and Mandelkow, E. (2016). Tau in physiology and pathology. *Nat. Rev. Neurosci.* 17 (1), 5–21. doi:10.1038/nrn.2015.1
- Ward, R. J., Zucca, F. A., Duyn, J. H., Crichton, R. R., and Zecca, L. (2014). The role of iron in brain ageing and neurodegenerative disorders. *Lancet. Neurol.* 13 (10), 1045–1060. doi:10.1016/S1474-4422(14)70117-6
- Xia, J., Si, H., Yao, W., Li, C., Yang, G., Tian, Y., et al. (2021). Research progress on the mechanism of ferroptosis and its clinical application. *Exp. Cell. Res.* 409 (2), 112932. doi:10.1016/j.yexcr.2021.112932
- Xie, Y., Song, X., Sun, X., Huang, J., Zhong, M., Lotze, M. T., et al. (2016). Identification of baicalein as a ferroptosis inhibitor by natural product library screening. *Biochem. Biophys. Res. Commun.* 473 (4), 775–780. doi:10.1016/j.bbrc.2016.03.052
- Xie, Y., Zhu, S., Song, X., Sun, X., Fan, Y., Liu, J., et al. (2017). The tumor suppressor p53 limits ferroptosis by blocking DPP4 activity. *Cell. Rep.* 20 (7), 1692–1704. doi:10.1016/j.celrep.2017.07.055
- Xu, G., Wang, H., Li, X., Huang, R., and Luo, L. (2021). Recent progress on targeting ferroptosis for cancer therapy. *Biochem. Pharmacol.* 190, 114584. doi:10.1016/j.bcp.2021.114584
- Yan, H. F., Zou, T., Tuo, Q. Z., Xu, S., Li, H., Belaidi, A. A., et al. (2021). Ferroptosis: Mechanisms and links with diseases. *Signal Transduct. Target. Ther.* 6 (1), 49. doi:10.1038/s41392-020-00428-9
- Yan, H., Yan, Y., Gao, Y., Zhang, N., Kumar, G., Fang, Q., et al. (2022). Transcriptome analysis of fasudil treatment in the APPsw/PSEN1dE9 transgenic (APP/PS1) mice model of Alzheimer's disease. *Sci. Rep.* 12 (1), 6625. doi:10.1038/s41598-022-10554-9
- Yan, N., and Zhang, J. (2019). Iron metabolism, ferroptosis, and the links with Alzheimer's disease. *Front. Neurosci.* 13, 1443. doi:10.3389/fnins.2019.01443
- Yang, W. S., and Stockwell, B. R. (2008). Synthetic lethal screening identifies compounds activating iron-dependent, nonapoptotic cell death in oncogenic-RAS-harboring cancer cells. *Chem. Biol.* 15 (3), 234–245. doi:10.1016/j.chembiol.2008.02.010
- Yoo, S. E., Chen, L., Na, R., Liu, Y., Rios, C., Van Remmen, H., et al. (2012). Gpx4 ablation in adult mice results in a lethal phenotype accompanied by neuronal loss in brain. *Free Radic. Biol. Med.* 52 (9), 1820–1827. doi:10.1016/j.freeradbiomed.2012.02.043
- Yuan, Y., Men, W., Shan, X., Zhai, H., Qiao, X., Geng, L., et al. (2020). Baicalein exerts neuroprotective effect against ischemic/reperfusion injury via alteration of NF- $\kappa$ B and LOX and AMPK/Nrf2 pathway. *Inflammopharmacology* 28 (5), 1327–1341. doi:10.1007/s10787-020-00714-6
- Zhang, Y. H., Wang, D. W., Xu, S. F., Zhang, S., Fan, Y. G., Yang, Y. Y., et al. (2018).  $\alpha$ -Lipoic acid improves abnormal behavior by mitigation of oxidative stress, inflammation, ferroptosis, and tauopathy in P301S Tau transgenic mice. *Redox Biol.* 14, 535–548. doi:10.1016/j.redox.2017.11.001
- Zhang, Z., Dmitrieva, N. I., Park, J. H., Levine, R. L., and Burg, M. B. (2004). High urea and NaCl carbonylate proteins in renal cells in culture and *in vivo*, and high urea causes 8-oxoguanine lesions in their DNA. *Proc. Natl. Acad. Sci. U. S. A.* 101 (25), 9491–9496. doi:10.1073/pnas.0402961101
- Zheng, H., Jiang, J., Xu, S., Liu, W., Xie, Q., Cai, X., et al. (2021). Nanoparticle-induced ferroptosis: Detection methods, mechanisms and applications. *Nanoscale* 13 (4), 2266–2285. doi:10.1039/d0nr08478f
- Zilka, O., Shah, R., Li, B., Friedmann Angeli, J. P., Griesser, M., Conrad, M., et al. (2017). On the mechanism of cytoprotection by ferrostatin-1 and liproxstatin-1 and the role of lipid peroxidation in ferroptotic cell death. *ACS Cent. Sci.* 3 (3), 232–243. doi:10.1021/acscentsci.7b00028





## OPEN ACCESS

## EDITED BY

Yanqing Liu,  
Columbia University, United States

## REVIEWED BY

Qian Wang,  
College of Staten Island, United States  
Lingli He,  
Harvard University, United States

## \*CORRESPONDENCE

Yinnong Jia,  
jiayinnong@kmmu.edu.cn

## SPECIALTY SECTION

This article was submitted to Molecular  
Diagnostics and Therapeutics,  
a section of the journal  
Frontiers in Molecular Biosciences

RECEIVED 10 June 2022

ACCEPTED 30 June 2022

PUBLISHED 26 August 2022

## CITATION

Tan Z, Huang H, Sun W, Li Y and Jia Y  
(2022), Current progress of ferroptosis  
study in ovarian cancer.  
*Front. Mol. Biosci.* 9:966007.  
doi: 10.3389/fmolb.2022.966007

## COPYRIGHT

© 2022 Tan, Huang, Sun, Li and Jia. This  
is an open-access article distributed  
under the terms of the [Creative  
Commons Attribution License \(CC BY\)](#).  
The use, distribution or reproduction in  
other forums is permitted, provided the  
original author(s) and the copyright  
owner(s) are credited and that the  
original publication in this journal is  
cited, in accordance with accepted  
academic practice. No use, distribution  
or reproduction is permitted which does  
not comply with these terms.

# Current progress of ferroptosis study in ovarian cancer

Zhuomin Tan, Hui Huang, Wenyan Sun, Ya Li and Yinnong Jia\*

Department of Pharmaceutical Sciences, School of Pharmaceutical Sciences and Yunnan Key  
Laboratory of Pharmacology for Natural Products, Kunming Medical University, Kunming, China

Tumors are the leading cause of death all over the world, among which ovarian cancer ranks the third in gynecological malignancies. The current treatment for ovarian cancer is liable to develop chemotherapy resistance and high recurrence rate, in which a new strategy is demanded. Ferroptosis, a newly discovered manner of regulatory cell death, is shown to be induced by massive iron-dependent accumulation of lipid reactive oxygen species. With the in-depth study of ferroptosis, its associated mechanism with various tumors is gradually elucidated, including ovarian tumor, which probably promotes the application of ferroptosis in treating ovarian cancer. To this end, this review will focus on the history and current research progress of ferroptosis, especially its regulation mechanism, and its potential application as a novel treatment strategy for ovarian cancer.

## KEYWORDS

ovarian cancer, ferroptosis, ROS, System-Xc<sup>-</sup>, FSP1-CoQ10-NAD (P) H, GCH1-BH4, inducer, inhibitor

## 1 Introduction

Malignant tumors, one of the major diseases that seriously endanger human health, are the leading cause of death and a major public health problem all over the world. The treatments for tumors commonly include surgical therapy, radiotherapy, and drug therapy (chemotherapy), which is referred to as systemic therapy.

Ovarian cancer ranks the third in incidence and the second in mortality rate among gynecological malignant tumors worldwide. Meanwhile, it is one of the three most diagnosed malignant tumors in the female reproductive system. As diagnosed, 90–95% of ovarian cancers are primary ovarian malignant tumors and 5–10% are primary metastatic ovarian malignancy detected at other proximal sites. Among primary ovarian malignant tumors, epithelial cutaneous ovarian cancer is most commonly observed, accounting for more than 90% (Brown et al., 2014), in which high-grade serous cancer (high-grade serous carcinoma, HGSC) accounts for 70% (Reid et al., 2017). Most ovarian cancer patients do not display specific symptoms at early onset, and 75% are identified as advanced stage at the time of diagnosis (Lheureux et al., 2019). In addition, most of them exhibit a poor prognosis because of drug resistance and adverse effects. Therefore, it remains a great challenge to realize early diagnosis and overcome drug resistance in the current investigation of ovarian cancer.

At present, comprehensive treatment in ovarian cancer is frequently adopted, that is, the initial surgical treatment, supplemented by chemotherapy with the diagnosis and

treatment has entered the era of accurate and individualized comprehensive disease management. At present, surgery is not only the most effective treatment to remove tumors but also a necessary method to confirm the diagnosis and specific stages by pathological analysis. Ovarian cancer patients at an early stage are treated with comprehensive staging surgery in order to completely remove the tumor and identify the specific stages, and patients at the advanced stage are treated with debulking surgery to remove tumor maximally (China Anti-Cancer Association Gynecological Cancer Professional Committee, 2021). Owing to the spread of most ovarian cancer in the early stage, surgery can barely remove all malignant lesions. In addition, the tumor volume of some advanced patients has decreased significantly after drug treatment, which facilitates surgery. Therefore, systemic chemotherapy has become the most important auxiliary therapy for ovarian cancer. At present, the first-line chemotherapy regimen for ovarian cancer is the administration of platinum drugs combined with paclitaxel, and the targeted drugs bevacizumab and PARP inhibitor are usually used for the maintenance of treatment. In recent years, the neoadjuvant chemotherapy (NACT) (van Driel et al., 2018) such as immunotherapy which utilizes inhibitors of immune examination point has become research hotspot, and gradually participates in ovarian cancer treatment.

In recent years, a new type of regulatory cell death (RCD) has been reported, somewhere between cell necrosis and apoptosis (Luo et al., 2021), which was first named ferroptosis in 2012. The cellular accumulation of lipid peroxides depending on the existence of iron eventually leads to cell ferroptosis. Cells that die in this way displayed unique characteristics, including increased mitochondrial membrane density, decreased or disappeared mitochondrial cristae, and reduced mitochondrial volume. Furthermore, ferroptosis has been reported to be

associated with tumors, neurological diseases, kidney injury, and other diseases (Li et al., 2020). However, current studies of the regulatory mechanism of ferroptosis, such as the Fenton reaction, reactive oxygen species (ROS) regulation mechanism, System-Xc<sup>-</sup>-GSH-GPX4 pathway, *p53*-related pathway, FSP1-COQ10-NAD (P) H pathway, Hippo pathway, and GCH1-BH4 pathway, are not enough. At present, research reports of ferroptosis in ovarian cancer are less than 100, including the cell iron level, transsulfuration pathway, and Hippo pathway with participating genes such as *p53*, SCD1, and FZD7. Some publications also explored the application of ferroptosis in treating patients with platinum and paclitaxel resistance. In the future, more targets and drugs related to ferroptosis are expected for the diagnosis, treatment, and prognosis of ovarian cancer. Therefore, we summarized the role of ferroptosis in tumors, especially ovarian cancer, to provide a new research direction and novel treatment strategy.

## 1.1 Research history of ferroptosis

In 2001, during the study of the role of glutamate oxidative toxicity on nerve cell death, researchers found that dead nerve cells presented features of cell necrosis and apoptosis and were prevented by macromolecular synthesis inhibitors. However, this type of death depends on the generation of oxidative stress, different from the classical mode of cell death, and is therefore named oxidative death (Tan et al., 2001). In 2003, Dolma et al. (2003) reported that when they were screening for genetically selective antitumor small molecule drugs, they identified a new compound (named erastin). They found cells treated with erastin did not induce DNA fragmentation, with no change in nuclear morphology observed, and this treatment was irreversible on

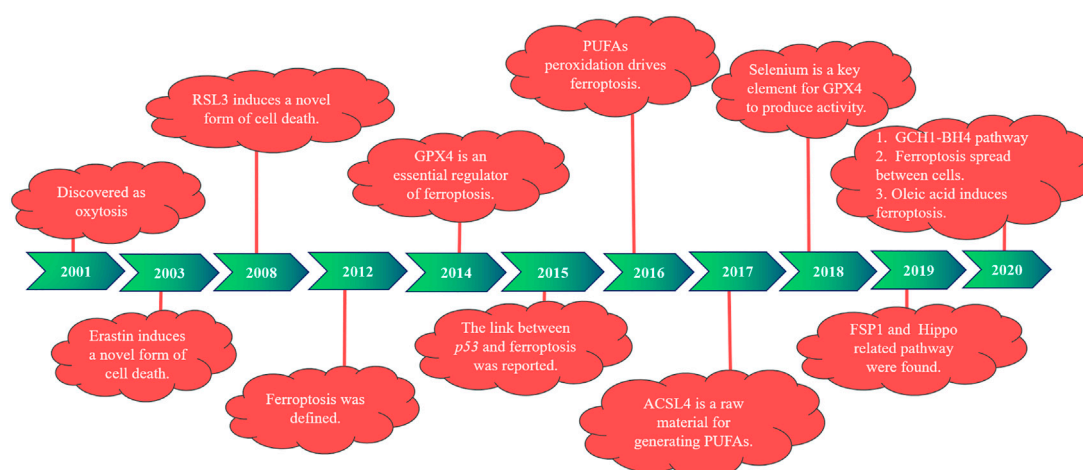


**FIGURE 1**

The development of ferroptosis at different time points.

cells. Therefore, researchers believe that erastin-induced a new nonapoptotic cell death. Then, in 2008, Yang and Stockwell (2008) used the oncogene RAS as a specific mutation in artificial lethal screening, and between the two new compounds identified (named RSL5 and RSL3), RSL3 can activate erastin-mediated cell death mechanisms and can be inhibited by iron complexes. In 2012, Dixon et al. (2012) defined ferroptosis for the first time when they found that the small molecule erastin in the cancer-causing RAS-selective lethal compound triggered a form of nonapoptotic cell death. This is iron-dependent, which is different from apoptosis, programmed necrosis, and other known forms of cell death, and is usually accompanied by a massive accumulation of ROS, oxidative stress). It was also found that erastin inhibited cellular uptake of cystine by targeting the cystine/glutamate reverse transporter, thereby reducing the synthesis of reduced glutathione (GSH) and depleting GSH, which can be inhibited by the lipophilic antioxidant small molecule iron statin (ferrostatin-1, Fer-1).

Studies have found that the deficiency of glutathione peroxidase 4 (GPX4) leads to the accumulation of lipid peroxidation and abnormal cell death, which was induced by oxidative stress and prevented by knocking down the AIF gene (Seiler et al., 2008). According to previous studies, GPX4 is widely expressed in mammals, belongs to one of the seven glutathione peroxidases in mammals, is the only known major antioxidant enzyme that directly reduces peroxidase in cell membranes and lipoproteins, and interacts with tocopherol (vitamin E) to inhibit lipid peroxidation (Yant et al., 2003). In 2014, GPX4 was selected by Yang et al. (2014) and was confirmed as a key regulator of ferroptosis activated by erastin and RSL3. Erastin deactivates GPX4 by exhausting GSH, leading to the production of cytoplasmic and lipid ROS, whereas RSL3 directly binds and inactivates GPX4, leading to ferroptosis, and can be inhibited by an RSL3 inhibitor, such as iron complexation (DFOM), a MEK inhibitor (U0126), and antioxidants. In 2015, Jiang et al. (2015) first reported a link between *p53* and ferroptosis. One year later, Yang et al. (2016) reported that peroxidation of polyunsaturated fatty acids (PUFAs) occurred under the regulation of phosphorylase G2 (PHKG2) and lipoxygenase, respectively. In 2017, Doll et al. (2017) identified acyl-CoA synthetase long-chain family member 4 (ACSL4) as a key determinant of ferroptosis sensitivity, which can be used as a predictive marker of ferroptosis in different cellular environments and is an essential raw material for the production of PUFAs. In the following year, Ingold et al. (2018) found that selenium is present in GPX4 as the amino acid selenocysteine at position 21 and plays an indispensable role in GPX4 activity.

Then, in 2019, Bersuker et al. (2019) and Doll et al. (2019) investigated the mechanism of ferroptosis suppressor protein 1 [FSP1, previously known as the apoptosis-inducing factor mitochondrial 2 (AIFM2)] in ferroptosis, identifying FSP1 as a potent ferroptosis resistance factor. At the same time, another

group (Wu et al., 2019; Yang et al., 2019) found that cell density was a nongenetic factor that could modulate the sensitivity of ferroptosis by regulating the Hippo pathway effector YAP/TAZ, and more specific regulatory mechanisms were subsequently found in kidney and ovarian cancer studies. In 2020, a new pathway of GCH1-BH4 was discovered (Kraft et al., 2020; Wei et al., 2020). Riegman et al. (2020) reported that cell swelling was observed with ferroptosis, suggesting that it is an osmotic process that can be prevented by the administration of osmoprotectants. Ferroptosis was also found to distribute between cells in a lipid peroxidation and iron-dependent manner, which was not prevented by treatment with osmoprotectants. It has also been shown that oleic acid in lymph protects melanoma cells from ferroptosis in an acyl-CoA synthetase long-chain family member 3 (ACSL3)-dependent manner and can increase their ability to form metastatic tumors (Ubellacker et al., 2020). The history of ferroptosis development is also demonstrated in Figure 1.

## 2 Regulatory mechanisms of ferroptosis

In this section, the key regulatory pathways and mechanisms of proteins involved in ferroptosis are elucidated (Figure 2), with an emphasis on the valuable targets for treatment.

### 2.1 Iron reacts with Fenton

As the name suggested, the occurrence of ferroptosis depends on the existence of iron, which is essential for the normal maintenance of mammalian cells. Ingested iron absorbed by duodenal epithelial cells and red blood cell lysis produce  $\text{Fe}^{2+}$ , and then, ceruloplasmin oxidizes  $\text{Fe}^{2+}$  to  $\text{Fe}^{3+}$ .  $\text{Fe}^{3+}$  forms a binding substance with transferrin (TF), which is then transported through transferrin receptor 1 (TFR1) on the cell membrane surface and then endocytosed into cells. Later,  $\text{Fe}^{3+}$  is detached from the TF of the endosome and is finally reduced to  $\text{Fe}^{2+}$  by six-transmembrane epithelial antigen of prostate 3 (STEAP3) and then transported to the cytoplasm through the divalent metal ion transporter 1 (DMT1). In addition,  $\text{Fe}^{2+}$  constitutes labile iron pool (LIP) in cells as free iron ions, most of which are transferred to the mitochondria to participate in the formation of iron-dependent protein complexes, iron-sulfur clusters, heme, and other metabolic processes. However, heme oxygenase 1 (HO-1) catalyzes heme degradation to produce free iron, whose overexpression is able to accelerate erastin-induced ferroptosis. On the other hand, if  $\text{Fe}^{2+}$  is in excess in cells, it is stored as ferritin and released by the ferritin complex when needed or transported extracellularly by ferroportin 1 (FPN1) (Rockfield et al., 2017).

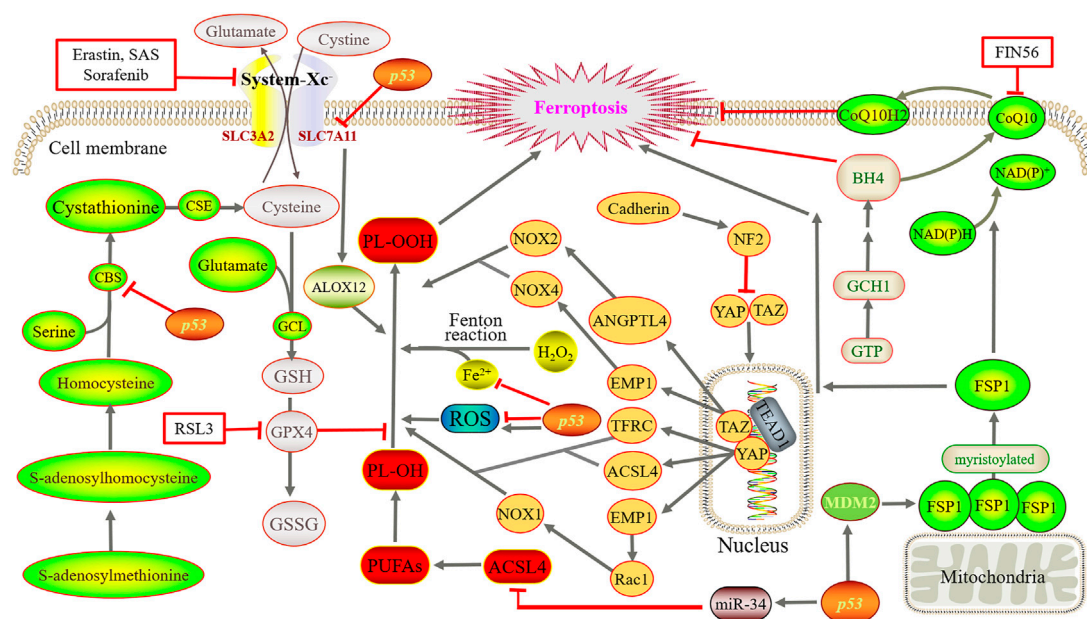


FIGURE 2

Main regulatory mechanisms of ferroptosis. Iron directs the Fenton reaction and induces large accumulation of ROS. Cystine is converted to cysteine for the synthesis of GSH. Then, GPX4 converts GSH to GSSG and reduces PL-OOH to PL-OH, thereby blocks the lipid peroxidation chain reaction. Using methionine as a sulfur donor, intermediate homocysteine, serine and cystathionine are converted into cysteine by the catalysis of CBS and CSE, simultaneously producing GSH. YAP and TAZ are abnormally activated, and bind to the TEAD after dephosphorylation. GCH1 overexpression promotes the generation of BH4. FSP1 oxidizes the terminal octadecylation modification of protein N to mediate lipid peroxidation. Simultaneously, FSP1 catalyzes the regeneration of ubiquinone and enters the circulation. By suppressing TFR1, ZIP14, ACSL4, SLC7A11 and CBS, *p53* reduce or increase ROS as well as transactivate MDM2.

It is well known that iron deficiency often causes anemia, but excessive iron may imbalance iron homeostasis, thus driving the Fenton reaction to produce biotoxicity. Iron and hydrogen peroxide oxidize multiple substrates in biotoxic reactions called the Fenton reaction, which is able to produce hydroxyl radicals and higher oxidized states of iron (Winterbourn, 1995). The simplest representation of the Fenton reaction is as follows:



Iron directs the Fenton reaction to that of the hydrogen peroxide ( $\text{H}_2\text{O}_2$ ) generation of a hydroxyl radical ( $\text{HO} \cdot$ ). When GPX4 is inhibited,  $\text{HO} \cdot$  causes PUFAs to produce peroxidized lipids, and then, oxygen further catalyzes lipid oxidation and disrupts the membrane (Green, 2019). Peroxidized lipids can also produce new free radicals under the catalysis of iron, undergo a chain reaction, and promote the further propagation of lipid peroxidation (Conrad and Pratt, 2019).

## 2.2 Reactive oxygen species

ROS include superoxide anions, hydrogen peroxide, singlet oxygen, and hydroxyl radicals, which drive lipid peroxidation

and kill cells by destroying lipids, proteins, and DNA (Lin et al., 2018). Tumor cell sustained growth and proliferation require “hypermetabolism,” and cells undergo metabolic reprogramming and abnormalities in mitochondrial function, eventually producing ROS and conducting proliferation signals to promote tumor development (Wang et al., 2019), but too much ROS may cause cell death. In this process, the mitochondrial electron transport chain produces electron leakage to generate a superoxide anion, NADPH oxidase on the cell membrane produces a superoxide anion, a superoxide anion forms  $\text{H}_2\text{O}_2$  under the action of superoxide dismutase, and  $\text{H}_2\text{O}_2$  is catalyzed by iron to produce  $\text{HO} \cdot$ , which further induces lipid peroxidation (large accumulation of ROS accumulation) and eventually leads to ferroptosis.

## 2.3 System-Xc<sup>-</sup>-GSH-GPX4 pathway

System-Xc<sup>-</sup> is a heterodimeric amino acid reverse transporter that is widely distributed on the phospholipid bilayer. It is formed by solute carrier family members 11 (xCT) and solute carrier family 3 member 2 (SLC3A2, also called CD98hc) by disulfide bonds, also known as a cystine/glutamate reverse transporter. The former is a



nutrient transporter protein that is frequently overexpressed in human malignancies (Koppula et al., 2018), and the latter uptakes extracellular cysteine while delivering equivalent amounts of glutamate to extracellular cells (Cao and Dixon, 2016). After cysteine enters the cell, cystine is converted to cysteine for the synthesis of GSH. Then, GPX4, which is active because of its selenocysteine content, converts GSH to oxidized GSH (GSSG) and reduces phospholipid hydrogen peroxide (PL-OOH) to phospholipid-alcohol (PL-OH), thereby blocking the lipid peroxidation chain reaction (Seibt et al., 2019). Studies have shown that erastin, sulfasalazine (SAS), and multiple kinase inhibitor sorafenib can block the function of xCT, deplete GSH, and thus induce ferroptosis (Gout et al., 2001; Dixon et al., 2012; Sun et al., 2016). However, the *p53* gene can downregulate cystine uptake by inhibiting SLC7A11 transcription, which limits intracellular GSH production (Yant et al., 2003).

In addition, studies have shown that cysteine, a nonessential amino acid, can be synthesized through the transsulfuration pathway in some mammalian cells and then binds glutamate to generate GSH under the action of glutamate cysteine ligase. Using methionine as a sulfur donor, intermediate homocysteine, serine, and cystathionine are converted into cysteine by the catalysis of cystathionine  $\beta$ -synthase (CBS) and cystathionine gamma-lyase (CSE), simultaneously producing GSH and the gas signaling molecule hydrogen sulfide (McBean, 2012; Sbodio et al., 2019). In addition, homocysteine can be derived from dietary methionine, which is converted to S-adenosine methionine and is then catalyzed by methyltransferase to produce S-adenosine and further generate homocysteine. In particular, CBS (also known as L-serine hydrolase) catalyzes the condensation of serine and homocysteine to form cystathionine. CSE (also known as L-cystathionine cysteine-lyase) is the only enzyme in mammals that can directly produce cysteine using the cystathionine generated by CBS.

## 2.4 *p53*-related pathway

The expression of *p53* in different species is highly conservative. Therefore, it is also called the guardian of genomes and cells, with a critical role. In 2015, it was reported by Jiang et al. (2015) for the first time that *p53* was related to ferroptosis, indicating its dual effect on ferroptosis as involving iron metabolism, lipid metabolism, amino acid metabolism, and ROS regulation. At present, ferroptosis can be classified into two main categories: GPX4-centered and *p53*-centered. As *p53* is a key regulator of cellular metabolism, it plays a vital role in ferroptosis regulation and is tightly related to ferroptosis initiation and progression (Liu and Gu, 2021; Liu and Gu, 2022). It is also related to the regulation mechanism in Section 2.1, Section 2.2, Section 2.3, and Section 2.5 of this review. It has been revealed that *p53* suppresses TFR1 and Zrt- and Irt-like protein 14 (ZIP14) to reduce cell iron intake and *p53* can also

be reduced or increased in different conditions (Liu and Gu, 2022). In addition, *p53* reduces ACSL4 by controlling miR-34 to suppress ferroptosis. On the one hand, *p53* can inhibit SLC7A11 and CBS to reduce the synthesis of GSH, ultimately inducing ferroptosis. On the other hand, it can promote the release of ALOX12 by reducing SLC7A11, which, in turn, causes lipid peroxidation and finally ferroptosis. Furthermore, *p53* can transactivate mouse double minute two homolog (MDM2), which activates FSP1 to promote ferroptosis.

## 2.5 FSP1-CoQ10-NAD (P) H pathway

GPX4 has long been recognized as a core regulatory protein that suppresses the occurrence of ferroptosis. In 2019, Bersuker et al. (2019) and Doll et al. (2019) reported FSP1 as an important ferroptosis regulator protein and confirmed that the FSP1-CoQ10-NAD (P) H pathway was independent of System-Xc<sup>-</sup>-GSH-GPX4 pathway and cooperated with it to inhibit ferroptosis lead by lipid peroxidation. Using expression cloning methods, AIFM2 was identified by Doll's group. This unknown inhibitory gene of ferroptosis was therefore renamed FSP1, which was originally described by Wu et al. (2002) as a proapoptotic gene. FSP1 is primarily attached to the outer mitochondrial membrane, and when octadecylation occurs, FSP1 moves to the plasma membrane.

FSP1 inhibition of ferroptosis is mediated by ubiquinone (CoQ10), which utilizes the terminal octadecylation modification of protein N to target cytoplasmic membrane, as an NADPH-dependent CoQ10 induces the redox function to cause oxidation or reduction. The oxidizing CoQ10 is a lipophilic radical trapper and functions as an antioxidant to inhibit lipid peroxidation to avoid further ferroptosis. The reduction reaction generates panthenol, which can capture free radicals and can further mediate lipid peroxidation to inhibit ferroptosis. At the same time, FSP1 catalyzes the regeneration of ubiquinone by NAD (P) H and takes the circulation. Studies also found (Shimada et al., 2016) that by binding and activating squalene synthase, small molecule compound FIN56 inhibits the methoxyeruc pathway synthesis of CoQ10, which causes the consumption of CoQ10 and induction of ferroptosis.

## 2.6 GCH1-BH4 pathway

It was reported that recently, a new pathway (the GCH1-BH4 protection pathway) was identified, which was parallel with and independent from the two classical pathways, namely, System-Xc<sup>-</sup>-GSH-GPX4 and FSP1-CoQ10-NAD (P) H (Li L. et al., 2021). By increasing its expression, CoQ10 can be elevated to slow down the progression of ferroptosis (Kraft et al., 2020). GTP cyclohydrolase 1 (GCH1), originating from GTP, is able to remove lipid peroxidation, and its overexpression promotes the generation of

tetrahydrobiopterin (BH4) and avoids RSL3-induced ferroptosis (Wei et al., 2020).

### 3 Application of ferroptosis in ovarian cancer

#### 3.1 Elevated iron levels

RCD plays a key role in the normal growth and development as well as maintaining homeostasis of multicellular organisms. Ferroptosis is a unique type of RCD, and many studies have demonstrated the relationship of ferroptosis was closely with tumor treatment. In particular, elevated iron levels are associated with the occurrence of various malignant tumors such as stem cell cancer, lung cancer, ovarian cancer, and renal cell cancer (Toyokuni, 2009; Xia et al., 2019). Studies have shown a soluble molybdenum compound called sodium molybdate that induced the elevation of LIP in ovarian cancer cells (Mao et al., 2022). In the tumor tissue of HGSC patients, the iron efflux pump ferroportin (FPN) decreases whereas TFR1 and TF increase. As a result, the intracellular level of iron is increased (Basuli et al., 2017). A similar situation was observed in genetic models of ovarian cancer tumor-initiating cells, suggesting that tumor cell intracellular iron levels are also elevated in the early stages of ovarian cancer. In a recent study, GPX4 knockout reduced iron levels and decreased interleukin-6 and tumor necrosis factor expression in ovarian cancer cells (Li D. et al., 2021). It suggests that we probably could interfere with the iron metabolism of tumor cells in the early stage of ovarian cancer to kill tumor cells.

#### 3.2 Genes

##### 3.2.1 *p53* gene

The *p53* gene expresses the *p53* protein, which acts as a DNA-binding transcription factor and selectively regulates the expression of certain *p53* transcriptional target genes. Studies have shown (McBean, 2012) that the inhibition of SLC7A11 expression reduced cystine uptake and sensitized ovarian cancer tumor cells to ferroptosis. However, *p53*<sup>3KR</sup> as an acetylation-deficient mutant of the *p53* protein fails to induce cell cycle arrest, senescence, and apoptosis, which completely retains the ability to regulate SLC7A11 expression and induce ferroptosis in tumor cells under oxidative stress. Furthermore, PARP inhibitors can inhibit SLC7A11 expression in a *p53*-dependent manner (Hong et al., 2021). Quartuccio et al. (2015) studied a mouse model of tubal epithelial cells with *p53* mutation, and the results showed that single *p53* mutation only migrated normal cells and normal cells transformed into tumor cells when combining *p53* mutation with the activation of K-ras. The expression of the *p53* gene also promotes ferroptosis induced by superparamagnetic iron oxide

(SPIO) with the incubation in human serum, which provides a theoretical basis for the development of iron nanomaterials as new tumor therapeutic drugs (Zhang Y. et al., 2021). According to the results, SPIO could also induce ferroptosis in human ovarian cancer stem cells by attenuated autophagy (Huang et al., 2020). Almost 96% of HGSC cases are detected with mutations in the *p53* gene. Therefore, the interference with *p53*-mediated metabolic regulation has a significant impact on the treatment of ovarian cancer.

##### 3.2.2 Stearyl-coenzyme A desaturase gene

Stearyl-coenzyme A desaturase (SCD) is also known as D9-fatty acyl-CoA desaturase, through which monounsaturated fatty acids are produced from saturated fatty acids. In humans, SCD includes two isoforms, namely, *SCD5* and *SCD1* (prevalent form). In ovarian cancer tumor cells, *SCD1* is highly expressed, and studies have shown that the inhibition or deletion of *SCD1* gene could induce apoptosis and ferroptosis. The coadministration of erastin with *SCD1* inhibitor A939572 in mice with ovarian cancer tumor cells was much more effective than that of a single drug (Carbone and Melino, 2019; Tesfay et al., 2019). In addition, treatment with the *SCD1* inhibitors MF-438, CAY10566, and A939572 increased the sensitivity of ovarian cancer cells to the ferroptosis inducers RSL3 and erastin (Wang et al., 2022a). Furthermore, *SCD1* can induce ferroptosis in cancer cells mediated by the Menin-MLL inhibitor MI-463 (Kato et al., 2020).

##### 3.2.3 *Frizzled-7*

Overexpression of *frizzled-7* (*FZD7*) can activate the oncogenic factor P63, upregulate GPX4, and avoid ferroptosis in cells. The expression of *FZD7* was directly associated with the expression of the GSH metabolism-related genes, namely, GSS, GSR, GPX2, and IDH (Wang et al., 2021a). Therefore, it is applicable to explore whether *FZD7* could be used as a novel biomarker to evaluate the sensitivity of platinum-resistant ovarian cancer cells to ferroptosis.

In addition, the solute carrier family (SLC) is associated with inducing ovarian cancer tumor cells. The anesthetic lidocaine downregulates the expression of SLC7A11 in a dose-dependent manner by promoting the intracellular expression of microRNA-382-5p (miR-382-5p), and the inhibition of miR-382-5p blocked ferroptosis in ovarian cancer cells (Sun et al., 2021). The *SNAIL2* gene can directly bind to the SLC7A11 promoter to regulate SLC7A11 expression (Jin et al., 2022). The tumor suppressor miR-424-5p inhibits ferroptosis in ovarian cancer by targeting ACSL4 (Ma et al., 2021).

#### 3.3 Transsulfuration pathway

Studies have confirmed that the high level of GSH (Nunes and Serpa, 2018) and the high expression of related proteases (Kigawa et al., 1998) are closely related to the chemotherapy

resistance of ovarian cancer. [Verschoor and Singh \(2013\)](#) treated a model derived from the tetracycline-induced overexpression of the proto-oncogene ETS-1 in ovarian cancer cells in 2008 with xCT inhibitors and inhibitors of the transsulfuration pathway. It was found that the overexpression of ETS-1 was accompanied by an increase in intracellular GSH and a significant reduction of GSH levels in models treated with transsulfuration pathway inhibitors. It indicates that the transsulfuration pathway plays an important role in GSH synthesis in ovarian cancer cells. Then, [Chakraborty et al. \(2015\)](#) found that the expression of CBS was increased in epithelial ovarian cancer cells (EOC) and silencing the genes of CBS could inhibit the migration and invasion of EOC tumor cells. [Liu et al. \(2020\)](#) found that the antioxidant transcription factor nuclear factor erythroid 2-related factor 2 (NRF2) upregulates CBS expression in erastin-resistant cells but causes ferroptosis after RNAi knockdown. It shows that the cell activation of the reverse transsulfuration pathway by NRF2/CBS enhances erastin-induced ferroptosis resistance. Thus, we can further think about the potential of the transsulfuration pathway to treat ovarian cancer with ferroptosis inducers. In this pathway, cysteine deprivation induced ferroptosis in tumor cells of ovarian clear cell carcinoma ([Novera et al., 2020](#)).

### 3.4 Hippo pathway

The Hippo pathway, consisting of a range of protein kinases and transcription factors regulated by cell-to-cell contact and cell density, is highly conserved in the evolution of both lower and higher animals. It is a potent inhibitory mechanism in tumor progression involved ([Sun and Chi, 2020](#); [Wang et al., 2021b](#)) in apoptosis as well as tumorigenesis, metastasis, and chemoresistance. Yes-associated protein 1 (YAP) and transcriptional coactivator with PDZ-binding motif (TAZ) are two major transcription coactivators of transcription enhancement-related domains (TEAD) in the Hippo pathway. They affect cell phenotypes that include promoting cell proliferation, self-renewal, and inhibiting apoptosis by regulating the expression of target genes. YAP/TAZ is considered a receptor of cell density. When cell density is low and cell-to-cell contact is limited, the Hippo pathway is turned off. YAP and TAZ are abnormally activated and translocated from the cytoplasm to the nucleus after dephosphorylation, where they bind to the transcription factor TEAD, trigger cell ferroptosis, and inhibit apoptosis. However, the opposite result occurs.

In epithelial malignant tumor cells, cadherin overexpression mediates high cell density-enhanced cell contacts that then activate the Hippo pathway through NF2 (also called merlin) tumor suppressor proteins, thereby inhibiting nuclear transposition and YAP activity, which ultimately inhibits sensitivity to ferroptosis. Among them, YAP promotes ferroptosis by upregulating ACSL4 and transferrin receptor

(TFRC), which can be inhibited by the small molecule CA3 ([Song et al., 2018](#)). In head and neck cancer, overexpression of epithelial membrane protein 1 (EMP1) regulates the expression of Rac1 and NADPH oxidase 1 (NOX 1) through the Hippo-YAP pathway, further promoting RSL3-induced ferroptosis ([Wang et al., 2022b](#)). Endogenous glutamate was reported to inhibit the iron-death sensitivity ([Zhang X. et al., 2021](#)) of lung adenocarcinoma by inhibiting ADCY10-dependent YAP. However, in malignant kidney tumor cells, TAZ is highly expressed and regulates EMP1 expression, which then induces NADPH oxidase 4 (NOX4) to regulate ferroptosis.

It has also shown that the relatively high activity of YAP/TAZ promotes the invasion and metastasis of ovarian cancer cells and is often associated with poor prognosis ([Yang and Chi, 2019](#)). Cell density-dependent TAZ is the determinant factor of ferroptosis sensitivity in ovarian cancer. However, regulation is different from the pathway in kidney cancer. In ovarian cancer, TAZ regulates the level of its direct target gene angiopoietin-like 4 (ANGPTL4) to manage the activity of NADPH oxidase 2 (NOX2), finally leading to ferroptosis ([Yang et al., 2020](#)). YAP promotes ferroptosis in ovarian cancer malignant tumor cells by regulating its direct target gene, E3 ubiquitin ligase S phase protein-associated protein 2 (SKP2) ([Yang W. H. et al., 2021](#)). Furthermore, discoidin domain receptor tyrosine kinase 2 (DDR2) is upregulated in recurrent breast tumor cells, with sensitivity to ferroptosis enhanced by YAP/TAZ activation, which is unknown in ovarian cancer ([Lin et al., 2021](#)). In serous ovarian cancer, the TEAD family plays an important role, in which TEAD1 acts as a cotranscription factor in the Hippo pathway and the reduced TEAD2 expression may increase the accumulation of ROS, leading to ferroptosis ([Ren et al., 2021](#)). The currently studied proteins and genes of ferroptosis, especially in ovarian cancer, are summarized in [Figure 3](#).

## 4 Ferroptosis-related drugs

At present, sorafenib is a United States FDA-approved ovarian cancer treatment agent that can induce ferroptosis ([Sun et al., 2017](#)). Other studies are still undergoing to develop new and effective ferroptosis-related drugs for ovarian cancer treatment.

### 4.1 Chemoresistance

The coadministration of platinum drugs with paclitaxel is the first-line drug treatment regimen for ovarian cancer. However, most ovarian cancer patients frequently develop chemoresistance, especially the resistance by taking platinum drugs, leading to recurrence. Platinum drugs are nonspecific drugs for affecting cell cycle that bind to DNA after entering tumor cells to form Pt-DNA complexes, producing intracellular

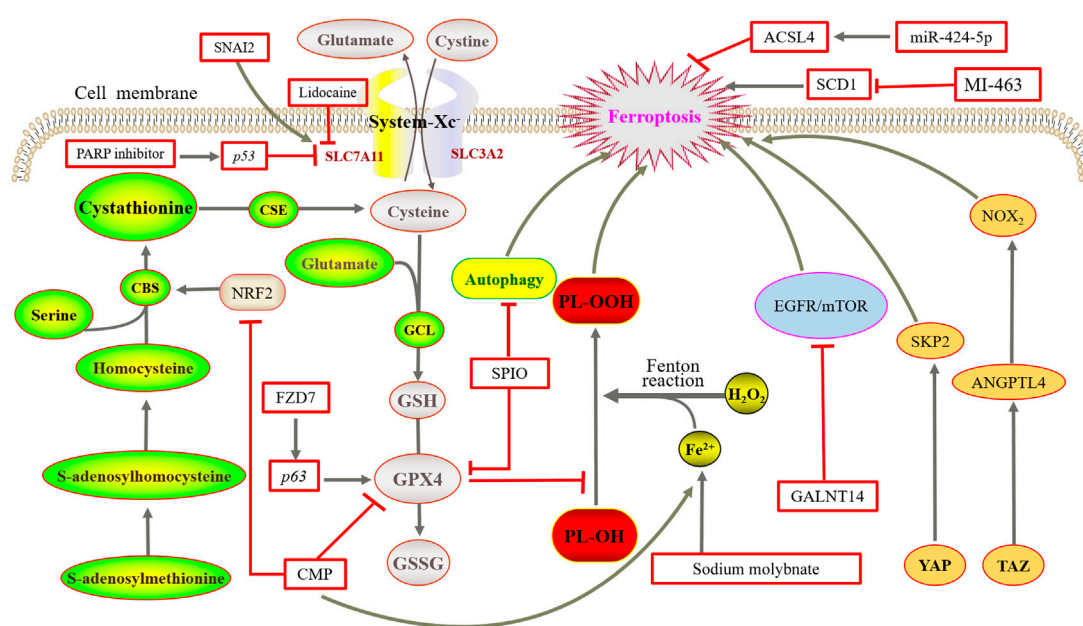


FIGURE 3

Mechanisms of ferroptosis in ovarian cancer. NRF2 upregulates CBS expression but causes ferroptosis after RNAi knockdown. Overexpression of FZD7 can activate the oncogenic factor *P63*, upregulate GPX4, and avoid undergoing ferroptosis. SPIO could also induce ferroptosis by attenuated autophagy. Sodium molybdate induced the elevation of LIP. The inhibition or deletion of *SCD1* gene could induce ferroptosis. GALNT14 inhibits the EGFR/mTOR pathway, thereby downregulating ferroptosis. TAZ regulates the level of ANGPTL4 to manage the activity of NOX2, and finally leads to ferroptosis. YAP promotes ferroptosis by regulating SKP2.

ROS, which leads to cell damage and death. A multicenter phase 2 randomized controlled trial evaluated the oral coadministration of sorafenib with topotecan as a maintenance treatment and found a statistically and clinically significant improvement in progression-free survival in patients with platinum-resistant ovarian cancer (Chekerov et al., 2018). Micelles made from arachidonic acid-conjugated amphipathic copolymers targeting GPX4 after wrapping of RSL3 enhance the ability of RSL3 to induce ferroptosis, suggesting that chemotherapy resistance could be overcome by reducing the dosage of platinum drugs used and coadministration with this copolymer (Konstorum et al., 2020).

The ferroptosis inducer erastin acts with cisplatin synergistically by ROS-mediated and activated apoptosis to inhibit the growth of ovarian cancer cells, and it could be used as a sensitizer to overcome cisplatin resistance (Cang et al., 2020; Cheng et al., 2021). A combination of cisplatin with mTOR inhibitors causes an additive effect of cell death, and GALNT14, a member of the family of acetyl-galactosyltransferases, regulates the stability of EGFR proteins to inhibit the EGFR/mTOR pathway, thereby downregulating self-induced ferroptosis in ovarian cancer cells (Li H.W. et al., 2022). This suggests that GALNT14 provides a strategy to overcome cisplatin resistance in ovarian cancer patients. The

MAP30 protein isolated from bitter melon also exhibits an effect on tumor treatment and can be used as a supplement to enhance the chemotherapy effect. It is a natural AMPK activator that induces ferroptosis consistent with cisplatin, enhancing the antitumor response and antichemo-resistance in ovarian cancer (Chan et al., 2020).

Furthermore, several studies have demonstrated that the acquired synthesis of cysteine and GSH affects carboplatin resistance in ovarian cancer. Lopes-Coelho et al. (2016) found that hepatocyte nuclear factor 1 $\beta$  (HNF1) promotes glutathione synthesis to avoid carboplatin resistance in ovarian clear cell carcinoma. By studying ovarian cancer cell lines, including ES2, OVCAR3, OVCAR8, A2780, and A2780cisR, Nunes et al. (2018) clarified that cysteine protects cells from hypoxia and carboplatin effect to develop ovarian cancer. Santos et al. (2019) hypothesized that chemotherapy resistance of carboplatin could be reversed by disrupting cysteine metabolism. They used selenium-containing Chrysin (SeChry) as a competitive inhibitor of xCT, testing the effect of SeChry on three different ovarian cancer cell lines (ES2, OVCAR3, and OVCAR8) and two nonmalignant cell lines (HaCaT and HK2). The results showed that SeChry depleted GSH and inhibited CBS, preventing the production of the antioxidant hydrogen sulfide. Then, a new nanomedicine is designed to improve the specificity of drugs to tumor cells,



which has achieved good effects in the treatment of ovarian cancer.

It was also shown that the upregulation of the drug efflux transporter ABCB1 easily led to relapse of resistance to docetaxel therapy, but the ovarian cancer cell cycle remained in the G2/M phase after coadministration with erastin, and the relapse of resistance was reversed (Zhou et al., 2019). Promyelocytic leukemia protein (PML) can increase lipid peroxidation, regulate mitochondrial metabolism and iron metabolism in tumor cells, and then enhance the chemosensitivity of HGSC (Gentric et al., 2019).

## 4.2 Other

Artemisinin (ARS) is a classic antimalarial drug and can fight tumors (Effertth, 2017). The cellular response of ARS and its derivatives to tumor cells involves multiple cell death modes, including apoptosis, autophagy, ferroptosis, and necrosis. Artesunate (ART), derived from *Artemisia annua* leaves, has potent antiproliferative and cytotoxic effects on ovarian cancer cells (Greenshields et al., 2017). The strong anticancer effects of ART include that low concentrations of ART lead to ROS-independent cell cycle arrest in the G1 phase and inhibition of mTOR signaling; high concentrations of ART lead to ROS production, mediated by apoptosis and ferroptosis.

Furthermore, the plant extract uronic acid can promote ferroptosis through the activation of the JNK/p53 signaling pathway (Ruan et al., 2021). Carboxymethylated pachyman (CMP) inhibited HO-1 signaling, xCT, and GPX4, as well as upregulated Fe<sup>2+</sup> expression by downregulating NRF2 expression, ultimately leading to the induction of ferroptosis in ovarian cancer cells. According to recent reports, sodium molybdate can modulate the production of nitric oxide to exhaust GSH, raise iron levels, and promote ferroptosis in ovarian cancer cells (Zheng et al., 2022). In the view of immunotherapy, it has found that checkpoint inhibitors induce CD8<sup>+</sup> T cells to trigger ferroptosis in mice bearing ovarian tumor (Immunotherapy Activates, 2019). Furthermore, the combination of the Menin-MLL inhibitor MI-463 with the thioredoxin reductase inhibitor auranofin could synergistically increase the mortality of ovarian cancer tumor cells (Jing et al., 2022).

## 5 Discussion and perspective

Ferroptosis, discovered as a novel type of RCD, occurs in an iron-dependent manner after massive accumulation of ROS, presenting features different from other well known forms of cell death such as apoptosis and autophagy. The reported regulatory mechanisms of ferroptosis include the Fenton

response, System-Xc<sup>-</sup>-GSH-GPX4 pathway, FSP1-CoQ10-NAD (P) H pathway, Hippo pathway, and GCH1-BH4 pathway. At present, most of these pathways have been studied extensively in malignant tumors, neurological diseases, and liver and kidney injury, except the latter two pathways, which are relatively rarely studied and showing no clear target or index for the treatment or prognosis in each disease. As a rising star, ferroptosis provides a new idea for the research of various diseases and plays a significantly important role in the remarkable success of tumor treatment. In recent years, a large number of studies have screened reliable mRNAs and genes to predict the prognosis of ovarian cancer patients by means of bioinformatics (Feng et al., 2022), comprehensive clinical analysis (Peng et al., 2021), and construction of ferroptosis-related gene models (Yang L. et al., 2021; Chen et al., 2021; Li X. X. et al., 2021; Zhang J. et al., 2021; Ye et al., 2021; You et al., 2021; Yu et al., 2021; Li Y. et al., 2022; Wang H. et al., 2022; Zou et al., 2022). It provides preciously applicable suggestions for exploring the therapeutic targets and prognostic indicators related to ferroptosis in ovarian cancer. At the same time, research of new compounds as inducers and inhibitors also provides a meaningful reference for the optimization of ovarian cancer treatment regimen. However, on the basis of the current research results, it is too soon to conclude the role of ferroptosis in the diagnosis, treatment, and prognosis of ovarian cancer for clinical purpose. In the future, inducers and inhibitors related to ferroptosis of ovarian cancer tumor cells, as well as the combined effects of new and classic drugs, the drug resistance of tumor cells, and the specific regulatory mechanisms, remain to be thoroughly studied.

## Author contributions

ZT and YJ designed the review and revised the manuscript. ZT and HH dedicated in drafting the manuscript and performed the literature review. WS and YL participated in sorting and organizing the sentences and figures.

## Funding

This review was supported by National Natural Science Foundation of China project (Grant No. 82160344) and Yunnan Fundamental Research Projects (Grant No. 202001AU070141 and Grant No.202101AY070001-068).

## Conflict of interest

The authors declare that the research was conducted in the absence of any commercial or financial relationships that could be construed as a potential conflict of interest.

## Publisher's note

All claims expressed in this article are solely those of the authors and do not necessarily represent those of their affiliated

## References

- Basuli, D., Tesfay, L., Deng, Z., Paul, B., Yamamoto, Y., NinG, G., et al. (2017). Iron addition: A novel therapeutic target in ovarian cancer. *Oncogene* 36 (29), 4089–4099. doi:10.1038/ncr.2017.11
- Bersuker, K., Hendricks, J. M., Li, Z., Magtanong, L., Ford, B., Tang, P. H., et al. (2019). The CoQ oxidoreductase FSP1 acts parallel to GPX4 to inhibit ferroptosis. *Nature* 575 (7784), 688–692. doi:10.1038/s41586-019-1705-2
- Brown, J., Friedlander, M., Backes, F. J., Harter, P., O'Connor, D. M., de la Motte Rouge, T., et al. (2014). Gynecologic Cancer Intergroup (GCI) consensus review for ovarian germ cell tumors. *Int. J. Gynecol. Cancer* 24 (9 Suppl. 3), S48–S54. doi:10.1097/IGC.0000000000000223
- Cang, W., Wu, A., Di, W., and Qiu, L. (2020). Study of the iron death activator Erastin for enhancing cisplatin sensitivity in ovarian cancer cells by activating apoptosis [J]. *Prog. Mod. Obstetrics Gynecol.* 29 (10), 730–733. doi:10.13283/j.cnki.xdfckjz.2020.10.030
- Cao, J. Y., and Dixon, S. J. (2016). Mechanisms of ferroptosis. *Cell. Mol. Life Sci.* 73 (11–12), 2195–2209. doi:10.1007/s00018-016-2194-1
- Carbone, M., and Melino, G. (2019). Stearoyl CoA desaturase regulates ferroptosis in ovarian cancer offering new therapeutic perspectives. *Cancer Res.* 79 (20), 5149–5150. doi:10.1158/0008-5472.CAN-19-2453
- Chakraborty, P. K., Xiong, X., Mustafa, S. B., Saha, S., Dhanasekaran, D., Mandal, N. A., et al. (2015). Role of cystathionine beta synthase in lipid metabolism in ovarian cancer. *Oncotarget* 6 (35), 37367–37384. doi:10.18632/oncotarget.5424
- Chan, D. W., Yung, M. M., Chan, Y. S., Xuan, Y., Yang, H., Xu, D., et al. (2020). MAP30 protein from *Momordica charantia* is therapeutic and has synergistic activity with cisplatin against ovarian cancer *in vivo* by altering metabolism and inducing ferroptosis. *Pharmacol. Res.* 161, 105157. doi:10.1016/j.phrs.2020.105157
- Chekerov, R., Hilpert, F., Mahner, S., El-Balat, A., Harter, P., De Gregorio, N., et al. (2018). Sorafenib plus topotecan versus placebo plus topotecan for platinum-resistant ovarian cancer (TRIAS): A multicentre, randomised, double-blind, placebo-controlled, phase 2 trial. *Lancet. Oncol.* 19 (9), 1247–1258. doi:10.1016/S1470-2045(18)30372-3
- Chen, R., Cao, J., Jiang, W., Wang, S., and Cheng, J. (2021). Upregulated expression of CYBRD1 predicts poor prognosis of patients with ovarian cancer. *J. Oncol.* 2021, 7548406. doi:10.1155/2021/7548406
- Cheng, Q., Bao, L., Li, M., Chang, K., and Yi, X. (2021). Erastin synergizes with cisplatin via ferroptosis to inhibit ovarian cancer growth *in vitro* and *in vivo*. *J. Obstet. Gynaecol. Res.* 47 (7), 2481–2491. doi:10.1111/jog.14779
- China Anti-Cancer Association Gynecological Cancer Professional Committee (2021). Ovarian malignant tumor diagnosis and treatment guide. *China Oncol.* 31 (6), 490–500. doi:10.19401/j.cnki.1007-3639.2021.06.07
- Conrad, M., and Pratt, D. A. (2019). The chemical basis of ferroptosis. *Nat. Chem. Biol.* 15 (12), 1137–1147. doi:10.1038/s41589-019-0408-1
- Dixon, S. J., Lemberg, K. M., Lamprecht, M. R., Skouta, R., Zaitsev, E. M., Gleason, C. E., et al. (2012). Ferroptosis: An iron-dependent form of nonapoptotic cell death. *Cell* 149 (5), 1060–1072. doi:10.1016/j.cell.2012.03.042
- Doll, S., Freitas, F. P., Shah, R., Aldrovandi, M., da Silva, M. C., Ingold, I., et al. (2019). FSP1 is a glutathione-independent ferroptosis suppressor. *Nature* 575 (7784), 693–698. doi:10.1038/s41586-019-1707-0
- Doll, S., Proneth, B., Tyurina, Y. Y., Panzilius, E., Kobayashi, S., Ingold, I., et al. (2017). ACSL4 dictates ferroptosis sensitivity by shaping cellular lipid composition. *Nat. Chem. Biol.* 13 (1), 91–98. doi:10.1038/nchembio.2239
- Dolma, S., Lessnick, S. L., Hahn, W. C., and Stockwell, B. R. (2003). Identification of genotype-selective antitumor agents using synthetic lethal chemical screening in engineered human tumor cells. *Cancer Cell* 3 (3), 285–296. doi:10.1016/s1535-6108(03)00050-3
- Efferth, T. (2017). From ancient herb to modern drug: *Artemisia annua* and artemisinin for cancer therapy. *Semin. Cancer Biol.* 46, 65–83. doi:10.1016/j.semcancer.2017.02.009
- Feng, S., Yin, H., Zhang, K., Shan, M., Ji, X., Luo, S., et al. (2022). Integrated clinical characteristics and omics analysis identifies a ferroptosis and iron-metabolism-related lncRNA signature for predicting prognosis and therapeutic responses in ovarian cancer. *J. Ovarian Res.* 15 (1), 10. doi:10.1186/s13048-022-00944-y
- Gentric, G., Kieffer, Y., Mieulet, V., Goundiam, O., Bonneau, C., Nemati, F., et al. (2019). PML-regulated mitochondrial metabolism enhances chemosensitivity in human ovarian cancers. *Cell Metab.* 29 (1), 156–173. e10. doi:10.1016/j.cmet.2018.09.002
- Gout, P. W., Buckley, A. R., Simms, C. R., and Bruchovsky, N. (2001). Sulfasalazine, a potent suppressor of lymphoma growth by inhibition of the x(c)-cystine transporter: A new action for an old drug. *Leukemia* 15 (10), 1633–1640. doi:10.1038/sj.leu.2402238
- Green, D. R. (2019). The coming decade of cell death research: Five riddles. *Cell* 177 (5), 1094–1107. doi:10.1016/j.cell.2019.04.024
- Greenshields, A. L., Shepherd, T. G., and Hoskin, D. W. (2017). Contribution of reactive oxygen species to ovarian cancer cell growth arrest and killing by the anti-malarial drug artesunate. *Mol. Carcinog.* 56 (1), 75–93. doi:10.1002/mc.22474
- Hong, T., Lei, G., Chen, X., Li, H., Zhang, X., Wu, N., et al. (2021). PARP inhibition promotes ferroptosis via repressing SLC7A11 and synergizes with ferroptosis inducers in BRCA-proficient ovarian cancer. *Redox Biol.* 42, 101928. doi:10.1016/j.redox.2021.101928
- Huang, Y., Lin, J., Xiong, Y., Chen, J., Du, X., Liu, Q., et al. (2020). Superparamagnetic iron oxide nanoparticles induce ferroptosis of human ovarian cancer stem cells by weakening cellular autophagy. *J. Biomed. Nanotechnol.* 16 (11), 1612–1622. doi:10.1166/jbnn.2020.2991
- Immunotherapy Activates (2019). Immunotherapy activates unexpected cell death mechanism. *Cancer Discov.* 9 (7), OF2. doi:10.1158/2159-8290.CD-NB2019-058
- Ingold, I., Berndt, C., Schmitt, S., Doll, S., Poschmann, G., Buday, K., et al. (2018). Selenium utilization by GPX4 is required to prevent hydroperoxide-induced ferroptosis. *Cell* 172 (3), 409–422. e21. doi:10.1016/j.cell.2017.11.048
- Jiang, L., Kon, N., Li, T., Wang, S. J., Su, T., Hibshoosh, H., et al. (2015). Ferroptosis as a p53-mediated activity during tumour suppression. *Nature* 520 (7545), 57–62. doi:10.1038/nature14344
- Jin, Y., Chen, L., Li, L., Huang, G., Huang, H., Tang, C., et al. (2022). SNAI2 promotes the development of ovarian cancer through regulating ferroptosis. *Bioengineered* 13 (3), 6451–6463. doi:10.1080/21655979.2021.2024319
- Jing, T., Guo, Y., and Wei, Y. (2022). Carboxymethylated pachyman induces ferroptosis in ovarian cancer by suppressing NRF1/HO-1 signaling. *Oncol. Lett.* 23 (5), 161. doi:10.3892/ol.2022.13281
- Kato, I., Kasukabe, T., and Kumakura, S. (2020). Menin-MLL inhibitors induce ferroptosis and enhance the anti-proliferative activity of auranofin in several types of cancer cells. *Int. J. Oncol.* 57 (4), 1057–1071. doi:10.3892/ijo.2020.5116
- Kigawa, J., Minagawa, Y., Cheng, X., and Terakawa, N. (1998). Gamma-glutamyl cysteine synthetase up-regulates glutathione and multidrug resistance-associated protein in patients with chemoresistant epithelial ovarian cancer. *Clin. Cancer Res.* 4 (7), 1737–1741.
- Konstorum, A., Tesfay, L., Paul, B. T., Torti, F. M., Laubenbacher, R. C., Torti, S. V., et al. (2020). Systems biology of ferroptosis: A modeling approach. *J. Theor. Biol.* 493, 110222. doi:10.1016/j.jtbi.2020.110222
- Koppula, P., Zhang, Y., Zhuang, L., and Gan, B. (2018). Amino acid transporter SLC7A11/xCT at the crossroads of regulating redox homeostasis and nutrient dependency of cancer. *Cancer Commun.* 38 (1), 12. doi:10.1186/s40880-018-0288-x
- Kraft, V. A. N., Bezjian, C. T., Pfeiffer, S., Ringelstetter, L., Müller, C., Zandkarimi, F., et al. (2020). GTP cyclohydrolase 1/tetrahydrobiopterin counteract ferroptosis through lipid remodeling. *ACS Cent. Sci.* 6 (1), 41–53. doi:10.1021/acscentsci.9b01063
- Lheureux, S., Gourley, C., Vergote, I., and Oza, A. M. (2019). Epithelial ovarian cancer. *Lancet* 393 (10177), 1240–1253. doi:10.1016/S0140-6736(18)32552-2
- Li, D., Zhang, M., and Chao, H. (2021). Significance of glutathione peroxidase 4 and intracellular iron level in ovarian cancer cells—“utilization” of ferroptosis mechanism. *Inflamm. Res.* 70 (10–12), 1177–1189. doi:10.1007/s00011-021-01495-6

- Li, H. W., Liu, M. B., Jiang, X., Song, T., Feng, S. X., Wu, J. Y., et al. (2022). GALNT14 regulates ferroptosis and apoptosis of ovarian cancer through the EGFR/mTOR pathway. *Future Oncol.* 18 (2), 149–161. doi:10.2217/fon-2021-0883
- Li, J., Cao, F., Yin, H. L., Huang, Z. J., Lin, Z. T., Mao, N., et al. (2020). Ferroptosis: Past, present and future. *Cell Death Dis.* 11 (2), 88. doi:10.1038/s41419-020-2298-2
- Li, L., Qiu, C., Hou, M., Wang, X., Huang, C., Zou, J., et al. (2021). Ferroptosis in ovarian cancer: A novel therapeutic strategy. *Front. Oncol.* 11, 665945. doi:10.3389/fonc.2021.665945
- Li, X. X., Xiong, L., Wen, Y., and Zhang, Z. J. (2021). Comprehensive analysis of the tumor microenvironment and ferroptosis-related genes predict prognosis with ovarian cancer. *Front. Genet.* 12, 774400. doi:10.3389/fgene.2021.774400
- Li, Y., Gong, X., Hu, T., and Chen, Y. (2022). Two novel prognostic models for ovarian cancer respectively based on ferroptosis and necroptosis. *BMC Cancer* 22 (1), 74. doi:10.1186/s12885-021-09166-9
- Lin, C. C., Yang, W. H., Lin, Y. T., Tang, X., Chen, P. H., Ding, C. C., et al. (2021). DDR2 upregulation confers ferroptosis susceptibility of recurrent breast tumors through the Hippo pathway. *Oncogene* 40 (11), 2018–2034. doi:10.1038/s41388-021-01676-x
- Lin, L. S., Song, J., Song, L., Ke, K., Liu, Y., Zhou, Z., et al. (2018). Simultaneous fenton-like ion delivery and glutathione depletion by MnO<sub>2</sub>-based nanoagent to enhance chemodynamic therapy. *Angew. Chem. Int. Ed. Engl.* 57 (18), 4902–4906. doi:10.1002/anie.201712027
- Liu, N., Lin, X., and Huang, C. (2020). Activation of the reverse transsulfuration pathway through NRF2/CBS confers erastin-induced ferroptosis resistance. *Br. J. Cancer* 122 (2), 279–292. doi:10.1038/s41416-019-0660-x
- Liu, Y., and Gu, W. (2022). p53 in ferroptosis regulation: the new weapon for the old guardian. *Cell Death Differ.* 29 (5), 895–910. doi:10.1038/s41418-022-00943-y
- Liu, Y., and Gu, W. (2021). The complexity of p53-mediated metabolic regulation in tumor suppression. *Semin. Cancer Biol.* S1044-579X(21)00060-2. doi:10.1016/j.semcancer.2021.03.010
- Lopes-Coelho, F., Gouveia-Fernandes, S., Gonçalves, L. G., Nunes, C., Faustino, I., Silva, F., et al. (2016). HNF1 $\beta$  drives glutathione (GSH) synthesis underlying intrinsic carboplatin resistance of ovarian clear cell carcinoma (OCCC). *Tumour Biol.* 37 (4), 4813–4829. doi:10.1007/s13277-015-4290-5
- Luo, M., Peng, H., and Guo, D. (2021). The mechanism of iron death and its application in tumor therapy [J]. *Chem. Life* 41 (01), 10–18. doi:10.13488/j.smhx.20200341
- Ma, L. L., Liang, L., Zhou, D., and Wang, S. W. (2021). Tumor suppressor miR-424-5p abrogates ferroptosis in ovarian cancer through targeting ACSL4. *Neoplasma* 68 (1), 165–173. doi:10.4149/neo\_2020\_200707N705
- Mao, G., Xin, D., Wang, Q., and Lai, D. (2022). Sodium molybdate inhibits the growth of ovarian cancer cells via inducing both ferroptosis and apoptosis. *Free Radic. Biol. Med.* 182, 79–92. doi:10.1016/j.freeradbiomed.2022.02.023
- McBean, G. J. (2012). The transsulfuration pathway: A source of cysteine for glutathione in astrocytes. *Amino Acids* 42 (1), 199–205. doi:10.1007/s00726-011-0864-8
- Novera, W., Lee, Z. W., Nin, D. S., Dai, M. Z. Y., Binte Idres, S., Wu, H., et al. (2020). Cysteine deprivation targets ovarian clear cell carcinoma via oxidative stress and iron-sulfur cluster biogenesis deficit. *Antioxid. Redox Signal.* 33 (17), 1191–1208. doi:10.1089/ars.2019.7850
- Nunes, S. C., Ramos, C., Lopes-Coelho, F., Sequeira, C. O., Silva, F., Gouveia-Fernandes, S., et al. (2018). Cysteine allows ovarian cancer cells to adapt to hypoxia and to escape from carboplatin cytotoxicity. *Sci. Rep.* 8 (1), 9513. doi:10.1038/s41598-018-27753-y
- Nunes, S. C., and Serpa, J. (2018). Glutathione in ovarian cancer: A double-edged sword. *Int. J. Mol. Sci.* 19 (7), 1882. doi:10.3390/ijms19071882
- Peng, J., Hao, Y., Rao, B., and Zhang, Z. (2021). A ferroptosis-related lncRNA signature predicts prognosis in ovarian cancer patients. *Transl. Cancer Res.* 10 (11), 4802–4816. doi:10.21037/tcr-21-1152
- Quartuccio, S. M., Karthikeyan, S., Eddie, S. L., Lantvit, D. D., O hAinmhire, E., Modi, D. A., et al. (2015). Mutant p53 expression in fallopian tube epithelium drives cell migration. *Int. J. Cancer* 137 (7), 1528–1538. doi:10.1002/ijc.29528
- Reid, B. M., Permut, J. B., and Sellers, T. A. (2017). Epidemiology of ovarian cancer: A review. *Cancer Biol. Med.* 14 (1), 9–32. doi:10.20892/j.issn.2095-3941.2016.0084
- Ren, X., Wang, X., Peng, B., Liang, Q., Cai, Y., Gao, K., et al. (2021). Significance of TEAD family in diagnosis, prognosis and immune response for ovarian serous carcinoma. *Int. J. Gen. Med.* 27 (14), 7133–7143. doi:10.2147/IJGM.S336602
- Riegman, M., Sagie, L., Galed, C., Levin, T., Steinberg, N., Dixon, S. J., et al. (2020). Ferroptosis occurs through an osmotic mechanism and propagates independently of cell rupture. *Nat. Cell Biol.* 22 (9), 1042–1048. doi:10.1038/s41556-020-0565-1
- Rockfield, S., Raffel, J., Mehta, R., Rehman, N., and Nanjundan, M. (2017). Iron overload and altered iron metabolism in ovarian cancer. *Biol. Chem.* 398 (9), 995–1007. doi:10.1515/hsz-2016-0336
- Ruan, F., Wang, Y., and Wang, J. (2021). To investigate the effect and mechanism of uric acid inducing iron death in OVCAR3 cells of ovarian cancer cell lines based on the JNK/p53 pathway [J]. *Chin. J. Traditional Chin. Med.* 39 (07), 62–64. + 267. doi:10.13193/j.issn.1673-7717.2021.07.016
- Santos, I., Ramos, C., Mendes, C., Sequeira, C. O., Tome, C. S., Fernandes, D. G. H., et al. (2019). Targeting glutathione and cystathionine  $\beta$ -synthase in ovarian cancer treatment by selenium-chrysin polyurea dendrimer nanoformulation. *Nutrients* 11 (10), 2523. doi:10.3390/nu11102523
- Sbodio, J. I., Snyder, S. H., and Paul, B. D. (2019). Regulators of the transsulfuration pathway. *Br. J. Pharmacol.* 176 (4), 583–593. doi:10.1111/bph.14446
- Seibt, T. M., Proneth, B., and Conrad, M. (2019). Role of GPX4 in ferroptosis and its pharmacological implication. *Free Radic. Biol. Med.* 133, 144–152. doi:10.1016/j.freeradbiomed.2018.09.014
- Seiler, A., Schneider, M., Förster, H., Roth, S., Wirth, E. K., Culmsee, C., et al. (2008). Glutathione peroxidase 4 senses and translates oxidative stress into 12/15-lipoxygenase dependent- and AIF-mediated cell death. *Cell Metab.* 8 (3), 237–248. doi:10.1016/j.cmet.2008.07.005
- Shimada, K., Skouta, R., Kaplan, A., Yang, W. S., Hayano, M., Dixon, S. J., et al. (2016). Global survey of cell death mechanisms reveals metabolic regulation of ferroptosis. *Nat. Chem. Biol.* 12 (7), 497–503. doi:10.1038/nchembio.2079
- Song, S., Xie, M., Scott, A. W., Jin, J., Ma, L., Dong, X., et al. (2018). A novel YAP1 inhibitor targets CSC-enriched radiation-resistant cells and exerts strong antitumor activity in esophageal adenocarcinoma. *Mol. Cancer Ther.* 17 (2), 443–454. doi:10.1158/1535-7163.MCT-17-0560
- Sun, D., Li, Y. C., and Zhang, X. Y. (2021). Lidocaine promoted ferroptosis by targeting miR-382-5p/SLC7A11 Axis in ovarian and breast cancer. *Front. Pharmacol.* 12, 681223. doi:10.3389/fphar.2021.681223
- Sun, J., Wei, Q., Zhou, Y., Wang, J., Liu, Q., Xu, H., et al. (2017). A systematic analysis of FDA-approved anticancer drugs. *BMC Syst. Biol.* 11 (Suppl. 5), 87. doi:10.1186/s12918-017-0464-7
- Sun, T., and Chi, J. T. (2020). Regulation of ferroptosis in cancer cells by YAP/TAZ and Hippo pathways: The therapeutic implications. *Genes Dis.* 8 (3), 241–249. doi:10.1016/j.gendis.2020.05.004
- Sun, X., Niu, X., Chen, R., He, W., Chen, D., Kang, R., et al. (2016). Metallothionein-1G facilitates sorafenib resistance through inhibition of ferroptosis. *Hepatology* 64 (2), 488–500. doi:10.1002/hep.28574
- Tan, S., Schubert, D., and Maher, P. (2001). Oxytosis: A novel form of programmed cell death. *Curr. Top. Med. Chem.* 1 (6), 497–506. doi:10.2174/1568026013394741
- Tesfay, L., Paul, B. T., Konstorum, A., Deng, Z., Cox, A. O., Lee, J., et al. (2019). Stearoyl-CoA desaturase 1 protects ovarian cancer cells from ferroptotic cell death. *Cancer Res.* 79 (20), 5355–5366. doi:10.1158/0008-5472.CAN-19-0369
- Toyokuni, S. (2009). Role of iron in carcinogenesis: Cancer as a ferrotoxic disease. *Cancer Sci.* 100 (1), 9–16. doi:10.1111/j.1349-7006.2008.01001.x
- Ubellacker, J. M., Tasdogan, A., Ramesh, V., Shen, B., Mitchell, E. C., Martin-Sandoval, M. S., et al. (2020). Lymph protects metastasizing melanoma cells from ferroptosis. *Nature* 585 (7823), 113–118. doi:10.1038/s41586-020-2623-z
- van Driel, W. J., Koole, S. N., Sikorska, K., Schagen van Leeuwen, J. H., Schreuder, H. W. R., Hermans, R. H. M., et al. (2018). Hyperthermic intraperitoneal chemotherapy in ovarian cancer. *N. Engl. J. Med.* 378 (3), 1363–1364. doi:10.1056/NEJMc1802033
- Verschuur, M. L., and Singh, G. (2013). Ets-1 regulates intracellular glutathione levels: Key target for resistant ovarian cancer. *Mol. Cancer* 12 (1), 138. doi:10.1186/1476-4598-12-138
- Wang, H., Cheng, Q., Chang, K., Bao, L., and Yi, X. (2022). Integrated analysis of ferroptosis-related biomarker signatures to improve the diagnosis and prognosis prediction of ovarian cancer. *Front. Cell Dev. Biol.* 9, 807862. doi:10.3389/fcell.2021.807862
- Wang, K., Jiang, J., Lei, Y., Zhou, S., Wei, Y., Huang, C., et al. (2019). Targeting metabolic-redox circuits for cancer therapy. *Trends biochem. Sci.* 44 (5), 401–414. doi:10.1016/j.tibs.2019.01.001
- Wang, Y., Zhang, L., Yao, C., Ma, Y., and Liu, Y. (2022b). Epithelial membrane protein 1 promotes sensitivity to RSL3-induced ferroptosis and intensifies gefitinib resistance in head and neck cancer. *Oxid. Med. Cell. Longev.* 2022, 4750671. doi:10.1155/2022/4750671

- Wang, Y., Zhao, G., Condello, S., Huang, H., Cardenas, H., Tanner, E. J., et al. (2021a). Frizzled-7 identifies platinum-tolerant ovarian cancer cells susceptible to ferroptosis. *Cancer Res.* 81 (2), 384–399. doi:10.1158/0008-5472.CAN-20-1488
- Wang, Y., Zhao, Y., Ye, T., Yang, L., Shen, Y., Li, H., et al. (2021b). Ferroptosis signaling and regulators in atherosclerosis. *Front. Cell Dev. Biol.* 9, 809457. doi:10.3389/fcell.2021.809457
- Wang, Y., Zhang, Y., Zhang, Y., Mou, J., and Wang, Y. (2022a). Progress in the treatment of stearyl-coenzymatic A desaturase 1 inhibitor in ovarian cancer [J]. *Chin. J. Pract. Diagnostic Ther.* 36 (05), 524–526. doi:10.13507/j.issn.1674-3474.2022.05.022
- Wei, X., Yi, X., Zhu, X. H., and Jiang, D. S. (2020). Posttranslational modifications in ferroptosis. *Oxid. Med. Cell. Longev.* 2020, 8832043. doi:10.1155/2020/8832043
- Winterbourn, C. C. (1995). Toxicity of iron and hydrogen peroxide: The Fenton reaction. *Toxicol. Lett.* 82–83, 969–974. doi:10.1016/0378-4274(95)03532-x
- Wu, J., Minikes, A. M., Gao, M., Bian, H., Li, Y., Stockwell, B. R., et al. (2019). Intercellular interaction dictates cancer cell ferroptosis via NF2-YAP signalling. *Nature* 572 (7769), 402–406. doi:10.1038/s41586-019-1426-6
- Wu, M., Xu, L. G., Li, X., Zhai, Z., and Shu, H. B. (2002). AMID, an apoptosis-inducing factor-homologous mitochondrion-associated protein, induces caspase-independent apoptosis. *J. Biol. Chem.* 277 (28), 25617–25623. doi:10.1074/jbc.M202285200
- Xia, X., Fan, X., Zhao, M., and Zhu, P. (2019). The relationship between ferroptosis and tumors: A novel landscape for therapeutic approach. *Curr. Gene Ther.* 19 (2), 117–124. doi:10.2174/1566523219666190628152137
- Yang, L., Tian, S., Chen, Y., Miao, C., Zhao, Y., Wang, R., et al. (2021). Ferroptosis-related gene model to predict overall survival of ovarian carcinoma. *J. Oncol.* 2021, 6687391. doi:10.1155/2021/6687391
- Yang, W. H., and Chi, J. T. (2019). Hippo pathway effectors YAP/TAZ as novel determinants of ferroptosis. *Mol. Cell. Oncol.* 7 (1), 1699375. doi:10.1080/23723556.2019.1699375
- Yang, W. H., Ding, C. C., Sun, T., Rupprecht, G., Lin, C. C., Hsu, D., et al. (2019). The Hippo pathway effector TAZ regulates ferroptosis in renal cell carcinoma. *Cell Rep.* 28 (10), 2501–2508. e4. doi:10.1016/j.celrep.2019.07.107
- Yang, W. H., Huang, Z., Wu, J., Ding, C. C., Murphy, S. K., Chi, J. T., et al. (2020). A TAZ-ANGPTL4-NOX2 Axis regulates ferroptotic cell death and chemoresistance in epithelial ovarian cancer. *Mol. Cancer Res.* 18 (1), 79–90. doi:10.1158/1541-7786.MCR-19-0691
- Yang, W. H., Lin, C. C., Wu, J., Chao, P. Y., Chen, K., Chen, P. H., et al. (2021). The Hippo pathway effector YAP promotes ferroptosis via the E3 ligase SKP2. *Mol. Cancer Res.* 19 (6), 1005–1014. doi:10.1158/1541-7786.MCR-20-0534
- Yang, W. S., Kim, K. J., Gaschler, M. M., Patel, M., Shchepinov, M. S., Stockwell, B. R., et al. (2016). Peroxidation of polyunsaturated fatty acids by lipoxygenases drives ferroptosis. *Proc. Natl. Acad. Sci. U. S. A.* 113 (34), E4966–E4975. doi:10.1073/pnas.1603244113
- Yang, W. S., SriRamaratnam, R., Welsch, M. E., Shimada, K., Skouta, R., Viswanathan, V. S., et al. (2014). Regulation of ferroptotic cancer cell death by GPX4. *Cell* 156 (1–2), 317–331. doi:10.1016/j.cell.2013.12.010
- Yang, W. S., and Stockwell, B. R. (2008). Synthetic lethal screening identifies compounds activating iron-dependent, nonapoptotic cell death in oncogenic-RAS-harboring cancer cells. *Chem. Biol.* 15 (3), 234–245. doi:10.1016/j.chembiol.2008.02.010
- Yant, L. J., Ran, Q., Rao, L., Van Remmen, H., Shibata, T., Belter, J. G., et al. (2003). The selenoprotein GPX4 is essential for mouse development and protects from radiation and oxidative damage insults. *Free Radic. Biol. Med.* 34 (4), 496–502. doi:10.1016/s0891-5849(02)01360-6
- Ye, Y., Dai, Q., Li, S., He, J., and Qi, H. (2021). A novel defined risk signature of the ferroptosis-related genes for predicting the prognosis of ovarian cancer. *Front. Mol. Biosci.* 8, 645845. doi:10.3389/fmolb.2021.645845
- You, Y., Fan, Q., Huang, J., Wu, Y., Lin, H., Zhang, Q., et al. (2021). Ferroptosis-related gene signature promotes ovarian cancer by influencing immune infiltration and invasion. *J. Oncol.* 2021, 9915312. doi:10.1155/2021/9915312
- Yu, Z., He, H., Chen, Y., Ji, Q., and Sun, M. (2021). A novel ferroptosis related gene signature is associated with prognosis in patients with ovarian serous cystadenocarcinoma. *Sci. Rep.* 11 (1), 11486. doi:10.1038/s41598-021-90126-5
- Zhang, J., Xi, J., Huang, P., and Zeng, S. (2021). Comprehensive analysis identifies potential ferroptosis-associated mRNA therapeutic targets in ovarian cancer. *Front. Med.* 8, 644053. doi:10.3389/fmed.2021.644053
- Zhang, X., Yu, K., Ma, L., Qian, Z., Tian, X., Miao, Y., et al. (2021). Endogenous glutamate determines ferroptosis sensitivity via ADCY10-dependent YAP suppression in lung adenocarcinoma. *Theranostics* 11 (12), 5650–5674. doi:10.7150/thno.55482
- Zhang, Y., Xia, M., Zhou, Z., Hu, X., Wang, J., Zhang, M., et al. (2021). p53 promoted ferroptosis in ovarian cancer cells treated with human serum incubated-superparamagnetic iron oxides. *Int. J. Nanomedicine* 16, 283–296. doi:10.2147/IJN.S282489
- Zheng, J., Guo, J., Wang, Y., Zheng, Y., Zhang, K., Tong, J., et al. (2022). Bioinformatic analyses of the ferroptosis-related lncRNAs signature for ovarian cancer. *Front. Mol. Biosci.* 8, 735871. doi:10.3389/fmolb.2021.735871
- Zhou, H. H., Chen, X., Cai, L. Y., Nan, X. W., Chen, J. H., Chen, X. X., et al. (2019). Erastin reverses ABCB1-mediated docetaxel resistance in ovarian cancer. *Front. Oncol.* 9, 1398. doi:10.3389/fonc.2019.01398
- Zou, J., Li, Y., Liao, N., Liu, J., Zhang, Q., Luo, M., et al. (2022). Identification of key genes associated with polycystic ovary syndrome (PCOS) and ovarian cancer using an integrated bioinformatics analysis. *J. Ovarian Res.* 15 (1), 30. doi:10.1186/s13048-022-00962-w





## OPEN ACCESS

## EDITED BY

Xin Wang,  
National Institutes of Health (NIH),  
United States

## REVIEWED BY

Jingquan He,  
Shenzhen Traditional Chinese Medicine  
Hospital, China  
Si-Yuan Song,  
Baylor College of Medicine,  
United States

## \*CORRESPONDENCE

Xiaobo Huang,  
drhuangxb@163.com  
Jingfen Shi,  
963725462@qq.com  
Yi Wang,  
w\_yi2022@163.com

<sup>†</sup>These authors share first authorship

## SPECIALTY SECTION

This article was submitted to Molecular  
Diagnostics and Therapeutics,  
a section of the journal  
Frontiers in Molecular Biosciences

RECEIVED 15 August 2022

ACCEPTED 02 September 2022

PUBLISHED 15 September 2022

## CITATION

Zhou Q, Yang L, Li T, Wang K, Huang X,  
Shi J and Wang Y (2022), Mechanisms  
and inhibitors of ferroptosis in psoriasis.  
*Front. Mol. Biosci.* 9:1019447.  
doi: 10.3389/fmolb.2022.1019447

## COPYRIGHT

© 2022 Zhou, Yang, Li, Wang, Huang,  
Shi and Wang. This is an open-access  
article distributed under the terms of the  
[Creative Commons Attribution License  
\(CC BY\)](#). The use, distribution or  
reproduction in other forums is  
permitted, provided the original  
author(s) and the copyright owner(s) are  
credited and that the original  
publication in this journal is cited, in  
accordance with accepted academic  
practice. No use, distribution or  
reproduction is permitted which does  
not comply with these terms.

# Mechanisms and inhibitors of ferroptosis in psoriasis

Qiao Zhou<sup>1,2,3†</sup>, Lijing Yang<sup>2,4†</sup>, Ting Li<sup>5†</sup>, Kaiwen Wang<sup>6</sup>,  
Xiaobo Huang<sup>7\*</sup>, Jingfen Shi<sup>8\*</sup> and Yi Wang<sup>7\*</sup>

<sup>1</sup>Health Management Center, Sichuan Academy of Medical Science and Sichuan Provincial People's Hospital, University of Electronic Science and Technology of China, Chengdu, China, <sup>2</sup>Department of Rheumatology and Immunology, Sichuan Academy of Medical Science and Sichuan Provincial People's Hospital, University of Electronic Science and Technology of China, Chengdu, China, <sup>3</sup>Clinical Immunology Translational Medicine Key Laboratory of Sichuan Province, Sichuan Provincial People's Hospital, University of Electronic Science and Technology of China, Chengdu, China, <sup>4</sup>School of Medicine, University of Electronic Science and Technology of China, Chengdu, China, <sup>5</sup>Department of Rheumatology, Wenjiang District People's Hospital, Chengdu, China, <sup>6</sup>School of Medicine, Faculty of Medicine and Health, The University of Leeds, Leeds, United Kingdom, <sup>7</sup>Department of Critical Care Medicine, Sichuan Academy of Medical Science and Sichuan Provincial People's Hospital, University of Electronic Science and Technology of China, Chengdu, China, <sup>8</sup>Department of Rheumatology and Immunology, Sichuan Academy of Medical Science and Sichuan Provincial People's Hospital, Wenjiang District People's Hospital, Chengdu, China

Psoriasis is a chronic inflammatory skin disease that features localized or widespread erythema, papules, and scaling. It is common worldwide and may be distributed throughout the whole body. The pathogenesis of psoriasis is quite complex and the result of the interplay of genetic, environmental and immune factors. Ferroptosis is an iron-dependent programmed death that is different from cell senescence, apoptosis, pyroptosis and other forms of cell death. Ferroptosis involves three core metabolites, iron, lipids, and reactive oxygen species (ROS), and it is primarily driven by lipid peroxidation. Ferrostatin-1 (Fer-1) is an effective inhibitor of lipid peroxidation that inhibited the changes related to ferroptosis in erastin-treated keratinocytes and blocked inflammatory responses. Therefore, it has a certain effect on the treatment of psoriatic lesions. Although ferroptosis is closely associated with a variety of human diseases, such as inflammatory diseases, no review has focused on ferroptosis in psoriasis. This mini review primarily focused on the pathogenesis of psoriasis, the mechanisms of ferroptosis, the connection between ferroptosis and psoriasis and ferroptosis inhibitors in psoriasis treatment. We discussed recent research advances and perspectives on the relationship between ferroptosis and psoriasis.

## KEYWORDS

psoriasis, ferroptosis, lipid metabolism, ferrostatin-1, treatment

## Introduction

Psoriasis (PsO) is a chronic, recurrent, and autoimmune skin disorder caused by multiple risk factors, including genetic and environmental factors (Pezzolo and Naldi, 2019; Kanda et al., 2020; Madden et al., 2020; Reid and Griffiths, 2020). The incidence of psoriasis varies greatly worldwide, with a global prevalence of approximately 2%–4%

(Liang et al., 2021) or approximately 125 million people (Armstrong and Read, 2020). According to the clinical features, PsO is divided into four types: vulgaris, arthrogryposis, pustular, and erythroderma (Navarini et al., 2017; Carrasquillo et al., 2020; Lo et al., 2020; Nast et al., 2020). Psoriatic lesions initially appear as red papules. With the development of the disease, the red plaques exhibit various morphologies, such as dot-like, map-like, or covered with thick, silvery-white scales (Raychaudhuri et al., 2014). Keratinocytes play an essential role in psoriasis, and their death amplifies the inflammatory effect. A recent study showed that keratinocytes in psoriatic lesions exhibited lipid peroxidation, which is related to a novel type of cell death, ferroptosis (Wen et al., 2019; Shou et al., 2021).

The Brent Stockwell Laboratory formally defined ferroptosis for the first time in 2012, and it is caused by lipid peroxidation due to the accumulation of reactive oxygen species (ROS) (Dixon et al., 2012). Lipids are organic substances that play critical roles in human tissues. Lipids form the cell membrane and participate in a variety of processes, including cell proliferation and apoptosis, inflammatory conditions, and immune responses (van Meer et al., 2008; Nowowiejska et al., 2021). Iron, lipids and ROS play important roles in cell survival. However, these factors lead to fatal damage when metabolic disorders occur (Liu and Gu, 2022). Ferroptosis is closely related to a variety of human diseases (Jiang et al., 2021), including tumors, septicemia, bacterial, and viral diseases, some neurodegenerative diseases and autoimmune diseases, such as systemic lupus erythematosus, inflammatory bowel diseases, and PsO, which we will discuss briefly in this review (Gunther et al., 2013; Li et al., 2021; Shou et al., 2021).

## Pathogenesis of psoriasis

The pathogenesis of psoriasis is extremely complicated and is currently believed that the development of the disease is caused by the joint action of genetic and environmental factors, which together result in inflammatory cell infiltration, keratinocyte proliferation, and T cell differentiation, etc. (Ogawa and Okada, 2020; Solmaz et al., 2020). The heritability of psoriasis is approximately 66%–90%, which is one of the highest heritability rates of multifactorial genetic diseases (Traks et al., 2019). Environmental factors, such as infection, obesity, nicotine dependence, etc., also induce and aggravate the progression of psoriasis (Madden et al., 2020; Karpinska-Mirecka et al., 2021; Reolid et al., 2021). For example, drip psoriasis is closely related to acute streptococcal infection, which indicates a link between psoriasis and bacterial infection (Madden et al., 2020; Zhou and Yao, 2022). Although the pathogenic etiology of psoriasis is not clear, psoriasis susceptibility genes are associated with immune mechanisms (Vicic et al., 2021; van de Kerkhof, 2022). The innate and adaptive immune systems play crucial roles (Xu and Zhang,

2017), especially CD4 and CD8 cells and the interleukin-23/T helper 17 pathway (Girolomoni et al., 2017; Ly et al., 2019; Iznardo and Puig, 2021). The abnormal activation and migration of specific T cells to the skin leads to the gradual accumulation of inflammatory cells (Xu and Zhang, 2017). Inflammatory cytokines produced by Th1 and Th22 cells, such as tumor necrosis factor (TNF), interleukin (IL)-17, and IL-22, all contribute to the inflammation. With the induction of IL-23, Th17 cells differentiate, proliferate and secrete IL-17, which disrupts the integrity of the skin barrier and induces keratinocyte hyperproliferation (Rendon and Schakel, 2019).

## Mechanisms of ferroptosis

As a new form of programmed cell death (Dixon et al., 2012), ferroptosis differs from other forms of cell death, such as pyroptosis, apoptosis or cellular senescence, and results in membrane damage and cell lysis (Riegman et al., 2020; Ding et al., 2021). Iron, lipids, and ROS maintain a steady state for cell survival (Liu and Gu, 2022). The accumulation of ROS causes lipid peroxidation and further induces ferroptosis (Stockwell, 2022). The detailed mechanisms of ferroptosis are illustrated below and shown in Figure 1.

## Lipid metabolism

Lipid metabolism is closely related to ferroptosis. As one of the basic elements, long-chain polyunsaturated fatty acids (PUFAs) participate in ferroptosis and are quite sensitive to lipid peroxidation (Li et al., 2020). Free PUFAs are esterified and form film phospholipids that transmit ferroptosis signals after oxidation. PUFAs are linked to coenzyme A (CoA) via the catalysis of acyl-CoA synthetase long-chain family member 4 (ACSL4) (Das, 2019). Lysophosphatidylcholine acetyltransferase 3 (LPCAT3) re-esterifies these products into phospholipids and integrates them into membrane phospholipids (Forcina and Dixon, 2019; Li and Li, 2020; Chen et al., 2021b; Liang et al., 2022). Lipid peroxidation leads to the destruction of the lipid layer, which causes cell damage and ferroptosis. Arachidonic acid (AA) is a key phospholipid that induces ferroptosis. ACSL4 and LPCAT3 are involved in the biosynthesis of phosphatidylethanolamine (PE) of adrenaline, a derivative of arachidonic acid, which activates PUFAs and acts as key phospholipids to induce ferroptosis (Stockwell, 2022). ACSL4 and LPCAT3 are also involved in the activation of PUFAs and the binding of them to local membrane lipids, which shows the necessity of PUFAs in the membrane binding environment to have fatal effects on peroxidation (Li et al., 2020; Stockwell, 2022). Because specific carbon atoms in lipids are susceptible to peroxidation, lipid peroxidation depends on the strength of its hydrocarbon bond (Li et al., 2020).

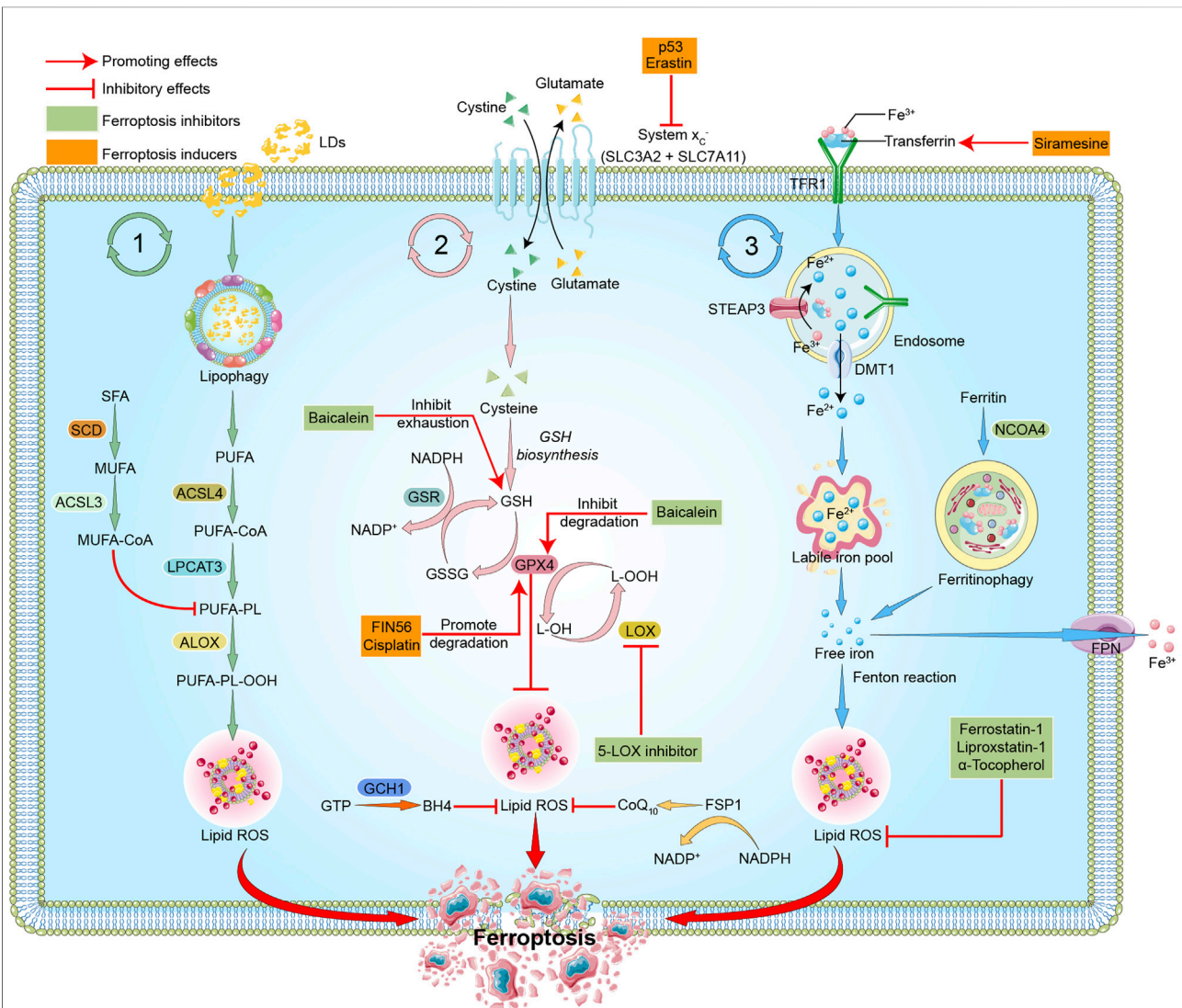


FIGURE 1

Mechanisms of ferroptosis. The three pathways represent lipid metabolism, antioxidant metabolism, and iron metabolism in ferroptosis, respectively. In lipid metabolism, LDs are degraded *via* lipophagy to release free fatty acids, including PUFAs. Accumulated PUFAs are catalyzed by ACSL4 to generate the key substrate PUFA-CoA, which is finally esterified into PUFA-PLs by LPCAT3. PUFA-PLs can be peroxidized to PUFA-PL-OOH through enzymatic and non-enzymatic lipid peroxidation reactions in the presence of bioactive iron. PLOOH can generate lipid hydroxyl radicals and lipid peroxy radicals, sensitizing the cell to ferroptosis. MUFAs, likely through MUFA-PLs from MUFA-CoA, can inhibit PUFA-PLs by replacing PUFA from phosphatidylethanolamine, thus reducing the available substrate for lipid peroxidation. In antioxidant metabolism, the two subunits SLC3A2 and SLC7A11 constitute the system Xc<sup>-</sup>, which is an amino acid antiporter that mediates the exchange of extracellular cystine and intracellular glutamate across the plasma membrane. After entering the cells, cystine is reduced to cysteine and participates in the synthesis of GSH, which serves the substrate of GPX4. GPX4 reduces cytotoxic lipid peroxide (L-OOH) to the corresponding alcohol (L-OH), thus inhibiting the formation of lipid peroxide and ferroptosis. GPX4 can also transform GSH into GSSG, and GSSG can be reduced to GSH under the action of GSR. FSP1-CoQ10 or GCH1-BH4 pathway inhibits ferroptosis independently of GSH. In iron metabolism, ferric iron (Fe<sup>3+</sup>) is bound to transferrin (TF) to form TF-Fe<sup>3+</sup>, which is then taken up by the TF receptor (TFR1). In endosomes, STEAP3 reduces Fe<sup>3+</sup> to Fe<sup>2+</sup>, which is then released to cytoplasm through DMT1, and stored in LIP or ferritin. Fe<sup>2+</sup> mediates the Fenton reaction, thereby promoting lipid peroxidation and ferroptosis. Excess Fe<sup>2+</sup> is oxidized to Fe<sup>3+</sup> by FPN. In addition, NCOA4-mediated ferritinophagy can increase LIP, thereby sensitizing the cell to ferroptosis through Fenton reaction. The target of ferroptosis inducers and inhibitors are also indicated. P53 and erastin can interfere with the synthesis of GSH by inhibiting system Xc<sup>-</sup>. FIN56 and cisplatin promote the degradation of GPX4. Siramesine increases the expression of transferrin in iron metabolism and increases the level of intracellular ferric iron. Baicalein inhibits GSH depletion, GPX4 degradation and lipid peroxidation. 5-LOX inhibitor inhibits the production of ROS. Ferostatin-1, Liproxstatin-1, and α-Tocopherol scavenge ROS and inhibit lipid peroxidation. Red arrows indicate promoting effects. Short lines with vertical end indicate inhibitory effect. The pink ball represents Fe<sup>3+</sup>. Blue balls represent Fe<sup>2+</sup>. Green triangles represent cystine. Yellow triangles represent glutamate. Light green triangles represent cysteine. Green boxes indicate ferroptosis inhibitors. Yellow boxes represent ferroptosis inducers. Abbreviations: ACSL3, acyl-CoA synthetase long chain family member 3; ACSL4, acyl-CoA synthetase long chain family member 4; ALOX, arachidonate lipoxygenase; BH4, tetrahydrobiopterin; CoA, coenzyme A; CoQ10, coenzyme Q10; DMT1, divalent metal transporter 1; FPN, ferroportin; FSP1, ferroptosis suppressor protein 1; GCH1, GTP cyclohydrolase 1; GPX4, glutathione peroxidase 4; GSH, glutathione; GSR, glutathione reductase; GSSG, oxidized glutathione; GTP, guanosine triphosphate; LDs, lipid droplets; LPCAT3,

(Continued)

**FIGURE 1 (Continued)**

lysophosphatidylcholine acyltransferase 3; LIP, labile iron pool; LOX, lipoxygenase; MUFA, monounsaturated fatty acid; NADP, nicotinamide-adenine-dinucleotide phosphate; NADPH, reduced nicotinamide adenine dinucleotide phosphate; NCOA4, nuclear receptor coactivator 4; OOH, hydroperoxides; PUFA, polyunsaturated fatty acid; PL, phospholipid; ROS, reactive oxygen species; SCD, stearoyl CoA desaturase; SFA, saturated fatty acids; SLC3A2, solute carrier family 3 member 2; SLC7A11, solute carrier family 7 member 11; STEAP3, the six-transmembrane epithelial antigen of prostate 3; TF, transferrin; TFR, transferrin receptor protein.

Peroxidation of specific membrane lipids could induce ferroptosis. The latest research shows that cytochrome P450 oxidoreductase is the driver of lipid peroxidation in ferroptosis (Stockwell et al., 2020). Once the production of lipid peroxides far exceeds the antioxidant scavenging capacity, the accumulated lipid peroxides attack the adjacent PUFAs to form new lipid peroxides, which leads to the enhancement of lipid peroxides (Chen et al., 2021a; Stockwell, 2022). Continuous peroxidation of PUFAs leads to changes in the physiological state of cell membranes, such as destruction of the stability and integrity of cell membranes, and ion homeostasis inside and outside of cells (Stockwell, 2022). The decomposition products of lipid peroxide further react with and destroy essential proteins of the human body (Li et al., 2020), which ultimately leads to ferroptosis.

## Iron metabolism

Iron ions are critical factors in the production of ROS *via* enzymatic or non-enzymatic reactions, and it participates in the process of lipid peroxidation and plays a crucial role in ferroptosis (Masaldan et al., 2019; Angelova et al., 2020; Jiang et al., 2021). The abnormal accumulation of free iron in the body often affects normal physiological processes and is a key signal of ferroptosis.  $\text{Fe}^{2+}$  is acquired from the intestinal absorption or red blood cells degradation. Under the action of ceruloplasmin,  $\text{Fe}^{2+}$  is oxidized to  $\text{Fe}^{3+}$ , which combines with transferrin (TF) on the cell membrane to form  $\text{TF-Fe}^{3+}$  complex *via* the membrane protein TF receptor 1 (TFR1) (Frazer and Anderson, 2014). The six-transmembrane epithelial antigen of prostate 3 (STEAP3) reduces  $\text{Fe}^{3+}$  to  $\text{Fe}^{2+}$ , and  $\text{Fe}^{2+}$  is normally stored in the labile iron pool (LIP) and ferritin, which is mediated by divalent metal transporter 1 (DMT1) or Zinc-Iron regulatory protein family 8/14 (ZIP8/14) (Li et al., 2020). Excess  $\text{Fe}^{2+}$  is oxidized to  $\text{Fe}^{3+}$  by ferroportin (FPN) (Li et al., 2020). LIP is the source of iron ions in the Fenton reaction (He et al., 2020; Lin et al., 2020). Excessive free iron in the cell mediates the Fenton reaction to produce a large amount of ROS, which further causes a cascade reaction, intensifies the lipid oxidation of the cell membrane, and induces ferroptosis (Shen et al., 2018). Ferrous iron may act as a cofactor of some enzymes that mediate lipid peroxidation and participate in the process of ferroptosis. Therefore, the physiological process of iron ions has an impact on the sensitivity of ferroptosis (Xia et al., 2021).

Silencing the TFR1 gene inhibited erastin-induced ferroptosis (Gao et al., 2015). It was also found that heat shock protein  $\beta$ -1 (HSPB1) inhibited ferroptosis by inhibiting TFR1 expression and reducing the intracellular iron concentration (Sun et al., 2015). In contrast, heme oxygenase-1 (HO-1) supplementation with iron accelerated erastin-induced ferroptosis (Kwon et al., 2015).

## Antioxidant metabolism

The antioxidant system is the critical determining factor of the occurrence of iron-induced cell death, and it inhibits the lipid peroxidation chain reaction by reducing lipid peroxides (Seibt et al., 2019). Under physiological conditions, antioxidant enzymes, including glutathione peroxidase 4 (GPX4), inhibit the production of oxidized lipids (Hong et al., 2022). GPX4, which is a glutathione (GSH)- and selenium-dependent glutathione peroxidase, could detoxify lipid hydroperoxides (Miao et al., 2022). GSH is a cysteine-containing tripeptide that exists as an intracellular antioxidant and primarily depends on system Xc-mediated cystine uptake and the concomitant reduction of cystine to cysteine (Ursini and Maiorino, 2020). System Xc- is an amino acid antiporter that is widely distributed in the phospholipid bilayer, and it is a heterodimer composed of two subunits, SLC7A11 and SLC3A2 (Ursini and Maiorino, 2020; Stockwell, 2022). Cysteine and glutamate enter and exit the cell via system Xc-. The absorbed cysteine participates in the synthesis of GSH *via* a reduction reaction. With the help of GSH as a cofactor, GPX4 converts GSH to oxidized glutathione disulfide (GSSG) and reduces cytotoxic lipid peroxide (L-OOH) to the corresponding alcohols (L-OH), thereby detoxifying peroxide products and preventing the accumulation of lipid ROS, making it an important inhibitor of ferroptosis (Friedmann Angeli et al., 2019; Stockwell, 2019; Li et al., 2020; Ursini and Maiorino, 2020; Miao et al., 2022; Stockwell, 2022).

The NADPH-FSP1 (ferroptosis suppressor protein 1)-CoQ<sub>10</sub> and GCH1 (guanosine triphosphate cyclohydrolase 1)-BH4 (tetrahydrobiopterin) pathways are also reported to be involved in inhibiting ferroptosis, with specific roles needed to be further elucidated (Zheng and Conrad, 2020). RAS-selective lethal 3 (RSL3) and the compounds DPI7 and DPI10 may be used as ferroptosis inducers by directly inhibiting the activity of GPX4, thus reducing the antioxidant capacity of cells and causing the



TABLE 1 The use of ferroptosis inducers and inhibitors in diseases.

Classification		Representatives	Mechanisms	Indications	References
Regulating oxidative stress	Inducers	Erastin	Produce ROS to damage mitochondria or affect GSH synthesis by inhibiting System Xc-	Diffuse large B cell lymphoma	(Kose et al. (2019), Zhao et al. (2020))
		FIN56	Produce ROS and induce ferroptosis by inhibiting GPX4	Glioblastoma	Zhang et al. (2021a)
	Inhibitors	Ferrostatin-1	Inhibit oxidative stress, reduce ROS and lipid peroxidation, and regulate oxidation related proteins such as up regulating GPX4 expression	Psoriasis	Zilka et al. (2017)
		Liproxstatin-1	Reduce mitochondrial ROS production, restore GPX4 level and inhibit lipid peroxidation	Myocardialischaemia/reperfusion	Zilka et al. (2017)
		$\alpha$ -Tocopherol	Damage the chain reaction of automatic oxidation, so as to resist oxidation	Myocardialischaemia/reperfusion	Zilka et al. (2017)
		5-LOX inhibitor	Inhibit glutamate toxicity and ferroptosis by inhibiting the production of ROS in the cytoplasm	Asthma	Yuan et al. (2016)
Iron metabolism	Inducers	Siramesine	Increase the expression of transferrin in iron metabolism and increase the level of intracellular ferric iron	Breast cancer	Ma et al. (2016)
	Inhibitors	Deferoxamine and other iron chelator	Bind free iron ions to inhibit ferroptosis	Thalassemia Major	Guerrero-Hue et al. (2019)
Others	Inducers	Cisplatin	Increase the level of intracellular ROS	Lung cancer	Guo et al. (2018)
	Inhibitors	Baicalein	Inhibit GSH depletion, GPX4 degradation and lipid peroxidation	Pancreatic cancer	Xie et al. (2016)

Abbreviations: GPX4, glutathione peroxidase 4; GSH, glutathione; LOX, lipoxygenase; ROS, reactive oxygen species; System Xc, sodium-independent, anionic amino acid transport system.

accumulation of ROS to exert ferroptosis (Yang et al., 2014; Magtanong et al., 2019). P53 downregulates the expression of SLC7A11 and inhibits the uptake of cystine by system Xc-, which may also lead to ferroptosis (Jiang et al., 2015; Liu et al., 2019; Liu and Gu, 2021; Liu and Gu, 2022).

## Ferroptosis in psoriasis

There is an intricate relationship between ferroptosis and inflammation in psoriatic lesions. Abnormal lipid expression and metabolism are frequently observed in patients with psoriasis, especially in keratinocytes from the psoriatic lesions (Benhadou et al., 2019; Shou et al., 2021). At the single-cell level, the lipid oxidation pathway was significantly upregulated in keratinocyte groups of psoriasis, and lipid peroxidation was enhanced during psoriasis (Shou et al., 2021). Compared to other cells, such as fibroblasts, macrophages, dendritic cells, endothelial cells, and T cells, the lipid oxidation activity in keratinocytes highly correlated with the Th22/Th17 pathway and had a time- and concentration-dependent effect on the stimulation of erastin-dependent ferroptosis (Orsmond et al., 2021; Shou et al., 2021).

Cell death related to ferroptosis was also reported to be activated in psoriatic lesions. For example, GPX4 was highly expressed in all layers of the epidermis in normal samples while under-expressed in psoriatic skin, and ACSL4 was highly expressed in the basal layer of the epidermis in psoriasis compared to the normal skin (Shou et al., 2021). The

expression of prostaglandin-endoperoxide synthase 2 (PTGS2) and transferrin receptor (TFRC) also increased significantly in psoriatic samples, while the expression of ferritin heavy chain 1 (FTH1) and ferritin light chain (FTL) decreased (Shou et al., 2021). PTGS2 is a potential biomarker for cells undergoing ferroptosis (Wu et al., 2022), and FTH1 and FTL is involved in the storage, entry and homeostasis of iron (Park and Chung, 2019). As a derivative of lipid peroxidation, 4-hydroxynonenol (4-HNE) is also increased in psoriatic lesions and enhances ferroptosis (Liu et al., 2020; Shou et al., 2021). GPX4 is a selenoprotein (Proneth and Conrad, 2019; Zhang et al., 2021b), and the exact reason for its reduced expression in psoriatic lesions is unknown. It is observed that selenium was decreased and related to the severity of psoriasis in patients with long disease duration, and selenium deficiency affects the biosynthesis of GPX4, which might explain the decreased antioxidant activity and susceptibility towards ferroptosis in psoriatic patients (Serwin et al., 2003; Ingold et al., 2018).

Ferroptosis not only promotes cell death, but also triggers inflammation in psoriatic keratinocytes. Several studies showed that ferroptosis triggers and amplifies a variety of inflammatory responses (Tsurusaki et al., 2019; Bebbler et al., 2020; Ren et al., 2020). It enhances inflammatory responses *via* the release of damage-associated molecular patterns (DAMPs) and alarmins (Chen et al., 2021a), which could further activate the immune cells and significantly stimulate the expression of inflammatory cytokines, making a complex link between the inflammatory response and ferroptosis in psoriatic lesions.

## Ferroptosis inhibitors in psoriasis treatment

Ferroptosis is involved in several pathophysiological processes and the development of miscellaneous conditions, including iron overload disease and myocardial diseases (Yang et al., 2020; Liu and Gu, 2021; Weber et al., 2021; Lai et al., 2022; Liu and Gu, 2022). Reasonable induction or inhibition of ferroptosis contributes to the treatment of these diseases. For example, the ferroptosis inducer erastin selectively kills tumor cells by regulating oxidative stress (Kose et al., 2019; Zhao et al., 2020). FIN56, siramesine, cisplatin and other inducers also improve the treatment of some diseases (Table 1) (Ma et al., 2016; Guo et al., 2018; Zhao et al., 2020; Zhang et al., 2021a).

However, ferroptosis inhibitors play an essential role, especially in psoriasis. There are many inhibitors, such as ferrostatin-1 (fer-1), liproxstatin-1 (lip-1) and  $\alpha$ -Tocopherol ( $\alpha$ -TOH) (Xie et al., 2016; Yuan et al., 2016; Zilka et al., 2017; Guerrero-Hue et al., 2019). Fer-1 and lip-1 are more effective compared to  $\alpha$ -TOH, which is a relatively weak ferroptosis inhibitor (Stockwell et al., 2017; Shah et al., 2018; Yao et al., 2019; Miotto et al., 2020).

Fer-1 was obtained from the high-throughput screening of a small molecule library. As an aromatic amine antioxidant, Fer-1 prevented erastin-induced lipid ROS production and inhibited ferroptosis in HT-1080 cells, but it did not inhibit the cell death induced by other lethal oxidative compounds, such as  $H_2O_2$  or apoptosis inducers (Armstrong and Read, 2020). Fer-1 reduces lipid peroxidation by inhibiting oxidative stress through downregulating prostaglandin endoperoxide synthase 2 and upregulating GPX4 and Nuclear factor E2 related factor 2 (NRF2) (Asano et al., 2017). In psoriatic keratinocytes, Fer-1 blocks the inflammatory responses and alleviates the skin lesions by inhibiting the lipid peroxidation (Kajarabille and Latunde-Dada, 2019; Miotto et al., 2020). Fer-1 was also demonstrated to eliminate erastin-induced death in keratinocytes and alleviate imiquimod-induced psoriasiform dermatitis in mice (Shou et al., 2021). The complex effect of Fer-1 against psoriasis-like inflammatory responses suggests that lipid peroxidation in psoriatic lesions also amplifies inflammatory responses, and the two act together to contribute to ferroptosis (Gong et al., 2019). Further studies need to identify key pathogenic mediators of this process and provide more specific and accurate therapeutic targets.

The level of mammalian targets of rapamycin (mTOR) signaling protein and the expression of mTOR complex 1 (mTORC1) was elevated in psoriatic skin (Raychaudhuri and Raychaudhuri, 2014). Through activating mTORC1, cystine and cysteine promotes the biosynthesis of not only GSH, but also GPX4, while inhibition of mTORC1 sensitizes cells to ferroptosis by decreasing the synthesis of GPX4, demonstrating a link between mTORC1 and ferroptosis (Zhang et al., 2021b; Conlon et al., 2021).

## Conclusion and perspective

Ferroptosis primarily consists of three components: 1) oxidation of PUFAs, 2) excess active iron, and 3) inactivation of GPX4 (Battaglia et al., 2020). Studies have shown that ferroptosis is closely associated with the development of several human diseases, including autoimmune diseases, tumors, infectious diseases, and neurodegenerative diseases, such as Alzheimer's disease (AD), Parkinson's disease (PD), and Huntington's disease (Qiu et al., 2020; Reichert et al., 2020; Lai et al., 2022). The current mini review focused on the mechanisms and treatment of psoriasis associated with ferroptosis and the therapeutic advances that contribute to the effective improvement of psoriatic skin manifestations, including skin thickness and scales, in the role of the inhibition of ferroptosis. Although studies on the role of ferroptosis in psoriasis are scarce, the limited available literature shows that ferroptosis inhibitors have good effects in the treatment of this disease.

However, as a novel cell death mechanism, many issues must be solved urgently. Current research results of ferroptosis in psoriasis are limited, and the specific role of ferroptosis in the occurrence and development of psoriasis is not known. The medical field faces challenges in psoriasis treatment, such as the side effects and adherence of medications. To promote the quality of life of psoriatic patients, we need more effective treatment strategies. Determining the specific connection of ferroptosis and PsO will facilitate targeted therapies and personalized treatment for psoriasis, provide guidance for precision medicine and achieve better therapeutic effects.

Taken together, ferroptosis has a close connection with psoriasis, and there should be more experimental data to support further investigations. Psoriasis treatment strategies based on ferroptosis research will provide great advances in the future and benefit psoriatic patients.

## Author contributions

YW, JS, and XH contributed to the conception and design of the work. QZ, LY, and TL drafted the manuscript. KW prepared the figure. YW, JS, and XH substantively revised the manuscript. All authors read and approved the final manuscript.

## Funding

This research was supported by the National Natural Science Foundation of China (81802504, 81872207), the Sichuan Science and Technology Bureau (2019YFS0439, 2020JDJQ0067, 2020JDR0118, 2021YJ0564, 2022YFH0005), the Science and Technology Innovation Project of Chengdu, China (No. 2021-

YF05-00225-SN), and a Sichuan Medical Association grant (No. Q19037).

## Conflict of interest

The authors declare that the research was conducted in the absence of any commercial or financial relationships that could be construed as a potential conflict of interest.

## References

- Angelova, P. R., Choi, M. L., Berezhnov, A. V., Horrocks, M. H., Hughes, C. D., De, S., et al. (2020). Alpha synuclein aggregation drives ferroptosis: An interplay of iron, calcium and lipid peroxidation. *Cell Death Differ.* 27, 2781–2796. doi:10.1038/s41418-020-0542-z
- Armstrong, A. W., and Read, C. (2020). Pathophysiology, clinical presentation, and treatment of psoriasis: A review. *Jama* 323, 1945–1960. doi:10.1001/jama.2020.4006
- Asano, M., Yamasaki, K., Yamauchi, T., Terui, T., and Aiba, S. (2017). Epidermal iron metabolism for iron salvage. *J. Dermatol. Sci.* 87, 101–109. doi:10.1016/j.jdermsci.2017.04.003
- Battaglia, A. M., Chirillo, R., Aversa, I., Sacco, A., Costanzo, F., and Biamonte, F. (2020). Ferroptosis and cancer: Mitochondria meet the "iron maiden" cell death. *Cells* 9, 1505. doi:10.3390/cells9061505
- Bebber, C. M., Muller, F., Prieto Clemente, L., Weber, J., and Von Karstedt, S. (2020). Ferroptosis in cancer cell biology. *Cancers (Basel)* 12, E164. doi:10.3390/cancers12010164
- Benhadou, F., Mintoff, D., and Del Marmol, V. (2019). Psoriasis: Keratinocytes or immune cells - which is the trigger? *Dermatology* 235, 91–100. doi:10.1159/000495291
- Carrasquillo, O. Y., Pabon-Cartagena, G., Falto-Aizpurua, L. A., Santiago-Vazquez, M., Cancel-Artau, K. J., Arias-Berrios, G., et al. (2020). Treatment of erythrodermic psoriasis with biologics: A systematic review. *J. Am. Acad. Dermatol.* 83, 151–158. doi:10.1016/j.jaad.2020.03.073
- Chen, X., Kang, R., Kroemer, G., and Tang, D. (2021a). Ferroptosis in infection, inflammation, and immunity. *J. Exp. Med.* 218, e20210518. doi:10.1084/jem.20210518
- Chen, X., Li, J., Kang, R., Klionsky, D. J., and Tang, D. (2021b). Ferroptosis: Machinery and regulation. *Autophagy* 17, 2054–2081. doi:10.1080/15548627.2020.1810918
- Conlon, M., Poltorack, C. D., Forcina, G. C., Armenta, D. A., Mallais, M., Perez, M. A., et al. (2021). A compendium of kinetic modulatory profiles identifies ferroptosis regulators. *Nat. Chem. Biol.* 17, 665–674. doi:10.1038/s41589-021-00751-4
- Das, U. N. (2019). Saturated fatty acids, mufas and pufas regulate ferroptosis. *Cell Chem. Biol.* 26, 309–311. doi:10.1016/j.chembiol.2019.03.001
- Ding, Y., Chen, X., Liu, C., Ge, W., Wang, Q., Hao, X., et al. (2021). Identification of A small molecule as inducer of ferroptosis and apoptosis through ubiquitination of Gpx4 in triple negative breast cancer cells. *J. Hematol. Oncol.* 14, 19. doi:10.1186/s13045-020-01016-8
- Dixon, S. J., Lemberg, K. M., Lamprecht, M. R., Skouta, R., Zaitsev, E. M., Gleason, C. E., et al. (2012). Ferroptosis: An iron-dependent form of nonapoptotic cell death. *Cell* 149, 1060–1072. doi:10.1016/j.cell.2012.03.042
- Forcina, G. C., and Dixon, S. J. (2019). Gpx4 at the crossroads of lipid homeostasis and ferroptosis. *Proteomics* 19, E1800311. doi:10.1002/pmic.201800311
- Frazer, D. M., and Anderson, G. J. (2014). The regulation of iron transport. *Biofactors* 40, 206–214. doi:10.1002/biof.1148
- Friedmann Angeli, J. P., Miyamoto, S., and Schulze, A. (2019). Ferroptosis: The greasy side of cell death. *Chem. Res. Toxicol.* 32, 362–369. doi:10.1021/acs.chemrestox.8b00349
- Gao, M., Monian, P., Quadri, N., Ramasamy, R., and Jiang, X. (2015). Glutaminolysis and transferrin regulate ferroptosis. *Mol. Cell* 59, 298–308. doi:10.1016/j.molcel.2015.06.011
- Girolomoni, G., Strohal, R., Puig, L., Bachelez, H., Barker, J., Boehncke, W. H., et al. (2017). The role of il-23 and the il-23/Th 17 immune Axis in the pathogenesis and treatment of psoriasis. *J. Eur. Acad. Dermatol. Venereol.* 31, 1616–1626. doi:10.1111/jdv.14433
- Gong, Y., Wang, N., Liu, N., and Dong, H. (2019). Lipid peroxidation and Gpx4 inhibition are common causes for myofibroblast differentiation and ferroptosis. *DNA Cell Biol.* 38, 725–733. doi:10.1089/dna.2018.4541
- Guerrero-Hue, M., Garcia-Caballero, C., Palomino-Antolin, A., Rubio-Navarro, A., Vazquez-Carballo, C., Herencia, C., et al. (2019). Curcumin reduces renal damage associated with rhabdomyolysis by decreasing ferroptosis-mediated cell death. *Faseb J.* 33, 8961–8975. doi:10.1096/fj.201900077R
- Gunther, C., Neumann, H., Neurath, M. F., and Becker, C. (2013). Apoptosis, necrosis and necroptosis: Cell death regulation in the intestinal epithelium. *Gut* 62, 1062–1071. doi:10.1136/gutjnl-2011-301364
- Guo, J., Xu, B., Han, Q., Zhou, H., Xia, Y., Gong, C., et al. (2018). Ferroptosis: A novel anti-tumor action for cisplatin. *Cancer Res. Treat.* 50, 445–460. doi:10.4143/crt.2016.572
- He, Y. J., Liu, X. Y., Xing, L., Wan, X., Chang, X., and Jiang, H. L. (2020). Fenton reaction-independent ferroptosis therapy via glutathione and iron redox couple sequentially triggered lipid peroxide generator. *Biomaterials* 241, 119911. doi:10.1016/j.biomaterials.2020.119911
- Hong, M., Rong, J., Tao, X., and Xu, Y. (2022). The emerging role of ferroptosis in cardiovascular diseases. *Front. Pharmacol.* 13, 822083. doi:10.3389/fphar.2022.822083
- Ingold, I., Berndt, C., Schmitt, S., Doll, S., Poschmann, G., Buday, K., et al. (2018). Selenium utilization by Gpx4 is required to prevent hydroperoxide-induced ferroptosis. *Cell* 172, 409–422. doi:10.1016/j.cell.2017.11.048
- Iznardo, H., and Puig, L. (2021). Exploring the role of il-36 cytokines as A new target in psoriatic disease. *Int. J. Mol. Sci.* 22, 4344. doi:10.3390/ijms22094344
- Jiang, L., Kon, N., Li, T., Wang, S. J., Su, T., Hibshoosh, H., et al. (2015). Ferroptosis as A P53-mediated activity during tumour suppression. *Nature* 520, 57–62. doi:10.1038/nature14344
- Jiang, X., Stockwell, B. R., and Conrad, M. (2021). Ferroptosis: Mechanisms, biology and role in disease. *Nat. Rev. Mol. Cell Biol.* 22, 266–282. doi:10.1038/s41580-020-00324-8
- Kajarabille, N., and Latunde-Dada, G. O. (2019). Programmed cell-death by ferroptosis: Antioxidants as mitigators. *Int. J. Mol. Sci.* 20, 4968. doi:10.3390/ijms20194968
- Kanda, N., Hoashi, T., and Saeki, H. (2020). Nutrition and psoriasis. *Int. J. Mol. Sci.* 21, 5405. doi:10.3390/ijms21155405
- Karpinska-Mirecka, A., Bartosinska, J., and Krasowska, D. (2021). The impact of hypertension, diabetes, lipid disorders, overweight/obesity and nicotine dependence on health-related quality of life and psoriasis severity in psoriatic patients receiving systemic conventional and biological treatment. *Int. J. Environ. Res. Public Health* 18, 13167. doi:10.3390/ijerph182413167
- Kose, T., Vera-Aviles, M., Sharp, P. A., and Latunde-Dada, G. O. (2019). Curcumin and (-)- epigallocatechin-3-gallate protect murine Min6 pancreatic beta-cells against iron toxicity and erastin-induced ferroptosis. *Pharm. (Basel)* 12, 26. doi:10.3390/ph12010026
- Kwon, M. Y., Park, E., Lee, S. J., and Chung, S. W. (2015). Heme oxygenase-1 accelerates erastin-induced ferroptotic cell death. *Oncotarget* 6, 24393–24403. doi:10.18632/oncotarget.5162
- Lai, B., Wu, C. H., Wu, C. Y., Luo, S. F., and Lai, J. H. (2022). Ferroptosis and autoimmune diseases. *Front. Immunol.* 13, 916664. doi:10.3389/fimmu.2022.916664

## Publisher's note

All claims expressed in this article are solely those of the authors and do not necessarily represent those of their affiliated organizations, or those of the publisher, the editors and the reviewers. Any product that may be evaluated in this article, or claim that may be made by its manufacturer, is not guaranteed or endorsed by the publisher.

- Li, D., and Li, Y. (2020). The interaction between ferroptosis and lipid metabolism in cancer. *Signal Transduct. Target. Ther.* 5, 108. doi:10.1038/s41392-020-00216-5
- Li, J., Cao, F., Yin, H. L., Huang, Z. J., Lin, Z. T., Mao, N., et al. (2020). Ferroptosis: Past, present and future. *Cell Death Dis.* 11, 88. doi:10.1038/s41419-020-2298-2
- Li, P., Jiang, M., Li, K., Li, H., Zhou, Y., Xiao, X., et al. (2021). Glutathione peroxidase 4-regulated neutrophil ferroptosis induces systemic autoimmunity. *Nat. Immunol.* 22, 1107–1117. doi:10.1038/s41590-021-00993-3
- Liang, D., Minikes, A. M., and Jiang, X. (2022). Ferroptosis at the intersection of lipid metabolism and cellular signaling. *Mol. Cell* 82, 2215–2227. doi:10.1016/j.molcel.2022.03.022
- Liang, X., Ou, C., Zhuang, J., Li, J., Zhang, F., Zhong, Y., et al. (2021). Interplay between skin microbiota dysbiosis and the host immune system in psoriasis: Potential pathogenesis. *Front. Immunol.* 12, 764384. doi:10.3389/fimmu.2021.764384
- Lin, L., Wang, S., Deng, H., Yang, W., Rao, L., Tian, R., et al. (2020). Endogenous labile iron pool-mediated free radical generation for cancer chemodynamic therapy. *J. Am. Chem. Soc.* 142, 15320–15330. doi:10.1021/jacs.0c05604
- Liu, P., Feng, Y., Li, H., Chen, X., Wang, G., Xu, S., et al. (2020). Ferrostatin-1 alleviates lipopolysaccharide-induced acute lung injury via inhibiting ferroptosis. *Cell. Mol. Biol. Lett.* 25, 10. doi:10.1186/s11658-020-00205-0
- Liu, Y., and Gu, W. (2022). P53 in ferroptosis regulation: The new weapon for the old guardian. *Cell Death Differ.* 29, 895–910. doi:10.1038/s41418-022-00943-y
- Liu, Y., and Gu, W. (2021). The complexity of P53-mediated metabolic regulation in tumor suppression. *Semin. Cancer Biol.* doi:10.1016/j.semcancer.2021.03.010
- Liu, Y., Tavana, O., and Gu, W. (2019). P53 modifications: Exquisite decorations of the powerful guardian. *J. Mol. Cell Biol.* 11, 564–577. doi:10.1093/jmcb/mjz060
- Lo, Y., Chiu, H. Y., and Tsai, T. F. (2020). Clinical features and genetic polymorphism in Chinese patients with erythrodermic psoriasis in A single dermatologic clinic. *Mol. Diagn. Ther.* 24, 85–93. doi:10.1007/s40291-019-00441-x
- Ly, K., Smith, M. P., Thibodeaux, Q., Reddy, V., Liao, W., and Bhutani, T. (2019). Anti il-17 in psoriasis. *Expert Rev. Clin. Immunol.* 15, 1185–1194. doi:10.1080/1744666X.2020.1679625
- Ma, S., Henson, E. S., Chen, Y., and Gibson, S. B. (2016). Ferroptosis is induced following siramesine and lapatinib treatment of breast cancer cells. *Cell Death Dis.* 7, E2307. doi:10.1038/cddis.2016.208
- Madden, S. K., Flanagan, K. L., and Jones, G. (2020). How lifestyle factors and their associated pathogenetic mechanisms impact psoriasis. *Clin. Nutr.* 39, 1026–1040. doi:10.1016/j.clnu.2019.05.006
- Magtanong, L., Ko, P. J., To, M., Cao, J. Y., Forcina, G. C., Tarangelo, A., et al. (2019). Exogenous monounsaturated fatty acids promote A ferroptosis-resistant cell state. *Cell Chem. Biol.* 26, 420–432. doi:10.1016/j.chembiol.2018.11.016
- Masaldan, S., Bush, A. I., Devos, D., Rolland, A. S., and Moreau, C. (2019). Striking while the iron is hot: Iron metabolism and ferroptosis in neurodegeneration. *Free Radic. Biol. Med.* 133, 221–233. doi:10.1016/j.freeradbiomed.2018.09.033
- Miao, Y., Chen, Y., Xue, F., Liu, K., Zhu, B., Gao, J., et al. (2022). Contribution of ferroptosis and Gpx4's dual functions to osteoarthritis progression. *Ebiomedicine* 76, 103847. doi:10.1016/j.ebiomed.2022.103847
- Miotto, G., Rossetto, M., Di Paolo, M. L., Orian, L., Venerando, R., Roveri, A., et al. (2020). Insight into the mechanism of ferroptosis inhibition by ferrostatin-1. *Redox Biol.* 28, 101328. doi:10.1016/j.redox.2019.101328
- Nast, A., Smith, C., Spuls, P. I., Avila Valle, G., Bata-Csorgo, Z., Boonen, H., et al. (2020). Euroguiderm guideline on the systemic treatment of psoriasis vulgaris - Part 1: Treatment and monitoring recommendations. *J. Eur. Acad. Dermatol. Venereol.* 34, 2461–2498. doi:10.1111/jdv.16915
- Navarini, A. A., Burden, A. D., Capon, F., Mrowietz, U., Puig, L., Koks, S., et al. (2017). European consensus statement on phenotypes of pustular psoriasis. *J. Eur. Acad. Dermatol. Venereol.* 31, 1792–1799. doi:10.1111/jdv.14386
- Nowowiejska, J., Baran, A., and Flisiak, I. (2021). Aberrations in lipid expression and metabolism in psoriasis. *Int. J. Mol. Sci.* 22, 6561. doi:10.3390/ijms22126561
- Ogawa, K., and Okada, Y. (2020). The current landscape of psoriasis genetics in 2020. *J. Dermatol. Sci.* 99, 2–8. doi:10.1016/j.jdermsci.2020.05.008
- Orsmond, A., Bereza-Malcolm, L., Lynch, T., March, L., and Xue, M. (2021). Skin barrier dysregulation in psoriasis. *Int. J. Mol. Sci.* 22, 10841. doi:10.3390/ijms221910841
- Park, E., and Chung, S. W. (2019). Ros-mediated autophagy increases intracellular iron levels and ferroptosis by ferritin and transferrin receptor regulation. *Cell Death Dis.* 10, 822. doi:10.1038/s41419-019-2064-5
- Pezzolo, E., and Naldi, L. (2019). The relationship between smoking, psoriasis and psoriatic arthritis. *Expert Rev. Clin. Immunol.* 15, 41–48. doi:10.1080/1744666X.2019.1543591
- Proneth, B., and Conrad, M. (2019). Ferroptosis and necroinflammation, A yet poorly explored link. *Cell Death Differ.* 26, 14–24. doi:10.1038/s41418-018-0173-9
- Qiu, Y., Cao, Y., Cao, W., Jia, Y., and Lu, N. (2020). The application of ferroptosis in diseases. *Pharmacol. Res.* 159, 104919. doi:10.1016/j.phrs.2020.104919
- Raychaudhuri, S. K., Mavarakis, E., and Raychaudhuri, S. P. (2014). Diagnosis and classification of psoriasis. *Autoimmun. Rev.* 13, 490–495. doi:10.1016/j.autrev.2014.01.008
- Raychaudhuri, S. K., and Raychaudhuri, S. P. (2014). Mtor signaling cascade in psoriatic disease: Double kinase mtor inhibitor A novel therapeutic target. *Indian J. Dermatol.* 59, 67–70. doi:10.4103/0019-5154.123499
- Reichert, C. O., De Freitas, F. A., Sampaio-Silva, J., Rokita-Rosa, L., Barros, P. L., Levy, D., et al. (2020). Ferroptosis mechanisms involved in neurodegenerative diseases. *Int. J. Mol. Sci.* 21, 8765. doi:10.3390/ijms211228765
- Reid, C., and Griffiths, C. E. M. (2020). Psoriasis and treatment: Past, present and future aspects. *Acta Derm. Venereol.* 100, Adv00032. doi:10.2340/00015555-3386
- Ren, J. X., Sun, X., Yan, X. L., Guo, Z. N., and Yang, Y. (2020). Ferroptosis in neurological diseases. *Front. Cell. Neurosci.* 14, 218. doi:10.3389/fncel.2020.00218
- Rendon, A., and Schakel, K. (2019). Psoriasis pathogenesis and treatment. *Int. J. Mol. Sci.* 20, 1475. doi:10.3390/ijms20061475
- Reolid, A., Munoz-Aceituno, E., Abad-Santos, F., Ovejero-Benito, M. C., and Dauden, E. (2021). Epigenetics in non-tumor immune-mediated skin diseases. *Mol. Diagn. Ther.* 25, 137–161. doi:10.1007/s40291-020-00507-1
- Riegman, M., Sagie, L., Galed, C., Levin, T., Steinberg, N., Dixon, S. J., et al. (2020). Ferroptosis occurs through an osmotic mechanism and propagates independently of cell rupture. *Nat. Cell Biol.* 22, 1042–1048. doi:10.1038/s41556-020-0565-1
- Seibt, T. M., Proneth, B., and Conrad, M. (2019). Role of Gpx4 in ferroptosis and its pharmacological implication. *Free Radic. Biol. Med.* 133, 144–152. doi:10.1016/j.freeradbiomed.2018.09.014
- Serwin, A. B., Wasowicz, W., Gromadzinska, J., and Chodyncka, B. O. (2003). Selenium status in psoriasis and its relations to the duration and severity of the disease. *Nutrition* 19, 301–304. doi:10.1016/s0899-9007(02)01081-x
- Shah, R., Shchepinov, M. S., and Pratt, D. A. (2018). Resolving the role of lipoxygenases in the initiation and execution of ferroptosis. *ACS Cent. Sci.* 4, 387–396. doi:10.1021/acscentsci.7b00589
- Shen, Z., Liu, T., Li, Y., Lau, J., Yang, Z., Fan, W., et al. (2018). Fenton-reaction-acceleratable magnetic nanoparticles for ferroptosis therapy of orthotopic brain tumors. *ACS Nano* 12, 11355–11365. doi:10.1021/acsnano.8b06201
- Shou, Y., Yang, L., Yang, Y., and Xu, J. (2021). Inhibition of keratinocyte ferroptosis suppresses psoriatic inflammation. *Cell Death Dis.* 12, 1009. doi:10.1038/s41419-021-04284-5
- Solmaz, D., Bakirci, S., Kimyon, G., Gunal, E. K., Dogru, A., Bayindir, O., et al. (2020). Impact of having family history of psoriasis or psoriatic arthritis on psoriatic disease. *Arthritis Care Res.* 72, 63–68. doi:10.1002/acr.23836
- Stockwell, B. R. (2019). A powerful cell-protection system prevents cell death by ferroptosis. *Nature* 575, 597–598. doi:10.1038/d41586-019-03145-8
- Stockwell, B. R. (2022). Ferroptosis turns 10: Emerging mechanisms, physiological functions, and therapeutic applications. *Cell* 185, 2401–2421. doi:10.1016/j.cell.2022.06.003
- Stockwell, B. R., Friedmann Angeli, J. P., Bayir, H., Bush, A. I., Conrad, M., Dixon, S. J., et al. (2017). Ferroptosis: A regulated cell death nexus linking metabolism, redox biology, and disease. *Cell* 171, 273–285. doi:10.1016/j.cell.2017.09.021
- Stockwell, B. R., Jiang, X., and Gu, W. (2020). Emerging mechanisms and disease relevance of ferroptosis. *Trends Cell Biol.* 30, 478–490. doi:10.1016/j.tcb.2020.02.009
- Sun, X., Ou, Z., Xie, M., Kang, R., Fan, Y., Niu, X., et al. (2015). Hspb1 as A novel regulator of ferroptotic cancer cell death. *Oncogene* 34, 5617–5625. doi:10.1038/onc.2015.32
- Traks, T., Keermann, M., Prans, E., Karelson, M., Loite, U., Koks, G., et al. (2019). Polymorphisms in IL36g gene are associated with plaque psoriasis. *BMC Med. Genet.* 20, 10. doi:10.1186/s12881-018-0742-2
- Tsurusaki, S., Tsuchiya, Y., Koumura, T., Nakasone, M., Sakamoto, T., Matsuoka, M., et al. (2019). Hepatic ferroptosis plays an important role as the trigger for initiating inflammation in nonalcoholic steatohepatitis. *Cell Death Dis.* 10, 449. doi:10.1038/s41419-019-1678-y
- Ursini, F., and Maiorino, M. (2020). Lipid peroxidation and ferroptosis: The role of gsh and Gpx4. *Free Radic. Biol. Med.* 152, 175–185. doi:10.1016/j.freeradbiomed.2020.02.027



- Van De Kerkhof, P. C. (2022). From empirical to pathogenesis-based treatments for psoriasis. *J. Invest. Dermatol.* 142, 1778–1785. doi:10.1016/j.jid.2022.01.014
- Van Meer, G., Voelker, D. R., and Feigenson, G. W. (2008). Membrane lipids: Where they are and how they behave. *Nat. Rev. Mol. Cell Biol.* 9, 112–124. doi:10.1038/nrm2330
- Vicic, M., Kastelan, M., Brajac, I., Sotosek, V., and Massari, L. P. (2021). Current concepts of psoriasis immunopathogenesis. *Int. J. Mol. Sci.* 22, 11574. doi:10.3390/ijms222111574
- Weber, B., Merola, J. F., Husni, M. E., Di Carli, M., Berger, J. S., and Garshick, M. S. (2021). Psoriasis and cardiovascular disease: Novel mechanisms and evolving therapeutics. *Curr. Atheroscler. Rep.* 23, 67. doi:10.1007/s11883-021-00963-y
- Wen, Q., Liu, J., Kang, R., Zhou, B., and Tang, D. (2019). The release and activity of Hmgb1 in ferroptosis. *Biochem. Biophys. Res. Commun.* 510, 278–283. doi:10.1016/j.bbrc.2019.01.090
- Wu, J., Xue, R., Wu, M., Yin, X., Xie, B., and Meng, Q. (2022). Nrf2-Mediated ferroptosis inhibition exerts A protective effect on acute-on-chronic liver failure. *Oxid. Med. Cell. Longev.* 2022, 4505513. doi:10.1155/2022/4505513
- Xia, J., Si, H., Yao, W., Li, C., Yang, G., Tian, Y., et al. (2021). Research progress on the mechanism of ferroptosis and its clinical application. *Exp. Cell Res.* 409, 112932. doi:10.1016/j.yexcr.2021.112932
- Xie, Y., Song, X., Sun, X., Huang, J., Zhong, M., Lotze, M. T., et al. (2016). Identification of baicalein as A ferroptosis inhibitor by natural product library screening. *Biochem. Biophys. Res. Commun.* 473, 775–780. doi:10.1016/j.bbrc.2016.03.052
- Xu, X., and Zhang, H. Y. (2017). The immunogenetics of psoriasis and implications for drug repositioning. *Int. J. Mol. Sci.* 18, 2650. doi:10.3390/ijms18122650
- Yang, L., Wang, H., Yang, X., Wu, Q., An, P., Jin, X., et al. (2020). Auranofin mitigates systemic iron overload and induces ferroptosis via distinct mechanisms. *Signal Transduct. Target. Ther.* 5, 138. doi:10.1038/s41392-020-00253-0
- Yang, W. S., Sriramaratnam, R., Welsch, M. E., Shimada, K., Skouta, R., Viswanathan, V. S., et al. (2014). Regulation of ferroptotic cancer cell death by Gpx4. *Cell* 156, 317–331. doi:10.1016/j.cell.2013.12.010
- Yao, X., Zhang, Y., Hao, J., Duan, H. Q., Zhao, C. X., Sun, C., et al. (2019). Deferoxamine promotes recovery of traumatic spinal cord injury by inhibiting ferroptosis. *Neural Regen. Res.* 14, 532–541. doi:10.4103/1673-5374.245480
- Yuan, H., Li, X., Zhang, X., Kang, R., and Tang, D. (2016). Identification of Acsf4 as A biomarker and contributor of ferroptosis. *Biochem. Biophys. Res. Commun.* 478, 1338–1343. doi:10.1016/j.bbrc.2016.08.124
- Zhang, X., Guo, Y., Li, H., and Han, L. (2021a). Fin56, A novel ferroptosis inducer, triggers lysosomal membrane permeabilization in A tfef-dependent manner in glioblastoma. *J. Cancer* 12, 6610–6619. doi:10.7150/jca.58500
- Zhang, Y., Swanda, R. V., Nie, L., Liu, X., Wang, C., Lee, H., et al. (2021b). Mtorc1 couples cyst(E)ine availability with Gpx4 protein synthesis and ferroptosis regulation. *Nat. Commun.* 12, 1589. doi:10.1038/s41467-021-21841-w
- Zhao, Y., Li, Y., Zhang, R., Wang, F., Wang, T., and Jiao, Y. (2020). The role of erastin in ferroptosis and its prospects in cancer therapy. *Onco. Targets. Ther.* 13, 5429–5441. doi:10.2147/OTT.S254995
- Zheng, J., and Conrad, M. (2020). The metabolic underpinnings of ferroptosis. *Cell Metab.* 32, 920–937. doi:10.1016/j.cmet.2020.10.011
- Zhou, S., and Yao, Z. (2022). Roles of infection in psoriasis. *Int. J. Mol. Sci.* 23, 6955. doi:10.3390/ijms23136955
- Zilka, O., Shah, R., Li, B., Friedmann Angeli, J. P., Griesser, M., Conrad, M., et al. (2017). On the mechanism of cytoprotection by ferrostatin-1 and liproxstatin-1 and the role of lipid peroxidation in ferroptotic cell death. *ACS Cent. Sci.* 3, 232–243. doi:10.1021/acscentsci.7b00028



## OPEN ACCESS

EDITED BY  
Guo Chen,  
China Pharmaceutical University, China

REVIEWED BY  
Hongri Gong,  
Nanjing University, China  
Xin Wang,  
National Institutes of Health (NIH),  
United States

\*CORRESPONDENCE  
Kegan Zhu,  
zhukegan@tmu.edu.cn

<sup>†</sup>These authors have contributed equally  
to this work

SPECIALTY SECTION  
This article was submitted to Molecular  
Diagnostics and Therapeutics,  
a section of the journal  
Frontiers in Molecular Biosciences

RECEIVED 28 June 2022  
ACCEPTED 25 July 2022  
PUBLISHED 20 September 2022

CITATION  
Hu D, Zhou Z, Wang J and Zhu K (2022),  
Screening of ferroptosis-related genes  
with prognostic effect in colorectal  
cancer by bioinformatic analysis.  
*Front. Mol. Biosci.* 9:979854.  
doi: 10.3389/fmolb.2022.979854

COPYRIGHT  
© 2022 Hu, Zhou, Wang and Zhu. This is  
an open-access article distributed  
under the terms of the [Creative  
Commons Attribution License \(CC BY\)](#).  
The use, distribution or reproduction in  
other forums is permitted, provided the  
original author(s) and the copyright  
owner(s) are credited and that the  
original publication in this journal is  
cited, in accordance with accepted  
academic practice. No use, distribution  
or reproduction is permitted which does  
not comply with these terms.

# Screening of ferroptosis-related genes with prognostic effect in colorectal cancer by bioinformatic analysis

Dongzhi Hu<sup>†</sup>, Zhengyang Zhou<sup>†</sup>, Junyi Wang<sup>†</sup> and Kegan Zhu<sup>\*</sup>

Key Laboratory of Cancer Prevention and Therapy, National Clinical Research Center for Cancer, Tianjin's Clinical Research Center for Cancer, Tianjin Medical University Cancer Institute and Hospital, Tianjin Medical University, Tianjin, China

Colorectal cancer (CRC) remains a common malignant tumor of digestive tract with high incidence rate and high mortality in the worldwide. The current clinical treatments of CRC often fail to achieve satisfactory results. Searching for more effective prediction or prognosis biomarkers, or developing more targeted therapeutic schedule may help to improve the outcomes of CRC patients. Here, we tried to study the effect of ferroptosis-related genes on CRC prognosis and make it clearer that ferroptosis has connection with immune environment. First, we obtained gene expression data of CRC and normal tissues, as well as corresponding clinical data from the Gene Expression Omnibus (GEO) database and the Cancer Genome Atlas (TCGA) database. The differentially expressed genes (DEGs) were intersected with ferroptosis-related gene set downloaded from FerrDb database, and 93 abnormally expressed ferroptosis-related genes were obtained. Then, these genes were analyzed for functional enrichment. Univariate Cox regression and multivariate Cox regression analyses were performed to establish prognostic model based on ferroptosis-related genes. In the process of exploring the correlation between prognostic genes and immune infiltration, we found that these genes were closely related to B cells, CD8<sup>+</sup> T cells, CD4<sup>+</sup> T cells, macrophages and other cells in CRC. In addition, we found a large proportion of plasma cells and macrophages in TCGA-COADREAD. Finally, a prognostic nomogram of ferroptosis-related genes was established, including age, sex, grade and other predicted values. To summary, we established a prognostic model of colorectal cancer (CRC) based on ferroptosis-related genes and further explored the relationship between these genes with immune microenvironment.

## KEYWORDS

colorectal cancer, ferroptosis, prognostic model, immune microenvironment, bioinformatic analysis

**Abbreviations:** CRC, colorectal cancer; GEO, Gene Expression Omnibus; TCGA, the Cancer Genome Atlas; DEGs, differentially expressed genes; ROS, reactive oxygen species; GO, gene ontology; PPI, protein-protein interaction; ROC, receiver operating characteristic; AUC, area under curve; CC, cellular components; MF, molecular functions; KEGG, Kyoto Encyclopedia of Genes; TIMER, Tumor Immune Estimation Resource.

## Introduction

According to statistics in 2021, colorectal cancer (CRC) ranks third in morbidity and second in mortality worldwide, seriously affects human health and brings heavy economic burden (Li et al., 2021; Rezapour et al., 2021; Sung et al., 2021). Especially in China, CRC is one of the most common malignancies after lung cancer, with increasing morbidity and mortality (Arnold et al., 2017; Zhou et al., 2021). Usually, the CRC patients only show symptoms at the advanced stage, which make it difficult in the early detection. In fact, many patients are already in advanced cancer when first diagnosed (Simon 2016; Dekker et al., 2019; Biller and Schrag 2021). Besides, no regular physical examination due to economic reasons or lack of awareness is also an important reason for the late diagnosis of CRC (Chen et al., 2019; Ladabaum et al., 2020). Patients with advanced CRC have poorer prognosis, whose five-year survival rate is only 10% (Brenner et al., 2014; Dekker et al., 2019). The common clinical treatments, including surgery, chemotherapy, and immunotherapy, all failed to achieve satisfactory results (Piawah and Venook 2019; Johdi and Sukor 2020; Biller and Schrag 2021). Therefore, it is urgent to screen for more effective biomarkers for early diagnosis and prognosis, or develop more potential therapeutic targets for CRC, as well as other tumors (Mohamed et al., 2020).

Ferroptosis, which was first proposed in 2012, is a non-apoptotic and iron-dependent form of cell death characterized by the accumulation of reactive oxygen species (ROS) (Dixon et al., 2012). It is significantly different from apoptosis, necrosis and autophagy in both cell morphology and cellular function, which are also important bases to distinguish them (Xie et al., 2016; Li et al., 2020). In recent years, there has been an increasing number of studies on ferroptosis. It has been reported that ferroptosis can be triggered by different physiological conditions or pathological stress (Mou et al., 2019; Jiang and Stockwell 2021). More and more evidences show that ferroptosis has a regulatory effect on the occurrence and development of many diseases (Dixon et al., 2012; Fearnhead and Vandenabeele 2017; Jiang and Stockwell 2021; Wu et al., 2021). It should be noted that ferroptosis also plays important roles in different cancers (Liang and Zhang 2019; Koppula et al., 2021). Moreover, the role of ferroptosis in immune microenvironment has attracted more and more attention recently (Stockwell and Jiang 2019; Wang et al., 2019; Chen and Kang 2021; Lu et al., 2021). Tumor microenvironment contains a large number of immune cells which act in chemotherapy and antitumor therapy of CRC, involving immune tolerance, immune escape and other processes (Wang et al., 2019). Tumor microenvironment may be a crucial bridge by which ferroptosis functions in cancers. Thus, a more in-depth study of the relationship between ferroptosis and immune cell infiltration may open a new way for immunotherapy of CRC.

Previous studies on ferroptosis in tumors mainly focused on the abnormally expressed ferroptosis-related genes, which have

close connections with tumors, by screening the relative database through bioinformatic analysis. Here, we want to further analyse ferroptosis-related factors that have connections with immune microenvironment. In our study, CRC expression data together with corresponding patients' information from TCGA and GEO databases were screened and cross-referenced with FerrDB database to identify differentially expressed genes (DEGs) associated with ferroptosis. The prognostic genes were further screened and prognostic model was established to predict the prognosis of CRC patients. Meanwhile, we analyzed the association between ferroptosis-related genes and tumor microenvironment in CRC, enhancing our understanding of the relationship between ferroptosis and immune cell abundance. In a word, our results provide a novel ferroptosis-related model for prognosis analysis of CRC patients and further verified the relationship between ferroptosis and immune microenvironment, which may contribute to the immunotherapy in the future.

## Materials and methods

### Data source

From the GEO database (<https://www.ncbi.nlm.nih.gov/geo>), we downloaded RNA expression data including normal and tumor tissues from GEO: GSE21510, GSE44861, GSE62321 and GSE79793, and obtained RNA expression data as well as clinical information of patients from GEO: GSE41258. All the above data are normalized by log<sub>2</sub>-scale transformation to ensure standardization. The gene symbols with multiple probes were calculated using mean expression levels. We also obtained the level three HTSEQ-FPKM format RNA sequencing data in CRC project from TCGA database (<https://www.cancer.gov/tcga/>), named TCGA-COADREAD. A total of 644 matched patients' clinical information and sample information were obtained. In addition, a total of 388 ferroptosis-related genes (including drivers, markers, and suppressors) were obtained from FerrDB database (<http://www.zhounan.org/ferrdb/legacy/index.html>) as candidate genes. Detailed information about these genes are shown in **Supplementary Table S1**. This study followed the publication guidelines of the GEO and TCGA databases.

### Identification of differentially expressed genes (DEGs)

We used R package "limma" in RStudio to detect the DEGs between tumor and normal tissue from GEO: GSE21510, GSE44861, GSE52321, GSE79793 with  $p$ -value < 0.05 and  $|\log_2FC| \geq 1$ . R package "Pheatmap" was applied to visualize the degree range of differences between the four datasets. Next,

we obtained 93 ferroptosis-related genes by intersecting DEGs and candidate genes.

## Functional analysis of ferroptosis-related genes

The GO and Kyoto Encyclopedia of Genes (KEGG) analysis were performed using a gene annotation and analysis resource Metascape (<https://metascape.org/gp/index.html#/main/step1>). The cutoff of the  $p$ -value was 0.01. Enriched terms were selected to construct the network, and similar terms were connected with edges. The cutoff value of similarity is 0.3. STRING (<http://string.embl.de/>) was used to predict PPI information. Then, we established PPI networks using Cytoscape. And the MCODE algorithm was performed to identify the key modules. The cutoff of the  $p$ -value was 0.05.

## Construction and validation of prognostic models

We used TCGA-COADREAD (as the training cohort) and GEO: GSE41258 datasets (as the validation cohort) to establish prognostic markers of ferroptosis-related genes. Univariate Cox analysis of OS was conducted to identify ferroptosis-related genes with significant prognostic value, and  $p$ -value < 0.05 was considered to be statistically significant. The independent prognostic factors were identified by multivariate Cox regression analysis. The prognostic model of ferroptosis-related genes was constructed according to the correlation coefficient of independent prognostic genes. Patients in the TCGA-COADREAD were divided into low-risk group and high-risk group according to the risk scoring algorithm obtained by multivariate Cox regression analysis, and the survival curve was drawn. The ROC curve was plotted using R package “time ROC”, and the prognostic efficiency was evaluated according to AUC.

## Immune analysis of ferroptosis-related prognostic genes

To determining the immune correlation of prognostic genes, we used TIMER2.0 database (<http://timer.cistrome.org/>) to analyze the relationship between prognostic genes and tumor immune infiltrating cells. Then, the R package “estimate” was used to calculate the immune score of TCGA-COADREAD to obtain the stromal score, immune score, and ESTIMATE score of prognostic genes. And a Kaplan-Meier survival curve was plotted to evaluate the relationship between immune score and patient survival time. CIBERSORTx (<https://cibersortx.stanford.edu/>) was used to evaluate the proportion of immune cell

infiltration in tissues from TCGA-COADREAD and GEO: GSE41258 datasets to clarify the relationship between prognostic genes and immune cell infiltration. In addition, we also used ssGSEA algorithm to calculate the distribution of various immune cells and draw violin plots.

## Construction of a nomogram

We used R package “rms” to plot the nomogram and calibration curves. A nomogram could provide survival probability for a specific outcome, and calibration curve (3-years OS) was used to visualize the observed rates against nomogram-predicted probabilities.

## Results

### Identification of DEGs associated with ferroptosis in CRC

Four GEO datasets were selected as data sources, and the information is listed in Table 1. Through the differential gene analysis, a total of 2,611 up-regulated genes ( $\log_2FC > 1$ ,  $p$ -value < 0.05) and 471 down-regulated genes ( $\log_2FC < 1$ ,  $p$ -value < 0.05) were obtained from GEO: GSE21510. A total of 141 genes showed upregulation and 261 genes showed downregulation were obtained from GEO: GSE44861. In addition, 254 genes with high expression and 715 genes with low expression were found in GEO: GSE62321, 46 genes with high expression and 241 genes with low expression were found in GEO: GSE79793. The heat maps of the four datasets are showed in Figure 1. The DEGs associated with ferroptosis were obtained by intermixing these DEGs with identified ferroptosis-related genes from FerrDb database. The Venn diagram displayed that there are 93 genes intersecting between five datasets (Figure 2A). All genes are listed in Supplementary Table S1.

We performed functional analysis by Metascape to investigate the underlying mechanisms of abnormally expressed ferroptosis-related genes in CRC. The gene ontology (GO) analysis results revealed that the dysregulated ferroptosis-related genes were mainly enriched in response to stimulus, metabolic process and positive regulation of biological process (Figures 2B,C). It is worth noting that immune system process was also enriched. It suggested that there may be a certain correlation between ferroptosis-gene set and tumor immune environment. In addition, we used the protein-protein interaction (PPI) network and Molecular Complex Detection (MCODE) plugin based on the Metascape to identify the significant modules in these ferroptosis-related genes. Module 1 involved PTEN, MDM2, HSPA5, AR, HNF4A, and MAPK9. Module 2 involved MAPK1, MDM4, GSK3B, STK11, MAPK8, PIK3CA, and PRKAA2. Module 3 involved SQTM1, ATG7, and



TABLE 1 The information of datasets from the GEO database.

Accession number	Platform	Samples	Experiment type	PMID
GEO:GSE21510	GPL570	46	Expression profiling by array	21,270,110
GEO:GSE 44861	GPL3921	94	Expression profiling by array	23,982,929
GEO:GSE62321	GPL97	30	Expression profiling by array	24,023,955
GEO:GSE79793	GPL14951	20	Expression profiling by array	28,595,259

ELAVL1 (Figure 2D). Besides, GeneMANIA database was used to verify the interaction of the relative proteins (Supplementary Figure S1A). We also analyzed the transcription factors of these ferroptosis-related genes using PASTAA and presented the top 30 genes in Table 2.

## The establishment and verification of a prognostic model

We obtained 644 standardized mRNA expression data and corresponding patients' information from TCGA-COADREAD, which were used to establish a predictive model based on ferroptosis-related genes. To improve the accuracy and reliability of the predictive model, GEO: GSE41258 from GEO was used as a validation cohort. Firstly, univariate Cox regression analysis was performed to detect genes significantly associated with prognosis. As shown in Figures 3A–E, five ferroptosis-related prognostic genes were identified from 93 screened genes, which were AGPS, ATG7, CEBPG, MAPK9, and MMD. Figure 3F displayed the forest map of univariate Cox regression analysis. The detailed information of these genes is showed in Table 2. By multivariate Cox regression analysis, ATG7, MAPK9, and MMD were identified as independent prognostic genes (Table 4). Then, we established a prognostic model based on multivariate Cox regression. A risk score for each patient was calculated as follows:  $(-0.397,447) (\beta_1) \times (\text{expression of ATG7}) + (-0.575,347) (\beta_2) \times (\text{expression of MAPK9}) + (-0.385,768) (\beta_3) \times (\text{expression of MMD})$ . Then, a high-risk group ( $n = 322$ ) and a low-risk group ( $n = 322$ ) were stratified based on the median of the risk score and survival curves were plotted. It was found that the survival time of patients in the low-risk group was significantly longer than that in the high-risk group (Figure 4A). Next, a receiver operating characteristic (ROC) curve was created to assess the prognosis prediction efficiency of the model. As shown in Figure 4B, we found that the area under curve (AUC) was 0.64 (1-year OS), 0.64 (3-years OS), and 0.71 (5-years OS) respectively, which suggested that the predictive effect of the model was acceptable. Furthermore, to evaluate the accuracy and reliability of this predictive model, we validated the power of the model in GEO: GSE41258. In Figure 4C, Kaplan-Meier plots demonstrated that the ferroptosis-related predictive model

successfully stratified CRC patients into the long-term OS and short-term OS group with significant difference ( $p = 0.023$ ). Similarly, the ROC curve indicated that the model had an ideal prediction effect (Figure 4D).

## Analysis of prognostic genes in CRC patients

Subsequently, we further analyzed these three prognostic genes, ATG7, MAPK9 and MMD. Table 3 shows that the three genes all belong to ferroptosis driver genes, which obviously have the function of promoting ferroptosis. As shown in Supplementary Figure S1B, the expression levels of ATG7 and MAPK9 were higher in CRC tissues than in normal tissues. The expression of MMD in normal tissues was higher than that in CRC tissues. In addition, we found that the expression of these genes decreased with tumor progression (Supplementary Figure S1C), but it was not statistically significant.

In the functional enrichment analysis, we got hints that these genes were involved in immune system processes. Therefore, it is necessary to further explore their relevance with immune infiltration. First, by using the tumor immune estimation resource (TIMER) 2.0 database, we found that these three prognostic genes were associated with B cells, CD8<sup>+</sup> T cells, CD4<sup>+</sup> T cells, macrophages, neutrophils, and myeloid dendritic cells in CRC (Supplementary Figure S2A–C4). Next, we calculated the stromal score, immune score, and ESTIMATE score for 644 patients in the TCGA-COADREAD through the ESTIMATE algorithm. The results showed that except the immune score of MMD, the other groups could be statistically divided into low group and high group (Figures 5A–C). Furthermore, Kaplan-Meier plots were performed based on the three scores, but there were no statistical significance between the low stromal/immune/ESTIMATE groups and high stromal/immune/ESTIMATE groups.

Next, we assessed the proportion of immune landscapes in the tumor. Based on the data of gene expression, CIBERSORT algorithm was used to explore the proportion of immune cells in TCGA-COADREAD and GEO: GSE41258 datasets. It was found that plasma cells and macrophages (including the M0, M1 and M2 subsets) accounted for a large proportion of infiltrating

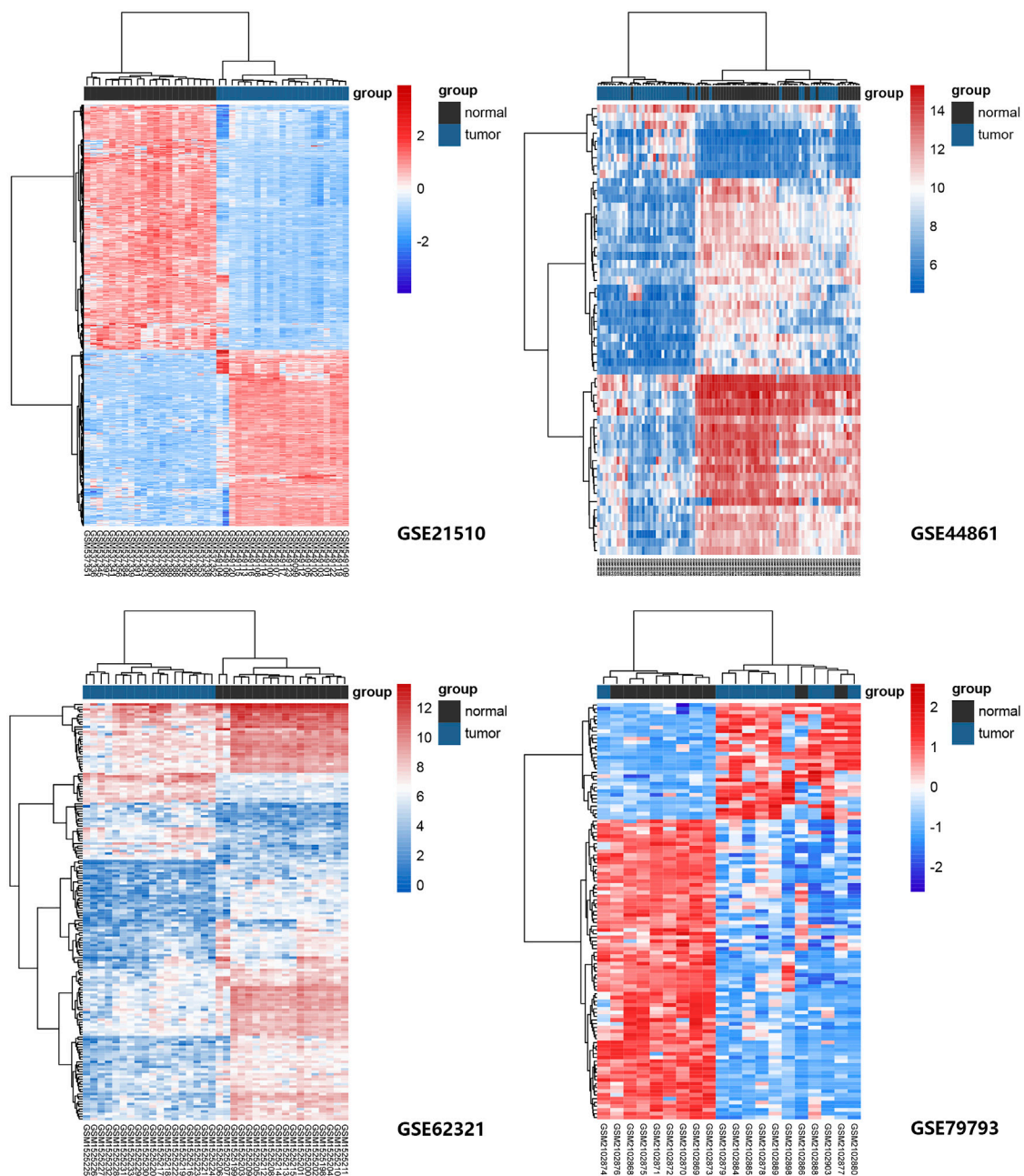


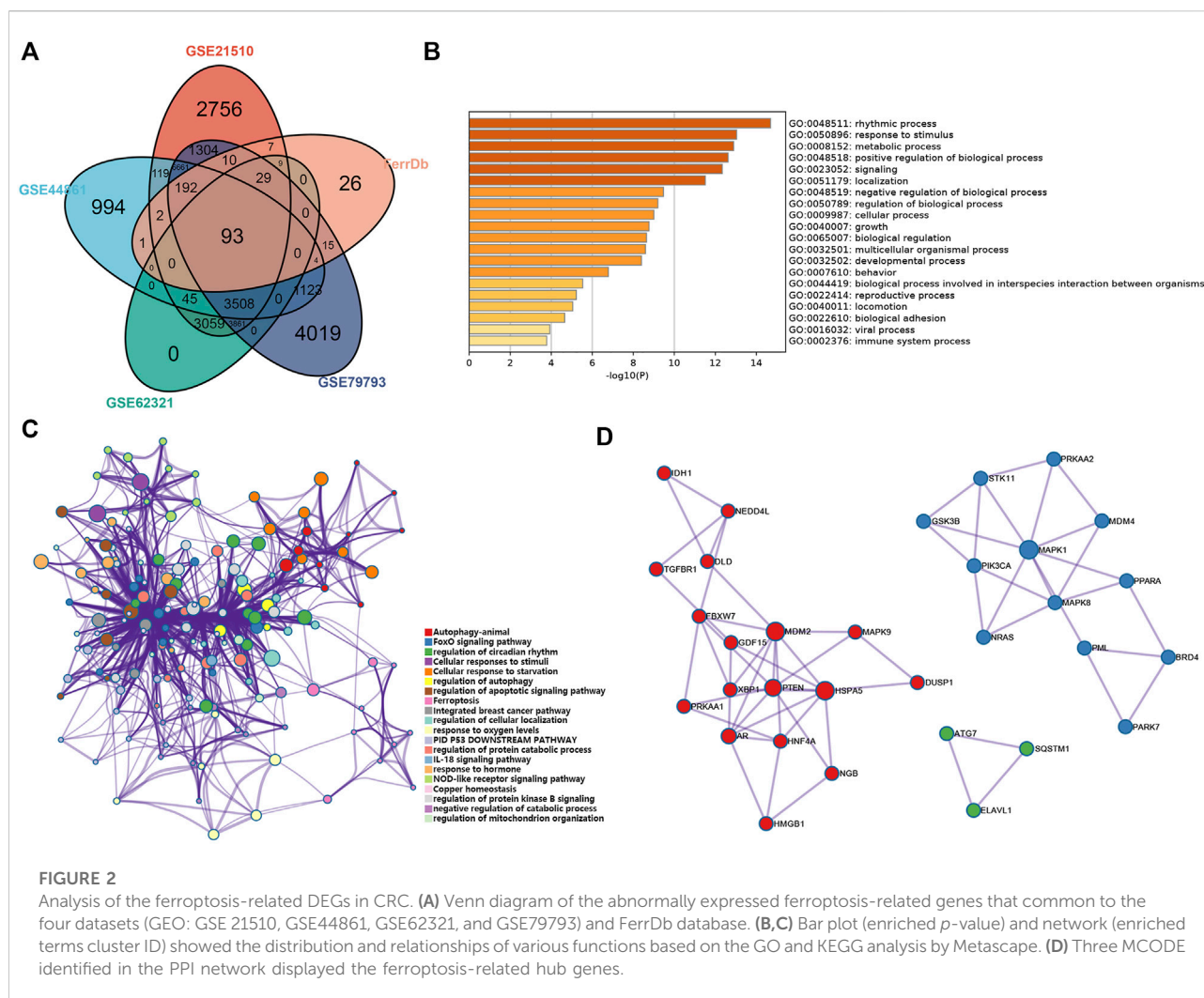
**FIGURE 1**

Heat maps of ferroptosis-related gene expression in normal and tumor samples in GEO: GSE21510, GSE44861, GSE62321, and GSE79793 datasets. The genes were clustered according to their expression levels. The red color represents high expression and the blue color represents low expression.

immune cells in TCGA-COADREAD (Supplementary Figure S3). We used the ssGSEA algorithm to draw the violin plots for visualizing the distribution of various immune cells between the low group and high group. And we found that the proportions of B cells, CD8<sup>+</sup> T cells, dendritic cells and macrophages were statistically significant (Figures 5D–F). In addition, M0, M1,

M2 macrophages, and plasma cells accounted for a large proportion of infiltrating immune cells in GEO: GSE41258, which was as same as the trend we found in TCGA-COADREAD (Supplementary Figure S4).

Furthermore, we explored the expression of PD-1 and CTLA4 in the low-risk group and high-risk group. It was



demonstrated that patients in the high-risk group had a higher expression level of PD-1 and a lower expression level of CTLA-4 in TCGA-COADREAD cohort (Figure 5G). But we noticed that the expression of PD-1 showed no statistical significance between the low-risk group and high-risk group. Additionally, PD-1 in GEO: GSE41258 exhibited consistency with TCGA-COADREAD, while CLTA4 exhibited the opposite trend (Figure 5H).

## Construction of the nomogram

Finally, we used the results of the multivariate analysis to establish a predictive ferroptosis-related prognostic nomogram. We used nomogram to predict the 1-year, 2-years, and 3-years OS for identifying the predictive value of age, gender, pathologic stage, TNM stage, and risk score (Figure 6A). This nomogram was used to evaluate the variables, which were based on patients' characteristics, including age, gender, TNM stage and risk score.

The predictive accuracy of OS can be judged by the calibrated curves. As shown in Figure 6B, the calibration curve for the predictive probabilities displayed an accordant agreement for the 3-years OS.

## Discussion

At the moment, surgical resection, chemotherapy, targeted therapy and immunotherapy are the main clinical treatments for CRC (Messersmith 2019; Modest et al., 2019; Biller and Schrag 2021). The option depends on the physical state and clinical characteristics of patients and the tumor stage (Benitez Majano et al., 2019; Roque-Castellano et al., 2020). Unfortunately, all these approaches are not ideal for patients with advanced CRC (Kim 2015). One choice of optimize the clinical treatment scheme is to explore more effective prognostic markers or therapeutic targets. Ferroptosis, a newly discovered type of cell death, is found to function in many cancers and is thought to

TABLE 2 The top 30 transcription factor of 93 ferroptosis-related genes from PASTAA.

Rank	Matrix	Transcription Factor	Association Score	p-Value
1	NFY_01	N/A	5.270	1.61e-04
2	MAZR_01	Mazr	4.116	1.90e-03
3	ATF4_Q2	Atf-4, Atf4	3.869	3.19e-03
4	TAXCREB_02	Creb, Deltacreb	3.580	5.71e-03
5	NRL_HAND	N/A	3.560	5.83e-03
6	NFY_Q6_01	Cbf-a, Cbf-b	3.559	5.86e-03
7	MMEF2_Q6	N/A	3.487	6.76e-03
8	IRF1_01	Irf-1	3.148	1.33e-02
9	NFY_Q6	Cbf-a, Cbf-b	3.131	1.37e-02
10	ARP1_01	Coup-tf2	3.076	1.49e-02
11	MTATA_B	N/A	3.042	1.64e-02
12	CRX_Q4	Crx, Rx	2.978	1.95e-02
13	FAC1_01	Fac1	2.940	2.05e-02
14	CREBP1CJUN_01	Atf-2, C-jun	2.877	2.29e-02
15	AMEF2_Q6	AmeF-2	2.823	2.52e-02
16	RFX1_02	Rfx1	2.816	2.57e-02
17	PBX1_03	N/A	2.802	2.65e-02
18	LYF1_01	N/A	2.718	3.15e-02
19	PITX2_Q2	Pitx2, Pitx2	2.516	4.50e-02
20	SREBP1_01	Srebp-1, Srebp-1a	2.509	4.55e-02
21	FOX_Q2	Foxd3, Foxf1	2.474	4.88e-02
22	BEL1_B	N/A	2.467	4.96e-02
23	MAF_Q6	N/A	2.380	5.81e-02
24	SRY_02	Sry	2.369	5.93e-02
25	CAAT_C	N/A	2.306	6.70e-02
26	CHOP_01	C/ebp, C/ebpalpha	2.283	6.88e-02
27	STAF_01	Staf	2.252	7.05e-02
28	ATF3_Q6	Atf3	2.241	7.52e-02
29	ATF_B	N/A	2.241	7.52e-02
30	LUN1_HAND	N/A	2.238	7.52e-02

have great potential for anti-tumor therapy (Tang et al., 2020; Wang et al., 2020). Recently, there are several researches have reported that ferroptosis activation could be benefit for tumor outcomes (Hassannia et al., 2019). For example, wang et al. (Wang et al., 2019) reported that cell ferroptosis is regulated by CD8<sup>+</sup> T cells, which can in turn affect the efficacy of tumor immunotherapy. Therefore, further study of ferroptosis-related genes in CRC may help to determine the tumor prognosis. Moreover, it is meaningful, to some degree, to make it clearer about the relationship between ferroptosis and tumor immune microenvironment, which can guide for the immunotherapy of CRC.

In our study, we focused on ferroptosis-related genes and their effect on prognosis and sought to explore the relationship between these genes and tumor immune microenvironment. First, we analyzed the DEGs in GEO:

GSE21510, GSE44861, GSE62321 and GSE79793 datasets, and intersected them with ferroptosis gene set in FerrDb database. We identified 93 ferroptosis-related genes in CRC this time. Functional analysis of these genes revealed that they were involved in immune system processes and may play roles in the immune microenvironment. Univariate Cox and multivariate Cox regression analysis were used to identify the most significant prognostic genes, which were ATG7, MAPK9 and MMD. Then, the risk score was calculated and the prognostic model was established, which was verified in GEO: GSE41258. Next, we found that these three ferroptosis-related prognostic genes were closely related to immune cells by using the TIMER 2.0 database. CIBERSORT algorithm was performed to evaluate the immune cell infiltration of the tumor immune microenvironment.



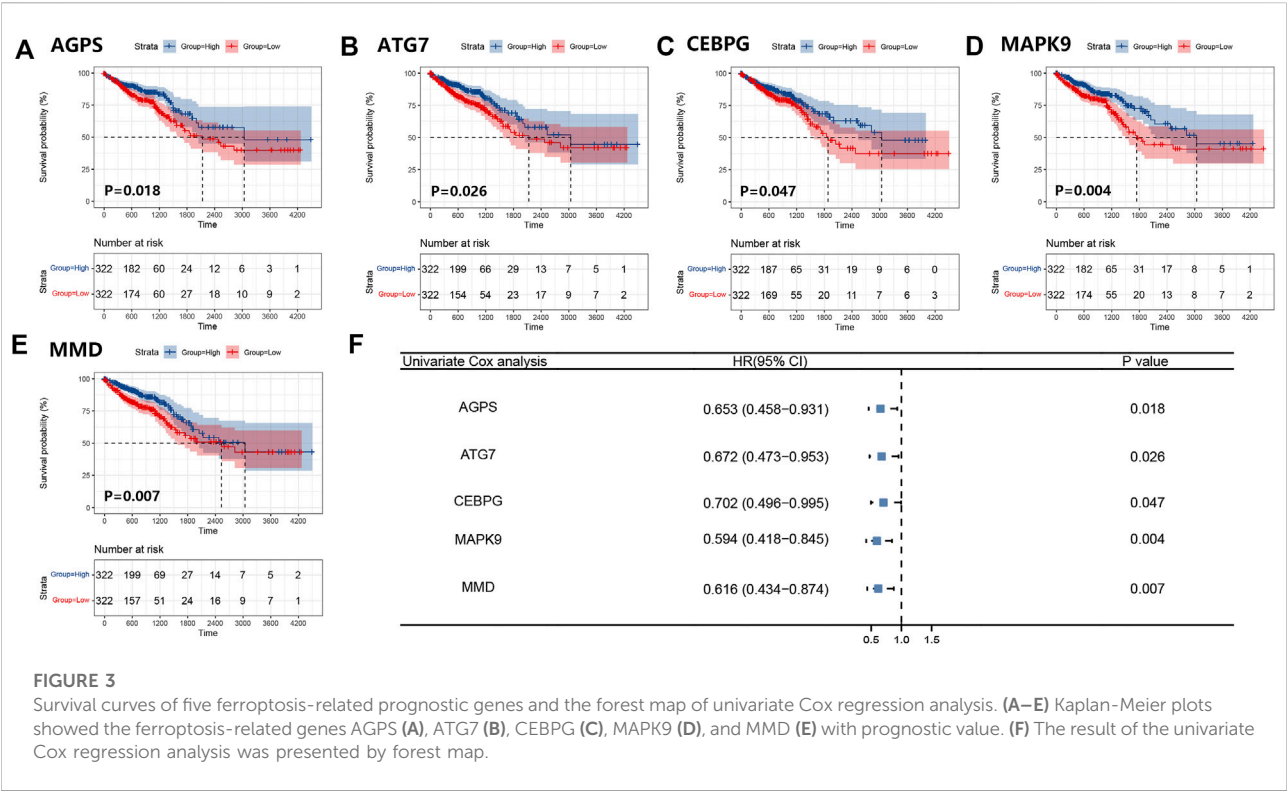


TABLE 3 The information of 10 prognostic genes.

Genes	Name	Ferroptosis Property	HGNC ID
AGPS	alkylglycerone phosphate synthase	Driver	327
ATG7	Autophagy related 7	Driver	16,935
CEBPG	CCAAT enhancer binding protein gamma	Marker	1837
MAPK9	Mitogen-activated protein kinase 9	Driver	6,886
MMD	monocyte to macrophage differentiation associated	Driver	7,153

TABLE 4 Multivariate Cox regression analysis of signature in TCGA-COADREAD cohort.

Variable	Coef	Exp (coef)	Se (coef)	Z	p value
ATG7	−0.397447	0.672033	0.185670	−2.141	0.03231
MAPK9	−0.575347	0.562510	0.193735	−2.970	0.00298
MMD	−0.385768	0.679928	0.190712	−2.023	0.04310

In recent years, there have been several bioinformatic studies about tumor associated ferroptosis-related genes in CRC. Moreover, some of them also explored the relationship between ferroptosis-related genes and immune microenvironment. Pan et al. reported a ferroptosis-related prognostic model based on

eight genes, AKR1C1, ALOX12, ATP5MC3, CARS1, HMGCR, CRYAB, FDFT1, and PHKG2. They divided the patients in two groups according to the expression pattern of these genes and CD8<sup>+</sup> T cells were significantly different in the two groups. They though it could be a biomarker for immune checkpoint therapy in CRC Patients (Yang and Zhou 2021). Zheng et al. established a prognostic risk signature based on 10 ferroptosis-related genes, ATG7, PGD, ATP6V1G2, DRD4, DUOX1, JDP2, NOX4, SLC2A3, TP63 and VEGFA. There were different immune landscapes between high and low risk groups (Yang et al., 2021). Besides, He et al. demonstrated that aberrantly expressed MT1G also affected the immune response of CRC patients (Peng et al., 2022). Immune escape is an important reason for tumor treatment failure and the change of tumor environment caused by ferroptosis may be responsible for it (Xu et al., 2020; Wang et al.,

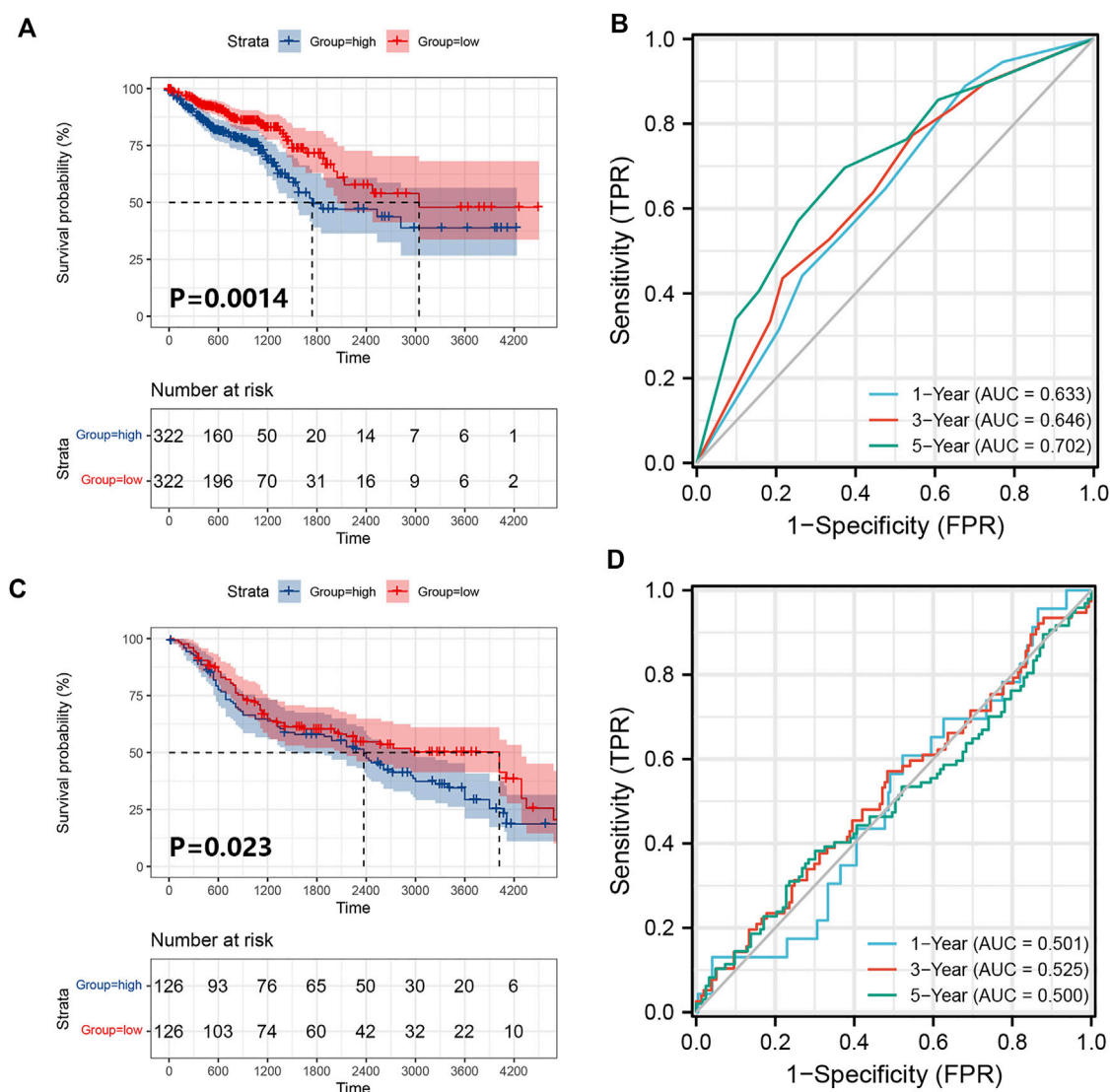
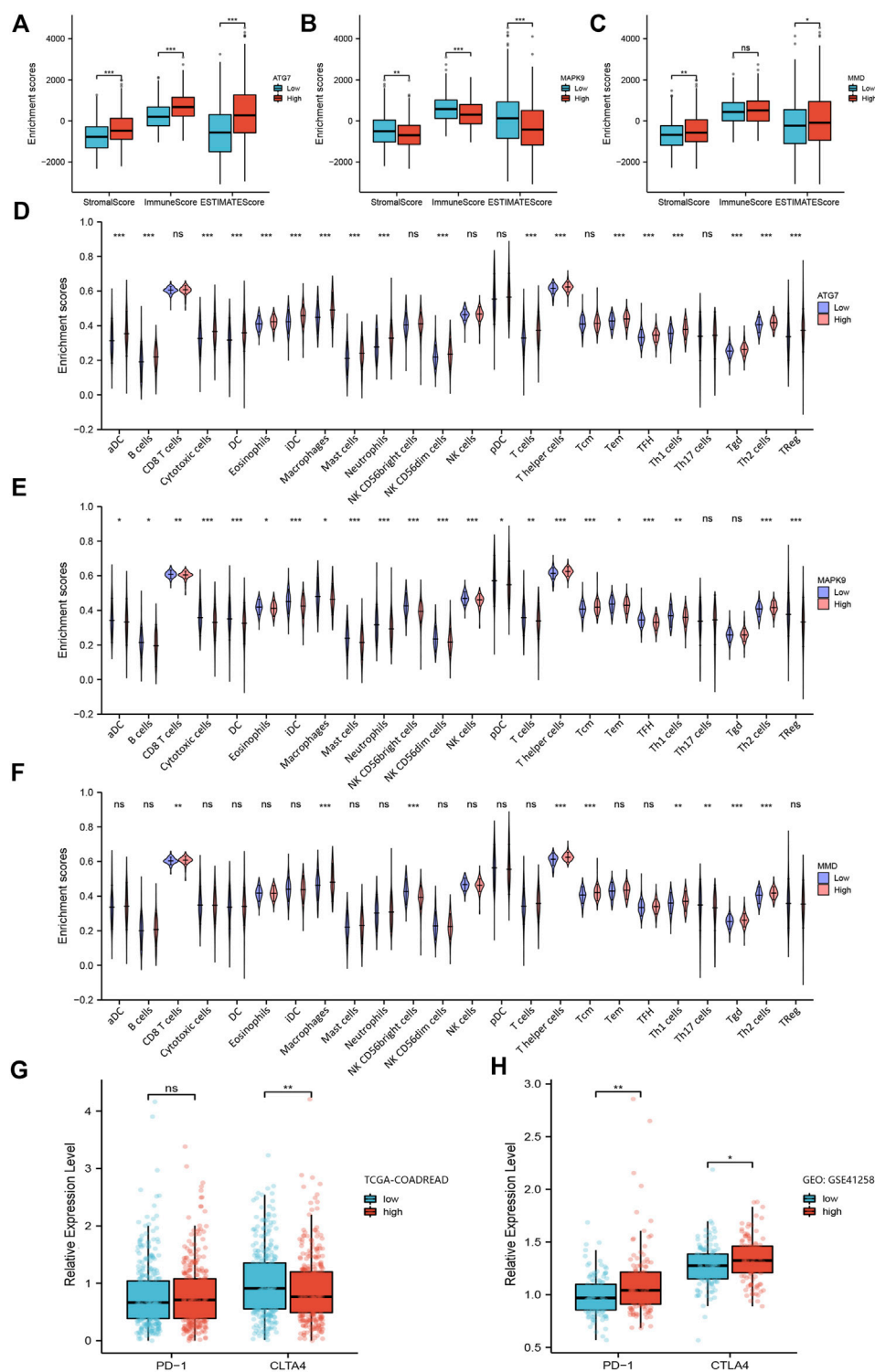


FIGURE 4

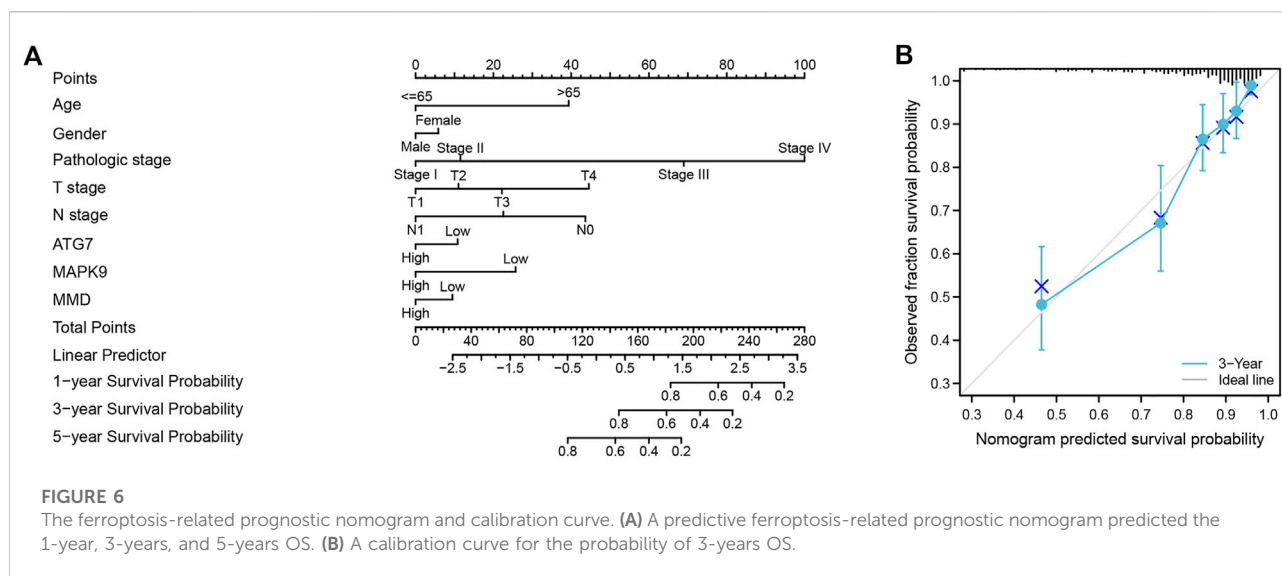
Establishment and verification of the prognostic model. (A) A prognostic model for patients with CRC based on the risk coefficients of ferroptosis-related genes ATG7, MAPK9 and MMD in TCGA-COADREAD. (B) The ROC curve of the three ferroptosis-related genes with the AUC in TCGA-COADREAD. (C) A prognostic model was established from three ferroptosis-related genes in the GEO: GSE41258. (D) The ROC curve of the three ferroptosis-related genes with the AUC in GEO: GSE41258.

2021). According to our results, the ATG7, MAPK9 and MMD were independent ferroptosis-related genes that can be used as prognosis markers. Furthermore, they may also be used as biomarkers to predict the response of immunotherapy and as one reference of determining CRC therapeutic strategy. This finding further strengthened the understanding that there is a close connection between ferroptosis and T cell immunity or cancer immunotherapy. This can further verify and improve the ferroptosis-related gene map currently and provide clinical potential from another point of view, which may benefit for the immunotherapy and prognosis of CRC in the future.

ATG7, an important member in the autophagy process, participates in autophagosome formation and maturation (Collier and Suomi 2021). It also plays important roles in cancer. It was reported that knockout of ATG7 could lead to a significant reduction in tumorigenesis in a mouse model of hepatocellular carcinoma (Cho et al., 2021). Besides, ATG7 can contribute to the survival of dormant breast cancer cells and metastatic tumor recurrence by activating autophagy (Vera-Ramirez et al., 2018). In addition, autophagy has been shown to promote the ferroptosis process through the ferritin pathway, which is naturally



**FIGURE 5** Analysis of the relationship between ferroptosis-related prognosis genes with immune microenvironment. (A–C) Box plots of ferroptosis-related genes ATG7, MAPK9 and MMD obtained by the ESTIMATE algorithm, showing their stromal score, immune score and ESTIMATE score. (D–F) Violin plots of ferroptosis-related genes ATG7, MAPK9 and MMD obtained by ssGSEA algorithm, showing the distribution of various immune cells between low group and high group. (G–H) The expression level of PD-1 and CTLA4 in the low-risk group and high-risk group in TCGA-COADREAD cohort and GEO: GSE41258, respectively. \*,  $p < 0.05$ ; \*\*,  $p < 0.01$ ; \*\*\*,  $p < 0.001$ .



regulated by ATG7 (Hou et al., 2016). The protein encoded by MAPK9 belong to the MAP kinase family and is involved in cell proliferation, differentiation, transcriptional regulation as well as other processes (Li et al., 2017). MAPK9 is most closely related to MAPK8, and both are known as C-Jun N-terminal kinase, which can block tumor suppressor p53 (Topisirovic et al., 2009; Barutcu and Girnius 2018). MAPK9 signaling pathway is reported to have regulatory roles in non-small cell lung cancer, bladder cancer, cholangiocarcinoma and other cancers (Hao et al., 2021; Huang et al., 2021; Teng et al., 2021). Meanwhile, it also has a great potential as the biomarker (Song et al., 2021). What's more, MAPK9 also functions in many immune-related diseases, suggesting that we could explore its role in the immune environment (Won et al., 2016; Naderi et al., 2019). MMD, first discovered in 1995, is named for its high expression in mature macrophages but not in monocytes (Rehli et al., 1995). Preferentially expressed in mature macrophages, MMD participates in the activation of macrophages with a carcinogenic role (Liu et al., 2012; Lin et al., 2020). There was a research that highlighted the value of miR-140-5p/MMD axis in non-small cell lung cancer (Li and He 2014). In this study, we also explored the significance of MMD in tumor immune microenvironment, which drew no attention previously.

In conclusion, our study established a prognostic model of CRC based on ferroptosis-related genes ATG7, MAPK9, and MMD and further verified its good predictive effect. The

establishment of this model and related immune analysis confirmed the influence of immune microenvironment on the prognosis of CRC, which may benefit for clinical diagnosis and outcome judgment of CRC in the future.

## Data availability statement

Publicly available datasets were analyzed in our study. This data can be found from the GEO database (<https://www.ncbi.nlm.nih.gov/geo/>), and TCGA database (<https://www.cancer.gov/tcga/>).

## Author contributions

DH, ZZ, JW, and KZ designed the study. DH, and ZZ carried out data acquisition and analysis. ZZ and JW wrote the manuscript and made figures. DH, and JW was involved in project management. KZ supervised the study. All authors read and approved the final manuscript.

## Funding

This work was supported by grants from Tianjin Science Foundation (Grant/Award Number: 19JCQNJC09600).



## Conflict of interest

The authors declare that the research was conducted in the absence of any commercial or financial relationships that could be construed as a potential conflict of interest.

## Publisher's note

All claims expressed in this article are solely those of the authors and do not necessarily represent those of their affiliated

organizations, or those of the publisher, the editors and the reviewers. Any product that may be evaluated in this article, or claim that may be made by its manufacturer, is not guaranteed or endorsed by the publisher.

## Supplementary material

The Supplementary Material for this article can be found online at: <https://www.frontiersin.org/articles/10.3389/fmolb.2022.979854/full#supplementary-material>

## References

- Arnold, M., Sierra, M. S., Laversanne, M., Soerjomataram, I., Jemal, A., and Bray, F. (2017). Global patterns and trends in colorectal cancer incidence and mortality. *Gut* 66 (4), 683–691. doi:10.1136/gutjnl-2015-310912
- Barutcu, S. A., Girmis, N., Vernia, S., and Davis, R. J. (2018). Role of the MAPK/cJun NH(2)-terminal kinase signaling pathway in starvation-induced autophagy. *Autophagy* 14 (9), 1586–1595. doi:10.1080/15548627.2018.1466013
- Benitez Majano, S., Di Girolamo, C., Rachet, B., Maringe, C., Guren, M. G., Glimelius, B., et al. (2019). Surgical treatment and survival from colorectal cancer in Denmark, England, Norway, and Sweden: A population-based study. *Lancet. Oncol.* 20 (1), 74–87. doi:10.1016/s1470-2045(18)30646-6
- Billir, L. H., and Schrag, D. (2021). Diagnosis and treatment of metastatic colorectal cancer: A review. *Jama* 325 (7), 669–685. doi:10.1001/jama.2021.0106
- Brenner, H., Kloor, M., and Pox, C. P. (2014). Colorectal cancer. *Lancet* 383 (9927), 1490–1502. doi:10.1016/s0140-6736(13)61649-9
- Chen, H., Li, N., Ren, J., Feng, X., Lyu, Z., Wei, L., et al. (2019). Participation and yield of a population-based colorectal cancer screening programme in China. *Gut* 68 (8), 1450–1457. doi:10.1136/gutjnl-2018-317124
- Chen, X., Kang, R., Kroemer, G., and Tang, D. (2021). Ferroptosis in infection, inflammation, and immunity. *J. Exp. Med.* 218 (6), e20210518. doi:10.1084/jem.20210518
- Cho, K. J., Shin, S. Y., Moon, H., Kim, B. K., and Ro, S. W. (2021). Knockdown of Atg7 suppresses Tumorigenesis in a murine model of liver cancer. *Transl. Oncol.* 14 (9), 101158. doi:10.1016/j.tranon.2021.101158
- Collier, J. J., Suomi, F., Olahova, M., McWilliams, T. G., and Taylor, R. W. (2021). Emerging roles of ATG7 in human health and disease. *EMBO Mol. Med.* 13 (12), e14824. doi:10.15252/emmm.202114824
- Dekker, E., Tanis, P. J., Vleugels, J. L. A., Kasi, P. M., and Wallace, M. B. (2019). Colorectal cancer. *Lancet* 394 (10207), 1467–1480. doi:10.1016/s0140-6736(19)32319-0
- Dixon, S. J., Lemberg, K. M., Lamprecht, M. R., Skouta, R., Zaitsev, E. M., Gleason, C. E., et al. (2012). Ferroptosis: An iron-dependent form of nonapoptotic cell death. *Cell* 149 (5), 1060–1072. doi:10.1016/j.cell.2012.03.042
- Fearnhead, H. O., Vandenabeele, P., and Vanden Berghe, T. (2017). How do we fit ferroptosis in the family of regulated cell death? *Cell Death Differ.* 24 (12), 1991–1998. doi:10.1038/cdd.2017.149
- Hao, J., Deng, H., Yang, Y., Chen, L., Wu, Q., Yao, P., et al. (2021). Downregulation of MCM8 expression restrains the malignant progression of cholangiocarcinoma. *Oncol. Rep.* 46 (5), 235. doi:10.3892/or.2021.8186
- Hassannia, B., Vandenabeele, P., and Vanden Berghe, T. (2019). Targeting ferroptosis to iron out cancer. *Cancer Cell* 35 (6), 830–849. doi:10.1016/j.ccell.2019.04.002
- Hou, W., Xie, Y., Song, X., Sun, X., Lotze, M. T., Zeh, H. J., 3rd, et al. (2016). Autophagy promotes ferroptosis by degradation of ferritin. *Autophagy* 12 (8), 1425–1428. doi:10.1080/15548627.2016.1187366
- Huang, H., Fan, X., Qiao, Y., Yang, M., and Ji, Z. (2021). Knockdown of KNTC1 inhibits the proliferation, migration and tumorigenesis of human bladder cancer cells and induces apoptosis. *Crit. Rev. Eukaryot. Gene Expr.* 31 (1), 49–60. doi:10.1615/CritRevEukaryotGeneExpr.2021037301
- Jiang, X., Stockwell, B. R., and Conrad, M. (2021). Ferroptosis: Mechanisms, biology and role in disease. *Nat. Rev. Mol. Cell Biol.* 22 (4), 266–282. doi:10.1038/s41580-020-00324-8
- Johdi, N. A., and Sukor, N. F. (2020). Colorectal cancer immunotherapy: Options and strategies. *Front. Immunol.* 11, 1624. doi:10.3389/fimmu.2020.01624
- Kim, J. H. (2015). Chemotherapy for colorectal cancer in the elderly. *World J. Gastroenterol.* 21 (17), 5158–5166. doi:10.3748/wjg.v21.i17.5158
- Koppula, P., Zhuang, L., and Gan, B. (2021). Cystine transporter slc7a11/xCT in cancer: Ferroptosis, nutrient dependency, and cancer therapy. *Protein Cell* 12 (8), 599–620. doi:10.1007/s13238-020-00789-5
- Ladabaum, U., Dominitz, J. A., Kahi, C., and Schoen, R. E. (2020). Strategies for colorectal cancer screening. *Gastroenterology* 158 (2), 418–432. doi:10.1053/j.gastro.2019.06.043
- Li, J., Yao, W., Zhang, L., Bao, L., Chen, H., Wang, D., et al. (2017). Genome-wide DNA methylation analysis in lung fibroblasts co-cultured with silica-exposed alveolar macrophages. *Respir. Res.* 18 (1), 91. doi:10.1186/s12931-017-0576-z
- Li, J., Cao, F., Yin, H. L., Huang, Z. J., Lin, Z. T., Mao, N., et al. (2020). Ferroptosis: Past, present and future. *Cell Death Dis.* 11 (2), 88. doi:10.1038/s41419-020-2298-2
- Li, N., Lu, B., Luo, C., Cai, J., Lu, M., Zhang, Y., et al. (2021). Incidence, mortality, survival, risk factor and screening of colorectal cancer: A comparison among China, Europe, and Northern America. *Cancer Lett.* 522, 255–268. doi:10.1016/j.canlet.2021.09.034
- Li, W., and He, F. (2014). Monocyte to macrophage differentiation-associated (MMD) targeted by miR-140-5p regulates tumor growth in non-small cell lung cancer. *Biochem. Biophys. Res. Commun.* 450 (1), 844–850. doi:10.1016/j.bbrc.2014.06.075
- Liang, C., Zhang, X., Yang, M., and Dong, X. (2019). Recent progress in ferroptosis inducers for cancer therapy. *Adv. Mat.* 31 (51), e1904197. doi:10.1002/adma.201904197
- Lin, W., Zhou, L., Liu, M., Zhang, D., Yan, Y., Chang, Y. F., et al. (2020). gga-miR-200b-3p promotes macrophage activation and differentiation via targeting monocyte to macrophage differentiation-associated in HD11 cells. *Front. Immunol.* 11, 563143. doi:10.3389/fimmu.2020.563143
- Liu, Q., Zheng, J., Yin, D. D., Xiang, J., He, F., Wang, Y. C., et al. (2012). Monocyte to macrophage differentiation-associated (MMD) positively regulates ERK and Akt activation and TNF- $\alpha$  and NO production in macrophages. *Mol. Biol. Rep.* 39 (5), 5643–5650. doi:10.1007/s11033-011-1370-5
- Lu, T., Xu, R., Li, Q., Zhao, J. Y., Peng, B., Zhang, H., et al. (2021). Systematic profiling of ferroptosis gene signatures predicts prognostic factors in esophageal squamous cell carcinoma. *Mol. Ther. Oncolytics* 21, 134–143. doi:10.1016/j.omto.2021.02.011
- Messersmith, W. A. (2019). NCCN guidelines updates: Management of metastatic colorectal cancer. *J. Natl. Compr. Canc. Netw.* 17 (5.5), 599–601. doi:10.6004/jnccn.2019.5014
- Modest, D. P., Pant, S., and Sartore-Bianchi, A. (2019). Treatment sequencing in metastatic colorectal cancer. *Eur. J. Cancer* 109, 70–83. doi:10.1016/j.ejca.2018.12.019
- Mohamed, A. A., Omar, A. A., El-Awady, R. R., Hassan, S. M. A., Eitah, W. M. S., Ahmed, R., et al. (2020). MiR-155 and MiR-665 role as potential non-invasive biomarkers for hepatocellular carcinoma in Egyptian patients with chronic hepatitis C virus infection. *J. Transl. Int. Med.* 8 (1), 32–40. doi:10.2478/jtim-2020-0006
- Mou, Y., Wang, J., Wu, J., He, D., Zhang, C., Duan, C., et al. (2019). Ferroptosis, a new form of cell death: Opportunities and challenges in cancer. *J. Hematol. Oncol.* 12 (1), 34. doi:10.1186/s13045-019-0720-y

- Naderi, N., Yousefi, H., Mollazadeh, S., Seyed Mikaeili, A., Keshavarz Norouzpour, M., Jazebi, M., et al. (2019). Inflammatory and immune response genes: A genetic analysis of inhibitor development in Iranian hemophilia A patients. *Pediatr. Hematol. Oncol.* 36 (1), 28–39. doi:10.1080/08880018.2019.1585503
- Peng, B., Peng, J., Kang, F., Zhang, W., Peng, E., and He, Q. (2022). Ferroptosis-related gene MT1G as a novel biomarker correlated with prognosis and immune infiltration in colorectal cancer. *Front. Cell Dev. Biol.* 10, 881447. doi:10.3389/fcell.2022.881447
- Piawah, S., and Venook, A. P. (2019). Targeted therapy for colorectal cancer metastases: A review of current methods of molecularly targeted therapy and the use of tumor biomarkers in the treatment of metastatic colorectal cancer. *Cancer* 125 (23), 4139–4147. doi:10.1002/cncr.32163
- Rehli, M., Krause, S. W., Schwarzfischer, L., Kreutz, M., and Andreessen, R. (1995). Molecular cloning of a novel macrophage maturation-associated transcript encoding a protein with several potential transmembrane domains. *Biochem. Biophys. Res. Commun.* 217 (2), 661–667. doi:10.1006/bbrc.1995.2825
- Rezapour, A., Nargesi, S., Mezginjad, F., Rashki Kemmak, A., and Bagherzadeh, R. (2021). The economic burden of cancer in Iran during 1995–2019: A systematic review. *Iran. J. Public Health* 50 (1), 35–45. doi:10.18502/ijph.v50i1.5070
- Roque-Castellano, C., Fariña-Castro, R., Nogués-Ramía, E. M., Artiles-Armas, M., and Marchena-Gómez, J. (2020). Colorectal cancer surgery in selected nonagenarians is relatively safe and it is associated with a good long-term survival: An observational study. *World J. Surg. Oncol.* 18 (1), 120. doi:10.1186/s12957-020-01895-8
- Simon, K. (2016). Colorectal cancer development and advances in screening. *Clin. Interv. Aging* 11, 967–976. doi:10.2147/cia.s109285
- Song, J., Liu, Y., Guan, X., Zhang, X., Yu, W., and Li, Q. (2021). A novel ferroptosis-related biomarker signature to predict overall survival of esophageal squamous cell carcinoma. *Front. Mol. Biosci.* 8, 675193. doi:10.3389/fmolb.2021.675193
- Stockwell, B. R., and Jiang, X. (2019). A physiological function for ferroptosis in tumor suppression by the immune system. *Cell Metab.* 30 (1), 14–15. doi:10.1016/j.cmet.2019.06.012
- Sung, H., Ferlay, J., Siegel, R. L., Laversanne, M., Soerjomataram, I., Jemal, A., et al. (2021). Global cancer statistics 2020: GLOBOCAN estimates of incidence and mortality worldwide for 36 cancers in 185 countries. *Ca. Cancer J. Clin.* 71 (3), 209–249. doi:10.3322/caac.21660
- Tang, R., Xu, J., Zhang, B., Liu, J., Liang, C., Hua, J., et al. (2020). Ferroptosis, necroptosis, and pyroptosis in anticancer immunity. *J. Hematol. Oncol.* 13 (1), 110. doi:10.1186/s13045-020-00946-7
- Teng, Z., Yao, J., Zhu, L., Zhao, L., and Chen, G. (2021). ZNF655 is involved in development and progression of non-small-cell lung cancer. *Life Sci.* 280, 119727. doi:10.1016/j.lfs.2021.119727
- Topisirovic, I., Gutierrez, G. J., Chen, M., Appella, E., Borden, K. L., and Ronai, Z. A. (2009). Control of p53 multimerization by Ubc13 is JNK-regulated. *Proc. Natl. Acad. Sci. U. S. A.* 106 (31), 12676–12681. doi:10.1073/pnas.0900596106
- Vera-Ramirez, L., Vodnala, S. K., Nini, R., Hunter, K. W., and Green, J. E. (2018). Autophagy promotes the survival of dormant breast cancer cells and metastatic tumour recurrence. *Nat. Commun.* 9 (1), 1944. doi:10.1038/s41467-018-04070-6
- Wang, W., Green, M., Choi, J. E., Gijón, M., Kennedy, P. D., Johnson, J. K., et al. (2019). CD8(+) T cells regulate tumour ferroptosis during cancer immunotherapy. *Nature* 569 (7755), 270–274. doi:10.1038/s41586-019-1170-y
- Wang, Y., Wei, Z., Pan, K., Li, J., and Chen, Q. (2020). The function and mechanism of ferroptosis in cancer. *Apoptosis* 25 (11–12), 786–798. doi:10.1007/s10495-020-01638-w
- Wang, Y., Hou, K., Jin, Y., Bao, B., Tang, S., Qi, J., et al. (2021). Lung adenocarcinoma-specific three-integrin signature contributes to poor outcomes by metastasis and immune escape pathways. *J. Transl. Int. Med.* 9 (4), 249–263. doi:10.2478/jtim-2021-0046
- Won, Y. H., Lee, M. Y., Choi, Y. C., Ha, Y., Kim, H., Kim, D. Y., et al. (2016). Elucidation of relevant neuroinflammation mechanisms using gene expression profiling in patients with amyotrophic lateral sclerosis. *PLoS One* 11 (11), e0165290. doi:10.1371/journal.pone.0165290
- Wu, X., Li, Y., Zhang, S., and Zhou, X. (2021). Ferroptosis as a novel therapeutic target for cardiovascular disease. *Theranostics* 11 (7), 3052–3059. doi:10.7150/thno.54113
- Xie, Y., Hou, W., Song, X., Yu, Y., Huang, J., Sun, X., et al. (2016). Ferroptosis: Process and function. *Cell Death Differ.* 23 (3), 369–379. doi:10.1038/cdd.2015.158
- Xu, J., Zhang, J., and Wang, J. (2020). The application of traditional Chinese medicine against the tumor immune escape. *J. Transl. Int. Med.* 8 (4), 203–204. doi:10.2478/jtim-2020-0032
- Yang, C., Huang, S., Cao, F., and Zheng, Y. (2021). Role of ferroptosis-related genes in prognostic prediction and tumor immune microenvironment in colorectal carcinoma. *PeerJ* 9, e11745. doi:10.7717/peerj.11745
- Yang, Y. B., Zhou, J. X., Qiu, S. H., He, J. S., Pan, J. H., and Pan, Y. L. (2021). Identification of a novel ferroptosis-related gene prediction model for clinical prognosis and immunotherapy of colorectal cancer. *Dis. Markers* 2021, 4846683. doi:10.1155/2021/4846683
- Zhou, J., Zheng, R., Zhang, S., Zeng, H., Wang, S., Chen, R., et al. (2021). Colorectal cancer burden and trends: Comparison between China and major burden countries in the world. *Chin. J. Cancer Res.* 33 (1), 1–10. doi:10.21147/j.issn.1000-9604.2021.01.01



## OPEN ACCESS

## EDITED BY

Yanqing Liu,  
Columbia University, United States

## REVIEWED BY

Xiaoling Chen,  
Purdue University, United States  
Qi Hu,  
University of Florida, United States  
Jingjie Yi,  
Columbia University, United States

## \*CORRESPONDENCE

Hui Li,  
huihui922@126.com

## SPECIALTY SECTION

This article was submitted to Molecular  
Diagnostics and Therapeutics,  
a section of the journal  
Frontiers in Molecular Biosciences

RECEIVED 25 August 2022

ACCEPTED 14 September 2022

PUBLISHED 27 September 2022

## CITATION

Maimaitizunong R, Wang K and Li H  
(2022), Ferroptosis and its emerging role  
in esophageal cancer.  
*Front. Mol. Biosci.* 9:1027912.  
doi: 10.3389/fmolb.2022.1027912

## COPYRIGHT

© 2022 Maimaitizunong, Wang and Li.  
This is an open-access article  
distributed under the terms of the  
[Creative Commons Attribution License](#)  
(CC BY). The use, distribution or  
reproduction in other forums is  
permitted, provided the original  
author(s) and the copyright owner(s) are  
credited and that the original  
publication in this journal is cited, in  
accordance with accepted academic  
practice. No use, distribution or  
reproduction is permitted which does  
not comply with these terms.

# Ferroptosis and its emerging role in esophageal cancer

Rezeye Maimaitizunong<sup>1</sup>, Kai Wang<sup>2</sup> and Hui Li<sup>3\*</sup>

<sup>1</sup>Department of Biochemistry and Molecular Biology, Basic Medicine School, Xinjiang Medical University, Urumqi, China, <sup>2</sup>Department of Medical Engineering and Technology, Xinjiang Medical University, Urumqi, China, <sup>3</sup>Central Laboratory of Xinjiang Medical University, Urumqi, China

The occurrence and development of tumors involve a series of life activities of cells, among which cell death has always been a crucial part in the research of tumor mechanisms and treatment methods. Ferroptosis is a non-apoptotic form of cell death, which is characterized by lipid peroxidation accumulation and further cell membrane rupture caused by excessive production of intracellular oxygen free radicals dependent on iron ions. Esophageal cancer is one of the common digestive tract tumors. Patients in the early stage are mainly treated with surgery, and the curative effect is awe-inspiring. However, surgery is far from enough for terminal patients, and it is the best choice to combine radiotherapy and chemotherapy before the operation or during the perioperative period. Although the treatment plan for patients with advanced esophageal cancer is constantly being optimized, we are disappointed at the still meager 5-year survival rate of patients and the poor quality of life. A series of complex problems, such as increased chemotherapy drug resistance and decreased radiotherapy sensitivity of esophageal cancer cells, are waiting for us to tackle. Perhaps ferroptosis can provide practical and feasible solutions and bring new hope to patients with advanced esophageal cancer. The occurrence of ferroptosis is related to the dysregulation of iron metabolism, lipid metabolism, and glutamate metabolism. Therefore, these dysregulated metabolic participant proteins and signaling pathways are essential entry points for using cellular ferroptosis to resist the occurrence and development of cancer cells. This review first introduced the main regulatory mechanisms of ferroptosis. It then summarized the current research status of ferroptosis in esophageal cancer, expecting to provide ideas for the research related to ferroptosis in esophageal cancer.

## KEYWORDS

ferroptosis, lipid peroxidation, antioxidant system, esophageal cancer, non-coding RNA

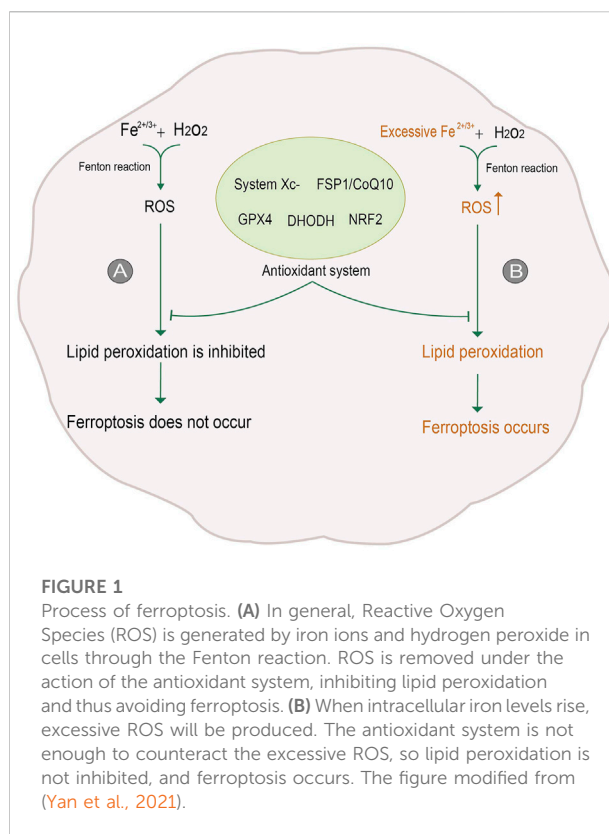
## Introduction

Cell death is a significant step in organism growth and development. Moreover, different forms of cell death are regulated differently; imbalanced regulation could be the first step in the occurrence and development of diseases. Traditionally, cell death can be classified into apoptosis, necrosis, and autophagy according to the change in mechanism and cell morphology (Kroemer et al., 2009). With the in-depth study of cell death, a non-

apoptotic form of cell death, namely ferroptosis, was first proposed in 2012. Ferroptosis is a process of oxidative damage after the accumulation of oxygen free radicals dependent on iron ions. Excessive iron ions in cells react with hydrogen peroxide to produce reactive Oxygen Species (ROS). Excessive ROS will attack polyunsaturated fatty acid (PUFA) in biomembrane to deprive hydrogen ions, making it into a peroxide state. Eventually, the lipids in cell membranes and intracellular organelles become lipid peroxide and rupture due to massive peroxidation, resulting in cell death (Dixon et al., 2012). In general, there are many sources of oxygen free radicals in cells, to eliminate these oxygen radicals, cells contain potent antioxidant mechanisms. Despite the protective mechanism, when too many oxygen radicals are produced, the balance is disrupted, and oxidative damage can occur, leading to further cell death (Jamar et al., 2017) (Figure 1).

The ferroptosis process is a complex and sophisticated life phenomenon that occurs under the joint control of multiple systems, multiple metabolism, and multiple genes. According to the data provided by the FerrDb database, 259 genes are involved in ferroptosis. Based on their roles in ferroptosis, they can be divided into ferroptosis driver genes, ferroptosis suppressor genes, and ferroptosis marker genes. Among them were 108 driver genes, 69 repressor genes and 111 marker genes. The total number of the three genes was significantly higher than 259. The reason was that 28 genes had multiple identities in the ferroptosis. These genes have become the focus of research on disease mechanisms. In malignant tumors, ferroptosis can be triggered to eliminate tumor cells, while inhibiting this process can prevent acute damage to normal cells and neurodegenerative diseases. For example, Erastin (ferroptosis inducer) was used to activate the ferroptosis pathway in acute myelogenous leukemia cells, which was found to be more sensitive to chemotherapy agents (Yu et al., 2015); Treatment of breast cancer cells with Siramesine and lapatinib enhanced the occurrence of ferroptosis (Ma et al., 2016); Sorafenib (an oncogenic kinase inhibitor) can effectively induce ferroptosis in different solid tumor cell lines (Lachaier et al., 2014). Among non-tumor diseases: the combined treatment of iron inhibin -1 and iron chelating agent (both ferroptosis inhibitors) significantly improved the heart failure of mice (Fang et al., 2019); After the mice with intracerebral hemorrhage were treated with iron inhibin -1, the neurological deficit, memory impairment and brain atrophy caused by intracerebral bleeding were significantly reduced (Chen et al., 2019). After treatment with liproxstatin-1 (ferroptosis inhibitor), liver lipid peroxidation and related cell death were obviously inhibited, thus reducing the severity of nonalcoholic steatohepatitis (Qi et al., 2020). In addition, more research results show that ferroptosis is an essential participant in disease occurrence and development, as well as malignant tumor deterioration and metastasis.

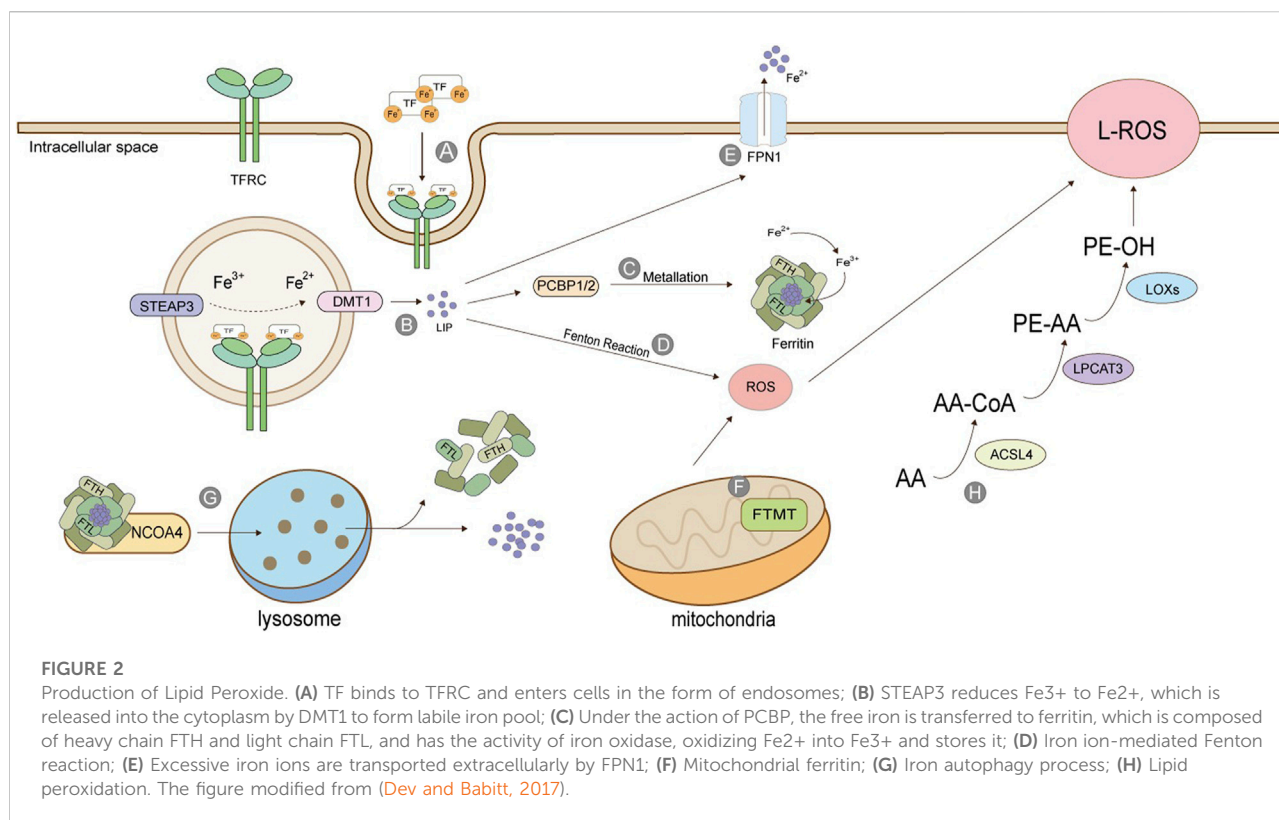
Since infinite proliferation and malignant metastasis are two characteristics of malignant tumors and two major problems in clinical treatment, inducing the death of tumor cells and



preventing the continued proliferation have been the primary means of clinical treatment of malignant tumors. The biggest problem faced by traditional treatment schemes, such as radiotherapy and chemotherapy, is that the sensitivity of tumor cells to radiotherapy decreases, and they are resistant to chemotherapy drugs. Therefore, some effective measures are urgently needed to reverse the insensitivity of tumor cells. Ferroptosis can help solve these problems. In light of such traditional treatment ideas as inducing tumor cell death, the answer given by ferroptosis is to cause tumor cell death by various mature ferroptosis inducers to prevent the infinite proliferation of cells. The FerrDb database shows 54 small molecular compounds that induce ferroptosis. For the problem of insensitivity to radiotherapy and chemotherapy, sensitivity can be enhanced by regulating the targets in the ferroptosis pathway. Therefore, the ferroptosis pathway is a valuable therapeutic target that deserves further investigation.

Esophageal cancer is one of the most common malignant tumors of the digestive tract in China. Due to its hidden incidence, most patients are already in the middle and late stages when they come to the hospital for treatment. Since the prognosis and survival rate of patients with early esophageal cancer is reasonable, improving the survival rate and quality of life of patients with mid and late-stage esophageal cancer has always been a complex problem that needs to be solved timely. Surgery





is only limited to patients in the non-advanced stage and is less effective for patients in the advanced stage (Nakajima et al., 2016). Treating patients with advanced esophageal squamous cell carcinoma aims to alleviate symptoms and prolong survival. For a long time, cytotoxic drug therapy has been the primary means of chemotherapy, molecular targeted therapy, immunotherapy, and so on. However, the antitumor activity of traditional chemotherapy drugs such as cisplatin and 5-fluorouracil is still insufficient to meet the clinical needs. Despite the rapid development of molecular targeted therapy and immunotherapy, the individual differences of tumor suppressor patients and other factors need to be further studied (Hirano and Kato, 2019). Therefore, finding reliable and effective gene targets will be the future research direction. The metabolic pathway involved in ferroptosis contains many gene regulatory points, which indicates that it can provide us with abundant targets to design good experiments and provide practical new ideas for clinical treatment.

## Main regulatory mechanism of ferroptosis

### Production of lipid peroxide

The most typical morphological changes of ferroptosis are membrane rupture, Outer mitochondrial membrane rupture,

reduction or deletion of mitochondrial cristae, etc. These membrane damage induced by ferroptosis is mainly due to the production of lipid peroxides. Therefore, the production of lipid peroxides can be broadly divided into iron ion absorption and Lipid peroxidation (Xie et al., 2016).

### Iron ions

Iron ions in the human body can be divided into exogenous iron and endogenous iron. Exogenous iron comes from food and diet; generally, Fe<sup>3+</sup>, which is transported to the cell membrane by transferrin (TF) in serum, combines with transferrin receptor TFRC and enters the cell in the form of endocytosis (Kwon et al., 2015). The metal reductase STEAP3 contained in the endosome is responsible for reducing Fe<sup>3+</sup> to Fe<sup>2+</sup>, which is then released into the cytoplasm under the action of divalent metal transporter (DMT1) to form labile iron pool (Figure 2). LIP has three destinations: most intracellular free iron transfers iron ions to ferritin by protein-protein interaction under the action of iron molecular chaperone PCBP1/2, also called metallization of ferritin. Ferritin is composed of heavy chain FTH and light chain FTL and has the activity of iron oxidase, which oxidizes Fe<sup>2+</sup> to Fe<sup>3+</sup> and stores it. The rest of cytoplasmic free iron undergoes a Fenton reaction with the cytosolic peroxide to mediate the production of ROS. Excess-free iron, in addition to these two uses, is excluded from the cell via the iron transporter 1 (FPN1) on the cell membrane (Anderson and

Frazer, 2017; Dev and Babitt, 2017; Aversa et al., 2018; Di Sanzo et al., 2018) (Figure 2).

The release of stored iron, mainly the iron release process of ferritin *in vivo*, is an essential source of endogenous iron. Ferritin in mitochondria is FTMT, which is not ubiquitous and especially maintains the iron ion homeostasis in mitochondria. As iron ion is necessary for mitochondria to synthesize heme and iron-sulfur clusters, controlling iron ion content by FTMT is also critical (Mancias et al., 2014; Mancias et al., 2015). Ferritin is directed to lysosomes by a nuclear receptor coactivator (NCOA4). It degrades the protein part under the action of lysosomal enzymes, releasing iron ions and stabilizing iron content in cells. This process is also called iron autophagy. When iron autophagy is excessive, the concentration of iron ions in the body rises, inducing ferroptosis (Fuhrmann et al., 2020). Iron ion absorption is a prerequisite for ferroptosis, and many genes will also participate in the regulation of this process. For example, in lung cancer cells, the inhibition of cysteine desulphurase (NFS1) will up-regulate the expression of transferrin receptor TFRC, thus accelerating iron ion absorption and precipitating ferroptosis (Alvarez et al., 2017). Fanconi anemia complementary group D2 (FANCD2) is a nuclear protein involved in repairing DNA damage, which can regulate many genes of iron metabolism, such as FTH1, TF, TFRC, FPN1, and STEAP3 (Song et al., 2016). Serine/threonine kinase ATM indirectly regulates the expression of ferritin and iron transporter 1 (FPN1) by holding the nuclear shift of metal-regulated transcription factor 1 (MTF1), thus controlling the process of ferroptosis (Chen et al., 2020).

### Lipid peroxidation

The activation of polyunsaturated fatty acids (PUFA) is the first step and the critical regulatory point of ferroptosis, which needs the catalysis of acyl-coenzyme A long synthetase chain family member 4 (ACSL4) and lysophosphatidylcholine acyltransferase 3 (LPCAT3) (Mou et al., 2019; Cheng et al., 2020). ACSL4 catalysis is specific to fatty acyl (Kagan et al., 2017). Arachidonic acid (AA) and epinephrine (AdA) can produce arachidonic acid coenzyme A (AA-CoA) and epinephrine coenzyme A (AdA-CoA) under the action of ACSL4. The latter two can be inserted into membrane phospholipids under the act of LPCAT3 to be converted into PE-AA and PE-AdA, and finally oxidized to form lipid peroxides under the catalysis of lipoxygenase (LOXs) (Dixon et al., 2015; Sha et al., 2021) (Figure 2).

### Antioxidant system

The occurrence of ferroptosis originates from the imbalance of oxidation and antioxidant regulation. The oxidation reaction takes place in cells, and there are many sources of oxygen free radicals. As the powerful antioxidant system constantly

counteracts these oxygen free radicals concurrently, generally, cells will not die because of excessive oxidative damage. To a large extent, the occurrence of ferroptosis can be attributed to the reduction of antioxidant capacity. When the antioxidant capacity of cells is weakened, even if the oxidative system of cells is not hyperactive, ROS produced by the general life activities of cells will cause the cells to die due to oxidative damage. Therefore, reducing antioxidant capacity is one of the critical mechanisms in ferroptosis. Glutathione (GSH) is one of the most abundant and powerful antioxidant molecules in cells and the leading force in the antioxidant system, whose metabolic disorder means the occurrence and development of ferroptosis. The systems XC - involved in GSH synthesis, GPX4 with GSH as an activating substrate, FSP1/CoQ10, DHODH, and others are presented below.

### Cystine/glutamate antitransporter (System Xc-)

System Xc- is a reverse transporter protein existing in the cell membrane, which transports glutamic acid out of the cell and cystine into the cell at the ratio of 1: 1 (Figure 3). This channel stops transporting when intracellular homocysteine and extracellular hyperglycemic acid are reached. This transporter is composed of light chain SLC7A11 (also called xCT) and heavy chain SLC3A2 (also called CD98), among which SLC7A11 plays a significant role in transport and accordingly determines the specificity of this system, and SLC3A2 is to stabilize SLC7A11. Cystine transported into cells is reduced to cysteine, one of the critical raw materials for synthesizing glutathione (GSH) and a rate-limiting precursor, which also acts as an antioxidant independently of GSH. GSH is synthesized from cysteine, glutamic acid, and glycine under the catalysis of  $\gamma$ -glutamylcysteine ligase (GCL) and glutathione synthetase (GSS), which is one of the most abundant antioxidant molecules in cells, also the number one molecule to resist ferroptosis. Its functions include maintaining intracellular redox balance, reducing oxygen free radicals, and maintaining the thiol state of the protein (Bassi et al., 2001; Dong et al., 2020; Lin et al., 2020; Koppula et al., 2021). Tables 1, 2 summarize the regulatory factors that regulate the two subunits in System Xc- respectively.

### Glutathione peroxidase 4 (GPX4)

GPX4 is the core protein that regulates ferroptosis in cells, and it depends on GSH to achieve a substantial antioxidant effect. GSH is the activated substrate of GPX4, which transfers its sulfhydryl group to GPX4, allowing GPX4 to acquire antioxidant function and become oxidized glutathione (GSSG). The activated GPX4 reduces phospholipid peroxide PLOOH to the corresponding phospholipid alcohol PLOH, reduces phospholipid peroxide in the membrane, and removes oxygen free radicals, thus resisting the ferroptosis of cells (Figure 3). When GSH is depleted, GPX4 is inactivated, and oxidative damage occurs, leading to excessive lipid peroxidation

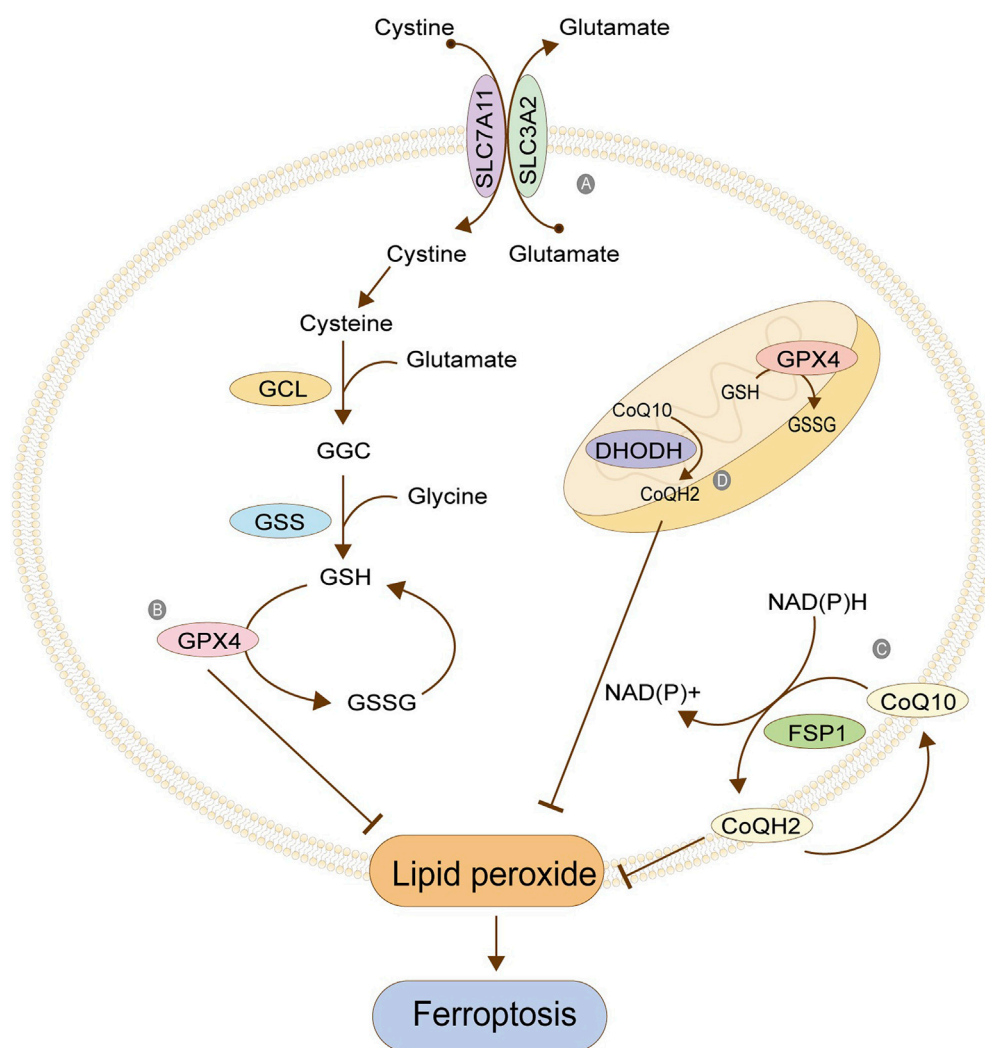


FIGURE 3

Antioxidant system. (A) Cystine/glutamate antitransporter; (B) Glutathione peroxidase 4; (C) FSP1/CoQ10; (D) Antioxidant system in mitochondria. The figure modified from (Anandhan et al., 2020).

and ferroptosis. GPX4, as an essential regulatory protein, is an important target of many ferroptosis inducers, the most typical of which is RSL3 (Maiorino et al., 2018; Bersuker et al., 2019; Xu et al., 2019; Zou et al., 2019). Table 3 summarizes other regulatory factors of GPX4.

### Ferroptosis-suppressor-protein 1 (FSP1)/coenzyme Q10 (CoQ10)

FSP1 is a GSH-independent ferroptosis regulator. When GSH antioxidant system is normal, the absence of FSP1 will still lead to lipid peroxidation. Therefore, it can be concluded that inhibiting lipid peroxidation mediated by FSP1 is parallel to the GSH system (Bersuker et al., 2019). FSP1 can be accurately localized on the cell membrane by its

myoacylation structure. Its oxidoreductase domain is a significant part of ferroptosis, which is responsible for reducing the CoQ10 to reduced coenzyme Q (CoQH2) in the cell membrane. CoQ10 is a mobile lipophilic electron carrier that exists in all biofilms. CoQ10 can be recycled in the cell membrane, thus playing a more lasting role. Its reduction is completed by FSP1, and the required hydrogen is provided by NAD (P) H. The CoQ10 can be used as a free radical collecting antioxidant (RTA) to capture the oxygen free radicals in the cell membrane and further prevent the peroxidation of phospholipids in the cell membrane (Figure 3). The FPS1/CoQ10 system is parallel to GPX4 and System Xc, maintaining cell redox balance (Takahashi et al., 1993; Bentinger et al., 2007)

TABLE 1 Regulatory factors of SLC7A11.

Regulatory factor	The regulation of SLC7A11	Cancer
Metformin	downregulate	Breast cancer (Yang et al., 2021)
SOX 2	upregulate	Lung Cancer (Wang X. et al., 2021)
Lidocaine	downregulate	Ovarian and Breast Cancer (Sun D. et al., 2021)
P53	downregulate	Multiple cancer cell lines (Jiang et al., 2015)
Triptolide	downregulate	Head and neck cancer (Cai et al., 2021)
BAP1	downregulate	Kidney cancer (Zhang et al., 2019)
miR-27a-3p	downregulate	Non-small cell lung cancer (Lu X. et al., 2021)
Tanshinone IIA	downregulate	Gastric cancer (Guan et al., 2020)
ATF3	downregulate	Multiple cancer cell lines (Wang et al., 2020)
IMCA	downregulate	Colorectal Cancer (Zhang et al., 2020)
YAP/TAZ	upregulate	hepatocellular carcinoma (Gao et al., 2021)
TalaA	downregulate	colorectal cancer (Xia et al., 2020)
BECN1	downregulate	Multiple cancer cell lines (Song et al., 2018)
YTHDC2	downregulate	lung adenocarcinoma (Ma et al., 2021)
METTL3	upregulate	lung adenocarcinoma (Xu et al., 2022)
AKR1B1	upregulate	lung cancer (Zhang K. R. et al., 2021)
Levobupivacaine	downregulate	Gastric Cancer (Zhang K. R. et al., 2021)
Bavachin	downregulate	Osteosarcoma (Luo et al., 2021)
SFN	downregulate	Small-cell lung cancer (Iida et al., 2021)

SOX2, Stem Cell Factor 2; BAP1, H2A deubiquitinase; ATF3, activating transcription factor 3; IMCA, benzopyran derivative 2-imino-6-methoxy-2H-chromene-3-Carbothioamide; YAP/TAZ, transcription factor; TalaA, Natural compound, ferroptosis inducer; BECN1, beclin 1; YTHDC2, M6A reader; METTL3, methyltransferase-like 3; AKR1B1, aldo-keto reductase family 1 member B1; SFN, Sulforaphane.

TABLE 2 Regulatory factors of SLC3A2.

Regulatory factor	The regulation of SLC3A2	Cancer
ZEB1	downregulate	Ovarian Cancer (Cui et al., 2018)
IMiDs	downregulate	multiple myeloma (Heider et al., 2021)
miR-21	upregulate	hepatocellular carcinoma (Li et al., 2019)
AR-v7	upregulate	castration resistant prostate cancer (Sugiura et al., 2021)
DIO1	upregulate	renal cancer (Popławski et al., 2017)
PTPRJ	downregulate	lung cancer (D'Agostino et al., 2018)
IFN $\gamma$	downregulate	hepatocellular carcinoma (Kong et al., 2021)
MYCN	upregulate	neuroblastoma in mice (Gamble et al., 2019)
ADC	downregulate	triple negative breast cancer (Montero et al., 2022)
FZKA	downregulate	Non-Small Cell Lung Cancer (Zhao Y. Y. et al., 2022)

ZEB1, Zinc finger E-box-binding homeobox 1; IMiDs, immunomodulatory drugs; AR-v7, androgen receptor splice variant-7; DIO1, Type 1 iodothyronine deiodinase; PTPRJ, receptor protein tyrosine phosphatase; IFN $\gamma$ ,  $\gamma$ Interferon- $\gamma$ ; MYCN, oncogene; ADC, antibody-drug conjugates; FZKA, Fuzheng Kang'ai decoction.

Antioxidant systems in mitochondria

GPX4 functions not only in the cytoplasm but also in the mitochondria. The antioxidant systems GPX4 and CoQ10/FSP1 in the cytoplasm are parallel. One exhibits down-regulation, and the other up-regulates its function, maintaining the overall antioxidant capacity of the cells. A similar phenomenon exists in mitochondria, where the GPX4 and the dihydroorotate dehydrogenase (DHODH) system maintain the balance (Figure 3). DHODH is a crucial enzyme involved in the *ab initio* synthesis of pyrimidine in

prokaryotic and eukaryotic organisms, which is of great significance in cell chromosome replication. In addition, the enzyme is also related to ATP and ROS production. The function of DHODH is similar to that of the CoQ10/FSP1 system in cells in that it mainly helps the reduction of ubiquinone into panthenol in mitochondria to provide antioxidants to eliminate lipid peroxides in the mitochondrial membrane, thereby protecting the integrity of the mitochondrial membrane. The two mitochondrial systems, GPX4 and DHODH,



TABLE 3 Regulatory factors of GPX4.

Regulatory factor	The regulation of GPX4	Cancer
RSL3	GPX4 Inactivation	Colorectal Cancer (Sui et al., 2018)
DMOCPTL	induced GPX4 ubiquitination	triple negative breast cancer (Ding et al., 2021)
FZD7	Indirectly upregulate GPX4	Ovarian Cancer (Wang R. et al., 2021)
Fin56	promote GPX4 protein degradation	bladder cancer (Sun Y. et al., 2021)
RB	GPX4 inactivation	colorectal cancer (Shen et al., 2021)
KLF2	transcriptional repression of GPX4	clear cell renal cell carcinoma (Lu Y. et al., 2021)
SFRS9	upregulate	Colorectal Cancer (Wang Y. et al., 2021)
circKIF4A	Indirectly upregulate GPX4	papillary thyroid cancer (Chen W. et al., 2021)
EBV	Indirectly upregulate GPX4	nasopharyngeal carcinoma (Yuan et al., 2022)
CREB	upregulate	lung adenocarcinoma (Wang Z. et al., 2021)
DHA	GPX4 Inactivation	glioblastoma (Yi et al., 2020)
GSTZ1	Indirectly downregulate GPX4	hepatocellular carcinoma (Wang Z. et al., 2021)
Metformin	Indirectly downregulate GPX4	breast cancer (Hou et al., 2021)
Apatinib	Indirectly downregulate GPX4	gastric cancer (Zhao et al., 2021)
Ketamine	Indirectly downregulate GPX4	Liver Cancer (He et al., 2021)

RSL3, ferroptosis inducer; DMOCPTL, a derivative of natural product parthenolide; FZD7, the Wnt receptor Frizzled-7; Fin56, ferroptosis inducer; RB, Resibufogenin; KLF2, Kruppel like factor 2; SFRS9, Serine and arginine rich splicing factor 9; circKIF4A, Circular RNA; EBV, Epstein-Barr virus; CREB, cAMP, response element-binding protein; DHA, Dihydroartemisinin; GSTZ1, Glutathione S-transferase zeta 1.

are complementary. One system suffers from functional decline, and the other enhances its function, maintaining the antioxidant capacity (Mohamad Fairus et al., 2017; Mao et al., 2021).

## Nuclear factor erythroid 2-related factor 2(NRF2)

As a stress-induced transcription factor, NRF2 plays a crucial role in maintaining the redox homeostasis of cells. Generally, NRF2 is at a low level in cells, which is maintained by Kelch-like ECH-related protein 1 (KEAP1). Under non-oxidative stress, KEAP1 binds to NRF2 to form a complex, which promotes the degradation of NRF2 by ubiquitination, thereby reducing the content of intracellular free NRF2. When cells are damaged by oxidation and other stress states, the KEAP1/NRF2 complex depolymerizes, releasing NRF2 (Kensler et al., 2007). A large amount of free intracellular NRF2 enters the nucleus. It binds with antioxidant response elements (ARE) located in the regulatory region to enhance the transcription of target genes (Figure 4), regulating their expression to rescue cells under stress (Ma et al., 2019). Most of the target genes regulated by NRF2 are involved in intracellular redox reactions, among which NRF2 regulates almost all the genes related to iron metabolism and glutathione metabolism. Table 4 summarizes the genes related to iron metabolism, glutathione metabolism, and other metabolism regulated by NRF2.

## P53 and ferroptosis

P53 is a well-known cancer suppressor gene, which mainly achieves its arrest action during cancer development through cell

cycle arrest, cell senescence, and apoptosis. Recently, more and more studies have shown that P53 has a close correlation with and a potent function in a novel death mod, ferroptosis, apart from its classical role mentioned above, which involves several vital molecules in the ferroptosis pathway, such as SLC7A11, alox12, GPx4 and so on.

These results suggest that P53 exerts a tumor suppressor effect by regulating the cell cycle and mediates ferroptosis by regulating ferroptosis-related molecules. SLC7A11 is one of the vital ferroptosis inhibiting molecules, which provides essential components for glutathione synthesis by transporting cystine, thus inhibiting the occurrence of ferroptosis. Studies have shown that P53 binds to the promoter region of SLC7A11 in many human cancer cell lines through experiment verification, thereby down-regulating its protein expression, reducing the inhibition of tumor cells on ferroptosis, and finally promoting ferroptosis. In addition, it was surprising to find in these studies that the mutant P53<sup>3KR</sup> (an acetylation-defensive mutant) lost the function of cell cycle arrest but ultimately retains the process of down-regulating SLC7A11. This study provides us with a new powerful function of P53 in tumor inhibition (Jiang et al., 2015). ALOX12(Arachidonate-12-Lipoxygenase) is a member of the lipoxygenase family, and its role in ferroptosis is mainly to realize lipid peroxidation (shown in Figure 2), which is also the initial step of ferroptosis. Studies have shown that ALOX12 is an essential molecule in ferroptosis mediated by P53. It was also found that the knock-out of Alox12 fails to affect the protein expression levels of P53 and the downstream targeted genes of P53, but it can eliminate P53-mediated ferroptosis (Chu et al., 2019). The

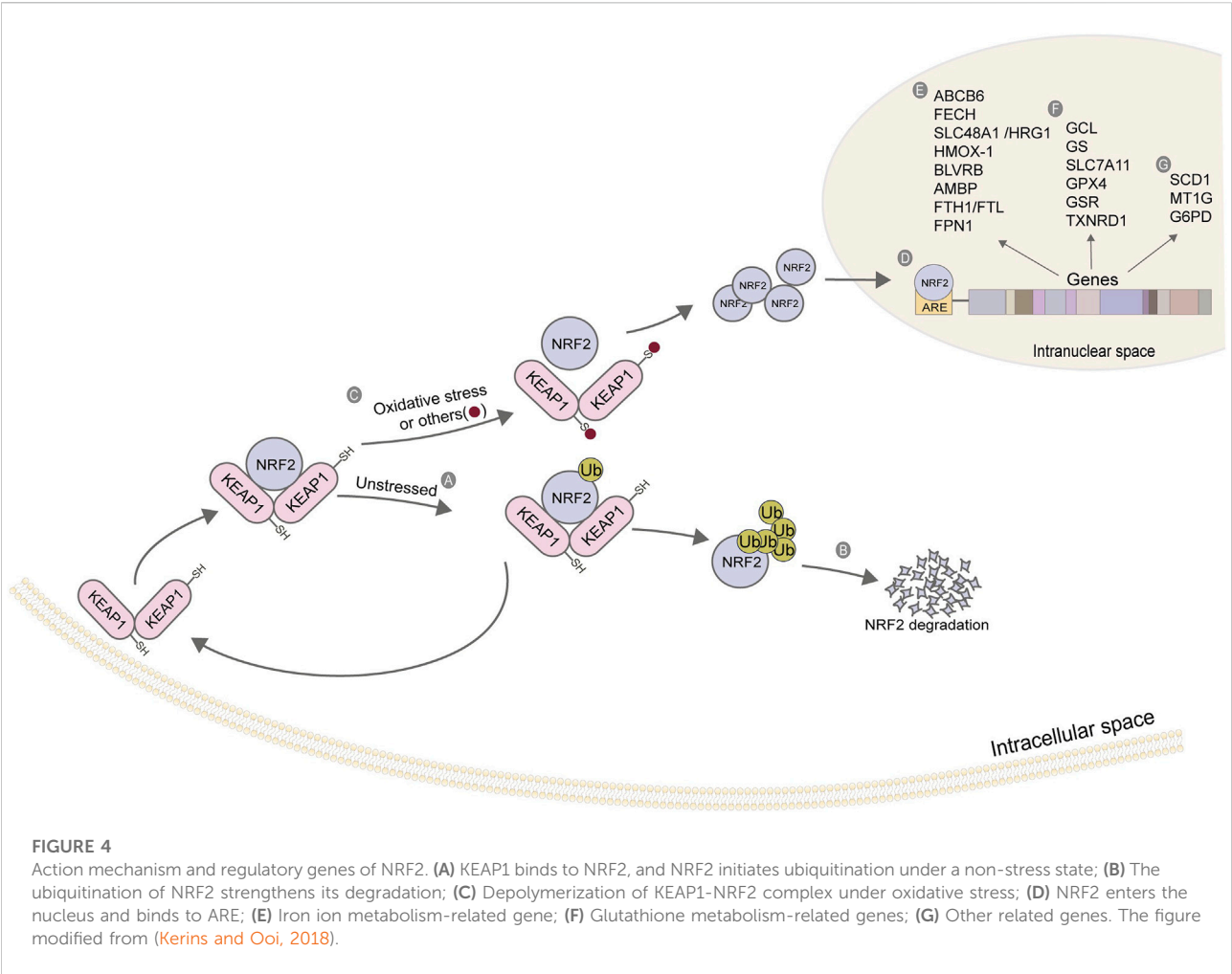


TABLE 4 Nrf2-regulated iron and glutathione metabolism related genes.

Gene abbreviation	Gene name	Involved metabolism
ABCB6	ATP binding cassette subfamily B member 6	Heme anabolism (Kerins and Ooi, 2018)
FECH	ferrochelatase	Heme anabolism (Kerins and Ooi, 2018)
SLC48A1/HRG1	Heme sensitive gene1	Heme catabolism (Kerins and Ooi, 2018)
HMOX-1	heme oxygenase	Heme catabolism (Kerins and Ooi, 2018)
BLVRB	biliverdin reductase B	Heme catabolism (Kerins and Ooi, 2018)
AMBP	alpha-1-microglobulin/bikunin precursor	Heme catabolism (Kerins and Ooi, 2018)
FTH1/FTL	ferritin heavy chain/light chain	iron storage (Kerins and Ooi, 2018)
FPN1	ferroportin1	iron mobilization (Kerins and Ooi, 2018)
GCL	glutamate-cysteine ligase	GSH anabolism (Lu, 2013)
GS	glutamyl synthetase	GSH anabolism (Lu, 2013)
SLC7A11	Solute Carrier Family 7	GSH anabolism (Dong et al., 2020)
GPX4	glutathione peroxidase 4	GSH reduction (Wang Q. et al., 2021)
GSR	Glutathione Reductase	GSH reduction (Hoffmann et al., 2017)
TXNRD1	Thioredoxin Reductase 1	GSH anabolism (Gao et al., 2020)
SCD1	Stearyl coenzyme A dehydrogenase-1	fatty acid metabolism (Huang et al., 2010)
MT1G	metallothionein (MT)-1G	MT1G-Nrf2/MT1G-P53-P21 pathway (Sun et al., 2016)
G6PD	glucose-6-phosphate dehydrogenase	Pentose phosphate pathway (Dodson et al., 2019)

regulatory relationship between P53 and GPX4 was reported by (Chen et al., 2021a). In the vascular endothelium induced by oxygen and glucose depletion (OGD) combined with high glucose (HG), P53 was regulated by the lncRNA Meg3 and accordingly unregulated. Then the highly expressed P53 entered the nucleus and combined with the regulatory region of GPX4 to down-regulate the expression of GPX4, finally preventing the scavenging effect of GPX4 on lipid peroxide. This study revealed the mechanism of lncRNA Meg3 inducing ferroptosis in vascular endothelial cells through the P53-GPX4 axis.

In 2021, studies reported the related mechanism of calcium-independent phospholipase iPLA2 $\beta$  inhibiting ferroptosis. iPLA2 $\beta$  has the detoxification effect of lipid peroxides, and iPLA2 $\beta$  can inhibit ROS-induced p53-driven ferroptosis in tumor cells. And p53-driven ferroptosis is independent of GPX4. The team first demonstrated that p53-driven ferroptosis independent of GPX4 in response to ROS-induced ferroptosis and subsequently revealed that loss of iPLA2 $\beta$  expression significantly increased the sensitivity of cancer cells to p53-dependent ferroptosis in response to ROS-induced ferroptosis. Although both GPX4 and iPLA2 $\beta$  inhibit ferroptosis by lipid peroxide detoxification, this study reveals the differences in the working principles of iPLA2 $\beta$  and GPX4 (Chen D. et al., 2021). Based on the above results, we can understand the powerful function of P53 in regulating ferroptosis. Liu et al. divided the mechanism of P53 regulating ferroptosis into two categories: canonical (GPX4-dependent) and non-canonical (GPX4-independent) and gave a very comprehensive summary. P53 by cell metabolism, iron ion, lipid metabolism, glutathione, and the synthesis of ROS aspects of regulation and control ferroptosis, in most cases, P53 promotes ferroptosis. As a result, the authors have also proposed several schemes to target P53 to treat tumors and neurodegenerative diseases through the ferroptosis pathway (Liu and Gu, 2022). Both the traditional tumor suppressor mechanism of P53 (cell cycle arrest, *etc.*) and the non-traditional tumor suppressor mechanism (promoting ferroptosis, *etc.*) are sufficient to make P53 the focus of targeted drug development. In the future, our research should focus on developing new targeted drugs using p53-mediated ferroptosis and combining traditional cancer therapies with p53-mediated ferroptosis, to propose therapeutic strategies with better efficacy. More and more studies are devoted to discovering the unconventional tumor-inhibiting mechanism of P53. To our surprise, many pieces of evidence demonstrate that P53 can achieve its tumor-inhibiting effect through ferroptosis. Based on this, we can continue to improve the clinical research of P53-mediated ferroptosis in the treatment of human cancer and further explore other potential mechanisms of p53.

## Study on ferroptosis in esophageal cancer

Esophageal cancer is the sixth most common cause of cancer death in the world, which can be divided into esophageal squamous cell carcinoma (ESCC) and esophageal adenocarcinoma (EAC) from the pathological point of view. Nearly 90% of esophageal cancer patients in the world are ESCC patients. The most unfortunate for esophageal cancer is that it is already in the middle and late stages with a poor prognosis at the time of diagnosis. The 5-year survival rate is less than 20% in developed countries and less than 5% in developing countries. Thus, early screening, diagnosis, and treatment for ESCC patients are critical (Jemal et al., 2011; Arnold et al., 2015; Codipilly et al., 2018). Clinical efforts have been devoted to finding marker molecules representing the early stage of cancer, whose characteristic changes can become a reliable signal, thus playing a predictive role and providing robust evidence for early screening of esophageal cancer patients.

In essence, ferroptosis is an oxidative damage process induced by the imbalance of oxidation and antioxidant systems. In 2014, Sehitogullar et al. detected the serum of 33 patients with ESCC after primary cancer resection to catch the oxidative stress level of ESCC patients. The results showed that the activities of glutathione peroxidase (GPXs), glutathione reductase (GR), and superoxide dismutase (SOD) in the ESCC group were lower than those in the control group. At the same time, the level of malondialdehyde (MDA) was significantly higher than that in the control group. This data set suggested that ESCC patients have a high level of oxidative stress (Sehitogullari et al., 2014). In 2020, Xiong et al. mentioned in their research that the expression level of SLC7A11 in cystine/glutamic acid transporter was significantly increased in ESCC patients, and it was verified by data mining analysis that SLC7A11 was a differentially expressed gene, and the survival prognosis of its highly expressed patients was poor. In addition, they preliminarily speculated that SLC7A11 might participate in ferroptosis through P53 and ROS metabolic pathways through functional enrichment analysis (Xiong et al., 2020). In 2019, Wang et al. proposed that the mutation of isocitrate dehydrogenase 1 (IDH1), a key enzyme in the tricarboxylic acid cycle, could enhance the sensitivity of ESCC KYSE170 cells to Erastin (ferroptosis inducer). Specifically, D-2-hydroxyglutaric acid, a metabolite produced by mutant IDH1 in tumor cells, reduces the expression of antioxidant GPX4 in tumor cells, thus enhancing the ferroptosis sensitivity induced by Erastin (Wang et al., 2019). Jiang et al. found that the expression level of DnaJ/Hsp40 homolog B subfamily 6 (DNAJB6) in ESCC tissue was lower than that in normal esophageal cancer tissues, and its expression level was negatively correlated with lymph node metastasis. The cancer inhibition effect of the DNJB6 was verified by *in vivo* and *in vitro* experiments. Through further mechanism research, they were

surprised to find that the overexpression of DNAJB6 gene was accompanied by a significant decrease in GPX4 and p-AKT protein levels. At the same time, the increase in lipid peroxidation level and the characteristic changes of ferroptosis in mitochondria were detected. Accordingly, they proposed for the first time compelling evidence that overexpression of DNAJB6 increased ferroptosis in esophageal cancer cells by down-regulating GPX4 (Jiang et al., 2020).

NRF2 is a well-known transcription factor that regulates antioxidant system proteins. In ESCC, NRF2 still upregulates the expression of SLC7A11 as its role as a transcription factor. The upregulated SLC7A11 is beneficial to the synthesis of intracellular GSH, further enhancing the resistance to ferroptosis. The inhibition of the ferroptosis pathway instead promotes the radioresistance of ESCCs (Feng et al., 2021). The team of Chen et al. identified a new neuropeptide-related ferroptosis pathway and found that neuropeptide LGI1 receptor ADAM23 not only inhibited the proliferation and migration of ESCCs but also upregulated the ferroptosis pathway. The mechanism may be that overexpressed ADAM23 promotes ferroptosis by consuming GPX4, SLC3A2, and SLC7A11. The up-regulation of ADAM23 is complete by the upstream ARHGEF26-AS1 (lncRNA) regulating miR-372-3p, positively regulating ADAM23 (Chen et al., 2021b).

## Ferroptosis of esophageal cancer cells induced by anticancer therapy

Radiotherapy has always been one of the effective treatments for patients with esophageal cancer, whose principle is DNA double bond breakage and cell cycle stagnation, which is well known. Recently, Lei et al. discovered that after radiotherapy, ROS level and ACSL4 level in FOL-1 cells of esophageal adenocarcinoma were significantly up-regulated, both of which were prerequisites for ferroptosis. At the same time, FOL-1 cells exhibited an adaptive response to radiotherapy by up-regulating the levels of SLC7A11 and GPX4. That is, radiotherapy can up-regulate both the promotion and the inhibition pathways of ferroptosis in FOL-1 cells. On these grounds, they further used inhibitors of SLC7A11 and GPX4 simultaneously with radiotherapy. They found that the sensitivity of FOL-1 to radiotherapy was improved, thus preliminarily revealing the close relationship between the ferroptosis pathway and radiotherapy (Lei et al., 2020). Terpenoids have attracted the attention of researchers because of their excellent pharmacological effects, such as anticancer, anti-inflammation, anti-oxidation, and so on (Ku and Lin, 2013). And Oridonin (Ori) is one of them. Zhang et al. verified Ori's anticancer activity to inhibit esophageal cancer cells' growth in their experiments and proposed the relationship between the anticancer activity of Ori and ferroptosis. After treating of ESCC cell TE-1 by Ori, intracellular iron ions, malondialdehyde (MDA)

levels, and ROS were significantly dose-dependent. In addition, metabolomics analysis showed that Ori significantly inhibited the  $\gamma$ -glutamyl cycle of TE-1 cells, decreasing intracellular glutathione synthesis and thus inducing the ferroptosis of cells (Zhang J. et al., 2021). The anticancer activity of isopropyl lactone in many cancers was confirmed, and its effect in esophageal cancer has been initially proposed in the study of Lu et al. They detected the impact of isopropyl lactone on inhibiting invasion and migration in ESCC Eca109 cells, which was mediated through such means as apoptosis and ferroptosis. After the isopropyl lactone treatment, the isopropyl lactone caused the apoptosis of cells by up-regulating the external apoptosis pathway of death receptor 5 (DR5) to activate cells and, simultaneously, caused ferroptosis by increasing intracellular ROS levels. To verify this, they treated Eca109 cells with ferroptosis inhibitor combined with isopropyl lactone and found that the cell death was saved and the cell viability was improved (Lu et al., 2018). Pentaaminolevulinic acid (5-ALA), a natural amino acid, is widely used in cancer treatment. Current research shows that 5-ALA induces ferroptosis through glutathione peroxidase 4 (GPX4) and HMOX1, and has an anti-tumor effect in ESCC (Shishido et al., 2021).

Preventing the continued proliferation of cancer cells and promoting the death of cancer cells is one of the primary purposes of anti-cancer treatment. As a cell death mode characterized by oxidative damage, ferroptosis has become an essential link in many cancer treatment drugs and means. In addition to their classical anti-tumor effects, the radiotherapy and classical anti-cancer drugs mentioned above have also been confirmed to promote ferroptosis of cancer cells by increasing ferroptosis-inducing factors such as intracellular iron ions and ROS, inhibiting GPX4 expression, reducing GSH content and the like, which is a beneficial and surprising discovery. According to these findings, the existing clinical anti-cancer treatments can be further enhanced, for example, chemoradiotherapy combined with ferroptosis inducer treatment which increases the mortality of cancer cells and also increases the sensitivity of cancer cells to chemoradiotherapy; the design of targeted drugs against ferroptosis inhibitory factors combined them with classical anticancer drug therapy to improve the ability of anti-cancer medications to promote ferroptosis of cancer cells.

## Prediction of the prognosis of esophageal cancer patients by ferroptosis-related genes (FRGs)

Lu et al. systematically identified FRGs TFRC, ATG5, ENPP2, SCP2, MAPK1, and PRKAA1 as valuable genes for predicting the prognosis of ESCC, among which SCP2, MAPK1, and PRKAA1 were identified as independent prognostic genes (Lu T. et al., 2021). Similarly, they identified ALOX12, ALOX12B, ANGPTL7, DRD4, MAPK9, SLC38A1, and



ZNF419 as prognostic FRGs in patients with ESCC, among which the expression of ALOX12, ANGPTL7, DRD4 and MAPK9 in ESCC was significantly decreased. In contrast, the expression of SLC38A1 and ZNF419 was significantly increased, but the expression of ALOX12B was not significantly different. On this basis, the researcher selected SLC38A1 with noticeable expression difference to further explore its influence on the proliferation and migration of ESCC cells and finally concluded that SLC38A1 promoted the proliferation and migration of ESCC cells (Song et al., 2021); Ye et al. identified SRC, FADS2, GLUD1, POLG, ANO6, SLC2A6, PTGS2, ALOXE3, etc. (Ye et al., 2021); Zhao et al. identified six FRGs with prognostic value in 112 ESCC samples (Zhao M. et al., 2022). Among them, the expressions of PRNP, SLC3A2, SLC39A8, and SLC39A14 were negatively correlated with the prognosis of ESCC patients, while the expressions of ATP6V0A1 and LCN2 were the opposite. They also evaluated the infiltration of immune cells, and the results showed that the expressions of ATP6V0A1, SLC39A14, SLC39A8, and LCN2 were positively associated with the infiltration of B cells. In contrast, the expressions of SLC3A2 and PRNP were negatively correlated with the infiltration of B cells. The same study also reported a significant correlation between 74 FRGs (Zhao Y. Y. et al., 2022) and the risk score of esophageal cancer patients, among which 32 genes were positively correlated with the risk score, with the top five genes being HIC1, ACSL3, NNMT, ANO6 and CDO1, and 42 genes were negatively correlated with the risk score, with the top five genes being HAMP, ALOX12B, MAFG, HILPDA and DUOX1 (Shi et al., 2021).

Many ferroptosis-related genes mentioned above have different prognostic values for esophageal cancer patients, even some of which can become independent prognostic factors. The deep exploration and further improvement of these genes can provide early signals for the occurrence and development of esophageal cancer, thereby helping the clinic to take preventive and therapeutic measures earlier. In addition, these ferroptosis-related genes with prognostic values are significantly related to the tumor immune microenvironment. Further, combined with the correlation of immune check inhibition points, this significant correlation can be used clinically to design a more reliable immunotherapy protocol to tap the potential of prognostic ferroptosis-related genes in immunotherapy of esophageal cancer.

## Non-coding RNA regulating FRGs in esophageal cancer cells

CircPVT1 is a circular non-coding RNA and a crucial regulatory factor in the pathogenesis of ESCC. For example, it can enhance the malignant phenotype of ESCC by regulating the miR-4663/Pax and PPAR axis, including the proliferation and invasion of ESCC cells

(Zhong et al., 2019). A recent study showed that circPVT1 was significantly upregulated in 5-fluorouracil-resistant ESCCs, and the knock-down of circPVT1 significantly reduced the expression levels of GPX4 and SLC7A11, which indicated that the overexpression of circPVT1 could upregulate the expression of GPX4 and SLC7A11, thus enhancing the ferroptosis resistance and chemotherapy drug resistance of cancer cells. In addition, their results also showed that CircPVT1 regulated the chemosensitivity of ESCCs through miR-30a-5p/FZD3 axis (Yao et al., 2021). Methylene selenite (MSA) is a selenium substituted compound which realizes the nuclear transfer of NRF2 by down-regulating the expression of Keap1 in ESCCs. The accumulation of NRF2 in the nucleus will strengthen its binding with antioxidant response elements (ARE), thus upregulating the expression of antioxidant-related genes. Further studies showed that miR-200a mainly mediated MSA's down-regulation of Keap1 expression. MSA firstly upregulates the expression of miR-200a, while Keap1 is the direct downstream target of miR-200a. Highly expressed miR-200a inhibits the expression of Keap1, resulting in increased nuclear metastasis of NRF2 and further enhancing the antioxidant activity of cells (Liu et al., 2015). Keap1 is also a direct target of miR-432-3p, which directly binds to the regulatory region of Keap1 and then down-regulates its expression, thereby positively regulating NRF2. Besides, miR-432-3p is over-expressed in primary ESCC, which is closely related to the decreased sensitivity of chemotherapeutic drugs such as cisplatin (CDDP) (Akdemir et al., 2017). Noncoding RNAs directly targeting NRF2 include miR-507 (Yamamoto et al., 2014) and MicroRNA-153-3p (Zuo et al., 2020). miR-507 inhibits the expression of NRF2 through direct targeting, thus inhibiting the carcinogenesis pathway mediated by NRF2. The author found that miR-507 was low in ESCC, thus losing its inhibitory effect on NRF2. To further determine the target genes regulated by NRF2, the expression of eight NRF2 transcription target genes which were obviously inhibited in ESCCs transfected with miR-507 was detected, which further determined the target genes regulated by NRF2, including SLC7A11; MiR-153-3p can inhibit the proliferation of food cells and enhance cisplatin resistance by down-regulating the expression of NRF2 in Eca-109 cells.

Non-coding RNA, as an important regulatory molecule in gene expression, regulates disease occurrence, development, and outcome. With the molecular mechanism of the ferroptosis pathway becoming more apparent, more and more related genes have been confirmed. The discovery and research of the upstream regulation mechanism of these genes have become a hot spot, among which non-coding RNA is widely studied. The non-coding RNA listed above affects the proliferation, invasion, and metastasis of esophageal cancer cells by regulating the ferroptosis pathway during the occurrence and development of esophageal cancer. On these grounds, corresponding detection means can be developed to detect the non-coding RAN with biomarker value in esophageal cancer patients at different stages, which can be applied to clinical diagnosis and staging. With its role in regulating the ferroptosis pathway, small molecular compounds that promote or prevent the

combination of non-coding RNA and target genes can be developed to intervene in the ferroptosis process in esophageal cancer cells.

## Summary and prospect

As the prognosis of early esophageal cancer patients is good, the early diagnosis of esophageal cancer is vital. For mid and late-stage patients, relying on surgery alone is infeasible, and the best treatment method is to combine chemoradiotherapy; however, radiotherapy insensitivity and chemotherapy drug resistance are often one of the main reasons that affect the treatment effect. Presently, the mechanism of ferroptosis in esophageal cancer is extensively studied, including such issues as some ferroptosis inducers combined with chemotherapy drugs have more obvious efficacy than that of the two drugs alone but also improve the sensitivity of chemotherapy drugs. Many ferroptosis-related genes have been verified as prognostic genes of esophageal cancer. The changes in their expression levels in different stages of esophageal cancer patients can provide beneficial information for clinics and robust evidence for clinicians to accurately diagnose and stage. In addition, by up-regulating or down-regulating the essential regulatory point genes in the ferroptosis pathway, the ferroptosis of esophageal cancer cells can be promoted utilizing elevated levels of intracellular iron ions, ROS, and lipid peroxidation, thereby achieving tumor inhibition. Secondly, combined with the current hot immune checkpoint treatment, the correlation between the differentially expressed genes related to ferroptosis and each immune checkpoint in esophageal cancer was analyzed to find out the genes with significant correlation for further design of immune checkpoint related immunotherapy.

The research on the mechanism of ferroptosis is deepening, but there are still more elaborate and complex networks of signal pathways waiting for us to explore. In future research, we need to reveal and analyze the molecular mechanism of ferroptosis in cells more comprehensively

from metabolism, immunity, and genetics perspectives. There is relatively little research on the mechanism of ferroptosis in esophageal cancer. Its research mainly focuses on predicting the prognosis of esophageal cancer patients, providing us with many potentially valuable genes. Next, the focus of our study should be to find out the most valuable FRGs from the data supplied by bioinformatics for in-depth mechanism research and dig out more mechanisms for regulating ferroptosis. The research results will provide clinical treatment strategies and powerful evidence in pharmacology to develop corresponding ferroptosis inhibitors or inducers. For cancer patients who have developed chemotherapy drug resistance, applying the ferroptosis mechanism in treatment will bring them new hope.

## Author contributions

HL conceptualized this review, decided on the content, and RM and HL wrote the manuscript. RM and KW prepared the figures. HL revised the manuscript. All authors read and approved the final manuscript and agreed to be accountable for all aspects of the work. All authors read and approved the final manuscript.

## Funding

This work was supported by the National Natural Science Foundation of China (81660459).

## Conflict of interest

The authors declare that the research was conducted in the absence of any commercial or financial relationships that could be construed as a potential conflict of interest.

## References

- Akdemir, B., Nakajima, Y., Inazawa, J., and Inoue, J. (2017). miR-432 induces NRF2 stabilization by directly targeting KEAP1. *Mol. Cancer Res.* 15, 1570–1578. doi:10.1158/1541-7786.MCR-17-0232
- Alvarez, S. W., Sviderskiy, V. O., Terzi, E. M., Papagiannakopoulos, T., Moreira, A. L., Adams, S., et al. (2017). NFS1 undergoes positive selection in lung tumours and protects cells from ferroptosis. *Nature* 551, 639–643. doi:10.1038/nature24637
- Anderson, G. J., and Frazer, D. M. (2017). Current understanding of iron homeostasis. *Am. J. Clin. Nutr.* 106, 1559S–1566S. doi:10.3945/ajcn.117.155804
- Anandhan, A., Dodson, M., Schmidlin, C. J., Liu, P., and Zhang, D. D. (2020). Breakdown of an ironclad defense system: The critical role of NRF2 in mediating ferroptosis. *Cell Chem. Biol.* 27, 436–447.
- Arnold, M., Soerjomataram, I., Ferlay, J., and Forman, D. (2015). Global incidence of oesophageal cancer by histological subtype in 2012. *Gut* 64, 381–387. doi:10.1136/gutjnl-2014-308124
- Aversa, I., Chirillo, R., Chiarella, E., Zolea, F., Di Sanzo, M., Biamonte, F., et al. (2018). Chemoresistance in H-ferritin silenced cells: The role of NF- $\kappa$ B. *Int. J. Mol. Sci.* 19, E2969. doi:10.3390/ijms19102969
- Bassi, M. T., Gasol, E., Manzoni, M., Pineda, M., Riboni, M., Martín, R., et al. (2001). Identification and characterisation of human xCT that co-expresses, with 4F2 heavy chain, the amino acid transport activity system xc. *Pflugers Arch.* 442, 286–296. doi:10.1007/s004240100537
- Bentinger, M., Brismar, K., and Dallner, G. (2007). The antioxidant role of coenzyme Q. *Mitochondrion* 7, S41–S50. doi:10.1016/j.mito.2007.02.006
- Bersuker, K., Hendricks, J. M., Li, Z., Magtanong, L., Ford, B., Tang, P. H., et al. (2019). The CoQ oxidoreductase FSP1 acts parallel to GPX4 to inhibit ferroptosis. *Nature* 575, 688–692. doi:10.1038/s41586-019-1705-2
- Cai, J., Yi, M., Tan, Y., Li, X., Li, G., Zeng, Z., et al. (2021). Natural product triptolide induces GSDME-mediated pyroptosis in head and neck cancer through suppressing mitochondrial hexokinase-II. *J. Exp. Clin. Cancer Res.* 40, 190. doi:10.1186/s13046-021-01995-7

- Chen, B., Chen, Z., Liu, M., Gao, X., Cheng, Y., Wei, Y., et al. (2019). Inhibition of neuronal ferroptosis in the acute phase of intracerebral hemorrhage shows long-term cerebroprotective effects. *Brain Res. Bull.* 153, 122–132. doi:10.1016/j.brainresbull.2019.08.013
- Chen, C., Huang, Y., Xia, P., Zhang, F., Li, L., Wang, E., et al. (2021a). Long noncoding RNA Meg3 mediates ferroptosis induced by oxygen and glucose deprivation combined with hyperglycemia in rat brain microvascular endothelial cells, through modulating the p53/GPX4 axis. *Eur. J. Histochem.* 65, 3224. doi:10.4081/ejh.2021.3224
- Chen, C., Zhao, J., Liu, J. N., and Sun, C. (2021b). Mechanism and role of the neuropeptide LGI1 receptor ADAM23 in regulating biomarkers of ferroptosis and progression of esophageal cancer. *Dis. Markers* 2021, 9227897. doi:10.1155/2021/9227897
- Chen, D., Chu, B., Yang, X., Liu, Z., Jin, Y., Kon, N., et al. (2021). iPLA2 $\beta$ -mediated lipid detoxification controls p53-driven ferroptosis independent of GPX4. *Nat. Commun.* 12, 3644. doi:10.1038/s41467-021-23902-6
- Chen, P. H., Wu, J., Ding, C. C., Lin, C. C., Pan, S., Bossa, N., et al. (2020). Kinome screen of ferroptosis reveals a novel role of ATM in regulating iron metabolism. *Cell Death Differ.* 27, 1008–1022. doi:10.1038/s41418-019-0393-7
- Chen, W., W., Fu, J., Chen, Y., Li, Y., Ning, L., Huang, D., et al. (2021). Circular RNA circKIF4A facilitates the malignant progression and suppresses ferroptosis by sponging miR-1231 and upregulating GPX4 in papillary thyroid cancer. *Aging (Albany NY)* 13, 16500–16512. doi:10.18632/aging.203172
- Cheng, J., Fan, Y. Q., Liu, B. H., Zhou, H., Wang, J. M., and Chen, Q. X. (2020). ACSL4 suppresses glioma cells proliferation via activating ferroptosis. *Oncol. Rep.* 43, 147–158. doi:10.3892/or.2019.7419
- Chu, B., Kon, N., Chen, D., Li, T., Liu, T., Jiang, L., et al. (2019). ALOX12 is required for p53-mediated tumour suppression through a distinct ferroptosis pathway. *Nat. Cell Biol.* 21, 579–591. doi:10.1038/s41556-019-0305-6
- Codipilly, D. C., Qin, Y., Dawsey, S. M., Kisiel, J., Topazian, M., Ahlquist, D., et al. (2018). Screening for esophageal squamous cell carcinoma: Recent advances. *Gastrointest. Endosc.* 88, 413–426. doi:10.1016/j.gie.2018.04.2352
- Cui, Y., Qin, L., Tian, D., Wang, T., Fan, L., Zhang, P., et al. (2018). ZEB1 promotes chemoresistance to cisplatin in ovarian cancer cells by suppressing SLC3A2. *Chemotherapy* 63, 262–271. doi:10.1159/000493864
- D'Agostino, S., Lanzillotta, D., Varano, M., Botta, C., Baldrini, A., Bilotta, A., et al. (2018). The receptor protein tyrosine phosphatase PTPRJ negatively modulates the CD98hc oncoprotein in lung cancer cells. *Oncotarget* 9, 23334–23348. doi:10.18632/oncotarget.25101
- Dev, S., and Babitt, J. L. (2017). Overview of iron metabolism in health and disease. *Hemodial. Int.* 21 (1), S6–s20. doi:10.1111/hdi.12542
- Di Sanzo, M., Chirillo, R., Aversa, I., Biamonte, F., Santamaria, G., Giovannone, E. D., et al. (2018). shRNA targeting of ferritin heavy chain activates H19/miR-675 axis in K562 cells. *Gene* 657, 92–99. doi:10.1016/j.gene.2018.03.027
- Ding, Y., Chen, X., Liu, C., Ge, W., Wang, Q., Hao, X., et al. (2021). Identification of a small molecule as inducer of ferroptosis and apoptosis through ubiquitination of GPX4 in triple negative breast cancer cells. *J. Hematol. Oncol.* 14, 19. doi:10.1186/s13045-020-01016-8
- Dixon, S. J., Lemberg, K. M., Lamprecht, M. R., Skouta, R., Zaitsev, E. M., Gleason, C. E., et al. (2012). Ferroptosis: An iron-dependent form of nonapoptotic cell death. *Cell* 149, 1060–1072. doi:10.1016/j.cell.2012.03.042
- Dixon, S. J., Winter, G. E., Musavi, L. S., Lee, E. D., Snijder, B., Rebsamen, M., et al. (2015). Human haploid cell genetics reveals roles for lipid metabolism genes in nonapoptotic cell death. *ACS Chem. Biol.* 10, 1604–1609. doi:10.1021/acscchembio.5b00245
- Dodson, M., Castro-Portuguez, R., and Zhang, D. D. (2019). NRF2 plays a critical role in mitigating lipid peroxidation and ferroptosis. *Redox Biol.* 23, 101107. doi:10.1016/j.redox.2019.101107
- Dong, H., Qiang, Z., Chai, D., Peng, J., Xia, Y., Hu, R., et al. (2020). Nrf2 inhibits ferroptosis and protects against acute lung injury due to intestinal ischemia reperfusion via regulating SLC7A11 and HO-1. *Aging (Albany NY)* 12, 12943–12959. doi:10.18632/aging.103378
- Dev, S., and Babitt, J. L. (2017). Overview of iron metabolism in health and disease. *Hemodial. Int.* 21 (1), S6–S20.
- Fang, X., Wang, H., Han, D., Xie, E., Yang, X., Wei, J., et al. (2019). Ferroptosis as a target for protection against cardiomyopathy. *Proc. Natl. Acad. Sci. U. S. A.* 116, 2672–2680. doi:10.1073/pnas.1821022116
- Feng, L., Zhao, K., Sun, L., Yin, X., Zhang, J., Liu, C., et al. (2021). SLC7A11 regulated by NRF2 modulates esophageal squamous cell carcinoma radiosensitivity by inhibiting ferroptosis. *J. Transl. Med.* 19, 367. doi:10.1186/s12967-021-03042-7
- Fuhrmann, D. C., Mondorf, A., Beifus, J., Jung, M., and Brüne, B. (2020). Hypoxia inhibits ferritinophagy, increases mitochondrial ferritin, and protects from ferroptosis. *Redox Biol.* 36, 101670. doi:10.1016/j.redox.2020.101670
- Gamble, L. D., Purgato, S., Murray, J., Xiao, L., Yu, D. M. T., Hanssen, K. M., et al. (2019). Inhibition of polyamine synthesis and uptake reduces tumor progression and prolongs survival in mouse models of neuroblastoma. *Sci. Transl. Med.* 11, eaau1099. doi:10.1126/scitranslmed.aau1099
- Gao, Q., Zhang, G., Zheng, Y., Yang, Y., Chen, C., Xia, J., et al. (2020). SLC27A5 deficiency activates NRF2/TXNRD1 pathway by increased lipid peroxidation in HCC. *Cell Death Differ.* 27, 1086–1104. doi:10.1038/s41418-019-0399-1
- Gao, R., Kalathur, R. K. R., Coto-Llerena, M., Ercan, C., Buechel, D., Shuang, S., et al. (2021). YAP/TAZ and ATF4 drive resistance to Sorafenib in hepatocellular carcinoma by preventing ferroptosis. *EMBO Mol. Med.* 13, e14351. doi:10.15252/emmm.202114351
- Guan, Z., Chen, J., Li, X., and Dong, N. (2020). Tanshinone IIA induces ferroptosis in gastric cancer cells through p53-mediated SLC7A11 down-regulation. *Biosci. Rep.* 40, BSR20201807. doi:10.1042/BSR20201807
- He, G. N., Bao, N. R., Wang, S., Xi, M., Zhang, T. H., and Chen, F. S. (2021). Ketamine induces ferroptosis of liver cancer cells by targeting lncRNA PVT1/miR-214-3p/GPX4. *Drug Des. devel. Ther.* 15, 3965–3978. doi:10.2147/DDDT.S332847
- Heider, M., Eichner, R., Stroth, J., Morath, V., Kuisl, A., Zecha, J., et al. (2021). The IMiD target CRBN determines HSP90 activity toward transmembrane proteins essential in multiple myeloma. *Mol. Cell* 81, 1170–1186.e10. doi:10.1016/j.molcel.2020.12.046
- Hirano, H., and Kato, K. (2019). Systemic treatment of advanced esophageal squamous cell carcinoma: Chemotherapy, molecular-targeting therapy and immunotherapy. *Jpn. J. Clin. Oncol.* 49, 412–420. doi:10.1093/jjco/hyz034
- Hoffmann, C., Dietrich, M., Herrmann, A. K., Schacht, T., Albrecht, P., and Methner, A. (2017). Dimethyl fumarate induces glutathione recycling by upregulation of glutathione reductase. *Oxid. Med. Cell. Longev.* 2017, 6093903. doi:10.1155/2017/6093903
- Hou, Y., Cai, S., Yu, S., and Lin, H. (2021). Metformin induces ferroptosis by targeting miR-324-3p/GPX4 axis in breast cancer. *Acta Biochim. Biophys. Sin.* 53, 333–341. doi:10.1093/abbs/gmaa180
- Huang, J., Tabbi-Anneni, I., Gunda, V., and Wang, L. (2010). Transcription factor Nrf2 regulates SHP and lipogenic gene expression in hepatic lipid metabolism. *Am. J. Physiol. Gastrointest. Liver Physiol.* 299, G1211–G1221. doi:10.1152/ajpgi.00322.2010
- Iida, Y., Okamoto-Katsuyama, M., Maruoka, S., Mizumura, K., Shimizu, T., Shikano, S., et al. (2021). Effective ferroptotic small-cell lung cancer cell death from SLC7A11 inhibition by sulforaphane. *Oncol. Lett.* 21, 71. doi:10.3892/ol.2020.12332
- Jamar, N. H., Kritsiligkou, P., and Grant, C. M. (2017). The non-stop decay mRNA surveillance pathway is required for oxidative stress tolerance. *Nucleic Acids Res.* 45, 6881–6893. doi:10.1093/nar/gkx306
- Jemal, A., Bray, F., Center, M. M., Ferlay, J., Ward, E., and Forman, D. (2011). Global cancer statistics. *Ca. Cancer J. Clin.* 61, 69–90. doi:10.3322/caac.20107
- Jiang, B., Zhao, Y., Shi, M., Song, L., Wang, Q., Qin, Q., et al. (2020). DNAJB6 promotes ferroptosis in esophageal squamous cell carcinoma. *Dig. Dis. Sci.* 65, 1999–2008. doi:10.1007/s10620-019-05929-4
- Jiang, L., Kon, N., Li, T., Wang, S. J., Su, T., Hibshoosh, H., et al. (2015). Ferroptosis as a p53-mediated activity during tumour suppression. *Nature* 520, 57–62. doi:10.1038/nature14344
- Kagan, V. E., Mao, G., Qu, F., Angeli, J. P., Doll, S., Croix, C. S., et al. (2017). Oxidized arachidonic and adrenic PEs navigate cells to ferroptosis. *Nat. Chem. Biol.* 13, 81–90. doi:10.1038/nchembio.2238
- Kensler, T. W., Wakabayashi, N., and Biswal, S. (2007). Cell survival responses to environmental stresses via the Keap1-Nrf2-ARE pathway. *Annu. Rev. Pharmacol. Toxicol.* 47, 89–116. doi:10.1146/annurev.pharmtox.46.120604.141046
- Kerins, M. J., and Ooi, A. (2018). The roles of NRF2 in modulating cellular iron homeostasis. *Antioxid. Redox Signal.* 29, 1756–1773. doi:10.1089/ars.2017.7176
- Kong, R., Wang, N., Han, W., Bao, W., and Lu, J. (2021). IFN $\gamma$ -mediated repression of system xc(-) drives vulnerability to induced ferroptosis in hepatocellular carcinoma cells. *J. Leukoc. Biol.* 110, 301–314. doi:10.1002/JLB.3MA1220-815RRR
- Koppula, P., Zhuang, L., and Gan, B. (2021). Cystine transporter slc7a11/xCT in cancer: Ferroptosis, nutrient dependency, and cancer therapy. *Protein Cell* 12, 599–620. doi:10.1007/s13238-020-00789-5
- Kroemer, G., Galluzzi, L., Vandenabeele, P., Abrams, J., Alnemri, E. S., Baehrecke, E. H., et al. (2009). Classification of cell death: Recommendations of the nomenclature committee on cell death 2009. *Cell Death Differ.* 16, 3–11. doi:10.1038/cdd.2008.150

- Ku, C. M., and Lin, J. Y. (2013). Anti-inflammatory effects of 27 selected terpenoid compounds tested through modulating Th1/Th2 cytokine secretion profiles using murine primary splenocytes. *Food Chem.* 141, 1104–1113. doi:10.1016/j.foodchem.2013.04.044
- Kwon, M. Y., Park, E., Lee, S. J., and Chung, S. W. (2015). Heme oxygenase-1 accelerates erastin-induced ferroptotic cell death. *Oncotarget* 6, 24393–24403. doi:10.18632/oncotarget.5162
- Lachiaer, E., Louandre, C., Godin, C., Saidak, Z., Baert, M., Diouf, M., et al. (2014). Sorafenib induces ferroptosis in human cancer cell lines originating from different solid tumors. *Anticancer Res.* 34, 6417–6422.
- Lei, G., Zhang, Y., Koppula, P., Liu, X., Zhang, J., Lin, S. H., et al. (2020). The role of ferroptosis in ionizing radiation-induced cell death and tumor suppression. *Cell Res.* 30, 146–162. doi:10.1038/s41422-019-0263-3
- Li, W., Dong, X., He, C., Tan, G., Li, Z., Zhai, B., et al. (2019). LncRNA SNHG1 contributes to sorafenib resistance by activating the Akt pathway and is positively regulated by miR-21 in hepatocellular carcinoma cells. *J. Exp. Clin. Cancer Res.* 38, 183. doi:10.1186/s13046-019-1177-0
- Lin, W., Wang, C., Liu, G., Bi, C., Wang, X., Zhou, Q., et al. (2020). SLC7A11/xCT in cancer: Biological functions and therapeutic implications. *Am. J. Cancer Res.* 10, 3106–3126.
- Liu, M., Hu, C., Xu, Q., Chen, L., Ma, K., Xu, N., et al. (2015). Methylseleninic acid activates Keap1/Nrf2 pathway via up-regulating miR-200a in human esophageal squamous cell carcinoma cells. *Biosci. Rep.* 35, e00256. doi:10.1042/BSR20150092
- Liu, Y., and Gu, W. (2022). p53 in ferroptosis regulation: the new weapon for the old guardian. *Cell Death Differ.* 29, 895–910. doi:10.1038/s41418-022-00943-y
- Lu, S. C. (2013). Glutathione synthesis. *Biochim. Biophys. Acta* 1830, 3143–3153. doi:10.1016/j.bbagen.2012.09.008
- Lu, T., Xu, R., Li, Q., Zhao, J. Y., Peng, B., Zhang, H., et al. (2021). Systematic profiling of ferroptosis gene signatures predicts prognostic factors in esophageal squamous cell carcinoma. *Mol. Ther. Oncolytics* 21, 134–143. doi:10.1016/j.omto.2021.02.011
- Lu, X., Kang, N., Ling, X., Pan, M., Du, W., and Gao, S. (2021). MiR-27a-3p promotes non-small cell lung cancer through slc7a11-mediated-ferroptosis. *Front. Oncol.* 11, 759346. doi:10.3389/fonc.2021.759346
- Lu, Y., Qin, H., Jiang, B., Lu, W., Hao, J., Cao, W., et al. (2021). KLF2 inhibits cancer cell migration and invasion by regulating ferroptosis through GPX4 in clear cell renal cell carcinoma. *Cancer Lett.* 522, 1–13. doi:10.1016/j.canlet.2021.09.014
- Lu, Z., Zhang, G., Zhang, Y., Hua, P., Fang, M., Wu, M., et al. (2018). Isoalantolactone induces apoptosis through reactive oxygen species-dependent upregulation of death receptor 5 in human esophageal cancer cells. *Toxicol. Appl. Pharmacol.* 352, 46–58. doi:10.1016/j.taap.2018.05.026
- Luo, Y., Gao, X., Zou, L., Lei, M., Feng, J., and Hu, Z. (2021). Bavachin induces ferroptosis through the STAT3/P53/slc7a11 Axis in osteosarcoma cells. *Oxid. Med. Cell. Longev.* 2021, 1783485. doi:10.1155/2021/1783485
- Ma, L., Chen, T., Zhang, X., Miao, Y., Tian, X., Yu, K., et al. (2021). The m(6)A reader YTHDC2 inhibits lung adenocarcinoma tumorigenesis by suppressing SLC7A11-dependent antioxidant function. *Redox Biol.* 38, 101801. doi:10.1016/j.redox.2020.101801
- Ma, N., Wei, W., Fan, X., and Ci, X. (2019). Farrerol attenuates cisplatin-induced nephrotoxicity by inhibiting the reactive oxygen species-mediated oxidation, inflammation, and apoptotic signaling pathways. *Front. Physiol.* 10, 1419. doi:10.3389/fphys.2019.01419
- Ma, S., Henson, E. S., Chen, Y., and Gibson, S. B. (2016). Ferroptosis is induced following siramesine and lapatinib treatment of breast cancer cells. *Cell Death Dis.* 7, e2307. doi:10.1038/cddis.2016.208
- Maiorino, M., Conrad, M., and Ursini, F. (2018). GPx4, lipid peroxidation, and cell death: Discoveries, rediscoveries, and open issues. *Antioxid. Redox Signal.* 29, 61–74. doi:10.1089/ars.2017.7115
- Mancias, J. D., Pontano Vaites, L., Nissim, S., Biancur, D. E., Kim, A. J., Wang, X., et al. (2015). Ferritinophagy via NCOA4 is required for erythropoiesis and is regulated by iron dependent HERC2-mediated proteolysis. *Elife* 4, e10308. doi:10.7554/eLife.10308
- Mancias, J. D., Wang, X., Gygi, S. P., Harper, J. W., and Kimmelman, A. C. (2014). Quantitative proteomics identifies NCOA4 as the cargo receptor mediating ferritinophagy. *Nature* 509, 105–109. doi:10.1038/nature13148
- Mao, C., Liu, X., Zhang, Y., Lei, G., Yan, Y., Lee, H., et al. (2021). DHODH-mediated ferroptosis defence is a targetable vulnerability in cancer. *Nature* 593, 586–590. doi:10.1038/s41586-021-03539-7
- Mohamad Fairus, A. K., Choudhary, B., Hosahalli, S., Kavitha, N., and Shatrah, O. (2017). Dihydroorotate dehydrogenase (DHODH) inhibitors affect ATP depletion, endogenous ROS and mediate S-phase arrest in breast cancer cells. *Biochimie* 135, 154–163. doi:10.1016/j.biochi.2017.02.003
- Montero, J. C., Calvo-Jiménez, E., Del Carmen, S., Abad, M., Ocaña, A., and Pandiella, A. (2022). Surfaceome analyses uncover CD98hc as an antibody drug-conjugate target in triple negative breast cancer. *J. Exp. Clin. Cancer Res.* 41, 106. doi:10.1186/s13046-022-02330-4
- Mou, Y., Wang, J., Wu, J., He, D., Zhang, C., Duan, C., et al. (2019). Ferroptosis, a new form of cell death: Opportunities and challenges in cancer. *J. Hematol. Oncol.* 12, 34. doi:10.1186/s13045-019-0720-y
- Nakajima, M., Kato, H., Miyazaki, T., Inose, T., Tanaka, N., Suzuki, S., et al. (2016). An absolute standardized uptake value is more useful than the decreased rate of uptake of FDG-PET to predict responses to neoadjuvant chemoradiotherapy for esophageal cancer. *Open J. Gastroenterol.* 06, 373–385. doi:10.4236/ojgas.2016.611040
- Popławski, P., Wiśniewski, J. R., Rijntjes, E., Richards, K., Rybicka, B., Köhrle, J., et al. (2017). Restoration of type 1 iodothyronine deiodinase expression in renal cancer cells downregulates oncoproteins and affects key metabolic pathways as well as anti-oxidative system. *PLoS One* 12, e0190179. doi:10.1371/journal.pone.0190179
- Qi, J., Kim, J. W., Zhou, Z., Lim, C. W., and Kim, B. (2020). Ferroptosis affects the progression of nonalcoholic steatohepatitis via the modulation of lipid peroxidation-mediated cell death in mice. *Am. J. Pathol.* 190, 68–81. doi:10.1016/j.ajpath.2019.09.011
- Sehitogullari, A., Aslan, M., Sayir, F., Kahraman, A., and Demir, H. (2014). Serum paraoxonase-1 enzyme activities and oxidative stress levels in patients with esophageal squamous cell carcinoma. *Redox Rep.* 19, 199–205. doi:10.1179/1351000214Y.00000000091
- Sha, W., Hu, F., Xi, Y., Chu, Y., and Bu, S. (2021). Mechanism of ferroptosis and its role in type 2 diabetes mellitus. *J. Diabetes Res.* 2021, 9999612. doi:10.1155/2021/9999612
- Shen, L. D., Qi, W. H., Bai, J. J., Zuo, C. Y., Bai, D. L., Gao, W. D., et al. (2021). Resibufogenin inhibited colorectal cancer cell growth and tumorigenesis through triggering ferroptosis and ROS production mediated by GPX4 inactivation. *Anat. Rec.* 304, 313–322. doi:10.1002/ar.24378
- Shi, X., Liu, X., Pan, S., Ke, Y., Li, Y., Guo, W., et al. (2021). A novel autophagy-related long non-coding RNA signature to predict prognosis and therapeutic response in esophageal squamous cell carcinoma. *Int. J. Gen. Med.* 14, 8325–8339. doi:10.2147/IJGM.S333697
- Shishido, Y., Amisaki, M., Matsumi, Y., Yakura, H., Nakayama, Y., Miyauchi, W., et al. (2021). Antitumor effect of 5-aminolevulinic acid through ferroptosis in esophageal squamous cell carcinoma. *Ann. Surg. Oncol.* 28, 3996–4006. doi:10.1245/s10434-020-09334-4
- Song, J., Liu, Y., Guan, X., Zhang, X., Yu, W., and Li, Q. (2021). A novel ferroptosis-related biomarker signature to predict overall survival of esophageal squamous cell carcinoma. *Front. Mol. Biosci.* 8, 675193. doi:10.3389/fmolb.2021.675193
- Song, X., Xie, Y., Kang, R., Hou, W., Sun, X., Epperly, M. W., et al. (2016). FANCD2 protects against bone marrow injury from ferroptosis. *Biochem. Biophys. Res. Commun.* 480, 443–449. doi:10.1016/j.bbrc.2016.10.068
- Song, X., Zhu, S., Chen, P., Hou, W., Wen, Q., Liu, J., et al. (2018). AMPK-mediated BECN1 phosphorylation promotes ferroptosis by directly blocking system X(c) activity. *Curr. Biol.* 28, 2388–2399. e5. doi:10.1016/j.cub.2018.05.094
- Sugiura, M., Sato, H., Okabe, A., Fukuyo, M., Mano, Y., Shinohara, K. I., et al. (2021). Identification of AR-V7 downstream genes commonly targeted by AR/AR-V7 and specifically targeted by AR-V7 in castration resistant prostate cancer. *Transl. Oncol.* 14, 100915. doi:10.1016/j.tranon.2020.100915
- Sui, X., Zhang, R., Liu, S., Duan, T., Zhai, L., Zhang, M., et al. (2018). RSL3 drives ferroptosis through GPX4 inactivation and ROS production in colorectal cancer. *Front. Pharmacol.* 9, 1371. doi:10.3389/fphar.2018.01371
- Sun, D., Li, Y. C., and Zhang, X. Y. (2021). Lidocaine promoted ferroptosis by targeting miR-382-5p/SLC7A11 Axis in ovarian and breast cancer. *Front. Pharmacol.* 12, 681223. doi:10.3389/fphar.2021.681223
- Sun, X., Niu, X., Chen, R., He, W., Chen, D., Kang, R., et al. (2016). Metallothionein-1G facilitates sorafenib resistance through inhibition of ferroptosis. *Hepatology* 64, 488–500. doi:10.1002/hep.28574
- Sun, Y., Berleth, N., Wu, W., Schlütermann, D., Deitersen, J., Stuhldreier, F., et al. (2021). Fin56-induced ferroptosis is supported by autophagy-mediated GPX4 degradation and functions synergistically with mTOR inhibition to kill bladder cancer cells. *Cell Death Dis.* 12, 1028. doi:10.1038/s41419-021-04306-2
- Takahashi, T., Okamoto, T., Mori, K., Sayo, H., and Kishi, T. (1993). Distribution of ubiquinone and ubiquinol homologues in rat tissues and subcellular fractions. *Lipids* 28, 803–809. doi:10.1007/BF02536234
- Wang, L., Liu, Y., Du, T., Yang, H., Lei, L., Guo, M., et al. (2020). ATF3 promotes erastin-induced ferroptosis by suppressing system Xc. *Cell Death Differ.* 27, 662–675. doi:10.1038/s41418-019-0380-z



- Wang, Q., Bin, C., Xue, Q., Gao, Q., Huang, A., Wang, K., et al. (2021). GSTZ1 sensitizes hepatocellular carcinoma cells to sorafenib-induced ferroptosis via inhibition of NRF2/GPX4 axis. *Cell Death Dis.* 12, 426. doi:10.1038/s41419-021-03718-4
- Wang, R., Xing, R., Su, Q., Yin, H., Wu, D., Lv, C., et al. (2021). Knockdown of SFRS9 inhibits progression of colorectal cancer through triggering ferroptosis mediated by GPX4 reduction. *Front. Oncol.* 11, 683589. doi:10.3389/fonc.2021.683589
- Wang, T. X., Liang, J. Y., Zhang, C., Xiong, Y., Guan, K. L., and Yuan, H. X. (2019). The oncometabolite 2-hydroxyglutarate produced by mutant IDH1 sensitizes cells to ferroptosis. *Cell Death Dis.* 10, 755. doi:10.1038/s41419-019-1984-4
- Wang, X., Chen, Y., Wang, X., Tian, H., Wang, Y., Jin, J., et al. (2021). Stem cell factor SOX2 confers ferroptosis resistance in lung cancer via upregulation of SLC7A11. *Cancer Res.* 81, 5217–5229. doi:10.1158/0008-5472.CAN-21-0567
- Wang, Y., Zhao, G., Condello, S., Huang, H., Cardenas, H., Tanner, E. J., et al. (2021). Frizzled-7 identifies platinum-tolerant ovarian cancer cells susceptible to ferroptosis. *Cancer Res.* 81, 384–399. doi:10.1158/0008-5472.CAN-20-1488
- Wang, Z., Zhang, X., Tian, X., Yang, Y., Ma, L., Wang, J., et al. (2021). CREB stimulates GPX4 transcription to inhibit ferroptosis in lung adenocarcinoma. *Oncol. Rep.* 45, 88. doi:10.3892/or.2021.8039
- Xia, Y., Liu, S., Li, C., Ai, Z., Shen, W., Ren, W., et al. (2020). Discovery of a novel ferroptosis inducer-talaroconvolutin A-killing colorectal cancer cells in vitro and in vivo. *Cell Death Dis.* 11, 988. doi:10.1038/s41419-020-03194-2
- Xie, Y., Hou, W., Song, X., Yu, Y., Huang, J., Sun, X., et al. (2016). Ferroptosis: Process and function. *Cell Death Differ.* 23, 369–379. doi:10.1038/cdd.2015.158
- Xiong, Y., Li, Y., Chengxiang, F., Qian, W., Zhang, W., Yi, Z., et al. (2020). Data mining analysis of SLC7A11 expression in esophageal cancer and its involvement in regulating ferroptosis through the P53/ROS Metabolic Pathway. *Carcinog. Teratogenesis Mutagen.* 32, 126–131. doi:10.3969/j.issn.1004-616x.2020.02.008
- Xu, T., Ding, W., Ji, X., Ao, X., Liu, Y., Yu, W., et al. (2019). Molecular mechanisms of ferroptosis and its role in cancer therapy. *J. Cell. Mol. Med.* 23, 4900–4912. doi:10.1111/jcmm.14511
- Xu, Y., Lv, D., Yan, C., Su, H., Zhang, X., Shi, Y., et al. (2022). METTL3 promotes lung adenocarcinoma tumor growth and inhibits ferroptosis by stabilizing SLC7A11 m(6)A modification. *Cancer Cell Int.* 22, 11. doi:10.1186/s12935-021-02433-6
- Yamamoto, S., Inoue, J., Kawano, T., Kozaki, K., Omura, K., and Inazawa, J. (2014). The impact of miRNA-based molecular diagnostics and treatment of NRF2-stabilized tumors. *Mol. Cancer Res.* 12, 58–68. doi:10.1158/1541-7786.MCR-13-0246-T
- Yan, B., Ai, Y., Sun, Q., Ma, Y., Cao, Y., Wang, J., et al. (2021). Membrane damage during ferroptosis is caused by oxidation of phospholipids catalyzed by the oxidoreductases POR and CYB5R1. *Mol. Cell* 81, 355–369.e10.
- Yang, J., Zhou, Y., Xie, S., Wang, J., Li, Z., Chen, L., et al. (2021). Metformin induces Ferroptosis by inhibiting UFMylation of SLC7A11 in breast cancer. *J. Exp. Clin. Cancer Res.* 40, 206. doi:10.1186/s13046-021-02012-7
- Yao, W., Wang, J., Meng, F., Zhu, Z., Jia, X., Xu, L., et al. (2021). Circular RNA CircPVT1 inhibits 5-fluorouracil chemosensitivity by regulating ferroptosis through MiR-30a-5p/FZD3 Axis in esophageal cancer cells. *Front. Oncol.* 11, 780938. doi:10.3389/fonc.2021.780938
- Ye, J., Wu, Y., Cai, H., Sun, L., Deng, W., Liang, R., et al. (2021). Development and validation of a ferroptosis-related gene signature and nomogram for predicting the prognosis of esophageal squamous cell carcinoma. *Front. Genet.* 12, 697524. doi:10.3389/fgene.2021.697524
- Yi, R., Wang, H., Deng, C., Wang, X., Yao, L., Niu, W., et al. (2020). Dihydroartemisinin initiates ferroptosis in glioblastoma through GPX4 inhibition. *Biosci. Rep.* 40, BSR20193314. doi:10.1042/BSR20193314
- Yu, Y., Xie, Y., Cao, L., Yang, L., Yang, M., Lotze, M. T., et al. (2015). The ferroptosis inducer erastin enhances sensitivity of acute myeloid leukemia cells to chemotherapeutic agents. *Mol. Cell. Oncol.* 2, e1054549. doi:10.1080/23723556.2015.1054549
- Yuan, L., Li, S., Chen, Q., Xia, T., Luo, D., Li, L., et al. (2022). EBV infection-induced GPX4 promotes chemoresistance and tumor progression in nasopharyngeal carcinoma. *Cell Death Differ.* 29, 1513–1527. doi:10.1038/s41418-022-00939-8
- Zhang, J., Wang, N., Zhou, Y., Wang, K., Sun, Y., Yan, H., et al. (2021). Oridonin induces ferroptosis by inhibiting gamma-glutamyl cycle in TE1 cells. *Phytother. Res.* 35, 494–503. doi:10.1002/ptr.6829
- Zhang, K. R., Zhang, Y. F., Lei, H. M., Tang, Y. B., Ma, C. S., Lv, Q. M., et al. (2021). Targeting AKR1B1 inhibits glutathione de novo synthesis to overcome acquired resistance to EGFR-targeted therapy in lung cancer. *Sci. Transl. Med.* 13, eabg6428. doi:10.1126/scitranslmed.abg6428
- Zhang, L., Liu, W., Liu, F., Wang, Q., Song, M., Yu, Q., et al. (2020). IMCA induces ferroptosis mediated by SLC7A11 through the AMPK/mTOR pathway in colorectal cancer. *Oxid. Med. Cell. Longev.* 2020, 1675613. doi:10.1155/2020/1675613
- Zhang, Y., Koppula, P., and Gan, B. (2019). Regulation of H2A ubiquitination and SLC7A11 expression by BAP1 and PRC1. *Cell Cycle* 18, 773–783. doi:10.1080/15384101.2019.1597506
- Zhao, L., Peng, Y., He, S., Li, R., Wang, Z., Huang, J., et al. (2021). Apatinib induced ferroptosis by lipid peroxidation in gastric cancer. *Gastric Cancer* 24, 642–654. doi:10.1007/s10120-021-01159-8
- Zhao, M., Li, M., Zheng, Y., Hu, Z., Liang, J., Bi, G., et al. (2022). Identification and analysis of a prognostic ferroptosis and iron-metabolism signature for esophageal squamous cell carcinoma. *J. Cancer* 13, 1611–1622. doi:10.7150/jca.68568
- Zhao, Y. Y., Yang, Y. Q., Sheng, H. H., Tang, Q., Han, L., Wang, S. M., et al. (2022). GPX4 plays a crucial role in Fuzheng Kang'ai decoction-induced non-small cell lung cancer cell ferroptosis. *Front. Pharmacol.* 13, 851680. doi:10.3389/fphar.2022.851680
- Zhong, R., Chen, Z., Mo, T., Li, Z., and Zhang, P. (2019). Potential Role of circPVT1 as a proliferative factor and treatment target in esophageal carcinoma. *Cancer Cell Int.* 19, 267. doi:10.1186/s12935-019-0985-9
- Zou, Y., Palte, M. J., Deik, A. A., Li, H., Eaton, J. K., Wang, W., et al. (2019). A GPX4-dependent cancer cell state underlies the clear-cell morphology and confers sensitivity to ferroptosis. *Nat. Commun.* 10, 1617. doi:10.1038/s41467-019-09277-9
- Zuo, J., Zhao, M., Fan, Z., Liu, B., Wang, Y., Li, Y., et al. (2020). MicroRNA-153-3p regulates cell proliferation and cisplatin resistance via Nrf-2 in esophageal squamous cell carcinoma. *Thorac. Cancer* 11, 738–747. doi:10.1111/1759-7714.13326



## OPEN ACCESS

## EDITED BY

Xin Wang,  
National Institutes of Health,  
United States

## REVIEWED BY

Yanqing Liu,  
Columbia University, United States  
Xiaoling Chen,  
Purdue University, United States

## \*CORRESPONDENCE

Yuehui Liu,  
liuyuehuiclark@21cn.com

## SPECIALTY SECTION

This article was submitted to Molecular  
Diagnostics and Therapeutics,  
a section of the journal  
Frontiers in Molecular Biosciences

RECEIVED 25 July 2022

ACCEPTED 20 September 2022

PUBLISHED 12 October 2022

## CITATION

Guo L, Zhang Q and Liu Y (2022), The  
role of microRNAs in ferroptosis.  
*Front. Mol. Biosci.* 9:1003045.  
doi: 10.3389/fmolb.2022.1003045

## COPYRIGHT

© 2022 Guo, Zhang and Liu. This is an  
open-access article distributed under  
the terms of the [Creative Commons  
Attribution License \(CC BY\)](#). The use,  
distribution or reproduction in other  
forums is permitted, provided the  
original author(s) and the copyright  
owner(s) are credited and that the  
original publication in this journal is  
cited, in accordance with accepted  
academic practice. No use, distribution  
or reproduction is permitted which does  
not comply with these terms.

# The role of microRNAs in ferroptosis

Liqing Guo<sup>1,2</sup>, Qingkun Zhang<sup>1</sup> and Yuehui Liu<sup>1\*</sup>

<sup>1</sup>Department of Otolaryngology, The Second Affiliated Hospital of Nanchang University, NanChang, China, <sup>2</sup>Jiangxi Province Key Laboratory of Molecular Medicine, Nanchang, China

Ferroptosis is a newly discovered type of programmed cell death, which is closely related to the imbalance of iron metabolism and oxidative stress. Ferroptosis has become an important research topic in the fields of cardiomyopathy, tumors, neuronal injury disorders, and ischemia perfusion disorders. As an important part of non-coding RNA, microRNAs regulate various metabolic pathways in the human body at the post-transcriptional level and play a crucial role in the occurrence and development of many diseases. The present review introduces the mechanisms of ferroptosis and describes the relevant pathways by which microRNAs affect cardiomyopathy, tumors, neuronal injury disorders and ischemia perfusion disorders through regulating ferroptosis. In addition, it provides important insights into ferroptosis-related microRNAs, aiming to uncover new methods for treatment of the above diseases, and discusses new ideas for the implementation of possible microRNA-based ferroptosis-targeted therapies in the future.

## KEYWORDS

ferroptosis, lipid peroxidation, microRNA, cardiomyopathy, tumor, neuronal injury disorder, ischemia perfusion disorder

## Introduction

Ferroptosis is a newly discovered programmed cell death mechanism with characteristics that are different from those of autophagy, apoptosis and necrosis. Several studies have demonstrated that ferroptosis is involved in the occurrence and development of cardiomyopathy, tumors, neuronal injury disorders, and ischemia perfusion disorders (Masaldan et al., 2019; Jiang et al., 2021; Van Coillie et al., 2022). MicroRNAs are a class of endogenous non-coding small RNA molecules, generally 21–25 nucleotides in length, which regulate various metabolic pathways in the human body at the post-transcriptional and translational levels, including regulation of tumor cell growth and induction of chemotherapy resistance (Ambros, 2001). Noncoding RNAs play a significant role in ferroptosis of various cells (Zhang X. et al., 2020; Zhi et al., 2021; Zuo et al., 2022). Previous reviews have mainly focused on the role of noncoding RNAs in cancer through regulating ferroptosis (Valashedi et al., 2022), but the role of microRNAs in other diseases through regulating ferroptosis has not been summarized.

The present review first discusses the mechanisms of ferroptosis and then summarizes the diseases and related pathways regulated by microRNAs through regulating ferroptosis. MicroRNAs have great potential as therapeutic targets. This report

provides reference information for more in-depth studies of microRNAs in the field of ferroptosis.

## Overview of ferroptosis

In 2012, Dixon et al. first used the concept of ferroptosis to describe the mode of cell death, which is caused by the accumulation of lipid peroxides (Dixon et al., 2012).

Ferroptosis is an iron-dependent mode of cell death that involves lipid reactive oxygen species (ROS) accumulation (Stockwell et al., 2017). The mechanism of its occurrence has been partially uncovered (Jhelum et al., 2020). First, the overloaded iron ions generate a lot of free hydroxyl groups *via* the Fenton reaction. Iron is a vital trace element involved in many physiological processes in the human body. Excess iron, however, increases the oxidative sensitivity of cells (Chen et al., 2019). Cells take up  $\text{Fe}^{3+}$  primarily through the transferrin receptor protein 1 complex (Gao et al., 2015). The six-transmembrane epithelial antigen of the prostate 3 (Steap3) reduces intracellular  $\text{Fe}^{3+}$  to  $\text{Fe}^{2+}$ . Ferroportin (FPN), also known as solute carrier family 40 member 1 (SLC40A1), is involved in the regulation of iron balance by expelling  $\text{Fe}^{2+}$  out of the cells (Geng et al., 2018). Overexpression of ferritin heavy chain1 (FTH1) inhibits erastin-induced ferroptosis by regulating  $\text{Fe}^{2+}$  (Gao et al., 2016; Hou et al., 2016).

Next, lipid peroxidation induction leads to lipid metabolism disorders, and the accumulation of lipid oxides and ROS is responsible for ferroptosis.  $\text{Fe}^{2+}$  overload causes a series of oxidative stress reactions in the cell, resulting in the destruction of the nucleus, membrane, organelles, and proteins. Esterified polyunsaturated fatty acids (PUFAs) are the most common substrates in lipid peroxidation (Kagan et al., 2017). Acyl-CoA synthetase long-chain family member 4 (ACSL4) is involved in the biosynthesis and reassembly of PUFAs on the cell membrane (Chen et al., 2021b). Lysophosphatidylcholine acyltransferase 3 then mediates PUFA activation to induce ferroptosis (Doll et al., 2017).

Finally, System  $\text{Xc}^-$  - glutathione - glutathione peroxidase 4 ( $\text{Xc}^-$ -GSH-GPX4) is considered a crucial antioxidant axis in ferroptosis.  $\text{Xc}^-$  complex is a cysteine-glutamate reverse transporter composed of two-subunit solute carrier family 7 member 11 (SLC7A11/xCT) along with solute carrier family 3 member 2 (SLC3A2) (Koppula et al., 2018). The main function of  $\text{Xc}^-$  is to regulate the transport balance of glutamate and cysteine and participate in the synthesis of GSH (Koppula et al., 2021). GSH is a cofactor for GPX4. It protects cells from oxidative damage. GPX4 is a selenoprotein that neutralizes toxic lipid peroxides and inhibits ferroptosis (Forcina and Dixon, 2019; Weaver and Skouta, 2022). GPX4 inactivation is a pivotal condition for the occurrence of ferroptosis (Jhelum et al., 2020). Large amounts of GSH are depleted, resulting in decreased glutathione peroxidase 4 (GPX4) activity. Certain

intracellular components, including oncoprotein activating transcription factor 4 (ATF4), nuclear factor erythroid 2-like factor 2 (NFE2L2/NRF2), and Beclin-1, can also regulate iron by affecting systems  $\text{Xc}^-$  and GSH death level (Habib et al., 2015; Song et al., 2018). In addition, the classic tumor suppressor gene P53 affects the occurrence and development of various diseases, such as tumors, by regulating GPX4-dependent and GPX4-independent ferroptosis pathways (Liu and Gu, 2022).

At present, numerous genetic hallmarks and protein hallmarks of ferroptosis are available for detection, but their specificity remains limited (Chen et al., 2021a).

Other auxiliary evidence, such as detection of cell activity, iron levels, GSH levels in cells and tissues, ROS and ROS product content, malondialdehyde (MDA), and mitochondrial membrane potential (MMP) is also often used to demonstrate the occurrence of ferroptosis. Moreover, changes in cell morphology, particularly mitochondrial morphology, observed under transmission electron microscopy, are the main features that distinguish ferroptosis from other forms of programmed cell death, such as apoptosis, autophagy, and necrosis. Mitochondrial shrinkage, high membrane density, diminished or absent cristae, and exterior membrane rupture are common in cells undergoing ferroptosis (Agmon and Stockwell, 2017; Stockwell, 2022).

More research on ferroptosis has continued to accumulate over the last few years. Ferroptosis has been shown to take part in the development of various diseases, such as tumors, cardiovascular diseases, and autoimmune diseases (Nguyen et al., 2020; Guo et al., 2022; Lai et al., 2022). Next, the role of microRNAs was explored in ferroptosis separately from microRNA-involved cardiomyopathy, tumors, nervous system diseases, and ischemia perfusion disorders.

## The role of microRNA in cardiomyopathy *via* regulating ferroptosis

As mentioned earlier, GPX4 is critical for the regulation of ferroptosis (Ursini et al., 2022). Zhuang et al. used an ischemia-reperfusion (I/R) rat model and cardiac fibrosis cell model induced by angiotensin II to determine that miR-375-3p promotes ferroptosis and accelerates cardiac fibrosis by inhibiting GPX4 (Zhuang et al., 2022). Fan et al. have showed that inhibition of miR-15a-5p decreases ferroptosis through GPX4 and thus alleviates myocardial injury in acute myocardial infarction (Fan et al., 2021). Inhibition of miR-1224 has also been found to alleviate hypoxia/reoxygenation myocardial injury by upregulating GPX4 (Li G. et al., 2021). GPX4 is a critical target in ferroptosis. MiR-375-3p, miR-15a-5p or miR-1224 inhibition may protect cardiomyocytes and alleviate myocardial injury by increasing GPX4 and decreasing ferroptosis. As a part of the  $\text{Xc}^-$  transporter, SLC7A11 also plays a significant role in the antioxidant system (Jyotsana et al., 2022). The study of Liu et al. inhibited cardiac

TABLE 1 The role of microRNA in cardiomyopathy via regulating ferroptosis.

microRNA name	Target gene	Cell model	Disease name	Effect on ferroptosis
miR-23a-3p	SLC7A11	H9c2	Atrial fibrillation	Promote ferroptosis
miR-375-3p	GPX4	Cardiac fibroblasts	Cardiac fibrosis	Promote ferroptosis
miR-190a-5p	GLS2	H9c2	Myocardial infarction	Suppress ferroptosis
miR-30d	ATG5	H9c2	Myocardial infarction	Promote ferroptosis
miR-1224	GPX4	H9c2	Myocardial H/R injury	Promote ferroptosis
miR-15a-5p	GPX4	HL-1	Myocardial infarction	Promote ferroptosis

fibroblast-derived exon-miR-23a-3p by using the exosome inhibitor GW4869, and inhibition of miR-23a-3p resulted in upregulation of SLC7A11, thereby reducing ferroptosis in H9c2 cardiomyocytes and preventing continued development of atrial flutter (Liu D. et al., 2022). It suggests that miR-23a-3p inhibition increases intracellular cystine and GSH levels, thereby neutralizing ROS and treating atrial fibrillation. Glutaminase 2 (GLS2) can cause ROS accumulation through mitochondria by accelerating glutamate formation (Matés et al., 2020). After myocardial infarction, cardiomyocytes often undergo cell death and pathological remodeling, which easily lead to heart failure (Duan, 2020). Zhou et al. have suggested that miR-190a-5p inhibits cardiomyocyte ferroptosis by inhibiting GLS2 and decreases the levels of ROS, MDA, and  $\text{Fe}^{2+}$  in H9c2 cells, thus playing a protective role in myocardial infarction (Zhou et al., 2021). MiR-190a-5p reduces lipid peroxidation by inhibiting GLS2 mRNA, thereby inhibiting ferroptosis and lowering the risk of myocardial infarction. Autophagy related protein 5 (ATG5) has been suggested to inhibit ferroptosis by inhibiting autophagy (Liang et al., 2022). Tang et al. have found that overexpression of miR-30d promotes ferroptosis after myocardial infarction by targeting ATG5, thus inhibiting autophagy in cardiomyocytes (Tang et al., 2020). Therefore, crosstalk may exist between ferroptosis and autophagy. The incidence of cardiovascular disease is high worldwide. Decreasing cardiomyocyte death and repairing damaged cardiac tissue are urgent clinical needs (Xu S. et al., 2021). Ferroptosis decreases reduces the overall cardioprotective effect of ischemia/reperfusion (I/R) injury. Ferroptosis suppression decreases inflammation and limits the extent of left ventricular remodeling after I/R injury (Komai et al., 2022).

Common clinical cardiovascular diseases include atherosclerosis, myocardial infarction, heart failure, and arrhythmia. Ferroptosis plays a vital role in the development of cardiovascular disease (Guo et al., 2022). The mechanism of microRNA in ferroptosis occurs through regulation of the antioxidant system and lipid oxidation. Most existing studies have shown that microRNA overexpression damages cardiomyocytes by promoting ferroptosis. However, because microRNAs have diverse functions, further research is needed

to reveal more details. Table 1 shows microRNAs that affect cardiomyopathy through regulating ferroptosis.

## The role of microRNA in tumors via regulating ferroptosis

GPX4 remains an important target of microRNAs in tumor diseases (Gao et al., 2022). The experiments by Xu et al. showed that miR-15a overexpression can inhibit cell proliferation, increase the release of lactate dehydrogenase, MDA,  $\text{Fe}^{2+}$ , and ROS, and then destroy MMP by inhibiting GPX4 in prostate cancer cells (Xu P. et al., 2022). In colorectal cancer cells, Liu et al. reported that miR-15a-3p overexpression can also promote ferroptosis by inhibiting GPX4 (Liu L. et al., 2022). Xu et al. found that miR-1287-5p still targets GPX4 to promote ferroptosis in osteosarcoma cells (Xu Z. et al., 2021). Deng et al. study suggested that miR-324-3p targets inhibition of GPX4, promotes ferroptosis in lung adenocarcinoma cells, and reverses their resistance to cisplatin (Deng et al., 2021). These microRNAs directly bound to the 3'-UTR of GPX4 mRNA and inhibited its expression, causing ROS accumulation in tumor cells and acting as tumor suppressor genes. Inhibition of the ATF4-HSPA5-GPX4 pathway reduces GPX4 levels and induces ferroptosis. Loss of ATF4 leads to increased ferroptosis (Chen et al., 2017; Zhu et al., 2017). The study by Bai et al. reported that miR-214-3p targets ATF4 to promote ferroptosis in hepatoma cells (Bai et al., 2020). Gomaa et al. found that overexpression of miR-4715-3p can inhibit aurora kinase A (AURKA) and GPX4, inducing ferroptosis in upper gastrointestinal adenocarcinoma cells (Gomaa et al., 2019). GPX4 content is a key factor in tumor ferroptosis, and these microRNAs have been shown to promote ferroptosis in various tumor cells by inhibiting target genes involved in GPX4 synthesis. Ferroptosis suppressor protein 1 (FSP1) exerts antioxidant effects parallel to GPX4, and FSP1-CoQ10-NAD(P)H is another pathway that inhibits ferroptosis (Bersuker et al., 2019; Doll et al., 2019). One experiment showed that exosomal miR-4443 targets methyltransferase 3 (METT3) to regulate FSP1 expression, thereby inhibiting ferroptosis in non-small cell lung cancer (Song et al., 2021). In the absence of GPX4,



FSP1 can be used as an oxidoreductase to inhibit ROS and alleviate ferroptosis.

SLC7A11 is widely expressed in various tumor tissues, and plays a significant role in inhibiting ferroptosis during the occurrence and development of tumors by controlling cysteine transport (Tang et al., 2022). Sun et al. found that the miR-34c-3p/SLC7A11 axis can potentiate erastin-induced ferroptosis in oral squamous cell carcinoma (Sun et al., 2022). Yadav et al. reported that overexpression of miR-5096 can promote ferroptosis by targeting SLC7A11 and inhibit breast cancer cell growth (Yadav et al., 2021). The study by Ni et al. showed that miR-375/SLC7A11 inhibits gastric cancer stem cells by triggering ferroptosis. They believe that miR-375 can reduce the stemness of gastric cancer cells by inducing ferroptosis (Ni et al., 2021). SLC3A2, like SLC11A7, is an important functional subunit of the  $Xc^-$  system (Liu M. et al., 2022). Hu et al. found that exosomal miR-142-3p secreted by hepatocellular carcinoma cells targets SLC3A2 to promote ferroptosis in MI-type macrophages, thus, accelerating the development of hepatocellular carcinoma (Hu et al., 2022). The microRNAs mentioned above reduced GSH levels by regulating cystine transport into tumor cells by targeting SLC7A11 and SLC3A2. Dickkopf-related protein 1 (DKK1) inhibits the occurrence of ferroptosis and protects cells from ferroptosis by enhancing the expression of SLC7A11 (Wu M. et al., 2022). Liao et al. found that miR-130b-3p targets DKK1 to inhibit ferroptosis in melanoma cells (Liao et al., 2021). MicroRNAs essentially regulated tumor ferroptosis via the antioxidant system, whether by regulating GPX4, FSP1, or GSH.

ACSL4 can promote lipid peroxidation of PUFAs to promote ferroptosis, and is also an important target of many microRNAs (Chen et al., 2021b; Liu et al., 2021). Bao et al. demonstrated that miR-670-3p can inhibit ferroptosis in glioblastoma cells by targeting ACSL4. Furthermore, miR-670-3p inhibitor-treated U87MG and A172 cells increase chemosensitivity to temozolomide (Bao et al., 2021). The study by Ma et al. showed that miR-424-5p targeting ACSL4 negatively regulates ferroptosis in ovarian cancer cells (Ma et al., 2021). They inhibited ROS production from PUFAs by targeting ACSL4 mRNA, thus resulting in ferroptosis inhibition.

Solute carrier family 1 member 5 (SLC1A5) transports glutamine into the cell during ferroptosis, and may increase cell sensitivity to ferroptosis (Xu F. et al., 2022; Zhu D. et al., 2022). Luo et al. reported that overexpression of miR-137, which results in decreased glutamine and MDA levels, can inhibit ferroptosis in melanoma cells by targeting SLC1A5 (Luo et al., 2018). Aspartate aminotransaminase (GOT1) is an enzyme involved in glutamate metabolism, which catalyzes the production of  $\alpha$ -ketoglutarate (Kremer et al., 2021). Zhang et al. have shown that overexpression of miR-9 inhibits ferroptosis in melanoma cells by directly binding to the 3'-UTR of GOT1 (Zhang et al., 2018). These findings suggest that miR-137 and miR-9 speed up the progression of

melanoma by inhibiting ferroptosis through reducing lipid peroxidation.

Iron-responsive element-binding protein 2 (IREB2) is related to intracellular iron ion concentration, and suppression of IREB2 can inhibit the level of  $Fe^{2+}$ , thus inhibiting ferroptosis (Li et al., 2022). Fan et al. showed that miR-19a inhibits ferroptosis in colorectal cancer cells HT29 by inhibiting IREB2 (Fan et al., 2022). Transferrin (TF) mediates  $Fe^{2+}$  entry into the cells, and TF blocking can reduce  $Fe^{2+}$  overload and inhibit ferroptosis (Pandurangi et al., 2022). Zheng et al. found that miR-545 inhibition can reduce ferroptosis in rectal cancer cells by regulating TF (Sixin Zheng, Lingling Hu, Qingwen Song et al., 2021). Intracellular  $Fe^{2+}$  can transport  $Fe^{2+}$  out of the cells via FPN1/SLC40A1. FPN participates in ferroptosis by regulating intracellular  $Fe^{2+}$  concentration (Hao et al., 2021; Wang et al., 2021; Pandurangi et al., 2022). Wei et al. reported that miR-302a-3p can strengthen ferroptosis in non-small cell lung cancer by targeting FPN (Wei et al., 2021). Zhu et al. showed that miR-4735-3p targets SLC40A1 to promote ferroptosis in clear cell renal cell carcinoma, thereby inhibiting tumor proliferation (Zhu C. et al., 2022). Ferroptosis is characterized by iron overload. Different microRNAs have different effects on iron metabolism target genes, resulting in ferroptosis regulation.

Tumor necrosis factor- $\alpha$ -induced protein 8 (TNFAIP8/TIPE) can participate in ferroptosis by inhibiting p53. One prior study showed that miR-539 overexpression can promote ferroptosis in colorectal cancer cells by inhibiting TIPE (Yang et al., 2021). Two studies by Tomita et al. demonstrated that miR-7-5p knockdown can reduce radioresistance in radioresistant cancer cells by regulating ferroptosis through changes in  $Fe^{2+}$  content (Tomita et al., 2019; Tomita et al., 2021). Tumor cells change their own microenvironment to achieve continuous proliferation (Xu et al., 2020), and microRNAs affect the proliferation of various tumor cells through the regulation of ferroptosis. The function of microRNA can be accomplished by the degradation or the translation inhibition of targeted mRNA after binding to the 3'-UTR region. However, this regulatory effect is complex, in that it presents two aspects of tumor-promoting and tumor-suppression. Table 2 lists microRNAs that affect tumors through regulating ferroptosis.

## The role of microRNA in neuronal injury disorder *via* regulating ferroptosis

FSP1 acts as a complementary antioxidant pathway and is also a target gene of microRNA-672-3p. Inhibition of miR-672-3p was reported to inhibit ferroptosis by upregulating FSP1, thereby promoting neural repair in spinal cord injury (Wang F. et al., 2022). The SLC7A11/GPX4 signaling pathway is a major antioxidant pathway in ferroptosis-induced nerve injury (Fu et al., 2022). Wang et al. reported that inhibition of miR-378a-3p reverses lead exposure-induced ferroptosis by targeting

TABLE 2 The role of microRNA in tumor *via* regulating ferroptosis.

microRNA name	Target gene	Cell model	Disease name	Effect on ferroptosis
miR-4735-3p	SLC40A1	786-O, A498	Cell Renal cell carcinoma	promote ferroptosis
miR-19a	IREB2	HT29	Colorectal cancer	Suppress ferroptosis
miR-142-3p	SLC3A2	HepG2,THP-1	Hepatocellular carcinoma caused hepatitis B virus	promote ferroptosis
miR-34c-3p	SLC7A11	SCC-25,CAL-27	Oral squamous cell carcinoma	promote ferroptosis
miR-15a	GPX4	LNCAP	Prostate cancer	promote ferroptosis
miR-545	TF	HT-29,HCT-116	Colorectal cancer	Suppress ferroptosis
miR-15a-3p	GPX4	HCT-116,CaCo2, HT29, KM12	Colorectal cancer	promote ferroptosis
miR-539	TIPE	HCT-116	Colorectal cancer	promote ferroptosis
miR-5096	SLC7A11	MDA-MB-468,MDA-MB-453, BT-549, MDA-MB-231,SKBR-3, T-47D, MCF-7, ZR-75	Breast cancer	promote ferroptosis
miR-1287-5p	GPX4	SaOS2, U2OS	Osteosarcoma	promote ferroptosis
miR-7-5p	-	HeLa,SAS	Cancer radioresistance	Suppress ferroptosis
miR-670-3p	ACSL4	U87MG, A172	Glioblastoma	Suppress ferroptosis
miR-302a-3p	Ferroportin	A549,H358,H1299, H1650	Non-small cell lung cancer	promote ferroptosis
miR-130b-3p	DKK1	A375,G-361	Melanoma	Suppress ferroptosis
miR-375	SLC7A11	SGC-7901,BGC-823	Gastric cancer	promote ferroptosis
miR-424-5p	ACSL4	HO8910,SKOV3	Ovarian cancer	Suppress ferroptosis
miR-214-3p	ATF4	HepG2,Hep3B	Hepatocellular carcinoma	promote ferroptosis
miR-4715-3p	AURKA	OE33, MKN45	Upper gastrointestinal cancers	promote ferroptosis
miR-9	GOT1	A375, G-361	Melanomma	Suppress ferroptosis
miR-137	SLC1A5	A375, G-361	Melanomma	Suppress ferroptosis
miR-324-3p	GPX4	A549	Lung adenocarcinoma	promote ferroptosis
miR-4443	METT3	A549-R,A549S	Non-small cell lung carcinoma	Suppress ferroptosis

TABLE 3 The role of microRNA in neuronal injury disorder *via* regulating ferroptosis.

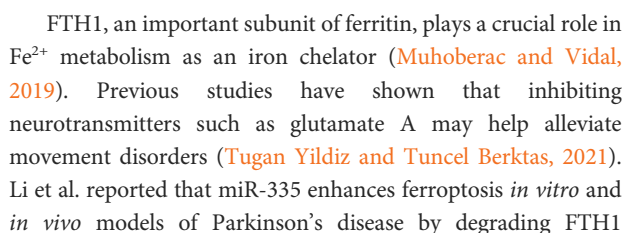
microRNA name	Target gene	Cell model	Disease name	Effect on ferroptosis
miR-378a-3p	SLC7A11	HT22	Nerve injury caused by lead exposure	promote ferroptosis
miR-672-3p	FSP1	HN,PC12	Spinal Cord Injury	promote ferroptosis
miR-194	Bach1	MSCs	Oxygen-glucose deprivation/reoxygenation-induced neuronal injury	Suppress ferroptosis
miR-335	FTTH1	PC12	Parkinson's disease	promote ferroptosis
miR-137	-	SH-SY5Y	Hemorrhagic stroke	Suppress ferroptosis
miR-212-5p	Ptgs2	HT-22,Neuro-2a	Traumatic brain injury	Suppress ferroptosis

SLC7A11 in HT22 cells (Wang W. et al., 2022). The two microRNAs mentioned above induced ferroptosis by inhibiting key molecules in the antioxidant pathway. It suggests that blocking them can reduce nerve cell death and alleviate specific neuronal injury disorders.

BTB and CNC homology 1(Bach1) is an oxidative stress-responsive transcription factor in ferroptosis, which promotes it by inhibiting the antioxidant system (GSH-GPX4 and FSP1-CoQ10 pathways) (Nishizawa et al., 2022). Li et al. showed that miR-194-loaded mesenchymal exosomes can inhibit

neurovascular endothelial cell ferroptosis by targeting Bach1, resulting in neuroprotection (Li X. et al., 2021). Prostaglandin peroxidase synthase-2(Ptgs2) is a regulatory gene in ferroptosis lipid oxidation (Macías-Rodríguez et al., 2020). Xiao et al. reported that overexpression of miR-212-5p overexpression can inhibit ferroptosis in neuronal cells by inhibiting Ptgs2, thereby attenuating traumatic brain injury (Xiao X. et al., 2019). Overall, miR-194 and miR-212-5p reduced ROS production or increased ROS decomposition by targeting key lipid peroxidation targets.

microRNA name	Target gene	Cell model	Disease name	Effect on ferroptosis
miR-124-3p	Steap3	BMMSCs	Liver ischemia reperfusion injury	Suppress ferroptosis
miR-214-3p	GPX4	Acute kidney injury mice and Acute kidney injury	Acute kidney injury induced by cisplatin	promote ferroptosis
miR-132	–	peripheral vessels of atherosclerosis, HUVECs	Atherosclerosis	promote ferroptosis
miR-3587	HMOX1	NRK-52E	Renal ischemia-reperfusion	promote ferroptosis
miR-182-5p	GPX4	Hk-2,TCMK-1	Ischemia/reperfusion kidney injury	promote ferroptosis
miR-378a-3p	SLC7A11			
miR-30b-5p	Pax3,SLC7A11	HTR-8, TEV-1	Preeclampsia	promote ferroptosis
miR-17-92	A20	HUVEC	Endothelial cell death	Suppress ferroptosis



frontiersin.org

important effects on ferroptosis and nerve damage. Therefore, ferroptosis in neurological diseases is increasingly being studied. Studies have shown that the roles of microRNAs in ferroptosis of neurological diseases are involved in the complex of bidirectional regulation of neurological diseases (Wu et al., 2018). Table 3 lists microRNAs that affect neuronal injury disorder through regulating ferroptosis.

## The role of microRNA in ischemia perfusion disorders *via* regulating ferroptosis

Ferroptosis is an important mechanism leading to I/R injury in multiple organs (Chen Y. et al., 2021). GPX4 and SLC7A11 are key ferroptosis enzymes that act as target genes for multiple microRNAs in ischemic perfusion disease. Cell and animal experiments by, Zhou et al. demonstrated that miR-214-3p inhibition inhibits ferroptosis through GPX4, thereby reducing renal tubular damage (Zhou et al., 2022). Ding et al. reported that miR-182-5p and miR-378a-3p contribute to the activation of ferroptosis in I/R renal injury by inhibiting GPX4 and SLC7A11 (Ding et al., 2020). Zhang et al. showed that miR-30b-5p targets paired box protein 3 (PAX3) and SLC7A11 to enhance trophoblast ferroptosis, and that miR-30b-5p inhibition alleviates symptoms in a rat model (Zhang H. et al., 2020). GPX4 and SLC7A11 are still important microRNA target genes in ischemic perfusion disorders. This is related to GPX4's critical antioxidant role in ferroptosis.

Steap3 is involved in ferroptosis as a key regulator of iron metabolism (Yan et al., 2021). A prior study demonstrated that miR-124-3p reduces the degree of ferroptosis in HO-1-modified bone marrow mesenchymal stem cells by inhibiting Steap3, alleviating the risk of hepatic I/R injury (Wu L. et al., 2022). Nuclear factor erythroid 2-related factor 2/heme oxygenase 1 (Nrf2/HO-1) signaling axis inhibits ROS generation and prevents oxidative stress damage (Yan et al., 2021). Tao et al. reported that miR-3587 inhibition could upregulate HO-1 by regulating HMOX1, thereby attenuating I/R-induced ferroptosis in kidney tissue (Tao et al., 2021). MiR3587 inhibition increases HO-1, a key antioxidant that reduces intracellular ROS and ferroptosis.

Xiao et al. found that miR-17-92 overexpression can affect ACSL4 expression by targeting tumor necrosis factor, alpha-induced protein 3(A20), thereby reducing ferroptosis in endothelial cells (Xiao F. J. et al., 2019). Liu et al. showed that miR-132 overexpression can accelerate the progression of atherosclerosis by reducing the level MMP, increasing ROS production, and promoting ferroptosis (Zexin et al., 2022). Ferroptosis is involved in the ischemic injury of various organs and tissues (von Samson-Himmelstjerna et al., 2022). Existing studies have shown that the mechanism through which microRNAs act on ischemic perfusion diseases mainly involve promotion of ferroptosis. Therefore, interventions may

potentially target microRNA to achieve protection of target organs. Table 4 lists microRNAs that affect ischemia perfusion disorders through regulating ferroptosis.

## Summary and outlook

Many studies have confirmed that microRNAs are involved in the occurrence of cardiomyopathy, tumors, neuronal injury disorder and ischemia perfusion disorders by promoting or inhibiting ferroptosis (Li N. et al., 2021; Maslov et al., 2022; Zuo et al., 2022). Figure 1 shows their relevant mechanisms. A significant number of studies have demonstrated that microRNAs can participate in the ferroptosis process through key targets, such as GPX4, SLC7A11, and ACSL4 (Chen et al., 2021b). Most of the current microRNA research explores its impact on a key target in the ferroptosis pathway alone, and does not explore the mechanism of action related to ferroptosis. The mechanism of microRNA's impact on disease through regulating ferroptosis remains largely unexplored. Therefore, it is still necessary to further analyze the relevant mechanisms of microRNA from the aspects of metabolic pathways and epigenetic modifications in order to be able to, intervene in the development of diseases.

## Author contributions

LG and QZ contributed to the preparation and writing of the manuscript. YL contributed to the editing of the manuscript.

## Funding

The study was supported by the National Natural Science Fund of China (grant No. 81760184 and 82060185) and Natural Science Fund of Jiangxi Province (grant No. 20192ACB20027).

## Conflict of interest

The authors declare that the research was conducted in the absence of any commercial or financial relationships that could be construed as a potential conflict of interest.

## Publisher's note

All claims expressed in this article are solely those of the authors and do not necessarily represent those of their affiliated organizations, or those of the publisher, the editors and the reviewers. Any product that may be evaluated in this article, or claim that may be made by its manufacturer, is not guaranteed or endorsed by the publisher.



## References

- Agmon, E., and Stockwell, B. R. (2017). Lipid homeostasis and regulated cell death. *Curr. Opin. Chem. Biol.* 39, 83–89. doi:10.1016/j.cbpa.2017.06.002
- Ambros, V. (2001). microRNAs: Tiny regulators with great potential. *Cell* 107, 823–826.
- Bai, T., Liang, R., Zhu, R., Wang, W., Zhou, L., and Sun, Y. (2020). MicroRNA-214-3p enhances erastin-induced ferroptosis by targeting ATF4 in hepatoma cells. *J. Cell Physiol.* 235 (7–8), 5637–5648. doi:10.1002/jcp.29496
- Bao, C., Zhang, J., Xian, S.-Y., and Chen, F. (2021). MicroRNA-670-3p suppresses ferroptosis of human glioblastoma cells through targeting ACSL4. *Free Radic. Res.* 55 (7), 743–754. doi:10.1080/10715762.2021.1962009
- Bersuker, K., Hendricks, J. M., Li, Z., Magtanong, L., Ford, B., Tang, P. H., et al. (2019). The CoQ oxidoreductase FSP1 acts parallel to GPX4 to inhibit ferroptosis. *Nature* 575 (7784), 688–692. doi:10.1038/s41586-019-1705-2
- Chen, D., Fan, Z., Rauh, M., Buchfelder, M., Eyupoglu, I. Y., and Savaskan, N. (2017). ATF4 promotes angiogenesis and neuronal cell death and confers ferroptosis in a xCT-dependent manner. *Oncogene* 36 (40), 5593–5608. doi:10.1038/onc.2017.146
- Chen, X., Comish, P. B., Tang, D., and Kang, R. (2021a). Characteristics and biomarkers of ferroptosis. *Front. Cell Dev. Biol.* 9, 637162. doi:10.3389/fcell.2021.637162
- Chen, X., Li, J., Kang, R., Klionsky, D. J., and Tang, D. (2021b). Ferroptosis: Machinery and regulation. *Autophagy* 17 (9), 2054–2081. doi:10.1080/15548627.2020.1810918
- Chen, Y., Fan, H., Wang, S., Tang, G., Zhai, C., and Shen, L. (2021c). Ferroptosis: A novel therapeutic target for ischemia-reperfusion injury. *Front. Cell Dev. Biol.* 9, 688605. doi:10.3389/fcell.2021.688605
- Chen, Y., Fan, Z., Yang, Y., and Gu, C. (2019). Iron metabolism and its contribution to cancer (Review). *Int. J. Oncol.* 54 (4), 1143–1154. doi:10.3892/ijo.2019.4720
- Deng, S. H., Wu, D. M., Li, L., Liu, T., Zhang, T., Li, J., et al. (2021). miR-324-3p reverses cisplatin resistance by inducing GPX4-mediated ferroptosis in lung adenocarcinoma cell line A549. *Biochem. Biophys. Res. Commun.* 549, 54–60. doi:10.1016/j.bbrc.2021.02.077
- Ding, C., Ding, X., Zheng, J., Wang, B., Li, Y., Xiang, H., et al. (2020). miR-182-5p and miR-378a-3p regulate ferroptosis in I/R-induced renal injury. *Cell Death Dis.* 11 (10), 929. doi:10.1038/s41419-020-03135-z
- Dixon, S. J., Lemberg, K. M., Lamprecht, M. R., Skouta, R., Zaitsev, E. M., Gleason, C. E., et al. (2012). Ferroptosis: An iron-dependent form of nonapoptotic cell death. *Cell* 149 (5), 1060–1072. doi:10.1016/j.cell.2012.03.042
- Doll, S., Freitas, F. P., Shah, R., Aldrovandi, M., da Silva, M. C., Ingold, I., et al. (2019). FSP1 is a glutathione-independent ferroptosis suppressor. *Nature* 575 (7784), 693–698. doi:10.1038/s41586-019-1707-0
- Doll, S., Proneth, B., Tyurina, Y. Y., Panzilius, E., Kobayashi, S., Ingold, I., et al. (2017). ACSL4 dictates ferroptosis sensitivity by shaping cellular lipid composition. *Nat. Chem. Biol.* 13 (1), 91–98. doi:10.1038/nchembio.2239
- Duan, B. (2020). Concise review: Harnessing iPSC-derived cells for ischemic heart disease treatment. *J. Transl. Int. Med.* 8 (1), 20–25. doi:10.2478/jtim-2020-0004
- Fan, H., Ai, R., Mu, S., Niu, X., Guo, Z., and Liu, L. (2022). MiR-19a suppresses ferroptosis of colorectal cancer cells by targeting IREB2. *Bioengineered* 13 (5), 12021–12029. doi:10.1080/21655979.2022.2054194
- Fan, K., Huang, W., Qi, H., Song, C., He, C., Liu, Y., et al. (2021). The Egr-1/miR-15a-5p/GPX4 axis regulates ferroptosis in acute myocardial infarction. *Eur. J. Pharmacol.* 909, 174403. doi:10.1016/j.ejphar.2021.174403
- Forcina, G. C., and Dixon, S. J. (2019). GPX4 at the crossroads of lipid homeostasis and ferroptosis. *Proteomics* 19 (18), e1800311doi:10.1002/pmic.201800311
- Fu, C., Wu, Y., Liu, S., Luo, C., Lu, Y., Liu, M., et al. (2022). Rehmannioside A improves cognitive impairment and alleviates ferroptosis via activating PI3K/AKT/Nrf2 and SLC7A11/GPX4 signaling pathway after ischemia. *J. Ethnopharmacol.* 289, 115021doi:10.1016/j.jep.2022.115021
- Gao, M., Fan, K., Chen, Y., Zhang, G., Chen, J., and Zhang, Y. (2022). Understanding the mechanistic regulation of ferroptosis in cancer: Gene matters. *J. Genet. Genomics.* doi:10.1016/j.jgg.2022.06.002
- Gao, M., Monian, P., Pan, Q., Zhang, W., Xiang, J., and Jiang, X. (2016). Ferroptosis is an autophagic cell death process. *Cell Res.* 26 (9), 1021–1032. doi:10.1038/cr.2016.95
- Gao, M., Monian, P., Quadri, N., Ramasamy, R., and Jiang, X. (2015). Glutaminolysis and transferrin regulate ferroptosis. *Mol. Cell* 59 (2), 298–308. doi:10.1016/j.molcel.2015.06.011
- Geng, N., Shi, B. J., Li, S. L., Zhong, Z. Y., Li, Y. C., Xua, W. L., et al. (2018). Knockdown of ferroportin accelerates erastin-induced ferroptosis in neuroblastoma cells. *Eur. Rev. Med. Pharmacol. Sci.* 22 (12), 3826–3836. doi:10.26355/eurrev\_201806\_15267
- Gomaa, A., Peng, D., Chen, Z., Soutto, M., Abouelezz, K., Corvalan, A., et al. (2019). Epigenetic regulation of AURKA by miR-4715-3p in upper gastrointestinal cancers. *Sci. Rep.* 9 (1), 16970doi:10.1038/s41598-019-53174-6
- Guo, Y., Zhang, W., Zhou, X., Zhao, S., Wang, J., Guo, Y., et al. (2022). Roles of ferroptosis in cardiovascular diseases. *Front. Cardiovasc. Med.* 9, 911564doi:10.3389/fcvm.2022.911564
- Habib, E., Linher-Melville, K., Lin, H. X., and Singh, G. (2015). Expression of xCT and activity of system xc(-) are regulated by NRF2 in human breast cancer cells in response to oxidative stress. *Redox Biol.* 5, 33–42. doi:10.1016/j.redox.2015.03.003
- Hao, L., Mi, J., Song, L., Guo, Y., Li, Y., Yin, Y., et al. (2021). SLC40A1 mediates ferroptosis and cognitive dysfunction in type 1 diabetes. *Neuroscience* 463, 216–226. doi:10.1016/j.neuroscience.2021.03.009
- Hou, W., Xie, Y., Song, X., Sun, X., Lotze, M. T., Zeh, H. J., 3rd, et al. (2016). Autophagy promotes ferroptosis by degradation of ferritin. *Autophagy* 12 (8), 1425–1428. doi:10.1080/15548627.2016.1187366
- Hu, Z., Yin, Y., Jiang, J., Yan, C., Wang, Y., Wang, D., et al. (2022). Exosomal miR-142-3p secreted by Hepatitis B virus (HBV)-hepatocellular carcinoma (HCC) cells promotes ferroptosis of M1-type macrophages through SLC3A2 and the mechanism of HCC progression. *J. Gastrointest. Oncol.* 13 (2), 754–767. doi:10.21037/jgo-21-916
- Jhelum, P., Santos-Nogueira, E., Teo, W., Haumont, A., Lenoël, I., Stys, P. K., et al. (2020). Ferroptosis mediates cuprizone-induced loss of oligodendrocytes and demyelination. *J. Neurosci.* 40 (48), 9327–9341. doi:10.1523/jneurosci.1749-20.2020
- Jiang, X., Stockwell, B. R., and Conrad, M. (2021). Ferroptosis: Mechanisms, biology and role in disease. *Nat. Rev. Mol. Cell Biol.* 22 (4), 266–282. doi:10.1038/s41580-020-00324-8
- Jyotsana, N., Ta, K. T., and DelGiorno, K. E. (2022). The role of cystine/glutamate antiporter slc7a11/xCT in the pathophysiology of cancer. *Front. Oncol.* 12, 858462doi:10.3389/fonc.2022.858462
- Kagan, V. E., Mao, G., Qu, F., Angeli, J. P., Doll, S., Croix, C. S., et al. (2017). Oxidized arachidonic and adrenic PEs navigate cells to ferroptosis. *Nat. Chem. Biol.* 13 (1), 81–90. doi:10.1038/nchembio.2238
- Komai, K., Kawasaki, N. K., Higa, J. K., and Matsui, T. (2022). The role of ferroptosis in adverse left ventricular remodeling following acute myocardial infarction. *Cells* 11 (9). doi:10.3390/cells11091399
- Koppula, P., Zhang, Y., Zhuang, L., and Gan, B. (2018). Amino acid transporter SLC7A11/xCT at the crossroads of regulating redox homeostasis and nutrient dependency of cancer. *Cancer Commun. (Lond)* 38 (1), 12. doi:10.1186/s40880-018-0288-x
- Koppula, P., Zhuang, L., and Gan, B. (2021). Cystine transporter slc7a11/xCT in cancer: Ferroptosis, nutrient dependency, and cancer therapy. *Protein Cell* 12 (8), 599–620. doi:10.1007/s13238-020-00789-5
- Kremer, D. M., Nelson, B. S., Lin, L., Yarosz, E. L., Halbrook, C. J., Kerk, S. A., et al. (2021). GOT1 inhibition promotes pancreatic cancer cell death by ferroptosis. *Nat. Commun.* 12 (1), 4860. doi:10.1038/s41467-021-24859-2
- Lai, B., Wu, C. H., Wu, C. Y., Luo, S. F., and Lai, J. H. (2022). Ferroptosis and autoimmune diseases. *Front. Immunol.* 13, 916664. doi:10.3389/fimmu.2022.916664
- Li, G., Jin, J., Liu, S., Ding, K., and Qian, C. (2021a). Inhibition of miR-1224 suppresses hypoxia/reoxygenation-induced oxidative stress and apoptosis in cardiomyocytes through targeting GPX4. *Exp. Mol. Pathol.* 121, 104645. doi:10.1016/j.yexmp.2021.104645
- Li, N., Jiang, W., Wang, W., Xiong, R., Wu, X., and Geng, Q. (2021b). Ferroptosis and its emerging roles in cardiovascular diseases. *Pharmacol. Res.* 166, 105466. doi:10.1016/j.phrs.2021.105466
- Li, Xinrong, Wenwen, S. I., Zhan, L. I., Xuelei, L. I. U., Shanyu, Y. E., et al. (2021). MiR-335 promotes ferroptosis by targeting ferritin heavy chain 1 in *in vivo* and *in vitro* models of Parkinson's disease. *Int. J. Mol. Med.* 47 (61), 1–11.
- Li, X., Wu, L., Tian, X., Zheng, W., Yuan, M., Tian, X., et al. (2022). MiR-29a-3p in exosomes from heme oxygenase-1 modified bone marrow mesenchymal stem cells alleviates steatotic liver ischemia-reperfusion injury in rats by suppressing ferroptosis via iron responsive element binding protein 2. *Oxid. Med. Cell Longev.* 2022, 6520789. doi:10.1155/2022/6520789
- Li, X., Zhang, X., Liu, Y., Pan, R., Liang, X., Huang, L., et al. (2021c). Exosomes derived from mesenchymal stem cells ameliorate oxygen-glucose deprivation/

reoxygenation-induced neuronal injury via transferring MicroRNA-194 and targeting Bach1. *Tissue Cell* 73, 101651. doi:10.1016/j.tice.2021.101651

Li, Y., Wang, J., Chen, S., Wu, P., Xu, S., Wang, C., et al. (2020). MiR-137 boosts the neuroprotective effect of endothelial progenitor cell-derived exosomes in oxyhemoglobin-treated SH-SY5Y cells partially via COX2/PGE2 pathway. *Stem Cell Res. Ther.* 11 (1). doi:10.1186/s13287-020-01836-y

Liang, Y., Deng, Y., Zhao, J., Liu, L., Wang, J., Chen, P., et al. (2022). Ferritinophagy is involved in experimental subarachnoid hemorrhage-induced neuronal ferroptosis. *Neurochem. Res.* 47 (3), 692–700. doi:10.1007/s11064-021-03477-w

Liao, Y., Jia, X., Ren, Y., Deji, Z., Gesang, Y., Ning, N., et al. (2021). Suppressive role of microRNA-130b-3p in ferroptosis in melanoma cells correlates with DKK1 inhibition and Nrf2-HO-1 pathway activation. *Hum. Cell* 34 (5), 1532–1544. doi:10.1007/s13577-021-00557-5

Liu, D., Yang, M., Yao, Y., He, S., Wang, Y., Cao, Z., et al. (2022a). Cardiac fibroblasts promote ferroptosis in atrial fibrillation by secreting exo-miR-23a-3p targeting SLC7A11. *Oxidative Med. Cell. Longev.* 2022, 1–31. doi:10.1155/2022/3961495

Liu, J., Kang, R., and Tang, D. (2021). Signaling pathways and defense mechanisms of ferroptosis. *Febs J.* doi:10.1111/febs.16059

Liu, L., Yao, H., Zhou, X., Chen, J., Chen, G., Shi, X., et al. (2022b). MiR-15a-3p regulates ferroptosis via targeting glutathione peroxidase GPX4 in colorectal cancer. *Mol. Carcinog.* 61 (3), 301–310. doi:10.1002/mc.23367

Liu, M., Kong, X. Y., Yao, Y., Wang, X. A., Yang, W., Wu, H., et al. (2022c). The critical role and molecular mechanisms of ferroptosis in antioxidant systems: A narrative review. *Ann. Transl. Med.* 10 (6), 368. doi:10.21037/atm-21-6942

Liu, Y., and Gu, W. (2022). p53 in ferroptosis regulation: the new weapon for the old guardian. *Cell Death Differ.* 29 (5), 895–910. doi:10.1038/s41418-022-00943-y

Luo, M., Wu, L., Zhang, K., Wang, H., Zhang, T., Gutierrez, L., et al. (2018). miR-137 regulates ferroptosis by targeting glutamine transporter SLC1A5 in melanoma. *Cell Death Differ.* 25 (8), 1457–1472. doi:10.1038/s41418-017-0053-8

Ma, L. L., Liang, L., Zhou, D., and Wang, S. W. (2021). Tumor suppressor miR-424-5p abrogates ferroptosis in ovarian cancer through targeting ACSL4. *Neoplasma* 68 (1), 165–173. doi:10.4149/neo\_2020\_200707N705

Macías-Rodríguez, R. U., Inzaugarat, M. E., Ruiz-Margáin, A., Nelson, L. J., Trautwein, C., and Cubero, F. J. (2020). Reclassifying hepatic cell death during liver damage: Ferroptosis-A novel form of non-apoptotic cell death? *Int. J. Mol. Sci.* 21 (5). doi:10.3390/ijms21051651

Masaldan, S., Bush, A. I., Devos, D., Rolland, A. S., and Moreau, C. (2019). Striking while the iron is hot: Iron metabolism and ferroptosis in neurodegeneration. *Free Radic. Biol. Med.* 133, 221–233. doi:10.1016/j.freeradbiomed.2018.09.033

Maslov, L. N., Popov, S. V., Naryzhnaya, N. V., Mukhomedzyanov, A. V., Kurbatov, B. K., Derkachev, I. A., et al. (2022). The regulation of necroptosis and perspectives for the development of new drugs preventing ischemic/reperfusion of cardiac injury. *Apoptosis*. doi:10.1007/s10495-022-01760-x

Matés, J. M., Campos-Sandoval, J. A., de Los Santos-Jiménez, J., and Márquez, J. (2020). Glutaminases regulate glutathione and oxidative stress in cancer. *Arch. Toxicol.* 94 (8), 2603–2623. doi:10.1007/s00204-020-02838-8

Muhoherac, B. B., and Vidal, R. (2019). Iron, ferritin, hereditary ferritinopathy, and neurodegeneration. *Front. Neurosci.* 13, 1195. doi:10.3389/fnins.2019.01195

Nguyen, T. H. P., Mahalakshmi, B., and Velmurugan, B. K. (2020). Functional role of ferroptosis on cancers, activation and deactivation by various therapeutic candidates-an update. *Chem. Biol. Interact.* 317, 108930. doi:10.1016/j.cbi.2019.108930

Ni, H., Qin, H., Sun, C., Liu, Y., Ruan, G., Guo, Q., et al. (2021). MiR-375 reduces the stemness of gastric cancer cells through triggering ferroptosis. *Stem Cell Res. Ther.* 12 (1), 325. doi:10.1186/s13287-021-02394-7

Nishizawa, H., Yamanaka, M., and Igarashi, K. (2022). Ferroptosis: Regulation by competition between NRF2 and BACH1 and propagation of the death signal. *Febs J.* doi:10.1111/febs.16382

Pandurangi, S. L., Chittineedi, P., Chikati, R., Lingareddy, J. R., Nagoor, M., and Ponnada, S. K. (2022). Role of dietary iron revisited: In metabolism, ferroptosis and pathophysiology of cancer. *Am. J. Cancer Res.* 12 (3), 974–985.

Song, X., Zhu, S., Chen, P., Hou, W., Wen, Q., Liu, J., et al. (2018). AMPK-mediated BECN1 phosphorylation promotes ferroptosis by directly blocking system X(c<sup>-</sup>) activity. *Curr. Biol.* 28 (15), 2388–2399. e2385. doi:10.1016/j.cub.2018.05.094

Song, Z., Jia, G., Ma, P., and Cang, S. (2021). Exosomal miR-4443 promotes cisplatin resistance in non-small cell lung carcinoma by regulating FSP1 m6A modification-mediated ferroptosis. *Life Sci.* 276, 119399. doi:10.1016/j.lfs.2021.119399

Stockwell, B. R. (2022). Ferroptosis turns 10: Emerging mechanisms, physiological functions, and therapeutic applications. *Cell* 185 (14), 2401–2421. doi:10.1016/j.cell.2022.06.003

Stockwell, B. R., Friedmann Angeli, J. P., Bayir, H., Bush, A. I., Conrad, M., Dixon, S. J., et al. (2017). Ferroptosis: A regulated cell death nexus linking metabolism, redox biology, and disease. *Cell* 171 (2), 273–285. doi:10.1016/j.cell.2017.09.021

Sun, K., Ren, W., Li, S., Zheng, J., Huang, Y., Zhi, K., et al. (2022). MiR-34c-3p upregulates erastin-induced ferroptosis to inhibit proliferation in oral squamous cell carcinomas by targeting SLC7A11. *Pathol. Res. Pract.* 231, 153778. doi:10.1016/j.prp.2022.153778

Tang, S., Wang, Y., Ma, T., Lu, S., Huang, K., Li, Q., et al. (2020). MiR-30d inhibits cardiomyocytes autophagy promoting ferroptosis after myocardial infarction. *Panminerva Med.* doi:10.23736/s0031-0808.20.03979-8

Tang, X., Chen, W., Liu, H., Liu, N., Chen, D., Tian, D., et al. (2022). Research progress on SLC7A11 in the regulation of cystine/cysteine metabolism in tumors. *Oncol. Lett.* 23 (2), 47. doi:10.3892/ol.2021.13165

Tao, W., Liu, F., Zhang, J., Fu, S., Zhan, H., and Qian, K. (2021). miR-3587 inhibitor attenuates ferroptosis following renal ischemia-reperfusion through HO-1. *Front. Mol. Biosci.* 8, 789927. doi:10.3389/fmolb.2021.789927

Tomita, K., Fukumoto, M., Itoh, K., Kuwahara, Y., Igarashi, K., Nagasawa, T., et al. (2019). MiR-7-5p is a key factor that controls radioresistance via intracellular Fe(2+) content in clinically relevant radioresistant cells. *Biochem. Biophys. Res. Commun.* 518 (4), 712–718. doi:10.1016/j.bbrc.2019.08.117

Tomita, K., Nagasawa, T., Kuwahara, Y., Torii, S., Igarashi, K., Roudkenar, M. H., et al. (2021). MiR-7-5p is involved in ferroptosis signaling and radioresistance through the generation of ROS in radioresistant HeLa and SAS cell lines. *Int. J. Mol. Sci.* 22 (15). doi:10.3390/ijms22158300

Tugan Yildiz, B., and Tuncel Berktaş, D. (2021). Experiences on the administration of botulinum toxin in movement disorders. *J. Transl. Int. Med.* 9 (1), 52–56. doi:10.2478/jtim-2021-0003

Ursini, F., Bosello Travain, V., Cozza, G., Miotto, G., Roveri, A., Toppo, S., et al. (2022). A white paper on Phospholipid Hydroperoxide Glutathione Peroxidase (GPx4) forty years later. *Free Radic. Biol. Med.* 188, 117–133. doi:10.1016/j.freeradbiomed.2022.06.227

Valashedi, M. R., Bamshad, C., Najafi-Ghalehlou, N., Nikoo, A., Tomita, K., Kuwahara, Y., et al. (2022). Non-coding RNAs in ferroptotic cancer cell death pathway: Meet the new masters. *Hum. Cell* 35 (4), 972–994. doi:10.1007/s13577-022-00699-0

Van Coillie, S., Van San, E., Goetschalckx, I., Wiernicki, B., Mukhopadhyay, B., Tonnus, W., et al. (2022). Targeting ferroptosis protects against experimental (multi)organ dysfunction and death. *Nat. Commun.* 13 (1), 1046. doi:10.1038/s41467-022-28718-6

von Samson-Himmelstjerna, F. A., Kolbrink, B., Riebeling, T., Kunzendorf, U., and Krautwald, S. (2022). Progress and setbacks in translating a decade of ferroptosis research into clinical practice. *Cells* 11 (14). doi:10.3390/cells11142134

Wang, F., Li, J., Zhao, Y., Guo, D., Liu, D., Chang, S. e., et al. (2022a). miR-672-3p promotes functional recovery in rats with contusive spinal cord injury by inhibiting ferroptosis suppressor protein 1. *Oxidative Med. Cell. Longev.* 2022, 1–19. doi:10.1155/2022/6041612

Wang, W., Shi, F., Cui, J., Pang, S., Zheng, G., and Zhang, Y. (2022b). MiR-378a-3p/SLC7A11 regulate ferroptosis in nerve injury induced by lead exposure. *Ecotoxicol. Environ. Saf.* 239. doi:10.1016/j.ecoenv.2022.113639

Wang, Y., Zhao, Y., Ye, T., Yang, L., Shen, Y., and Li, H. (2021). Ferroptosis signaling and regulators in atherosclerosis. *Front. Cell Dev. Biol.* 9, 809457. doi:10.3389/fcell.2021.809457

Weaver, K., and Skouta, R. (2022). The selenoprotein glutathione peroxidase 4: From molecular mechanisms to novel therapeutic opportunities. *Biomedicines* 10 (4). doi:10.3390/biomedicines10040891

Wei, D., Ke, Y. Q., Duan, P., Zhou, L., Wang, C. Y., and Cao, P. (2021). MicroRNA-302a-3p induces ferroptosis of non-small cell lung cancer cells via targeting ferroptin. *Free Radic. Res.* 55 (7), 821–830. doi:10.1080/10715762.2021.1947503

Wu, J. R., Tuo, Q. Z., and Lei, P. (2018). Ferroptosis, a recent defined form of critical cell death in neurological disorders. *J. Mol. Neurosci.* 66 (2), 197–206. doi:10.1007/s12031-018-1155-6

Wu, J. Y., and Prentice, H. (2021). Potential new therapeutic intervention for ischemic stroke. *J. Transl. Int. Med.* 9 (1), 1–3. doi:10.2478/jtim-2021-0014

Wu, L., Tian, X., Zuo, H., Zheng, W., Li, X., Yuan, M., et al. (2022a). miR-124-3p delivered by exosomes from heme oxygenase-1 modified bone marrow mesenchymal stem cells inhibits ferroptosis to attenuate ischemia-reperfusion injury in steatotic grafts. *J. Nanobiotechnology* 20 (1). doi:10.1186/s12951-022-01407-8

- Wu, M., Zhang, X., Zhang, W., Chiou, Y. S., Qian, W., Liu, X., et al. (2022b). Cancer stem cell regulated phenotypic plasticity protects metastasized cancer cells from ferroptosis. *Nat. Commun.* 13 (1), 1371. doi:10.1038/s41467-022-29018-9
- Xiao, F. J., Zhang, D., Wu, Y., Jia, Q. H., Zhang, L., Li, Y. X., et al. (2019a). miRNA-17-92 protects endothelial cells from erastin-induced ferroptosis through targeting the A20-ACSL4 axis. *Biochem. Biophys. Res. Commun.* 515 (3), 448–454. doi:10.1016/j.bbrc.2019.05.147
- Xiao, X., Jiang, Y., Liang, W., Wang, Y., Cao, S., Yan, H., et al. (2019b). miR-212-5p attenuates ferroptotic neuronal death after traumatic brain injury by targeting Ptg2. *Mol. Brain* 12 (1), 78. doi:10.1186/s13041-019-0501-0
- Xu, F., Wang, H., Pei, H., Zhang, Z., Liu, L., Tang, L., et al. (2022a). SLC1A5 prefers to play as an accomplice rather than an opponent in pancreatic adenocarcinoma. *Front. Cell Dev. Biol.* 10, 800925. doi:10.3389/fcell.2022.800925
- Xu, J., Zhang, J., and Wang, J. (2020). The application of traditional Chinese medicine against the tumor immune escape. *J. Transl. Int. Med.* 8 (4), 203–204. doi:10.2478/jtim-2020-0032
- Xu, P., Wang, Y., Deng, Z., Tan, Z., and Pei, X. (2022b). MicroRNA-15a promotes prostate cancer cell ferroptosis by inhibiting GPX4 expression. *Oncol. Lett.* 23 (2), 67. doi:10.3892/ol.2022.13186
- Xu, S., Qiu, Y., and Tao, J. (2021a). The challenges and optimization of cell-based therapy for cardiovascular disease. *J. Transl. Int. Med.* 9 (4), 234–238. doi:10.2478/jtim-2021-0017
- Xu, Z., Chen, L., Wang, C., Zhang, L., and Xu, W. (2021b). MicroRNA-1287-5p promotes ferroptosis of osteosarcoma cells through inhibiting GPX4. *Free Radic. Res.* 55 (11–12), 1119–1129. doi:10.1080/10715762.2021.2024816
- Yadav, P., Sharma, P., Sundaram, S., Venkatraman, G., Bera, A. K., and Karunakaran, D. (2021). SLC7A11/xCT is a target of miR-5096 and its restoration partially rescues miR-5096-mediated ferroptosis and anti-tumor effects in human breast cancer cells. *Cancer Lett.* 522, 211–224. doi:10.1016/j.canlet.2021.09.033
- Yan, Y., Liang, Q., Xu, Z., Huang, J., Chen, X., Cai, Y., et al. (2021). Downregulated ferroptosis-related gene STEAP3 as a novel diagnostic and prognostic target for hepatocellular carcinoma and its roles in immune regulation. *Front. Cell Dev. Biol.* 9, 743046. doi:10.3389/fcell.2021.743046
- Yang, Y., Lin, Z., Han, Z., Wu, Z., Hua, J., Zhong, R., et al. (2021). miR-539 activates the SAPK/JNK signaling pathway to promote ferroptosis in colorectal cancer by directly targeting TIPE. *Cell Death Discov.* 7 (1), 272. doi:10.1038/s41420-021-00659-x
- Zexin, L., (2022). MicroRNA-132 promotes atherosclerosis by inducing mitochondrial oxidative stress-mediated ferroptosis. *Nan Fang. Yi Ke Da Xue Xue Bao* 421, 143–149. doi:10.12122/j.issn.1673-4254.2022.01.18
- Zhang, H., He, Y., Wang, J. X., Chen, M. H., Xu, J. J., Jiang, M. H., et al. (2020a). miR-30-5p-mediated ferroptosis of trophoblasts is implicated in the pathogenesis of preeclampsia. *Redox Biol.* 29, 101402. doi:10.1016/j.redox.2019.101402
- Zhang, K., Wu, L., Zhang, P., Luo, M., Du, J., Gao, T., et al. (2018). miR-9 regulates ferroptosis by targeting glutamic-oxaloacetic transaminase GOT1 in melanoma. *Mol. Carcinog.* 57 (11), 1566–1576. doi:10.1002/mc.22878
- Zhang, X., Wang, L., Li, H., Zhang, L., Zheng, X., and Cheng, W. (2020b). Crosstalk between noncoding RNAs and ferroptosis: New dawn for overcoming cancer progression. *Cell Death Dis.* 11 (7), 580. doi:10.1038/s41419-020-02772-8
- Zheng, S., Hu, L., Qingwen Song, Y. S., Yin, G., Zhu, H., and Wencheng Kong, C. Z. (2021). miR-545 promotes colorectal cancer by inhibiting transferring in the non-normal ferroptosis signaling. *AGING* 13 (24), 26137–26147.
- Zhi, Y., Gao, L., Wang, B., Ren, W., Liang, K. X., and Zhi, K. (2021). Ferroptosis holds novel promise in treatment of cancer mediated by non-coding RNAs. *Front. Cell Dev. Biol.* 9, 686906. doi:10.3389/fcell.2021.686906
- Zhou, J., Xiao, C., Zheng, S., Wang, Q., Zhu, H., Zhang, Y., et al. (2022). MicroRNA-214-3p aggravates ferroptosis by targeting GPX4 in cisplatin-induced acute kidney injury. *Cell Stress Chaperones.* doi:10.1007/s12192-022-01271-3
- Zhou, X., Zhuo, M., Zhang, Y., Shi, E., Ma, X., and Li, H. (2021). miR-190a-5p regulates cardiomyocytes response to ferroptosis via directly targeting GLS2. *Biochem. Biophys. Res. Commun.* 566, 9–15. doi:10.1016/j.bbrc.2021.05.100
- Zhu, C., Song, Z., Chen, Z., Lin, T., Lin, H., Xu, Z., et al. (2022a). MicroRNA-4735-3p facilitates ferroptosis in clear cell renal cell carcinoma by targeting SLC40A1. *Anal. Cell. Pathol.* 2022, 1–12. doi:10.1155/2022/4213401
- Zhu, D., Wu, S., Li, Y., Zhang, Y., Chen, J., Ma, J., et al. (2022b). Ferroptosis-related gene SLC1A5 is a novel prognostic biomarker and correlates with immune infiltrates in stomach adenocarcinoma. *Cancer Cell Int.* 22 (1), 124. doi:10.1186/s12935-022-02544-8
- Zhu, S., Zhang, Q., Sun, X., Zeh, H. J., Lotze, M. T., Kang, R., et al. (2017). HSPA5 regulates ferroptotic cell death in cancer cells. *Cancer Res.* 77 (8), 2064–2077. doi:10.1158/0008-5472.Can-16-1979
- Zhuang, Y., Yang, D., Shi, S., Wang, L., Yu, M., Meng, X., et al. (2022). MiR-375-3p promotes cardiac fibrosis by regulating the ferroptosis mediated by GPX4. *Comput. Intell. Neurosci.* 2022, 1–12. doi:10.1155/2022/9629158
- Zuo, Y. B., Zhang, Y. F., Zhang, R., Tian, J. W., Lv, X. B., Li, R., et al. (2022). Ferroptosis in cancer progression: Role of noncoding RNAs. *Int. J. Biol. Sci.* 18 (5), 1829–1843. doi:10.7150/ijbs.66917



## OPEN ACCESS

## EDITED BY

Xin Wang,  
National Institutes of Health (NIH),  
United States

## REVIEWED BY

Min Wan,  
Cornell University, United States  
Enchao Qiu,  
Thomas Jefferson University,  
United States  
Xianyi Cai,  
Huazhong University of Science and  
Technology, China

## \*CORRESPONDENCE

Xiangyan Li,  
xiangyan\_li1981@163.com  
Jia Mi,  
mijia8201@126.com

\*These authors have contributed equally  
to this work

## SPECIALTY SECTION

This article was submitted to Molecular  
Diagnostics and Therapeutics,  
a section of the journal  
Frontiers in Molecular Biosciences

RECEIVED 23 September 2022

ACCEPTED 20 October 2022

PUBLISHED 03 November 2022

## CITATION

Wang Y, Zhang Z, Jiao W, Wang Y,  
Wang X, Zhao Y, Fan X, Tian L, Li X and  
Mi J (2022), Ferroptosis and its role in  
skeletal muscle diseases.  
*Front. Mol. Biosci.* 9:1051866.  
doi: 10.3389/fmolb.2022.1051866

## COPYRIGHT

© 2022 Wang, Zhang, Jiao, Wang,  
Wang, Zhao, Fan, Tian, Li and Mi. This is  
an open-access article distributed  
under the terms of the [Creative  
Commons Attribution License \(CC BY\)](#).  
The use, distribution or reproduction in  
other forums is permitted, provided the  
original author(s) and the copyright  
owner(s) are credited and that the  
original publication in this journal is  
cited, in accordance with accepted  
academic practice. No use, distribution  
or reproduction is permitted which does  
not comply with these terms.

# Ferroptosis and its role in skeletal muscle diseases

Ying Wang<sup>1†</sup>, Zepeng Zhang<sup>2†</sup>, Weikai Jiao<sup>1</sup>, Yanyan Wang<sup>3</sup>,  
Xiuge Wang<sup>3</sup>, Yunyun Zhao<sup>3</sup>, Xuechun Fan<sup>1</sup>, Lulu Tian<sup>4</sup>,  
Xiangyan Li<sup>5\*</sup> and Jia Mi<sup>3\*</sup>

<sup>1</sup>College of Traditional Chinese Medicine, Changchun University of Chinese Medicine, Changchun, China, <sup>2</sup>Research Center of Traditional Chinese Medicine, The First Affiliated Hospital of Changchun University of Chinese Medicine, Changchun, China, <sup>3</sup>Department of Endocrinology, The First Affiliated Hospital of Changchun University of Chinese Medicine, Changchun, China, <sup>4</sup>School of Life Sciences, Zhejiang Chinese Medical University, Hangzhou, China, <sup>5</sup>Northeast Asia Research Institute of Traditional Chinese Medicine, Key Laboratory of Active Substances and Biological Mechanisms of Ginseng Efficacy, Changchun University of Chinese Medicine, Changchun, China

Ferroptosis is characterized by the accumulation of iron and lipid peroxidation products, which regulates physiological and pathological processes in numerous organs and tissues. A growing body of research suggests that ferroptosis is a key causative factor in a variety of skeletal muscle diseases, including sarcopenia, rhabdomyolysis, rhabdomyosarcoma, and exhaustive exercise-induced fatigue. However, the relationship between ferroptosis and various skeletal muscle diseases has not been investigated systematically. This review's objective is to provide a comprehensive summary of the mechanisms and signaling factors that regulate ferroptosis, including lipid peroxidation, iron/heme, amino acid metabolism, and autophagy. In addition, we tease out the role of ferroptosis in the progression of different skeletal muscle diseases and ferroptosis as a potential target for the treatment of multiple skeletal muscle diseases. This review can provide valuable reference for the research on the pathogenesis of skeletal muscle diseases, as well as for clinical prevention and treatment.

## KEYWORDS

ferroptosis, mechanism, sarcopenia, rhabdomyolysis, rhabdomyosarcoma, fatigue, myositis

## 1 Introduction

As proposed by Dixon in 2012, ferroptosis is a novel method of regulatory cell death (RCD) (Dixon et al., 2012). Ferroptosis is characterized by the accumulation of iron ions and products of lipid peroxidation, which are different from the currently known mechanisms for cell death, such as apoptosis, pyroptosis, necrosis, and autophagy (Dixon et al., 2012; Latunde-Dada, 2017; Li J. et al., 2020). Ferroptosis, on the other hand, displays unique morphological changes, such as mitochondrial shrinkage, an increase in membrane density, and diminished or absent mitochondrial cristae (Dixon et al., 2012; Yu et al., 2017). As research advances, the interaction among amino acids, lipids, and iron metabolism is considered to be the key to ferroptosis, and a number of related signaling pathways, genes, proteins, and organelles have been



identified (Chen et al., 2017; Badgley et al., 2020; Zhang H. et al., 2020; Venkatesh et al., 2020; Yu et al., 2020; Li Y. et al., 2021; Kong et al., 2021). Furthermore, genes associated with autophagy, such as *nuclear receptor coactivator 4* (NCOA4) and *fanconi anemia complementation group D2* (FANCD2), have also been discovered as key regulators of ferroptosis (Hou et al., 2016; Song et al., 2016). Meanwhile, numerous studies have demonstrated that ferroptosis plays a crucial role in cancer, diabetes mellitus, chronic kidney disease, heart failure, and other disease processes, offering a promising perspective for future clinical treatment (Chen X. et al., 2019; Li D. et al., 2020; Mao et al., 2021; Wang et al., 2022).

Skeletal muscle is the largest organ of the human body (accounting for about 40% of the body weight) (Janssen et al., 2000), which is crucial for maintaining body movements, posture and essential movements (such as swallowing and breathing), glucose intake and temperature regulation (Ferrannini et al., 1988; Meyer et al., 2002; Fluck and Hoppeler, 2003; Klaus et al., 2005; Shiozu et al., 2015; Kanezaki et al., 2021). Meanwhile, the storage of amino acids and the secretion of muscle cytokines are also the key functions of skeletal muscle (Wolfe, 2006; Argiles et al., 2016; Hoffmann and Weigert, 2017). The former can provide the substrate needed for the generation of energy and protein in the body (Garber et al., 1976; Perez-Sala et al., 1987; Perriello et al., 1997; Hyde et al., 2005), and the latter can participate in a versatile of physiological and pathological processes such as inflammation regulation, insulin sensitivity, tumor growth inhibition and cognitive improvement (Pedersen and Febbraio, 2008; Hong et al., 2009; Ellingsgaard et al., 2011; Hojman et al., 2011; Wrann et al., 2013). The importance of skeletal muscle bestows the life-threatening perniciousness on skeletal muscle diseases. Among the diseases, not only do sarcopenia, rhabdomyolysis (RML), rhabdomyosarcoma (RMS) and exhaustive exercise-induced fatigue (EEIF) and other skeletal muscle diseases seriously affect the quality of life and body function of patients, but they can also induce or develop into a variety of acute/chronic diseases, such as diabetes, fractures, hypercalcemia and acute kidney injury (AKI) (Kawasaki et al., 1998; Lima et al., 2008; Liu et al., 2014; Oliveira and Vaz, 2015; Tsekoura et al., 2017; Welch et al., 2020). Therefore, it is an urgent medical problem to clarify the pathogenesis of different skeletal muscle diseases and seek effective therapeutic targets. Recent studies have found that ferroptosis is an important RCD that induces skeletal muscle cell death and prevents skeletal muscle proliferation and differentiation (Guerrero-Hue et al., 2019; Ding et al., 2021; Huang et al., 2021). At the same time, ferroptosis is repeatedly reported to be associated with skeletal muscle disease processes such as sarcopenia, RML, RMS, and EEIF (Guerrero-Hue et al., 2019; Dachert et al., 2020; Huang et al., 2021; Xiao et al., 2022). The exact role of ferroptosis in these diseases, however, has not been systematically elucidated.

In this review, the biological mechanisms and key regulators of ferroptosis that have been published so far will be elaborated on. What will also be summarized is the research progress of ferroptosis in various skeletal muscle diseases and possible related therapeutic target strategies, aiming to provide valuable information and new directions for ferroptosis to participate in the pathogenesis and treatment of skeletal muscle diseases.

## 2 The regulatory mechanism of ferroptosis

### 2.1 Lipid peroxidation and ferroptosis

As shown in current research, ferroptosis is caused by the accumulation of lipid peroxides and their decomposition products (Dixon et al., 2012; Yang and Stockwell, 2016; Feng and Stockwell, 2018). It is therefore important to understand the mechanisms of lipid peroxide production and clearance for the purpose of comprehending ferroptosis regulation.

#### 2.1.1 Lipid peroxide production

Reactive oxygen species (ROS) are a group of highly active chemicals containing oxygen, including superoxide anion, hydrogen peroxide (H<sub>2</sub>O<sub>2</sub>), hydroxyl radical and peroxy radical (Bayir, 2005; Yang et al., 2013). ROS produced in physiological process can regulate tissue homeostasis and transduce cell signal transduction (Rhee et al., 2000; Zhang H. et al., 2013; Zhang et al., 2016; Ferreira et al., 2018). The intracellular antioxidant system strictly monitors the generation and elimination of the ROS to maintain balance (He et al., 2017). When the oxidation and antioxidant systems are out of balance, a large amount of ROS produced will react with polyunsaturated fatty acids (PUFAs) in membrane phospholipids to form lipid peroxidation, which will change the fluidity and permeability of cell membrane and eventually lead to cell death (Farmer and Mueller, 2013; Catala and Diaz, 2016; Su et al., 2019). Ferroptosis, named for its iron ion dependence, is a typical representative of this cell death mode (Dixon et al., 2012; Yang and Stockwell, 2016). Fenton reaction, a non-enzymatic reaction mediated by iron, can promote the lipid peroxidation of PUFAs in membrane lipids by producing highly toxic hydroxyl radicals, thereby inducing ferroptosis (He et al., 2020). Enzymatic reaction is another important way to cause lipid peroxidation of PUFAs (Yamamoto, 1991; Lee et al., 2021). During enzymatic reaction, the esterification of free PUFAs and the insertion of these molecules into membrane phospholipids are achieved by Acyl-CoA synthetase long-chain family member 4 (ACSL4) and Lysophosphatidylcholine acyltransferase 3 (LPCAT3) (Dixon et al., 2015; Yuan et al., 2016a; Doll et al., 2017). Subsequently, lipoxygenase catalyzes lipid peroxidation of membrane phospholipids, which results in ferroptosis (Yang et al., 2016). Meanwhile, malondialdehyde (MDA) and

4-hydroxy-nonenal (4-HNE), which are produced during lipid peroxide degradation, can have adverse effects on the structure and function of proteins and nucleic acids (Ayala et al., 2014). Reducing lipid peroxidation has thus become a core step in the regulation of ferroptosis.

### 2.1.2 Role of antioxidant system in ferroptosis

Lipid peroxidation mediated by ROS can lead to ferroptosis (Su et al., 2019). The three important intracellular antioxidant systems, GSH system, CoQ10 system and BH4 system, are essential for scavenging ROS and maintaining redox stability (Schafer and Buettner, 2001; James et al., 2004; Mugoni et al., 2013; Hatem et al., 2014; Jazvinscak Jembrek et al., 2014; Xue et al., 2017). In a variety of studies, they have also been proved to be a crucial defense to protect cells from lipid peroxidation induced ferroptosis (Bersuker et al., 2019; Kraft et al., 2020; Chen et al., 2022b). Hence, in the following discussion, we will focus on the role of these three antioxidant systems in ferroptosis.

#### 2.1.2.1 Glutathione system and ferroptosis

Glutathione (GSH) is a tripeptide composed of glutamate, cysteine and glycine, and also a paramount antioxidant in cells (Meister and Anderson, 1983). Glutathione peroxidase 4 (GPX4) is a selenoprotein with selenocysteine as its active center (Flohe et al., 1973; Rotruck et al., 1973; Ingold et al., 2018). GPX4 can convert toxic lipid hydroperoxides (L-OOH) into non-toxic lipid alcohol (L-OH) to prevent the accumulation of Fe<sup>2+</sup> dependent lipid ROS on membrane lipids, thus playing a strong role in inhibiting ferroptosis (Imai and Nakagawa, 2003; Ursini and Maiorino, 2020). The transformation relies on the electrons provided by the process of GSH conversion into glutathione disulfide (GSSG) (Deponte, 2013). Subsequently, GSSG regenerates GSH under the catalysis of glutathione reductase (GR) and cofactor NADPH/H<sup>+</sup>, so as to continuously and circularly play an antioxidant role (Lu, 2009). Cysteine is the rate limiting substrate for GSH synthesis, and its availability directly affects the intracellular GSH level (Lu, 2009). Heavy chain solute carrier family 3 member 2 (SLC3A2, also known as CD98hc) and light chain solute carrier family 7 member 11 (SLC7A11, also known as XCT) construct the crucial amino acid transporter known as the cysteine/glutamate antiporter (system Xc<sup>-</sup>) (Bridges et al., 2012). Under system Xc<sup>-</sup>, cystine is exchanged 1:1 with intracellular glutamate and quickly reduced to cysteine for GSH synthesis and antioxidant defense (Mandal et al., 2010; Lewerenz et al., 2013). As a result, inhibiting the impairment of cystine uptake caused by system Xc<sup>-</sup> can directly result in GSH depletion and GPX4 inactivation, which contributes to the induction of ferroptosis. Erastin is a representative of this ferroptosis trigger mechanism and has been widely used in ferroptosis induction experiments (Zhao Y. et al., 2020; Wang et al., 2020). Meanwhile, numerous researches results have proved that blocking System Xc<sup>-</sup> to induce ferroptosis of cancer cells is an important mechanism

for sorafenib to play an anti-cancer role (Li Y. et al., 2020; Li Z. J. et al., 2021), which provides a promising direction for inhibiting tumor growth.

In addition, in some mammalian cells, another way to maintain the supply of cysteine is the activation of transsulfuration pathway (McBean, 2012; Eriksson et al., 2015). Specifically, methionine, a sulfur donor from the diet, is converted into homocysteine (Mosharov et al., 2000; Sbodio et al., 2019). Then, homocysteine is condensed with serine under the catalysis of cystathionine  $\beta$ -synthase (CBS) to produce cystathionine, which finally produces cysteine through the action of cystathionine gamma-lyase (CSE) (Sbodio et al., 2019). It was found that cells with cysteinyl tRNA synthetase deletion can resist ferroptosis induced by erastin by up regulating genes and metabolites (cystathionine) in the transsulfuration pathway (Hayano et al., 2016). It is suggested that the transsulfuration pathway may be an alternative in inhibiting ferroptosis during cysteine deprivation. Further, cysteine produced by trans-sulfuration or uptake pathway combines with glutamate through GSH synthesis rate limiting enzyme glutamate cysteine ligase (GCL) (Lu, 2009). After the combination, GSH is finally synthesized under the catalysis of glutamate synthase (GSS) (Lu, 2009). The study found that GCL inhibition can induce ferroptosis of cancer cells (Nishizawa et al., 2018; Qin et al., 2021), contributing a new strategy for the development of cancer drugs.

#### 2.1.2.2 Coenzyme Q 10 system with ferroptosis

Coenzyme Q 10 (CoQ10, also known as ubiquinone) is a potent fat-soluble antioxidant that has been found in several recent studies to be involved in the regulation of ferroptosis (Laredj et al., 2014; Bersuker et al., 2019; Doll et al., 2019). Specifically, ferroptosis suppressor protein 1 (FSP1) is recruited to the plasma membrane by myristoylated and reduce CoQ10 to ubiquinol (CoQ10H2) by using NAD (P) H, thereby trapping lipid peroxidation free radicals to prevent lipid peroxidation (Bersuker et al., 2019). It is worth noting that although CoQ10 exists in almost all lipid membranes of cells, only CoQ10 outside mitochondria can inhibit ferroptosis under FSP1 dependent modification (Stockwell, 2019). Bersuker et al. found that FSP1 is a necessary factor to maintain tumor cell activity and growth under the condition of GPX4 knockout, and its expression is positively related to the resistance of cells to GPX4 inhibitors (Bersuker et al., 2019). It is indicated that FSP1/CoQ10/NAD(P)H pathway is a parallel and complementary regulatory mechanism of ferroptosis with GSH/GPX4 pathway.

The mevalonate pathway is essential for ferroptosis regulation because its metabolic intermediate, isopentenyl pyrophosphate, is indispensable for CoQ10 and GPX4 biosynthesis (Holstein and Hohl, 2004; Moosmann and Behl, 2004; Friedmann Angeli and Conrad, 2018). It was found that ferroptosis inducing 56 can induce ferroptosis by degrading GPX4 and consuming CoQ10, which is achieved by interfering

with the mevalonate pathway (Shimada et al., 2016). Therefore, it is necessary to further explore the regulatory effect of mevalonate pathway in ferroptosis.

### 2.1.2.3 Tetrahydrobiopterin system and ferroptosis

Tetrahydrobiopterin (BH4) has been found in recent studies to be a potent radical-trapping antioxidant that protects cells from ferroptosis by blocking lipid peroxidation transmission and acts independently of the GSH-dependent GPX4 protective pathway (Kraft et al., 2020; Soula et al., 2020). Guanosine triphosphate cyclohydrolase-1 (GCH1), the rate-limiting enzyme of BH4 synthesis, regenerates BH4 by catalyzing guanosine triphosphate (Thony et al., 2000). It was found that up-regulation of GCH1 restored the resistance of BH4-deficient cells to RSL3, indicating that GCH1 expression is decisive in the effectiveness of BH4 (Soula et al., 2020). In addition, BH4 may increase CoQ10 levels by converting phenylalanine into tyrosine, which provides a new perspective for its involvement in ferroptosis regulation (Kraft et al., 2020). However, the exact mechanism of BH4 system involved in the regulation of ferroptosis is still unclear, and further research is needed.

## 2.2 Iron metabolism and ferroptosis

Iron is a trace element necessary to maintain human life and health, and plays many essential physiological functions, including metabolism, oxygen transport, antioxidant reactions, electron transport, and DNA synthesis (Dlouhy and Outten, 2013). To maintain iron homeostasis, the body tightly regulates iron metabolism (including iron acquisition, utilization, storage, and efflux) (Wang and Pantopoulos, 2011). However, the destruction of iron homeostasis can lead to unstable iron accumulation and catalyze Fenton reaction, thus inducing ferroptosis (Winterbourn, 1995; Dixon et al., 2012; Henning et al., 2022). Therefore, regulation of iron metabolism is vital for the ferroptosis process.

### 2.2.1 Cellular iron metabolism and ferroptosis

A complex formed by transferrin (TF) containing iron and the transferrin receptor (TFRC) on the cell membrane enters the endosome through endocytosis under physiological conditions (Andrews, 2000; Hentze et al., 2010). An endosome containing the complex is acidified to promote the release of  $\text{Fe}^{3+}$  from TF, which is then reduced to  $\text{Fe}^{2+}$  by six-transmembrane epithelial antigen of prostate 3 (Steap3) (Ohgami et al., 2005), and the iron is transported to the unstable labile iron pool in the cytoplasm by the divalent metal transporter 1 (DMT1) (Fleming et al., 1998). Studies have shown that TFRC and DMT1 overexpression can promote unstable iron accumulation and trigger lipid peroxidation, thus becoming key regulators of ferroptosis

(Song et al., 2021a; Zhang H. et al., 2021; Guo et al., 2021; Lu et al., 2021). Additionally, the high expression of heat shock protein beta-1 (HSPB1) prevents ferroptosis by inhibiting TFRC-mediated iron absorption (Chen et al., 2006; Sun et al., 2015). Ferritin is the major cytoplasmic iron storage protein complex, which includes ferritin light chain (FTL) and ferritin heavy chain 1 (FTH1) (Knovich et al., 2009). Ferroptosis can be inhibited by the ferroxidase activity of FTH1, which converts  $\text{Fe}^{2+}$  captured by ferritin into  $\text{Fe}^{3+}$  in order to reduce the production of ROS (Theil, 2013). A number of studies have confirmed that high expression of FTH1 can reduce susceptibility to ferroptosis *in vivo* and *in vitro*, respectively (Tian et al., 2020; Kong et al., 2021). Mammalian cells release iron through ferroportin 1 (FPN1) (Nemeth et al., 2004; Ward and Kaplan, 2012). A high level of FPN1 expression can promote iron efflux and protect cells from ferroptosis (Zhao X. et al., 2020; Tian et al., 2021). The iron regulatory protein 1/2 (IRP1/2) can bind to the iron responsive element (IRE) to regulate the expression of various iron metabolism proteins (DMT1, TFRC, FPN, FTH1/FTL), which is responsible for regulating iron homeostasis in cells (Aziz and Munro, 1987; Koeller et al., 1989; Xu et al., 2018; Xu M. et al., 2022). By promoting the expression of IRP1/2, the ferroptosis inducers erastin and RSL3 increase the susceptibility of melanoma cells to ferroptosis (Yao et al., 2021).

In general, each regulatory link in cellular iron metabolism affects the intracellular iron content and therefore contributes to ferroptosis.

### 2.2.2 Mitochondrial iron metabolism and ferroptosis

Iron metabolism in mitochondria is crucial to the control of cellular iron homeostasis. Iron transported from endosomes, cytosols, or ferritin traverses the outer membrane and inner membrane of mitochondria to reach the mitochondrial matrix, where it is utilized for the biosynthesis of heme and iron sulfur clusters or stored by mitochondrial ferritin (FtMt) to maintain cellular iron homeostasis (Paul et al., 2017). Mitoferrin 1/2 (Mfrn1/2) is a crucial component in facilitating iron transport across the inner mitochondrial membrane during this process (Paradkar et al., 2009). Studies have shown that reduced Mfrn expression may minimize ferroptosis by ameliorating mitochondrial iron excess (An et al., 2022; Zhang T. et al., 2022). Not only does FtMt store free iron in mitochondria, but it can also transport cytoplasmic iron to mitochondria, which is essential for controlling mitochondrial iron metabolism (Corsi et al., 2002; Drysdale et al., 2002). *In vivo* and *in vitro*, overexpression of FtMt abolished erastin-induced ferroptosis (Wang et al., 2016). In addition, the mitochondrial outer membrane protein CDGSH iron sulfur domain 1 (CISD1) was reported to reduce the sensitivity of liver cancer cells to erastin by inhibiting mitochondrial iron

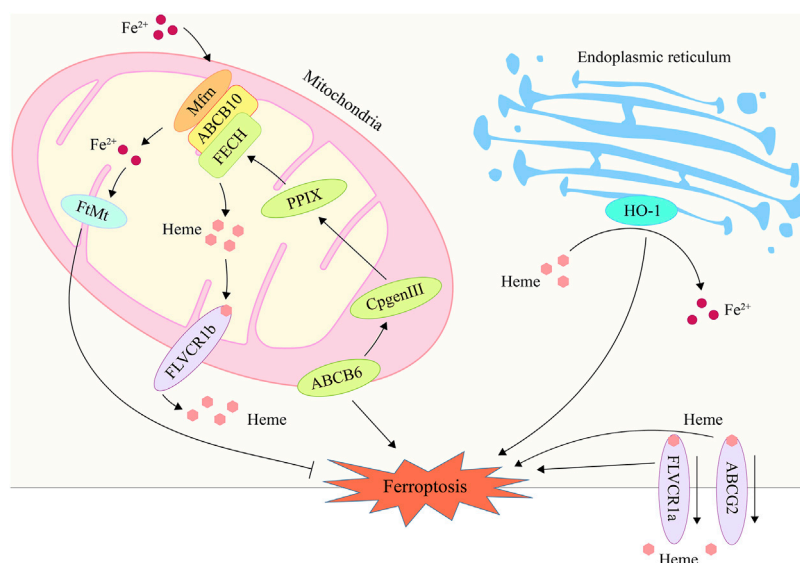


**FIGURE 1**

The processes of heme metabolism and mitochondrial iron metabolism are implicated in ferroptosis. In the endoplasmic reticulum, HO-1 degrades heme and releases iron ions, hence raising intracellular iron content and promoting ferroptosis. ABCB6 stimulates heme production by transferring CPgenIII from the cytosol to the mitochondrial membrane gap, a process that may play a role in ferroptosis. By exporting heme via the plasma membrane, ABCG2 and FLVCR1 contribute to the control of ferroptosis. Mfn is capable of transporting iron through the inner membrane and into the mitochondrial matrix, hence elevating the iron concentration in mitochondria and inducing ferroptosis. FtMt may store free iron in mitochondria, hence reducing iron concentration and inhibiting ferroptosis. HO-1, heme oxygenase 1; ABCB6, ATP-binding cassette subfamily B member 6; ABCG2, ATP-binding cassette subfamily G member 2; Mfn, mitoferrin; FtMt, mitochondrial ferritin.

overload mediated lipid peroxidation (Yuan et al., 2016b), providing a new target for cancer treatment.

## 2.3 Heme metabolism and ferroptosis

Heme is the primary source of functional iron in the human body and a crucial component of erythropoiesis (Chung et al., 2012; Hooda et al., 2014). Therefore, the maintenance of systemic iron homeostasis requires the maintenance of a normal heme metabolism. The up-regulation of heme oxygenase 1 (HO-1), a crucial enzyme that degrades heme to liberate iron, can participate in ferroptosis induction by increasing intracellular iron levels (Tenhunen et al., 1968; Han et al., 2022). HO-1 inhibitor zinc protoporphyrin IX was discovered to counteract erastin-induced ferroptosis in HT-1080 fibrosarcoma cells (Kwon et al., 2015). HO-1-deficient proximal tubular cells, however, are very vulnerable to ferroptosis produced by erastin and RAS-selective lethal 3 (RSL3), which may be correlated to elevated heme levels after HO-1 deletion (Adedoyin et al., 2018). Heme metabolism related genes such as ATP-binding cassette subfamily B member 6 (ABCB6), Feline leukemia virus subgroup C receptor 1 (FLVCR1) and ATP-binding cassette subfamily G member 2 (ABCG2) were also found to be associated with ferroptosis (Tang et al., 2020; Zhang et al., 2020; Kawai et al., 2022). ABCB6 can transport

the coproporphyrinogen III (CPgenIII) precursor of heme synthesis from the cytosol to the mitochondria, which is a key gene for heme synthesis (Krishnamurthy et al., 2006). As is shown in a research, low expression of ABCB6 in hepatocellular carcinoma may reduce the sensitivity of cancer cells to ferroptosis by reducing heme production (Zhang et al., 2020). Another study found that ABCB6 and FLVCR1 (an important carrier of cell surface heme output) were strongly positive and synergetic in tumor tissue, and were significantly down regulated after erastin intervention (Quigley et al., 2004; Keel et al., 2008; Tang et al., 2020). These results suggest that the heme content in cancer cells may affect their sensitivity to ferroptosis. In addition, as another important executor of heme export, part of ABCG2's heme output capacity was found to be related to ferroptosis in recent studies (Desuzinges-Mandon et al., 2010; Kawai et al., 2022). But there is still no substantive research to support this finding yet. In general, heme metabolism is a promising research direction in the regulation mechanism of ferroptosis, which needs more attention and research (Figure 1; Table 1).

## 2.4 Amino acid metabolism and ferroptosis

Amino acid metabolism is closely related to ferroptosis, one of the main reasons is that it participates in GSH synthesis (Te



TABLE 1 Heme metabolism related genes and ferroptosis.

Gene	Protein name	Function	Relationship with ferroptosis	References
ABCB6	ATP binding cassette subfamily B member 6	Transport CPgenIII from the cytosol to the mitochondria to promote heme synthesis	Low expression of ABCB6 might promote ferroptosis through reducing iron consumption by inhibit heme synthesis	Krishnamurthy et al. (2006); Zhang et al. (2020); Tang et al. (2020)
FLVCR1(a/b)	Feline leukemia virus subgroup C receptor 1	Export heme	Low expression of FLVCR1 increases tumor cell sensitivity to erastin by reducing iron-containing heme export	Quigley et al. (2004); Keel et al. (2008); Tang et al. (2020)
ABCG2	ATP-binding cassette subfamily G member 2	Export heme	Regulation of heme output involved in ferroptosis	Desuzinges-Mandon et al. (2010); Kawai et al. (2022)
HO-1	Heme oxygenase 1	Breaks down heme to produce free iron, biliverdin and CO Protect cells from oxidative stress	Promotes free iron release to enhance cellular ferroptosis sensitivity Ferroptosis is regulated by Nrf2/HO-1 axis	Tenhunen et al. (1968); Han et al. (2022); Kwon et al. (2015) Niu et al. (2020); Chen et al. (2021b); Li et al. (2021b); Lv et al. (2021)

Braake et al., 2008; Sikilidis et al., 2014; Sun et al., 2018; Xu Y. et al., 2022). In addition to the above-mentioned cysteine, glutamate is another essential amino acid for GSH synthesis, and glutaminolysis is one of its sources (Whillier et al., 2011). By encouraging the conversion of glutamine to glutamate and boosting the synthesis of GSH, glutaminase 2 (GLS2) improves the antioxidant capacity of cells (Xiang et al., 2013). The ferroptosis resistance of cardiomyocytes can be significantly increased by targeted regulation of GLS2, according to studies (Zhou et al., 2021). However, a new regulatory mechanism for glutamate neurotoxicity is provided by the fact that high glutamate levels cause ferroptosis in neuronal cells by interfering with cystine uptake (Olney, 1971; Murphy et al., 1989; Jiang et al., 2020). Additionally, it has been demonstrated that the downstream metabolite of glutaminolysis,  $\alpha$ -ketoglutarate, is involved in the production of lipid ROS, raising the possibility that ferroptosis influenced by glutaminolysis (Gao et al., 2015). Meanwhile, compound 968, a glutaminolysis inhibitor, can significantly reduce erastin sensitivity under cystine deficiency (Gao et al., 2015), further demonstrated the necessity of glutaminolysis for ferroptosis. It is interesting to note that the ferroptosis inhibitor ferrostatin-1 (Fer-1) completely restored the sharply decreased glutamine level under RSL3 intervention (Rodriguez-Graciani et al., 2022). Based on the aforementioned findings, it is possible that the amino acid environment in which cells are located plays a role in the bidirectional regulation of ferroptosis by glutaminolysis.

Other amino acids, such as branched chain amino acids, tryptophan and lysine, is pivotal in ferroptosis (Chepikova et al., 2020; Wang K. et al., 2021; Zeitler et al., 2021). It was shown that the branched-chain amino acid aminotransferase two and lysine oxidase can participate in the ferroptosis process by antagonizing the system  $Xc^-$  inhibition and promoting  $H_2O_2$  generation, respectively (Chepikova et al., 2020; Wang K. et al., 2021). Meanwhile, the tryptophan metabolite indole-3-pyruvate was recently found to negatively regulate ferroptosis through direct

free radical depletion and upregulation of antioxidant genes (SLC7A11 and HO-1) (Zeitler et al., 2021). In addition, despite no relevant research report that arginine, serine and glycine participate in the regulation of ferroptosis, the three amino acids have shown the potential to fight ferroptosis in some studies (Possemato et al., 2011; Ye et al., 2014; Sen et al., 2018), which needs more exploration and excavation.

## 2.5 Other ferroptosis regulatory proteins

### 2.5.1 Nuclear factor erythroid 2-related factor 2

Nuclear factor erythroid 2-related factor 2 (Nrf2) is a crucial transcription factor for cell antioxidants and a crucial ferroptosis regulator (Dodson et al., 2019; Anandhan et al., 2020). To stop lipid peroxides-mediated ferroptosis, Nrf2 can directly control the expression level of the GPX4 protein and important genes for GSH synthesis, such as the catalytic and regulatory subunits of glutamate cysteine ligase (GCLC/GCLM), GSS, GR, and XCT (Chan and Kwong, 2000; Madduma Hewage et al., 2017; Feng et al., 2021; Scibior et al., 2021; Lu et al., 2022). Meanwhile, with the ability of targeting key genes (*FTH1*, *FPN1*) that regulate iron metabolism, Nrf2 can participate in the process of ferroptosis by affecting intracellular iron levels (Harada et al., 2011; Liu et al., 2020). In addition, Nrf2 also regulate the key genes of heme metabolism *ABCB6*, *ABCG2*, *HO-1* and *heme responsive gene-1* to participate in the process of ferroptosis (Hubner et al., 2009; Singh et al., 2010; Campbell et al., 2013; Dong et al., 2020). Among them, HO-1 is not only the key enzyme to decompose heme, but also an important antioxidant (Tenhunen et al., 1968; Niu et al., 2020). Multiple studies have shown that activating the antioxidant response axis Nrf2/HO-1 is a crucial means of inhibiting ferroptosis and ameliorating myocardial ischemia-reperfusion injury, ulcerative colitis, and acute lung injury

(Chen et al., 2021b; Li J. et al., 2021; Lv et al., 2021). Kelch-like ECH-associated protein 1 (Keap1) is a substrate adaptor protein of E3 ubiquitin ligase, which tightly controls the activity of Nrf2 by way of the ubiquitin-proteasome system (Furukawa and Xiong, 2005; Yamamoto et al., 2018). In order to prevent Nrf2 degradation and to promote its nuclear translocation and maintain cellular redox homeostasis, p62 can bind to Keap1 in a competitive manner (Tan et al., 2021). Studies have shown that one of the effective ways to treat liver cancer, endometrial hyperplasia, and protect neurons is by mediating the p62/Keap1/Nrf2 pathway to regulate ferroptosis (Sun et al., 2016; Zhang M. et al., 2021; Li et al., 2022). Owing to that Nrf2 is extensive in the regulation of ferroptosis, targeting Nrf2 is of great significance in the treatment of ferroptosis related diseases.

### 2.5.2 P53

A crucial tumor suppressor gene called p53 is involved in the cell cycle, aging, apoptosis, and autophagy (Ong and Ramasamy, 2018). But more and more research has revealed that p53 also plays a significant part in controlling ferroptosis (Zhang Y. et al., 2021; Gao et al., 2021; Lei et al., 2021). Study has indicated that, as a direct target gene of p53, spermidine/spermine N1-acetyltransferase 1 (SAT1) can up-regulate arachidonate 15-lipoxygenase to promote ferroptosis due to accumulation of lipid peroxidation under ROS-induced stress (Ou et al., 2016). Other studies have shown that up-regulated p53 can affect GSH synthesis by inhibiting the expression of its downstream target gene SLC7A11, thereby inducing ferroptosis (Jiang et al., 2015; Guan et al., 2020). Meanwhile, by suppressing the expression of SLC7A11, p53 can indirectly activate the positive regulator of ferroptosis arachidonate 12-lipoxygenase (ALOX12) to promote ferroptosis (Chu et al., 2019). Additionally, p53 can facilitate dipeptidyl-peptidase 4's (DPP4) nuclear translocation and join forces with it to form the DPP4-p53 complex, which lowers DPP4-dependent lipid peroxidation and inhibits ferroptosis in colorectal cancer cells (Xie et al., 2017). It has been suggested that p53 may mediate glutaminolysis to take part in the ferroptosis process because the essential enzyme for glutamine catabolism, GLS2, is also a direct target gene of p53 (Hu et al., 2010; Suzuki et al., 2010).

### 2.5.3 Nuclear receptor coactivator 4

One important mechanism for ferritin degradation is ferritinophagy, which can encourage the release of iron and provide a substrate for ferroptosis (Gao et al., 2016; Hou et al., 2016). A crucial regulator of ferritinophagy, NCOA4, can specifically bind to the surface arginine of FTH1 and promote ferritin degradation by lysosomes and autophagosomes (Mancias et al., 2014; Gryzik et al., 2017). Ferritinophagy also involves the traditional *autophagy-related*

*gene 3* (Atg3), Atg5, and Atg7, which are significant players (Hou et al., 2016). Knockout of Atg5, Atg7 or NCOA4 can effectively inhibited ferritin degradation to reduce erastin-induced ferroptosis (Hou et al., 2016). Furthermore, a new ferroptosis inhibitor compound 9a was found to block ferroptosis by disrupting the interaction of NCOA4-FTH1 (Fang et al., 2021), which opens up a new access for the development of ferroptosis inhibitors.

### 2.5.4 Fanconi anemia complementation group D2

As a nuclear protein involved in DNA damage repair, FANCD2 was discovered to be a key gene in autophagy-dependent ferroptosis (Nakanishi et al., 2002; Miao et al., 2022). Furthermore, FANCD2 mediates ferroptosis independently of autophagy (Song et al., 2016). The deletion of FANCD2 increases iron overload and lipid peroxidation in erastin-induced ferroptosis of bone marrow mesenchymal stem cells, which is associated with restricted expression of GPX4, FTH1, and upregulation of TFR1 (Song et al., 2016). It offers a novel approach to alleviating the side effects of bone marrow damage brought on by cancer treatment.

### 2.5.5 CDGSH iron sulfur domain 1

Recent research indicates that the outer mitochondrial membrane protein CDGSH iron sulfur domain 1 (CISD1) can inhibit mitochondrial iron uptake and lipid peroxidation, thereby negatively regulating erastin-induced ferroptosis (Yuan et al., 2016b). Meanwhile, pioglitazone inhibits iron-mediated mitochondrial lipid peroxidation and subsequent ferroptosis by binding CISD1 and stabilizing iron-sulfur clusters (Yuan et al., 2016b). Another study showed that the ferroptosis-related gene CISD1 is anticipated to become one of the novel biomarkers for predicting the prognosis of breast cancer patients, thereby providing a new target for cancer therapy (Wang D. et al., 2021) (Figure 2).

## 3 The role of ferroptosis in skeletal muscle diseases

Ferroptosis has been widely concerned by researchers since its discovery, and has proved to play a pivotal role in the progress of human diseases in various systems, such as tumors, cardiovascular and cerebrovascular diseases, nervous system diseases, respiratory diseases and digestive diseases (Do Van et al., 2016; Fang et al., 2019; Badgley et al., 2020; Ma et al., 2020b; Guan et al., 2020; Bao et al., 2021; Wu et al., 2021; Zheng et al., 2021; Liu T. et al., 2022; Bao et al., 2022; Zhang Y. et al., 2022). In recent years, the functions of ferroptosis in a variety of skeletal muscle diseases has attracted the attention of researchers, and has been reported to be an overriding participant in the physiological and pathological processes

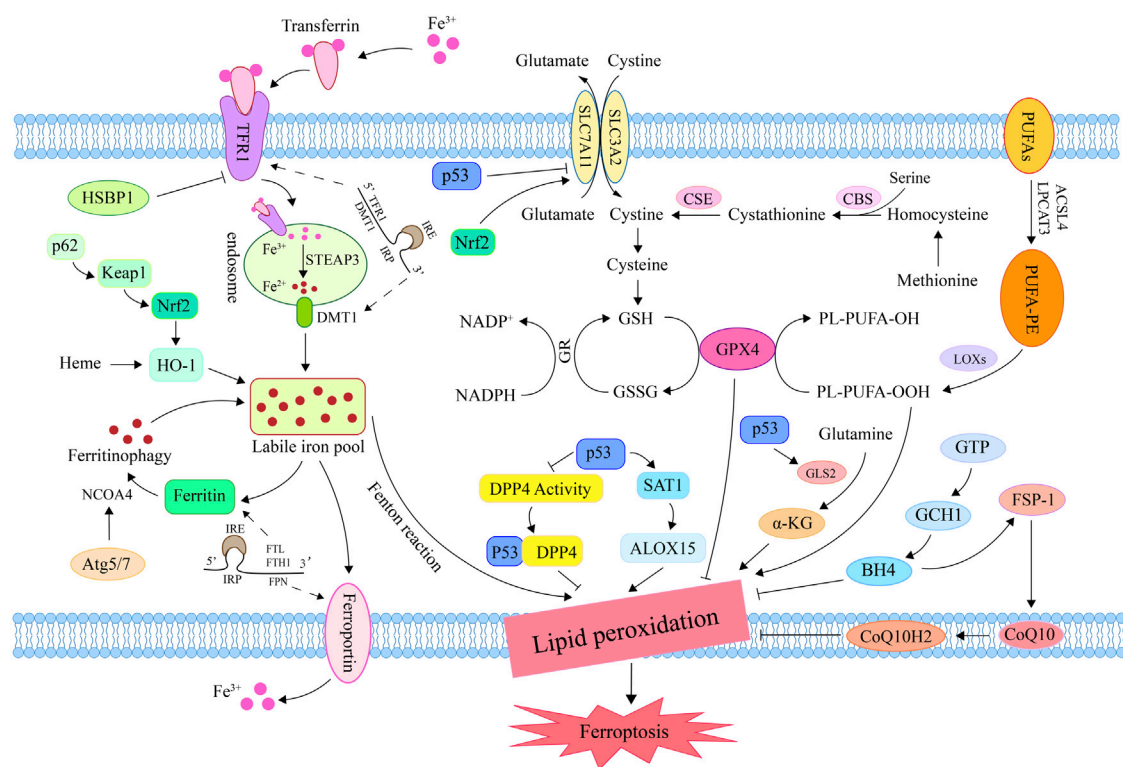


FIGURE 2

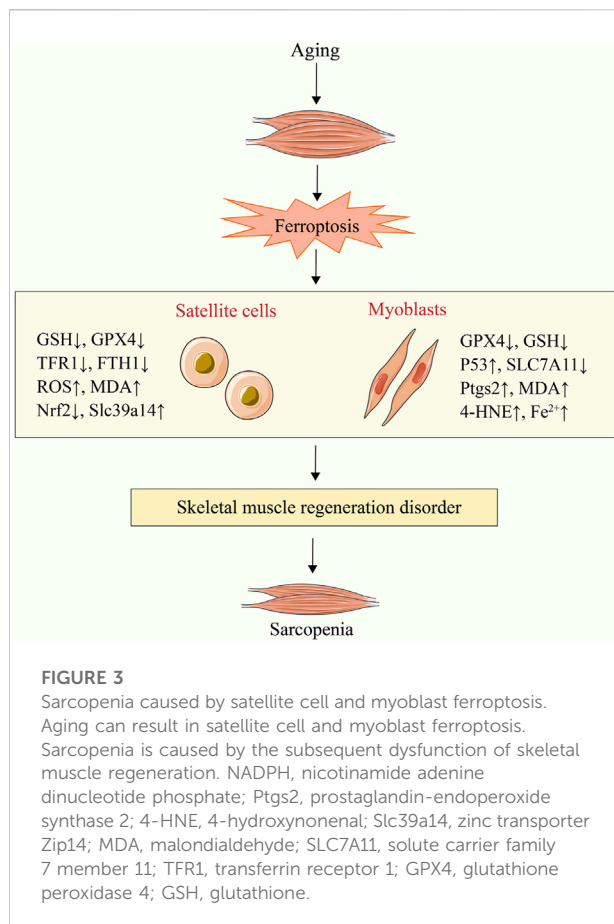
Mechanisms for regulating ferroptosis. Iron in circulation binds to TFR1 and enters the endosome via endocytosis; then, STEAP3 converts  $\text{Fe}^{3+}$  to  $\text{Fe}^{2+}$ . DMT1 transports  $\text{Fe}^{2+}$  into the cell in order to promote unstable iron accumulation and induce ferroptosis via the Fenton reaction. Methionine generates cysteine under the action of CBS and CSE for GSH synthesis. Inhibition of system Xc<sup>-</sup> reduced GSH synthesis and inactivated GPX4, promoting lipid peroxide accumulation and inducing ferroptosis. Under the catalysis of ACSL4, LPCAT3, and LOX, PUFA lipid peroxidation resulted in ferroptosis. By promoting iron release, the ferritin autophagy-related genes Atg5, Atg7, and NCOA4 induce ferroptosis. By influencing genes related to iron/heme metabolism and amino acid metabolism, Nrf2 plays a significant role in the regulation of ferroptosis. By inhibiting DPP4 activity and systemic SLC7A11 expression, or by activating SAT1 and GLS2, p53 can induce ferroptosis. FSP1 prevents lipid peroxidation by converting CoQ10 to CoQ10H2, thereby inhibiting ferroptosis. GCH1 blocks the chain propagation of lipid peroxidation by catalyzing GTP to generate BH4. TFR1, transferrin receptor 1; DMT1, divalent metal transporter 1; CBS, cystathionine  $\beta$ -synthase; CSE, cystathionine gamma-lyase; GSH, glutathione; GPX4, glutathione peroxidase 4; ACSL4, Acyl-CoA synthetase long-chain family member 4; LPCAT3, lysophosphatidylcholine acyltransferase 3; LOX, lipoxygenase; PUFA, polyunsaturated fatty acid; Atg5, autophagy-related gene 3; Atg7, autophagy-related gene 7; NCOA4, nuclear receptor coactivator 4; Nrf2, nuclear factor erythroid 2-related factor 2; DPP4, dipeptidyl-peptidase 4; SLC7A11, solute carrier family 7 member 11; SAT1, spermidine/spermine N1-acetyltransferase 1; GLS2, glutaminase 2; FSP1, ferroptosis suppressor protein 1; CoQ10, ubiquinone; CoQ10H2, ubiquinol; GCH1, GTP cyclohydrolase-1; GTP, Guanosine triphosphate; BH4, tetrahydrobiopterin.

such as sarcopenia, RML, RMS, and EEIF (Guerrero-Hue et al., 2019; Dachtel et al., 2020; Huang et al., 2021; Xiao et al., 2022). Therefore, we summarized the functions of ferroptosis in the pathogenesis of these skeletal muscle diseases.

### 3.1 Ferroptosis and sarcopenia

Sarcopenia is an age-related degenerative loss of skeletal muscle strength and quality (Cruz-Jentoft et al., 2010). The main mechanism of its occurrence and development is the imbalance of muscle synthesis and degradation (Tan et al., 2020a), which is closely related to the decline of satellite cells (SCs) number/function (Brack et al., 2005; Budai et al., 2018).

SCs are embryonic muscle stem cells located beneath the basal layer of muscle fibers and are in a quiescent state (Mauro, 1961; Yin et al., 2013). When muscle is damaged, SCs are activated and will proliferate into myoblasts, which will then differentiate and fuse to exert a powerful ability to promote muscle regeneration and repair damage (Aziz et al., 2012; Chen F. et al., 2019). However, some researches indicates that the number and function of SCs decline significantly with age, which would severely impair their capacity for self-renewal and regeneration and would lead to sarcopenia (Day et al., 2010; Jang et al., 2011; Sousa-Victor et al., 2014). Previous research has demonstrated that unstable iron accumulation existed in aging skeletal muscle and could promote muscle damage in mice by down-regulating SCs markers (paired box 7, myogenic differentiation antigen and myogenic factor 5)



and inhibiting C2C12 myoblast differentiation (Ikeda et al., 2019). Another study found changes in ferroptosis related factors such as HO-1, SAT1 and prostaglandin-endoperoxide synthase 2 (Ptgs2) in muscle samples of elderly people with sarcopenia (Ding et al., 2021). It is suggested that SCs and C2C12 myoblasts may participate in sarcopenia disease through ferroptosis, which has been verified in several recent studies.

TFR1 is an important factor in the activation, proliferation, and maintenance of SCs, whereas the expression of TFR1 is significantly decreased in aging skeletal muscle (DeRuisseau et al., 2013; Ding et al., 2021). The research demonstrates that deletion of the *TFR1* gene can promote zinc transporter Zip14 (Slc39a14) to absorb non-heme iron and down-regulate GPX4, Nrf2, and FTH1 to increase unstable iron accumulation and lipid peroxidation level, thereby inducing ferroptosis in skeletal muscle cells and impairing their regeneration (Ding et al., 2021). As is shown in another study, in animal models with sarcopenia, C2C12 myoblasts had age-related iron accumulation (Huang et al., 2021). Simultaneously, the activation of p53/SLC7A11 axis can induce ferroptosis of C2C12 myoblasts to

hinder their differentiation into myotubes and to promote the progression of sarcopenia, which can be reversed by the ferroptosis inhibitors fer-1 and DFO (Huang et al., 2021). Targeted regulation of SCs/myoblast ferroptosis is therefore anticipated to become a new treatment strategy for sarcopenia. In addition, the CSE derivative hydrogen sulfide can inhibit the acetylation modification of ALOX12, prevent lipid peroxidation of phospholipid membrane, and protect myoblasts from ferroptosis (Wang Y. et al., 2021). It provides a new target for preventing ferroptosis in aging skeletal muscle, although the relationship to primary sarcopenia was not explored (Figure 3).

### 3.2 Ferroptosis and rhabdomyolysis

RML is an acute clinical syndrome caused by the injury of skeletal muscle cells and the release of intracellular components (such as myoglobin and creatine kinase) into the systemic circulation (Lindner and Zierz, 2003; Stahl et al., 2020). It is exhibited in study that ferroptosis of skeletal muscle cells induced by the inhibition of the antioxidant axis Nrf2-XCT/GPX4 is one of the potential mechanisms of atorvastatin-induced muscle-related symptoms (muscle weakness, pain, cramps, and RML) (Zhang Q. et al., 2022). It suggests that ferroptosis may be related to the disease progression of RML. AKI is a common complication of RML and one of the leading causes of death in RML patients (Ahmad et al., 2021). A study reported that iron deficiency could exacerbate RML-induced AKI by evoking lipid peroxidation through catalytic heme-iron (Zhao et al., 2021b). Another study found that the related characteristics of ferroptosis include decreased GSH levels and the accumulation of lipid peroxidation products MDA, 4-HNE and iron occurred in RML mice (Guerrero-Hue et al., 2019). Simultaneously, fer-1 has a significant improvement effect on muscle cell death, renal function and structure of RML mice compared to zVAD (an apoptosis inhibitor) and RIPK3-knockout mice (necroptosis pathway deficiency) (Guerrero-Hue et al., 2019). These results suggest that ferroptosis is a paramount pathogenic factor in RML and its associated renal injury. Furthermore, curcumin, a powerful antioxidant, has been reported to improve the AKI associated with RML by increasing the ferroptosis resistance of cells (Guerrero-Hue et al., 2019), which opens a new way for the treatment of RML syndrome.

RML is also one of the major types of exertional heat stroke (EHS)-related muscle damage (Epstein and Yanovich, 2019; Laitano et al., 2021). The experimental results revealed that high levels of iron content, ferroptosis markers (Ptgs2, MDA), and typical ferroptotic mitochondrial morphological changes would happen in the muscle tissue of RML mice after EHS (He et al., 2022). Through further study *in vivo* and



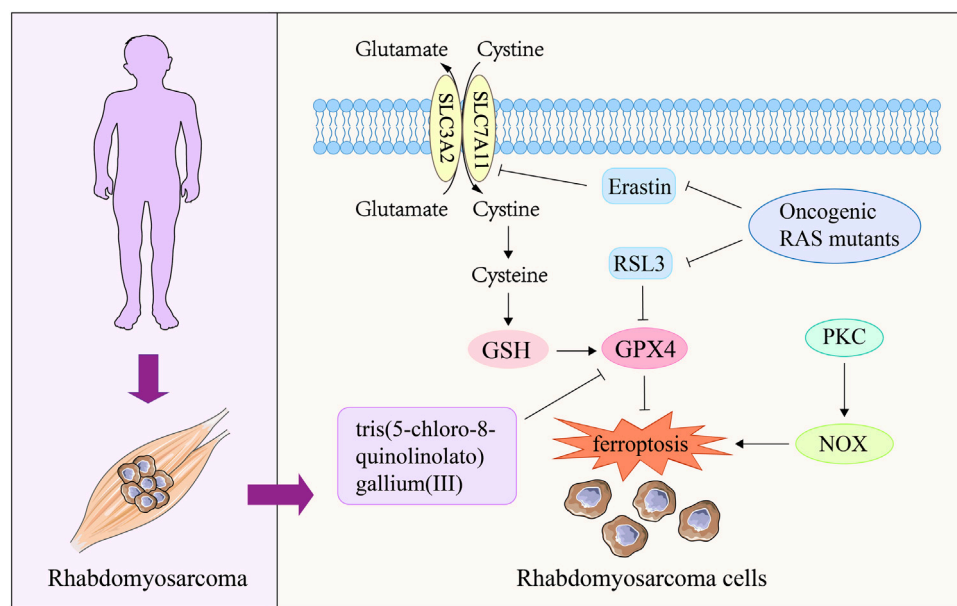


**FIGURE 4**

The role of ferroptosis in rhabdomyosarcoma. Oncogenic RAS mutants are the key mediator of RMS disease, which can block the ferroptosis of RMS cells induced by erastin and RSL3. The complex tris(5-chloro-8-quinolinolato) gallium (III) can induce ferroptosis in RMS cells by reducing GPX4 expression, thereby exerting therapeutic effects on RMS. The activation of PKC-NOX pathway can participate in the process of RMS disease by increasing the ferroptosis resistance of RMS cells. PKC, protein kinase C; NOX, NADPH oxidases; GPX4, glutathione peroxidase 4; GSH, glutathione.

*in vitro*, it is found that post-EHS-mediated ferroptosis of skeletal muscle cells depended on the up-regulation of ACSL4, the key gene for lipid modeling, and rosiglitazone (ACSL4 inhibitor) treatment could significantly reduce the skeletal muscle injury caused by EHS (He et al., 2022). Inhibition of ferroptosis by targeting ACSL4, therefore, may be a novel approach to prevent RML after EHS.

### 3.3 Ferroptosis and rhabdomyosarcoma

Characterized by poor survival and high recurrence, RMS is a malignant soft tissue tumor that occurs mostly in children and adolescents (Kramer et al., 1983; Ognjanovic et al., 2009; Dantonello et al., 2013; Egas-Bejar and Huh, 2014). Recent study has reported that RMS is sensitive to oxidative stress (Chen et al., 2013). Ferroptosis, as a novel mode of cell death induced by oxidative stress (Wu et al., 2018), has received attention in current RMS research. Research shows that erastin and RSL3, as common ferroptosis-inducing compounds, can cause ferroptosis of RMS cells through GSH consumption and GPX4 inactivation respectively (Codenotti et al., 2018; Dachert et al., 2020). Notably, inhibition of protein kinase C (PKC) isoform PKC $\alpha$  and its downstream target gene NADPH oxidases (NOX) isoforms

(NOX1/4) can significantly protect RMS cells from erastin-induced ferroptosis, providing a new perspective for the treatment of RMS (Dachert et al., 2020). Activation of RAS-related signaling pathways is a key cause of RMS occurrence and recurrence (Zhang et al., 2013; Shern et al., 2014). It was found that ectopic expression of oncogenic RAS mutants (NRAS12V, KRAS12V and HRAS12V) significantly reduced the sensitivity of RMS13 cell line to erastin and RSL3 (Schott et al., 2015). This suggests that one of the pathways by which RAS drives the occurrence and progression of RMS is to confer ferroptosis resistance to RMS cells. In addition, a recent work found that tris (5-chloro-8-quinolinolato) gallium (III) complex had an active anti proliferation effect on RMS cells, and its efficacy decreased under the co incubation of fer-1 (Hreusova et al., 2022). Meanwhile, cells treated with tris (5-chloro-8-quinolinolato) gallium (III) complex presented typical characteristics of ferroptosis, such as down-regulation of GPX4 expression and accumulation of lipid peroxide (Hreusova et al., 2022). These results suggest that ferroptosis may be a potential mechanism for this compound to exert RMS therapeutic effect. In general, targeting RMS cell ferroptosis is a promising researching direction in clinical treatment. However, at present, the research on ferroptosis and RMS is mainly conducted *in vitro*, and further intervention on

TABLE 2 Therapeutic strategies for skeletal muscle diseases associated with ferroptosis.

Target	Protein/reagent	Mechanisms	Diseases	References
<b>Inducers</b>				
GPX4	RSL3, tris(5-chloro-8-quinolinolato) gallium (III)	Inhibits GPX4, leading to accumulation of lipid peroxides	RMS	Codenotti et al. (2018); Hreusova et al. (2022)
SLC7A11	P53, erastin	Decreased cystine uptake, causing GSH depletion	Sarcopenia, RMS	Huang et al. (2021); Codenotti et al. (2018); Dachert et al. (2020)
Nrf2	Atorvastatin	Inhibits Nrf2, increases lipid peroxidation levels	RML	Zhang et al. (2022e)
<b>Inhibitors</b>				
Nrf2	Trilobatin	Promotes Nrf2 nuclear translocation, increases GSH levels	EEIF	Xiao et al. (2022)
ACSL4	Rosiglitazone	Down-regulate ACSL4 and reduce the production of lipid peroxidation	RML	He et al. (2022)
Iron	DFO	Chelates iron	Sarcopenia	Huang et al. (2021)
Lipid peroxidation	Fer-1	Inhibition of lipid peroxidation	Sarcopenia, RML, RMS	Huang et al. (2021); Guerrero-Hue et al. (2019); Hreusova et al. (2022)
PKCa	Gö6976	Inhibits the expression of PKCa	RMS	Dachert et al. (2020)
NOX1/4	GKT137831	Inhibits NOX1/4, reduce the production of lipid peroxidation	RMS	Dachert et al. (2020)

ferroptosis *in vivo* is needed to fully investigate the relationship between ferroptosis and RMS (Figure 4).

### 3.4 Ferroptosis and exhaustive exercise-induced fatigue

EEIF refers to the inability of muscles to generate force due to prolonged and/or strenuous exercise, which not only reduces quality of life, but also promotes the development of fatigue itself, and even causes organic changes (Dalsgaard et al., 2004; da Rocha et al., 2018; Hou et al., 2020). Under physiological conditions, skeletal muscle fibers continuously produce ROS at a slow rate and increase during muscle contraction, which will be offset by the antioxidant system to maintain the balance of its production and removal (Reid, 2008). However, it is found in many research that long and/or strenuous exercise will cause a sharp ROS increase in skeletal muscle (Davies et al., 1982; Reid et al., 1992). Meanwhile, this activity dependent increase of ROS will induce lipid peroxidation of cell membrane and damage the healthy tissue, thus aggravating muscle fatigue during strenuous exercise (Dillard et al., 1978; Alessio et al., 1988). Therefore, ferroptosis may be a new type of cell death that participates in the physiological and pathological process of EEIF except apoptosis (Sun Y. et al., 2016; Liu S. et al., 2022). Excitingly, a recent report explored the relationship between ferroptosis and EEIF (Xiao et al., 2022). The experimental data showed that there were characteristics related to ferroptosis in skeletal muscle of EEIF mice, such as accumulation of iron, lipid peroxide, decreased expression of GPX4 and GSH, suggesting that ferroptosis may participate in the process of EEIF disease (Xiao et al., 2022).

Trilobatin, as a natural food additive, has been reported to be anti-fatigue role by reducing the production of ROS and MDA, increasing the activity of GPX4 and the level of GSH, which is related to the inhibition of ferroptosis by the activation of Nrf2/ARE signaling pathway (Xiao et al., 2022). Based on the above, the high-level ROS produced in skeletal muscle after prolonged and/or strenuous exercise may increase the loss of muscle cells by activating ferroptosis, thereby promoting EEIF. Although there is limited evidence to support this view, it provides a new direction for the treatment of EEIF, which is worthy of more in-depth exploration from researchers in related fields.

### 3.5 Ferroptosis and idiopathic inflammatory myopathies

IIMs are a group of autoimmune diseases characterized by muscle inflammation (Parkes et al., 2015; Lundberg et al., 2016). Polymyositis (PM) and dermatomyositis (DM) are the two most common types of IIMs with high mortality (Yang et al., 2020). However, the role of ferroptosis in IIMs remains unclear. Vitamin E and selenium are important antioxidants that prevent lipid peroxidation with the effect of resisting ferroptosis (Conrad and Proneth, 2020; Hu et al., 2021; Tuo et al., 2021). It was found that a patient with chronic malabsorption and selective IgA deficiency lacking vitamin E and selenium appeared PM when receiving iron glucan treatment, which was related to lipid peroxidation caused by free iron activated free radicals (Foulkes et al., 1991). Ferritin is the main site of iron storage in the body, and elevated levels indicate iron accumulation in the body (Cook et al., 1974;

Harrison, 1977; Worwood, 1987). Many population surveys based on PM/DM have found that the severity and prognosis of PM/DM and its complications (interstitial lung disease) were related to ferritinemia (Gono et al., 2010; Kawasumi et al., 2014; Ishizuka et al., 2016). In addition, mitochondrial dysfunction, as a landmark event of termination of ferroptosis and the main cause of ROS accumulation, has been reported as an important pathogenic mechanism of IIMs (Meyer et al., 2017; Boehler et al., 2019). Based on this, it is logical to speculate that ferroptosis is involved in the occurrence and development of IIM, and further exploration is needed to clarify the exact role ferroptosis plays in IIM (Table 2).

## 4 Conclusion and prospect

This review summarizes the regulatory mechanism of ferroptosis and its role in the progression of different skeletal muscle diseases. As mentioned above, in addition to the three classical regulatory pathways for ferroptosis in lipid, iron, and amino acid metabolism, a number of signal regulators and autophagy-related genes, such as *Nrf2*, *p53*, *NCOA4*, *FANCD2*, and *CISD1*, are also essential ferroptosis players. With the deepening of research, ferroptosis has been proved to be overriding in some muscle mass and dysfunction diseases, including sarcopenia, RML and EEIF. Skeletal muscle, composed of skeletal muscle cells, is an important organ to maintain human posture, exercise, energy metabolism and secretion of muscle cytokines. Therefore, it is of great significance to inhibit the ferroptosis of skeletal muscle cells in the treatment of sarcopenia, RML, EEIF and other diseases. However, in terms of RMS and other malignant tumor tissues, the key to prevent cancer occurrence and recurrence is to actively promote the ferroptosis of cancer cells. It is concluded that unstable iron accumulation, increase of lipid peroxide, inactivation of GPX4, inhibition of system  $Xc^-$  and depletion of GSH are common causes of ferroptosis in skeletal muscle diseases. The regulatory mechanisms and targets involved include P53/SLC7A11 axis, Nrf2-xCT/GPX4 axis, TFR1, ACSL4, PKC $\alpha$  and NOX1/4. These ferroptosis related targets were found to be an important way in distinct skeletal muscle disease treatment drugs to inhibit ferroptosis (Trilobatin and Rosiglitazone) or induce ferroptosis [tris (5-chloro-8-quinolinolato) gallium (III) and atorvastatin]. Their effects were similar to those of known ferroptosis interventions such as erastin, RSL3, and fer-1. However, it is not clear whether these regulatory factors are specific targets of therapeutic drugs for skeletal muscle diseases.

Due to the limitation of current literature, our review of ferroptosis and skeletal muscle disease is not very comprehensive. However, there are still some exploratory suggestions worth putting forward. Ferroptosis is a regulatory mechanism that is promising for the treatment of sarcopenia, RML, RMS and EEIF. Whereas the exploration of the correlation between these diseases and ferroptosis is still in its infancy. Meanwhile,

ferroptosis may also be a breakthrough for us to overcome the problems in treatment skeletal muscle-related intractable diseases such as IIMs. Of note, in the treatment of RMS and other skeletal muscle diseases, it is necessary to properly promote and inhibit ferroptosis to intervene the disease process. Therefore, when treating cancer and skeletal muscle related diseases with ferroptosis as a target, we should pay attention to balancing the two-way effects of ferroptosis treatment drugs on cancer tissues and healthy tissues. This is especially critical for the treatment of cancer patients with skeletal muscle disease, and it is also the focus and difficulty in drug development. Moreover, several genes associated with heme metabolism, such as ABCB6, FLVCR1, and ABCG2, appear to significantly influence ferroptosis, providing profound reference for the study on ferroptosis regulatory targets in skeletal muscle diseases, which needs more exploration and excavation.

## Author contributions

YW and ZZ conceived the framework of the review and wrote the manuscript. WJ, YW, XW, YZ, XF, and LT added and checked references. XL and JM reviewed and improved the manuscript. All authors contributed to the article and approved the submitted version.

## Funding

This work was supported by the National Natural Science Foundation of China (No: 82205039), the Innovation Team and Talents Cultivation Program of National Administration of Traditional Chinese Medicine (No: ZYYCXTD-D-202001), the Jilin Scientific and Technological Development Program (20200201305JC, 20190101010JH) and the Education Department of Jilin Province (JJKH20200882KJ).

## Conflict of interest

The authors declare that the research was conducted in the absence of any commercial or financial relationships that could be construed as a potential conflict of interest.

## Publisher's note

All claims expressed in this article are solely those of the authors and do not necessarily represent those of their affiliated organizations, or those of the publisher, the editors and the reviewers. Any product that may be evaluated in this article, or claim that may be made by its manufacturer, is not guaranteed or endorsed by the publisher.

## References

- Adedoyin, O., Boddu, R., Traylor, A., Lever, J. M., Bolisetty, S., George, J. F., et al. (2018). Heme oxygenase-1 mitigates ferroptosis in renal proximal tubule cells. *Am. J. Physiol. Ren. Physiol.* 314 (5), F702–F714. doi:10.1152/ajprenal.00044.2017
- Ahmad, S., Anees, M., Elahi, I., and Fazal, E. M. (2021). Rhabdomyolysis leading to acute kidney injury. *J. Coll. Physicians Surg. Pak.* 31 (2), 235–237. doi:10.29271/jcpsp.2021.02.235
- Alessio, H. M., Goldfarb, A. H., and Cutler, R. G. (1988). MDA content increases in fast- and slow-twitch skeletal muscle with intensity of exercise in a rat. *Am. J. Physiol.* 255 (1), C874–C877. doi:10.1152/ajpcell.1988.255.6.C874
- An, J. R., Su, J. N., Sun, G. Y., Wang, Q. F., Fan, Y. D., Jiang, N., et al. (2022). Liraglutide alleviates cognitive deficit in db/db mice: Involvement in oxidative stress, iron overload, and ferroptosis. *Neurochem. Res.* 47 (2), 279–294. doi:10.1007/s11064-021-03442-7
- Anandhan, A., Dodson, M., Schmidlin, C. J., Liu, P., and Zhang, D. D. (2020). Breakdown of an ironclad defense system: The critical role of NRF2 in mediating ferroptosis. *Cell Chem. Biol.* 27 (4), 436–447. doi:10.1016/j.chembiol.2020.03.011
- Andrews, N. C. (2000). Iron homeostasis: Insights from genetics and animal models. *Nat. Rev. Genet.* 1 (3), 208–217. doi:10.1038/35042073
- Argiles, J. M., Campos, N., Lopez-Pedrosa, J. M., Rueda, R., and Rodriguez-Manas, L. (2016). Skeletal muscle regulates metabolism via interorgan crosstalk: Roles in health and disease. *J. Am. Med. Dir. Assoc.* 17 (9), 789–796. doi:10.1016/j.jamda.2016.04.019
- Ayala, A., Munoz, M. F., and Arguelles, S. (2014). Lipid peroxidation: Production, metabolism, and signaling mechanisms of malondialdehyde and 4-hydroxy-2-nonenal. *Oxid. Med. Cell. Longev.* 2014, 360438. doi:10.1155/2014/360438
- Aziz, A., Sebastian, S., and Dilworth, F. J. (2012). The origin and fate of muscle satellite cells. *Stem Cell Rev. Rep.* 8 (2), 609–622. doi:10.1007/s12015-012-9352-0
- Aziz, N., and Munro, H. N. (1987). Iron regulates ferritin mRNA translation through a segment of its 5' untranslated region. *Proc. Natl. Acad. Sci. U. S. A.* 84 (23), 8478–8482. doi:10.1073/pnas.84.23.8478
- Badgley, M. A., Kremer, D. M., Maurer, H. C., DelGiorno, K. E., Lee, H. J., Purohit, V., et al. (2020). Cysteine depletion induces pancreatic tumor ferroptosis in mice. *Science* 368 (6486), 85–89. doi:10.1126/science.aaw9872
- Bao, C., Liu, C., Liu, Q., Hua, L., Hu, J., Li, Z., et al. (2022). Liproxstatin-1 alleviates LPS/L13-induced bronchial epithelial cell injury and neutrophilic asthma in mice by inhibiting ferroptosis. *Int. Immunopharmacol.* 109, 108770. doi:10.1016/j.intimp.2022.108770
- Bao, W. D., Pang, P., Zhou, X. T., Hu, F., Xiong, W., Chen, K., et al. (2021). Loss of ferroportin induces memory impairment by promoting ferroptosis in Alzheimer's disease. *Cell Death Differ.* 28 (5), 1548–1562. doi:10.1038/s41418-020-00685-9
- Bayir, H. (2005). Reactive oxygen species. *Crit. Care Med.* 33 (12), S498–S501. doi:10.1097/01.ccm.0000186787.64500.12
- Bersuker, K., Hendricks, J. M., Li, Z., Magtanong, L., Ford, B., Tang, P. H., et al. (2019). The CoQ oxidoreductase FSP1 acts parallel to GPX4 to inhibit ferroptosis. *Nature* 575 (7784), 688–692. doi:10.1038/s41586-019-1705-2
- Boehler, J. F., Horn, A., Novak, J. S., Li, N., Ghimbovschi, S., Lundberg, I. E., et al. (2019). Mitochondrial dysfunction and role of harakiri in the pathogenesis of myositis. *J. Pathol.* 249 (2), 215–226. doi:10.1002/path.5309
- Brack, A. S., Bildsoe, H., and Hughes, S. M. (2005). Evidence that satellite cell decrement contributes to preferential decline in nuclear number from large fibres during murine age-related muscle atrophy. *J. Cell Sci.* 118 (20), 4813–4821. doi:10.1242/jcs.02602
- Bridges, R. J., Natale, N. R., and Patel, S. A. (2012). System xc(-) cystine/glutamate antiporter: An update on molecular pharmacology and roles within the CNS. *Br. J. Pharmacol.* 165 (1), 20–34. doi:10.1111/j.1476-5381.2011.01480.x
- Budai, Z., Balogh, L., and Sarang, Z. (2018). Altered gene expression of muscle satellite cells contributes to accelerated sarcopenia in mice. *Curr. Aging Sci.* 11 (3), 165–172. doi:10.2174/1874609811666180925104241
- Campbell, M. R., Karaca, M., Adamski, K. N., Chorley, B. N., Wang, X., and Bell, D. A. (2013). Novel hematopoietic target genes in the NRF2-mediated transcriptional pathway. *Oxid. Med. Cell. Longev.* 2013, 120305. doi:10.1155/2013/120305
- Catala, A., and Diaz, M. (2016). Editorial: Impact of lipid peroxidation on the physiology and pathophysiology of cell membranes. *Front. Physiol.* 7, 423. doi:10.3389/fphys.2016.00423
- Chan, J. Y., and Kwong, M. (2000). Impaired expression of glutathione synthetic enzyme genes in mice with targeted deletion of the Nrf2 basic-leucine zipper protein. *Biochim. Biophys. Acta* 1517 (1), 19–26. doi:10.1016/s0167-4781(00)00238-4
- Chen, F., Zhou, J., Li, Y., Zhao, Y., Yuan, J., Cao, Y., et al. (2019a). YY1 regulates skeletal muscle regeneration through controlling metabolic reprogramming of satellite cells. *EMBO J.* 38 (10), e99727. doi:10.15252/embj.201899727
- Chen, H., Cao, L., Han, K., Zhang, H., Cui, J., Ma, X., et al. (2022b). Patulin disrupts SLC7A11-cystine-cysteine-GSH antioxidant system and promotes renal cell ferroptosis both *in vitro* and *in vivo*. *Food Chem. Toxicol.* 166, 113255. doi:10.1016/j.fct.2022.113255
- Chen, H., Zheng, C., Zhang, Y., Chang, Y. Z., Qian, Z. M., and Shen, X. (2006). Heat shock protein 27 downregulates the transferrin receptor 1-mediated iron uptake. *Int. J. Biochem. Cell Biol.* 38 (8), 1402–1416. doi:10.1016/j.biocel.2006.02.006
- Chen, M. S., Wang, S. F., Hsu, C. Y., Yin, P. H., Yeh, T. S., Lee, H. C., et al. (2017). CHAC1 degradation of glutathione enhances cystine-starvation-induced necroptosis and ferroptosis in human triple negative breast cancer cells via the GCN2-eIF2 $\alpha$ -ATF4 pathway. *Oncotarget* 8 (70), 114588–114602. doi:10.18632/oncotarget.23055
- Chen, X., Stewart, E., Shelat, A. A., Qu, C., Bahrami, A., Hatley, M., et al. (2013). Targeting oxidative stress in embryonal rhabdomyosarcoma. *Cancer Cell* 24 (6), 710–724. doi:10.1016/j.ccr.2013.11.002
- Chen, X., Xu, S., Zhao, C., and Liu, B. (2019b). Role of TLR4/NADPH oxidase 4 pathway in promoting cell death through autophagy and ferroptosis during heart failure. *Biochem. Biophys. Res. Commun.* 516 (1), 37–43. doi:10.1016/j.bbrc.2019.06.015
- Chen, Y., Wang, J., Li, J., Zhu, J., Wang, R., Xi, Q., et al. (2021b). Astragalus polysaccharide prevents ferroptosis in a murine model of experimental colitis and human Caco-2 cells via inhibiting NRF2/HO-1 pathway. *Eur. J. Pharmacol.* 911, 174518. doi:10.1016/j.ejphar.2021.174518
- Chepkova, O. E., Malin, D., Strekalova, E., Lukasheva, E. V., Zamyatnin, A. A., Jr., and Cryns, V. L. (2020). Lysine oxidase exposes a dependency on the thioredoxin antioxidant pathway in triple-negative breast cancer cells. *Breast Cancer Res. Treat.* 183 (3), 549–564. doi:10.1007/s10549-020-05801-4
- Chu, B., Kon, N., Chen, D., Li, T., Liu, T., Jiang, L., et al. (2019). ALOX12 is required for p53-mediated tumour suppression through a distinct ferroptosis pathway. *Nat. Cell Biol.* 21 (5), 579–591. doi:10.1038/s41556-019-0305-6
- Chung, J., Chen, C., and Paw, B. H. (2012). Heme metabolism and erythropoiesis. *Curr. Opin. Hematol.* 19 (3), 156–162. doi:10.1097/MOH.0b013e328351c48b
- Codenotti, S., Poli, M., Asperti, M., Zizioli, D., Marampon, F., and Fanzani, A. (2018). Cell growth potential drives ferroptosis susceptibility in rhabdomyosarcoma and myoblast cell lines. *J. Cancer Res. Clin. Oncol.* 144 (9), 1717–1730. doi:10.1007/s00432-018-2699-0
- Conrad, M., and Proneth, B. (2020). Selenium: Tracing another essential element of ferroptotic cell death. *Cell Chem. Biol.* 27 (4), 409–419. doi:10.1016/j.chembiol.2020.03.012
- Cook, J. D., Lipschitz, D. A., Miles, L. E., and Finch, C. A. (1974). Serum ferritin as a measure of iron stores in normal subjects. *Am. J. Clin. Nutr.* 27 (7), 681–687. doi:10.1093/ajcn/27.7.681
- Corsi, B., Cozzi, A., Arosio, P., Drysdale, J., Santambrogio, P., Campanella, A., et al. (2002). Human mitochondrial ferritin expressed in HeLa cells incorporates iron and affects cellular iron metabolism. *J. Biol. Chem.* 277 (25), 22430–22437. doi:10.1074/jbc.M105372200
- Cruz-Jentoft, A. J., Baeyens, J. P., Bauer, J. M., Boirie, Y., Cederholm, T., Landi, F., et al. (2010). Sarcopenia: European consensus on definition and diagnosis: Report of the European working group on sarcopenia in older people. *Age Ageing* 39 (4), 412–423. doi:10.1093/ageing/afq034
- da Rocha, A. L., Teixeira, G. R., Pinto, A. P., de Moraes, G. P., Oliveira, L. D. C., de Vicente, L. G., et al. (2018). Excessive training induces molecular signs of pathologic cardiac hypertrophy. *J. Cell. Physiol.* 233 (11), 8850–8861. doi:10.1002/jcp.26799
- Dachert, J., Ehrenfeld, V., Habermann, K., Dolgikh, N., and Fulda, S. (2020). Targeting ferroptosis in rhabdomyosarcoma cells. *Int. J. Cancer* 146 (2), 510–520. doi:10.1002/ijc.32496
- Dalsgaard, M. K., Ott, P., Dela, F., Juul, A., Pedersen, B. K., Warberg, J., et al. (2004). The CSF and arterial to internal jugular venous hormonal differences during exercise in humans. *Exp. Physiol.* 89 (3), 271–277. doi:10.1113/expphysiol.2003.026922
- Dantonello, T. M., Int-Veen, C., Schuck, A., Seitz, G., Leuschner, I., Nathrath, M., et al. (2013). Survival following disease recurrence of primary localized alveolar rhabdomyosarcoma. *Pediatr. Blood Cancer* 60 (8), 1267–1273. doi:10.1002/pbc.24488
- Davies, K. J., Quintanilha, A. T., Brooks, G. A., and Packer, L. (1982). Free radicals and tissue damage produced by exercise. *Biochem. Biophys. Res. Commun.* 107 (4), 1198–1205. doi:10.1016/s0006-291x(82)80124-1



- Day, K., Shefer, G., Shearer, A., and Yablonka-Reuveni, Z. (2010). The depletion of skeletal muscle satellite cells with age is concomitant with reduced capacity of single progenitors to produce reserve progeny. *Dev. Biol.* 340 (2), 330–343. doi:10.1016/j.ydbio.2010.01.006
- Deponte, M. (2013). Glutathione catalysis and the reaction mechanisms of glutathione-dependent enzymes. *Biochim. Biophys. Acta* 1830 (5), 3217–3266. doi:10.1016/j.bbagen.2012.09.018
- DeRuisseau, K. C., Park, Y. M., DeRuisseau, L. R., Cowley, P. M., Fazen, C. H., and Doyle, R. P. (2013). Aging-related changes in the iron status of skeletal muscle. *Exp. Gerontol.* 48 (11), 1294–1302. doi:10.1016/j.exger.2013.08.011
- Desuzinges-Mandon, E., Arnaud, O., Martinez, L., Huche, F., Di Pietro, A., and Falson, P. (2010). ABCG2 transports and transfers heme to albumin through its large extracellular loop. *J. Biol. Chem.* 285 (43), 33123–33133. doi:10.1074/jbc.M110.139170
- Dillard, C. J., Litov, R. E., Savin, W. M., Dumelin, E. E., and Tappel, A. L. (1978). Effects of exercise, vitamin E, and ozone on pulmonary function and lipid peroxidation. *J. Appl. Physiol. Respir. Environ. Exerc. Physiol.* 45 (6), 927–932. doi:10.1152/jappl.1978.45.6.927
- Ding, H., Chen, S., Pan, X., Dai, X., Pan, G., Li, Z., et al. (2021). Transferrin receptor 1 ablation in satellite cells impedes skeletal muscle regeneration through activation of ferroptosis. *J. Cachexia Sarcopenia Muscle* 12 (3), 746–768. doi:10.1002/jcsm.12700
- Dixon, S. J., Lemberg, K. M., Lamprecht, M. R., Skouta, R., Zaitsev, E. M., Gleason, C. E., et al. (2012). Ferroptosis: An iron-dependent form of nonapoptotic cell death. *Cell* 149 (5), 1060–1072. doi:10.1016/j.cell.2012.03.042
- Dixon, S. J., Winter, G. E., Musavi, L. S., Lee, E. D., Snijder, B., Rebsamen, M., et al. (2015). Human haploid cell genetics reveals roles for lipid metabolism genes in nonapoptotic cell death. *ACS Chem. Biol.* 10 (7), 1604–1609. doi:10.1021/acscchembio.5b00245
- Dlouhy, A. C., and Outten, C. E. (2013). The iron metallome in eukaryotic organisms. *Mater. Ions Life Sci.* 12, 241–278. doi:10.1007/978-94-007-5561-1\_8
- Do Van, B., Gouel, F., Jonneaux, A., Timmerman, K., Gele, P., Petraut, M., et al. (2016). Ferroptosis, a newly characterized form of cell death in Parkinson's disease that is regulated by PKC. *Neurobiol. Dis.* 94, 169–178. doi:10.1016/j.nbd.2016.05.011
- Dodson, M., Castro-Portuguez, R., and Zhang, D. D. (2019). NRF2 plays a critical role in mitigating lipid peroxidation and ferroptosis. *Redox Biol.* 23, 101107. doi:10.1016/j.redox.2019.101107
- Doll, S., Freitas, F. P., Shah, R., Aldrovandi, M., da Silva, M. C., Ingold, I., et al. (2019). FSP1 is a glutathione-independent ferroptosis suppressor. *Nature* 575 (7784), 693–698. doi:10.1038/s41586-019-1707-0
- Doll, S., Proneth, B., Tyurina, Y. Y., Panzilius, E., Kobayashi, S., Ingold, I., et al. (2017). ACSL4 dictates ferroptosis sensitivity by shaping cellular lipid composition. *Nat. Chem. Biol.* 13 (1), 91–98. doi:10.1038/nchembio.2239
- Dong, H., Qiang, Z., Chai, D., Peng, J., Xia, Y., Hu, R., et al. (2020). Nrf2 inhibits ferroptosis and protects against acute lung injury due to intestinal ischemia reperfusion via regulating SLC7A11 and HO-1. *Aging (Albany NY)* 12 (13), 12943–12959. doi:10.18632/aging.103378
- Drysdale, J., Arosio, P., Invernizzi, R., Cazzola, M., Volz, A., Corsi, B., et al. (2002). Mitochondrial ferritin: A new player in iron metabolism. *Blood Cells Mol. Dis.* 29 (3), 376–383. doi:10.1006/bcmd.2002.0577
- Egas-Bejar, D., and Huh, W. W. (2014). Rhabdomyosarcoma in adolescent and young adult patients: Current perspectives. *Adolesc. Health Med. Ther.* 5, 115–125. doi:10.2147/AHMT.S44582
- Ellingsgaard, H., Hauselmann, I., Schuler, B., Habib, A. M., Baggio, L. L., Meier, D. T., et al. (2011). Interleukin-6 enhances insulin secretion by increasing glucagon-like peptide-1 secretion from L cells and alpha cells. *Nat. Med.* 17 (11), 1481–1489. doi:10.1038/nm.2513
- Epstein, Y., and Yanovich, R. (2019). *N. Engl. J. Med.* 380 (25), 2449–2459. doi:10.1056/NEJMra1810762
- Eriksson, S., Prigge, J. R., Talago, E. A., Arner, E. S., and Schmidt, E. E. (2015). Dietary methionine can sustain cytosolic redox homeostasis in the mouse liver. *Nat. Commun.* 6, 6479. doi:10.1038/ncomms7479
- Fang, X., Wang, H., Han, D., Xie, E., Yang, X., Wei, J., et al. (2019). Ferroptosis as a target for protection against cardiomyopathy. *Proc. Natl. Acad. Sci. U. S. A.* 116 (7), 2672–2680. doi:10.1073/pnas.1821022116
- Fang, Y., Chen, X., Tan, Q., Zhou, H., Xu, J., and Gu, Q. (2021). Inhibiting ferroptosis through disrupting the NCOA4-FTH1 interaction: A new mechanism of action. *ACS Cent. Sci.* 7 (6), 980–989. doi:10.1021/acscentsci.0c01592
- Farmer, E. E., and Mueller, M. J. (2013). ROS-mediated lipid peroxidation and RES-activated signaling. *Annu. Rev. Plant Biol.* 64, 429–450. doi:10.1146/annurev-arplant-050312-120132
- Feng, H., and Stockwell, B. R. (2018). Unsolved mysteries: How does lipid peroxidation cause ferroptosis? *PLoS Biol.* 16 (5), e2006203. doi:10.1371/journal.pbio.2006203
- Feng, L., Zhao, K., Sun, L., Yin, X., Zhang, J., Liu, C., et al. (2021). SLC7A11 regulated by NRF2 modulates esophageal squamous cell carcinoma radiosensitivity by inhibiting ferroptosis. *J. Transl. Med.* 19 (1), 367. doi:10.1186/s12967-021-03042-7
- Ferrannini, E., Simonson, D. C., Katz, L. D., Reichard, G., Jr., Bevilacqua, S., Barrett, E. J., et al. (1988). The disposal of an oral glucose load in patients with non-insulin-dependent diabetes. *Metabolism* 37 (1), 79–85. doi:10.1016/0026-0495(88)90033-9
- Ferreira, C. A., Ni, D., Rosenkrans, Z. T., and Cai, W. (2018). Scavenging of reactive oxygen and nitrogen species with nanomaterials. *Nano Res.* 11 (10), 4955–4984. doi:10.1007/s12274-018-2092-y
- Fleming, M. D., Romano, M. A., Su, M. A., Garrick, L. M., Garrick, M. D., and Andrews, N. C. (1998). Nramp2 is mutated in the anemic belgrade (b) rat: Evidence of a role for Nramp2 in endosomal iron transport. *Proc. Natl. Acad. Sci. U. S. A.* 95 (3), 1148–1153. doi:10.1073/pnas.95.3.1148
- Flohe, L., Gunzler, W. A., and Schock, H. H. (1973). Glutathione peroxidase: A selenoenzyme. *FEBS Lett.* 32 (1), 132–134. doi:10.1016/0014-5793(73)80755-0
- Fluck, M., and Hoppeler, H. (2003). Molecular basis of skeletal muscle plasticity--from gene to form and function. *Rev. Physiol. Biochem. Pharmacol.* 146, 159–216. doi:10.1007/s10254-002-0004-7
- Foulkes, W. D., Sewry, C., Calam, J., and Hodgson, H. J. (1991). Rhabdomyolysis after intramuscular iron-dextran in malabsorption. *Ann. Rheum. Dis.* 50 (3), 184–186. doi:10.1136/ard.50.3.184
- Friedmann Angeli, J. P., and Conrad, M. (2018). Selenium and GPX4, a vital symbiosis. *Free Radic. Biol. Med.* 127, 153–159. doi:10.1016/j.freeradbiomed.2018.03.001
- Furukawa, M., and Xiong, Y. (2005). BTB protein Keap1 targets antioxidant transcription factor Nrf2 for ubiquitination by the Cullin 3-Roc1 ligase. *Mol. Cell Biol.* 25 (1), 162–171. doi:10.1128/MCB.25.1.162-171.2005
- Gao, J., Li, Y., and Song, R. (2021). SIRT2 inhibition exacerbates p53-mediated ferroptosis in mice following experimental traumatic brain injury. *Neuroreport* 32 (12), 1001–1008. doi:10.1097/WNR.0000000000001679
- Gao, M., Monian, P., Pan, Q., Zhang, W., Xiang, J., and Jiang, X. (2016). Ferroptosis is an autophagic cell death process. *Cell Res.* 26 (9), 1021–1032. doi:10.1038/cr.2016.95
- Gao, M., Monian, P., Quadri, N., Ramasamy, R., and Jiang, X. (2015). Glutaminolysis and transferrin regulate ferroptosis. *Mol. Cell* 59 (2), 298–308. doi:10.1016/j.molcel.2015.06.011
- Garber, A. J., Karl, I. E., and Kipnis, D. M. (1976). Alanine and glutamine synthesis and release from skeletal muscle. I. Glycolysis and amino acid release. *J. Biol. Chem.* 251 (3), 826–835. doi:10.1016/s0021-9258(17)33859-0
- Gono, T., Kawaguchi, Y., Hara, M., Masuda, I., Katsumata, Y., Shinozaki, M., et al. (2010). Increased ferritin predicts development and severity of acute interstitial lung disease as a complication of dermatomyositis. *Rheumatol. Oxf.* 49 (7), 1354–1360. doi:10.1093/rheumatology/keq073
- Gryzik, M., Srivastava, A., Longhi, G., Bertuzzi, M., Gianoncelli, A., Carmona, F., et al. (2017). Expression and characterization of the ferritin binding domain of Nuclear Receptor Coactivator-4 (NCOA4). *Biochim. Biophys. Acta. Gen. Subj.* 1861, 2710–2716. doi:10.1016/j.bbagen.2017.07.015
- Guan, Z., Chen, J., Li, X., and Dong, N. (2020). Tanshinone IIA induces ferroptosis in gastric cancer cells through p53-mediated SLC7A11 down-regulation. *Biosci. Rep.* 40 (8), BSR20201807. doi:10.1042/BSR20201807
- Guerrero-Hue, M., Garcia-Caballero, C., Palomino-Antolin, A., Rubio-Navarro, A., Vazquez-Carballo, C., Herencia, C., et al. (2019). Curcumin reduces renal damage associated with rhabdomyolysis by decreasing ferroptosis-mediated cell death. *FASEB J.* 33 (8), 8961–8975. doi:10.1096/fj.201900077R
- Guo, S., Chen, Y., Xue, X., Yang, Y., Wang, Y., Qiu, S., et al. (2021). TRIB2 desensitizes ferroptosis via  $\beta$ TrCP-mediated TFRC ubiquitination in liver cancer cells. *Cell Death Discov.* 7 (1), 196. doi:10.1038/s41420-021-00574-1
- Han, S., Lin, F., Qi, Y., Liu, C., Zhou, L., Xia, Y., et al. (2022). HO-1 contributes to luteolin-triggered ferroptosis in clear cell renal cell carcinoma via increasing the labile iron pool and promoting lipid peroxidation. *Oxid. Med. Cell. Longev.* 2022, 3846217. doi:10.1155/2022/3846217
- Harada, N., Kanayama, M., Maruyama, A., Yoshida, A., Tazumi, K., Hosoya, T., et al. (2011). Nrf2 regulates ferroportin 1-mediated iron efflux and counteracts lipopolysaccharide-induced ferroportin 1 mRNA suppression in macrophages. *Arch. Biochem. Biophys.* 508 (1), 101–109. doi:10.1016/j.abb.2011.02.001
- Harrison, P. M. (1977). Ferritin: An iron-storage molecule. *Semin. Hematol.* 14 (1), 55–70.

- Hatem, E., Berthonaud, V., Dardalhon, M., Lagniel, G., Baudouin-Cornu, P., Huang, M. E., et al. (2014). Glutathione is essential to preserve nuclear function and cell survival under oxidative stress. *Free Radic. Biol. Med.* 75 (1), S25–S26. doi:10.1016/j.freeradbiomed.2014.10.746
- Hayano, M., Yang, W. S., Corn, C. K., Pagano, N. C., and Stockwell, B. R. (2016). Loss of cysteinyl-tRNA synthetase (CARS) induces the transsulfuration pathway and inhibits ferroptosis induced by cystine deprivation. *Cell Death Differ.* 23 (2), 270–278. doi:10.1038/cdd.2015.93
- He, L., He, T., Farrar, S., Ji, L., Liu, T., and Ma, X. (2017). Antioxidants maintain cellular redox homeostasis by elimination of reactive oxygen species. *Cell. Physiol. Biochem.* 44 (2), 532–553. doi:10.1159/000485089
- He, S., Li, R., Peng, Y., Wang, Z., Huang, J., Meng, H., et al. (2022). ACSL4 contributes to ferroptosis-mediated rhabdomyolysis in exertional heat stroke. *J. Cachexia Sarcopenia Muscle* 13 (3), 1717–1730. doi:10.1002/jcsm.12953
- He, Y. J., Liu, X. Y., Xing, L., Wan, X., Chang, X., and Jiang, H. L. (2020). Fenton reaction-independent ferroptosis therapy via glutathione and iron redox couple sequentially triggered lipid peroxide generator. *Biomaterials* 241, 119911. doi:10.1016/j.biomaterials.2020.119911
- Henning, Y., Blind, U. S., Larafa, S., Matschke, J., and Fandrey, J. (2022). Hypoxia aggravates ferroptosis in RPE cells by promoting the Fenton reaction. *Cell Death Dis.* 13 (7), 662. doi:10.1038/s41419-022-05121-z
- Hentze, M. W., Muckenthaler, M. U., Galy, B., and Camaschella, C. (2010). Two to tango: Regulation of mammalian iron metabolism. *Cell* 142 (1), 24–38. doi:10.1016/j.cell.2010.06.028
- Hoffmann, C., and Weigert, C. (2017). Skeletal muscle as an endocrine organ: The role of myokines in exercise adaptations. *Cold Spring Harb. Perspect. Med.* 7 (11), a029793. doi:10.1101/cshperspect.a029793
- Hojman, P., Dethlefsen, C., Brandt, C., Hansen, J., Pedersen, L., and Pedersen, B. K. (2011). Exercise-induced muscle-derived cytokines inhibit mammary cancer cell growth. *Am. J. Physiol. Endocrinol. Metab.* 301 (3), E504–E510. doi:10.1152/ajpendo.00520.2010
- Holstein, S. A., and Hohl, R. J. (2004). Isoprenoids: Remarkable diversity of form and function. *Lipids* 39 (4), 293–309. doi:10.1007/s11745-004-1233-3
- Hong, E. G., Ko, H. J., Cho, Y. R., Kim, H. J., Ma, Z., Yu, T. Y., et al. (2009). Interleukin-10 prevents diet-induced insulin resistance by attenuating macrophage and cytokine response in skeletal muscle. *Diabetes* 58 (11), 2525–2535. doi:10.2337/db08-1261
- Hooda, J., Shah, A., and Zhang, L. (2014). Heme, an essential nutrient from dietary proteins, critically impacts diverse physiological and pathological processes. *Nutrients* 6 (3), 1080–1102. doi:10.3390/nu6031080
- Hou, W., Xie, Y., Song, X., Sun, X., Lotze, M. T., Zeh, H. J., 3rd, et al. (2016). Autophagy promotes ferroptosis by degradation of ferritin. *Autophagy* 12 (8), 1425–1428. doi:10.1080/15548627.2016.1187366
- Hou, Y., Tang, Y., Wang, X., Ai, X., Wang, H., Li, X., et al. (2020). Rhodiola Crenulata ameliorates exhaustive exercise-induced fatigue in mice by suppressing mitophagy in skeletal muscle. *Exp. Ther. Med.* 20 (4), 3161–3173. doi:10.3892/etm.2020.9072
- Hreusova, M., Novohradsky, V., Markova, L., Kosthunova, H., Potocnak, I., Brabec, V., et al. (2022). Gallium(III) complex with cloxyquin ligands induces ferroptosis in cancer cells and is a potent agent against both differentiated and tumorigenic cancer stem rhabdomyosarcoma cells. *Bioinorg. Chem. Appl.* 2022, 3095749. doi:10.1155/2022/3095749
- Hu, Q., Zhang, Y., Lou, H., Ou, Z., Liu, J., Duan, W., et al. (2021). GPX4 and vitamin E cooperatively protect hematopoietic stem and progenitor cells from lipid peroxidation and ferroptosis. *Cell Death Dis.* 12 (7), 706. doi:10.1038/s41419-021-04008-9
- Hu, W., Zhang, C., Wu, R., Sun, Y., Levine, A., and Feng, Z. (2010). Glutaminase 2, a novel p53 target gene regulating energy metabolism and antioxidant function. *Proc. Natl. Acad. Sci. U. S. A.* 107 (16), 7455–7460. doi:10.1073/pnas.1001006107
- Huang, Y., Wu, B., Shen, D., Chen, J., Yu, Z., and Chen, C. (2021). Ferroptosis in a sarcopenia model of senescence accelerated mouse prone 8 (SAMP8). *Int. J. Biol. Sci.* 17 (1), 151–162. doi:10.7150/ijbs.53126
- Hubner, R. H., Schwartz, J. D., De Bishnu, P., Ferris, B., Omberg, L., Mezey, J. G., et al. (2009). Coordinate control of expression of Nrf2-modulated genes in the human small airway epithelium is highly responsive to cigarette smoking. *Mol. Med.* 15 (7–8), 203–219. doi:10.2119/molmed.2008.00130
- Hyde, R., Hajduch, E., Powell, D. J., Taylor, P. M., and Hundal, H. S. (2005). Ceramide down-regulates System A amino acid transport and protein synthesis in rat skeletal muscle cells. *FASEB J.* 19 (3), 461–463. doi:10.1096/fj.04-2284jfe
- Ikeda, Y., Satoh, A., Horinouchi, Y., Hamano, H., Watanabe, H., Imao, M., et al. (2019). Iron accumulation causes impaired myogenesis correlated with MAPK signaling pathway inhibition by oxidative stress. *FASEB J.* 33 (8), 9551–9564. doi:10.1096/fj.201802724RR
- Imai, H., and Nakagawa, Y. (2003). Biological significance of phospholipid hydroperoxide glutathione peroxidase (PHGPx, GPx4) in mammalian cells. *Free Radic. Biol. Med.* 34 (2), 145–169. doi:10.1016/s0891-5849(02)01197-8
- Ingold, I., Berndt, C., Schmitt, S., Doll, S., Poschmann, G., Buday, K., et al. (2018). Selenium utilization by GPX4 is required to prevent hydroperoxide-induced ferroptosis. *Cell* 172 (3), 409–422. doi:10.1016/j.cell.2017.11.048
- Ishizuka, M., Watanabe, R., Ishii, T., Machiyama, T., Akita, K., Fujita, Y., et al. (2016). Long-term follow-up of 124 patients with polymyositis and dermatomyositis: Statistical analysis of prognostic factors. *Mod. Rheumatol.* 26 (1), 115–120. doi:10.3109/14397595.2015.1054081
- James, A. M., Smith, R. A., and Murphy, M. P. (2004). Antioxidant and prooxidant properties of mitochondrial Coenzyme Q. *Arch. Biochem. Biophys.* 423 (1), 47–56. doi:10.1016/j.abb.2003.12.025
- Jang, Y. C., Sinha, M., Cerletti, M., Dall’Osso, C., and Wagers, A. J. (2011). Skeletal muscle stem cells: Effects of aging and metabolism on muscle regenerative function. *Cold Spring Harb. Symp. Quant. Biol.* 76, 101–111. doi:10.1101/sqb.2011.76.010652
- Janssen, I., Heymsfield, S. B., Wang, Z. M., and Ross, R. (2000). Skeletal muscle mass and distribution in 468 men and women aged 18–88 yr. *J. Appl. Physiol.* 89 (1), 81–88. doi:10.1152/jappl.2000.89.1.81
- Jazvinskac Jembrek, M., Vlainic, J., Radovanovic, V., Erhardt, J., and Orsolic, N. (2014). Effects of copper overload in P19 neurons: Impairment of glutathione redox homeostasis and crosstalk between caspase and calpain protease systems in ROS-induced apoptosis. *Biometals* 27 (6), 1303–1322. doi:10.1007/s10534-014-9792-x
- Jiang, L., Kon, N., Li, T., Wang, S. J., Su, T., Hibshoosh, H., et al. (2015). Ferroptosis as a p53-mediated activity during tumour suppression. *Nature* 520 (7545), 57–62. doi:10.1038/nature14344
- Jiang, T., Cheng, H., Su, J., Wang, X., Wang, Q., Chu, J., et al. (2020). Gastrodin protects against glutamate-induced ferroptosis in HT-22 cells through Nrf2/HO-1 signaling pathway. *Toxicol. Vitro* 62, 104715. doi:10.1016/j.tiv.2019.104715
- Kanezaki, M., Terada, K., Tanabe, N., Shima, H., Hamakawa, Y., and Sato, S. (2021). Effects of sarcopenia on ventilatory behavior and the multidimensional nature of dyspnea in patients with chronic obstructive pulmonary disease. *J. Am. Med. Dir. Assoc.* 22 (4), 827–833. doi:10.1016/j.jamda.2021.01.081
- Kawai, K., Hirayama, T., Imai, H., Murakami, T., Inden, M., Hozumi, I., et al. (2022). Molecular imaging of labile heme in living cells using a small molecule fluorescent probe. *J. Am. Chem. Soc.* 144 (9), 3793–3803. doi:10.1021/jacs.1c08485
- Kawasaki, H., Takayama, J., Nagasaki, K., Yamaguchi, K., and Ohira, M. (1998). Hypercalcemia in children with rhabdomyosarcoma. *J. Pediatr. Hematol. Oncol.* 20 (4), 327–329. doi:10.1097/00043426-199807000-00009
- Kawasumi, H., Gono, T., Kawaguchi, Y., Kaneko, H., Katsumata, Y., Hanaoka, M., et al. (2014). IL-6, IL-8, and IL-10 are associated with hyperferritinemia in rapidly progressive interstitial lung disease with polymyositis/dermatomyositis. *Biomed. Res. Int.* 2014, 815245. doi:10.1155/2014/815245
- Keel, S. B., Doty, R. T., Yang, Z., Quigley, J. G., Chen, J., Knoblaugh, S., et al. (2008). A heme export protein is required for red blood cell differentiation and iron homeostasis. *Science* 319 (5864), 825–828. doi:10.1126/science.1151133
- Klaus, S., Rudolph, B., Dohrmann, C., and Wehr, R. (2005). Expression of uncoupling protein 1 in skeletal muscle decreases muscle energy efficiency and affects thermoregulation and substrate oxidation. *Physiol. Genomics* 21 (2), 193–200. doi:10.1152/physiolgenomics.00299.2004
- Knovich, M. A., Storey, J. A., Coffman, L. G., Torti, S. V., and Torti, F. M. (2009). Ferritin for the clinician. *Blood Rev.* 23 (3), 95–104. doi:10.1016/j.blre.2008.08.001
- Koeller, D. M., Casey, J. L., Hentze, M. W., Gerhardt, E. M., Chan, L. N., Klausner, R. D., et al. (1989). A cytosolic protein binds to structural elements within the iron regulatory region of the transferrin receptor mRNA. *Proc. Natl. Acad. Sci. U. S. A.* 86 (10), 3574–3578. doi:10.1073/pnas.86.10.3574
- Kong, N., Chen, X., Feng, J., Duan, T., Liu, S., Sun, X., et al. (2021). Baicalin induces ferroptosis in bladder cancer cells by downregulating FTH1. *Acta Pharm. Sin. B* 11 (12), 4045–4054. doi:10.1016/j.apsb.2021.03.036
- Kraft, V. A. N., Bezjian, C. T., Pfeiffer, S., Ringelstetter, L., Muller, C., Zandkarimi, F., et al. (2020). GTP cyclohydrolase 1/tetrahydrobiopterin counteract ferroptosis through lipid remodeling. *ACS Cent. Sci.* 6 (1), 41–53. doi:10.1021/acscentsci.9b01063
- Kramer, S., Meadows, A. T., Jarrett, P., and Evans, A. E. (1983). Incidence of childhood cancer: Experience of a decade in a population-based registry. *J. Natl. Cancer Inst.* 70 (1), 49–55.
- Krishnamurthy, P. C., Du, G., Fukuda, Y., Sun, D., Sampath, J., Mercer, K. E., et al. (2006). Identification of a mammalian mitochondrial porphyrin transporter. *Nature* 443 (7111), 586–589. doi:10.1038/nature05125

- Kwon, M. Y., Park, E., Lee, S. J., and Chung, S. W. (2015). Heme oxygenase-1 accelerates erastin-induced ferroptotic cell death. *Oncotarget* 6 (27), 24393–24403. doi:10.18632/oncotarget.5162
- Laitano, O., Oki, K., and Leon, L. R. (2021). The role of skeletal muscles in exertional heat stroke pathophysiology. *Int. J. Sports Med.* 42 (8), 673–681. doi:10.1055/a-1400-9754
- Laredj, L. N., Licitra, F., and Puccio, H. M. (2014). The molecular genetics of coenzyme Q biosynthesis in health and disease. *Biochimie* 100, 78–87. doi:10.1016/j.biochi.2013.12.006
- Latunde-Dada, G. O. (2017). Ferroptosis: Role of lipid peroxidation, iron and ferritinophagy. *Biochim. Biophys. Acta. Gen. Subj.* 1861 (8), 1893–1900. doi:10.1016/j.bbagen.2017.05.019
- Lee, J. Y., Kim, W. K., Bae, K. H., Lee, S. C., and Lee, E. W. (2021). Lipid metabolism and ferroptosis. *Biol. (Basel)* 10 (3), 184. doi:10.3390/biology10030184
- Lei, G., Zhang, Y., Hong, T., Zhang, X., Liu, X., Mao, C., et al. (2021). Ferroptosis as a mechanism to mediate p53 function in tumor radiosensitivity. *Oncogene* 40 (20), 3533–3547. doi:10.1038/s41388-021-01790-w
- Lewerenz, J., Hewett, S. J., Huang, Y., Lambros, M., Gout, P. W., Kalivas, P. W., et al. (2013). The cystine/glutamate antiporter system x(c)(-) in health and disease: From molecular mechanisms to novel therapeutic opportunities. *Antioxid. Redox Signal.* 18 (5), 522–555. doi:10.1089/ars.2011.4391
- Li, D., Jiang, C., Mei, G., Zhao, Y., Chen, L., Liu, J., et al. (2020b). Quercetin alleviates ferroptosis of pancreatic beta cells in type 2 diabetes. *Nutrients* 12 (10), E2954. doi:10.3390/nut12102954
- Li, J., Cao, F., Yin, H. L., Huang, Z. J., Lin, Z. T., Mao, N., et al. (2020a). Ferroptosis: Past, present and future. *Cell Death Dis.* 11 (2), 88. doi:10.1038/s41419-020-2298-2
- Li, J., Lu, K., Sun, F., Tan, S., Zhang, X., Sheng, W., et al. (2021b). Panaxydol attenuates ferroptosis against LPS-induced acute lung injury in mice by Keap1-Nrf2/HO-1 pathway. *J. Transl. Med.* 19 (1), 96. doi:10.1186/s12967-021-02745-1
- Li, M. Y., Dai, X. H., Yu, X. P., Zou, W., Teng, W., Liu, P., et al. (2022). Scalp acupuncture protects against neuronal ferroptosis by activating the p62-keap1-nrf2 pathway in rat models of intracranial haemorrhage. *J. Mol. Neurosci.* 72 (1), 82–96. doi:10.1007/s12031-021-01890-y
- Li, Y., Yan, H., Xu, X., Liu, H., Wu, C., and Zhao, L. (2020c). Erastin/sorafenib induces cisplatin-resistant non-small cell lung cancer cell ferroptosis through inhibition of the Nrf2/xCT pathway. *Oncol. Lett.* 19 (1), 323–333. doi:10.3892/ol.2019.11066
- Li, Y., Zeng, X., Lu, D., Yin, M., Shan, M., and Gao, Y. (2021a). Erastin induces ferroptosis via ferroportin-mediated iron accumulation in endometriosis. *Hum. Reprod.* 36 (4), 951–964. doi:10.1093/humrep/deaa363
- Li, Z. J., Dai, H. Q., Huang, X. W., Feng, J., Deng, J. H., Wang, Z. X., et al. (2021c). Artesunate synergizes with sorafenib to induce ferroptosis in hepatocellular carcinoma. *Acta Pharmacol. Sin.* 42 (2), 301–310. doi:10.1038/s41401-020-0478-3
- Lima, R. S., da Silva Junior, G. B., Liborio, A. B., and Daher Ede, F. (2008). Acute kidney injury due to rhabdomyolysis. *Saudi J. Kidney Dis. Transpl.* 19 (5), 721–729.
- Lindner, A., and Zierz, S. (2003). Rhabdomyolysis and myoglobinuria. *Nervenarzt* 74 (6), 505–515. doi:10.1007/s00115-003-1518-1
- Liu, C. K., Leng, X., Hsu, F. C., Kritchevsky, S. B., Ding, J., Earnest, C. P., et al. (2014). The impact of sarcopenia on a physical activity intervention: The lifestyle interventions and independence for elders pilot study (LIFE-P). *J. Nutr. Health Aging* 18 (1), 59–64. doi:10.1007/s12603-013-0369-0
- Liu, S., Meng, F., Zhang, D., Shi, D., Zhou, J., Guo, S., et al. (2022b). Lonicera caerulea berry polyphenols extract alleviates exercise fatigue in mice by reducing oxidative stress, inflammation, skeletal muscle cell apoptosis, and by increasing cell proliferation. *Front. Nutr.* 9, 853225. doi:10.3389/fnut.2022.853225
- Liu, T., Xu, P., Ke, S., Dong, H., Zhan, M., Hu, Q., et al. (2022a). Histone methyltransferase SETDB1 inhibits TGF-beta-induced epithelial-mesenchymal transition in pulmonary fibrosis by regulating SNAIL expression and the ferroptosis signaling pathway. *Arch. Biochem. Biophys.* 715, 109087. doi:10.1016/j.ab.2021.109087
- Liu, Z., Lv, X., Song, E., and Song, Y. (2020). Fostered Nrf2 expression antagonizes iron overload and glutathione depletion to promote resistance of neuron-like cells to ferroptosis. *Toxicol. Appl. Pharmacol.* 407, 115241. doi:10.1016/j.taap.2020.115241
- Lu, H., Xiao, H., Dai, M., Xue, Y., and Zhao, R. (2022). Britanin relieves ferroptosis-mediated myocardial ischaemia/reperfusion damage by upregulating GPX4 through activation of AMPK/GSK3β/Nrf2 signalling. *Pharm. Biol.* 60 (1), 38–45. doi:10.1080/13880209.2021.2007269
- Lu, S. C. (2009). Regulation of glutathione synthesis. *Mol. Asp. Med.* 30 (1–2), 42–59. doi:10.1016/j.mam.2008.05.005
- Lu, Y., Yang, Q., Su, Y., Ji, Y., Li, G., Yang, X., et al. (2021). MYCN mediates TFRC-dependent ferroptosis and reveals vulnerabilities in neuroblastoma. *Cell Death Dis.* 12 (6), 511. doi:10.1038/s41419-021-03790-w
- Lundberg, I. E., Miller, F. W., Tjarnlund, A., and Bottai, M. (2016). Diagnosis and classification of idiopathic inflammatory myopathies. *J. Intern. Med.* 280 (1), 39–51. doi:10.1111/joim.12524
- Lv, Z., Wang, F., Zhang, X., Zhang, X., Zhang, J., and Liu, R. (2021). Etomidate attenuates the ferroptosis in myocardial ischemia/reperfusion rat model via Nrf2/HO-1 pathway. *Shock* 56 (3), 440–449. doi:10.1097/SHK.0000000000001751
- Ma, S., Sun, L., Wu, W., Wu, J., Sun, Z., and Ren, J. (2020b). USP22 protects against myocardial ischemia-reperfusion injury via the SIRT1-p53/slc7a11-dependent inhibition of ferroptosis-induced cardiomyocyte death. *Front. Physiol.* 11, 551318. doi:10.3389/fphys.2020.551318
- Madduma Hewage, S. R. K., Piao, M. J., Kang, K. A., Ryu, Y. S., Fernando, P., Oh, M. C., et al. (2017). Galangin activates the ERK/AKT-Driven Nrf2 signaling pathway to increase the level of reduced glutathione in human keratinocytes. *Biomol. Ther.* 25 (4), 427–433. doi:10.4062/biomolther.2016.112
- Mancias, J. D., Wang, X., Gygi, S. P., Harper, J. W., and Kimmelman, A. C. (2014). Quantitative proteomics identifies NCOA4 as the cargo receptor mediating ferritinophagy. *Nature* 509 (7498), 105–109. doi:10.1038/nature13148
- Mandal, P. K., Seiler, A., Perisic, T., Kolle, P., Banjac Canak, A., Forster, H., et al. (2010). System x(c)- and thioredoxin reductase 1 cooperatively rescue glutathione deficiency. *J. Biol. Chem.* 285 (29), 22244–22253. doi:10.1074/jbc.M110.121327
- Mao, C., Liu, X., Zhang, Y., Lei, G., Yan, Y., Lee, H., et al. (2021). DHODH-mediated ferroptosis defence is a targetable vulnerability in cancer. *Nature* 593 (7860), 586–590. doi:10.1038/s41586-021-03539-7
- Mauro, A. (1961). Satellite cell of skeletal muscle fibers. *J. Biophys. Biochem. Cytol.* 9, 493–495. doi:10.1083/jcb.9.2.493
- McBean, G. J. (2012). The transsulfuration pathway: A source of cysteine for glutathione in astrocytes. *Amino Acids* 42 (1), 199–205. doi:10.1007/s00726-011-0864-8
- Meister, A., and Anderson, M. E. (1983). Glutathione. *Annu. Rev. Biochem.* 52, 711–760. doi:10.1146/annurev.bi.52.070183.003431
- Meyer, A., Laverny, G., Allenbach, Y., Grelet, E., Ueberschlager, V., Echaniz-Laguna, A., et al. (2017). IFN-beta-induced reactive oxygen species and mitochondrial damage contribute to muscle impairment and inflammation maintenance in dermatomyositis. *Acta Neuropathol.* 134 (4), 655–666. doi:10.1007/s00401-017-1731-9
- Meyer, C., Dostou, J. M., Welle, S. L., and Gerich, J. E. (2002). Role of human liver, kidney, and skeletal muscle in postprandial glucose homeostasis. *Am. J. Physiol. Endocrinol. Metab.* 282 (2), E419–E427. doi:10.1152/ajpendo.00032.2001
- Miao, H., Ren, Q., Li, H., Zeng, M., Chen, D., Xu, C., et al. (2022). Comprehensive analysis of the autophagy-dependent ferroptosis-related gene FANCD2 in lung adenocarcinoma. *BMC Cancer* 22 (1), 225. doi:10.1186/s12885-022-09314-9
- Moosmann, B., and Behl, C. (2004). Selenoproteins, cholesterol-lowering drugs, and the consequences: Revisiting of the mevalonate pathway. *Trends Cardiovasc. Med.* 14 (7), 273–281. doi:10.1016/j.tcm.2004.08.003
- Mosharov, E., Cranford, M. R., and Banerjee, R. (2000). The quantitatively important relationship between homocysteine metabolism and glutathione synthesis by the transsulfuration pathway and its regulation by redox changes. *Biochemistry* 39 (42), 13005–13011. doi:10.1021/bi001088w
- Mugoni, V., Postel, R., Catanzaro, V., De Luca, E., Turco, E., Digilio, G., et al. (2013). Ubiad1 is an antioxidant enzyme that regulates eNOS activity by CoQ10 synthesis. *Cell* 152 (3), 504–518. doi:10.1016/j.cell.2013.01.013
- Murphy, T. H., Miyamoto, M., Sastre, A., Schnaar, R. L., and Coyle, J. T. (1989). Glutamate toxicity in a neuronal cell line involves inhibition of cystine transport leading to oxidative stress. *Neuron* 2 (6), 1547–1558. doi:10.1016/0896-6273(89)90043-3
- Nakanishi, K., Taniguchi, T., Ranganathan, V., New, H. V., Moreau, L. A., Stotsky, M., et al. (2002). Interaction of FANCD2 and NBS1 in the DNA damage response. *Nat. Cell Biol.* 4 (12), 913–920. doi:10.1038/ncb879
- Nemeth, E., Tuttle, M. S., Powelson, J., Vaughn, M. B., Donovan, A., Ward, D. M., et al. (2004). Hepcidin regulates cellular iron efflux by binding to ferroportin and inducing its internalization. *Science* 306 (5704), 2090–2093. doi:10.1126/science.1104742
- Nishizawa, S., Araki, H., Ishikawa, Y., Kitazawa, S., Hata, A., Soga, T., et al. (2018). Low tumor glutathione level as a sensitivity marker for glutamate-cysteine ligase inhibitors. *Oncol. Lett.* 15 (6), 8735–8743. doi:10.3892/ol.2018.8447
- Niu, T., Fu, G., Zhou, J., Han, H., Chen, J., Wu, W., et al. (2020). Floridosiside exhibits antioxidant properties by activating Ho-1 expression via P38/erk mapk pathway. *Mar. Drugs* 18 (2), E105. doi:10.3390/md18020105



- Ognjanovic, S., Linabery, A. M., Charbonneau, B., and Ross, J. A. (2009). Trends in childhood rhabdomyosarcoma incidence and survival in the United States, 1975–2005. *Cancer* 115 (18), 4218–4226. doi:10.1002/cncr.24465
- Ohgami, R. S., Campagna, D. R., Greer, E. L., Antiochos, B., McDonald, A., Chen, J., et al. (2005). Identification of a ferrireductase required for efficient transferrin-dependent iron uptake in erythroid cells. *Nat. Genet.* 37 (11), 1264–1269. doi:10.1038/ng1658
- Oliveira, A., and Vaz, C. (2015). The role of sarcopenia in the risk of osteoporotic hip fracture. *Clin. Rheumatol.* 34 (10), 1673–1680. doi:10.1007/s10067-015-2943-9
- Olney, J. W. (1971). Glutamate-induced neuronal necrosis in the infant mouse hypothalamus. An electron microscopic study. *J. Neuropathol. Exp. Neurol.* 30 (1), 75–90. doi:10.1097/00005072-197101000-00008
- Ong, A. L. C., and Ramasamy, T. S. (2018). Role of Sirtuin1-p53 regulatory axis in aging, cancer and cellular reprogramming. *Ageing Res. Rev.* 43, 64–80. doi:10.1016/j.arr.2018.02.004
- Ou, Y., Wang, S. J., Li, D., Chu, B., and Gu, W. (2016). Activation of SAT1 engages polyamine metabolism with p53-mediated ferroptotic responses. *Proc. Natl. Acad. Sci. U. S. A.* 113 (44), E6806–E6812. doi:10.1073/pnas.1607152113
- Paradkar, P. N., Zumbrennen, K. B., Paw, B. H., Ward, D. M., and Kaplan, J. (2009). Regulation of mitochondrial iron import through differential turnover of mitoferrin 1 and mitoferrin 2. *Mol. Cell. Biol.* 29 (4), 1007–1016. doi:10.1128/MCB.01685-08
- Parkes, J. E., Day, P. J., Chinoy, H., and Lamb, J. A. (2015). The role of microRNAs in the idiopathic inflammatory myopathies. *Curr. Opin. Rheumatol.* 27 (6), 608–615. doi:10.1097/BOR.0000000000000225
- Paul, B. T., Manz, D. H., Torti, F. M., and Torti, S. V. (2017). Mitochondria and iron: Current questions. *Expert Rev. Hematol.* 10 (1), 65–79. doi:10.1080/17474086.2016.1268047
- Pedersen, B. K., and Febbraio, M. A. (2008). Muscle as an endocrine organ: Focus on muscle-derived interleukin-6. *Physiol. Rev.* 88 (4), 1379–1406. doi:10.1152/physrev.90100.2007
- Perez-Sala, D., Parrilla, R., and Ayuso, M. S. (1987). Key role of L-alanine in the control of hepatic protein synthesis. *Biochem. J.* 241 (2), 491–498. doi:10.1042/bj2410491
- Perriello, G., Nurjhan, N., Stumvoll, M., Bucci, A., Welle, S., Dailey, G., et al. (1997). Regulation of gluconeogenesis by glutamine in normal postabsorptive humans. *Am. J. Physiol.* 272, E437–E445. doi:10.1152/ajpendo.1997.272.3.E437
- Possemato, R., Marks, K. M., Shaul, Y. D., Pacold, M. E., Kim, D., Birsoy, K., et al. (2011). Functional genomics reveal that the serine synthesis pathway is essential in breast cancer. *Nature* 476 (7360), 346–350. doi:10.1038/nature10350
- Qin, Z., Ou, S., Xu, L., Sorensen, K., Zhang, Y., Hu, D. P., et al. (2021). Design and synthesis of isothiocyanate-containing hybrid androgen receptor (AR) antagonist to downregulate AR and induce ferroptosis in GSH-Deficient prostate cancer cells. *Chem. Biol. Drug Des.* 97 (5), 1059–1078. doi:10.1111/cbdd.13826
- Quigley, J. G., Yang, Z., Worthington, M. T., Phillips, J. D., Sabo, K. M., Sabath, D. E., et al. (2004). Identification of a human heme exporter that is essential for erythropoiesis. *Cell* 118 (6), 757–766. doi:10.1016/j.cell.2004.08.014
- Reid, M. B. (2008). Free radicals and muscle fatigue: Of ROS, canaries, and the IOC. *Free Radic. Biol. Med.* 44 (2), 169–179. doi:10.1016/j.freeradbiomed.2007.03.002
- Reid, M. B., Haack, K. E., Franchek, K. M., Valberg, P. A., Kobzik, L., and West, M. S. (1992). Reactive oxygen in skeletal muscle. I. Intracellular oxidant kinetics and fatigue *in vitro*. *J. Appl. Physiol.* 73 (5), 1797–1804. doi:10.1152/jappl.1992.73.5.1797
- Rhee, S. G., Bae, Y. S., Lee, S. R., and Kwon, J. (2000). Hydrogen peroxide: A key messenger that modulates protein phosphorylation through cysteine oxidation. *Sci. STKE* 2000 (53), pe1. doi:10.1126/stke.2000.53.pe1
- Rodriguez-Graciani, K. M., Chapa-Dubocq, X. R., Ayala-Arroyo, E. J., Chaves-Negron, I., Jang, S., Chorna, N., et al. (2022). Effects of ferroptosis on the metabolome in cardiac cells: The role of glutaminolysis. *Antioxidants (Basel)* 11 (2), 278. doi:10.3390/antiox11020278
- Rotruck, J. T., Pope, A. L., Ganther, H. E., Swanson, A. B., Hafeman, D. G., and Hoekstra, W. G. (1973). Selenium: Biochemical role as a component of glutathione peroxidase. *Science* 179 (4073), 588–590. doi:10.1126/science.179.4073.588
- Sbodio, J. I., Snyder, S. H., and Paul, B. D. (2019). Regulators of the transsulfuration pathway. *Br. J. Pharmacol.* 176 (4), 583–593. doi:10.1111/bph.14446
- Schafer, F. Q., and Buettner, G. R. (2001). Redox environment of the cell as viewed through the redox state of the glutathione disulfide/glutathione couple. *Free Radic. Biol. Med.* 30 (11), 1191–1212. doi:10.1016/s0891-5849(01)00480-4
- Schott, C., Graab, U., Cuvelier, N., Hahn, H., and Fulda, S. (2015). Oncogenic RAS mutants confer resistance of RMS13 rhabdomyosarcoma cells to oxidative stress-induced ferroptotic cell death. *Front. Oncol.* 5, 131. doi:10.3389/fonc.2015.00131
- Scibior, A., Wojda, I., Wnuk, E., Pietrzyk, L., and Plewa, Z. (2021). Response of cytoprotective and detoxifying proteins to vanadate and/or magnesium in the rat liver: The nrf2-keap1 system. *Oxid. Med. Cell. Longev.* 2021, 8447456. doi:10.1155/2021/8447456
- Sen, N., Cross, A. M., Lorenzi, P. L., Khan, J., Gryder, B. E., Kim, S., et al. (2018). EWS-FLI1 reprograms the metabolism of Ewing sarcoma cells via positive regulation of glutamine import and serine-glycine biosynthesis. *Mol. Carcinog.* 57 (10), 1342–1357. doi:10.1002/mc.22849
- Shern, J. F., Chen, L., Chmielecki, J., Wei, J. S., Patidar, R., Rosenberg, M., et al. (2014). Comprehensive genomic analysis of rhabdomyosarcoma reveals a landscape of alterations affecting a common genetic axis in fusion-positive and fusion-negative tumors. *Cancer Discov.* 4 (2), 216–231. doi:10.1158/2159-8290.CD-13-0639
- Shimada, K., Skouta, R., Kaplan, A., Yang, W. S., Hayano, M., Dixon, S. J., et al. (2016). Global survey of cell death mechanisms reveals metabolic regulation of ferroptosis. *Nat. Chem. Biol.* 12 (7), 497–503. doi:10.1038/nchembio.2079
- Shiozu, H., Higashijima, M., and Koga, T. (2015). Association of sarcopenia with swallowing problems, related to nutrition and activities of daily living of elderly individuals. *J. Phys. Ther. Sci.* 27 (2), 393–396. doi:10.1589/jpts.27.393
- Sikalidis, A. K., Mazar, K. M., Lee, J. I., Roman, H. B., Hirschberger, L. L., and Stipanuk, M. H. (2014). Upregulation of capacity for glutathione synthesis in response to amino acid deprivation: Regulation of glutamate-cysteine ligase subunits. *Amino Acids* 46 (5), 1285–1296. doi:10.1007/s00726-014-1687-1
- Singh, A., Wu, H., Zhang, P., Happel, C., Ma, J., and Biswal, S. (2010). Expression of ABCG2 (BCRP) is regulated by Nrf2 in cancer cells that confers side population and chemoresistance phenotype. *Mol. Cancer Ther.* 9 (8), 2365–2376. doi:10.1158/1535-7163.MCT-10-0108
- Song, Q., Peng, S., Sun, Z., Heng, X., and Zhu, X. (2021a). Temozolomide drives ferroptosis via a DMT1-dependent pathway in glioblastoma cells. *Yonsei Med. J.* 62 (9), 843–849. doi:10.3349/ymj.2021.62.9.843
- Song, X., Xie, Y., Kang, R., Hou, W., Sun, X., Epperly, M. W., et al. (2016). FANCD2 protects against bone marrow injury from ferroptosis. *Biochem. Biophys. Res. Commun.* 480 (3), 443–449. doi:10.1016/j.bbrc.2016.10.068
- Soula, M., Weber, R. A., Zilka, O., Alwaseem, H., La, K., Yen, F., et al. (2020). Metabolic determinants of cancer cell sensitivity to canonical ferroptosis inducers. *Nat. Chem. Biol.* 16 (12), 1351–1360. doi:10.1038/s41589-020-0613-y
- Sousa-Victor, P., Gutarra, S., Garcia-Prat, L., Rodriguez-Ubreva, J., Ortet, L., Ruiz-Bonilla, V., et al. (2014). Geriatric muscle stem cells switch reversible quiescence into senescence. *Nature* 506 (7488), 316–321. doi:10.1038/nature13013
- Stahl, K., Rastelli, E., and Schoser, B. (2020). A systematic review on the definition of rhabdomyolysis. *J. Neurol.* 267 (4), 877–882. doi:10.1007/s00415-019-09185-4
- Stockwell, B. R. (2019). A powerful cell-protection system prevents cell death by ferroptosis. *Nature* 575 (7784), 597–598. doi:10.1038/d41586-019-03145-8
- Su, L. J., Zhang, J. H., Gomez, H., Murugan, R., Hong, X., Xu, D., et al. (2019). Reactive oxygen species-induced lipid peroxidation in apoptosis, autophagy, and ferroptosis. *Oxid. Med. Cell. Longev.* 2019, 5080843. doi:10.1155/2019/5080843
- Sun, X., Ou, Z., Chen, R., Niu, X., Chen, D., Kang, R., et al. (2016). Activation of the p62-Keap1-NRF2 pathway protects against ferroptosis in hepatocellular carcinoma cells. *Hepatology* 63 (1), 173–184. doi:10.1002/hep.28251
- Sun, X., Ou, Z., Xie, M., Kang, R., Fan, Y., Niu, X., et al. (2015). HSPB1 as a novel regulator of ferroptotic cancer cell death. *Oncogene* 34 (45), 5617–5625. doi:10.1038/onc.2015.32
- Sun, Y., Cui, D., Zhang, Z., Zhang, T., Shi, J., Jin, H., et al. (2016b). Attenuated oxidative stress following acute exhaustive swimming exercise was accompanied with modified gene expression profiles of apoptosis in the skeletal muscle of mice. *Oxid. Med. Cell. Longev.* 2016, 8381242. doi:10.1155/2016/8381242
- Sun, Y., Zheng, Y., Wang, C., and Liu, Y. (2018). Glutathione depletion induces ferroptosis, autophagy, and premature cell senescence in retinal pigment epithelial cells. *Cell Death Dis.* 9 (7), 753. doi:10.1038/s41419-018-0794-4
- Suzuki, S., Tanaka, T., Poyurovsky, M. V., Nagano, H., Mayama, T., Ohkubo, S., et al. (2010). Phosphate-activated glutaminase (GLS2), a p53-inducible regulator of glutamine metabolism and reactive oxygen species. *Proc. Natl. Acad. Sci. U. S. A.* 107 (16), 7461–7466. doi:10.1073/pnas.1002459107
- Tan, C. T., Chang, H. C., Zhou, Q., Yu, C., Fu, N. Y., Sabapathy, K., et al. (2021). MOAP-1-mediated dissociation of p62/SQSTM1 bodies releases Keap1 and suppresses Nrf2 signaling. *EMBO Rep.* 22 (1), e50854. doi:10.15252/embr.202050854
- Tan, K. T., Ang, S. J., and Tsai, S. Y. (2020a). Sarcopenia: Tilting the balance of protein homeostasis. *Proteomics* 20 (5–6), e1800411. doi:10.1002/pmic.201800411



- Tang, B., Zhu, J., Li, J., Fan, K., Gao, Y., Cheng, S., et al. (2020). The ferroptosis and iron-metabolism signature robustly predicts clinical diagnosis, prognosis and immune microenvironment for hepatocellular carcinoma. *Cell Commun. Signal.* 18 (1), 174. doi:10.1186/s12964-020-00663-1
- Te Braake, F. W., Schierbeek, H., de Groof, K., Vermes, A., Longini, M., Buonocore, G., et al. (2008). Glutathione synthesis rates after amino acid administration directly after birth in preterm infants. *Am. J. Clin. Nutr.* 88 (2), 333–339. doi:10.1093/ajcn/88.2.333
- Tenhunen, R., Marver, H. S., and Schmid, R. (1968). The enzymatic conversion of heme to bilirubin by microsomal heme oxygenase. *Proc. Natl. Acad. Sci. U. S. A.* 61 (2), 748–755. doi:10.1073/pnas.61.2.748
- Theil, E. C. (2013). Ferritin: The protein nanocage and iron biomineral in health and in disease. *Inorg. Chem.* 52 (21), 12223–12233. doi:10.1021/ic400484n
- Thony, B., Auerbach, G., and Blau, N. (2000). Tetrahydrobiopterin biosynthesis, regeneration and functions. *Biochem. J.* 347 Pt 1, 1–16. doi:10.1042/bj3470001
- Tian, H., Xiong, Y., Zhang, Y., Leng, Y., Tao, J., Li, L., et al. (2021). Activation of NRF2/FPN1 pathway attenuates myocardial ischemia-reperfusion injury in diabetic rats by regulating iron homeostasis and ferroptosis. *Cell Stress Chaperones* 27 (2), 149–164. doi:10.1007/s12192-022-01257-1
- Tian, Y., Lu, J., Hao, X., Li, H., Zhang, G., Liu, X., et al. (2020). FTH1 inhibits ferroptosis through ferritinophagy in the 6-OHDA model of Parkinson's disease. *Neurotherapeutics* 17 (4), 1796–1812. doi:10.1007/s13311-020-00929-z
- Tsekoura, M., Kastrinis, A., Katsoulaki, M., Billis, E., and Gliatis, J. (2017). Sarcopenia and its impact on quality of life. *Adv. Exp. Med. Biol.* 987, 213–218. doi:10.1007/978-3-319-57379-3\_19
- Tuo, Q. Z., Masaldan, S., Southon, A., Mawal, C., Ayton, S., Bush, A. I., et al. (2021). Characterization of selenium compounds for anti-ferroptotic activity in neuronal cells and after cerebral ischemia-reperfusion injury. *Neurotherapeutics* 18 (4), 2682–2691. doi:10.1007/s13311-021-01111-9
- Ursini, F., and Maiorino, M. (2020). Lipid peroxidation and ferroptosis: The role of GSH and GPx4. *Free Radic. Biol. Med.* 152, 175–185. doi:10.1016/j.freeradbiomed.2020.02.027
- Venkatesh, D., O'Brien, N. A., Zandkarimi, F., Tong, D. R., Stokes, M. E., Dunn, D. E., et al. (2020). MDM2 and MDMX promote ferroptosis by PPAR $\alpha$ -mediated lipid remodeling. *Genes Dev.* 34 (7–8), 526–543. doi:10.1101/gad.334219.119
- Wang, D., Wei, G., Ma, J., Cheng, S., Jia, L., Song, X., et al. (2021b). Identification of the prognostic value of ferroptosis-related gene signature in breast cancer patients. *BMC Cancer* 21 (1), 645. doi:10.1186/s12885-021-08341-2
- Wang, J., and Pantopoulos, K. (2011). Regulation of cellular iron metabolism. *Biochem. J.* 434 (3), 365–381. doi:10.1042/BJ20101825
- Wang, J., Wang, Y., Liu, Y., Cai, X., Huang, X., Fu, W., et al. (2022). Ferroptosis, a new target for treatment of renal injury and fibrosis in a 5/6 nephrectomy-induced CKD rat model. *Cell Death Discov.* 8 (1), 127. doi:10.1038/s41420-022-00931-8
- Wang, K., Zhang, Z., Tsai, H. I., Liu, Y., Gao, J., Wang, M., et al. (2021d). Branched-chain amino acid aminotransferase 2 regulates ferroptotic cell death in cancer cells. *Cell Death Differ.* 28 (4), 1222–1236. doi:10.1038/s41418-020-00644-4
- Wang, L., Liu, Y., Du, T., Yang, H., Lei, L., Guo, M., et al. (2020). ATF3 promotes erastin-induced ferroptosis by suppressing system Xc $^+$ . *Cell Death Differ.* 27 (2), 662–675. doi:10.1038/s41418-019-0380-z
- Wang, Y. Q., Chang, S. Y., Wu, Q., Gou, Y. J., Jia, L., Cui, Y. M., et al. (2016). The protective role of mitochondrial ferritin on erastin-induced ferroptosis. *Front. Aging Neurosci.* 8, 308. doi:10.3389/fnagi.2016.00308
- Wang, Y., Yu, R., Wu, L., and Yang, G. (2021c). Hydrogen sulfide guards myoblasts from ferroptosis by inhibiting ALOX12 acetylation. *Cell. Signal.* 78, 109870. doi:10.1016/j.cellsig.2020.109870
- Ward, D. M., and Kaplan, J. (2012). Ferroportin-mediated iron transport: Expression and regulation. *Biochim. Biophys. Acta* 1823 (9), 1426–1433. doi:10.1016/j.bbamcr.2012.03.004
- Welch, A. A., Hayhoe, R. P. G., and Cameron, D. (2020). The relationships between sarcopenic skeletal muscle loss during ageing and macronutrient metabolism, obesity and onset of diabetes. *Proc. Nutr. Soc.* 79 (1), 158–169. doi:10.1017/S0029665119001150
- Whillier, S., Garcia, B., Chapman, B. E., Kuchel, P. W., and Raftos, J. E. (2011). Glutamine and alpha-ketoglutarate as glutamate sources for glutathione synthesis in human erythrocytes. *FEBS J.* 278 (17), 3152–3163. doi:10.1111/j.1742-4658.2011.08241.x
- Winterbourn, C. C. (1995). Toxicity of iron and hydrogen peroxide: The Fenton reaction. *Toxicol. Lett.* 82–83, 969–974. doi:10.1016/0378-4274(95)03532-x
- Wolfe, R. R. (2006). The underappreciated role of muscle in health and disease. *Am. J. Clin. Nutr.* 84 (3), 475–482. doi:10.1093/ajcn/84.3.475
- Worwood, M. (1987). The diagnostic value of serum ferritin determinations for assessing iron status. *Haematol. (Budap)* 20 (4), 229–235.
- Wrann, C. D., White, J. P., Salogiannis, J., Laznik-Bogoslavski, D., Wu, J., Ma, D., et al. (2013). Exercise induces hippocampal BDNF through a PGC-1 $\alpha$ /FNDC5 pathway. *Cell Metab.* 18 (5), 649–659. doi:10.1016/j.cmet.2013.09.008
- Wu, A., Feng, B., Yu, J., Yan, L., Che, L., Zhuo, Y., et al. (2021). Fibroblast growth factor 21 attenuates iron overload-induced liver injury and fibrosis by inhibiting ferroptosis. *Redox Biol.* 46, 102131. doi:10.1016/j.redox.2021.102131
- Wu, C., Zhao, W., Yu, J., Li, S., Lin, L., and Chen, X. (2018). Induction of ferroptosis and mitochondrial dysfunction by oxidative stress in PC12 cells. *Sci. Rep.* 8 (1), 574. doi:10.1038/s41598-017-18935-1
- Xiang, L., Xie, G., Liu, C., Zhou, J., Chen, J., Yu, S., et al. (2013). Knock-down of glutaminase 2 expression decreases glutathione, NADH, and sensitizes cervical cancer to ionizing radiation. *Biochim. Biophys. Acta* 1833 (12), 2996–3005. doi:10.1016/j.bbamcr.2013.08.003
- Xiao, R., Wei, Y., Zhang, Y., Xu, F., Ma, C., Gong, Q., et al. (2022). Trilobatin, a naturally occurring food additive, ameliorates exhaustive exercise-induced fatigue in mice: Involvement of Nrf2/ARE/ferroptosis signaling pathway. *Front. Pharmacol.* 13, 913367. doi:10.3389/fphar.2022.913367
- Xie, Y., Zhu, S., Song, X., Sun, X., Fan, Y., Liu, J., et al. (2017). The tumor suppressor p53 limits ferroptosis by blocking DPP4 activity. *Cell Rep.* 20 (7), 1692–1704. doi:10.1016/j.celrep.2017.07.055
- Xu, H., Liu, X., Xia, J., Yu, T., Qu, Y., Jiang, H., et al. (2018). Activation of NMDA receptors mediated iron accumulation via modulating iron transporters in Parkinson's disease. *FASEB J.* 32, 6100–6111. doi:10.1096/fj.20180060RR
- Xu, M., Li, Y., Meng, D., Zhang, D., Wang, B., Xie, J., et al. (2022b). 6-Hydroxydopamine induces abnormal iron sequestration in BV2 microglia by activating iron regulatory protein 1 and inhibiting hepcidin release. *Biomolecules* 12 (2), 266. doi:10.3390/biom12020266
- Xu, Y., Li, Y., Li, J., and Chen, W. (2022a). Ethyl carbamate triggers ferroptosis in liver through inhibiting GSH synthesis and suppressing Nrf2 activation. *Redox Biol.* 53, 102349. doi:10.1016/j.redox.2022.102349
- Xue, J., Yu, C., Sheng, W., Zhu, W., Luo, J., Zhang, Q., et al. (2017). The nrf2/GCH1/BH4 Axis Ameliorates radiation-induced skin injury by modulating the ROS cascade. *J. Invest. Dermatol.* 137 (10), 2059–2068. doi:10.1016/j.jid.2017.05.019
- Yamamoto, M., Kensler, T. W., and Motohashi, H. (2018). The KEAP1-NRF2 system: A thiol-based sensor-effector apparatus for maintaining redox homeostasis. *Physiol. Rev.* 98 (3), 1169–1203. doi:10.1152/physrev.00023.2017
- Yamamoto, S. (1991). Enzymatic lipid peroxidation: Reactions of mammalian lipoxygenases. *Free Radic. Biol. Med.* 10 (2), 149–159. doi:10.1016/0891-5849(91)90008-q
- Yang, W. S., Kim, K. J., Gaschler, M. M., Patel, M., Shchepinov, M. S., and Stockwell, B. R. (2016). Peroxidation of polyunsaturated fatty acids by lipoxygenases drives ferroptosis. *Proc. Natl. Acad. Sci. U. S. A.* 113 (34), E4966–E4975. doi:10.1073/pnas.1603244113
- Yang, W. S., and Stockwell, B. R. (2016). Ferroptosis: Death by lipid peroxidation. *Trends Cell Biol.* 26 (3), 165–176. doi:10.1016/j.tcb.2015.10.014
- Yang, X., Hao, Y., Zhang, X., Geng, Y., Ji, L., Li, G., et al. (2020). Mortality of Chinese patients with polymyositis and dermatomyositis. *Clin. Rheumatol.* 39 (5), 1569–1579. doi:10.1007/s10067-019-04910-w
- Yang, Y., Bazhin, A. V., Werner, J., and Karakhanova, S. (2013). Reactive oxygen species in the immune system. *Int. Rev. Immunol.* 32 (3), 249–270. doi:10.3109/08830185.2012.755176
- Yao, F., Cui, X., Zhang, Y., Bei, Z., Wang, H., Zhao, D., et al. (2021). Iron regulatory protein 1 promotes ferroptosis by sustaining cellular iron homeostasis in melanoma. *Oncol. Lett.* 22 (3), 657. doi:10.3892/ol.2021.12918
- Ye, J., Fan, J., Venneti, S., Wan, Y. W., Pawel, B. R., Zhang, J., et al. (2014). Serine catabolism regulates mitochondrial redox control during hypoxia. *Cancer Discov.* 4 (12), 1406–1417. doi:10.1158/2159-8290.CD-14-0250
- Yin, H., Price, F., and Rudnicki, M. A. (2013). Satellite cells and the muscle stem cell niche. *Physiol. Rev.* 93 (1), 23–67. doi:10.1152/physrev.00043.2011
- Yu, H., Guo, P., Xie, X., Wang, Y., and Chen, G. (2017). Ferroptosis, a new form of cell death, and its relationships with tumorous diseases. *J. Cell. Mol. Med.* 21 (4), 648–657. doi:10.1111/jcmm.13008
- Yu, Y., Jiang, L., Wang, H., Shen, Z., Cheng, Q., Zhang, P., et al. (2020). Hepatic transferrin plays a role in systemic iron homeostasis and liver ferroptosis. *Blood* 136 (6), 726–739. doi:10.1182/blood.2019002907
- Yuan, H., Li, X., Zhang, X., Kang, R., and Tang, D. (2016b). C1SD1 inhibits ferroptosis by protection against mitochondrial lipid

peroxidation. *Biochem. Biophys. Res. Commun.* 478 (2), 838–844. doi:10.1016/j.bbrc.2016.08.034

Yuan, H., Li, X., Zhang, X., Kang, R., and Tang, D. (2016a). Identification of ACSL4 as a biomarker and contributor of ferroptosis. *Biochem. Biophys. Res. Commun.* 478 (3), 1338–1343. doi:10.1016/j.bbrc.2016.08.124

Zeitler, L., Fiore, A., Meyer, C., Russier, M., Zanella, G., Suppmann, S., et al. (2021). Anti-ferroptotic mechanism of IL4i1-mediated amino acid metabolism. *Elife* 10, e64806. doi:10.7554/eLife.64806

Zhang, H., Deng, T., Liu, R., Ning, T., Yang, H., Liu, D., et al. (2020b). CAF secreted miR-522 suppresses ferroptosis and promotes acquired chemo-resistance in gastric cancer. *Mol. Cancer* 19 (1), 43. doi:10.1186/s12943-020-01168-8

Zhang, H., Gomez, A. M., Wang, X., Yan, Y., Zheng, M., and Cheng, H. (2013b). ROS regulation of microdomain Ca(2+) signalling at the dyads. *Cardiovasc. Res.* 98 (2), 248–258. doi:10.1093/cvr/cvt050

Zhang, H., Ostrowski, R., Jiang, D., Zhao, Q., Liang, Y., Che, X., et al. (2021a). Hepcidin promoted ferroptosis through iron metabolism which is associated with DMT1 signaling activation in early brain injury following subarachnoid hemorrhage. *Oxid. Med. Cell. Longev.* 2021, 9800794. doi:10.1155/2021/9800794

Zhang, J., Wang, X., Vikash, V., Ye, Q., Wu, D., Liu, Y., et al. (2016). ROS and ROS-mediated cellular signaling. *Oxid. Med. Cell. Longev.* 2016, 4350965. doi:10.1155/2016/4350965

Zhang, J., Zhang, X., Li, J., and Song, Z. (2020). Systematic analysis of the ABC transporter family in hepatocellular carcinoma reveals the importance of ABCB6 in regulating ferroptosis. *Life Sci.* 257, 118131. doi:10.1016/j.lfs.2020.118131

Zhang, M., Linardic, C. M., and Kirsch, D. G. (2013). RAS and ROS in rhabdomyosarcoma. *Cancer Cell* 24 (6), 689–691. doi:10.1016/j.ccr.2013.11.015

Zhang, M., Zhang, T., Song, C., Qu, J., Gu, Y., Liu, S., et al. (2021c). Guizhi Fuling Capsule ameliorates endometrial hyperplasia through promoting p62-Keap1-NRF2-mediated ferroptosis. *J. Ethnopharmacol.* 274, 114064. doi:10.1016/j.jep.2021.114064

Zhang, Q., Qu, H., Chen, Y., Luo, X., Chen, C., Xiao, B., et al. (2022e). Atorvastatin induces mitochondria-dependent ferroptosis via the modulation of nrf2-xCT/GPx4 Axis. *Front. Cell Dev. Biol.* 10, 806081. doi:10.3389/fcell.2022.806081

Zhang, T., Sun, L., Hao, Y., Suo, C., Shen, S., Wei, H., et al. (2022a). ENO1 suppresses cancer cell ferroptosis by degrading the mRNA of iron regulatory protein 1. *Nat. Cancer* 3 (1), 75–89. doi:10.1038/s43018-021-00299-1

Zhang, Y., Xia, M., Zhou, Z., Hu, X., Wang, J., Zhang, M., et al. (2021d). p53 promoted ferroptosis in ovarian cancer cells treated with human serum incubated-superparamagnetic iron oxides. *Int. J. Nanomedicine* 16, 283–296. doi:10.2147/IJN.S282489

Zhang, Y., Zheng, L., Deng, H., Feng, D., Hu, S., Zhu, L., et al. (2022d). Electroacupuncture alleviates LPS-induced ARDS through  $\alpha 7$  nicotinic acetylcholine receptor-mediated inhibition of ferroptosis. *Front. Immunol.* 13, 832432. doi:10.3389/fimmu.2022.832432

Zhao, S., Wang, X., Zheng, X., Liang, X., Wang, Z., Zhang, J., et al. (2021b). Iron deficiency exacerbates cisplatin- or rhabdomyolysis-induced acute kidney injury through promoting iron-catalyzed oxidative damage. *Free Radic. Biol. Med.* 173, 81–96. doi:10.1016/j.freeradbiomed.2021.07.025

Zhao, X., Liu, Z., Gao, J., Li, H., Wang, X., Li, Y., et al. (2020a). Inhibition of ferroptosis attenuates busulfan-induced oligospermia in mice. *Toxicology* 440, 152489. doi:10.1016/j.tox.2020.152489

Zhao, Y., Li, Y., Zhang, R., Wang, F., Wang, T., and Jiao, Y. (2020b). The role of erastin in ferroptosis and its prospects in cancer therapy. *Onco. Targets. Ther.* 13, 5429–5441. doi:10.2147/OTT.S254995

Zheng, H., Shi, L., Tong, C., Liu, Y., and Hou, M. (2021). circSnx12 is involved in ferroptosis during heart failure by targeting miR-224-5p. *Front. Cardiovasc. Med.* 8, 656093. doi:10.3389/fcvm.2021.656093

Zhou, X., Zhuo, M., Zhang, Y., Shi, E., Ma, X., and Li, H. (2021). miR-190a-5p regulates cardiomyocytes response to ferroptosis via directly targeting GLS2. *Biochem. Biophys. Res. Commun.* 566, 9–15. doi:10.1016/j.bbrc.2021.05.100



## OPEN ACCESS

## EDITED BY

Yanqing Liu,  
Columbia University, United States

## REVIEWED BY

Xiaoling Chen,  
Purdue University, United States  
Huiwang Zhan,  
Johns Hopkins University, United States  
Qi Hu,  
University of Florida, United States

## \*CORRESPONDENCE

Jong-Kai Hsiao,  
jongkai@tzuchi.com.tw

## SPECIALTY SECTION

This article was submitted to Molecular Diagnostics and Therapeutics, a section of the journal Frontiers in Molecular Biosciences

RECEIVED 16 September 2022

ACCEPTED 14 November 2022

PUBLISHED 07 December 2022

## CITATION

Tseng H-C, Kuo C-Y, Liao W-T, Chou T-S and Hsiao J-K (2022), Indocyanine green as a near-infrared theranostic agent for ferroptosis and apoptosis-based, photothermal, and photodynamic cancer therapy. *Front. Mol. Biosci.* 9:1045885. doi: 10.3389/fmolb.2022.1045885

## COPYRIGHT

© 2022 Tseng, Kuo, Liao, Chou and Hsiao. This is an open-access article distributed under the terms of the [Creative Commons Attribution License \(CC BY\)](https://creativecommons.org/licenses/by/4.0/). The use, distribution or reproduction in other forums is permitted, provided the original author(s) and the copyright owner(s) are credited and that the original publication in this journal is cited, in accordance with accepted academic practice. No use, distribution or reproduction is permitted which does not comply with these terms.

# Indocyanine green as a near-infrared theranostic agent for ferroptosis and apoptosis-based, photothermal, and photodynamic cancer therapy

Hsiang-Ching Tseng<sup>1,2</sup>, Chan-Yen Kuo<sup>2</sup>, Wei-Ting Liao<sup>2</sup>, Te-Sen Chou<sup>1,2</sup> and Jong-Kai Hsiao<sup>1,3\*</sup>

<sup>1</sup>Department of Medical Imaging, Taipei Tzu Chi General Hospital, Buddhist Tzu-Chi Medical Foundation, New Taipei City, Taiwan, <sup>2</sup>Department of Research, Taipei Tzu Chi General Hospital, Buddhist Tzu-Chi Medical Foundation, New Taipei City, Taiwan, <sup>3</sup>School of Medicine, Tzu Chi University, Hualien, Taiwan

Ferroptosis is a recently discovered programmed cell death pathway initiated by reactive oxygen species (ROS). Cancer cells can escape ferroptosis, and strategies to promote cancer treatment are crucial. Indocyanine green (ICG) is a near-infrared (NIR) fluorescent molecule used in the imaging of residual tumor removal during surgery. Growing attention has been paid to the anticancer potential of ICG-NIR irradiation by inducing ROS production and theranostic effects. Organic anion transmembrane polypeptide (OATP) 1B3 is responsible for ICG metabolism. Additionally, the overexpression of OATP1B3 has been reported in several cancers. However, whether ICG combined with NIR exposure can cause ferroptosis remains unknown and the concept of treating OATP1B3-expressing cells with ICG-NIR irradiation has not been validated. We then used ICG as a theranostic molecule and an OATP1B3-transfected fibrosarcoma cell line, HT-1080 (HT-1080-OATP1B3), as a cell model. The HT-1080-OATP1B3 cell could promote the uptake of ICG into the cytoplasm. We observed that the HT-1080-OATP1B3 cells treated with ICG and exposed to 808-nm laser irradiation underwent apoptosis, as indicated by a reduction in mitochondrial membrane potential, and upregulation of cleaved Caspase-3 and Bax but downregulation of Bcl-2 expression. Moreover, lipid ROS production and consequent ferroptosis and

**Abbreviations:** BSA, bovine serum albumin; BCA, bicinchoninic acid; CCCP, carbonyl cyanide 3-chlorophenylhydrazone; DMEM, dulbecco's modified eagle's medium; DCFH-DA, 2',7'-dichlorofluorescein diacetate; DAPI, 4,6-diamidino-2-phenylindole; DFO, deferoxamine mesylate salt; FBS, fetal bovine serum; GPX4, glutathione peroxidase 4; ICG, indocyanine green; IHC, immunohistochemistry; IACUC, institutional animal care and use committee; MMP, mitochondrial membrane potential; MTT, 3-[4,5-dimethylthiazol-2-yl]-2,5-diphenyl tetrazolium bromide; NIR, near-infrared; OATP, organic anion transmembrane polypeptide; PDT, photodynamic therapy; PBS, phosphate-buffered saline; PBST, phosphate-buffered saline with Tween-20; PI, propidium iodide; ROS, reactive oxygen species; ROI, region of interest; SLC7A11, a subunit of the system xc-cystine/glutamate antiporter.

hyperthermic effect were noted after ICG and laser administration. Finally, *in vivo* study findings also revealed that ICG with 808-nm laser irradiation has a significant effect on cancer suppression. ICG is a theranostic molecule that exerts synchronous apoptosis, ferroptosis, and hyperthermia effects and thus can be used in cancer treatment. Our findings may facilitate the development of treatment modalities for chemo-resistant cancers.

#### KEYWORDS

indocyanine green, organic anion transmembrane polypeptide, near-infrared, theranostic effect, apoptosis, ferroptosis

## 1 Introduction

Indocyanine green (ICG), an infrared fluorescent dye, has been widely used in clinical settings to determine liver function before liver resection and to visualize the retinal vasculature for decades (Lu and Hsiao, 2021). Recently, ICG has been employed for the *in vivo* imaging of tumors because of its near-infrared (NIR) fluorescent capability that enables deep tissue penetration and cancer detection (Wu et al., 2018; Wu et al., 2019a; Wu et al., 2019b). Moreover, studies have reported the feasibility of using ICG, in combination with NIR phototherapy that produces reactive oxygen species (ROS) with sequential apoptosis, for the detection of hepato-cellular carcinoma (Radzi et al., 2012; Shirata et al., 2017). A study indicated that ICG potentiates the photothermal effect (Porcu et al., 2016). Due to its safety, antitumor properties, and deep tissue penetration ability, ICG has the potential to be used as an anticancer molecule.

Our previous study reported ICG is metabolized by organic anion transporting polypeptide 1B3 (OATP1B3) (Wu et al., 2018). OATP1B3 regulates anion transportation into the cytoplasm and is physiologically expressed in the liver (Shitara, 2011). Furthermore, OATP1B3 is highly expressed in various cancer cells (Imai et al., 2013). However, the prognostic role of OATP1B3 in cancer remains unclear. Therefore, targeting OATP1B3-expressing cancer cells by ICG, observing these tumor cells through imaging modalities, and killing them can be a beneficial cancer treatment strategy.

Fibrosarcoma is an uncommon malignancy that has a poor response toward chemotherapy (Donato Di Paola and Nielsen, 2002). Apart from complete resection, the eradication of residual fibrosarcoma by chemotherapy alone is difficult. Only 4%–11% of patients with advanced fibrosarcoma benefitted from chemotherapy (Augsburger et al., 2017). Hence, a new strategy for treating fibrosarcoma is required. HT-1080 cells originated from patients with fibrosarcoma have been examined extensively (Rasheed et al., 1974; Daigeler et al., 2008; Hsiao et al., 2013; Wu et al., 2018). Although OATP1B3 has a restricted expression toward liver, we previously transfected HT-1080 cells with OATP1B3, which successfully transported ICG into the cytoplasm (Wu et al., 2018). In this study, we evaluated the photothermal and photodynamic effects of ICG and their benefits for treating chemo-resistant cancer by using HT-1080 cells overexpressing OATP1B3.

Ferroptosis is an iron-dependent, programmed cell death mechanism that occurs after exposure to excess reactive oxygen species (Dixon et al., 2012; Liang et al., 2019; Su et al., 2020). Ferroptosis is entirely different from apoptosis, necrosis, and autophagy (Ye et al., 2020). Cancer cells resistant to apoptosis after chemotherapy might be vulnerable to ferroptosis (Xu et al., 2019). Strategies inducing ferroptosis in cancer cells have been evaluated. Studies have reported the efficacy of some anti-cancer drugs, such as sorafenib and erastin, in promoting ferroptosis in both the cancer cell culture and tumor xenograft (Dixon et al., 2012; Lachaier et al., 2014). ICG, in combination with infrared irradiation, was reported to be effective in generating reactive oxygen species in cell culture (Wang et al., 2019a). Nevertheless, the feasibility of using ICG and infrared irradiation to induce ferroptosis for treating cancer has not been examined. This study examined the feasibility of using ICG and infrared irradiation to treat fibrosarcoma cells and elucidated underlying cell death pathways. The findings of this study can facilitate the development of novel cancer therapies.

## 2 Materials and methods

### 2.1 Cell line and culture

HT-1080 cells were cultured in Dulbecco's modified Eagle's medium (DMEM) (Thermo Fisher Scientific, Waltham, MA, United States) supplemented with 10% fetal bovine serum (FBS) (Biologic Industries, Cromwell, CT, United States), 100 U/mL of penicillin, and 100 µg/ml of streptomycin (Invitrogen, Carlsbad, CA, United State). A stable cell line, OATP1B3-expressing HT-1080 cells were constructed through lentivirus transduction as described previously (Wu et al., 2018). All the cells were maintained in a humidified atmosphere of 5% CO<sub>2</sub> at 37°C and passaged with 0.5% trypsin (Thermo Fisher Scientific) for 1.5 min at 80%–90% confluence.

### 2.2 Cellular uptake of ICG

Crystalline ICG (molecular weight of ICG sodium iodide, 924.9 g/mol) was purchased from Sigma Aldrich (St. Louis, MO,



United States). A 2 mM ICG stock solution in water was prepared and separated into several aliquots and stored at  $-20^{\circ}\text{C}$ . The ICG signal detection was performed using both a microplate reader and fluorescence microscope. To evaluate the transportability of ICG by using SpectraMax M5 system (Molecular Devices, Sunnyvale, CA, United States),  $2.5 \times 10^4$  cells were seeded in 96-well plates for 1 day before the addition of 20 and 200  $\mu\text{g/ml}$  ICG for 2 h. Excess ICG was removed by washing the cells three times with phosphate-buffered saline (PBS). The intensity signal was measured at the excitation and emission wavelengths of 780 and 830 nm, respectively, under shaking for 2 s and normalized to that of the control group. In addition, we visualized the ICG signal by using a fluorescence microscope (Leica Microsystems DMI6000 B, Wetzlar, Germany). A 49030-ET-ICG filter cube (Chroma Technology, Olching, Germany) was chosen to detect the intensity of ICG. In total,  $5 \times 10^5$  cells were seeded in six-well plates for 1 day before 50  $\mu\text{g/ml}$  ICG was added for distinct time points. Then, the cells were washed three times with PBS after ICG incubation and fixed with 4% formaldehyde. Finally, the slides were mounted in SlowFade Gold Antifade Reagent with 4,6-diamidino-2-phenylindole (DAPI) (Thermo Fisher Scientific).

## 2.3 *In vitro* PDT

The OATP1B3-expressing cells were seeded in 96-multiwell microplates at  $2.5 \times 10^4$  cells/100  $\mu\text{l}$  medium/well. The cells were divided into four groups: control (without ICG treatment and laser irradiation), ICG only (without laser irradiation), laser only (without ICG treatment), and PDT (with both ICG treatment and laser irradiation). The supernatant of the cells treated with ICG for 4 h was removed, and the cells were carefully washed with PBS to eliminate any remaining dye. Finally, each well was covered with a drug-free medium. Homogeneous irradiation was successively performed using laser diodes emitting light at 808 nm with a maximum optical output power of 15 W. The effects of laser irradiation with different fluence rates and times were examined. The irradiation conditions were as follows: One of the fluence rates was adjusted to 0.098  $\text{W/cm}^2$ , and the energy density was 54  $\text{J/cm}^2$ . The other fluence rate was adjusted to 0.2  $\text{W/cm}^2$ , and the energy density was 60  $\text{J/cm}^2$ . The laser diodes were set 1 cm below the microplate. In addition, a second NIR irradiation was conducted 24 h after the first irradiation, and each well was replaced with fresh medium and incubated for 0, 24, 48, and 72 h.

## 2.4 Reactive oxygen species detection

To evaluate ROS synthesis, DCFH-DA was employed to examine intracellular ROS generation. Briefly, the cells exposed to ICG and NIR irradiation were incubated with

10  $\mu\text{M}$  DCFH-DA in 200  $\mu\text{l}$  DMEM for 30 min at  $37^{\circ}\text{C}$ . Subsequently, the cells were washed three times with PBS. For the positive group, the cells were treated with 10  $\mu\text{M}$   $\text{H}_2\text{O}_2$  for 2 h before DCFH-DA treatment. All data were acquired either using a fluorescence reader or a fluorescent cell imager (ZOE, Bio-Rad, Hercules, CA, United States). To investigate the lipid ROS levels of these cells, the cells were incubated with 2  $\mu\text{M}$  C11-BODIPY 581/591 (Thermo Fisher Scientific, Waltham, MA, United States) in a culture medium for 1 h and then washed with PBS. After trypsinization, the cells were harvested and processed for flow cytometry (BD Bioscience, San Jose, CA, United States) at an excitation wavelength of 488 nm combined with an emission wavelength of 517–527 nm.

## 2.5 Mitochondrial membrane potential measurement

The apoptosis signaling pathway is triggered when cells are under a toxic or an unfavorable environment. MMP decreases during apoptosis. Therefore, MMP can serve as an early indicator of cell apoptosis. The method used for MMP measurement was based on a previous study (Smiley et al., 1991). The cells were washed with PBS after treatment with ICG and NIR laser irradiation. The cells were then incubated with the JC-1 dye (Thermo Fisher Scientific) at  $37^{\circ}\text{C}$  for 30 min in a cell culture incubator. Finally, the fluorescence intensity was analyzed using a fluorescence microscope and a fluorescence spectrometer. The cells treated with 50  $\mu\text{M}$  carbonyl cyanide 3-chlorophenylhydrazone (CCCP) were used as positive controls because CCCP is a common MMP disruptor.

## 2.6 Annexin V and propidium iodide staining

After distinct treatment (group1: control; group2: ICG only; group3: laser only; group4: PDT), cells were harvested and washed twice in cold PBS, and resuspended in annexin V-FITC and PI (Elabscience Biotechnology Inc., Houston, TX, USA) for 30 min in the dark. Cells were then measured with a flow cytometer (BD Bioscience, San Jose, CA, United States) equipped with an air-cooled argon laser that emitted at 488 nm. Data from at least  $10^4$  cells were analyzed with FlowJo software.

## 2.7 Thermal observation and imaging analysis

In brief, 200  $\mu\text{l}$  of sample solutions containing different ICG concentrations were added into 96-well plates and exposed to an 808-nm laser for different time courses. After ICG-NIR treatment, thermal images were captured using an IR

FlexCam Thermal Imager *TI55* (FLUKE, Everett, WA, United States). The HT-1080-OATP1B3 cells treated with ICG but not exposed to 808-nm laser were used as a negative control. All images were analyzed using the open-source image processing software (Fluke Connect) downloaded from the website (<https://www.fluke.com/en-us/products/fluke-software/connect>). The temperature values for quantification were circled within the edge of the thermal signal.

## 2.8 Cell viability assay

Viability was examined using the MTT assay. MTT is reduced to purple formazan in living cells by mitochondrial reductase. The morphology of the cells in the control, ICG, NIR laser, and PDT groups was examined using a phase-contrast microscope (Eclipse TS100; Nikon, Tokyo, Japan). Then, the MTT reagent was added to each well with the medium at a final concentration of 0.5 mg/ml. After incubation at 37°C for 4 h under a 5% CO<sub>2</sub> atmosphere, the medium was aspirated from 96-well plates carefully and substituted with an equal volume of solubilizer buffer (DMSO) to dissolve the formazan crystals. The absorbance of the formazan product was evaluated at a wavelength of 570 nm by using a fluorescence plate reader. The results are indicated as the percentage of data obtained with control cultures.

## 2.9 Western blotting

A total of  $1 \times 10^6$  cells were harvested from six-well plates and lysed using the following steps. The cells were collected, washed with PBS, and lysed using RIPA lysis buffer (Pierce, Rockford, IL, United States) containing 1% Sigma protease cocktail for 30 min at 4°C. The lysates were centrifuged at  $12,000 \times g$  at 4°C to obtain solubilized cellular proteins. The protein concentration was measured using a bicinchoninic acid (BCA) protein assay (Pierce, Rockford, IL, United States). Each lane of 12% SDS-PAGE was loaded with 30 µg of the total protein extract, and the proteins were electrotransferred onto nitrocellulose membranes (Sartorius, Göttingen, Germany). The membranes were blocked with 5% nonfat milk and 1% bovine serum albumin (BSA, Biologic Industries, Cromwell, CT, United States) in tris-buffered saline with Tween 20. Subsequently, the blots were probed with specific primary antibodies against PARP-1 (1:200, Santa Cruz Biotechnology, Dallas, TX, United States), Caspase-3 (1:1000, Cell Signaling, Danvers, MA, United States), Bim (1:1000, Cell Signaling, Danvers, MA, USA), Bcl-2 (1:1000, Cell Signaling, Danvers, MA, United States), Bax (1:1000, Cell Signaling, Danvers, MA, USA), GPX4 (1:1000, Cell Signaling, Danvers, MA, United States), SLC7A11 (1:1000, ABclonal, Woburn, MA, United States), and  $\beta$ -actin (1:4000, Cell signaling separately

at 4°C overnight, followed by incubation with HRP-conjugated goat anti-rabbit IgG (1:5000, Zymed, San Francisco, CA, United States) for 1 h at room temperature. The same membrane was reprobed with  $\beta$ -actin as a loading control. Protein bands were detected through enhanced chemiluminescence (Millipore-Sigma, Billerica, MA, United States) by using the BioSpectrum 810 Imaging System (UVP, CA, United States).

## 2.10 Tumor xenografts

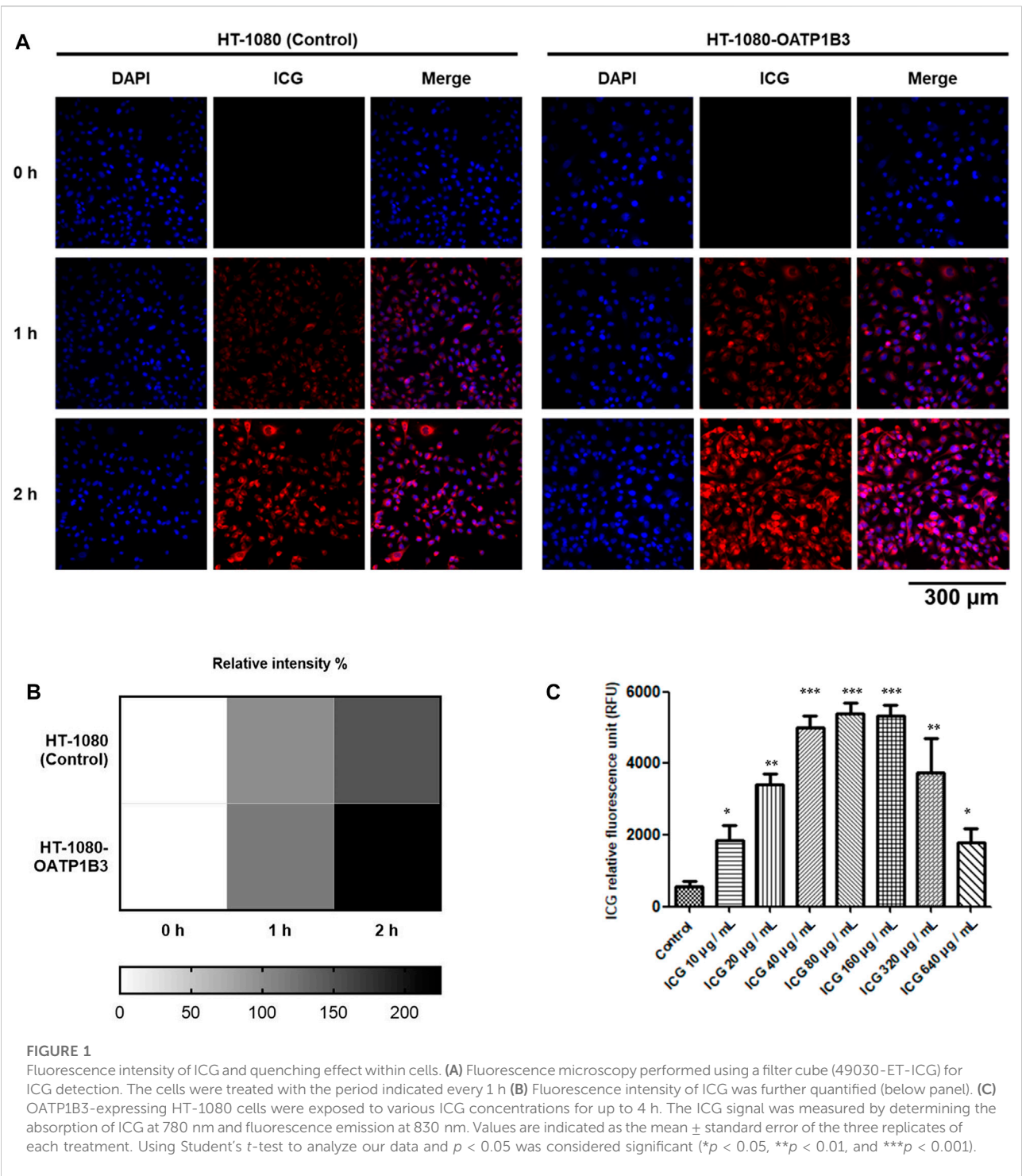
Female BALB/cAnN.Cg-FoxnlNu/CrlNarl nude mice (aged 6–8 weeks) were purchased from the National Laboratory Animal Center (Taiwan). A total of  $1 \times 10^6$  OATP1B3-expressing HT-1080 cells in 100 µl of DMEM were injected subcutaneously in the bilateral flank. The xenografts were inspected twice a week during the 2 weeks following cell implantation. If a subcutaneous nodule could be visualized, the xenograft size was recorded, and *in vivo* PDT experiments were initiated.

## 2.11 *In vivo* imaging and PDT

After the nude mice were subcutaneously administered the tumor cells for 2 weeks, they were anesthetized with isoflurane and intraperitoneally injected with 10 mg/kg of ICG (solvent: ddH<sub>2</sub>O). Following the administration of ICG, the trend of the ICG signal in the mice was traced through *in vivo* fluorescence imaging at 1, 4, 7, 24, and 28 h post-injection by using the IVIS50 imaging system (Xenogen, Perkin Elmer, MA, United States). The transplanted tumor was illuminated at an excitation wavelength of 780 nm, and fluorescence was obtained using an 845-nm filter. The model mice were prepared as aforementioned for *in vivo* PDT (as shown in [Supplementary Figure S2B](#)). Irradiation with a near-infrared laser source (High Power LED driver, THORLABS, Münchener, Germany) was performed 24 h post-injection, and the laser source was placed 1 cm above the xenograft tumor. The fluence rate was 1 W/cm<sup>2</sup>, and the irradiation time was 10 min. Subsequently, the tumor volume was measured every 2 days until day 8. The tumor sizes were calculated using the following formula: [(longest length)  $\times$  (shortest)<sup>2</sup>]/2 with a digital caliper.

## 2.12 Immunohistochemistry

Tumor tissues were fixed with 10% formalin and were prepared as paraffin-embedded sections (5-µm thick). Slide sections were deparaffinized in xylene (Allegiance Healthcare Corporation, McGaw Park, IL, United States) and then hydrated by passing through graded alcohol to water.



Endogenous peroxidase was blocked using 0.3% hydrogen peroxide for 10 min. After a short wash with phosphate-buffered saline with Tween-20 (PBST), the tissue samples were blocked with 5% BSA at room temperature for 1 h. The samples were then incubated with rabbit polyclonal 4 Hydroxynonenal (4-HNE) antibody (dilution 1:200 in 1%

BSA; Thermo Fisher Scientific) at 4°C overnight. Furthermore, after a short wash in PBST, the slides were incubated using the EnVision kit (Agilent Technologies Inc., Santa Clara, CA) and were counterstained with hematoxylin. All cover slides were visualized using the ECLIPSE TE2000-U microscope (Nikon, NY, United States).

## 2.13 Statistics

Each experiment was performed at least in three biological replicates. Data are presented as means  $\pm$  standard errors (SEM). In addition, statistical analysis was performed using Student's *t* test, Duncan's new multiple range tests, and Newman–Keuls and Dunnett's multiple comparison tests to determine differences (\**p* < 0.05; \*\**p* < 0.01; \*\*\**p* < 0.001) *via* GraphPad Prism.

## 3 Results

### 3.1 *In vitro* ICG uptake and quenching effect

Although previous studies have reported that OATP1B3 can uptake ICG (Wu et al., 2018), the quenching effect of ICG within cells has not been addressed in detail. Therefore, we investigated the quenching property of ICG and examined its transportability in OATP1B3-expressing HT-1080 cells. After treating control and OATP1B3-expressing HT-1080 cells with 50  $\mu$ g/ml of ICG for 0, 1, and 2 h, respectively, the OATP1B3-expressing HT-1080 cells were observed to have a stronger ICG signal than did the control cells, as indicated by fluorescence microscopy findings (Figures 1A). Furthermore, the ICG intensity enhanced with an increase in ICG treatment time. Supplementary Figure S1 presents the flow cytometry results of the uptake of ICG by OATP1B3-expressing HT-1080 cells. To examine the quenching property of ICG within the HT-1080 cells, we treated them with a series of concentrations of ICG and then monitored their relative fluorescence unit by using a spectrometer. The data indicated that the fluorescent signal significantly decreased when the ICG concentration was >160  $\mu$ g/ml (Figure 1C), which may lead to some responses because the energy emission of ICG interfered at such conditions.

### 3.2 Detection of reactive oxygen species production

To evaluate responses after ICG–NIR administration, we conducted a cytochemical analysis by using 2',7'-dichlorofluorescein diacetate (DCFH-DA) to examine ROS production. As presented in Figure 2, higher ROS production was observed in the cells treated with ICG–NIR than in the cells treated with ICG alone. Moreover, the cells treated with 200  $\mu$ g/ml of ICG exhibited markedly enhanced fluorescence intensity under low-fluence or high-fluence laser irradiation. Compared to the 200  $\mu$ g/mL ICG treated group, the ROS production of the 20  $\mu$ g/mL ICG treated group is less significant. Additionally, the findings of quantitative analysis indicated that treatment with 200  $\mu$ g/ml of ICG–NIR considerably increased ROS production,

implying that the quenching effect of ICG might be a significant factor contributing to effective photodynamic therapy (PDT). For semi-quantitative determination of the NIR laser effect toward ICG treated cells and for future clinical translation, we did low and high fluence laser irradiation to the ICG treated cells. We found a dose-responsive ROS production effect between the low and high fluence NIR Laser treated group.

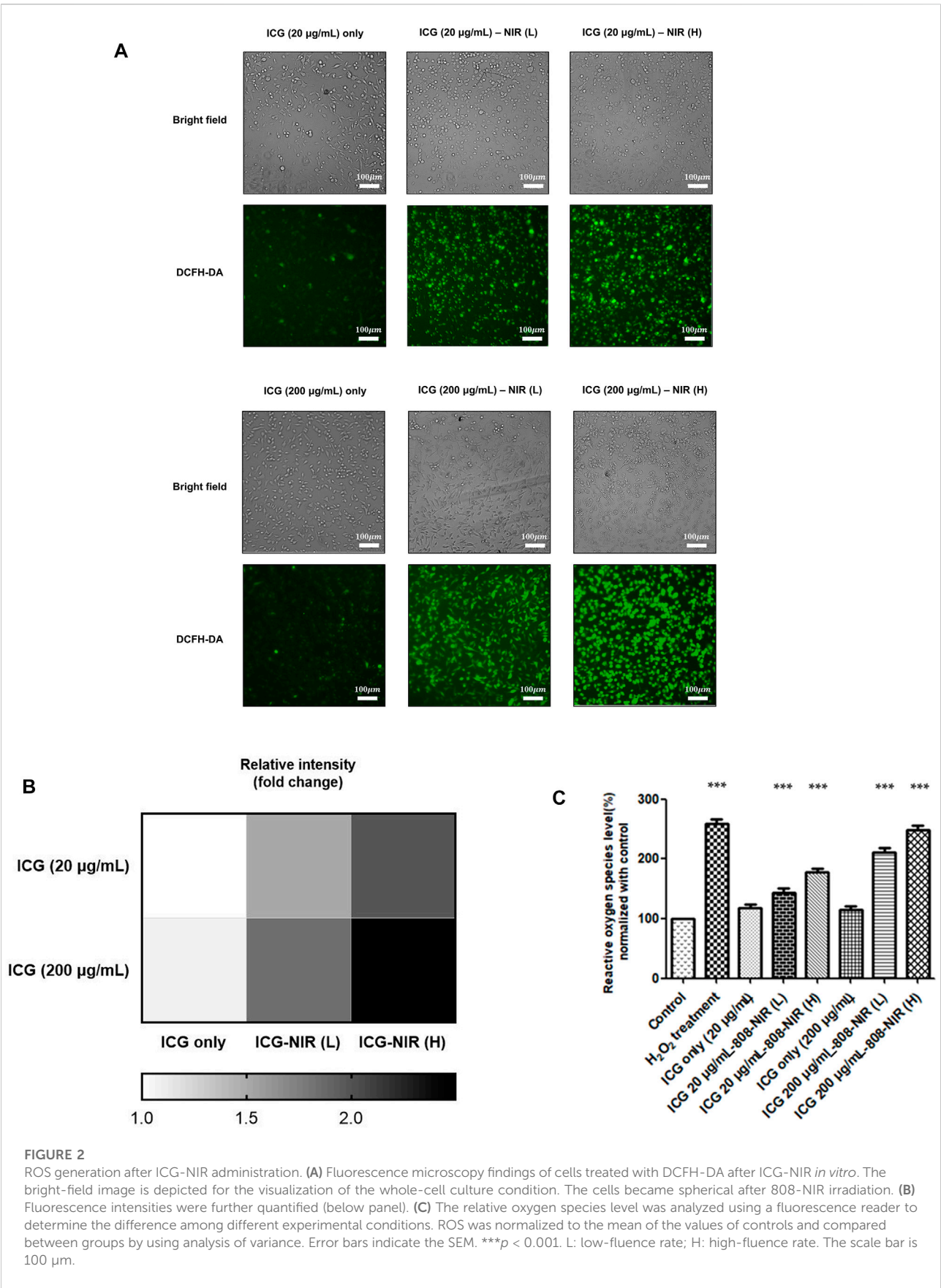
### 3.3 ICG-near-infrared exposure reduced mitochondrial membrane potential and induced apoptosis

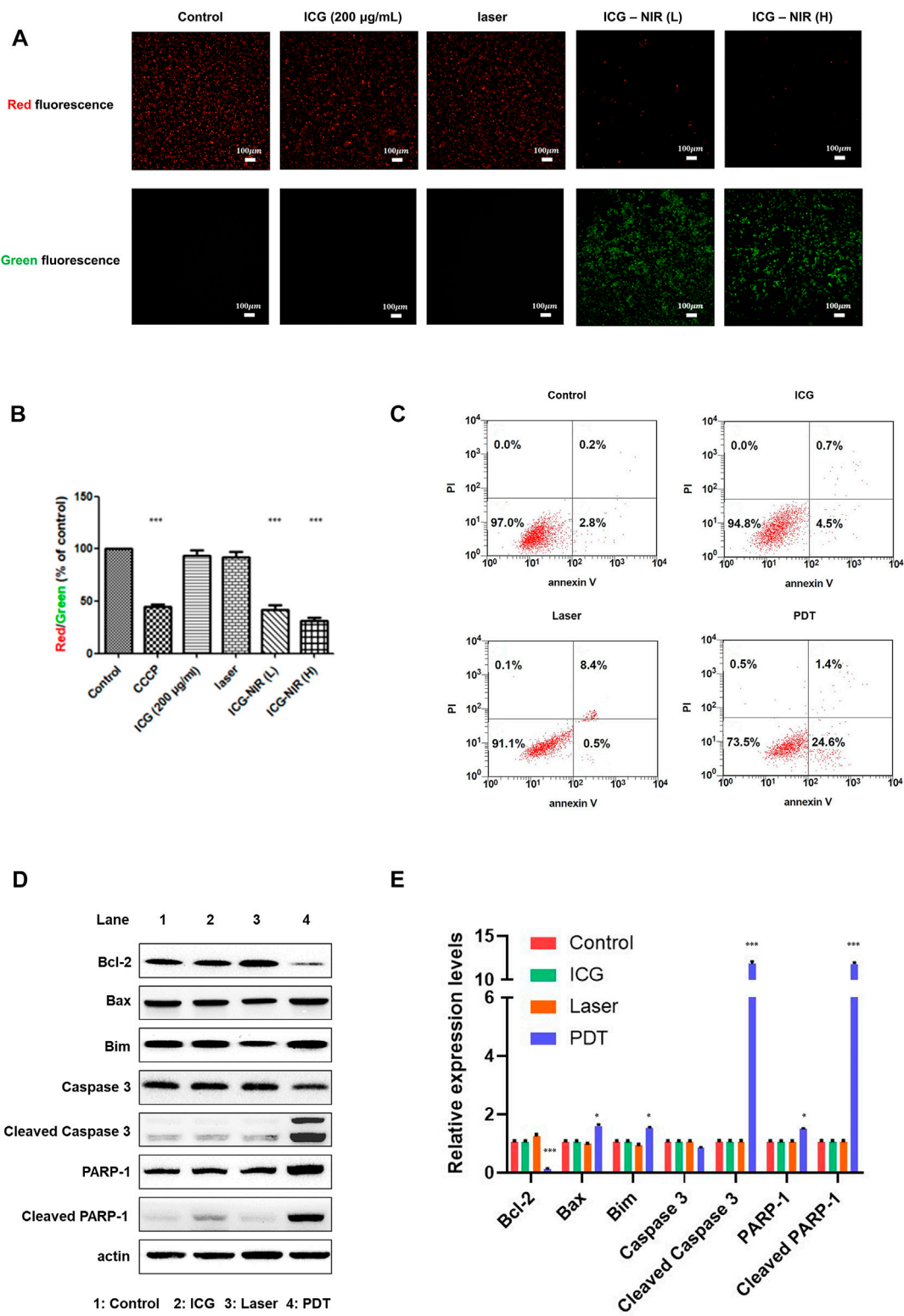
Several studies have reported that ROS causes oxidative damage in the mitochondria and affects their function (Guo et al., 2013; Murphy, 2013; Ježek et al., 2018). Thus, we looked into mitochondrial membrane potential (MMP) by treating the cells with the JC-1 dye to determine changes. The results revealed that ICG–NIR exposure promoted mitochondrial depolarization in the OATP1B3-expressing HT-1080 cells. Furthermore, ICG–NIR exerted a significantly stronger effect on mitochondrial depolarization than did control (Figure 3B). A decreased red (–590 nm) to green (–529 nm) fluorescence intensity ratio in response to ICG–NIR exposure for mitochondrial depolarization was noted in fluorescence images (Figure 3A). In addition, fluorescence images indicated that ICG–NIR irradiation induced higher ROS production within the OATP1B3-expressing HT-1080 cells and resulted in ROS accumulation in response to mitochondrial dysfunction. These results implied that the loss of MMP is a signal of stress and may release apoptotic factors, leading to cell death. To further understand ICG–NIR exposure impaired MMP and triggered apoptosis in OATP1B3-expressing HT-1080 cells, we examined cell apoptosis by using the annexin V assay. The number of apoptotic cells increased dramatically after ICG–NIR administration (Figure 3C). Moreover, the expression levels of cell apoptosis-related genes were also studied through Western blotting. The results showed an increase in cleaved PARP-1, cleaved Caspase-3, Bax and Bim but a decrease in Bcl-2 was observed under ICG–NIR irradiation (Figures 3D,E). In summary, our results implied that PDT treatment following of ROS accumulation attenuated MMP and induced cell death *via* apoptosis.

### 3.4 Photothermal assessment

The photothermal heating capacity of ICG was evaluated in an aqueous dispersion. The temperature variation was recorded under continuous laser irradiation (1 W/cm<sup>2</sup>) for 2, 4, 8, and 16 min, respectively, after treatment with the ICG concentrations of 25, 50, 100, and 200  $\mu$ g/mL. As depicted in Figure 4, the temperature was higher under the laser condition than under the



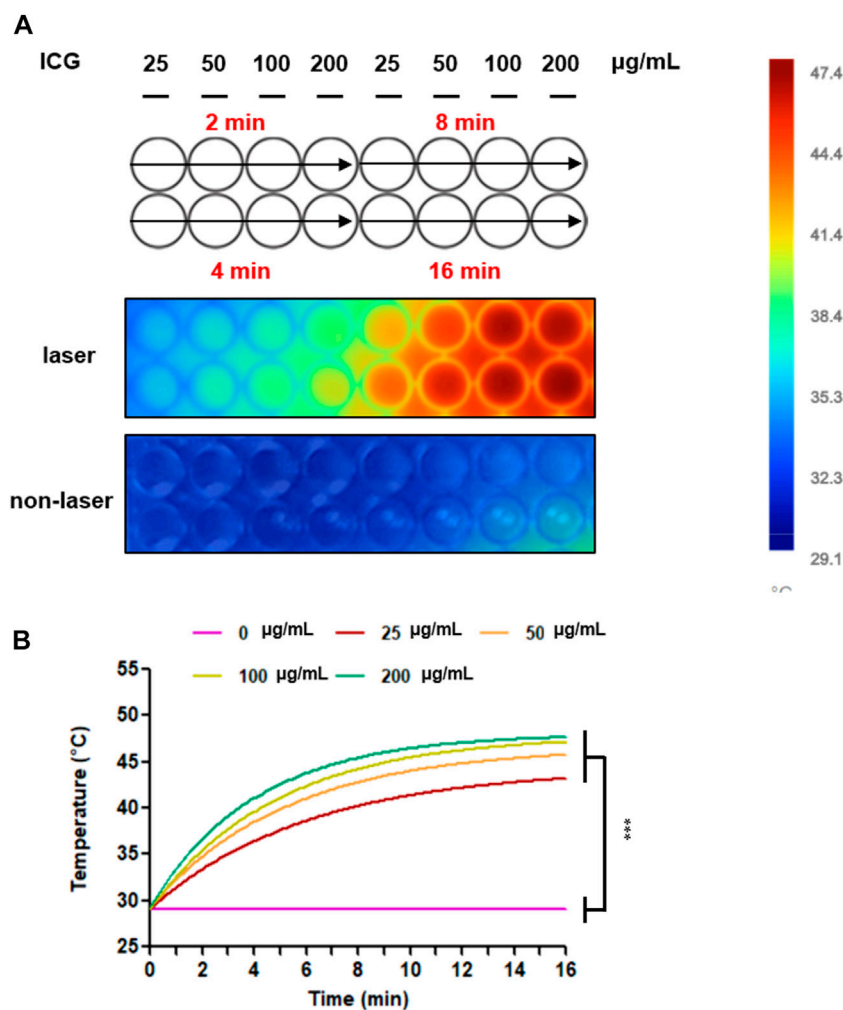




**FIGURE 3** MMP measurement and cell apoptosis analysis post-ICG-NIR administration. (A) Fluorescence images of red and green were examined to determine whether mitochondria were healthy after the addition of the JC-1 dye *in vitro*. (B) We used a fluorescence reader and calculated the red (~590 nm)/green (~529 nm) fluorescence intensity ratio. Significant MMP changes between with and without ICG-NIR administration were observed. MMP was normalized to the mean of the values of controls and compared between groups by using analysis of variance. (C) Cell (Continued)

**FIGURE 3 (Continued)**

apoptosis was detected through the annexin V assay. The *x*-axis was the annexin V signal which represented the expression of phosphatidylserine on the membrane when cells underwent apoptosis. The *y*-axis was the PI signal which represented the loss of membrane integrity of cells undergoing necrosis. The lower left, upper left, lower right, and upper right portions respectively indicate viable, necrotic, apoptotic, and secondary necrotic cells. **(D)** Apoptosis-associated proteins were analyzed in OATP1B3-expressing HT-1080 cells with different treatment. **(E)** Western blotting assays were done in triplicate, then all data were further quantified. Error bars indicate the SEM. \**p* < 0.05, \*\**p* < 0.01, and \*\*\**p* < 0.001. The scale bar is 100  $\mu$ m.

**FIGURE 4**

Temperature increases after treatment with ICG and 808-nm laser irradiation. **(A)** Changes in the thermal images of colors were examined *in vitro* by using an infrared thermal imaging camera. The bar displayed the temperature scale to distinguish the temperature variation. **(B)** The thermal heating curves were analyzed and quantified using Fluke Connect. Temperature increases between the laser and non-laser conditions. The data are presented as the mean  $\pm$  SEM; *n* = 3 per group (\*\*\**p* < 0.001).

non-laser condition. Furthermore, at the same laser power density, the temperature of the OATP1B3-expressing HT-1080 cells treated with 200  $\mu$ g/ml ICG increased from 29.1 to 47.4°C;

this finding is consistent with that of software analysis and quantification. Similar increases in temperature were noted in the remaining treatment groups (25, 50, and 100  $\mu$ g/ml),



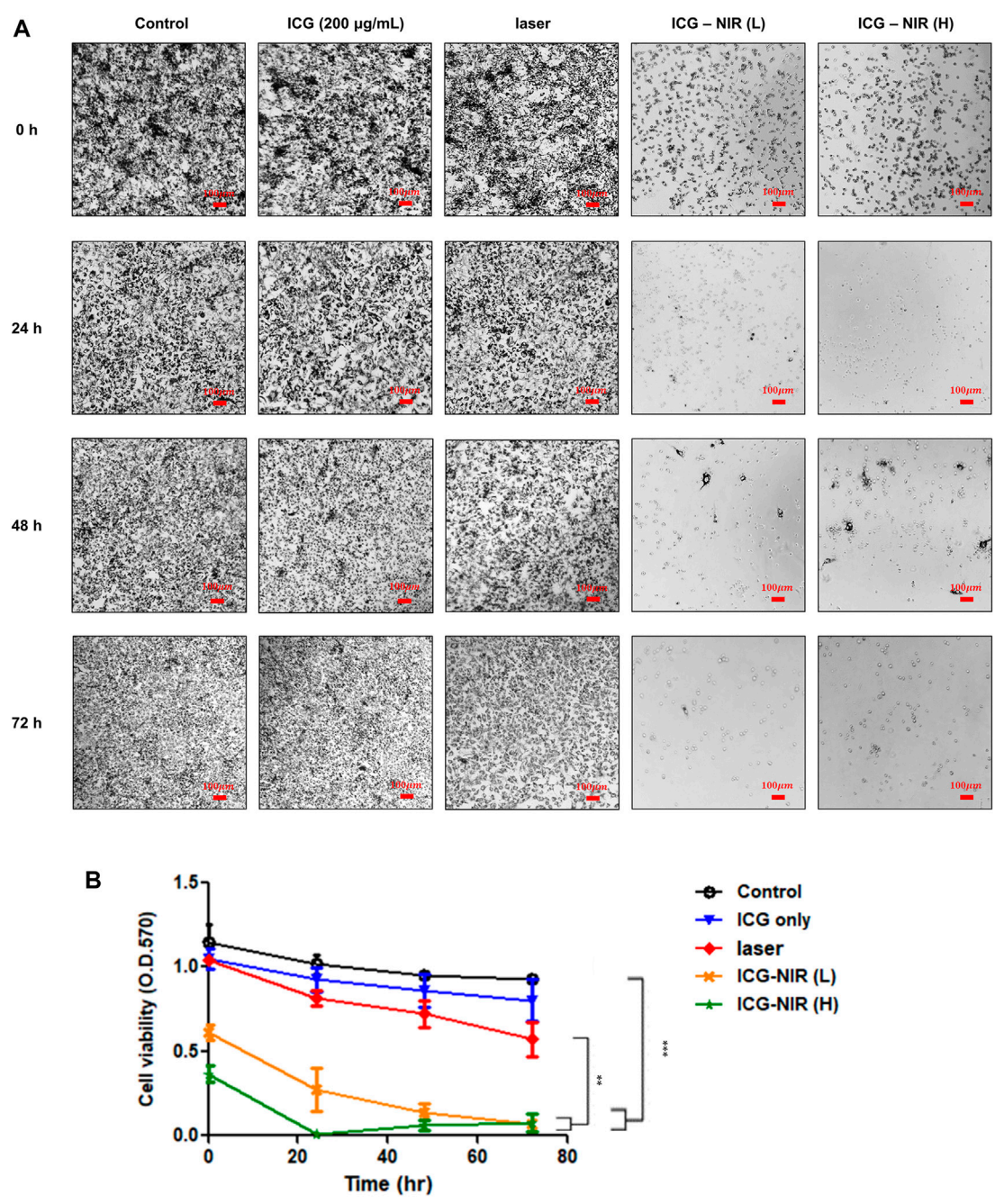


**FIGURE 5** MTT metabolism of OATP1B3-expressing HT-1080 cells after ICG treatment and irradiation *in vitro*. **(A)** Cell viability was examined using the MTT assay. Morphological changes and formazan crystal formation in the OATP1B3-expressing HT-1080 cells were observed under a light microscope. Control, untreated cells; ICG, cells treated with ICG (200  $\mu\text{g/mL}$ ); Laser only, cells exposed to 808-nm NIR; ICG-NIR, cells treated with both ICG and 808-nm light exposure; L, cells exposed to low-fluence laser irradiation; H, cells exposed with high-fluence laser irradiation. **(B)** A significant difference was observed in cell viability between the ICG-NIR and control groups. Data represent the findings of three separate experiments, and values are presented as the mean  $\pm$  standard error. \*\*\* $p < 0.001$ . The scale bar is 100  $\mu\text{m}$ .



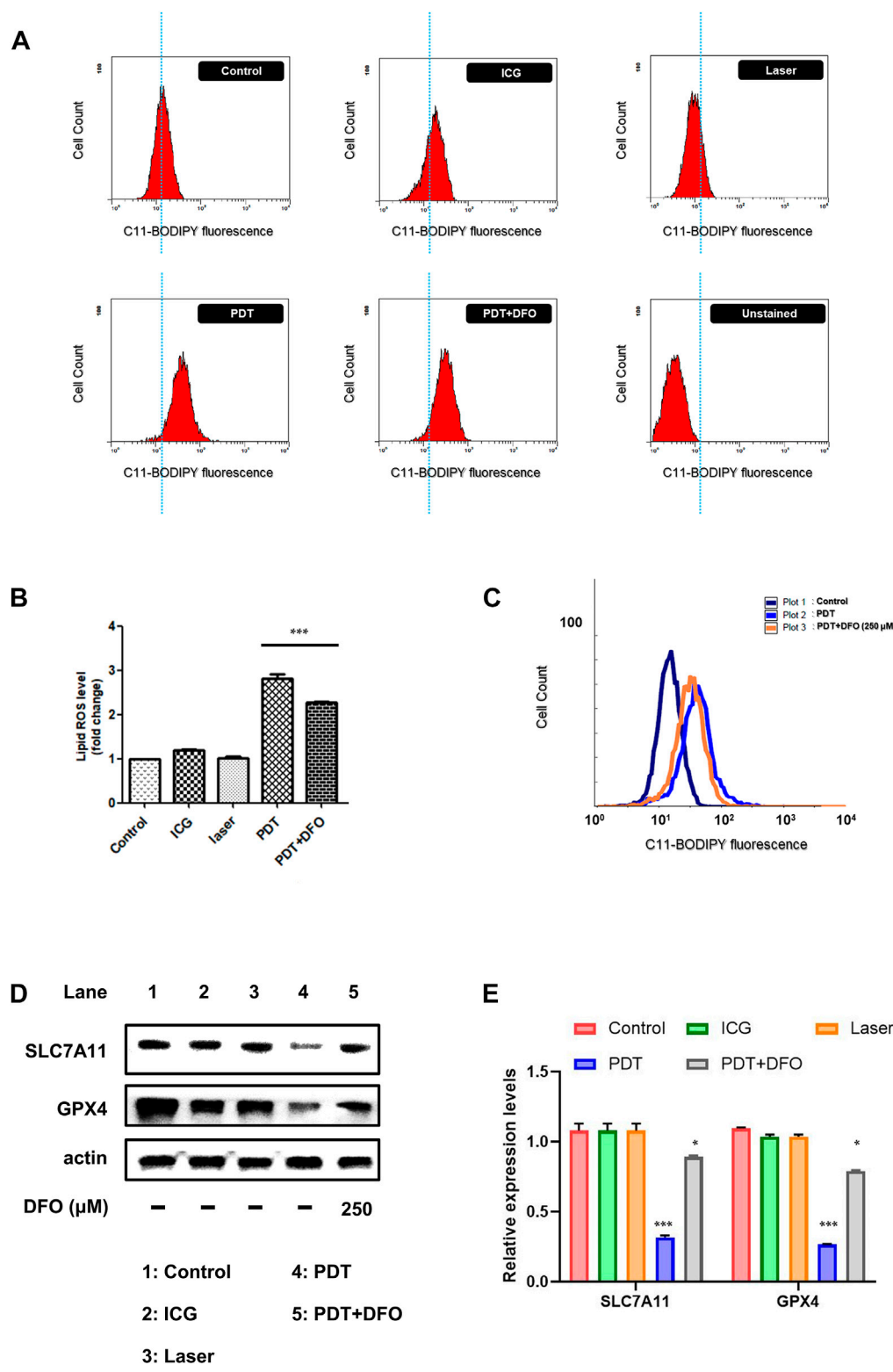


**FIGURE 6** ICG-NIR irradiation induced cell death through the ferroptosis pathway. **(A)** Changes in the cellular lipid ROS levels of control (with C11-BODIPY staining), ICG (cells treated with 200 μg/ml ICG only), laser (cells treated with 808-nm laser only), PDT (cells incubated with ICG and then exposed to 808-nm laser), PDT + DFO (cells treated with PDT and 250 μM DFO), and unstained (cells without C11-BODIPY staining) groups. **(B)** Bar graph showing the mean fluorescence intensity of lipid ROS generation. **(C)** Representative flow cytometry histogram with an overlay of the three groups indicating that DFO alleviated ICG-NIR-induced ferroptosis. **(D)** Changes in the protein expression of SLC7A11 and GPX4. β-Actin was used as an internal control. **(E)** Western blotting assays were further quantified. Error bars represent the SEM from three independent replicates ( $n = 3$ ). \*\*\* $p < 0.001$ .

indicating that the OATP1B3-expressing HT-1080 cells treated with ICG exhibited a favorable hyperthermic effect upon 808-nm laser irradiation.

### 3.5 Evaluation of cell viability after ICG and near-infrared laser irradiation

To determine whether ICG-NIR treatment reduces the cell population and causes cell death, we performed the 3-[4,5-dimethylthiazol 2-yl]-2,5-diphenyl tetrazolium bromide (MTT) assay. Purple formazan crystals were formed only in live treated cells because of the presence of mitochondrial reductases. As presented in [Figure 5A](#), the formation of formazan crystals in the ICG-NIR group was fewer than that in the control group, as observed under a light microscope. Moreover, we examined the absorbance of this colored solution at 570 nm ([Figure 5B](#)). The results revealed that fewer viable cells were present in the ICG-NIR group, indicating that the suppression of cell survival following ICG-NIR treatment was effective.

### 3.6 Ferroptosis occurred upon ICG-near-infrared irradiation

*In vitro* photodynamic therapy (PDT) caused the death of the OATP1B3-expressing HT-1080 cells; this finding is consistent with that of the cell viability assay ([Figure 5](#)). To elucidate whether other mechanisms through which ICG-NIR irradiation affects cell survival, we reviewed previous studies ([Wang et al., 2019b](#); [Chen et al., 2022](#)). The OATP1B3-expressing cells treated with ICG-NIR may have a higher tendency to undergo ferroptosis owing to the overall higher active metabolism and higher ROS load. We first measured the lipid ROS level to verify our hypothesis because studies have demonstrated that ferroptosis results from lipid peroxidation ([Zuo et al., 2020](#); [Jiang et al., 2021](#)). The results of flow cytometry ([Figure 6A](#)) indicated that the lipid ROS level was higher in the PDT group than in either the control, ICG, or laser group. We then performed Western blotting to examine the protein expression of SLC7A11 and GPX4 because both of these proteins were reported to serve as biomarkers for ferroptosis ([Jiang et al., 2021](#)). When SLC7A11 and GPX4 are dysfunctional, lipid transforms into lipid ROS with O<sub>2</sub> and Fe<sup>2+</sup>, resulting in lipid ROS attacking intracellular biomolecules and finally killing cells. Our results indicated that the expression of SLC7A11 and GPX4 was downregulated ([Figure 6D](#), lane 1 vs. lane 4 and [Figure 6E](#)) in the PDT group compared with the ICG and laser groups. In addition, we examined if ICG-NIR irradiation leads to ferroptosis by using deferoxamine mesylate salt (DFO, an iron chelator), a ferroptosis inhibitor, in this study. DFO could directly regulate iron metabolism to inhibit ferroptosis. As presented in [Figures 6B,C](#), the lipid ROS level was attenuated

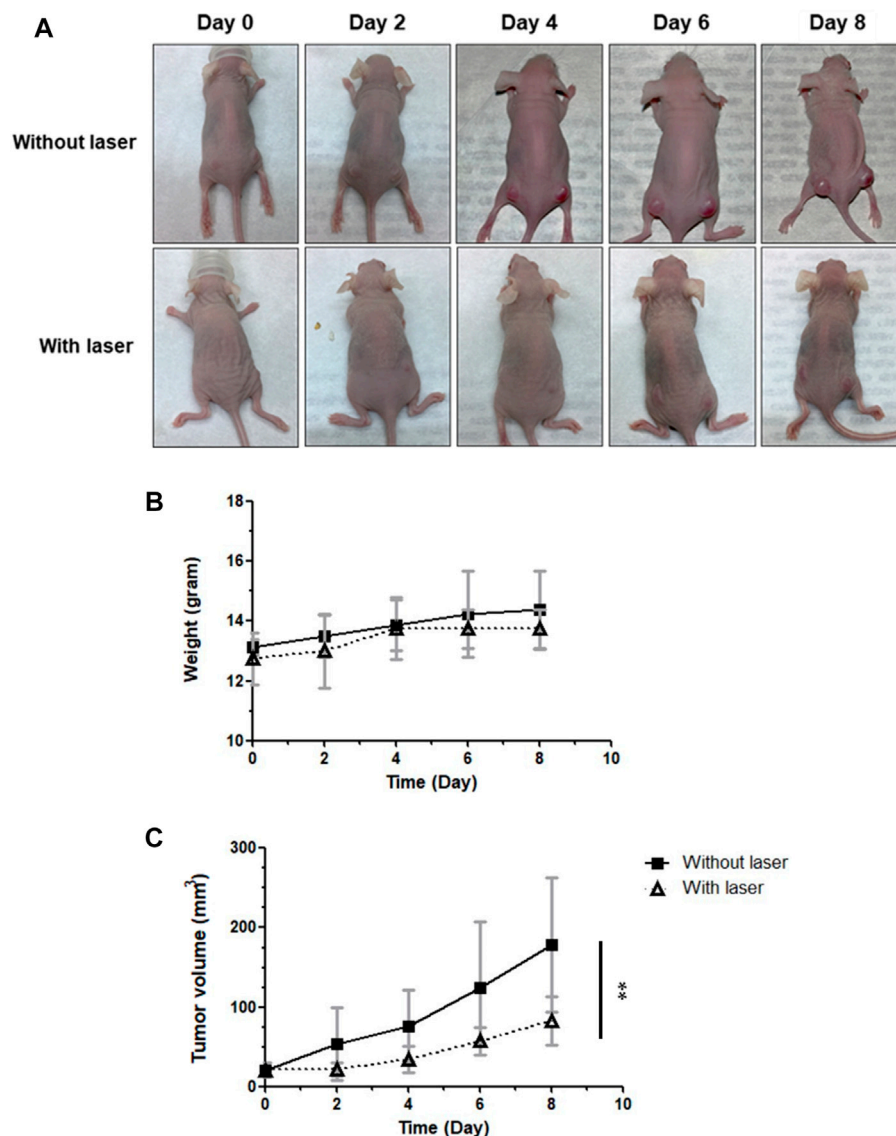
in the presence of DFO. Furthermore, DFO reversed the downregulation of GPX4 and SLC7A11 induced by ICG-NIR ([Figure 6D](#), lane 5 and 6e). The findings suggested that the OATP1B3-expressing cells die upon ICG-NIR administration at least partially through the ferroptosis pathway.

### 3.7 *In vivo* PDT of nude mice with subcutaneous tumors

On the basis of the findings of ICG-NIR treatment *in vitro*, we investigated the effects of tumor therapy *in vivo*. The mice were divided into two groups: group 1 (control; ICG treatment without laser irradiation) and group 2 (PDT; ICG treatment with laser irradiation). On the basis of IVIS results presented in [Supplementary Figure S3](#), we applied laser treatment to the tumor 24 h after the administration of ICG. After conducting different therapies, tumor volumes were measured every 2 days. Finally, we sacrificed mice for obtaining tumors. Specimens were collected, and lipid peroxidation was examined through immunohistochemical (IHC) staining ([Supplementary Figure S4](#)). During the treatment, no marked difference in weight changes was noted among the groups, suggesting minimal damage by PDT ([Figure 7B](#)). However, as presented in [Figures 7A,C](#) marked difference in tumor volumes was observed between the groups receiving ICG without laser irradiation and ICG with laser irradiation, implying that ICG-NIR exerted a tumor inhibitory effect on the OATP1B3-expressing cells. The digital photos of mice in distinct groups were obtained to illustrate the therapeutic effect visually ([Figure 7A](#)).

## 4 Discussion

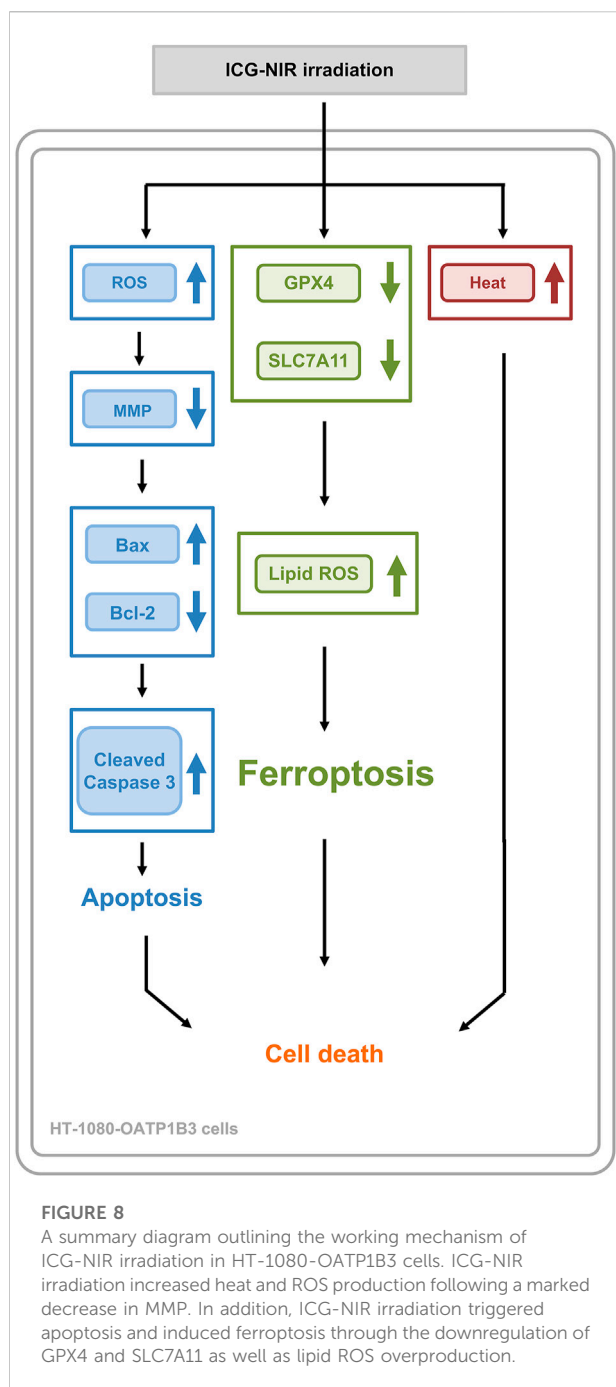
This study demonstrated the multiple anticancer properties of ICG. ICG exhibited photothermal and photodynamic effects, eventually causing apoptosis and ferroptosis. Multimodal and combination cancer therapies have changed the landscape of anticancer treatment ([Meric-Bernstam et al., 2021](#); [Gugenheim et al., 2022](#)). Various medications focusing on different cancer-specific pathways increase patient survival. ICG can be used in multimodal or combination anticancer therapy for several reasons. First, ICG has been clinically used for decades. Its broad therapeutic range and safety were reported ([Lu and Hsiao, 2021](#)). Second, because ICG is stimulated at the infrared activation range, it may penetrate deeper into cancer tissues where visible light cannot reach. Third, we previously observed that the metabolism of ICG is regulated by several transmembrane proteins such as the OATP family. Moreover, OATP proteins are expressed in several cancer cells ([Thakkar et al., 2013](#); [Morio et al., 2018](#); [Chen et al., 2020](#)), making ICG a potential theranostic molecule.

**FIGURE 7**

Effect of PDT on antitumor capabilities *in vivo*. ICG was administered every day following laser irradiation. The tumor volumes and body weights were measured at indicated times. **(A)** Representative photos of HT-1080-OATP1B3-bearing mice receiving PDT. **(B)** Body weights of mice after treatment. **(C)** Relative tumor change curves during 808-nm laser irradiation. The results are presented as the mean  $\pm$  SEM ( $n = 8$  per group,  $**p < 0.01$  between the laser and non-laser groups.).

A relationship exists between OATP1B3 and cancers. OATP1B3 is highly expressed in breast, gastrointestinal tract, lung, prostate, colon, and pancreatic cancers (Abe et al., 2001; Monks et al., 2007; Muto et al., 2007; Hamada et al., 2008; Lee et al., 2008; Kounnis et al., 2011). Furthermore, OATP1B3 protein expression is positively correlated with the clinicopathological features of patients with cancer and has a predictive value. Hence, examining ICG-treated OATP1B3-expressing cells exposed to laser irradiation might facilitate the development of cancer therapies. This study proposed that the elevated ROS level and photothermal effect mediated the cell

death of the OATP1B3-expressing cells after ICG-NIR administration. These findings have been reported previously (Sheng et al., 2018), indicating that OATP1B3-expressing cells can be a significant target during PDT because they have a more substantial capacity of intaking ICG. Although other studies have indicated that oxidative stress, hyperthermic effect, and repeated NIR laser exposure play essential roles in the effectiveness of PDT (Dolmans et al., 2003; Brown et al., 2004; Wu et al., 2020), our findings indicated that the quenching effect of ICG may be another critical factor underlying the anti-tumor effect of ICG-NIR therapy due to higher ROS production.



ICG strongly absorbs NIR irradiation; thus, it can convert absorbed light energy into ROS and heat. This study examined mechanisms through which ICG-NIR treatment causes ROS production and heat generation in OATP1B3-expressing cells. Our results indicated that high ROS accumulation in cells led to a decrease in MMP, followed by the initiation of apoptosis (Ly et al., 2003). In addition, the OATP1B3-expressing cells became more spherical, and cell viability decreased and cell death increased in a time-dependent manner. Similar results or

tendencies have been demonstrated in other studies examining the effects of photosensitizers on various cell lines (Zhang et al., 2019; Jiang et al., 2020; Park et al., 2020).

Our results also indicated that ICG-NIR administration caused death in the OATP1B3-expressing cells through ferroptosis. This unique modality of cell death, driven by iron-dependent phospholipid peroxidation, is regulated by multiple cellular metabolic pathways. Accumulating research has implied that many cancer cells show increased susceptibility to ferroptosis, and ferroptosis induction can be explored as an anticancer therapy (Zuo et al., 2020; Jiang et al., 2021). However, this newly discovered form of cell death and its connection with cancer should be examined. Essential regulators of ferroptosis, such as a crucial inhibitor of phospholipid peroxidation, glutathione peroxidase 4 (GPX4), and the system  $x_c^-$  cystine/glutamate antiporter (a transmembrane protein complex containing subunits SLC7A11 and SLC3A2), inhibit ferroptosis by contributing to GPX4 activity. Our findings suggested that ICG-NIR treatment induced ferroptosis through the regulation of GPX4 and SLC7A11 and the accumulation of lipid ROS, as indicated by the results of the Western blot and C11-BODIPY fluorescence staining (Figure 6) in the OATP1B3-expressing cells.

Given its optical absorbance in the NIR region, ICG has been widely used in fluorescence imaging. *In vivo* imaging offers a unique approach to visualizing the dynamic distribution of ICG within the whole body. Our imaging data demonstrated that ICG was incorporated explicitly into and visualized in the subcutaneous xenograft OATP1B3-expressing tumors of mice 24 h post intraperitoneal injection (Supplementary Figure S3A). The background uptake in most tissues has been low because OATP1B3 exhibits restricted tissue expression (Svoboda et al., 2011). Moreover, PDT induced ROS production and suppressed tumor growth *in vivo* (Supplementary Figure S4 and Figure 7B). The 4HNE antibody is a promising antigen because it can be targeted to evaluate cellular ROS levels in tissues through IHC (Hu et al., 2020). Thus, we used 4HNE to detect oxidative stress-mediated lipid peroxidation. The IHC results indicated that OATP1B3-expressing tumors had a significantly high readout for ROS after ICG-NIR therapy.

Compared with other studies, the anti-tumor effect of PDT combined with ICG in our model mice was stronger because of the sufficient accumulation of ICG in OATP1B3-expressing tumors. The inadequate accumulation of ICG in tumors would adversely affect tumor growth prevention. Nevertheless, this study has some limitations. First, for measuring tumor sizes, our method should be improved because of the presence of measurement errors and anthropogenic factors. In the future, measurements conducted through imaging can synergistically provide information to delineate tumor size, scope, and guiding therapy accurately. In addition, the size of tumors is the major factor limiting the application of the findings of the present study to clinical practice. ICG-NIR therapy was found to be effective only for small tumors. Therefore, ICG-NIR treatment combined



with other therapeutic tools may be necessary for clinical use. As for *in vivo* cell line-derived xenograft, we only compared the NIR effect of OATP1B3-expressing HT-1080 cells after ICG injection, we didn't perform the comparison between HT-1080 and OATP1B3-expressing HT-1080 cells. The reason is that there is endogenous uptake of ICG of HT-1080 cells that might interfere with our interpretation of the ICG effect (Wu et al., 2018). However, the endogenous uptake of ICG in many cancer cells could be used as an advantage in future ICG-NIR irradiation treatment. Further study regarding the role of endogenous ICG in these cancer cells and the possibility of treatment through the ferroptosis pathway should be investigated.

Our findings have several implications for cancer treatment. With the progress in optics and robotic mechanics, more effective surgical instruments have been increasingly used in tumor surgery. In combination with these techniques, ICG has been used by surgeons to visualize undissected, residual tumors (Kaplan-Marans et al., 2019; Baiocchi et al., 2021). These tumors could be ablated by infrared laser through the aforementioned mechanisms. Additionally, ICG can be easily encapsulated into nanocomposites as a small molecule, making the implementation of a cancer-specific, multiple functionality theranostic strategy possible (Wang et al., 2017; Wang et al., 2019a). Finally, for cancer cells exhibiting anti-ferroptotic mechanisms or expressing cancer-type OATP1B3, our findings on the ferroptotic effect of ICG and ICG metabolism might contribute to eradication of cancer cells.

## 5 Conclusion

In addition to the photodynamic and photothermal effect, ICG with NIR irradiation successfully enhanced the death of the OATP1B3-expressing cells through apoptosis and ferroptosis. Furthermore, the quenching effect of ICG may be a crucial factor in effective PDT due to the higher production of ROS and the severe loss of MMP. The multiple mechanisms of cancer therapy (Figure 8) in a single molecule can provide conceptual and mechanistic insights into cancer theranostic strategy.

## Data availability statement

The original contributions presented in the study are included in the article/Supplementary Material, further inquiries can be directed to the corresponding author.

## Ethics statement

The animal study was reviewed and approved by Institutional Animal Care and Use Committee (IACUC) of Taipei Tzu Chi

General Hospital, Buddhist Tzu Chi Medical Foundation (102-IACUC-024).

## Author contributions

J-KH and C-YK designed and guided the whole study, and H-CT carried out most of the experiments and data collection; T-SC performed H&E staining and IHC analysis. W-TL performed fluorescence microscopy and created the graphical abstract. H-CT and T-SC performed animal experiments. H-CT and C-YK analyzed the data. J-KH and H-CT wrote and edited the manuscript.

## Funding

This research was funded in part by the Taiwan Ministry of Science and Technology (MOST-110-2314-B-303-013-MY3, approved in Aug. 2021) and Taipei Tzu Chi Hospital (TCRD-TPE-109-35, approved in Jan. 2019, TCRD-TPE-106-34, approved in Jan. 2017).

## Acknowledgments

The authors thank the staff of the Eighth Core Labs, Department of Medical Research, National Taiwan University, and Hsu-Liang Hsieh's lab (Institute of Plant Biology, College of Life Science, National Taiwan University) for providing facility and technical support. We thank the Core Laboratory of the Taipei Tzu Chi Hospital, Buddhist Tzu Chi Medical Foundation, for assistance with the laboratory studies. We also appreciate the work of the research assistant Xin-Hui Wang from the Instrument Center at National Taiwan University for IVIS measurements.

## Conflict of interest

The authors declare that the research was conducted in the absence of any commercial or financial relationships that could be construed as a potential conflict of interest.

## Publisher's note

All claims expressed in this article are solely those of the authors and do not necessarily represent those of their affiliated organizations, or those of the publisher, the editors and the reviewers. Any product that may be evaluated in this article, or claim that may be made by its manufacturer, is not guaranteed or endorsed by the publisher.

## Supplementary material

The Supplementary Material for this article can be found online at: <https://www.frontiersin.org/articles/10.3389/fmolb.2022.1045885/full#supplementary-material>

### SUPPLEMENTARY FIGURE S1

HT-1080 OATP1B3-expressing cells after ICG incubation.

### SUPPLEMENTARY FIGURE S2

Schematic diagram of the NIR laser source for *in vitro* and *in vivo* PDT.

### SUPPLEMENTARY FIGURE S3

*In vivo* fluorescence imaging in ICG-treated mice with subcutaneous tumors.

### SUPPLEMENTARY FIGURE S4

Histological analysis of subcutaneous tumors in ICG-NIR treated mice.

## References

- Abe, T., Unno, M., Onogawa, T., Tokui, T., Noriko Kondo, T., Nakagomi, R., et al. (2001). LST-2, A human liver-specific organic anion transporter, determines methotrexate sensitivity in gastrointestinal cancers. *Gastroenterology* 120, 1689–1699. doi:10.1053/GAST.2001.24804
- Augsburger, D., Nelson, P. J., Kalinski, T., Udelnow, A., Knösel, T., Hofstetter, M., et al. (2017). Current Diagnostics and treatment of fibrosarcoma –perspectives for future therapeutic targets and strategies. *Oncotarget* 8, 104638–104653. doi:10.18632/ONCOTARGET.20136
- Baiocchi, G. L., Guercioni, G., Vettoretto, N., Scabini, S., Millo, P., Muratore, A., et al. (2021). ICG fluorescence imaging in colorectal surgery: A snapshot from the ical study group. *BMC Surg.* 21, 190. doi:10.1186/S12893-021-01191-6
- Brown, S. B., Brown, E. A., and Walker, I. (2004). The present and future role of photodynamic therapy in cancer treatment. *Lancet. Oncol.* 5, 497–508. doi:10.1016/S1470-2045(04)01529-3
- Chen, C., Wang, Z., Jia, S., Zhang, Y., Ji, S., Zhao, Z., et al. (2022). Evoking highly immunogenic ferroptosis aided by intramolecular motion-induced photo-hyperthermia for cancer therapy. *Adv. Sci.* 2022, 2104885. doi:10.1002/ADVS.202104885
- Chen, S., Li, K., Jiang, J., Wang, X., Chai, Y., Zhang, C., et al. (2020). Low expression of organic anion-transporting polypeptide 1B3 predicts a poor prognosis in hepatocellular carcinoma. *World J. Surg. Oncol.* 18, 127–213. doi:10.1186/s12957-020-01891-y
- Daigeler, A., Brenzel, C., Bulut, D., Geisler, A., Hilgert, C., Lehnhardt, M., et al. (2008). TRAIL and taurodine induce apoptosis and decrease proliferation in human fibrosarcoma. *J. Exp. Clin. Cancer Res.* 27, 82. doi:10.1186/1756-9966-27-82
- Dixon, S. J., Lemberg, K. M., Lamprecht, M. R., Skouta, R., Zaitsev, E. M., Gleason, C. E., et al. (2012). Ferroptosis: An iron-dependent form of non-apoptotic cell death. *Cell* 149, 1060–1072. doi:10.1016/j.CELL.2012.03.042
- Dolmans, D. E. J. G., Fukumura, D., and Jain, R. K. (2003). Photodynamic therapy for cancer. *Nat. Rev. Cancer* 3, 380–387. doi:10.1038/nrc1071
- Donato Di Paola, E., and Nielsen, O. S. (2002). The EORTC soft tissue and bone sarcoma group. *Eur. J. cancer.* Oxford, England, 38, 138–141. doi:10.1016/S0959-8049(01)00444-0
- Gugenheim, J., Crovetto, A., and Petrucciani, N. (2022). Neoadjuvant therapy for pancreatic cancer. *Updat. Surg.* 74, 35–42. doi:10.1007/S13304-021-01186-1
- Guo, C. Y., Sun, L., Chen, X. P., and Zhang, D. S. (2013). Oxidative stress, mitochondrial damage and neurodegenerative diseases. *Neural Regen. Res.* 8, 2003–2014. doi:10.3969/j.issn.1673-5374.2013.21.009
- Hamada, A., Sissung, T., Price, D. K., Danesi, R., Chau, C. H., Sharifi, N., et al. (2008). Effect of SLC01B3 haplotype on testosterone transport and clinical outcome in caucasian patients with androgen-independent prostatic cancer. *Clin. Cancer Res.* 14, 3312–3318. doi:10.1158/1078-0432.CCR-07-4118
- Hsiao, J.-K., Law, B., Weissleder, R., and Tung, C.-H. (2013). *In-vivo* imaging of tumor associated urokinase-type plasminogen activator activity. *J. Biomed. Opt.* 11, 34013. doi:10.1117/1.2204029
- Hu, J., Pauer, G. J., Hagstrom, S. A., Bok, D., DeBenedictis, M. J., Bonilha, V. L., et al. (2020). Evidence of complement dysregulation in outer retina of stargardt disease donor eyes. *Redox Biol.* 37, 101787. doi:10.1016/j.REDOX.2020.101787
- Imai, S., Kikuchi, R., Tsuruya, Y., Naoi, S., Nishida, S., Kusuhara, H., et al. (2013). Epigenetic regulation of organic anion transporting polypeptide 1b3 in cancer cell lines. *Pharm. Res.* 30, 2880–2890. doi:10.1007/s11095-013-1117-1
- Ježek, J., Cooper, K. F., and Strich, R. (2018). Reactive oxygen species and mitochondrial dynamics: The yin and yang of mitochondrial dysfunction and cancer progression. *Antioxidants* 7, 13. doi:10.3390/ANTIOX7010013
- Jiang, X., Du, B., Huang, Y., Yu, M., and Zheng, J. (2020). Cancer photothermal therapy with ICG-conjugated Gold nanoclusters. *Bioconjugate Chem.* 31, 1522–1528. doi:10.1021/ACS.BIOCONJCHEM.0C00172/SUPPL\_FILE/BC0C00172\_SI\_001
- Jiang, X., Stockwell, B. R., and Conrad, M. (2021). Ferroptosis: Mechanisms, biology and role in disease. *Nat. Rev. Mol. Cell Biol.* 22, 266–282. doi:10.1038/s41580-020-00324-8
- Kaplan-Marans, E., Fulla, J., Tomer, N., Bilal, K., and Palese, M. (2019). Indocyanine green (ICG) in urologic surgery. *Urology* 132, 10–17. doi:10.1016/j.UROLOGY.2019.05.008
- Kounnis, V., Ioachim, E., Svoboda, M., Tzakos, A., Sainis, I., Thalhammer, T., et al. (2011). Expression of organic anion-transporting polypeptides 1B3, 1B1, and 1A2 in human pancreatic cancer reveals a new class of potential therapeutic targets. *Oncotargets Ther.* 4, 27–32. doi:10.2147/OTT.S16706
- Lachaier, E., Louandre, C., Godin, C., Saidak, Z., Baert, M., Diouf, M., et al. (2014). Sorafenib induces ferroptosis in human cancer cell lines originating from different solid tumors. *Anticancer Res.* 34, 6417–6422.
- Lee, W., Belkhir, A., Lockhart, A. C., Merchant, N., Glaeser, H., Harris, E. I., et al. (2008). Overexpression of OATP1B3 confers apoptotic resistance in colon cancer. *Cancer Res.* 68, 10315–10323. doi:10.1158/0008-5472.CAN-08-1984
- Liang, C., Zhang, X., Yang, M., and Dong, X. (2019). Recent progress in ferroptosis inducers for cancer therapy. *Adv. Mat.* 31, 1904197. doi:10.1002/ADMA.201904197
- Lu, C. H., and Hsiao, J. K. (2021). Indocyanine green: An old drug with novel applications. *Tzu Chi Med. J.* 33, 317–322. doi:10.4103/tcmj.tcmj\_216\_20
- Ly, J. D., Grubb, D. R., and Lawen, A. (2003). The mitochondrial membrane potential (Deltapsi(m)) in apoptosis; an update. *Apoptosis* 8, 115–128. doi:10.1023/A:1022945107762
- Meric-Bernstam, F., Larkin, J., Tabernero, J., and Bonini, C. (2021). Enhancing anti-tumour efficacy with immunotherapy combinations. *Lancet (London, Engl.* 397, 1010–1022. doi:10.1016/S0140-6736(20)32598-8
- Monks, N. R., Liu, S., Xu, Y., Yu, H., Bendelow, A. S., and Moscow, J. A. (2007). Potent cytotoxicity of the phosphatase inhibitor microcystin LR and microcystin analogues in OATP1B1- and OATP1B3-expressing HeLa cells. *Mol. Cancer Ther.* 6, 587–598. doi:10.1158/1535-7163.MCT-06-0500
- Morio, H., Sun, Y., Harada, M., Ide, H., Shimoza, O., Zhou, X., et al. (2018). Cancer-type OATP1B3 mRNA in extracellular vesicles as a promising candidate for a serum-based colorectal cancer biomarker. *Biol. Pharm. Bull.* 41, 445–449. doi:10.1248/BBP.B17-00743
- Murphy, M. P. (2013). Mitochondrial dysfunction indirectly elevates ROS production by the endoplasmic reticulum. *Cell Metab.* 18, 145–146. doi:10.1016/j.CMET.2013.07.006
- Muto, M., Onogawa, T., Suzuki, T., Ishida, T., Rikiyama, T., Katayose, Y., et al. (2007). Human liver-specific organic anion transporter-2 is a potent prognostic factor for human breast carcinoma. *Cancer Sci.* 98, 1570–1576. doi:10.1111/J.1349-7006.2007.00570.X
- Park, T., Lee, S., Amaty, R., Cheong, H., Moon, C., Kwak, H. D., et al. (2020). ICG-loaded PEGylated BSA-silver nanoparticles for effective photothermal cancer therapy. *Int. J. Nanomedicine* 15, 5459–5471. doi:10.2147/IJN.S255874
- Porcu, E. P., Salis, A., Gavini, E., Rassu, G., Maestri, M., and Giunchedi, P. (2016). Indocyanine green delivery systems for tumour detection and treatments. *Biotechnol. Adv.* 34, 768–789. doi:10.1016/j.BIOTECHADV.2016.04.001
- Radzi, R., Osaki, T., Tsuka, T., Imagawa, T., Minami, S., Nakayama, Y., et al. (2012). Photodynamic hyperthermal therapy with indocyanine green (ICG) induces apoptosis and cell cycle arrest in B16F10 murine melanoma cells. *J. Vet. Med. Sci.* 74, 545–551. doi:10.1292/JVMS.11-0464
- Rasheed, S., Nelson-Rees, W. A., Toth, E. M., Arnstein, P., and Gardner, M. B. (1974). Characterization of a newly derived human sarcoma cell line (HT-1080).

- Cancer* 33, 1027–1033. doi:10.1002/1097-0142(197404)33:4<1027::AID-CNCR2820330419>3.0.CO;2-Z
- Sheng, D., Liu, T., Deng, L., Zhang, L., Li, X., Xu, J., et al. (2018). Perfluorooctyl bromide & indocyanine green Co-loaded nanoliposomes for enhanced multimodal imaging-guided phototherapy. *Biomaterials* 165, 1–13. doi:10.1016/j.BIOMATERIALS.2018.02.041
- Shitara, C., Kaneko, J., Inagaki, Y., Kokudo, T., Sato, M., Kiritani, S., et al. (2017). Near-infrared photothermal/photodynamic therapy with indocyanine green induces apoptosis of hepatocellular carcinoma cells through oxidative stress. *Sci. Rep.* 7, 13958. doi:10.1038/S41598-017-14401-0
- Shitara, Y. (2011). Clinical importance of OATP1B1 and OATP1B3 in drug-drug interactions. *Drug Metab. Pharmacokinet.* 26, 220–227. doi:10.2133/DMPK.DMPK-10-RV-094
- Smiley, S., Reers, M., Mottola-Hartshorn, C., Lin, M., Chen, A., Smith, T., et al. (1991). Intracellular heterogeneity in mitochondrial membrane potentials revealed by a J-aggregate-forming lipophilic cation JC-1. *Proc. Natl. Acad. Sci. U. S. A.* 88 (9), 3671–3675. doi:10.1073/pnas.88.9.3671
- Su, Y., Zhao, B., Zhou, L., Zhang, Z., Shen, Y., Lv, H., et al. (2020). Ferroptosis, a novel pharmacological mechanism of anti-cancer drugs. *Cancer Lett.* 483, 127–136. doi:10.1016/J.CANLET.2020.02.015
- Svoboda, M., Riha, J., Wlcek, K., Jaeger, W., and Thalhammer, T. (2011). Organic anion transporting polypeptides (OATPs): Regulation of expression and function. *Curr. Drug Metab.* 12, 139–153. doi:10.2174/138920011795016863
- Thakkar, N., Kim, K., Jang, E. R., Han, S., Kim, K., Kim, D., et al. (2013). A cancer-specific variant of the SLC01B3 gene encodes a novel human organic anion transporting polypeptide 1B3 (OATP1B3) localized mainly in the cytoplasm of colon and pancreatic cancer cells. *Mol. Pharm.* 10, 406–416. doi:10.1021/MP3005353
- Wang, M., Xiao, Y., Li, Y., Wu, J., Li, F., Ling, D., et al. (2019). Reactive oxygen species and near-infrared light dual-responsive indocyanine green-loaded nanohybrids for overcoming tumour multidrug resistance. *Eur. J. Pharm. Sci.* 134, 185–193. doi:10.1016/J.EJPS.2019.04.021
- Wang, Y., Xie, Y., Li, J., Peng, Z. H., Sheinin, Y., Zhou, J., et al. (2017). Tumor-penetrating nanoparticles for enhanced anticancer activity of combined photodynamic and hypoxia-activated therapy. *ACS Nano* 11, 2227–2238. doi:10.1021/ACS.NANO.6B08731
- Wang, Z., Ju, Y., Ali, Z., Yin, H., Sheng, F., Lin, J., et al. (2019). Near-infrared light and tumor microenvironment dual responsive size-switchable nanocapsules for multimodal tumor theranostics. *Nat. Commun.* 10, 4418–4512. doi:10.1038/s41467-019-12142-4
- Wu, M.-R., Huang, Y.-Y., and Hsiao, J.-K. (2019). Role of sodium taurocholate cotransporting polypeptide as a new reporter and drug-screening platform: Implications for preventing hepatitis B virus infections. *Mol. Imaging Biol.* 22 (2), 313–323. doi:10.1007/s11307-019-01373-y
- Wu, M.-R., Huang, Y.-Y., and Hsiao, J.-K. (2019). Use of indocyanine green (ICG), a medical near infrared dye, for enhanced fluorescent imaging—comparison of organic anion transporting polypeptide 1B3 (OATP1B3) and sodium-taurocholate cotransporting polypeptide (NTCP) reporter genes. *Molecules* 24, 2295. doi:10.3390/molecules24122295
- Wu, M.-R., Liu, H.-M., Lu, C.-W., Shen, W.-H., Lin, I.-J., Liao, L.-W., et al. (2018). Organic anion-transporting polypeptide 1B3 as a dual reporter gene for fluorescence and magnetic resonance imaging. *FASEB J.* 32, 1705–1715. doi:10.1096/fj.201700767R
- Wu, X., Suo, Y., Shi, H., Liu, R., Wu, F., Wang, T., et al. (2020). Deep-tissue photothermal therapy using laser illumination at NIR-IIa window. *Nano-Micro Lett.* 12, 38–13. doi:10.1007/s40820-020-0378-6
- Xu, T., Ding, W., Ji, X., Ao, X., Liu, Y., Yu, W., et al. (2019). Molecular mechanisms of ferroptosis and its role in cancer therapy. *J. Cell. Mol. Med.* 23, 4900–4912. doi:10.1111/JCMM.14511
- Ye, Z., Liu, W., Zhuo, Q., Hu, Q., Liu, M., Sun, Q., et al. (2020). Ferroptosis: Final destination for cancer? *Cell Prolif.* 53, e12761. doi:10.1111/CPR.12761
- Zhang, X., Li, Y., Wei, M., Liu, C., and Yang, J. (2019). Cetuximab-modified silica nanoparticle loaded with ICG for tumor-targeted combinational therapy of breast cancer. *Drug Deliv.* 26, 129–136. doi:10.1080/10717544.2018.1564403
- Zuo, S., Yu, J., Pan, H., and Lu, L. (2020). Novel insights on targeting ferroptosis in cancer therapy. *Biomark. Res.* 8, 50. doi:10.1186/S40364-020-00229-W

# Frontiers in Molecular Biosciences

Explores biological processes in living organisms  
on a molecular scale

Focuses on the molecular mechanisms  
underpinning and regulating biological processes  
in organisms across all branches of life.

## Discover the latest Research Topics

[See more →](#)

### Frontiers

Avenue du Tribunal-Fédéral 34  
1005 Lausanne, Switzerland  
[frontiersin.org](https://frontiersin.org)

### Contact us

+41 (0)21 510 17 00  
[frontiersin.org/about/contact](https://frontiersin.org/about/contact)



### Frontiers in Molecular Biosciences

